

CHEMICAL & PHARMACEUTICAL BULLETIN

Vol. 35, No. 3

March 1987

Regular Articles

[Chem. Pharm. Bull.]
35(3) 933-940 (1987)

Estimation of Cation Binding of Arabate by Conductivity Measurement¹⁾

CHIKAKO YOMOTA*^a and MASAYUKI NAKAGAKI^b

*National Institute of Hygienic Sciences, Osaka,^a 1-1-43 Hoenzaka,
Higashi-ku, Osaka 540, Japan and Faculty of Pharmaceutical
Sciences, Kyoto University,^b Yoshida-Shimoadachi-cho,
Sakyo-ku, Kyoto 606, Japan*

(Received August 8, 1986)

The cation binding behavior of arabate was investigated by conductivity measurements with reference to the various colligative properties of arabate reported previously. The equivalent conductance of arabic anion, A_p , was found to be about $6 (\Omega^{-1} \cdot \text{cm}^{-1} \cdot \text{eq}^{-1})$ from the conductivity titration curves of arabic acid with tetra-*n*-butylammonium hydroxide (TBA-OH). Using the value of $A_p=6$, cation binding of arabate was estimated by the conductivity measurement of TBA-arabate at a constant concentration of 1.2×10^{-2} (eq/kg) in the presence of various added salts, and the binding curves were found to be of Langmuir type. Since the saturated amounts of cation binding, x_{∞} , were observed to be similar to each other among cations of the same valency, since they increased with the valence number of cations, the interactions of arabate with cations were suggested to be due to electrostatic force. The present results are discussed in terms of the estimation methods of cation binding behavior of arabate.

Keywords—gum arabic; arabic acid; conductivity measurement; cation binding

Introduction

Arabate, which is the main component of gum arabic, is a typical polyelectrolyte, and is widely used as a food additive and a pharmaceutical material²⁾ because of its particular characteristics arising from its branched anionic heteropolysaccharide structure with a very low charge density, as discussed previously.³⁾ Among many useful characteristics of arabate, its emulsifying ability and binding capacity are excellent. In contrast to the extensive investigations on the physicochemical properties of linear polyelectrolytes, relatively little is known about arabate.

Recently, gum arabic has been in short supply worldwide because of under-production in the Republic of Sudan, which is a main producing country. Thus, it would be desirable to develop a substitute for gum arabic. First, however, the physicochemical characteristics of arabate must be established.

In the previous paper, such colligative properties of arabate as the osmotic coefficient, ϕ ,³⁾ the counterion activity coefficient, γ_+ ³⁾ and the transport parameter, f ,⁴⁾ were investigated

to cast a light on the fundamental properties of the branched polyelectrolyte, and the counterion binding of arabate was elucidated in detail.

In the present work, the characteristic behavior of arabate with counterions was further studied with tetra-*n*-butyl ammonium arabate (TBA-arabate) because the interaction of the TBA ion with arabate can be neglected due to the complete dissociation resulting from the large size of the TBA ion under the present experimental conditions,^{5,6)} and so the amount of cation binding to arabate can be directly calculated by using conductivity measurement.⁷⁻⁹⁾ This method seems to be simple and convenient than the others based on the colligative properties of arabate, when comparing the cation-binding characteristics of various polyelectrolytes similar to gum arabic with those of arabate. Methods for estimation of cation binding based on the colligative properties are discussed.

Materials and Methods

Arabic acid was purified from a batch of crude *Acacia senegal* gum (F1-08), which was a gift from San-ei Chemicals Engineering Co., as reported previously.³⁾ TBA-arabate was prepared by adding a calculated amount of extra pure TBA hydroxide, purchased from Tokyo Kasei Co., to the purified arabic acid solution. All other chemicals were of reagent grade and were used without further purification. Water used in this experiment was twice-distilled after being passed through an ion-exchange column.

Conductivity Measurements and Cation Binding to Polyanion—Conductivity measurements were performed at 25 ± 0.01 °C with Jones' type cells and with a Metrohm Konduktoskope E 365 B. The specific conductance of anionic polyelectrolyte solution, κ , is expressed by the following equation:

$$1000 \cdot \kappa = f \cdot m_p (A_p + A_c) \quad (1)$$

where m_p is the polymer concentration in equivalents (eq/l), f is the transport parameter, that is, the ratio of free counterion to polyanion in the electric field, A_p is the limiting equivalent conductance of polyanion and A_c is the limiting equivalent conductance of counterion. On adding a salt, C_s , to the anionic polyelectrolyte solution, some cations of the added salt will be bound to the polyanion, resulting in an increase of free counterions corresponding to pC_m , where C_m is the concentration of the bound cation and p is the cation exchange parameter with a value of less than 1.0. Then, the specific conductance in a salt-added system, κ' , is expressed as follows:

$$1000 \cdot \kappa' = (m_p f - (1-p)C_m)A_p + (m_p f + pC_m)A_c + (C_s - C_m)A_+ + C_s A_- \quad (2)$$

where A_+ is the limiting equivalent conductance of the added cation and A_- is that of the added anion. The increment of specific conductance induced by the addition of a salt to the anionic polyelectrolyte solution, $\Delta\kappa$, is therefore given by Eq. 1 and Eq. 2 as follows:

$$1000 \cdot \Delta\kappa = C_m((p-1)A_p + pA_c - A_+) + C_s(A_+ + A_-) \quad (3)$$

Equation 3 indicates that C_m can be obtained by measuring both conductance and the value of p , which is dependent on the dissociation constant. In this experiment, TBA ion was used as a counterion. As this ion cannot be bound to carboxyl groups of the polymers due to the steric hindrance arising from the large molecular size of the tetrabutyl group, f can be assumed to be nearly equal to unity, and therefore, the value of p is negligible. Substituting $p=0$ into Eq. 3, Eq. 3' is obtained:

$$C_s A_s - 1000 \cdot \Delta\kappa = C_m(A_p + A_+) \quad (3')$$

where A_s is given as $A_s = (A_+ + A_-)$.

Provided that the TBA ion can dissociate completely in such a polyanion-counterion system when arabic acid is titrated with TBA-OH, the specific conductance of the solution, κ , at any degree of neutralization, should be given by the following equation:

$$1000 \cdot \kappa = C_H A_H + C_{TBA} A_{TBA} + \alpha m_p A_p \quad (4)$$

According to Eq. 4, the contribution of a cation should be expressed as $1000 \cdot \kappa_+ = C_H A_H + C_{TBA} A_{TBA}$, and this leads to

$$1000(\kappa - \kappa_+) = \alpha m_p A_p \quad (5)$$

When the values of C_H , C_{TBA} , A_H and A_{TBA} are found, A_p can be obtained according to Eq. 5.

Results

Estimation of Equivalent Conductance of Arabic Acid

To obtain the value of the equivalent conductance, Λ_p , according to Eq. 4 described in Materials and Methods, arabic acid was titrated with TBA-OH or NaOH and the pH and conductance changes were measured against the degree of neutralization, α , at a constant arabic acid concentration of 0.0162 (eq/l). The results obtained are shown in Fig. 1. The pH titration curves of arabic acid with TBA-OH or NaOH were approximately the same at all degrees of neutralization, indicating similar degrees of ionization for both counterions. Conductometric titration curves, which are also shown in Fig. 1, were both gently concave as is characteristic of weak acids, but not strong acids, whose conductances show a linear decrease with neutralization and a sharp increase after $\alpha=1.0$. However, a different counterion showed a remarkably different titration curve, due mainly to the difference of equivalent conductances. By using the pH and conductometric titration curves shown in Fig. 1, and the literature values¹⁰⁾ of Λ_H and Λ_{TBA} , which are 349.8 and 19.5, respectively, the equivalent conductance, Λ_p , given by Eq. 4 was calculated graphically (Fig. 2). Here, $(\kappa - \kappa_+)$ and Λ_p were plotted against α , where $(\kappa - \kappa_+)$ is the difference between the observed specific conductance of the polymer-counterion system (κ) and that of the counterion alone (κ_+).

As is clear from Fig. 2, the value of $(\kappa - \kappa_+)$ increased sharply at a lower degree of neutralization and became constant at about $\alpha=0.3$. On the other hand, the value of Λ_p decreased gently with neutralization, became constant with an extrapolated value of 6.0 ($\Omega^{-1} \cdot \text{cm}^{-1} \cdot \text{eq}^{-1}$).

Specific Conductance of Arabate in a Salt-Added System and Cation Binding

The conductance of TBA-arabate solution was measured in the presence of KCl, NaCl, LiCl, CaCl₂, BaCl₂, MgCl₂ and LaCl₃. In the present experiments, the final concentration of arabate was always kept constant at 1.2×10^{-3} (eq/l).

First, the specific conductance of arabate solution, κ , was measured in the presence of monovalent salts, and the results obtained are shown in Fig. 3. It is clear that the value of $\Delta\kappa$

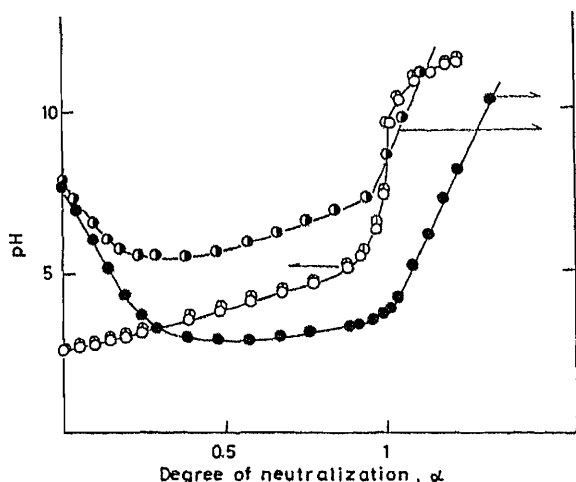


Fig. 1. pH and Conductometric Titration Curves of Arabic Acid

(○, ●), neutralized with tetrabutylammonium hydroxide; (⊙, ⊙) neutralized with sodium hydroxide.

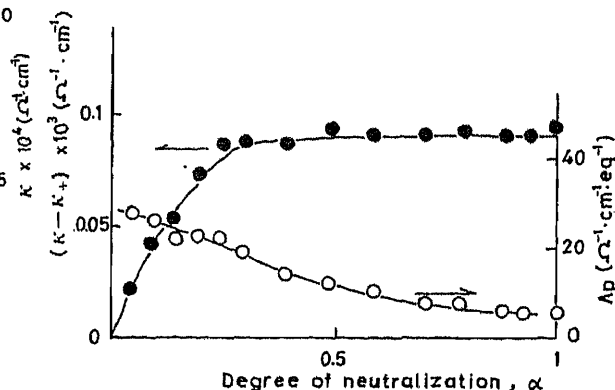


Fig. 2. Apparent Specific Conductance of Arabic Ion ($\kappa - \kappa_+$), and Equivalent Conductance of Arabic Ion, Λ_p , as a Function of Degree of Neutralization

Each value was calculated from the conductometric titration curve of arabic acid with TBA-OH shown in Fig. 1.

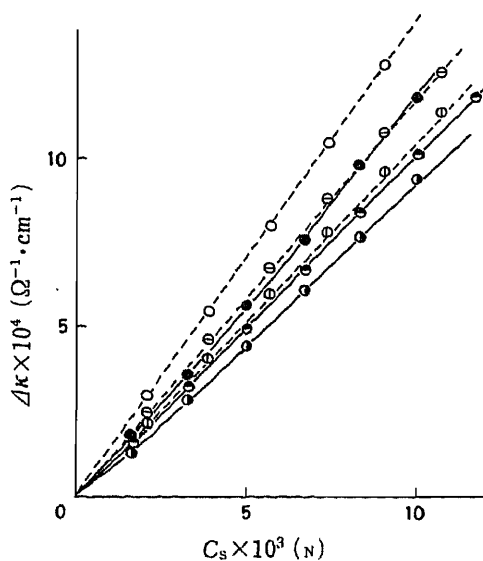


Fig. 3. Increment of Specific Conductance of Arabate-Salt Solutions *versus* Added Salt Concentration

The broken lines indicate the specific conductance of corresponding simple salt solutions in the absence of polymer. $m_p, 1.2 \times 10^{-2}$ eq/l; (O, ●), KCl; (◻, ◼), NaCl; (△, ▽), LiCl.

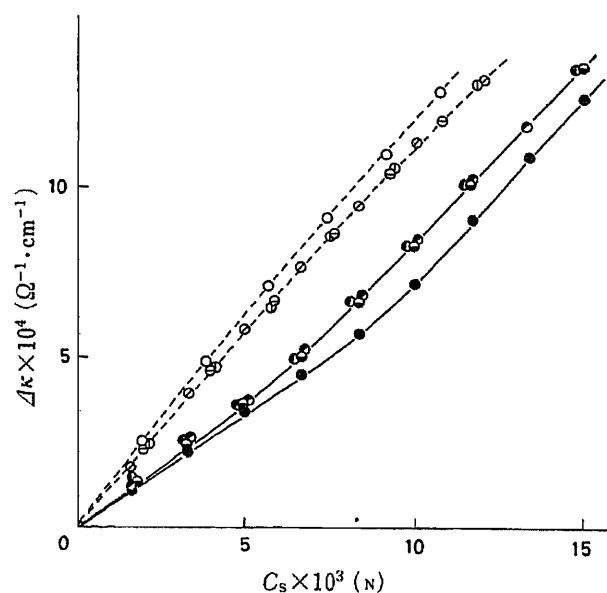


Fig. 4. Increment of Specific Conductance of Arabate-Salt Solutions *versus* Added Salt Concentration

The broken lines indicate the specific conductance of corresponding simple salt solutions. $m_p, 1.2 \times 10^{-2}$ eq/l; (◻, ◼), CaCl₂; (△, ▽), MgCl₂; (◇, ◇), BaCl₂; (○, ●), LaCl₃.

(solid line) increased linearly with increasing concentration of monovalent ion over the added salt concentration range from 1.5×10^{-3} to 1.2×10^{-2} (N). The slopes of the linear plots were in the order of $K > Na > Li$, reflecting the difference in the degree of association. The broken lines in Fig. 3 show the observed specific conductances of the corresponding simple salt solutions in the absence of arabate. The results indicate that the degree of binding of monovalent cations to arabate increased with increasing concentration of added salt, since the conductance difference between the solid line and the corresponding broken one may be due to the binding of the added cation to arabate.

Next, in the presence of divalent and trivalent salts, the specific conductance of arabate solution, κ , was measured at various concentrations of added salts, C_s . The results obtained are shown in Fig. 4.

The specific conductances increased linearly with C_s at low concentrations of added salts and bended up near the middle concentration tested in the present experiments so that the slopes of the solid lines got close to those of the broken lines which show the specific conductance of the corresponding simple salt solution in the absence of arabate. This may be mainly due to the saturation of cation binding to arabate, as will be discussed below.

As for the cation binding, the differences between the slopes of the solid lines and the corresponding broken ones in Fig. 4 as compared with those of Fig. 3 strongly suggest that the amount of monovalent cation binding to arabate is less than that of divalent or trivalent cations.

To clarify the characteristics of cation binding to arabate, the amount of binding, C_m , of the cation to arabate in relation to C_s was calculated according to Eq. 3 in Materials and Methods, by using the observed values shown in Fig. 3 and Fig. 4. In the use of Eq. 3', literature values of limiting equivalent conductance of various cations were taken from Robinson and Stokes¹⁰; K, 73.5; Na, 50.1; Li, 38.7; Ca, 59.5; Ba, 63.6; Mg, 53.1; La, 69.7. The value of $C_s A_s$ was obtained by measurement. The results obtained are shown in Fig. 5,

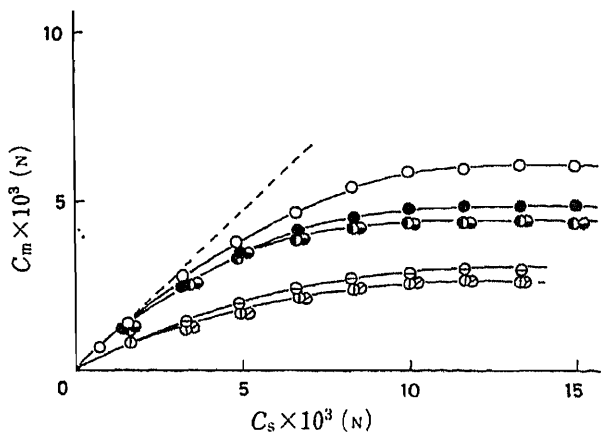


Fig. 5. The Relation between the Amount of Bound Cations, C_m , and the Concentration of Added Salt, C_s
 ○, LaCl_3 ; ●, BaCl_2 ; ◐, CaCl_2 ; ●, MgCl_2 ; ○, NaCl ; ◐, KCl ; ◐, LiCl .

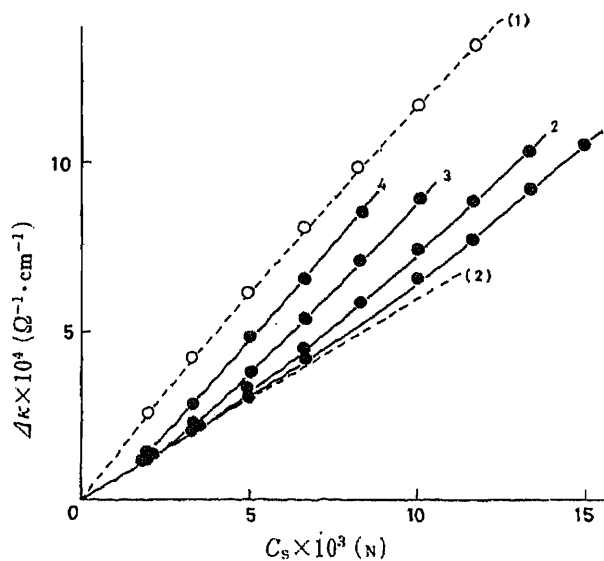


Fig. 6. Increment of Specific Conductance of Arabate- CaCl_2 Solutions versus Added CaCl_2 Concentration at Various Arabate Concentrations

Arabate concentration, m_p (eq/l): 1, 1.24×10^{-2} ; 2, 8.3×10^{-3} ; 3, 5.3×10^{-3} ; 4, 1.7×10^{-3} .
 The broken line (1) indicates the specific conductances of CaCl_2 solutions and the broken line (2) shows the conductivity contribution of Cl^- ions.

where the amount of bound cation is plotted against the concentration of the added salts. Each curve was of typical Langmuir type, and the saturated amount of cation bound to arabate was dependent on the cationic valences in the order of $\text{La}^{3+} > \text{Ba}^{2+} > \text{Ca}^{2+} \approx \text{Mg}^{2+} > \text{Na}^+ > \text{K}^+ > \text{Li}^+$.

Considering that the broken line in Fig. 5 reflects complete cation binding to arabate, it is clear from Fig. 5 that at very low concentrations of added salts, divalent and trivalent cations were bound to arabate completely but monovalent cations were not.

Dependency of Degree of Cation Binding on Arabate Concentration

The effect of arabate concentration on the cation binding to arabate was examined in the cases of NaCl and CaCl_2 . In Fig. 6, the specific conductance of arabate solution at various concentrations is plotted against the concentration of CaCl_2 . The broken line (1) in Fig. 6 shows the specific conductance of CaCl_2 solution in the absence of arabate and the broken line (2) gives the conductivity contribution of Cl^- ion in the specific conductance of CaCl_2 solution. In the relatively low concentration range of C_s , the values, $\Delta\kappa$, of various arabate solutions were approximately in agreement with the broken line (2), which means that in these regions almost all of the added calcium ions were bound to arabate.

The amount of calcium bound to arabate was calculated at various concentrations of arabate with use of Eq. 3', and the results obtained are shown in Fig. 7, where C_m is plotted against C_s . At all concentrations of arabate, the binding curves seemed to be of Langmuir type because of the saturation. The numerical values of x_∞ and k at various arabate concentrations, m_p , were therefore calculated in the presence of CaCl_2 and NaCl based on the Langmuir-type binding curve given by the following equation,

$$x = \frac{x_\infty \cdot kC_f}{1 + kC_f} \tag{6}$$

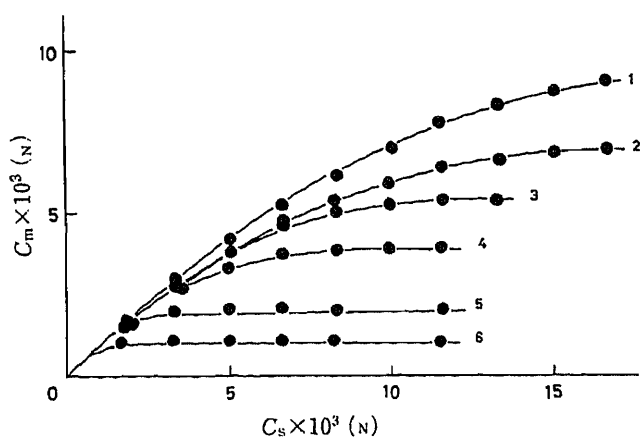


Fig. 7. The Relation of the Amount of Bound Cations C_m and the Concentration of CaCl_2 at Various Arabate Concentrations

Arabate concentration, m_p (eq/l): 1, 2.49×10^{-3} ; 2, 1.66×10^{-2} ; 3, 1.24×10^{-2} ; 4, 8.3×10^{-3} ; 5, 3.3×10^{-3} ; 6, 1.7×10^{-3} .

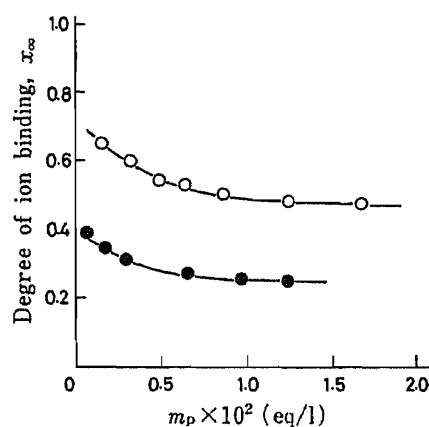


Fig. 8. Degree of Cation Binding to Arabate Estimated by Conductivity Measurement, x_∞

●, NaCl; ○, CaCl_2 .

TABLE I. Numerical Values of x_∞ and k in Eq. 6 at Various Arabate Concentrations, m_p , in the Cases of NaCl and CaCl_2

Added salt	m_p (eq/l)	k	x_∞ (mol/eq)
CaCl_2	2.49×10^{-2}	1.05	0.40
	1.66×10^{-2}	1.16	0.43
	0.83×10^{-2}	2.50	0.50
	0.33×10^{-2}	4.24	0.59
	0.17×10^{-2}	3.68	0.68
NaCl	1.25×10^{-2}	0.34	0.25
	0.66×10^{-2}	0.34	0.28
	0.33×10^{-2}	0.69	0.33

where k is the binding constant, C_f is the equilibrium concentration of added salt, x is the amount of binding defined as $x = C_m/m_p$ and x_∞ is the saturated amount of binding. The results are presented in Table I. These results are illustrated graphically in Fig. 8, where the saturated amounts of sodium and/or calcium, x_∞ , are plotted against arabate concentration. As is clear from Fig. 8, x_∞ increased gradually with decreasing arabate concentration.

Discussion

We have investigated the conductometric behavior of TBA–arabate and found that the binding characteristics of arabate with the counterions were of Langmuir type, indicating that the interaction was due to the electrostatic force. This result is fundamentally in good agreement with the results reported in the previous papers.^{3,4} From these results, it is possible to estimate the degree of cation binding to arabate. As shown in Fig. 9, in the cases of Na^+ and Ca^{2+} as a mono- and divalent cations, respectively, the degrees of cation binding to arabate were not always in good agreement with each other. The reasons for this may be differences in the methods of estimation based on various parameters such as the counterion activity coefficient, γ_+ , the osmotic coefficient, ϕ , the transport parameter, f , and the saturated amount of cation binding, x_∞ . This point will be discussed below.

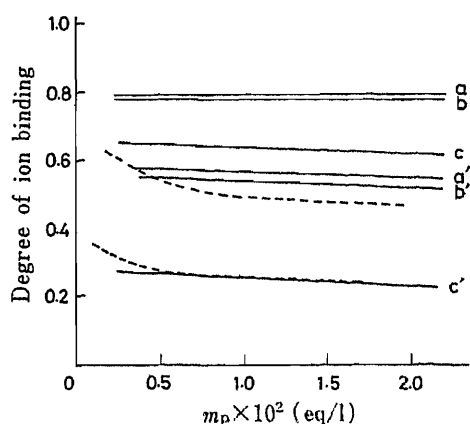


Fig. 9. Degree of Cation Binding for Arabate Estimated from Various Measurements

Calcium, a, $1-\phi$; b, $1-\gamma_+$; c, $1-f$

Sodium, a', $1-\phi$; b', $1-\gamma_+$; c', $1-f$

The broken lines indicate the x_{∞} values from Fig. 8.

Among these parameters, γ_+ and ϕ are obtained from an assay system based on the thermodynamic characteristics of arabate, whereas, f and x_{∞} are obtained from conductivity measurements. Thus, the values of $(1-\gamma_+)$ and $(1-\phi)$ shown in Fig. 9, will be essentially equivalent. It is also suggested that $(1-f)$ will be roughly equivalent to x_{∞} . In fact, the degree of Na^+ binding to arabate was, as expected, in the order of $x_{\infty} \approx (1-f) < (1-\gamma_+) \approx (1-\phi)$. In the case of Ca^{2+} , however, unexpected results were obtained. That is, x_{∞} was smaller than $(1-f)$ and the degree of binding was in the order of $x_{\infty} < (1-f) < (1-\gamma_+) \approx (1-\phi)$.

Although the reasons for such a marked difference between x_{∞} and $(1-f)$ are not clear at present, the different experimental conditions used may be involved. The value of f was obtained by the conductivity measurement of arabate solution in the absence of added salts. In this case, the value of the equivalent conductance of arabic anion, Λ_p , was determined by the transference measurement as $\Lambda_p = 4.4$. On the other hand, the value of x_{∞} was obtained by the conductivity measurement of arabate solution in the presence of added salts as $\Lambda_p = 6$. Considering that the value of Λ_p is reported to depend on the type of counterion,¹¹⁾ different counterions will give different values of Λ_p . In our experiments, sodium arabate was used for the transference measurement and TBA-arabate for the conductivity measurement. The difference may be attributable to the low value of x_{∞} compared to $(1-f)$, as shown in Fig. 9.

In addition, the different ionic strength brought about by the absence or presence of added salts may be one of the more important factors affecting the degree of cation binding. In the present work, as in the work on $(1-f)$ reported previously, the literature value of Λ_+ at infinite dilution was used because it is impossible to get an accurate value at finite concentration in the presence of added salts in addition to polyelectrolyte. It is well known that the equivalent conductance of an electrolyte solution is dependent on the ionic strength and that this dependency is much larger in a polyvalent salt system than in a monovalent salt one. Therefore, at such a high ionic strength as used in the present work, the practical value of Λ_+ should be smaller than the literature value used, and the deviation would be larger in the case of CaCl_2 than NaCl .

In the present work, we investigated the cation binding behavior of arabate by the conductivity measurement with reference to the various colligative properties of arabate, and found that the behavior estimated from any one of the 4 parameters was essentially the same in the concentration ranges tested. This is because for both Na^+ and Ca^{2+} , as shown in Fig. 9, the broken lines indicating the conductivity measurements and the solid lines indicating the others were parallel to each other except at very low concentrations of added salts. This good relationship seems to be very important when arabic acid-like substances are to be selected from among various polyelectrolytes and polysaccharides similar to gum arabic, because this conductance titration method is very simple and can be carried out easily without any special techniques or instruments. Therefore, we believe that this method may have some advantages

over the other three methods, at last in the preliminary experiments.

References

- 1) This work was presented at the 101st Annual Meeting of the Pharmaceutical Society of Japan, Kumamoto, 1981.
- 2) R. L. Whistler, "Industrial Gums," 2nd Ed., Academic Press Inc., New York, 1973, pp. 197—263.
- 3) C. Yomota, S. Okada, K. Mochida and M. Nakagaki, *Chem. Pharm. Bull.*, **32**, 3793 (1984).
- 4) C. Yomota, S. Okada and M. Nakagaki, *Yakugaku Zasshi*, **106**, 653 (1986).
- 5) H. P. Gregor and M. Frederick, *J. Polymer Sci.*, **23**, 451 (1957).
- 6) H. P. Gregor, D. H. Gold and M. Frederick, *J. Polymer Sci.*, **23**, 467 (1957).
- 7) A. Ikegami and N. Imai, *J. Polymer Sci.*, **56**, 133 (1962).
- 8) H. Noguchi, K. Gekko and S. Makino, *Macromolecules*, **6**, 438 (1973).
- 9) K. Gekko, "Solution Properties of Polysaccharides," ACS Symposium Series, American Chemical Society, 1981, pp. 415—438.
- 10) R. A. Robinson and R. H. Stokes, "Electrolyte Solutions," Butterworths, London, 1959, pp. 463—465.
- 11) N. Shavit, *Isr. J. Chem.*, **11**, 236 (1973).

[Chem. Pharm. Bull.]
[35(3) 941—947 (1987)]

Theoretical Study of Oxygen Atom (^1D) Insertion into Methane

MITSUO NAKAJIMA, MINORU TSUDA* and SETSUKO OIKAWA

Laboratory of Bio-physical Chemistry, Faculty of Pharmaceutical Sciences,
Chiba University, Chiba 260, Japan

(Received August 15, 1986)

Ab initio molecular orbital configuration interaction calculations were carried out on the intrinsic reaction coordinate (IRC) path of the reaction $\text{CH}_4 + \text{O}(^1\text{D}) \rightarrow \text{CH}_3\text{OH}$. The oxygen atom (^1D) approaches methane along the C_3 rotational axis of C_{3v} symmetry on the lowest potential energy path of the ground state. The ground state and four kinds of excited states of methanol originate from $\text{CH}_4 + \text{O}(^1\text{D})$. The reaction system of $\text{CH}_4 + \text{O}(^1\text{S})$ generates a higher excited state than those from $\text{CH}_4 + \text{O}(^1\text{D})$. It was confirmed that the ground state function along the IRC path can be approximately expressed by the Hartree Fock function near the saddle point. The increase of antibonding σ^* character with the C–O bond formation is the origin of the elevation of energies and the splitting of the five excited states.

Keywords—oxygen atom (^1D); oxidation; *ab initio*; molecular orbital method; configuration interaction; intrinsic reaction coordinate; methane; methanol

Introduction

Recent developments in research on plasma chemistry as well as on chemical carcinogenesis require a precise understanding of the elementary reaction of an oxygen atom with hydrocarbons. Oxygen plasma is widely used, especially in the semiconductor industry.¹⁾ Further, in carcinogenesis by polynuclear aromatic hydrocarbons, the ultimate carcinogens are generated through oxidation by cytochrome P-450.²⁾

It has been experimentally established that $\text{O}(^1\text{D})$ can be inserted into a paraffinic C–H bond,³⁾ while $\text{O}(^1\text{S})$ only abstracts a hydrogen atom.⁴⁾ The singlet oxygen atom adds stereospecifically to olefin double bonds,⁵⁾ whereas triplet oxygen atom addition results in some loss of the reactant's geometrical isomeric purity.⁶⁾

Bader *et al.* reported *ab initio* self-consistent field (SCF) potential energy surfaces for the cycloaddition reactions $\text{C}_2\text{H}_4(^1\text{A}_{1g}) + \text{O}(^1\text{D}$ and $^3\text{P})$.⁶⁾ Dupuis *et al.* carried out *ab initio* multiconfiguration Hartree Fock (MCHF) calculations to characterize the reactants, the transition state, and the products of the electrophilic addition of $\text{O}(^3\text{P})$ to the π bond of ethylene.⁷⁾ Walch and Dunning calculated the barrier height and transition state geometry for the reaction $\text{CH}_4 + \text{O}(^3\text{P}) \rightarrow \text{CH}_3 + \text{OH}$ by using polarization configuration interaction (POL-CI) wave functions with the valence double zeta plus polarization basis set.⁸⁾ However, there has been no theoretical research on the insertion of $\text{O}(^1\text{D})$ into a paraffinic C–H bond.

This paper describes *ab initio* molecular orbital configuration interaction (MO CI) calculations on the barrier height, transition state geometry and geometrical change following the lowest potential energy path of the reaction $\text{CH}_4 + \text{O}(^1\text{D}) \rightarrow \text{CH}_3\text{OH}$.

Method

All the structures reported in the present research were fully optimized according to the energy gradient method by using the spin-restricted Hartree Fock (RHF) wave function. The MCHF wave function was also used for confirmation of the saddle point. The optimized structures were analyzed in terms of their harmonic vibrational

frequencies. Zero and one imaginary frequency were employed as the criteria for potential minima and saddle points, respectively. Basis sets used are Pople's STO-3G⁹⁾ and his double zeta quality 3-21G.¹⁰⁾ The potential energy hypersurface was constructed with $3N-6$ dimensional mass-weighted Cartesian coordinates, where N is the number of atoms contained in the reaction system. On the hypersurface, the saddle point was decided at the RHF level firstly, and then the intrinsic reaction coordinate (IRC)¹¹⁾ was calculated starting from the saddle point. The lowest potential energy reaction path obtained was elaborated by the CI method using the graphical unitary group approach (GUGA)¹²⁾; *i.e.*, the electronic state functions were expressed by a linear combination of the electronic configuration functions obtained by promoting one or more electrons from the occupied MO to the unoccupied ones.

Computer programs used were GAUSSIAN80 for geometry optimization and GAMESS for vibrational analysis and CI calculation. The program for the IRC was written by us, utilizing GAUSSIAN80 in the energy eigenvalue and eigenvector as well as the energy gradient calculations.

Results and Discussion

Approach of Oxygen Atom(¹D) to Methane at the Initial Stage of Insertion

A unique route of approach of a free oxygen atom(¹D) to methane is determined, provided that the insertion of O(¹D) into a C-H bond follows the lowest potential energy path. The IRC path which starts from the saddle point and goes toward the separation to O(¹D) and CH₄ gives the atomic configuration changes of the reaction system following the route of approach. The IRC and the atomic configuration changes are shown in Figs. 1 and 2, respectively. The structure at the saddle point belongs to the point group C_s. As shown in Fig. 2, the extrapolation of the atomic configuration changes to $-5.0 \text{ \AA} \cdot \text{amu}^{1/2}$ converges to the structure belonging to the point group C_{3v}, where oxygen, carbon and H₂ atoms are on the

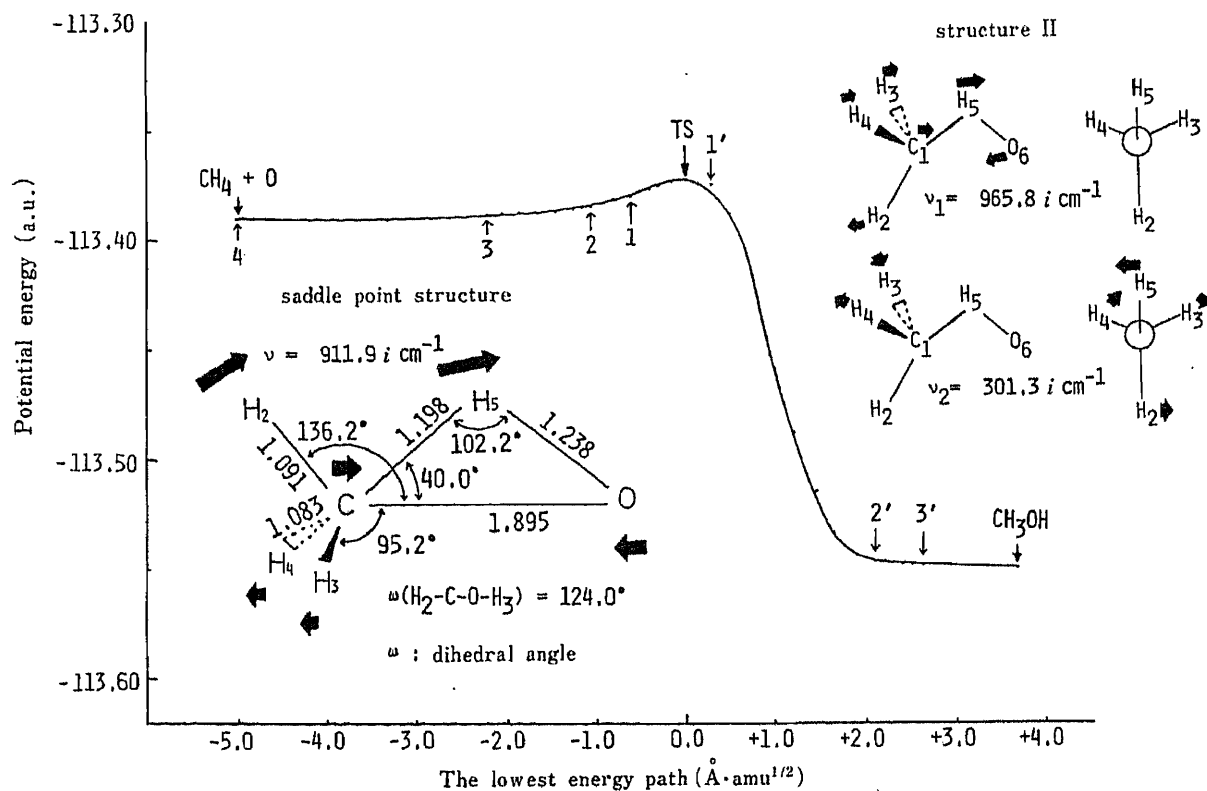


Fig. 1. The Potential Energy Change along the IRC Path in Insertion of O(¹D) into a C-H Bond of Methane

The saddle point (TS) structure is shown with the normal mode of vibration of imaginary frequency, and 1, 2, 3, 4 and 1', 2', 3' correspond to the structure changes in Figs. 2 and 3, respectively. The pseudo-saddle point structure II has two kinds of normal mode of vibration of imaginary frequency, one of which (ν_2) produces the real saddle point structure.

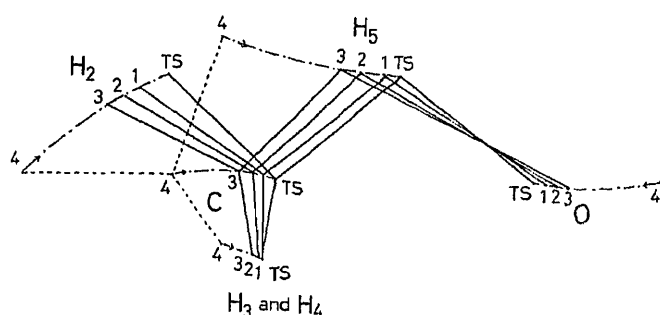


Fig. 2. The Unique Route of Approach of $O(^1D)$ to Methane along the IRC Path at the Initial Stage of Insertion

Each of the structures 1, 2, 3 and 4 corresponds to the same point on the IRC path in Fig. 1.

TABLE I. Potential Energies (a.u.) of the Saddle Point Structure and the Pseudo Saddle Point Structure II

	Total energy	Electronic energy	Nuclear repulsion energy
Saddle point structure	-113.37150	-148.62576	35.25426
Pseudo saddle point structure II	-113.36918	-148.53253	35.16334

three-fold rotational axis C_3 . (For numbering of hydrogen atoms, see Fig. 1.)

Structure Changes along the Lowest Potential Energy Path

The oxygen atom (1D) approaches methane along the C_3 rotational axis, on which the H_2 and C atoms lie. One of the three H atoms on the symmetrical positions, H_5 in Fig. 1, moves as if it were pulled by the $O(^1D)$ atom, and the structure of the reaction system changes to C_s . The details of the structure change are shown in Fig. 2. At the saddle point, the angles $\angle H_5CO$, $\angle H_3CO$, and $\angle H_2CO$ are 40.0, 95.2 and 136.2°, respectively, although the first and the second angles had the same values (70.5°) and the third was 180.0° in the C_{3v} structure. The unique normal mode of vibration of imaginary frequency is shown in Fig. 1, where methanol is produced by forward displacement following the arrows, and $O(^1D)$ and methane are regenerated by backward movement.

We can imagine another transition state structure II which also belongs to the point group C_s . Pudzianowski and Loew reported the structure II at the saddle point in their MINDO/3 calculation.¹³⁾ However, the structure II has two imaginary frequencies, one of which has the normal mode of vibration (ν_2) leading to the real saddle point structure (Fig. 1). As shown in Table I, the structure II having smaller nuclear repulsion energy is unstable in terms of total energy compared with the real saddle point structure because of its comparative instability in electronic energy.

Starting from the saddle point, first, the reaction system produces methanol in substantial *cis*-conformation with respect to the positions of H_2 and H_5 , and second, the $C-O$ bond rotates suddenly to form the real conformation of methanol near the end of the reaction process. The situation is shown in Fig. 3, where the positional changes of H_2 , H_3 and H_4 around the $C-O$ bond are shown.

The symmetrical plane of the reaction system at the saddle point is maintained during the IRC calculation because of the symmetrical gradients. For this reason, sometimes it happens that no lowest energy path is obtained. In order to avoid this difficulty, the $C-O$ bond was rotated by 5° near the saddle point and then the IRC calculation was performed. This rotation gave the point 1' projected from the smooth curve near the saddle point in Fig. 1.

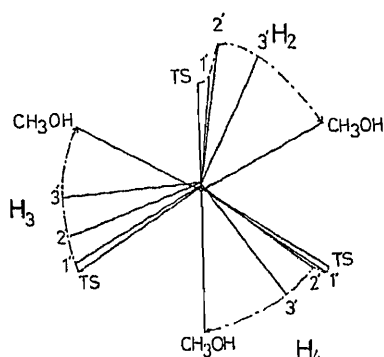


Fig. 3. The Rotation of the C-O Bond to Form the Real Conformation of CH_3OH Near the End of the Reaction of $\text{CH}_4 + \text{O}(^1\text{D})$

Each of the structures 1', 2' and 3' corresponds to the same point on the IRC path in Fig. 1.

Comparing Figs. 1 and 3, one can see that the C-O bond rotation takes place mainly at the final stage of energy stabilization of the reaction system.

Validity of the IRC at the HF Level

Since five electronic states are generated in the reaction $\text{CH}_4 + \text{O}(^1\text{D})$ because of the quinary degeneration of the lowest singlet state of the oxygen atom, it is important to confirm that the HF calculation reproduces the real lowest potential energy path.

Reproducibility of ^1D and ^1S States of Oxygen Atom Perturbed by Methane in CI Calculation—The ^1D and ^1S states of an isolated oxygen atom can be expressed by a linear combination of the singly and the doubly excited electronic configuration functions (SD-CI). The energy separation between ^1D and ^1S is 51 kcal/mol by STO-3G SD-CI calculation, which reproduces exactly the experimental value.¹⁴⁾ However, perturbation by methane at the initial stage of the insertion reaction, where the distance between the oxygen atom and carbon of methane is 3.6 Å, requires the addition of the triply and the quadruply excited electronic configuration functions (SDTQ-CI) at least for the expression of the ^1D and ^1S states of the oxygen atom. The same requirement of SDTQ-CI was also found in the case of the oxygen atom (^1D) perturbed by a hydrogen molecule.

Potential Energy Change along the IRC Path in SDTQ-CI Calculation—SDTQ-CI calculations were performed along the IRC path of Fig. 1, and the results are shown in Fig. 4. The total profile of the lowest potential energy path in Fig. 4 is substantially the same as that in Fig. 1, although the saddle point position moved slightly from D to C. The structures of the reaction system at D and C are substantially the same. The activation energy, the energy difference between the saddle point and the reactants, is 10 kcal/mol in the RHF calculation and 13 kcal/mol in the SDTQ-CI calculation.

The STO-3G MCHF calculations showed that the gradients on the potential energy hypersurface at the points B and C in Fig. 4 ensured the regeneration of the oxygen atom and methane. On the other hand, the gradient at D favored the methanol formation. Therefore, the saddle point exists between C and D in this level calculation. The 3-21G RHF calculations also gave the same conclusion.

As an oxygen atom approaches methane, the energy levels of the quinary degenerated ^1D state separate gradually and the ground state and four excited states are formed. $\text{O}(^1\text{S})$ produces the A' state of the reaction system, which always has the highest potential energy. Neither a crossing nor an avoid-crossing takes place on the IRC path among the six potential energy surfaces generated from the ^1D and ^1S states of the oxygen atom (Fig. 4). Since the potential energy increases monotonously with the progress of insertion in every surface except the lowest one, $\text{O}(^1\text{S})$ inserts itself into the C-H bond only when the transition takes place to the lowest energy hypersurface which arises from the ^1D state. Experiment showed that $\text{O}(^1\text{S})$ abstracts an H atom.⁴⁾

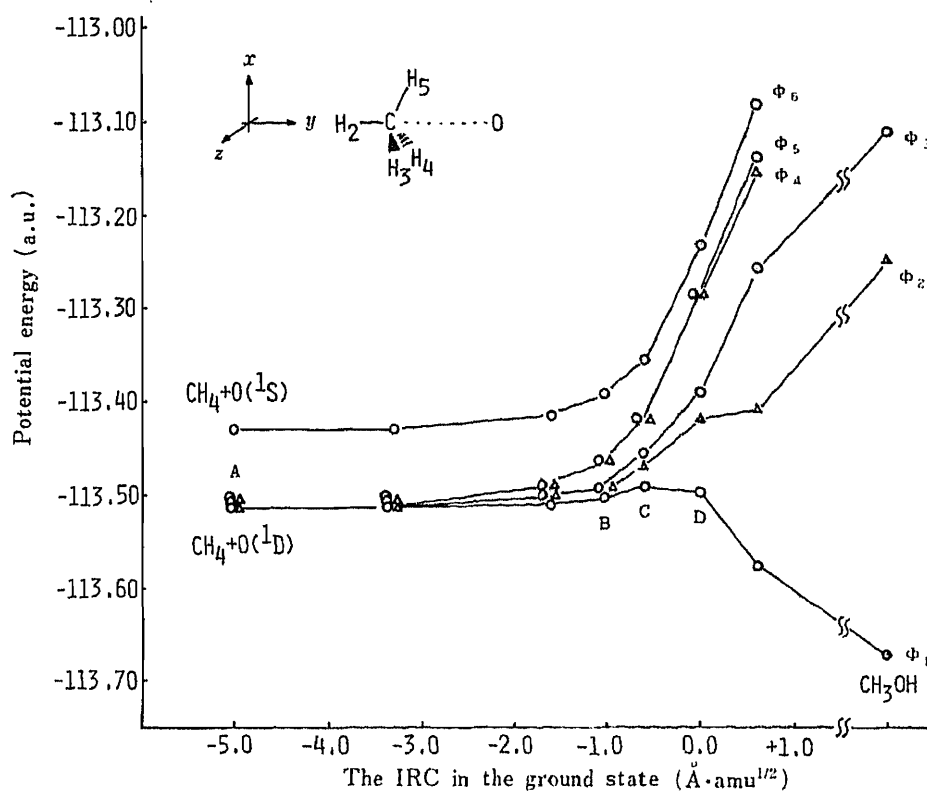


Fig. 4. The Potential Energy Changes of the Six Electronic States That Arise from the O (1D and 1S) + CH_4 Reaction along the IRC Path on the Ground State Hypersurface

The electronic state from O(1S) always keeps the highest energy (cf. Table II).

Electronic Configuration in the Lowest Potential Energy Path and the Origin of the Elevation of Energy at the Excited States—Now, we shall consider the validity of the IRC in the HF level calculation. The singlet oxygen atom ($1S$) $^2(2S)$ $^2(2P)$ 4 has the lowest state 1D expressed as $2Pz^2Px^2 - Px^2Py^2 - Py^2Pz^2$, Px^2PyPz , Py^2PzPx , Pz^2PxPy and $Pz^2Px^2 - Pz^2Py^2$ as well as the second lowest state 1S , $Px^2Py^2 + Py^2Pz^2 + Pz^2Px^2$. (Note these expressions are very similar to $2Z^2 - X^2 - Y^2$, YZ , ZX , XY and $X^2 - Y^2$ for d atomic orbitals and $X^2 + Y^2 + Z^2$ for s atomic orbital, although the superscript 2 is the number of occupied electrons in the case of the oxygen atom but an exponent in the case of the atomic orbital.) The state functions of the reaction system at the initial stage of the reaction, at $-5.0 \text{ \AA} \cdot \text{amu}^{1/2}$ in Fig. 4, where the distance between the oxygen atom and carbon of methane is 3.6 \AA , are expressed approximately by the function of oxygen atom, because the electronic configuration functions mainly contributing to these state functions are comprised of the LUMO(Y), HOMO(X) and second HOMO(Z). The main components of MO Y, X and Z are Py, Px and Pz atomic orbitals of the oxygen atom, respectively (Table II).

The state functions expressing the reaction system at the points A, C and D of Fig. 4 are listed in Table II with the MOs, Y, X and Z, which are always LUMO, HOMO and the second HOMO, respectively, in these structures of the reaction system. The MO energy is also given for each MO in Table II. In the lowest energy path, the electronic state is expressed approximately as $2Z^2X^2 - X^2Y^2 - Y^2Z^2$ at the initial stage of the reaction, A. The contribution of the configuration function Z^2X^2 increases gradually with the progress of insertion of the oxygen atom into the C-H bond. At the saddle point, C, the contribution of Z^2X^2 reaches 87.0%. These state functions shown in Table II support the validity of the IRC in the HF level

TABLE II. The Main Configuration Functions Contributing to Each Electronic State at A, C and D in Fig. 4

	O + CH ₄ (-5.0) (A)	CI-TS (-0.6) (C)	TS (0.0) (D)
$\phi_1(A')$	= 0.8054 [$\cdots Z^2X^2$] -0.4282 [$\cdots Z^2Y^2$] -0.3562 [$\cdots X^2Y^2$]	0.9330 [$\cdots Z^2X^2$] -0.1834 [$\cdots Z^2Y^2$] -0.1942 [$\cdots X^2Y^2$]	0.9472 [$\cdots Z^2X^2$] -0.1114 [$\cdots Z^2Y^2$]
$\phi_2(A'')$	= 0.9802 [$\cdots ZY^2Y$]	0.9655 [$\cdots ZX^2Y$]	0.9467 [$\cdots ZX^2Y$]
$\phi_3(A')$	= 0.9800 [$\cdots Z^2XY$]	0.9582 [$\cdots Z^2XY$]	0.9329 [$\cdots Z^2XY$]
$\phi_4(A'')$	= 0.9800 [$\cdots ZXY^2$]	0.9486 [$\cdots ZXY^2$]	0.9208 [$\cdots ZXY^2$]
$\phi_5(A')$	= 0.6723 [$\cdots Z^2Y^2$] -0.7120 [$\cdots X^2Y^2$]	0.6424 [$\cdots Z^2Y^2$] -0.6980 [$\cdots X^2Y^2$]	0.5316 [$\cdots Z^2Y^2$] -0.7534 [$\cdots X^2Y^2$]
$\phi_6(A')$	= 0.5433 [$\cdots Z^2X^2$] 0.5588 [$\cdots Z^2Y^2$] 0.5612 [$\cdots X^2Y^2$]	0.6583 [$\cdots Z^2Y^2$] 0.6104 [$\cdots X^2Y^2$]	0.7304 [$\cdots Z^2Y^2$] 0.5125 [$\cdots X^2Y^2$]
MO Z (2a')	= 0.9999 O _{2PZ} -0.0064 C _{2PZ} (-0.4073)	0.9921 O _{2PZ} -0.0886 C _{2PZ} (-0.3730)	0.9894 O _{2PZ} -0.0955 C _{2PZ} (-0.3543)
MO X (7a')	= 0.9995 O _{2PX} 0.0192 C _{2PX} (-0.4071)	0.9413 O _{2PX} -0.1615 C _{2PX} (-0.3686)	0.8831 O _{2PX} -0.2035 C _{2PX} (-0.3462)
MO Y (8a')	= 0.9999 O _{2PY} -0.0048 C _{2PY} (0.2356)	0.9417 O _{2PY} 0.2097 C _{2PY} (0.2776)	0.9004 O _{2PY} 0.4005 C _{2PY} (0.3138)

\cdots means $(1a')^2(2a')^2(3a')^2(4a')^2(5a')^2(1a'')^2(6a')^2$ in [$\cdots X^2Y^2$], etc. X, Y and Z are MO X, MO Y and MO Z, respectively. MO Y becomes an antibonding σ^* MO at the points C and D. MO energy (a.u.) is given in parentheses for each MO.

calculation since the HF state function is always Z^2X^2 throughout the lowest energy reaction path. This result also justifies the HF level MNDO and MINDO/3 type semiempirical calculations on the insertion of an oxygen atom into C-H.¹³⁾

Only the lowest potential energy hypersurface gives the ground state of methanol and all others lead to excited states of the methanol, provided that the reaction path is restricted to the IRC (Fig. 4). A remarkable feature found in the state functions leading to the excited states is a large contribution of MO Y. At the saddle point, C, MO Y has an antibonding character σ^* with respect to the C-O bond where the lobe of Py AO of oxygen couples out of phase with that of carbon. The antibonding character of MO Y increases with the progress of methanol formation from C to D as shown in Table II. (The contributions of other AOs are negligible in MO Y.) The marked contrast in the contribution of MO Y between the electronic state function for the lowest potential energy hypersurface and those for the five excited states suggests strongly that the main origin of the elevation of the energy levels in the excited states is increase of the antibonding σ^* character in the C-O bond which is produced with the progress of methanol formation.

Acknowledgment The authors thank the Computer Center, Institute for Molecular Science, Okazaki, for the use of an M-200H computer and the Library program GAMESS. The computation was also carried out at the Computer Center, the University of Tokyo, and the Computer Center, Chiba University.

References

- 1) For example, M. Tsuda, S. Oikawa and A. Suzuki, "Microcircuit Engineering 80," ed. by R. P. Kramer, Delft Univ. Press, Amsterdam, 1981, p. 553.

- 2) D. Thakker, H. Yagi, W. Levin, A. W. Wood, A. H. Conney and D. M. Jerina, "Bioactivation of Foreign Compounds," ed. by M. W. Anders, Academic Press, New York, 1985, p. 177.
- 3) G. Paraskevopovlos and R. J. Cvetanovic, *J. Chem. Phys.*, **50**, 590 (1969).
- 4) H. Yamasaki and R. J. Cvetanovic, *J. Chem. Phys.*, **41**, 3703 (1964).
- 5) R. F. W. Bader and J. I. Generosa, *Can. J. Chem.*, **43**, 1631 (1965).
- 6) R. F. W. Bader, M. E. Stephens and R. A. Gangi, *Can. J. Chem.*, **55**, 2755 (1977).
- 7) M. Dupuis, J. J. Wendoloski, T. Tanaka and W. A. Lester, Jr., *J. Chem. Phys.*, **76**, 481 (1982).
- 8) S. P. Walch and T. H. Dunning, Jr., *J. Chem. Phys.*, **72**, 3221 (1980).
- 9) W. J. Hehre, R. F. Stewart and J. A. Pople, *J. Chem. Phys.*, **51**, 2657 (1969).
- 10) J. S. Binkley, J. A. Pople and W. J. Hehre, *J. Am. Chem. Soc.*, **102**, 939 (1980).
- 11) a) K. Fukui, *J. Phys. Chem.*, **74**, 4161 (1970); b) K. Fukui, S. Kato and H. Fujimoto, *J. Am. Chem. Soc.*, **97**, 1 (1975).
- 12) I. Shavitt, "The Unitary Group," ed. by J. Hinze, Springer-Verlag, New York, 1981, p. 51.
- 13) A. T. Pudzianowski and G. H. Loew, *J. Am. Chem. Soc.*, **102**, 5449 (1980).
- 14) "Kagaku-benran Kiso-hen," 3rd Ed., Vol. 2, ed. by K. Hata, Chem. Soc. Jpn., Tokyo, 1984, p. 572 (in Japanese, cited from S. Baskin and J. O. Stoner, Jr., "Atomic Energy Levels and Grotrian Diagrams," Vol. 1, North Holland, 1975 and Addenda, 1978).

[Chem. Pharm. Bull.]
35(3) 948-956 (1987)

A Stereoselective Synthesis of a Stable Prostacyclin Analogue; *dl*-3-Oxa-9(*O*)-methano- $\Delta^{6(9\alpha)}$ -prostaglandin I₁

KOICHI KOJIMA,* KAZUO KOYAMA, SHIGEO AMEMIYA
and SHINICHI SAITO

Chemical Research Laboratories, Sankyo Co., Ltd., 1-2-58 Hiromachi,
Shinagawa-ku, Tokyo 140, Japan

(Received June 30, 1986)

A prostacyclin analogue, *dl*-3-oxa-9(*O*)-methano- $\Delta^{6(9\alpha)}$ -prostaglandin I₁ (**1a**), has been synthesized. The key step for this synthesis is a new, one-step conversion reaction of the (hydroxymethyl)cyclopropylketone group in **8** and **21** to the γ,δ -unsaturated ketone **9** and **22**, respectively, with iodotrimethylsilane.

Keywords—isocarbacyclin; prostacyclin analogue; iodotrimethylsilane; cyclopropane ring; bicyclo[3.3.0]octane

Many prostacyclin analogues have been synthesized in attempts to develop therapeutically useful agents.¹⁾ In 1983, Shibasaki *et al.*^{2a,b)} reported the synthesis of 9(*O*)-methano- $\Delta^{6(9\alpha)}$ -prostaglandin I₁ (isocarbacyclin) (**2**), which was found to be more potent than well-known 9(*O*)-methanoprostacyclin (carbacyclin) (**3**) in inhibiting platelet aggregation.^{2a)} Since then, many syntheses of **2** and its derivatives have been reported.^{2c-g)} We³⁾ have also described the synthesis of *dl*-isocarbacyclin (**2**) and its derivatives *via* a different route. Aiming at

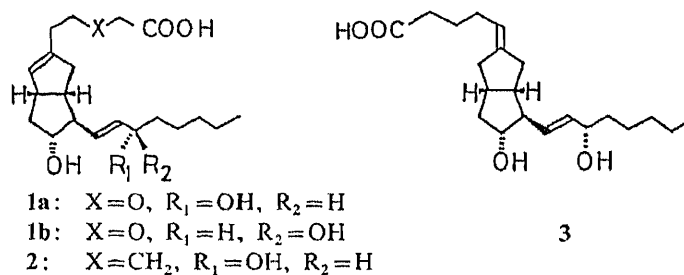


Chart 1

synthesizing a biologically more stable isocarbacyclin analogue, we thought of blocking the β -oxidation reaction of the carboxylic acid side chain (α -side chain) by replacement of the C-3 methylene group with an oxygen atom. The β -oxidation reaction of the α -side chain is well-known as one of the main metabolic pathways of prostaglandins, and results in the loss of biological activity. 3-Oxa analogues of both PGE₁^{4a)} and carbacyclin^{4b)} have already been synthesized. We now report the synthesis of a 3-oxa analogue of isocarbacyclin, *dl*-3-oxa-9(*O*)-methano- $\Delta^{6(9\alpha)}$ -prostaglandin I₁ (**1a**), using a new, one-step conversion reaction.

For the synthesis of 3-oxa-9(*O*)-methano- $\Delta^{6(9\alpha)}$ -prostaglandin I₁ (**1a**), we investigated a new, regioselective method for the introduction of the 6(9α)-double bond (prostaglandin numbering). Our basic approach was as follows; if the (hydroxymethyl)cyclopropylketone group could be converted to the γ,δ -unsaturated ketone group in one step, the double bond at the 6(9α) position would be introduced regioselectively (**21**→**22**). In order to realize this

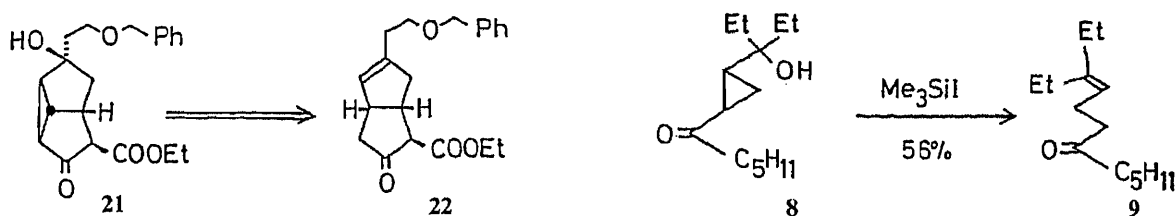


Chart 2

approach, we firstly investigated a model reaction using the simple acyclic compound (**8**) with iodotrimethylsilane (Me₃SiI). Treatment of **8** with 2.5 eq of Me₃SiI in toluene at 25 °C afforded the desired γ,δ -unsaturated ketone (**9**), together with liberation of iodine, in 56% yield⁵⁾ (Chart 2). Compound **8** was synthesized from methyl 4-oxo-2-nonenoate (**4**)⁶⁾ as illustrated in Chart 3.

As for the mechanism of this reaction, two routes (route A and B) might be possible (Chart 4). Route A: The cyclopropane ring in **8** was cleaved⁷⁾ by Me₃SiI and the hydroxy

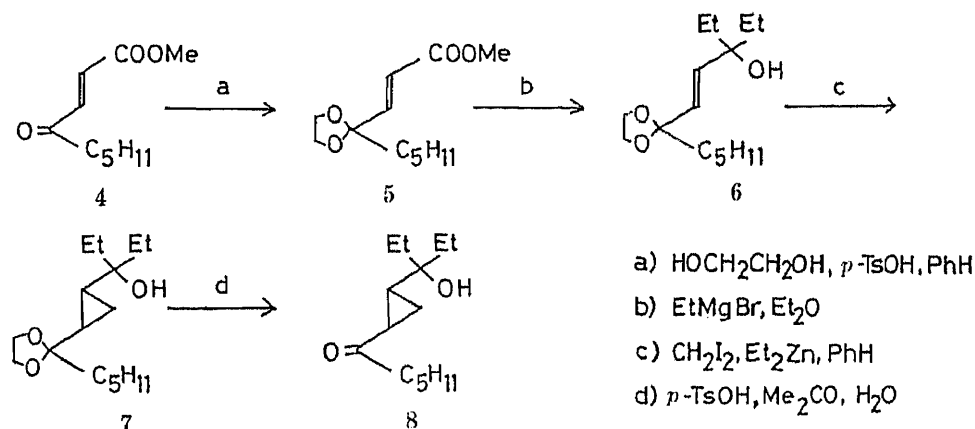


Chart 3

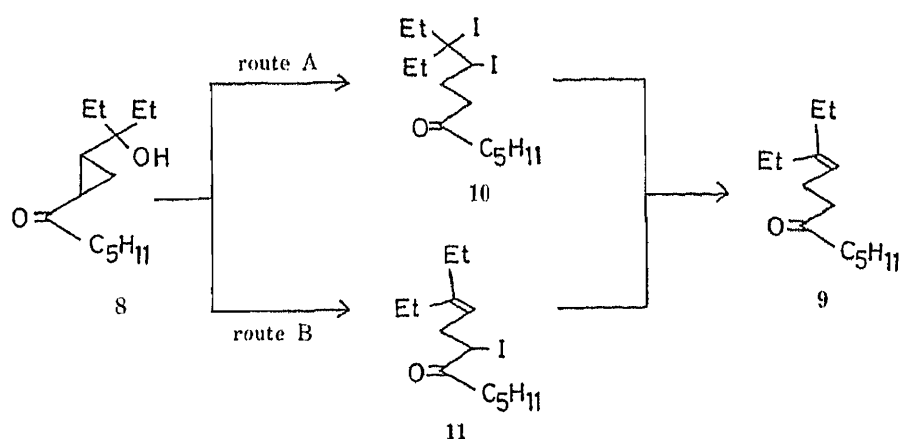


Chart 4

group was substituted⁸⁾ by iodide ion to afford the 1,2-diodide (**10**), which might be converted⁹⁾ to the olefin (**9**). Route B: The cyclopropyl carbinol moiety in **8** was converted¹⁰⁾ to the γ -iodo olefin (**11**) by treatment with Me₃SiI, and **11** might be converted¹¹⁾ to **9** with further Me₃SiI. The following results indicate that route A is more probable than route B.

Similar reaction of **8** with Me_3SiI under ice-cooling in place of room temperature, followed by quenching of the reaction mixture with aqueous sodium thiosulfate solution after 10 min, gave a crude mixture of **9** and a new, more polar product. All attempts to isolate this new product failed. However, thin layer chromatographic (TLC) analysis of the crude mixture obtained above in chloroform at room temperature showed that the more polar product was slowly converted to the olefin (**9**) with liberation of iodine. It is known that a 1,2-diiodide is unstable and loses iodine to afford an olefin.⁹ Thus, we assigned this new product as the 1,2-diiodide (**10**), namely an intermediate of this reaction.

Now, we have applied this new, one-step conversion reaction to the synthesis of *dl*-3-oxa-9(*O*)-methano- $\Delta^{6(9\alpha)}$ -prostaglandin I_1 (**1a**). The key compound **21** was easily synthesized from the mono-acetal (**12**)¹² as follows (Chart 5). The Wittig-Honer reaction of **12** with

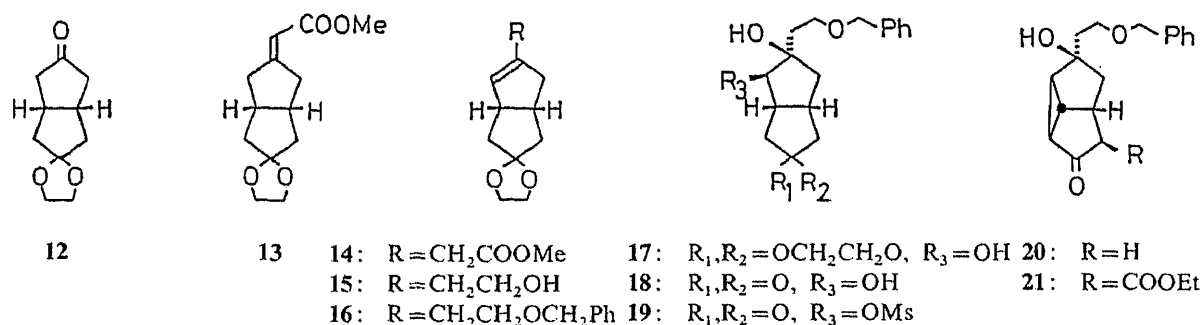


Chart 5

trimethyl phosphonoacetate [$(\text{MeO})_2\text{P}(\text{O})\text{CH}_2\text{COOMe}$] and sodium hydride in 1,2-dimethoxyethane (DME) gave the α, β -unsaturated ester (**13**). Isomerization of the *exo*-double bond in **13** to the *endo*-double bond was easily accomplished by treatment with lithium diisopropylamide (LDA) and hexamethylphosphoric triamide (HMPA)¹³ in tetrahydrofuran (THF) at -78°C to give **14**. Reduction of the ester group in **14** with lithium aluminum hydride (LiAlH_4) gave the alcohol (**15**), which was treated with benzyl bromide and sodium hydride in *N,N*-dimethylformamide (DMF) to give the benzyl ether (**16**) in 85% yield from **12**. Oxidation of the double bond in **16** with *N*-methylmorpholine *N*-oxide¹⁴ and a catalytic amount of osmium tetroxide (OsO_4) gave the β -diol (**17**) in 95% yield. Treatment of **17** with HCl aq. in acetone gave the ketone (**18**), which was then converted to the mono-mesylate (**19**) with methanesulfonyl chloride (MsCl) and triethylamine (Et_3N) in methylene chloride. Cyclopropanation of the mono-mesylate (**19**) with potassium *tert*-butoxide (*tert*- BuOK) in THF at room temperature afforded the tricyclic compound **20** in 73% yield. Finally, treatment of **20** with LDA and then ethoxyformylimidazole¹⁵ in THF at -78°C yielded the desired tricyclic β -ketoester (**21**) in 84% yield.

We then investigated the key step, the one step conversion reaction (Chart 6). Similar treatment of the tricyclic β -ketoester (**21**) with Me_3SiI in toluene at 25°C afforded the desired olefin (**22**) in 45% yield. Under the reaction conditions used, the benzyl group in **21** remained intact. The bicyclo[3.3.0]octane structure of **22** was confirmed by synthesizing **22** through the following reactions: acid treatment of **16** gave the ketone (**23**), which was treated with diethyl carbonate and sodium hydride in 1,4-dioxane to give **22** along with the isomeric β -ketoester after chromatographic separation.

Similar treatment of the tricyclic ketone (**20**) afforded the olefin (**23**) in 43% yield.

We now had the desired intermediate (**22**), which was then converted into *dl*-3-oxa-9(*O*)-methano- $\Delta^{6(9\alpha)}$ -prostaglandin I_1 (**1a**) by the following sequence of reactions (Chart 7). Reduction of the ketone group in **22** with sodium borohydride (NaBH_4) in ethanol,³ followed by protection of the hydroxy group as the tetrahydropyranyl ether, afforded **25** in 79% yield.

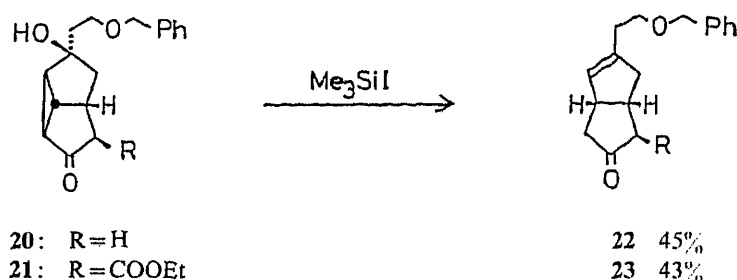


Chart 6

After reduction of the ester group in **25** with LiAlH_4 in THF, the obtained alcohol (**26**) was oxidized to the aldehyde (**27**) with excess sulfur trioxide (SO_3) pyridine complex and Et_3N in dimethylsulfoxide (DMSO). The Wittig reaction of **27** with tributyl 2-oxoheptylidene phosphorane [$\text{Bu}_3\text{P}=\text{CHCO}_2\text{C}_7\text{H}_{11}$] in ether at room temperature gave the α,β -unsaturated ketone (**28**) in 86% yield from the ester (**25**). Reduction of the ketone group in **28** with NaBH_4 in the presence of cerium(III) chloride (CeCl_3) in methanol gave the more polar 15α -alcohol (**29a**) (PG numbering) and the less polar 15β -alcohol (**29b**) in 65% and 33% yields, respectively. Protection of the hydroxy group in the 15α -alcohol (**29a**) with dihydropyran (DHP) and *p*-toluenesulphonic acid (*p*-TsOH) in methylene chloride, followed by treatment with excess sodium metal in liquid ammonia at -78°C gave the alcohol (**31**) in 88% yield from **29a**. Alkylation of the alcohol (**31**) with lithium chloroacetate ($\text{ClCH}_2\text{COOLi}$) afforded the carboxylic acid **32** in 85% yield. Finally, removal of the protective groups of **32** with camphorsulphonic acid in aqueous acetone gave *dl*-3-oxa-9(*O*)-methano- $\Delta^{6(9\alpha)}$ -prostaglandin I_1 (**1a**), mp $72\text{--}74^\circ\text{C}$, in 74% yield.

By using a sequence of reactions similar to that described for the synthesis of **1a**, the 15β -alcohol (**29b**) was led to the 15β -isomer (**1b**).

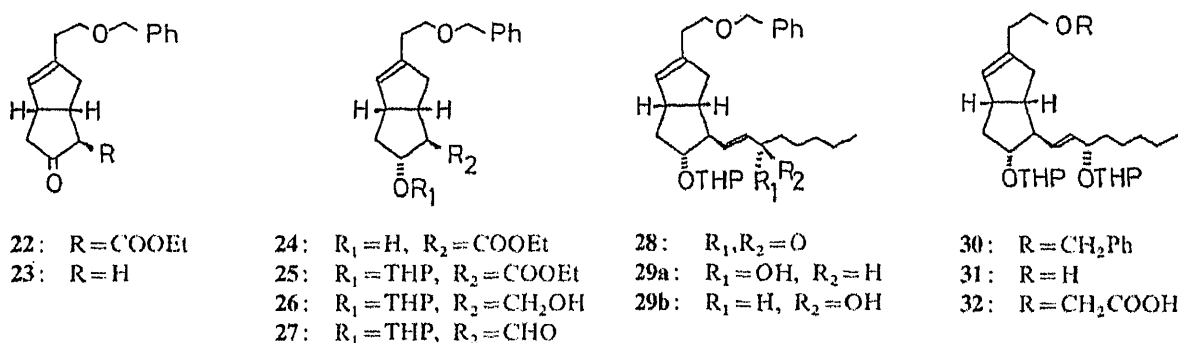


Chart 7

dl-3-Oxa-9(*O*)-methano- $\Delta^{6(9\alpha)}$ -prostaglandin I_1 (**1a**) (IC_{50} : 23 ng/ml) was found to be a more potent inhibitor of adenosine diphosphate-induced platelet aggregation than (+)-carbacyclin (**3**), using rabbit platelet-rich plasma. In a preliminary experiment, **1a** was found to be more stable than isocarbacyclin (**2**) in an *in vitro* experimental model for β -oxidation using liver homogenate. Details will be published elsewhere.

Experimental

Melting points are uncorrected. Infrared (IR) spectra were recorded with a JASCO A-102 spectrophotometer. Proton nuclear magnetic resonance ($^1\text{H-NMR}$) spectra were recorded with a Varian T-60A (60 MHz) or EM-390 (90 MHz) spectrometer in deuteriochloroform, with tetramethylsilane as internal reference. Mass spectra (MS) were

obtained with a JEOL JMS-01SG or JMS-G300 mass spectrometer. Removal of solvents *in vacuo* was accomplished with a rotating flash evaporator at 20–30 mmHg and usually at 35–50 °C. Plates for thin layer chromatography (TLC) were Silica gel 60 F-254 (E. Merck AG) and spots were visualized by spraying a solution of 0.5% vanillin in 20% ethanol in sulfuric acid (v/v), followed by heating. Columns for ordinary chromatography were prepared with Silica gel 60 (70–230 mesh or 230–400 mesh, E. Merck AG). In general, reactions were carried out under a nitrogen stream.

Methyl 4,4-Ethylenedioxy-2-nonenolate (5)—A mixture of methyl 4-oxo-2-nonenolate (4)⁶ (4.860 g), ethyleneglycol (15 ml) and *p*-TsOH (150 mg) in benzene (60 ml) was heated under reflux using a Dean–Stark apparatus for 5 h. The reaction mixture was diluted with benzene, washed with 5% NaHCO₃ aq. and brine, and dried over Na₂SO₄. Removal of the solvent *in vacuo* gave an oily residue, which was purified by silica gel column chromatography. Elution with 2–3% AcOEt in hexane (v/v) afforded **5** (6.020 g) as a colorless oil. IR (neat): 1725, 1660 cm⁻¹. ¹H-NMR (CDCl₃) δ: 3.76 (3H, s, COOMe), 3.92 (4H, s, OCH₂CH₂O), 6.06 (1H, d, *J* = 16 Hz, olefinic-H), 6.80 (1H, d, *J* = 16 Hz, olefinic-H). MS *m/z*: 229 (M⁺ + 1), 197, 157.

3-Ethyl-6,6-ethylenedioxy-4-undecen-3-ol (6)—A solution of **5** (6.020 g) in Et₂O (60 ml) was added to stirred EtMgBr reagent [prepared from Mg metal (3.20 g) and EtBr (9.9 ml) in Et₂O (160 ml)] at room temperature. The reaction mixture was stirred for 30 min, quenched with NH₄Cl aq., and then extracted with Et₂O. The extracts were washed with brine and dried over Na₂SO₄. Removal of the solvent gave an oily residue, which was purified by silica gel column chromatography. Elution with 4–6% AcOEt in hexane (v/v) afforded **6** (4.140 g) as a colorless oil. IR (neat): 3300, 1460 cm⁻¹. ¹H-NMR (CDCl₃) δ: 3.90 (4H, s, OCH₂CH₂O), 5.45 (1H, d, *J* = 16 Hz, olefinic-H), 5.80 (1H, d, *J* = 16 Hz, olefinic-H). MS *m/z*: 257 (M⁺ + 1), 227, 185.

1-(1-Ethyl-1-hydroxypropyl)-2-(1,1-ethylenedioxyhexyl)cyclopropane (7)—CH₂I₂ (3.9 ml) was added to a stirred solution of **6** (4.140 g) and Et₂Zn (1 M solution in hexane, 48.5 ml) in benzene (90 ml) at room temperature, and the whole was stirred for 12 h. The reaction mixture was poured into water and extracted with Et₂O. The extracts were washed with brine and dried over Na₂SO₄. Removal of the solvent *in vacuo* gave an oily residue, which was purified by silica gel column chromatography. Elution with 6–8% AcOEt in hexane (v/v) afforded **7** (2.460 g) as a colorless oil. IR (neat): 3510, 1460 cm⁻¹. ¹H-NMR (CDCl₃) δ: 3.95 (4H, s, OCH₂CH₂O). MS *m/z*: 241 (M⁺ – Et), 199.

1-(1-Ethyl-1-hydroxypropyl)-2-(1-oxohexyl)cyclopropane (8)—A solution of **7** (2.460 g) and *p*-TsOH (50 mg) in a mixture of acetone (50 ml) and water (25 ml) was stirred at room temperature for 30 min. The reaction mixture was diluted with AcOEt, washed with 5% NaHCO₃ aq. and brine, and dried over Na₂SO₄. Removal of the solvent *in vacuo* gave an oily residue, which was purified by silica gel column chromatography. Elution with 5–7% AcOEt in hexane (v/v) afforded **8** (1.770 g) as a colorless oil. IR (neat): 3500, 1685, 1460 cm⁻¹. ¹H-NMR (CDCl₃) δ: 2.53 (2H, t, *J* = 6 Hz, COCH₂CH₂), 4.90–5.40 (1H, m, olefinic-H). MS *m/z*: 197 (M⁺ – Et).

3-Ethyl-7-oxo-3-dodecene (9)—Me₃SiI (0.31 ml) was added dropwise to a stirred solution of **8** (200 mg) in toluene (20 ml) at 25 °C, and the whole was stirred for 1 h. Sodium thiosulfate aq. was added to the reaction mixture, and which was extracted with Et₂O. The extracts were washed with brine and dried over Na₂SO₄. Removal of the solvent gave an oily residue, which was purified by silica gel column chromatography. Elution with 1% AcOEt in hexane (v/v) afforded **9** (105 mg) as a colorless oil. IR (neat): 1710, 1460 cm⁻¹. ¹H-NMR (CDCl₃) δ: 2.39 (4H, t, *J* = 6 Hz, CH₂COCH₂CH₂), 4.90–5.40 (1H, m, olefinic-H). MS *m/z*: 210 (M⁺), 154, 127.

(1S*,5R*)-3-Methoxycarbonylmethyliden-7,7-ethylenedioxybicyclo[3.3.0]octane (13)—A solution of **12** (20.00 g) in DME (60 ml) was added to a stirred ylide solution [prepared from trimethyl phosphonoacetate (20.00 g) and 55% NaH in oil (3.83 g) in DME (900 ml)] under ice-cooling, and the whole was stirred for 29 h at room temperature. The reaction mixture was poured into brine and extracted with AcOEt. The extracts were washed with brine and dried over Na₂SO₄. Removal of the solvent *in vacuo* gave an oily residue, which was purified by silica gel column chromatography. Elution with 3–8% AcOEt in hexane (v/v) afforded **13** (23.60 g) as a colorless oil. IR (neat): 1720, 1660 cm⁻¹. ¹H-NMR (CDCl₃) δ: 3.68 (3H, s, COOMe), 3.88 (4H, s, OCH₂CH₂O), 5.80 (1H, m, olefinic-H). MS *m/z*: 238 (M⁺), 207.

(1S*,5R*)-3-Methoxycarbonylmethyl-7,7-ethylenedioxybicyclo[3.3.0]oct-2-ene (14)—A solution of **13** (15.26 g) in THF (86 ml) was added to a stirred solution of LDA [prepared from 15% *n*-BuLi in hexane solution (56 ml), diisopropylamine (13.5 ml) and HMPA (16.7 ml) in THF (66 ml)] at –78 °C, and the whole was stirred for 40 min at the same temperature. The reaction mixture was quenched with NH₄Cl aq., poured into brine, and extracted with AcOEt. The extracts were washed with brine and dried over Na₂SO₄. Removal of the solvent *in vacuo* gave an oily residue, which was purified by silica gel column chromatography. Elution with 4–20% AcOEt in hexane (v/v) afforded **14** (15.05 g) as a colorless oil. IR (neat): 1745 cm⁻¹. ¹H-NMR (CDCl₃) δ: 3.68 (3H, s, COOMe), 3.88 (4H, s, OCH₂CH₂O), 5.47 (1H, m, olefinic-H). MS *m/z*: 238 (M⁺), 188, 166.

(1S*,5R*)-3-(2-Hydroxyethyl)-7,7-ethylenedioxybicyclo[3.3.0]oct-2-ene (15)—A solution of **14** (14.96 g) in THF (250 ml) was added dropwise to a stirred suspension of LiAlH₄ (3.57 g) in THF (125 ml) under ice-cooling. The reaction mixture was stirred for 25 min, then quenched with 4% NaOH aq. (15 ml). The reaction mixture was stirred at room temperature for another 1 h, and then the precipitate was filtered off. Removal of the solvent of the filtrate *in vacuo* gave an oily residue, which was purified by silica gel column chromatography. Elution with 25–55% AcOEt in hexane (v/v) afforded **15** (12.42 g) as a colorless oil. IR (neat): 3450 cm⁻¹. ¹H-NMR (CDCl₃) δ: 3.88 (4H, s,

OCH₂CH₂O), 5.35 (1H, m, olefinic-H). MS *m/z*: 210 (M⁺), 180.

(1S*,5R*)-3-(2-Benzyloxyethyl)-7,7-ethylenedioxybicyclo[3.3.0]oct-2-ene (16)——A solution of 15 (15.00 g) in DMF (25 ml) was added dropwise to a stirred suspension of 55% NaH in oil (4.60 g) in DMF (50 ml) under ice-cooling. The reaction mixture was stirred for 30 min at room temperature. Benzyl bromide (10 ml) was added dropwise to the reaction mixture, and the whole was stirred for 20 min at room temperature. The reaction mixture was poured into water and extracted with Et₂O. The extracts were washed with brine and dried over Na₂SO₄. Removal of the solvent gave an oily residue, which was purified by silica gel column chromatography. Elution with 3–10% AcOEt in hexane (v/v) afforded 16 (21.40 g) as a colorless oil. IR (neat): 1105 cm⁻¹. ¹H-NMR (CDCl₃) δ: 3.88 (4H, s, OCH₂CH₂O), 4.50 (2H, s, OCH₂Ph), 5.31 (1H, brs, olefinic-H), 7.35 (5H, s, arom.-H). MS *m/z*: 300 (M⁺).

(1S*,2R*,3R*,5R*)-3-(2-Benzyloxyethyl)-7,7-ethylenedioxybicyclo[3.3.0]octane-2,3-diol (17)——A solution of 16 (20.00 g) in acetone (100 ml) was added to a solution of OsO₄ (100 mg) and *N*-methylmorpholine *N*-oxide (10.00 g) in a mixture of *tert*-BuOH (150 ml), acetone (100 ml) and water (100 ml) at room temperature, and the whole was stirred for 6 h. Na₂S₂O₄ was added to the reaction mixture and filtered off. The filtrate was evaporated *in vacuo* and the residue was purified by silica gel column chromatography. Elution with 3–10% AcOEt in hexane (v/v) afforded 17 (20.90 g) as crystals. Recrystallization from AcOEt–hexane gave an analytical sample, mp 56–58 °C. *Anal.* Calcd for C₁₉H₂₆O₅: C, 68.24; H, 7.84. Found: C, 67.97; H, 7.78. IR (KBr): 3440, 1110 cm⁻¹. ¹H-NMR (CDCl₃) δ: 3.88 (4H, s, OCH₂CH₂O), 4.52 (2H, s, OCH₂Ph), 7.36 (5H, s, arom.-H). MS *m/z*: 334 (M⁺), 316.

(1R*,5S*,6R*,7R*)-7-(2-Benzyloxyethyl)-6,7-dihydroxybicyclo[3.3.0]octan-3-one (18)——A solution of 17 (20.80 g) in a mixture of acetone (100 ml), water (50 ml) and conc. HCl (3 ml) was stirred for 30 min at room temperature. The reaction mixture was poured into brine and extracted with AcOEt. The extracts were washed with brine and dried over Na₂SO₄. Removal of the solvent *in vacuo* gave an oily residue, which was purified by silica gel column chromatography. Elution with 3–10% AcOEt in hexane (v/v) afforded 18 (18.00 g) as crystals. Recrystallization from AcOEt–hexane gave an analytical sample, mp 91–93 °C. *Anal.* Calcd for C₁₇H₂₂O₄: C, 70.32; H, 7.64. Found: C, 70.11; H, 7.69. IR (KBr): 3440, 1735 cm⁻¹. ¹H-NMR (CDCl₃) δ: 4.52 (2H, s, OCH₂Ph), 7.36 (5H, s, arom.-H). MS *m/z*: 290 (M⁺), 272, 216.

(1R*,5S*,6R*,7R*)-7-(2-Benzyloxyethyl)-7-hydroxy-5-methanesulphonyloxybicyclo[3.3.0]octan-3-one (19)——MsCl (5.5 ml) was added to a stirred solution of 18 (17.90 g) and Et₃N (13 ml) in CH₂Cl₂ (350 ml) under ice-cooling, and the whole was stirred for 50 min. The reaction mixture was poured into brine and extracted with AcOEt. The extracts were washed with brine and dried over Na₂SO₄. Removal of the solvent *in vacuo* gave 19 (22.51 g) as crystals. Recrystallization from AcOEt–hexane gave an analytical sample, mp 90–92 °C. *Anal.* Calcd for C₁₈H₂₄O₆S: C, 58.67; H, 6.57. Found: C, 58.49; H, 6.50. IR (KBr): 3400, 1730 cm⁻¹. ¹H-NMR (CDCl₃) δ: 3.02 (3H, s, CH₃SO₂), 4.52 (2H, s, OCH₂Ph), 7.36 (5H, s, arom.-H). MS *m/z*: 368 (M⁺).

(1R*,4S*,5S*,6R*,7R*)-7-(2-Benzyloxyethyl)-7-hydroxytricyclo[3.3.0.0^{4,6}]octan-3-one (20)——*tert*-BuOK (3.51 g) was added to a stirred solution of 19 (7.681 g) in THF (300 ml) at room temperature, and the whole was stirred for 20 min at room temperature. After neutralization of the reaction mixture with AcOH, the whole was poured into water and extracted with AcOEt. The extracts were washed with water and dried over Na₂SO₄. Removal of the solvent *in vacuo* gave an oily residue, which was purified by silica gel column chromatography. Elution with 30–60% AcOEt in hexane (v/v) afforded 20 (4.170 g) as a colorless oil. IR (neat): 3455, 1720 cm⁻¹. ¹H-NMR (CDCl₃) δ: 4.55 (2H, s, OCH₂Ph), 7.35 (5H, s, arom.-H). MS *m/z*: 272 (M⁺), 254.

Ethyl(1S*,2R*,3S*,5S*,6R*,7R*)-7-(2-Benzyloxyethyl)-7-hydroxy-3-oxotricyclo[3.3.0.0^{4,6}]octane-2-carboxylate (21)——A solution of 20 (4.002 g) in THF (70 ml) was added dropwise to a stirred solution of LDA [prepared from diisopropylamine (5.3 ml) and 15% solution of *n*-BuLi in hexane (22.0 ml) in THF (240 ml)] at –78 °C. The mixture was stirred for 20 min, a solution of ethoxyformylimidazole¹⁵⁾ (4.00 g) in THF (45 ml) was added, and the whole was stirred for 15 min at –78 °C. After neutralization with AcOH, the reaction mixture was poured into water, and extracted with AcOEt. The extracts were washed with 5% HCl aq. and brine, and then dried over Na₂SO₄. Removal of the solvent *in vacuo* gave an oily residue, which was purified by silica gel column chromatography. Elution with 25–50% AcOEt in hexane (v/v) afforded 21 (4.262 g) as a colorless oil. IR (neat): 3500, 1735, 1715 cm⁻¹. ¹H-NMR (CDCl₃) δ: 1.22 (3H, t, *J* = 7 Hz, OCH₂CH₃), 4.11 (2H, q, *J* = 7 Hz, OCH₂CH₃), 4.49 (2H, s, OCH₂Ph), 7.28 (5H, s, arom.-H). MS *m/z*: 344 (M⁺), 326.

Ethyl (1S*,2R*,5S*)-7-(2-Benzyloxyethyl)-3-oxobicyclo[3.3.0]oct-6-en-2-carboxylate (22)——Me₃SiI (3.1 ml) was added dropwise to a stirred solution of 21 (3.010 g) in toluene (200 ml) over 30 min at 25 °C. The mixture was stirred for 30 min, and sodium thiosulfate aq. was added. The reaction mixture was extracted with Et₂O. The extracts were washed with brine and dried over Na₂SO₄. Removal of the solvent gave an oily residue, which was purified by silica gel column chromatography. Elution with 4–5% AcOEt in hexane (v/v) afforded 22 (1.290 g) as a colorless oil. IR (neat): 1755, 1720, 1655, 1620 cm⁻¹. ¹H-NMR (CDCl₃) δ: 1.27 (3H, t, *J* = 7 Hz, OCH₂CH₃), 4.15 (2H, q, *J* = 7 Hz, OCH₂CH₃), 4.46 (2H, s, OCH₂Ph), 5.20 (1H, brs, olefinic-H), 7.25 (5H, s, arom.-H). MS *m/z*: 328 (M⁺), 283, 238.

(1R*,5S*)-7-(2-Benzyloxyethyl)bicyclo[3.3.0]oct-6-en-3-one (23)——A solution of 16 (2.600 g) in a mixture of acetone (20 ml), water (8 ml) and conc. HCl (0.5 ml) was stirred for 1 h at room temperature. The reaction mixture was poured into brine and extracted with AcOEt. The extracts were washed with brine and dried over Na₂SO₄. Removal

of the solvent *in vacuo* gave an oily residue, which was purified by silica gel column chromatography. Elution with 7–10% AcOEt in hexane (v/v) afforded **23** (2.100 g) as a colorless oil. IR (neat): 1740 cm^{-1} . $^1\text{H-NMR}$ (CDCl_3) δ : 4.46 (2H, s, OCH_2Ph), 5.28 (1H, br s, olefinic-H), 7.30 (5H, s, arom.-H). MS m/z : 256 (M^+), 166.

Treatment of 23 with $(\text{EtO})_2\text{CO}$ and NaH—A solution of **23** (1.102 g) in dioxane (10 ml) was added dropwise to a stirred mixture of 55% NaH in oil (940 mg) and $(\text{EtO})_2\text{CO}$ (17 ml) in dioxane (30 ml) at 80 °C, and the whole was stirred for 30 min at the same temperature. After neutralization, the reaction mixture was poured into water and extracted with AcOEt. The extracts were washed with water and dried over Na_2SO_4 . Removal of the solvent *in vacuo* gave an oily residue, which was purified by silica gel column chromatography. Elution with 5% AcOEt in hexane (v/v) afforded **22** (280 mg), and elution with 6% AcOEt in hexane (v/v) afforded the isomeric ester (226 mg) as a colorless oil.

Treatment of 20 with Me_3SiH —Similar treatment of **20** (200 mg) with Me_3SiH (0.25 ml) in toluene (20 ml) afforded the olefin **23** (80 mg) as a colorless oil.

Ethyl (1*S,2*R**,3*R**,5*S**)-7-(2-Benzyloxyethyl)-3-hydroxybicyclo[3.3.0]oct-6-ene-2-carboxylate (24)**— NaBH_4 (330 mg) was added to a stirred solution of **22** (1.281 g) in ethanol (25 ml) under ice-cooling, and the whole was stirred for 30 min. The reaction mixture was poured into brine and extracted with AcOEt. The extracts were washed with brine and dried over Na_2SO_4 . Removal of the solvent *in vacuo* gave an oily residue, which was purified by silica gel column chromatography. Elution with 15–20% AcOEt in hexane (v/v) afforded **24** (1.060 g) as a colorless oil. IR (neat): 3450, 1730 cm^{-1} . $^1\text{H-NMR}$ (CDCl_3) δ : 1.22 (3H, t, $J=7$ Hz, OCH_2CH_3), 4.09 (2H, q, $J=7$ Hz, OCH_2CH_3), 4.46 (2H, s, OCH_2Ph), 5.26 (1H, br s, olefinic-H), 7.30 (5H, s, arom.-H). MS m/z : 330 (M^+), 312.

Ethyl (1*S,2*R**,3*R**,5*S**)-3-(2-Benzyloxyethyl)-3-(tetrahydropyran-2-yl)oxybicyclo[3.3.0]oct-6-ene-2-carboxylate (25)**—A mixture of **24** (2.201 g), DHP (0.93 ml) and a catalytic amount of *p*-TsOH in CH_2Cl_2 (60 ml) was stirred under ice-cooling for 30 min. The reaction mixture was diluted with CH_2Cl_2 , washed with 5% NaHCO_3 aq. and brine, and dried over Na_2SO_4 . Removal of the solvent *in vacuo* gave an oily residue, which was purified by silica gel column chromatography. Elution with 5–10% AcOEt in hexane (v/v) afforded **25** (2.620 g) as a colorless oil. IR (neat): 1730 cm^{-1} . $^1\text{H-NMR}$ (CDCl_3) δ : 1.26 (3H, t, $J=6$ Hz, $\text{CH}_3\text{CH}_2\text{O}$), 4.14 (2H, q, $J=6$ Hz, $\text{CH}_3\text{CH}_2\text{O}$), 4.52 (2H, s, OCH_2Ph), 4.65 (1H, br s, OCHO), 5.35 (1H, br s, olefinic-H), 7.36 (5H, s, arom.-H). MS m/z : 414 (M^+), 330.

(1*S,5*S**,6*S**,7*R**)-3-(2-Benzyloxyethyl)-6-hydroxymethyl-7-(tetrahydropyran-2-yl)oxybicyclo[3.3.0]oct-2-ene (26)**—A solution of **25** (2.580 g) in THF (15 ml) was added to a stirred suspension of LiAlH_4 (400 mg) in THF (50 ml) under ice-cooling, and the whole was stirred for 30 min, and then quenched with 4% NaOH aq. (1.6 ml). The reaction mixture was stirred at room temperature for another 1 h, and the precipitate was filtered off. Removal of the solvent of the filtrate *in vacuo* gave an oily residue, which was purified by silica gel column chromatography. Elution with 20–25% AcOEt in hexane (v/v) afforded **26** (2.620 g) as a colorless oil. IR (neat): 3470, 1080 cm^{-1} . $^1\text{H-NMR}$ (CDCl_3) δ : 4.52 (2H, s, OCH_2Ph), 5.37 (1H, br s, olefinic-H), 7.35 (5H, s, arom.-H). MS m/z : 372 (M^+), 354, 288.

(1*S,5*S**,6*R**,7*R**)-3-(2-Benzyloxyethyl)-6-formyl-7-(tetrahydropyran-2-yl)oxybicyclo[3.3.0]oct-2-ene (27)**—A solution of SO_3 pyridine complex (2.500 g) in DMSO (15 ml) was added to a stirred mixture of **26** (2.140 g) and Et_3N (10.0 ml) in DMSO (20 ml) at room temperature. After being stirred for 45 min, the reaction mixture was poured into water and extracted with AcOEt. The extracts were washed with water and dried over Na_2SO_4 . Removal of the solvent *in vacuo* gave almost pure aldehyde (**27**) (2.061 g) as a pale yellow oil. The crude material was used for the subsequent step without purification. IR (neat): 1720 cm^{-1} . $^1\text{H-NMR}$ (CDCl_3) δ : 4.52 (2H, s, OCH_2Ph), 4.65 (1H, br s, OCHO), 5.37 (1H, br s, olefinic-H), 7.37 (5H, s, arom.-H), 9.77 (1H, d, $J=4$ Hz, CHO). MS m/z : 370 (M^+), 286, 268.

(1*S,5*S**,6*S**,7*R**)-3-(2-Benzyloxyethyl)-6-[3-oxo-1(*E*)-octenyl]-7-(tetrahydropyran-2-yl)oxybicyclo[3.3.0]oct-2-ene (28)**—Tributyl 2-oxoheptylidene phosphorane (2.36 g) in Et_2O (10 ml) was added to a solution of **27** (2.032 g) in Et_2O (20 ml), and the mixture was stirred for 5 h at room temperature, then evaporated to dryness. The residue was purified by silica gel column chromatography. Elution with 4–6% AcOEt in hexane (v/v) afforded **28** (2.358 g) as a colorless oil. IR (neat): 1695, 1670, 1625 cm^{-1} . $^1\text{H-NMR}$ (CDCl_3) δ : 4.52 (2H, s, OCH_2Ph), 5.37 (1H, br s, olefinic-H), 6.17 (1H, dd, $J=3, 12$ Hz, olefinic-H), 6.75–7.05 (1H, m, olefinic-H), 7.36 (5H, s, arom.-H). MS m/z : 382 ($\text{M}^+ - 84$), 364.

(1*S,5*S**,6*S**,7*R**)-3-(2-Benzyloxyethyl)-6-[3(*S**)-hydroxyoct-1(*E*)-enyl]-7-(tetrahydropyran-2-yl)oxybicyclo[3.3.0]oct-2-ene (29a)** and **(1*S**,5*S**,6*S**,7*R**)-3-(2-Benzyloxyethyl)-6-[3(*R**)-hydroxyoct-1(*E*)-enyl]-7-(tetrahydropyran-2-yl)oxybicyclo[3.3.0]oct-2-ene (29b)**— NaBH_4 (280 mg) was added to a stirred solution of **28** (2.318 g) and $\text{CeCl}_3 \cdot 7\text{H}_2\text{O}$ (2.22 g) in methanol (40 ml) under ice-cooling. After 30 min of stirring, the excess reagent was decomposed by adding AcOH, and the reaction mixture was diluted with brine and extracted with AcOEt. The extracts were washed with brine and dried over Na_2SO_4 . Removal of the solvent *in vacuo* gave an oily residue, which was purified by silica gel column chromatography. Elution with 10% AcOEt in hexane (v/v) afforded **29b** (762 mg) as a colorless oil, and then elution with 12% AcOEt in hexane (v/v) afforded **29a** (1.510 g) as a colorless oil. Compound **29a**; IR (neat): 3450 cm^{-1} . $^1\text{H-NMR}$ (CDCl_3) δ : 4.52 (2H, s, OCH_2Ph), 4.68 (1H, br s, OCHO), 5.35 (1H, br s, olefinic-H), 5.60 (2H, m, olefinic-H), 7.36 (5H, s, arom.-H). MS m/z : 468 (M^+), 450, 406. Compound **29b**; IR (neat): 3440 cm^{-1} . $^1\text{H-NMR}$ (CDCl_3) δ : 4.52 (2H, s, OCH_2Ph), 4.70 (1H, br s, OCHO), 5.36 (1H, br s, olefinic-H), 5.60 (2H,

m, olefinic-H), 7.36 (5H, s, arom.-H). MS m/z : 468 (M^+), 450, 406.

(1*S**,5*S**,6*S**,7*R**)-3-(2-Benzoyloxyethyl)-6-[3(*S**)-(tetrahydropyran-2-yl)oxyoct-1(*E*)-enyl]-7-(tetrahydropyran-2-yl)oxybicyclo[3.3.0]oct-2-ene (30)—A mixture of 29a (1.489 g), DHP (0.44 ml) and a catalytic amount of *p*-TsOH in CH_2Cl_2 (15 ml) was stirred under ice-cooling for 1 h. The reaction mixture was diluted with CH_2Cl_2 , washed with 5% NaHCO_3 aq. and water, and dried over Na_2SO_4 . Removal of the solvent *in vacuo* gave an oily residue, which was purified by silica gel chromatography. Elution with 6–10% AcOEt in hexane (v/v) afforded 30 (1.721 g) as a colorless oil. IR (neat): 2950, 1020 cm^{-1} . $^1\text{H-NMR}$ (CDCl_3) δ : 4.53 (2H, s, OCH_2Ph), 4.73 (2H, brs, OCHO), 5.37 (1H, brs, olefinic-H), 5.60 (2H, m, olefinic-H), 7.37 (5H, s, arom.-H). MS m/z : 450 ($M^+ - 102$), 406.

(1*S**,5*S**,6*S**,7*R**)-3-(2-Hydroxyethyl)-6-[3(*S**)-(tetrahydropyran-2-yl)oxyoct-1(*E*)-enyl]-7-(tetrahydropyran-2-yl)oxybicyclo[3.3.0]oct-2-ene (31)—Excess sodium metal was added to a stirred solution of 30 (1.690 g) in a mixture of liquid ammonia (80 ml) and THF (30 ml) at -78°C until a blue color persisted, and the whole was stirred for 20 min. The reaction was quenched by the addition of NH_4Cl , and ammonia was evaporated off at room temperature under a stream of N_2 . Water was added to the residue and extracted with Et_2O . The extracts were washed with brine and dried over Na_2SO_4 . Removal of the solvent gave an oily residue, which was purified by silica gel column chromatography. Elution with 20–30% AcOEt in hexane (v/v) afforded 31 (1.273 g) as a colorless oil. IR (neat): 3450 cm^{-1} . $^1\text{H-NMR}$ (CDCl_3) δ : 4.71 (2H, brs, OCHO), 5.43 (1H, brs, olefinic-H), 5.60 (2H, m, olefinic-H). MS m/z : 360 ($M^+ - 102$), 316, 276.

dl-3-Oxa-9(*O*)-methano- $\Delta^{6(9\alpha)}$ -prostaglandin I_1 11,15-Bis(tetrahydropyran-2-yl)ether (32)—A 15% solution of *n*-BuLi in hexane (3.1 ml) was added to a stirred solution of 31 (1.240 g) in THF (6 ml) under ice-cooling. The mixture was stirred for 10 min, DMF (3 ml), DMSO (3 ml), $\text{ClCH}_2\text{COOLi}$ (540 mg) and NaI (2.00 g) were added to the reaction mixture, and the whole was stirred for 8 h at room temperature. The reaction mixture was diluted with water, acidified with 3% HCl aq. and extracted with AcOEt. The extracts were washed with brine and dried over Na_2SO_4 . Removal of the solvent *in vacuo* gave an oily residue, which was purified by acid-washed silica gel column chromatography. Elution with 20–30% AcOEt in hexane (v/v) afforded 32 (1.186 g) as a colorless oil. IR (neat): 1760, 1740 cm^{-1} . $^1\text{H-NMR}$ (CDCl_3) δ : 4.12 (2H, s, OCH_2COOH), 4.74 (2H, brs, OCHO), 5.38 (1H, brs, olefinic-H), 5.60 (2H, m, olefinic-H), 8.17 (1H, s, COOH). MS m/z : 418 ($M^+ - 102$), 374, 334.

dl-3-Oxa-9(*O*)-methano- $\Delta^{6(9\alpha)}$ -prostaglandin I_1 (1a)—A mixture of 32 (528 mg) and camphorsulphonic acid (50 mg) in acetone (20 ml) and water (10 ml) was stirred at 40°C for 2 h. The reaction mixture was poured into water and extracted with AcOEt. The extracts were washed with brine and dried over Na_2SO_4 . Removal of the solvent gave a crystalline residue, which was recrystallized from AcOEt–hexane to give 1a (265 mg), mp $72-74^\circ\text{C}$. Anal. Calcd for $\text{C}_{20}\text{H}_{32}\text{O}_5$: C, 68.15; H, 9.15. Found: C, 68.01; H, 8.97. IR (CHCl_3): 3400, 1730, 972 cm^{-1} . $^1\text{H-NMR}$ (CDCl_3) δ : 2.70–3.20 (1H, m, $\text{C}_9\text{-H}$), 3.67 (2H, t, $J=6$ Hz, OCH_2CH_2), 4.07 (2H, s, OCH_2COOH), 5.40–5.55 (3H, m, olefinic-H). MS m/z : 334 ($M^+ - 18$), 316, 290. TLC: $R_f=0.48$ [AcOEt:AcOH = 10:1 (v/v)].

15 β -Isomer (1b) of 1a—Similar treatment of the 15 β -alcohol (29b) through the reaction sequence described for the synthesis of 1a gave 1b as a colorless viscous oil. IR (neat): 3350, 1730 cm^{-1} . $^1\text{H-NMR}$ (CDCl_3) δ : 3.67 (2H, t, $J=6$ Hz, OCH_2CH_2), 4.09 (2H, s, OCH_2COOH), 5.40–5.55 (3H, m, olefinic-H). MS m/z : 334 ($M^+ - 18$), 316, 290. TLC: $R_f=0.56$ [AcOEt:AcOH = 10:1 (v/v)].

Acknowledgement The authors thank Dr. T. Oshima, Sankyo Co., Ltd., for testing biological activities.

References and Notes

- 1) P. A. Aristoff, "Advances in Prostaglandin, Thromboxane and Leukotriene Research," Vol. 14, ed. by J. E. Pike and D. R. Morton, Jr., Raven Press, New York, 1985, p. 309; R. C. Nickolson, M. H. Town and H. Vorbrüggen, *Med. Res. Rev.*, **5**, 1 (1985).
- 2) a) M. Shibasaki, Y. Torisawa and S. Ikegami, *Tetrahedron Lett.*, **24**, 3493 (1983); b) M. Shibasaki, H. Fukasawa and S. Ikegami, *ibid.*, **24**, 3497 (1983); c) M. Sodeoka and M. Shibasaki, *Chem. Lett.*, 1984, 579; d) Y. Torisawa, H. Okabe, M. Shibasaki and S. Ikegami, *ibid.*, 1984, 1069; e) Y. Ogawa and M. Shibasaki, *Tetrahedron Lett.*, **25**, 1067 (1984); f) T. Mase, M. Sodeoka and M. Shibasaki, *ibid.*, **25**, 5087 (1984); g) Y. Torisawa, H. Okabe and S. Ikegami, *J. Chem. Soc., Chem. Commun.*, 1984, 1602.
- 3) Sankyo Co., Ltd., Japan. Patent Appl. 83-136625 (1983) [*Chem. Abstr.*, **104**, 33934b (1986)]; K. Koyama and K. Kojima, *Chem. Pharm. Bull.*, **32**, 2866 (1984).
- 4) a) G. L. Bundy, F. Lincoln, N. Nelson, J. E. Pike and W. Schneider, *Ann. N. Y. Acad. Sci.*, **180**, 76 (1971); N. A. Nelson, R. W. Jackson, A. T. Au, D. J. Wynalda and E. Nishizawa, *Prostaglandins*, **10**, 795 (1975); D. R. Morton, J. L. Thompson, *J. Org. Chem.*, **43**, 2102 (1978); b) P. A. Aristoff, A. W. Harrison and A. M. Huber, *Tetrahedron Lett.*, **25**, 3955 (1984); P. A. Aristoff, P. D. Johnson and A. W. Harrison, *J. Am. Chem. Soc.*, **107**, 7967 (1985); W. Skuballa, E. Schillinger, C.-St. Sturzebecher and H. Vorbrüggen, *J. Med. Chem.*, **29**, 313 (1986).
- 5) Similar treatment of $(\text{CH}_3)_2\text{C}(\text{OH})\underset{\text{CH}_2}{\text{C}}\text{H}-\text{CHCOCH}_3$ with Me_3SiI afforded $(\text{CH}_3)_2\text{C}=\text{CHCH}_2\text{CH}_2\text{COCH}_3$ in 27% yield.
- 6) M. Nakayama, S. Shinke, Y. Matsushita, S. Ohira and S. Hayashi, *Bull. Chem. Soc. Jpn.*, **52**, 184 (1979).

- 7) The ring opening of cyclopropyl ketones by iodotrimethylsilane to afford γ -iodo ketones was reported: R. D. Miller and D. R. McKean, *J. Org. Chem.*, **46**, 2412 (1981).
- 8) M. E. Jung and P. L. Ornstein, *Tetrahedron Lett.*, **18**, 2659 (1977).
- 9) P. Bladon and L. N. Owen, *J. Chem. Soc.*, **1950**, 598.
- 10) G. Balme, G. Fournet and J. Gore, *Tetrahedron Lett.*, **27**, 1907 (1986).
- 11) T.-L. Ho, *Synth. Commun.*, **9**, 665 (1979).
- 12) K. C. Nicolaou, W. J. Sipio, R. L. Magolda, S. Seitz and W. E. Barnett, *Chem. Commun.*, **1978**, 1067; M. Shibasaki, J. Ueda and S. Ikegami, *Tetrahedron Lett.*, **20**, 433 (1979).
- 13) J. H. Herrmann, G. R. Kieczkowski and R. H. Schlessinger, *Tetrahedron Lett.*, **14**, 2433 (1973).
- 14) V. VanRheenen, R. C. Kelly and D. Y. Cha, *Tetrahedron Lett.*, **17**, 1973 (1976).
- 15) H. A. Staab, *Justus Liebigs Ann. Chem.*, **609**, 83 (1957).

[Chem. Pharm. Bull.]
35(3) 957-969 (1987)

A Quantitative Analysis of Proton Nuclear Magnetic Relaxation: Conformation Analysis of Substituted 5,1-Benzothiazocine and Its Homologue

HIDEYUKI HARUYAMA,* SADA0 SATO, KAYOKO KAWAZOE,
and MICHIO KONDO

*Analytical and Metabolic Research Laboratories, Sankyo Co., Ltd.,
1-2-58, Hiromachi, Shinagawa-ku, Tokyo 140, Japan*

(Received July 17, 1986)

In addition to variable-temperature experiments and the analysis of vicinal coupling constants, a quantitative treatment of T_1 values and nuclear Overhauser effect (NOE) factors was applied to the conformation analysis of novel heterocycles, substituted 4,1-benzothiazepine (**1**) and 5,1-benzothiazocine (**2**). The most probable conformations of the seven- and eight-membered rings of **1** and **2**, respectively, could be distinguished by comparing the observed T_1 values and NOE factors with those calculated for several possible conformers.

By the quantitative analysis of T_1 values at -90.2°C and at room temperature (24.5°C), **1** was found to be in an equilibrium state of rapid ring inversion between two chair forms in the ratio of 0.7:0.3 (at 24.5°C), and the major conformer was the chair form with 5-methyl group equatorial.

The X-ray analysis of **2** showed that the eight-membered ring adopted a boat-boat like conformation in the crystal. Although this conformation seemed to be consistent with most of the observed relaxation data obtained in solution, the significant shielding effect expected on H_{4a} was not observed. By a systematic search of the conformers, a boat-chair like conformer was found to satisfy all the observed relaxation and shielding data.

Keywords— $^1\text{H-NMR}$; spin-lattice relaxation time; NOE; X-ray analysis; conformation analysis; 4,1-benzothiazepine derivative; 5,1-benzothiazocine derivative

Introduction

Analyses of the stable conformations and related dynamic processes of cyclic molecules in solution constitute an interesting area of nuclear magnetic resonance (NMR) spectroscopy.¹⁾ Extensive studies have been done on six-membered ring systems, while a rather limited number of studies exist on more-than-six-membered ring systems. This paper describes the conformational analysis of novel seven-(**1**) and eight-(**2**) membered heterocycles, which have been synthesized by Sato *et al.* as a part of their search for new heterocyclic compounds with biological activities.²⁾ In addition to the conventional variable-temperature experiments and the analysis of vicinal coupling constants, a quantitative treatment of the spin-lattice relaxation time (T_1) values and nuclear Overhauser effect (NOE) factors was applied. The spin-lattice relaxation rate of an organic molecule in solution is a function of molecular motion and intramolecular dipole-dipole interactions. The latter is closely related to the molecular conformation, *i.e.*, intramolecular interproton distances. The molecular motion must be anisotropic, but the authors have shown that this quantity can be treated as a single parameter just for the purpose of getting the best coincidence between the calculated and observed T_1 values.³⁾ This corresponds to an assumption of isotropic molecular tumbling. Based on this assumption, the configuration of a nitrile group in saframycin A was determined successfully⁴⁾ and the details of the treatment were described therein. Using that procedure, the most probable conformations of the seven- and eight-membered rings of **1** and

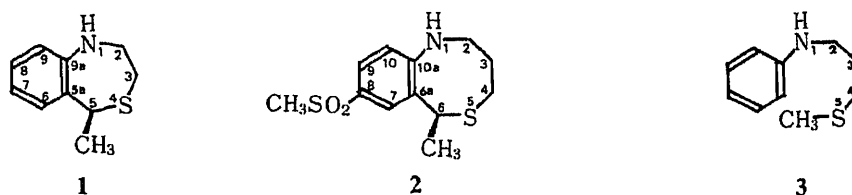


Chart 1

2, respectively, could be distinguished by comparing the observed T_1 values and NOE factors with those calculated for the several possible conformers. Other physical quantities were of course taken into account to avoid reaching incorrect conclusions.

The $^1\text{H-NMR}$ spectrum of **1** (in CD_3OD) showed two sets of signals with an intensity ratio of 0.84:0.16 at -90.2°C . The quantitative analysis of T_1 and NOE data allowed us to assign to the major component a chair conformation with the 5-methyl group in the equatorial position, while the minor component took an inverted chair form. Based on a rapid ring inversion between these two chair forms, the T_1 values and vicinal coupling constants at 24.5°C could be explained well.

As for **2**, which shows an inhibitory activity against gastric secretion,⁵⁾ an X-ray analysis was carried out. The X-ray derived boat-boat like conformer seemed to reproduce the observed relaxation parameters at 24.5°C , but the significant shielding effect on H_{4a} , which was expected in this conformation, was not observed. By a systematic search of the conformers, a boat-chair like conformer was found to satisfy all the observed relaxation and shielding parameters. Therefore, **2** was concluded to take a boat-chair like conformation in solution.

Results and Discussion

5-Methyl-4,1-benzothiazepine (**1**)

Chemical Shifts and Coupling Constants—The chemical shifts and coupling constants measured in CDCl_3 and CD_3OD are summarized in Tables I and II. The assignments could be readily made on the basis of decoupling experiments and NOE measurements.

At ambient temperature ($24 \pm 0.5^\circ\text{C}$), only one set of signals could be observed (see Fig. 1(a)). Methylene protons on C_2 and C_3 were differentiated by comparing the chemical shifts with those of related molecules, and the assignment was confirmed by NOE measurement in CD_3OD , where a 5% signal enhancement was observed at H_{3b} (δ : 2.92) on irradiating H_5 .

The assignment of aromatic protons was readily made from their coupling patterns and NOE experiments in CD_3OD . The irradiation of 5-methyl protons at δ : 1.67 caused (a) 25% signal enhancement of a double doublet at δ : 7.16 and -5% signal enhancement of a double triplet at δ : 6.91. This observation is consistent with a linear arrangement of 5- CH_3 , H_6 , and H_7 in space, leading to the assignment of δ : 7.16 and 6.91 to H_6 and H_7 , respectively. Thus, another double triplet at 7.03 ppm and a double doublet at 6.91 ppm (in CD_3OD) could be assigned to H_8 and H_9 , respectively.

The coupling constants obtained for the protons on the seven-membered ring could not be explained by any single conformation.

At a lower temperature, the $^1\text{H-NMR}$ spectrum in CD_3OD was found to consist of two sets of sharp signals (see Fig. 1(b)). This indicates the presence of a slow conversion process between two different conformers in the solution. The ratio of them was estimated from the integrated intensities to be 0.84:0.16 at -90.2°C .

On irradiating a triplet at δ : 2.59, a doublet at δ : 3.57 and a triplet at δ : 3.11 changed to a singlet and a doublet, respectively, while on irradiating a triplet at δ : 3.11, a doublet at δ : 2.71

and a triplet at δ : 2.59 changed to a singlet and a doublet, respectively. From these decoupling experiments, two pairs of methylene signals for the major conformer could be readily differentiated. The assignment of these signals could be done by referring to the assignment of the spectra at 24.5 °C.

The assignment of the signals belonging to the minor component was made on the basis of the following assumption; when two conformers are in equilibrium with rapid interconversion, the observed chemical shifts should be described by an equation similar to Eq. 1, where J_{obs} , J_M , and J_m in Eq. 1 should be replaced by the corresponding chemical shift values. By using this relation, the assignment of the minor component signals for H_{2b} , H_9 , and 5- CH_3 could be done from the chemical shifts of these protons at 24.5 °C and those for the major component at -90.2 °C.

The magnitude of the vicinal coupling constants showed that H_{2a} and H_{3b} were in *trans* and H_{2b} and H_{3a} were in *gauche* relation in the major conformer (M). These observations are consistent with either a chair or a boat form of the seven-membered ring for both major and minor components, but the possibility of a twist conformation is negligible.

To differentiate the above alternatives, a quantitative interpretation of T_1 s was carried out.

TABLE I. ¹H-NMR Chemical Shifts for 1

Protons	at 24.5 °C		at -90.2 °C	
	δ_{CDCl_3}	δ_{CD_3OD}	$\delta_M^a)$	$\delta_m^b)$
H_{2a}	3.12	3.00	2.59	— ^{c)}
H_{2b}	3.47	3.39	3.57	— ^{c)}
H_{3a}	2.90	2.85	2.71	— ^{c)}
H_{3b}	2.97	2.92	3.11	2.49
H_5	4.19	4.14	4.10	3.89
5-Me	1.72	1.67	1.61	1.72
H_6	7.20	7.16	7.23	7.23
H_7	6.97	6.91	7.00	7.00
H_8	7.08	7.03	7.08	7.08
H_9	6.84	6.91	6.97	6.80

Chemical shifts are given relative to internal TMS as a reference. a) Major conformer (M) in CD_3OD . b) Minor conformer (m) in CD_3OD . c) Not identified.

TABLE II. Coupling Constants (Hz) for 1 (at 24.5 °C)

	$J_{obs}^a)$	$J_{obs}^b)$	$J_{cal}^c)$
$J_{2a,3a}$	2.6	2.2	2.6
$J_{2a,3b}$	8.8	8.4	8.3
$J_{2b,3a}$	6.2	6.6	5.1
$J_{2b,3b}$	2.6	2.3	2.6
$J_{2a,2b}$	12.8	13.1	
$J_{3a,3b}$	14.1	13.8	
$J_{5,5-Me}$	7.7	7.4	
$J_{6,7}$	7.8	8.1	
$J_{6,8}$	1.5	1.7	
$J_{7,8}$	7.8	7.3	
$J_{7,9}$	1.5	1.5	
$J_{8,9}$	7.8	7.8	

a) In $CDCl_3$. b) In CD_3OD . c) Calculated according to the procedure described in the text.

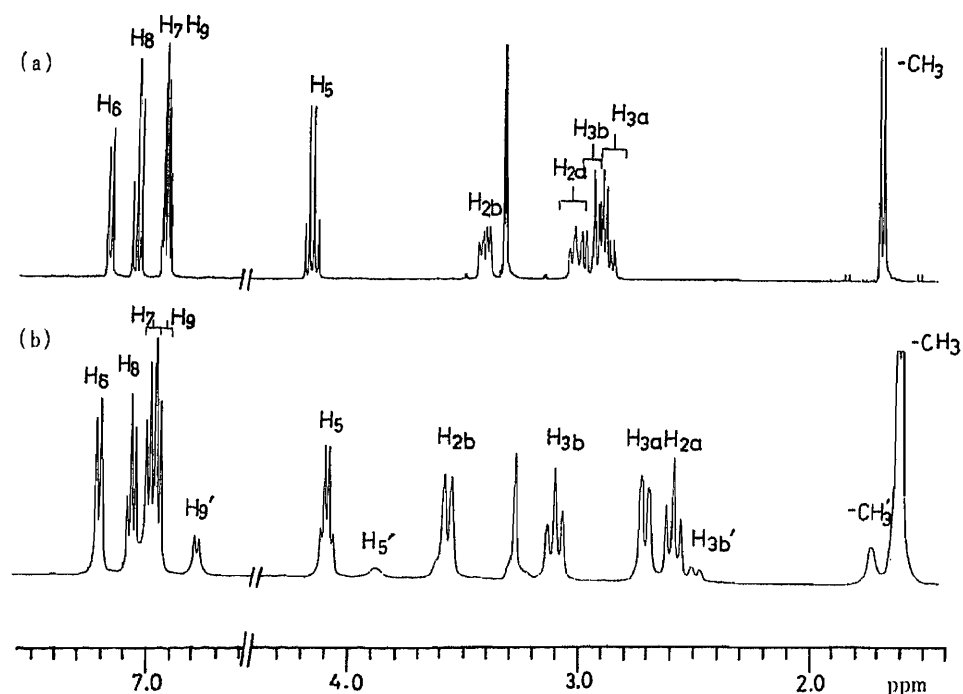


Fig. 1. $^1\text{H-NMR}$ Spectra for **1** in CD_3OD

(a) at room temperature (24.5°C), (b) at -90.2°C , where signals assigned to the minor component are denoted by prime (').

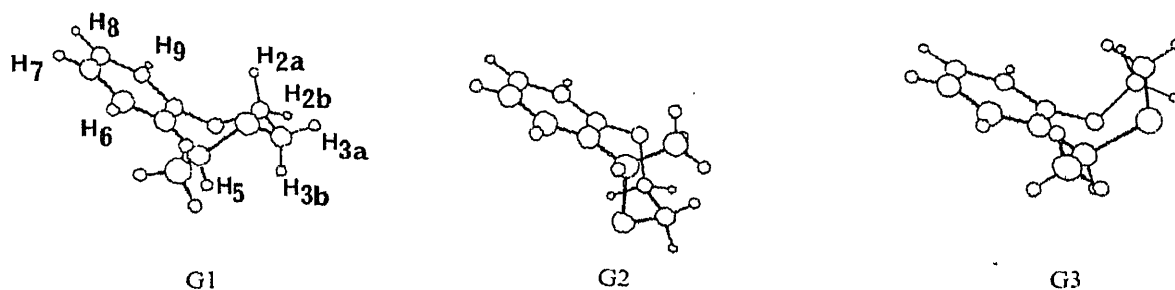


Fig. 2. Possible Conformers for **1**

Quantitative Analysis of T_1 Values at -90.2°C —The $^1\text{H-T}_1$ values measured at -90.2°C are summarized in Table III. The calculation of the T_1 values was carried out for the geometries of two chair forms and one boat form, which are illustrated in Fig. 2. The effective τ_c value necessary for the calculation was obtained in the process as the value giving the best agreement between the observed and calculated T_1 values.⁵⁾ Though $\tau_c = 1.0 \times 10^{-10}$ and 0.7×10^{-9} s were possible, $\tau_c = 0.7 \times 10^{-9}$ s was taken, because the negative NOE described below required $\omega\tau_c > 1.0$.⁶⁾

The calculated results are given in the third column of Table III. The T_1 values for H_5 and H_6 are very sensitive to the conformation, because interproton distances between H_5 and its neighboring protons depend on the seven-membered ring conformation as can be readily understood from the model geometries shown in Fig. 2. The best agreement between the observed and calculated T_1 values was given by the chair conformation with the 5-methyl group equatorial (conformer G1). This was consistent with the NOE observed at H_{3a} and H_{3b} on irradiating H_5 (Fig. 3).

On the assumption of a ring inversion process between M and m, the minor component

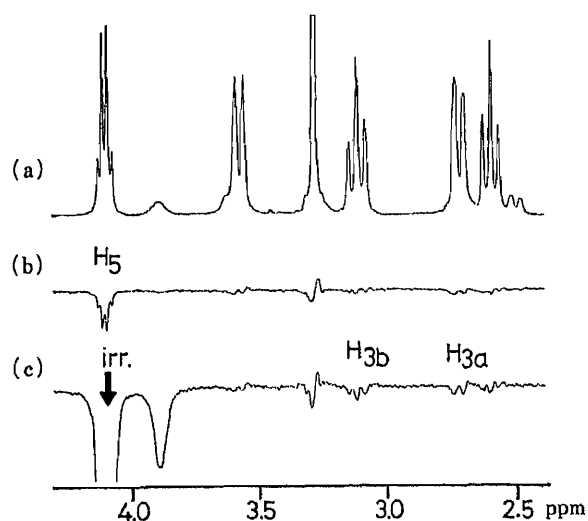


Fig. 3. NOE Difference Spectra for 1 at -90.2°C (CD_3OD)

(a), control; (b) and (c), spectra obtained on irradiation of the 5-methyl protons and H_5 , respectively.

TABLE III. Observed and Calculated T_1 Values^{a)} for 1 (at -90.2°C)

Protons	T_1^{obs}	T_1^{cal}		
		G1	G2	G3
H_{2a}	0.40	0.40	0.39	0.37
H_{2b}	0.38	0.37	0.36	0.40
H_{3a}	0.36	0.33	0.22	0.39
H_{3b}	0.36	0.35	0.34	0.39
H_5	0.83	0.70	0.88	1.15
H_6	0.76	0.62	1.40	0.50
H_8	1.73	1.79	1.80	1.79
S-Me	0.24	0.21	0.20	0.21
$q^b)$		0.13	0.25	0.19

a) The correlation times, $\tau_c = \tau_c^{\text{Mc}} = 0.7 \times 10^{-9}$ s were assumed. T_1 values for H_7 and H_9 protons were not included in the analysis because of signal overlapping, which prevent the accurate T_1 measurement of these protons.

$$b) \quad q = \sqrt{\frac{1}{n} \sum_{i=1}^n \left[\left(\frac{1}{T_{1,i}^{\text{obs}}} - \frac{1}{T_{1,i}^{\text{cal}}} \right) / \frac{1}{T_{1,i}^{\text{obs}}} \right]^2}$$

where n is the number of protons under consideration, and $T_{1,i}^{\text{obs}}$ and $T_{1,i}^{\text{cal}}$ mean the observed and calculated T_1 values for H_i proton. The smallest q value leads to the best agreement between the observed and calculated T_1 values.³⁰⁾

(m) can be assigned as the corresponding inverted chair with the 5-methyl group axial (the conformer G2, see Fig. 2). If the minor component m were G3, the signal assigned to H_{3b} , would be a triplet. The possibility of G3 was, therefore, ruled out.

Quantitative Analysis of T_1 Values at 24.5°C —In order to confirm the equilibrium between the conformers G1 and G2, the vicinal coupling constants and T_1 values were analyzed quantitatively based on the assumption of rapid interconversion of the seven-membered ring between G1 and G2. On this assumption, the observed vicinal coupling constants can be described by Eq. 1,

$$J_{\text{obs}} = J_M \cdot P_M + J_m \cdot P_m \quad (1)$$

where P_M and P_m are the molar fractions of the major and the minor component, respectively.

TABLE IV. Observed and Calculated T_1 Values^{d)} for **1** (at 24.5 °C)

Protons	T_1^{obs}	T_1^{cal}		
		I ^{b)}	II ^{c)}	III ^{d)}
H _{2a}	2.5	3.0	3.1	2.7
H _{2b}	2.7	2.9	2.8	3.1
H _{3a}	2.7	2.4	2.7	1.8
H _{3b}	2.7	2.5	2.4	2.8
H ₅	8.1	7.6	7.1	9.3
H ₆	6.9	6.6	5.6	11.1
H ₇	14.3	11.7	11.8	11.7
H ₈	14.5	13.6	13.6	13.6
H ₉	18.2	22.3	22.4	22.0
Me	2.4	2.5	2.5	2.5
q		0.09		

a) $\tau_c = \tau_c^{\text{Me}} = 1.0 \times 10^{-11}$ s were assumed. b) Calculated assuming equilibrium between the conformers G1 and G2. For details, see the text. c) Calculated assuming G1 geometry (chair with equatorial 5-Me). d) Calculated assuming G2 geometry (chair with axial 5-Me).

The most satisfactory agreement between the observed J values and those calculated by Eq. 1 could be attained with $P_M = 0.7$ ($P_m = 0.3$), using J_M and J_m taken from the observed coupling constants at -90.2 °C; 10.8 Hz for J_{trans} and 2.6 Hz for J_{gauche} , respectively (see Table II).

When the molecule is rapidly converting, as mentioned above, the interproton distances appearing in the relaxation equation must be replaced by the effective values described by Eq. 2,⁷⁾

$$\frac{1}{\langle r^6 \rangle_{\text{av}}} = \frac{1}{r_M^6} \cdot P_M + \frac{1}{r_m^6} \cdot P_m \quad (2)$$

The third column of Table IV shows the calculated T_1 values using the molar ratio $P_M = 0.7$ ($P_m = 0.3$) and the effective interproton distances calculated from the geometries G1 and G2. The agreement between the observed and calculated T_1 values was excellent, and this is consistent with the rapid interconversion of the seven-membered ring between the two chair forms (G1 and G2). Although a quantitative treatment was not done, the above mentioned NOE observed between H₅ and H_{3b} is consistent with the conclusion that 70% of the molecules were in the G1 conformation.

8-Methylsulfonyl-5,1-benzothiazocine (**2**)

Chemical Shifts and Coupling Constants—¹H-NMR measurement was made in CDCl₃ and CD₃OD. The spectral assignments given in Tables V and VI were based on the extensive decoupling experiments. No significant solvent effect was observed either on the chemical shifts or on the coupling constants. The variable-temperature experiment showed no spectral change except line broadening due to increased viscosity in the range from 24.5 to -90.2 °C (Fig. 4). Thus, it may be safely concluded that **2** adopts a single conformation in solution.

The vicinal coupling constants about C₂-C₃ and C₃-C₄ were analyzed using the Karplus-type Eq. 3.⁸⁾

$$J^{\text{vic}} = 7 - \cos \varphi + 5 \cos 2\varphi \quad (3)$$

The dihedral angles (φ) which are consistent with the observed coupling constants are illustrated in Fig. 5. The possible eight-membered ring conformation of **2**, therefore, should satisfy these constraints of the dihedral angles as well as the constraint of the dihedral angle C₆-C_{6a}-C_{10a}-N₁ = 0°.

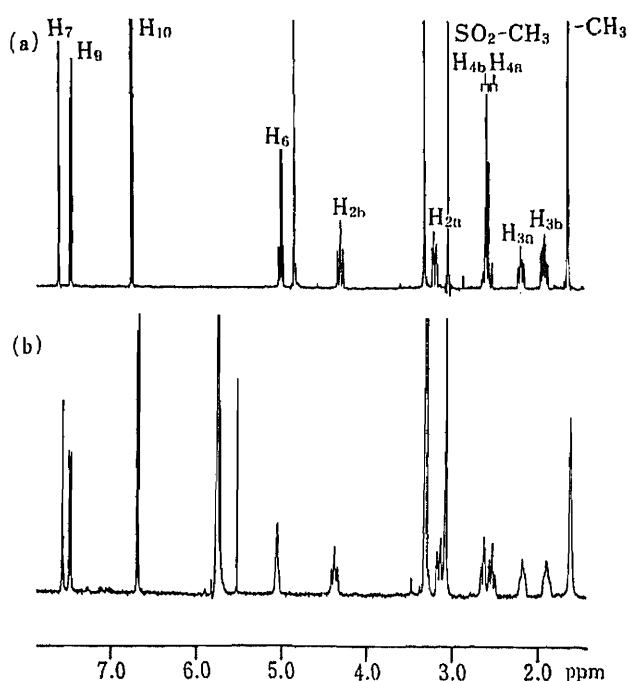


Fig. 4. $^1\text{H-NMR}$ Spectra for **2** in CD_3OD
(a) at room temperature (24.5°C), (b) at -90.2°C .

TABLE V. $^1\text{H-NMR}$ Chemical Shifts for **2** and **3**

Protons	2		3^{a)}
	δ_{CDCl_3}	$\delta_{\text{CD}_3\text{OD}}$	δ_{CDCl_3}
H_{2a}	3.24	3.23 (3.12)	3.20
H_{2b}	4.20	4.34 (4.35)	
H_{3a}	2.14	2.17 (2.15)	1.80
H_{3b}	1.92	1.90 (1.88)	
H_{4a}	2.53	2.60 (2.54)	2.55
H_{4b}	2.62	2.64 (2.63)	
H_6	4.89	5.04 (5.03)	2.06 ^{b)}
H_7	7.70	7.63 (7.53)	6.55—7.35 ^{c)}
H_9	7.53	7.49 (7.44)	
H_{10}	6.65	6.79 (6.66)	
6-Me	1.68	1.65 (1.60)	
SO_2Me	3.02	3.03 (3.05)	

Spectra were taken at ambient temperature ($24.5 \pm 0.5^\circ\text{C}$) and at -90.2°C (in parentheses). Chemical shifts are given relative to internal TMS as a reference. ^{a)} Values reported in the literature.²⁾ ^{b)} δ_{H} for CH_3S^- . ^{c)} δ_{H} for aromatic protons.

According to the procedure described in the experimental section, the six conformers (G1, G2, G3, G3', G4, and G4') shown in Fig. 6, which satisfy the above mentioned dihedral constraints, were derived. In these conformers, the eight-membered ring adopts boat-boat (BB), boat-chair (BC), or twist boat-chair (TBC) form.⁹⁾

Unambiguous differentiation of the most probable conformer among them could be done by quantitative analysis of T_1 values and NOE factors.

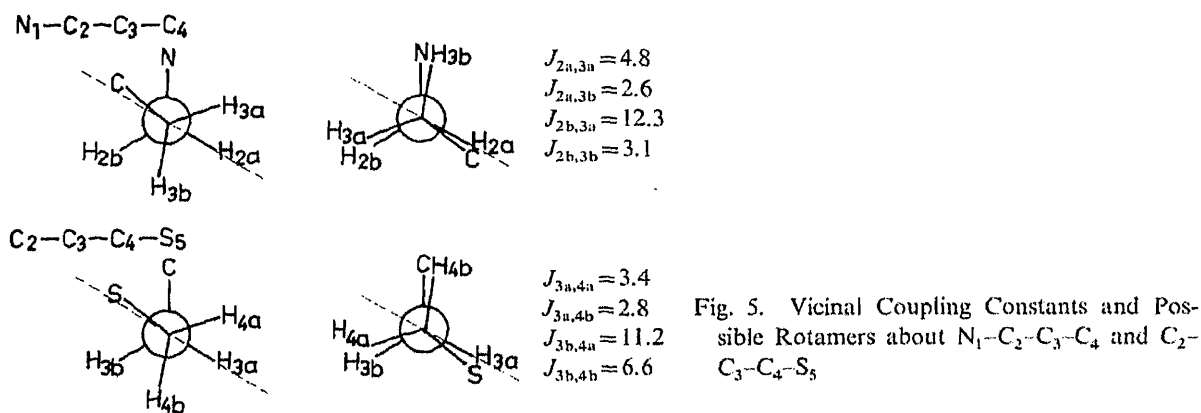
Quantitative Analysis of T_1 Values and NOE Factors—Some typical partially relaxed Fourier-transformed (PRFT) spectra for **2** are given in Fig. 7. The observed T_1 values and NOE factors are summarized in Tables VII and VIII, respectively.

The relaxation times of the methylene protons except H_{2b} take very similar values in the range from 0.99 to 1.2 s, because the T_1 value of a methylene proton is determined dominantly

TABLE VI. Coupling Constants (Hz) for **2** (at 24.5 °C)

	J_{obs}		$J_{\text{cal}}^a)$	
	(CDCl ₃)	(CD ₃ OD)	G5	G2
$J_{2a,3a}$	4.4	4.8	4.6 (55.9°)	4.7 (55.2°)
$J_{2a,3b}$	2.9	2.6	4.0 (-59.9°)	3.7 (-62.5°)
$J_{2b,3a}$	12.2	12.3	12.8 (171.2°)	12.9 (173.6°)
$J_{2b,3b}$	2.8	3.1	4.7 (55.4°)	4.6 (56.0°)
$J_{3a,4a}$	3.3	3.4	5.5 (49.8°)	5.9 (47.5°)
$J_{3a,4b}$	2.8	2.8	3.9 (-60.4°)	2.9 (-68.8°)
$J_{3b,4a}$	11.1	11.2	12.6 (169.3°)	12.3 (165.2°)
$J_{3b,4b}$	5.6	6.6	5.6 (49.3°)	5.7 (48.9°)
$J_{2a,2b}$	15.5	15.5		
$J_{3a,3b}$	13.8	13.0		
$J_{4a,4b}$	15.4	14.6		
$J_{6,6-\text{Me}}$	6.8	6.8		
$J_{7,9}$	2.1	2.1		
$J_{9,10}$	8.5	8.4		

a) The vicinal coupling constants were calculated according to Eq. 3. Dihedral angles used for the calculation are shown in parentheses; these values were taken from the X-ray analysis for G5 and from the calculated geometry for G2.



by the contribution of its geminal proton.⁷⁾ An evidently short T_1 value of H_{2b} (0.62 s) suggests the presence of another proton, in addition to H_{2a} , contributing to H_{2b} relaxation. This is consistent with the NOE observed at H_{2b} on irradiating H_6 . Thus, the eight-membered ring of **2** should take a conformation in which H_6 is located close to H_{2b} . Among the six conformers, G1 and G2 satisfy this condition (see Fig. 6), while the others do not.

The T_1 values and NOE factors expected for the conformers given in Fig. 6 were calculated assuming $\tau_c = 0.15 \times 10^{-10}$ s for the methyl protons ($\tau_c^{\text{Me}})^{3b)}$ and $\tau_c = 0.25 \times 10^{-10}$ s for all other protons.³⁾ The results are given in Tables VII and VIII. None of the conformers G3, G3', G4 and G4' could explain either the observed NOEs or the T_1 values, while the agreement between observed and calculated T_1 values and NOE factors is very satisfactory for G1 conformer. As to G2 conformer, the T_1 agreement was also satisfactory for all the protons other than H_7 . The observed T_1 disagreement for H_7 may be ascribed to the ambiguity in the effective interproton distances between H_7 and the 6-methyl protons due to the internal rotation of the methyl group.¹¹⁾

Comparison of the X-Ray Derived Conformation with Those Derived from ¹H-NMR—In

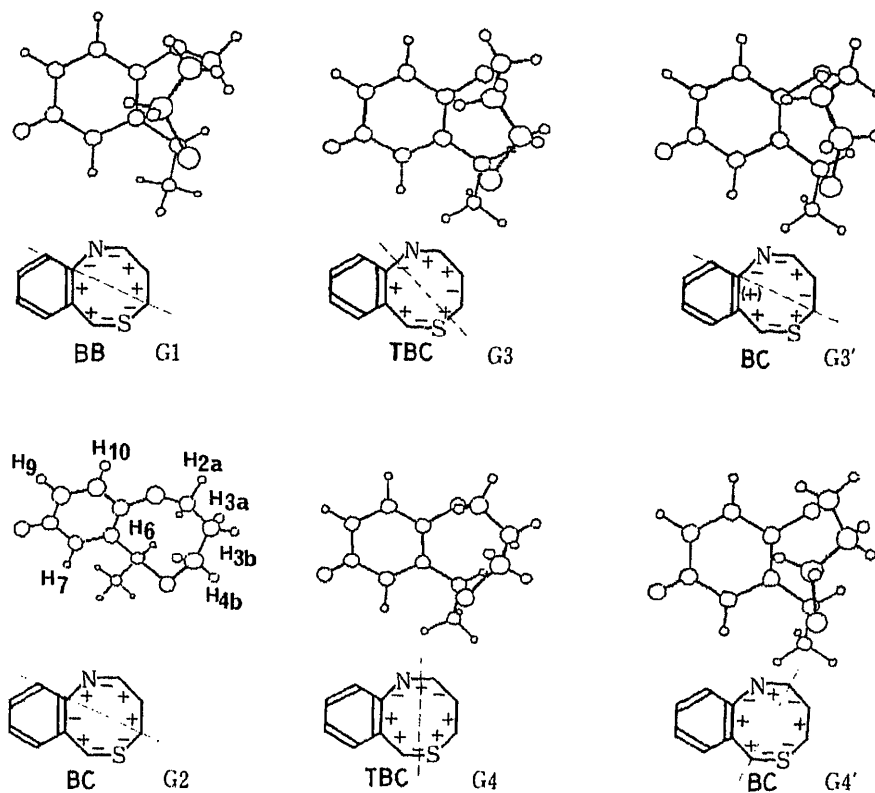


Fig. 6. Six Possible Conformers for 2

The signs of the dihedral angles and the location of the symmetry (denoted by ---), which define the conformation of the eight-membered ring^{9,10} are shown. As for the dihedral angle, $C_6-C_{6a}-C_{10a}-N$, a small deviation from the ideal value of 0° was used to define the conformation. In $G3'$, the sign of the dihedral angle in the parenthesis was assumed to classify its eight-membered ring into one of the conformations defined by Hendrickson *et al.*; the actually observed value was -5.3° .

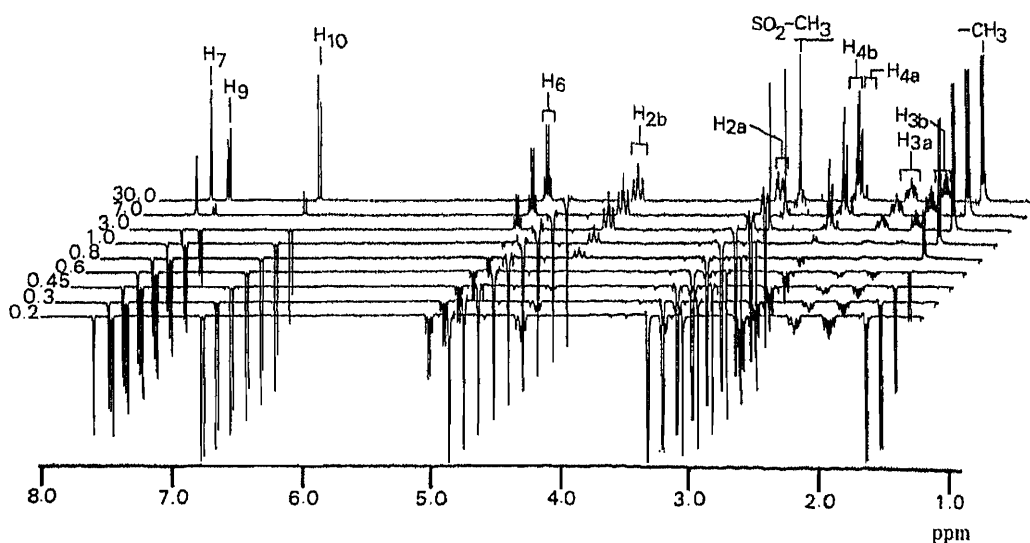


Fig. 7. Typical Partially Relaxed Spectra for 2 in CD_3OD

order to compare the conformation in solution with that in crystals, X-ray analysis of 2 was carried out. The ORTEP drawing of 2 is given in Fig. 8. The final atomic coordinates are presented in Table IX.¹²⁾ The comparison of dihedral angles revealed that the eight-membered

TABLE VII. Observed and Calculated T_1 Values for 2 (at 24.5 °C)

Protons	T_1^{obs}	T_1^{cal}						
		G1	G2	G5	G3	G3'	G4	G4'
H _{2a}	1.08	1.15	1.16	1.08	1.01	0.97	0.98	1.06
H _{2b}	0.62	0.75	0.63	0.65	1.02	1.05	0.99	0.98
H _{3a}	0.99	0.99	0.96	0.93	1.05	0.78	0.76	0.94
H _{3b}	1.00	0.95	0.96	0.92	0.84	0.94	0.55	0.85
H _{4a}	1.16	1.10	1.14	1.08	0.79	0.99	1.00	0.97
H _{4b}	1.16	1.12	1.11	1.04	0.96	1.05	0.96	0.97
H ₆	1.50	1.45	1.11	1.33	2.39	3.73	0.92	3.10
H ₇	3.85	3.23	2.00	3.16	3.88	3.03	3.75	3.36
H ₉	6.78	7.11	6.88	6.94	7.81	7.09	7.05	7.14
H ₁₀	6.58	6.28	6.48	6.60	5.88	6.03	6.31	5.39
6-Me	0.90	0.98	0.93	0.96	0.96	0.93	0.89	0.94
q		0.09	0.37	0.10	0.25	0.28	0.37	0.25

The correlation times, $\tau_c = 0.25 \times 10^{-10}$ s, and $\tau_c^{\text{Me}} = 0.15 \times 10^{-10}$ s, were assumed.

TABLE VIII. Observed and Calculated NOE Factors for 2

Protons	Irr.	Obs.	η_{obs}	η_{cal}					
				G1	G2	G5	G3	G3'	G4
H ₆	H _{2a}	-0.05	-0.07	-0.08	-0.07	---	0.04	---	---
	H _{2b}	0.21	0.19	0.24	0.21	---	-0.01	---	---
	H _{3a}	---	---	---	---	---	---	0.23	0.07
	H _{3b}	---	---	---	---	---	---	-0.07	-0.02
	H _{4a}	---	---	---	---	0.10	---	---	---
	H _{4b}	---	---	---	---	-0.03	---	---	---
	6-Me	0.02	0.03	0.02	0.02	0.02	0.02	0.02	0.02
6-Me	H ₆	0.19	0.16	0.12	0.11	0.21	0.30	0.11	0.26
	H ₇	0.38	0.45	0.49	0.45	0.47	0.46	0.47	0.45

$\eta = (I_{\text{irr}} - I_{\text{n}}) / I_{\text{n}}$, where I_{n} and I_{irr} are peak intensities of control and irradiated spectra, respectively.

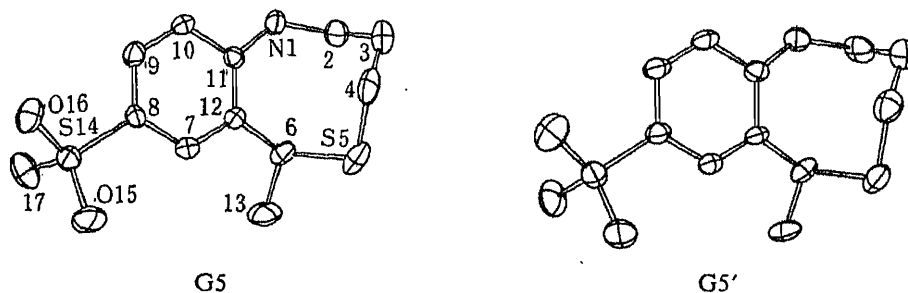


Fig. 8. An ORTEP Drawing of 2 Derived from X-Ray Analysis

The conformations of the two independent molecules in an asymmetric unit are shown.¹³⁾ The atomic numbering used in Table IX is given to the unprimed molecule.

TABLE IX. Fractional Atomic Coordinates ($\times 10^4$) and Thermal Parameters (\AA^2) for **2**, with Estimated Standard Deviations in Parentheses

Atom	<i>x</i>	<i>y</i>	<i>z</i>	<i>B</i> _{eq}
N(1)	826 (5)	5016 (10)	11379 (8)	3.17 (26)
C(2)	24 (8)	4575 (11)	11568 (11)	3.83 (37)
C(3)	-684 (8)	5815 (15)	11353 (13)	5.45 (47)
C(4)	-1245 (8)	6539 (13)	9819 (13)	4.95 (45)
S(5)	-1990 (2)	5401 (3)	8177 (3)	4.45 (9)
C(6)	-1034 (6)	4372 (10)	8094 (10)	2.93 (31)
C(7)	-34 (6)	5825 (10)	7439 (9)	2.52 (29)
C(8)	846 (6)	6550 (10)	7812 (9)	2.37 (28)
C(9)	1666 (6)	6698 (10)	9317 (10)	2.62 (30)
C(10)	1631 (6)	6216 (10)	10457 (9)	2.39 (28)
C(11)	730 (6)	5458 (10)	10098 (9)	2.19 (27)
C(12)	-97 (6)	5266 (9)	8572 (9)	2.30 (27)
C(13)	-1642 (8)	3808 (14)	6476 (11)	4.47 (39)
S(14)	901 (2)	7161 (3)	6360 (2)	2.76 (7)
O(15)	-117 (5)	7441 (9)	5006 (8)	4.10 (25)
O(16)	1644 (5)	8317 (8)	6975 (8)	4.27 (27)
C(17)	1427 (9)	5730 (13)	5973 (13)	5.31 (47)
N(1')	6063 (5)	3148 (10)	11316 (8)	3.25 (27)
C(2')	5797 (8)	2991 (13)	12395 (10)	4.07 (37)
C(3')	5415 (9)	4352 (15)	12668 (12)	5.26 (46)
C(4')	4455 (8)	4999 (12)	11222 (12)	4.73 (43)
S(5')	3365 (2)	3821 (3)	10085 (3)	4.40 (9)
C(6')	3755 (7)	2586 (10)	9181 (11)	3.42 (35)
C(7')	3915 (6)	3790 (10)	7288 (9)	2.35 (28)
C(8')	4460 (6)	4403 (10)	6796 (10)	2.64 (30)
C(9')	5537 (6)	4511 (10)	7826 (10)	2.87 (31)
C(10')	6015 (6)	4118 (10)	9280 (10)	2.72 (30)
C(11')	5490 (6)	3526 (10)	9842 (9)	2.47 (29)
C(12')	4381 (6)	3353 (9)	8735 (9)	2.29 (28)
C(13')	2752 (7)	1927 (12)	7854 (12)	3.82 (36)
S(14')	3820 (2)	4892 (3)	4910 (2)	3.06 (7)
O(15')	2794 (5)	5425 (10)	4379 (7)	4.48 (26)
O(16')	4458 (6)	5870 (9)	4774 (9)	5.74 (33)
C(17')	3643 (9)	3339 (13)	3904 (12)	5.08 (46)

$$B_{eq} = (4/3) \cdot \sum_i \sum_j \beta_{ij} a_i \cdot a_j$$

TABLE X. Estimated Shielding by the Phenyl Ring in Several Conformations of **2**

Geometry	H _{4a}	H _{4b}	$\Delta\delta_{\text{cal}}^{a)}$	$\Delta\delta_{\text{obs}}^{a)}$
G5	-0.85	-0.14	-0.71	
G5' ^{b)}	-0.84	-0.16	-0.68	
G2	-0.09	-0.05	-0.14	-(0.04-0.09)

a) $\Delta\delta = \delta_{\text{H4a}} - \delta_{\text{H4b}}$. b) Another conformation in the crystals.¹³⁾

ring of **2** adopts a G1-type conformation (BB form).¹³⁾ The T_1 values and NOE factors calculated for the X-ray derived geometry (G5) are also given in Tables VII and VIII.

In this X-ray derived conformer (G5) as well as the model geometry G1, significant ring current shifts are expected at H_{4a}, because H_{4a} is located in the shielding region of the benzene ring, while H_{4b} may be slightly shielded. According to the method of Johnson and Bovey,¹⁴⁾

the chemical shift difference between H_{4a} and H_{4b} was estimated to be *ca.* 0.7 ppm (see Table X). However, this is inconsistent with the observation that $\Delta\delta$ between H_{4a} and H_{4b} is less than 0.1 ppm. The chemical shifts of H_{4a} and H_{4b} are similar to the values of methylene protons at C_4 in **3**,²⁾ which is free from the ring current effects.

On the other hand, the ring current shifts calculated for the G2 conformation (BC form) are consistent with the observations, as shown in Table X. The vicinal coupling constants calculated for this conformation also satisfy the observed values (see Table VI).

Taking into account the above-mentioned ambiguity involved in the estimation of interproton distances, the absence of the ring current effect on H_{4a} and H_{4b} leads to the conclusion that the eight-membered ring of **2** takes a BC form (G2 conformation) in solution instead of the BB form in crystals, although the G1 conformation (BB form) or the conformation in crystals could also satisfy the observed vicinal coupling constants as well as T_1 s and NOEs (see Tables VI, VII and VIII, respectively). The interproton distance between H_{2b} and H_6 , estimated from the T_1 value of H_6 , is *ca.* $1.85 + 0.5 \text{ \AA}$, which could explain the low field shift of H_{2b} by the steric compression effect.¹⁵⁾

Experimental

Materials—5-Methyl-4,1-benzothiazepine (**1**) and 6-methyl-8-methylsulfonyl-5,1-benzothiazocine (**2**) were supplied by Dr. Tomita of our Chemical Laboratories. After the NH protons were replaced with deuterium,⁴⁾ the compounds were dissolved in CD_3OD or $CDCl_3$ to the concentration of *ca.* 0.5% (w/v) and degassed by repeating freeze-pump-thaw cycles.

NMR—¹H-NMR spectra were obtained on a JEOL GX-400 spectrometer operating at 399.6 MHz. Generally, 64 FIDs were accumulated using 16000 data points for a spectral width of 4000 Hz (¹H). For the variable-temperature experiments, a JEOL GVT1 system was used. The temperature was directly read on the meter and not calibrated. The measurement and the analysis of T_1 s and NOEs were carried out as reported previously.⁴⁾

Geometry Generation—The coordinates of the possible conformers, for which the T_1 values and NOEs were calculated, were obtained by either the distance geometry method⁴⁾ or by the following procedure.

Assume a virtual acyclic linear molecule with n atoms corresponding to an n -membered ring. The bond lengths and bond angles were fixed at the standard values for the relevant atoms. Then the ring closure test was carried out for the various combinations of the dihedral angles. In order to make the test less laborious, some of the dihedral angles were restricted to the ranges required from the vicinal coupling constants, while the others were varied in the range from -120 to 120° in steps of 10 or 20° .

The ring closure was judged first by the criterion of whether the terminal atoms of this acyclic molecule (1st and n th atom) could be located within the relevant bond lengths $\pm 0.4 \text{ \AA}$, and then, the bond angles resulting from the ring formation were checked. If these values were chemically reasonable, the molecular mechanics calculation was carried out to refine the coordinates.

The computer program for these treatments and calculations is included in our RSCA system.

X-Ray Analysis of 2—A crystal of dimensions $0.6 \times 0.4 \times 0.2$ mm, obtained from ethyl acetate, was used for the X-ray reflection intensity measurements. Crystal data are as follows: $C_{12}N_17NO_2S_2$, monoclinic, $P2_1$, $Z=4$, $a=16.103(3)$, $b=9.487(2)$, $c=10.903(2) \text{ \AA}$, $\beta=126.30(1)^\circ$, $D_{calc.}=1.34 \text{ g/cm}^3$.

Intensity data were recorded on a Rigaku AFC-5R with a graphite-monochromated CuK_α radiation, using the $\theta-2\theta$ scan technique ($2\theta \leq 128^\circ$). The 2260 independent reflections ($F_o \geq 2\sigma(F_o)$) were corrected for Lorentz and polarization factors but not for absorption.

The structure was solved by MULTAN¹⁶⁾ and refined by the block-diagonal least-squares method. Hydrogen atoms were located from difference Fourier synthesis. The final least-squares refinement, with anisotropic temperature factors for the non-hydrogen atoms and isotropic temperature factors for the hydrogen atoms, lowered the R -value to 0.060.

Acknowledgement The authors wish to thank Dr. Kuniyuki Tomita for supplying purified materials and for his valuable suggestion.

References and Notes

- 1) M. Oki, "Applications of Dynamic NMR Spectroscopy to Organic Chemistry," VCH Publishers, Deerfield Beach, 1985, pp. 287—323.

- 2) S. Sato, K. Tomita, H. Fujita, and Y. Sato, *Heterocycles*, **22**, 1045 (1984).
- 3) In this paper, the calculation of T_1 values was carried out under the assumption of isotropic tumbling, where the correlation time of the isotropic tumbling was treated as an adjustable parameter which was adjusted so that the best agreement between observed and calculated T_1 values could be obtained. Under this assumption, a set of T_1 values can be taken as reflecting the spatial distribution of protons, because T_1 values have a more significant dependency on interproton distances rather than the correlation times. Due to the dependency on the sixth power of interproton distance, the agreement between observed and calculated T_1 values is practically determined by the difference of the geometries (interproton distances) instead of the intrinsically existing anisotropy of the molecular motion. In support of the above-mentioned procedure, the analysis of the ^{13}C - T_1 values of **2** gave the averaged correlation times of the C-H vectors, $(0.26 \pm 0.02) \times 10^{-10}$ s (unpublished data), which was very similar to the effective value obtained in the text (0.25×10^{-10} s).
- 4) a) H. Haruyama, H. Kurihara, and M. Kondo, *Chem. Pharm. Bull.*, **33**, 905 (1985); b) H. Haruyama and M. Kondo, *Chem. Pharm. Bull.*, **35**, 170 (1987).
- 5) S. Kobayashi, M. Miyamoto, Y. Shimada, K. Endo, F. Asai, and T. Ito, *Jpn. J. Pharmacol.*, **36**, Suppl. 89p (1984).
- 6) A. A. Bothner-By, "Biological Applications of Magnetic Resonance," ed. by R. G. Shulman, Academic Press, Inc., New York, 1979, pp. 178-187.
- 7) J. H. Noggle and R. E. Schirmer, "The Nuclear Overhauser Effect," Academic Press, Inc., New York, 1971.
- 8) A. A. Bothner-By, *Adv. Magn. Reson.*, **1**, 195 (1965).
- 9) According to the definition of Hendrickson,¹⁰⁾ the eight-membered ring conformation of **2** was classified in terms of the signs of the dihedral angles and the location of the symmetry in the ring (mirror planes or twofold axes).
- 10) J. B. Hendrickson, *J. Am. Chem. Soc.*, **89**, 7047 (1967).
- 11) R. Rowan, III, J. A. McCammon, and B. D. Sykes, *J. Am. Chem. Soc.*, **96**, 4773 (1974).
- 12) The following data are available from one of the authors (S. S.) upon request; tables of bond lengths, bond angles, anisotropic thermal parameters for non-hydrogen atoms, hydrogen atom parameters, and observed and calculated structure factors.
- 13) The X-ray analysis of **2** revealed that two independent molecules were present in an asymmetric unit cell. The difference of the geometries for these two molecules (referring to G5 and G5') was not significant. As for the thiazocine rings, the maximum and average deviations of the corresponding torsion angles are 8.0 and 2.6°, respectively. According to the categories adopted in this paper, the conformations of the thiazocine rings are classified as BB form, where the sign of the individual torsion angle is coincident with that of the corresponding torsion angle of G1 and the maximum deviations of the corresponding torsion angles are ca. 15°. Therefore, the X-ray derived conformation can be considered to be very similar to the model geometry G1. The calculated relaxation parameters are given only for G5, while the calculated ring-current effects are presented for both geometries (see Table X).
- 14) C. E. Johnson, Jr. and F. A. Bovey, *J. Chem. Phys.*, **29**, 1012 (1958).
- 15) a) S. Winstein, P. Carter, F. A. L. Anet, and A. J. R. Bourn, *J. Am. Chem. Soc.*, **87**, 5247 (1965); b) J. E. Baldwin and R. K. Pinschmidt, Jr., *ibid.*, **92**, 5247 (1970).
- 16) P. Main, L. Lessinger, M. M. Woolfson, G. Germain, and J. P. Declercq, MULTAN74. A System of Computer Programs for the Automatic Solution of Crystal Structures from X-Ray Diffraction Data. Universities of York, England, and Louvain, Belgium, 1974.

[Chem. Pharm. Bull.]
35(3) 970-979 (1987)

Syntheses of 24,25-Dihydroxyvitamin D₂, 24,25-Dihydroxy-22-dehydrovitamin D₃, 25-Hydroxy-24-oxo-22-dehydrovitamin D₃ and 22,24,25-Trihydroxyvitamin D₃¹⁾

KOTOMI KATSUMI,^a TOSHIO OKANO,^a YURIE ONO,^a EMIKO MAEGAKI,^a
KUMIKO NISHIMURA,^a MIZUE BABA,^a TADASHI KOBAYASHI,*^a
OKIKO MIYATA,^b TAKEAKI NAITO,^b
and ICHIYA NINOMIYA^b

*Departments of Hygienic Sciences^a and Medicinal Chemistry,^b
Kobe Women's College of Pharmacy, Motoyamakita-machi,
Higashinada-ku, Kobe 658, Japan*

(Received July 28, 1986)

Four vitamin D₂ and D₃ metabolites, 24,25-dihydroxyvitamin D₂ (**8**), 24,25-dihydroxy-22-dehydrovitamin D₃ (**10**), 25-hydroxy-24-oxo-22-dehydrovitamin D₃ (**12**) and 22,24,25-trihydroxyvitamin D₃ (**14**), were synthesized from ergosterol (**1**) *via* the hydroxyketone (**4**) as a common key intermediate.

Keywords—24,25-dihydroxyvitamin D₂; 24,25-dihydroxy-22-dehydrovitamin D₃; 25-hydroxy-24-oxo-22-dehydrovitamin D₃; 22,24,25-trihydroxyvitamin D₃; vitamin D; ergosterol; high-performance liquid chromatography

There are two of vitamin D,²⁾ namely D₂ and D₃, which differ in the side chain structure but have practically the same biological activity in mammals, including human beings. These two vitamins are known to be similarly metabolized to 25-hydroxyvitamin D (25-OH-D) in the liver and subsequently to 1 α ,25-dihydroxyvitamin D [1 α ,25-(OH)₂-D] or 24R,25-dihydroxyvitamin D [24R,25-(OH)₂-D] in the kidney when plasma calcium concentrations are lower or higher than normal.³⁾ Many studies have been done on the further metabolism of 25-OH-D₃ and 1 α ,25-(OH)₂-D₃. The 26,23-lactone,⁴⁾ 23-hydroxy,⁵⁾ 23,24-dihydroxy,⁶⁾ 24,26-dihydroxy,⁶⁾ 23-oxo,⁶⁾ 24-oxo^{6,7)} and 23-hydroxy-24-oxo⁸⁻¹⁰⁾ derivatives of 25-OH-D₃ and 26,23-lactone,¹¹⁾ 23-hydroxy¹²⁾ and 24-oxo^{13,14)} derivatives of 1 α ,25-(OH)₂-D have been isolated and identified as *in vivo* or *in vitro* metabolites. The mechanisms of metabolism have been well discussed^{15,16)} and some of the isolated metabolites were chemically synthesized.¹⁷⁻²¹⁾ However, few reports have appeared on the metabolism of vitamin D₂, and the metabolic fate of the double bond at the 22-position and the methyl group at the 24S-position in the side chain of vitamin D₂ remains to be clarified. We now report the syntheses of four potential metabolites, 24,25-(OH)₂-D₂ (**8**), 24,25-dihydroxy-22-dehydrovitamin D₃ [Δ^{22} -24,25-(OH)₂-D₃] (**10**), 25-hydroxy-24-oxo-22-dehydrovitamin D₃ [Δ^{22} -24-oxo-25-OH-D₃] (**12**) and 22,24,25-trihydroxyvitamin D₃ [22,24,25-(OH)₃-D₃] (**14**).

First, we investigated the synthesis of 24,25-(OH)₂-D₂ (**8**). Though the synthesis of **8** from stigmasterol was reported by Jones *et al.*,^{22,23)} their synthetic route is rather complicated. Therefore, we have developed an improved synthesis of **8** by modification of their procedure. As shown in Chart 1, ergosterol (**1**) was converted into the known 20-aldehyde (**3**) *via* a route involving protection of the 5,7-diene group and ozonolysis according to Barton *et al.*²⁴⁾ Aldol condensation of **3** with 3-methyl-3-(tetrahydropyran-2-yloxy)butan-2-one proceeded very smoothly to afford the hydroxyketone (**4a** and **4b**) as a diastereomeric mixture; **4a**

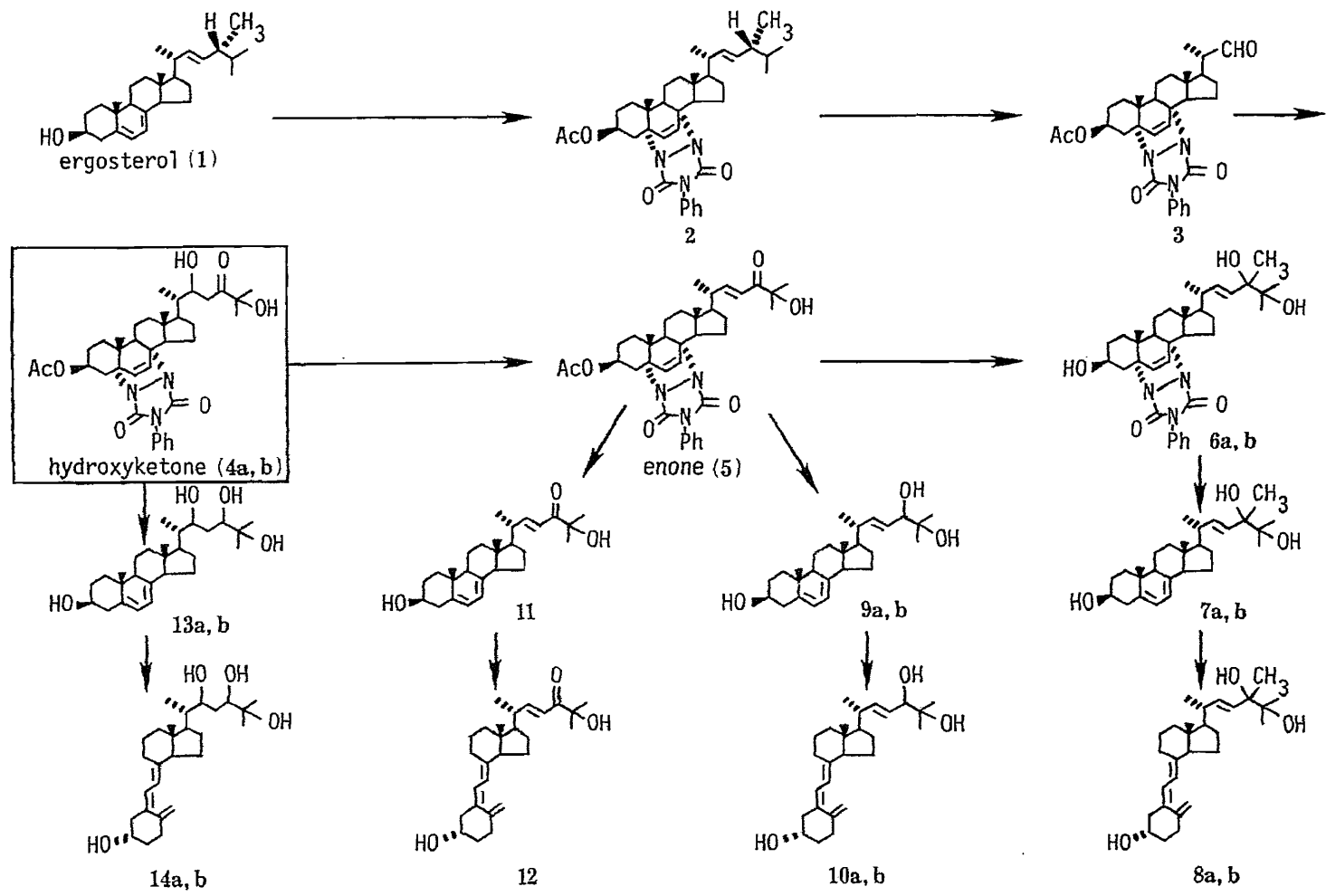


Chart 1. Synthetic Scheme

and **4b** were separated, both as colorless crystals, by preparative thin layer chromatography (TLC) using silica gel. The yields of the less polar (**4a**: $R_f=0.33$) and more polar (**4b**: $R_f=0.19$) 22-isomers were 18 and 21%, respectively, though their stereochemistry at the 22-position has not been clarified. Dehydration of a mixture of **4a** and **4b** with *p*-toluenesulfonic acid afforded the known enone (**5**) in 90% yield, which exhibited the proton nuclear magnetic resonance ($^1\text{H-NMR}$) signals of two newly formed olefinic protons at 6.36 (d, $J=15$ Hz, 23-H) and 7.03 (dd, $J=15, 8$ Hz, 22-H). The conversion of **3** to **5** was carried out according to Eyley and Williams,²⁵ who obtained **5** directly without isolation of **4**. Methylation of **5** with methyllithium afforded the methylated 24,25-glycols (**6**) in 60% yield, and these were refluxed with lithium aluminum hydride (LiAlH_4) in tetrahydrofuran (THF) to afford the desired 24,25-dihydroxyprovitamin D_2 [$24,25\text{-(OH)}_2\text{-pro-D}_2$, **7a** and **7b**] as a mixture of diastereomers in 70% yield.

The two diastereomers were completely separated by high-performance liquid chromatography (HPLC) on a Zorbax SIL column with 2.5% isopropanol in *n*-hexane as the mobile phase, as shown in Fig. 1, to afford the respective diastereomers in almost equal amounts; the less polar (peak 1) was confirmed to be (24*S*)-24,25-(OH)₂-pro-D₂ (**7a**) and the more polar compound (peak 2) to be the (24*R*)-isomer (**7b**) by converting them into the corresponding 24,25-(OH)₂-D₂ (**8a** and **8b**) by ultraviolet (UV) irradiation followed by thermal isomerization. Figure 2 shows the HPLC profiles of **7a** and **7b** before and after photochemical and thermal isomerization as representatives of the provitamin forms (**7**, **9**, **11** and **13**).

When **7a** and **7b** were irradiated by a monochromatic UV ray at 295 nm obtained from a spectroirradiator, the peaks decreased while those of the respective previtamin forms (**15a** and **15b**) with retention times of 46.3 and 49.4 min increased. Upon thermal isomerization by refluxing the irradiated ethanolic solutions for 2 h, the previtamin peaks were converted to those of the vitamin D forms (**8a** and **8b**) with retention times of 32.0 and 34.0 min, respectively. These products were purified by HPLC. The eluates corresponding to the respective peaks were carefully collected and the solvent was evaporated off under reduced pressure to give the respective vitamins (**8a** and **8b**) in pure form.

On co-chromatography (HPLC) with authentic **8a** and **8b**, kindly donated by Dr. Y. Mazur and Dr. G. Jones, the purified vitamins showed retention times of 32.0 and 34.0 min, and were confirmed to be (24*S*)-24,25-(OH)₂-D₂ (**8a**) and (24*R*)-24,25-(OH)₂-D₂ (**8b**), respectively.

Secondly, we synthesized Δ^{22} -24,25-(OH)₂-D₃ (**10a** and **10b**). Δ^{22} -24,25-(OH)₂-pro-D₃ (**9a** and **9b**) was produced from the enone (**5**) by a double reduction procedure. Reduction of **5**

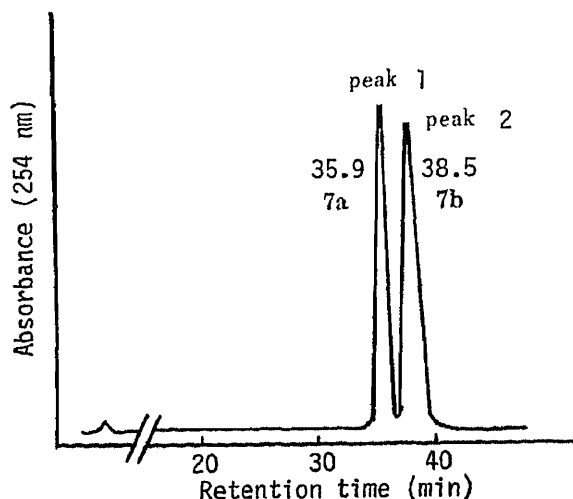


Fig. 1. HPLC Separation of the Diastereomeric Mixture of 24,25-(OH)₂-D₂ (**7a** and **7b**)

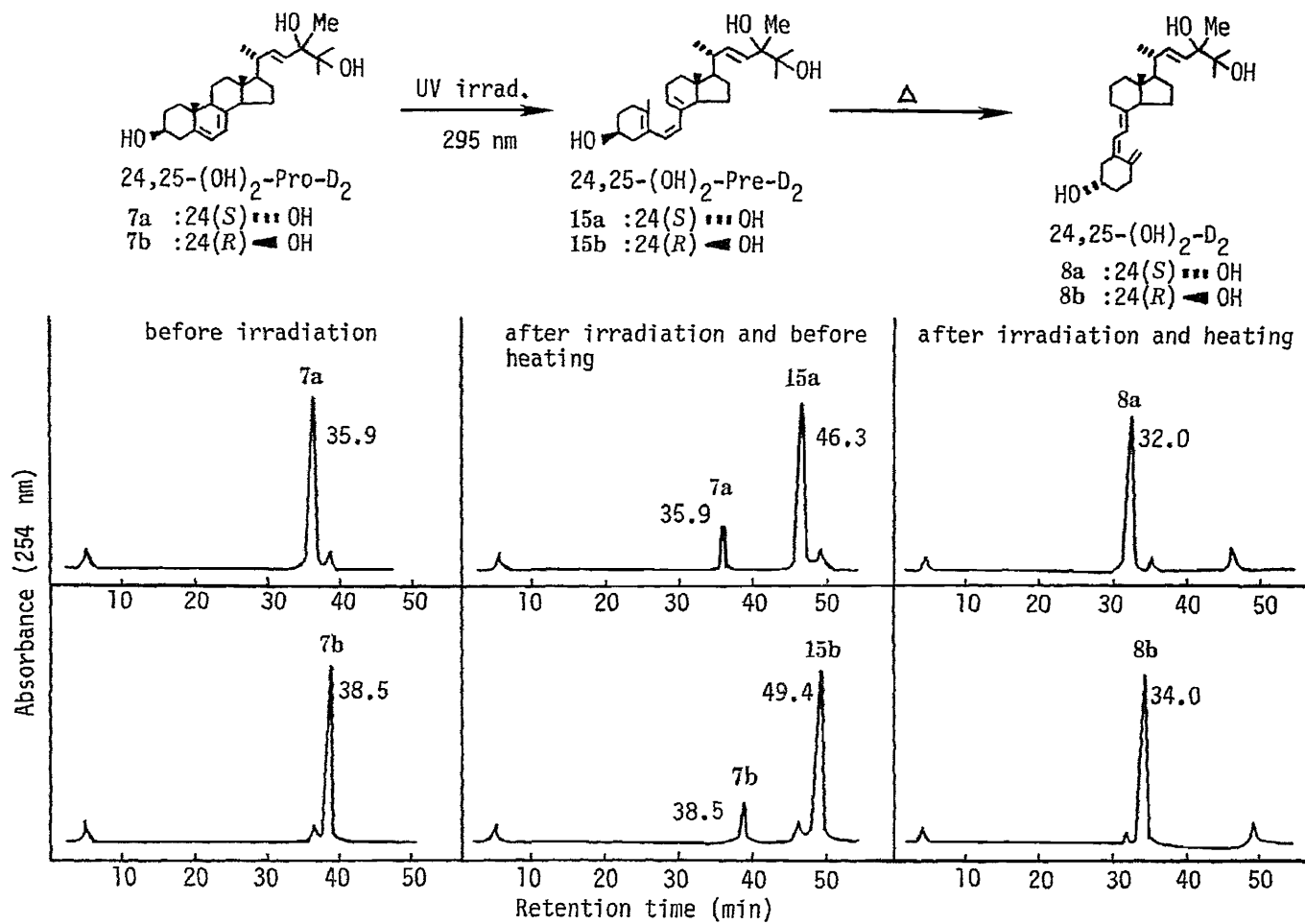


Fig. 2. HPLC Profiles of 7a and 7b before and after Photochemical and Thermal Isomerization

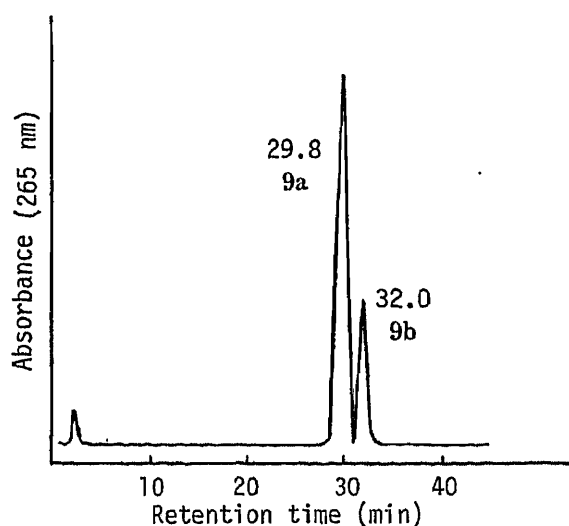


Fig. 3. HPLC Separation of the Diastereomeric Mixture of the 24-ol Provitamins (**9a** and **9b**)

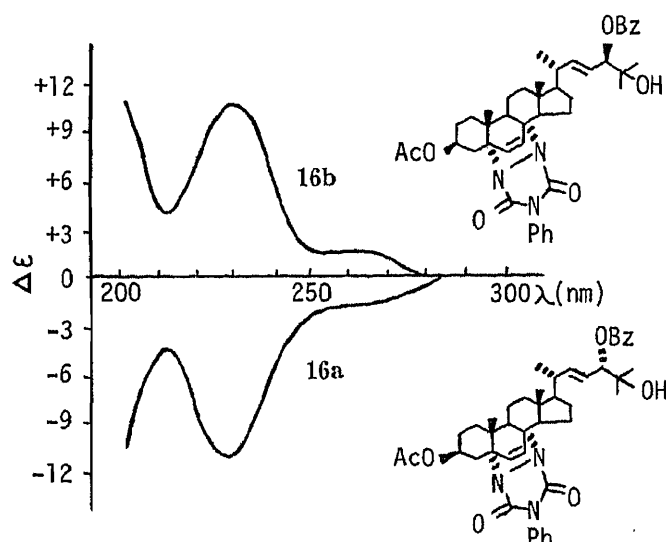


Fig. 4. CD Spectra of the 24-Benzoates (**16a** and **16b**)

with LiAlH_4 in THF afforded the two provitamins (**9a** and **9b**) in the ratio of 3:1. On the other hand, chemoselective reduction of the carbonyl group at the 24-position in **5** with lithium tri-*sec*-butylborohydride (L-selectride) in THF at -78°C followed by deprotection of the triazoline ring with LiAlH_4 gave **9a** and **9b** in the ratio of 6:1; these products were separated by HPLC on a Zorbax SIL column with 5.5% isopropanol in *n*-hexane as a mobile phase, as shown in Fig. 3. The absolute configurations at the 24-position of **9a** and **9b** were assigned as 24*S* and 24*R*, respectively, on the basis of the following considerations.

Since the 24*S*-isomer of 24,25-(OH)₂-pro-D₂ (**7a**) was eluted faster than the 24*R*-isomer (**7b**) on HPLC, as shown in Fig. 1, we considered that the faster and later peaks observed in Fig. 3 might also be due to the 24*S*- and 24*R*-isomers of the provitamin forms (**9a** and **9b**), respectively. The faster elution of the 24*S*-isomers (**7a** and **9a**) than the respective 24*R*-isomers (**7b** and **9b**) is in good agreement with the results on the analogous epimers of 24-hydroxyderivatives of the vitamin D₃ series reported by Sai *et al.*²⁶⁾ The provitamin D forms (**9a** and **9b**) were converted into the respective benzoates (**16a** and **16b**), and their circular dichroism (CD) spectra were measured. As shown in Fig. 4, a strongly negative Cotton curve in **16a** and a positive one in **16b** were observed. Therefore, the prediction of the "exciton chirality method" developed by Gonnella *et al.*²⁷⁾ is that **9a** and **9b** have 24*S* and 24*R*

configurations, respectively.

As mentioned above, the reduction of **5** with the two hydride reagents resulted in the preferential formation of the 24*S*-ol (**9a**) rather than the 24*R*-ol (**9b**). Sai *et al.*²⁶⁾ have also reported that the reduction of the Δ^{22} -24-one system in the vitamin D₃ series with sodium borohydride gave the (24*S*)-24-alcohol as the major product. The preferential formation of **9a** over **9b** can be explained as follows. The most stable conformation for the enone (**5**) may be that shown in Chart 2, in which the 20-hydrogen is *syn* to the *s-cis* enone system involving hydrogen bonding with the 25-hydroxyl group. Hydride ion would attack the carbonyl group preferentially from the *re*-face due to the presence of the more bulky steroidal skeleton than the methyl group in **5**. When we used L-selectride as a bulky hydride agent, stereoselectivity in the reduction of the enone system increased, as described above. Corey *et al.*²⁸⁾ reported the same effect on the chirality at the α -position in hydride reduction of the α,β -unsaturated enone system.

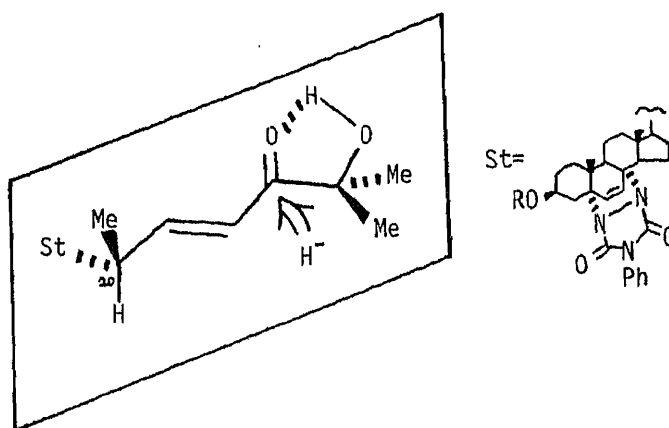


Chart 2. Presumed Mechanism of the Reduction of **5**

As in the syntheses of **8a** and **8b**, the provitamins (**9a** and **9b**) were converted into the respective vitamin forms (**10a** and **10b**) upon UV irradiation followed by thermal isomerization.

Finally, we also synthesized Δ^{22} -25-OH-24-oxo-D₃ (**12**) and 22,24,25-(OH)₃-D₃ (**14a** and **14b**). The enone (**5**) was heated at 120 °C in ethylene glycol in the presence of anhydrous K₂CO₃ to afford Δ^{22} -25-OH-24-oxo-pro-D₃ (**11**) as a result of retro-1,4-cycloaddition. On the other hand, reduction of each of the two separated hydroxyketones (**4a** and **4b**) with LiAlH₄ in THF afforded the respective 22,24,25-(OH)₃-pro-D₃ (**13a** and **13b**). The compounds were characterized spectrally except for their absolute configurations at the 22- and 24-positions. The provitamin D forms (**11**, **13a** and **13b**) thus obtained were similarly converted into the respective vitamin D forms (**12**, **14a** and **14b**) upon UV irradiation followed by thermal isomerization.

Experimental

All melting points were measured on a micro hot-stage apparatus (Yanagimoto) and are uncorrected. ¹H-NMR spectra were obtained on a Varian XL-200 spectrometer in CDCl₃ with tetramethylsilane as an internal standard. Mass spectra (MS) were recorded on a JEOL LMS-01SG or a Hitachi M-80 spectrometer. UV spectra were obtained on a Hitachi 323 spectrophotometer in ethanol and infrared (IR) spectra were recorded on a Hitachi IR-215 spectrometer in CHCl₃. CD spectra were obtained on a JASCO J500C spectropolarimeter in ethanol. Preparative TLC was carried out on precoated plates of silica gel (Kieselgel 60F₂₅₄, 2 or 0.5 mm thickness, Merck). HPLC was performed on a Shimadzu LC-3A or LC-4A high-performance liquid chromatograph equipped with a Shimadzu SPD 2AS detector (set at 265 nm, 0.005 absorbance unit full scale) or a Shimadzu UVD-2 (set at 254 nm, 0.001 absorbance

unit full scale) and a Zorbax SIL column (4.6 i.d. \times 250 mm or 6.2 i.d. \times 250 mm, DuPont) with 2.5 or 5.5% isopropanol in *n*-hexane as a mobile phase. The following abbreviations are used: s=singlet, d=doublet, t=triplet, q=quartet, m=multiplet, br=broad, THF=tetrahydrofuran, DHP=dihydropyran, LiAlH₄=lithium aluminum hydride.

3 β -Acetoxy-22,25-dihydroxy-5 α ,8 α -(3,5-dioxo-4-phenyl-1,2,4-triazolidino)cholesta-6-en-24-one (4a and 4b)—A solution of *n*-butyllithium (0.3 ml of 15% solution in *n*-hexane) was added to a cooled (-78°C) solution of diisopropylamine (75 mg, 0.7 mmol) in dry THF (3 ml) with stirring. A solution of 3-methyl-3-(tetrahydropyran-2-yloxy)butan-2-one²⁵⁾ (68 mg, 0.67 mmol) in dry THF (2 ml) was then added dropwise at -78°C over 15 min. The mixture was stirred at the same temperature for 1 h and then a solution of the 20-aldehyde (3)²⁴⁾ (200 mg, 0.36 mmol) in dry THF (4 ml) was added. After being stirred at -78°C for 2 h, the reaction mixture was brought back to room temperature. Diethyl ether (Et₂O) and water were added and the whole was vigorously shaken, then allowed to stand at room temperature. The separated organic layer was washed with brine, dried (Na₂SO₄) and evaporated. The resulting residue was dissolved in THF (10 ml) containing 1.5 N HCl (2 ml) and allowed to stand at room temperature for 3 h. Et₂O was added, and the solution was washed with 5% Na₂CO₃ solution and brine, dried (Na₂SO₄), and evaporated to give crude 4, which was subjected to preparative TLC (developing solvent: Et₂O-acetone, 97:3). The band of *R*_f 0.32 was scraped off and extracted with CHCl₃-MeOH. Removal of the solvent under reduced pressure gave the less polar hydroxyketone (4a) as colorless crystals (42 mg, 18%); mp 143–145.5 $^\circ\text{C}$ (Et₂O-*n*-hexane). High-resolution MS *m/z*: Calcd for C₂₇H₄₀O₃ (M⁺ - PhC₂N₃O₂ - CH₃COOH): 412.2974. Found: 412.2970. ¹H-NMR δ : 0.85 (3H, s, 13-Me), 1.00 (3H, s, 10-Me), 1.00 (3H, d, *J*=6 Hz, 20-Me), 1.38 (6H, s, 25-Me₂), 2.03 (3H, s, 3-OAc), 4.22 (1H, m, 22-H), 5.48 (1H, m, 3 α -H), 6.30, 6.46 (each 1H, d, *J*=8 Hz, 6- and 7-H), 7.44 (5H, m, Ar).

The band of *R*_f 0.19 on preparative TLC was scraped off and extracted with CHCl₃-MeOH to give the more polar hydroxyketone (4b) (49 mg, 21%); mp 153–154 $^\circ\text{C}$ (Et₂O-*n*-hexane) as colorless crystals. High-resolution MS *m/z*: Calcd for C₂₇H₄₀O₃ (M⁺ - PhC₂N₃O₂ - CH₃COOH): 412.2975. Found: 412.2974. ¹H-NMR δ : 0.82 (3H, s, 13-Me), 0.99 (3H, d, *J*=6 Hz, 20-Me), 1.00 (3H, s, 10-Me), 1.38 (6H, s, 25-Me₂), 2.03 (3H, s, 3-OAc), 2.50 (1H, dd, *J*=17, 2.5 Hz, 23-H), 2.92 (1H, dd, *J*=17, 9 Hz, 23-H), 4.27 (1H, br d, *J*=9.5 Hz, 22-H), 5.48 (1H, m, 3-H), 6.28, 6.46 (each 1H, d, *J*=8 Hz, 6- and 7-H), 7.42 (5H, m, Ar).

(22E)-3 β -Acetoxy-25-hydroxy-5 α ,8 α -(3,5-dioxo-4-phenyl-1,2,4-triazolidino)cholesta-6,22-dien-24-one (5)—A mixture of the hydroxyketones (4a and 4b) (100 mg, 0.15 mmol) was dissolved in benzene and a small amount of *p*-toluenesulfonic acid was added. This mixture was stirred at room temperature for 2 h, and solid K₂CO₃ was added for neutralization. The mixture was extracted with benzene and the extract was dried (Na₂SO₄). Removal of the solvent gave the enone (5) as a colorless glass (90 mg, 90%). High-resolution MS *m/z*: Calcd for C₂₇H₃₈O₂ (M⁺ - PhC₂N₃O₂ - CH₃COOH): 394.2869. Found: 394.2860. IR ν_{max} cm⁻¹: 3400, 1750, 1730, 1700. ¹H-NMR δ : 0.83 (3H, s, 13-Me), 0.98 (3H, s, 10-Me), 1.12 (3H, d, *J*=6 Hz, 20-Me), 1.38 (6H, s, 25-Me₂), 2.02 (3H, s, 3-OAc), 3.24 (1H, m, 9-H), 5.45 (1H, m, 3 α -H), 6.25, 6.42 (each 1H, d, *J*=8 Hz, 6- and 7-H), 6.36 (1H, d, *J*=15 Hz, 23-H), 7.03 (1H, dd, *J*=15, 8 Hz, 22-H), 7.42 (5H, m, Ar).

(22E)-3 β ,24,25-Trihydroxy-5 α ,8 α -(3,5-dioxo-4-phenyl-1,2,4-triazolidino)ergosta-6,22-diene (6)—A solution of methylolithium (0.6 mmol/ml) in Et₂O (2 ml) was added with stirring to a solution of the enone (5) (100 mg, 0.16 mmol) in THF (5 ml) at 0 $^\circ\text{C}$ under argon. The solution was brought back to room temperature, stirred for 0.5 h and then treated with 5% HCl solution. The reaction mixture was extracted with ethyl acetate, and the extract was dried (Na₂SO₄) and evaporated. The crude product was purified by preparative TLC (developing solvent: CH₂Cl₂-MeOH=9:1) to give the 24,25-glycol (6) (57 mg, 60%) as a colorless glass. High-resolution MS *m/z*: Calcd for C₂₈H₄₄O₃ (M⁺ - PhC₂N₃O₂): 428.3287. Found: 428.3229. IR ν_{max} cm⁻¹: 3500, 1730, 1700. ¹H-NMR δ : 0.84 (3H, s, 13-Me), 0.99 (3H, s, 10-Me), 1.07 (3H, d, *J*=6 Hz, 20-Me), 1.20 (6H, s, 25-Me₂), 1.28 (3H, s, 24-Me), 4.48 (1H, m, 3 α -H), 5.60 (2H, m, 22- and 23-H), 6.26, 6.42 (each 1H, d, *J*=8 Hz, 6- and 7-H), 7.46 (5H, m, Ar).

(22E)-3 β ,24,25-Trihydroxyergosta-5,7,22-triene (7a and 7b)—The 24,25-glycol (6) (20 mg, 0.03 mmol) in dry THF (5 ml) was treated with LiAlH₄ (21 mg, 0.56 mmol) under reflux for 3 h. After cooling, the excess reagent was destroyed by adding a few drops of water. The mixture was extracted with ethyl acetate, dried (Na₂SO₄) and evaporated. The crude product was purified by HPLC on a Zorbax SIL column (4.6 i.d. \times 250 mm) with 2.5% isopropanol in *n*-hexane as a mobile phase at a flow rate of 2.0 ml/min to give (24*S*)-24,25-(OH)₂-pro-D₂ (7a) (4.2 mg, 33%) as a colorless glass and (24*R*)-24,25-(OH)₂-pro-D₂ (7b) (4.3 mg, 34%) as a colorless glass.

7a: High-resolution MS *m/z*: Calcd for C₂₈H₄₄O₃: 428.3289. Found: 428.3271. UV $\lambda_{\text{max}}^{\text{EtOH}}$ nm: 264, 272, 281, 292. IR ν_{max} cm⁻¹: 3500, 1600. ¹H-NMR δ : 0.64 (3H, s, 13-Me), 0.96 (3H, s, 10-Me), 1.07 (3H, d, *J*=6 Hz, 20-Me), 3.66 (1H, m, 3 α -H), 5.42 (1H, m, 6- or 7-H), 5.60 (3H, m, 22,23-H and 6- or 7-H).

7b: High-resolution MS *m/z*: Calcd for C₂₈H₄₄O₃: 428.3289. Found: 428.3273. UV $\lambda_{\text{max}}^{\text{EtOH}}$ nm: 264, 272, 281, 292. IR ν_{max} cm⁻¹: 3500, 1600. ¹H-NMR δ : 0.64 (3H, s, 13-Me), 0.96 (3H, s, 10-Me), 1.07 (3H, d, *J*=6 Hz, 20-Me), 3.67 (1H, m, 3 α -H), 5.42 (1H, m, 6- or 7-H), 5.60 (3H, m, 22,23-H and 6- or 7-H).

(24*S*)-24,25-Dihydroxyvitamin D₂ (8a)—A solution (4 ml) of (24*S*)-24,25-(OH)₂-pro-D₂ (7a) in ethanol (0.5 mg/ml) was placed in a quartz cell (10 \times 10 \times 40 mm) in a spectroirradiator and irradiated with monochromatic light at 295 nm. The irradiated solution was refluxed for 2 h and the solvent was evaporated off. The crude product was purified by HPLC under the same conditions as above to give (24*S*)-24,25-(OH)₂-D₂ (8a) (0.2 mg, 10%) as a

colorless glass: High-resolution MS m/z : Calcd for $C_{28}H_{44}O_3$: 428.3288. Found: 428.3307. UV $\lambda_{\max}^{\text{EtOH}}$ nm: 265; $\lambda_{\min}^{\text{EtOH}}$ nm: 228. $^1\text{H-NMR}$ δ : 0.50 (3H, s, 13-Me), 0.98 (3H, d, $J=6$ Hz, 20-Me), 1.14, 1.16, 1.20 (each 3H, s, 24-Me and 25-Me₂), 3.88 (1H, m, 3 α -H), 4.76, 4.99 (each 1H, br s, 19-H₂), 5.50 (2H, m, 22- and 23-H), 5.97, 6.20 (each 1H, d, $J=11$ Hz, 6- and 7-H).

(24R)-24,25-Dihydroxyvitamin D₂ (8b)—As described for the conversion of 7a to 8a, (24R)-24,25-(OH)₂-pro-D₂ (7b) (2.0 mg, 0.005 mmol) was converted into (24R)-24,25-(OH)₂-D₂ (8b) (0.2 mg, 10%) as a colorless glass: High-resolution MS m/z : Calcd for $C_{28}H_{44}O_3$: 428.3287. Found: 428.3271. UV $\lambda_{\max}^{\text{EtOH}}$ nm: 265; $\lambda_{\min}^{\text{EtOH}}$ nm: 228. $^1\text{H-NMR}$ δ : 4.84, 5.08 (each 1H, br s, 19-H₂), 5.64 (2H, m, 22- and 23-H).

(22E)-3 β ,24,25-Trihydroxycholesta-5,7,22-trienes (9a and 9b) Reduction with LiAlH₄—The enone (5) (60 mg, 0.1 mmol) in dry THF was treated with LiAlH₄ (70 mg, 1.8 mmol) under reflux for 3 h. After cooling, the excess reagent was destroyed by adding a few drops of water. The mixture was extracted with ethyl acetate, and the extract was dried (Na₂SO₄) and evaporated. The crude product was purified by HPLC on a Zorbax SIL column (4.6 i.d. \times 250 mm) with 5.5% isopropanol in *n*-hexane as a mobile phase at a flow rate of 1.0 ml/min to give (24S)- Δ^{22} -24,25-(OH)₂-pro-D₃ (9a) (18.5 mg, 45%) and (24R)- Δ^{22} -24,25-(OH)₂-pro-D₃ (9b) (7 mg, 17%) as colorless crystals.

9a: mp 203–204 °C (MeOH-*n*-hexane). High-resolution MS m/z : Calcd for $C_{27}H_{42}O_3$: 414.3131. Found: 414.3112. UV $\lambda_{\max}^{\text{EtOH}}$ nm: 292, 280, 272, 262. $^1\text{H-NMR}$ δ : 0.64 (3H, s, 13-Me), 0.94 (3H, s, 10-Me), 1.06 (3H, d, $J=6$ Hz, 20-Me), 1.13 and 1.18 (each 3H, s, 25-Me₂), 3.62 (1H, m, 3 α -H), 3.82 (1H, d, $J=7$ Hz, 24-H), 5.42 (2H, m, 22- or 23- and 6- or 7-H), 5.62 (2H, m, 22- or 23- and 6- or 7-H).

9b: mp 206–207 °C (MeOH-*n*-hexane). High-resolution MS m/z : Calcd for $C_{27}H_{42}O_3$: 414.3132. Found: 414.3111. UV $\lambda_{\max}^{\text{EtOH}}$ nm: 292, 280, 272, 262. $^1\text{H-NMR}$ δ : 0.64 (3H, s, 13-Me), 0.95 (3H, s, 10-Me), 1.08 (3H, d, $J=6$ Hz, 20-Me), 1.16 and 1.20 (each 3H, s, 25-Me₂), 3.64 (1H, m, 3 α -H), 3.86 (1H, d, $J=7$ Hz, 24-H), 5.42 (2H, m, 22- or 23- and 6- or 7-H), 5.60 (2H, m, 22- or 23- and 6- or 7-H).

(22E)-3 β ,24,25-Trihydroxycholesta-5,7,22-trienes (9a and 9b). Reduction with L-Selectride and LiAlH₄—The enone (5) (15 mg, 0.024 mmol) was dissolved in dry THF (2 ml) and 0.03 ml (0.03 mmol) of 1.0 M L-selectride solution in THF was slowly added at –78 °C. The reaction mixture was kept at –78 °C for 2 h with stirring, then brought back to room temperature, and the hydrolyzed with 0.01 ml of 3 N NaOH solution. The organoborane was then decomposed with 0.01 ml of 30% H₂O₂. The reaction mixture was extracted with Et₂O, washed with water, dried (Na₂SO₄) and evaporated to give 3 β ,24,25-trihydroxy-5 α ,8 α -(3,5-dioxo-4-phenyl-1,2,4-triazolidino)cholesta-6,22-diene (17) (10 mg, 71%) as a colorless glass. $^1\text{H-NMR}$ δ : 0.83 (3H, s, 13-Me), 0.98 (3H, s, 10-Me), 1.06 (3H, d, $J=6$ Hz, 20-Me), 1.13 and 1.20 (each 3H, s, 25-Me₂), 3.82 (6/7H, d, $J=7$ Hz, 24-H), 3.86 (1/7H, d, $J=7$ Hz, 24-H), 4.46 (1H, m, 3-H), 5.46 (1H, dd, $J=15, 7$ Hz, 23-H), 5.65 (1H, dd, $J=15, 8$ Hz, 22-H), 6.28 and 6.44 (each 1H, d, $J=8$ Hz, 6- and 7-H), 7.40 (5H, m, Ar).

This triol (17) (5 mg, 0.008 mmol) in dry THF (5 ml) was treated with LiAlH₄ (9.3 mg, 0.24 mmol) under reflux for 3 h. The crude product was purified by HPLC using a Zorbax SIL column (4.6 i.d. \times 250 mm) with 5.5% isopropanol in *n*-hexane as a mobile phase at a flow rate of 1.0 ml/min to give 9a (1.9 mg, 57%) and 9b (0.3 mg, 9%).

3 β -Acetoxy-24-benzoyloxy-25-hydroxy-5 α ,8 α -(3,5-dioxo-4-phenyl-1,2,4-triazolidino)cholesta-6,22-dienes (16a and 16b)—Methanol (1 ml) and NaBH₄ (1.7 mg, 0.045 mmol) were added to a solution of the enone (5) (15 mg, 0.024 mmol) in dry THF (1 ml). The mixture was kept at room temperature for 2 h with stirring, then extracted with ethyl acetate. The extract was evaporated to give a residue, which was dissolved in CHCl₃ (2 ml). Benzoyl chloride (0.03 ml) was added, and the resulting reaction mixture was stirred in the presence of *N,N*-diisopropyl ethylamine at room temperature for 3 h. The usual work-up (CHCl₃ extraction) and purification by HPLC on a Zorbax SIL column (4.6 i.d. \times 250 mm) with 8% isopropanol in *n*-hexane as a mobile phase at a flow rate of 0.4 ml/min gave the 24S-benzoate (16a) (4 mg, 24%) as a colorless glass and the 24R-benzoate (16b) (3.8 mg, 22%) as a colorless glass.

16a: $^1\text{H-NMR}$ δ : 2.04 (3H, s, 3-OAc), 5.32 (1H, d, $J=8$ Hz, 24-H), 5.50 (2H, m, 22- or 23-H and 3 α -H), 5.76 (1H, m, 22- or 23-H), 6.26 and 6.42 (2H, d, $J=8$ Hz, 6- and 7-H), 7.48 (8H, m, Ar), 8.10 (2H, d, $J=8$ Hz, Ar).

16b: $^1\text{H-NMR}$ δ : 0.82 (3H, s, 13-Me), 1.00 (3H, s, 10-Me), 1.06 (3H, d, $J=6$ Hz, 20-Me), 1.28 (6H, s, 25-Me₂), 2.02 (3H, s, 3-OAc), 5.32 (1H, d, $J=8$ Hz, 24-H), 5.50 (2H, m, 22- or 23-H and 3 α -H), 5.76 (1H, m, 22- or 23-H), 6.28 and 6.44 (each 1H, d, $J=8$ Hz, 6- and 7-H), 7.48 (8H, m, Ar), 8.10 (2H, d, $J=8$ Hz, Ar).

Upon reduction with LiAlH₄, the benzoates (16a and 16b) thus isolated were unambiguously converted into the respective alcohols (9a and 9b), which were identical with the respective alcohols prepared directly by reduction of the enone (5) with LiAlH₄.

(22E)-24,25-Dihydroxy-22-dehydrovitamin D₃ (10a and 10b)—In the same manner as described for the synthesis of 8, (24S)- Δ^{22} -24,25-(OH)₂-pro-D₃ (9a) and (24R)- Δ^{22} -24,25-(OH)₂-pro-D₃ (9b) (each 4 mg, 0.01 mmol) were converted into (24S)- Δ^{22} -25-(OH)₂-D₃ (10a) as a colorless glass (0.6 mg, 15%) and (24R)- Δ^{22} -(24R)-24,25-(OH)₂-D₃ (10b) as a colorless glass (0.6 mg, 15%), respectively.

10a: High-resolution MS m/z : Calcd for $C_{27}H_{42}O_3$: 414.3131. Found: 414.3125. UV $\lambda_{\max}^{\text{EtOH}}$ nm: 265; $\lambda_{\min}^{\text{EtOH}}$ nm: 228. $^1\text{H-NMR}$ δ : 0.56 (3H, s, 13-Me), 1.04 (3H, d, $J=6$ Hz, 20-Me), 1.16 and 1.20 (each 3H, s, 25-Me₂), 3.86 (1H, d, $J=7$ Hz, 24-H), 3.96 (1H, m, 3 α -H), 4.84 and 5.07 (each 1H, br s, 19-H₂), 5.44 (1H, dd, $J=15, 7$ Hz, 23-H), 5.64 (1H, dd, $J=15, 8$ Hz, 22-H), 6.04 and 6.26 (each 1H, d, $J=11$ Hz, 6- and 7-H).

10b: High-resolution MS m/z : Calcd for $C_{27}H_{42}O_3$: 414.3132. Found: 414.3132. UV $\lambda_{\max}^{\text{EtOH}}$ nm: 265; $\lambda_{\min}^{\text{EtOH}}$ nm:

228. $^1\text{H-NMR}$ δ : 0.56 (3H, s, 13-Me), 1.05 (3H, d, $J=6$ Hz, 20-Me), 1.16 and 1.20 (each 3H, s, 25-Me₂), 3.83 (1H, d, $J=7$ Hz, 24-H), 3.96 (1H, m, 3 α -H), 4.83 and 5.06 (each 1H, br s, 19-H₂), 5.42 (1H, dd, $J=15, 7$ Hz, 23-H), 5.60 (1H, dd, $J=15, 8$ Hz, 22-H), 6.05 and 6.25 (each 1H, d, $J=11$ Hz, 6- and 7-H).

(22*E*)-3 β ,25-Dihydroxycholesta-5,7,22-trien-24-one (11)—A mixture of the enone (5) (20 mg, 0.03 mmol), anhydrous K₂CO₃ and furan (2.8 g, 0.04 mmol) in ethylene glycol was heated at 120 °C for 5 h under N₂. The mixture was then extracted with ethyl acetate, and the extract was washed with 5% HCl, saturated aqueous Na₂CO₃ and brine, and dried (Na₂SO₄). After evaporation of the solvent, the crude product was purified by HPLC on a Zorbax SIL column (4.6 i.d. \times 250 mm) with 2.5% isopropanol in *n*-hexane as a mobile phase at a flow rate of 1.5 ml/min to give the Δ^{22} -25-OH-24-oxo-pro-D₃ (11) (7 mg, 54%) as a colorless glass. High-resolution MS m/z : Calcd for C₂₇H₄₀O₃: 412.2974. Found: 412.2969. UV $\lambda_{\text{max}}^{\text{EtOH}}$ nm: 292, 282, 272, 262. $^1\text{H-NMR}$ δ : 0.51 (3H, s, 13-Me), 0.93 (3H, s, 10-Me), 1.02 (3H, d, $J=6$ Hz, 20-Me), 1.38 and 1.40 (each 3H, s, 25-Me₂), 3.64 (1H, m, 3 α -H), 5.40 and 5.58 (each 1H, m, 6- and 7-H), 6.40 (1H, d, $J=15$ Hz, 23-H), 7.10 (1H, dd, $J=15, 9$ Hz, 22-H).

(22*E*)-25-Hydroxy-24-oxo-22-dehydrovitamin D₃ (12)—In the same manner as described for the synthesis of 8, Δ^{22} -25-OH-24-oxo-pro-D₃ (11) (0.5 mg, 0.001 mmol) was converted into Δ^{22} -25-OH-24-oxo-D₃ (12) (0.015 mg, 3%) as a colorless glass. High-resolution MS m/z : Calcd for C₂₇H₄₀O₃: 412.2976. Found: 412.2989. UV $\lambda_{\text{max}}^{\text{EtOH}}$ nm: 265; $\lambda_{\text{min}}^{\text{EtOH}}$ nm: 228.

3 β ,22,24,25-Tetrahydroxycholesta-5,7-diene (13a and 13b)—A solution of the hydroxyketone (4a) (40 mg, 0.06 mmol) in dry THF (10 ml) was treated with LiAlH₄ (70 mg, 1.8 mmol) under reflux for 3 h. After cooling, excess reagent was destroyed by adding a few drops of water. The mixture was extracted with ethyl acetate, and the extract was dried (Na₂SO₄) and evaporated. The crude product was purified by HPLC on a Zorbax SIL column (6.2 i.d. \times 250 mm) with 15% isopropanol in *n*-hexane as a mobile phase at a flow rate of 1.7 ml/min to give the 22,24,25-(OH)₃-pro-D₃ (13a) (18 mg, 70%) as a colorless glass. High-resolution MS m/z : Calcd for C₂₇H₄₄O₄: 432.3236. Found: 432.3234. UV $\lambda_{\text{max}}^{\text{EtOH}}$ nm: 292, 280, 272, 262. $^1\text{H-NMR}$ δ : 0.64 (3H, s, 13-Me), 0.94 (3H, s, 10-Me), 0.98 (3H, d, $J=6$ Hz, 20-Me), 1.18 and 1.21 (each 3H, s, 25-Me₂), 3.60 (2H, m, 3 α - and 22-H), 3.94 (1H, m, 24-H), 5.40 and 5.58 (each 1H, m, 6- and 7-H).

In the same manner as described for 13a, the hydroxyketone (4b) (40 mg, 0.06 mmol) was converted into 22,24,25-(OH)₃-pro-D₃ (13b) (18 mg, 70%) as a colorless glass. High-resolution MS m/z : Calcd for C₂₇H₄₄O₄: 432.3237. Found: 432.3230. UV $\lambda_{\text{max}}^{\text{EtOH}}$ nm: 292, 280, 272, 262. $^1\text{H-NMR}$ δ : 0.63 (3H, s, 13-Me), 0.94 (3H, s, 10-Me), 0.98 (3H, d, $J=6$ Hz, 20-Me), 1.16 and 1.20 (each 3H, s, 25-Me₂), 3.60 (2H, m, 3 α - and 22-H), 3.96 (1H, d-like, $J=7$ Hz, 24-H) 5.42 and 5.58 (each 1H, m, 6- and 7-H).

22,24,25-Trihydroxyvitamin D₃ (14a and 14b)—In the same manner as described for the synthesis of 8, 22,24,25-(OH)₃-pro-D₃ (13a) (4 mg, 0.01 mmol) was converted into 22,24,25-(OH)₃-D₃ (14a). The crude product was purified by HPLC on a Zorbax SIL column (4.6 i.d. \times 250 mm) with 5.5% isopropanol in *n*-hexane as a mobile phase at a flow rate of 1.7 ml/min to give 14a as a colorless glass. High-resolutions MS m/z : Calcd for C₂₇H₄₄O₄: 432.3237. Found: 432.3217. UV $\lambda_{\text{max}}^{\text{EtOH}}$ nm: 265; $\lambda_{\text{min}}^{\text{EtOH}}$ nm: 228. $^1\text{H-NMR}$ δ : 0.56 (3H, s, 13-Me), 0.97 (3H, d, $J=6$ Hz, 20-Me), 1.20 and 1.24 (each 3H, s, 25-Me₂), 3.60 (1H, m, 22- or 24-H), 4.00 (2H, m, 22- or 24-H and 3 α -H), 4.85 and 5.08 (each 1H, br s, 19-H₂), 6.07 and 6.27 (each 1H, d, $J=11$ Hz, 6- and 7-H).

Similarly, 13b (4 mg, 0.01 mmol) was converted into 14b as a colorless glass. High-resolution MS m/z : Calcd for C₂₇H₄₄O₄: 432.3236. Found: 432.3235. UV $\lambda_{\text{max}}^{\text{EtOH}}$ nm: 265; $\lambda_{\text{min}}^{\text{EtOH}}$ nm: 228. $^1\text{H-NMR}$ δ : 0.54 (3H, s, 13-Me), 0.98 (3H, d, $J=6$ Hz, 20-Me), 1.17 and 1.21 (each 3H, s, 25-Me₂), 3.73 (3H, m, 3 α -, 22- and 24-H), 4.84 and 5.06 (each 1H, br s, 19-H₂), 6.05 and 6.25 (each 1H, d, $J=11$ Hz, 6- and 7-H).

Acknowledgements The authors wish to thank Dr. Yehuda Mazur of the Weizmann Institute of Science, Israel, and Dr. Glenville Jones of Queen's University, Canada, for kind gifts of authentic samples of (24*S*)- and (24*R*)-24,25-(OH)₂-D₂ (8a and 8b) and valuable advice. The authors also wish to thank Dr. Makiko Sugiura and Dr. Kayoko Saiki of Kobe Women's College of Pharmacy for $^1\text{H-NMR}$ and MS measurements, and Dr. Yasuho Nishii and Dr. Isao Matsunaga of Chugai Pharmaceutical Co., Ltd., for their continuous encouragement and valuable advice.

References and Notes

- 1) A part of this work was presented in a preliminary report: K. Katsumi, T. Okano, T. Kobayashi, O. Miyata, T. Naito, and I. Ninomiya, *Chem. Pharm. Bull.*, **32**, 3744 (1984).
- 2) Vitamin D is used as a general name for vitamins D₂ and D₃.
- 3) H. F. DeLuca, *J. Lab. Clin. Med.*, **87**, 7 (1976).
- 4) J. K. Wichmann, H. F. DeLuca, H. K. Schnoes, R. L. Horst, R. M. Shepard, and N. A. Jorgensen, *Biochemistry*, **18**, 4775 (1979).
- 5) Y. Tanaka, H. F. DeLuca, H. K. Schnoes, N. Ikekawa, and T. Eguchi, *Proc. Natl. Acad. Sci. U.S.A.*, **78**, 4805 (1981).
- 6) J. K. Wichmann, H. K. Schnoes, and H. F. DeLuca, *Biochemistry*, **20**, 7385 (1981).

- 7) Y. Takasaki, N. Horiuchi, N. Takahashi, E. Abe, T. Shinki, and T. Suda, *Biochem. Biophys. Res. Commun.*, **95**, 177 (1980).
- 8) E. Meyer, G. S. Reddy, J. R. Kruse, G. Popjak, and A. W. Norman, *Biochem. Biophys. Res. Commun.*, **109**, 370 (1982).
- 9) E. Meyer, G. S. Reddy, R. A. S. Chandratna, W. H. Okamura, J. R. Kruse, G. Popjak, J. E. Bishop, and A. W. Norman, *Biochemistry*, **22**, 1798 (1983).
- 10) G. Jones, M. Kung, and K. Kano, *J. Biol. Chem.*, **258**, 12920 (1983).
- 11) N. Ohnuma, K. Bannai, H. Yamaguchi, Y. Hashimoto, and A. W. Norman, *Arch. Biochem. Biophys.*, **204**, 387 (1980).
- 12) R. L. Horst, P. M. Wovkulich, E. G. Baggiolini, M. R. Uskokovic, G. W. Engstrom, and J. L. Napoli, *Biochemistry*, **23**, 3937 (1984).
- 13) S. Yamada, M. Ohmori, H. Takayama, Y. Takasaki, and T. Suda, *J. Biol. Chem.*, **258**, 457 (1983).
- 14) E. Meyer, J. E. Bishop, R. A. S. Chandraratna, W. H. Okamura, J. R. Kruse, S. Popjak, N. Ohnuma, and A. W. Norman, *J. Biol. Chem.*, **258**, 13458 (1983).
- 15) Y. Tanaka, J. K. Wichmann, H. E. Paaren, H. K. Schnoes, and H. F. DeLuca, *Proc. Natl. Acad. Sci. U.S.A.*, **77**, 6411 (1980).
- 16) N. Ohnuma and A. W. Norman, *J. Biol. Chem.*, **257**, 8261 (1982).
- 17) Y. Takasaki, T. Suda, S. Yamada, M. Ohmori, and H. Takayama, *J. Biol. Chem.*, **257**, 3732 (1982).
- 18) D. S. Morris, D. H. Williams, and A. F. Morris, *J. Org. Chem.*, **46**, 3422 (1981).
- 19) N. Ikekawa, T. Eguchi, and Y. Hirano, *J. Chem. Soc., Chem. Commun.*, **1981**, 1157.
- 20) Y. Hirano, N. Ikekawa, Y. Tanaka, and H. F. DeLuca, *Chem. Pharm. Bull.*, **29**, 2254 (1981).
- 21) N. Ikekawa, Y. Hirano, M. Ishiguro, J. Oshida, T. Eguchi, and S. Miyasaka, *Chem. Pharm. Bull.*, **28**, 2852 (1980).
- 22) G. Jones, A. Rosenthal, D. Segev, Y. Mazur, F. Frolow, Y. Hafion, D. Rabinovich, and Z. Shakked, *Biochemistry*, **18**, 1094 (1979).
- 23) G. Jones, A. Rosenthal, D. Segev, Y. Mazur, F. Frolow, Y. Hafion, D. Rabinovich, and Z. Shakked, *Tetrahedron Lett.*, **1979**, 177.
- 24) D. H. R. Barton, T. Shioiri, and D. A. Widdowson, *J. Chem. Soc. C*, **1971**, 1968.
- 25) S. C. Eyley and D. H. Williams, *J. Chem. Soc., Perkin Trans. 1*, **1976**, 727.
- 26) H. Sai, S. Takatsuto, N. Ikekawa, Y. Tanaka, C. Smith, and H. F. DeLuca, *Chem. Pharm. Bull.*, **32**, 3866 (1984).
- 27) N. C. Gonnella, K. Nakanishi, V. S. Martin, and B. Sharpless, *J. Am. Chem. Soc.*, **104**, 3775 (1982).
- 28) E. J. Corey, S. M. Albonico, U. Koelliker, T. K. Schaaf, and R. K. Varma, *J. Am. Chem. Soc.*, **93**, 1491 (1971).

[Chem. Pharm. Bull.]
35(3) 980-985 (1987)

Chemical Transformation of Protoberberines. XII.¹⁾ A Novel Synthesis of Rhoeadine Alkaloids. An Alternative Synthesis of a Key Intermediate, Benzindenoazepine, for a Synthesis of (\pm)-*cis*-Alpinigenine and (\pm)-*cis*-Alpinine from Palmatine²⁾

MIYOJI HANAOKA,* MITSURU INOUE, NOBUYUKI KOBAYASHI,
and SHINGO YASUDA

Faculty of Pharmaceutical Sciences, Kanazawa University,
Takara-machi, Kanazawa 920, Japan

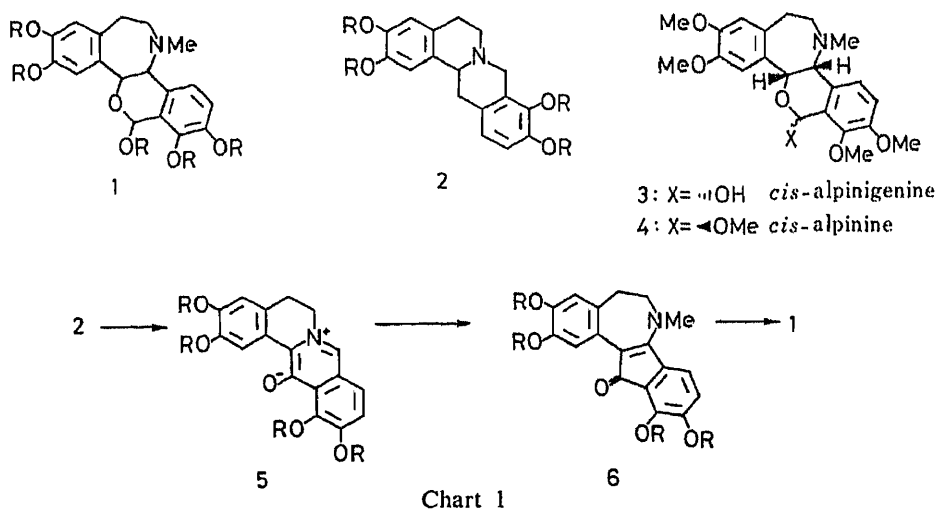
(Received August 5, 1986)

A formal synthesis of (\pm)-*cis*-alpinigenine (**3**) and (\pm)-*cis*-alpinine (**4**) was achieved by conversion of palmatine (**7**) into the key intermediate, benzindenoazepine (**16**), via the ring D-inverted 2,3,11,12-tetraoxygenated phenolbetaine (**14**) and the 8,14-cycloberbine (**15**) through photooxygenation, photochemical valence isomerization, and regioselective C-N bond cleavage of **15** as crucial reactions.

Keywords—rhoeadine alkaloid; protoberberine alkaloid; *cis*-alpinigenine; *cis*-alpinine; palmatine; benzindenoazepine framework; 8,14-cycloberbine; photooxygenation; photochemical isomerization; regioselective C-N bond cleavage

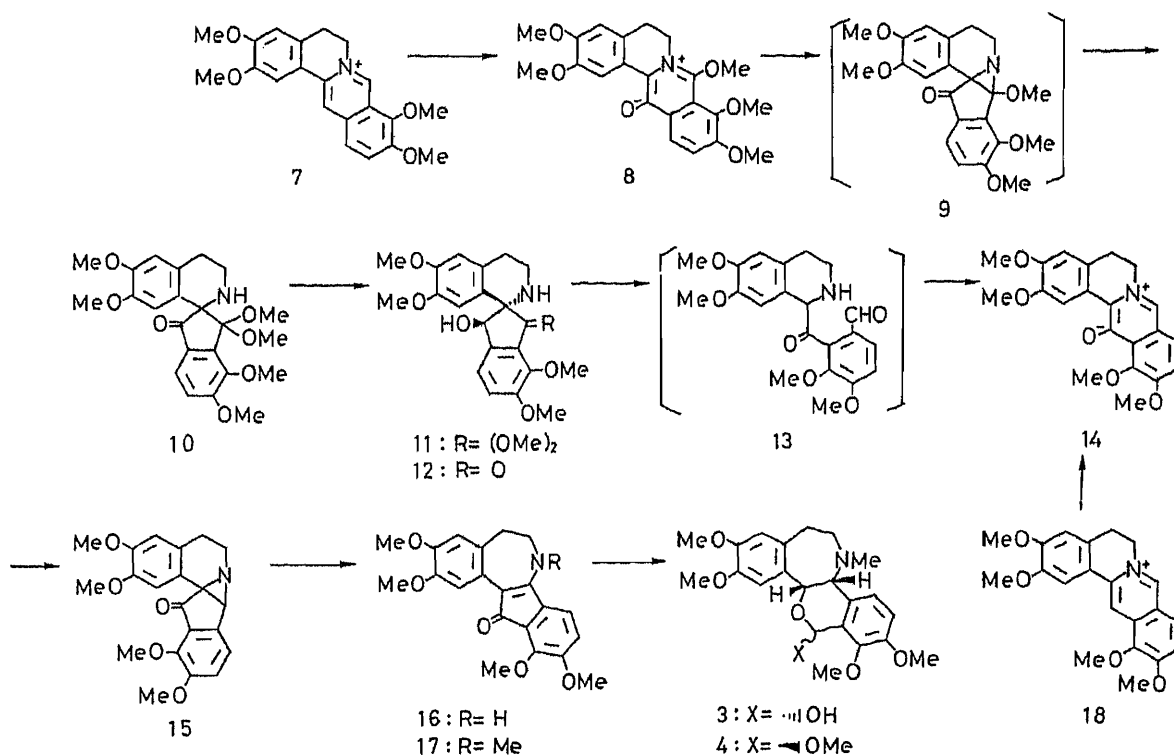
Rhoeadine alkaloids (**1**)³⁾ possess a unique framework having a benzazepine system fused with a six-membered hemiacetal or acetal. These alkaloids have been shown to be biosynthesized from the corresponding protoberberines (**2**).⁴⁻⁶⁾ Among several successful syntheses,⁷⁻¹²⁾ those through benzindenoazepines^{9,10,12)} such as **6** (R = Me)¹⁰⁾ are of great interest from the viewpoints of both biosynthesis and chemical transformation.

On the basis of biogenetic considerations, we planned a novel synthetic route to rhoeadine alkaloids (Chart 1). The protoberberine (**2**) is transformed to the ring D-inverted protoberberine (**5**) and then to the benzindenoazepine (**6**), which has already been converted to rhoeadine alkaloids (**1**).



In the previous papers, we have demonstrated a convenient transformation of a natural 2,3,9,10-tetraoxygenated protoberberine (**2**) into a ring D-inverted unnatural 2,3,11,12-tetraoxygenated protoberberine (**5**) *via* a spirobenzylisoquinoline,¹³⁾ as well as an efficient synthesis of a benzindenoazepine system from a protoberberinephenolbetaine *via* an 8,14-cycloberbine.^{2,14)} Now we describe a novel and convenient synthesis of the key intermediate, benzindenoazepine (**6**), for total synthesis of (\pm)-*cis*-alpinigenine (**3**)¹⁵⁾ and (\pm)-*cis*-alpinine (**4**)¹⁵⁾ from a protoberberine alkaloid, palmatine (**7**) according to our novel pathway mentioned above.

Irradiation of palmatine (**7**) in methanol in the presence of sodium methoxide and rose bengal with a halogen lamp in a stream of oxygen at 0 °C followed by alumina column chromatography afforded 8-methoxypalmatinephenolbetaine (**8**)¹⁶⁾ in 60% yield. The structure of **8** was well established by the appearance of a low-field signal due to H-1 at δ 9.26 ppm as well as five methoxy signals in the proton nuclear magnetic resonance (¹H-NMR) spectrum. Further irradiation¹⁷⁾ of **8** in methanol with a mercury lamp in a stream of nitrogen effected valence isomerization to give the presumed intermediate (**9**), which immediately decomposed to afford the spirobenzylisoquinoline (**10**) in 81% yield through solvolysis in methanol. The product showed a carbonyl band at 1710 cm⁻¹ in the infrared (IR) spectrum and a high-field signal due to H-1 at δ 6.28 ppm (diagnostic of a spirobenzylisoquinoline skeleton)¹⁸⁾ and six methoxy signals in the ¹H-NMR spectrum. Sodium borohydride reduction of **10** afforded stereoselectively¹⁷⁾ the hydroxy-acetal (**11**) in a quantitative yield. The *trans* relationship between the nitrogen and the hydroxy group in **11** was supported by the H-13 signal at δ 4.92 ppm in the ¹H-NMR spectrum.¹⁷⁾ Deacetalization of **11** with 10% hydrochloric acid afforded quantitatively the hydroxy-ketone (**12**).



On exposure to 10% sodium hydroxide in ethanol,¹³⁾ **12** underwent retro-aldol reaction, recyclization, and dehydration successively to afford the expected ring D-inverted protoberberine (**14**) *via* the keto-aldehyde (**13**) in a quantitative yield. The structure of **14** was

supported by the chemical shift of an AB-quartet (7.38 and 7.25 ppm) due to the protons on ring D in comparison with that (8.52 and 7.43 ppm) of **8**.

The structure of **14** was fully confirmed by an alternative and conventional synthesis. The protoberberine (**18**)¹⁹⁾ was synthesized starting from 3,4-dimethoxyphenethylamine and 2,3-dimethoxyphenylacetic acid by a modification of the reported method.²⁰⁾ Reduction of **18** with lithium aluminum hydride (LAH) in tetrahydrofuran (THF) followed by oxidation with *m*-chloroperbenzoic acid (*m*-CPBA) in dichloromethane afforded the betaine (**14**) in 63% yield. The product was identical with that obtained above.

Thus, we succeeded in the ring D inversion of palmatine (**7**) to the protoberberine (**14**), and therefore the next step is the transformation of **14** to the benzindenoazepine framework.

Irradiation¹⁷⁾ of **14** in methanol with a mercury lamp in a stream of nitrogen afforded the 8,14-cycloberberine (**15**) in 78% yield; this product showed a singlet due to the proton on the aziridine ring at δ 3.79 ppm in the ¹H-NMR spectrum. Treatment of **15** with *p*-toluenesulfonic acid (*p*-TsOH)¹⁴⁾ effected regioselective C₁₄-N bond cleavage to afford the benzindenoazepine (**16**) in 58% yield. The product showed a band due to a vinylogous amide at 1655 cm⁻¹ in the IR spectrum. On treatment with dimethyl sulfate in hexamethylphosphoric amide (HMPA) and benzene, **16** produced the *N*-methyl derivative (**17**) in 78% yield. The product was identical with an authentic sample¹⁰⁾ in IR and ¹H-NMR spectra and thin layer chromatographic behavior. Since **17** has already been converted to (\pm)-*cis*-alpinigenine (**3**) and (\pm)-*cis*-alpinine (**4**),¹⁰⁾ the present synthesis of **17** amounts to a formal synthesis of these alkaloids.

Thus, we have developed a novel synthesis of (\pm)-*cis*-alpinigenine and (\pm)-*cis*-alpinine and have provided a new general method for synthesis of rhoeadine alkaloids.

Experimental

Melting points were determined on a Yanagimoto micro melting point apparatus and are uncorrected. Organic extracts were dried over anhydrous Na₂SO₄ and concentrated *in vacuo*. Column chromatography was carried out with alumina (Aluminiumoxid 90, Aktivitätsstufe II—III, 70—230 mesh, Merck) and silica gel (Kieselgel 60, 70—230 mesh, Merck). Preparative thin-layer chromatography (pTLC) was performed on alumina (Aluminiumoxid GF₂₅₄, Typ 60/E, Merck). IR spectra were measured with a JASCO A-102 spectrometer, mass spectra (MS) with a Hitachi M-80 spectrometer, and ¹H-NMR spectra with a JEOL FX-100 spectrometer in CDCl₃ using tetramethylsilane as an internal standard, unless otherwise stated. Irradiation was carried out with a 100W high-pressure mercury or halogen lamp with a Pyrex filter (Riko Kagaku Co.).

5,6-Dihydro-2,3,8,9,10-pentamethoxydibenzo[*a,g*]quinolizinium-13-olate (8-Methoxypalmatinephenolbetaine) (8)
—Palmatinium chloride (**7**) (505 mg) and rose bengal (1% methanol solution, 0.1 ml) were dissolved in a solution of methanol (50 ml) containing sodium methoxide (prepared from Na, 100 mg), and the resulting solution was irradiated with a halogen lamp at 0°C for 20 min in a stream of oxygen. The reaction solution was adjusted to pH 7—8 with conc. HCl and concentrated at 30—35°C. Aqueous K₂CO₃ was added to the residue and the mixture was extracted with CH₂Cl₂. The CH₂Cl₂ layer was washed with sat. NaCl, dried, and concentrated. The residue was chromatographed on Al₂O₃ with CH₂Cl₂ and CH₂Cl₂-MeOH (99:1). The fraction eluted with CH₂Cl₂-MeOH was concentrated and the residue was washed with AcOEt to give the betaine (**8**) (310 mg, 60%) as an orange powder. MS *m/z* (%): 397 (M⁺, 53), 382 (100). High-resolution MS *m/z*: Calcd for C₂₂H₂₃NO₆: 397.1523. Found: 397.1511. ¹H-NMR δ : 9.26 (1H, s, C₁-H), 8.52, 7.43 (2H, AB-q, *J*=9.5 Hz, C₁₂- and C₁₁-H), 6.70 (1H, s, C₄-H), 4.66 (2H, t, *J*=5.5 Hz, C₆-H), 4.03 (6H, s, OCH₃ × 2), 4.00 (3H, s, OCH₃), 3.91 (6H, s, OCH₃ × 2), 3.01 (2H, t, *J*=5.5 Hz, C₅-H).

2,3,8,8,9,10-Hexamethoxynorochotensan-13-one (10)²¹⁾—A solution of the betaine (**8**) (309 mg) in MeOH (200 ml) was irradiated with an Hg lamp at 0°C for 1 h in a stream of nitrogen. The solvent was evaporated off and the residue was chromatographed on Al₂O₃ with CH₂Cl₂ to give the spirobenzylisoquinoline (**10**) (272 mg, 81%) as colorless needles, mp 168—169°C (MeOH). IR $\nu_{\text{max}}^{\text{CHCl}_3}$ cm⁻¹: 1710 (CO). MS *m/z* (%): 429 (M⁺, 91), 414 (77), 398 (62), 382 (100). ¹H-NMR δ : 7.63, 7.22 (2H, AB-q, *J*=8.5 Hz, C₁₂- and C₁₁-H), 6.60 (1H, s, C₄-H), 6.28 (1H, s, C₁-H), 3.99, 3.90, 3.84, 3.46, 3.33, 3.21 (each 3H, s, OCH₃ × 6). *Anal.* Calcd for C₂₃H₂₇NO₇: C, 64.32; H, 6.34, N, 3.26. Found: C, 64.12; H, 6.31; N, 3.34.

rel-(13R,14S)-2,3,8,8,9,10-Hexamethoxynorochotensan-13-ol (11)—Sodium borohydride (100 mg) was added portionwise to a stirred solution of the ketone (**10**) (134 mg) in MeOH (10 ml)-CHCl₃ (3 ml) under ice cooling, and the mixture was stirred at the same temperature for 2 h. The solvents were evaporated off and the residue was taken

up in CHCl_3 . The CHCl_3 layer was washed with sat. NaCl, dried, and concentrated. The residue was chromatographed on Al_2O_3 with CH_2Cl_2 to afford the alcohol (11) (131 mg, 98%) as colorless plates, mp 147–148°C (iso- Pr_2O). IR $\nu_{\text{max}}^{\text{CHCl}_3} \text{ cm}^{-1}$: 3550 (OH). MS m/z (%): 416 ($\text{M}^+ - 15$, 46), 399 (32), 368 (100). $^1\text{H-NMR}$ δ : 7.11 (1H, dd, $J = 8.5$, 1 Hz, $\text{C}_{12}\text{-H}$), 7.00 (1H, d, $J = 8.5$ Hz, $\text{C}_{11}\text{-H}$), 6.62 (1H, s, $\text{C}_4\text{-H}$), 6.13 (1H, s, $\text{C}_1\text{-H}$), 4.92 [1H, dd, $J = 10$, 1 Hz, $\text{C}_{13}\text{-H}$ (\rightarrow d, $J = 1$ Hz, by addition of D_2O)], 3.89, 3.86, 3.84, 3.36, 3.35, 3.20 (each 3H, s, $\text{OCH}_3 \times 6$). Anal. Calcd for $\text{C}_{23}\text{H}_{29}\text{NO}_7$: C, 64.02; H, 6.77; N, 3.25. Found: C, 63.84; H, 6.83; N, 3.30.

rel-(13R,14S)-13-Hydroxy-2,3,9,10-tetramethoxynorochotensan-8-one (12)—Hydrochloric acid (10%, 6 ml) was added to a solution of the acetal (11) (110 mg) in MeOH (6 ml) and the reaction mixture was heated under reflux for 1 h. After evaporation of the MeOH, the residue was made alkaline with aqueous K_2CO_3 and extracted with CH_2Cl_2 . The CH_2Cl_2 layer was washed with sat. NaCl, dried, and concentrated. The crude hydroxy-ketone (12) (98 mg, 100%) was recrystallized from iso- Pr_2O to give colorless plates, mp 127.5–129.5°C. IR $\nu_{\text{max}}^{\text{CHCl}_3} \text{ cm}^{-1}$: 3550 (OH), 1710 (CO). MS m/z (%): 385 (M^+ , 100), 326 (45), 192 (47). $^1\text{H-NMR}$ δ : 7.38 (1H, dd, $J = 8$, 0.7 Hz, $\text{C}_{12}\text{-H}$), 7.30 (1H, d, $J = 8$ Hz, $\text{C}_{11}\text{-H}$), 6.66 (1H, s, $\text{C}_4\text{-H}$), 5.96 (1H, s, $\text{C}_1\text{-H}$), 5.16 (1H, d, $J = 0.7$ Hz, $\text{C}_{13}\text{-H}$), 4.03, 3.94, 3.84, 3.47 (each 3H, s, $\text{OCH}_3 \times 4$). Anal. Calcd for $\text{C}_{21}\text{H}_{23}\text{NO}_6$: C, 65.44; H, 6.02; N, 3.63. Found: C, 65.41; H, 5.98; N, 3.52.

5,6-Dihydro-2,3,11,12-tetramethoxydibenzo[*a,g*]quinolizinium-13-olate (14)—1) A solution of the hydroxy-ketone (12) (116 mg) and 10% aqueous NaOH (2 ml) in EtOH (6 ml) was heated under reflux with stirring for 40 min. The EtOH was evaporated off and the residue was extracted with CH_2Cl_2 . The CH_2Cl_2 layer was washed with sat. NaCl, dried, and concentrated. The residue was chromatographed on Al_2O_3 with CH_2Cl_2 -MeOH (49:1) to afford the betaine (14) (110 mg, 100%) as yellow needles, mp 162–164°C (MeOH). MS m/z (%): 367 (M^+ , 85), 352 (100), 334 (33). High-resolution MS m/z : Calcd for $\text{C}_{21}\text{H}_{21}\text{NO}_5$: 367.1417. Found: 367.1413. $^1\text{H-NMR}$ δ : 9.15 (1H, s, $\text{C}_1\text{-H}$), 7.40 (1H, s, $\text{C}_8\text{-H}$), 7.38, 7.25 (2H, AB-q, $J = 8$ Hz, $\text{C}_9\text{-}$ and $\text{C}_{10}\text{-H}$), 6.64 (1H, s, $\text{C}_4\text{-H}$), 4.36 (2H, t, $J = 5.5$ Hz, $\text{C}_6\text{-H}$), 4.02, 3.97, 3.88, 3.47 (each 3H, s, $\text{OCH}_3 \times 4$), 2.30 (2H, t, $J = 5.5$ Hz, $\text{C}_5\text{-H}$).

2) The quaternary base (18) (2.216 g) was added portionwise to an ice-cooled suspension of LAH (1.0 g) in THF (50 ml), and the reaction mixture was stirred at room temperature for 3 h in a stream of nitrogen. Excess LAH was decomposed with water and inorganic precipitates were filtered off through a filter cell and washed with CH_2Cl_2 . The filtrate and washings were concentrated and the residue was chromatographed on Al_2O_3 with CH_2Cl_2 to afford the dihydro base (1.529 g). A solution of *m*-CPBA (1.32 g) in CH_2Cl_2 (20 ml) was added dropwise to a stirred solution of the above dihydro base in CH_2Cl_2 (50 ml) at -20°C for 15 min in a stream of nitrogen, and the mixture was stirred for a further 1 h at the same temperature. The reaction temperature was allowed to rise to 0°C , finely powdered Na_2SO_3 (2 g) was added to the reaction solution and the mixture was stirred vigorously at room temperature for 1 h. The inorganic precipitates were filtered off and the filtrate was concentrated to dryness. The residue was treated as described in 1) to afford the betaine (14) (1.064 g, 63%) which was identical with that obtained in 1).

2,3,11,12-Tetramethoxy-8,14-cycloberbin-13-one (15)—A solution of the betaine (14) (110 mg) in MeOH (150 ml) was irradiated with an Hg lamp at room temperature for 1 h in a stream of nitrogen. The solvent was evaporated off and the residue was chromatographed on SiO_2 with C_6H_6 -AcOEt (4:1) to afford the cycloberbine (15) (85.4 mg, 78%) as pale yellow prisms, mp 157.5–158.5°C (MeOH). IR $\nu_{\text{max}}^{\text{CHCl}_3} \text{ cm}^{-1}$: 1710 (CO). MS m/z : 367 (M^+). $^1\text{H-NMR}$ δ : 7.40 (1H, s, $\text{C}_1\text{-H}$), 7.17, 7.02 (2H, AB-q, $J = 8$ Hz, $\text{C}_9\text{-}$ and $\text{C}_{10}\text{-H}$), 6.67 (1H, s, $\text{C}_4\text{-H}$), 4.04, 3.91 (each 3H, s, $\text{OCH}_3 \times 2$), 3.87 (6H, s, $\text{OCH}_3 \times 2$), 3.79 (1H, s, $\text{C}_8\text{-H}$). Anal. Calcd for $\text{C}_{21}\text{H}_{21}\text{NO}_5$: C, 68.65; H, 5.76; N, 3.81. Found: C, 68.42; H, 5.77; N, 3.52.

5,6,7,13-Tetrahydro-2,3,11,12-tetramethoxybenz[*d*]indeno[1,2-*b*]azepin-13-one (16)²²⁾—A solution of the cycloberbine (15) (105.7 mg) and *p*-TsOH (71 mg) in anhyd. C_6H_6 (10 ml) was heated under reflux for 1.5 h with stirring. The C_6H_6 was evaporated off and the residue was taken up in CHCl_3 . The CHCl_3 layer was washed with aqueous K_2CO_3 , water, dried, and concentrated. The residue was chromatographed on pTLC (Al_2O_3 , CHCl_3) to afford the azepine (16) (61 mg, 58%) as red prisms, mp 234–237°C (MeOH). IR $\nu_{\text{max}}^{\text{CHCl}_3} \text{ cm}^{-1}$: 3425 (NH), 1655 (CO). MS m/z (%): 367 (M^+ , 100), 352 (45). $^1\text{H-NMR}$ δ : 8.06 (1H, s, $\text{C}_1\text{-H}$), 6.76, 6.68 (2H, AB-q, $J = 8$ Hz, $\text{C}_9\text{-}$ and $\text{C}_{10}\text{-H}$), 6.53 (1H, s, $\text{C}_4\text{-H}$), 4.03, 3.92, 3.87, 3.83 (each 3H, s, $\text{OCH}_3 \times 4$), 3.90–3.60 (2H, m, $\text{C}_6\text{-H}$), 3.05–2.95 (2H, m, $\text{C}_5\text{-H}$). Anal. Calcd for $\text{C}_{21}\text{H}_{21}\text{NO}_5$: C, 68.65; H, 5.76; N, 3.81. Found: C, 68.40; H, 5.82; N, 3.81.

5,6,7,13-Tetrahydro-2,3,11,12-tetramethoxy-7-methylbenz[*d*]indeno[1,2-*b*]azepin-13-one (17)—Sodium hydride (40 mg, 50% mineral oil dispersion) was added to a solution of the azepine (16) (59 mg) in HMPA (0.5 ml) and anhyd. C_6H_6 (2 ml). The resulting solution was stirred at room temperature for 15 min. Dimethyl sulfate (3 drops) was added to the stirred solution and stirring was continued at room temperature for 1 h. Aqueous NH_3 (28%, 1 ml) was added to the reaction mixture and stirring was continued at room temperature for 30 min. The reaction mixture was extracted with CHCl_3 . The CHCl_3 layer was washed with water, dried, and evaporated to dryness. The residue was subjected to pTLC [Al_2O_3 , C_6H_6 -AcOEt (4:1)] to afford the *N*-methyl derivative (17) (48 mg, 78%) as reddish purple prisms, mp 164–166°C (MeOH) (lit.¹⁰⁾ mp 159–161°C). IR $\nu_{\text{max}}^{\text{CHCl}_3} \text{ cm}^{-1}$: 1650 (CO). MS m/z (%): 381 (M^+ , 100), 366 (53). $^1\text{H-NMR}$ δ : 7.81 (1H, s, $\text{C}_1\text{-H}$), 7.01, 6.66 (2H, AB-q, $J = 8$ Hz, $\text{C}_9\text{-}$ and $\text{C}_{10}\text{-H}$), 6.54 (1H, s, $\text{C}_4\text{-H}$), 4.01, 3.94, 3.87, 3.85 (each 3H, s, $\text{OCH}_3 \times 4$), 3.95–3.60 (2H, m, $\text{C}_6\text{-H}$), 3.40 (3H, s, NCH_3), 3.00–2.80 (2H, m, $\text{C}_5\text{-H}$). Anal. Calcd for $\text{C}_{22}\text{H}_{23}\text{NO}_5$: C, 69.28; H, 6.08; N, 3.67. Found: C, 69.18; H, 6.13; N, 3.39. The product was identical with an authentic specimen¹⁰⁾ (IR and $^1\text{H-NMR}$ spectra, and mixed melting point).

5,6-Dihydro-2,3,11,12-Tetramethoxydibenzo[*a,g*]quinolinium Iodide (18)—A mixture of 3,4-dimethoxyphenethylamine (8.00 g) and 2,3-dimethoxyphenylacetic acid (7.50 g) was heated at 190 °C for 5 h under an Ar atmosphere. The reaction mixture was recrystallized from MeOH to afford *N*-(3,4-dimethoxyphenethyl)-2,3-dimethoxyphenylacetamide (11.5 g, 83%) as colorless needles, mp 138–138.5 °C (lit.^{20a} mp 130–130.5 °C). IR $\nu_{\max}^{\text{CHCl}_3}$ cm^{-1} : 1650 (CO). MS *m/z*: 359 (M^+). ¹H-NMR δ : 7.11–6.53 (6H, m, Ar-H), 5.88 (1H, br s, NH), 3.87, 3.85, 3.83, 3.78 (each 3H, s, OCH₃ × 4), 3.53 (2H, s, COCH₂), 3.39 (2H, t, *J* = 6.5 Hz, NHCH₂), 2.67 (2H, t, *J* = 6.5 Hz, ArCH₂CH₂). *Anal.* Calcd for C₂₀H₂₅NO₅: C, 66.83; H, 7.01; N, 3.90. Found: C, 66.83; H, 7.08; N, 3.92.

Phosphorus oxychloride (47 g) was added to a solution of the amide (9.3 g) in anhyd. C₆H₆ (140 ml), and the resulting mixture was heated under reflux for 6 h with stirring. The C₆H₆ and excess POCl₃ were evaporated off. The residue was poured into ice-water, made alkaline with K₂CO₃, and extracted with CHCl₃. The CHCl₃ layer was washed with water, dried, and concentrated to leave the oily imine (8.5 g, 96%). Sodium borohydride (1.2 g) was added portionwise to a solution of the imine (8.5 g) in MeOH (130 ml) and stirring was continued at room temperature for 6 h. The MeOH was evaporated off and the residue was taken up in CHCl₃. The CHCl₃ layer was washed with water, dried, and concentrated to leave the oily amine (8.5 g, quant.). A solution of the crude amine (8.5 g) and 37% HCHO (105 ml) in AcOH (105 ml) was heated under reflux for 6 h with stirring. The solvents were evaporated off and the residue was taken up in CHCl₃. The CHCl₃ layer was washed with aqueous K₂CO₃, water, dried, and concentrated to leave the tetrahydroprotoberberine (8.2 g, 97%) which was recrystallized from MeOH to afford pale yellow plates, mp 167–167.5 °C (lit.^{19a} mp 162–163 °C). MS *m/z*: 355 (M^+). ¹H-NMR δ : 6.81 (1H, s, C₁-H), 6.79 (2H, s, C₉- and C₁₀-H), 6.62 (1H, s, C₄-H), 3.92, 3.87, 3.85, 3.81 (each 3H, s, OCH₃ × 4). *Anal.* Calcd for C₂₁H₂₅NO₄: C, 70.96; H, 7.09; N, 3.94. Found: C, 70.95; H, 7.10; N, 4.03.

A solution of I₂ (7.3 g) in EtOH (40 ml) was added dropwise to a refluxing solution of the tetrahydroprotoberberine (3.0 g) and AcOK (4.7 g) in EtOH (200 ml) with stirring for 1 h, and stirring was continued at the same temperature for 1.5 h. After the reaction mixture had cooled to room temperature, the precipitates were collected by filtration. Sulfur dioxide gas was passed through a suspension of the precipitates in water (20 ml) for 2 h with stirring. The yellow precipitates were collected by filtration to give the quaternary base (18) (3.9 g, quant.) as yellow needles, mp 201–202 °C (MeOH). ¹H-NMR (DMSO-*d*₆) δ : 9.88 (1H, s, C₈-H), 8.65 (1H, s, C₁₃-H), 8.28, 7.95 (2H, AB-q, *J* = 9.3 Hz, C₉- and C₁₀-H), 7.74 (1H, s, C₁-H), 7.12 (1H, s, C₄-H), 4.80 (2H, t, *J* = 5.5 Hz, C₆-H), 4.14, 4.02, 3.97, 3.89 (each 3H, s, OCH₃ × 4), 3.24 (2H, t, *J* = 5.5 Hz, C₅-H).

Acknowledgement The authors are grateful to Professor R. Rodrigo, University of Waterloo, Canada, for providing the authentic sample of the benzindenoazepine (17) and its ¹H-NMR spectrum. Financial support from the Ministry of Education, Science and Culture of Japan in the form of a Grant-in-Aid for Scientific Research is also gratefully acknowledged.

References and Notes

- 1) Part XI: M. Hanaoka, W. J. Cho, M. Marutani, and C. Mukai, *Chem. Pharm. Bull.*, **35**, 195 (1987).
- 2) A part of this work was published in a preliminary communication: M. Hanaoka, M. Inoue, S. Sakurai, Y. Shimada, and S. Yasuda, *Chem. Pharm. Bull.*, **30**, 1110 (1982).
- 3) C. T. Montgomery, B. K. Cassels, and M. Shamma, *J. Nat. Prod.*, **46**, 441 (1983).
- 4) A. R. Battersby and J. Staunton, *Tetrahedron*, **30**, 1707 (1974).
- 5) C. Tani and K. Tagahara, *Yakugaku Zasshi*, **97**, 93 (1977).
- 6) H. Rönisch, *Phytochemistry*, **16**, 691 (1977).
- 7) From protoberberine: B. Nalliah, R. H. Manske, and R. Rodrigo, *Tetrahedron Lett.*, **1974**, 2853; S. Prabhakar, A. M. Lobo, and I. M. C. Oliveila, *J. Chem. Soc., Chem. Commun.*, **1977**, 419; S. Prabhakar, A. M. Lobo, M. R. Tavares, and I. M. C. Oliveila, *J. Chem. Soc., Perkin Trans. 1*, **1981**, 1273.
- 8) From phthalideisoquinoline: W. Klötzer, S. Teitel, and A. Brossi, *Helv. Chim. Acta*, **54**, 2057 (1971); *idem, ibid.*, **55**, 2228 (1972); R. Hohlbrugger and W. Klötzer, *Chem. Ber.*, **112**, 849 (1979).
- 9) From spirobenzylisoquinoline: H. Irie, S. Tani, and H. Yamane, *J. Chem. Soc., Perkin Trans. 1*, **1972**, 2986.
- 10) K. Orito, R. H. Manske, and R. Rodrigo, *J. Am. Chem. Soc.*, **96**, 1944 (1974).
- 11) I. Ahmad and V. Sniekus, *Can. J. Chem.*, **60**, 2678 (1982).
- 12) G. Blaskó, S. F. Hussain, A. J. Freyer, and M. Shamma, *Tetrahedron Lett.*, **22**, 3127 (1981).
- 13) M. Hanaoka, M. Inoue, M. Takahashi, and S. Yasuda, *Heterocycles*, **19**, 31 (1982); *idem, Chem. Pharm. Bull.*, **32**, 4431 (1984).
- 14) M. Hanaoka, M. Inoue, K. Nagami, Y. Shimada, and S. Yasuda, *Heterocycles*, **19**, 313 (1982); M. Hanaoka, S. K. Kim, M. Inoue, K. Nagami, Y. Shimada, and S. Yasuda, *Chem. Pharm. Bull.*, **33**, 1434 (1985); N. Murugesan, G. Blaskó, R. D. Minard, and M. Shamma, *Tetrahedron Lett.*, **22**, 3131 (1981); G. Blaskó, V. Elango, N. Murugesan, and M. Shamma, *J. Chem. Soc., Chem. Commun.*, **1981**, 1246.
- 15) M. Shamma and J. A. Weiss, *J. Chem. Soc., Chem. Commun.*, **1968**, 212; H. Rönisch, *Tetrahedron Lett.*, **1972**, 4431.

-
- 16) 8-Methoxyberberinephenolbetaine: M. Hanaoka, C. Mukai, and Y. Arata, *Heterocycles*, **6**, 895 (1977); *idem*, *Chem. Pharm. Bull.*, **31**, 947 (1983); J. L. Moniot and M. Shamma, *J. Am. Chem. Soc.*, **98**, 6714 (1976); *idem*, *J. Org. Chem.*, **44**, 4337 (1979).
 - 17) M. Hanaoka, C. Mukai, K. Nagami, K. Okajima, and S. Yasuda, *Chem. Pharm. Bull.*, **32**, 2230 (1984).
 - 18) R. M. Preisner and M. Shamma, *J. Nat. Prod.*, **43**, 305 (1980).
 - 19) a) H. Irie, K. Akagi, S. Tani, K. Yabusaki, and H. Yamane, *Chem. Pharm. Bull.*, **21**, 855 (1973); b) D. Greenslade and R. Ramage, *Tetrahedron*, **33**, 927 (1977).
 - 20) a) E. Späth and E. Mosettig, *Justus Liebigs Ann. Chem.*, **433**, 138 (1923); b) S. Chakravarti and M. Swaminathan, *J. Indian Chem. Soc.*, **11**, 107 (1934).
 - 21) All spirobenzylisoquinolines in this paper were named and numbered according to the spirobenzylisoquinoline alkaloid skeleton, ochotensan.²³⁾
 - 22) The numbering of the benzindenoazepines described in this paper is in accord with that for protoberberines.
 - 23) M. Shamma, "The Isoquinoline Alkaloids—Chemistry and Pharmacology," Academic Press, New York, 1972, p. 381.

[Chem. Pharm. Bull.]
[35(3) 986—995 (1987)]

Synthesis of 5 α -Cholestan-6-one Derivatives with Some Substituents at the C-1, C-2, or C-3 Position

SUGURU TAKATSUTO*^a and NOBUO IKEKAWA*^b

Department of Chemistry, Joetsu University of Education,^a Joetsu, Niigata 943, Japan
and Department of Chemistry, Tokyo Institute of Technology,^b
Ookayama, Meguro-ku, Tokyo 152, Japan

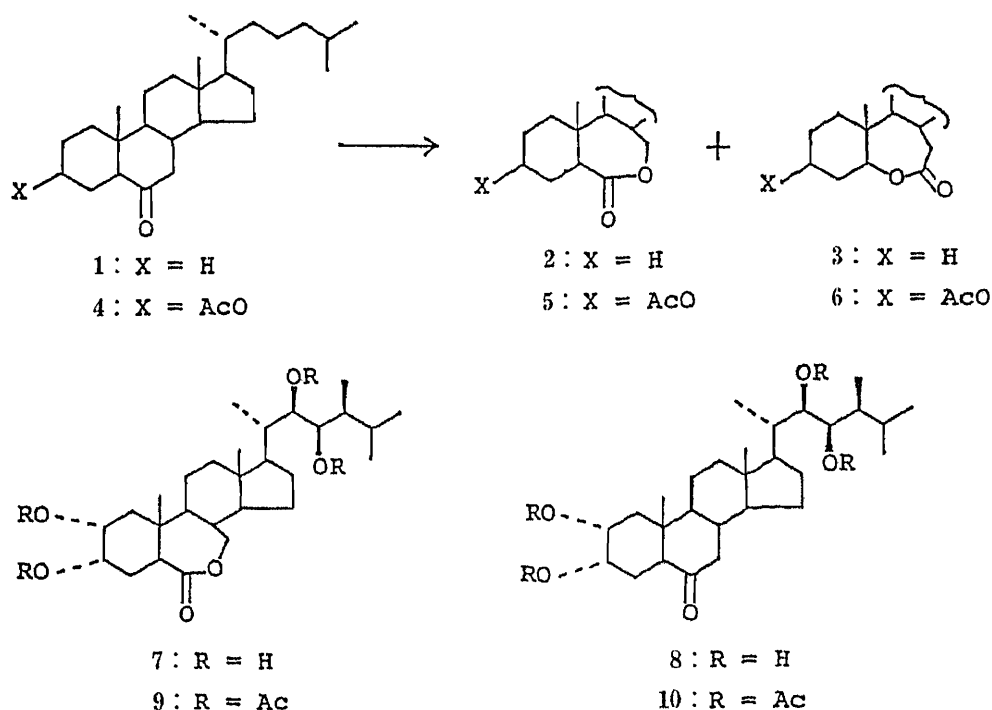
(Received August 13, 1986)

In order to investigate the regioselectivity of Baeyer–Villiger oxidation, thirty 5 α -cholestan-6-one derivatives with various substituents (methyl, hydrogen, acetoxymethyl, methoxy, acetyloxy, benzyloxy, trifluoroacetyloxy, *p*-toluenesulfonyloxy) at the C-1, C-2, or C-3 position were synthesized from cholesterol. The 6-oxo functional group of 5 α -cholestan-6-one derivatives was introduced *via* hydroboration. The 3 β -derivatives were readily obtained by using the native 3 β -hydroxyl group of cholesterol. The 3 α -isomers were obtained by inversion of the configuration of the 3 β -tosylate **24** with tetra-*n*-butylammonium acetate in refluxing 2-butanone. The 2 β -isomers were derived from the 2-ene **43** by bromohydrination, LiAlH₄ reduction, and esterification. The 2 β - to 2 α -hydroxyl group inversion was achieved by Birch reduction of the 2-oxo steroid **51**. The 1 α -derivatives were derived from the known 6 β -acetoxy-1 α -hydroxy-5 α -cholest-2-ene (**57**).

Keywords—Baeyer–Villiger oxidation; regioselectivity; 5 α -cholestan-6-one derivative; hydroboration; configuration inversion; methoxymethyl group

In Baeyer–Villiger oxidation, the migratory aptitude of alkyl groups with retention of configuration is in the order of tertiary > secondary > primary, as expected from their relative abilities to stabilize an electron-deficient, tetrahedral transition state. It was reported that upon the oxidation of 5 α -cholestan-6-one (**1**) with peracid, the 6-oxalactone **3** was obtained as a major product and its regioisomeric 7-oxalactone **2** as a minor product.¹⁾ On the other hand, in the case of 3 β -acetoxy-5 α -cholestan-6-one (**4**) the major product was not the 6-oxalactone **6** but the 7-oxalactone **5**.¹⁾ During the course of our synthesis of brassinolide (**7**) and castasterone (**8**), naturally occurring plant growth hormonal steroids, we also observed a similar unusual phenomenon in the Baeyer–Villiger oxidation of (22*R*,23*R*,24*S*)-2 α ,3 α ,22,23-tetraacetoxy-5 α -ergostan-6-one (**10**); the C-7 carbon migrated more readily than the C-5 carbon, affording the 7-oxalactone **9** with *ca.* 90% regioselectivity.²⁾ This high regioselectivity, which can be ascribed to the effect of not only the 3 α -acetoxy but also the 2 α -acetoxy group, prompted us to investigate the regioselectivity of the Baeyer–Villiger oxidation of 5 α -cholestan-6-one derivatives in more detail. We have prepared thirty 5 α -cholestan-6-one derivatives with various substituents at the C-1, C-2, or C-3 position from cholesterol (**11**) and reported the regioselectivity of Baeyer–Villiger oxidation of them.³⁾ In this paper, we present details of the synthesis of the 5 α -cholestan-6-one derivatives (**4**, **13**–**16**, **18**–**20**, **22**, **26**–**30**, **32**, **38**, **41**, **42**, **46**, **47**, **49**, **50**, **53**–**56**, **60**–**63**).

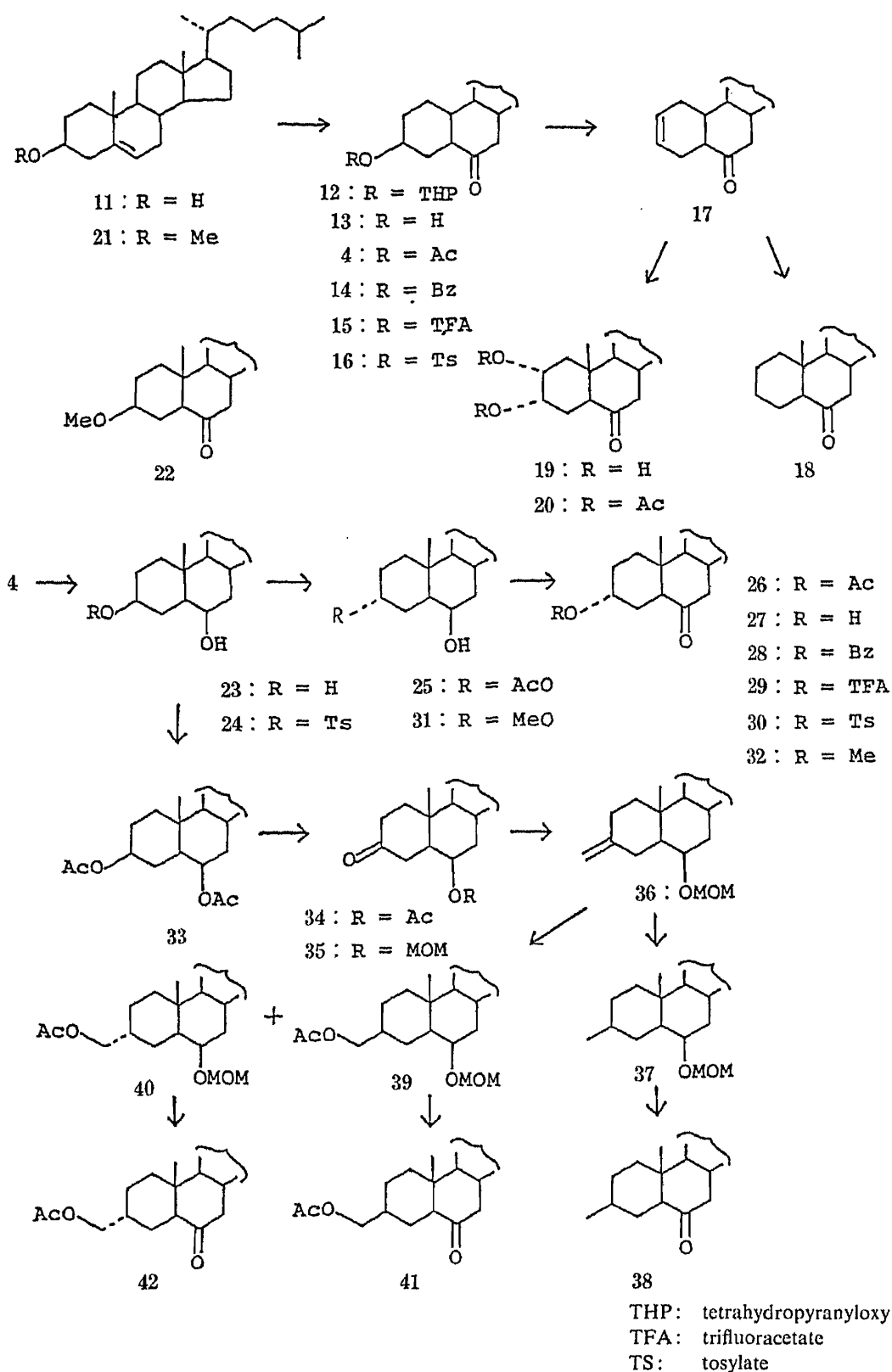
The 5 α -cholestan-6-one derivatives (**4**, **13**–**16**) with substituents at the 3 β -position were prepared from the known 3 β -tetrahydropyranyloxy-5 α -cholestan-6-one (**12**).⁴⁾ Acid hydrolysis of **12** gave 3 β -hydroxy-5 α -cholestan-6-one (**13**), which was converted into the corresponding acetate **4**, the benzoate **14**, the trifluoroacetate **15**, and the tosylate **16**. 3 β -Methoxy-5 α -cholestan-6-one (**22**) was synthesized from cholesterol methyl ether (**21**) as follows. Hydroboration of **21** with BH₃–tetrahydrofuran (THF) complex, followed by



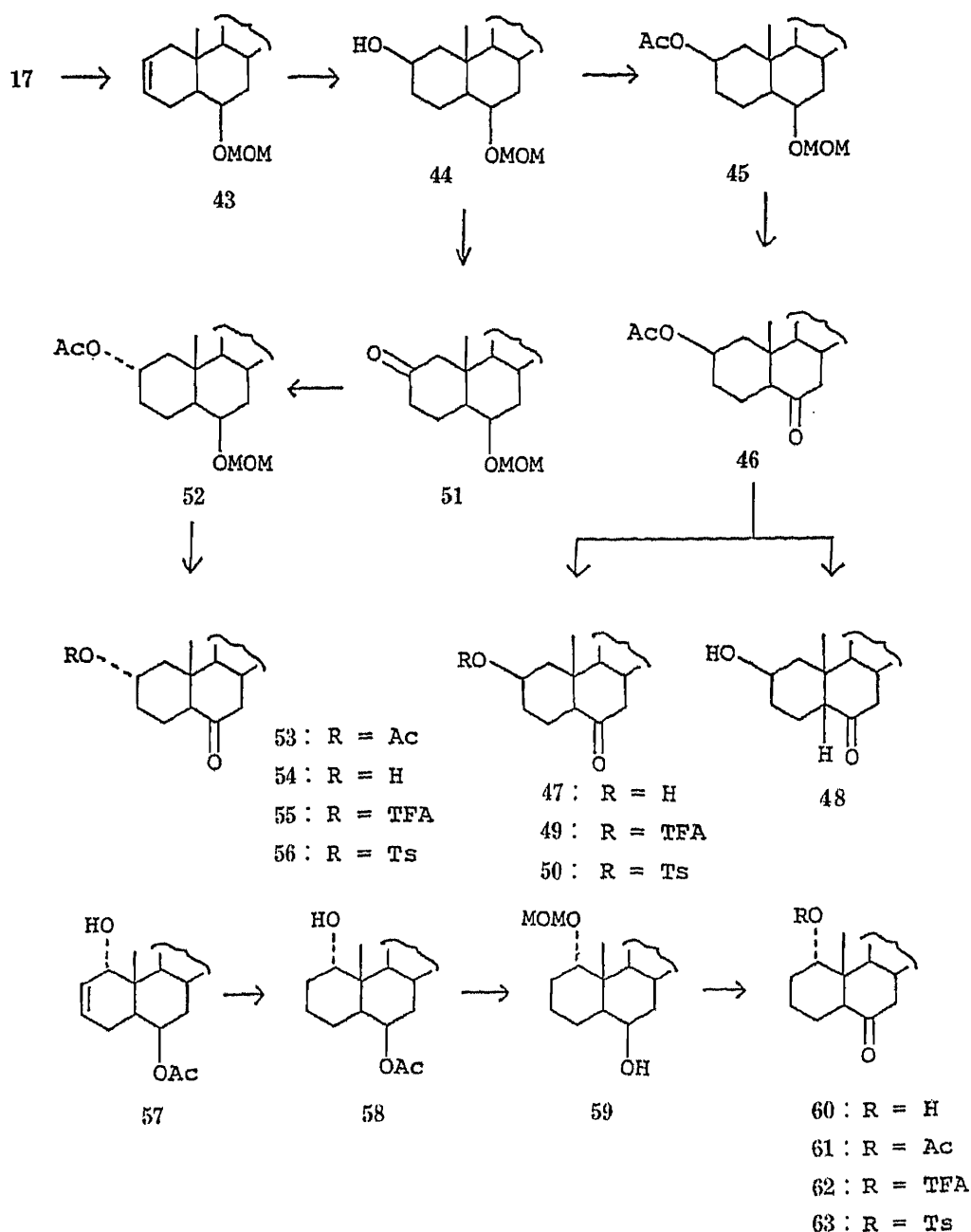
alkaline H_2O_2 oxidation gave 6α -hydroxy- 3β -methoxy- 5α -cholestane, which, without purification, was oxidized with Jones reagent. The 6-ketone **22** was obtained in 80% yield after chromatography.

The next target compounds were 5α -cholestan-6-one (**18**), $2\alpha,3\alpha$ -dihydroxy- 5α -cholestan-6-one (**19**), and $2\alpha,3\alpha$ -diacetoxy- 5α -cholestan-6-one (**20**). These 6-oxo steroids were prepared from the tosylate **16** according to our procedure used for the synthesis of brassinolide (**7**).²⁾ Thus, treatment of **16** with lithium bromide in refluxing dimethylformamide gave the 2-ene **17** in 95% yield. Hydrogenation provided 5α -cholestan-6-one (**18**), quantitatively. Stereoselective α -face hydroxylation of **17** was carried out with a catalytic amount of osmium tetroxide and an excess of *N*-methylmorpholine *N*-oxide in *tert*-BuOH-THF- H_2O (10:3:1) to afford the $2\alpha,3\alpha$ -diol **19**, which was then acetylated. The $2\alpha,3\alpha$ -diacetate **20** was obtained in 87% yield from **17**.

Next, we synthesized 5α -cholestan-6-one derivatives substituted at the 3α -position. Attempted inversion reaction of the 3β -tosylate **16** with various reagents (AcOK or AcONa/dimethylformamide (DMF) or dimethyl sulfoxide (DMSO), BzONa/DMF or DMSO, KO_2 /18-crown-6/DMF-DMSO) and the Mitsunobu reaction of the 3β -ol **13** turned out to be fruitless because of the low yield of the inversion product. Therefore, we adopted the reported method,⁵⁾ which involves the inversion reaction of the 3β -tosyl- 6β -ol **24** with tetra-*n*-butylammonium acetate. The substrate **24** was obtained as follows. Reduction of **13** with lithium aluminum hydride and recrystallization from ethyl acetate gave crystalline $3\beta,6\beta$ -dihydroxy- 5α -cholestane (**23**) in 75% yield. Other stereoisomers were removed by recrystallization. Treatment of **23** with 1.14 eq of *p*-toluenesulfonyl chloride and pyridine gave the 3β -monotosylate **24** in 91% yield. Heating of **24** with tetra-*n*-butylammonium acetate and 2-butanone at reflux temperature gave the inversion product **25**, which was then oxidized with Jones reagent to afford 3α -acetoxy- 5α -cholestan-6-one (**26**) in 50% yield. Saponification of **26** with 5% KOH/MeOH gave the 3α -ol **27**, which was converted into the benzoate **28**, the trifluoroacetate **29**, and the tosylate **30**. Refluxing of **24** with methanol also gave the inversion product **31**. Jones oxidation of **31** gave 3α -methoxy- 5α -cholestan-6-one (**32**) in 50% yield.



The 3 β -methyl, 3 α - and 3 β -acetoxyethyl derivatives **38**, **41**, **42** of 5 α -cholestan-6-one were next synthesized. Acetylation of **23** gave the 3 β ,6 β -diacetate **33**. Selective saponification of the 3 β -acetyl group followed by Jones oxidation provided the known 6 β -acetoxy-5 α -



cholestan-3-one (34)⁴¹ in 76% yield. After exchange of the acetyl group in 34 with a methoxymethyl (MOM) group, the 3-oxo compound 35 was submitted to Wittig reaction with methylenetriphenylphosphorane to give the olefin 36 in 73% yield from 34. Hydrogenation of 36 provided the saturated compound 37 as a single product. The 3 β -configuration was expected from the less hindered, α -face attack of hydrogen. Removal of the MOM group with conc. HCl was followed by Jones oxidation to give 3 β -methyl-5 α -cholestan-6-one (38) in 90% yield. Hydroboration of 36, followed by alkaline H₂O₂ oxidation yielded, after acetylation, two separable products. Chromatographic separation gave the less polar 3 α compound 40 and the more polar 3 β compound 39, in 50 and 27% yields, respectively. These were converted, as described for 38, into the corresponding 3 α -6-oxo steroid 42 (δ_{H} 4.04 (2H, d, $J=8$ Hz, $-\text{CH}_2-\text{OAc}$)) and 3 β -6-oxo steroid 41 (δ_{H} 3.90 (2H, d, $J=5$ Hz, $-\text{CH}_2-\text{OAc}$)), respectively. The stereochemical assignment of 41 and 42 was based on the relative chemical shift due to the

acetoxy methylene in the proton nuclear magnetic resonance ($^1\text{H-NMR}$) spectra. The 3α -isomer should have lower chemical shift than the 3β -isomer because of the 1,3-diaxial interaction between the acetoxymethyl and 1α - and 5α -hydrogens.

Next we describe the synthesis of 5α -cholestan-6-one derivatives with C-2 substituents. Reduction of 5α -cholest-2-en-6-one (**17**) with lithium aluminum hydride was followed by protection of the resulting 6β -ol as the MOM ether to give **43**. Bromohydrination of **43** with *N*-bromosuccinimide/ H_2O followed by reduction with lithium aluminum hydride provided the 2β -ol **44** (δ_{H} 4.10 (1H, m, $W_{1/2}$ = 8 Hz, 2α -H)) in 50% yield from **17**. The reaction possibly proceeded *via* the $2\beta,3\beta$ -epoxide, which suffered further reduction in *trans*-diaxial fashion. Acetylation of **44**, removal of the MOM group, and oxidation with pyridinium chlorochromate in the presence of sodium acetate gave 2β -acetoxy- 5α -cholestan-6-one (**46**) in 79% yield. Saponification of **46** with 5% KOH/MeOH under reflux provided the less polar 5α compound **47** (19%, δ_{H} 4.15 (1H, m, $W_{1/2}$ = 8 Hz, 2α -H)) and the more polar 5β compound **48** (69%, δ_{H} 3.78 (1H, m, $W_{1/2}$ = 24 Hz, 2α -H)). 2β -Hydroxy- 5α -cholestan-6-one (**47**) was converted into the trifluoroacetate **49** and the tosylate **50**.

The 2α -isomers **53**–**56** were prepared as follows. Jones oxidation of **44** gave the 2-oxo compound **51**. This was treated with Li/NH_3 -EtOH and subsequently quenched with dry ammonium chloride to afford, after acetylation, the 2α -acetate **52** (δ_{H} 4.90 (1H, m, $W_{1/2}$ = 24 Hz, 2β -H)) as a single product in 86% yield from **44**. Regeneration of the 6-oxo functionality gave 2α -acetoxy- 5α -cholestan-6-one (**53**) in 95% yield. 2α -Hydroxy- 5α -cholestan-6-one (**54**), obtained by saponification of **53**, was converted into the trifluoroacetate **55** and the tosylate **56**.

The 6-oxo steroids with 1α -substituents were prepared from the known 6β -acetoxy- 1α -hydroxy- 5α -cholest-2-ene (**57**),⁶⁾ which was obtained from **34** according to the reported method.⁶⁾ Hydrogenation of **57** gave 6β -acetoxy- 1α -hydroxy- 5α -cholestane (**58**). Protection of the 1α -hydroxyl group of **58** as the MOM ether was followed by saponification to provide the 6β -ol **59**. This was submitted to Jones oxidation and then acid hydrolysis to afford 1α -hydroxy- 5α -cholestan-6-one (**60**) in 80% overall yield. The alcohol **60** was converted into the acetate **61**, the trifluoroacetate **62**, and the tosylate **63**.

Experimental

Melting points were determined with a hot-stage microscope and are uncorrected. Infrared (IR) spectra were taken with a Hitachi 260-10 spectrometer in chloroform solution. $^1\text{H-NMR}$ spectra were taken with a Hitachi R-24A (60 MHz) or JEOL PS-100 (100 MHz) spectrometer in deuteriochloroform solution with tetramethylsilane as an internal standard. Column chromatography was done on Kieselgel 60 F_{254} (Merck, 70–230 mesh) and analytical thin layer chromatography (TLC) was carried out on precoated Kieselgel 60 F_{254} (Merck, 0.25 mm thickness). Work-up refers to dilution with water, extraction with the organic solvent indicated in parenthesis, washing of the extract to neutrality, drying over anhydrous magnesium sulfate, filtration, and removal of the solvent under reduced pressure. The following abbreviations are used; ether, diethyl ether; MeOH, methanol; EtOAc, ethyl acetate; CHCl_3 , chloroform; CH_2Cl_2 , dichloromethane.

3 β -Hydroxy-5 α -cholestan-6-one (13)—The crude 3β -tetrahydropyranyloxy- 5α -cholestan-6-one (31 g) obtained from cholesterol (**11**) according to the reported method⁴⁾ was treated with 6 M HCl (50 ml) and THF (400 ml) at room temperature for 1 h. Work-up (ether) and chromatography on silica gel (150 g) with benzene-EtOAc (10:1) gave the 3β -ol **13** (22.4 g, 75% from **11**), mp 142–144 °C (MeOH). IR ν_{max} cm^{-1} : 1710. $^1\text{H-NMR}$ δ : 0.66 (3H, s, 18-H_3), 0.74 (3H, s, 19-H_3), 0.85 (6H, d, J = 6 Hz, 26-H_3 , 27-H_3), 3.54 (1H, m, 3-H). *Anal.* Calcd for $\text{C}_{27}\text{H}_{46}\text{O}_2$: C, 80.54; H, 11.52. Found: C, 80.60; H, 11.54.

3 β -Acetoxy-5 α -cholestan-6-one (4)—The 3β -ol **13** (225 mg, 0.498 mmol) in pyridine (1 ml) was treated with acetic anhydride (1 ml) at room temperature overnight. Work-up (EtOAc) and chromatography on silica gel (20 g) with benzene gave the acetate **4** (182 mg, 82%), mp 129–130 °C (MeOH). $^1\text{H-NMR}$ δ : 0.67 (3H, s, 18-H_3), 0.80 (3H, s, 19-H_3), 0.85 (6H, d, J = 6 Hz, 26-H_3 , 27-H_3), 2.00 (3H, s, acetyl), 4.83 (1H, m, 3-H). *Anal.* Calcd for $\text{C}_{29}\text{H}_{48}\text{O}_3$: C, 78.32; H, 10.88. Found: C, 78.56; H, 10.85.

3 β -Benzoyloxy-5 α -cholestan-6-one (14)—The 3β -ol **13** (320 mg, 0.796 mmol) in pyridine (2 ml) was treated with benzoyl chloride (0.2 ml) at room temperature overnight. Work-up (EtOAc) and chromatography on silica gel (20 g)

with benzene gave the benzoate **14** (368 mg, 94%), mp 172–174 °C (MeOH). ¹H-NMR δ: 0.67 (3H, s, 18-H₃), 0.81 (3H, s, 19-H₃), 0.85 (6H, d, *J* = 6 Hz, 26-H₃, 27-H₃), 4.85 (1H, m, 3-H), 7.30–7.60 (3H, m, benzoyl), 7.90–8.10 (2H, m, benzoyl). *Anal.* Calcd for C₃₄H₅₀O₃: C, 80.58; H, 9.95. Found: C, 80.68; H, 9.93.

3β-Trifluoroacetoxy-5α-cholestan-6-one (15)—The 3β-ol **13** (402 mg, 1.0 mmol) in CHCl₃–pyridine (1 : 1, 2 ml) was treated with trifluoroacetic anhydride (0.3 ml) at room temperature overnight. Work-up (EtOAc) and chromatography on silica gel (20 g) with benzene gave the trifluoroacetate **15** (403 mg, 84%), mp 143–145 °C (CHCl₃–MeOH). ¹H-NMR δ: 0.66 (3H, s, 18-H₃), 0.79 (3H, s, 19-H₃), 0.86 (6H, d, *J* = 6 Hz, 26-H₃, 27-H₃), 4.86 (1H, m, 3-H). *Anal.* Calcd for C₂₉H₄₅F₃O₃: C, 69.85; H, 9.10. Found: C, 69.77; H, 8.98.

3β-p-Toluenesulfonyloxy-5α-cholestan-6-one (16)—The 3β-ol **13** (4.02 g, 10.0 mmol) in pyridine (30 ml) was treated with *p*-toluenesulfonyl chloride (3.8 g, 20.0 mmol) at room temperature overnight. Work-up (EtOAc) and chromatography on silica gel (100 g) with benzene gave the tosylate **16** (5.0 g, 90%), mp 175–177 °C (MeOH). ¹H-NMR δ: 0.63 (3H, s, 18-H₃), 0.71 (3H, s, 19-H₃), 0.85 (6H, d, *J* = 6 Hz, 26-H₃, 27-H₃), 0.90 (3H, d, *J* = 6 Hz, 21-H₃), 2.45 (3H, s, tosyl), 4.50 (1H, m, 3-H), 7.40 (2H, d, *J* = 8 Hz, tosyl), 7.90 (2H, d, *J* = 8 Hz, tosyl). *Anal.* Calcd for C₃₄H₅₂O₄S: C, 73.34; H, 9.41. Found: C, 73.46; H, 9.50.

5α-Cholest-2-en-6-one (17)—The 3β-tosylate **16** (25 g, 45 mmol) in dimethylformamide (70 ml) was treated with anhydrous lithium bromide (10 g, 115 mmol) under reflux for 1 h. Work-up (EtOAc) and chromatography on silica gel (100 g) with benzene gave the 2-ene **17** (16.4 g, 95%), mp 97–98 °C (MeOH). IR ν_{max} cm⁻¹: 1710. ¹H-NMR δ: 0.65 (3H, s, 18-H₃), 0.67 (3H, s, 19-H₃), 0.84 (6H, d, *J* = 6 Hz, 26-H₃, 27-H₃), 5.53 (2H, m, 2-H, 3-H). *Anal.* Calcd for C₂₇H₄₄O: C, 84.31; H, 11.53. Found: C, 84.37; H, 11.33.

5α-Cholestan-6-one (18)—The 2-ene **17** (300 mg, 0.781 mmol) in EtOAc (20 ml) was treated with 5% Pd–C (30 mg) under a hydrogen atmosphere at room temperature overnight. Filtration and removal of the solvent gave 5α-cholestan-6-one (**18**) (300 mg), mp 97–98 °C (MeOH). ¹H-NMR δ: 0.66 (3H, s, 18-H₃), 0.72 (3H, s, 19-H₃), 0.85 (6H, d, *J* = 6 Hz, 26-H₃, 27-H₃).

2α,3α-Dihydroxy-5α-cholestan-6-one (19)—The 2-ene **17** (1.0 g, 2.6 mmol) in *tert*-BuOH–THF–H₂O (10 : 3 : 1, 10 ml) was treated with osmium tetroxide (20 mg) and *N*-methylmorpholine *N*-oxide (750 mg, 6.4 mmol) at room temperature overnight. Work-up (CH₂Cl₂) and chromatography on silica gel (30 g) with benzene–EtOAc (1 : 2) gave the 2α,3α-diol **19** (0.97 g, 89%), mp 206–207 °C (CHCl₃–MeOH).

2α,3α-Diacetoxy-5α-cholestan-6-one (20)—The 2α,3α-diol **19** (400 mg, 0.957 mmol) in pyridine (5 ml) was treated with acetic anhydride (4 ml) at 60 °C overnight. Work-up (EtOAc) and chromatography on silica gel (30 g) with benzene–EtOAc (25 : 1) gave the diacetate **20** (470 mg, 98%), mp 152–153 °C (MeOH). ¹H-NMR δ: 0.68 (3H, s, 18-H₃), 0.84 (3H, s, 19-H₃), 0.88 (6H, d, *J* = 6 Hz, 26-H₃, 27-H₃), 0.92 (3H, d, *J* = 6 Hz, 21-H₃), 1.99 (3H, s, acetyl), 2.08 (3H, s, acetyl), 2.56 (1H, dd, *J* = 9, 6 Hz, 5α-H), 4.92 (1H, m, *W*_{1/2} = 22 Hz, 2β-H), 5.36 (1H, m, *W*_{1/2} = 7 Hz, 3β-H). *Anal.* Calcd for C₃₁H₅₀O₅: C, 74.06; H, 10.02. Found: C, 74.03; H, 9.94.

3β-Methoxy-5α-cholestan-6-one (22)—Cholesterol methyl ether (**21**) (500 mg, 1.25 mmol) in THF (7 ml) was treated with 1 M BH₃–THF complex solution (3 ml) at room temperature for 6 h. Then, the reaction mixture was treated with 3 M NaOH (0.5 ml) and 30% H₂O₂ (0.5 ml) at room temperature for 1 h. Work-up (ether) gave a crude product. This in acetone (5 ml) was treated with 2 eq of Jones reagent at room temperature for 15 min. Work-up (ether) and chromatography on silica gel (20 g) with benzene gave the 6-oxo compound **22** (415 mg, 80%), mp 132–135 °C (MeOH–ether). ¹H-NMR δ: 0.66 (3H, s, 18-H₃), 0.75 (3H, s, 19-H₃), 0.85 (6H, d, *J* = 6 Hz, 26-H₃, 27-H₃), 3.00 (1H, m, 3-H), 3.36 (1H, s, –OCH₃). *Anal.* Calcd for C₂₈H₄₈O₂: C, 81.25; H, 11.29. Found: C, 81.18; H, 11.33.

6β-Hydroxy-3β-p-toluenesulfonyloxy-5α-cholestane (24)—3β-Acetoxy-5α-cholestan-6-one (**4**) (10 g, 22.5 mmol) in THF (50 ml) was treated with lithium aluminum hydride (2.0 g, 52.6 mmol) at room temperature for 1 h. Water was carefully added to decompose the excess hydride. Filtration and removal of the solvent gave a crude product, which was recrystallized from EtOAc to afford the 3β,6β-diol **23** (6.7 g, 75%), mp 189–190 °C. The diol **23** (6.5 g, 16.1 mmol) in pyridine (20 ml) was treated with *p*-toluenesulfonyl chloride (3.5 g, 18.4 mmol) at room temperature overnight. Work-up (ether) and chromatography on silica gel (70 g) with benzene gave the 3β-monotosylate **24** (7.96 g, 91%), mp 139–140 °C (hexane–EtOAc). ¹H-NMR δ: 0.66 (3H, s, 18-H₃), 0.90 (3H, s, 19-H₃), 2.41 (3H, s, tosyl), 3.72 (1H, m, *W*_{1/2} = 8 Hz, 6α-H), 4.50 (1H, m, 3-H), 7.30 (2H, d, *J* = 8 Hz, tosyl), 7.78 (2H, d, *J* = 8 Hz, tosyl). *Anal.* Calcd for C₃₄H₅₄O₄S: C, 73.07; H, 9.74. Found: C, 73.15; H, 9.44.

3α-Acetoxy-5α-cholestan-6-one (26)—The tosylate **24** (6.7 g, 12.3 mmol) in 2-butanone (120 ml) was treated with tetra-*n*-butylammonium acetate (13 g, 43.2 mmol) under reflux for 20 h. Work-up (ether) and chromatography on silica gel (100 g) with benzene–EtOAc (100 : 1) gave the 3α-acetate **25** (3.13 g, 57%), mp 144–146 °C (MeOH) (lit.⁵ mp 135–136 °C). ¹H-NMR δ: 0.69 (3H, s, 18-H₃), 0.86 (6H, d, *J* = 6 Hz, 26-H₃, 27-H₃), 0.90 (3H, d, *J* = 6 Hz, 21-H₃), 1.01 (3H, s, 19-H₃), 2.03 (3H, s, acetyl), 3.71 (1H, m, *W*_{1/2} = 7 Hz, 6α-H), 5.08 (1H, m, *W*_{1/2} = 7 Hz, 3β-H). This product **25** (3.2 g, 7.17 mmol) in acetone (100 ml) was treated with 1 eq of Jones reagent at room temperature for 10 min. Work-up (ether) gave the 6-oxo steroid **26** (3.1 g), mp 106.5–107.5 °C (ether–MeOH) (lit.⁵ mp 107–108 °C). ¹H-NMR δ: 0.68 (3H, s, 18-H₃), 0.75 (3H, s, 19-H₃), 0.86 (6H, d, *J* = 6 Hz, 26-H₃, 27-H₃), 0.90 (3H, d, *J* = 6 Hz, 21-H₃), 2.04 (3H, s, acetyl), 2.54 (1H, dd, *J* = 11, 5 Hz, 5α-H), 5.09 (1H, m, *W*_{1/2} = 7 Hz, 3β-H). *Anal.* Calcd for C₂₉H₄₈O₃: C, 78.32; H, 10.88. Found: C, 78.52; H, 10.95.

3α-Hydroxy-5α-cholestan-6-one (27)—The acetate **26** (2.34 g, 5.04 mmol) in MeOH (50 ml) was treated with

5% KOH/MeOH (20 ml) at room temperature for 3 h. Work-up (ether) and chromatography on silica gel (30 g) with benzene-EtOAc (50:1) gave the 3 α -ol 27 (1.5 g, 72%), mp 158–160°C (ether-MeOH) (lit.⁵⁾ mp 160°C. IR ν_{\max} cm⁻¹: 1712. ¹H-NMR δ : 0.64 (3H, s, 18-H₃), 0.71 (3H, s, 19-H₃), 0.85 (6H, d, J =6 Hz, 26-H₃, 27-H₃), 0.89 (3H, d, J =6 Hz, 21-H₃), 4.12 (1H, m, $W_{1/2}$ =8 Hz, 3 β -H).

3 α -Benzyloxy-5 α -cholestan-6-one (28)—The 3 α -ol 27 (300 mg, 0.746 mmol) was converted, as described for 14, into the benzoate 28 (374 mg, 98%), mp 137–138°C (ether-MeOH). ¹H-NMR δ : 0.66 (3H, s, 18-H₃), 0.79 (3H, s, 19-H₃), 0.85 (6H, d, J =6 Hz, 26-H₃, 27-H₃), 2.67 (1H, dd, J =11, 5 Hz, 5 α -H), 5.36 (1H, m, $W_{1/2}$ =8 Hz, 3 β -H), 7.30–7.60 (3H, m, benzoyl), 7.90–8.10 (2H, m, benzoyl). *Anal.* Calcd for C₃₄H₅₀O₃: C, 80.58; H, 9.95. Found: C, 80.57; H, 9.92.

3 α -Trifluoroacetoxy-5 α -cholestan-6-one (29)—The 3 α -ol 27 (300 mg, 0.746 mmol) was converted, as described for 15, into the trifluoroacetate 29 (324 mg, 87%), mp 105–106°C (CHCl₃-MeOH). ¹H-NMR δ : 0.68 (3H, s, 18-H₃), 0.78 (3H, s, 19-H₃), 0.84 (6H, d, J =6 Hz, 26-H₃, 27-H₃), 2.54 (1H, dd, J =10, 6 Hz, 5 α -H), 5.33 (1H, m, $W_{1/2}$ =8 Hz, 3 β -H). *Anal.* Calcd for C₂₉H₄₅F₃O₃: C, 69.85; H, 9.10. Found: C, 70.10; H, 8.87.

3 α -*p*-Toluenesulfonyloxy-5 α -cholestan-6-one (30)—The 3 α -ol 27 (193 mg, 0.48 mmol) was converted, as described for 16, into the tosylate 30 (253 mg, 95%), mp 146–147°C (ether-MeOH). ¹H-NMR δ : 0.62 (3H, s, 18-H₃), 0.65 (3H, s, 19-H₃), 0.85 (6H, d, J =6 Hz, 26-H₃, 27-H₃), 2.39 (3H, s, tosyl), 2.54 (1H, dd, J =12, 5 Hz, 5 α -H), 4.74 (1H, m, $W_{1/2}$ =8 Hz, 3 β -H), 7.28 (2H, d, J =8 Hz, tosyl), 7.72 (2H, d, J =8 Hz, tosyl). *Anal.* Calcd for C₃₄H₅₂O₄S: C, 73.34; H, 9.41. Found: C, 73.40; H, 9.23.

3 α -Methoxy-5 α -cholestan-6-one (32)—The mixture of the tosylate 24 (1.0 g, 1.79 mmol) and MeOH (50 ml) was refluxed for 2 d. Work-up (ether) and chromatography on silica gel (20 g) with benzene-EtOAc (20:1) gave the 3 α -methoxy-6 β -ol 31 (390 mg, 54%), oil. ¹H-NMR δ : 0.68 (3H, s, 18-H₃), 0.85 (6H, d, J =6 Hz, 26-H₃, 27-H₃), 1.00 (3H, s, 19-H₃), 3.29 (3H, s, -OCH₃), 3.55 (1H, m, $W_{1/2}$ =8 Hz, 3 β -H), 3.73 (1H, m, $W_{1/2}$ =7 Hz, 6 α -H). This in acetone (10 ml) was oxidized with Jones reagent to give the 6-oxo compound 32 (380 mg), mp 107–108.5°C (MeOH). ¹H-NMR δ : 0.65 (3H, s, 18-H₃), 0.73 (3H, s, 19-H₃), 0.85 (6H, d, J =6 Hz, 26-H₃, 27-H₃), 3.29 (3H, s, -OCH₃), 3.53 (1H, m, $W_{1/2}$ =8 Hz, 3 β -H). *Anal.* Calcd for C₂₈H₄₈O₂: C, 81.25; H, 11.29. Found: C, 80.87; H, 11.41.

3 β ,6 β -Diacetoxy-5 α -cholestane (33)—The 3 β ,6 β -diol 23 (9.0 g, 22.28 mmol) in pyridine (100 ml) was treated with acetic anhydride (50 ml) at room temperature for 40 h. Work-up (EtOAc) and chromatography on silica gel (100 g) with benzene gave the diacetate 33 (9.86 g, 91%), mp 137–138°C (MeOH). ¹H-NMR δ : 0.68 (3H, s, 18-H₃), 0.85 (6H, d, J =6 Hz, 26-H₃, 27-H₃), 0.90 (3H, d, J =6 Hz, 21-H₃), 1.00 (3H, s, 19-H₃), 2.01 (3H, s, acetyl), 2.03 (3H, s, acetyl), 4.75 (1H, m, 3-H), 4.95 (1H, m, 6-H).

6 β -Acetoxy-5 α -cholestan-3-one (34)—The diacetate 33 (8.56 g, 17.5 mmol) in THF-MeOH (1:2, 150 ml) was treated with 5% KOH/MeOH (40 ml) at room temperature for 45 min. Work-up (ether) gave a crude product, which was dissolved in acetone (200 ml). Then, Jones reagent (1 eq) was added and stirring was continued for 10 min. Work-up (ether) and chromatography on silica gel (100 g) with benzene-EtOAc (50:1) gave the 3-oxo steroid 34 (6.5 g, 83%), mp 97–99°C (MeOH) (lit.⁵⁾ mp 99–102°C). ¹H-NMR δ : 0.70 (3H, s, 18-H₃), 0.85 (6H, d, J =6 Hz, 26-H₃, 27-H₃), 0.90 (3H, d, J =6 Hz, 21-H₃), 1.14 (3H, s, 19-H₃), 2.02 (3H, s, acetyl), 4.85 (1H, m, 6-H). *Anal.* Calcd for C₂₉H₄₈O₃: C, 78.32; H, 10.88. Found: C, 78.19; H, 10.88.

6 β -Methoxymethoxy-3-methylene-5 α -cholestane (36)—The 6 β -acetate 34 (3.0 g, 6.76 mmol) in dioxane (10 ml) was treated with 5% KOH/MeOH (30 ml) at 70°C for 17 h. Work-up (ether) gave a crude product (2.8 g). This in dioxane (20 ml) was treated with chloromethyl methyl ether (4 ml) and diethylcyclohexylamine (5 ml) at room temperature for 4 h. Work-up (EtOAc) and chromatography on silica gel (50 g) with benzene-EtOAc (20:1) gave the methoxymethyl ether 35 (2.33 g, 76%).

A solution of *n*-butyl lithium in hexane (5.7 ml, 8.89 mmol) was added to a solution of methyltriphenylphosphonium iodide (2.5 g, 6.19 mmol) in THF (10 ml) at 0°C. The mixture was stirred at room temperature for 10 min. Then, a solution of the ketone 35 (2.3 g, 5.16 mmol) in THF (10 ml) was added to the ylide solution. The mixture was stirred at room temperature for 1 h. Work-up (EtOAc) and chromatography on silica gel (30 g) with benzene-EtOAc (50:1) gave the olefin 36 (2.2 g, 96%), oil. ¹H-NMR δ : 0.69 (3H, s, 18-H₃), 1.02 (3H, s, 19-H₃), 3.33 (3H, s, -OCH₃), 3.58 (1H, m, 6-H), 4.55 (4H, m, -OCH₂O-, =CH₂).

3 β -Methyl-5 α -cholestan-6-one (38)—The olefin 36 (300 mg, 0.676 mmol) was hydrogenated, as described for 18, to give 6 β -methoxymethoxy-3 β -methyl-5 α -cholestane (300 mg). This in THF (5 ml) was treated with conc. HCl (0.2 ml) at 50°C for 5 h. Work-up (ether) gave a crude product, which was oxidized with Jones reagent to give the 3 β -methyl steroid 38 (260 mg, 98%), mp 102–104°C (MeOH). ¹H-NMR δ : 0.65 (3H, s, 18-H₃), 0.68 (3H, s, 19-H₃), 0.85 (6H, d, J =6 Hz, 26-H₃, 27-H₃). *Anal.* Calcd for C₂₈H₄₈O: C, 83.93; H, 12.07. Found: C, 83.87; H, 12.01.

3 α - and 3 β -Acetoxymethyl-5 α -cholestan-6-one (42 and 41)—The olefin 36 (1.0 g, 2.25 mmol) in THF (10 ml) was treated with 1 M BH₃-THF complex solution (6 ml) at room temperature for 1.5 h. Water was carefully added to decompose the excess reagent. Then, 2 M NaOH (3 ml) and 30% H₂O₂ (3 ml) were added. Stirring was continued at room temperature for 1 h. Work-up (ether) followed by acetylation with acetic anhydride (4 ml) and pyridine (5 ml) at room temperature for 18 h gave two separable products. Work-up (EtOAc) and chromatography on silica gel (50 g) with benzene-EtOAc (100:1) gave the less polar product 40 (570 mg, 50%) and the more polar product 39 (310 mg, 27%).

The less polar acetate **40** (570 mg) in THF (10 ml) was treated with 6 M HCl (2 ml) at room temperature for 15 h and then treated with Jones reagent in acetone (10 ml). Work-up (ether) and chromatography on silica gel (30 g) with benzene-EtOAc (100:1) gave the 3 α -compound **42**, mp 68–72 °C (MeOH-ether). ¹H-NMR δ : 0.65 (3H, s, 18-H₃), 0.74 (3H, s, 19-H₃), 0.85 (6H, d, $J=6$ Hz, 26-H₃, 27-H₃), 2.02 (3H, s, acetyl), 4.04 (2H, d, $J=8$ Hz, -CH₂-OAc). *Anal.* Calcd for C₃₀H₅₀O₃: C, 78.55; H, 10.99. Found: C, 78.47; H, 10.92.

The more polar acetate **39** (310 mg) was similarly converted into the 6-oxo compound **41** (210 mg, 71%), amorphous solid. ¹H-NMR δ : 0.65 (3H, s, 18-H₃), 0.70 (3H, s, 19-H₃), 0.85 (6H, d, $J=6$ Hz, 26-H₃, 27-H₃), 2.02 (3H, s, acetyl), 3.90 (2H, d, $J=5$ Hz, -CH₂-OAc).

6 β -Methoxymethoxy-5 α -cholest-2-ene (43)—5 α -Cholest-2-en-6-one (**17**) (17 g, 44.3 mmol) in THF (300 ml) was treated with lithium aluminum hydride (2.0 g, 52.6 mmol) at room temperature for 1 h. Water was carefully added to decompose the excess hydride. Filtration and removal of the solvent gave a crude product (17 g). This crude product was dissolved in dioxane (260 mg) and diethylcyclohexylamine (25 ml). Chloromethyl methyl ether (10 ml) was added to the solution. The mixture was stirred at 50 °C for 3 h. Work-up (ether) and chromatography on silica gel (100 g) with benzene gave the product **43** (15.2 g, 80%), mp 75–76 °C (MeOH). ¹H-NMR δ : 0.68 (3H, s, 18-H₃), 0.88 (6H, d, $J=6$ Hz, 26-H₃, 27-H₃), 0.92 (3H, s, 19-H₃), 3.37 (3H, s, -OCH₃), 3.66 (1H, m, $W_{1/2}=8$ Hz, 6 α -H), 4.63 (2H, dd, $J=10, 7$ Hz, -OCH₂O-), 5.52 (2H, m, 2-H, 3-H). *Anal.* Calcd for C₂₉H₅₀O₂: C, 80.87; H, 11.70. Found: C, 80.94; H, 11.66.

6 β -Methoxymethoxy-5 α -cholestan-2 β -ol (44)—The 2-ene **43** (8.8 g, 20.5 mmol) in glyme-H₂O (15:1, 160 ml) was treated with *N*-bromosuccinimide (5.0 g, 24.5 mmol) at room temperature for 1 h. Work-up (ether) gave a crude product, which in THF (150 ml) was treated with lithium aluminum hydride (1.5 g, 39.5 mmol) under reflux for 2 h. Work-up (ether) and chromatography on silica gel (50 g) with benzene-EtOAc (50:1) gave the 2 β -ol **44** (5.5 g, 60%), mp 140–141 °C (MeOH). ¹H-NMR δ : 0.69 (3H, s, 18-H₃), 0.88 (6H, d, $J=6$ Hz, 26-H₃, 27-H₃), 0.91 (3H, s, 19-H₃), 3.37 (3H, s, -OCH₃), 3.65 (1H, m, $W_{1/2}=8$ Hz, 6-H), 4.15 (1H, m, $W_{1/2}=8$ Hz, 2 α -H), 4.62 (1H, dd, $J=10, 7$ Hz, -OCH₂O-). *Anal.* Calcd for C₂₉H₅₂O₃: C, 77.62; H, 11.68. Found: C, 77.85; H, 11.50.

2 β -Acetoxy-5 α -cholestan-6-one (46)—The 2 β -ol **44** (3.14 g, 7.0 mmol) in pyridine (7 ml) was treated with acetic anhydride (5 ml) at room temperature overnight. Work-up (EtOAc) gave a crude product (3.3 g). This in THF (60 ml) was treated with 6 M HCl (6 ml) at 50 °C for 3 h. Work-up (ether) gave a crude product, which was dissolved in CH₂Cl₂ (100 ml). Then, sodium acetate (800 mg) and pyridinium chlorochromate (2.4 g, 11.2 mmol) were added to the solution. The reaction mixture was stirred at room temperature for 30 min, and ether (500 ml) was added. Filtration through a column of Florisil (20 g), elution with ether, and removal of the solvent gave a crude product (2.8 g). Chromatography on silica gel (40 g) with benzene-EtOAc (100:1) gave the 2 β -acetoxy-6-ketone **46** (2.4 g, 77%), mp 154–155 °C (MeOH). ¹H-NMR δ : 0.65 (3H, s, 18-H₃), 0.84 (6H, d, $J=6$ Hz, 26-H₃, 27-H₃), 0.88 (3H, s, 19-H₃), 2.00 (3H, s, acetyl), 5.05 (1H, m, $W_{1/2}=9$ Hz, 2 α -H). *Anal.* Calcd for C₂₉H₄₈O₃: C, 78.32; H, 10.88. Found: C, 78.58; H, 10.79.

2 β -Hydroxy-5 α -cholestan-6-one (47) and 2 β -Hydroxy-5 β -cholestan-6-one (48)—The acetate **46** (4.6 g, 10.3 mmol) in THF-MeOH (1:1, 60 ml) was treated with 5% KOH/MeOH (10 ml) under reflux for 1 h. Work-up (ether) and chromatography on silica gel (150 g) with benzene-EtOAc (25:1) gave the less polar 5 α -steroid **47** (780 mg, 19%), mp 196–197 °C (MeOH). ¹H-NMR δ : 0.68 (3H, s, 18-H₃), 0.86 (6H, d, $J=6.5$ Hz, 26-H₃, 27-H₃), 1.00 (3H, s, 19-H₃), 0.90 (3H, d, $J=6$ Hz, 21-H₃), 4.16 (1H, m, $W_{1/2}=9$ Hz, 2 α -H). *Anal.* Calcd for C₂₇H₄₆O₂: C, 80.54; H, 11.52. Found: C, 80.64; H, 11.55.

Further elution with the same solvent gave the more polar 5 β -steroid **48** (2.86 g, 69%), amorphous solid. ¹H-NMR δ : 0.66 (3H, s, 18-H₃), 0.86 (6H, d, $J=6$ Hz, 26-H₃, 27-H₃), 0.91 (3H, d, $J=6$ Hz, 21-H₃), 0.92 (3H, s, 19-H₃), 3.76 (1H, m, $W_{1/2}=24$ Hz, 2 α -H). *Anal.* Calcd for C₂₇H₄₆O₂: C, 80.54; H, 11.52. Found: C, 80.61; H, 11.57.

2 β -Trifluoroacetoxy-5 α -cholestan-6-one (49)—The 2 β -ol **47** (94 mg, 0.234 mmol) was converted, as described for **15**, into the trifluoroacetate **49** (105 mg, 80%), mp 176–177 °C (acetone). ¹H-NMR δ : 0.64 (3H, s, 18-H₃), 0.88 (3H, s, 19-H₃), 5.30 (1H, m, $W_{1/2}=8$ Hz, 2 α -H). *Anal.* Calcd for C₂₉H₄₅F₃O₃: C, 69.85; H, 9.10. Found: C, 70.02; H, 9.14.

2 β -*p*-Toluenesulfonyloxy-5 α -cholestan-6-one (50)—The 2 β -ol **47** (100 mg, 0.249 mmol) was converted, as described for **16**, into the tosylate **50** (115 mg, 83%), mp 153–155 °C (MeOH-ether). ¹H-NMR δ : 0.62 (3H, s, 18-H₃), 0.85 (6H, d, $J=6$ Hz, 26-H₃, 27-H₃), 0.98 (3H, s, 19-H₃), 2.40 (3H, s, tosyl), 5.43 (1H, m, $W_{1/2}=8$ Hz, 2 α -H), 7.30 (2H, d, $J=8$ Hz, tosyl), 7.72 (2H, d, $J=8$ Hz, tosyl). *Anal.* Calcd for C₃₄H₅₂O₄S: C, 73.34; H, 9.41. Found: C, 73.28; H, 9.56.

6 β -Methoxymethoxy-5 α -cholestan-2-one (51)—The 2 β -ol **44** (3.0 g, 6.72 mmol) in acetone (50 ml) was treated with 1 eq of Jones reagent at room temperature for 10 min. Work-up (ether) gave the 2-oxo steroid **51** (3.0 g), mp 89–90 °C (MeOH). IR ν_{\max} cm⁻¹: 1710. ¹H-NMR δ : 0.65 (3H, s, 18-H₃), 0.84 (6H, d, $J=6$ Hz, 26-H₃, 27-H₃), 0.89 (3H, s, 19-H₃), 3.29 (3H, s, -OCH₃), 3.70 (1H, m, $W_{1/2}=8$ Hz, 6-H), 4.55 (2H, dd, $J=10, 7$ Hz, -OCH₂O-). *Anal.* Calcd for C₂₉H₅₀O₃: C, 77.97; H, 11.28. Found: C, 78.15; H, 11.06.

2 α -Acetoxy-6 β -methoxymethoxy-5 α -cholestane (52)—A solution of the 2-oxo steroid **51** (2.76 g, 6.18 mmol) in THF (80 ml) was added to a solution of liquid ammonia (160 ml) and ethanol (10 ml) at -78 °C under an argon atmosphere. Then, small pieces of lithium (2.0 g) were added portionwise. The mixture was stirred at -78 °C for

30 min. Then, dry ammonium chloride (50 g) was added portionwise to the reaction mixture at -78°C . Work-up (ether) gave a crude product, which in pyridine (20 ml) was treated with acetic anhydride (10 ml) at room temperature overnight. Work-up (EtOAc) and chromatography on silica gel (60 g) with benzene gave the 2 α -acetate **52** (2.62 g, 91%), mp $79-80^{\circ}\text{C}$ (MeOH). $^1\text{H-NMR}$ δ : 0.69 (3H, s, 18-H₃), 0.86 (6H, d, $J=6$ Hz, 26-H₃, 27-H₃), 1.02 (3H, s, 19-H₃), 1.99 (3H, s, acetyl), 3.30 (3H, s, -OCH₃), 3.60 (1H, m, $W_{1/2}=7$ Hz, 6 α -H), 4.50 (2H, dd, $J=10, 7$ Hz, -OCH₂O-), 4.85 (1H, m, $W_{1/2}=24$ Hz, 2 β -H). *Anal.* Calcd for C₃₁H₅₄O₄: C, 75.87; H, 11.09. Found: C, 75.32; H, 11.03.

2 α -Acetoxy-5 α -cholestan-6-one (53)—The methoxymethoxy ether **52** (2.4 g, 4.92 mmol) was deprotected and oxidized, as described for **42**, to give the 6-oxo steroid **53** (2.08 g, 95%), mp $154-156^{\circ}\text{C}$ (MeOH). $^1\text{H-NMR}$ δ : 0.65 (3H, s, 18-H₃), 0.79 (3H, s, 19-H₃), 0.85 (6H, d, $J=6$ Hz, 26-H₃, 27-H₃), 2.01 (3H, s, acetyl), 4.91 (1H, m, $W_{1/2}=24$ Hz, 2 β -H). *Anal.* Calcd for C₂₉H₄₈O₃: C, 78.32; H, 10.88. Found: C, 78.47; H, 10.84.

2 α -Hydroxy-5 α -cholestan-6-one (54)—The acetate **53** (790 mg, 1.78 mmol) in THF-MeOH (2:1, 30 ml) was treated with 5% KOH/MeOH (4 ml) at room temperature for 1 h. Work-up (ether) gave the 2 α -ol **54** (715 mg), mp $162-164^{\circ}\text{C}$ (MeOH). $^1\text{H-NMR}$ δ : 0.66 (3H, s, 18-H₃), 0.74 (3H, s, 19-H₃), 0.85 (6H, d, $J=6$ Hz, 26-H₃, 27-H₃), 3.72 (1H, m, 2-H). *Anal.* Calcd for C₂₇H₄₆O₂: C, 80.54; H, 11.52. Found: C, 80.77; H, 11.36.

2 α -Trifluoroacetoxy-5 α -cholestan-6-one (55)—The 2 α -ol **53** (145 mg, 0.361 mmol) was converted, as described for **15**, into the trifluoroacetate **55** (178 mg, 98%), mp $136-137.5^{\circ}\text{C}$ (MeOH). $^1\text{H-NMR}$ δ : 0.65 (3H, s, 18-H₃), 0.80 (3H, s, 19-H₃), 0.85 (6H, d, $J=6$ Hz, 26-H₃, 27-H₃), 5.05 (1H, m, 2-H). *Anal.* Calcd for C₂₉H₄₅F₃O₃: C, 69.85; H, 9.10. Found: C, 69.94; H, 9.08.

2 α -*p*-Toluenesulfonyloxy-5 α -cholestan-6-one (56)—The 2 α -ol **54** (145 mg, 0.361 mmol) was converted, as described for **16**, into the tosylate **56** (180 mg, 93%), mp $178-180^{\circ}\text{C}$ (MeOH). $^1\text{H-NMR}$ δ : 0.63 (3H, s, 18-H₃), 0.69 (3H, s, 19-H₃), 0.85 (6H, d, $J=6$ Hz, 26-H₃, 27-H₃), 2.45 (3H, s, tosyl), 4.60 (1H, m, 2-H), 7.32 (2H, d, $J=8$ Hz, tosyl), 7.78 (2H, d, $J=8$ Hz, tosyl). *Anal.* Calcd for C₃₄H₅₂O₄S: C, 73.34; H, 9.41. Found: C, 73.29; H, 9.43.

1 α -Methoxymethoxy-5 α -cholestan-6 β -ol (59)—The allylic alcohol **57**⁶¹ (2.63 g, 5.92 mmol) in EtOAc (100 ml) was hydrogenated with 5% Pd-C (50 mg) at room temperature under a hydrogen atmosphere overnight. Filtration and removal of the solvent gave the saturated compound **58** (2.63 g), oil. $^1\text{H-NMR}$ δ : 0.69 (3H, s, 18-H₃), 0.85 (6H, d, $J=6$ Hz, 26-H₃, 27-H₃), 0.94 (3H, s, 19-H₃), 2.03 (3H, s, acetyl), 3.65 (1H, m, $W_{1/2}=6$ Hz, 1 β -H), 5.08 (1H, m, $W_{1/2}=8$ Hz, 6 α -H). This product was dissolved in dioxane (20 ml) and diethylcyclohexylamine (10 ml). Then, chloromethyl methyl ether (4 ml) was added to the solution. The mixture was stirred at 50°C for 3 h. Work-up (EtOAc) gave a crude product, which in dioxane (20 ml) was treated with 5% KOH/MeOH (10 ml) under reflux overnight. Work-up (ether) and chromatography on silica gel (50 g) with benzene-EtOAc (100:1) gave the 6 β -ol **59** (2.12 g, 80%), oil. $^1\text{H-NMR}$ δ : 0.68 (3H, s, 18-H₃), 0.85 (6H, d, $J=6$ Hz, 26-H₃, 27-H₃), 0.97 (3H, s, 19-H₃), 3.39 (3H, s, -OCH₃), 3.83 (1H, m, $W_{1/2}=8$ Hz, 1 β -H), 4.50 (2H, dd, $J=10, 7$ Hz, -OCH₂O-).

1 α -Hydroxy-5 α -cholestan-6-one (60)—The 6 β -ol **59** (2.1 g, 4.69 mmol) in acetone (50 ml) was treated with Jones reagent (1 eq) at room temperature for 10 min. Work-up (ether) gave a crude product, which in THF (30 ml) was treated with 6 M HCl (6 ml) at room temperature overnight. Work-up (ether) and chromatography on silica gel (50 g) with benzene-EtOAc (50:1) gave the 1 α -ol **60** (1.8 g, 95%), mp $186-187^{\circ}\text{C}$ (acetone). IR ν_{max} cm^{-1} : 1713. $^1\text{H-NMR}$ δ : 0.65 (3H, s, 18-H₃), 0.73 (3H, s, 19-H₃), 0.85 (6H, d, $J=6$ Hz, 26-H₃, 27-H₃), 3.76 (1H, m, $W_{1/2}=8$ Hz, 1 β -H). *Anal.* Calcd for C₂₇H₄₆O₂: C, 80.54; H, 11.52. Found: C, 80.61; H, 11.31.

1 α -Acetoxy-5 α -cholestan-6-one (61)—The 1 α -ol **60** (184 mg, 0.458 mmol) was acetylated with pyridine (2 ml) and acetic anhydride (1 ml) at room temperature overnight. Work-up (EtOAc) and chromatography gave the 1 α -acetate **61** (172 mg, 85%), mp $105-106^{\circ}\text{C}$ (MeOH). $^1\text{H-NMR}$ δ : 0.65 (3H, s, 18-H₃), 0.80 (3H, s, 19-H₃), 0.86 (6H, d, $J=6$ Hz, 26-H₃, 27-H₃), 2.08 (3H, s, acetyl), 4.85 (1H, m, $W_{1/2}=6$ Hz, 1 β -H). *Anal.* Calcd for C₂₉H₄₈O₃: C, 78.32; H, 10.88. Found: C, 78.28; H, 10.70.

1 α -Trifluoroacetoxy-5 α -cholestan-6-one (62)—The 1 α -ol **60** (184 mg, 0.458 mmol) was converted, as described for **15**, into the trifluoroacetate **62** (240 mg, 98%), mp $107-108^{\circ}\text{C}$ (MeOH). $^1\text{H-NMR}$ δ : 0.64 (3H, s, 18-H₃), 0.82 (3H, s, 19-H₃), 0.85 (6H, d, $J=6$ Hz, 26-H₃, 27-H₃), 5.05 (1H, m, $W_{1/2}=6$ Hz, 1 β -H). *Anal.* Calcd for C₂₉H₄₅F₃O₃: C, 69.85; H, 9.10. Found: C, 70.15; H, 8.94.

1 α -*p*-Toluenesulfonyloxy-5 α -cholestan-6-one (63)—The 1 α -ol **60** (180 mg, 0.448 mmol) was converted, as described for **16**, into the tosylate **63** (236 mg, 95%), mp $139-141^{\circ}\text{C}$ (MeOH). $^1\text{H-NMR}$ δ : 0.62 (3H, s, 18-H₃), 0.75 (3H, s, 19-H₃), 0.85 (6H, d, $J=6$ Hz, 26-H₃, 27-H₃), 2.42 (3H, s, tosyl), 4.78 (1H, m, $W_{1/2}=6$ Hz, 1 β -H), 7.35 (2H, d, $J=8$ Hz, tosyl), 7.80 (2H, d, $J=8$ Hz, tosyl). *Anal.* Calcd for C₃₄H₅₂O₄S: C, 73.34; H, 9.41. Found: C, 73.09; H, 9.37.

References

- 1) a) R. C. Cookson, R. P. Gandhi, and R. M. Southam, *J. Chem. Soc. C*, **1968**, 2494; b) M. S. Ahmad, G. Moinuddin, and I. A. Khan, *J. Org. Chem.*, **43**, 163 (1978).
- 2) a) M. Ishiguro, S. Takatsuto, M. Morisaki, and N. Ikekawa, *J. Chem. Soc., Chem. Commun.*, **1980**, 962; b) S. Takatsuto, N. Yazawa, M. Ishiguro, M. Morisaki, and N. Ikekawa, *J. Chem. Soc., Perkin Trans. 1*, **1984**, 139; The high regio-selectivity was also pointed out by other groups; c) M. J. Thompson, N. B. Mandava, J. L. Flippen-Anderson, J. F. Worley, S. R. Dutky, W. E. Robbins, and W. R. Lusby, *J. Org. Chem.*, **44**, 5002 (1979);

-
- d) S. Fung and J. B. Siddall, *J. Am. Chem. Soc.*, **102**, 6580 (1980).
- 3) S. Takatsuto and N. Ikekawa, *Tetrahedron Lett.*, **24**, 917 (1983).
- 4) M. Morisaki, A. Saika, K. Bannai, M. Sawamura, J. Rubio-Lightbourn, and N. Ikekawa, *Chem. Pharm. Bull.*, **23**, 3272 (1975).
- 5) D. N. Jones, R. Grayshan, A. Hinchcliffe, and D. E. Kime, *J. Chem. Soc. C*, **1969**, 1208.
- 6) M. Ishiguro, A. Kajikawa, T. Haruyama, Y. Ogura, M. Okubayashi, M. Morisaki, and N. Ikekawa, *J. Chem. Soc., Perkin Trans. 1*, **1975**, 2295.

[Chem. Pharm. Bull.]
35(3) 996—1015(1987)

Synthesis of Carbapenems with a Sulfonyl Group in the C-6 Side-Chain and Their Biological Activity¹⁾

NORIKAZU TAMURA,* HIDEAKI NATSUGARI, YASUHIKO KAWANO,
YOSHIHIRO MATSUSHITA, KOUICHI YOSHIOKA,
and MICHIIHIKO OCHIAI

Central Research Division, Takeda Chemical Industries, Ltd.,
Yodogawa-ku, Osaka 532, Japan

(Received August 22, 1986)

A new type of 5,6-*cis*-carbapenems (racemic) having a sulfonyl group in the C-6 side-chain were synthesized by employing the synthetic methodology reported in our previous papers, and an alternative stereocontrolled synthesis of these 5,6-*cis*-carbapenems was achieved starting from 8-oxo-7-azabicyclo[4.2.0]oct-3-ene (14) *via* an intramolecular aldol condensation as the key step. Chiral 5,6-*cis*-carbapenems were also synthesized from (1*S*,6*R*)-8-oxo-7-azabicyclo[4.2.0]oct-3-ene (29), which was derived from *cis*-1,2,5,6-tetrahydrophthalic anhydride. The carbapenems thus obtained proved to be highly stable to the mouse kidney homogenate, and most of them showed good antibacterial activity as well as potent β -lactamase inhibitory activity.

Keywords—carbapenem; C-19393 derivative; aldol condensation; sulfonyl group; antibacterial activity; dehydropeptidase; mouse kidney homogenate; β -lactamase inhibitory activity

Since the discovery of thienamycin, many naturally occurring and synthetic carbapenem antibiotics have been reported.²⁾ Some of them possess highly potent, broad-spectrum *in vitro* antibacterial activity. However, because of their susceptibility to renal dehydropeptidase,³⁾ synthesis of carbapenems which are stable to the enzyme while retaining their excellent antibacterial activity has been desired.

In previous papers⁴⁾ we described a stereoselective synthesis of 5,6-*cis*-carbapenems related to C-19393⁵⁾ (carpetimycin⁶⁾) *via* reductive desulfurization utilizing an organotin hydride, and found that the antibacterial activity of 5,6-*cis*-carbapenems having a bulky substituent at the C-6 position is generally more potent than that of the 5,6-*trans*-isomers. By applying this synthetic methodology, versatile introduction of various new substituents into the C-6 position on the carbapenem nucleus seemed possible. As a part of our research program on the modification of the C-6 substituent to obtain a carbapenem with improved biological properties, we planned to synthesize a carbapenem having a sulfonyl group in the C-6 side-chain, expecting that the bulkiness and high polarity of the sulfonyl group might affect the interaction between the carbapenem and the enzyme. Here we report the synthesis and biological properties of carbapenems with a sulfonyl group in the C-6 side-chain.

Chemistry

Chart 1 shows the synthetic route to the *cis*-azetidinones (3a-1, 3b-1, 3c-1) from 2,2-dimethyl-3-oxa-1-azabicyclo[4.2.0]octan-8-one (1).⁷⁾ The β -lactam 1 was converted into the aldolization products (2a, 2b, 2c) by sulfonylation with lithium diisopropylamide (LDA) and diphenyl disulfide followed by an aldol reaction with methylthioacetaldehyde,⁸⁾ 3-thiacyclopentanone⁹⁾ and 4-thiacyclohexanone, respectively (79—83% yield). The aldolization products (2a, 2b, 2c) were subjected to desulfurization using triphenyltin hydride⁴⁾ in the presence of azobisisobutyronitrile (AIBN) (0.2 eq) to give the *cis*-isomers (3a-1, 3b-1, 3c-1) predominantly

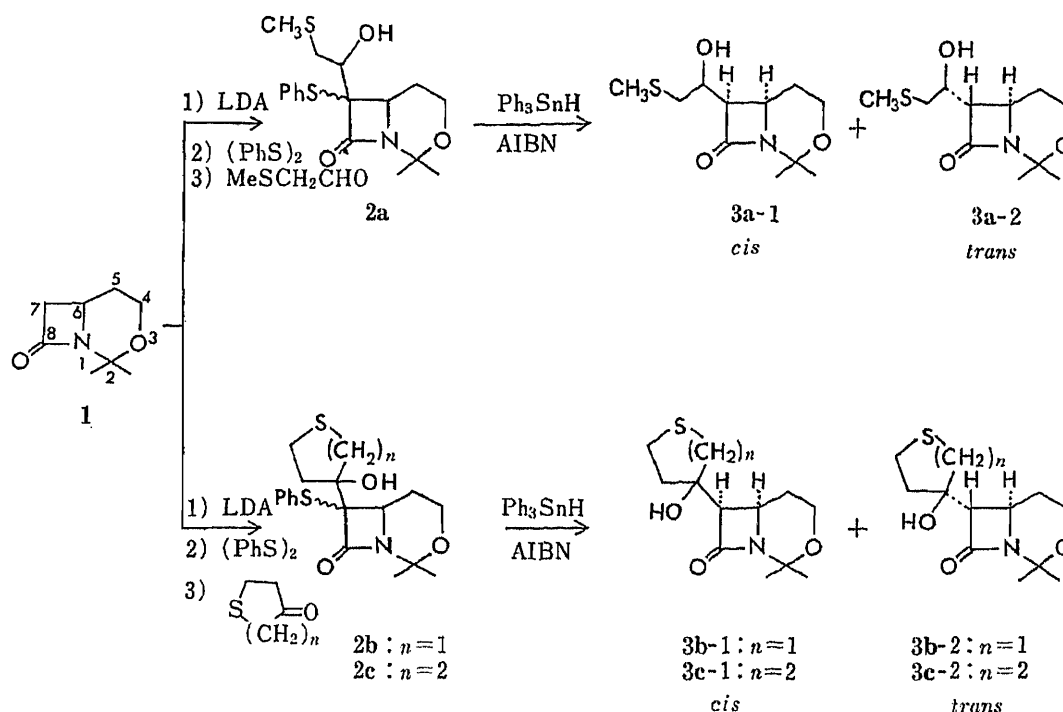


Chart 1

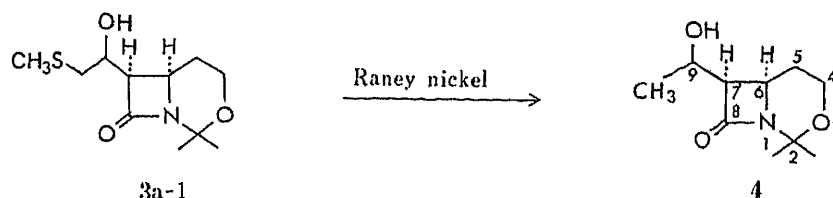


Chart 2

together with a small amount of the *trans*-isomers (**3a-2**, **3b-2**, **3c-2**) (*cis*:*trans* = 71:29—90:10). The *cis* and *trans*-isomers were separated by chromatography on silica gel. In this reaction, reductive cleavage of only the phenylthio group took place to give **3** selectively, whereas the alkylthio group in the C-7 side-chain of **2a**, **2b**, **2c** remained intact (Table II).

The relative configuration at the C-9 position of **3a-1** was confirmed by converting the compound into the desulfurized compound **4** (Chart 2). The nuclear magnetic resonance (NMR) spectrum of **4** was identical with that of the compound with R^* C-9 configuration.¹⁰ Therefore the relative configuration of the C-9 position of **3a-1** was determined to be S^* .¹¹

The exclusive formation of S^* is likely to be consistent with Martel *et al.*'s prediction¹² based on a six-membered transition state mechanism. The configuration of the C-9 position of **3b** has not been determined yet. Chart 3 shows the preparation of carbapenem **13a** from **3a-1**. The hydroxy group of **3a** was protected with a methoxyethoxymethyl (MEM) group.¹³ Oxidation of **5a** with *m*-chloroperbenzoic acid (*m*-CPBA) gave the sulfone **6a** (76%), which was converted into the carboxylic acid **7a** by Jones oxidation.⁴ The unstable carboxylic acid **7a** was transformed into the keto-ester **8a** (53%),¹⁴ which was converted into the diazo keto-ester **9a** (89%). Removal of the MEM group from **9a** was effected with titanium tetrachloride to form the cyclization precursor **10a** quantitatively. Construction of the carbapenem ring was achieved by the rhodium-catalyzed carbene insertion reaction.¹⁵ Reaction of **11a** with diphenyl chlorophosphate followed by treatment with *N*-acetylcysteamine in the presence of a base¹⁶ gave the carbapenem ester **12a** (Table VII). The *p*-nitrobenzyl (PNB) group of **12a** was

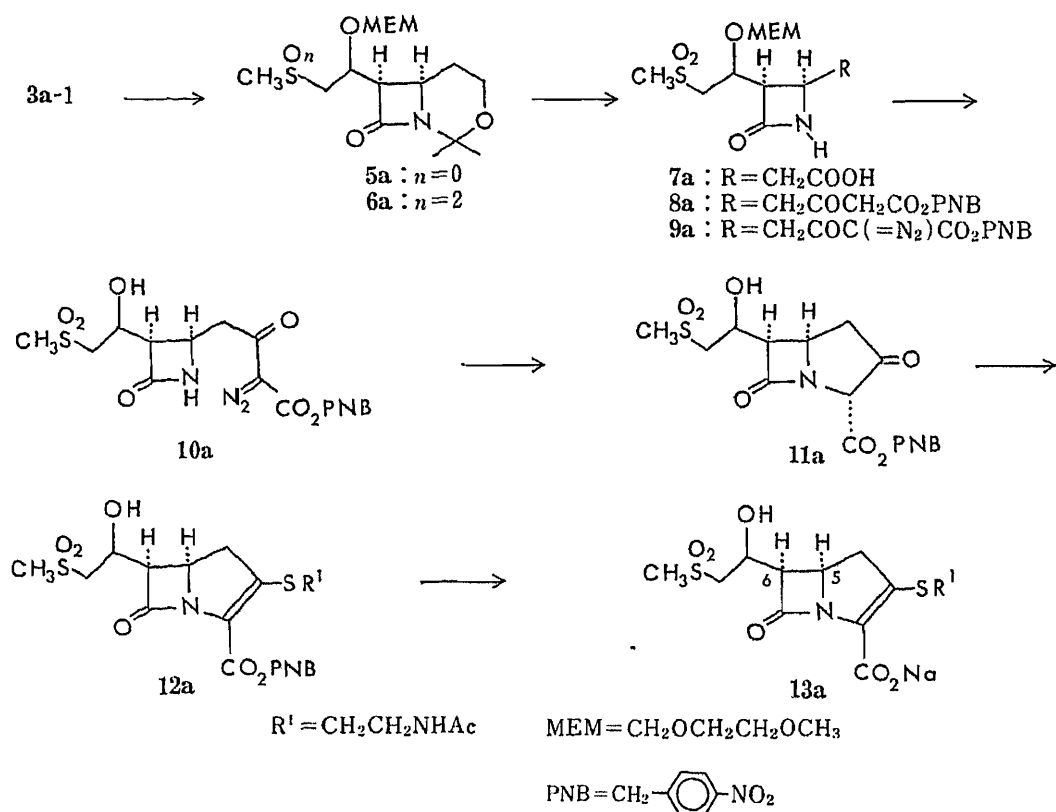


Chart 3

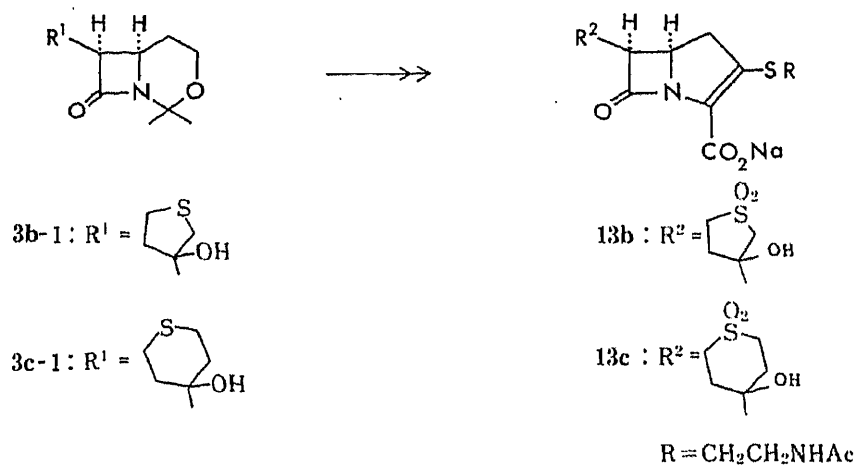


Chart 4

removed by hydrogenolysis using 10% palladium-charcoal to give the carboxylic acid (or sodium salt) of the carbapenem **13a**. The carbapenems (**13b** and **13c**) were also obtained from **3b-1** and **3c-1**, respectively, by a process similar to that employed for the conversion of **3a-1** into **13a** (Chart 4).

Our attention was then directed to establishing a new synthetic method in which the use of LDA and organotin hydride, and a tedious chromatographic separation of *cis* and *trans* isomers, could be avoided. Easily available *cis*-substituted 8-oxo-7-azabicyclo[4.2.0]oct-3-ene (**14**)¹⁷⁾ seemed to be a promising starting material for this purpose. A few syntheses of 5,6-*cis*-

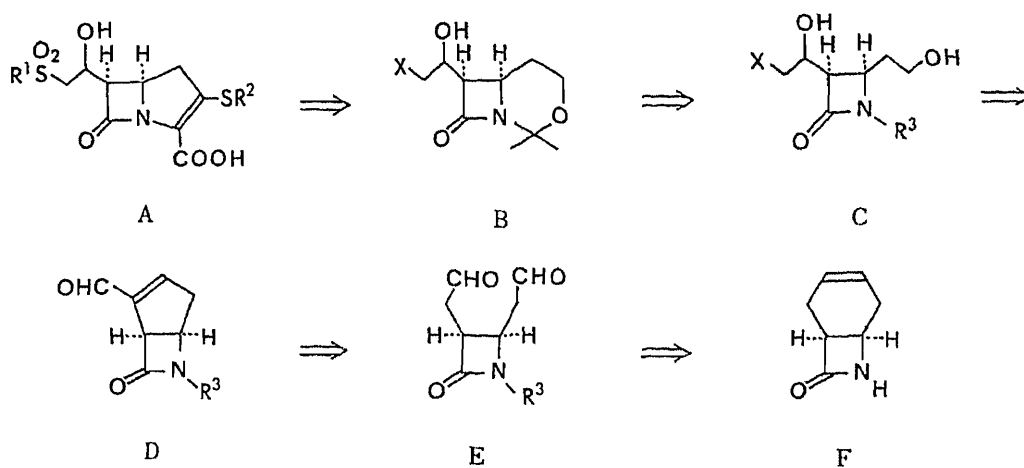


Chart 5

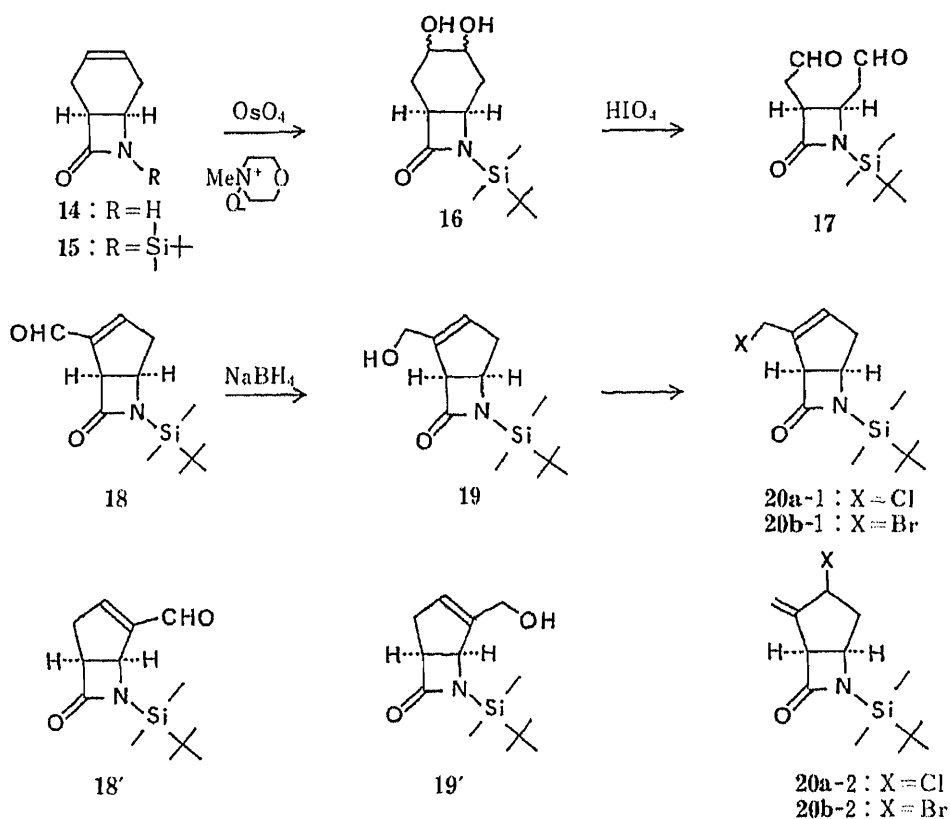


Chart 6

carbapenems from **14** have already been reported,¹⁸⁾ but these syntheses do not permit the introduction of a hydroxy group into the C-8 position of the side-chain. Key features of our retrosynthetic plan (Chart 5) include i) regioselective generation of the α,β -unsaturated aldehyde **D** via an intramolecular aldol condensation of the dialdehyde **E**, ii) conversion of **D** into the diol **C**, iii) formation of the bicyclic β -lactam **B**, and iv) synthesis of the carbapenem **A** from **B** by the same procedure as described before (Chart 3).

The synthesis of **20** was carried out as shown in Chart 6. After the protection of the amide nitrogen of the β -lactam **14** the silylated β -lactam **15** was subjected to osmylation with OsO_4 - N -methylmorpholine N -oxide¹⁹⁾ to furnish a diol **16**. The diol **16** was subsequently treated

with $\text{HIO}_4 \cdot 2\text{H}_2\text{O}$ to give a rather unstable dialdehyde **17** quantitatively. In the intramolecular aldol condensation, there is a possibility of the formation of two regioisomers (**18** and **18'**). Actually, by effecting the reaction with morpholine–camphoric acid,²⁰⁾ a *ca.* 1 : 1 mixture of **18** and **18'** was obtained (the ratio was determined by NMR after reduction with NaBH_4 to **19** and **19'**). On the other hand, treatment of **17** with piperidine–acetic acid²¹⁾ afforded **18** highly regioselectively but in a low yield (after reduction with NaBH_4 , **19** was isolated in 16% yield). An exclusive formation of the regioisomer **18** was achieved in a good yield by treating **17** with dibenzylammonium trifluoroacetate.²²⁾ Reduction of **18**, without purification, with NaBH_4 gave **19** in 57% yield from **16** (the other regioisomer **19'** was not observed by ^{13}C -NMR or high performance liquid chromatography (HPLC)). We presumed that this high regioselectivity might be due to the bulkiness of the *tert*-butyldimethylsilyl group. Ozonolysis of **15** also gave **17** which contained unidentified impurities (checked by thin layer chromatography (TLC)) and the subsequent aldol reaction, without purification, effected with dibenzylammonium trifluoroacetate afforded **19** in only 19% yield.

Treatment of **19** with thionyl chloride gave a mixture of two chlorinated isomers **20a-1** and **20a-2** in a ratio of *ca.* 1 : 1 (determined by NMR). Compound **20a-2** was formed *via* allylic rearrangement. Then, **19** was treated with *N*-bromosuccinimide–dimethylsulfide²³⁾ to afford the bromide **20b-1** in 67% yield without concomitant formation of the allylic rearranged product **20b-2**. Ozonolysis of **20b-1** and subsequent reduction with NaBH_4 gave the diol **21** in 97% yield (for the side-chain stereochemistry, *vide post*), from which the silyl group was removed with potassium fluoride to furnish the diol **22** in 92% yield. The diol **22** was treated with 2,2-dimethoxypropane to give the acetonide **23** in 63% yield. Since the bromo atom in the side-chain is susceptible to nucleophiles, **23** serves as a versatile intermediate for preparing a new type of carbapenems with a variety of functional groups in the C-6 side-chain. The acetonide **23** was converted into the sulfenyl compound **24** in a good yield by treatment with a thiol compound in the presence of a base (Chart 7). Preparation of the carbapenems **13** from **24** was achieved in the same manner as shown in Chart 3.

Since the synthesis of the racemic 5,6-*cis*-carbapenem was established, we concentrated our efforts on the synthesis of optically active 5,6-*cis*-carbapenems. Chart 8 shows the synthesis of the desired chiral bicyclic β -lactam **29** from the racemic compound **25**, which was derived from commercially available *cis*-1,2,5,6-tetrahydrophthalic anhydride. Enantiomer resolution of the racemic compound **25** with cinchonidine provided the chiral half ester **26a**²⁴⁾ and its enantiomer **26b**.²⁴⁾ The half ester **26a** was converted into **27** by Curtius rearrangement

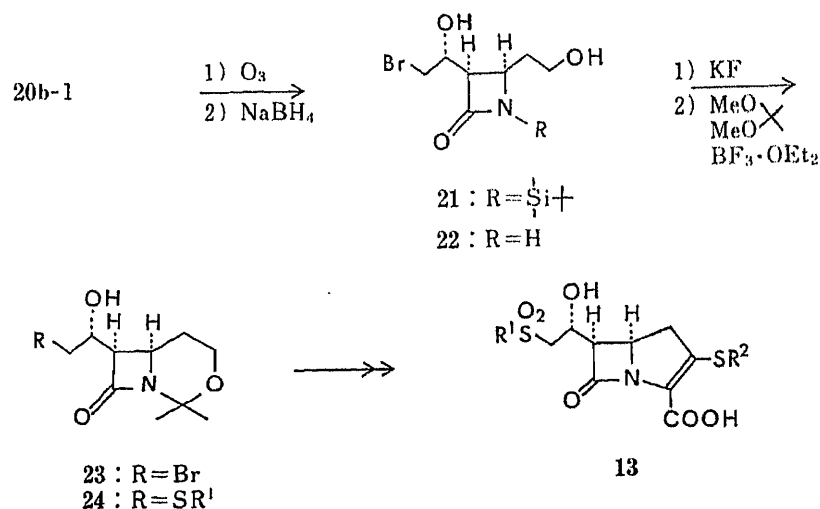


Chart 7

in 79% yield, and **27** was then hydrolyzed to the β -amino acid **28** in 76% yield. The β -amino acid **28** was transformed into the optically active β -lactam **29**²⁵⁾ with $\text{Ph}_3\text{P}-(\text{PyS})_2/\text{CH}_3\text{CN}$.²⁶⁾ On the other hand, **26b** was also converted into **29** via esterification (92%), hydrolysis (93%), Curtius rearrangement (96%), and deprotection (73%). By the strategy we have described here, both the enantiomers (**26a** and **26b**) resolved from **25** are wholly utilized in preparing the optically active compound **29**.

The same sequence of reactions employed in the preparation of **23** from **14** was applied to the optically active compound **29** to give the desired optically active β -lactam **36**. The stereochemistry of **36** was confirmed to be 6*R*, 7*R*, 9*R* by a single crystal X-ray analysis.²⁷⁾ The

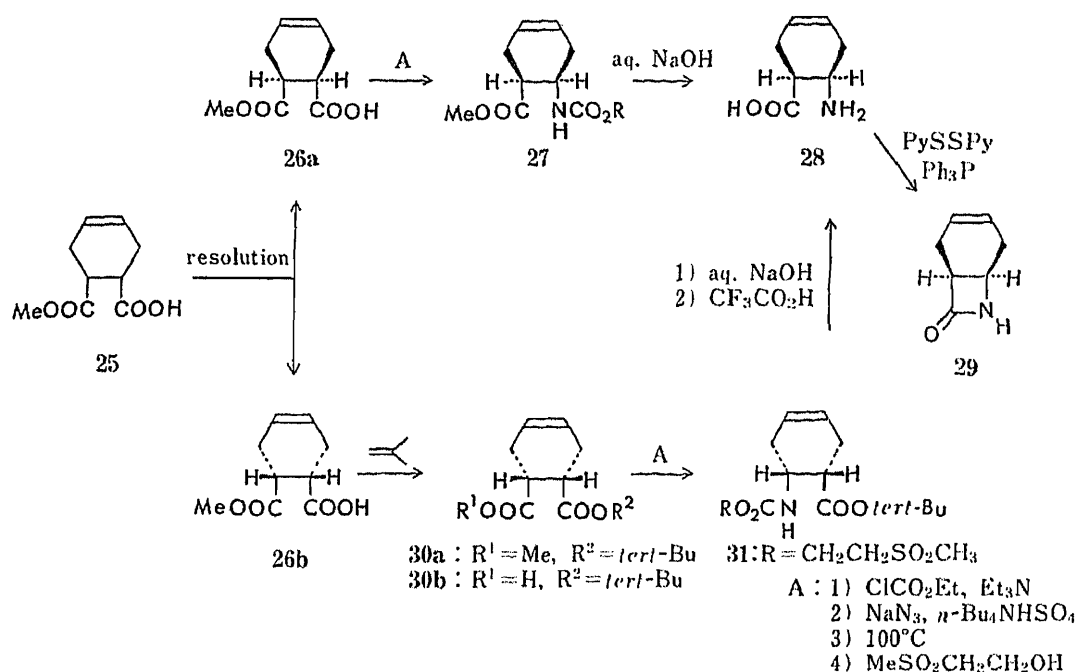


Chart 8

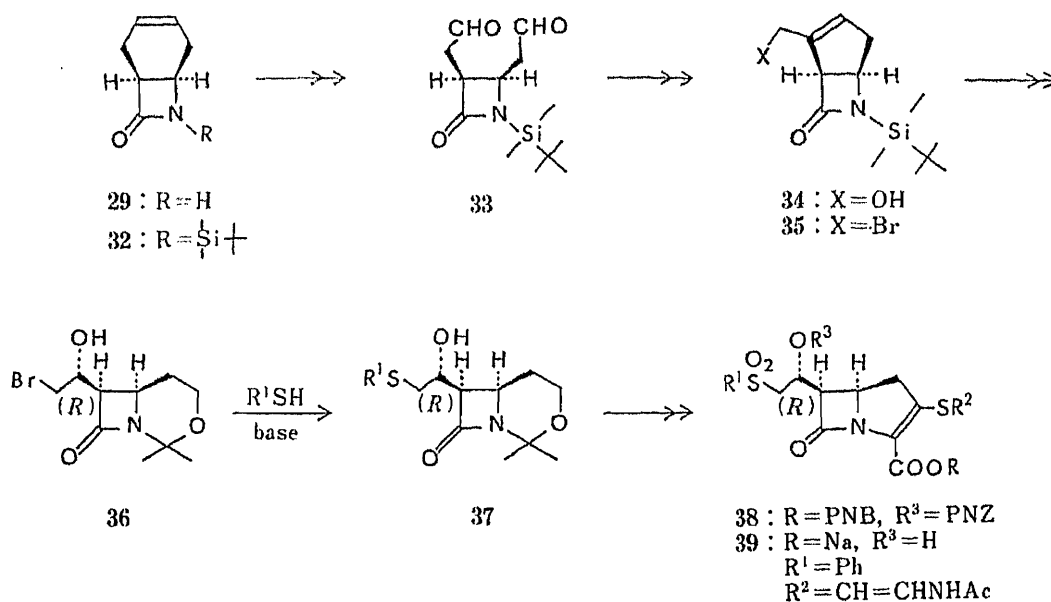
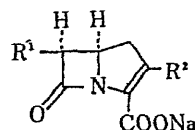


Chart 9

TABLE I. Biological Activities of Carbapenems with a Sulfonyl Group in the C-6 Side-Chain



Biological activities	Compound					
	R ¹	SCH ₂ CH ₂ NHAc 13b-1	SCH=CHNHAc 13b-2	SCH ₂ CH ₂ NHAc 13a	SCH=CHNHAc 39	SCH=CHNHAc C-19393 H ₂
Antibacterial activity						
<i>in vitro</i> (MIC: μg/ml: 10 ⁸ CFU) ^{a)}						
<i>S. aureus</i> FDA 209P		3.13	1.56	1.56	1.56	0.78
<i>E. coli</i> O-111		0.39	0.39	0.39	0.78	0.1
<i>C. freundii</i> IFO 12681		3.13	1.56	3.13	1.56	0.2
<i>K. pneumoniae</i> DT		3.13	0.78	1.56	3.13	0.78
<i>in vivo</i> (ED ₅₀ : mg/kg) ^{b)}						
<i>E. coli</i> O-111		0.329	0.39	—	—	50
β-Lactamase inhibitory activity						
(ID ₅₀ : μg/ml) ^{c)}						
Source and type of β-lactamase						
<i>S. aureus</i> 1840	PCase ^{d)}	0.14	0.0022	0.21	0.65	43
<i>E. coli</i> TN 713	PCase	0.014	0.0035	3.2	> 5	3.0
<i>E. cloacae</i> TN 1282	CSase ^{e)}	0.19	0.040	0.025	0.12	34
<i>P. vulgaris</i> GN 4413	CSase	0.25	0.055	1.7	2.5	0.60
Half-life in mouse kidney homogenate (min)		> 120	> 120	> 120	> 120	15

a) The MICs were determined by a standard dilution method in Trypticase soy agar (BBL).²⁸⁾ b) Protective effect against experimental intraperitoneal infection in mice. c) The ID₅₀s (concentrations required to cause 50% inhibition) were determined by microiodometric method.²⁹⁾ d, e) PCase, penicillinase; CSase, cephalosporinase.

reduction of the ozonide of **35** with NaBH_4 was proved to proceed selectively to give **9R** stereochemistry. Optically active carbapenems with a sulfonyl group in the C-6 side-chain (**39**) were synthesized from **36** by applying the same sequence of reactions as employed for the synthesis of the racemic compound (Chart 9).

Biological Activity

The *in vitro* antibacterial activity of the carbapenems with a sulfonyl group in the C-6 side-chain against several bacteria is shown in Table I. Their β -lactamase inhibitory (BLI) activity and stability to the mouse kidney homogenate are also given. It should be stressed that these carbapenems are highly stable to the mouse kidney homogenate (half-life > 120 min), which should reasonably reflect the behavior towards renal dehydropeptidase. Most of the compounds showed good antibacterial activity as well as strong BLI activity. Carbapenems **13a-1** and **13b-2** showed a good *in vivo* protective effect in mouse infected with *Escherichia coli* O-111, which seems to reflect the *in vitro* antibacterial activity.

Experimental

Melting points were determined with a Yanagimoto melting point apparatus and are uncorrected. Infrared (IR) spectra were measured with a Hitachi 215 spectrophotometer. $^1\text{H-NMR}$ spectra were taken on a Varian EM-390 (90 MHz) and a JEOL GK-400FT (400 MHz) spectrometer, and $^{13}\text{C-NMR}$ spectra were measured with a JEOL GK-400FT (100 MHz) spectrometer with tetramethylsilane as an internal standard. Abbreviations are follows: s = singlet; br s = broad singlet; d = doublet; dd = doublet of doublets; t = triplet; q = quartet. Ultraviolet (UV) spectra were taken with a Hitachi 557 spectrophotometer. Extracted solutions were dried over sodium sulfate. The MICs (minimum inhibitory concentrations) were determined by a standard dilution method in Trypticase soy agar (BBL) as described previously.²⁸⁾ The BLI activity were determined as described previously and expressed in terms of ID_{50} , the concentration required to inhibit β -lactamase activity by 50%.²⁹⁾

7-(1-Hydroxy-2-methylthioethyl)-2,2-dimethyl-3-oxa-7-phenylthio-1-azabicyclo[4.2.0]octan-8-one (2a) and 7-(1-Hydroxythiacycloalkyl)-2,2-dimethyl-3-oxa-7-phenylthio-1-azabicyclo[4.2.0]octan-8-one (2b, c)—As a typical example, the preparation of **2a** from **1** is described. A solution of 2,2-dimethyl-3-oxa-1-azabicyclo[4.2.0]octan-8-one (**1**) (1.00 g, 6.45 mmol) in dry tetrahydrofuran (THF) (20 ml) was added at -78°C to a solution of LDA, prepared from *n*-butyl lithium (9.6 ml of 15% hexane solution, 14.7 mmol) and diisopropylamine (2.2 ml, 15.7 mmol) under a nitrogen atmosphere, and the mixture was stirred for 15 min at -78°C . A solution of diphenyl disulfide (1.42 g, 6.50 mmol) in dry THF (6 ml) was added dropwise to this enolate over 5 min at -78°C . The mixture was stirred for 15 min at this temperature, then methylthioacetaldehyde³⁰⁾ (1.16 g, 12.9 mmol) was added. The mixture was stirred for 30 min and poured into a mixture of 3% acetic acid (60 ml) and AcOEt (60 ml) at 0°C with stirring. The organic phase was separated and the aqueous phase was further extracted with AcOEt. The combined extracts were washed successively with 0.5N NaOH, water and sat. aq. NaCl, and dried. After evaporation of the solvent, the residue was subjected to chromatography on silica gel. Elution with hexane-AcOEt (1:2, v/v) gave **2a** (1.88 g, 83%) as colorless crystals (a mixture of two isomers at C-7). Compounds **2b** and **2c** were synthesized in a similar manner, by using 3-thiacyclopentanone³¹⁾ and 4-thiacyclohexanone, respectively, in place of methylthioacetaldehyde. The stereochemistry of **2b** at C-9 has not been determined.

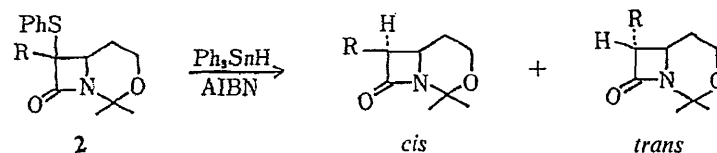
2a: Colorless prism, mp $83\text{--}85^\circ\text{C}$. Yield 83%. IR $\nu_{\text{max}}^{\text{KBr}} \text{cm}^{-1}$: 1730. $^1\text{H-NMR}$ (CDCl_3) δ : isomer A: 0.79, 1.58 (each 3H, $2 \times s$, $2 \times \text{Me}$), 1.6—2.0 (2H, m, $\text{C}_5\text{-H}_2$), 2.15 (3H, s, SMe), 2.89 (2H, d, $J=7.5$ Hz, CH_2S), 3.3—4.0 (3H, m, $\text{C}_4\text{-H}_2$, $\text{C}_6\text{-H}$), 4.31 (1H, dd, $J=7.5$, 4.8 Hz, SCH_2CH), 7.2—7.6 (5H, m, aromatic protons). Isomer B: 1.47, 1.76 (each 3H, $2 \times s$, $2 \times \text{Me}$), 1.91 (3H, s, SMe), 1.6—2.0 (2H, m, $\text{C}_5\text{-H}_2$), 2.96 (2H, m, CH_2S), 3.7—4.0 (3H, m, $\text{C}_4\text{-H}_2$, $\text{C}_6\text{-H}$), 4.13 (1H, dd, $J=5.1$, 10.5 Hz, SCH_2CH), 7.2—7.7 (5H, m, aromatic protons). *Anal.* Calcd for $\text{C}_{17}\text{H}_{23}\text{NO}_3\text{S}_2$: C, 57.76; H, 6.56; N, 3.96; S, 18.14. Found: C, 57.69; H, 6.68; N, 4.14; S, 18.38.

2b: Colorless oil. Yield 83%. IR $\nu_{\text{max}}^{\text{liquid}} \text{cm}^{-1}$: 1740. $^1\text{H-NMR}$ (CDCl_3) δ : 1.46, 1.56 (each 3H, $2 \times s$, $2 \times \text{Me}$), 1.5—1.9 (2H, m, $\text{C}_5\text{-H}_2$), 2.2—2.4 (2H, m, CH_2), 2.8—3.2 (4H, m, CH_2SCH_2), 3.8—4.2 (3H, m, $\text{C}_4\text{-H}_2$, $\text{C}_6\text{-H}$), 7.1—7.9 (5H, m, aromatic protons).

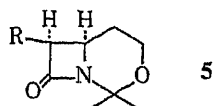
2c: Colorless prism, mp $191\text{--}192^\circ\text{C}$. Yield 79%. IR $\nu_{\text{max}}^{\text{KBr}} \text{cm}^{-1}$: 1730. $^1\text{H-NMR}$ (CDCl_3) δ : 1.38, 1.48 (each 3H, $2 \times s$, $2 \times \text{Me}$), 1.6 (2H, m, $\text{C}_5\text{-H}_2$), 1.7—3.3 (8H, m, $4 \times \text{CH}_2$), 3.7—4.2 (3H, m, $\text{C}_4\text{-H}_2$, $\text{C}_6\text{-H}$), 7.1—7.9 (5H, m, aromatic protons). *Anal.* Calcd for $\text{C}_{19}\text{H}_{25}\text{NO}_3\text{S}_2$: C, 60.13; H, 6.64; N, 3.69; S, 16.89. Found: C, 60.39; H, 6.49; N, 3.68; S, 17.17.

7-(1-Hydroxy-2-methylthioethyl)-2,2-dimethyl-3-oxa-1-azabicyclo[4.2.0]octan-8-one (3a) and 7-(1-Hydroxythiacycloalkyl)-2,2-dimethyl-3-oxa-1-azabicyclo[4.2.0]octan-8-one (3b, c)—As a typical example, the preparation of **3a** from **2a** is described. A mixture of **2a** (1.32 g, 3.73 mmol), AIBN (120 mg, 0.73 mmol), triphenyltin hydride (2.62 g,

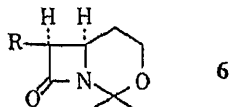
TABLE II. 2,2-Dimethyl-7-(substituted-alkyl)-3-oxa-1-azabicyclo[4.2.0]octan-8-ones (3)



Compound	R	Stereo-chemistry at C(6) and C(7)	Yield (%)	mp (°C)	IR cm^{-1} (KBr)	NMR (CDCl_3) δ	Analysis (%) Found (Calcd)			
							C	H	N	S
3a-1		<i>cis</i>	70	91—92.5	1720	1.38, 1.72 (each 3H, 2 × s, 2 × CH ₃), 2.15 (3H, s, SCH ₃), 1.5—2.2 (2H, m, CH ₂), 2.68 (2H, d, <i>J</i> =6 Hz, SCH ₂), 3.33 (1H, dd, <i>J</i> =6.8, 5.3 Hz, CH—CO), 3.6—4.0 (3H, m, OCH ₂ , CH—N), 4.12 (1H, m, CH—N)	53.85 (53.85)	7.81 (7.81)	5.82 (5.71)	13.06 (13.07)
3a-2		<i>trans</i>	19	106—107	1740	1.40, 1.71 (each 3H, 2 × s, 2 × CH ₃), 2.12 (3H, s, SCH ₃), 1.5—2.1 (2H, m, CH ₂), 2.3—3.2 (3H, m, SCH ₂ , CH—CO), 3.5—4.2 (4H, m, OCH ₂ , CH—N, CH—O)	54.03 (53.85)	7.92 (7.81)	5.70 (5.71)	12.77 (13.07)
3b-1		<i>cis</i>	80	113—115	1740	1.40, 1.74 (each 3H, 2 × s, 2 × CH ₃), 1.6—2.2 (2H, m, CH ₂), 2.5—3.2 (6H, m, 3 × CH ₂), 3.36 (1H, d, <i>J</i> =6 Hz, CHCO), 3.7—4.1 (3H, m, CHN, CH ₂ O)	56.28 (56.01)	7.35 (7.44)	5.40 (5.44)	12.65 (12.46)
3b-2		<i>trans</i>	9	145—147	1720	1.40, 1.69 (each 3H, 2 × s, 2 × CH ₃), 1.6—2.0 (2H, m, CH ₂), 2.3—3.2 (7H, m, 2 × CH ₂ , CH—CO), 3.5—4.0 (3H, m, CHN, CH ₂ O)	56.13 (56.01)	7.38 (7.44)	5.37 (5.44)	
3c-1		<i>cis</i>	64	133—134	1740	1.38, 1.73 (each 3H, 2 × s, 2 × CH ₃), 1.6—3.3 (10H, m, 5 × CH ₂), 3.20 (1H, d, <i>J</i> =6 Hz, CH—CO), 3.6—3.9 (3H, m, OCH ₂ , CH—N)	57.30 (57.54)	7.85 (7.80)	5.42 (5.16)	12.05 (11.81)
3c-2		<i>trans</i>	26	163—164	1720	1.40, 1.71 (each 3H, 2 × s, 2 × CH ₃), 1.6—3.3 (10H, m, 5 × CH ₂), 2.81 (1H, d, <i>J</i> =2 Hz, CH—CO), 3.55 (1H, m, CH—N), 3.7—3.9 (2H, m, OCH ₂)	57.21 (57.54)	7.87 (7.80)	5.49 (5.16)	

TABLE III. (6*R**,7*R**)-2,2-Dimethyl-7-[1-(2-methoxyethoxymethoxy)substituted alkyl]-3-oxa-1-azabicyclo[4.2.0]octan-8-ones (5)

Compound	R	IR cm^{-1} (liquid)	NMR (CDCl_3) δ
5a		1750	1.37, 1.70 (each 3H, 2 \times s, 2 \times CH_3), 2.14 (3H, s, SCH_3), 1.5—2.1 (2H, m, CH_2), 2.75 (2H, dd, $J=5.3, 5.3$ Hz, SCH_2), 3.38 (3H, s, OCH_3), 3.4—4.0 (8H, m, 3 \times OCH_2 , CH-CO , CH-N), 4.2 (1H, m, CH-O), 4.87 (2H, m, OCH_2O)
5b		1745	1.38, 1.71 (each 3H, 2 \times s, 2 \times CH_3), 1.70 (2H, m, CH_2), 2.0—3.2 (6H, m, 3 \times CH_2), 3.17 (1H, d, $J=5$ Hz, CH-CO), 3.38 (3H, s, OCH_3), 3.3—3.9 (7H, m, 3 \times OCH_2 , CH-N), 4.90 (2H, br s, OCH_2O)
5c		1745	1.38, 1.71 (each 3H, 2 \times s, 2 \times CH_3), 1.5—3.1 (10H, m, 5 \times CH_2), 3.38 (3H, s, OCH_3), 3.0—4.0 (8H, m, 3 \times OCH_2 , CH-CO , CH-N), 4.93 (2H, m, OCH_2O)

TABLE IV. (6*R**,7*R**)-2,2-Dimethyl-7-(substituted-sulfonylalkyl)-3-oxa-1-azabicyclo[4.2.0]octan-8-ones (6)

Compound	R	Yield ^{a)} (%)	IR cm^{-1} (liquid)	NMR (CDCl_3) δ
6a		76	1745	1.37, 1.70 (each 3H, 2 \times s, 2 \times CH_3), 2.14 (3H, s, SCH_3), 1.5—2.1 (2H, m, CH_2), 2.75 (2H, dd, $J=5.3, 5.3$ Hz, SCH_2), 3.38 (3H, s, OCH_3), 3.4—4.0 (8H, m, 3 \times OCH_2 , CH-CO , CH-N), 4.2 (1H, m, CH-O), 4.87 (2H, m, OCH_2O)
6b		86	1750	1.38, 1.69 (each 3H, 2 \times s, 2 \times CH_3), 1.9 (2H, m, CH_2), 3.36 (3H, s, OCH_3), 3.0—4.0 (12H, m, 2 \times SO_2CH_2 , 3 \times OCH_2 , CH-CO , CH-N), 4.86 (2H, s, OCH_2O)
6c		Quantitatively	1740	1.38, 1.70 (each 3H, 2 \times s, 2 \times CH_3), 1.6—3.0 (8H, m, 3 \times CH_2 , CHSO_2CH), 3.1—4.0 (10H, m, CHSO_2CH , 3 \times OCH_2 , CH-CO , CH-N), 3.36 (3H, s, OCH_3), 5.01 (2H, m, OCH_2O)

a) Overall yields from 3.

7.46 mmol) and acetone (45 ml) was refluxed for 5 h under a nitrogen atmosphere. After further addition of triphenyltin hydride (1.00 g, 2.84 mmol), the mixture was refluxed for an additional 14 h. The solvent was evaporated off and the residue was subjected to chromatography on silica gel. Elution with hexane–AcOEt (4:1—1:1, v/v) afforded the *cis*-azetidinones 3a-1 (643 mg, 70%) and the *trans*-azetidinone 3a-2 (172 mg, 19%), each as colorless prisms. Compounds 2b and 2c were desulfurized to give 3b and 3c, respectively, in a similar manner. The results are summarized in Table II.

Desulfurization of 3a-1—A mixture of 3a-1 (80 mg, 0.33 mmol), Raney nickel (Kawaken Fine Chemical,

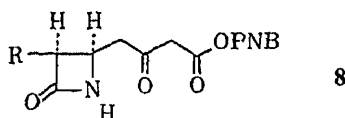
NDHT-90) (1 ml) and THF (7 ml) was refluxed for 5 h. The Raney nickel was filtered off and the filtrate was concentrated. The concentrate was subjected to chromatography on silica gel. Elution with AcOEt-hexane (1:1—2:1, v/v) afforded **4** as a colorless oil (44 mg, 67%). ¹H-NMR (acetone-*d*₆) δ: 1.15 (3H, d, *J*=6 Hz, Me), 1.36, 1.63 (each 3H, 2 × s, 2 × Me), 1.8 (2H, m, C₅-H₂), 2.8 (1H, br s, OH), 3.05 (1H, dd, *J*=5, 7.5 Hz, C₇-H), 3.6—4.3 (4H, m, C₄-H, C₆-H, CH-O).

(6*R**,7*R**)-7-[1-(2-Methoxyethoxymethoxy)-2-methylthioethyl]-2,2-dimethyl-3-oxa-1-azabicyclo[4.2.0]octan-8-one (**5a**) and (6*R**,7*R**)-7-[1-(2-Methoxyethoxymethoxy)thiacycloalkyl]-2,2-dimethyl-3-oxa-1-azabicyclo[4.2.0]octan-8-one (**5b**, **c**)—As a typical example, the preparation of **5a** from **3a** is described. A mixture of the azetidinone **3a** (286 mg, 1.17 mmol) diisopropylethylamine (0.63 ml, 3.62 mmol), 2-(methoxyethoxy)methyl (MEM) chloride (0.42 ml, 3.67 mmol) and CH₂Cl₂ (8.5 ml) was allowed to stand at room temperature for 140 h under a nitrogen atmosphere. The mixture was then washed successively with water, 2% acetic acid, sat. aq. NaHCO₃, water and sat. aq. NaCl, and dried. The solvent was evaporated off to give the azetidinone **5a** (quantitatively) as a pale yellow oil, which was used in the subsequent oxidation without further purification. The results are summarized in Table III.

(6*R**,7*R**)-7-[1-(2-Methoxyethoxymethoxy)-2-methylsulfonyl-ethyl]-2,2-dimethyl-3-oxa-1-azabicyclo[4.2.0]octan-8-one (**6a**) and (6*R**,7*R**)-7-[1-(2-Methoxyethoxymethoxy)thiacycloalkyl-*S,S*-dioxide]-2,2-dimethyl-3-oxa-1-azabicyclo[4.2.0]octan-8-one (**6b**, **c**)—As a typical example, the preparation of **6a** from **5a** is described. A solution of **5a** prepared from **3a-1** (274 mg, 1.12 mmol) in CH₂Cl₂ (9 ml) was treated at 0 °C with *m*-CPBA (*ca.* 70%) (597 mg). After being stirred for 2 h, the mixture was washed successively with sat. aq. NaHCO₃, water and sat. aq. NaCl. The organic phase was dried and evaporated. The residue was subjected to chromatography on silica gel. Elution with AcOEt afforded **6a** (310 mg, 76% from **3a-1**) as a colorless oil. The azetidinones **6b** and **6c** were similarly prepared from **5b** and **5c**, respectively. The results are summarized in Table IV.

(3*R**,4*R**)-4-Carboxymethyl-3-[1-(2-methoxyethoxymethoxy)-2-methylsulfonyl-ethyl]azetidin-2-one (**7a**) and (3*R**,4*R**)-4-Carboxymethyl-3-[1-(2-methoxyethoxymethoxy)thiacycloalkyl-*S,S*-dioxide]azetidin-2-one (**7b**, **c**)—As a typical example, the preparation of **7a** from **6a** is described. An 8*N* solution of Jones reagent (0.43 ml) was added dropwise to a stirred, cooled (0 °C) solution of the azetidinone **6a** (226 mg, 0.73 mmol) in acetone (4 ml). The mixture was stirred for 7 h at 0 °C. After the addition of isopropyl alcohol (0.3 ml), the mixture was stirred for 10 min at 0 °C

TABLE V. (3*R**,4*R**)-3-(Substituted-sulfonylalkyl)-4-(*p*-nitrobenzyloxycarbonyl)-2-oxopropyl)azetidin-2-ones (**8**)



Compound	R	Yield ^{a)} (%)	IR cm ⁻¹ (liquid)	NMR (CDCl ₃) δ
8a		53	1720, 1760	2.96 (3H, s, SO ₂ CH ₃), 3.11 (2H, d, <i>J</i> =7 Hz, CH ₂ CO), 3.33 (3H, s, OCH ₃), 3.57 (2H, s, COCH ₂ CO), 3.1—4.0 (7H, m, OCH ₂ CH ₂ O, SO ₂ CH ₂ , CHCO), 4.1 (1H, m, CH-N), 4.4 (1H, m, CH-O), 4.83 (2H, s, OCH ₂ O), 5.25 (2H, s, OCH ₂ Ar), 6.33 (1H, br, NH), 7.50 (2H, d, <i>J</i> =9 Hz, arom H), 8.20 (2H, d, <i>J</i> =9 Hz, arom H)
8b		71	1720—1750	2.6 (2H, m, CH ₂), 3.30 (3H, s, OCH ₃), 3.59 (2H, s, CO-CH ₂ CO), 3.2—3.9 (11H, m, OCH ₂ CH ₂ O, 2 × SO ₂ CH ₂ , CH-CO, CH ₂ CO), 4.2 (1H, m, CHN), 4.76 (2H, s, CH ₂ Ar), 6.86 (1H, br, NH), 7.55 (2H, d, <i>J</i> =9 Hz, arom H), 8.22 (2H, d, <i>J</i> =9 Hz, arom H)
8c		60	1720—1750	2.0—3.0 (6H, m, 2 × CH ₂ , CHSCH), 3.34 (3H, s, OCH ₃), 3.63 (2H, s, COCH ₂ CO), 3.1—3.9 (9H, m, CH ₂ CO, CHCO, OCH ₂ CH ₂ O, CHSCH), 4.2 (1H, m, CHN), 4.92 (2H, m, OCH ₂ O), 5.30 (2H, s, OCH ₂ Ar), 6.5 (1H, br, NH), 7.54 (2H, d, <i>J</i> =9 Hz, arom H), 8.23 (2H, d, <i>J</i> =9 Hz, arom H)

a) The yields are based on **6**.

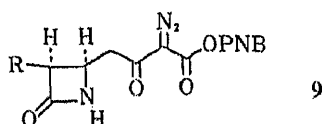
and was then diluted with CH_2Cl_2 (10 ml). Insoluble materials were filtered off and the filtrate was concentrated. The concentrate was dissolved in CHCl_3 (10 ml) and the solution was dried and evaporated to dryness to give the acid **7a** (205 mg, 82%) as a colorless oil. Similar oxidation of the azetidinones **6b** and **6c** gave the acids **7b** and **7c**, respectively. These compounds were used in the subsequent reactions without purification. IR $\nu_{\text{max}}^{\text{liquid}} \text{cm}^{-1}$: 1700—1760.

(3*R**,4*R**)-3-[1-(2-Methoxyethoxymethoxy)-2-methylsulfonyl ethyl]-4-(*p*-nitrobenzyloxycarbonyl-2-oxopropyl)-azetidin-2-one (**8a**) and (3*R**,4*R**)-3-[1-(2-Methoxyethoxymethoxy)thiacycloalkyl-*S,S*-dioxide]-4-(*p*-nitrobenzyloxycarbonyl-2-oxopropyl)azetidin-2-one (**8b, c**)—As a typical example, the preparation of **8a** from **7a** is described. *N,N*-Carbonyldiimidazole (132 mg, 0.814 mmol) was added to a solution of the acid **7a** (230 mg, 0.68 mmol) in dry THF (9 ml). After the mixture had been stirred for 6 h at room temperature under a nitrogen atmosphere, magnesium *p*-nitrobenzyl malonate (407 mg, 0.81 mmol) was added. The mixture was stirred for 20 h at room temperature under a nitrogen atmosphere and was then diluted with AcOEt and washed successively with dil. HCl, water, sat. aq. NaHCO_3 , and water. The organic phase was dried, the solvent was evaporated off, and the residue was chromatographed on silica gel. Elution with AcOEt gave the azetidinone **8a** (187 mg, 53%) as a pale yellow oil. The results are summarized in Table V.

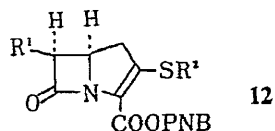
(3*R**,4*R**)-4-[3-(Diazo-3-(*p*-nitrobenzyloxycarbonyl)-2-oxopropyl)-3-[1-(2-methoxyethoxymethoxy)-2-methylsulfonyl ethyl]azetidin-2-one (**9a**) and (3*R**,4*R**)-4-[3-Diazo-3-(*p*-nitrobenzyloxycarbonyl)-2-oxopropyl]-3-[1-(2-methoxyethoxymethoxy)thiacycloalkyl-*S,S*-dioxide]azetidin-2-one (**9b, c**)—As a typical example, the preparation of **9a** from **8a** is described. A solution of *p*-toluenesulfonyl azide (84 mg, 0.43 mmol) in dry acetonitrile (1 ml) and Et_3N (0.19 ml, 1.36 mmol) were added to a stirred, cooled (0 °C) solution of the azetidinone **8a** (187 mg, 0.36 mmol) in dry acetonitrile (6 ml). After being stirred for 1 h at room temperature, the mixture was diluted with AcOEt, washed with sat. aq. NaCl, and dried. After evaporation of the solvent, then residue was chromatographed on silica gel. Elution with AcOEt gave the diazo-azetidinone **9a** (172 mg, 89%) as a pale yellow oil. The diazo-azetidinones **9b** and **9c** were synthesized in a similar manner. The results are summarized in Table VI.

p-Nitrobenzyl (5*R**,6*R**)-2-Acetamidoethylthio-6-[1-hydroxy-2-methylsulfonyl ethyl]-2-carbapenam-3-carboxylate (**12a**) and *p*-Nitrobenzyl (5*R**,6*R**)-2-(Substituted)thio-6-(1-hydroxythiacycloalkyl-*S,S*-dioxide)-2-carbapenam-3-carboxylate (**12b, c**)—As a typical example, the preparation of **12b-1** from **9b** is described. Titanium tetrachloride (1.30 ml, 11.8 mmol) was added to a stirred, cooled (0 °C) solution of the diazo-azetidinone **9b** (72 mg, 0.13 mmol) in CH_2Cl_2 (18 ml) under a nitrogen atmosphere. The mixture was stirred vigorously for 1 h at 0 °C, then AcOEt (30 ml) was added, and the reaction mixture was stirred for an additional 1 h at 0 °C and poured into a stirred, cooled (0 °C)

TABLE VI. (3*R**,4*R**)-3-(Substituted-sulfonylalkyl)-4-[3-diazo-3-(*p*-nitrobenzyloxycarbonyl)-2-oxopropyl]azetidin-2-ones (**9**)



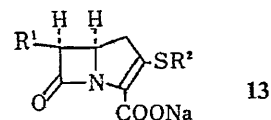
Compound	R	Yield (%)	IR cm^{-1} (liquid)	NMR (CDCl_3) δ
9a		89	2140, 1750	2.96 (3H, s, SO_2CH_3), 3.35 (3H, s, OCH_3), 3.2—4.0 (9H, m, CHCO , CH_2CO , $\text{OCH}_2\text{CH}_2\text{O}$, SO_2CH_2), 4.15 (1H, m, CHN), 4.35 (1H, m, CH-O), 4.87 (2H, ABq, $J=10.5$, 7.5 Hz, OCH_2O), 5.33 (2H, s, OCH_2Ar), 6.21 (1H, br, NH), 7.51 (2H, d, $J=9$ Hz, arom H), 8.23 (2H, d, $J=9$ Hz, arom H)
9b		90	2140, 1760	2.6 (2H, m, CH_2), 3.31 (3H, s, OCH_3), 3.0—3.9 (11H, m, $\text{CH}_2\text{SO}_2\text{CH}_2$, $\text{OCH}_2\text{CH}_2\text{O}$, CH_2CO , CHCO), 4.2 (1H, m, CHN), 4.83 (2H, br, OCH_2O), 5.26 (2H, s, OCH_2Ar), 6.40 (1H, br, NH), 7.54 (2H, d, $J=9$ Hz, arom H), 8.24 (2H, d, $J=9$ Hz, arom H)
9c		98	2140, 1760	2.1—3.0 (6H, m, $2 \times \text{CH}_2$, CHSCH), 3.36 (3H, s, OCH_3), 3.3—3.9 (9H, m, CH_2CO , CHCO , $\text{OCH}_2\text{CH}_2\text{O}$, CHSCH), 4.2 (1H, m, CHN), 4.93 (2H, br, OCH_2O), 5.38 (2H, s, OCH_2Ar), 6.4 (1H, br, NH), 7.54 (2H, d, $J=9$ Hz, arom H), 8.26 (2H, d, $J=9$ Hz, arom H)

TABLE VII. *p*-Nitrobenzyl 2-Carbapenem-3-carboxylates (12)

Compound	R ¹	R ²	Yield ^{a)} (%)	IR cm ⁻¹ (state)	UV (EtOH) nm	NMR (acetone- <i>d</i> ₆) δ
12a		CH ₂ CH ₂ NHAc	32	1765 (KBr)	267 320	— ^{b)}
12b-1		CH ₂ CH ₂ NHAc	32	1770 (liquid)	269 320	1.90 (3H, s, COCH ₃), 2.7 (2H, m, CH ₂), 2.8—3.8 (10H, m, 2 × SO ₂ CH ₂ , CH ₂ , SCH ₂ CH ₂ N), 4.08 (1H, d, <i>J</i> = 6 Hz, CHCO), 4.4 (1H, m, CHN), 5.38 (2H, ABq, <i>J</i> = 22, 14 Hz, OCH ₂ Ar), 7.4 (1H, m, NH), 7.78 (2H, d, <i>J</i> = 9 Hz, arom H), 8.25 (2H, d, <i>J</i> = 9 Hz, arom H)
12b-2			36	1765 (KBr)	230 265 326	1.97 (3H, s, COCH ₃), 2.45 (2H, m, CH ₂), 2.7—3.9 (6H, m, 2 × SO ₂ CH ₂ , CH ₂), 4.06 (1H, d, <i>J</i> = 6 Hz, CHCO), 4.4 (1H, m, CHN), 5.38 (2H, ABq, <i>J</i> = 22, 14 Hz, OCH ₂ Ar), 5.9 (1H, d, <i>J</i> = 14 Hz, SCH=C), 7.17 (1H, dd, <i>J</i> = 14, 13 Hz, SC=CHN), 7.73 (2H, d, <i>J</i> = 9 Hz, arom H), 8.21 (2H, d, <i>J</i> = 9 Hz, arom H), 9.76 (1H, d, <i>J</i> = 13 Hz, NH)
12c		CH ₂ CH ₂ NHAc	25	1770 (KBr)	268 319	1.90 (3H, s, COCH ₃), 2.1—3.7 (14H, m, 5 × CH ₂ , SCH ₂ CH ₂ N), 3.84 (1H, d, <i>J</i> = 6 Hz, CHCO), 4.4 (1H, m, CHN), 5.40 (2H, ABq, <i>J</i> = 24, 14 Hz, OCH ₂ Ar), 7.4 (1H, m, NH), 7.78 (2H, d, <i>J</i> = 9 Hz, arom H), 8.23 (2H, d, <i>J</i> = 9 Hz, arom H)

a) Overall yields from 9. b) Not measured. Insoluble in CDCl₃ or acetone-*d*₆.

TABLE VIII. Sodium 2-Carbapenem-3-carboxylate (13)



Compound ^{a)}	R ¹	R ²	Yield ^{b)} (%)	IR cm ⁻¹ (KBr)	UV (H ₂ O) nm (E _{1%} ^{1cm})	NMR (D ₂ O) δ
13a		CH ₂ CH ₂ NHAc	36	1760	299 (169)	2.15 (3H, s, COCH ₃), 3.31 (3H, s, SO ₂ CH ₃), 3.0—4.1 (9H, m, SO ₂ CH ₂ , CH ₂ , SCH ₂ CH ₂ N, CHCO), 4.4 (1H, m, CHN), 4.8 (1H, m, CH-O)
13b-1		CH ₂ CH ₂ NHAc	26	1750	298 (134)	2.01 (3H, s, COCH ₃), 2.5 (2H, m, CH ₂), 2.8—3.9 (10H, m, 2 × SO ₂ CH ₂ , CH ₂ , SCH ₂ CH ₂ N), 4.00 (1H, d, J=6 Hz, CHCO), 4.4 (1H, m, CHN)
13b-2			41	1755	229 (312) 306 (312)	2.20 (3H, s, COCH ₃), 2.65 (2H, m, CH ₂), 3.0—4.0 (6H, m, CH ₂ , 2 × SO ₂ CH ₂), 4.12 (1H, d, J=6 Hz, CHCO), 4.50 (1H, m, CHN), 6.15 (1H, d, J=13 Hz, SCH=CHN), 7.28 (1H, d, J=13 Hz, SCH=CHN)
13c		CH ₂ CH ₂ NHAc	39	1750	300 (166)	2.13 (3H, s, COCH ₃), 2.2—3.9 (14H, m, 5 × CH ₂ , SCH ₂ CH ₂ N), 3.97 (1H, d, J=6 Hz, CHCO), 4.4 (1H, m, CHN)

a) All the compounds were obtained as colorless powders. b) Yields were calculated on the basis of the anhydrous sodium salts obtained by hydrogenolysis of the corresponding *p*-nitrobenzyl esters.

mixture of 20% K_2CO_3 (50 ml) and AcOEt (20 ml). Insoluble materials were filtered off, the organic phase was separated and the aqueous phase was further extracted with AcOEt. The combined extracts were washed successively with water, 20% K_2CO_3 , water, sat. aq. $NaHCO_3$, water and sat. aq. NaCl, and dried. Evaporation of the solvent gave the diazo-ester **10b** as a pale yellow oil (IR $\nu_{max}^{liquid} cm^{-1}$: 2140, 1750, 1720). The unstable compound **10b** was used in the subsequent reactions without purification. A mixture of the diazo-azetidinone **10b**, a catalytic amount of rhodium (II) diacetate (5 mg), dry THF (4 ml), and dry benzene (6 ml) was heated at 80°C for 7 min under a nitrogen atmosphere. After being cooled to room temperature, the mixture was evaporated to dryness to give the 2-oxocarbapenam (**11b**) as a foam (IR $\nu_{max}^{KBr} cm^{-1}$: 1770, 1720), which was used in the subsequent reactions without purification. Diisopropylethylamine (0.016 ml, 0.09 mmol) and diphenyl chlorophosphate (0.019 ml, 0.09 mmol) were added to a stirred, cooled (0°C) solution of the 2-oxocarbapenam (**11b**) in dry acetonitrile (6 ml) under an argon atmosphere. The mixture was stirred for 1.5 h at 0°C and then diisopropylethylamine (0.016 ml, 0.09 mmol) and *N*-acetylcysteamine (11 mg, 0.09 mmol) were added. After being stirred for 1 h at 0°C and allowed to stand at -20°C for 14 h, the mixture was diluted with AcOEt, washed with water, and dried. After evaporation of the solvent the residue was subjected to chromatography on Florisil. Elution with acetone-chloroform (1:1, v/v) afforded **12b-1** as a pale yellow foam. Other compounds (**12**) listed in Table VII were synthesized in the same manner. Compound **12b-2** was prepared by using the silver salt of the thiol derivative.

Deprotection of the *p*-Nitrobenzyl Group of the Carbapenam Esters (12**) by Hydrogenolysis**—As a typical example, the preparation of **13b-1** from **12b-1** is described. A mixture of **12b-1** (57 mg, 0.11 mmol) and 10% palladium-charcoal (50 mg) in THF (5 ml), pH 7.0 phosphate buffer (2.6 ml) and water (2.6 ml) was stirred under a hydrogen atmosphere at room temperature for 1.5 h. The catalyst was filtered off, and the filtrate was washed with AcOEt and concentrated under reduced pressure. The concentrate was subjected to chromatography on Diaion HP-20 using water as an eluent. The fractions ($\lambda_{max}^{H_2O}$ 298 nm) were collected and lyophilized to give **13b-1** as a colorless powder. The compounds listed in Table VIII were similarly prepared from the corresponding carbapenam esters.

(1*S,6*R**)-3,4-*cis*-7-*tert*-Butyldimethylsilyl-3,4-dihydroxy-7-azabicyclo[4.2.0]oct-8-one (**16**)**—A solution of the silylated β -lactam **15** (4.70 g, 20 mmol) in acetone (10 ml) was added to a solution of *N*-methylmorpholine *N*-oxide (3.40 g, 25 mmol), water (24 ml) and OsO_4 (106 mg, 0.4 mmol) in *tert*-BuOH (4 ml) at 0°C under an argon atmosphere with stirring. The mixture was stirred for 13 h under an argon atmosphere at room temperature in the dark. A solution of $NaHSO_3$ (4.3 g) in water (20 ml) was added with stirring. After 10 min, magnesium silicate (15 g) was added to the mixture and vigorous stirring was continued for a further 10 min. The precipitate was filtered off and the filtrate was extracted with $CHCl_3$. The extracts were dried and evaporated. The residue was subjected to chromatography on silica gel. Elution with AcOEt afforded the diol **16** (3.40 g, 63%) as colorless crystals, mp 83–85°C. *Anal.* Calcd for $C_{13}H_{25}NO_3Si$: C, 57.53; H, 9.28; N, 5.16. Found: C, 57.84; H, 9.66; N, 4.92. IR $\nu_{max}^{KBr} cm^{-1}$: 1730, 1700. 1H -NMR ($CDCl_3$) δ : 0.23 (6H, s, 2 \times SiMe), 0.96 (9H, s, 3 \times Me), 1.8–2.4 (4H, m, 2 \times CH_2), 3.18 (2H, br s, 2 \times OH), 3.43 (1H, m, C_7 -H), 3.6–4.3 (3H, m, C_3 -H, C_4 -H, C_6 -H).

The Dialdehyde **17**—A solution of the diol **16** (2.08 g, 7.66 mmol) in freshly distilled THF (60 ml) was treated with periodic acid (2.16 g, 9.48 mmol) at 0°C with stirring. The mixture was stirred at room temperature for 45 min, diluted with water and extracted with $CHCl_3$. The extract was washed with water, dried and concentrated to give the aldehyde **17** quantitatively as an oily substance. The unstable dialdehyde was used in the subsequent reactions without purification. IR $\nu_{max}^{liquid} cm^{-1}$: 1730.

Intramolecular Aldol Condensation of the Dialdehyde **17**—1) Method A: A solution of the dialdehyde **17**, which was derived from the diol **16** (2.08 g, 7.66 mmol), in dry benzene (140 ml) was treated with dibenzylammonium trifluoroacetate (465 mg, 1.49 mmol). The mixture was heated at 60°C for 50 min under an argon atmosphere. Methanol (30 ml) and $NaBH_4$ (540 mg, 14 mmol) were added to the mixture and the mixture was stirred for 1.5 h at room temperature. After evaporation of the solvent, AcOEt and dil. HCl were added to the residue and insoluble materials were filtered off. The organic phase was separated and the aqueous phase was further extracted with AcOEt. The combined extracts were washed successively with water and sat. aq. NaCl, dried and evaporated under reduced pressure. The residue was subjected to chromatography on silica gel. Elution with AcOEt- $CHCl_3$ (1:1, v/v) afforded (1*S**,5*R**)-6-*tert*-butyldimethylsilyl-2-hydroxymethyl-7-oxo-6-azabicyclo[3.2.0]hept-2-ene (**19**) (1.104 g, 57%) as a pale yellow oil. IR $\nu_{max}^{liquid} cm^{-1}$: 1720. 1H -NMR (400 MHz, $CDCl_3$) δ : 0.224 (3H, s, SiMe), 0.235 (3H, s, SiMe), 0.956 (9H, s, 3 \times Me), 2.253 (1H, br s, OH), 2.451–2.583 (2H, m, C_4 - H_2), 4.063–4.125 (2H, m, C_1 -H, C_5 -H), 4.294 (2H, s, CH_2OH), 5.603–5.614 (1H, m, C_3 -H). ^{13}C -NMR ($CDCl_3$) δ : -5.17 (s, $SiCH_3$), -5.59 (s, $SiCH_3$), 26.23 (q, 3 \times CH_3), 37.27 (t, C_4), 52.52 (d, C_5), 60.73 (t, CH_2O), 63.99 (d, C_1), 125.48 (d, C_3), 140.72 (s, C_2), 175.79 (s, C_7).

2) Method B: One drop each of piperidine and AcOH was added to a solution of the dialdehyde **17**, which was derived from **16** (392 mg, 1.44 mmol), in dry benzene (15 ml). The mixture was heated at 60°C for 45 min under an argon atmosphere. After cooling, MeOH (5 ml) and $NaBH_4$ (60 mg, 1.59 mmol) were added to the reaction mixture and the mixture was stirred for 1 h at room temperature. After evaporation of the solvent, AcOEt and dil. HCl were added to the residue and insoluble materials were filtered off. The organic phase was separated and the aqueous phase was further extracted with AcOEt. The combined extracts were washed successively with water and sat. aq. NaCl, dried and concentrated. The residue was subjected to chromatography on silica gel. Elution with AcOEt- $CHCl_3$ (1:1, v/v) afforded **19** (58 mg, 16%) as a pale yellow oil.

3) Method C: Morpholine (0.90 ml, 10.32 mmol), camphoric acid (2410 mg, 12.04 mmol) and hexamethylphosphoramide (HMPA) (0.45 ml) were added to a solution of the aldehyde **17**, which was derived from **16** (480 mg, 1.77 mmol), in dry Et₂O (40 ml) at 0 °C with vigorous stirring. The mixture was stirred at 0 °C under an argon atmosphere for 23 h, then the reaction mixture was diluted with water and extracted with Et₂O. The extracts were washed with a large amount of water, dried and concentrated. The residue was dissolved in MeOH (20 ml) and treated with NaBH₄ (75 mg, 1.98 mmol), and the mixture was stirred for 1 h at room temperature. After evaporation of the solvent, AcOEt and dil. HCl were added to the residue and insoluble materials were filtered off. The organic phase was separated and the aqueous phase was further extracted with AcOEt. The combined extracts were washed successively with water and sat. aq. NaCl, dried and concentrated under reduced pressure. The concentrate was subjected to chromatography on silica gel. Elution with AcOEt-CHCl₃ (1:1, v/v) afforded a mixture of the two regioisomers **19** and **19'** (130 mg, 29%) as a pale yellow oil. The two isomers could not be separated. IR $\nu_{\max}^{\text{liquid}} \text{ cm}^{-1}$: 1720. ¹H-NMR (CDCl₃) δ : 0.23 (6H, s, 2 × SiMe), 0.94 (9H, s, 3 × Me), 2.3–2.8 (3H, m, CH₂, OH), 3.7–4.4 (4H, m, C₁-H, C₂-H, CH₂O), 5.59 (0.5H, br s, olefinic proton), 5.87 (0.5H, br s, olefinic proton).

Chlorination of 19—Thionyl chloride (0.029 ml, 0.40 mmol) was added to a stirred, cooled (0 °C) solution of the azetidinone **19** (100 mg, 0.39 mmol) in CHCl₃ (1 ml). After being stirred for 4 h at 0 °C, the mixture was poured into ice-water and CHCl₃ and extracted with CHCl₃. The combined extracts were dried and evaporated. The residue was subjected to chromatography on silica gel. Elution with CHCl₃ afforded an inseparable mixture of **20a-1** and **20a-2** (43 mg, 41%) as an oily substance. IR $\nu_{\max}^{\text{liquid}} \text{ cm}^{-1}$: 1720. ¹H-NMR (CDCl₃) δ : 0.23 (6H, s, 2 × SiMe), 0.95 (9H, s, 3 × Me), 2.54 (2H, m, C₄-H₂), 4.0–4.3 (3.5H, m, C₅-H, CH₂Cl of **20a-1**, CHCl of **20a-2**), 5.37 (0.5H, dd, *J* = 2, 6 Hz, olefinic proton of **20a-2**), 5.73 (0.5H, br s, olefinic proton of **20a-1**). The stereochemistry at C-3 of **20a-2** could not be determined.

(1S*,5R*)-2-Bromomethyl-6-tert-butyl dimethylsilyl-7-oxo-6-azabicyclo[3.2.0]hept-2-ene (20b-1)—Dimethyl sulfide (0.27 ml, 3.68 mmol) was added dropwise to a solution containing *N*-bromosuccinimide (555 mg, 3.12 mmol) in dry CH₂Cl₂ (10 ml) at 0 °C over a period of 3 min. The mixture was cooled to –20 °C, and the azetidinone **19** (526 mg, 3.68 mmol) in CH₂Cl₂ (5 ml) was added dropwise. Then the reaction mixture was warmed to 0 °C and stirred for 3 h, diluted with AcOEt and poured into ice-water. The organic phase was washed successively with water and sat. aq. NaCl, and dried. After evaporation of the solvent, the residue was subjected to chromatography on silica gel. Elution with CHCl₃ afforded the bromide **20b-1** (444 mg, 67%) as a pale yellow oil. IR $\nu_{\max}^{\text{liquid}} \text{ cm}^{-1}$: 1740. ¹H-NMR (CDCl₃) δ : 0.23 (6H, s, 2 × SiMe), 0.93 (9H, s, 3 × Me), 2.53 (2H, m, C₄-H₂), 3.9–4.4 (4H, m, C₁-H, C₅-H, CH₂Br), 5.76 (1H, m, C₃-H).

Synthesis of 19 via Ozonolysis of 15—A solution of **15** (373 mg, 1.57 mmol) in dry CH₂Cl₂ (15 ml) was ozonized at –78 °C in an acetone-dry ice bath, until the solution turned blue, at which time the ozone was replaced by a stream of dry nitrogen gas. After treatment with Me₂S (1 ml), the solution was evaporated to dryness to give the dialdehyde **18**, which was converted into **19** (75 mg, 19%) by Method A.

(3R*,4R*)-3-[(1R*)-2-Bromo-1-hydroxyethyl]-1-tert-butyl dimethylsilyl-4-(2-hydroxyethyl)azetidin-2-one (21)—A solution of **20b-1** (444 mg, 1.40 mmol) in MeOH (13 ml) was ozonized at –78 °C in an acetone-dry ice bath, until the solution turned blue, at which time the ozone was replaced by a stream of dry nitrogen gas. The reaction mixture was warmed to –40 °C, NaBH₄ (50 mg, 1.32 mmol) was added, and the mixture was stirred for 1 h at room temperature. After evaporation of the solvent, AcOEt and dil. HCl were added to the residue and the organic phase was separated. The aqueous phase was further extracted with AcOEt. The combined extracts were washed successively with water and sat. aq. NaCl, and dried. The solvent was evaporated off to afford the diol **21** (478 mg, 97%) as a pale yellow oil. IR $\nu_{\max}^{\text{liquid}} \text{ cm}^{-1}$: 1740. ¹H-NMR (CDCl₃) δ : 0.23 (6H, s, 2 × SiMe), 0.97 (9H, s, 3 × Me), 2.0 (2H, m, CH₂), 3.3–4.4 (7H, m, OCH₂, C₃-H, C₄-H, CH₂Br, H-C-O).

(3R*,4R*)-3-[(1R*)-2-Bromo-1-hydroxyethyl]-4-(2-hydroxyethyl)azetidin-2-one (22)—Potassium fluoride (346 mg, 5.96 mmol) was added to a solution of **21** (1050 mg, 2.98 mmol) in dry MeOH (20 ml) and the reaction mixture was stirred for 1 h at room temperature. The solvent was evaporated off, and the residue was purified by chromatography on silica gel. Elution with AcOEt-MeOH (20:1, v/v) afforded **22** (656 mg, 93%) as a colorless oil. IR $\nu_{\max}^{\text{liquid}} \text{ cm}^{-1}$: 1740. ¹H-NMR (acetone-*d*₆) δ : 1.7–2.1 (2H, m, CH₂), 3.1–4.2 (7H, m, CH₂O, CH-O, C₃-H, C₄-H, CH₂Br), 7.2 (1H, br s, NH).

(6R*,7R*)-7-[(1R*)-2-Bromo-1-hydroxyethyl]-2,2-dimethyl-3-oxo-8-oxa-1-azabicyclo[4.2.0]octane (23)—Dimethoxypropane (0.44 ml, 3.58 mmol) and one drop of BF₃·OEt₂ were added to a solution of **22** (656 mg, 2.76 mmol) in dry CH₂Cl₂ (10 ml) and the reaction mixture was stirred for 1.5 h at room temperature. The mixture was poured into pH 6.86 buffer and extracted with CH₂Cl₂. The organic phase was washed with sat. aq. NaCl, dried and concentrated. The concentrate was subjected to chromatography on silica gel. Elution with hexane-AcOEt (1:1, v/v) afforded the acetonide **23** (482 mg, 63%) as colorless prisms, mp 133–135 °C. Anal. Calcd for C₁₀H₁₆BrNO₃: C, 43.18; H, 5.80; N, 5.04. Found: C, 43.34; H, 5.59; N, 5.11. IR $\nu_{\max}^{\text{KBr}} \text{ cm}^{-1}$: 1740. ¹H-NMR (CDCl₃) δ : 1.40, 1.69 (each 3H, 2 × s, 2 × Me), 1.7–2.0 (2H, m, C₅-H₂), 2.50 (1H, br s, OH), 3.29 (1H, dd, *J* = 11, 6 Hz, C₇-H), 3.5–4.3 (6H, m, C₄-H₂, C₆-H, CH-O, CH₂Br).

(6R*,7R*)-7-[(1R*)-1-Hydroxy-2-(methylthio)ethyl]-2,2-dimethyl-8-oxo-3-oxa-1-azabicyclo[4.2.0]octane (24a)—An aqueous solution of sodium methylthiolate (15%) (0.60 ml) was added to a solution of **23** (239 mg,

0.859 mmol) in dimethylformamide (DMF) (10 ml) and the reaction mixture was stirred for 1 h at room temperature under an argon atmosphere. AcOEt and water were added to the mixture and the aqueous phase was extracted with AcOEt. The organic phase was washed successively with water and sat. aq. NaCl, and dried. After evaporation of the solvent, the residue was subjected to chromatography on silica gel. Elution with hexane-AcOEt (1:1, v/v) afforded **24a** (190 mg, 90%) as colorless prisms, mp 75–76 °C. *Anal.* Calcd for $C_{11}H_{19}NO_3S$: C, 53.85; H, 7.81; N, 5.71. Found: C, 53.86; H, 7.91; N, 5.61. IR $\nu_{\max}^{KBr} \text{ cm}^{-1}$: 1740. $^1\text{H-NMR}$ (acetone- d_6) δ : 1.41, 1.64 (each 3H, 2 \times s, 2 \times Me), 1.8–2.0 (2H, m, $C_5\text{-H}_2$), 2.16 (3H, s, SMe), 2.58 (1H, dd, $J=14$, 7.5 Hz, SCH), 2.98 (1H, dd, $J=14$, 3.2 Hz, SCH), 3.39 (1H, dd, $J=10.3$, 5.2 Hz, $C_7\text{-H}$), 3.6–4.3 (6H, m, $C_4\text{-H}_2$, $C_6\text{-H}$, CH-O, CH_2Br).

(6R*,7R*)-2,2-Dimethyl-7-[(1R*)-2-methylthio-1-(p-nitrobenzyloxycarbonyloxy)ethyl]-8-oxo-3-oxa-1-azabicyclo[4.2.0]octane (5a-2)—Dimethylaminopyridine (495 mg, 4.05 mmol) and *p*-nitrobenzyl chloroformate (436 mg, 2.02 mmol) were added to a solution of **24a** (333 mg, 1.36 mmol) in CH_2Cl_2 (20 ml) at 0 °C under an argon atmosphere. The reaction mixture was stirred for 18 h at room temperature. After evaporation of the solvent, AcOEt and dil. HCl were added to the residue. The organic phase was separated, washed successively with water and sat. aq. NaCl, and dried. After evaporation of the solvent, the residue was subjected to chromatography on silica gel. Elution with hexane-AcOEt (2:1–1:1, v/v) afforded **5a-2** (420 mg, 73%) as a colorless oil and unreacted **24a** (39 mg). IR $\nu_{\max}^{\text{liquid}} \text{ cm}^{-1}$: 1760, 1740. $^1\text{H-NMR}$ (CDCl_3) δ : 1.38, 1.70 (each 3H, 2 \times s, 2 \times Me), 1.7–2.0 (2H, m, $C_5\text{-H}$), 2.13 (3H, s, SMe), 2.71 (1H, dd, $J=14$, 7.5 Hz, SCH), 3.17 (1H, dd, $J=14$, 3 Hz, SCH), 3.5–4.0 (4H, m, $C_4\text{-H}_2$, $C_6\text{-H}$, $C_7\text{-H}$), 5.25 (1H, m, CH-O), 5.26 (2H, s, CH_2Ar), 7.51 (2H, d, $J=9$ Hz, aromatic protons), 8.21 (2H, d, $J=9$ Hz, aromatic protons).

(6R*,7R*)-7-[(1R*)-2-Methylsulfonyl-1-(p-nitrobenzyloxycarbonyloxy)ethyl]-2,2-dimethyl-8-oxo-3-oxa-1-azabicyclo[4.2.0]octane (6a-2)—Starting from **5a-2**, **6a-2** was obtained as a colorless oil. Yield 97%. IR $\nu_{\max}^{\text{liquid}} \text{ cm}^{-1}$: 1770–1730. $^1\text{H-NMR}$ (CDCl_3) δ : 1.39, 1.70 (each 3H, 2 \times s, 2 \times Me), 1.7–2.0 (2H, m, $C_5\text{-H}$), 3.00 (3H, s, SO_2Me), 3.1–4.0 (4H, m, SO_2CH_2 , $C_4\text{-H}_2$, $C_6\text{-H}$, $C_7\text{-H}$), 5.26 (2H, s, CH_2Ar), 5.64 (1H, m, CH-O), 7.51 (2H, d, $J=9$ Hz, aromatic protons), 8.20 (2H, d, $J=9$ Hz, aromatic protons).

(3R*,4R*)-3-[(1R*)-2-Methylsulfonyl-1-(p-nitrobenzyloxycarbonyloxy)ethyl]-4-[3-(p-nitrobenzyloxycarbonyl)-2-oxopropyl]azetidin-2-one (8a-2)—Starting from **6a-2**, **8a-2** was obtained as a pale yellow foam. Yield 57%. IR $\nu_{\max}^{KBr} \text{ cm}^{-1}$: 1755, 1720. $^1\text{H-NMR}$ (acetone- d_6) δ : 3.00 (3H, s, SO_2Me), 3.13 (2H, d, $J=6.3$ Hz, CH_2CO), 3.66 (2H, s, COCH_2CO), 3.0–4.0 (3H, m, SO_2CH_2 , $C_3\text{-H}$), 4.15 (1H, m, $C_4\text{-H}$), 5.28 (2H, s, CH_2Ar), 5.30 (2H, s, CH_2Ar), 5.66 (1H, m, CH-O), 7.40 (1H, br s, NH), 7.63 (2H, d, $J=9$ Hz, aromatic protons), 8.18 (2H, d, $J=9$ Hz, aromatic protons).

(3R*,4R*)-4-[3-Diazo-3-(p-nitrobenzyloxycarbonyl)-2-oxopropyl]-3-[(1R*)-2-methylsulfonyl-1-(p-nitrobenzyloxycarbonyl)ethyl]azetidin-2-one (9a-2)—Starting from **8a-2**, **9a-2** was obtained quantitatively as crystals. IR $\nu_{\max}^{KBr} \text{ cm}^{-1}$: 2140, 1770, 1730.

***p*-Nitrobenzyl (5R*,6R*)-2-(2-Acetamidoethylthio)-6-[(1R*)-2-methylsulfonyl-1-(p-nitrobenzyloxycarbonyloxy)ethyl]-2-carbapenam-3-carboxylate (12a-2)**—Starting from **9a-2**, **12a-2** was obtained as a pale yellow oil. Yield 36%. IR $\nu_{\max}^{\text{liquid}} \text{ cm}^{-1}$: 1760, 1710, 1660. UV $\lambda_{\max}^{\text{EtOH}}$ nm: 267, 320. $^1\text{H-NMR}$ (acetone- d_6) δ : 2.10 (3H, s, COMe), 3.05 (3H, s, SO_2Me), 3.36 (2H, d, $J=6$ Hz, SO_2CH_2), 2.8–4.0 (6H, m, $C_1\text{-H}$, $\text{SCH}_2\text{CH}_2\text{N}$), 4.1–4.7 (2H, m, $C_5\text{-H}$, $C_6\text{-H}$), 5.36 (2H, s, CH_2Ar), 5.37 (2H, ABq, $J=23$, 14 Hz, CH_2Ar), 5.80 (1H, m, CH-O), 7.30 (1H, br s, NH), 7.63 (2H, d, $J=9$ Hz, aromatic protons), 7.73 (2H, d, $J=9$ Hz, aromatic protons), 8.18 (4H, d, $J=9$ Hz, aromatic protons).

Sodium (5R*,6R*)-2-(2-Acetamidoethylthio)-6-[(1R*)-1-hydroxy-2-(methylsulfonyl)ethyl]-2-carbapenam-3-carboxylate (13a-2)—Starting from **12a-2**, **13a-2** was obtained as a powder. Yield 24%. IR $\nu_{\max}^{KBr} \text{ cm}^{-1}$: 1750. UV $\lambda_{\max}^{\text{EtOH}}$ nm: 298 ($\epsilon=4060$, $E_{1\text{cm}}^{1\%}=98$). $^1\text{H-NMR}$ (D_2O) δ : 2.13 (3H, s, COMe), 3.30 (3H, s, SO_2Me), 2.8–3.8 (8H, m, $C_1\text{-H}$, $\text{SCH}_2\text{CH}_2\text{N}$, SO_2CH_2), 3.97 (1H, dd, $J=10$, 5 Hz, $C_6\text{-H}$), 4.3–4.9 (2H, m, $C_5\text{-H}$, CH-O).

1-Methyl Hydrogen (1R,2S)-1,2-Cyclohex-4-ene Dicarboxylate (26b)—Racemic 1-methyl hydrogen 1,2-*cis*-1,2-cyclohex-4-ene dicarboxylate (82.3 g, 0.464 mol) and cinchonidine (136.3 g, 0.463 mol) were dissolved in MeOH (400 ml) and insoluble materials were filtered off. The filtrate was concentrated and dissolved in acetone (150 ml), and the solution was allowed to stand for 4 d at 5 °C. The resulting precipitate was collected by filtration and washed with acetone. The precipitate was dissolved in a mixture of MeOH (75 ml) and acetone (150 ml). The solution was allowed to stand at 5 °C for 1 d. The resulting precipitate was collected by filtration, and washed with acetone to afford the cinchonidine salt of **26** [mp 156–157 °C, $[\alpha]_{\text{D}}^{24} -88.4^\circ$ ($c=0.57$, MeOH)]. This salt was suspended in AcOEt (300 ml) and the solution was washed successively with 1 N HCl (twice) and sat. aq. NaCl, and dried. After evaporation of the solvent, the chiral half ester **26b** (22 g, 27%) was obtained as a pale yellow oil. $[\alpha]_{\text{D}}^{25} -3.44^\circ$ ($c=1.685$ CHCl_3). $^1\text{H-NMR}$ (CDCl_3) δ : 2.1–2.9 (4H, m, 2 \times CH_2), 2.9–3.2 (2H, $C_1\text{-H}$, $C_2\text{-H}$), 3.70 (3H, s, OMe), 5.67 (2H, s, olefinic protons), 11.68 (1H, s, COOH).

1-Methyl Hydrogen (1S,2R)-1,2-Cyclohex-4-ene Dicarboxylate (26a)—The mother liquor of the cinchonidine salt of the half ester was dissolved in AcOEt (100 ml) and the solution was washed with 1 N HCl and sat. aq. NaCl, dried and concentrated. After filtration of insoluble materials, the chiral half ester **26a** (23 g, 28%) was obtained as a pale yellow oil. $[\alpha]_{\text{D}}^{25} +3.36^\circ$ ($c=1.24$, CHCl_3).

Methyl (1S,2R)-2-[(2-Methylsulfonyl)ethoxycarbonylamino]-1-cyclohex-4-ene Carboxylate (27)—Triethylamine (11 g, 0.108 mol) and ethyl chloroformate (11.8 g, 0.108 mol) were added to a solution of the chiral half ester

26a (18.82 g, 0.102 mol) in CH_2Cl_2 (350 ml) at -20°C , and the mixture was stirred for 40 min at -20°C . A solution of sodium azide (14 g, 0.216 mol) in water (75 ml) and tetrabutylammonium hydrogen sulfate (7.3 g, 0.0216 mol) were added to the mixture and the mixture was stirred for 1 h at 0°C . The organic phase was separated and the aqueous phase was further extracted with CH_2Cl_2 . The combined extracts were washed with sat. aq. NaCl and dried. After evaporation of the solvent, the residue was dissolved in toluene (150 ml). The solution was stirred at 100°C for 15 min. After cooling, a solution of 2-methylsulfonylethanol (31.7 g, 0.255 mol) in THF (150 ml) and 1,4-diazabicyclo[2.2.2]octane (DABCO) (2.6 g, 0.0255 mol) were added. The reaction mixture was allowed to stand at room temperature for 18 h. The solvent was evaporated off and the residue was subjected to chromatography on silica gel. Elution with hexane-AcOEt (1:2, v/v) afforded **27** (24.6 g, 79%) as crystals, mp $90-92^\circ\text{C}$. *Anal.* Calcd for $\text{C}_{12}\text{H}_{19}\text{NO}_6\text{S}$: C, 47.20; H, 6.27; N, 4.59. Found: C, 47.10; H, 6.36; N, 4.57. IR $\nu_{\text{max}}^{\text{KBr}} \text{cm}^{-1}$: 1725, 1705, 1530. $^1\text{H-NMR}$ (CDCl_3) δ : 2.0–2.6 (4H, m, $2 \times \text{CH}_2$), 2.6–2.9 (1H, m, $\text{C}_1\text{-H}$), 2.98 (3H, s, SO_2Me), 3.33 (2H, t, $J=5$ Hz, SO_2CH_2), 3.68 (3H, s, OMe), 4.0–4.4 (1H, m, $\text{C}_2\text{-H}$), 4.49 (2H, t, $J=5$ Hz, CO_2CH_2), 5.63 (2H, s, olefinic protons).

tert-Butyl (1S,2R)-2-[(2-Methylsulfonyl)ethoxycarbonylamino]-1-cyclohex-4-ene Carboxylate (31)—Isobutene was bubbled into a mixture of **26b** (25.7 g, 0.139 mol), CH_2Cl_2 (280 ml) and sulfuric acid (1.5 ml) for 30 min at 0°C with stirring. The mixture was allowed to stand for 3 d. After further bubbling of isobutene for 30 min, the mixture was allowed to stand for 1 d. After evaporation of the solvent, the residue was dissolved in Et_2O (300 ml) and the organic phase was washed successively with aq. NaHCO_3 and sat. aq. NaCl, then dried. After evaporation of the solvent, the diester (**30a**) (30.6 g, 92%) was obtained as a colorless oil. The diester **30a** (30.6 g, 0.127 mol) was dissolved in MeOH (250 ml) and a solution of NaOH (8.34 g, 0.209 mol) in water (100 ml) was added. The mixture was allowed to stand for 20 h at room temperature. After evaporation of the solvent, the residue was dissolved in water and washed with Et_2O . Conc. HCl (21.5 ml, 0.212 mol) was added to the aqueous phase, which was extracted with Et_2O . The organic phase was washed with sat. aq. NaCl and dried. After evaporation of the solvent, the half ester **30b** (26.9 g, 93%) was obtained as colorless crystals. The half ester **30b** was transformed into **31** (39.3 g, 96%) as a colorless oil in a manner similar to that described for the preparation of **27** from **26**. IR $\nu_{\text{max}}^{\text{liquid}} \text{cm}^{-1}$: 1725, 1520. $^1\text{H-NMR}$ (CDCl_3) δ : 1.44 (9H, s, CMe_3), 2.0–2.9 (5H, m, $2 \times \text{CH}_2$, $\text{C}_1\text{-H}$), 2.97 (3H, s, SO_2Me), 3.32 (2H, t, $J=5$ Hz, SO_2CH_2), 4.0–4.4 (1H, m, $\text{C}_2\text{-H}$), 4.48 (2H, t, $J=5$ Hz, CO_2CH_2), 5.5–5.8 (2H, m, olefinic protons).

(1S,2R)-2-Amino-1-cyclohex-4-ene Carboxylic Acid (28)—a) A 1 N NaOH solution (10 ml, 10 mmol) was added to a solution of **27** (1.53 g, 5 mmol) in MeOH (25 ml) and the mixture was stirred for 12 h. After further addition of 1 N NaOH (3 ml, 3 mmol), the mixture was stirred for 4 h. The precipitate was dissolved in water and IRA-401 ion exchange resin (OH^- type, wet 49 ml) was added to the solution. The mixture was stirred and the resin was collected by filtration and washed with water. The desired fraction, obtained by eluting the column containing the resin with 5% AcOH (200 ml), was concentrated. The concentrate was dissolved in water and the solution was stirred with Dowex 50W (H^+ , 15 ml). The desired fraction, obtained by eluting the column containing the resin with 5% aq. ammonia, was evaporated. Acetone was added to the residue and the resulting precipitate was collected by filtration and washed with acetone to give **28** (532 mg, 76%) as colorless crystals. $[\alpha]_{\text{D}}^{25} + 36.4^\circ$ ($c=0.45$, H_2O).

b) Aqueous 5 N NaOH (15 ml) was added to a mixture of **31** (8.69 g, 25 mmol), dioxane (210 ml) and MeOH (75 ml). The reaction mixture was stirred for 15 min at room temperature, AcOH (4.6 ml, 75 mmol) was added, and the mixture was concentrated. Aqueous NaHCO_3 was added to the residue and the aqueous phase was extracted with CHCl_3 . The organic phase was washed with water and dried. After evaporation of the solvent, trifluoroacetic acid (15 ml) was added to the residue and allowed to stand for 24 h at room temperature. Dowex 50W (H^+ , 75 ml) and water (50 ml) were added to the mixture at 0°C . After being stirred at 0°C for 1 h, the resin was collected by filtration. The desired fraction, collected by eluting the column containing the resin with 5% aq. ammonia (300 ml), provided **28** (2.56 g, 73%) as crystals, mp 225°C (dec). *Anal.* Calcd for $\text{C}_7\text{H}_{11}\text{NO}_2 \cdot 1/2\text{H}_2\text{O}$: C, 55.98; H, 8.06; N, 9.33. Found: C, 55.55; H, 7.93; N, 9.31. IR $\nu_{\text{max}}^{\text{KBr}} \text{cm}^{-1}$: 1700, 1620, 1550. $^1\text{H-NMR}$ ($\text{CDCl}_3\text{-CF}_3\text{COOH}$) δ : 2.3–3.0 (4H, m, $2 \times \text{CH}_2$), 3.0–3.4 (1H, m, $\text{C}_1\text{-H}$), 3.8–4.3 (1H, m, $\text{C}_2\text{-H}$), 5.5–6.1 (2H, m, olefinic protons), 7.15 (2H, br s, NH_2) $[\alpha]_{\text{D}}^{25} + 36.6^\circ$ ($c=0.56$, H_2O).

(1S,6R)-8-Oxo-7-azabicyclo[4.2.0]oct-3-ene (29)—A mixture of **28** (424 mg, 3 mmol), triphenylphosphine (997 mg, 3.8 mmol), 2,2'-dipyridyl disulfide (838 mg, 3.8 mmol), manganese oxide (652 mg, 7.5 mmol) and acetonitrile (60 ml) were refluxed for 3.5 h with vigorous stirring. After cooling, insoluble materials were filtered off and the filtrate was concentrated. The residue was subjected to chromatography on silica gel. Elution with hexane-AcOEt (1:2, v/v) afforded the β -lactam **29** (251 mg, 68%) as a colorless prism, mp $163-164^\circ\text{C}$. $[\alpha]_{\text{D}}^{25} - 28.6^\circ$ ($c=0.585$, CHCl_3). *Anal.* Calcd for $\text{C}_7\text{H}_9\text{NO}$: C, 68.27; H, 7.37; N, 11.37. Found: C, 68.04; H, 7.29; N, 11.23. IR $\nu_{\text{max}}^{\text{KBr}} \text{cm}^{-1}$: 1730, 1700. $^1\text{H-NMR}$ (CDCl_3) δ : 2.0–2.8 (4H, m, $2 \times \text{CH}_2$), 3.35 (1H, m, $\text{C}_1\text{-H}$), 3.98 (1H, m, $\text{C}_6\text{-H}$), 5.6–6.3 (3H, m, NH, olefinic protons).

(1S,6R)-7-tert-Butyldimethylsilyl-8-oxo-7-azabicyclo[4.2.0]oct-3-ene (32)—The β -lactam **29** (251 mg, 2.04 mmol) was dissolved in DMF (9 ml). *tert*-Butyldimethylsilyl chloride (498 mg, 3.3 mmol) and Et_3N (0.46 ml, 3.3 mmol) were added to the solution at 0°C and the mixture was stirred for 1.5 h at room temperature, then poured into ice-water. The aqueous phase was extracted with AcOEt. The combined extracts were washed with sat. aq. NaCl, and dried. After evaporation of the solvent, the residue was subjected to chromatography on silica gel. Elution with hexane-AcOEt (6:1, v/v) afforded **33** (484 mg, quantitatively) as a colorless oil. $[\alpha]_{\text{D}}^{25} - 45.9^\circ$ ($c=1.43$, EtOH). IR

$\nu_{\max}^{\text{liquid}} \text{ cm}^{-1}$: 1745, 1725. $^1\text{H-NMR}$ (CDCl_3) δ : 0.23 (6H, s, $2 \times \text{Me}$), 0.96 (9H, s, CMe_3), 1.8—2.7 (4H, m, $2 \times \text{CH}_2$), 3.2—3.5 (1H, m, $\text{C}_1\text{-H}$), 3.8—4.0 (1H, m, $\text{C}_6\text{-H}$), 5.5—6.1 (2H, m, olefinic protons).

(1*S*,5*R*)-6-*tert*-Butyldimethylsilyl-2-hydroxymethyl-7-oxo-6-azabicyclo[3.2.0]hept-2-ene (34)—Compound 34 was prepared from optically active 16 in the same manner as that described for the preparation of the racemic compound 19. Yield 40%.

(1*S*,5*R*)-2-Bromomethyl-6-*tert*-butyldimethylsilyl-7-oxo-6-azabicyclo[3.2.0]hept-2-ene (35)—Compound 35 was prepared from 34 in the same manner as that described for the preparation of the racemic compound 20b-1. Yield 66%.

(6*R*,7*R*)-2,2-Dimethyl-7-[(1*R*)-2-bromo-1-hydroxyethyl]-8-oxo-3-oxa-1-azabicyclo[4.2.0]octane (36)—Compound 36 was prepared from optically active 22 in the same manner as that described for the preparation of the racemic 23. Yield 71%, mp 141—142°C. *Anal.* Calcd for $\text{C}_{10}\text{H}_{16}\text{BrNO}_3$: C, 43.18; H, 5.80; N, 5.04. Found: C, 43.12; H, 5.79; N, 5.04. $[\alpha]_{\text{D}}^{25} + 13.0^\circ$ ($c=0.54$, CHCl_3). NMR and IR spectra were identical with those of the racemic compound 23.

(6*R*,7*R*)-7-[(1*R*)-1-Hydroxy-2-(phenylthio)ethyl]-2,2-dimethyl-8-oxo-3-oxa-1-azabicyclo[4.2.0]octane (37)—Compound 37 was prepared from 36 quantitatively as a pale yellow oil. IR $\nu_{\max}^{\text{liquid}} \text{ cm}^{-1}$: 1740. $^1\text{H-NMR}$ (CDCl_3) δ : 1.36, 1.69 (each 3H, $2 \times \text{s}$, $2 \times \text{Me}$), 1.7—2.0 (2H, m, $\text{C}_5\text{-H}_2$), 2.7 (1H, brs, OH), 2.83 (2H, dd, $J=14$, 9 Hz, CH_2S), 3.23 (1H, dd, $J=11$, 6 Hz, $\text{C}_7\text{-H}$), 3.5—4.2 (4H, m, $\text{C}_4\text{-H}_2$, $\text{C}_6\text{-H}$, CH-O), 7.1—7.5 (5H, m, aromatic protons).

p-Nitrobenzyl (5*R*,6*R*)-2-(2-Acetamidovinylthio)-6-[(1*R*)-1-hydroxy-2-(phenylsulfonyl)ethyl]-2-carbapenem-3-carboxylate (38)—Compound 38 was prepared from the optically active 10 in a manner similar to that described for the preparation of the racemic compound 12. Yield 56%. IR $\nu_{\max}^{\text{liquid}} \text{ cm}^{-1}$: 1770, 1700, 1620. UV $\lambda_{\max}^{\text{EtOH}} \text{ nm}$: 263, 325. $^1\text{H-NMR}$ (acetone- d_6) δ : 1.97 (3H, s, COMe), 3.30 (2H, dd, $J=15$, 9 Hz, SO_2CH_2), 3.5—4.0 (3H, m, $\text{C}_1\text{-H}$, $\text{C}_6\text{-H}$), 4.1—4.7 (2H, m, $\text{C}_5\text{-H}$, CH-O), 5.36 (2H, ABq, $J=24$, 15 Hz, OCH_2Ar), 5.94 (1H, d, $J=14$ Hz, $\text{SCH}=\text{C}$), 7.18 (1H, dd, $J=14$, 11 Hz, $\text{NCH}=\text{C}$), 7.5—8.1 (5H, m, aromatic protons), 7.71 (2H, d, $J=9$ Hz, aromatic protons), 8.20 (2H, d, $J=9$ Hz, aromatic protons), 9.47 (1H, d, $J=11$ Hz, NH).

Sodium (5*R*,6*R*)-2-(2-Acetamidovinylthio)-6-[(1*R*)-1-hydroxy-2-(phenylsulfonyl)ethyl]-2-carbapenem-3-carboxylate (39)—Compound 39 was prepared from 38 in the same manner as that described for the preparation of the racemic compound 13. Yield 33%. IR $\nu_{\max}^{\text{KBr}} \text{ cm}^{-1}$: 1755, 1670. UV $\lambda_{\max}^{\text{H}_2\text{O}} \text{ nm}$: 218 ($\epsilon=17650$, $E_{1\text{cm}}^1=372$), 305 ($\epsilon=8780$, $E_{1\text{cm}}^1=185$). $^1\text{H-NMR}$ (D_2O) δ : 2.20 (3H, s, COMe), 3.15 (2H, d, $J=9$ Hz, SO_2CH_2), 3.6—4.1 (3H, m, $\text{C}_1\text{-H}_2$, $\text{C}_6\text{-H}$), 4.2—4.8 (2H, m, $\text{C}_5\text{-H}$, CH-O), 6.13 (1H, d, $J=13$ Hz, $\text{SCH}=\text{C}$), 7.28 (1H, d, $J=13$ Hz, $\text{NCH}=\text{C}$), 7.8—8.2 (5H, m, aromatic protons).

Acknowledgement The authors thank Dr. K. Morita of this Division for his encouragement throughout this work. Thanks are also due to Dr. M. Kondo and Dr. K. Okonogi for the biological evaluation.

References and Notes

- 1) Part of this paper was presented at the 106th Annual Meeting of the Pharmaceutical Society of Japan, Chiba, April 1986; Abstracts of Papers, p. 491. Preliminary communication: N. Tamura, Y. Kawano, Y. Matsushita, K. Yoshioka, and M. Ochiai, *Tetrahedron Lett.*, **27**, 3749 (1986).
- 2) R. W. Ratcliffe and G. Albers-Schönberg, "The Chemistry of Thienamycin and Other Carbapenem Antibiotics," *Chemistry and Biology of β -Lactam Antibiotics*, Vol. 2, ed. by R. B. Morin and M. Gorman, Academic Press, New York, 1982, pp. 227—313; T. Kametani, *Heterocycles*, **17**, 463 (1982) and references cited therein.
- 3) H. Kropp, J. G. Sundelf, R. Hajdu, and F. M. Kahan, *Antimicrob. Agents Chemother.*, **22**, 62 (1982); J. S. Kahan, F. M. Kahan, R. Goegelman, S. A. Currie, M. Jackson, E. O. Stapley, T. W. Miller, A. K. Miller, D. Hendlin, S. Mochales, S. Hernandez, H. B. Woodruff, and J. Birnbaum, *J. Antibiot.*, **32**, 1 (1979).
- 4) H. Natsugari, Y. Matsushita, N. Tamura, K. Yoshioka, and M. Ochiai, *J. Chem. Soc., Perkin Trans. 1*, **1983**, 403; H. Natsugari, Y. Matsushita, N. Tamura, K. Yoshioka, M. Kondo, K. Okonogi, M. Kuno, and M. Ochiai, *J. Antibiot.*, **36**, 855 (1983).
- 5) A. Imada, Y. Nozaki, K. Kintaka, K. Okonogi, K. Kitano, and S. Harada, *J. Antibiot.*, **33**, 1417 (1980).
- 6) M. Nakayama, A. Iwasaki, S. Kimura, T. Mizoguchi, S. Tanabe, A. Murakami, M. Okuchi, H. Itoh, Y. Saino, F. Kobayashi, and T. Mori, *J. Antibiot.*, **33**, 1388 (1980).
- 7) D. B. R. Johnston, S. M. Schmitt, F. A. Bouffard, and B. G. Christensen, *J. Am. Chem. Soc.*, **100**, 313 (1978); F. A. Bouffard, D. B. R. Johnston, and B. G. Christensen, *J. Org. Chem.*, **45**, 1130 (1980).
- 8) E. Y. Wick, T. Yamanishi, K. C. Wertheimer, J. E. Hoff, B. E. Proctor, and S. A. Goldblith, *Agriculture and Food Chemistry*, **9**, 1175 (1961).
- 9) F. A. Buitter, J. H. S. Weiland, and H. Wynberg, *Recueil*, **83**, 1160 (1964).
- 10) F. A. Bouffard, D. B. R. Johnston, and B. G. Christensen, *J. Org. Chem.*, **45**, 1130 (1980).
- 11) The sulfur atom in the side-chain changed the sequence, see: R. S. Cahn, C. K. Ingold, and V. Prelog, *Angew. Chem. Int. Ed. Engl.*, **5**, 385 (1966).

- 12) A. Martel, J. Colletette, J. Banville, J.-P. Daris, P. Lapointe, B. Belleau, and M. Menard, *Can. J. Chem.*, **61**, 613 (1983).
- 13) E. J. Corey, J.-L. Gras, and P. Ulrich, *Tetrahedron Lett.*, **1976**, 809. The *p*-nitrobenzyloxycarbonyl (PNZ) group was also used for this purpose (see Experimental).
- 14) D. W. Brooks, L. D.-Lu, and S. Masamune, *Angew. Chem. Int. Ed. Engl.*, **18**, 72 (1979).
- 15) R. W. Ratcliffe, T. N. Saltzmann, and B. G. Christensen, *Tetrahedron Lett.*, **21**, 31 (1980).
- 16) M. Sletzinger, T. Liu, R. A. Reamer, and I. Shinkai, *Tetrahedron Lett.*, **21**, 4221 (1980).
- 17) L. A. Paquette and T. Kakihana, *J. Am. Chem. Soc.*, **90**, 3897 (1968).
- 18) A. J. G. Baxter, K. H. Dickinson, P. M. Roberts, T. C. Smale, and R. Southgate, Ger. Offen., 2811514 (1979) [*Chem. Abstr.*, **90**, 22800w (1979)]; J. H. Bateson, R. I. Hickling, P. M. Roberts, T. C. Smale, and R. Southgate, *J. Chem. Soc., Chem. Commun.*, **1980**, 1084.
- 19) V. VanRheenen, R. C. Kelly, and R. Y. Cha, *Tetrahedron Lett.*, **1976**, 1973.
- 20) T. Harayama, M. Takatani, and Y. Inubushi, *Chem. Pharm. Bull.*, **28**, 1276 (1980).
- 21) R. B. Woodward, F. Sondheimer, D. Taub, K. Heusler, and W. M. McLamore, *J. Am. Chem. Soc.*, **74**, 4223 (1952).
- 22) E. J. Corey, R. L. Danheiser, S. Chandrasekaran, P. Siret, G. E. Keck, and J.-L. Gras, *J. Am. Chem. Soc.*, **100**, 8031 (1978).
- 23) E. J. Corey, C. U. Kim, and M. Takeda, *Tetrahedron Lett.*, **1972**, 4339.
- 24) M. Schneider, N. Engel, P. Hönicke, G. Heineman, and H. Görisch, *Angew. Chem. Int. Ed. Engl.*, **23**, 67 (1984); H.-J. Gais and K. L. Lukas, *ibid.*, **23**, 142 (1984).
- 25) After completion of this work, Ohno *et al.* reported the synthesis of **29** from **26a**, which was obtained by an enzymatic procedure: M. Kurihara, K. Kamiyama, S. Kobayashi, and M. Ohno, *Tetrahedron Lett.*, **26**, 5831 (1985).
- 26) S. Kobayashi, T. Iimori, T. Izawa, and M. Ohno, *J. Am. Chem. Soc.*, **103**, 2406 (1981).
- 27) We thank Dr. K. Kamiya and Mr. Y. Wada of this Division for this analysis.
- 28) K. Tsuchiya, M. Kida, M. Kondo, H. Ono, M. Takeuchi, and T. Nishi, *Antimicrob. Agents Chemother.*, **14**, 557 (1978).
- 29) K. Okonogi, Y. Nozaki, A. Imada, and M. Kuno, *J. Antibiot.*, **34**, 212 (1981).

[Chem. Pharm. Bull.]
[35(3)1016-1029(1987)]

Selective Deoxygenation *via* Regioselective Thioacylation of Non-protected Glycopyranosides by the Dibutyltin Oxide Method¹⁾

MOHAMMED EKRAMUL HAQUE,^a TOHRU KIKUCHI,^{*a} KIMIHIRO KANEMITSU,^b
and YOSHISUKE TSUDA^{*.b}

*Research Institute for Wakan-Yaku (Oriental Medicines), Toyama Medical and
Pharmaceutical University,^a 2630 Sugitani, Toyama 930-01, Japan and
Faculty of Pharmaceutical Sciences, Kanazawa University,^b
13-1 Takara-machi, Kanazawa 920, Japan*

(Received August 25, 1986)

Regioselective thioacylation of some non-protected glycopyranosides (Me α -D-Glc, Me β -D-Glc, Me α -D-Xyl, Me β -D-Xyl) was examined by the dibutyltin oxide method, using phenoxythiocarbonyl chloride as the thioacylating agent. This method gave the mono-thionocarbonates regioselectively in high yields. Acetylation of these thionocarbonates followed by deoxygenation with tributyltin hydride smoothly gave the corresponding deoxy derivatives, except for the primary thionocarbonates. Similar treatment of the pyranosides that have a *cis*-vicinal glycol (Me α -D-Gal, Me β -D-Gal, Me β -L-Ara, and Ph α -L-Ara) led to the formation of cyclic thionocarbonates, which on acetylation followed by olefination with trimethyl phosphite afforded the unsaturated derivatives in satisfactory yields. On deacetylation and subsequent hydrogenation over platonic oxide, they gave the corresponding dideoxy derivatives quantitatively. The compounds thus prepared were identified by analyses of their proton and carbon-13 nuclear magnetic resonance spectra.

Keywords—glycopyranoside; regioselective thioacylation; dibutyltin oxide; deoxygenation; *cis*-vicinal glycol; thionocarbonate; cyclic thionocarbonate; deoxy, dideoxy sugar; unsaturated sugar; ¹³C-NMR

Introduction

Thiocarbonyl esters of the secondary alcohols are reduced by tributyltin hydride to give the deoxygenated derivatives, usually in high yields.²⁾ In the cases of poly-hydroxy compounds (such as carbohydrates), protection of those hydroxyl groups which need not be involved in the reaction is necessary prior to the thioacylation. In our previous paper we reported the regioselective acylation³⁾ and alkylation⁴⁾ of some non-protected glycopyranosides by using tin compounds. From those results, it is evident that the method using dibutyltin oxide permits regioselective acylation and alkylation of a particular secondary hydroxyl group instead of a primary hydroxyl group, and thus thioacylation is also expected to occur in a similar manner. This reaction, in combination with deoxygenation, should allow the preparation of deoxy sugars regioselectively, providing useful intermediates for the synthesis of natural products from easily available carbohydrates. However, the utility of this approach needs to be established.

In this paper, we describe the selective deoxygenation of some non-protected glycopyranosides *via* regioselective thioacylation by the dibutyltin oxide method.

Results and Discussion

Thioacylation

Among the reagents tested for thioacylation, phenoxythiocarbonyl chloride⁵⁾ was found

to be the most suitable for the preparation of monothionocarbonates by the Bu_2SnO method. Thioacylation with other reagents, such as *p*-methoxythiobenzoyl chloride, requires prolonged reaction time (5–6 h) and elevated temperature, even in the presence of catalysts (for example, 4-dimethylaminopyridine). Under such vigorous conditions, the yields of the desired products as well as the selectivity were reduced, and in most cases, migration of the thioacyl group also occurred. Moreover, an appreciable formation of di-*p*-methoxythionobenzoate was observed.

On the other hand, when phenoxythiocarbonyl chloride was used, the regioselectivity as well as the yields of the monothionocarbonates were excellent and the dithionocarbonates were not formed. For example, the stannylene derivative of methyl β -D-xylopyranoside (**11**), when reacted with 1.1 mol eq of phenoxythiocarbonyl chloride in dioxane at room temperature, gave the 4-thionocarbonate (**12a**) quantitatively within 1 h, without any catalyst.

Identification of each product and determination of the product composition were done as described in a previous paper³⁾ by analysis of the carbon-13 nuclear magnetic resonance (¹³C-NMR) spectra (Table I). In most cases, the monothionocarbonates obtained by the reaction could be completely analyzed by taking account of the thioacylation shifts (estimated from the acylation shift rule) with respect to the non-acylated compounds. Moreover, the proton nuclear magnetic resonance (¹H-NMR) signals of all methine protons could be completely assigned by successive proton decoupling experiments on the acetylated derivatives (see Experimental).

Stannylation was carried out with Bu_2SnO (1.5 mol eq) in refluxing dry methanol as described in a previous paper.³⁾ In parallel with the result of acylation, methyl α -D-

TABLE I. ¹³C-Chemical Shifts of Monothionocarbonates and Cyclic Thionocarbonates of Some Hexo- and Pentopyranosides and Their Thioacylation Shift Values (in Parentheses) in Pyridine-*d*₅

Thionocarbonate	C-1	C-2	C-3	C-4	C-5	C-6	OMe	C=S
Me α -D-Glc (1)	101.3	73.7	75.3	72.0	74.0	62.7	55.0	
2-Phenyl thionocarbonate (2a)	96.7 (-4.6)	84.3 (+10.6)	71.7 (-3.6)	72.0 (0)	74.1 (+0.1)	62.1 (-0.6)	54.9 (-0.1)	195.8
Me β -D-Glc (4)	105.5	74.9	78.2	71.4	78.2	62.6	56.7	
6-Phenyl thionocarbonate (5)	105.7 (+0.2)	74.9 (0)	78.2 (0)	71.2 (-0.2)	74.7 (-3.5)	62.6 (+12.1)	56.8 (+0.1)	195.6
Me α -D-Xyl (6)	101.5	73.7	75.5	71.4	63.1		55.1	
2-Phenyl thionocarbonate (7a)	97.1 (-4.4)	84.4 (+10.7)	72.3 (-3.2)	71.4 (0)	62.9 (-0.2)		55.1 (0)	195.9
4-Phenyl thionocarbonate (8a)	101.4 (-0.1)	73.6 (-0.1)	71.6 (-3.9)	83.0 (+11.6)	57.9 (-5.2)		55.4 (+0.3)	195.7
Me β -D-Xyl (11)	106.0	74.6	78.1	70.9	67.0		56.6	
4-Phenyl thionocarbonate (12a)	106.0 (0)	74.8 (+0.2)	74.3 (-3.8)	82.9 (+12.0)	62.0 (-5.0)		56.8 (+0.2)	195.6
Me α -D-Gal (15)	101.5	70.3	71.5	70.8	72.4	62.5	55.0	
3,4-Thionocarbonate (16a)	99.8 (-1.7)	67.9 (-2.4)	83.4 (+11.9)	81.2 (+10.4)	68.6 (-3.8)	60.8 (-1.7)	55.6 (+0.6)	192.6
Me β -D-Gal (13)	106.1	72.3	75.1	70.1	76.8	62.2	56.6	
3,4-Thionocarbonate (14a)	103.6 (-2.5)	71.4 (-0.9)	84.8 (+9.7)	80.8 (+10.7)	72.9 (-3.9)	61.0 (-1.2)	56.6 (0)	192.6
Me β -L-Ara (20)	102.0	70.4	70.8	70.0	63.8		55.3	
3,4-Thionocarbonate (21a)	99.7 (-2.3)	68.6 (-1.8)	82.9 (+12.1)	80.9 (+10.9)	57.6 (-6.2)		55.8 (+0.5)	192.5
Ph α -L-Ara (18)	102.7	72.0	74.4	69.3	67.2			
3,4-Thionocarbonate (19a)	99.2 (-2.5)	70.2 (-1.8)	83.7 (+9.3)	79.6 (+10.3)	61.6 (-5.6)			192.4

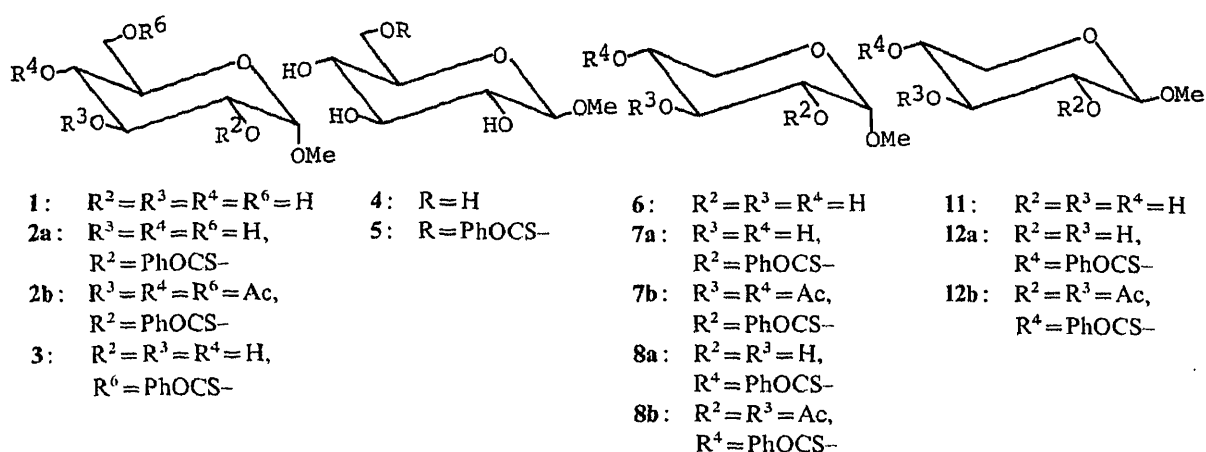


Chart 1

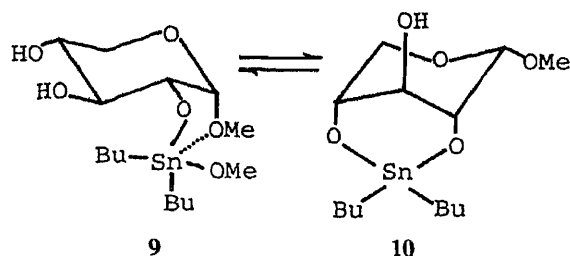


Chart 2

glucopyranoside (1) on stannylation followed by thioacylation with phenoxythiocarbonyl chloride at room temperature gave the 2- and 6-thionocarbonates (2a and 3) in 83.0% yield, the 2-thionocarbonate (2a) was the major product and the 6-thionocarbonate was the minor product (Table II). On similar treatment, methyl β -D-glucopyranoside (4) gave the 6-thionocarbonate (5) as the sole product in 84.8% yield (Table II).

Reduced regioselectivity in thioacylation was observed for methyl α -D-xylopyranoside (6), which yielded the 2- and 4-thionocarbonates (7a and 8a) in the ratio of 54:46 (Table II). This result is parallel with that of acylation³⁾ and could be ascribed to a partial contribution of the cyclic tin intermediate 10 besides the major contribution of 9.

On the other hand, it is interesting that the thioacylation of the pyranosides that have a *cis*-vicinal glycol produced the cyclic thionocarbonates in high yields. The direct preparation of cyclic thionocarbonates from non-protected sugars by using other reagents, such as thiocarbonyldiimidazole⁶⁾ or thiophosgene⁷⁾ gave poor results, so the above method represents a facile procedure to obtain the cyclic thionocarbonates without protecting the other hydroxyl groups. The formation of cyclic thionocarbonates, however, reduces the regioselectivity of deoxygenation, but these products should be useful as intermediates for the synthesis of unsaturated and dideoxy sugars. The mechanism of cyclic thionocarbonate formation is shown in Chart 3.

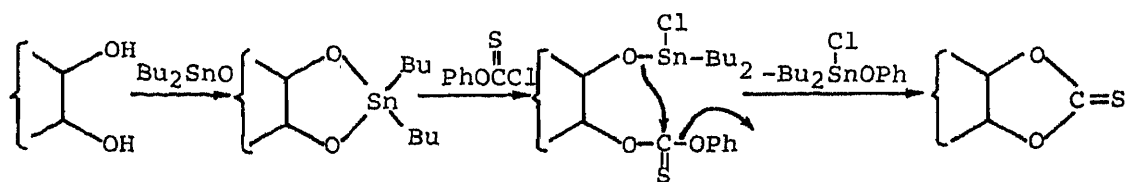


Chart 3

Thus, methyl β -D-galactopyranoside (**13**) on stannylation followed by thioacylation gave a cyclic thionocarbonate (**14a**) as a syrup in 85.3% yield with a trace of other thionocarbonates. This compound (**14a**) exhibited no aromatic proton signals in its $^1\text{H-NMR}$ spectrum, but a signal at δ 192.6 due to $\text{C}=\text{S}$ was observed in the $^{13}\text{C-NMR}$ spectrum. On acetylation it gave the 2,6-diacetate (**14b**) quantitatively as colorless needles, mp 94—96 °C. This compound showed two acetyl signals in its $^1\text{H-NMR}$ spectrum and the H-2 and H-6 signals appeared at low field compared with those of the parent compound (**14a**). On similar treatment, methyl α -D-galactopyranoside (**15**) produced the 3,4-cyclic thionocarbonate (**16a**) and 6-thionocarbonate (**17**) in the ratio of 71 : 29 with a combined yield of 71.5%. On acetylation, **16a** gave the 2,6-diacetate (**16b**) quantitatively as colorless needles, mp 131—132 °C. The identity of this compound was confirmed by detailed examination of its $^1\text{H-NMR}$ spectrum.

Pentopyranosides, such as phenyl α -L-arabinopyranoside (**18**) and methyl β -L-arabinopyranoside (**20**) also undergo thioacylation as described above to produce the corresponding 3,4-cyclic thionocarbonates **19a** (colorless needles, mp 202—203 °C) and **21a** (syrup) in 94.9% and 83.2% yields, respectively (Table III). These products were completely analyzed by successive proton decoupling experiments on their acetylated derivatives **19b** and **21b** and from the $^{13}\text{C-NMR}$ spectra.

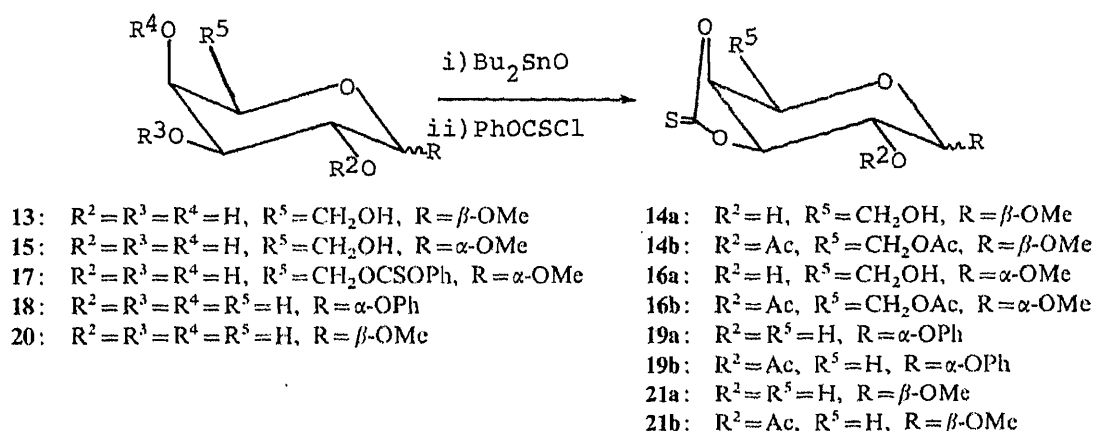


Chart 4

Deoxygenation

The acetates of the above thionocarbonates undergo smooth deoxygenation when heated at 75—100 °C with 1—1.5 mol eq of Bu_3SnH in toluene with the addition of a catalytic amount of 2,2-azobisisobutyronitrile (AIBN). Under these conditions, methyl α -D-glucopyranoside 2-thionocarbonate 3,4,6-triacetate (**2b**) gave the 2-deoxy compound (**22b**) in 75.6% yield. This compound exhibited no aromatic proton signals in its $^1\text{H-NMR}$ spectrum, but it showed two up-field proton signals at δ 2.28 (1H, dd, $J=5.5$ and 13.0 Hz) and at δ 1.24 (1H, ddd, $J=3.5$, 12.0, and 13.0 Hz) due to H-2 protons, which were again confirmed by successive proton decoupling experiments. In the $^{13}\text{C-NMR}$ spectrum, the C-2 carbon signal appeared at δ 39.0.

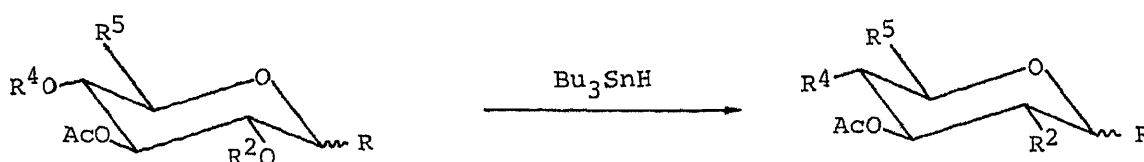
Similarly, the 2- and 4-thionocarbonate diacetates, (**7b**) and (**8b**), of methyl α -D-xylopyranoside (**6**) and the 4-thionocarbonate diacetate (**12b**) of methyl β -D-xylopyranoside (**11**) were deoxygenated to the corresponding deoxy derivatives in the yields given in Table II. The structures of these products were also confirmed by analyses of the $^1\text{H-}$ and $^{13}\text{C-NMR}$ spectra (Table IV).

The secondary thionocarbonates were smoothly reduced to the corresponding deoxy derivatives. However, the primary thionocarbonates produced the deoxy compounds in poor

TABLE II. Yields and Percentage Compositions of the Mono-thionocarbonates and the Deoxy Derivatives of the Glycopyranosides That Do Not Have a *cis*-Vicinal Glycol System

Starting material	Mono-thionocarbonate		Deoxy derivatives		
	Yield (%)	Composition ^{a)}	Yield (%)		
Me α -D-Glc (1)	83.0	2-Ester (2a)	93.5	2-Deoxy (22b)	75.6
		6-Ester (3)	6.5	—	—
Me β -D-Glc (4)	84.8	6-Ester (5)	100.0	—	—
Me α -D-Xyl (6)	76.3	2-Ester (7a)	54.0	2-Deoxy (23)	91.6
		4-Ester (8a)	46.0	4-Deoxy (24)	83.2
Me β -D-Xyl (11)	97.4	4-Ester (12a)	100.0	4-Deoxy (25)	82.6

a) Composition was determined by measuring the OMe peak areas in the ¹H-NMR spectra.



- 2b: R⁴ = Ac, R⁵ = CH₂OAc, R² = PhOCS-, R = α -OMe 22b: R⁴ = OAc, R⁵ = CH₂OAc, R² = H, R = α -OMe
 7b: R⁴ = Ac, R⁵ = H, R² = PhOCS-, R = α -OMe 23: R⁴ = OAc, R² = R⁵ = H, R = α -OMe
 8b: R² = Ac, R⁵ = H, R⁴ = PhOCS-, R = α -OMe 24: R² = OAc, R⁴ = R⁵ = H, R = α -OMe
 12b: R² = Ac, R⁵ = H, R⁴ = PhOCS-, R = β -OMe 25: R² = OAc, R⁴ = R⁵ = H, R = β -OMe

Chart 5

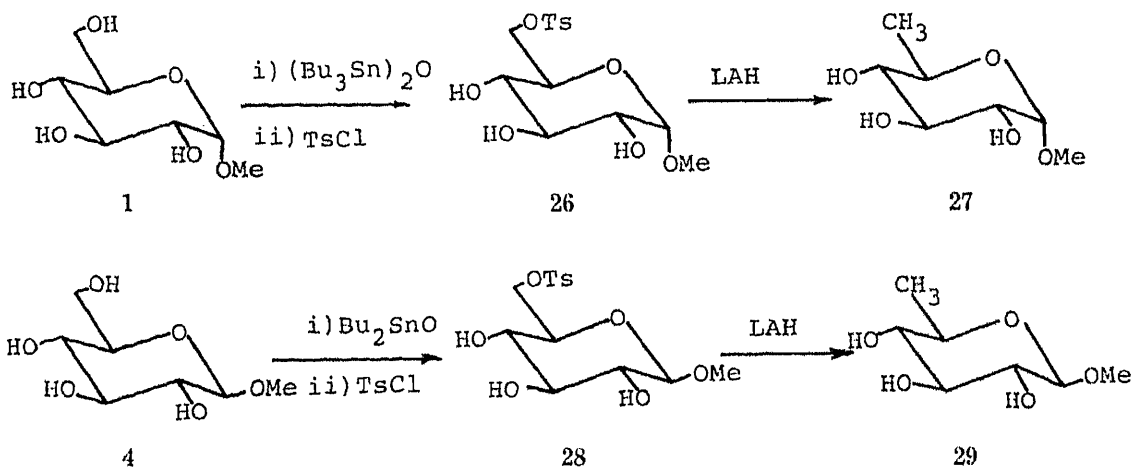


Chart 6

yields [for example, the 6-thionocarbonates of α - and β -D-glucopyranoside (3 and 5) and methyl α -D-galactopyranoside (17)], clearly because of the lesser stability of the primary relative to the secondary carbon radical.⁸⁾

On the other hand, primary tosylates undergo smooth deoxygenation with an excess of lithium aluminum hydride (LAH) in refluxing tetrahydrofuran (THF). Thus, tosylation of methyl α -D-glucopyranoside (1) by using the $(\text{Bu}_3\text{Sn})_2\text{O}$ method,³⁾ gave the 6-tosylate (26) as the major product, which on reduction with an excess of LAH gave the corresponding 6-deoxy compound (27) in 71% yield. Tosylation of methyl β -D-glucopyranoside (4) by using the Bu_2SnO method produced the 6-tosylate (28) in 92.4% yield, and this was also reduced to

the corresponding 6-deoxy compound in 68% yield. These 6-deoxy compounds were characterized by analyses of their ^1H - and ^{13}C -NMR spectra.

The cyclic thionocarbonates, produced from the pyranosides with a *cis*-vicinal glycol, undergo radical deoxygenation by Bu_3SnH , but in these cases two deoxy compounds were formed, thus reducing the yield as well as the selectivity of deoxygenation. By using this method, the 3,4-cyclic thionocarbonate acetates of methyl α - and β -D-galactopyranosides were deoxygenated to the corresponding 3- and 4-deoxy derivatives in the yields shown in Table III. The products were identified and characterized by analyses of their ^1H - and ^{13}C -NMR spectra.

3,4-Cyclic thionocarbonate acetates of pentopyranosides, such as phenyl α -L-

TABLE III. Yields and Percentage Compositions of the Cyclic Thionocarbonates, Deoxy, Unsaturated, and Dideoxy Derivatives of the Pyranosides Which Possess a *cis*-Vicinal Glycol System

Starting material	3,4-Thionocarbonate Yield (%)	Deoxy compound		Unsaturated compound Yield (%)	Dideoxy compound Yield (%)
		Yield (%)	3-Deoxy:4-Deoxy		
Me β -D-Gal (13)	(14a) 85.3	56.0	(30) 57:(31) 43	(41b) 65.6	(42) (96)
Me α -D-Gal (15)	(16a) 62.6	56.6	(32) 67:(33) 33	(43b) 55.1	(44) 100
Ph α -L-Ara (18)	(19a) 94.9	73.6	(34) 74:(35) 26	(45b) 75.6	(46) 99
Me β -L-Ara (20)	(21a) 83.2	57.3	(36) 50:(37) 50	(47b) 64.8	(48) 99

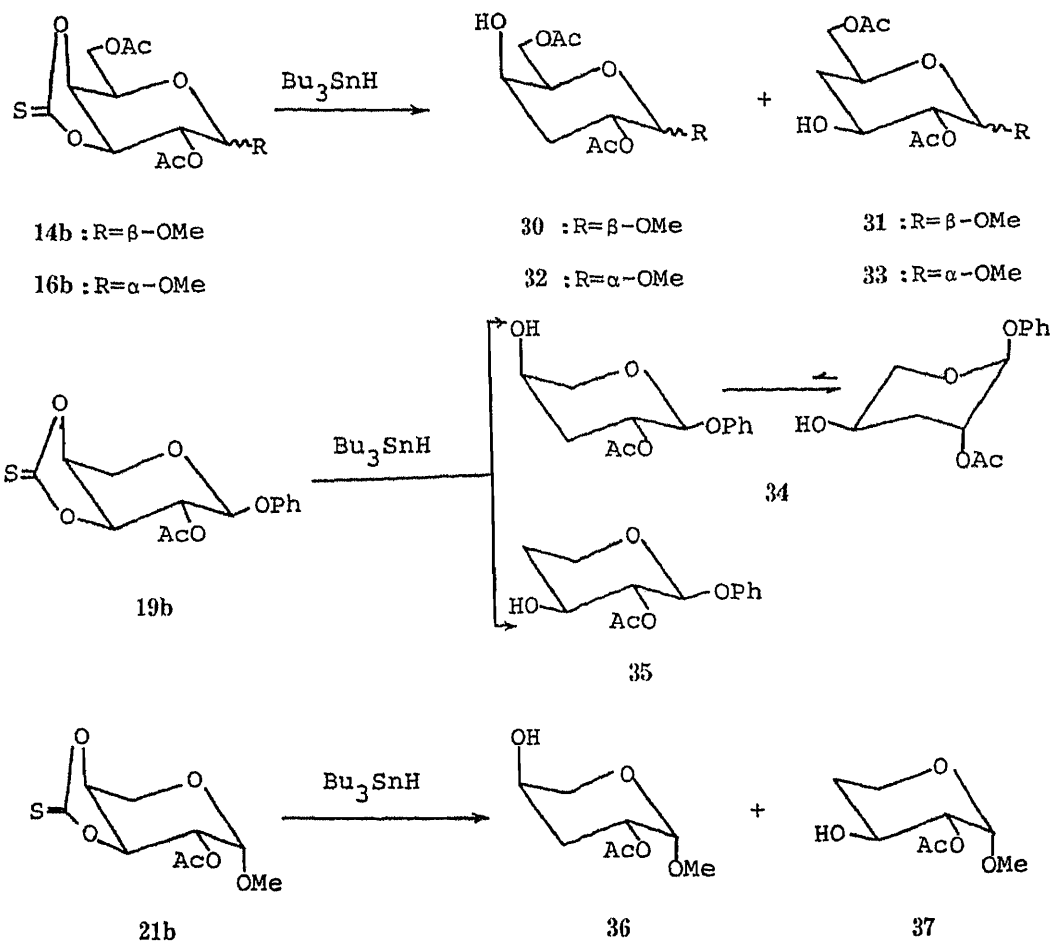


Chart 7

arabinopyranoside (**18**) and methyl β -L-arabinopyranoside (**20**) also undergo similar deoxygenation to give the corresponding 3- and 4-deoxy derivatives in the yields given in Table III. From the $^1\text{H-NMR}$ spectra the 3-deoxy derivative (**34**) of phenyl α -L-arabinopyranoside was found to be in the $1C$ conformation, since its anomeric proton signal appeared at δ 5.71 as a doublet with $J=2.5$ Hz. Spectral data for the deoxy sugars are listed in Table IV.

It should be noted that when this deoxygenation reaction was carried out at a higher temperature and/or a higher concentration of the reagent, undesired side reactions were observed. For example, when **21b** was treated with an excess of Bu_3SnH (5 mol eq) at 100°C , the methyldene derivative (**38**) and a compound tentatively assigned as **39**, mp $117\text{--}119^\circ\text{C}$, were the major products. The reaction with 1.5 mol eq of the reagent at 100°C produced four products, **36**, **38**, **39**, and **40**, of which **40** is the acetyl migration product from the expected 4-deoxy derivative (**37**).⁹⁾ The best result was obtained by the reaction of **21b** with 1.5 mol eq of Bu_3SnH at 75°C , where the expected **36** and **37** were produced in a ratio of 1:1 with the combined yield of 56.7% (see Table III). Details of the above side reactions and the structure

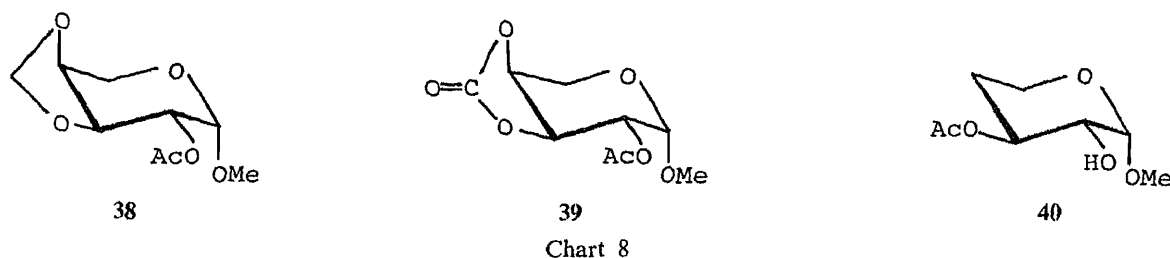


TABLE IV. ^{13}C -Chemical Shifts of Deoxy Derivatives of Some Hexo- and Pentopyranosides in Pyridine- d_5

Deoxy sugars of	C-1	C-2	C-3	C-4	C-5	C-6	OMe	CH_3	C=O
2-Deoxy sugars of									
Me α -D-Glc (22b)	99.2	39.0	69.5	74.4 ^{a)}	73.6 ^{a)}	62.9	54.4		
Me α -D-Xyl 3,4-diAc (23)	98.5	34.9	68.8 ^{a)}	69.9 ^{a)}	59.8		54.8	20.7	160.9
								20.9	170.1
3-Deoxy sugars of									
Me α -D-Gal 2,6-diAc (32)	97.3	67.7	32.3	66.1	69.2	64.8	54.8	20.7	170.4
								20.9	170.7
Me β -D-Gal 2,6-diAc (30)	103.7	68.7	36.6	65.6	76.4	64.5	56.0	21.0	169.7
								21.7	169.9
Ph α -L-Ara 2-Ac (34)	95.1	70.2	33.6	66.2	61.6			20.9	170.1
Me β -L-Ara 2-Ac (36)	97.9	68.1	32.0	65.9	64.8		55.1	21.0	170.3
4-Deoxy sugars of									
Me α -D-Gal 2,6-diAc (33)	98.4	76.9	65.0	36.8	66.4	66.3	54.9	20.7	170.5
								20.9	170.8
Me β -D-Gal 2,6-diAc (31)	102.5	76.7	70.4 ^{a)}	36.6	69.3 ^{a)}	66.1	56.2	20.6	170.1
								21.0	170.4
Me α -D-Xyl 2,3-diAc (24)	98.3	72.8	68.2	31.3	57.3		55.0	20.7	170.1
								20.8	170.4
Me β -D-Xyl 2,3-diAc (25)	102.1	72.2	70.9	30.3	60.2		56.2	20.8	169.8
								20.8	170.2
Ph α -L-Ara 2-Ac (35)	100.2	76.3	69.3	34.0	61.7			20.9	170.1
Me β -L-Ara 2-Ac (37)	98.7	76.9	65.3	34.9	58.3		55.0	21.0	170.8
Me β -L-Ara 3-Ac (40)	101.6	71.6	71.6	31.2	57.5		55.0	20.9	170.5
6-Deoxy sugars of									
Me α -D-Glc (27)	101.4	74.0	75.1	77.4	68.5	18.6	55.0		
Me β -D-Glc (29)	105.4	75.2	78.2	72.9	76.8	18.6	56.6		

a) Assignments may be interchanged in each row.

determinations of the by-products will be presented in a separate paper.

Olefination and Hydrogenation

The acetates of the cyclic thionocarbonates synthesized in a foregoing section undergo olefination according to the Corey-Winter method,¹⁰⁾ to produce the unsaturated sugars in satisfactory yields. Thus the 3,4-cyclic thionocarbonate 2,6-diacetate (**14b**) of methyl β -D-galactopyranoside, when heated under reflux in trimethylphosphite, gave the corresponding unsaturated derivative (**41b**) (65.6%) as colorless needles, mp 78–80°C. In the ¹H-NMR spectrum it showed low-field signals at δ 5.91 (1H, ddd, $J=1.2, 1.8,$ and 10.4 Hz) due to H-3 and at δ 5.85 (1H, ddd, $J=2.4, 3.0,$ and 10.4 Hz) due to H-4, confirming the presence of a double bond between the 3- and 4-positions. Moreover, in the ¹³C-NMR spectrum two low-field signals due to C-3 and C-4 appeared at δ 129.2 and 124.7, respectively (Table V). Deacetylation with NaOMe in MeOH followed by hydrogenation over PtO₂ in MeOH produced the 3,4-dideoxy derivative (**42**) quantitatively. This compound showed four high-field proton signals due to H₂-3 and H₂-4 between δ 1.45 to 2.12 as multiplets, and in the ¹³C-NMR spectrum the C-3 and C-4 carbon signals appeared at δ 29.0 and 26.0, respectively (Table V).

The 3,4-cyclic thionocarbonate 2,6-diacetate (**16b**) of methyl α -D-galactopyranoside also produced the unsaturated compound (**43b**) in 55.1% yield. The site of unsaturation between C-3 and C-4 was confirmed by analysis of the ¹H-NMR spectrum and from ¹H-¹³C shift correlation studies. This compound (**43b**) on deacetylation followed by hydrogenation gave the 3,4-dideoxy compound (**44**) quantitatively.

The 3,4-cyclic thionocarbonate acetates of pentopyranosides, such as phenyl α -L-arabinopyranoside (**19b**) and methyl β -L-arabinopyranoside (**21b**), undergo similar olefina-

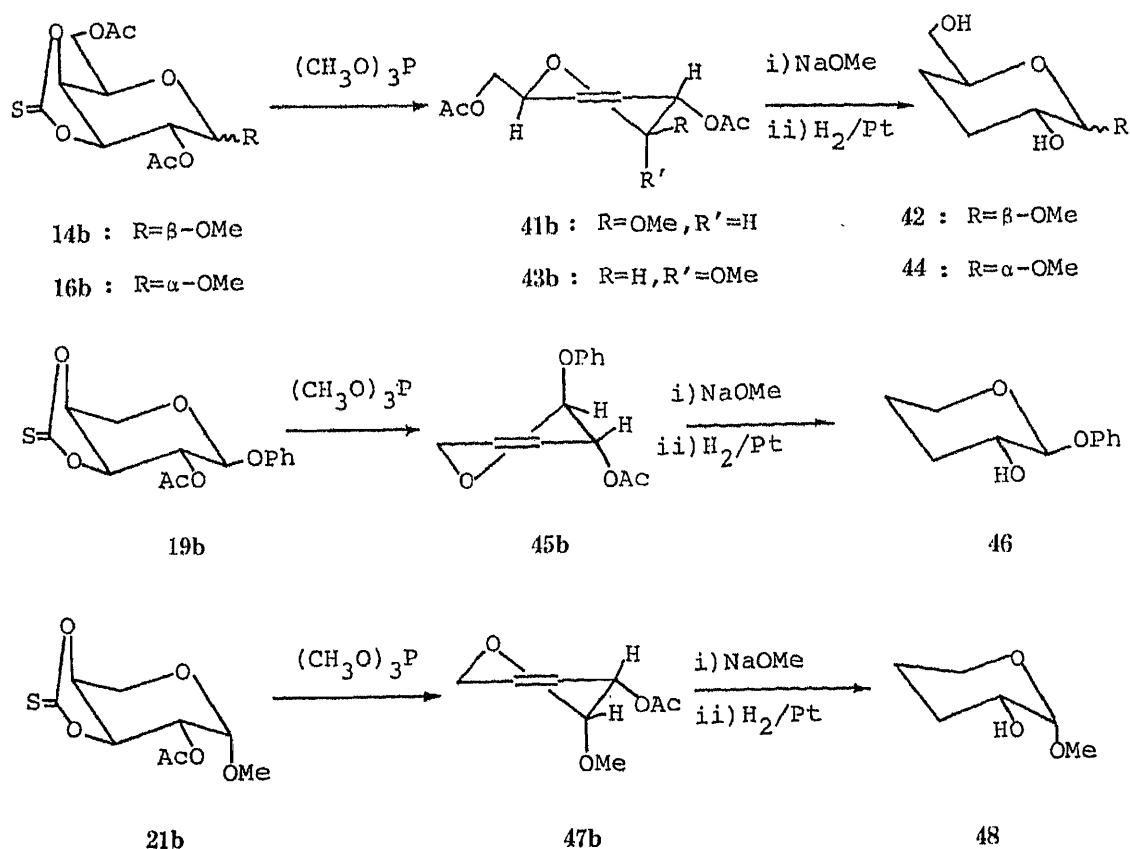


Chart 9

TABLE V. ^{13}C -NMR Chemical Shifts of Some Unsaturated Glycopyranosides and Their Dideoxy Derivatives in CDCl_3

Compounds		C-1	C-2	C-3	C-4	C-5	C-6	OMe	Me	C=O
Me β -D-Gal										
3-Enoside, 2,6-diAc	(41b)	100.1	67.3	129.2	124.7	71.6	65.9	56.2	21.0	170.0
3-Enoside	(41a)	103.7	66.9	128.4	127.6	75.5	65.0	56.7	20.8	170.1
3,4-Dideoxy	(42)	106.4	69.8	29.0	26.0	76.5	65.2	56.9		
Me α -D-Gal										
3-Enoside, 2,6-diAc	(43b)	95.9	66.7	127.9	124.3	66.5	65.3	56.0	20.9	170.7
3-Enoside	(43a)	98.2	64.3	128.9	126.4	69.0	64.9	56.1	20.8	170.4
3,4-Dideoxy	(44)	99.4	68.2	27.1	26.0	68.5	65.5	55.1		
Ph α -L-Ara										
3-Enoside, 2-Ac	(45b)	95.9	65.8	131.4	120.1	59.8			21.0	170.2
3-Enoside	(45a)	98.6	64.5	129.3	124.2	60.9				
3,4-Dideoxy	(46)	100.8	68.0	27.7	22.3	63.5				
Me β -L-Ara										
3-Enoside, 2-Ac	(47b)	96.1	66.5	129.3	121.8	60.2		56.1	21.0	170.6
3-Enoside	(47a)	98.1	64.2	129.0	127.0	60.0		56.1		
3,4-Dideoxy	(48)	99.7	68.0	27.5	24.0	59.5		55.1		

tion to produce the corresponding unsaturated derivatives (**45b** and **47b**) in 75.6 and 64.8% yields, respectively. In both cases, the site of unsaturation was between the C-3 and C-4 positions. Compound **45b** was found to be in the 1H_0 conformation, since the anomeric proton signal appeared at δ 5.56 as a broad singlet in the ^1H -NMR spectrum. On deacetylation followed by hydrogenation, **45b** and **47b** gave the corresponding dideoxy derivatives **46** and **48** quantitatively, as confirmed by analyses of their ^1H - and ^{13}C -NMR spectra. From the ^1H -NMR spectrum, **46** was found to be in the $C1$ conformation, since its anomeric proton signal appeared at δ 5.03 as a doublet with $J = 5.2$ Hz.

Conclusion

The glycopyranosides whose hydroxyl groups are all *trans* oriented are regioselectively mono-thioacylated by the Bu_2SnO method and are deoxygenated to the corresponding deoxy derivatives in high yields. In the cases of pyranosides which possess a *cis*-vicinal glycol system, this method produces the cyclic thionocarbonates, which are smoothly deoxygenated to the dideoxy sugars through the unsaturated derivatives. The deoxy, unsaturated, and dideoxy sugars thus obtained should be useful intermediates for syntheses of complex molecules having chiral centers.

Experimental

Melting points were determined on a Yanaco micro hot stage melting point apparatus and are uncorrected. Infrared (IR) spectra were recorded in KBr discs on a Jasco IRA-2 spectrometer and the data are given in cm^{-1} . Unless otherwise stated, ^1H -NMR (400 MHz) spectra and ^{13}C -NMR spectra (100 MHz) were recorded with a JEOL JNM GX400 FT NMR spectrometer in pyridine- d_5 solution with tetramethylsilane as an internal standard, and the chemical shifts are given in δ values. Concentrations were about 0.1–0.3 mmol/ml. Column chromatography was performed on Wakogel C-200. For thin layer chromatography (TLC) Kieselgel 60F₂₅₄ precoated plates were used and spots were developed by spraying 1% $\text{Ce}(\text{SO}_4)_2$ in 10% H_2SO_4 and heating the plates at 100 °C until coloration took place.

Thioacylation of Pyranosides (General Procedure)—Glycopyranoside (0.3–0.9 mmol) and Bu_2SnO (1.5 mol eq) in dry MeOH (10–25 ml) were heated under reflux until the mixture became homogeneous and clear (about 1 h). The mixture was refluxed for an additional 2 h, then the solvent was evaporated off *in vacuo* to leave a glassy solid,

which was dissolved in dioxane (10–25 ml). Phenoxythiocarbonyl chloride (1.1 mol eq) was added dropwise to the stirred solution at room temperature. When the tin complex was insoluble in dioxane (in the cases of Me α -D-Gal and Me β -D-Gal), it was suspended in dioxane. The mixture became clear upon addition of phenoxythiocarbonyl chloride. Maximum conversion was checked by TLC. After 1–1.5 h, the solvent was evaporated off *in vacuo* to leave a syrupy residue, which was subjected to column chromatography for further separation.

Deoxygenation (General Procedure)—The mono-thionocarbonates or cyclic thionocarbonates obtained by the above procedure were acetylated with acetic anhydride and pyridine in a usual manner. The acetates (100–300 mg) thus obtained were dissolved in toluene (10–15 ml), Bu_3SnH (1.1–1.5 mol eq) was added, and the mixture was heated at 75–100 °C with the addition of catalytic amount of AIBN for 1–3.5 h. The solvent was evaporated off *in vacuo* to leave a syrup, which was chromatographed for further separation and purification.

Olefination and Hydrogenation (General Procedure)—The cyclic thionocarbonate obtained by the thioacylation of the pyranosides which possesses a *cis*-vicinal glycol was acetylated with acetic anhydride and pyridine in a usual manner. The acetate (20–200 mg) was dissolved in trimethyl phosphite (3–5 ml) and heated under reflux for 70 h. Saturated Na_2CO_3 aq. was added to the cooled mixture and the mixture was extracted with CH_2Cl_2 . The organic extract was dried and concentrated *in vacuo* to leave a residue, which was purified by silica gel column chromatography with benzene–AcOEt. The unsaturated sugar (30–60 mg) thus obtained was deacetylated with 0.2 N NaOMe (0.3–0.6 ml) in MeOH (2.5–5 ml) at room temperature for 20–30 min. The reaction mixture was then made just neutral by adding Dowex 50 \times 8 (H^+) and filtered. The filtrate was concentrated *in vacuo* to leave a residue, which was subjected to hydrogenation over PtO_2 in MeOH for 4–5 h without further purification. The catalyst was removed by filtration, the filtrate was carefully concentrated *in vacuo* and the residue was subjected to preparative TLC.

Methyl α -D-Glucopyranoside 2-Phenylthionocarbonate (2a)—Needles from AcOEt–light petroleum, mp 128–129 °C. $^1\text{H-NMR}$ (200 MHz): 7.06–7.36 (5H, m, ArH), 5.79 (1H, dd, $J = 3.9, 10.0$ Hz, H-2), 5.51 (1H, d, $J = 3.9$ Hz, H-1), 4.37 (1H, t, $J = 10.0$ Hz, H-3), 3.39 (3H, s, OMe). IR: 3400, 2900, 1040. Anal. Calcd for $\text{C}_{14}\text{H}_{18}\text{O}_7\text{S}$: C, 50.90; H, 5.50. Found: C, 50.96; H, 5.54.

The 3,4,6-triacetate (2b) was a syrup. $^1\text{H-NMR}$ (200 MHz, CDCl_3): 7.03–7.44 (5H, m, ArH), 5.62 (1H, dd, $J = 10.0, 10.5$ Hz, H-3), 5.42 (1H, dd, $J = 4.0, 10.0$ Hz, H-2), 5.18 (1H, d, $J = 4.0$ Hz, H-1), 5.09 (1H, t, $J = 10.5$ Hz, H-4), 4.00–4.36 (3H, m, H-5 and H-6), 3.46 (3H, s, OMe), 2.02, 2.03, and 2.09 (3H each, s, OAc).

The 6-phenylthionocarbonate (3) was also formed, but was not isolated; it showed an OMe signal at δ 3.35.

Methyl β -D-Glucopyranoside 6-Phenylthionocarbonate (5)—Syrup. $^1\text{H-NMR}$: 7.17–7.41 (5H, m, ArH), 5.38 (1H, dd, $J = 0.8, 11.4$ Hz, H-6), 5.17 (1H, dd, $J = 5.5, 11.4$ Hz, H-6), 4.72 (1H, d, $J = 7.6$ Hz, H-1), 4.22 (1H, t, $J = 8.0$ Hz, H-3), 4.13 (2H, m, H-4, 5), 4.01 (1H, dd, $J = 7.6, 8.0$ Hz, H-2), 3.62 (3H, s, OMe). High resolution (HR) MS m/z Calcd for $\text{C}_{13}\text{H}_{18}\text{O}_7\text{S}$: 318.0773. Found: 318.0772.

Methyl α -D-Xylopyranoside 2-Phenylthionocarbonate (7a)—Needles from hexane–AcOEt, mp 130–131 °C. $^1\text{H-NMR}$: 7.12–7.36 (5H, m, ArH), 5.80 (1H, dd, $J = 3.5, 9.5$ Hz, H-2), 5.49 (1H, d, $J = 3.5$ Hz, H-1), 4.71 (1H, t, $J = 9.5$ Hz, H-3), 4.27 (1H, m, H-4), 3.95–4.08 (2H, m, H-5), 3.38 (3H, s, OMe). IR: 3400, 2900, 1040. Anal. Calcd for $\text{C}_{13}\text{H}_{16}\text{O}_6\text{S}$: C, 52.00; H, 5.37. Found: C, 51.96; H, 5.39.

The 3,4-diacetate (7b) forms needles from hexane–ether, mp 139–140 °C. $^1\text{H-NMR}$ (CDCl_3): 7.07–7.44 (5H, m, ArH), 5.65 (1H, t, $J = 9.5$ Hz, H-3), 5.39 (1H, dd, $J = 3.7, 9.5$ Hz, H-2), 5.14 (1H, d, $J = 3.7$ Hz, H-1), 5.05 (1H, ddd, $J = 5.8, 9.5, 10.7$ Hz, H-4), 3.84 (1H, dd, $J = 5.8, 10.7$ Hz, H-5eq), 3.66 (1H, t, $J = 10.7$ Hz, H-5ax), 3.47 (3H, s, OMe), 2.05 and 2.08 (3H each, s, OAc). IR: 2950, 1740, 1040. Anal. Calcd for $\text{C}_{17}\text{H}_{20}\text{O}_8\text{S}$: C, 53.12; H, 5.25. Found: C, 53.02; H, 5.31.

Methyl α -D-Xylopyranoside 4-Phenylthionocarbonate (8a)—Needles from hexane–AcOEt, mp 115–116 °C. $^1\text{H-NMR}$: 7.17–7.36 (5H, m, ArH), 5.80 (1H, ddd, $J = 5.8, 9.2, 10.5$ Hz, H-4), 5.07 (1H, d, $J = 3.5$ Hz, H-1), 4.67 (1H, t, $J = 9.2$ Hz, H-3), 4.26 (1H, dd, $J = 5.8, 10.5$ Hz, H-5eq), 4.14 (1H, dd, $J = 3.5, 9.2$ Hz, H-2), 3.83 (1H, t, $J = 10.5$ Hz, H-5ax), 3.41 (3H, s, OMe). IR: 2900, 2400, 1040. Anal. Calcd for $\text{C}_{13}\text{H}_{16}\text{O}_6\text{S}$: C, 52.00; H, 5.31. Found: C, 51.99; H, 5.40.

The 2,3-diacetate (8b) forms needles from hexane–AcOEt, mp 145–147 °C. $^1\text{H-NMR}$ (CDCl_3): 7.05–7.43 (5H, m, ArH), 5.67 (1H, t, $J = 9.5$ Hz, H-3), 5.50 (1H, ddd, $J = 6.0, 9.5, 10.5$ Hz, H-4), 4.89–4.92 (2H, m, H-1 and H-2), 4.07 (1H, dd, $J = 6.0, 10.7$ Hz, H-5eq), 3.76 (1H, t, $J = 10.7$ Hz, H-5ax), 3.43 (3H, s, OMe), 2.08 and 2.10 (3H each, s, OAc). IR: 2950, 1740, 1040. Anal. Calcd for $\text{C}_{17}\text{H}_{20}\text{O}_8\text{S}$: C, 53.12; H, 5.25. Found: C, 52.85; H, 5.11.

Methyl β -D-Xylopyranoside 4-Phenylthionocarbonate (12a)—Leaflets from hexane–AcOEt, mp 136–137 °C. $^1\text{H-NMR}$ (200 MHz): 7.16–7.43 (5H, m, ArH), 5.88 (1H, dt, $J = 5.5, 9.5$ Hz, H-4), 4.67 (1H, d, $J = 7.5$ Hz, H-1), 4.61 (1H, dd, $J = 5.5, 11.5$ Hz, H-5eq), 4.48 (1H, t, $J = 9.5$ Hz, H-3), 4.08 (1H, dd, $J = 7.5, 9.5$ Hz, H-2), 3.71 (1H, dd, $J = 9.5, 11.5$ Hz, H-5ax), 3.59 (3H, s, OMe). IR: 3400, 2900, 1040. Anal. Calcd for $\text{C}_{13}\text{H}_{16}\text{O}_6\text{S}$: C, 52.00; H, 5.37. Found: C, 52.19; H, 5.49.

The 2,3-diacetate (12b) forms needles from hexane–ether, mp 126–127 °C. $^1\text{H-NMR}$ (CDCl_3): 7.07–7.44 (5H, m, ArH), 5.45 (1H, dt, $J = 4.5, 7.5$ Hz, H-4), 5.35 (1H, t, $J = 7.5$ Hz, H-3), 4.96 (1H, dd, $J = 6.0, 7.5$ Hz, H-2), 4.50 (1H, d, $J = 6.0$ Hz, H-1), 4.35 (1H, dd, $J = 4.5, 12.2$ Hz, H-5eq), 3.62 (1H, dd, $J = 7.5, 12.2$ Hz, H-5ax), 3.49 (3H, s, OMe), 2.09 (6H, s, OAc \times 2). IR: 2950, 1740, 1040. Anal. Calcd for $\text{C}_{17}\text{H}_{20}\text{O}_8\text{S}$: C, 53.12; H, 5.25. Found: C, 52.87; H, 5.30.

Methyl β -D-Galactopyranoside 3,4-Thionocarbonate (14a)—Syrup. $^1\text{H-NMR}$: 5.57 (1H, dd, $J=2.0, 7.5$ Hz, H-4), 5.48 (1H, dd, $J=6.0, 7.5$ Hz, H-3), 4.78 (1H, d, $J=7.0$ Hz, H-1), 4.51 (1H, dt, $J=2.0, 8.0$ Hz, H-5), 4.30—4.34 (2H, m, H₂-6), 4.21 (1H, dd, $J=6.0, 7.0$ Hz, H-2), 3.51 (3H, s, OMe).

The 2,6-diacetate (14b) forms needles from benzene-AcOEt, mp 94—96 °C. $^1\text{H-NMR}$ (CDCl_3): 4.97—5.15 (3H, m, H-2, 3, 4), 4.75 (1H, br d, $J=ca. 6.0$ Hz, H-1), 4.44 (1H, dd, $J=6.4, 11.5$ Hz, H-6), 4.31 (1H, dd, $J=6.4, 11.5$ Hz, H-6), 4.18 (1H, dt, $J=2.0, 6.4$ Hz, H-5), 3.45 (3H, s, OMe), 2.12 and 2.14 (3H each, s, OAc). IR: 1810, 1740, 1040. *Anal.* Calcd for $\text{C}_{12}\text{H}_{16}\text{O}_8\text{S}$: C, 45.00; H, 5.04. Found: C, 45.45; H, 5.10.

Methyl α -D-Galactopyranoside 3,4-Thionocarbonate (16a)—Syrup. $^1\text{H-NMR}$: 5.52—5.57 (1H, m, H-4), 5.50 (1H, t, $J=7.0$ Hz, H-3), 5.20 (1H, d, $J=4.0$ Hz, H-1), 4.56 (1H, dt, $J=2.0, 7.0$ Hz, H-5), 4.31 (1H, dd, $J=4.0, 7.0$ Hz, H-2), 4.24—4.28 (2H, m, H₂-6), 3.42 (3H, s, OMe).

The 2,6-diacetate (16b) forms needles from hexane- CH_2Cl_2 , mp 131—132 °C. $^1\text{H-NMR}$ (CDCl_3): 5.07 (1H, t, $J=7.0$ Hz, H-3), 5.02 (1H, d, $J=3.7$ Hz, H-1), 4.94—4.98 (2H, m, H-2 and H-4), 4.42 (1H, dd, $J=7.0, 11.5$ Hz, H-6), 4.37 (1H, dd, $J=6.0, 11.5$ Hz, H-6), 4.23 (1H, ddd, $J=2.5, 6.0, 7.0$ Hz, H-5), 3.42 (3H, s, OMe), 2.12 and 2.16 (3H each, s, OAc). IR: 1720, 1140, 1020. *Anal.* Calcd for $\text{C}_{12}\text{H}_{16}\text{O}_8\text{S}$: C, 45.00; H, 5.04. Found: C, 44.82; H, 5.00.

The 6-phenylthionocarbonate (17) was also formed, but was not isolated; it showed an OMe signal at δ 3.47.

Phenyl α -L-Arabinopyranoside 3,4-Thionocarbonate (19a)—Needles from AcOEt, mp 202—203 °C. $^1\text{H-NMR}$: 6.99—7.35 (5H, m, ArH), 5.60 (1H, d, $J=6.0$ Hz, H-1), 5.52 (1H, dd, $J=6.0, 8.0$ Hz, H-3), 5.40 (1H, ddd, $J=2.5, 3.0, 8.5$ Hz, H-4), 4.55 (1H, t, $J=6.0$ Hz, H-2), 4.50 (1H, dd, $J=2.5, 14.0$ Hz, H-5eq), 4.30 (1H, dd, $J=3.0, 14.0$ Hz, H-5ax). IR: 3350, 2950, 1080. *Anal.* Calcd for $\text{C}_{12}\text{H}_{12}\text{O}_5\text{S}$: C, 53.73; H, 4.51. Found: C, 53.97; H, 4.55.

The 2-acetate (19b) forms needles from hexane-ether- CH_2Cl_2 , mp 118—120 °C. $^1\text{H-NMR}$ (CDCl_3): 7.00—7.34 (5H, m, ArH), 5.43 (1H, d, $J=4.0$ Hz, H-1), 5.33 (1H, t, $J=4.0$ Hz, H-2), 5.11 (1H, dd, $J=4.0, 8.0$ Hz, H-4), 5.02 (1H, dd, $J=4.0, 8.0$ Hz, H-3), 4.24 (1H, dd, $J=4.0, 14.0$ Hz, H-5), 4.04 (1H, dd, $J=4.0, 14.0$ Hz, H-5). IR: 2950, 1740, 1040. *Anal.* Calcd for $\text{C}_{14}\text{H}_{14}\text{O}_6\text{S}$: C, 54.19; H, 4.55. Found: C, 53.89; H, 4.57.

Methyl β -L-Arabinopyranoside 3,4-Thionocarbonate (21a)—Syrup. $^1\text{H-NMR}$: 5.38 (1H, t, $J=7.0$ Hz, H-3), 5.21 (1H, dd, $J=2.5, 7.0$ Hz, H-4), 4.96 (1H, d, $J=3.4$ Hz, H-1), 4.32 (1H, dd, $J=3.4, 7.0$ Hz, H-2), 4.17 (1H, d, $J=14.0$ Hz, H-5eq), 4.06 (1H, dd, $J=2.5, 14.0$ Hz, H-5ax), 3.36 (3H, s, OMe).

The 2-acetate (21b) forms needles from hexane-AcOEt, mp 120—121 °C. $^1\text{H-NMR}$ (CDCl_3): 5.05 (1H, t, $J=7.3$ Hz, H-3), 4.98 (1H, d, $J=3.7$ Hz, H-1), 4.95 (1H, dd, $J=2.7, 7.3$ Hz, H-4), 4.92 (1H, dd, $J=3.7, 7.3$ Hz, H-2), 4.20 (1H, d, $J=14.3$ Hz, H-5eq), 3.96 (1H, dd, $J=2.7, 14.3$ Hz, H-5ax), 3.42 (3H, s, OMe), 2.16 (3H, s, OAc). IR: 1740, 1050, 1000. *Anal.* Calcd for $\text{C}_9\text{H}_{12}\text{O}_6\text{S}$: C, 43.55; H, 4.87. Found: C, 43.62; H, 4.93.

Methyl 2-Deoxy- α -D-arabino-hexopyranoside 3,4,6-Triacetate (22b)—Syrup. $^1\text{H-NMR}$ (CDCl_3): 5.26—5.40 (1H, m, H-3), 5.03 (1H, t, $J=10.0$ Hz, H-4), 4.87 (1H, d, $J=3.5$ Hz, H-1), 4.33 (1H, dd, $J=5.0, 12.0$ Hz, H-6), 4.08 (1H, dd, $J=2.5, 12.0$ Hz, H-6), 3.92—4.01 (1H, m, H-5), 3.37 (3H, s, OMe), 2.28 (1H, dd, $J=5.5, 13.0$ Hz, H-2eq), 1.24 (1H, ddd, $J=3.5, 12.0, 13.0$ Hz, H-2ax), 2.03, 2.06 and 2.12 (3H each, s, OAc).

On deacetylation it gave methyl 2-deoxy- α -D-arabino-hexopyranoside (22a) as needles from AcOEt, mp 89—90 °C. $^1\text{H-NMR}$: 4.96 (1H, d, $J=3.5$ Hz, H-1), 4.34 (1H, dd, $J=5.5, 11.5$ Hz, H-3), 3.36 (3H, s, OMe), 2.46 (1H, dd, $J=5.5, 13.0$ Hz, H-2eq), 2.02 (1H, ddd, $J=3.5, 11.5, 13.0$ Hz, H-2ax). *Anal.* Calcd for $\text{C}_7\text{H}_{14}\text{O}_5$: C, 47.18; H, 7.92. Found: C, 47.04; H, 7.75.

Methyl 2-Deoxy- α -D-threo-pentopyranoside 3,4-Diacetate (23)—Syrup. $^1\text{H-NMR}$: 5.57 (1H, ddd, $J=5.0, 9.5, 10.0$ Hz, H-4), 5.17 (1H, dt, $J=5.0, 9.5$ Hz, H-3), 4.79 (1H, dd, $J=2.5, 3.5$ Hz, H-1), 3.93 (1H, dd, $J=5.0, 11.0$ Hz, H-5eq), 3.68 (1H, dd, $J=10.0, 11.0$ Hz, H-5ax), 2.29 (3H, s, OMe), 2.33 (1H, ddd, $J=2.5, 5.0, 13.0$ Hz, H-2eq), 1.82 (1H, ddd, $J=3.5, 9.5, 13.0$ Hz, H-2ax), 2.00 and 2.02 (3H each, s, OAc). HR-MS m/z Calcd for $\text{C}_{10}\text{H}_{16}\text{O}_6$: 232.0947. Found: 232.0951.

Methyl 4-Deoxy- β -L-threo-pentopyranoside 2,3-Diacetate (24)—Syrup. $^1\text{H-NMR}$: 5.60 (1H, ddd, $J=5.5, 10.0, 12.0$ Hz, H-3), 5.16 (1H, dd, $J=3.4, 10.0$ Hz, H-2), 5.12 (1H, d, $J=3.4$ Hz, H-1), 3.70 (1H, dt, $J=2.5, 12.0$ Hz, H-5ax), 3.58 (1H, ddd, $J=1.8, 5.5, 12.0$ Hz, H-5eq), 3.30 (3H, s, OMe), 2.05—2.11 (1H, m, H-4eq), 1.78 (1H, ddd, $J=5.5, 12.0, 12.5$ Hz, H-4ax), 2.00 and 2.01 (3H each, s, OAc). HR-MS m/z Calcd for $\text{C}_{10}\text{H}_{16}\text{O}_6$: 232.0947. Found: 232.0950.

Methyl 4-Deoxy- α -L-threo-pentopyranoside 2,3-Diacetate (25)—Syrup. $^1\text{H-NMR}$: 5.22—5.25 (2H, m, H-2 and H-3), 4.49 (1H, d, $J=6.7$ Hz, H-1), 3.94 (1H, dt, $J=3.8, 12.0$ Hz, H-5ax), 3.84 (1H, ddd, $J=1.0, 2.8, 12.0$ Hz, H-5eq), 3.43 (3H, s, OMe), 2.05—2.11 (1H, m, H-4), 1.68—1.78 (1H, m, H-4), 1.99 and 2.01 (3H each, s, OAc). HR-MS m/z Calcd for $\text{C}_{10}\text{H}_{16}\text{O}_6$: 232.0947. Found: 232.0954.

Methyl 6-O-Tosyl- α -D-glucopyranoside (26)—Needles from AcOEt, mp 118—120 °C. $^1\text{H-NMR}$: 8.00 (2H, d, $J=7.6$ Hz, ArH), 7.20 (2H, d, $J=7.6$ Hz, ArH), 5.04 (1H, d, $J=3.7$ Hz, H-1), 4.92 (1H, d, $J=10.5$ Hz, H-6), 4.77 (1H, dd, $J=5.8, 10.5$ Hz, H-6), 4.44 (1H, t, $J=8.9$ Hz, H-3), 4.50 (1H, dd, $J=5.8, 8.9$ Hz, H-5), 3.97—4.05 (2H, m, H-2 and H-4), 3.36 (3H, s, OMe), 2.17 (3H, s, Me). IR: 3400, 2920, 1351, 1340, 1195, 1160. *Anal.* Calcd for $\text{C}_{14}\text{H}_{20}\text{O}_8\text{S}$: C, 48.27; H, 5.79. Found: C, 48.23; H, 7.81.

Methyl 6-Deoxy- α -D-glucopyranoside (27)—Methyl α -D-glucopyranoside 6-tosylate (1.4 g) and LiAlH_4 (0.73 g, 4.4 mol eq) in THF (100 ml) were refluxed for 16 h. After decomposition of the excess reagent by sat. Na_2SO_4 aq., the mixture was filtered and the residue was extracted several times with hot AcOEt. The residue was decomposed by adding 1 N HCl and neutralized with NaHCO_3 , then concentrated to dryness, and the residue was extracted

thoroughly with hot EtOH–AcOEt. All organic extracts were combined and concentrated to dryness and the residue was chromatographed in AcOEt. The AcOEt and AcOEt–EtOH (99 : 1) eluates gave **27** in 71% yield (550 mg) as needles from AcOEt, mp 96–98 °C (lit. mp 99 °C).¹¹ ¹H-NMR: 5.05 (1H, d, $J=3.7$ Hz, H-1), 4.42 (1H, t, $J=9.2$ Hz, H-3), 4.09–4.14 (1H, m, H-5), 4.08 (1H, dd, $J=3.7, 9.2$ Hz, H-2), 3.67 (1H, t, $J=9.2$ Hz, H-4), 3.41 (3H, s, OMe), 1.58 (3H, d, $J=6.4$ Hz, 6-Me).

Methyl 6-O-Tosyl-β-D-glucopyranoside (28)—Syrup. ¹H-NMR: 7.99 (2H, d, $J=8.0$ Hz, ArH), 4.93 (1H, d, $J=10.0$ Hz, H-6), 4.74 (1H, dd, $J=4.5, 10.0$ Hz, H-6), 4.61 (1H, d, $J=8.0$ Hz, H-1), 4.11 (1H, t, $J=8.0$ Hz, H-3), 3.94–4.07 (2H, m, H-4 and H-5), 3.89 (1H, t, $J=8.0$ Hz, H-2), 3.52 (3H, s, OMe), 2.18 (3H, s, Me).

On acetylation it gave a triacetate as colorless needles from hexane–CH₂Cl₂, mp 173–175 °C. ¹H-NMR (CDCl₃): 7.78 (2H, d, $J=8.0$ Hz, ArH), 7.35 (2H, d, $J=8.0$ Hz, ArH), 5.17 (1H, t, $J=9.5$ Hz, H-3), 4.91 (1H, t, $J=9.5$ Hz, H-4), 4.89 (1H, dd, $J=8.0, 9.5$ Hz, H-2), 4.38 (1H, d, $J=8.0$ Hz, H-1), 4.13 (1H, dd, $J=3.0, 11.0$ Hz, H-6), 4.08 (1H, dd, $J=5.5, 11.0$ Hz, H-6), 3.75 (1H, ddd, $J=3.0, 5.5, 9.5$ Hz, H-5), 3.44 (3H, s, OMe), 2.46 (3H, s, Me), 1.98, 2.00, and 2.03 (3H each s, OAc). IR: 2900, 1740, 1350, 1175. Anal. Calcd for C₂₀H₂₆O₁₁S: C, 50.63; H, 5.53. Found: C, 50.35; H, 5.54.

Methyl 6-Deoxy-β-D-glucopyranoside (29)—Reduction of **28** with LAH was carried out as described for **27**, in 68% yield. After isolation, the product was crystallized from AcOEt as needles, mp 132–133 °C (lit. mp 130–131 °C).¹¹ ¹H-NMR: 4.61 (1H, d, $J=7.6$ Hz, H-1), 4.10 (1H, t, $J=7.6$ Hz, H-3), 3.97 (1H, t, $J=7.6$ Hz, H-2), 3.65–3.80 (2H, m, H-4, 5), 3.61 (3H, s, OMe), 1.61 (3H, d, $J=5.5$ Hz, 6-Me). IR: 3400, 2900. Anal. Calcd for C₇H₁₄O₅: C, 47.18; H, 7.92. Found: C, 46.94; H, 7.92.

Methyl 3-Deoxy-β-D-xyllo-hexopyranoside 2,6-Diacetate (30)—Syrup. ¹H-NMR: 4.93–5.06 (1H, m, H-2), 4.38 (1H, d, $J=6.5$ Hz, H-1), 4.34 (1H, dd, $J=6.5, 12.0$ Hz, H-6), 4.22 (1H, dd, $J=6.5, 12.0$ Hz, H-6), 3.91 (1H, br s, H-4), 3.76 (1H, dt, $J=1.0, 6.5$ Hz, H-5), 3.52 (3H, s, OMe), 2.34–2.45 (1H, m, H-3), 1.58–1.72 (1H, m, H-3), 2.06–2.16 (3H each s, OAc). HR-MS m/z Calcd for C₁₁H₁₈O₇: 262.1052. Found: 262.1059.

Methyl 4-Deoxy-β-D-xyllo-hexopyranoside 2,6-Diacetate (31)—Syrup. ¹H-NMR: 5.27 (1H, dd, $J=8.0, 9.0$ Hz, H-2), 4.54 (1H, d, $J=8.0$ Hz, H-1), 4.22–4.38 (2H, m, H₂-6), 3.82–3.94 (2H, m, H-3 and H-5), 3.48 (3H, s, OMe), 2.22 (1H, ddd, $J=2.0, 5.5, 12.5$ Hz, H-4eq), 1.86 (1H, t, $J=12.5$ Hz, H-4ax), 1.98 and 1.99 (3H each s, OAc). HR-MS m/z Calcd for C₁₁H₁₈O₇: 262.1052. Found: 262.1057.

Methyl 3-Deoxy-α-D-xyllo-hexopyranoside 2,6-Diacetate (32)—Syrup. ¹H-NMR: 5.75 (1H, ddd, $J=3.7, 5.2, 12.0$ Hz, H-2), 5.17 (1H, d, $J=3.7$ Hz, H-1), 4.70 (1H, dd, $J=7.6, 11.3$ Hz, H-6), 4.60 (1H, dd, $J=4.6, 11.3$ Hz, H-6), 4.25 (1H, br s, H-4), 4.18 (1H, dd, $J=4.6, 7.6$ Hz, H-5), 3.44 (3H, s, OMe), 2.37 (1H, dt, $J=5.2, 12.0$ Hz, H-3ax), 2.13 (1H, ddd, $J=3.2, 5.2, 12.0$ Hz, H-3eq), 1.99 and 2.03 (3H each s, OAc). HR-MS m/z Calcd for C₁₁H₁₈O₇: 262.1052. Found: 262.1047.

Methyl 4-Deoxy-α-D-xyllo-hexopyranoside 2,6-Diacetate (33)—Syrup. ¹H-NMR: 5.21 (1H, d, $J=3.7$ Hz, H-1), 5.15 (1H, dd, $J=3.7, 10.0$ Hz, H-2), 4.56 (1H, ddd, $J=2.0, 5.0, 10.0$ Hz, H-3), 4.25–4.33 (2H, m, H₂-6), 4.12–4.18 (1H, m, H-5), 3.36 (3H, s, OMe), 2.27 (1H, ddd, $J=2.0, 5.0, 12.5$ Hz, H-4eq), 1.88 (1H, ABq, $J=12.5$ Hz, H-4ax), 1.97 and 2.03 (3H each s, OAc). HR-MS m/z Calcd for C₁₁H₁₈O₇: 262.1052. Found: 262.1049.

Phenyl 3-Deoxy-β-L-threo-pentopyranoside 2-Acetate (34)—Syrup. ¹H-NMR: 7.04–7.40 (5H, m, ArH), 5.71 (1H, d, $J=2.5$ Hz, H-1), 5.46 (1H, dt, $J=2.5, 3.5$ Hz, H-2), 4.39–4.54 (1H, m, H-4), 4.01 (1H, br s, H-5), 3.98 (1H, d, $J=3.0$ Hz, H-5), 2.26 (2H, dd, $J=3.5, 7.5$ Hz, H₂-3), 2.08 (3H, s, OAc). HR-MS m/z Calcd for C₁₂H₁₆O₈: 240.0998. Found: 240.1001.

Phenyl 4-Deoxy-α-L-threo-pentopyranoside 2-Acetate (35)—Syrup. ¹H-NMR: 7.02–7.37 (5H, m, ArH), 5.54 (1H, t, $J=8.0$ Hz, H-2), 5.30 (1H, d, $J=8.0$ Hz, H-1), 4.16–4.28 (1H, m, H-3), 4.02–4.12 (1H, m, H-5), 3.65 (1H, dt, $J=2.5, 11.0$ Hz, H-5), 1.88–2.21 (2H, m, H-4), 2.01 (3H, s, OAc). HR-MS m/z Calcd for C₁₂H₁₆O₈: 240.0998. Found: 240.1000.

Treatment of 21b with Tributyltin Hydride—i) With excess Bu₃SnH: A toluene solution (12 ml) of **21b** (80 mg), Bu₃SnH (470 mg, 5 mol eq), and AIBN (4 mg) was heated at 100 °C for 1 h in an argon atmosphere with stirring. Chromatography of the product in benzene–ethyl acetate gave **38** (syrup, 44 mg), **39** (mp 117–119 °C, 20 mg), and trace amounts of **40** and **36**.

ii) With 1.5 mol eq of Bu₃SnH at 100 °C: **21b** (100 mg) in toluene (15 ml) was deoxygenated with Bu₃SnH (175 mg) as described above. Four compounds were obtained after chromatography; **38** (30 mg), **39** (25 mg), **40** (syrup, 22 mg), and **36** (syrup, 10 mg) slightly contaminated with **37**.

iii) With 1.5 mol eq of Bu₃SnH at 75 °C: **21b** (150 mg) in toluene (23 ml) was deoxygenated with Bu₃SnH (261 mg) and AIBN (6 mg) at 75 °C for 1 h. Chromatography of the product gave **38** (35 mg) (contaminated with the other compounds), **39** (27 mg), and an inseparable mixture of **37** and **36** (51 mg). The ¹H- and ¹³C-NMR spectra of **37** were obtained by subtraction of the spectra of **36** from those of the mixture, and confirmed by comparisons of the COSY and C–H COSY spectra of the mixture and those of the pure **36**. The ratio (1 : 1) was determined from the intensity ratio of the OMe peaks.

Methyl 3,4-O-Methylidene-β-L-arabinopyranoside 2-Acetate (38)—Syrup. ¹H-NMR (CDCl₃): 5.21 and 5.00 (1H each, s, –OCH₂O–), 4.85 (1H, d, $J=3.5$ Hz, H-1), 4.83 (1H, dd, $J=3.5, 7.5$ Hz, H-2), 4.37 (1H, dd, $J=5.5, 7.5$ Hz, H-3), 4.07 (1H, d, $J=13.5$ Hz, H-5ax), 4.04 (1H, dd, $J=3, 5.5$ Hz, H-4), 3.92 (1H, dd, $J=3.0, 13.5$ Hz, H-5eq), 3.40

(3H, s, OMe), 2.15 (3H, s, OAc). $^{13}\text{C-NMR}$ (CDCl_3): 170.5 (C=O), 97.1 (C-1), 94.6 ($-\text{OCH}_2\text{O}-$), 74.5, 72.3, 70.2 (C-2, 3, 4), 58.2 (C-5), 55.6 (OMe), 21.0 (OAc). HR-MS m/z Calcd for $\text{C}_9\text{H}_{14}\text{O}_6$: 218.0786. Found: 218.0790.

Methyl β -L-Arabinopyranoside 3,4-Carbonate 2-Acetate (39)—Colorless needles from hexane- CH_2Cl_2 , mp 117–119°C. $^1\text{H-NMR}$: 5.43 (1H, dd, $J=3.7, 7.3$ Hz, H-2), 5.27 (1H, t, $J=7.3$ Hz, H-3), 5.17 (1H, dd, $J=2.7, 7.3$ Hz, H-4), 5.16 (1H, d, $J=3.7$ Hz, H-1), 4.17 (1H, d, $J=14.3$ Hz, H-5eq), 3.98 (1H, dd, $J=2.7, 14.3$ Hz, H-5ax), 3.29 (3H, s, OMe), 1.99 (3H, s, OAc). $^{13}\text{C-NMR}$: 169.9 ($\text{CH}_3\text{C}=\text{O}$), 154.4 ($\text{C}=\text{O}$), 96.6 (C-1), 75.9 (C-4), 74.7 (C-3), 70.8 (C-2), 57.7 (C-5), 55.8 (OCH_3), 20.5 ($\text{CH}_3\text{C}=\text{O}$). IR: 1814, 1724. Anal. Calcd for $\text{C}_9\text{H}_{12}\text{O}_7$: C, 46.55; H, 5.21. Found: C, 46.73; H, 5.29.

Methyl 4-Deoxy- β -L-threo-pentopyranoside 3-Acetate (40)—Syrup. $^1\text{H-NMR}$: 5.56 (1H, dt, $J=5.0, 10.5$ Hz, H-3), 5.06 (1H, d, $J=4$ Hz, H-1), 4.00 (1H, dd, $J=4.0, 10.0$ Hz, H-2), 3.74 (1H, dt, $J=12.0, 2.0$ Hz, H-5ax), 3.60 (1H, ddd, $J=2.0, 5.0, 12.0$ Hz, H-5eq), 3.37 (3H, s, OMe), 2.09 (1H, ddt, $J=12.5, 5.0, 2.0$ Hz, H-4eq), 2.01 (3H, s, OAc), 1.76 (1H, ddt, $J=12.5, 5.0, 10.5$ Hz, H-4ax). HR-MS m/z Calcd for $\text{C}_8\text{H}_{14}\text{O}_5$: 190.0841. Found: 190.0845.

Methyl 4-Deoxy- β -L-threo-pentopyranoside 2-Acetate (37)— $^1\text{H-NMR}$: 5.14 (1H, br d, $J=3.5$ Hz, H-1), 5.12 (1H, dd, $J=3.5, 9$ Hz, H-2), 4.46 (1H, ddd, $J=5, 9, 11$ Hz, H-3), 3.79 (1H, dt, $J=12.0, 2.5$ Hz, H-5ax), 3.65 (1H, ddd, $J=2.0, 5.5, 12.0$ Hz, H-5eq), 3.33 (3H, s, OMe), 2.12 (1H, ddt, $J=12.5, 5.0, 2.5$ Hz, H-4eq), 1.97 (3H, s, OAc), 1.95 (1H, ddt, $J=5.0, 11.0, 12.5$ Hz, H-4ax).

Methyl 3-Deoxy- α -L-threo-pentopyranoside 2-Acetate (36)—Syrup. $^1\text{H-NMR}$: 5.74 (1H, ddd, $J=3, 5, 11.5$ Hz, H-2), 5.06 (1H, br d, $J=3$ Hz, H-1), 4.20–4.24 (1H, m, H-4), 3.92 (1H, dd, $J=2, 12$ Hz, H-5ax), 3.77 (1H, dd, $J=2, 12.0$ Hz, H-5eq), 3.41 (3H, s, OMe), 2.33 (1H, ddd, $J=3, 11.5, 12.5$ Hz, H-3ax), 2.23 (1H, ddd, $J=4, 5, 12.5$ Hz, H-3eq), 1.99 (3H, s, OAc). HR-MS m/z Calcd for $\text{C}_8\text{H}_{14}\text{O}_5$: 190.0841. Found: 190.0848.

Methyl 3,4-Dideoxy- β -D-erythro-hex-3-enopyranoside 2,6-Diacetate (41b)—Needles from isopropyl ether, mp 78–80°C. $^1\text{H-NMR}$ (CDCl_3): 5.91 (1H, ddd, $J=1.2, 1.8, 10.4$ Hz, H-3), 5.85 (1H, ddd, $J=2.4, 3.0, 10.4$ Hz, H-4), 5.14–5.17 (1H, m, H-2), 4.62 (1H, d, $J=4.9$ Hz, H-1), 4.48–4.54 (1H, m, H-5), 4.19 (1H, dd, $J=6.4, 11.3$ Hz, H-6), 4.15 (1H, dd, $J=5.2, 11.3$ Hz, H-6), 3.50 (3H, s, OMe), 2.09 and 2.10 (3H each, s, OAc). IR: 1800, 1720. Anal. Calcd for $\text{C}_{11}\text{H}_{16}\text{O}_6$: C, 54.09; H, 6.60. Found: C, 54.02; H, 6.63.

Methyl 3,4-Dideoxy- β -D-erythro-hex-3-enopyranoside (41a)—Syrup. $^1\text{H-NMR}$ (CDCl_3): 5.86 (1H, dt, $J=10.2, 2.4$ Hz, H-3), 5.74 (1H, dt, $J=10.2, 1.8$ Hz, H-4), 4.42 (1H, d, $J=5.8$ Hz, H-1), 4.36–4.41 (1H, m, H-5), 4.08 (1H, dt, $J=5.8, 2.4$ Hz, H-2), 3.76 (1H, dd, $J=3.2, 12.0$ Hz, H-6), 3.62 (1H, dd, $J=6.0, 12.0$ Hz, H-6), 3.57 (3H, s, OMe).

Methyl 3,4-Dideoxy- β -D-erythro-hexopyranoside (42)—Volatile liquid. $^1\text{H-NMR}$ (CDCl_3): 4.14 (1H, d, $J=7.6$ Hz, H-1), 3.59–3.63 (3H, m, H-5 and H-2-6), 3.56 (3H, s, OMe), 3.39 (1H, ddd, $J=5.5, 7.6, 10.5$ Hz, H-2), 2.12 (1H, ddd, $J=2.5, 5.5, 10.5$ Hz, H-3), 1.59–1.67 (1H, m, H-3), 1.45–1.58 (2H, m, H-2-4). HR-MS m/z Calcd for $\text{C}_7\text{H}_{14}\text{O}_4$: 162.0892. Found: 162.0895.

Methyl 3,4-Dideoxy- α -D-erythro-hex-3-enopyranoside 2,6-Diacetate (43b)—Colorless liquid. $^1\text{H-NMR}$ (CDCl_3): 5.84 (1H, dt, $J=10.7, 2.1$ Hz, H-3), 5.75 (1H, dt, $J=10.7, 2.1$ Hz, H-4), 5.30–5.34 (1H, m, H-2), 5.11 (1H, d, $J=4.2$ Hz, H-1), 4.36–4.42 (1H, m, H-5), 4.18 (2H, d, $J=4.9$ Hz, H-2-6), 3.50 (3H, s, OMe), 2.10 and 2.12 (3H each, s, OAc).

Methyl 3,4-Dideoxy- α -D-erythro-hex-3-enopyranoside (43a)—Volatile liquid. $^1\text{H-NMR}$ (CDCl_3): 5.81 (1H, dt, $J=10.4, 2.1$ Hz, H-3), 5.69 (1H, dt, $J=10.4, 2.1$ Hz, H-4), 4.92 (1H, d, $J=4.6$ Hz, H-1), 4.19–4.26 (2H, m, H-2, 5), 3.74 (1H, dd, $J=3.0, 11.3$ Hz, H-6), 3.60 (1H, dd, $J=6.1, 11.3$ Hz, H-6), 3.53 (3H, s, OMe).

Methyl 3,4-Dideoxy- α -D-erythro-hexopyranoside (44)—Volatile liquid. $^1\text{H-NMR}$ (CDCl_3): 4.70 (1H, d, $J=3.7$ Hz, H-1), 3.72–3.79 (1H, m, H-5), 3.62 (1H, dd, $J=3.4, 11.6$ Hz, H-6), 3.59–3.63 (1H, m, H-2), 3.51 (1H, dd, $J=6.7, 11.6$ Hz, H-6), 3.45 (3H, s, OMe), 1.90 (1H, ddd, $J=4.0, 5.5, 11.5$ Hz, H-3eq), 1.71 (1H, dddd, $J=4.0, 8.0, 11.5, 11.9$ Hz, H-3ax), 1.61 (1H, ddd, $J=3.4, 4.0, 11.9$ Hz, H-4eq), 1.48 (1H, dddd, $J=4.0, 8.0, 11.9, 11.9$ Hz, H-4ax). HR-MS m/z Calcd for $\text{C}_7\text{H}_{14}\text{O}_4$: 162.0892. Found: 162.0898.

Phenyl 3,4-Dideoxy- β -D-glycero-pent-3-enopyranoside 2-Acetate (45b)—Syrup. $^1\text{H-NMR}$ (CDCl_3): 7.27–7.32 (2H, m, ArH), 7.01–7.09 (3H, m, ArH), 6.17 (1H, dt, $J=2.5, 10.0$ Hz, H-4), 4.94–4.98 (1H, m, H-3), 5.56 (1H, br s, H-1), 5.18 (1H, br d, $J=4.0$ Hz, H-2), 4.28 (1H, dd, $J=2.5, 17.0$ Hz, H-5), 4.02 (1H, dd, $J=2.5, 17.0$ Hz, H-5).

Phenyl 3,4-Dideoxy- β -D-glycero-pent-3-enopyranoside (45a)—Syrup. $^1\text{H-NMR}$ (CDCl_3): 7.00–7.32 (5H, m, ArH), 6.00 (2H, s, H-3 and H-4), 5.47 (1H, d, $J=2.1$ Hz, H-1), 4.24 (1H, dd, $J=2.0, 17.5$ Hz, H-5ax), 4.15 (1H, dd, $J=1.2, 17.5$ Hz, H-5eq), 4.08 (1H, br s, H-2).

Phenyl 3,4-Dideoxy- β -D-glycero-pentopyranoside (46)—Volatile oil. $^1\text{H-NMR}$ (CDCl_3): 7.00–7.31 (5H, m, ArH), 5.03 (1H, d, $J=5.2$ Hz, H-1), 3.96 (1H, ddd, $J=3.5, 6.3, 11.5$ Hz, H-5), 3.76 (1H, ddd, $J=4.0, 5.2, 7.8$ Hz, H-2), 3.58 (1H, ddd, $J=3.0, 7.6, 11.5$ Hz, H-5), 2.20 (1H, m, H-3), 1.84 (1H, m, H-4), 1.69 (1H, ddd, $J=4.3, 7.8, 12.5$ Hz, H-3), 1.58–1.66 (1H, m, H-4). HR-MS m/z Calcd for $\text{C}_{11}\text{H}_{14}\text{O}_3$: 194.0943. Found: 194.0949.

Methyl 3,4-Dideoxy- α -D-glycero-pent-3-enopyranoside 2-Acetate (47b)—Highly volatile liquid. $^1\text{H-NMR}$ (CDCl_3): 5.95 (1H, dt, $J=10.4, 2.4$ Hz, H-4), 4.66 (1H, dd, $J=2.4, 10.4$ Hz, H-3), 5.30 (1H, m, H-2), 4.93 (1H, d, $J=4.0$ Hz, H-1), 4.23 (1H, dd, $J=2.4, 16.8$ Hz, H-5), 4.08 (1H, dd, $J=2.4, 16.8$ Hz, H-5), 3.50 (3H, s, OMe), 2.12 (3H, s, OAc).

Methyl 3,4-Dideoxy- α -D-glycero-pent-3-enopyranoside (47a)—Highly volatile liquid. $^1\text{H-NMR}$ (CDCl_3): 5.82

(1H, dt, $J=10.5, 2.4$ Hz, H-4), 5.73 (1H, dd, $J=2.1, 10.5$ Hz, H-3), 4.77 (1H, d, $J=4.0$ Hz, H-1), 4.17—4.21 (1H, m, H-2), 4.14 (1H, dd, $J=2.4, 16.8$ Hz, H-5), 4.02 (1H, dd, $J=2.4, 16.8$ Hz, H-5), 3.53 (3H, s, OMe).

Methyl 3,4-Dideoxy- α -D-glycero-pentopyranoside (48)—Highly volatile liquid. $^1\text{H-NMR}$ (CDCl_3): 4.58 (1H, d, $J=3.1$ Hz, H-1), 3.61—3.69 (1H, m, H-2), 3.42—3.53 (2H, m, H₂-5), 3.45 (3H, s, OMe), 1.79—1.85 (1H, m, H-3), 1.62—1.75 (3H, m, H-3 and H₂-4). HR-MS m/z Calcd for $\text{C}_6\text{H}_{12}\text{O}_3$: 132.0787. Found: 132.0792.

Acknowledgement One of the author (M. E. H.) is grateful to the Ministry of Education, Science and Culture of Japan for a scholarship. We also thank Miss Y. Ito for technical assistance for some experiments. This work was supported in part by a Grant-in-Aid for Developmental Research (No. 58870102, 1983 and 1984) to Y. T. and K. K. from Ministry of Education, Science and Culture of Japan.

References and Notes

- 1) Utilization of Sugars in Organic Syntheses, XVII. Part XVI: M. E. Haque, T. Kikuchi, K. Kanemitsu, and Y. Tsuda, *Chem. Pharm. Bull.*, **34**, 430 (1986).
- 2) a) D. H. R. Barton and S. W. McCombie, *J. Chem. Soc., Perkin Trans. 1*, **1975**, 1574; b) D. H. R. Barton and R. Subramanian, *ibid.*, **1977**, 1718; c) T. S. Fuller and R. V. Stick, *Aust. J. Chem.*, **33**, 2509 (1980); d) D. H. R. Barton and R. Subramanian, *J. Chem. Soc., Chem. Commun.*, **1977**, 867; e) D. H. R. Barton and R. V. Stick, *J. Chem. Soc., Perkin Trans. 1*, **1975**, 1773.
- 3) Y. Tsuda, M. E. Haque, and K. Yoshimoto, *Chem. Pharm. Bull.*, **31**, 1612 (1983).
- 4) M. E. Haque, T. Kikuchi, K. Yoshimoto, and Y. Tsuda, *Chem. Pharm. Bull.*, **33**, 2243 (1985).
- 5) a) M. Miyazaki and K. Nakahashi, Jpn. Tokkyo Koho, 1322 (1957) [*Chem. Abstr.*, **52**, 4684g (1958)]; b) M. J. Robins, J. S. Wilson, and F. Hansske, *J. Am. Chem. Soc.*, **105**, 4059 (1983).
- 6) H. A. Staab and G. Walther, *Justus Liebigs Ann. Chem.*, **657**, 98 (1962).
- 7) B. Classon, P. J. Gregg, and T. Norberg, *Acta Chem. Scand.*, **B38**, 195 (1984).
- 8) a) C. Walling, "Free Radicals in Solution," Wiley, New York, 1959; b) Ingold and B. P. Roberts, "Free Radical Substitution Reaction," Wiley-Interscience, New York, 1971.
- 9) Occurrence of a facile *trans*-acyl migration between O-2 and O-3 in pyranosides has been proved [K. Yoshimoto and Y. Tsuda, *Chem. Pharm. Bull.*, **31**, 4324 (1983)].
- 10) E. J. Corey and R. A. E. Winter, *J. Am. Chem. Soc.*, **85**, 2677 (1963).
- 11) M. E. Evans, L. Long, Jr., and F. W. Parrish, *J. Org. Chem.*, **33**, 1074 (1968).

[Chem. Pharm. Bull.]
[35(3)1030-1035(1987)]

Synthesis of 2-Substituted 5-(1-Oxido-4-pyridyl)- and 5-(1-Oxido-2-pyridyl)-1,3,4-thiadiazole Derivatives by Substitution of 2-Methylsulfonyl Group with Various Nucleophiles

KOUHEI TOYOOKA, YASUSHI KAWASHIMA, and SEIJU KUBOTA*

Faculty of Pharmaceutical Sciences, University of Tokushima,
Shomachi, Tokushima 770, Japan

(Received August 28, 1986)

The synthesis of 2-substituted 5-(1-oxido-4-pyridyl)-(4a—10a) and 5-(1-oxido-2-pyridyl)-1,3,4-thiadiazole derivatives (4b—10b) by substitution reaction of 5-(1-oxido-4-pyridyl)- (3a) and 5-(1-oxido-2-pyridyl)-2-methylsulfonyl-1,3,4-thiadiazole (3b) is described. 5-(1-Oxido-4-pyridyl)- (9a) and 5-(1-oxido-2-pyridyl)-1,3,4-thiadiazole (9b) could be reduced with sodium dithionite to 2-(4-pyridyl)- (11c) and 2-(2-pyridyl)-1,3,4-thiadiazole (11d).

Keywords—2,3-dihydro-1,3,4-thiadiazole; oxidation; methylsulfonyl-1,3,4-thiadiazole; nucleophilic substitution; nucleophile; substituted 1,3,4-thiadiazole; hydrolysis; sodium borohydride; (1-oxidopyridyl)-1,3,4-thiadiazole; sodium dithionite

The most common procedure for the synthesis of 2,5-disubstituted 1,3,4-thiadiazoles is based on cyclization of acylated thiosemicarbazides or compounds with similar structures.¹⁾ Nucleophilic substitution reaction of 1,3,4-thiadiazole derivatives with strong electron-withdrawing substituents in the 2-position is a valuable procedure for preparing 2,5-disubstituted 1,3,4-thiadiazole derivatives which are not readily obtainable by the common procedures.

A substituent such as a halogen atom²⁾ or nitro group³⁾ in 1,3,4-thiadiazole derivatives can be readily displaced by nucleophiles, due to the low electron density at the carbon atoms in the 1,3,4-thiadiazole ring. It has also been reported that methylsulfonyl groups at carbons with low electron density in heterocyclic compounds can be displaced with nucleophiles.⁴⁾ 2-Hydrazino-5-phenyl-1,3,4-thiadiazole has been prepared by hydrazinolysis of 2-methylsulfonyl-5-phenyl-1,3,4-thiadiazole.⁵⁾

Previously, we have reported that acetylation of both pyridine-carbaldehyde methylthio(thiocarbonyl)hydrazones (1a,1b) with acetic anhydride gave the 2,3-dihydro-1,3,4-thiadiazoles (2a,2b) and oxidation of 2a,2b with an excess of 30% hydrogen peroxide in acetic acid gave 2-methylsulfonyl-5-(1-oxido-pyridyl)-1,3,4-thiadiazoles (3a, 3b) in good yields⁶⁾ (Chart 1).

We here report on the substitution reaction of the 2-methylsulfonyl-1,3,4-thiadiazoles

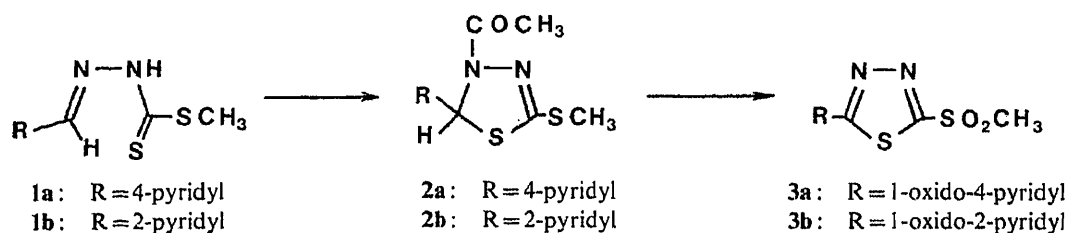


Chart 1

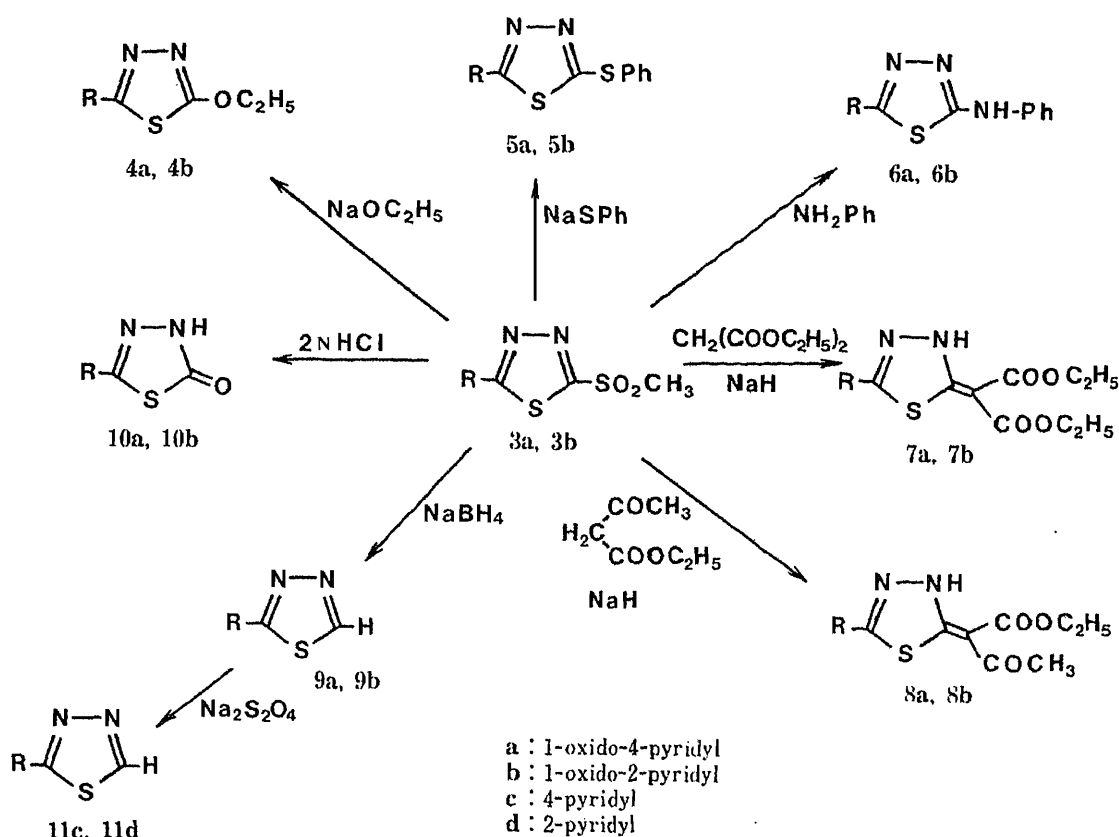


Chart 2

(3a,3b) with various nucleophiles. Treatment of 3a with sodium ethoxide in EtOH or with thiophenol in the presence of sodium hydride at room temperature gave 2-ethoxy- (4a) or 2-phenylthio-5-(1-oxido-4-pyridyl)-1,3,4-thiadiazole (5a) in 77% or 78% yield, respectively. Reaction of 3a with aniline at elevated temperature gave 2-anilino-5-(1-oxido-4-pyridyl)-1,3,4-thiadiazole (6a). Reaction of 3a with diethyl malonate or ethyl acetoacetate in the presence of sodium hydride afforded diethyl 5-(1-oxido-4-pyridyl)-2,3-dihydro-1,3,4-thiadiazol-2-ylidenemalonate (7a) or ethyl 1-(5-(1-oxido-4-pyridyl)-2,3-dihydro-1,3,4-thiadiazol-2-ylidene)-1-acetylacetate (8a) in 83% or 81% yield, respectively. The infrared (IR) spectra of compounds 7a and 8a showed NH absorptions at 3210 and 3230 cm^{-1} , respectively. The proton nuclear magnetic resonance ($^1\text{H-NMR}$) spectra of compounds 7a (δ_{H} 13.54) and 8a (δ_{H} 13.60) also indicate the presence of NH protons. These results show that 7a and 8a exist as the 2,3-dihydro-1,3,4-thiadiazole tautomers. Reaction of 3a with NaBH_4 at room temperature gave 2-(1-oxido-4-pyridyl)-1,3,4-thiadiazole (9a) by substitution of the 2-methylsulfonyl group with a hydride anion. Hydrolysis of 3a with 2N HCl under reflux gave 5-(1-oxido-4-pyridyl)-2,3-dihydro-1,3,4-thiadiazol-2-one (10a). The structures of compounds 4a—10a were supported by the analytical and spectral data (Table I).

Similar treatment of 3b with the nucleophiles described above also gave 2-substituted 5-(1-oxido-2-pyridyl)-1,3,4-thiadiazoles (4b—10b). The structures of compounds 4b—10b were also supported by the analytical and spectral data (Table II).

It has been reported that pteridine N-oxides could be easily reduced to pteridine by treatment with sodium dithionite ($\text{Na}_2\text{S}_2\text{O}_4$).⁷⁾ In fact, reduction of 9a with 8 eq of $\text{Na}_2\text{S}_2\text{O}_4$ in 50% aqueous EtOH under reflux for 15 min gave 2-(4-pyridyl)-1,3,4-thiadiazole (11c) in 94% yield, while treatment of 9b with 30 eq of $\text{Na}_2\text{S}_2\text{O}_4$ in 50% aqueous EtOH under reflux for 1 h gave 2-(2-pyridyl)-1,3,4-thiadiazole (11d)⁸⁾ in only 56% yield.

TABLE I. 2-Substituted 5-(1-Oxido-4-pyridyl)-1,3,4-thiadiazoles (4a—10a)

Compd. No.	Yield (%)	mp (°C) (Recrystn. solvent)	IR $\nu_{\max}^{\text{KBr}} \text{cm}^{-1}$			¹ H-NMR signals (ppm) (<i>J</i> =Hz)	Formula	Analysis (%)			MS <i>m/z</i> (<i>M</i> ⁺)
			NH	CO	N—O			Calcd	(Found)	C	
4a	77	159—161 (EtOH)			1260 ^{a)}	1.42 (3H, t, <i>J</i> =7, CH ₂ CH ₃), 4.56 (2H, q, <i>J</i> =7, CH ₂ CH ₃), 7.81 (2H, dd, <i>J</i> =2, 7, PyH), 8.29 (2H, dd, <i>J</i> =2, 7, PyH)	C ₉ H ₉ N ₃ O ₂ S	48.42 (48.45)	4.06 4.02	18.82 18.92	223
5a	78	141—143 (EtOH)			1285 ^{a)}	7.40—8.00 (5H, m, ArH), 7.87 (2H, dd, <i>J</i> =2, 7, PyH), 8.30 (2H, dd, <i>J</i> =2, 7, PyH)	C ₁₃ H ₉ N ₃ OS ₂	54.34 (54.38)	3.16 3.00	14.62 14.65	287
6a	87	274—276 (EtOH)	3240		1245 ^{a)}	6.90—7.76 (5H, m, ArH), 7.85 (2H, dd, <i>J</i> =2, 7, PyH), 8.29 (2H, dd, <i>J</i> =2, 7, PyH), 10.99 (1H, br s, NH)	C ₁₂ H ₁₀ N ₄ OS	57.76 (57.74)	3.73 3.62	20.73 20.54	270
7a	83	185—187 (dec.) (EtOH)	3210	1640 1625	1260 ^{b)}	1.35 (6H, t, <i>J</i> =7, CH ₂ CH ₃), 4.29 (4H, q, <i>J</i> =7, CH ₂ CH ₃), 7.67 (2H, dd, <i>J</i> =2, 7, PyH), 8.23 (2H, dd, <i>J</i> =2, 7, PyH), 13.54 (1H, br s, NH)	C ₁₄ H ₁₅ N ₃ O ₅ S	49.85 (49.49)	4.48 4.49	12.46 12.22	337
8a	81	205—207 (dec.) (EtOH)	3230	1630 1585	1240 ^{b)}	1.41 (3H, t, <i>J</i> =7, CH ₂ CH ₃), 2.58 (3H, s, COCH ₃), 4.37 (2H, q, <i>J</i> =7, CH ₂ CH ₃), 7.75 (2H, dd, <i>J</i> =2, 7, PyH), 8.26 (2H, dd, <i>J</i> =2, 7, PyH), 13.60 (1H, br s, NH)	C ₁₃ H ₁₃ N ₃ O ₄ S	50.81 (51.11)	4.26 4.27	13.67 13.37	307
9a	82	156—159 (dec.) (EtOH)			1255 ^{a)}	8.03 (2H, dd, <i>J</i> =2, 7, PyH), 8.37 (2H, dd, <i>J</i> =2, 7, PyH), 9.72 (1H, s, C ₂ -H)	C ₇ H ₅ N ₃ OS	46.92 (46.90)	2.81 2.64	23.45 23.19	179
10a	80	280—281 (MeOH)	3110	1660	1240 ^{c)}		C ₇ H ₅ N ₃ O ₂ S	43.07 (42.79)	2.58 2.47	21.53 21.51	195

Abbreviations: br s, broad singlet; dd, doublet of doublets; m, multiplet; q, quartet; s, singlet; t, triplet. a) In DMSO-*d*₆. b) In CDCl₃. c) Not soluble in DMSO-*d*₆ or in CDCl₃.

TABLE II. 2-Substituted 5-(1-Oxido-2-pyridyl)-1,3,4-thiadiazoles (4b—10b)

Compd. No.	Yield (%)	mp (°C) (Recrystn. solvent)	IR $\nu_{\max}^{\text{KBr}} \text{cm}^{-1}$			¹ H-NMR signals (ppm) (<i>J</i> =Hz)	Formula	Analysis (%)			MS <i>m/z</i> (<i>M</i> ⁺)
			NH	CO	N-O			Calcd	Found	N	
4b	98	183—184 (EtOH)			1245 ^a	1.50 (3H, t, <i>J</i> =7, CH ₂ CH ₃), 4.55 (2H, q, <i>J</i> =7, CH ₂ CH ₃), 7.56—7.74 (2H, m, PyH), 8.38—8.60 (2H, m, PyH)	C ₉ H ₉ N ₃ O ₂ S	48.42 (48.62)	4.06 (3.96)	18.82 (18.99)	223
5b	97	172—174 (EtOH)			1250 ^a	7.40—7.90 (7H, m, ArH), 8.40—8.65 (2H, m, PyH)	C ₁₃ H ₉ N ₃ OS ₂	54.34 (54.39)	3.16 (2.90)	14.62 (14.71)	287
6b	82	275—278 (dec.) (EtOH)	3250		1250 ^a	6.92—7.80 (7H, m, ArH), 8.40—8.58 (2H, m, PyH), 10.85 (1H, brs, NH)	C ₁₂ H ₁₀ N ₄ OS	57.76 (57.82)	3.73 (3.59)	20.73 (20.78)	270
7b	74	182—184 (dec.) (EtOH)	3190	1640 1620	1240 ^b	1.36 (6H, t, <i>J</i> =7, CH ₂ CH ₃), 4.28 (4H, q, <i>J</i> =7, CH ₂ CH ₃), 7.30—7.56 (2H, m, PyH), 8.20—8.50 (2H, m, PyH), 14.01 (1H, brs, NH)	C ₁₄ H ₁₅ N ₃ O ₅ S	49.85 (49.75)	4.48 (4.61)	12.46 (12.16)	337
8b	64	217—220 (dec.) (EtOH)	3190	1635 1585	1250 ^b	1.41 (3H, t, <i>J</i> =7, CH ₂ CH ₃), 2.59 (3H, s, COCH ₃), 4.36 (2H, q, <i>J</i> =7, CH ₂ CH ₃), 7.34—7.56 (2H, m, PyH), 8.26—8.56 (2H, m, PyH), 12.00—14.50 (1H, br, NH)	C ₁₃ H ₁₃ N ₃ O ₄ S	50.81 (50.51)	4.26 (3.96)	13.67 (13.56)	307
9b	76	192—193 (EtOH)			1255 ^a	7.59—7.78 (2H, m, PyH), 8.54—8.73 (2H, m, PyH), 9.75 (1H, s, C ₂ -H)	C ₇ H ₅ N ₃ OS	46.92 (46.83)	2.81 (2.63)	23.45 (23.40)	179
10b	95	270—272 (dec.) (Benzene-MeOH)	3080	1670	1240 ^a	7.50—7.64 (2H, m, PyH), 8.06—8.50 (2H, m, PyH), 13.75 (1H, brs, NH)	C ₇ H ₅ N ₃ O ₂ S	43.07 (43.04)	2.58 (2.37)	21.53 (21.29)	195

Abbreviations: br, broad; brs, broad singlet; m, multiplet; q, quartet; s, singlet; t, triplet. ^a In DMSO-*d*₆. ^b In CDCl₃.

Experimental

Melting points were determined by the capillary method and are uncorrected. IR spectra were recorded on a Hitachi 215 spectrometer. ¹H-NMR spectra were recorded on a JEOL PS-100 spectrometer using tetramethylsilane as an internal standard. Mass spectra (MS) were measured with a JEOL D-300 instrument. For column chromatography, Silica gel 60 (230–400 mesh, Nakarai Chemicals, Ltd.) was employed. Yields, melting points, analytical and spectral data for 4a–10a and 4b–10b are given in Tables I and II, respectively.

2-Ethoxy-5-(1-oxido-4-pyridyl)- (4a) and 2-Ethoxy-5-(1-oxido-2-pyridyl)-1,3,4-thiadiazole (4b)—General Procedure: A suspension of 3a or 3b (150 mg, 0.58 mmol) in EtOH (5 ml) was added dropwise to a stirred solution of EtONa (1.74 mmol) in EtOH (4 ml) at room temperature. After 1 h, the mixture was neutralized with HCl/EtOH solution and concentrated under reduced pressure. The residue was chromatographed on a silica gel column (CHCl₃–MeOH, 20:1, v/v). Evaporation of the eluates gave a solid, which was crystallized from EtOH to give 4a or 4b.

2-Phenylthio-5-(1-oxido-4-pyridyl)- (5a) and 5-(1-Oxido-2-pyridyl)-1,3,4-thiadiazole (5b)—General Procedure: A suspension of sodium hydride (105 mg, 2.62 mmol, 60% dispersion in oil, washed twice with ether) in dry tetrahydrofuran (THF 4 ml) was added dropwise to a stirred solution of thiophenol (285 mg, 2.59 mmol) in dry THF (4 ml) at room temperature. After 1 h, a suspension of 3a or 3b (300 mg, 1.17 mmol) in dry THF (7 ml) was added dropwise to the solution of the sodium salt of thiophenol at room temperature. After being stirred for 15 min, the mixture was neutralized with aqueous acetic acid, and concentrated under reduced pressure. The residue was chromatographed on a silica gel column (CHCl₃–acetone, 20:1, v/v). Evaporation of the eluates gave a solid, which was crystallized from EtOH to give 5a or 5b.

2-Anilino-5-(1-oxido-4-pyridyl)- (6a) and 2-Anilino-5-(1-oxido-2-pyridyl)-1,3,4-thiadiazole (6b)—General Procedure: A mixture of 3a or 3b (150 mg, 0.58 mmol) and aniline (1 ml) was stirred at 110–130 °C for 5 h. The mixture was chromatographed on a silica gel column (CHCl₃–MeOH, 20:1, v/v). Evaporation of the eluates gave a solid, which was crystallized from EtOH to give 6a or 6b.

Diethyl 5-(1-Oxido-4-pyridyl)- (7a) and Diethyl 5-(1-Oxido-2-pyridyl)-2,3-dihydro-1,3,4-thiadiazol-2-ylidene-malonate (7b)—General Procedure: A suspension of sodium hydride (117 mg, 2.93 mmol, 60% dispersion in oil, washed twice with ether) in dry THF (4 ml) was added dropwise to a stirred solution of diethyl malonate (470 mg, 2.93 mmol) in dry THF (4 ml) at room temperature. After 1 h, a suspension of 3a or 3b (150 mg, 0.58 mmol) in dry THF (7 ml) was added dropwise to the solution of the sodium salt of diethyl malonate at room temperature. After being stirred for 3 h, the mixture was neutralized with aqueous acetic acid, and concentrated under reduced pressure. The residue was chromatographed on a silica gel column (CHCl₃–MeOH, 20:1, v/v). Evaporation of the eluates gave a solid, which was crystallized from EtOH to give 7a or 7b.

Ethyl 1-(5-(1-Oxido-4-pyridyl)- (8a) and Ethyl 1-(5-(1-Oxido-2-pyridyl)-2,3-dihydro-1,3,4-thiadiazol-2-ylidene)-1-acetylacetate (8b)—General Procedure: A suspension of sodium hydride (117 mg, 2.93 mmol, 60% dispersion in oil, washed twice with ether) in dry THF (4 ml) was added dropwise to a stirred solution of ethyl acetoacetate (380 mg, 2.92 mmol) in dry THF (4 ml) at room temperature. After 1 h, a suspension of 3a or 3b (150 mg, 0.58 mmol) in dry THF (7 ml) was added dropwise to the solution of the sodium salt of ethyl acetoacetate at room temperature. After being stirred at 70 °C for 1 h, the mixture was neutralized with aqueous acetic acid, and concentrated under reduced pressure. The residue was chromatographed on a silica gel column (CHCl₃–MeOH, 20:1, v/v). Evaporation of the eluates gave a solid, which was crystallized from EtOH to give 8a or 8b.

2-(1-Oxido-4-pyridyl)- (9a) and 2-(1-Oxido-2-pyridyl)-1,3,4-thiadiazole (9b)—General Procedure: NaBH₄ (for 3a, 56 mg, 1.48 mmol; for 3b, 90 mg, 2.38 mmol) was added portionwise to a stirred suspension of 3a or 3b (150 mg, 0.58 mmol) in EtOH (4 ml) at 0 °C. After being stirred at room temperature for 1 h, the mixture was neutralized with acetic acid, and concentrated under reduced pressure. The residue was chromatographed on a silica gel column (CHCl₃–MeOH, 20:1, v/v). Evaporation of the eluates gave a solid, which was crystallized from EtOH to give 9a or 9b.

5-(1-Oxido-4-pyridyl)- (10a) and 5-(1-Oxido-2-pyridyl)-2,3-dihydro-1,3,4-thiadiazol-2-one (10b)—General Procedure: A mixture of 3a or 3b (150 mg, 0.58 mmol) and 2 N HCl (7 ml) was refluxed for 3 h. The mixture was neutralized with saturated K₂CO₃ aqueous solution. i) For 3a: The resulting solid was collected by filtration and washed with hot MeOH to give 10a. ii) For 3b: The mixture was concentrated under reduced pressure. The residue was chromatographed on a silica gel column (CHCl₃–MeOH, 20:1, v/v). Evaporation of the eluates gave a solid, which was crystallized from benzene–MeOH to give 10b.

2-(4-Pyridyl)-1,3,4-thiadiazole (11c)—A mixture of 9a (100 mg, 0.56 mmol) and Na₂S₂O₄ (780 mg, 4.48 mmol) in 50% aqueous EtOH (8 ml) was refluxed for 15 min. The mixture was extracted with CHCl₃ (3 × 50 ml). The combined extract was washed with brine, and dried over Na₂SO₄. After removal of the solvent by evaporation, the residue was crystallized from ether to give 11c (86 mg, 94%) as colorless crystals, mp 112–114 °C. IR(KBr): 1600 cm⁻¹. ¹H-NMR (DMSO-*d*₆) δ: 7.98 (2H, dd, ArH), 8.80 (2H, dd, ArH), 9.82 (1H, s, C₂-H). *Anal.* Calcd for C₇H₅N₃S: C, 51.52; H, 3.09; N, 25.75. Found: C, 51.57; H, 2.96; N, 25.72.

2-(2-Pyridyl)-1,3,4-thiadiazole (11d)—A mixture of 9b (100 mg, 0.56 mmol) and Na₂S₂O₄ (2.918 g, 16.76 mmol) in 50% aqueous EtOH (15 ml) was refluxed for 1 h. The mixture was extracted with CHCl₃ (3 × 80 ml). The combined

extract was washed with brine, and dried over Na_2SO_4 . After removal of the solvent by evaporation, the residue was chromatographed on a silica gel column (CHCl_3 -MeOH, 50:1, v/v). Evaporation of the eluates gave a solid, which was crystallized from petroleum ether to give 11d (51 mg, 56%), mp 80 – 82°C (lit.⁸⁾ 83 – 84°C).

Acknowledgement The authors wish to thank Mrs. M. Ohe for elemental analyses, and Mrs. Y. Yoshioka for MS. This work was supported in part by a grant from the Ministry of Education, Science and Culture, Japan.

References

- 1) G. Korins, "Comprehensive Heterocyclic Chemistry," Vol. 6, ed. by Kevine T. Potts, Pergamon Press Ltd., 1984, pp. 545–577.
- 2) A. Alemagna, T. Bacchetti, and P. Beltrame, *Tetrahedron*, **24**, 3209 (1968); T. Saito, N. Saheki, M. Hatanaka, and T. Ishimaru, *J. Heterocycl. Chem.*, **20**, 73 (1983).
- 3) H. Newman, E. L. Evans, and B. Angier, *Tetrahedron Lett.*, **1968**, 5829.
- 4) E. Hayashi and Y. Tamura, *Yakugaku Zasshi*, **90**, 594 (1970); E. Hayashi, T. Higashino, E. Oishi, and M. Sano, *ibid.*, **87**, 687 (1967); E. Hayashi and T. Watanabe, *ibid.*, **88**, 94 (1968); A. Yamane, A. Matsuda, and T. Ueda, *Chem. Pharm. Bull.*, **28**, 150 (1980); A. Matsuda, Y. Nomoto, and T. Ueda, *ibid.*, **27**, 183 (1979).
- 5) K. Fujii, H. Yoshikawa, and M. Yuasa, *Yakugaku Zasshi*, **74**, 1056 (1954).
- 6) S. Kubota, K. Toyooka, H. K. Misra, M. Kawano, and M. Shibuya, *J. Chem. Soc., Perkin Trans. 1*, **1983**, 2957.
- 7) B. DeCroix, M. J. Strauss, A. DeFusco, and D. C. Palmer, *J. Org. Chem.*, **44**, 1700 (1979).
- 8) P. Hemmerich, B. Prijs, and H. Erlenmeyer, *Helv. Chim. Acta*, **41**, 2058 (1958).

[Chem. Pharm. Bull.]
35(3)1036—1043(1987)

Studies on Griseolic Acid Derivatives. IV.¹⁾ Synthesis and Phosphodiesterase Inhibitory Activity of Acylated Derivatives of Griseolic Acid²⁾

YOSHINOBU MUROFUSHI,^a MISAKO KIMURA,^a YASUTERU IJIMA,^b
MITSUO YAMAZAKI^b and MASAKATSU KANEKO*^a

*Chemical Research Laboratories^a and Biological Research Laboratories,^b
Sankyo Co., Ltd., 2-58, Hiromachi 1-chome,
Shinagawa-ku, Tokyo 140, Japan*

(Received August 29, 1986)

Mono-, di- or triacylated griseolic acid derivatives were synthesized by selective acylation or by selective hydrolysis of the polyacylated derivatives. The inhibitory activities of these compounds against adenosine 3',5'-cyclic monophosphate or guanosine 3',5'-cyclic monophosphate phosphodiesterase were investigated to clarify the structure activity relationship. Acylation of the amino group of the adenine moiety greatly reduced the inhibitory activity. On the other hand, acylation of the hydroxy groups at the 7'- and 2'-position had relatively little effect on the inhibitory activity.

Keywords—griseolic acid; selective partial acylation; adenosine 3',5'-cyclic monophosphate; guanosine 3',5'-cyclic monophosphate; phosphodiesterase; inhibition

Introduction

Griseolic acid is a new nucleoside type compound which was isolated from the culture broth of *Streptomyces griseoaurantiacus* SANK 63479.³⁾ Its structure was subsequently determined as **1** by X-ray crystallographic analysis.⁴⁾

As illustrated, griseolic acid, which seems to be derived from adenosine and tartaric acid, has an adenine base, a bicyclic ring in its sugar moiety and two carboxylic acid groups. Thus, its structure is very similar to that of adenosine 3',5'-cyclic monophosphate (cAMP).

We have reported that griseolic acid is a strong competitive inhibitor of cAMP and guanosine 3',5'-cyclic monophosphate (cGMP) phosphodiesterases (PDE), and thus it increases the level of 3',5'-cyclic nucleotides in the tissues of treated animals.⁵⁾ It seems to act as an antagonist for PDE, probably because its structure is very similar to that of a 3',5'-cyclic nucleotide. It is well-known that cAMP, which is widely distributed in animal tissues, functions as a second messenger for and mediates the effects of a large number of hormones; as a result, cAMP has a variety of important physiological and biochemical roles.

From this background, we have investigated the relationship between the structures of griseolic acid derivatives and their inhibitory activities against PDE. In this paper, we wish to report a synthetic method for acylated derivatives and an examination of their inhibitory activities against cyclic nucleotide PDE.

Synthesis

An interest in the structure-activity relationship of griseolic acid has prompted us to synthesize various partially acylated derivatives. Moreover, these compounds should be good intermediates for synthesizing other derivatives of griseolic acid, as will be reported elsewhere. We therefore developed methods for regioselective acylation of each functional group of

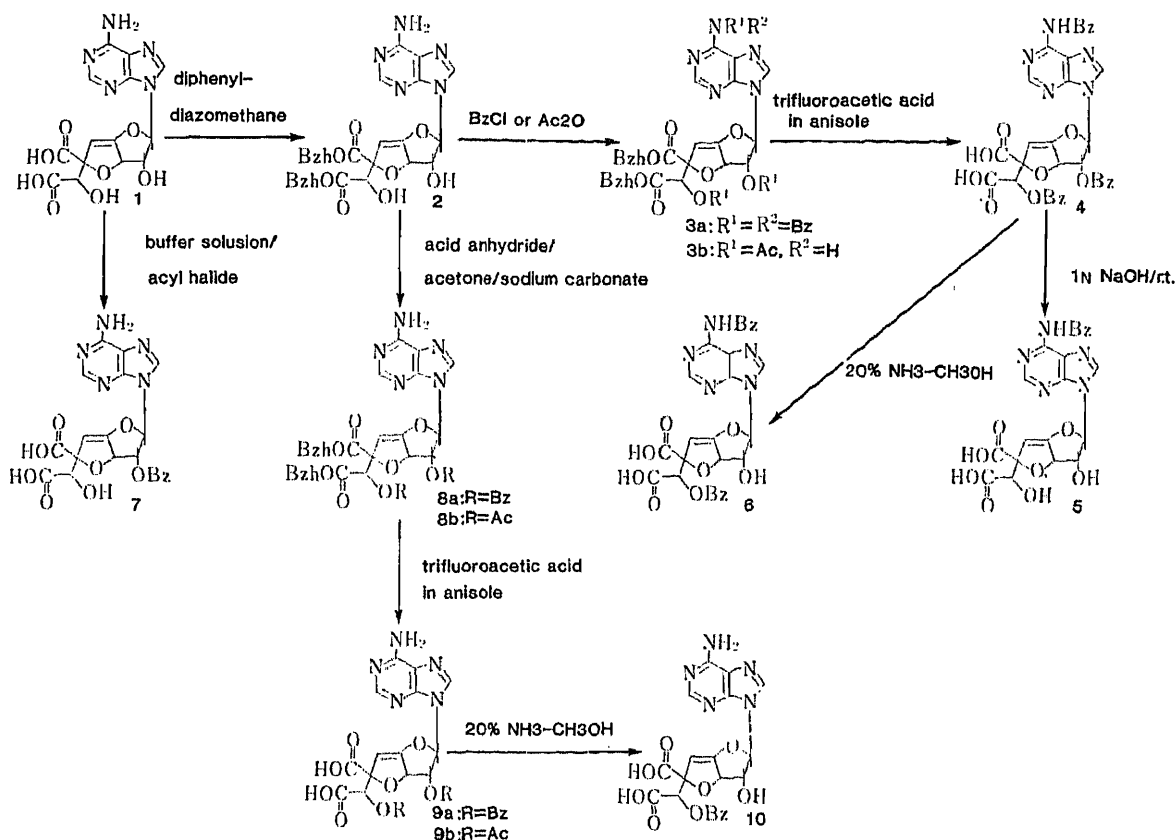


Fig. 1

griseolic acid.

N⁶,O^{2'},O^{7'}-Tribenzoylated Derivative (4)—In order to synthesize the title compounds, the general method⁶⁾ of acylation for nucleosides, that is, reaction with acid anhydride or acyl halide in pyridine, was applied to griseolic acid. However, the reaction mixture turned dark-brown and the starting material seemed to decompose. The desired compound was not formed. It seemed likely that this decomposition might be due to the double bond and carboxylic acid groups in the sugar moiety of griseolic acid.

Thus, we looked for a suitable protecting group, which could be removed under acidic conditions, for the two carboxylic acid groups. A benzhydryl group was found to be suitable for this purpose.

Dibenzhydryl griseolate (**2**) was obtained in good yield by reacting **1** with diphenyl-diazomethane in acetone containing water for 16 h at room temperature. This benzhydryl ester **2** was then benzoylated according to the general method⁷⁾ to give the **N⁶,N⁶,O^{2'},O^{7'}-tetrabenzoylated derivative (3a)**. Removal of the benzhydryl groups with trifluoroacetic acid in the presence of anisole gave the tribenzoyl compound (**4**).⁸⁾ Under these reaction conditions, not only the carboxy-protecting groups, but also one of the **N⁶**-benzoyl groups were simultaneously removed quantitatively. Consequently, it is considered that this method is available for preparing an acylated adenine nucleoside-type compound which has only one acyl group at the **N⁶**-position. It has been well recognized that, in the proton nuclear magnetic resonance (¹H-NMR) spectrum, the signal of the hydrogen bound to the carbon atom carrying an acyloxy group of the nucleoside is usually observed at significantly lower field as compared to that of the original hydroxy nucleoside. The NMR signals of 2'-H and 7'-H of **4** were observed at about 1.3 ppm lower field than those of **1**, as shown in Table I. Furthermore, the ultraviolet (UV) spectrum of **4** showed a peak at 277 nm which was very similar to that of

*N*⁶-benzoyladenoside.¹⁰⁾ These results and the elemental analysis data support the structure of **4**.

***N*⁶-Benzoylated Derivative (5)**—It has been well recognized that an acyl group attached to the amino group of adenosine is difficult to remove in alkaline conditions above pH 13, at which point the amido proton dissociates. On the other hand, the acyl group of the hydroxy group in the sugar moiety is easily hydrolyzed.¹¹⁾ Thus, the *N*⁶-monobenzoyl derivative (**5**) was obtained in 75% yield by selective hydrolysis of the *N*⁶,*O*^{2'},*O*^{7'}-tribenzoylated derivative **4**. As shown in Table I, the NMR signals of 2'-H and 7'-H of **5** do not show any significant downfield shift as compared to those of **1**. This fact, together with a UV spectrum whose λ_{max} is almost the same as that of *N*⁶-benzoyladenosine,¹⁰⁾ and the elemental analysis data support the identification of **5** as *N*⁶-benzoylgriseolic acid.

***O*^{2'}-Benzoylated Derivative (7)**—Although selective acylation of the primary hydroxy group of a nucleoside is possible in some cases, it is generally difficult to selectively acylate one hydroxy group of a molecule having two secondary ones. In the case of *p*-toluenesulfonylation, the authors have found that 2'-*p*-toluenesulfonyl-5'-adenylic acid can be obtained selectively by reacting 5'-adenylic acid with *p*-toluenesulfonyl chloride in the presence of sodium hydroxide in aqueous dioxane.¹²⁾ We expected that the carboxylic acid moieties of **1** might play the same role as the phosphate group of 5'-AMP in an acylation and would give the *O*^{2'}-acyl derivative. As expected, *O*^{2'}-benzoylgriseolic acid **7** was obtained in good yield by reacting **1** with benzoyl chloride in a mixture of ethyl acetate and 5M aqueous trisodium phosphate. A 1.3 ppm low-field shift of the NMR signal of 2'-H clearly supports the structure of **7**.

***O*^{2'}, *O*^{7'}-Diacylated Derivatives (9a and 9b)**—Acylation of adenine nucleoside with acid anhydride usually gives a product acylated at hydroxyl groups in the sugar moiety as a main product.¹³⁾ The benzhydryl ester **2** was treated with benzoic anhydride in acetone in the presence of sodium carbonate at refluxing temperature to give the dibenzoate **8a**. Removal of the benzhydryl groups with trifluoroacetic acid in the presence of anisole gave di-*O*-benzoylgriseolic acid (**9a**). The structure of this compound was determined from the NMR and UV spectra and elemental analysis.

***O*^{7'}-Acylated Derivative (10)**—Since all attempts of selective introduction of an acyl group at the *O*^{7'} position failed, we tried to remove the *O*^{2'}-benzoyl group of **9a**. The *O*^{2'}-benzoyl group of **9a** was selectively removed by treatment with 20% methanolic ammonia in an ice bath for 2 h to give the *O*^{7'}-benzoyl derivative **10** in good yield. The structure of this compound was determined from the NMR and UV spectra and elemental analysis. It seems likely that the resistance of the *O*^{7'}-acyl group to hydrolysis is due to participation of the neighboring carboxylic acid group at the 9' position.

As shown in Fig. 2, the carboxy anion at the 9' position can attack the carbon atom of the benzoyl carbonyl group to form a dioxolane structure. This dioxolane anion may be stabilized by forming an ion pair with an ammonium cation. This type of dioxolane formation

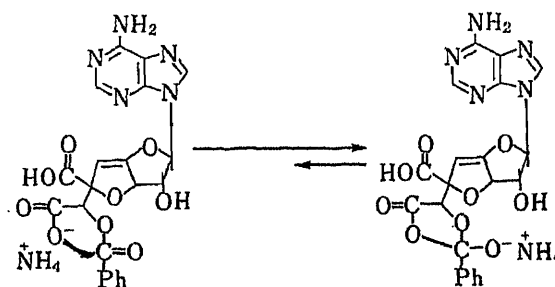


Fig. 2

TABLE I. ¹H-NMR Signals of 2'-H and 7'-H in Griseolic Acid Derivatives

Compound No.		1	2	3a	3b	4	5	6	7	8a	8b	9a	9b	10
δ ppm (DMSO- <i>d</i> ₆)	2'-H	4.61	4.68	5.75	6.04	5.92	4.72	4.76	5.90	5.93	5.70	5.87	5.64	4.71
	7'-H	4.52	4.93	5.99	6.13	5.79	4.56	5.82	4.45	6.16	5.98	5.80	5.64	5.82

TABLE II. PDE Inhibitory Activity of Griseolic Acid Derivatives

Compound No.		1	4	5	6	7	9a	9b	10
IC ₅₀	cAMP	0.16	74	13	33	6.8	3.2	9.3	0.31
(μM)	cGMP	0.63	116	72	111	48	90	243	2.9
	cAMP/cGMP	0.25	0.64	0.18	0.30	0.14	0.04	0.04	0.10

of acylated α -hydroxy carboxylic acid has been reported by Arcelli and Concilio.¹⁴⁾

***N*⁶, *O*⁷-Dibenzoylated Derivative (6)**—Compound 4 was treated in the same manner as described for the synthesis of 10 to give the title compound 6 in low yield. This low yield may be due to partial removal of the *N*⁶-acyl group under these reaction conditions. The structure of this compound was determined from the NMR spectrum, in which the signal of 7'-H is shifted downfield about 1.3 ppm compared to that of 1, and the UV spectrum, which is similar to that of 4, in addition to elemental analysis.

PDE Inhibitory Activity

As shown in Table II, the PDE inhibitory activity of griseolic acid seems to be weakened by acylation. Comparing the cAMP PDE inhibitory activity of the monobenzoylated derivative, the *N*⁶-benzoylated one 5 and the *O*^{2'}-benzoylated one 7 show about 80 times and 40 times less activity, respectively, whereas the inhibitory activity of the *O*^{7'}-benzoylated one (10) is decreased only two times. In addition, the *N*⁶,*O*^{7'}-dibenzoylated derivative 6 shows about 200 times less activity, whereas the *O*^{2'},*O*^{7'}-dibenzoylated one (9a) shows only 20 times less activity. Further, the inhibitory activity of the *N*⁶,*O*^{2'},*O*^{7'}-tribenzoylated compound 4 is reduced about 460 times. A similar tendency was observed in the inhibitory activity on cGMP PDE. Thus, it seems likely that the amino group at the 6-position plays a very important role at the binding site of PDE. In contrast, the sugar hydroxy groups, especially that at the 7'-position, do not play a significant role.

These findings are consistent with the conclusion of Severin *et al.*¹⁵⁾ that the amino group in the adenine moiety of cAMP was involved in binding with PDE. An investigation on the synthesis and PDE inhibitory activity of griseolic acid derivatives having various functional groups at the 6-position of the adenine moiety instead of the amino group is in progress in our laboratory to clarify more precisely the mode of action at the binding site of PDE.

Experimental

General—Melting points were determined using a Yanagimoto melting point apparatus and are uncorrected. NMR spectra were obtained with a Varian EM-390 spectrometer (90 MHz) and the chemical shifts are expressed in ppm from tetramethylsilane as internal standard; s, singlet; d, doublet; t, triplet; dd, doublet of doublets; m, multiplet; br d, broad doublet. UV spectra were obtained using a Hitachi 200-20 spectrophotometer. The thin layer chromatography (TLC) was carried out on Merck silica gel F₂₅₄ pre-coated TLC plates, layer thickness 0.25 mm, and spots were visualized by UV irradiation or by spraying with 30% aqueous sulfuric acid followed by heating. Ordinary chromatography was performed by the rapid chromatography method¹⁶⁾ using Merck silica gel (Kieselgel 60 Art. 9385).

Dibenzhydryl Griseolate (2)—Griseolic acid (10 g) was suspended in a mixture of 400 ml of acetone and 50 ml of water. To this was added a solution of 15.4 g of diphenyldiazomethane in 100 ml of acetone, and the mixture was stirred for 16 h at room temperature. The reaction product was then added dropwise to 2 l of hexane. The resulting powdery substance was collected by filtration, washed with 500 ml of hexane, and dried at 55–65 °C for 10 h under a pressure of 1–2 mmHg to yield 17.95 g (95.5%) of **2** as a white powder. UV (methanol) λ_{max} nm (ϵ): 258 (11800). NMR (DMSO- d_6) δ ppm: 8.37 (1H, s, 2 or 8-H), 8.18 (1H, s, 2 or 8-H), 6.58 (1H, s, 1'-H), 4.68 (1H, d, $J=6.0$ Hz, 2'-H), 6.35 (1H, dd, $J=6.0, 3.0$ Hz, 3'-H), 5.27 (1H, d, $J=3.0$ Hz, 5'-H), 4.93 (1H, s, 7'-H). *Anal.* Calcd for $C_{40}H_{33}N_5O_8 \cdot 1/2H_2O$: C, 66.66; H, 4.75; N, 9.72. Found: C, 66.67; H, 4.60; N, 9.59.

Dibenzhydryl N^6, N^6, O^2, O^7 -Tetrabenzoylgriseolate (3a)—Compound **2** (17.8 g) was dissolved in anhydrous pyridine. Then 18.5 ml of benzoyl chloride was added, with ice-cooling, and the mixture was kept standing at room temperature for 16 h, with protection from moisture. The reaction product was then ice-cooled, and 10 ml of water was added. The mixture was stirred at room temperature for 1 h. The solvent was then distilled off under reduced pressure. The residue was dissolved in a mixture of 100 ml of ethyl acetate and 50 ml of water, and the ethyl acetate layer was separated. This separated layer was washed with dilute hydrochloric acid, water, an aqueous solution of sodium bicarbonate, and a saturated aqueous solution of sodium chloride, in that order. The organic solution was separated and dried over anhydrous magnesium sulfate. The solvent was distilled off under reduced pressure to leave a pale yellowish residue. This residue was dissolved in a small quantity of methylene chloride, to which ethanol was added. The solvent was slowly distilled off under reduced pressure with an aspirator, leaving a yellowish powdery substance. This substance was collected by filtration, washed with ethanol and then dried to yield 26.4 g of **3a** in the form of a yellowish powder in a yield of 92.5%. A sample for analysis was obtained by purifying the powder by silica gel column chromatography with a 10% (v/v) solution of acetone in benzene. UV (methanol) λ_{max} nm (ϵ): 273 (22000). NMR (DMSO- d_6) δ ppm: 8.89 (1H, s, 2 or 8-H), 8.63 (1H, s, 2 or 8-H), 6.04 (1H, d, $J=6.6$ Hz, 2'-H), 6.63 (1H, dd, $J=6.6, 3.0$ Hz, 3'-H), 5.63 (1H, d, $J=3.0$ Hz, 5'-H), 6.13 (1H, s, 7'-H). *Anal.* Calcd for $C_{68}H_{49}N_5O_{12}$: C, 72.39; H, 4.38; N, 6.21. Found: C, 72.13; H, 4.40; N, 6.30.

Dibenzhydryl N^6, O^2, O^7 -Triacetylgriseolate (3b)—Compound **2** (1.06 g) was dissolved in 10 ml of anhydrous pyridine, then 1.13 ml of acetic anhydride was added, with ice-cooling. The mixture was stirred for 30 min under ice-cooling and left standing at 50 °C for 16 h. Methanol (20 ml) was added with ice-cooling, and the whole was stirred for 30 min. The solvent was distilled off under reduced pressure. Ethanol and water were added to the residue and the solvent was then distilled off. This process was repeated 4 times until the odor of pyridine could no longer be perceived. Subsequently, the product was dissolved in 15 ml of benzene, and the resulting solution was lyophilized to yield 1.21 g (96.6%) of **3b** as a crude product. This yellowish powder can be used as such for subsequent reactions, but a sample for analysis was obtained by silica gel column chromatography using methylene chloride containing 1% (v/v) methanol as the eluent. UV (methanol) λ_{max} nm (ϵ): 262 (15400), 280 sh (7900). NMR (DMSO- d_6) δ ppm: 8.65 (1H, s, 2 or 8-H), 8.59 (1H, s, 2 or 8-H), 7.00 (1H, s, 1'-H), 5.75 (1H, d, $J=6.0$ Hz, 2'-H), 6.49 (1H, dd, $J=6.0, 3.0$ Hz, 3'-H), 5.35 (1H, d, $J=3.0$ Hz, 5'-H), 5.99 (1H, s, 7'-H). *Anal.* Calcd for $C_{46}H_{39}N_5O_{11}$: C, 65.94; H, 4.69; N, 8.36. Found: C, 65.49; H, 4.46; N, 8.30.

N^6, O^2, O^7 -Tribenzoylgriseolic Acid (4)—Compound **3a** (26.2 g) was dissolved in 52 ml of anisole. Trifluoroacetic acid (52 ml) was then added, with ice-cooling, and the mixture was stirred for 4 h at room temperature. The solvent was distilled off under reduced pressure, and the residue was dissolved in acetone. Toluene was added to the acetone solution and distilled off; this process was repeated 3 times. The residue was dissolved in 150 ml of acetone and the solution was slowly poured into 2.5 l of hexane with stirring. The resulting precipitate was collected by filtration, washed with hexane, and dried to yield 17 g of a white powder, which was dissolved in a mixture of 350 ml of ethyl acetate and 60 ml of water, and treated with activated carbon. Sodium bicarbonate (8 eq) dissolved in 90 ml of water was added to this solution with stirring, and the mixture was stirred for 2 h. The resulting solid was collected by filtration, to yield 17.7 g of **4** in an impure form. This was recrystallized from a 1:8 (v/v) mixture of water and acetone, using activated carbon, to yield 15.7 g (91.9%) of the disodium salt of **4**. UV (methanol) λ_{max} nm (ϵ): 228 (39800), 277 (24900). NMR (DMSO- d_6) δ ppm: 8.85 (2H, s, 2 or 8-H), 6.98 (1H, s, 1'-H), 5.74 (1H, br d, $J=6.0$ Hz, 2'-H), 6.48 (1H, dd, $J=6.0, 3.0$ Hz, 3'-H), 5.25 (1H, d, $J=3.0$ Hz, 5'-H), 6.47 (1H, s, 7'-H). *Anal.* Calcd for $C_{35}H_{23}N_5Na_2O_{11} \cdot H_2O$: C, 55.78; H, 3.34; N, 9.29; Na, 6.10. Found: C, 55.43; H, 3.59; N, 9.23; Na, 6.21; mp 238–241 °C (dec.).

The disodium salt of **4** (5.2 g) was suspended in a mixture of 300 ml of ethyl acetate and 108 ml of water, and the suspension was stirred until there was hardly any insoluble material left. The pH of the suspension was then adjusted to 1.3 by addition of 3 N hydrochloric acid, under ice-cooling. The organic layer was separated, washed with a saturated aqueous solution of sodium chloride and dried over anhydrous magnesium sulfate. The solvent was then distilled off until the organic layer was concentrated to 270 ml. Hexane (270 ml) was added to the condensate, and the resulting white powdery substance was collected by filtration, washed with hexane and dried to yield 4.37 g (89.4%) of **4**. UV (50% (v/v) aqueous methanol) λ_{max} nm (ϵ): 232 (41400), 278 (27700). NMR (DMSO- d_6) δ ppm: 8.88 (1H, s, 2 or 8-H), 8.77 (1H, s, 2 or 8-H), 7.10–8.20 (16H, m, 1'-H), 5.92 (1H, d, $J=6.0$ Hz, 2'-H), 6.47 (1H, dd, $J=6.0, 3.0$ Hz, 3'-H), 5.43 (1H, d, $J=3.0$ Hz, 5'-H), 5.79 (1H, s, 7'-H). *Anal.* Calcd for $C_{35}H_{27}N_5O_{12}$: C, 59.24; H, 3.84; N, 9.87. Found: C, 59.48; H, 3.65; N, 9.78.

***N*⁶-Benzoylgriseolic Acid (5)**—The disodium salt of **4** (1.47 g) was dissolved in a 1 N aqueous solution of sodium hydroxide, and the solution was left standing for 15 h at room temperature. Ethyl acetate (30 ml) was then added and the pH of the solution was adjusted to 2.0 by addition of 2 N hydrochloric acid, under ice-cooling. Insoluble material formed. The mixture was stirred for a further 20 min, and the precipitate was collected by filtration and recrystallized from aqueous acetone to yield 725 mg (75.0%) of **5** as pale yellow crystals. UV (methanol) λ_{\max} nm (ϵ): 278 (25400). NMR (DMSO-*d*₆) δ ppm: 8.87 (1H, s, 2 or 8-H), 8.74 (1H, s, 2 or 8-H), 6.67 (1H, m, 1'-H), 4.72 (1H, br d, $J=6.0$ Hz, 2'-H), 6.08 (1H, dd, $J=6.0, 3.0$ Hz, 3'-H), 5.18 (1H, d, $J=3.0$ Hz, 5'-H), 4.56 (1H, s, 7'-H). *Anal.* Calcd for C₂₁H₁₇N₅O₉·1/2H₂O: C, 51.22; H, 3.68; N, 14.22. Found: C, 51.63; H, 3.74; N, 14.36.

***N*⁶,*O*⁷-Dibenzoylgriseolic Acid (6)**—The disodium salt of **4** (1.7 g) was dissolved with ice-cooling in 17 ml of a 0.5 N aqueous solution of sodium hydroxide, and the mixture was stirred for 1 h. The pH of the solution was then adjusted to 1 by addition of 3 N hydrochloric acid. Acetone and a solution of 1.5 g of diphenyldiazomethane in 10 ml of acetone were added, and the mixture was stirred for 50 min at room temperature. The reaction mixture was treated in the conventional manner to yield 0.92 g of dibenzhydryl *N*⁶,*O*⁷-dibenzoylgriseolate. This compound was dissolved in 8 ml of anisole. Trifluoroacetic acid (8 ml) was then added, under ice-cooling, and the mixture was left standing for 30 min at room temperature. The reaction mixture was treated in the same manner as described for **9b** to yield 515 mg (37.9%) of **6**. UV (50% (v/v) aqueous methanol) λ_{\max} nm (ϵ): 279 (23200). NMR (DMSO-*d*₆) δ ppm: 8.83 (1H, s, 2 or 8-H), 8.73 (1H, s, 2 or 8-H), 7.39 (2H, s, protons of benzene), 6.69 (1H, m, 1'-H), 4.76 (1H, d, $J=6.0$ Hz, 2'-H), 6.08 (1H, dd, $J=6.0, 3.0$ Hz, 3'-H), 5.20 (1H, d, $J=3.0$ Hz, 5'-H), 5.82 (1H, s, 7'-H). *Anal.* Calcd for C₂₈H₂₁N₅O₁₀·2/3H₂O + 1/3C₆H₆: C, 57.60; H, 3.89; N, 11.20. Found: C, 57.56; H, 3.90; N, 10.96.

***O*²-Benzoylgriseolic Acid (7)**—Griseolic acid (6.81 g) was dissolved in 120 ml of a 0.5 M aqueous solution of trisodium phosphate. Ethyl acetate (120 ml) was then added. The mixture was stirred and ice-cooled whilst 18 ml of benzoyl chloride was added, and the whole was then stirred for a further 3 h. The reaction product was transferred into a separating funnel, the aqueous layer was separated, and the organic layer was washed with 20 ml of water. The aqueous layer and the washings were combined and washed with 50 ml of ethyl acetate. A further 100 ml of ethyl acetate was added to the aqueous layer, whose pH was then adjusted to 2.0 by adding concentrated hydrochloric acid, under ice-cooling. A solid substance formed, but the mixture was left standing overnight in a refrigerator. The solid substance was collected by filtration, washed with a small quantity of water, and then dried to yield 7.60 g (87.5%) of **7**. UV (methanol) λ_{\max} nm (ϵ): 230 (17600), 257 (16000). NMR (DMSO-*d*₆) δ ppm: 8.43 (1H, s, 2 or 8-H), 8.33 (1H, s, 2 or 8-H), 7.48 (2H, s, NH₂), 7.27 (1H, s, 1'-H), 5.90 (1H, d, $J=6.0$ Hz, 2'-H), 6.41 (1H, dd, $J=6.0, 3.0$ Hz, 3'-H), 5.28 (1H, d, $J=3.0$ Hz, 5'-H), 4.55 (1H, s, 7'-H). *Anal.* Calcd for C₂₁H₁₇N₅O₉·1/2H₂O: C, 51.22; H, 3.68; N, 14.22. Found: C, 51.03; H, 3.43; N, 14.25.

Dibenzhydryl *O*²,*O*⁷-Dibenzoylgriseolate (8a)—Compound **3** (7.11 g) was dissolved in 200 ml of acetone. Anhydrous benzoic anhydride (22.6 g) and anhydrous sodium carbonate (27.6 g) were then added, and the mixture was refluxed for 7 h. Insoluble inorganic substances were filtered off, and the solvent was distilled from the filtrate under reduced pressure to yield a pale yellow caramel-like residue. The residue was purified by a silica gel column chromatography using methylene chloride containing 1% (v/v) methanol as the eluent to yield 4.3 g (46.7%) of **8a**. UV (methanol) λ_{\max} nm (ϵ): 257 (19500), 280 sh (5500). NMR (DMSO-*d*₆) δ ppm: 8.43 (1H, s, 2 or 8-H), 8.17 (1H, s, 2 or 8-H), 7.09 (2H, s, NH₂), 5.93 (1H, d, $J=6.0$ Hz, 2'-H), 6.85 (1H, dd, $J=6.0, 3.0$ Hz, 3'-H), 5.57 (1H, d, $J=3.0$ Hz, 5'-H), 6.16 (1H, s, 7'-H). *Anal.* Calcd for C₅₄H₄₁N₅O₁₀·1/2H₂O: C, 69.81; H, 4.56; N, 7.54. Found: C, 69.93; H, 4.46; N, 7.50.

Dibenzhydryl *O*²,*O*⁷-Diacetylgriseolate (8b)—Compound **2** (1.37 g) was suspended in 20 ml of anhydrous pyridine, and 0.94 ml of acetic anhydride was added, with ice-cooling. The mixture was then stirred whilst protecting it from moisture. Ethanol was added to the reaction product, whilst ice-cooling, and the mixture was stirred for 30 min. The residue obtained by distilling the solvent from the reaction product under reduced pressure was dissolved in 30 ml of chloroform, and the solution was washed with water. The organic layer was separated and the solvent was distilled off under reduced pressure. The resulting residue was purified by preparative thin layer chromatography using benzene containing 10% (v/v) methanol as the developing solvent to yield 936 mg (61.3%) of **8b** as a white solid. UV (methanol) λ_{\max} nm (ϵ): 257 (15400). NMR (DMSO-*d*₆) δ ppm: 8.35 (1H, s, 2 or 8-H), 8.13 (1H, s, 2 or 8-H), 7.2—8.8 (22H, m, protons of NH₂ and benzhydryl groups), 6.92 (1H, s, 1'-H), 5.70 (1H, d, $J=6.0$ Hz, 2'-H), 6.60 (1H dd, $J=6.0, 3.0$ Hz, 3'-H), 5.28 (1H, d, $J=3.0$ Hz, 5'-H), 5.98 (1H, s, 7'-H). *Anal.* Calcd for C₄₄H₃₇N₅O₁₀·1/2H₂O: C, 65.66; H, 4.76; N, 8.70. Found: C, 65.61; H, 4.46; N, 8.17.

***O*²,*O*⁷-Dibenzoylgriseolic Acid (9a)**—Compound **8a** (2.80 g) was dissolved in 10 ml of anisole. Trifluoroacetic acid (10 ml) was then added, under ice-cooling, and the mixture was left standing at room temperature for 1 h. The residue obtained by distilling off the solvent under reduced pressure was dissolved in acetone, toluene was added, and then the solvent was distilled off. This process was repeated 3 times. The resulting yellowish caramel-like substance was dissolved in 20 ml of acetone, and this solution was slowly poured into 200 ml of hexane, with stirring. The mixture was then stirred for 30 min, and the precipitate was collected by filtration. The precipitate was suspended in 20 ml of a 5% (w/v) aqueous solution of sodium bicarbonate and 20 ml of water. Ethyl acetate (50 ml) was added and the pH of the mixture was adjusted to 0.5—1.0 by the addition of concentrated hydrochloric acid so as to completely dissolve the precipitate. The pH of this solution was then adjusted to 2.0 by addition of sodium bicarbonate, and the

resulting white crystalline substance was collected by filtration, washed with 100 ml of water and 100 ml of hexane, and then dried to yield 1.75 g (98%) of **9a** as a white powder. UV (methanol) λ_{\max} nm (ϵ): 230 (28000), 256 (17700). NMR (DMSO- d_6) δ ppm: 8.48 (1H, s, 2 or 8-H), 8.32 (1H, s, 2 or 8-H), 7.2–7.8 (12H, m, protons of NH_2 and benzoyl groups), 7.15 (1H, s, 1'-H), 5.87 (1H, d, $J=6.0$ Hz, 2'-H), 6.51 (1H dd, $J=6.0, 3.0$ Hz, 3'-H), 5.40 (1H, d, $J=3.0$ Hz, 5'-H), 5.80 (1H, s, 7'-H). *Anal.* Calcd for $\text{C}_{28}\text{H}_{21}\text{N}_5\text{O}_{10} \cdot 1/2\text{H}_2\text{O}$: C, 56.38; H, 3.72; N, 11.74. Found: C, 56.06; H, 3.94; N, 11.26.

O²,O⁷-Diacetylgriseolic Acid (9b)—Compound **8b** (1.0 g) was dissolved in 10 ml of anisole. Trifluoroacetic acid (10 ml) was then added, under ice-cooling, and the mixture was left standing at room temperature for 30 min. The solvent was distilled from the product under reduced pressure. The resulting residue was dissolved in acetone. Toluene was added to the solution for extraction, and then distilled off under reduced pressure; this process was repeated 3 times to leave a pale yellowish residue. The residue was dissolved in 10 ml of acetone, and this solution was slowly poured into 250 ml of hexane with stirring. The resulting white precipitate was collected by filtration, washed with hexane, and dried. The precipitate was dissolved in 10 ml of saturated aqueous solution of sodium bicarbonate, with ice-cooling. The mixture was acidified by addition of 3N hydrochloric acid, and a white precipitate was formed. On further addition of hydrochloric acid to pH 0.5–1.0, the precipitate dissolved again to yield a clear solution. This clear solution was subjected to reverse phase column chromatography using a prepacked column RP-8 (Merck), which was washed with water and then eluted with a 10% (v/v) aqueous solution of acetonitrile. The main peaks of the eluate were collected to leave 412 mg (71.1%) of **9b** as a pale yellowish powder. UV (methanol) λ_{\max} nm (ϵ): 257 (15400). NMR (DMSO- d_6) δ ppm: 8.37 (1H, s, 2 or 8-H), 8.23 (1H, s, 2 or 8-H), 7.41 (2H, s, NH_2), 6.85 (1H, s, 1'-H), 5.64 (1H, d, $J=6.0$ Hz, 2'-H), 6.24 (1H, dd, $J=6.0, 3.0$ Hz, 3'-H), 5.13 (1H, d, $J=3.0$ Hz, 5'-H), 5.64 (1H, s, 7'-H). *Anal.* Calcd for $\text{C}_{18}\text{H}_{17}\text{N}_5\text{O}_{10} \cdot 2\text{H}_2\text{O}$: C, 43.46; H, 3.85; N, 14.08. Found: C, 43.70; H, 3.99; N, 14.92.

O⁷-Benzoylgriseolic Acid (10)—Compound **9a** (1.174 g) was dissolved in a 20% (w/v) solution of ammonia in methanol, and the solution was left standing for 2 h, with ice-cooling. The solvent was distilled off under reduced pressure to yield a white precipitate, which was suspended in a mixture of 30 ml of water and 30 ml of diethyl ether. Concentrated hydrochloric acid was added to this suspension until the pH was within the range of 0–1. Initially, a white insoluble material was formed, then it quickly dissolved. The aqueous layer was separated, washed with 30 ml of diethyl ether, and then transferred to a beaker, to which solid sodium bicarbonate was added until the pH of the mixture reached 2.0. The resulting white precipitate was collected by filtration and dried to yield a white powdery substance, which was recrystallized from aqueous acetone to yield 700 mg (72.9%) of **10** as a white powder. UV (methanol) λ_{\max} nm (ϵ): 210 (31900), 227 (20000), 257 (17500). NMR (DMSO- d_6) δ ppm: 8.42 (1H, s, 2 or 8-H), 8.26 (1H, s, 2 or 8-H), 7.44 (1H, s, NH_2), 5.59 (1H, s, 1'-H), 4.71 (1H, d, $J=6.0$ Hz, 2'-H), 6.11 (1H, dd, $J=6.0, 3.0$ Hz, 3'-H), 5.17 (1H, d, $J=3.0$ Hz, 5'-H), 5.82 (1H, s, 7'-H). *Anal.* Calcd for $\text{C}_{21}\text{H}_{17}\text{N}_5\text{O}_9 \cdot 2\text{H}_2\text{O}$: C, 48.55; H, 4.07; N, 13.48. Found: C, 48.90; H, 3.75; N, 13.61.

PDE Inhibitory Activity

The test was carried out following essentially the method of Pichard and Cheung.¹⁷⁾ The rat brains were homogenized using glass-glass or glass-Teflon homogenizers with four volumes of cold 0.17 M Tris-HCl buffer, pH 7.4, containing 5 mM MgSO_4 . The homogenate was then centrifuged at $100000 \times g$ at 0°C for 1 h. The clear supernatant solution was stored at -20°C and used as a cAMP PDE preparation. Prior to use, this solution was diluted 100–150 times with 40 mM Tris-HCl buffer (pH 7.5). The reaction mixture (total volume, 0.1 ml), consisting of 40 mM Tris-HCl buffer (pH 7.5), 5 mM MgSO_4 , 50 μM CaCl_2 , 20 μM of snake venom (*Crotalus atrox*, Sigma), 0.14 μM [¹⁴C] cAMP, test material and enzyme solution, was incubated at 30°C for 20 min. At the end of this time, the reaction mixture was treated with Amberlite IRP-58 resin and the level of residual radioactivity of adenosine was determined. The experiment was carried out at a number of concentration levels of each active compound, and from the results, the 50% inhibition value (IC_{50}) was calculated.

A similar experiment was carried out with cGMP as the substrate instead of cAMP. The IC_{50} value toward cGMP PDE was also calculated.

Acknowledgment The authors wish to express their thanks to Dr. H. Nakao, the Director of the Chemical Research Laboratories, for his encouragement and advice, and to Drs. T. Hiraoka and T. Miyadera for their valuable suggestions.

References and Notes

- 1) The previous paper of this series was published in *Nucleic Acid Research Symposium Series*, No. 17, 45 (1986).
- 2) This paper is dedicated to Professor Morio Ikehara on the occasion of his retirement from Osaka University in March, 1986.
- 3) F. Nakagawa, T. Okazaki, A. Naito, Y. Iijima and M. Yamazaki, *J. Antibiot.*, **38**, 823 (1985).
- 4) S. Takahashi, F. Nakagawa, K. Kawazoe, Y. Furukawa, S. Sato, C. Tamura and T. Naito, *J. Antibiot.*, **38**, 830 (1985).
- 5) Y. Iijima, F. Nakagawa, S. Handa, T. Oda, A. Naito and M. Yamazaki, *FEBS Lett.*, **192**, 179 (1985).

- 6) H. Weber and H. G. Khorana, *J. Mol. Biol.*, **72**, 219 (1972); R. I. Zhdanov and S. M. Zhenodarova, *Synthesis*, **1975**, 222; L. R. Lewis, R. K. Robins and C. C. Cheng, *J. Med. Chem.*, **7**, 200 (1964).
- 7) M. J. Robins and R. K. Robins, *J. Am. Chem. Soc.*, **87**, 4934 (1965).
- 8) G. C. Stelakatos, A. Paganou and L. Zervas, *J. Chem. Soc. C*, **1966**, 1191.
- 9) Y. Ishido, N. Sakairi, K. Okazaki and N. Nakazaki, *J. Chem. Soc., Perkin Trans. 1*, **1980**, 563.
- 10) R. H. Hall, *Biochemistry*, **3**, 769 (1964).
- 11) R. K. Ralph and H. G. Khorana, *J. Am. Chem. Soc.*, **83**, 2926 (1961).
- 12) M. Kaneko, M. Kimura, T. Nishimura and B. Shimizu, *Chem. Pharm. Bull.*, **25**, 2482 (1977); M. Ikehara and S. Uesugi, *Tetrahedron Lett.*, **59**, 713 (1970).
- 13) L. N. Nikolenko, W. N. Nesawibatko, A. F. Usatiy and M. N. Semjenowa, *Tetrahedron Lett.*, **59**, 5193 (1970).
- 14) A. Arcelli and C. Concilio, *J. Chem. Soc., Perkin Trans. 2*, **1977**, 1563; *idem*, *Ann. Chim.*, **58**, 881 (1968).
- 15) E. S. Severin, N. N. Gulyaev, T. V. Bulargina and M. N. Kochetkava, *Ad. Enzyme Regul.*, **17**, 251 (1979).
- 16) W. C. Still, M. Kahn and A. Mitra, *J. Org. Chem.*, **43**, 2923 (1978).
- 17) A. L. Pichard and W. Y. Cheung, *J. Biol. Chem.*, **251**, 5726 (1976).

[Chem. Pharm. Bull.]
[35(3)1044—1048(1987)]

Amino Acids and Peptides. VIII.¹⁾ A Water-Soluble Active Ester, Phenolsulfonic Acid Derivative

KOICHI KAWASAKI,* TOSHIKI TSUJI, MITSUKO MAEDA,
TATSUYA MATSUMOTO, and KATSUHIKO HIRASE

*Faculty of Pharmaceutical Sciences, Kobe-Gakuin University, Ikawadani-cho,
Nishi-ku, Kobe 673, Japan*

(Received September 1, 1986)

N-Protected amino acid 4-phenolsulfonic acid derivative esters, such as 2,6-dibromo-4-sulfophenyl ester sodium salt, 2,6-dichloro-4-sulfophenyl ester potassium salt and 2-nitro-4-sulfophenyl ester sodium salt, were prepared. These esters are water-soluble active esters, and were applied for the synthesis of Leu-enkephalin.

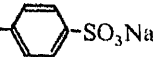
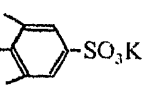
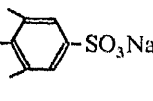
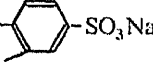
Keywords—water-soluble active ester; 2,6-dichloro-4-sulfophenyl ester; 2,6-dibromo-4-sulfophenyl ester; 2-nitro-4-sulfophenyl ester; peptide synthesis; Leu-enkephalin

Water-soluble active esters, such as water-soluble carbodiimide,²⁾ may be advantageous in peptide synthesis for easy purification of the product by an extraction procedure. In the preceding paper,³⁾ *p*-trimethylammonio-phenyl ester was examined as a water-soluble active ester. The ester had good reactivity, but its purification was rather difficult and it was somewhat unstable. Here we report water-soluble active esters, substituted 4-sulfophenyl esters, which are easier to purify and more stable than *p*-trimethylammonio-phenyl ester. During our study, Aldwin and Nitecki⁴⁾ reported the use of 2-nitro-4-sulfophenyl ester for a protein-protein crosslinking reaction in the pH range of 6—8 in aqueous media. They prepared *N*-maleimido-6-aminocaproic acid 2-nitro-4-sulfophenyl ester and used it as a crosslinking reagent.

Since 4-phenolsulfonic acid is a strong acid and may cleave acid-labile protecting groups, its salt was examined as an ester component. *tert*-Butoxycarbonylalanine (Boc-Ala-OH) was easily deblocked by 4-phenolsulfonic acid but was stable to sodium 4-phenolsulfonate. Boc-Ala 4-sulfophenyl ester sodium salt [Boc-Ala-OPS (Na)] was first prepared and was reacted with phenylalanine methyl ester. No reaction was observed, which suggested that an electron-attracting group should be introduced onto the phenyl ring to increase the reactivity of the 4-sulfophenyl ester. 2,6-Dichloro-4-sulfophenyl ester potassium salt [OPS (Cl, K)], 2,6-dibromo-4-sulfophenyl ester sodium salt [OPS (Br, Na)] and 2-nitro-4-sulfophenyl ester sodium salt [OPS (NO₂, Na)], each of which has an electron-attracting group on the phenyl ring, were examined as water-soluble active esters.

Potassium 3,5-dichloro-4-phenolsulfonate,⁵⁾ sodium 3,5-dibromo-4-phenolsulfonate⁶⁾ and sodium 3-nitro-4-phenolsulfonate⁷⁾ were prepared from potassium (or sodium) 4-phenolsulfonate according to the known methods. Esterification of benzyloxycarbonylalanine (Z-Ala-OH) and the 4-phenolsulfonic acid derivative was done with dicyclohexylcarbodiimide (DCC)⁸⁾ in dimethylformamide (DMF) to afford Z-Ala-OPS (Cl, K), Z-Ala-OPS (Br, Na) and Z-Ala-OPS (NO₂, Na). All these esters were water-soluble and had good reactivity. Each ester was reacted with phenylalanine methyl ester to form Z-Ala-Phe-OMe in reasonable yield as shown in Table I. No side reaction was observed and the product was easily purified by extraction with ethyl acetate followed by washing out of the unnecessary

TABLE I. Yields of Z-Ala-Phe-OMe Prepared from Z-Ala Ester and H-Phe-OMe

Esters	Yields (%)
Z-Ala-O-  -SO ₃ Na	0
Z-Ala-O-  -SO ₃ K	72
Z-Ala-O-  -SO ₃ Na	66
Z-Ala-O-  -SO ₃ Na	74

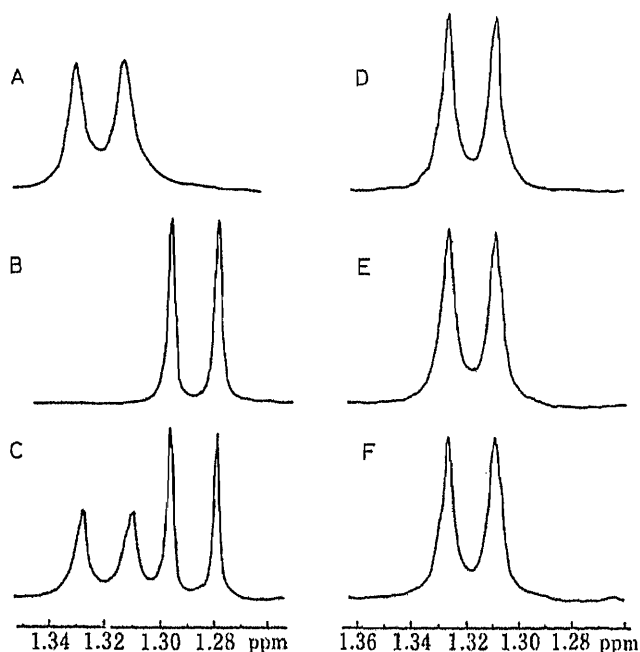


Fig. 1. NMR Spectra Showing the Methyl Signals of Ala in Z-Ala-Phe-OMe

Solvent: CDCl₃. A: standard L-L. B: standard D-L. C: standard L-L + standard D-L. D: prepared by the OPS (Cl, K) method. E: prepared by the OPS (Br, Na) method. F: prepared by the OPS (NO₂, Na) method.

material with 5% sodium carbonate, 5% citric acid and water.

Nuclear magnetic resonance (NMR) spectra of the synthetic Z-Ala-Phe-OMe were measured to examine the occurrence of racemization during the reactions according to the method reported by Weinstein and Pritchard.⁹⁾ The methyl signal of Ala in Z-Ala-Phe-OMe was compared with those of standard Z-L-Ala-L-Phe-OMe^{9,10)} and Z-D-Ala-L-Phe-OMe⁹⁾ as shown in Fig. 1. The methyl signal of Ala in Z-L-Ala-L-Phe-OMe appeared at 1.34 ppm, while the methyl signal of Ala in Z-D-Ala-L-Phe-OMe appeared at 1.29 ppm. A mixture of Z-L-Ala-L-Phe-OMe and Z-D-Ala-L-Phe-OMe showed signals at 1.32 and 1.29 ppm. All methyl signals of Ala in Z-Ala-Phe-OMe prepared by three different phenolsulfonic acid derivative ester procedures appeared at 1.32 ppm and no signal was observed at 1.29 ppm. The results suggested that these phenolsulfonic acid derivative esters are applicable to peptide synthesis.

Next, application of the phenolsulfonic acid derivative ester was examined. Leucine-

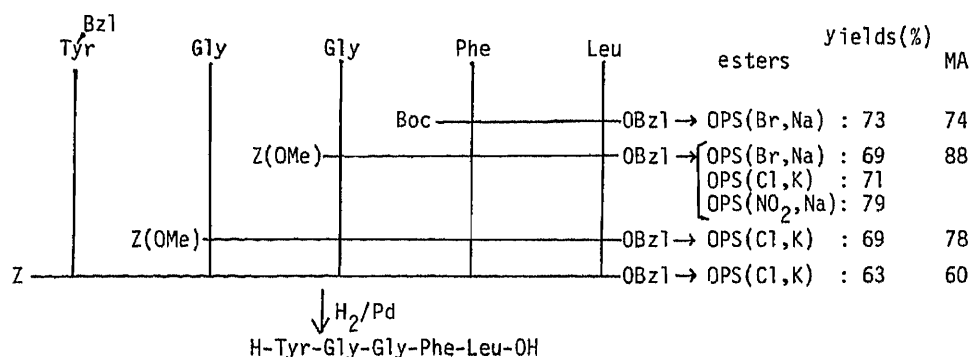


Fig. 2. Synthetic Scheme for Leu-enkephalin

MA: mixed anhydride method. Boc and Z(OMe) groups were removed by TFA treatment prior to the coupling reaction.

enkephalin was synthesized by these active ester methods and the coupling yields were compared with those of the mixed anhydride method¹¹⁾ reported in the preceding paper,³⁾ as shown in Fig. 2. The coupling reactions of the esters with amine components were done in DMF at room temperature, and the protected synthetic intermediates were purified easily by extraction. No side reaction was observed and the yields were comparable with those of the mixed anhydride method. *N*-Benzyloxycarbonyl-*O*-benzyltyrosine 2,6-dichloro-4-sulfophenyl ester potassium salt [Z-Tyr(Bzl)-OPS(Cl, K)] was not readily soluble in water but it could be removed from the reaction mixture by washing with water and recrystallization from methanol.

The reactivity of the phenolsulfonic acid derivative esters in aqueous media was also examined. Z-Ala-OPS(Cl, K), Z-Ala-OPS(Br, Na) and Z-Ala-OPS(NO₂, Na) were each reacted with glycine methyl ester in water to give Z-Ala-Gly-OMe. The precipitation of the product occurred immediately after the addition of the active ester to the aqueous solution of glycine methyl ester. The coupling yields were 73% by the OPS(Cl, K) method, 65% by the OPS(Br, Na) method and 79% by the OPS(NO₂, Na) method, and the products were identical with an authentic sample prepared by the known method.¹²⁾

The phenolsulfonic acid derivative esters may be useful not only for peptide synthesis but also for the acylation of proteins in aqueous media.

Experimental

Melting points are uncorrected. Solvent systems for ascending thin-layer chromatography (TLC) on Silica gel G (type 60, E. Merck) are indicated as follows: $R_f^1 = \text{BuOH}-\text{AcOH}-\text{H}_2\text{O}$ (4:1:5, upper phase), $R_f^2 = \text{BuOH}-\text{pyridine}-\text{AcOH}-\text{H}_2\text{O}$ (4:1:1:2), $R_f^3 = \text{CHCl}_3-\text{MeOH}-\text{H}_2\text{O}$ (8:3:1, lower phase), $R_f^4 = \text{AcOEt}-\text{benzene}$ (1:1). NMR spectra were taken in CDCl_3 on a Bruker AM-400 (400 MHz).

Treatment of Boc-Ala-OH with 4-Phenolsulfonic Acid—Boc-Ala-OH (100 mg, 0.53 mm) dissolved in MeOH (0.5 ml) and 4-phenolsulfonic acid (92 mg, 0.53 mm) dissolved in MeOH (5 ml) were combined and the mixture was stirred at room temperature. To examine the deblocking of Boc-Ala-OH, the mixture was checked by TLC (R_f^3 system). The spot of Boc-Ala-OH disappeared within 2 h and the spot of H-Ala-OH appeared.

Boc-Ala-OH was also treated with sodium 4-phenolsulfonate under the same conditions and the deblocking of Boc-Ala-OH was not observed.

General Procedure for Preparation of *N*-Protected Amino Acid 4-Phenolsulfonic Acid Derivative Ester—DCC (4.94 g, 24 mm) was added to a DMF solution (30 ml) of *N*-protected amino acid (20 mm) at -10°C and the mixture was stirred for 20 min. 4-Phenolsulfonic acid derivative (20 mm) dissolved in DMF (30 ml) was then added to the mixture and the whole was stirred overnight in a cold room. The resulting precipitate was filtered off and the filtrate was evaporated down. The residue was extracted with H_2O , and the aqueous layer was washed with ether and lyophilized. The residue was recrystallized from a suitable solvent.

Z-Ala-OPS(Na)—Prepared according to the general procedure. Recrystallized from ethanol. Yield 74%, mp $> 300^\circ\text{C}$, R_f^3 0.45, $[\alpha]_D^{25} - 32.0^\circ$ ($c = 1.0$, DMF). Anal. Calcd for $\text{C}_{17}\text{H}_{16}\text{NNaO}_7\text{S}$: C, 50.9; H, 4.0; N, 3.5. Found:

C, 50.9; H, 4.0; N, 3.4.

Z-Ala-OPS (Br, Na)—Prepared according to the general procedure. Recrystallized from propanol. Yield 78%, mp 243 °C (dec), R_f^3 0.38, $[\alpha]_D^{25}$ -12.2° ($c=1.0$, DMF). *Anal.* Calcd for $C_{17}H_{14}Br_2NNaO_7S$: C, 36.5; H, 2.5; N, 2.5. Found: C, 36.7; H, 2.7; N, 2.7.

Z-Ala-OPS (Cl, K)—Prepared according to the general procedure. Recrystallized from a mixture of MeOH and EtOH. Yield 69%, mp > 300 °C R_f^3 0.43, $[\alpha]_D^{25}$ -18.1° ($c=1.0$, DMF). *Anal.* Calcd for $C_{17}H_{14}Cl_2KNO_7S$: C, 42.0; H, 2.9; N, 2.9. Found: C, 41.7; H, 3.1; N, 2.7.

Z-Ala-OPS (NO₂, Na)—Prepared according to the general procedure. Recrystallized from MeOH. Yield 65%, mp > 300 °C, R_f^3 0.35, $[\alpha]_D^{25}$ -31.2° ($c=1.0$, DMF). *Anal.* Calcd for $C_{17}H_{15}N_2NaO_9S$: C, 45.7; H, 3.4; N, 6.3. Found: C, 45.6; H, 3.5; N, 6.0.

Boc-Phe-OPS (Br, Na)—Prepared according to the general procedure. Recrystallized from a mixture of MeOH and EtOH. Yield 66%, mp > 300 °C, R_f^3 0.57, $[\alpha]_D^{25}$ -44.2° ($c=1.0$, DMF). *Anal.* Calcd for $C_{20}H_{20}Br_2NNaO_7S$: C, 36.5; H, 2.5; N, 2.0. Found: C, 36.6; H, 2.7; N, 1.8.

Z(OMe)-Gly-OPS(Cl, K)—Prepared according to the general procedure. Recrystallized from EtOH. Yield 81%, mp > 300 °C, R_f^3 0.45. *Anal.* Calcd for $C_{17}H_{14}Cl_2KNO_8S$: C, 40.6; H, 2.8; N, 2.8. Found: C, 40.4; H, 3.0; N, 2.5.

Z(OMe)-Gly-OPS(Br, Na)—Prepared according to the general procedure. Recrystallized from EtOH. Yield 68%, mp > 300 °C R_f^3 0.45. *Anal.* Calcd for $C_{17}H_{14}BrNNaO_8S \cdot H_2O$: C, 34.4; H, 2.7; N, 2.4. Found: C, 34.3; H, 2.7; N, 2.5.

Z(OMe)-Gly-OPS(NO₂, Na)—Prepared according to the general procedure. Recrystallized from a mixture of MeOH and EtOH. Yield 77%, mp > 300 °C, R_f^3 0.43. *Anal.* Calcd for $C_{17}H_{15}N_2NaO_{10}S \cdot 1/2H_2O$: C, 43.3; H, 3.4; N, 5.9. Found: C, 43.4; H, 3.4; N, 6.1.

Z-Tyr(Bzl)-OPS (Cl, K)—Z-Tyr (Bzl)-OH and HOPS (Cl, K) were reacted with DCC according to the general procedure. After removal of the precipitated urea, the solvent was evaporated off and the residue was extracted with H₂O. Precipitation occurred when the aqueous layer was washed with ether and the precipitate was collected by filtration and recrystallized from MeOH. Yield 66%, mp > 300 °C, R_f^3 0.71, $[\alpha]_D^{25}$ -41.0° ($c=1.0$, DMF). *Anal.* Calcd for $C_{30}H_{24}Cl_2KNO_8S$: C, 53.9; H, 3.6; N, 2.1. Found: C, 53.7; H, 3.9; N, 1.9.

General Procedure for Peptide Synthesis with 4-Sulfophenyl Ester Derivative—An *N*-protected amino acid 4-sulfophenyl ester derivative and an amino component (1 : 1 in molar ratio) were dissolved in DMF and the solution was stirred at room temperature for 15 h. The solvent was evaporated off and the residue was extracted with AcOEt. The AcOEt layer was washed successively with 5% citric acid, 5% Na₂CO₃ and H₂O, and dried over Na₂SO₄. The AcOEt was evaporated off and the residue was recrystallized from a suitable solvent.

Z-Ala-Phe-OMe—prepared according to the general procedure. Recrystallized from AcOEt-petroleum ether. a) OPS (Cl, K) method: Yield 72%, mp 101–103 °C, R_f^4 0.87, $[\alpha]_D^{22}$ -8.1° ($c=1.0$, EtOH). *Anal.* Calcd for $C_{21}H_{24}N_2O_5$: C, 65.6; H, 6.3; N, 7.3. Found: C, 65.8; H, 6.3; N, 7.1. Amino acid ratios in an acid hydrolysate: Ala 1.00, Phe 0.96 (recovery of Ala, 84%). b) OPS (Br, Na) method: Yield 66%, mp 103–104 °C, R_f^4 0.87, $[\alpha]_D^{28}$ -8.4° ($c=1.0$, EtOH). Amino acid ratio in an acid hydrolysate, Ala 1.00, Phe 0.97 (recovery of Ala, 89%). c) OPS(NO₂, Na) method: Yield 74%, mp 102–103 °C, R_f^4 0.87, $[\alpha]_D^{29}$ -8.9° ($c=1.0$, EtOH). Amino acid ratio in an acid hydrolysate, Ala 1.00, Phe 1.05 (recovery of Ala, 89%). [lit.¹²] mp 99–100 °C, $[\alpha]_D^{22}$ -9.3° ($c=1.0$, EtOH).

Z-Ala-OPS (Na) was also reacted with H-Phe-OMe but no reaction was observed.

Boc-Phe-Leu-OBzl—Boc-Phe-OPS (Br, Na) (1.67 g, 2.2 mm) and H-Leu-OBzl [prepared from its tosylate (787 mg, 2 mm) by treatment with Et₃N] were reacted according to the general procedure. Recrystallized from a mixture of ether and petroleum ether. Yield 688 mg (73%), mp 86–87 °C, R_f^3 0.95, R_f^4 0.86, $[\alpha]_D^{24}$ -23.0° ($c=1.0$, MeOH). *Anal.* Calcd for $C_{27}H_{36}N_2O_5$: C, 69.2; H, 7.7; N, 6.0. Found: C, 69.0; H, 7.7; N, 5.9. Amino acid ratio in an acid hydrolysate: Phe 1.00, Leu 1.06 (recovery of Phe, 86%).

Boc-Phe-Leu-OBzl was also prepared from Boc-Phe-OH (2 g 7.5 mm) and H-Leu-OBzl tosylate (2.68 g, 6.8 mm) in DMF by the mixed anhydride method in the usual manner.¹¹ Yield 2.36 g (74%), mp 87–88 °C, R_f^3 0.86, $[\alpha]_D^{27}$ -25.7° ($c=1.0$, MeOH). Amino acid ratios in an acid hydrolysate: Ala 1.00, Leu 0.99 (recovery of Ala, 89%).

Z(OMe)-Gly-Phe-Leu-OBzl—Z(OMe)-Gly-OPS (Cl, K) (1 g, 2 mm) was reacted with H-Phe-Leu-OBzl [prepared from 852 mg of Boc-Phe-Leu-OBzl (1.8 mm) by trifluoroacetic acid (TFA) treatment followed by Et₃N treatment] according to the general procedure. Recrystallized from AcOEt-petroleum ether. Yield 787 mg (71%), mp 136–137 °C, R_f^3 0.93, R_f^4 0.76, $[\alpha]_D^{28}$ -10.3° ($c=1.0$, MeOH). *Anal.* Calcd for $C_{33}H_{39}N_3O_7$: C, 67.2; H, 6.7; N, 7.1. Found: C, 67.1; H, 6.7; N, 6.8. Amino acid ratios in an acid hydrolysate: Gly 1.00, Phe 1.02 (recovery of Gly, 88%).

Z(OMe)-Gly-Phe-Leu-OBzl was also prepared by the OPS (Br, Na) method and the OPS (NO₂, Na) method. The yields were 69% by the OPS (Br, Na) method and 79% by the OPS (NO₂, Na) method. The products were identical with those prepared by the OPS (Cl, K) method and the mixed anhydride method.³¹

Z(OMe)-Gly-Gly-Phe-Leu-OBzl—Z(OMe)-Gly-OPS (Cl, K) (603 mg, 1.2 mm) was reacted with H-Gly-Phe-Leu-OBzl [prepared from 590 mg of Z(OMe)-Gly-Phe-Leu-OBzl (1 mm) by TFA treatment followed by Et₃N treatment] according to the general procedure. Recrystallized from a mixture of AcOEt and petroleum ether. Yield 445 mg (69%), mp 147–150 °C, R_f^3 0.69, $[\alpha]_D^{28}$ -15.8° ($c=1.0$, MeOH). *Anal.* Calcd for $C_{35}H_{42}N_4O_8$: C, 65.0; H, 6.6;

N, 8.7. Found: C, 64.9; H, 6.5; N, 8.5. Amino acid ratios in an acid hydrolysate: Gly 2.00, Phe 0.99, Leu 1.03 (recovery of Gly, 84%).

Z-Tyr(Bzl)-Gly-Gly-Phe-Leu-OBzl—Z-Tyr (Bzl)-OPS (Cl, K) (620 mg, 0.93 mm) and H-Gly-Gly-Phe-Leu-OBzl [prepared from 500 mg of Z(OMe)-Gly-Phe-Leu-OBzl (0.77 mm) by TFA treatment followed by Et₃N treatment] were reacted in DMF (8 ml) at 30 °C for 48 h. The solvent was evaporated off and the residue was washed successively with 5% Na₂CO₃, 5% citric acid and H₂O. The material was purified by Sephadex LH 20 column (2.5 × 80 cm) chromatography using a mixture of MeOH and dioxane (1 : 1) as the eluent. Yield 424 mg (63%), mp 146—150 °C, *R*_f³ 0.91, [α]_D²⁵ -24.2° (*c* = 1.0, DMF). *Anal.* Calcd for C₅₀H₅₅N₅O₉: C, 69.0; H, 6.4; N, 7.9. Found: C, 69.0; H, 6.3; N, 7.9. Amino acid ratios in an acid hydrolysate: Tyr 0.86, Gly 2.00, Phe 0.96, Leu 1.02 (recovery of Gly, 88%).

H-Tyr-Gly-Gly-Phe-Leu-OH—Prepared from its protected derivative (435 mg) by catalytic hydrogenation as described in the preceding paper.³⁾ Yield 220 mg (79%), mp 201—205 °C, *R*_f¹ 0.76, [α]_D²⁰ -24.9° (*c* = 1.0, DMF). *Anal.* Calcd for C₂₈H₃₇N₅O₇: C, 60.5; H, 6.7; N, 12.6. Found: C, 60.2; H, 6.8; N, 12.2. Amino acid ratios in an acid hydrolysate: Tyr 0.81, Gly 2.00, Phe 1.04, Leu 1.06 (recovery of Gly, 88%). [lit.³⁾; mp 202—206 °C, [α]_D²² -23.4° (*c* = 1.0, DMF)].

Preparation of Z-Ala-Gly-OMe by the Phenolsulfonic Acid Derivative Ester Methods in H₂O—Z-Ala phenolsulfonic acid derivative ester (2.1 mm) was added to a solution of H-Gly-OMe (2.1 mm, prepared from its HCl salt by addition of Et₃N) in H₂O (5 ml). Precipitation of the product occurred immediately and the mixture was stirred over night. The product was extracted from the mixture with AcOEt and the AcOEt layer was washed successively with 5% citric acid, 5% Na₂CO₃ and H₂O, and dried over Na₂SO₄. The solvent was evaporated off and the residue was recrystallized from a mixture of AcOEt and petroleum ether.

a) OPS (Cl, K) Method: Yield 73%, mp 98—100 °C, [α]_D²⁹ -23.5° (*c* = 1.0, MeOH), *R*_f⁴ 0.49. Amino acid ratio in an acid hydrolysate, Ala 1.03, Gly 1.00 (recovery of Gly, 86%). *Anal.* Calcd for C₁₄H₁₈N₂O₅: C, 57.1; H, 6.2; N, 9.5. Found: C, 57.0; H, 6.2; N, 9.6.

b) OPS (Br, Na) Method: Yield 65%, mp 98—100 °C, [α]_D²⁷ -27.0° (*c* = 1.0, MeOH), *R*_f⁴ 0.49. Amino acid ratios in an acid hydrolysate, Ala 0.98, Gly 1.00 (recovery of Gly, 91%).

c) OPS (NO₂, Na) Method: Yield 79%, mp 98—101 °C, [α]_D²⁸ -27.8° (*c* = 1.0, MeOH), *R*_f⁴ 0.49. Amino acid ratio in an acid hydrolysate, Ala 1.04, Gly 1.00 (recovery of Gly, 88%). (lit.¹²⁾ Z-Ala-Gly-OMe: mp 98—99 °C, [α]_D¹⁵ -25.1° (*c* = 5, MeOH)].

References and Notes

- 1) Standard abbreviations are used for amino acids, protecting groups, and peptides [*Eur. J. Biochem.*, **138**, 9 (1984)].
- 2) J. C. Sheehan, P. A. Cruickshank, and G. L. Boshart, *J. Org. Chem.*, **26**, 2525 (1956).
- 3) T. Tsuji, S. Okusada, M. Maeda, and K. Kawasaki, *Chem. Pharm. Bull.*, **34**, 2214 (1986).
- 4) L. Aldwin and E. Nitecki, "Peptides. Structure and Function," Proceedings of the 9th American Peptide Symposium, ed. by C. M. Deber, V. J. Hruby, and K. D. Kopple, Pierce Chemical Comp., Rockford, Illinois, 1985, pp. 31—33.
- 5) H. Kolbe and F. Gauhe, *Ann. Chem. Pharm.*, **147**, 71 (1867).
- 6) H. E. Armstrong and F. D. Brown, *J. Chem. Soc.*, **25**, 857 (1872).
- 7) R. King, *J. Chem. Soc.*, **119**, 2105 (1921).
- 8) J. C. Sheehan and G. P. Hess, *J. Am. Chem. Soc.*, **77**, 1067 (1955).
- 9) B. Weinstein and A. E. Pritchard, *J. Chem. Soc., Perkin Trans. 1*, **1972**, 1015.
- 10) E. Schröder, *Justus Liebigs Ann. Chem.*, **679**, 207 (1964).
- 11) J. R. Vaughan, Jr. and R. L. Osato, *J. Am. Chem. Soc.*, **74**, 676 (1952).
- 12) L. Zervas, D. Borovas, and E. Gazis, *J. Am. Chem. Soc.*, **85**, 3660 (1963).

[Chem. Pharm. Bull.]
35(3)1049—1057(1987)

Reaction of Aromatic *N*-Oxides with Dipolarophiles.¹⁾ XII. Stereoselective *exo* Cycloaddition of 3,5-Lutidine *N*-Oxide with *N*-Substituted Maleimides and a Frontier Molecular Orbital and Mechanistic Study

TAKUZO HISANO,* KAZUNOBU HARANO, TOSHIKAZU MATSUOKA,
HIROTOSHI YAMADA and MASAHIKO KURIHARA

*Faculty of Pharmaceutical Sciences, Kumamoto University,
5-1 Oe-honmachi, Kumamoto 862, Japan*

(Received September 9, 1986)

Pericyclic reactions of 3,5-lutidine *N*-oxide with *N*-phenylmaleimides were investigated. The primary cycloadducts are thermally labile and undergo 1,5-sigmatropic rearrangement to give the 2,3-dihydropyridine derivatives. The proton nuclear magnetic resonance structural assignment of the 1,5-sigmatropy products implies that the primary cycloaddition proceeds through an *exo* transition state. The reaction behavior is discussed in terms of frontier molecular orbital theory, based on MINDO/3 and CNDO/2 calculations and kinetic data. It was concluded that the reaction falls into the category of a 'normal-type' cycloaddition and the *exo* cycloaddition is brought about by the unfavorable secondary orbital interaction.

Keywords—1,3-dipolar cycloaddition; 3,5-lutidine *N*-oxide; *N*-phenylmaleimide; kinetics; frontier molecular orbital; *exo* cycloaddition; 1,5-sigmatropy; substituent effect

Introduction

1,3-Dipolar cycloaddition is a valuable tool for the construction of five-membered heterocyclic ring systems.²⁾ The classical approach to the reaction was revised by Sustmann³⁾ and Houk⁴⁾ from the frontier molecular orbital (FMO) theoretical point of view.⁵⁾ In our continuing studies on the 1,3-dipolar cycloaddition reaction of aromatic *N*-oxides with dipolarophiles,⁶⁾ we have examined the cycloaddition of pyridine *N*-oxides with phenyl isocyanates and showed that the observed cycloaddition behavior can be rationalized in terms of the following controlling factors: (1) highest occupied molecular orbital (HOMO)–lowest unoccupied molecular orbital (LUMO) interaction, (2) secondary orbital interaction, (3) aromaticity, (4) charge-transfer (CT) complexation. From the frontier molecular orbital viewpoint based on the CNDO/2,⁷⁾ MINDO/2,⁸⁾ and MINDO/3⁹⁾ calculation data, we have sought a new and more reactive synthon applicable to the 1,3-dipolar cycloaddition of aromatic *N*-oxides. In this connection, we previously communicated the reaction of *N*-phenylmaleimides (II) with 3,5-dimethylpyridine *N*-oxide (3,5-lutidine *N*-oxide) (I) to afford 2,3-dihydropyridine-type cycloadducts (III) arising from 1,5-sigmatropy of the primary *exo* cycloadducts.¹⁰⁾

We now discuss the reaction in detail with newly obtained data in order to clarify the overall nature of the reaction.

Results and Discussion

The CNDO/2 method has been used with success to predict the cycloaddition reactivity

TABLE I. FMO Energy Levels^{a)} of the Addends (I and IIa–k)

Compd.	MINDO/3		CNDO/2	
	HOMO	LUMO	HOMO	LUMO
Pyridine <i>N</i> -oxide	-8.762	0.546	-10.549	2.246
Lutidine <i>N</i> -oxide (I)	-8.662	0.596	-10.420	2.396
<i>N</i> -Substituted maleimides				
H	-10.485	-0.470		
<i>p</i> -MeOC ₆ H ₄ - (IIb)			-13.416	0.882
<i>p</i> -MeC ₆ H ₄ - (IIe)			-13.614	0.873
Ph- (IIa)			-13.861	0.837
<i>p</i> -ClC ₆ H ₄ - (IIh)			-13.563	0.634
<i>p</i> -NO ₂ C ₆ H ₄ - (IIk)			-13.245	0.448
PhN=C=O	-8.552	0.915		

a) eV.

of various types of 1,3-dipoles and dipolarophiles. In this study, therefore, CNDO/2 calculations were performed to estimate the relative reactivity of pyridine *N*-oxides with *N*-substituted maleimides. The molecular geometries of the parent molecules of pyridine *N*-oxide and maleimide were determined by a semiempirical self-consistent field molecular orbital method based on the MINDO/3 approximation combined with geometrical optimization by the Fletcher–Powell method.⁹⁾ The resulting geometries were then used for the CNDO/2 calculations of substituted molecules. The optimized geometry and dipole moment of pyridine *N*-oxide are in agreement with the observed values determined by X-ray crystallographic analyses.¹¹⁾ The calculation data are summarized in Table I.

As can be seen in Table I, the 1,3-dipolar reaction of 3,5-lutidine *N*-oxide (I) with *N*-substituted maleimides (II) falls into the category of a normal-type reaction in Sustmann's classification,³⁾ wherein the dominant interaction occurs between the HOMO of I and the LUMO of II, indicating that a dipolarophile bearing an electron-accepting substituent would show a high reactivity toward 3,5-lutidine *N*-oxide (I).

In the reaction of pyridine *N*-oxides with phenyl isocyanates previously reported from our laboratory, we could not establish the stereochemistry of the cycloaddition transition state from the structure of the reaction products, because the dipolarophiles have a linear

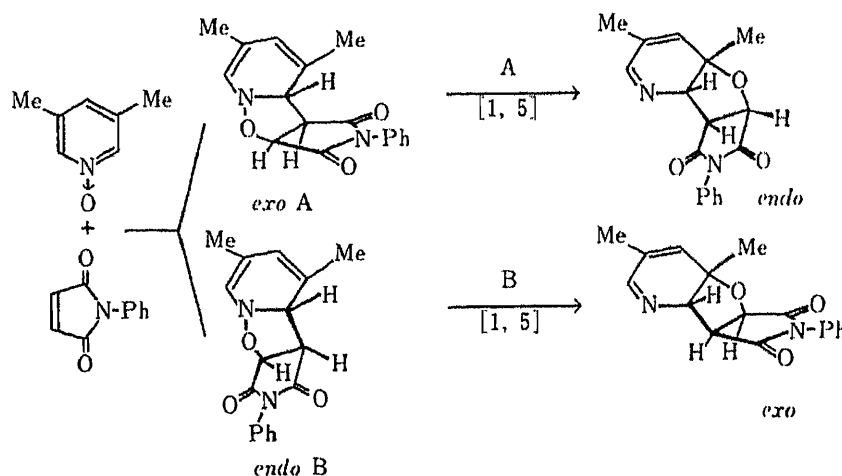


Chart 1

TABLE IIa. Cycloadducts from the 1,3-Dipolar Reaction of 3,5-Dimethylpyridine *N*-Oxide with *N*-Substituted Maleimides^{a)}

Adduct ^{b)}	R	mp (°C)	Yield (%)	IR (cm ⁻¹) ^{c)} C=O
IIIa	C ₆ H ₅ -	172.5—173.5	40.2	1715
IIIb	<i>p</i> -MeOC ₆ H ₄ -	187—188	36.5	1700
IIIc	<i>o</i> -MeC ₆ H ₄ -	185—186	56.2	1710—1715
III d	<i>m</i> -MeC ₆ H ₄ -	179—180	40.2	1715
IIIe	<i>p</i> -MeC ₆ H ₄ -	187—188	38.7	1715
III f	<i>o</i> -ClC ₆ H ₄ -	162—163	42.8	1715—1720
III g	<i>m</i> -ClC ₆ H ₄ -	175	40.5	1710
III h	<i>p</i> -ClC ₆ H ₄ -	209	25.2	1710
III i	<i>o</i> -NO ₂ C ₆ H ₄ -	207—208	46.3	1730—1735
III j	<i>m</i> -NO ₂ C ₆ H ₄ -	231—232	44.9	1720
III k	<i>p</i> -NO ₂ C ₆ H ₄ -	186—187	34.7	1715—1720
III l	<i>n</i> -C ₄ H ₉ -	119—120	37.5	1710
III m	CH ₃ -	184—185	32.8	1682
III n	α -Naphthyl	231—232	30.0	1715—1720

a) Refluxed for 10h. b) Colorless needles. c) KBr.

TABLE IIb. Analytical and Mass Spectral Data for the Cycloadducts (IIIa—n)

Compd.	Formula	Anal. Calcd (Found)			MS <i>m/z</i> (M ⁺)
		C	H	N	
IIIa	C ₁₇ H ₁₆ N ₂ O ₃	68.91 (68.80)	5.44 (5.51)	9.45 (9.40)	296
IIIb	C ₁₈ H ₁₈ N ₂ O ₄	66.25 (65.98)	5.56 (5.46)	8.56 (8.66)	326
IIIc	C ₁₈ H ₁₈ N ₂ O ₃	69.67 (69.33)	5.80 (5.84)	9.00 (8.98)	310
III d	C ₁₈ H ₁₈ N ₂ O ₃	69.67 (69.76)	5.80 (5.90)	9.00 (9.07)	310
IIIe	C ₁₈ H ₁₈ N ₂ O ₃	69.67 (69.75)	5.80 (6.11)	9.00 (9.13)	310
III f	C ₁₇ H ₁₅ ClN ₂ O ₃	61.72 (61.83)	4.54 (4.53)	8.47 (8.45)	330
III g	C ₁₇ H ₁₅ ClN ₂ O ₃	61.72 (61.59)	4.54 (4.47)	8.47 (8.93)	330
III h	C ₁₇ H ₁₅ ClN ₂ O ₃	61.72 (62.03)	4.54 (4.77)	8.47 (8.57)	330
III i	C ₁₇ H ₁₅ N ₃ O ₅	59.82 (59.98)	4.43 (4.61)	12.31 (12.34)	341
III j	C ₁₇ H ₁₅ N ₃ O ₅	59.82 (59.85)	4.43 (4.58)	12.31 (12.35)	341
III k	C ₁₇ H ₂₅ N ₃ O ₅	59.82 (60.21)	4.43 (4.51)	12.31 (12.32)	341
III l	C ₁₅ H ₂₀ N ₂ O ₃	65.20 (65.44)	7.29 (7.36)	10.14 (10.23)	276
III m	C ₁₂ H ₁₄ N ₂ O ₃	61.53 (61.13)	6.02 (5.98)	11.96 (12.11)	234
III n	C ₂₁ H ₁₈ N ₂ O ₃	72.83 (72.96)	5.20 (5.43)	8.09 (8.14)	346

structure and both the transition states (*exo* and *endo* addition) give the same product. On the other hand, in the reaction of pyridine *N*-oxides with substituted maleimides (II), it may be possible to discuss the stereochemistry of the transition state because of the rigid ring structures of both addends.

Refluxing a mixture of 3,5-lutidine *N*-oxide (I) and a slight excess of the *N*-substituted maleimides (IIa—n) in toluene for 10 h resulted in the formation of crystalline products (IIIa—n, respectively). The spectral data, physical constants and elemental analyses of the cycloadducts (IIIa—n) are summarized in Tables IIa—c.

The infrared (IR) spectra of III showed characteristic bands at 1690—1720 cm⁻¹, suggesting the presence of an unconjugated imido carbonyl group. The mass spectra (MS) of III exhibited molecular peaks corresponding to the 1 : 1 cycloadducts. Four *sp*³ carbons were

TABLE IIc. $^1\text{H-NMR}$ Spectral Data for the Cycloadducts (IIIa—n)

$^1\text{H-NMR}$ (in CDCl_3) ppm	
IIIa	1.33 (3H, s, C_{7a} -Me), 1.88 (3H, d, $J=2$ Hz, C_6 -Me), 4.01 (1H, t, $J=8$ Hz, C_3 -H), 4.35 (1H, dd, $J=8$, 2 Hz, C_{3a} -H), 4.86 (1H, d, $J=8$ Hz, C_2 -H), 5.88 (1H, t, $J=2$ Hz, C_7 -H), 6.93—7.66 (5H, m, -Ar), 7.80 (1H, t, $J=2$ Hz, C_5 -H)
IIIb	1.31 (3H, s, C_{7a} -Me), 1.84 (3H, d, $J=1.5$ Hz, C_6 -Me), 3.82 (1H, s, -OMe), 4.05 (1H, dd, $J=9.6$, 7.2 Hz, C_3 -H), 4.37 (1H, dd, $J=9.6$, 1.5 Hz, C_{3a} -H), 4.91 (1H, d, $J=7.2$ Hz, C_2 -H), 5.91 (1H, t, $J=1.5$ Hz, C_7 -H), 6.83—7.22 (4H, m, -Ar), 7.83 (1H, t, $J=1.5$ Hz, C_5 -H)
IIIc	1.38 (3H, s, C_{7a} -Me), 1.95 (3H, d, $J=1.8$ Hz, C_6 -Me), 2.14 and 2.21 (3H, s, -Ar-Me), ^{a)} 3.99—4.50 (2H, m, C_3 -H, C_{3a} -H), 4.87—5.06 (1H, m, C_2 -H), 6.02 (1H, m, C_7 -H), 6.97—7.35 (4H, m, -Ar), 7.85—8.98 (1H, m, C_5 -H)
III d	1.37 (3H, s, C_{7a} -Me), 1.90 (3H, d, $J=1.8$ Hz, C_6 -Me), 2.39 (3H, s, -Ar-Me), 4.09 (1H, dd, $J=9.6$, 7.6 Hz, C_3 -H), 4.42 (1H, dd, $J=9.6$, 2.4 Hz, C_{3a} -H), 4.95 (1H, d, $J=7.6$ Hz, C_2 -H), 5.96 (1H, dd, $J=2.4$, 1.8 Hz, C_7 -H), 6.95—7.39 (4H, m, Ar), 7.87 (1H, t, $J=2.4$ Hz, C_5 -H)
IIIe	1.31 (3H, s, C_{7a} -Me), 1.83 (3H, d, $J=2$ Hz, C_6 -Me), 2.35 (3H, s, -Ar-Me), 4.02 (1H, dd, $J=9$, 8 Hz, C_3 -H), 4.35 (1H, dd, $J=9$, 2 Hz, C_{3a} -H), 4.88 (1H, d, $J=8$ Hz, C_2 -H), 5.88 (1H, t, $J=2$ Hz, C_7 -H), 6.90—7.35 (4H, m, Ar), 7.79 (1H, t, $J=2$ Hz, C_5 -H) ^{b)}
III f	1.38 (3H, s, C_{7a} -Me), 1.96 (3H, d, $J=1.8$ Hz, C_6 -Me), 4.04—4.48 (2H, m, C_3 -H and C_{3a} -H), 4.86—5.11 (1H, m, C_2 -H), 5.97 (1H, m, C_7 -H), 7.08—7.56 (4H, m, -Ar), 7.85—7.93 (1H, m, C_5 -H)
III g	1.34 (3H, s, C_{7a} -Me), 1.87 (3H, d, $J=1.5$ Hz, C_6 -Me), 4.09 (1H, dd, $J=8.9$, 7.5 Hz, C_3 -H), 4.38 (1H, dd, $J=8.9$, 1.5 Hz, C_{3a} -H), 4.94 (1H, d, $J=7.5$ Hz, C_2 -H), 5.94 (1H, t, $J=1.5$ Hz, C_7 -H), 7.10—7.45 (4H, m, -Ar), 7.81 (1H, t, $J=1.5$ Hz, C_5 -H)
III h	1.35 (3H, s, C_{7a} -Me), 1.82 (3H, d, $J=2$ Hz, C_6 -Me), 4.03 (1H, dd, $J=9$, 7 Hz, C_3 -H), 4.33 (1H, dd, $J=9$, 2 Hz, C_{3a} -H), 4.89 (1H, d, $J=7$ Hz, C_2 -H), 5.88 (1H, t, $J=2$ Hz, C_7 -H), 7.10—7.60 (4H, m, -Ar), 7.80 (1H, t, $J=2$ Hz, C_5 -H)
III i	1.35 (3H, s, C_{7a} -Me), 1.91 (3H, d, $J=1.2$ Hz, C_6 -Me), 4.01—4.50 (2H, m, C_3 -H and C_{3a} -H), 4.95—5.10 (1H, m, C_2 -H), 5.98 (1H, m, C_7 -H), 7.25—8.27 (5H, m, -Ar and C_5 -H)
III j	1.39 (3H, s, C_{7a} -Me), 1.93 (3H, d, $J=1$ Hz, C_6 -Me), 4.17 (1H, dd, $J=9$, 7.2 Hz, C_3 -H), 4.43 (1H, dd, $J=9$, 2 Hz, C_{3a} -H), 5.03 (1H, d, $J=7.2$ Hz, C_2 -H), 5.99 (1H, dd, $J=2$, 1 Hz, C_7 -H), 7.05—8.40 (4H, m, -Ar), 7.88 (1H, t, $J=2$ Hz, C_5 -H)
III k	1.36 (3H, s, C_{7a} -Me), 1.87 (3H, d, $J=2$ Hz, C_6 -Me), 4.16 (1H, dd, $J=8.8$, 7.2 Hz, C_3 -H), 4.40 (1H, dd, $J=8.8$, 2 Hz, C_{3a} -H), 4.99 (1H, d, $J=7.2$ Hz, C_2 -H), 5.96 (1H, t, $J=2$ Hz, C_7 -H), 7.40—8.43 (4H, m, -Ar), 7.82 (1H, t, $J=2$ Hz, C_5 -H)
III l	0.95 (3H, t, $J=6.6$ Hz, aliphatic Me), 1.35 (3H, s, C_{7a} -Me), 1.10—1.70 (4H, m, - CH_2CH_2 -), 1.90 (3H, d, $J=2$ Hz, C_6 -Me), 3.46 (2H, t, $J=7.2$ Hz, N-CH_2 -), 3.99 (1H, dd, $J=8.4$, 7.2 Hz, C_3 -H), 4.34 (1H, dd, $J=8.4$, 2 Hz, C_{3a} -H), 4.82 (1H, d, $J=7.2$ Hz, C_2 -H), 5.89 (1H, t, $J=2$ Hz, C_7 -H), 7.79 (1H, t, $J=2$ Hz, C_5 -H)
III m	1.47 (3H, s, Me), 2.02 (3H, d, $J=1.2$ Hz, Me), 3.09 (3H, s, N-Me), 4.13 (1H, dd, $J=9.6$, 7.2 Hz, C_3 -H), 4.46 (1H, dd, $J=9.6$, 2.4 Hz, C_{3a} -H), 4.97 (1H, d, $J=7.2$ Hz, C_2 -H), 6.02 (1H, dd, $J=2.4$, 1.2 Hz, C_7 -H), 7.94 (1H, t, $J=2.4$ Hz, C_5 -H)
III n	1.39 (3H, s, Me), 1.96 (3H, brs, Me), 4.0—4.6 (2H, m, C_3 and C_{3a} -H), 4.85—5.30 (1H, m, C_2 -H), 6.04 (1H, dd, $J=1.5$ Hz, C_7 -H), 7.1—8.2 (8H, m, Ar and C_5 -H) ^{c)}

a) The methyl group of $\alpha\text{-Me-C}_6\text{H}_4$ - was observed as a split peak. This may result from restricted rotation about the N-Ar bond. b) The high-resolution $^1\text{H-NMR}$ (400 MHz) spectrum indicates that the C_7 proton is coupled with the C_6 -methyl proton ($J=1.46$ Hz) and with the C_5 proton ($J=2.2$ Hz), which is again coupled with the C_{3a} proton ($J=2.2$ Hz). c) The data can be interpreted in terms of a 1:1 mixture of conformational isomers.

observed in the carbon-13 nuclear magnetic resonance ($^{13}\text{C-NMR}$) spectrum of III,¹²⁾ suggesting that the product (III) is not the primary adduct (three sp^3 carbons) but the rearranged product (see Chart 1). Further, the proton nuclear magnetic resonance ($^1\text{H-NMR}$) spectra of III exhibited ABX patterns due to three *cis*-oriented methine protons ($J_{2,3}=7$ —8 Hz, $J_{3,3a}=8$ —9 Hz).¹³⁾

The $^1\text{H-NMR}$ spectra of the products exhibited essentially the same spectral patterns attributable to an ABX spin system. The coupling constants were evaluated by first-order analysis assuming it to be an AMX system. In the case of the cycloadduct from 1 and *N*-(α -

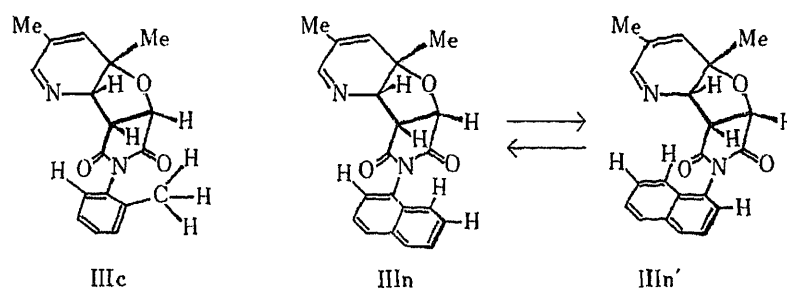


Chart 2

TABLE III. Solvent Effect and Activation Parameters for 1,3-Dipolar Reaction of I with IIa in Bromobenzene

Temp. (°C)	Solvent (E_T) ^{a)}	$k \times 10^6$ ($M^{-1} \cdot s^{-1}$)	ΔE (kcal/mol)	ΔS^\ddagger (e.u.)
100	Toluene	(33.9)	1.95	
100	Bromobenzene	(37.5)	3.07	
100	Acetophenone	(41.3)	2.96	
100	Sulfolane	(44.0)	2.93	
110	Bromobenzene		4.96	
120	Bromobenzene		11.0	20.0
130	Bromobenzene		21.4	-35

a) See ref. 16.

TABLE IV. Activation Parameters for Typical 1,3-Dipolar Cycloaddition Reactions

Reaction ^{a)}	ΔE (kcal/mol)	ΔS^\ddagger (e.u.)
3,5-Lutidine <i>N</i> -oxide + <i>N</i> -phenylmaleimide ^{b)}	20.0	-35
Pyridine <i>N</i> -oxide + phenyl isocyanate ^{c)}	20.0	-30
<i>C,C</i> -Biphenylene- <i>N</i> (α)-(p-chlorophenyl)- <i>N</i> (β)-cyanoazomethine imine +		
ethyl acrylate	12.5	-35
styrene	15.6	-31
phenyl isocyanate	12.1	-33
<i>N</i> -Phenyl- <i>C</i> -methylsydnone +		
ethyl cinnamate	18.3	-32
dimethyl acetylenedicarboxylate	14.7	-31
<i>C'</i> -Phenyl- <i>N</i> -methylnitron +		
methyl methacrylate	15.7	-32
2-vinylpyridine	18.3	-30

a) See ref. 2a. b) This study. c) See ref. 5a.

tolyl) maleimide or *N*-naphthylmaleimide, a distorted ABX pattern was observed. This may be caused by restricted rotation about the N-Ar bond, which can be recognized by the presence of a temperature effect (Chart 2).

From these data, we can safely say that IIIa—n are *endo* 2,3-dihydropyridine-type cycloadducts formed from the primary *exo*[4 + 2] π cycloadducts by 1,5-sigmatropic rearrangement (Chart 1).

In order to examine the cycloaddition behavior of 3,5-lutidine *N*-oxide (I) towards *N*-substituted maleimides (II), kinetic measurements¹⁴⁾ were carried out. The second-order rate

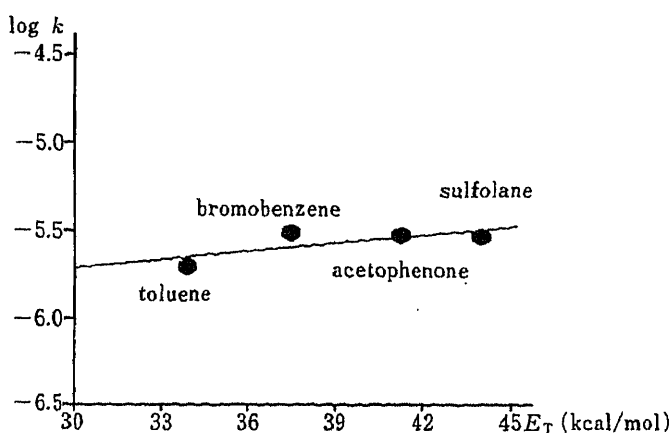


Fig. 1. Plots of k vs. E_T Values for the Reaction of I with IIa
 $\alpha=0.016$.

TABLE V. Substituent Effect in 1,3-Dipolar Cycloaddition of I with II

<i>p</i> -Substituent	σ_p^+	$k \times 10^6$ ($M^{-1} \cdot s^{-1}$)
OMe	-0.12	9.65
Me	-0.311	10.3
H	0.0	10.9
Cl	0.114	8.88
NO ₂	0.790	13.1

The correlation coefficient (r) excluding Cl is 0.992. Slope (ρ)=0.0859.

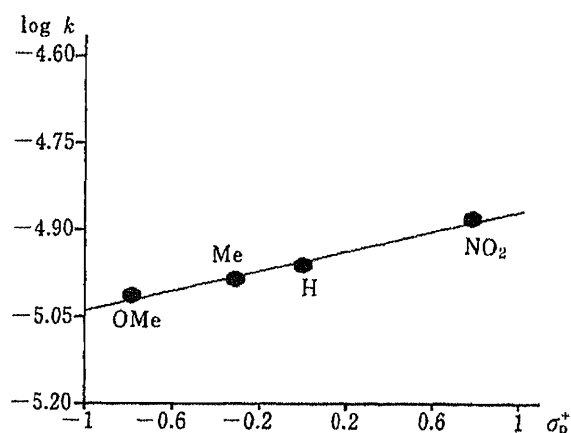


Fig. 2. Plots of k vs. σ_p^+ for the Reaction of I with II
 $\rho=0.086$.

constants of the reaction of I with IIa in several solvents at various temperatures were obtained by following the disappearance of I by high-performance liquid phase chromatography (HPLC) using methyl *o*- or *p*-nitrobenzoate as an internal standard.

The energy of activation (ΔE) for the reaction of I with IIa is 20 kcal/mol,¹⁵⁾ moderately higher than the average for 1,3-dipolar reactions, while the entropy of activation, $\Delta S^\ddagger = -35$ e.u., lying within the range reported for the typical 1,3-dipolar cycloaddition, suggests a highly ordered transition state.^{2a)}

Next, the solvent effect was investigated. As a scale of solvent ionizing power for clarification of the degree of charge separation in the transition state, the E_T values of Reichardt¹⁶⁾ have been successfully employed in studying the effect of solvent on the rate of reaction. As illustrated in Fig. 1, plots of $\log k$ against E_T values show a linear relationship with a very small slope (only 1.56×10^{-2}), comparable to those of typical concerted reactions.^{6a,17)} The small response to variation of solvent ionizing power rules out an intermediate involving any significant degree of charge separation.

The substituent effect of the *N*-phenylmaleimides (II) on the reaction rates were also examined by plotting the logarithm of $\log k(x)$ against σ_p^+ .¹⁸⁾ The plots show a linear correlation. The magnitude of the slope, the ρ -value, is assumed to be an indication of the narrowness of the HOMO-LUMO energy gap. The ρ -value is very small (1.20×10^{-1}), indicating that the FMO energy separation is relatively large, and the positive value indicates that the reaction falls into the category of normal-type cycloaddition. The results hitherto

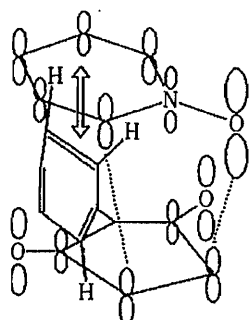


Fig. 3. Steric Interactions for the *endo* Cyclo-addition

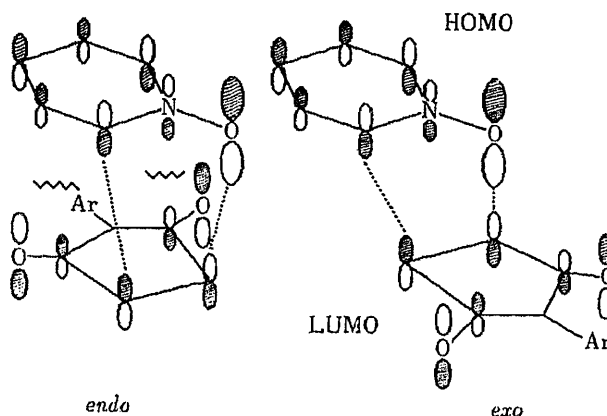


Fig. 4. Frontier Orbitals and Secondary Interactions for the Cycloaddition of I with II

TABLE VI. Frontier Orbital Energies and Coefficients for 3,5-Lutidine *N*-Oxide and Protonated 3,5-Lutidine *N*-Oxide Calculated by the MINDO/3 Method

	ArN→O	ArN→O···H ⁺ ^{a)}
FMO energy level (eV)		
LUMO	0.60	-4.11
HOMO	-8.66	-13.73
HOMO coefficient		
O	-0.590	-0.430
N	0.298	0.428
C ₂	0.363	0.156
Net charge		
O	-0.639	-0.446
N	0.723	0.596
C ₂	-0.201	0.123

^{a)} The donor-acceptor hydrogen-bond distance (NH···O) is assumed to be 2.0 Å.

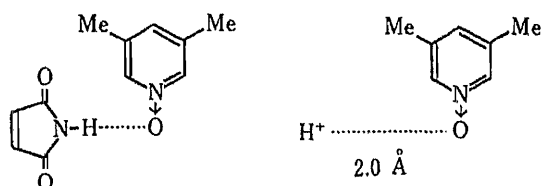


Fig. 5. Hydrogen Bonding between I and II

mentioned are fully in accordance with the concerted reaction behavior.

At first glance, it seems reasonable to attribute the *exo* addition to steric repulsion between the pyridine moiety of the 1,3-dipole and the *N*-aryl group of the dipolarophile, in which the *N*-aryl ring and the imide ring can not be coplanar (they lie in a nearly perpendicular disposition) (Fig. 3). However, this assumption is not acceptable because the dipolarophile bearing the *N*-methyl or *N*-(*n*-butyl) substituent shows a similar cycloaddition behavior to give the *endo* 1,5-sigmatropy product *via* *exo* cycloaddition. These facts indicate that electronic factors may be operative in stabilization of the transition state.

The frontier orbital interactions for *exo* and *endo* transition states are depicted in Fig. 4. As can be seen in Fig. 4, the secondary interactions of the frontier orbitals in the *endo*-transition state are antibonding, indicating that the reaction passing through the *exo*-transition state is more favorable than that passing through the *endo* one.

Interestingly, the parent maleimide did not react with 3,5-lutidine *N*-oxide (I) under the conditions used in the case of *N*-phenyl maleimide (IIa). This anomaly may be explained by taking into consideration the stabilization by the hydrogen bonding between the oxygen atom of I and the acidic hydrogen (-CONHCO-) of the imido group. The hydrogen bonding should

cause a considerable decrease of the FMO energies of I and retardation of the reactivity. This assumption was confirmed by MINDO/3 calculations on a pair of model compounds (I and protonated 3,5-lutidine *N*-oxide). The calculations indicate that the hydrogen bonding stabilizes the frontier orbital energies and diminishes the frontier coefficient magnitudes and the net charges of the nitron moiety, and these changes are very unfavorable for the normal-type interaction (HOMO of I-LUMO of II) (see Table VI).

The involvement of charge-transfer complexes in cycloaddition has been suggested, and it has been proposed that charge transfer plays an important role in stabilizing the transition state.¹⁹⁾ In our previous paper,^{6c)} we clarified the influence of charge transfer on the site selectivity and the reactivity for 1,3-dipolar cycloaddition of 3-methylpyridine (picoline) *N*-oxide with phenyl isocyanates. In the reaction studied here, the reaction mixture of I and IIa (110 °C) showed a weak absorption beyond 550 nm (tailing), which is characteristic of a charge-transfer interaction. This finding suggests that charge-transfer complexation occurs only to a small extent, and this must be a consequence of the steric disadvantage¹⁹⁾ of nonplanar *N*-phenylmaleimide, in which the phenyl and the imido rings can not be coplanar.

Finally, mention should be made of 1,5-sigmatropy of the primary cycloadducts. MINDO/3 calculations on model cycloadducts of pyridine *N*-oxide with ethylene indicate that the heat of formation (ΔH_f) of the 1,5-sigmatropy product is 26.7 kcal/mol smaller than that of the primary one, suggesting the primary adduct to be thermodynamically less stable. The FMO view on the facility of the rearrangement is that the interaction of the LUMO of the σ bond with the HOMO of the diene is assisted by the low-lying LUMO of the N-O σ bond.

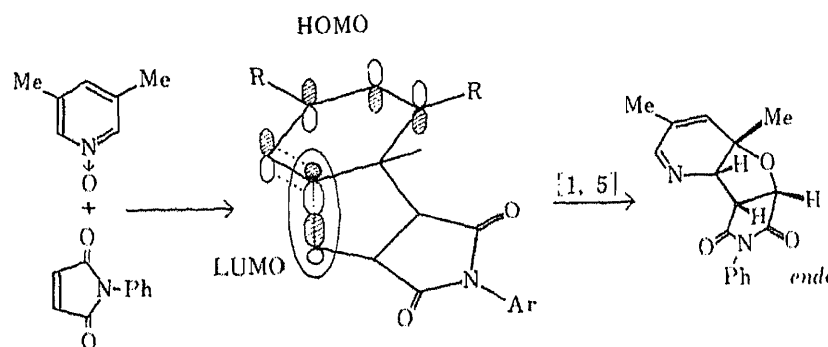


Chart 3

Experimental

All melting points are uncorrected. Nuclear magnetic resonance spectra were taken with Hitachi R-600, JNM-C-60H and GX-400 spectrometers (¹³C-NMR) for *ca.* 10% (w/v) solution with tetramethylsilane (TMS) as an internal standard; chemical shifts are expressed in δ values. IR spectra were recorded on a JASCO IR-G infrared spectrophotometer equipped with a grating. Mass spectra were taken with a JEOL JMS-O1SG double-focussing spectrometer operating at an ionization potential of 75 eV. High performance liquid chromatographic analyses (HPLC) were performed on a JASCO FAMILIC 100N chromatograph equipped with a ultraviolet detector and a column of Fine Pak SIL C12.

Molecular orbital calculations were performed on a FACOM M-382 computer in the Computer Center of Kyushu University.

Cycloaddition of I with IIa (General Procedure)—A solution of I (0.01 mol) and IIa (0.01 mol) in toluene (10 ml) was refluxed for 10 h. The solvent was evaporated off under reduced pressure. The residue was chromatographed on silica gel (2.5 cm i.d. column, 60 g) with ethyl acetate to give IIIa as colorless needles. Recrystallization from ethyl acetate gave an analytically pure sample. The physical and spectral data are summarized in Tables IIa—c.

Kinetics—A solution of I (5.00×10^{-3} mol), II (5.00×10^{-2} mol) and benzophenone (2.49×10^{-4} mol) in 5 ml of bromobenzene was placed in a ground-glass stoppered tube and immersed in a thermostated oil bath (Tokyo Rika

Kikai, HB 200B) controlled to 0.05 °C. The rates were followed at a given temperature by measuring the decrease of I by HPLC. Methyl *o*-nitrobenzoate was used as an internal standard.

Acknowledgement This work was supported in part by a Grant-in Aid for Scientific Research from the Ministry of Education, Science and Culture, Japan. The authors wish to express their thanks to the members of the Analytical Department of this faculty for microanalyses and spectral measurements.

References and Notes

- 1) Part XI: T. Hisano, K. Harano, R. Fukuoka, T. Matsuoka, K. Muraoka and I. Shinohara, *Chem. Pharm. Bull.*, **34**, 1485 (1986).
- 2) a) R. Huisgen, *Angew. Chem.*, **75**, 742 (1963); b) *Idem*, *Angew. Chem. Int. Ed. Engl.*, **2**, 565 (1963); c) *Idem*, *J. Org. Chem.*, **41**, 403 (1976).
- 3) R. Sustmann, *Tetrahedron Lett.*, **1971**, 2717, 2721.
- 4) K. N. Houk, "Pericyclic Reactions," Vol. 2, ed. by A. P. Marchand and R. E. Lehr, Academic Press, New York, 1977, Chapter IV.
- 5) a) H. Fujimoto and K. Fukui, "Chemical Reactivity and Reactions," Wiley, New York, 1974; b) K. Fukui, "Kagaku Hanno To Denshi No Kido (Chemical Reactions and Electron Orbitals)," Maruzen, Tokyo, 1976.
- 6) a) K. Harano, F. Suematsu, T. Matsuoka and T. Hisano, *Chem. Pharm. Bull.*, **32**, 543 (1984); b) T. Matsuoka, M. Shinada, F. Suematsu, K. Harano and T. Hisano, *ibid.*, **32**, 2077 (1984); c) K. Harano, R. Kondo, M. Murase, T. Matsuoka and T. Hisano, *ibid.*, **34**, 966 (1986).
- 7) J. A. Pople and D. L. Beveridge, "Approximate Molecular Orbital Theory," McGraw-Hill, New York, 1970.
- 8) M. J. S. Dewar and E. Haselbach, *J. Am. Chem. Soc.*, **92**, 590 (1970).
- 9) M. J. S. Dewar, MINDO/3 Program 279, "Quantum Chemistry Program Exchange (QCPE)," Indiana University, 1975.
- 10) T. Matsuoka, K. Harano and T. Hisano, *Chem. Pharm. Bull.*, **31**, 2948 (1983).
- 11) E. Ochiai, "Aromatic Amine Oxides," Elsevier Publishing Co., Amsterdam, 1967, p. 89.
- 12) The ¹³C-NMR spectral data of IIIe are as follows; 18.71, 21.19, 25.25, 50.60, 66.55, 75.02 and 79.59 ppm.
- 13) The calculated spectrum of the *exo* sigmatropy product is clearly inconsistent with the observed one for the *endo* isomer.
- 14) The previously reported data¹⁰⁾ for DMF and nitrobenzene solvents are erroneous because maleimides decompose in polar solvents on prolonged heating.
- 15) The *AE* is estimated to be about 5 kcal/mol greater than the average value for the reaction with nitrones.
- 16) a) K. Dimroth, C. Reichardt, T. Siepmann and F. Bohlmann, *Ann. Chem.*, **661**, 1 (1963); b) K. Dimroth, C. Reichardt and A. Schweig, *ibid.*, **669**, 95 (1963); c) C. Reichardt, *Angew. Chem.*, **77**, 30 (1965); d) C. Reichardt, *Pure Appl. Chem.*, **54**, 1967 (1982).
- 17) M. Yasuda, K. Harano and K. Kanematsu, *J. Org. Chem.*, **45**, 2368 (1980).
- 18) H. C. Brown and Y. Okamoto, *J. Am. Chem. Soc.*, **80**, 4979 (1958).
- 19) M. Yasuda, K. Harano and K. Kanematsu, *J. Org. Chem.*, **46**, 3836 (1981) and references cited therein.

[Chem. Pharm. Bull.]
35(3)1058-1069(1987)

Synthesis and Application of Imidazole Derivatives. Synthesis of (1-Methyl-1*H*-imidazol-2-yl)methanol Derivatives and Conversion into Carbonyl Compounds

SHUNSAKU OHTA,* SATOSHI HAYAKAWA, KAZUKO NISHIMURA,
and MASAO OKAMOTO

*Kyoto Pharmaceutical University, Misasagi-nakauchicho 5,
Kyoto 607, Japan*

(Received September 10, 1986)

(1-Methyl-1*H*-imidazol-2-yl)methanol derivatives (**4** and **7**) were prepared by treating carbonyl compounds with 2-lithio-1-methyl-1*H*-imidazole (**2**) or by treating 2-acyl-1*H*-imidazoles (**3**) with organometallic reagents or sodium borohydride. The alcohols (**4** and **7**) were convertible into the carbonyl compounds *via* the corresponding quaternary salts (**8** and **10**). The stable (1-methyl-1*H*-imidazol-2-yl)methanol system, $R-C(OH)-\underline{C=N-CH=CH-NCH_3}$, can be regarded as a masked form of the carbonyl group as well as a synthon of the group.

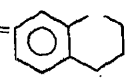
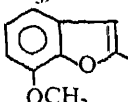
Keywords—(1-methyl-1*H*-imidazol-2-yl)methanol; 2-acyl-1-methyl-1*H*-imidazole; carbonyl compound synthesis; β -ketoester; protecting group; latent functionality; symmetric ketone; dihydrojasnone

1-Acyl-1*H*-imidazoles have been widely applied in organic synthesis as an important active acyl species.^{1,2)} On the other hand, 2-acyl-1-methyl-1*H*-imidazoles (**3**) have been little studied in regard to synthesis or their synthetic applications. In the previous paper, we reported syntheses of 2-acyl-1-methyl-1*H*-imidazoles (**3**) by treatment of various pyrrolidine amides (**1**) with 1-methyl-2-lithio-1*H*-imidazole, as well as the use of **3** as an active acyl source,³⁾ and conversion of the imidazole ring in **3** into the imidazolium form having a superior leaving ability. This paper mainly deals with synthesis of (1-methyl-1*H*-imidazol-2-yl)methanol derivatives (**4** and **7**) starting from the 2-acylimidazole (**3**) and further conversions of these products into carbonyl compounds by making use of the imidazolium group as a leaving group.

In the literature, (1-methyl-1*H*-imidazol-2-yl)methanol derivatives (**4** and **7**) have been prepared by treatment of aldehydes or ketones with 2-lithio-1-methyl-1*H*-imidazole (**2**),⁴⁾ and in one example by a Grignard reaction of 2-formyl-1-methyl-1*H*-imidazole (**3a**) with 4-phenoxyphenylmagnesium bromide.⁵⁾ We attempted to use a similar Grignard reaction to prepare **4** and **7** from various 2-acylimidazoles (**3**).³⁾ For example, the 2-cyclohexylcarbonylimidazole (**3d**) was added to an excess (more than two equivalents) of an ethereal benzylmagnesium bromide solution to give **7d** in 79.0% yield. Lithium reagents such as phenyllithium and lithium enolate were also usable instead of the Grignard reagent without difficulty. The secondary alcohols (**4**) were also obtained by reduction of the 2-acylimidazoles (**3**) with sodium borohydride as well as by Grignard reactions of the 2-formylimidazole (**3a**). Table I gives the yields and various data for the (1-methyl-1*H*-imidazol-2-yl)methanol derivatives (**4** and **7**).

In view of the superior leaving ability of the 2-imidazolium moiety, we considered that the structures of **4** and **7** can be regarded as a protected form of carbonyl group, such as *gem*-cyanohydrin. It was reported by Breslow that benzaldehyde was produced upon treatment of

TABLE I. Synthesis of the Substituted 2-Imidazolylmethanols (4 and 7)

Entry	Starting material	Nucleophile	Product	mp or bp (°C) Appearance (Recryst. solv.)	Isolated yield (%)
1	Piperonal (5a)	2	4a (R ¹ = 3,4-methylene- dioxypyhenyl)	mp 127—128.5 Needles (Et ₂ O)	85.7
2	3c	NaBH ₄			98.0
3	3a	CH ₂ =CHCH ₂ MgBr		4b (R ¹ = allyl)	bp 158 (3 mmHg)
4	<i>cyclo</i> -C ₆ H ₁₁ CHO (5d)	2	4c (R ¹ = <i>cyclo</i> -C ₆ H ₁₁)	mp 109.5—111 Needles (EtOAc- <i>n</i> -hexane)	76.0
5	3d	NaBH ₄			98.0
6	3a	<i>cyclo</i> -C ₆ H ₁₁ MgBr			63.0
7	<i>n</i> -C ₆ H ₁₃ CHO (5c)	2	4d (R ¹ = <i>n</i> -C ₆ H ₁₃)	mp 109.5—111 Needles (EtOAc- <i>n</i> -hexane)	70.3
8	3e	NaBH ₄			98.0
9	3a	<i>n</i> -C ₆ H ₁₃ MgBr			73.2
10	Citronellal (5b)	2	4e [R ¹ = Me ₂ CH(CH ₂) ₂ - CHMeCH ₂ -]	bp 112 (0.02 mmHg)	88.0
12	Benzophenone (6a)	2	7a (R ¹ = C ₆ H ₅) (R ² = C ₆ H ₅)	mp 194—194.5 Needles (EtOH)	90.2
13	3b	C ₆ H ₅ Li		7b (R ¹ = C ₆ H ₅) (R ² = CH ₃)	mp 151—152 Needles (Isopropanol)
14	Acetophenone (6c)	2	7c (R ¹ = C ₆ H ₅) (R ² = <i>n</i> -C ₄ H ₉)	mp 151—152 Needles (CCl ₄)	92.3
15	3b	<i>n</i> -BuLi		7d (R ¹ = <i>cyclo</i> -C ₆ H ₁₁) (R ² = C ₆ H ₅ CH ₂)	mp 151.5—152 Needles (CCl ₄)
16	Valerophenone (6d)	2	7e (R ¹ , R ² = )	mp 185—186 Needles (CCl ₄)	82.2
17	3d	C ₆ H ₅ CH ₂ MgBr	7f (R ¹ = 3,4-methylene- dioxypyhenyl) (R ² = <i>tert</i> -BuOCOCH ₂)	mp 123—125 Needles (CCl ₄)	83.0
18	1-Tetralone (6e)	2	7g (R ¹ = 3,4-methylene- dioxypyhenyl) (R ² = CH ₃ CHCOOCH ₃)	mp 125.5—127.5 Prisms (CCl ₄)	90.4
19	3c	LiCH ₂ COO- <i>tert</i> -Bu	7h (R ¹ = <i>n</i> -C ₆ H ₁₃) (R ² = <i>tert</i> -BuOCOCH ₂)	mp 125.5—127.5 Prisms (CCl ₄)	72.5
20	3c	CH ₃ CHCOOCH ₃ Li	7i (R ¹ = CH ₃) (R ² = <i>n</i> -C ₆ H ₁₃)	mp 123—125 Needles (<i>n</i> -Hexane)	90.7
21	3e	LiCH ₂ COO- <i>tert</i> -Bu	7j (R ¹ = CH ₃) (R ² = )	mp 170.5—172 Leaflets (EtOAc)	63.4
22	2-Octanone (6b)	2		mp 61.5—63 Needles (<i>n</i> -Hexane)	84.5
23	2-Acetyl-7-methoxy- benzo[<i>b</i>]furan (6f)	2		mp 170.5—172 Leaflets (EtOAc)	78.7

3,4-dimethyl-2-(hydroxyphenylmethyl)thiazolium salt with an organic base, but the reaction was reported as a qualitative, not a preparative, one.⁶⁾ Quaternization of the alcohols 4a and 7a proceeded easily on refluxing them in ethyl acetate solution in the presence of an excess of

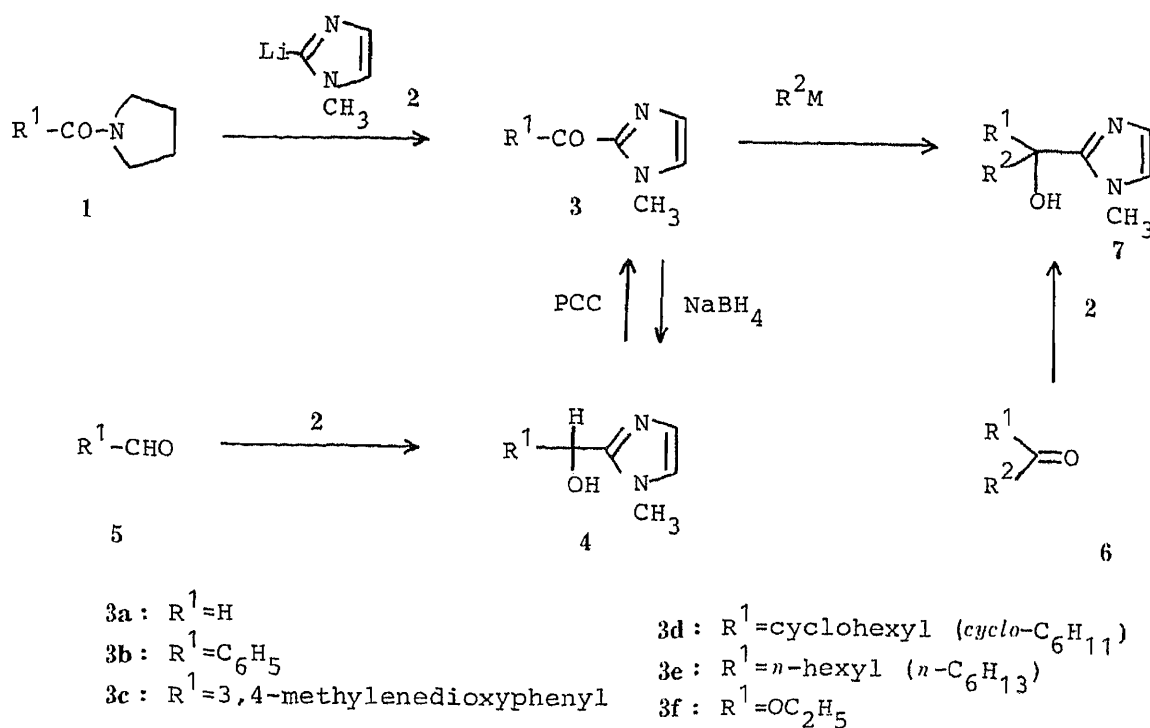


Chart 1

methyl iodide to give the corresponding crystalline imidazolium salt (**8a** and **10a**, respectively) in almost quantitative yields. First, the reactivity of the imidazolium salt **8a** were examined. When **8a** was treated with 10% potassium carbonate at 60 °C for 2 h, benzophenone was quantitatively produced, as expected (method A). In the cases of other imidazolymethanols (**4** and **7**), the corresponding imidazolium salts (**10**) were used without purification in the treatment with 10% potassium carbonate. As shown in Table II, the ketones were satisfactorily reduced. A possible reaction mechanism is illustrated in Chart 3, where removal of the proton from hydroxy group by the alkali occurs in an initial stage of the conversion of **8** to ketone and the equilibrium (a) seems to incline to the right.⁷⁾ Although the method A was applicable to producing aromatic aldehydes from the corresponding imidazolium salts such as **10a**, the method was not effective for producing aliphatic aldehydes, such as citronellal, from the imidazolium salt **10d**, probably because the initial equilibrium (a) incline to the left owing to lower steric repulsion in **10** than **8** (Chart 3). When stronger alkali, 0.1 N sodium hydroxide, was used instead of 10% potassium carbonate, a considerable amount of citronellal was formed. However, in that case, thin-layer chromatography (TLC) of the crude product demonstrated that the desired aldehyde was contaminated by by-products which were presumably formed by aldol condensation reaction and possible subsequent reactions. Thus, an excess of sodium 6-aminocaproate was added to the reaction mixture in order to trap the aldehyde in the aqueous phase as the corresponding Schiff base⁸⁾ (method B). As shown in Table II, formation of aldehydes proceeded satisfactorily. In method B, it is presumed that the equilibrium (a) may incline to the right owing to removal of the produced aldehyde by trapping with 6-aminocaproate through formation of the corresponding Schiff base, as well as owing to decomposition of the imidazolium counterpart *via* a pseudo-base (C) induced by the strong alkali (Chart 3).

When the imidazolium salt (**7a**) was treated with sodium hypochlorite in 20% acetic acid, benzophenone was obtained in high yield (method C). Since this procedure does not include a quaternization step, we expected that it might be generally applicable. However, in the case of

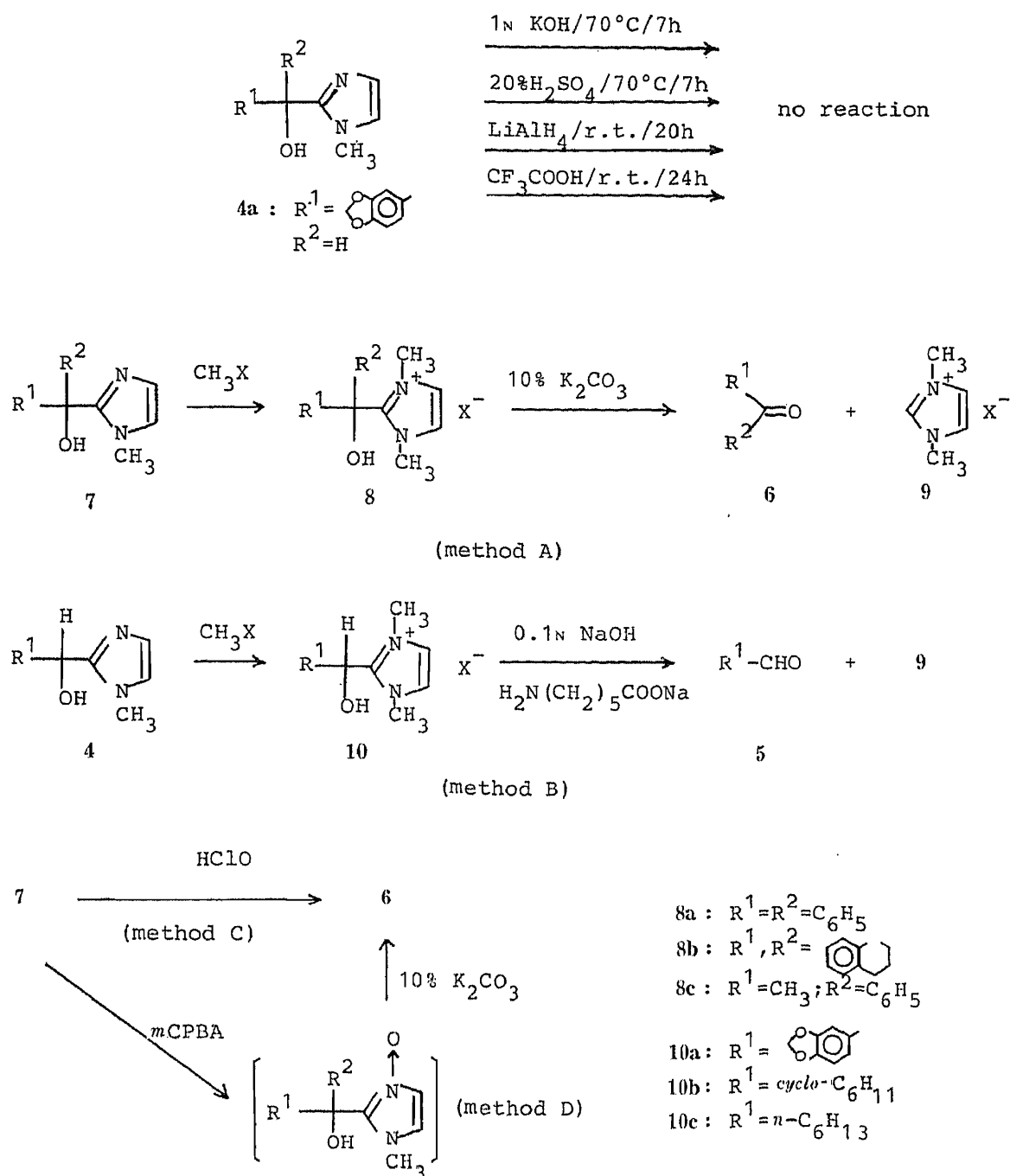
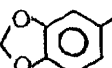
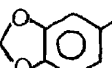
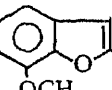


Chart 2

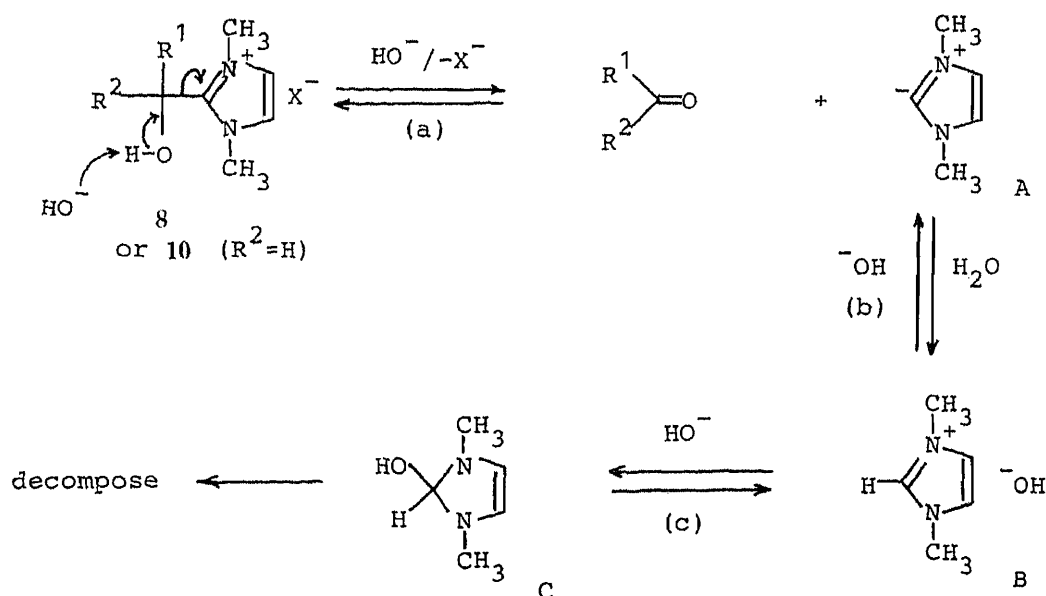
the imidazolylmethanol (7b), acetophenone produced was contaminated by a small amount (15%) of chlorinated acetophenone, so that the usefulness of the procedure seems to be restricted. The oxidation of 7c with *m*-chloroperbenzoic acid followed by treatment with 10% potassium carbonate also afforded the corresponding ketone in almost quantitative yield, but the reaction did not proceed satisfactorily in other cases (method D) (Table II).

When the carbinol (7c) was refluxed in ethyl acetate in the presence of methyl iodide, we observed a gradual formation of valerophenone, the yield of which reached 86% after prolonged reflux (3 d). 1,3-Dimethyl-1*H*-imidazolium iodide (9) could also be isolated in 63% yield, indicating that the C-C bond fission occurs in a hydrolytic manner but not through any

TABLE II. Formation of the Carbonyl Compounds (5 and 6) by Methods A—D

Entry	Starting material	Method	Product	Yield ^{a)} (%)
1	7a	A	Benzophenone (6a)	96.6 (quant.)
2	7a	C	Benzophenone (6a)	(quant.)
3	7a	D	Benzophenone (6a)	80.0
4	7b	A	Acetophenone (6c) ^{b)}	(quant.)
5	7b	C	Acetophenone (6c)	(80.0)
6	7c	A	Valerophenone (6d)	(quant.)
7	7c	D	Valerophenone (6d)	(quant.)
8	7d	A	R ¹ = <i>cyclo</i> -C ₆ H ₁₁ ; R ² = benzyl (6g)	90.0
9	7e	A	1-Tetralone (6e)	(quant.)
10	7f	A	 -COCH ₂ COO- <i>tert</i> -Bu (6h)	70.3
11	7g	A	 -COCHCOO- <i>tert</i> -Bu CH ₃ (6i)	85.7
12	7h	A	CH ₃ (CH ₂) ₅ COCH ₂ COO- <i>tert</i> -Bu (6j)	87.7
13	7i	A	2-Octanone (6b)	(quant.)
14	7j	A	 -COCH ₃ (6f)	(quant.)
15	4a	A	Piperonal (5a)	(quant.)
16	4a	B	Piperonal (5a)	(47.1)
17	4c	B	R ¹ = <i>cyclo</i> -C ₆ H ₁₁ (5d)	(84.4)
18	4d	B	<i>n</i> -Heptanol (5c)	(83.9)
19	4e	A	Citronellal (5b)	(nil)
20	4e	B	Citronellal (5b)	74.5 (79.0)

a) Yields in parentheses were obtained by GLC and those without parentheses are isolated yields. b) α -Chloroacetophenone was also produced in 5–15% yield.



other process such as autoxidation.

Stability of the imidazolyl methanol derivatives (**4a**) under various severe conditions was examined as follows in order to evaluate the characteristics of the molecular system as protecting group for the carbonyl group: 1 N KOH/CH₃OH/70°C/7 h; 20% H₂SO₄/70°C/7 h; NaBH₄/CH₃OH/room temperature (r.t.)/20 h; LiAlH₄/THF/r.t./N₂/20 h; CF₃COOH/r.t./24 h; H₂/5% Pd-C/C₂H₅OH/1 atmosphere (atm)/r.t./18 h. Fortunately, it was found on the bases of gas-liquid layer chromatography (GLC) that the substrate (**4a**) survived almost intact under all of these conditions. It is noteworthy that the imidazolymethanols (**4c** and **7c**), which might be expected to undergo relatively easy dehydration, were almost intact after treatment with 20% sulfuric acid at 70°C for 7 h probably because the first protonation on the imidazole nitrogen prevented the second protonation on hydroxy group owing to repulsion between the two positive charges. Thus, we can use the imidazolmethanols (**4** and **7**) as a characteristic protecting group for the carbonyl group.

If the secondary imidazolymethanols (**4**) can be oxidized to the 2-acylimidazoles (**3**), various aldehydes may be convertible into ketones and active acyls by applying the present methodology, including the procedure in the previous report.³⁾ Although pyridinium chlorochromate oxidation of **4a** proceeded in 84.3% yield, the other imidazolymethanols (**4**) gave the 2-acyl derivatives in very low yield probably because of losses during extraction of the product. We are now investigating more convenient oxidation procedures.

Next, preparations of dihydrojasnone (**16**),⁹⁾ a constituent of bergamot oil, was examined as an application of the present methodology. 1-(4,4-Ethylenedioxybutanoyl)-pyrrolidine (**11**) was treated with 2-lithio-1-methyl-1*H*-imidazole (**2**) to give the corresponding 2-acylimidazole (**12**) in 79.1% yield.³⁾ A Grignard reaction of the acylimidazole (**12**) with an excess of *n*-hexylmagnesium bromide proceeded satisfactorily to afford the crystalline carbinol (**13**) in 92.6% yield, and **13** was treated with 10% hydrochloric acid for several minutes to give a ketocarbinol (**14**). Treatment of the ketocarbinol (**14**) according to method A, described above, furnished the diketone (**15**) in 97.4% yield; this product was firstly reported as an intermediate for the synthesis of dihydrojasnone (**16**) by Stork and Borche.¹⁰⁾ In our experiment, a direct Grignard reaction of the ketal amide **11** with *n*-hexylmagnesium bromide resulted in formation of a complex mixture consisting of **11** (about 60%), the corresponding ketone (2-ethylenedioxyundecan-5-one; about 20%) and several

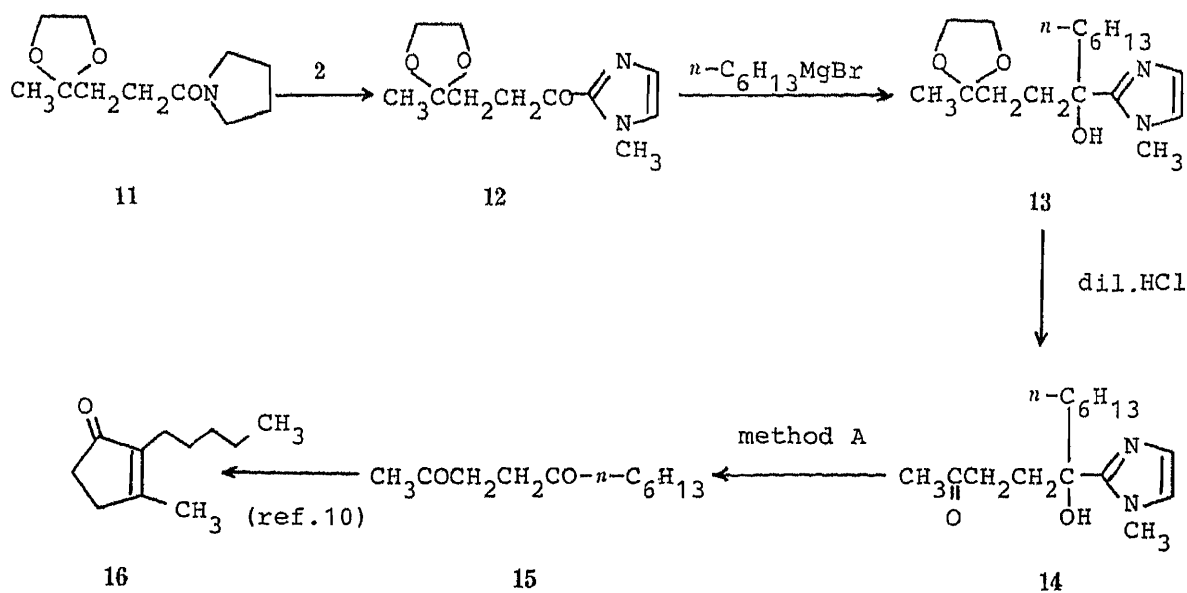


Chart 4

unidentified products. This result may be explained in terms of interference by the ketal function with the approach of the Grignard reagent and several known side reactions in the Bouveault ketone synthesis.¹¹⁾

Finally, syntheses of symmetric ketones were attempted. For example, 2-ethoxycarbonyl-1-methyl-1*H*-imidazole (**3f**)⁵⁾ was treated with an excess of an ethereal solution of cyclohexylmagnesium bromide to give the corresponding symmetrically disubstituted imidazolylmethanol (**7l**; R¹ = R² = cyclohexyl) in 81.9% yield. The imidazolylmethanol (**7l**) was treated according to method A to produce dicyclohexylketone (**6l**) in 78.9% yield. Other examples listed in Table III also proceeded satisfactorily except for **7n**. The reaction of ethyl formate with Grignard reagent has been well known as a convenient preparation method for symmetrically substituted secondary alcohols,¹²⁾ and the present reaction may provide a new and general procedure for linking two molecules of the same Grignard reagent with one carbonyl group.

In conclusion, the present methodology should be useful in organic synthesis not only as a protecting group for the carbonyl group but also as a synthon of various carbonyl compounds. Characteristic features of the present methodology can be summarized as follows. i) An excess of Grignard reagent and reducing agent (NaBH₄) can be used in their reaction with the 2-acyl-1*H*-imidazole (**3**). ii) The resulting imidazolylmethanols (**4** and **7**) can

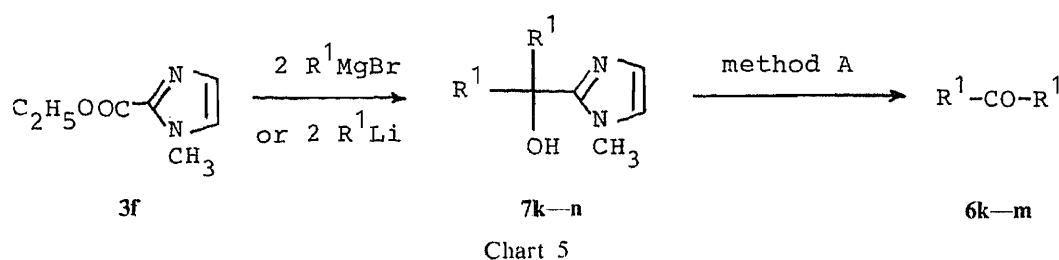
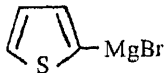
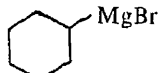
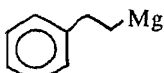
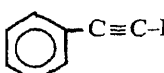


TABLE III. Conversion of 2-Ethoxycarbonyl-1-methyl-1*H*-imidazole (**3f**) into Symmetrically Substituted Ketones *via* Symmetrically Disubstituted Carbionols (**7**)

Entry	R ¹ MgBr or R ¹ Li	7 (R ¹ = R ²)			6 (R ¹ = R ²)	
		mp (°C) Appearance (Recryst. solv.)	Yield (%)	Method	mp or bp (°C) (Lit. value) (Reference)	Yield (%)
1	 MgBr	7k 180.5—182 (dec.) Needles (CCl ₄)	92.6	A	6k mp 87—88.5 (mp 87—88) (Ref. 14)	Quant.
2	 MgBr	7l 153.5—155 Needles (EtOAc- <i>n</i> -hexane)	81.9	A	6l bp 130—135 (5 mmHg) [bp 158—161 (10 mmHg)] (Ref. 15)	78.9
3	 MgBr	7m 152—153 Needles (AcOEt)	85.0	D	6m bp 140—145 (3 mmHg) [bp 225 (15 mmHg)] (Ref. 16)	70.5
4	 C≡C-Li	7n 178—179 Prisms (CH ₃ OH)	88.8	A	^{a)}	—

a) A resinous material was produced.

be regarded as protected forms of carbonyl compounds, which are stable under various severe conditions and can be deprotected under relatively selective reaction conditions. Thus, the present carbonyl group protection system [$-\text{C}(\text{OH})-\text{C}=\text{N}-\text{CH}=\text{CH}-\text{N}(\text{CH}_3)$] is a new type, different from the known carbonyl protecting systems such as ketal, acetal, thioketal and *gem*-cyanohydrin. iii) The 2-acylimidazoles (**3**) can be regarded as synthons of various carbonyl compounds. iv) Imidazole compounds are extractable with aqueous acid, so they can be easily separated from neutral and acidic compounds. We are now investigating syntheses of several natural products as further applications of the present methodology.

Experimental

All melting points are uncorrected. Infrared (IR) spectra were taken with a Shimadzu IR-410 spectrometer. Proton nuclear magnetic resonance ($^1\text{H-NMR}$) spectra were recorded on a Varian CFT-20 spectrometer using tetramethylsilane as an internal standard and the chemical shifts are given in δ -values (ppm). Abbreviations of $^1\text{H-NMR}$ signal patterns are as follows: s (singlet); d (doublet); t (triplet); q (quartet); m (multiplet); br (broad). High-resolution mass spectra (HRMS) and low-resolution mass spectra (MS) were both taken with a Hitachi RMU-2 spectrometer. Ultraviolet (UV) spectra in ethanolic solutions were recorded on a Shimadzu-200S spectrometer. Oily products and low-melting-point products were purified by vacuum distillation with a Kugel-Rohr distillation apparatus.

General Procedure for Synthesis of (1-Methyl-1*H*-imidazol-2-yl)-methanol Derivatives—a) 2-(1-Hydroxyheptyl)-1-methyl-1*H*-imidazole (**4d**): *n*-Butyllithium (1.6 M in hexane; 10 mmol) was added to a solution of 1-methyl-1*H*-imidazole (0.82 g, 10 mmol) in tetrahydrofuran (THF) at -78°C under an N_2 atmosphere and the mixture was stirred for 5 min. *n*-Heptanal (1.14 g, 10 mmol) was added dropwise to the solution and the mixture was stirred for 30 min while warming to ambient temperature (the cooling bath was removed). Ether (30 ml) and 10% HCl (10 ml) were added, and the aqueous layer was washed with ether (5 ml) and basified with solid K_2CO_3 . The separated oil was extracted with ethyl acetate. The organic layer was evaporated after drying with Na_2SO_4 to give an oily residue, which was purified by vacuum distillation. bp₃ 132°C . Yield, 1.38 g (70.3%). IR (CHCl_3): 3160 cm^{-1} (OH). $^1\text{H-NMR}$ (CDCl_3) δ : 0.86 (t, 3H, CH_3CH_2 -, $J=8\text{ Hz}$), 1.05–1.65 (m, 8H, $\text{CH}_3(\text{CH}_2)_4$ -), 1.83 (t, 2H, $-\text{CH}_2\text{CH}(\text{OH})$ -, $J=8\text{ Hz}$), 3.68 (s, 3H, NCH_3), 4.00 (br, 1H, OH), 4.67 (t, 1H, $-\text{CH}(\text{OH})$ -, $J=8\text{ Hz}$), 6.76 and 6.86 (d each, 1H each, imidazole H, $J=1\text{ Hz}$ each). Elemental analysis was performed with the corresponding methiodide (**10c**) as described below.

b) 2-(1-Cyclohexyl-1-hydroxy-2-phenylethyl)-1-methyl-1*H*-imidazole (**7d**): 2-Cyclohexylcarbonyl-1-methyl-1*H*-imidazole (**3d**; 0.96 g, 5 mmol) was added under ice-cooling to a stirred ethereal solution of benzylmagnesium bromide, which was prepared from benzyl bromide (1.71 g, 10 mmol), magnesium metal (468 mg, 20 mgatom) and ether (10 ml). The mixture was stirred at room temperature for 2 h and filtered. The mixture was acidified with 10% HCl and the aqueous layer was washed with ether then basified with solid K_2CO_3 . Separated material was extracted with ethyl acetate. Evaporation of the solution after drying with Na_2SO_4 gave a crystalline residue, which was recrystallized from CCl_4 to give colorless needles. mp 185 – 186°C . Yield, 1.18 g (83.0%). IR (CHCl_3): 3520 (OH), 3350 cm^{-1} (OH). $^1\text{H-NMR}$ (CDCl_3) δ : 0.95–2.20 (m, 11H, cyclohexyl H), 3.12 (s, 1H, OH), 3.25 (d, 2H, $-\text{CH}_2\text{C}_6\text{H}_5$, $J=8\text{ Hz}$), 3.43 (s, 3H, NCH_3), 6.55–7.30 (m, 7H, imidazole H and C_6H_5 -). Anal. Calcd for $\text{C}_{18}\text{H}_{24}\text{N}_2\text{O}$: C, 76.02; H, 8.51; N, 9.85. Found: C, 76.18; H, 8.47; N, 10.07.

c) 2-(Diphenylhydroxymethyl)-1-methyl-1*H*-imidazole (**7a**): Phenyllithium solution (2.4 M in ether, 6 mmol) was added to a solution of 2-benzoyl-1-methyl-1*H*-imidazole (**3b**; 0.93 g, 5 mmol) in tetrahydrofuran (THF; 10 ml) at -78°C and the solution was stirred for 10 min followed by stirring for 30 min while warming to ambient temperature (the cooling bath and removed). Ether (30 ml) and 10% HCl (10 ml) were added and the aqueous layer was washed with ether and basified with solid K_2CO_3 . The precipitated solid was filtered off and recrystallized from ethanol to give colorless needles. mp 194 – 194.5°C . Yield, 1.19 g (90.2%). IR (CHCl_3): 3370 cm^{-1} (OH). $^1\text{H-NMR}$ ($\text{DMSO}-d_6$) δ : 3.35 (s, 3H, NCH_3), 6.74 (s, 1H, OH), 6.73 and 7.11 (d each, 2H, imidazole H, $J=1\text{ Hz}$ each), 7.00–7.50 (m, 10H, $\text{C}_6\text{H}_5 \times 2$). Anal. Calcd for $\text{C}_{17}\text{H}_{16}\text{N}_2\text{O}$: C, 77.25; H, 6.10; N, 10.60. Found: C, 77.24; H, 5.88; N, 10.50.

d) 2-[(*tert*-Butoxycarbonylmethyl)hydroxy(3,4-methylenedioxyphenyl)methyl]-1-methyl-1*H*-imidazole (**7f**): *tert*-Butyl acetate (385 mg, 3.3 mmol) was added to a solution of lithium diisopropylamide (3 mmol) in THF at -78°C under N_2 and the solution was stirred for 5 min. 1-Methyl-2-piperonyloyl-1*H*-imidazole (**3c**; 0.69 g, 3 mmol) was added to the solution and the mixture was stirred for 5 min. Stirring was continued for 30 min while the mixture was warmed to ambient temperature (the cooling bath was removed). Water (5 ml) and ethyl acetate (30 ml) were added and the organic layer was washed with water ($5\text{ ml} \times 2$). Removal of the solvent after drying with Na_2SO_4 gave a crystalline residue, which was purified on a short silica gel column (ethyl acetate as an eluting solvent) followed by recrystallization from CCl_4 to give colorless prisms. mp 125.5 – 127.5°C . Yield, 755 mg (72.5%). IR (CHCl_3): 3420 (OH), 1700 cm^{-1} (C=O). $^1\text{H-NMR}$ (CDCl_3) δ : 1.45 (s, 9H, $-\text{C}(\text{CH}_3)_3$), 2.66 and 3.41 (d each, 1H each, $-\text{CH}_2\text{COO}-$,

$J=20$ Hz each), 3.40 (s, 3H, NCH_3), 5.84 (s, 1H, $-\text{OH}$), 5.93 (s, 2H, $-\text{OCH}_2\text{O}-$), 6.60—6.90 (m, 5H, imidazole H and Ar-H). *Anal.* Calcd for $\text{C}_{18}\text{H}_{22}\text{N}_2\text{O}_5$: C, 62.42; H, 6.40; N, 8.09. Found: C, 62.56; H, 6.53; N, 7.96.

e) 2-[(3,4-Methylenedioxyphenyl)hydroxymethyl]-1-methyl-1*H*-imidazole (**4a**): NaBH_4 (0.3 g) was added to a solution of **3c** (0.5 g) in methanol (15 ml) and the mixture was stirred at room temperature for 0.5 h. The solvent was evaporated off and the residue was extracted with ethyl acetate. The organic layer was washed with water (5 ml), and evaporated after drying with Na_2SO_4 to give a crystalline residue, which was recrystallized from ether. mp 127.5—128.5 °C. Yield, quantitative. IR (CHCl_3): 3120 cm^{-1} (OH). $^1\text{H-NMR}$ (CDCl_3) δ : 3.40 (s, 3H, NCH_3), 5.79 (s, 1H, $-\text{CH}(\text{OH})-$), 5.91 (s, 2H, $-\text{OCH}_2\text{O}-$), 5.65 (br, 1H, $-\text{OH}$), 6.50—7.00 (m, 5H, imidazole H and Ar-H). Elemental analysis was performed with the corresponding methiodide (**10a**) as described below. Physical and spectral data for other imidazolylmethanols (**4** and **7**) are listed in Table I and below.

2-(1-Hydroxybut-3-enyl)-1-methyl-1*H*-imidazole (**4b**): IR (CHCl_3): 3110 (OH), 1642 cm^{-1} (C=C). HRMS m/z : Calcd for $\text{C}_8\text{H}_{12}\text{N}_2\text{O}$ = 152.0960. $^1\text{H-NMR}$ (CDCl_3) δ : 2.68 (m, 2H, $-\text{CH}_2\text{C}(\text{OH})-$), 3.69 (s, 3H, NCH_3), 4.30 (br, 1H, $-\text{OH}$), 4.74 (t, 1H, $-\text{CH}(\text{OH})-$, $J=9$ Hz), 4.85—5.23 (m, 2H, $\text{CH}_2=$), 5.50—6.10 (m, 1H, $\text{CH}_2=\text{CH}-$), 6.77 and 6.87 (d each, 1H each, imidazole H, $J=2$ Hz each).

2-(Cyclohexylhydroxymethyl)-1-methyl-1*H*-imidazole (**4c**): IR (CHCl_3): 3100 cm^{-1} (OH). $^1\text{H-NMR}$ (CDCl_3) δ : 0.60—2.20 (m, 11H, *cyclo*- C_6H_{11}), 3.66 (s, 3H, NCH_3), 4.20 (br, 1H, $-\text{OH}$), 4.37 (d, 2H, $-\text{CH}(\text{OH})-$, $J=10$ Hz), 6.75 and 6.89 (d each, 1H each, imidazole H, $J=1$ Hz each). *Anal.* Calcd for $\text{C}_{11}\text{H}_{18}\text{N}_2\text{O}$: C, 68.01; H, 9.34; N, 14.42. Found: C, 67.97; H, 9.11; N, 14.36.

2-(3,7-Dimethyl-1-hydroxyoct-6-enyl)-1-methyl-1*H*-imidazole (**4e**): IR (CHCl_3): 3200 cm^{-1} (OH). $^1\text{H-NMR}$ (CDCl_3) δ : 0.93 (d, 3H, $\text{CH}_3\text{CH}-$, $J=8$ Hz), 1.00—2.20 (m, 13H, $(\text{CH}_2)_2\text{C}=\text{CH}(\text{CH}_2)_2\text{CH}(\text{CH}_3)\text{CH}_2-$), 3.68 (s, 3H, NCH_3), 4.79 (t, 1H, $-\text{CH}(\text{OH})-$, $J=9$ Hz), 5.02 (t, 1H, $-\text{CH}=\text{CH}-$, $J=7$ Hz), 6.86 and 6.77 (d each, 1H each, imidazole H, $J=1$ Hz each). *Anal.* Calcd for $\text{C}_{14}\text{H}_{24}\text{N}_2\text{O}$: C, 71.14; H, 10.23; N, 11.85. Found: C, 70.99; H, 10.68; N, 11.87.

2-(1-Hydroxy-1-phenylethyl)-1-methyl-1*H*-imidazole (**7b**): IR (KBr): 3170 cm^{-1} (OH). $^1\text{H-NMR}$ ($\text{DMSO}-d_6$) δ : 1.82 (s, 3H, $\text{CH}_3\text{C}(\text{OH})-$), 3.25 (s, 3H, NCH_3), 6.04 (s, 1H, $-\text{OH}$), 6.79 and 7.00 (d each, 2H, Imidazole H, $J=1$ Hz each), 7.00—7.45 (m, 5H, Ar-H). Elemental analysis was performed with the corresponding methiodide (**8c**) as described below.

2-(1-Hydroxy-1-phenyl-1-pentyl)-1-methyl-1*H*-imidazole (**7c**): IR (CHCl_3): 3600, 3300 cm^{-1} (OH). $^1\text{H-NMR}$ (CDCl_3) δ : 0.85 (t, 3H, CH_3CH_2- , $J=8$ Hz), 1.00—1.60 (m, 4H, $-(\text{CH}_2)_2\text{CH}_2\text{C}(\text{OH})-$), 2.39 (t, 2H, $-\text{CH}_2\text{C}(\text{OH})-$, $J=10$ Hz), 3.10 (br, 1H, OH), 3.26 (s, 3H, NCH_3), 6.75 and 6.92 (d each, 1H each, imidazole H, $J=1$ Hz each), 7.10—7.50 (m, 5H, Ar-H). *Anal.* Calcd for $\text{C}_{15}\text{H}_{20}\text{N}_2\text{O}$: C, 73.74; H, 8.25; N, 11.47. Found: C, 73.76; H, 8.41; N, 11.42.

2-(1-Hydroxy-1,2,3,4-tetrahydro-1-naphthyl)-1-methyl-1*H*-imidazole (**7e**): IR (CHCl_3): 3470 cm^{-1} (OH). $^1\text{H-NMR}$ (CDCl_3) δ : 1.70—2.30 (m, 4H, $-\text{C}(\text{OH})\text{CH}_2\text{CH}_2-$), 2.65—3.10 (m, 3H, $-\text{OH}$ and $\text{C}_6\text{H}_4\text{CH}_2-$), 3.05 (s, 3H, NCH_3), 6.80 and 6.97 (d each, 1H each, imidazole H, $J=1$ Hz each), 6.65—7.31 (m, 4H, Ar-H). *Anal.* Calcd for $\text{C}_{14}\text{H}_{16}\text{N}_2\text{O}$: C, 73.66; H, 7.06; N, 12.27. Found: C, 73.74; H, 6.95; N, 12.24.

2-[Hydroxy(3,4-methylenedioxyphenyl)(1-methoxycarbonyl)ethyl]methyl-1-methyl-1*H*-imidazole (**7g**): A diastereomeric mixture was obtained as a viscous material, purification of which for analysis was difficult. IR (CHCl_3): 3450 (OH), 1710 cm^{-1} (C=O). $^1\text{H-NMR}$ (CDCl_3) δ : 1.02 and 1.41 (s each, total 3H, $\text{CH}_3\text{CHCOO}-$), 3.20—4.20 (m, 7H, $-\text{NCH}_3$ and $-\text{CHCOOCH}_3$), 5.13 and 5.33 (s each, total 1H, $-\text{OH}$), 5.93 (s, 2H, $-\text{OCH}_2\text{O}-$), 6.50—6.90 (m, 5H, Ar-H).

2-(1-*tert*-Butoxycarbonyl-2-hydroxy-2-octyl)-1-methyl-1*H*-imidazole (**7h**): A viscous oil was obtained, purification of which for analysis was difficult. IR (CHCl_3): 3410 (OH), 1700 cm^{-1} (C=O). $^1\text{H-NMR}$ (CDCl_3) δ : 0.83 (t, 3H, CH_3CH_2- , $J=6$ Hz), 0.95—1.30 (m, 8H, $\text{CH}_3(\text{CH}_2)_4-$), 1.41 (s, 9H, $-\text{C}(\text{CH}_3)_3$), 1.60—2.00 (m, 2H, $-\text{CH}_2\text{C}(\text{OH})-$), 2.57 and 3.32 (d each, 1H each, $-\text{CH}_2\text{COO}-$, $J=21$ Hz each), 3.85 (s, 3H, NCH_3), 5.11 (s, 1H, $-\text{OH}$), 6.73 and 6.83 (d each, 2H, imidazole H, $J=1$ Hz each).

2-(2-Hydroxyhept-2-yl)-1-methyl-1*H*-imidazole (**7i**): IR (CHCl_3): 3600, 3200 cm^{-1} (OH). $^1\text{H-NMR}$ (CDCl_3) δ : 0.85 (t, 3H, CH_3CH_2- , $J=6$ Hz), 1.00—1.50 (m, 8H, $\text{CH}_3(\text{CH}_2)_4-$), 1.61 (s, 3H, $\text{CH}_3\text{C}(\text{OH})-$), 1.70—2.00 (m, 2H, $-\text{CH}_2\text{C}(\text{OH})-$), 3.35 (br, 1H, OH), 3.78 (s, 3H, NCH_3), 6.77 and 6.84 (d each, 1H each, imidazole H, $J=1$ Hz each). *Anal.* Calcd for $\text{C}_{12}\text{H}_{22}\text{N}_2\text{O}$: C, 68.53; H, 10.54; N, 13.32. Found: C, 68.78; H, 10.63; N, 13.57.

2-[1-Hydroxy-1-(8-methoxybenzo[*b*]furan-2-yl)ethyl]-1-methyl-1*H*-imidazole (**7j**): IR (CHCl_3): 3570, 3100 cm^{-1} (OH). $^1\text{H-NMR}$ (CDCl_3) δ : 2.09 (s, 3H, $\text{CH}_3\text{C}(\text{OH})-$), 3.60 (s, 3H, NCH_3), 3.95 (s, 3H, OCH_3), 4.08 (br, 1H, $-\text{OH}$), 6.40—7.30 (m, 6H, Ar-H). *Anal.* Calcd for $\text{C}_{15}\text{H}_{16}\text{N}_2\text{O}_3$: C, 66.16; H, 5.92; N, 10.29. Found: C, 66.24; H, 6.15; N, 10.28.

1,3-Dimethyl-2-(1-hydroxy-1-phenylethyl)-1-methyl-1*H*-imidazolium Iodide (8c**) (Typical Procedure for Synthesis of the Quaternary Salt **8** and **10**)**—A suspension of 2-(1-hydroxy-1-phenylethyl)-1-methyl-1*H*-imidazole (**7b**; 1.01 g, 5 mmol) in ethyl acetate (25 ml) was refluxed under N_2 for 2 h in the presence of methyl iodide (5 ml). Removal of the solvent gave a crystalline residue, which was recrystallized from CH_2Cl_2 -ether to give leaflets. mp 141—143 °C. Yield, quantitative. IR (CHCl_3): 3200 cm^{-1} (OH). $^1\text{H-NMR}$ (CDCl_3) δ : 2.26 (s, 3H, $\text{CH}_3\text{C}(\text{OH})-$), 3.89 (s, 6H, $2 \times \text{NCH}_3$), 5.75 (s, 1H, $-\text{OH}$), 7.00—7.60 (m, 7H, imidazole H and Ar-H). *Anal.* Calcd for $\text{C}_{13}\text{H}_{17}\text{IN}_2\text{O}$: C, 45.36; H, 4.98; N, 8.14. Found: C, 45.60; H, 5.13; N, 8.21. Physical and spectral data of other isolated quaternary salts are as follows.

1,3-Dimethyl-2-(1-hydroxy-1,2,3,4-tetrahydronaphth-1-yl)-1*H*-imidazolium Iodide (**8b**): Colorless leaflets from ethyl acetate, mp 195—202.5 °C. IR (KBr): 3250 cm⁻¹ (OH). ¹H-NMR (DMSO-*d*₆) δ: 1.60—2.35 (m, 4H, -C(OH)CH₂CH₂-), 2.70—3.0 (m, 2H, -C₆H₄CH₂-), 3.59 (s, 6H, NCH₃ × 2), 6.80 (br, 1H, -OH), 6.90—7.72 (m, 6H, Ar-H). *Anal.* Calcd for C₁₅H₁₉IN₂O: 48.66; H, 5.17; 7.57. Found: C, 48.77; H, 5.44; N, 7.73.

1,3-Dimethyl-2-[hydroxy(3,4-methylenedioxyphenyl)-methyl]-1*H*-imidazolium Iodide (**10a**): Colorless needles from ethanol-ether, mp 167—169 °C. IR (KBr): 3200 cm⁻¹ (OH). ¹H-NMR (DMSO-*d*₆) δ: 3.81 (s, 6H, NCH₃ × 2), 6.05 (s, 2H, -OCH₂O-), 6.35 (s, 1H, -CH(OH)-), 6.67—7.02 (m, 3H, Ar-H), 7.71 (s, 2H, imidazole H). *Anal.* Calcd for C₁₃H₁₅IN₂O₃: C, 41.73; H, 4.04; N, 7.49. Found: C, 41.84; H, 4.03; N, 7.52.

1,3-Dimethyl-2-cyclohexyl-1-hydroxymethyl-1*H*-imidazolium Iodide (**10b**): Colorless needles from acetone-ether, mp 123—124 °C. IR (CHCl₃): 3280 cm⁻¹ (OH). ¹H-NMR (CDCl₃) δ: 0.70—2.30 (m, 1H, *cyclo*-C₆H₁₁-), 4.02 (s, 6H, NCH₃ × 2), 4.93 (m, 1H, -CH(OH)-), 5.04 (s, 1H, -OH), 7.42 (s, 2H, imidazole H). *Anal.* Calcd for C₁₂H₂₁IN₂O: C, 42.97; H, 6.30; N, 9.39. Found: C, 43.04; H, 6.26; N, 9.09.

1,3-Dimethyl-2-(1-hydroxyheptyl)-1*H*-imidazolium Iodide (**10c**): Colorless leaflets from ethyl acetate, mp 105.5—107 °C. IR (CHCl₃): 3300 cm⁻¹ (OH). ¹H-NMR (CDCl₃) δ: 0.88 (t, 3H, CH₃CH₂-, *J* = 8 Hz), 1.02—2.10 (m, 10H, CH₂ (CH₂)₅-), 4.01 (s, 6H, NCH₃ × 2), 5.09 (d, 1H, -OH, 5 Hz), 5.10—5.40 (m, 1H, -CH(OH)-), 7.41 (s, 2H, imidazole H). *Anal.* Calcd for C₁₂H₂₃IN₂O: C, 42.61; H, 6.85; N, 8.28. Found: C, 42.46; H, 7.08; N, 8.26.

Typical Procedure for Method A [Example: Formation of Benzophenone (6a)]—A suspension of 1-methyl-2-(diphenylhydroxymethyl)-1*H*-imidazole (**7a**; 1.32 g, 5 mmol) in ethyl acetate (25 ml) was refluxed for 2 h in the presence of methyl iodide (5 ml) followed by evaporation of the solvent and the reagent. Benzene and 10% K₂CO₃ were added to the crystalline residue and the mixture was warmed at 60 °C with stirring under an N₂ atmosphere for 2 h. Evaporation of the organic layer after drying with Na₂SO₄ gave a crystalline residue, which was distilled under vacuum to afford benzophenone. bp 160 °C (10 mmHg). Yield, 0.88 g (96.6%).

Typical Procedure for Method B [Example: Formation of Citronellal (5b)]—A solution of 2-(1-hydroxy-3,7-dimethyloct-6-en-1-yl)-1-methyl-1*H*-imidazole (**4e**; 2.36 g, 10 mmol) in ethyl acetate (25 ml) was refluxed for 2 h in the presence of methyl iodide (10 ml), followed by evaporation of the volatile portion, to give a crystalline residue, to which 6-amino-1-caproic acid (5.24 g, 40 mmol), 1 N NaOH (50 ml) and benzene (20 ml) were added. The two-layer solution was stirred at 80 °C under an N₂ atmosphere for 5 h, then acidified with 10% HCl and extracted with benzene. The organic layer was evaporated after drying with Na₂SO₄ to give an oily residue, which was distilled under vacuum. bp 80 °C (3 mmHg). Yield, 1.15 g (74.5%).

Typical Procedure for Method C [Formation of Acetophenone (6e)]—A 5% sodium hypochlorite solution (5 ml) was added dropwise to a solution consisting of **7b** (0.606 g, 3 mmol) and 20% acetic acid, and the mixture was stirred for 15 min, becoming turbid. The product was extracted with ether (30 ml) and the ethereal layer was washed with 10% HCl, water and 10% K₂CO₃, followed by drying with Na₂SO₄. Naphthalene (30 mg) was added to the solution. GLC analysis showed the presence of acetophenone in 85% yield as well as α-chloroacetophenone in 5% yield. Work-up after overnight stirring of the reaction mixture gave acetophenone in 80% yield and α-chloroacetophenone in 15% yield. GLC conditions: column packing (5% SE-30; 2 m × 3 mm i.d.); carrier gas (N₂; 50 ml/min); column temperature (100—200 °C); injection port (flame ionization detector (FID); 200 °C).

General Procedure for Method D (Formation of Benzophenone)—*m*-Chloroperbenzoic acid (520 mg; 3 mmol) was added to a stirred solution of 2-(diphenylhydroxymethyl)-1-methyl-1*H*-imidazole (**7a**; 792 mg; 3 mmol) in CH₂Cl₂ (6 ml) and the mixture was stirred overnight followed by treatment of the mixture with 10% K₂CO₃ (10 ml) under stirring for 3 h. The dichloromethane solution was shaken with 5% Na₂S₂O₃, water, 10% HCl and 10% K₂CO₃ (5 ml each). Removal of the solvent after drying with Na₂SO₄ gave an oily residue, which was distilled under vacuum. bp 160 °C (1 mmHg). Yield, 480 mg (88.0%).

Decomposition of 2-(1-*n*-Butyl-1-hydroxy-1-phenylmethyl)-1-methyl-1*H*-imidazole (7c**)**—A mixture consisting of the imidazolylmethanol (**7c**; 2.00 g), methyl iodide (5 ml), water (0.5 ml) and ethyl acetate (50 ml) was refluxed under N₂ for 31 h. The solvent was evaporated off and the residue was extracted repeatedly with ether. Removal of the solvent by distillation gave an oily residue, which was distilled under vacuum. bp 130 °C (10 mmHg). Yield, 1.14 g (86.0%). The product was identical with an authentic sample of valerophenone. The residue after the extraction with ether crystallized on standing and it was recrystallized from isopropanol-ethyl acetate to give hygroscopic needles. mp 96—100 °C (in a sealed tube). Yield, 1.16 g (63.0%). The product was identified as 1,3-dimethyl-1*H*-imidazolium iodide by comparison of the IR spectra with that of a sample obtained by quaternization of 1-methyl-1*H*-imidazole with methyl iodide.

Stability Test of 2-[(3,4-Methylenedioxyphenyl)hydroxymethyl]-1-methyl-1*H*-imidazole (4a**)**—a) A solution of **4a** (200 mg) in 20% H₂SO₄ was heated at 85 °C for 7 h then basified with solid K₂SO₃. The separated material was extracted with ethyl acetate (20 and 10 ml) and the organic layer was dried with Na₂SO₄. Removal of the solvent under reduced pressure gave a crystalline residue, which was shown to be identical with **4a** by IR and TLC comparisons. mp 126—128 °C. Yield, 198 mg (99.0%).

b) A mixture consisting of **4a** (200 mg), 1 N KOH (2 ml) and ethanol (5 ml) was refluxed at 85 °C and then the solvent was evaporated off. The residue was extracted with ethyl acetate and the solution was washed with water followed by drying with Na₂SO₄. Removal of the solvent gave a crystalline residue, which was shown to be identical

with **4a** in the same manner as in i). mp 126—129 °C. Yield, 170 mg (85.0%).

c) NaBH_4 (30 mg) was added to a solution of **4a** (50 mg) in methanol (1.5 ml) followed by stirring at room temperature overnight. The solvent was evaporated off, and then ethyl acetate (20 ml) and water (5 ml) were added to the residue. The organic layer was dried with Na_2SO_4 . Removal of the solvent gave a crystalline residue, which was shown to be identical with **4a** by IR and TLC comparisons. mp 122—126 °C. Yield, 50 mg (quantitative).

d) The imidazolylmethanol (**4a**; 232 mg) was hydrogenated in ethanol (5 ml) in the presence of 5% Pd-C (500 mg) under usual pressure for 2 h. Hydrogen uptake was not observed. The reaction mixture was filtered and the filtrate was evaporated under reduced pressure to give a crystalline residue, which was identified as **4a** by IR and TLC comparisons. mp 123—128 °C. Yield, 204 mg (88.0%).

e) The imidazolylmethanol (**4a**; 232 mg) was added to a suspension of LiAlH_4 (76 mg) in THF (2 ml) and the mixture was stirred for 20 h. Water (1 ml) and ethyl acetate (10 ml) were added to the resulting mixture and the organic layer was dried with Na_2SO_4 . Removal of the solvent under reduced pressure gave a crystalline residue, which was identified as **4a** by IR and TLC comparisons. mp 122—127 °C. Yield, 206 mg (88.8%).

f) A solution of **4a** (200 mg) in trifluoroacetic acid (2 ml) was stirred at room temperature for 24 h followed by evaporation of the reagent under reduced pressure. The residue was basified with 10% K_2CO_3 and extracted with ethyl acetate. Removal of the solvent after drying with Na_2SO_4 gave a crystalline residue, which was identical with **4a** on the basis of IR and TLC comparisons. mp 124—128 °C. Yield, 201 mg (quantitative).

Oxidation of 2-(3,4-Methylenedioxyphenyl)hydroxymethyl-1-methyl-1H-imidazole (4a)—Powdered pyridinium chlorochromate (1.72 g, 8 mmol) was added to a solution of the alcohol (**4a**; 928 mg, 4 mmol) in CH_2Cl_2 (20 ml) and the mixture was stirred for 30 min. Ether (50 ml) was added and the supernatant was passed through a column packed with Florisil. Evaporation of the eluate gave a crystalline mass. The residual chromium deposit was treated with 10% NaOH (30 ml) followed by extraction with EtOAc (30 ml \times 3). The solvent was evaporated off after drying with Na_2SO_4 to give a crystalline residue. The combined crude product was recrystallized from CCl_4 . The product was identical with **3c**. mp 104—108 °C. (lit. mp 105—107 °C).³⁾ Yield, 775 mg (84.3%).

2-(2,2-Ethylenedioxy-5-hydroxy-5-undecyl)-1-methyl-1H-imidazole (13)—2-(4,4-Ethylenedioxy-pentanoyl)-1-methyl-1H-imidazole (**12**; 1.12 g, 5 mmol)³⁾ was added at 0 °C to an ethereal solution of *n*-hexylmagnesium bromide [prepared from *n*-hexyl bromide (1.65 g, 10 mmol), magnesium (486 mg, 20 mg atom) and ether (10 ml)]. The residual magnesium metal was removed after stirring of the mixture for 2 h at room temperature followed by addition of ether (30 ml) and 10% HCl (10 ml). The aqueous layer was basified with solid K_2CO_3 and separated organic material was extracted with ethyl acetate (30 and 20 ml). Evaporation of the solvent under reduced pressure after drying with Na_2SO_4 gave a crystalline residue, which was passed through a short silica gel column with ethyl acetate. Resultant solid was recrystallized from CCl_4 -*n*-hexane to give colorless needles. mp 73—74 °C. Yield, 1.44 g (92.6%). IR (CHCl_3): 3380 cm^{-1} (OH). $^1\text{H-NMR}$ (CDCl_3) δ : 0.60—2.15 (m, 20H, $\text{CH}_3\text{CCH}_2\text{CH}_2\text{C}(\text{CH}_2)_5\text{CH}_3$), 3.74 (s, 3H NCH_3), 3.90 (s, 4H, $-\text{OCH}_2\text{CH}_2\text{O}-$), 4.26 (s, 1H, OH), 6.78 and 6.89 (d each, 1H each, imidazole H, $J=1$ Hz each). *Anal.* Calcd for $\text{C}_{17}\text{H}_{30}\text{N}_2\text{O}_3$: C, 65.77; H, 9.74; N, 9.02. Found: C, 65.63; H, 9.60; N, 8.87.

2-(5-Hydroxy-2-oxo-5-undecyl)-1-methyl-1H-imidazole (14)—The imidazolylmethanol (**13**; 930 mg, 3 mmol) was dissolved in 10% HCl (15 ml) and the solution was stirred for 15 min followed by basification with solid K_2CO_3 . The separated material was extracted with ethyl acetate (30 and 20 ml) and the organic layer was dried with Na_2SO_4 . Removal of the solvent gave a crystalline residue, which was recrystallized from ether-*n*-hexane. mp 76—78 °C. Yield, 772 mg (96.7%). IR (CHCl_3): 3410 cm^{-1} (OH). $^1\text{H-NMR}$ (CDCl_3) δ : 0.84 (t, 3H, CH_3CH_2- , $J=9$ Hz), 3.71 (s, 3H, NCH_3), 4.41 (s, 1H, $-\text{OH}$), 6.78 and 6.87 (d each, 1H each, imidazole H, $J=1$ Hz each), 1.00—2.60 (m, 17H, other protons). *Anal.* Calcd for $\text{C}_{15}\text{H}_{26}\text{N}_2\text{O}_2$: C, 67.63; H, 9.84; N, 10.52. Found: C, 67.84; H, 9.70; N, 10.65.

2,5-Undecadione (15)—Method A was used, starting from the ketonic imidazolylmethanol (**14**; 532 mg, 2 mmol), dimethyl sulphate (303 mg, 2.4 mmol) and ethyl acetate (4 ml). The oily product was purified by vacuum distillation. bp 95—100 °C (1 mmHg) [lit. bp 70 °C (0.2 mmHg)].¹³⁾ Yield, 358 mg (97.4%). This product was characterized as **15** on the basis of the following spectral data. IR (CHCl_3): 1715 cm^{-1} (C=O) [lit. value: 1715 cm^{-1} (neat)].¹³⁾ MS m/z : M^+ = 184. $^1\text{H-NMR}$ (CDCl_3) δ : 0.87 (t, 3H, CH_3CH_2- , $J=8$ Hz), 1.10—1.85 (m, 8H, $\text{CH}_3(\text{CH}_2)_4-$), 2.10 (s, 3H, $\text{CH}_3\text{CO}-$), 2.44 (t, 2H, $-\text{COCH}_2(\text{CH}_2)_4-$), 2.68 (s, 4H $-\text{COCH}_2\text{CH}_2\text{CO}-$).

General Procedure for Synthesis of Symmetric Ketones [Example: Di-2-thienylketone (6k)]—A solution of 2-butoxycarbonyl-1-methyl-1H-imidazole (**3f**; 385 mg, 2.5 mmol)⁵⁾ in ether (10 ml) was added at 0 °C to a stirred solution of 2-thienylmagnesium bromide [prepared from 2-bromothiophene (0.97 ml, 10 mmol), magnesium metal (486 mg, 20 mg atom) and ether (10 ml)]. A usual work-up for the Grignard reaction as described above afforded the corresponding imidazolylmethanol (**7k**) as a crystalline product, which was recrystallized from CCl_4 as colorless needles. mp 180.5—182 °C. Yield, 690 mg (92.6%). IR (KBr): 3500—4000 cm^{-1} (OH). $^1\text{H-NMR}$ (CDCl_3) δ : 3.30 (s, 1H, $-\text{OH}$), 3.47 (s, 3H, NCH_3), 6.77—7.45 (m, 8H, Ar-H). *Anal.* Calcd for $\text{C}_{13}\text{H}_{12}\text{OS}_2$: C, 56.50; H, 4.38; N, 10.14. Found: C, 56.25; H, 4.37; N, 9.95.

Treatment of the Imidazolylmethanols (4c and 7c) with 20% Sulfuric Acid—a) A solution of 2-(cyclohexylhydroxymethyl)-1-methyl-1H-imidazole (**4c**; 200 mg) in 20% H_2SO_4 was heated at 70 °C for 7 h and then basified with solid K_2CO_3 . The separated material was extracted with ethyl acetate and the organic layer was dried with NaSO_4 . Removal of the solvent under reduced pressure gave a crystalline residue, which was recrystallized from

ethyl acetate-*n*-hexane to give colorless needles. The product was identified as **4c** by IR and TLC comparisons. mp 108–110°C. Yield, 168 mg (84.0%).

b) 2-(Butylhydroxyphenylmethyl)-1-methyl-1*H*-imidazole (**7c**; 200 mg) was reacted as described for a), resulting in a recovery of **7c** in 89.0% yield. mp 151–152°C.

References and Notes

- 1) H. A. Staab, *Angew. Chem. Int. Ed. Engl.*, **74**, 351 (1962); H. A. Staab and W. Rohr, "Newer Methods of Organic Chemistry," ed. by Foerst, Vol. V, Academic Press, New York, 1968, p. 61.
- 2) For review: S. Ohta and M. Okamoto, *Yuki Gosei Kagaku Kyokai Shi*, **41**, 38 (1983).
- 3) S. Ohta, S. Hayakawa, H. Moriwaki, S. Harada, and M. Okamoto, *Chem. Pharm. Bull.*, **34**, 4916 (1986); S. Ohta, S. Hayakawa, H. Moriwaki, S. Tsuboi, and M. Okamoto, *Heterocycles*, **23**, 1759 (1985).
- 4) N. J. Curtis and R. S. Brown, *J. Org. Chem.*, **45**, 4038 (1980).
- 5) G. F. Kathawara, U. S. Patent 4031233 [*Chem. Abstr.*, **87**, 102332y (1977)].
- 6) R. Breslow, *J. Am. Chem. Soc.*, **80**, 3719 (1958); R. Breslow and E. McNelis, *ibid.*, **81**, 3080 (1959).
- 7) In the preliminary report, we tentatively proposed a reaction mechanism, in which initial attack of the hydroxide ion occurred at the 2-position of the imidazolium salt (**8** and **10**) to produce a pseudo-base as an intermediate. The present mechanism seems to account for the difference of reactivities between the imidazolium salts (**8** and **10**) more reasonably than the previous mechanism. [S. Ohta, S. Hayakawa, K. Nishimura, and M. Okamoto, *Tetrahedron Lett.*, **25**, 3251 (1984).]
- 8) S. Ohta and M. Okamoto, *Chem. Pharm. Bull.*, **28**, 1976 (1980).
- 9) T.-L. Ho, *Synth. Commun.*, **4**, 265 (1974) and references cited therein.
- 10) G. Stork and R. Borch, *J. Am. Chem. Soc.*, **86**, 935 (1964).
- 11) G. A. Olah, G. K. S. Prakash, and M. Arvanaghi, *Synthesis*, **1984**, 228 and references cited therein.
- 12) G. H. Coleman and D. Craig, "Organic Syntheses," Coll. Vol. II, ed. by A. H. Blatt, John Wiley and Sons, Inc., New York, 1943, p. 179.
- 13) A. Hosomi, A. Shirahata, Y. Araki, and H. Sakurai, *J. Org. Chem.*, **46**, 4631 (1981).
- 14) "Beilstein Handbuch der Organischen Chemie," H-19, p. 135.
- 15) C. Hell and O. Schael, *Chem. Ber.*, **40**, 4163 (1907).
- 16) F. Fichter and H. Schiess, *Chem. Ber.*, **34**, 1999 (1901).

[Chem. Pharm. Bull.]
35(3)1070—1075(1987)

Alkaloidal Constituents of *Hymenocallis rotata* HERB. (Amaryllidaceae)

MASARU KIHARA,^a TOMOMI KOIKE,^a YASUHIRO IMAKURA,^a
KIYOSHI KIDA,^a TETSURO SHINGU,^b
and SHIGERU KOBAYASHI*^a

*Faculty of Pharmaceutical Sciences, Tokushima University,^a Shomachi, Tokushima 770,
Japan and Faculty of Pharmaceutical Sciences, Kobe Gakuin University,^b
Ikawadani, Nishi-ku, Kobe 673, Japan*

(Received September 12, 1986)

Two new alkaloids, demethylmaritidine (4) and (–)-*N*-demethyllycoramine (5), were isolated from the bulbs of *Hymenocallis rotata* HERB. (Amaryllidaceae) together with eleven known bases, vittatine (6), alkaloid-13 (7), 3-epimacronine (8), ismine (9), pretazettine (10), lycoramine (11), lycorine (12), tazettine (13), haemanthamine (14), galanthamine (15), and *N*-demethylgalanthamine (16).

Keywords—*Hymenocallis rotata*; Amaryllidaceae; demethylmaritidine; (–)-*N*-demethyllycoramine; vittatine; alkaloid-13; 3-epimacronine; ismine; pretazettine; *N*-demethylgalanthamine

We previously reported¹⁾ the isolation of leucotamine (1), *O*-methylleucotamine (2) and 3-*O*-acetylgingimiorine (3) from *Leucojum aetivum* L. (Amaryllidaceae). This paper reports the isolation of new alkaloids, demethylmaritidine (4) and (–)-*N*-demethyllycoramine (5), together with eleven known alkaloids, vittatine (6), alkaloid-13 (7), 3-epimacronine (8), ismine (9), pretazettine (10), lycoramine (11), lycorine (12), tazettine (13), haemanthamine (14), galanthamine (15), and *N*-demethylgalanthamine (16) from the bulbs of *Hymenocallis rotata* HERB. (Amaryllidaceae). Boit and Dopke²⁾ isolated 12–15 along with hipeastrine and homolycorine from this plant.

Crude basic material extracted from fresh bulbs of *H. rotata* HERB. by the method of Wildman and Bailey³⁾ was subjected to preparative thin layer chromatography (PTLC), as described in Experimental, to give compounds 4–16.

Compound 4, a new alkaloid, was isolated as colorless prisms from acetone, mp 139–140 °C, C₁₆H₁₉NO₃ and [α]_D +22.9° (MeOH). This base gave a violet color with ferric chloride reagent. The infrared (IR) spectrum showed absorption due to a hydroxy group at 3380 cm⁻¹. In the proton nuclear magnetic resonance (¹H-NMR) spectrum, the assignment of two aromatic protons (10-H and 7-H), *O*-methyl protons (9-OMe), two olefinic protons (1-H and 2-H), and methylene protons (6-H₂) was achieved by nuclear magnetic double resonance (NMDR) analysis: irradiation at δ 3.74 (OCH₃) gave a 9.8% nuclear Overhauser effect (NOE) increment at δ 7.00 (10-H); irradiation at δ 7.00 resulted in a 15% NOE increment in the signal of 1-H (δ 6.71). Monitoring the signal of 1-H showed an internuclear double resonance (INDOR) peak at δ 6.11 (2-H), which was monitored to give INDOR peaks at δ 6.71 and 4.46 (3-H). On monitoring the signal at δ 1.83 (4-H_α), INDOR peaks were found at δ 2.26 (4-H_β), 4.46 (3-H) and 3.73 (4a-H). Monitoring the signal of the other aromatic proton (7-H) at δ 6.76 showed an INDOR peak at δ 4.44 (6-H_α). From these findings, compound 4 was concluded to have the partial formula A (see Chart 1). The similarity of the mass spectrum (MS) to that of crinine (17)⁴⁾ suggested the presence of a crinine-type skeleton or its antipode (as in maritidine

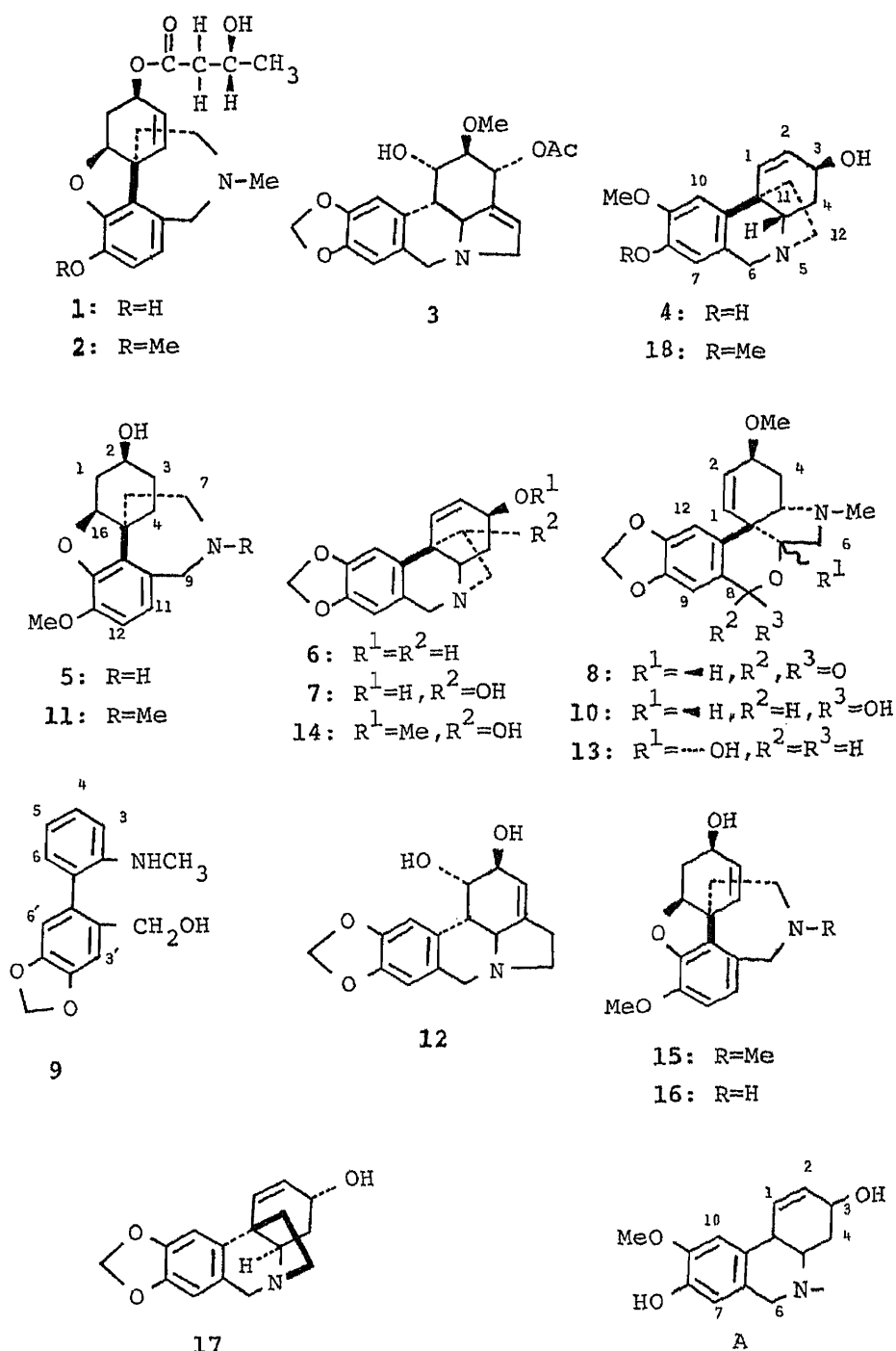


Chart 1

(18)). The ethylene bridge of 11-C and 12-C was concluded to have an α -configuration since the optical rotatory dispersion (ORD) curve of compound 4 showed a positive Cotton effect at 286 nm, similar to that of maritidine (18).⁵⁾ In the ¹H-NMR spectrum, the coupling constant (5.5 Hz) between 2-H and 3-H and the absence of an allylic coupling between 1-H and 3-H (as in the case of 18) suggested that 3-H has α -configuration. From these findings, compound 4 was concluded to be *O*-demethylmaritidine (4). Stereochemical evidence for this conclusion was obtained by conversion of 4 to maritidine (18) by methylation with diazomethane. The resulting product (mp 247–249 °C) was found to be identical with

maritidine (**18**)^{6,7)} by comparison of spectral (IR and ¹H-NMR) data.

Compound 5, a new base, was isolated as pale yellow prisms, mp 123—124 °C, C₁₆H₂₁NO₃, [α]_D -39.1° (CHCl₃). The IR spectrum showed absorptions due to a hydroxy group at 3550 cm⁻¹ and a secondary amino group at 3360 cm⁻¹. The ¹H-NMR spectrum showed the presence of aromatic protons (2H, singlet), and a methoxy group, but no signal due to an olefinic proton or an *N*-methyl group. The MS of compound 5 was similar to that of lycoramine (**11**). From these spectral data, compound 5 was assigned as (-)-*N*-demethyllycoramine (**5**). This assignment was supported by the fact that compound 5 had a similar optical rotation ([α]_D -39.1°) to that ([α]_D +38.2° (CHCl₃)) of (+)-*N*-demethyllycoramine,⁸⁾ except for its sign. For confirmation of this assignment, compound 5 was converted to lycoramine (**11**) as follows: treatment of compound 5 with boric acid, formalin, and sodium borohydride (NaBH₄) gave an *N*-methylated product, which was found to be identical with authentic **11** by direct comparison of the IR and ¹H-NMR spectra and by the mixed melting point test. Thus, compound 5 was concluded to be (-)-*N*-demethyllycoramine (**5**).

Compound 6 was isolated as colorless needles, C₁₆H₁₇NO₃, mp 204—205 °C, [α]_D +23.6° (CHCl₃). Its ¹H-NMR data (see Experimental) were very similar to those for crinine (**17**).⁹⁾ The IR spectrum (KBr) of compound 6 was identical with that of crinine (**17**).⁹⁾ The ORD curve (with a positive Cotton effect at 304 nm) for compound 6 and that (with a negative Cotton effect at 303 nm) for crinine (**17**) were antipodal. On the basis of these findings and of the fact that physical data for compound 6 were in good agreement with those reported for vittatine,¹⁰⁾ compound 6 was established to be vittatine (**6**).

Compound 7 (mp 236—237 °C, C₁₆H₁₇NO₄, [α]_D +14.3° (MeOH)) and compound 8 (amorphous powder, C₁₈H₁₉NO₅, [α]_D +225.6° (CHCl₃)) were established to be alkaloid-13 (**7**) and 3-epimacronine (**8**), respectively, on the basis of the facts that their ¹H-NMR and IR spectra were identical with those reported for **7**,^{11,12)} and **8**.¹³⁾

Compound 9, C₁₅H₁₅NO₃, was isolated as an amorphous powder. Its IR spectrum showed the presence of a hydroxy group, aromatic rings and a methylenedioxy group (see Experimental). The ¹H-NMR spectrum showed signals due to methylenedioxy protons at δ 5.98, *N*-methyl protons at δ 2.72, and six aromatic protons, of which two singlets at δ 7.04 and 6.68 indicated the presence of a 1,2,4,5-tetrasubstituted aromatic ring, and two double doublets at δ 6.80 and 6.75 and two double double doublets at δ 7.30 and 7.00 showed the presence of a second 1,2-disubstituted aromatic ring. From these findings and the ultraviolet (UV) spectrum (see Experimental), compound 9 was assigned as ismine (**9**).¹⁴⁾ This assignment was confirmed by conversion of compound 9 to its picrate, C₁₅H₁₅NO₃·C₆H₃N₃O₇, mp 156—157 °C.¹⁴⁾

Compounds 10 (amorphous; hydrochloride mp 227—229 °C (dec.)), 11 (mp 106—107 °C), 12 (mp 238—241 °C), 13 (mp 209—210 °C), 14 (mp 196—198 °C), 15 (oil), and 16 (mp 152—154 °C) were identified as pretazettine (**10**),¹⁵⁾ lycoramine (**11**),¹⁶⁾ lycorine (**12**),^{1,17)} tazettine (**13**),^{13,18)} haemanthamine (**14**),^{15,19)} galanthamine (**15**),¹⁾ *N*-demethylgalanthamine (**16**),²⁰⁾ respectively, by direct comparison of spectral data and by mixed melting point tests.

Experimental

All melting points are given as uncorrected values. The spectrophotometers used were a Hitachi IR-215 for IR spectra, a JEOL JMS-D 300 for MS, a Shimadzu UV-200 for UV spectra, a Union PM-201 for optical rotation, a JASCO ORD/UV-5 spectrometer for ORD, and a JEOL JNM-PS-100 or a Hitachi R-22 for ¹H-NMR spectra with tetramethylsilane (TMS) as an internal standard. The plates used for PTLC were coated with silica gel (Kieselgel, PF₂₅₄ Merck). The following solvent systems were used: 1) CHCl₃-MeOH-H₂O (70:15:2), 2) CHCl₃-Et₂NH (20:1), 3) CHCl₃-Et₂NH (40:1), 4) CHCl₃-MeOH (40:1), 5) CHCl₃-MeOH (10:1), 6) CHCl₃-MeOH (8:1), 7) CHCl₃-MeOH (5:1), 8) ether-MeOH (2:1), 9) benzene-Et₂NH (20:1). UV light, I₂ vapor and Dragendorff reagents

were used for location of compounds.

Isolation of Alkaloids—Following the method of Wildman and Bailey,³¹ fresh bulbs (9.8 kg) of this plant collected in our Faculty plot were ground in 99% EtOH in a mixer. The insoluble material was extracted three times with 371 of 99% EtOH. The ethanolic extract was evaporated to approximately 31 *in vacuo*, acidified (pH 4) with tartaric acid, and washed with ether to remove neutral and acidic materials. The acidic aqueous solution was made basic (pH 7.3) with conc. NH₄OH and extracted three times with 600 ml of CHCl₃. The extract was evaporated *in vacuo* to give crude alkaloid I (2.10 g, 0.021% yield). The above aqueous solution (pH 7.3) was made more basic (pH 8.0) and extracted three times with 800 ml of CHCl₃ to give crude alkaloids II (2.64 g, 0.027% yield). The aqueous solution (pH 8.0) was made more basic (pH 10.0) and treated similarly to yield crude alkaloids III (3.82 g, 0.039%). Crude alkaloids I (2.10 g from pH 7.3) were subjected to PTLC (solvent 1) to give five fractions: I-A, *Rf* 0.07—0.18; I-B, *Rf* 0.37—0.49; I-C, *Rf* 0.49—0.57; I-D, *Rf* 0.57—0.65, and I-E, *Rf* 0.65—1.00. Fraction I-A was further subjected to PTLC (solvent 2) to give pretazettine (10) (an amorphous material (41.7 mg). On PTLC (MeOH), I-B gave crude *N*-demethylgalanthamine (16, 37.4 mg; *Rf* 0—0.30) and vittatine (6, 26.2 mg; *Rf* 0.30—0.43). Fraction I-C was treated with CHCl₃ to give lycorine (12, 12.3 mg) as CHCl₃-insoluble material; the CHCl₃-soluble material was subjected to PTLC (solvent 2) to give lycoramine (11, 5.1 mg; *Rf* 0.69—0.71). Fraction I-D was subjected to PTLC (solvent 8) to give haemanthamine (14, 68 mg; *Rf* 0.43—0.61) and galanthamine (15, 6.2 mg; *Rf* 0.06—0.20). On PTLC (solvent 5), fraction I-E gave tazettine (13, 22.4 mg; *Rf* 0.41—0.44).

Crude alkaloids II (2.64 g) were subjected to PTLC (solvent 6) to give three fractions: II-A, *Rf* 0—0.15; II-B, *Rf* 0.15—0.27, and II-C, *Rf* 0.27—0.36. Fraction II-A was subjected to PTLC (solvent 2) to give crude demethylmaritidine (4, 56 mg; *Rf* 0.05—0.13), alkaloid-13 (7, 146 mg; *Rf* 0.13—0.18), pretazettine (10) as an amorphous material (537.6 mg, total 579.3 mg; *Rf* 0.56—0.65) and tazettine (13, 733 mg, total 755.6 mg; *Rf* 0.65—0.70). On PTLC (solvent 9), fraction II-B gave (–)-*N*-demethyllycoramine (5, 179.8 mg; *Rf* 0.24—0.36). Fraction II-C was subjected to PTLC (solvent 3) to give *N*-demethylgalanthamine (16, 33.3 mg, total 70.7 mg; *Rf* 0.64—0.68).

Crude alkaloids III (3.82 g) were subjected to PTLC (solvent 6) to give two fractions: III-A, *Rf* 0.66—0.80, and III-B, *Rf* 0.80—0.89. Fraction III-A was purified by PTLC (solvent 4) to afford ismine (9) as an amorphous powder (53.5 mg). On PTLC (CHCl₃), III-B gave 3-epimacronine (8, 8 mg; *Rf* 0.31—0.41).

Demethylmaritidine (4)—This crude base 4 (56.1 mg) was recrystallized from acetone to give prisms, mp 139—141 °C. [α]_D²³ + 22.9° (*c* = 0.31, MeOH). IR $\nu_{\text{max}}^{\text{KBr}}$ cm⁻¹: 3380, 1500. ¹H-NMR (pyridine-*d*₅) δ : 7.00 (1H, s, 10-H), 6.76 (1H, s, 7-H), 6.71 (1H, d, *J* = 9 Hz, 1-H), 6.11 (1H, ddd, *J* = 9, 5.5, 1 Hz, 2-H), 4.44 and 3.79 (each 1H, d, *J* = 16 Hz, 6-H₂), 4.46 (1H, dd, *J* = 5.5, 4 Hz, 3-H), 3.74 (3H, s, OCH₃), 3.73 (1H, dd, *J* = 12, 4 Hz, 4a-H), 3.43 and 2.88 (each 1H, m, 12-H₂), 2.26 (1H, ddd, *J* = 12, 4, 1 Hz, 4-H _{β}), 1.98 (2H, m, 11-H₂), 1.83 (1H, ddd, *J* = 12, 12, 4 Hz, 4-H _{α}). ORD (*c* = 0.0061, MeOH) M^{23} (nm): +1340° (350), +1790° (330), +3130° (310), +6270° (300) (peak), 0° (286), -2240° (274) (trough), 0° (258), +1790° (250), +4300° (240). MS *m/z* (%): 273 (M⁺, 30), 256 (14), 255 (64), 254 (100), 230 (10), 218 (5), 201 (25), 189 (17), 175 (10), 174 (6). High MS *m/z*: Calcd for C₁₆H₁₉NO₃: 273.1365. Found: 273.1360.

Methylation of Demethylmaritidine (4)—A mixture of 4 (9.7 mg), MeOH (1 ml) and ethereal CH₂N₂ left to stand for 3 d. Evaporation of the mixture gave a crude product (11.1 mg). This product was purified by PTLC (solvent 7) and crystallized from acetone-CHCl₃ to give maritidine (17) as colorless prisms (3.8 mg), mp 247—249 °C (dec.) (lit.^{7a} mp 253—256 °C). [α]_D²⁰ + 22.6° (*c* = 0.22, MeOH) (lit.^{7a} [α]_D²⁰ + 25.1° (MeOH)). IR $\nu_{\text{max}}^{\text{KBr}}$ cm⁻¹: 3350, 1600, 1510. ¹H-NMR (DMSO-*d*₆) δ : 6.98 (1H, s, 10-H), 6.69 (1H, d, *J* = 11 Hz, 1-H), 6.66 (1H, s, 7-H), 5.83 (1H, dd, *J* = 11, 5 Hz, 2-H), 4.77 (1H, d, *J* = 6 Hz, OH), 4.57 and 3.80 (each 1H, d, *J* = 16 Hz, 6-H₂), 4.17 (1H, br s, 3-H), 3.75 and 3.69 (each 3H, s, 2 × OCH₃). High MS *m/z*: Calcd for C₁₇H₂₁NO₃: 287.1521. Found: 287.1515.

(–)-*N*-Demethyllycoramine (5)—Crude 5 (179.8 mg) was recrystallized from acetone as colorless prisms (95.6 mg), mp 123—124 °C. [α]_D²⁹ - 39.1° (*c* = 0.95, CHCl₃). IR $\nu_{\text{max}}^{\text{KBr}}$ cm⁻¹: 3550, 3360. ¹H-NMR (CDCl₃) δ : 6.61 (2H, s, 11- and 12-H), 4.32 (1H, t, *J* = 3 Hz, 16-H), 4.04 (1H, m, 2-H), 3.90 (2H, s, 9-H₂), 3.80 (3H, s, OCH₃). MS *m/z* (%): 275 (M⁺, 15), 274 (22), 257 (100), 246 (2), 228 (22), 202 (81), 174 (73). High MS *m/z*: Calcd for C₁₆H₂₁NO₃: 275.1521. Found: 275.1579. *Anal.* Calcd for C₁₆H₂₁NO₃ · H₂O: C, 65.51; H, 7.90; N, 4.78. Found: C, 65.80; H, 7.98; N, 4.76.

Methylation of (–)-*N*-Demethyllycoramine (5)—A solution of H₃BO₃ (18.5 mg) and formalin (0.15 ml) in MeOH (1.45 ml) was added to a solution of 5 (11.4 mg) in MeOH (1.45 ml), and the mixture was stirred for 5 min. NaBH₄ (43.9 mg) was added and stirring was continued for 1 h. After addition of CH₃COOH (0.15 ml) and H₂O (4.77 ml), the mixture was concentrated *in vacuo*. The residue was made basic (pH 11) with NH₄OH and extracted with CHCl₃. The extract was washed with H₂O, dried and evaporated to give a crude product (10.2 mg). This product was crystallized from ether to give 11 as colorless needles, mp 107—110 °C. This compound was identical with an authentic sample of 11 described below as judged by direct comparison.

Vittatine (6)—The crude base 6 (26.2 mg) was crystallized from acetone as colorless needles, mp 204—205 °C (lit.¹⁰ mp 207—208 °C). [α]_D²² + 23.6° (*c* = 0.47, CHCl₃) (lit.¹⁰ [α]_D²⁵ + 26° (*c* = 0.5, CHCl₃)). IR $\nu_{\text{max}}^{\text{KBr}}$ cm⁻¹: 3150, 1500, 1480. ¹H-NMR (CDCl₃) δ : 6.86 (1H, s, 10-H), 6.60 (1H, d, *J* = 10 Hz, 1-H), 6.48 (1H, s, 7-H), 5.96 (1H, dd, *J* = 10, 5 Hz, 2-H), 4.40 and 3.74 (each 1H, d, *J* = 16 Hz, 6-H₂), 4.36 (1H, m, 3-H), 2.42 (1H, s, OH). ORD (*c* = 0.0049, MeOH) M^{22} (nm): +894° (350), +3240° (320), +6030° (304) (peak), 0° (293), -5800° (280) (trough), -5590° (270) (peak), -6930° (254) (trough), 0° (244), +5590° (240). High MS *m/z*: Calcd for C₁₆H₁₇NO₃: 271.1208. Found: 271.1209.

Alkaloid-13(7)—The crude base **7** (146 mg) was recrystallized from MeOH–acetone as colorless needles, mp 236–237°C (lit.¹¹ mp 248–250°C, lit.¹² mp 235–237°C). $[\alpha]_D^{26} + 14.3^\circ$ ($c=0.49$, MeOH) (lit.¹¹ $[\alpha]_D^{21} + 12^\circ$ ($c=0.9$, MeOH)). IR $\nu_{\max}^{\text{KBr}} \text{cm}^{-1}$: 3350, 1500, 1480. $^1\text{H-NMR}$ (CDCl_3) δ : 7.00 (1H, s, 10-H), 6.63 (1H, s, 7-H), 6.46 (1H, d, $J=10$ Hz, 1-H), 6.24 (1H, dd, $J=10, 4$ Hz, 2-H), 5.94 (2H, s, OCH_2O), 4.52 and 3.94 (each 1H, d, $J=16$ Hz, 6-H₂). High MS m/z : Calcd for $\text{C}_{16}\text{H}_{17}\text{NO}_4$; 287.1157. Found: 287.1153.

3-Epimacronine (8)—Pale yellow powder (8 mg) (lit.¹³ mp 125–127°C). $[\alpha]_D^{28} + 225.6^\circ$ ($c=0.15$, CHCl_3) (lit.¹³ $[\alpha]_D^{17} + 267.0^\circ$ ($c=0.54$, CHCl_3)). IR $\nu_{\max}^{\text{KBr}} \text{cm}^{-1}$: 1710, 1610, 1500. $^1\text{H-NMR}$ (CDCl_3) δ : 7.52 (1H, s, 9-H), 6.73 (1H, s, 12-H), 5.97 (1H, d, $J=10$ Hz, 2-H), 5.44 (1H, ddd, $J=10, 2, 2$ Hz, 1-H), 6.01 (2H, s, OCH_2O), 4.43 (1H, dd, $J=11, 8$ Hz, 6a-H), 4.12 (1H, m, 3-H), 3.40 (3H, s, OCH_3), 3.16 (1H, dd, $J=11, 10$ Hz, 6-H₂), 3.10 (1H, m, 4a-H), 2.76 (1H, dd, $J=10, 8$ Hz, 6-H₂), 2.50 (3H, s, N-CH₃). High MS m/z : Calcd for $\text{C}_{18}\text{H}_{19}\text{NO}_5$; 329.1263. Found: 329.1266.

Ismine (9)—Amorphous powder (lit.¹⁴ mp 99.5–100.5°C). IR $\nu_{\max}^{\text{KBr}} \text{cm}^{-1}$: 3400, 1600, 1580, 1040, 930. UV $\lambda_{\max}^{\text{MeOH}} \text{nm}$ ($\log \epsilon$): 241 (4.04), 292 (3.74). UV $\lambda_{\min}^{\text{MeOH}} \text{nm}$ ($\log \epsilon$): 268 (3.42). $^1\text{H-NMR}$ (CDCl_3) δ : 7.30 and 7.00 (each 1H, ddd, $J=7, 7, 2$ Hz, 5- and 4-H), 7.04 and 6.68 (each 1H, s, 3'- and 6'-H), 6.80 and 6.75 (each 1H, dd, $J=7, 2$ Hz, 6- and 3-H), 5.98 (2H, s, OCH_2O), 4.21 (2H, s, Ar-CH₂-OH), 3.00 (2H, br s, NH and OH), 2.72 (3H, s, N-CH₃). High MS m/z : Calcd for $\text{C}_{15}\text{H}_{15}\text{NO}_3$; 257.1052. Found: 257.1050. This amorphous powder was converted to its picrate as yellow prisms, mp 156–153°C (dec.) (from EtOH) (lit.¹⁴ mp 158–159°C). Anal. Calcd for $\text{C}_{21}\text{H}_{18}\text{N}_4\text{O}_{10}$: C, 51.85; H, 3.73; N, 11.52. Found: C, 51.71; H, 3.59; N, 11.15.

Pretazettine (10)—This amorphous base (**10**) (579.3 mg) was crystallized as colorless prisms of its hydrochloride, mp 227–229°C (from EtOH). Anal. Calcd for $\text{C}_{18}\text{H}_{21}\text{NO}_5 \cdot \text{HCl}$; C, 58.76; H, 6.03; N, 3.81. Found: C, 58.65; H, 6.11; N, 3.50. This hydrochloride was identical with authentic pretazettine hydrochloride¹⁵ as judged by direct comparison.

Lycoramine (11)—The crude base **11** (5.1 mg) was crystallized from ether as colorless needles, mp 106–107°C. IR $\nu_{\max}^{\text{KBr}} \text{cm}^{-1}$: 3200, 1610, 1590, 1495. $^1\text{H-NMR}$ (CDCl_3) δ : 6.61 (2H, s, 11- and 12-H), 4.00 and 3.60 (each 1H, d, $J=14$ Hz, 9-H₂), 3.99 (1H, m, 2-H), 3.80 (3H, s, OCH_3), 2.92 (1H, s, OH), 2.35 (3H, s, N-CH₃). MS m/z (%): 289 (M^+ , 65), 288 (100), 271 (2), 246 (4), 232 (11), 228 (6), 216 (7), 202 (15), 187 (14), 174 (10). This base was identical with authentic **11**¹⁶ as judged by direct comparison.

Lycorine (12)—The melting point of this base **12** (3.4 mg), 238–241°C (dec.) (from EtOH), was not depressed by admixture with an authentic sample¹⁷ of **12** and its IR spectrum was identical with that of authentic **12**.¹⁷

Tazettine (13)—The crude base **13** (755.6 mg) was recrystallized from EtOH as colorless needles, mp 209–210°C (dec.). Anal. Calcd for $\text{C}_{18}\text{H}_{21}\text{NO}_5$; C, 65.24; H, 6.39; N, 4.23. Found: C, 65.11; H, 6.53; N, 4.12. This base was identical with authentic **13**¹³ as judged by direct comparison.

Haemanthamine (14)—The base (**14**, 41.9 mg), mp 196–198°C, $[\alpha]_D^{22} + 15.9^\circ$ ($c=0.25$, MeOH) was obtained by recrystallization of crude base (68.0 mg) from EtOH. High MS m/z : Calcd for $\text{C}_{17}\text{H}_{19}\text{NO}_4$; 301.1313. Found: 301.1309. This compound **14** was identical with authentic **14**¹⁵ as judged by direct comparison.

Galanthamine (15)—This base **15** (6.2 mg), an oil (lit.¹⁸ mp 125–126°C), was shown to be identical with authentic **15**¹⁹ by comparisons of TLC behavior, and ORD and $^1\text{H-NMR}$ spectral data.

N-Demethylgalanthamine (16)—The crude base **16** (70.7 mg) was crystallized from acetone as colorless needles, mp 152–153°C. $[\alpha]_D^{21} - 72.9^\circ$ ($c=0.29$, CHCl_3). High MS m/z : Calcd for $\text{C}_{16}\text{H}_{19}\text{NO}_3$; 273.1365. Found: 273.1332. This base **16** was found to be identical with authentic **16**²⁰ as judged by direct comparison.

Acknowledgement This work was supported by a Grant-in-Aid for Scientific Research from the Ministry of Education, Science, and Culture of Japan.

References

- 1) S. Kobayashi, M. Kihara, K. Yuasa, Y. Imakura, T. Shingu, A. Kato, and T. Hashimoto, *Chem. Pharm. Bull.*, **33**, 5258 (1985).
- 2) H. G. Boit and W. Dopke, *Naturwissenschaften*, **45**, 315 (1958).
- 3) W. C. Wildman and D. T. Bailey, *J. Org. Chem.*, **33**, 3749 (1968).
- 4) A. M. Duffield, R. T. Aplin, H. Budzikiewicz, Carl Djerassi, C. F. Murphy, and W. C. Wildman, *J. Am. Chem. Soc.*, **87**, 4902 (1965).
- 5) G. G. DeAngelis and W. C. Wildman, *Tetrahedron Lett.*, **1969**, 729.
- 6) N. A. Schwartz and R. A. Holton, *J. Am. Chem. Soc.*, **92**, 1090 (1970).
- 7) a) S. Yamada, K. Tomioka, and K. Koga, *Tetrahedron Lett.*, **1976**, 57; b) K. Tomioka, K. Koga, and S. Yamada, *Chem. Pharm. Bull.*, **25**, 2681 (1977).
- 8) S. M. Laiho and H. M. Fales, *J. Am. Chem. Soc.*, **86**, 4434 (1964).
- 9) S. Kobayashi, T. Tokumoto, M. Kihara, Y. Imakura, T. Shingu, and Z. Taira, *Chem. Pharm. Bull.*, **32**, 3015 (1984).
- 10) H. G. Boit and H. Emke, *Chem. Ber.*, **90**, 369 (1957).
- 11) W. C. Wildman, C. Brown, K. H. Michel, D. Bailey, N. Heimer, R. Shaffer, and C. Murphy, *Pharmazie*, **22**, 725

-
- (1967).
- 12) F. Sandberg and K. H. Michel, *Lloydia*, **26**, 78 (1963).
 - 13) S. Kobayashi, M. Kihara, T. Shingu, and K. Shingu, *Chem. Pharm. Bull.*, **28**, 2924 (1980).
 - 14) R. J. Hight, *J. Org. Chem.*, **26**, 4767 (1961).
 - 15) S. Kobayashi, H. Ishikawa, M. Kihara, T. Shingu, and T. Hashimoto, *Chem. Pharm. Bull.*, **25**, 2244 (1977).
 - 16) S. Kobayashi, K. Yuasa, Y. Imakura, M. Kihara, and T. Shingu, *Chem. Pharm. Bull.*, **28**, 3433 (1980).
 - 17) S. Kobayashi, S. Takeda, H. Ishikawa, H. Matsumoto, M. Kihara, T. Shingu, A. Numata, and S. Uyeo, *Chem. Pharm. Bull.*, **24**, 1537 (1976).
 - 18) W. C. Wildman and C. J. Kaufman, *J. Am. Chem. Soc.*, **76**, 5815 (1954).
 - 19) H. M. Fales, L. D. Giuffrida, and W. C. Wildman, *J. Am. Chem. Soc.*, **78**, 4145 (1956).
 - 20) S. Kobayashi, H. Ishikawa, M. Kihara, T. Shingu, and S. Uyeo, *Chem. Pharm. Bull.*, **24**, 2553 (1976).

[Chem. Pharm. Bull.]
35(3)1076-1084(1987)]

Studies on Peptides. CXLVIII.^{1,2)} Application of a New Deprotecting Procedure with Trimethylsilyl Trifluoromethanesulfonate for the Syntheses of Two Porcine Spinal Cord Peptides, Neuromedin U-8 and Neuromedin U-25

NOBUTAKA FUJII,^a OSAMU IKEMURA,^a SUSUMU FUNAKOSHI,^a HISAYUKI MATSUO,^b
TOMIO SEGAWA,^c YOSHIHIRO NAKATA,^c ATSUKO INOUE,^c
and HARUAKI YAJIMA*^a

*Faculty of Pharmaceutical Sciences, Kyoto University,^a Sakyo-ku, Kyoto 606, Japan,
Department of Biochemistry and Anesthesiology, Miyazaki Medical College,^b
Kiyotake, Miyazaki 889-16, Japan and Institute of Pharmaceutical Sciences,
School of Medicine, Hiroshima University,^c Hiroshima 734, Japan*

(Received September 19, 1986)

The usefulness of a new deprotecting procedure was demonstrated in the solution syntheses of two porcine spinal cord peptides, designated neuromedin U-8 and neuromedin U-25. Protected neuromedin U-8 (8-residue peptide), prepared by condensation of two fragments, served as a C-terminal amino component for the synthesis of neuromedin U-25 (25-residue peptide). Onto this fragment, five peptide fragments were successively condensed by the azide procedure to construct the entire amino acid sequence of neuromedin U-25, a possible biosynthetic precursor of neuromedin U-8. All protecting groups were cleaved from protected neuromedin U-8 and neuromedin U-25 by 1 M trimethylsilyl trifluoromethanesulfonate-thioanisole in trifluoroacetic acid. The results were compared with those obtained by trifluoromethanesulfonic acid deprotection. In terms of contractile activity in rat uterus, neuromedin U-25 was twice as active as neuromedin U-8.

Keywords—porcine spinal cord peptide; neuromedin U-8; neuromedin U-25; thioanisole-mediated deprotection; trifluoromethanesulfonic acid deprotection; deprotecting reagent; trimethylsilyl trifluoromethanesulfonate; uterus contractile activity

Recently, we³⁾ found that trimethylsilyl trifluoromethanesulfonate (trimethylsilyl triflate, TMSOTf) cleaved various protecting groups currently employed in peptide synthesis more readily than TFMSA.⁴⁾ By using this newly found deprotecting reagent, we synthesized two peptides isolated by Minamino *et al.*⁵⁾ from porcine spinal cord; an 8-residue peptide and a 25-residue peptide, designated neuromedin U-8 and neuromedin U-25, respectively. Their sequence analysis revealed that U-25 contained the U-8 sequence, preceded by paired Arg residues, a typical biosynthetic processing signal.⁶⁾ Thus, U-8 is thought very likely to be processed biologically from U-25. Their C-terminal amide structures were confirmed by the solid phase synthesis.⁵⁾ Following our syntheses of neuromedins B, C,⁷⁾ K and L,⁸⁾ we synthesized U-8 and U-25 in order to examine the relationship between structure and function of these neurocandidate peptides. In combination with the TFA-labile Z(OMe) group,⁹⁾ amino acid derivatives bearing protecting groups removable by 1 M TFMSA-thioanisole/TFA⁴⁾ were employed, *i.e.*, Arg (Mts),¹⁰⁾ Asp(OBzl), Glu (OBzl), and Lys (Z). Later it was found that these side chain protecting groups could be cleaved more smoothly when TFMSA was replaced by TMSOTf.³⁾ Thus, in the final steps of the syntheses, deprotections were performed in two ways and the results were compared. Six peptide fragments served to construct the entire amino acid sequence of U-25, as shown in Fig. 1. U-8 was ob-

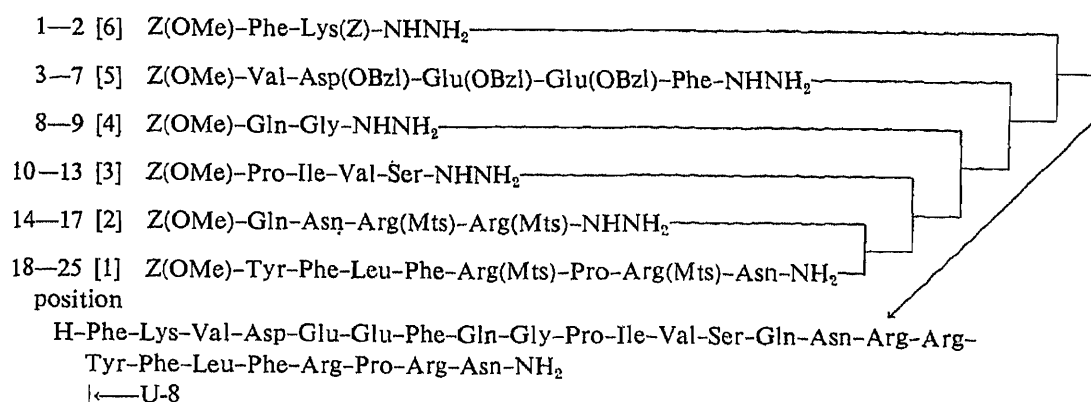


Fig. 1. Synthetic Route to Neuromedin U-25

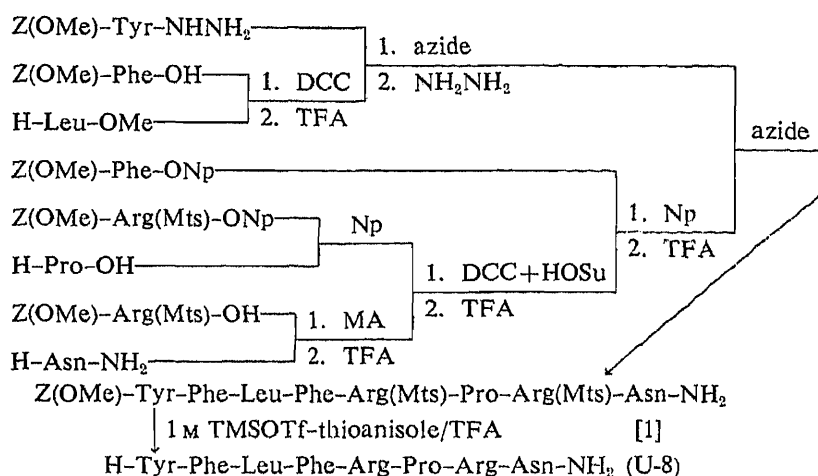


Fig. 2. Synthetic Scheme for the Protected Octapeptide Amide [1] and U-8

tained by deprotection of the C-terminal octapeptide fragment [1].

Fragment [1], Z(OMe)-Tyr-Phe-Leu-Phe-Arg(Mts)-Pro-Arg(Mts)-Asn-NH₂ (positions 18—25 of U-25, protected U-8), was prepared, according to the scheme shown in Fig. 2, by azide condensation¹¹⁾ of two components, Z(OMe)-Phe-Arg(Mts)-Pro-Arg(Mts)-Asn-NH₂ (component 1) and Z(OMe)-Tyr-Phe-Leu-NHNH₂ (component 2). First, Z(OMe)-Arg(Mts)-Pro-OH, prepared by the Np method,¹²⁾ was condensed by DCC in the presence of HOSu¹³⁾ with a TFA-treated sample of Z(OMe)-Arg(Mts)-Asn-NH₂ prepared by the mixed anhydride (MA) method.¹⁴⁾ The resulting protected tetrapeptide amide was treated with TFA, then condensed with Z(OMe)-Phe-OH by the Np method to give component 1. Component 2 was prepared by the azide condensation of Z(OMe)-Tyr-NHNH₂ with a TFA-treated sample of Z(OMe)-Phe-Leu-OMe,¹⁵⁾ followed by the usual hydrazine treatment of the resulting protected tripeptide ester. The purity of fragment [1], prepared by condensation of these two components, was ascertained by thin layer chromatography (TLC), elemental analysis and amino acid analysis after 6N HCl hydrolysis, as was done with other fragments. This protected octapeptide [1] served as a key intermediate for the synthesis of U-25, and its deprotection with 1 M TMSOTf-thioanisole/TFA afforded U-8. In this deprotecting step, the time required for complete removal of the two Mts groups from protected U-8 was less than 60 min in an ice-bath, while removal by 1 M TFMSA-thioanisole/TFA required 120 min.

Fragment [2], Z(OMe)-Gln-Asn-Arg(Mts)-Arg(Mts)-NHNH₂ (positions 14—17), was prepared by stepwise Np additions of two residues, Asn and Gln, to a TFA-treated sample of

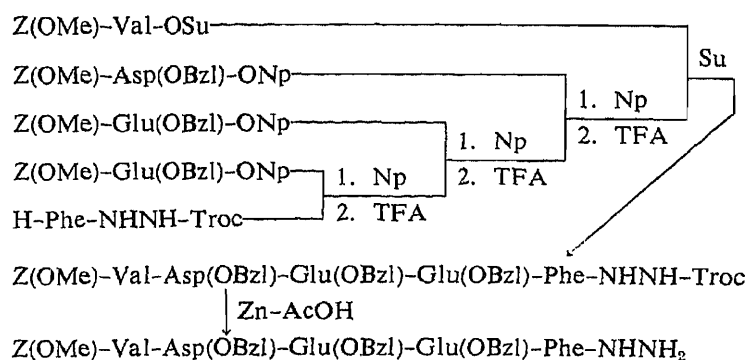


Fig. 3. Synthetic Scheme for the Protected Pentapeptide Hydrazide [5] (Positions 3—7)

Z(OMe)-Arg(Mts)-Arg(Mts)-OMe,¹⁶⁾ followed by the usual hydrazine treatment of the resulting protected tetrapeptide ester. Fragment [3], Z(OMe)-Pro-Ile-Val-Ser-NHNH₂ (position 10—13), was prepared in a stepwise manner also starting from a TFA-treated sample of Z(OMe)-Val-Ser-OMe.¹⁷⁾ The active Np and the MA methods were employed to introduce two residues, Ile and Pro, respectively and the resulting tetrapeptide ester was converted to [3] by hydrazine treatment as stated above. Fragment [4], Z(OMe)-Gln-Gly-NHNH₂ (positions 8—9), was easily obtained by hydrazine treatment of the known dipeptide ester, Z(OMe)-Gln-Gly-OMe.¹⁸⁾

Fragment [5], Z(OMe)-Val-Asp(OBzl)-Glu(OBzl)-Glu(OBzl)-Phe-NHNH₂ (positions 3—7) was prepared in a stepwise manner starting from H-Phe-NHNH-Troc as shown in Fig. 3. The Np method was employed for condensations of two Glu(OBzl) and one Asp(OBzl) residues and the Su method¹⁹⁾ for Z(OMe)-Val-OH. The Troc group was removed from the resulting protected pentapeptide derivative by treatment with Zn powder²⁰⁾ to give [5]. The N-terminal fragment, Z(OMe)-Phe-Lys(Z)-NHNH₂ (positions 1 and 2), was prepared by the usual hydrazine treatment of the corresponding dipeptide ester, which was easily prepared by the Np method.

Six peptide fragments thus obtained were assembled successively by the azide procedure to minimize racemization. DMF was employed as a solvent, and the amount of the acyl component was increased from 1.2 to 2 equivalents as chain elongation progressed. The products were purified either by precipitation from DMF with an appropriate solvent, such as AcOEt or MeOH or by gel-filtration on Sephadex LH-20 using DMF as an eluant. Throughout the synthesis, Leu was used as a diagnostic amino acid in acid hydrolysis in order to ascertain the homogeneity of each product. Recovery of Leu was compared with those of newly added amino acids after each condensation. Thus, satisfactory incorporation of each fragment was ascertained (Table I).

In the final step, protected U-25 was treated with 1 M TMSOTf-thioanisole/TFA in the presence of *m*-cresol and EDT in an ice-bath for 60 min to remove all protecting groups employed. The deprotected peptide was briefly treated with dil. ammonia to reverse any possible N→O shift²¹⁾ at the Ser residue. In this step, ammonium fluoride was added to ensure the complete hydrolysis of the O-trimethylsilyl groups possibly attached at the Ser and Tyr residues. The treated peptide was purified by gel-filtration on Sephadex G-25, followed by reversed-phase high performance liquid chromatography (HPLC) on a TSK-GEL LS-410KG column using isocratic elution of 26% acetonitrile in 0.1% TFA. Synthetic U-25 thus purified exhibited a sharp single spot on TLC and a single peak in analytical HPLC and behaved as a single component on disc isoelectrophoresis. Its 6 N HCl hydrolysate (Table I) and its leucine-aminopeptidase (LAP) digest contained amino acids in the ratios predicted by theory. The

TABLE I. Amino Acid Ratios in 6N HCl Hydrolysates of Synthetic Neuromedin U-25 and Its Intermediates

	Protected peptides						Syn. U-25	Residue
	18—25	14—25	10—25	8—25	3—25	1—25		
Asp	1.03	2.20	2.16	1.95	3.30	3.29	3.02	(3)
Ser			0.94	0.79	0.92	0.82	0.78	(1)
Glu		1.09	1.10	2.01	4.46	4.47	4.02	(4)
Gly				1.02	1.14	1.11	1.14	(1)
Val			0.72	0.73	1.64	1.94	1.87	(2)
Ile			0.69	0.75	0.80	0.93	0.94	(1)
Leu	1.00	1.00	1.00	1.00	1.00	1.00	1.00	(1)
Tyr	0.94	0.97	0.97	0.98	0.96	1.02	1.01	(1)
Phe	1.99	2.11	2.07	1.97	3.19	4.10	3.71	(4)
Lys						0.93	1.04	(1)
Arg	2.07	4.38	4.28	3.92	4.24	4.03	3.84	(4)
Pro	0.97	1.07	2.09	1.99	2.15	2.35	1.93	(2)
Recov. (%)	92	83	80	90	80	85	78	

overall yield from protected U-25 in the present new deprotecting procedure was 52%. For comparison, deprotection by using 1 M TFMSA-thioanisole/TFA was carried out. Protected U-25 was treated with the above reagents for 150 min, then purified as stated above, except for ammonium fluoride treatment. The overall yield in this experiment was 47%. To determine optimal deprotecting conditions, we preliminarily treated a small amount of each sample with either one of the reagents and examined the purity of the product by HPLC. The rate of deprotection by TMSOTf was clearly faster than that by TFMSA. In preparative experiments, U-8 and U-25 were obtained in better yields by the new procedure than by the TFMSA deprotecting procedure as stated above. On the basis of these experimental results, we consider that our new deprotecting procedure with TMSOTf is applicable to practical peptide synthesis, and is superior to the previous TFMSA deprotecting procedure.

The biological activity of neuromedin U-25 on rat uterus contraction was compared with that of U-8. Isolated uterus from female rats of the Wistar strain (about 200 g body weight) was suspended in a bath containing modified Locke-Ringer solution (35 °C) bubbled with 95% O₂-5% CO₂ and the contraction was recorded with a recticorder (KN 260, Natsume Seisakusho Co., Ltd.) via an isotonic transducer (KN 259). With regard to uterus stimulating activity (molar basis), neuromedin U-25 was about twice as potent as neuromedin U-8.

Experimental

General experimental procedures described herein are essentially the same as described in part CXXXIX²²⁾ of this series. Prior to condensation, the N^α-Z(OMe) group was removed by treatment with TFA in the presence of anisole. The active ester reaction was performed at room temperature. An azide was prepared with isoamyl nitrite and the reaction was performed at 4 °C. A mixed anhydride (MA) was prepared with isobutyl chloroformate, then the reaction was performed in an ice-bath. Unless otherwise stated, products were purified by one of the following procedures. A (extraction procedure): The product was dissolved in AcOEt. The organic phase was washed with 5% citric acid, 5% NaHCO₃ and H₂O-NaCl, dried over Na₂SO₄ and concentrated. The residue was recrystallized or precipitated from appropriate solvents. B (washing procedure): After evaporation of the solvent, the residue was treated with 5% citric acid and ether, then the resulting powder was washed with 5% citric acid, 5% NaHCO₃ and H₂O, and recrystallized or precipitated from appropriate solvents. C (gel-filtration procedure): The product partially purified by procedure B was dissolved in a small amount of DMF and a solution was applied to a column of Sephadex LH-20, which was eluted with DMF. Fractions (6.5 ml each) corresponding to the front main peak (monitored by ultraviolet absorption (UV) measurement at 275 nm) were combined and the solvent was removed by

evaporation *in vacuo*. The residue was precipitated from DMF with ether.

R_f values in TLC performed on silica gel (Kieselgel G, Merck) refer to the following solvent systems: *R_{f1}* CHCl₃-MeOH (10:0.5), *R_{f2}* CHCl₃-MeOH-H₂O (8:3:1), *R_{f3}* *n*-BuOH-AcOH-pyridine-H₂O (4:1:1:2), *R_{f4}* *n*-BuOH-AcOH-pyridine-H₂O (30:6:20:24). HPLC was conducted with a Waters 204 compact model. LAP was purchased from Sigma (Lot. No. L-6007).

Z(OMe)-Arg(Mts)-Asn-NH₂—The title compound was prepared by the MA method and purified by procedure B, followed by precipitation from DMF with AcOEt; yield 86%, mp 191–195 °C, $[\alpha]_D^{25} -5.3^\circ$ ($c=0.9$, DMF), *R_{f2}* 0.61. *Anal.* Calcd for C₂₈H₃₉N₇O₈S: C, 53.07; H, 6.20; N, 15.47. Found: C, 53.40; H, 6.34; N, 15.16.

Z(OMe)-Arg(Mts)-Pro-OH—A mixture of DCC (5.67 g, 27.5 mmol), Z(OMe)-Arg(Mts)-OH (13.01 g, 25.0 mmol) and *N_p*-OH (5.06 g, 27.5 mmol) in THF (150 ml) was stirred for 5 h. The filtered solution was added to a solution of H-Pro-OH (8.64 g, 75.0 mmol) in H₂O (30 ml) containing Et₃N (13.9 ml, 0.1 mol) and the mixture was stirred for 24 h. The solvent was evaporated off and the residue was dissolved in 5% NH₄OH. The aqueous phase, after being washed with AcOEt, was acidified with 5% citric acid and the resulting precipitate was extracted with AcOEt. The extract was washed with H₂O-NaCl, dried over Na₂SO₄ and concentrated. The residue was recrystallized from AcOEt and ether; yield 12.30 g (80%), mp 101–104 °C, $[\alpha]_D^{25} -23.3^\circ$ ($c=0.9$, MeOH), *R_{f2}* 0.54. *Anal.* Calcd for C₂₉H₃₉N₅O₈S: C, 56.38; H, 6.36; N, 11.34. Found: C, 56.38; H, 6.41; N, 11.41.

Z(OMe)-Arg(Mts)-Pro-Arg(Mts)-Asn-NH₂—A mixture of Z(OMe)-Arg(Mts)-Pro-OH (10.19 g, 16.5 mmol), SuOH (2.09 g, 18.2 mmol) and DCC (3.75 g, 18.2 mmol) in THF (100 ml) was stirred for 5 h and filtered. The filtrate was added to a solution of a TFA-treated sample of Z(OMe)-Arg(Mts)-Asn-NH₂ (9.51 g, 15.0 mmol) and Et₃N (4.59 ml, 32.9 mmol) in DMF (100 ml) and the mixture was stirred overnight. The solvent was removed by evaporation and the residue was purified by procedure B, followed by precipitation from DMF with AcOEt; yield 12.58 g (78%), mp 137–139 °C, $[\alpha]_D^{23} -18.7^\circ$ ($c=1.0$, DMF), *R_{f2}* 0.58. *Anal.* Calcd for C₄₈H₆₈N₁₂O₁₂S₂·H₂O: C, 53.02; H, 6.49; N, 15.46. Found: C, 53.10; H, 6.65; N, 15.28.

Z(OMe)-Phe-Arg(Mts)-Pro-Arg(Mts)-Asn-NH₂ (Positions 21–25)—A mixture of Z(OMe)-Phe-ONp (4.32 g 9.60 mmol), Et₃N (2.45 ml, 17.6 mmol) and a TFA-treated sample of the above protected tetrapeptide amide (8.55 g, 8.0 mmol) in DMF (100 ml) was stirred overnight and concentrated. The residue was purified by procedure B, followed by precipitation from DMF with AcOEt; yield 7.59 g (78%), mp 144–147 °C, $[\alpha]_D^{23} -15.7^\circ$ ($c=1.0$, DMF), *R_{f2}* 0.68. Amino acid ratios in a 6 N HCl hydrolysate: Phe 1.00, Arg 2.05, Pro 0.95, Asp 1.00 (recovery of Asp, 83%). *Anal.* Calcd for C₅₇H₇₇N₁₃O₁₃S₂·1/2H₂O: C, 55.86; H, 6.42; N, 14.86. Found: C, 55.74; H, 6.39; N, 14.75.

Z(OMe)-Tyr-Phe-Leu-OMe—The azide [prepared from 6.47 g (18.0 mmol) of Z(OMe)-Tyr-NHNH₂] in DMF (60 ml) and Et₃N (2.51 ml, 18.0 mmol) were added to an ice-chilled solution of a TFA-treated sample of Z(OMe)-Phe-Leu-OMe²⁰ⁱ (6.85 g, 15.0 mmol) in DMF (60 ml) containing Et₃N (2.09 ml, 15 mmol), then the solution was stirred overnight and the solvent was removed by evaporation. The residue was purified by procedure A, followed by recrystallization from AcOEt and ether; yield 7.90 g (85%), mp 183–185 °C, $[\alpha]_D^{23} -28.8^\circ$ ($c=1.8$, MeOH), *R_{f1}* 0.37. *Anal.* Calcd for C₃₄H₄₁N₃O₈·1/2H₂O: C, 64.95; H, 6.73; N, 6.68. Found: C, 65.07; H, 6.74; N, 6.92.

Z(OMe)-Tyr-Phe-Leu-NHNH₂ (Positions 18–20)—The above tripeptide ester (6.20 g, 10.0 mmol) in MeOH (60 ml) was treated with 80% hydrazine hydrate (1.90 ml, 3 eq) at room temperature overnight. The solution was concentrated and the residue was precipitated from DMF with MeOH, yield 5.32 g (86%), mp 224–226 °C, $[\alpha]_D^{23} -37.0^\circ$ ($c=1.0$, DMF), *R_{f2}* 0.59. Amino acid ratios in a 6 N HCl hydrolysate: Tyr 0.97, Phe 1.01, Leu 1.00 (recovery of Leu, 93%). *Anal.* Calcd for C₃₃H₄₁N₅O₇: C, 63.96; H, 6.67; N, 11.30. Found: C, 63.88; H, 6.59; N, 11.27.

Z(OMe)-Tyr-Phe-Leu-Phe-Arg(Mts)-Pro-Arg(Mts)-Asn-NH₂ [1] (Positions 18–25)—The azide [prepared from 3.72 g (6 mmol) of Z(OMe)-Tyr-Phe-Leu-NHNH₂] in DMF (40 ml) and Et₃N (0.84 ml, 6 mmol) were added to an ice-chilled solution of a TFA-treated sample of Z(OMe)-Phe-Arg(Mts)-Pro-Arg(Mts)-Asn-NH₂ (4.87 g, 4.0 mmol) in DMF (50 ml) containing Et₃N (0.56 ml, 4.0 mmol). The solution was stirred overnight and concentrated. The residue was purified by procedure B, followed by precipitation from DMF with AcOEt; yield 4.88 g (74%), $[\alpha]_D^{23} -49.5^\circ$ ($c=1.0$, DMF), *R_{f2}* 0.57. Amino acid ratios in a 6 N HCl hydrolysate: Tyr 0.91, Phe 1.94, Leu 0.97, Arg 2.01, Pro 0.95, Asp 1.00 (recovery of Asp, 95%). *Anal.* Calcd for C₈₁H₁₀₆N₁₆O₁₇S₂·3/2H₂O: C, 58.36; H, 6.59; N, 13.45. Found: C, 58.16; H, 6.59; N, 13.68.

Z(OMe)-Asn-Arg(Mts)-Arg(Mts)-OMe—A mixture of Z(OMe)-Asn-ONp (3.51 g, 8.40 mmol), Et₃N (2.15 ml, 15.4 mmol) and a TFA-treated sample of Z(OMe)-Arg(Mts)-Arg(Mts)-OMe¹⁶ⁱ (6.11 g, 7.0 mmol) in DMF (100 ml) was stirred overnight and concentrated. The residue was purified by procedure A, followed by recrystallization from MeOH and ether; yield 5.64 g (82%), mp 127–130 °C, $[\alpha]_D^{23} -13.9^\circ$ ($c=1.4$, MeOH), *R_{f2}* 0.64. *Anal.* Calcd for C₄₄H₆₂N₁₀O₁₂S₂·3/2H₂O: C, 52.11; H, 6.46; N, 13.81. Found: C, 52.26; H, 6.39; N, 13.31.

Z(OMe)-Gln-Asn-Arg(Mts)-Arg(Mts)-OMe—A mixture of Z(OMe)-Gln-ONp (4.66 g, 10.8 mmol), Et₃N (2.75 ml, 19.8 mmol) and a TFA-treated sample of the above protected tripeptide (8.88 g, 9.0 mmol) in DMF (120 ml) was stirred overnight and concentrated. The residue was purified by procedure B, followed by precipitation from DMF with AcOEt; yield 7.22 g (72%), mp 125–128 °C, $[\alpha]_D^{23} -13.8^\circ$ ($c=1.3$, DMF), *R_{f2}* 0.56. *Anal.* Calcd for C₄₉H₇₀N₁₂O₁₄S₂·1/2H₂O: C, 52.34; H, 6.37; N, 14.95. Found: C, 52.45; H, 6.71; N, 14.85.

Z(OMe)-Gln-Asn-Arg(Mts)-Arg(Mts)-NHNH₂[2] (Positions 14–17)—The above protected tetrapeptide

ester (3.92 g, 3.51 mmol) in DMF (40 ml) was treated with 80% hydrazine hydrate (1.1 ml, 5 eq) at room temperature overnight. The solvent was removed by evaporation and the residue was precipitated from DMF with MeOH; yield 3.15 g (80%), mp 146–148 °C, $[\alpha]_D^{23} -6.0^\circ$ ($c=0.7$, DMF), R_f 0.55. Amino acid ratios in a 6N HCl hydrolysate: Glu 1.00, Asp 1.03, Arg 1.99 (recovery of Glu, 83%). *Anal.* Calcd for $C_{48}H_{70}N_{14}O_{13}S_2 \cdot H_2O$: C, 50.87; H, 6.40; N, 17.30. Found: C, 50.74; H, 6.23; N, 17.29.

Z(OMe)-Ile-Val-Ser-OMe—A mixture of Z(OMe)-Ile-ONp (7.50 g, 18.0 mmol), Et_3N (4.60 ml, 33.0 mmol) and a TFA-treated sample of Z(OMe)-Val-Ser-OMe¹⁷⁾ (5.74 g, 15.0 mmol) in DMF (100 ml) was stirred overnight and concentrated. The residue was purified by procedure B, followed by precipitation from DMF with ether; yield 6.53 g (88%), mp 225–228 °C, $[\alpha]_D^{23} -2.2^\circ$ ($c=0.9$, DMF), R_f 0.88. *Anal.* Calcd for $C_{24}H_{37}N_3O_8$: C, 58.17; H, 7.53; N, 8.48. Found: C, 58.35; H, 7.75; N, 8.74.

Z(OMe)-Pro-Ile-Val-Ser-OMe—A MA [prepared from 4.97 g (10.8 mmol) of Z(OMe)-Pro-OH·DCHA] in THF (50 ml) was added to an ice-chilled solution of a TFA-treated sample of the above protected tripeptide ester (4.46 g, 9.0 mmol) in DMF (50 ml) containing Et_3N (1.25 ml, 9.0 mmol) and the solution was stirred for 5 h. The solution was concentrated and the residue was purified by procedure B, followed by precipitation from DMF with AcOEt; yield 4.03 g (76%), mp 217–219 °C, $[\alpha]_D^{23} -34.1^\circ$ ($c=0.9$, DMF), R_f 0.82. *Anal.* Calcd for $C_{29}H_{44}N_4O_9$: C, 58.77; H, 7.48; N, 9.45. Found: C, 58.93; H, 7.63; N, 9.62.

Z(OMe)-Pro-Ile-Val-Ser-NHNH₂ [3] (Positions 10–13)—The above protected tetrapeptide ester (5.93 g, 10.0 mmol) in DMF (100 ml) was treated with 80% hydrazine hydrate (3.13 ml, 5 eq) overnight. The solvent was evaporated off and the residue was precipitated from DMF with MeOH; yield 5.22 g (88%), mp 244–247 °C, $[\alpha]_D^{23} -26.1^\circ$ ($c=1.3$, DMF), R_f 0.58. Amino acid ratios in a 6N HCl hydrolysate: Pro 0.98, Ile 1.02, Val 0.97, Ser 1.00 (recovery of Ser, 86%). *Anal.* Calcd for $C_{28}H_{44}N_6O_8$: C, 56.74; H, 7.48; N, 14.18. Found: C, 56.48; H, 7.47; N, 14.00.

Z(OMe)-Gln-Gly-NHNH₂ [4] (Positions 8–9)—Z(OMe)-Gln-Gly-OMe¹⁸⁾ (3.81 g, 10.0 mmol) in DMF (30 ml) was treated with 80% hydrazine hydrate (3.13 ml, 5 eq) as stated above and purified by precipitation from DMF with MeOH; yield 3.13 g (82%), mp 195–197 °C, $[\alpha]_D^{23} -2.1^\circ$ ($c=0.9$, DMF), R_f 0.38. Amino acid ratios in a 6N HCl hydrolysate: Glu 0.98, Gly 1.00 (recovery of Gly, 90%). *Anal.* Calcd for $C_{16}H_{23}N_5O_6$: C, 50.39; H, 6.08; N, 18.36. Found: C, 50.29; H, 5.97; N, 18.54.

Z(OMe)-Glu(OBzl)-Phe-NHNH-Troc—A mixture of Z(OMe)-Glu(OBzl)-ONp (11.29 g, 21.6 mmol), Et_3N (5.52 ml, 39.6 mmol) and a TFA-treated sample of Z(OMe)-Phe-NHNH-Troc (9.34 g, 18.0 mmol) in DMF (150 ml) was stirred overnight and concentrated. The product was purified by procedure A, followed by recrystallization from MeOH; yield 9.75 g (73%), mp 151–154 °C, $[\alpha]_D^{23} -16.4^\circ$ ($c=0.8$, DMF), R_f 0.78. *Anal.* Calcd for $C_{33}H_{45}Cl_3N_4O_9$: C, 53.70; H, 4.78; N, 7.59. Found: C, 53.89; H, 4.76; N, 7.63.

Z(OMe)-Glu(OBzl)-Glu(OBzl)-Phe-NHNH-Troc—A mixture of Z(OMe)-Glu(OBzl)-ONp (5.96 g, 11.4 mmol), Et_3N (2.91 ml, 20.9 mmol) and a TFA-treated sample of the above dipeptide derivative (7.01 g, 9.50 mmol) in DMF (100 ml) was stirred overnight and concentrated. The product was purified by procedure A, followed by recrystallization from MeOH; yield 7.64 g (84%), mp 120–121 °C, $[\alpha]_D^{23} -12.5^\circ$ ($c=1.0$, DMF), R_f 0.75. *Anal.* Calcd for $C_{45}H_{48}Cl_3N_5O_{12}$: C, 56.46; H, 5.05; N, 7.32. Found: C, 56.37; H, 5.22; N, 7.70.

Z(OMe)-Asp(OBzl)-Glu(OBzl)-Glu(OBzl)-Phe-NHNH-Troc—A mixture of Z(OMe)-Asp(OBzl)-ONp (4.27 g, 8.40 mmol), Et_3N (2.15 ml, 15.4 mmol) and a TFA-treated sample of the above protected tripeptide derivative (6.70 g, 7.0 mmol) in DMF (100 ml) was stirred overnight and concentrated. The product was purified by procedure A, followed by precipitation from DMF with ether; yield 6.53 g (80%), mp 130–133 °C, $[\alpha]_D^{23} -10.6^\circ$ ($c=1.0$, DMF), R_f 0.50. *Anal.* Calcd for $C_{56}H_{59}Cl_3N_6O_{15}$: C, 57.86; H, 5.12; N, 7.23. Found: C, 58.00; H, 5.09; N, 7.28.

Z(OMe)-Val-Asp(OBzl)-Glu(OBzl)-Glu(OBzl)-Phe-NHNH-Troc—A mixture of Z(OMe)-Val-OSu (2.27 g, 6.0 mmol), Et_3N (1.53 ml, 11.0 mmol) and a TFA-treated sample of the above protected tetrapeptide derivative (5.81 g, 5.0 mmol) in DMF (100 ml) was stirred overnight and concentrated. The product was purified by procedure B, followed by precipitation from DMF with AcOEt; yield 4.93 g (78%), mp 208–211 °C, $[\alpha]_D^{23} -26.7^\circ$ ($c=0.8$, DMF), R_f 0.75. *Anal.* Calcd for $C_{61}H_{68}Cl_3N_7O_{16}$: C, 58.07; H, 5.43; N, 7.77. Found: C, 57.90; H, 5.48; N, 7.98.

Z(OMe)-Val-Asp(OBzl)-Glu(OBzl)-Glu(OBzl)-Phe-NHNH₂ [5] (Positions 3–7)—The above Troc-derivative (3.78 g, 3.0 mmol) in DMF-AcOH (40 ml-10 ml) was treated with Zn powder (1.96 g, 10 eq) at room temperature for 8 h. The solution was filtered, the filtrate was concentrated, and the residue was treated with 3% EDTA. The resulting powder was washed with 5% $NaHCO_3$ and H_2O and precipitated from DMF with MeOH; yield 2.67 g (82%), mp 215–217 °C, $[\alpha]_D^{23} -21.4^\circ$ ($c=1.0$, DMF), R_f 0.59. Amino acid ratios in a 6N HCl hydrolysate: Val 0.89, Asp 1.04, Glu 2.11, Phe 1.00 (recovery of Phe, 82%). *Anal.* Calcd for $C_{58}H_{67}N_7O_{14}$: C, 64.13; H, 6.22; N, 9.03. Found: C, 63.92; H, 6.11; N, 8.97.

Z(OMe)-Phe-Lys(Z)-OMe—The title compound was prepared by the Np method and purified by procedure B, followed by precipitation from DMF with ether; yield 85%, mp 137–138 °C, $[\alpha]_D^{23} -31.0^\circ$ ($c=0.8$, DMF), R_f 0.79. *Anal.* Calcd for $C_{33}H_{39}N_3O_8$: C, 65.44; H, 6.49; N, 6.94. Found: C, 65.37; H, 6.41; N, 6.81.

Z(OMe)-Phe-Lys(Z)-NHNH₂ [6] (Position 1–2)—The above protected dipeptide ester was treated with 80% hydrazine hydrate (5 eq) as stated above and the product was purified by precipitation from DMF with MeOH; yield 87%, mp 180–183 °C, $[\alpha]_D^{23} -24.5^\circ$ ($c=0.9$, DMF), R_f 0.63. Amino acid ratios in a 6N HCl hydrolysate: Phe 1.07, Lys 1.00 (recovery of Lys, 80%). *Anal.* Calcd for $C_{32}H_{39}N_5O_7$: C, 63.46; H, 6.49; N, 11.56. Found: C, 63.44; H,

6.47; N, 11.50.

Z(OMe)-Gln-Asn-Arg(Mts)-Arg(Mts)-Tyr-Phe-Leu-Phe-Arg(Mts)-Pro-Arg(Mts)-Asn-NH₂ (Positions 14–25)—The azide [prepared from 2.68 g (2.40 mmol) of fragment [2]] in DMF (40 ml) and Et₃N (0.40 ml, 2.88 mmol) were added to an ice-chilled solution of a TFA-treated sample of fragment [1] (3.28 g, 2.0 mmol) in DMF (30 ml) containing Et₃N (0.28 ml, 2.0 mmol) and the mixture, after being stirred for 24 h, was concentrated. The product was purified by procedure B, followed by precipitation from DMF with EtOH; yield 3.55 g (69%), mp 176–180 °C, $[\alpha]_D^{23} -17.9^\circ$ ($c=1.1$, DMF), R_f 0.56. *Anal.* Calcd for C₁₂₀H₁₆₄N₂₈O₂₇S₄·3H₂O: C, 55.15; H, 6.56; N, 15.01. Found: C, 55.32; H, 6.73; N, 14.70.

Z(OMe)-Pro-Ile-Val-Ser-Gln-Asn-Arg(Mts)-Arg(Mts)-Tyr-Phe-Leu-Phe-Arg(Mts)-Pro-Arg(Mts)-Asn-NH₂ (Positions 10–25)—The azide [prepared from 1.20 g (2.03 mmol) of fragment [3]] in DMF (10 ml) and Et₃N (0.34 ml, 2.44 mmol) were added to an ice-chilled solution of a TFA-treated sample of the above protected dodecapeptide amide (4.00 g, 1.56 mmol) in DMF (40 ml) containing Et₃N (0.22 ml, 1.56 mmol) and the mixture, after being stirred for 24 h, was concentrated. The product was purified by procedure B, followed by precipitation from DMF with MeOH; yield 3.21 g (69%), mp 203–206 °C, $[\alpha]_D^{23} -47.1^\circ$ ($c=0.4$, DMF), R_f 0.47. *Anal.* Calcd for C₁₃₉H₁₉₆N₃₂O₃₂S₄·4H₂O: C, 55.14; H, 6.79; N, 14.81. Found: C, 54.87; H, 6.86; N, 14.63.

Z(OMe)-Gln-Gly-Pro-Ile-Val-Ser-Gln-Asn-Arg(Mts)-Arg(Mts)-Tyr-Phe-Leu-Phe-Arg(Mts)-Pro-Arg(Mts)-Asn-NH₂ (Positions 8–25)—The azide [prepared from 0.76 g (2.0 mmol) of fragment [4]] in DMF (10 ml) and Et₃N (0.33 ml, 2.4 mmol) were added to an ice-chilled solution of a TFA-treated sample of the above hexadecapeptide amide (2.96 g, 1.0 mmol) in DMF (30 ml) containing Et₃N (0.14 ml, 1.0 mmol) and the mixture, after being stirred for 24 h, was concentrated. The product was purified by procedure B, followed by precipitation from DMF with MeOH; yield 2.70 g (86%), mp 188–192 °C, $[\alpha]_D^{23} -11.0^\circ$ ($c=0.8$, DMF), R_f 0.46. *Anal.* Calcd for C₁₄₆H₂₀₇N₃₅O₃₅S₄·5H₂O: C, 54.27; H, 6.77; N, 15.18. Found: C, 54.11; H, 6.58; N, 14.99.

Z(OMe)-Val-Asp(OBzl)-Glu(OBzl)-Glu(OBzl)-Phe-Gln-Gly-Pro-Ile-Val-Ser-Gln-Asn-Arg(Mts)-Arg(Mts)-Tyr-Phe-Leu-Phe-Arg(Mts)-Pro-Arg(Mts)-Asn-NH₂ (Positions 3–25)—The azide [prepared from 276 mg (0.26 mmol) of fragment [5]] in DMF (10 ml) and Et₃N (43 μl, 0.31 mmol) were added to an ice-chilled solution of a TFA-treated sample of the above protected octadecapeptide (400 mg, 0.13 mmol) in DMF (15 ml) containing Et₃N (18 μl, 0.13 mmol) and the mixture, after being stirred for 24 h, was concentrated. The product was purified by procedure C, followed by precipitation from DMF with MeOH; yield 430 mg (84%), mp 246–248 °C, $[\alpha]_D^{23} -46.7^\circ$ ($c=0.4$, DMF), R_f 0.60. *Anal.* Calcd for C₁₉₅H₂₆₂N₄₀O₄₆S₄·9H₂O: C, 55.86; H, 6.73; N, 13.36. Found: C, 55.60; H, 6.54; N, 13.16.

Z(OMe)-Phe-Lys(Z)-Val-Asp(OBzl)-Glu(OBzl)-Glu(OBzl)-Phe-Gln-Gly-Pro-Ile-Val-Ser-Gln-Asn-Arg(Mts)-Arg(Mts)-Tyr-Phe-Leu-Phe-Arg(Mts)-Pro-Arg(Mts)-Asn-NH₂, Protected U-25—The azide [prepared

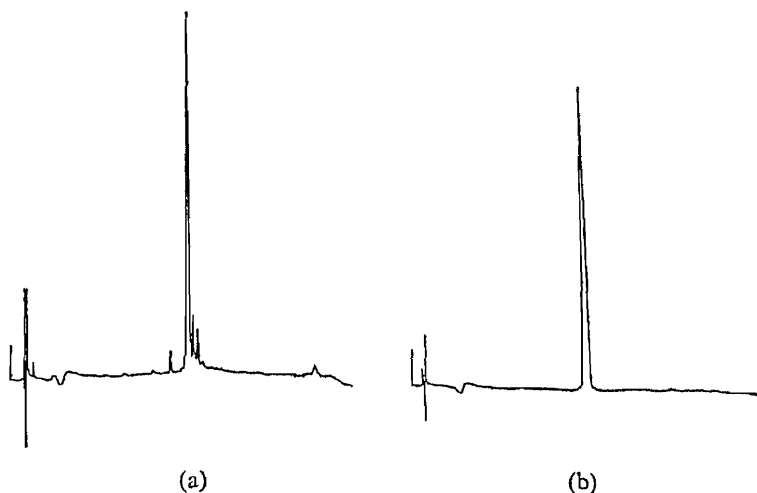


Fig. 4. HPLC of Synthetic Neuromedin U-25
a), crude sample; b), purified sample.



Fig. 5. Disc Isoelectrofocusing of Synthetic Neuromedin U-25

from 135 mg (0.20 mmol) of fragment [6] in DMF (10 ml) and Et₃N (28 μ l, 0.20 mmol) were added to an ice-chilled solution of a TFA-treated sample of the above tricosapeptide (403 mg, 0.10 mmol) in DMF (15 ml) containing Et₃N (14 μ l, 0.10 mmol) and the solution, after being stirred for 24 h, was concentrated. The product was purified by procedure C; yield 350 mg (79%), mp 238–240°C, $[\alpha]_D^{23}$ -9.1° ($c=0.8$, DMF), R_f^2 0.54. *Anal.* Calcd for C₂₁₈H₂₈₉N₄₃O₅₀S₄·4H₂O: C, 58.02; H, 6.63; N, 13.35. Found: C, 58.13; H, 6.58; N, 13.11.

Synthetic U-25—(a) Protected U-25 (50 mg) was treated with 1 M TMSOTf–thioanisole/TFA (2.25 ml, 200 eq) in the presence of *m*-cresol (118 μ l, 100 eq) and EDT (18.9 μ l, 20 eq) in an ice-bath for 60 min, then dry ether was added. The resulting powder was collected by centrifugation, washed with dry ether and dissolved in H₂O (10 ml). Under cooling with ice, the pH of the filtered solution was adjusted to 8.0 with 5% NH₄OH, and 1 M NH₄F/H₂O (282 μ l, 25 eq) was added. After 30 min, the solution was adjusted to pH 6.0 with 1 N AcOH. The solution was applied to a column of Sephadex G-25 (3.3 \times 103 cm), which was eluted with the same solvent. The fractions (9.2 ml each) corresponding to the front main peak (tube Nos. 39–49, monitored by UV absorption measurement at 275 nm) were collected and the solvent was removed by lyophilization to give a powder; yield 34.6 mg (98%). A part of the crude product (17 mg) thus obtained was purified by HPLC on a TSK-GEL LS-410KG column (21.5 \times 300 mm), by isocratic elution with 26% acetonitrile in 0.1% TFA aq. at a flow rate of 8.0 ml per min. The eluate corresponding to the main peak (retention time 33 min, Fig. 4-a) was collected. The rest of the sample was similarly purified by HPLC. The eluates were combined and the solvent was removed by evaporation. The residue was applied to a column of Sephadex G-25 (1.8 \times 55 cm), which was eluted with 0.1 N AcOH. The desired fractions (monitored as described above) were collected and the solvent was removed by lyophilization to give a fluffy white powder, yield 18.5 mg (53%). The overall yield from protected U-25 was 52%; $[\alpha]_D^{28}$ -78.6° ($c=0.4$, H₂O), a single spot on TLC: R_f^3 0.39, R_f^4 0.46. The retention time was 25 min in HPLC on an analytical Nucleosil 5C18 column (4.0 \times 150 mm), eluted with a gradient of acetonitrile (15% to 40%, 40 min) in 0.1% TFA aq. at a flow rate of 0.8 ml per min (Fig. 4-b). The mobility in disc isoelectrofocusing on 7.5% polyacrylamide gel containing Pharmalyte (pH 3–10) was 6.3 cm from the origin toward the cathodic end of the gel, after running at 200 V for 4 h (Fig. 5). Amino acid ratios in a 6 N HCl hydrolysate are listed in Table I. Amino acid ratios in a LAP digest (numbers in parentheses are theoretical): Asp 0.97 (1), Ser 0.96 (1), Glu 1.83 (2), Pro 1.70 (2), Gly 0.94 (1), Val 1.71 (2), Ile 0.90 (1), Leu 1.00 (1), Tyr 0.92 (1), Phe 3.42 (4), Lys 0.99 (1), Arg 3.37 (4), Asn and Gln were not determined (recovery of Leu, 70%).

(b) Protected U-25 (100 mg) was treated with 1 M TFMSA–thioanisole/TFA (4.5 ml) in the presence of *m*-cresol (0.24 ml, 100 eq) and EDT (37.7 μ l, 20 eq) in an ice-bath for 150 min, then dry ether was added. The resulting powder was treated with 5% NH₄OH at pH 8.0 for 30 min and purified by gel-filtration on Sephadex G-25, followed by HPLC as stated above; yield 33.2 mg (47% from the protected peptide). A mixture of the samples obtained in (a) and (b) emerged as a single peak (retention time 25 min) from a Nucleosil 5C18 HPLC column (4.0 \times 150 mm), which was eluted with a gradient of acetonitrile (15% to 40%, 40 min) in 0.1% TFA aq. at a flow rate of 0.8 ml per min. Amino acid ratios in a 6 N HCl hydrolysate: Asp 2.87, Ser 0.80, Glu 3.92, Gly 1.01, Val 1.68, Ile 0.89, Leu 1.00, Tyr 1.04, Phe 3.78, Lys 0.92, Arg 3.81, Pro 1.96 (recovery of Leu, 69%).

Synthetic U-8—(a) Protected U-8 (50 mg) was treated with 1 M TMSOTf–thioanisole in TFA (0.9 ml, 30 eq) in the presence of *m*-cresol (48 μ l, 15 eq) in an ice-bath for 60 min, then dry ether was added. The deprotected peptide was treated with 5% NH₄OH containing NH₄F (10 eq) at pH 8.0, then submitted to gel-filtration on Sephadex G-10 (2.8 \times 87 cm) as stated above. Yield 28.3 mg (84%). The final purification was achieved similarly by HPLC on a TSK-GEL LS-410KG column (21.5 \times 300 mm) using isocratic elution with 22% acetonitrile in 0.1% TFA aq. The purified peptide (retention time 50 min) was passed through a column of Sephadex G-10 using 0.1 N AcOH and finally lyophilized to give a fluffy powder; yield 14.4 mg (51%), overall yield from the protected peptide was 42%. $[\alpha]_D^{28}$ -44.7° ($c=0.2$, H₂O), a single spot on TLC: R_f^3 0.55, R_f^4 0.75. The retention time was 20 min in HPLC on a Cosmosil 5C18 column (4 \times 150 mm) on gradient elution with acetonitrile (15–40%, 40 min) in 0.1% TFA aq. at a flow rate of 0.8 ml/min; Amino acid ratios in a 6 N HCl hydrolysate and a LAP digest (numbers in parentheses): Asp 1.01, Leu 1.00 (1.00), Tyr 0.99 (0.93), Phe 1.97 (1.89), Arg 1.91 (1.73), Pro 0.99 (0.86), Asn was not determined, recovery of Leu 81% (79%).

(b) Protected U-8 (200 mg) was treated with 1 M TFMSA–thioanisole/TFA (3.7 ml, 30 eq) in the presence of *m*-cresol (0.4 ml, 30 eq) in an ice-bath for 120 min, then dry ether was added. The deprotected peptide was treated with 5% NH₄OH at pH 8.0 and then purified by gel-filtration on Sephadex G-10, followed by HPLC as described above; yield 43.3 mg (32%). A mixture of the samples obtained in (a) and (b) emerged as a single peak (retention time, 20 min) from a Cosmosil 5C18 HPLC column on gradient elution with acetonitrile (15% to 40%, 40 min) in 0.1% TFA aq. at a flow rate of 0.8 ml per min. Amino acid ratios in a 6 N HCl hydrolysate: Asp 1.03, Leu 1.00, Pro 0.97, Tyr 0.94, Phe 1.99, Arg 2.07 (recovery of Leu, 72%).

References and Notes

- 1) Part CXLVII: K. Akaji, M. Tanaka, S. Sumi, M. Kogire, K. Takaori, R. Doi, K. Inoue, T. Tobe, M. Moriga, M. Aono, and H. Yajima, *Chem. Pharm. Bull.*, **34**, 535 (1987).
- 2) Amino acids used in this investigation are of the L-configuration. The following abbreviations are used:

- Z = benzyloxycarbonyl, Z(OMe) = *p*-methoxybenzyloxycarbonyl, Mts = mesitylenesulfonyl, Troc = 2,2,2-trichloroethyloxycarbonyl, Np = *p*-nitrophenyl, Su = *N*-hydroxysuccinimidyl, DCC = dicyclohexylcarbodiimide, TFMSA = trifluoromethanesulfonic acid, TFA = trifluoroacetic acid, THF = tetrahydrofuran, DMF = dimethylformamide, EDT = ethanedithiol, EDTA = ethylenediaminetetraacetic acid disodium salts.
- 3) N. Fujii, A. Otaka, O. Ikemura, K. Akaji, S. Funakoshi, Y. Hayashi, Y. Kuroda, and H. Yajima, *J. Chem. Soc., Chem. Commun.*, in press.
 - 4) H. Yajima, N. Fujii, H. Ogawa, and H. Kawatani, *J. Chem. Soc., Chem. Commun.*, **1974**, 107; H. Yajima and N. Fujii, in "The Peptides, Analysis, Synthesis, Biology," Vol. 5, ed. by E. Gross and J. Meienhofer, Academic Press, New York, 1983, p. 65.
 - 5) N. Minamino, K. Kangawa, and H. Matsuo, *Biochem. Biophys. Res. Commun.*, **130**, 1078 (1985).
 - 6) S. Nakanishi, A. Inoue, T. Kita, M. Nakamura, S. N. Cohen, and S. Numa, *Nature* (London), **278**, 423 (1979); D. F. Steiner, P. S. Quinn, S. J. Chan, J. Marsh, and H. S. Tager, *Ann. N. Y. Acad. Sci.*, **343**, 1 (1980).
 - 7) N. Fujii, S. Futaki, K. Akaji, H. Yajima, A. Inoue, and T. Segawa, *Chem. Pharm. Bull.*, **33**, 3731 (1985).
 - 8) N. Fujii, Y. Hayashi, S. Katakura, K. Akaji, H. Yajima, A. Inoue, and T. Segawa, *Int. J. Peptide Protein Res.*, **26**, 121 (1985).
 - 9) F. Weygand and K. Hunger, *Chem. Ber.*, **95**, 1 (1962).
 - 10) H. Yajima, M. Takeyama, J. Kanaki, and K. Mitani, *J. Chem. Soc., Chem. Commun.*, **1978**, 482.
 - 11) J. Honzl and J. Rudinger, *Coll. Czech. Chem. Commun.*, **26**, 2333 (1961).
 - 12) M. Bodanszky and V. du Vigneaud, *J. Am. Chem. Soc.*, **81**, 5688 (1959).
 - 13) E. Wünsch and F. Dress, *Chem. Ber.*, **99**, 110 (1966).
 - 14) J. R. Vaughan, Jr., *J. Am. Chem. Soc.*, **73**, 3547 (1951); T. Wieland, W. Kern, and R. Sehering, *Ann. Chem.*, **569**, 117 (1950); R. A. Boissonnas, *Helv. Chim. Acta*, **34**, 874 (1951).
 - 15) T. Nakajima, T. Yasuhara, Y. Hirai, C. Kitada, M. Fujino, M. Takeyama, K. Koyama, and H. Yajima, *Chem. Pharm. Bull.*, **26**, 1222 (1978).
 - 16) H. Yajima, K. Akaji, K. Mitani, N. Fujii, S. Funakoshi, H. Adachi, M. Oishi, and Y. Akazawa, *Int. J. Peptide Protein Res.*, **14**, 169 (1979).
 - 17) Y. Mori, K. Koyama, Y. Kiso, and H. Yajima, *Chem. Pharm. Bull.*, **24**, 2788 (1976).
 - 18) H. Ogawa, M. Sugiura, H. Yajima, H. Sakurai, and K. Tsuda, *Chem. Pharm. Bull.*, **26**, 1549 (1978).
 - 19) G. W. Anderson, J. E. Zimmerman, and F. M. Callahan, *J. Am. Chem. Soc.*, **85**, 3039 (1963).
 - 20) R. B. Woodward, K. Heusler, J. Gosteli, P. Naegeli, W. Oppolzer, R. Ramage, S. Ranganathan, and H. Vorbrüggen, *J. Am. Chem. Soc.*, **88**, 852 (1966); H. Yajima and Y. Kiso, *Chem. Pharm. Bull.*, **19**, 420 (1971).
 - 21) S. Sakakibara, "Chemistry and Biochemistry of Amino Acids, Peptides and Proteins," ed. by B. Weinstein, Marcel Dekker, New York, Vol. 1, 1971, p. 51; M. Fujino, M. Wakimasu, S. Shinagawa, C. Kitada, and H. Yajima, *Chem. Pharm. Bull.*, **26**, 539 (1978).
 - 22) N. Fujii, M. Sakurai, K. Akaji, M. Nomizu, H. Yajima, K. Mizuta, M. Aono, M. Moriga, K. Inoue, R. Hosotani, and T. Tobe, *Chem. Pharm. Bull.*, **34**, 2397 (1986).

[Chem. Pharm. Bull.]
[35(3)1085—1092(1987)]

Synthesis of 6,5'-Cyclo-2',5'-dideoxypyrimidine Nucleosides (Nucleosides and Nucleotides. LXXII¹⁾)

YUKARI SUZUKI, AKIRA MATSUDA,
and TOHRU UEDA*

*Faculty of Pharmaceutical Sciences, Hokkaido University,
Kita-12, Nishi-6, Kita-ku, Sapporo 060, Japan*

(Received September 26, 1986)

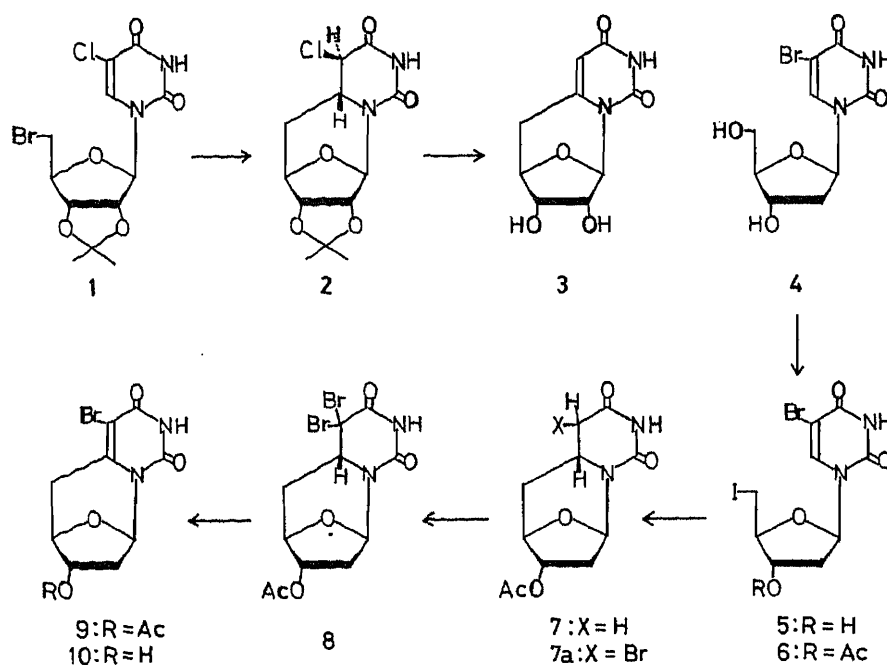
6,5'-Cyclo-2',5'-dideoxyuridine and 6,5'-cyclo-5'-deoxythymidine, pyrimidine deoxynucleosides fixed in the *anti* conformation, were synthesized. The key intermediate, 3'-*O*-acetyl-5-chloro-2',5'-dideoxy-5'-iodouridine (**12**), prepared from 2'-deoxyuridine, was cyclized by treatment with tributyltin hydride to the 6,5'-cyclo derivative (**13**), then dehydrochlorinated to furnish, after de-*O*-acetylation, 6,5'-cyclo-2',5'-dideoxyuridine (**14**). For the synthesis of 6,5'-cyclo-5'-deoxythymidine, 3'-*O*-acetyl-2',5'-dideoxy-5'-iodo-5-phenylthiomethyluridine (**22**) was prepared from 2'-deoxyuridine and this compound was cyclized by treatment with tributyltin hydride to yield, after de-*O*-acetylation, 6,5'-cyclo-5'-deoxythymidine (**24**).

Keywords—cyclonucleoside; C-cyclouridine; 6,5'-cyclo-2',5'-dideoxyuridine; 6,5'-cyclo-5'-deoxythymidine; 5-bromo-6,5'-cyclo-2',5'-dideoxyuridine; radical cyclization; tributyltin hydride; NMR; CD

We have reported the synthesis of a number of carbon-bridged cyclonucleosides for studies of the conformation of nucleosides and their interactions with enzymes which require nucleosides and nucleotides.²⁾ For example, 6,5'-cyclo-5'-deoxyuridine 2',3'-cyclic phosphate, a uridine cyclic phosphate conformationally fixed in the *anti* form, was found to be a substrate for pancreatic ribonuclease.³⁾ For the purpose of studying the conformational preference of the substrates of deoxynucleoside phosphorylases, the 2'-deoxy derivatives of 6,5'-cyclouridines appear to be useful candidates. This paper deals with synthetic studies of such compounds, such as 6,5'-cyclo-5'-deoxythymidine.

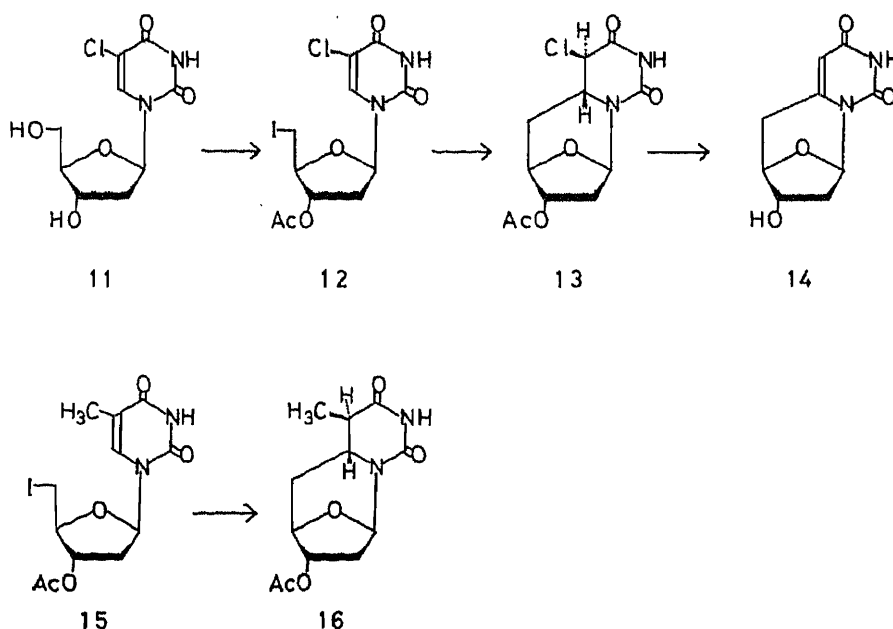
The key synthetic step we have developed for 6,5'-cyclization in uridine and cytidine is the generation of a radical at the 5'-position of 5'-deoxy-5'-halogeno-5-halogenouridine derivatives (for example, **1**) and successive intramolecular radical addition to the double bond at the 5,6-position, giving a 6,5'-cyclo-5,6-dihydro-5-halogenouridine (**2**). The dehydrohalogenation of **2** furnishes the product (**3**) after deprotection.³⁾ For the synthesis of the 2'-deoxy compound, the deoxygenation of the 2'-hydroxyl of **3** seemed to be an appropriate route. However, several attempts at the 2'-deoxygenation of **3** were unsuccessful despite the various methods available for 2'-deoxygenation in ribonucleosides.⁴⁾ Therefore, we started the synthesis from 2'-deoxyuridine derivatives. Since 5-bromo-2'-deoxyuridine (BUDR, **4**) is commercially available, we used this compound.

Treatment of **4** with triphenylphosphine and iodine⁵⁾ in dimethylformamide (DMF) afforded the 5'-deoxy-5'-iodo compound (**5**), which was converted to the 3'-*O*-acetate (**6**). Cyclization of **6** by dropwise addition of a mixture of tributyltin hydride (Bu₃SnH) and azobisisobutyronitrile (AIBN) in toluene under reflux proceeded slowly, and after addition of an excess of the reagents, the main product was 5'-*O*-acetyl-6,5'-cyclo-2',5'-dideoxy-5,6-dihydrouridine (**7**). It is conceivable that as the radical addition proceeded rather slowly with 2'-deoxyribosides, the initially formed 5-bromo-6,5'-cyclo-5,6-dihydro compound (**7a**) was



easily further reduced by Bu_3SnH to 7. An attempt at the re-bromination of 7 at the 5-position by bromine in carbon tetrachloride resulted in the formation of the 5,5-dibromo (8) and 5-bromouridine (9) compounds as an inseparable mixture. Treatment of the mixture with sodium methoxide afforded 5-bromo-6,5'-cyclo-2',5'-dideoxyuridine (10), a fixed model of BUDR in an *anti* conformation.

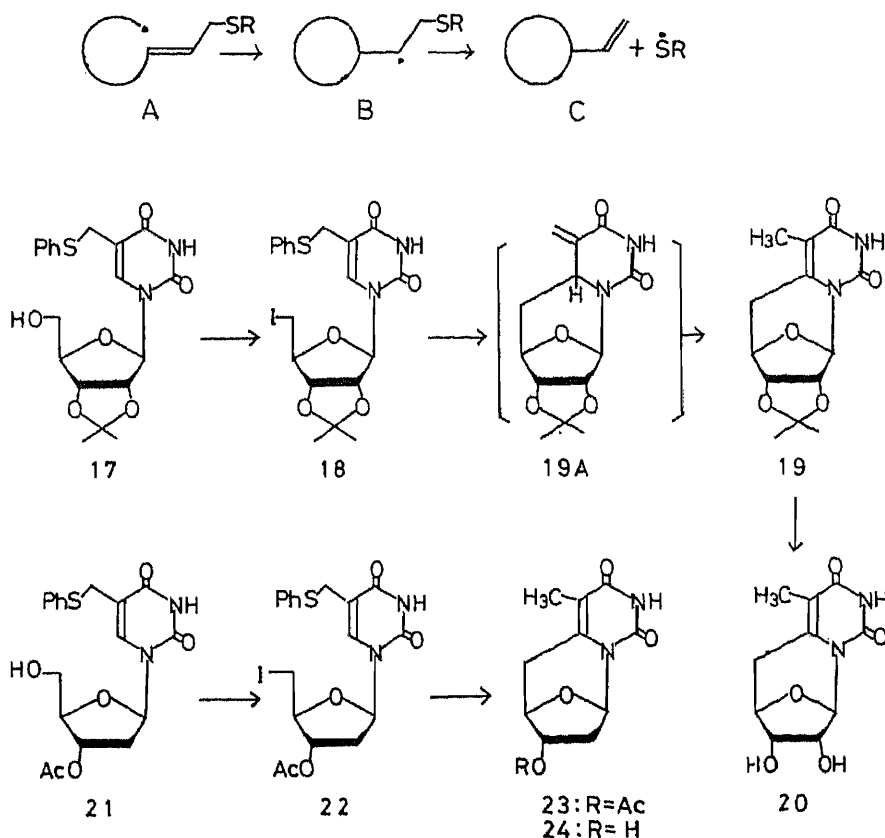
Since the bromo function reacted too easily with Bu_3SnH in the above reaction, we next selected 5-chloro-2'-deoxyuridine (11) as the starting material. Compound 11, prepared from 3',5'-di-*O*-acetyl-2'-deoxyuridine by chlorination with *N*-chlorosuccinimide followed by deacetylation, was converted to 3'-*O*-acetyl-2',5'-dideoxy-5'-iodouridine (12) by a similar route to that described above, or by 5'-*O*-tosylation, 3'-*O*-acetylation, and successive displacement of the tosyl group with sodium iodide. The latter method seems to be more suitable for large-



scale preparations. Cyclization of **12** by addition of Bu_3SnH and AIBN in toluene under reflux afforded the desired 5-chloro-6,5'-cyclo-5,6-dihydrouridine (**13**) in 75% yield. The structure of **13** was confirmed on the basis of nuclear magnetic resonance (NMR) and mass spectra (MS). The stereochemistry of the radical addition (*cis*-5,6-addition to give a compound with a 6(*R*)-configuration) was similar to that found previously in the uridine series.³⁾ Treatment of **13** with sodium methoxide in methanol gave 6,5'-cyclo-2',5'-dideoxyuridine (**14**).

In enzymatic studies of deoxynucleoside phosphorylases, the thymidine counterpart of **14** is required. Although treatment of 3'-*O*-acetyl-5'-deoxy-5'-iodothymidine (**15**)⁶⁾ with Bu_3SnH and AIBN afforded 6,5'-cyclo-5,6-dihydrothymidine (**16**), several attempts at the regeneration of the 5,6-double bond of **16** were unfruitful. Therefore we investigated another approach which involves the 6,5'-radical cyclization of a 5-phenylthiomethyluridine derivative, since it has been reported⁷⁾ that some alkylthiomethylalkenes (A) cyclize to give an intermediate (B) in which the alkylthiyl becomes a radical leaving group to give the vinylcycloalkane (C). To test this possibility, 2',3'-*O*-isopropylideneuridine was converted to the 5-phenylthiomethyl derivative (**17**) by the known procedure,⁸⁾ and **17** was 5'-*O*-mesylated and then substituted with sodium iodide to give 5'-deoxy-5'-iodo-2',3'-*O*-isopropylidene-5-phenylthiomethyluridine (**18**). Treatment of **18** with Bu_3SnH and AIBN in refluxing toluene gave the 6,5'-cyclo-5-methyluridine (**19**), in good yield, rather than the 5-methylene-5,6-dihydro compound (**19A**), which would be the presumed intermediate. Compound **19** was deprotected to furnish 6,5'-cyclo-5'-deoxy-5-methyluridine (**20**). The structure of **20** was fully confirmed by instrumental analysis (see Experimental).

Based on the above findings, 2'-deoxyuridine was converted to its 5-phenylthiomethyl derivative (**21**) by the sequence of hydroxymethylation, acetylation, substitution with



thiophenoxide, and finally deacetylation. Compound **21** was then converted to 3'-*O*-acetyl-2', 5'-dideoxy-5'-iodo-5-phenylthiomethyluridine (**22**) by the normal procedure. Radical cyclization of **22** with Bu_3SnH and AIBN gave the expected cyclothymidine (**23**) in 76% yield, and this was deacetylated to furnish 6,5'-cyclo-5'-deoxythymidine (**24**). The structure of **24** was also fully confirmed by instrumental analysis. The circular dichroism (CD) spectrum of **24** was similar to those of compounds in the *ribo* series, such as 6,5'-cyclo-5'-deoxyuridine,³ exhibiting a strong positive band at the main absorption region. Studies on the biological activities of 6,5'-cyclo-2',5'-dideoxypyrimidine nucleosides will be the subject of a future communication.

Experimental

Melting points were determined on a Yanagimoto MP-3 micromelting point apparatus and are uncorrected. The $^1\text{H-NMR}$ spectra were recorded on a JEOL FX-100FT or FX-270FT spectrometer in an appropriate solvent with tetramethylsilane as an internal standard. Chemical shifts are reported in ppm (δ), and signals are described as s (singlet), d (doublet), t (triplet), m (multiplet), or br (broad). All exchangeable protons were confirmed by addition of D_2O . Ultraviolet (UV) spectra were recorded on a Shimadzu UV-260 spectrophotometer. MS were measured on a JEOL D-300 spectrometer. CD spectra were recorded on a JASCO J-500A spectropolarimeter at room temperature. Silica gel used for column chromatography was Merck Kieselgel 60 (70–230 mesh).

5-Bromo-2',5'-dideoxy-5'-iodouridine (5)—Triphenylphosphine (9.86 g, 37.5 mmol) and I_2 (4.76 g, 37.5 mmol) were mixed in DMF (30 ml) at room temperature for 15 min. Compound **4** (7.63 g, 25 mmol) was added to the solution and the mixture was stirred overnight at room temperature. MeOH was added, the solvent was removed *in vacuo*, and the residue was dissolved in a small volume of MeOH, which was absorbed on silica gel. The gel was dried and placed on top of a column of silica gel. The column was washed with CHCl_3 , then eluted with 4% MeOH– CHCl_3 . The eluate was concentrated and the residue was crystallized from MeOH to give **5** (3.85 g, 37%), mp 160–161 °C (dec.). UV $\lambda_{\text{max}}^{\text{H}_2\text{O}}$ nm: 269.5. MS m/z : 418, 416 (M^+). NMR ($\text{DMSO}-d_6$): 11.87 (1H, br s, HN-3), 8.10 (1H, s, H-6), 6.16 (1H, t, $J_{1,2'} = 5.6$ Hz, H-1'), 4.16 (1H, m, H-3'), 3.83 (1H, m, H-4'), 3.50 (2H, m, HO-3',5'), 2.23 (2H, m, H-2'). Anal. Calcd for $\text{C}_9\text{H}_{10}\text{BrI N}_2\text{O}_4$: C, 25.98; H, 2.42; N, 6.73. Found: C, 26.15; H, 2.42; N, 6.73.

3'-O-Acetyl-5-bromo-2',5'-dideoxy-5'-iodouridine (6)—A mixture of **5** (3.85 g, 9.3 mmol), Ac_2O (1.75 ml, 18.6 mmol) and a catalytic amount of 4-dimethylaminopyridine in acetonitrile (50 ml) was stirred at room temperature for 9 h. MeOH was added to the solution, the solvent was removed *in vacuo* and the residue was crystallized from EtOH to give **6** (3.79 g, 89%), mp 152–153 °C. UV $\lambda_{\text{max}}^{\text{MeOH}}$ nm: 277. MS m/z : 460, 458 (M^+), 269 (M^+ – base). NMR (CDCl_3): 8.16 (1H, br s, HN-3), 7.25 (1H, s, H-6), 6.27 (1H, t, $J_{1,2'} = 5.6$ Hz, H-1'), 5.35 (1H, m, H-3'), 4.11 (1H, m, H-4'), 3.92 (2H, s, H-5'), 2.40 (2H, m, H-2'), 2.10 (3H, s, Ac). Anal. Calcd for $\text{C}_{11}\text{H}_8\text{BrI N}_2\text{O}_5$: C, 28.66; H, 2.87; N, 6.08. Found: C, 28.71; H, 2.58; N, 6.00.

3'-O-Acetyl-6,5'-cyclo-2',5'-dideoxy-5,6-dihydrouridine (7)—A mixture of Bu_3SnH (0.485 ml, 1.8 mmol) and AIBN (30 mg) in toluene (3 ml) was added dropwise to a suspension of **6** (688.5 mg, 1.5 mmol) in toluene (150 ml) at reflux under an Ar atmosphere over a period of 1 h. The mixture was further refluxed for 2 h, and the solvent was removed *in vacuo*. The residue was crystallized from EtOH to give **7** (285.8 mg, 75%), mp 238–239 °C. MS m/z : 254 (M^+). NMR (CDCl_3): 7.57 (1H, br s, HN³), 6.36 (1H, d, $J_{1,2'a} = 5.0$ Hz, H-1'), 5.15 (1H, m, H-3'), 4.47 (1H, dd, $J_{4,5'a} = 1.9$ Hz, $J_{4,5'b} = 4.0$ Hz, H-4'), 3.61 (1H, tt, $J_{5'a,6} = 11.8$ Hz, $J_{5'b,6} = 4.6$ Hz, $J_{5a,6} = 12.5$ Hz, $J_{5b,6} = 4.2$ Hz, H-6), 2.74 (1H, dd, $J_{gem} = 16.8$ Hz, H-5b), 2.52 (1H, dd, H-5a), 2.34 (2H, m, H-2'), 2.10 (3H, s, Ac), 1.96 (1H, ddd, $J_{gem} = 13.4$ Hz, H-5'a), 1.79 (1H, m, H-5'b). Anal. Calcd for $\text{C}_{11}\text{H}_{14}\text{N}_2\text{O}_5$: C, 51.97; H, 5.50; N, 11.01. Found: C, 52.08; H, 5.42; N, 10.84.

3'-O-Acetyl-5,5-dibromo-6,5'-cyclo-2',5'-dideoxy-5,6-dihydrouridine (8) and 3'-O-Acetyl-5-bromo-6,5'-cyclo-2',5'-dideoxyuridine (9)—A mixture of **7** (508 mg, 2 mmol) and *N*-bromosuccinimide (856 mg, 4.8 mmol) in CCl_4 was refluxed for 4 h, the solvent was removed *in vacuo* and the residue was partitioned between CHCl_3 and H_2O . The organic layer was separated and dried over Na_2SO_4 , and the solvent was evaporated off to leave a mixture of **8** and **9** as a foam, which was used in the next step without further purifications. MS m/z : 412, 410, 408 (M^+ of **8**), 332, 330 (M^+ of **9**). UV $\lambda_{\text{max}}^{\text{MeOH}}$ nm: 281.3.

5-Bromo-6,5'-cyclo-2',5'-dideoxyuridine (10)—A mixture of **8** and **9** (456 mg, *ca.* 1.1 mmol) was dissolved in MeOH (5 ml), 1 *N* NaOMe in MeOH (2.3 ml) was added, and the solution was stirred for 5 h at room temperature. The solution was neutralized by addition of Dowex 50 (H^+ form), the resin was filtered off, the filtrate was concentrated, and the residue was crystallized from EtOH to give **10** (253 mg, 78%), mp 195–196 °C (dec.). MS m/z : 290, 288 (M^+). UV $\lambda_{\text{max}}^{\text{MeOH}}$ nm (ϵ): 283.3 (9565). CD (H_2O) [θ] nm +148000 (281). NMR ($\text{DMSO}-d_6$): 11.71 (1H, br s, HN³), 6.21 (1H, d, $J_{1,2'a} = 5.4$ Hz, H-1'), 5.27 (1H, d, $J = 4.4$ Hz, HO-3'), 4.47 (1H, d, $J_{2'b,3'} = 6.6$ Hz, H-3'), 4.26 (1H, m, H-4'), 3.05 (2H, dd, H-5'), 1.94 (2H, m, H-2'). Anal. Calcd for $\text{C}_9\text{H}_9\text{BrN}_2\text{O}_4$: C, 37.40; H, 3.14; Br, 28.53; N, 9.69. Found: C, 37.43; H, 3.35; Br, 27.16; N, 9.62.

5-Chloro-2'-deoxyuridine (11)—A mixture of 3',5'-di-*O*-acetyl-2'-deoxyuridine (15.7 g, 49 mmol) and *N*-chlorosuccinimide (7.85 g, 58.8 mmol) in AcOH (100 ml) was stirred at 80 °C overnight. The solvent was removed *in vacuo* and the residue was partitioned between CHCl₃ and H₂O. The organic layer was dried over Na₂SO₄ and the solvent was evaporated off. The residue was dissolved in MeOH saturated with NH₃ (200 ml) and the mixture was stirred overnight at room temperature. The solvent was removed and the residue was crystallized from EtOH to give **11**⁹¹ (8.41 g, 65%), mp 181—183 °C (mp 178—179.5 °C⁹¹). MS *m/z*: 264, 262 (M⁺). UV λ_{max}^{MeOH} nm: 277. NMR (DMSO-*d*₆): 11.76 (1H, brs, HN³), 8.31 (1H, s, H-6), 6.11 (1H, t, *J* = 6.6 Hz, H-1'), 5.21 (1H, dd, *J*_{2',3'} = 5.0 Hz, *J*_{2',3'} = 4.4 Hz, H-3'), 5.16 (1H, t, HO-5'), 4.25 (1H, m, H-4'), 3.80 (1H, d, HO-3'), 3.60 (2H, br d, H-5'), 2.14 (2H, t, H-2'). *Anal.* C₉H₁₁ClN₂O₅ requires: C, 41.16; H, 4.22; N, 10.67. Found: C, 41.13; H, 4.25; N, 10.49.

3'-*O*-Acetyl-5-chloro-2',5'-dideoxy-5'-iodouridine (12)—Method a: A mixture of triphenylphosphine (7.86 g, 30 mmol) and I₂ (7.62 g, 30 mmol) in DMF (30 ml) was stirred for 15 min. Then, **11** (5.25 g, 15 mmol) was added and the solution was stirred overnight at room temperature. The solvent was removed and the residue was dissolved in a small volume of MeOH, and adsorbed on silica gel. The gel was dried and placed on top of a column of silica gel (4 × 70 cm). The column was washed with CHCl₃, then eluted with 8% MeOH-CHCl₃. The eluate was concentrated and the residue was crystallized from EtOH to give 5-chloro-2',5'-dideoxy-5'-iodouridine (6.88 g, 37%), mp 177—178 °C. MS *m/z*: 374, 372 (M⁺). NMR (DMSO-*d*₆): 11.89 (1H, brs, HN³), 8.02 (1H, s, H-6), 6.15 (1H, t, *J*_{1',2'} = 6.6 Hz, H-1'), 5.48 (1H, d, *J* = 4.15 Hz, HO-3'), 4.22 (1H, m, H-3'), 3.85 (1H, m, H-4'), 3.49 (2H, m, H-5'), 2.37 (1H, dd, H-2'a), 2.19 (1H, ddd, H-2'b). The compound (1.36 g, 3.7 mmol) was then added to Ac₂O (0.76 ml, 7.3 mmol) containing a catalytic amount of DMAP in acetonitrile (15 ml), and the mixture was stirred overnight at room temperature. MeOH was added, the solvent was removed, and the residue was crystallized from EtOH to give **12** (1.39 g, 92%), mp 153—154 °C. MS *m/z*: 416, 414 (M⁺), 269 (sugar⁺). NMR (CDCl₃): 8.79 (1H, brs, HN³), 8.06 (1H, s, H-6), 6.28 (1H, dd, *J*_{1',2'} = 5.6 Hz, *J*_{1',2'a} = 7.1 Hz, H-1'), 5.05 (1H, m, H-3'), 3.94 (1H, m, H-4'), 3.58 (2H, m, H-5'), 2.41 (2H, m, H-2'), 2.12 (3H, s, Ac). *Anal.* Calcd for C₁₁H₁₂ClIN₂O₅: 31.87; H, 2.92; Cl, 8.55; I, 30.61. N, 6.76. Found: C, 31.91; H, 2.90; Cl, 8.58; I, 30.71; N, 6.83.

Method b: Compound **11** (2.51 g, 9.6 mmol) in pyridine (30 ml) was treated with TsCl (2.0 g, 10.5 mmol) in an ice-water bath overnight. The solvent was removed *in vacuo* and the residue was crystallized from EtOH to give the 5'-*O*-tosylate (1.70 g, 42%), mp 169—170 °C (dec.). MS *m/z*: 390, 388 (M⁺). This tosylate (1.67 g, 4.0 mmol) was then added to Ac₂O (0.57 ml, 6 mmol) containing a catalytic amount of DMAP in acetonitrile (50 ml) and the solution was stirred at room temperature for 2 h. MeOH was added to the solution and the solvent was removed *in vacuo*. The residue was dried by co-distillation twice with benzene and then dissolved in 2-butanone (50 ml). NaI (750 mg, 5 mmol) was added and the solution was refluxed for 1 h. The solvent was removed *in vacuo* and the residue was partitioned between CHCl₃ and H₂O. The organic layer was dried over Na₂SO₄, the solvent was removed *in vacuo*, and the residue was crystallized from EtOH to give **12** (1.52 g, 92%). The physical constants were identical with those of the product obtained by method a.

3'-*O*-Acetyl-5-chloro-6,5'-cyclo-2',5'-dideoxy-5(*R*),6(*R*)-dihydrouridine (13)—A mixture of Bu₃SnH (0.81 ml, 3 mmol) and AIBN (40 mg) in toluene (3 ml) was added dropwise to a suspension of **12** (1.03 g, 2.5 mmol) in toluene (100 ml) under reflux in an Ar atmosphere over a period of 50 min. The mixture was further refluxed for 2 h, and the solvent was removed *in vacuo*. The residue was crystallized from EtOH to give **13** (540 mg, 75%), mp 146—147 °C. MS *m/z*: 290, 288 (M⁺), 253 (M⁺ - Cl). NMR (CDCl₃): 7.56 (1H, brs, NH³), 6.34 (1H, dd, *J*_{1',2'} = 5.0 Hz, *J*_{1',2'a} = 1.5 Hz, H-1'), 5.15 (1H, m, H-3'), 4.56 (1H, m, H-4'), 4.28 (1H, d, *J*_{5,6} = 11.3 Hz, H-5), 3.62 (1H, tt, *J*_{5'a,6} = 11.4 Hz, *J*_{5'b,6} = 6.1 Hz, H-6), 2.33 (3H, m, H-2',5'a), 2.10 (3H, s, Ac), 1.85 (1H, ddd, *J*_{5'a,b} = 13.7 Hz, H-5'b). *Anal.* Calcd for C₁₁H₁₃ClN₂O₅: C, 47.77; H, 4.54; N, 9.70. Found: C, 47.57; H, 4.40; N, 9.65.

6,5'-Cyclo-2',5'-dideoxyuridine (14)—A solution of **13** (288 mg, 1 mmol) and 1 *N* NaOMe (in MeOH, 2.2 ml) in MeOH (10 ml) was refluxed for 2 h. The solution was neutralized by addition of 1 *N* HCl, the solvent was evaporated off, and the residue was crystallized from EtOH to give **14** (168 mg, 80%), mp 247—249 °C. MS *m/z*: 210 (M⁺). UV λ_{max}^{H₂O} nm (ε): 269.9 (10600). CD (H₂O) [θ] nm: +1.84 × 10⁴ (269.5). NMR (DMSO-*d*₆): 11.15 (1H, brs, HN³), 6.20 (1H, d, *J*_{1',2'a} = 5.1 Hz, H-1'), 5.68 (1H, s, H-5), 5.38 (1H, brs, HO-3'), 4.39 (1H, d, *J*_{2',3'} = 6.8 Hz, H-3'), 4.23 (1H, dd, *J*_{4',5'a} = 7.1 Hz, *J*_{4',5'b} = 3.2 Hz, H-4'), 3.14 (1H, dd, *J*_{2'a,b} = 12.0 Hz, H-2'a), 2.74 (1H, ddd, H-2'b), 2.39 (1H, m, H-5'a), 5'a), 1.95 (1H, m, H-5'b). *Anal.* Calcd for C₉H₁₀N₂O₄: 51.43; H, 4.80; N, 13.33. Found: C, 51.00; H, 4.78; N, 13.13.

3'-*O*-Acetyl-5'-deoxy-5'-iodothymidine (15)—A solution of thymidine (4.84 g, 20 mmol) and TsCl (4.57 g, 24 mmol) in pyridine (30 ml) was stirred in an ice-water bath for 3.5 h. Water was added to the solution and the solvent was removed *in vacuo*. The residue was dried by co-distillation with toluene several times and crystallized from EtOH to give the 5'-*O*-tosylate (3.43 g, 8.7 mmol, 44%), which was dissolved in acetonitrile (200 ml). Ac₂O (1.78 ml, 17.4 mmol) and a catalytic amount of DMAP were added and the solution was stirred for 30 min. MeOH was added to the mixture and the solvent was removed *in vacuo*. The residue was dissolved in 2-butanone (100 ml), NaI (1.57 g, 10 mmol) was added, and the mixture was refluxed for 5 h. The solvent was evaporated off and the residue was partitioned between CHCl₃ and H₂O. The organic layer was dried over Na₂SO₄ and the solvent was removed *in vacuo*. The residue was crystallized from EtOH to give **15**⁶⁾ (2.88 g, 84%), mp 132—133 °C (lit.⁶⁾ 131 °C). UV λ_{max}^{MeOH} nm: 264.4. NMR (CDCl₃): 9.20 (1H, brs, HN³), 7.60 (1H, d, *J*_{5-Me,6} = 1.2 Hz, H-6), 6.33 (1H, t, *J*_{1',2'} = 8.3 Hz, H-1'), 5.04 (1H, m, H-3'), 3.90 (1H, dd, *J*_{4',5'a} = 3.9 Hz, *J*_{4',5'b} = 3.3 Hz, H-4'), 3.56 (2H, m, H-5'), 2.30

(2H, m, H-2'), 2.20 (3H, s, Ac), 1.97 (3H, s, Me-5). *Anal.* $C_{12}H_{15}IN_2O_5$ requires: C, 36.57; H, 3.84; N, 7.11. Found: C, 36.73; H, 3.86; N, 6.89.

3'-O-Acetyl-6,5'-cyclo-5'-deoxy-5(R),6(R)-dihydrothymidine (16)—A mixture of Bu_3SnH (1.4 mmol) and AIBN (100 mg) in toluene (8 ml) was added dropwise over a period of 1.5 h to a solution of **15** (2.37 g, 6 mmol) in toluene (200 ml) under reflux in an Ar atmosphere. The mixture was refluxed for 2 h and the solvent was removed *in vacuo*. The residue was crystallized from EtOH to give **16** (678 mg, 42%), mp 164–165 °C. *MS* m/z : 269 (M^+). NMR ($CDCl_3$): 7.48 (1H, brs, HN^3), 6.38 (1H, dd, $J_{1',2',b} = 1.7$ Hz, $J_{1',2',a} = 4.4$ Hz, H-1'), 5.13 (1H, m, H-3'), 4.50 (1H, dd, $J_{4',5',a} = 4.2$ Hz, $J_{4',5',b} = 2.0$ Hz, H-4'), 3.25 (1H, tt, $J_{5',a,b} = 11.5$ Hz, $J_{5',b,6} = 4.9$ Hz, $J_{5,6} = 11.5$ Hz, H-6), 2.42 (1H, dd, H-5'b), 2.32 (1H, m, H-5), 2.09 (3H, s, Ac), 2.05 (1H, ddd, $J_{5',a,b} = 13.5$ Hz, H-5'a), 1.74 (1H, ddd, $J_{2',a,b} = 13.7$ Hz, H-2'a), 1.36 (1H, ddd, H-2'b), 1.24 (3H, d, Me-5). *Anal.* Calcd for $C_{12}H_{16}N_2O_5 \cdot 0.25H_2O$: C, 52.94; H, 6.01; N, 10.27. Found: C, 52.87; H, 5.95; N, 10.27.

2',3'-O-Isopropylidene-5-phenylthiomethyluridine (17)—A mixture of 2',3'-O-isopropylideneuridine (10 g, 35 mmol), pyrrolidine (14.7 ml, 176 mmol) and 35% formaldehyde (15.1 ml, 171 mmol) in H_2O (180 ml) was refluxed for 1 h. The solution was concentrated and the residue was dried by co-distillation with toluene several times. The final residue was taken up in acetonitrile (100 ml), PhSH (3.85 ml, 35 mmol) was added, and the mixture was refluxed for 4 h. The solvent was removed *in vacuo* and the residue was taken up in $CHCl_3$ and applied to a column of silica gel (7 × 25 cm). The column was washed with $CHCl_3$, then eluted with 4% MeOH- $CHCl_3$. The eluate was concentrated and the residue was crystallized from EtOH to give **17** (9.35 g, 66%), mp 144–145 °C. *MS* m/z : 406 (M^+), 391 ($M^+ - Me$), 297 ($M^+ - SPh$), 174 (sugar⁺). UV λ_{max}^{MeOH} nm: NMR ($CDCl_3$): 8.70 (1H, brs, HN^3), 7.30 (5H, m, Ph), 7.15 (1H, s, H-6), 5.57 (1H, d, $J_{1',2'} = 2.4$ Hz, H-1'), 4.77 (2H, m, H-2',3'), 4.12 (1H, m, H-4'), 3.80 (4H, m, H-5' and CH_2 -5), 2.30 (1H, t, HO-5'), 1.55, 1.34 (3H each, s, iso-Pr). *Anal.* Calcd for $C_{19}H_{22}N_2O_6S$: C, 56.15; H, 5.46; N, 6.89; S, 7.89. Found: C, 56.08; H, 5.54; N, 6.86; S, 7.86.

5'-Deoxy-5'-iodo-2',3'-O-isopropylidene-5-phenylthiomethyluridine (18)—MsCl (0.26 ml, 1.2 mmol) was added to a solution of **17** (405 mg, 1 mmol) in pyridine (5 ml) under cooling in an ice-bath, and the solution was then stirred at room temperature for 1 h. A small volume of H_2O was added and the solvent was removed *in vacuo*. The residue was partitioned between AcOEt and H_2O , the organic layer was dried over Na_2SO_4 , and the solvent was evaporated off to leave the 5'-O-mesylate as a foam (450 mg, 93%). The mesylate (1.57 g, 3.2 mmol) was dissolved in 2-butanone (50 ml) containing NaI (576 mg, 3.8 mmol) and the solution was refluxed for 4 h. The solvent was removed *in vacuo* and the residue was partitioned between AcOEt and H_2O . The organic layer was dried over Na_2SO_4 and the solvent was evaporated off to leave **18** (1.56 g, 94%) as a foam. *MS* m/z : 516 (m^+), 501 ($M^+ - Me$), 407 ($M^+ - PhS$). NMR ($CDCl_3$): 9.00 (1H, brs, HN^3), 7.35 (5H, m, Ph), 6.96 (1H, s, H-6), 5.61 (1H, d, $J_{1',2'} = 1.5$ Hz, H-1'), 4.59 (2H, m, H-2',3'), 3.81 (3H, m, H-4' and CH_2 -5), 3.34 (2H, m, H-5'), 1.55, 1.34 (3H each, s, iso-Pr).

6,5'-Cyclo-5'-deoxy-2',3'-O-isopropylidene-5-methyluridine (19)—A mixture of Bu_3SnH (0.59 ml, 3.0 mmol) and AIBN (50 mg) in toluene (5 ml) was added dropwise over a period of 2 h to a solution of **18** (1.18 g, 2.3 mmol) in toluene (200 ml) under reflux in an Ar atmosphere. The solution was further refluxed for 2 h, then the solvent was evaporated off. The residue was dissolved in a small volume of $CHCl_3$ and applied to a column of silica gel (5 × 10 cm). After washing of the column with $CHCl_3$, **19** was eluted with 4% MeOH- $CHCl_3$. The eluate was concentrated and the residue was crystallized from EtOH to give 479 mg (74%), mp 237–238 °C. *MS* m/z : 280 (M^+), 265 ($M^+ - Me$). UV λ_{max}^{MeOH} nm: 271.7. NMR ($CDCl_3$): 8.35 (1H, brs, HN^3), 6.22 (1H, s, H-1'), 4.64 (3H, brs, H-2',3',4'), 3.12 (1H, dd, $J_{4',5',a} = 7.1$ Hz, $J_{5',a,b} = 18.6$ Hz, H-5'a), 2.77 (1H, d, H-5'b), 1.83 (3H, s, Me-5), 1.52, 1.32 (3H each, s, iso-Pr). *Anal.* Calcd for $C_{13}H_{16}N_2O_5$: C, 55.71; H, 5.75; N, 10.00. Found: C, 55.71; H, 6.02; N, 9.93.

6,5'-Cyclo-5'-deoxy-5-methyluridine (20)—A suspension of **19** (280 mg, 1 mmol) in trifluoroacetic acid (20 ml) was stirred at room temperature during which time a solution was formed. The solvent was removed *in vacuo*, and the residue was taken up in a small volume of MeOH and adsorbed on silica gel. This gel was dried and placed on top of a column of silica gel, which was eluted with 16% MeOH- $CHCl_3$. The eluate was concentrated and the residue was crystallized from EtOH to give **20** (223 mg, 93%), mp 281–282 °C. *MS* m/z : 240 (M^+). UV $\lambda_{max}^{H_2O}$ nm (ϵ): 275.4 (9100). CD (H_2O) [θ] nm: $+1.03 \times 10^4$ (270). NMR ($DMSO-d_6$): 11.22 (1H, brs, HN^3), 5.82 (1H, d, $J_{1',2'} = 1.0$ Hz, H-1'), 5.35, 5.11 (1H each, d, HO-2',3'), 4.43 (1H, d, $J_{2',3'} = 6.1$ Hz, H-2'), 3.31 (2H, brs, H-3',4'), 2.88 (1H, dd, $J_{4',5',a} = 5.4$ Hz, $J_{5',a,b} = 17.6$ Hz, H-5'a), 2.76 (1H, d, H-5'b), 1.67 (3H, s, Me-5). *Anal.* Calcd for $C_{10}H_{12}N_2O_5$: C, 49.71; H, 5.03; N, 11.66. Found: C, 49.52; H, 5.11; N, 11.49.

3'-O-Acetyl-2'-deoxy-5-phenylthiomethyluridine (21)—A mixture of 2'-deoxyuridine (11.4 g, 33 mmol) and paraformaldehyde (6 g) in 0.5 N Et_3N in H_2O (125 ml) was stirred at 60 °C. Paraformaldehyde (9 g and 6 g) was added after 1 d and 2 d, respectively, and after 3 d the solution was concentrated. The residue was dried by co-distillation with benzene several times. The final residue was dissolved in pyridine (100 ml), Ac_2O (40 ml) was added, and the solution was stirred overnight at room temperature. A small volume of MeOH was added and the solution was concentrated *in vacuo*. The residue was partitioned between $CHCl_3$ and H_2O . The organic layer was dried over Na_2SO_4 and the solvent was evaporated off *in vacuo*. The residue (4.4 g, 11.5 mmol) was dissolved in DMF (10 ml); PhSH (3.8 ml, 34.5 mmol) and Et_3N (4.8 ml, 29 mmol) were added, and the mixture was stirred overnight at 60 °C. The whole was partitioned between AcOEt and H_2O . The organic layer was separated, and dried over Na_2SO_4 , and the solvent was removed *in vacuo*. The residue was dissolved in MeOH saturated with NH_3 (100 ml) and kept

overnight at room temperature. The solvent was removed *in vacuo*, and the residue was dissolved in MeOH and adsorbed on silica gel. This gel was dried and placed on top of a silica gel column (4 × 20 cm), which was eluted with 20% MeOH-CHCl₃. The eluate was concentrated to leave the 5-phenylthiomethyl derivative (3.15 g, 30%) as a foam. MS *m/z* 318 (M⁺). NMR (DMSO-*d*₆): 11.43 (1H, br s, HN³), 7.68 (1H, s, H-6), 7.31 (5H, m, Ph), 6.09 (1H, t, *J*_{1',2'} = 7.3 Hz, H-1'), 5.19 (1H, d, HO-3'), 4.97 (1H, m, HO-5'), 4.14 (1H, m, H-3'), 3.80 (2H, s, CH₂-5), 3.75 (1H, m, H-4'), 3.50 (2H, d, *J*_{4,5} = 4.6 Hz, H-5'), 1.96 (1H, m, H-2'a), 1.75 (1H, m, H-2'b). The compound (1.20 g, 3.8 mmol) and dimethoxytrityl chloride (1.34 g, 4.0 mmol) were dissolved in pyridine (20 ml) and the solution was stirred for 30 min at room temperature. The solvent was removed *in vacuo* and the residue was partitioned between CHCl₃ and H₂O. The organic layer was dried over Na₂SO₄ and concentrated *in vacuo*. The residue was chromatographed on silica gel (4 × 10 cm) and eluted with 10% MeOH-CHCl₃. The eluate was concentrated and the residue was taken up in pyridine (30 ml). Ac₂O (0.8 ml, 7.8 mmol) was added and the solution was stirred overnight at room temperature. The solvent was evaporated off and the residue was dried by co-distillation with toluene several times. The final residue was dissolved in CHCl₃ (300 ml) and cooled. A solution of 2% benzenesulfonic acid in MeOH (125 ml) was added and the mixture was kept for 10 min in an ice-water bath. The solution was neutralized by addition of 5% NaHCO₃, and CHCl₃ (400 ml) was added. The separated organic layer was dried over Na₂SO₄, the solvent was removed *in vacuo*, and the residue was chromatographed on silica gel (4 × 10 cm). The eluate with 10% MeOH in CHCl₃ was concentrated to leave **21** as a foam. MS *m/z*: 392 (M⁺), 283 (M⁺ - PhS). NMR (CDCl₃): 9.46 (1H, br s, HN³), 7.51 (1H, s, H-6), 7.2 (5H, m, Ph), 6.23 (1H, dd, *J* = 6.1, 8.4 Hz, H-1'), 5.22 (1H, m, H-3'), 4.00 (1H, m, H-4'), 3.81 (4H, m, H-5' and CH₂S), 2.25 (1H, m, H-2'a), 2.09 (3H, s, Ac), 2.00 (1H, m, H-2'b).

3'-O-Acetyl-2',5'-dideoxy-5'-iodo-5-phenylthiomethyluridine (22)—Compound **21** (663 mg, 1.7 mmol) and MsCl (0.16 ml, 2.0 mmol) in pyridine (10 ml) were stirred for 9 h at room temperature. The solvent was removed *in vacuo* and the residue was partitioned between CHCl₃ and H₂O. The organic layer was separated and dried over Na₂SO₄, and the solvent was removed to leave the 5'-*O*-mesylate (671 mg, 85%) as a foam. MS *m/z*: 470 (M⁺), 374 (M⁺ - MsO), 361 (M⁺ - PhS). NMR (CDCl₃): 9.02 (1H, br s, HN³), 7.20 (5H, m, Ph), 6.78 (1H, s, H-6), 6.24 (1H, dd, *J*_{1',2'} = 5.6, *J*_{1',2'a} = 7.2 Hz, H-1'), 4.44 (1H, m, H-3'), 3.80 (2H, s, CH₂S), 3.40 (2H, d, *J* = 3.7 Hz, H-5'), 3.12 (1H, m, H-4'), 3.04 (3H, s, CH₃SO₃), 2.30 (1H, m, H-2'b), 2.12 (3H, s, Ac), 1.88 (1H, m, H-2'a). A solution of the 5'-*O*-mesyl derivative (490 mg, 1.1 mmol) and NaI (202 mg, 1.3 mmol) in 2-butanone (20 ml) was refluxed for 4 h. The solvent was removed *in vacuo* and the residue was partitioned between CHCl₃ and H₂O. The organic layer was separated, the solvent was removed, and the residue was chromatographed on silica gel with 2% MeOH-CHCl₃. The eluate was concentrated to leave **22** (500 mg, 89%) as a foam. MS *m/z*: 502 (M⁺), 393 (M⁺ - PhS). NMR (CDCl₃): 9.30 (1H, br s, HN³), 7.20 (5H, m, Ph), 6.78 (1H, s, H-6), 6.20 (1H, dd, *J*_{1',2'} = 6.0 Hz, *J*_{1',2'a} = 9.0 Hz, H-1'), 3.90 (1H, m, H-3'), 3.76 (5H, m, H-4',5' and CH₂S), 3.14 (1H, m, H-4'), 2.36—1.75 (2H, m, H-2'), 2.09 (3H, s, Ac).

3-O-Acetyl-6,5'-cyclo-5'-deoxythymidine (23)—A mixture of Bu₃SnH (0.23 ml, 0.85 mmol) and AIBN (50 mg) in toluene (4.5 ml) was added dropwise to a solution of **22** (356.4 mg, 0.7 mmol) in toluene (100 ml) over a period of 1.5 h under reflux in an Ar atmosphere. The mixture was further refluxed for 2 h, then the solvent was removed *in vacuo*. The residue was chromatographed on silica gel with 1% MeOH-CHCl₃. The eluate was concentrated and the residue was crystallized from EtOH to give **23** (143.5 mg, 76%), mp 209—210 °C. MS *m/z*: 266 (M⁺). UV λ_{max}^{MeOH} nm: 270.6. NMR (CDCl₃): 7.99 (1H, br s, HN³), 6.47 (1H, d, *J*_{1',2'a} = 5.5 Hz, H-1'), 5.08 (1H, dd, *J*_{2',3'} = 2.9 Hz, *J*_{2',3'} = 6.6 Hz, H-3'), 4.68 (1H, d, *J*_{4',5'a} = 6.6 Hz, H-4'), 3.30 (1H, dd, *J*_{n,b} = 19.1 Hz, H-5'a), 3.04 (1H, d, H-5'b), 2.60 (1H, ddd, H-2'b), 2.33 (1H, dd, *J*_{n,b} = 12.3 Hz, H-2'a), 2.10 (3H, s, Ac), 1.92 (3H, s, CH₃-5). *Anal.* Calcd for C₁₂H₁₄N₂O₅: C, 54.13; H, 5.30; N, 10.52. Found: C, 53.93; H, 5.33; N, 10.24.

6,5'-Cyclo-5'-deoxythymidine (24)—A suspension of **23** (133 mg, 0.5 mmol) in MeOH saturated with NH₃ (10 ml) was stirred overnight at room temperature. The solvent was evaporated off and the residue was crystallized from EtOH to give **24** (73 mg, 70%), mp 232—233 °C. MS *m/z*: 224 (M⁺). UV λ_{max}^{MeOH} nm (*a*): 274.4. (9700). CD (H₂O) [θ] nm: +18400 (270). NMR (CD₃OD): 6.41 (1H, dd, *J*_{1',2'b} = 2.2 Hz, *J*_{1',2'a} = 6.6 Hz, H-1'), 6.27 (1H, d, *J*_{2',3'} = 6.2 Hz, H-3'), 4.38 (1H, m, H-4'), 2.52 (2H, m, H-5'), 2.12 (2H, m, H-2'), 1.96 (3H, s, CH₃-5). *Anal.* Calcd for C₁₀H₁₂N₂O₄: C, 53.57; H, 5.34; N, 12.50. Found: C, 53.77; H, 5.17; N, 12.52.

Acknowledgement This work was supported in part by a Grant-in-Aid for Scientific Research from the Ministry of Education, Science and Culture, Japan, and a grant from the Uchara Memorial Fund for Life Sciences.

References and Notes

- 1) Part LXXI: A. Matsuda and T. Ueda, *Nucleosides Nucleotides*, in press (1987).
- 2) For example see: a) T. Ueda, *Nucleosides Nucleotides*, **4**, 67 (1985) and references cited therein; b) T. Sano and T. Ueda, *Chem. Pharm. Bull.*, **34**, 423 (1986); c) A. Matsuda and T. Ueda, *Chem. Pharm. Bull.*, **34**, 1573 (1986); d) H. Usui, A. Matsuda, and T. Ueda, *Chem. Pharm. Bull.*, **34**, 1961 (1986).
- 3) T. Ueda, H. Usui, S. Shuto, and H. Inoue, *Chem. Pharm. Bull.*, **32**, 3410 (1984).
- 4) For example see: a) M. J. Robins and J. S. Wilson, *J. Am. Chem. Soc.*, **103**, 932 (1981); b) K. Fukukawa, T.

-
- Ueda, and T. Hirano, *Chem. Pharm. Bull.*, **29**, 597 (1981); c) K. Pankiewicz, A. Matsuda, and K. A. Watanabe, *J. Org. Chem.*, **47**, 485 (1982); d) K. Fukukawa, T. Ueda, and T. Hirano, *Chem. Pharm. Bull.*, **31**, 1842 (1983).
- 5) J. P. H. Verheyden and J. G. Moffatt, *J. Org. Chem.*, **35**, 2319 (1970).
 - 6) A. M. Michelson and A. R. Todd, *J. Chem. Soc.*, **1953**, 951.
 - 7) Y. Ueno, K. Chino, and M. Okawara, *Tetrahedron Lett.*, **23**, 2575 (1982).
 - 8) S. S. Jones, C. B. Reese, and A. Ubasawa, *Synthesis*, **1982**, 259.
 - 9) D. W. Visser, D. M. Frisch, and B. Huang, *Biochem. Pharmacol.*, **5**, 157 (1960).

[Chem. Pharm. Bull.]
35(3)1093—1097(1987)

Structure Cristalline d'un Nouvel Agent Inotrope, la Bis-cyclopropyl-méthyl-1,4-piperazine (Bis-chlorhydrate)

NGUYEN HUY DUNG,^a BERNARD VIOSSAT,^b MICHEL CUGNON DE SÉVRI-COURT^c
et MAX ROBBA^{*,c}

Laboratoire de Chimie Minérale et Structurale, U.E.R. des Sciences Pharmaceutiques,^a 1, rue Vaubénard, 14032 Caen Cedex, France, Laboratoire de Chimie Générale, U.E.R. de Médecine et Pharmacie,^b 34, rue du Jardin des Plantes, 86034 Poitiers Cedex, France, et Laboratoire de Chimie Thérapeutique, U.E.R. des Sciences Pharmaceutiques,^c 1, rue Vaubénard, 14032 Caen Cedex, France

(Reçu le 24 juillet, 1986)

The crystal and molecular structure of 1,4-bis-(cyclopropylmethyl)piperazine dihydrochloride has been determined by single-crystal X-ray diffraction analysis. The crystals are monoclinic, space group $P2_1/c$, with $a = 11.641(7)$, $b = 7.017(2)$, $c = 9.32(4)$ Å, $\beta = 107.99(6)^\circ$, $Z = 2$. The structure was solved by direct methods. The hydrogen atoms were included in the refinement. The final R value is 0.035 for 1513 reflections considered to be observed. The bond distances and angles are in good agreement with the expected values. The 1,4-bis-cyclopropylmethylpiperazinium (2^+) ion has the "chair" conformation with a symmetry center. The crystal packing is due to the electrostatic attraction between chloride and nitrogen atoms, reinforced by hydrogen bonds.

Keywords—X-ray analysis; crystal structure; chair conformation; 1,4-bis-cyclopropyl-methylpiperazinium (2^+) ion

Le traitement de l'insuffisance cardiaque congestive continue d'être dominé par les glucosides digitaliques, ce qui justifie la recherche d'autres agents cardiotoniques. Sélectionnée parmi une cinquantaine de dérivés ayant fait l'objet de brevets déposés par Robba et Aurousseau¹⁾ au nom de la firme INNOTHERA, la bis-cyclopropylméthyl-1,4 piperazine²⁾ dont l'activité inotrope positive a été mise en évidence chez l'Homme dans des cardiomyopathies non obstructives³⁾ est actuellement en phase clinique I. Elle a été soumise à une étude radioacristallographique à l'état de bischlorhydrate.

Détermination de la Structure Cristalline

Le cristal choisi a pour dimensions: $280 \times 220 \times 180$ μm . Les paramètres de la maille élémentaire déterminés à partir de 24 réflexions avec le rayonnement $\text{MoK}_\alpha(6,8 < \theta < 14,3^\circ)$ ont pour valeurs: $a = 11,641(7)$; $b = 7,017(2)$; $c = 9,32(4)$ Å; $\beta = 107,99(6)^\circ$. $V = 701,7$ Å³; $Z = 2$; $D_m = 1,28(2)$; $D_x = 1,26$ Mg · m⁻³; $\mu = 0,440$ mm⁻¹ (MoK_α); $M_r = 267,2$; groupe spatial $P2_1/c$; $F(000) = 288$.

Les intensités ont été mesurées sur un diffractomètre automatique CAD-4 ENRAF-NONIUS, avec un balayage $\omega - 2\theta$, d'amplitude $s^\circ = 0,80 + 0,35 \tan \theta$. $1 \leq \theta \leq 35^\circ$; $-18 \leq h \leq 18$; $0 \leq k \leq 11$; $0 \leq l \leq 14$. Les réflexions 400, 040 et 002 ont été choisies pour contrôler les intensités. L'écart-type relatif moyen sur les intensités est de 0,02; 2712 réflexions indépendantes ont été mesurées; 1513 d'entre elles répondant au critère $I > 3\sigma(I)$ ont été retenues pour l'affinement.

Aucune correction d'absorption n'a été effectuée.

La structure a été résolue par les méthodes directes à l'aide de MULTAN 80.⁴⁾ L'affinement basé sur F a été effectué par la méthode des moindres carrés à l'aide d'un programme à matrice complète.⁵⁾ Les facteurs de diffusion corrigés des f' et f'' sont issus de "International Tables of Crystallography"⁶⁾; au cours de l'affinement, il a été tenu compte des corrections réelles de diffusion anormale pour Cl, N et C. Les positions des atomes non-

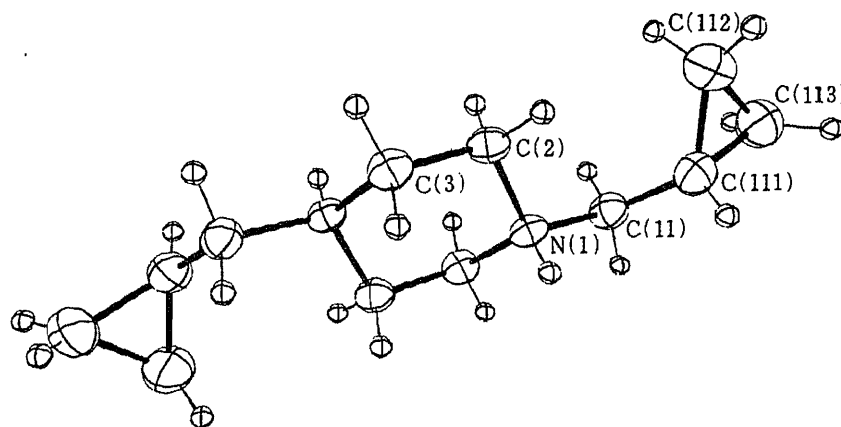


Fig. 1. Vue en Perspective du Cation (Bis-cyclopropyl-méthyl-1,4)pipérazinium (2⁺)

Les ellipsoïdes d'agitation thermique correspondent à 50% de probabilité.

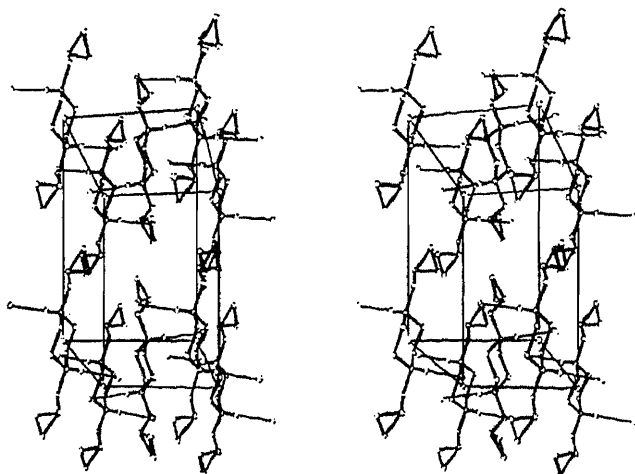


Fig. 2. Vue Stéréoscopique du Contenu de la Maille Élémentaire

hydrogène ainsi que les facteurs d'agitation thermique anisotrope ont été affinés. Les positions des atomes d'hydrogène ont été localisées avec la série de Fourier des différences $F_o - F_c$ puis affinées. Les facteurs d'agitation thermique des atomes d'hydrogène ont été laissés fixes et correspondent à ceux de l'atome porteur. Voici les valeurs obtenues à l'issue du dernier affinement: $R=0,035$; $R_w=0,038$ avec le schéma de pondération: $w=1/\sigma^2(F)$; la valeur maximale du rapport Δ/σ est égale à 0,64.

Les valeurs maximale et minimale de la densité électronique dans la série de FOURIER finale des différences valent 0,13 et $-0,09 e \cdot \text{Å}^{-3}$.

Les distances et angles valentiels ont été calculés à l'aide du programme ORFFE 3,⁷⁾ les distances aux plans moyens par le programme NRC.⁸⁾ Le dessin du cation (bis-cyclopropylméthyl-1,4)pipérazinium (2⁺) (voir Fig. 1) et la vue stéréoscopique de la maille élémentaire (Fig. 2) ont été obtenus à l'aide du programme ORTEP.⁹⁾

Les coordonnées atomiques relatives sont rassemblées dans le Tableau I, les principales distances interatomiques et les angles valentiels dans le Tableau II. La Fig. 1 représente une vue en perspective du cation (bis-cyclopropylméthyl-1,4) pipérazinium (2⁺) et précise la numérotation atomique utilisée. Ce cation présente un centre de symétrie (qui coïncide avec celui du groupe spatial), à la différence du cation *N*-méthyl pipérazinium (2⁺) dans le complexe de la *N*-méthyl pipérazine avec la phénylbutazone¹⁰⁾; en effet, ce dernier cation

TABLEAU I. Coordonnées Atomiques, Facteurs de Temperature Equivalents et Ecart-Types (Entre Parenthèses)

	<i>x</i>	<i>y</i>	<i>z</i>	<i>B</i> _{eq} (Å ²)
Cl	0,17254 (5)	0,55345 (6)	0,04662 (5)	3,2
N(1)	0,1246 (1)	-0,0223 (2)	-0,0008 (1)	2,1
C(2)	0,0955 (2)	0,0460 (3)	0,1399 (2)	2,5
C(3)	-0,0247 (1)	-0,0334 (2)	0,1422 (2)	2,4
C(11)	0,2439 (2)	0,0516 (3)	-0,0112 (2)	2,7
C(111)	0,3481 (2)	-0,0101 (3)	0,1228 (2)	3,2
C(112)	0,3873 (2)	0,1114 (4)	0,2659 (3)	4,5
C(113)	0,4616 (2)	0,1058 (4)	0,1580 (3)	4,3
H(N1)	0,135 (2)	-0,144 (4)	0,006 (3)	2,1
H(C2A)	0,162 (2)	0,002 (4)	0,233 (3)	2,5
H(C2B)	0,093 (2)	0,186 (4)	0,136 (3)	2,5
H(C3A)	-0,043 (2)	0,009 (4)	0,232 (3)	2,5
H(C3B)	-0,026 (2)	-0,179 (4)	0,141 (3)	2,5
H(C11A)	0,236 (2)	0,190 (4)	-0,015 (3)	2,7
H(C11B)	0,248 (2)	-0,002 (4)	-0,108 (3)	2,7
H(C111)	0,355 (2)	-0,141 (4)	0,132 (3)	3,2
H(C112A)	0,419 (3)	0,049 (4)	0,369 (4)	4,5
H(C112B)	0,342 (3)	0,231 (5)	0,269 (3)	4,5
H(C113A)	0,540 (3)	0,042 (5)	0,190 (3)	4,4
H(C113B)	0,458 (3)	0,221 (5)	0,090 (4)	4,4

$$B_{\text{eq}} = \frac{4}{3} \sum_i \sum_j \beta_i \beta_j \vec{a}_i \cdot \vec{a}_j$$

possède un plan de symétrie passant par les atomes d'azote et perpendiculaire au plan des atomes de carbone. Dans le composé cité en titre, le noyau pipérazinium (2⁺) présente une conformation de type chaise. Les distances C-N et C-C intracycliques sont très voisines de celles décrites dans le bichlorhydrate de pipérazine monohydrate¹¹⁾ qui présente une symétrie $\bar{1}$. Les distances C-C et C-N de l'ion pipérazinium (2⁺) ont des valeurs respectivement égales à 1,527 Å d'une part, 1,490 et 1,509 Å d'autre part.

Ces valeurs sont nettement supérieures à celles décrites dans l'hexahydrate de pipérazine¹²⁾ de symétrie 2/*m*: 1,491 Å pour la liaison C-C et 1,458 Å pour la liaison C-N.

La double charge cationique est apportée par les protons rattachés aux deux atomes d'azote du noyau pipérazine. Les atomes N(1) et N(1') sont situés de part et d'autre du plan moyen défini par les atomes C(2), C(3) et leurs centrosymétriques, à une distance égale à 0,681(1) Å. Les angles de liaison endocycliques ont une valeur moyenne de 110,3(9)°. La distance N(1)-C(11) reliant le noyau pipérazine au groupement méthylène en pont est un peu plus longue que les valeurs couramment admises pour les liaisons du type N(sp³)-C(sp³). En revanche, la distance C(11)-C(111) reliant ce pont au cyclopropane est plus courte que la longueur habituelle C(sp³)-C(sp³) et peut être comparée à celles rencontrées dans le chloro-1 phénylsulfonyle-1, diméthyl-2,3 cyclopropane¹³⁾: 1,511 et 1,515 Å. Les distances C-C à l'intérieur du cyclopropane sont plus courtes que les valeurs observées pour des simples liaisons de type paraffinique; elles sont très voisines de celles observées dans le dérivé précédemment cité.¹³⁾ Les angles endocycliques sont très proches de 60°. Le plan du cyclopropane (Tableau III) fait un angle de 29,70° avec le plan moyen du cycle pipérazine (défini par C(2), C(3) et leurs homologues centrosymétriques).

L'électroneutralité du composé est assurée par les ions Cl⁻ qui sont liés aux protons H⁺ rattachés aux atomes d'azote par la liaison hydrogène: N(1)-H(N1)···Clⁱⁱ: 3,034(1) Å et 174(2)° avec le code de symétrie ii: (*x*, -1 + *y*, *z*).

TABLEAU II.

a) Distances interatomiques (Å) et angles (°)			
Distances (Å)		Angles (°)	
N(1)-C(2)	1,492 (2)	C(2)-N(1)-C(3 ⁱ)	108,8 (1)
N(1)-C(3 ⁱ)	1,489 (2)	C(2)-N(1)-C(11)	113,4 (1)
N(1)-C(11)	1,512 (2)	C(3 ⁱ)-N(1)-C(11)	110,2 (1)
C(2)-C(3)	1,512 (2)	N(1)-C(2)-C(3)	110,4 (1)
C(11)-C(111)	1,489 (3)	C(2)-C(3)-N(1 ⁱ)	111,8 (1)
C(111)-C(112)	1,497 (3)	N(1)-C(11)-C(111)	112,5 (1)
C(111)-C(113)	1,500 (3)	C(11)-C(111)-C(112)	119,4 (2)
C(112)-C(113)	1,490 (3)	C(11)-C(111)-C(113)	117,3 (2)
N(1)-H(N1)	0,86 (3)	C(112)-C(111)-C(113)	59,6 (2)
C(2)-H(C2A)	1,00 (2)	C(111)-C(112)-C(113)	60,3 (1)
C(2)-H(C2B)	0,98 (3)	C(112)-C(113)-C(111)	60,1 (2)
C(3)-H(C3A)	0,95 (3)		
C(3)-H(C3B)	1,02 (3)		
C(11)-H(C11A)	0,98 (3)		
C(11)-H(C11B)	0,97 (3)		
C(111)-H(C111)	0,92 (3)		
C(112)-H(C112A)	0,99 (3)		
C(112)-H(C112B)	1,00 (3)		
C(113)-H(C113A)	0,97 (3)		
C(113)-H(C113B)	1,01 (3)		
b) Liaison hydrogene			
	N(1)-H-C1 ⁱⁱ	3,034(1)Å, 174 (2)°	
c) Liaisons intermoleculaires ($d < 3,60$ Å) et écarts-type			
	Cl-C(2 ⁱⁱⁱ)	3,571(1)Å	
	C(113)-C(113 ^{iv})	3,567(5)Å	

Code de symétrie, i: $-x, -y, -z$. ii: $x, 1-y, z$. iii: $x, 1/2-y, -1/2+z$. iv: $1-x, -y, -z$.

TABLEAU III. Equations des Différents Plans Moyens (Pondérés à Partir des Écarts-Type sur les Positions Atomiques), Distances des Atomes à ces Plans Moyens et Angle Dièdre entre Plans

a) Paramètres rapportés à un système de coordonnées cartésiennes en Å				
	l	m	n	p
Cycle A	-0,3687	0,9291	-0,0283	0
Cycle B	0,3830	-0,7673	0,5144	2,0178
b) Distances des atomes aux plans moyens (les écarts-type sont mis entre parenthèses)				
Cycle A défini par les atomes suivants: C(2), C(2 ⁱ), C(3), C(3 ⁱ)				
Distance de N(1) au cycle A: -0,681(1)Å				
Cycle B défini par les atomes C(111), C(112), C(113)				
c) Angle dièdre (A, B) = 150°				

Plans moyens $lX + mY + nZ = p$.

La Fig. 2 représente une vue stéréoscopique du contenu de la maille élémentaire; l'empilement des molécules sous forme d'entités isolées s'effectue selon la direction \vec{a} . La cohésion cristalline est assurée par les contacts de van der Waals habituels. Les paramètres d'agitation thermique anisotrope des atomes non hydrogène sont rassemblés dans le Tableau IV.

En conclusion, l'étude radiocristallographique de la bis-cyclopropylméthylpipérazine a

TABLEAU IV. Parametres d'Agitation Thermique Anisotrope ($\times 10^3$)

Atomes	β_{11}	β_{22}	β_{33}	β_{12}	β_{13}	β_{23}
Cl	9,52 (4)	9,68 (8)	10,80 (5)	0,81 (5)	3,77 (4)	0,56 (6)
N(1)	5,7 (1)	8,9 (2)	6,7 (1)	0,5 (1)	2,6 (1)	0,2 (1)
C(2)	6,2 (1)	13,7 (3)	6,2 (2)	-0,2 (2)	2,6 (1)	-0,7 (2)
C(3)	6,3 (1)	12,9 (3)	6,1 (2)	0,4 (2)	2,6 (1)	1,2 (2)
C(11)	5,9 (1)	13,3 (3)	9,6 (2)	-0,5 (2)	3,5 (1)	-0,6 (2)
C(111)	6,3 (1)	14,3 (4)	12,6 (2)	0,9 (2)	2,5 (2)	-0,8 (2)
C(112)	8,1 (2)	28,2 (6)	12,1 (3)	0,0 (3)	1,6 (2)	-4,1 (3)
C(113)	6,5 (2)	22,6 (5)	17,5 (4)	-1,2 (2)	2,7 (2)	-3,2 (4)

$$T = \exp\{-h^2\beta_{11} + k^2\beta_{22} + l^2\beta_{33} + 2hk\beta_{12} + 2hl\beta_{13} + 2kl\beta_{23}\}.$$

permis de préciser la conformation chaise du cycle pipérazinique ainsi que la configuration trans di-équatoriale des deux substituants cyclaniques. L'hétérocycle est caractérisé par la présence d'un centre d'inversion et par l'absence d'un plan de symétrie à la différence de la *N*-méthylpipérazine citée précédemment¹⁰⁾ qui présente simultanément ces deux éléments de symétrie. Nous pouvons ainsi entreprendre l'étude du mécanisme de l'activité hémodynamique de ce nouvel agent inotrope.

References

- 1) M. Robba et M. Arousseau, Brevet Français, Fr. Patent N° 8021527 (1980), Brevet Européen, Fr. Patent N° 50072 (1981), Brevet Américain, U. S. Patent 4.474.783 (1981), Brevet Japonais, Japan. Patent 163681 (1981).
- 2) G. Leclerc, *Drugs of the Future*, **10**, 907 (1985).
- 3) D. Mesangeau, I. Azancot, J. Haring, M. Maamer et M. Arousseau, First Pharmacological Findings on INO 2628 CZ: a New Inotropic Agent with Bis-cyclopropylmethylpiperazine Structure, Abstracts of Papers, 8th International Congress Pharmacology, Tokyo, July 1981, p. 908.
- 4) P. Main, S. J. Fiske, S. E. Hull, L. Lessinger, G. Germain, J. P. Declercq et M. M. Woolfson, MULTAN a System of Computer Programs for the Automatic Solution of Crystal Structures from X-Ray Diffraction Data, Université de York, Angleterre et Louvain, Belgique.
- 5) W. R. Busing, *Acta Cryst.*, **A27**, 683 (1971).
- 6) International Tables for X-Ray Crystallography, Tome IV, Kynoch Press, Birmingham, 1974, pp. 72--75.
- 7) W. R. Busing, K. O. Martin et H. A. Levy, ORFFE 3, Oak Ridge, National Laboratory, Tennessee, 1971.
- 8) F. R. Ahmed, S. R. Hall, M. E. Pippy et C. P. Huber, NRC Crystallography Programs for the IBM/360 System-World List of Crystallography Computer Programs, Utrecht, Oosthoek, 1966, p. 52.
- 9) C. K. Johnson, ORTEP. Report ORNL-3794. Oak Ridge, National Laboratory, Tennessee, 1965.
- 10) J. Toussaint, O. Dideberg et L. Dupont, *Acta Cryst.*, **B30**, 590 (1974).
- 11) C. Rerat, *Acta Cryst.*, **13**, 459 (1960).
- 12) D. Schwartzbach, *J. Chem. Phys.*, **48**, 4134 (1968).
- 13) W. Saenger et H. Schwalbe, *J. Org. Chem.*, **36**, 3401 (1971).

[Chem. Pharm. Bull.]
35(3)1098-1104(1987)

Efficient Synthetic Method for Ethyl (+)-(2*S*,3*S*)-3-[(*S*)-3-Methyl-1-(3-methylbutylcarbamoyl)butylcarbamoyl]-2-oxiranecarboxylate (EST), a New Inhibitor of Cysteine Proteinases

MASAHARU TAMAI,^a CHIHIRO YOKOO,^{*a} MITSUO MURATA,^a
KIYOSHI OGUMA,^a KAORU SOTA,^a EISUKE SATO,^b
and YUICHI KANAOKA^b

Research Center, Taisho Pharmaceutical Co., Ltd.,^a 1-403 Yoshino-cho, Ohmiya,
Saitama 330, Japan and Faculty of Pharmaceutical Sciences,
Hokkaido University,^b Kita-ku, Sapporo 060, Japan

(Received August 21, 1986)

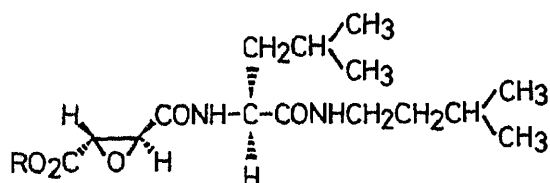
Ethyl (+)-(2*S*,3*S*)-3-[(*S*)-3-methyl-1-(3-methylbutylcarbamoyl)butylcarbamoyl]-2-oxiranecarboxylate (EST; **1a**) is expected to be useful as an oral therapeutic agent for muscular dystrophy on the basis of its potent inhibitory activities against the cysteine proteinases involved in the myofibrillar protein degradation that occurs in the disease. Through extensive investigations aimed at developing a new synthetic method for **1a** that would be suitable for industrial application, it has been found that L-arginine can be used as a new, efficient resolving agent to obtain optically pure L-*trans*-epoxysuccinic acid (**3a**), and the active ester method using *p*-nitrophenol is very effective in the coupling reaction of ethyl L-*trans*-epoxysuccinate (**7a**) and L-leucine isoamylamide (**8a**) because of the extremely low formation of by-products.

To examine the contribution of the stereochemistry of the *trans*-epoxysuccinic acid and leucine moieties to the inhibitory activity against cysteine proteinases, the diastereomers (**1b-d**) of **1a** were synthesized by a similar method and the rate constants of inactivation of papain by **1a-d** were measured. Compound **1a**, having L-*trans*-epoxysuccinic acid and L-leucine moieties, showed the most potent activity among them.

Keywords—synthesis; L-*trans*-epoxysuccinic acid; L-leucine isoamylamide; optical resolution; arginine; active ester method; inhibitor; cysteine proteinase; muscular dystrophy

Ethyl (+)-(2*S*,3*S*)-3-[(*S*)-3-methyl-1-(3-methylbutylcarbamoyl)butylcarbamoyl]-2-oxiranecarboxylate (EST; **1a**) is an ester derivative of (+)-(2*S*,3*S*)-3-[(*S*)-3-methyl-1-(3-methylbutylcarbamoyl)butylcarbamoyl]-2-oxiranecarboxylic acid (E-64-c; **2**),¹⁾ which is a potent inhibitor of cysteine proteinases.^{2,3)}

Compound **2** is expected to be a new type of therapeutic agent for muscular dystrophy on the basis of recent data suggesting that the progressive loss of muscle proteins in this disease arises because of a marked increase of intracellular cysteine proteinases such as calcium-activated neutral protease and lysosomal cathepsins.^{4,5)} However, the low absorbability of **2** from the intestine was one of the problems to be solved for practical use, since an oral drug is desirable for long-term use in chronic diseases, such as muscular dystrophy. Compound **1a**



EST (**1a**): R = C₂H₅
E-64-c (**2**): R = H

Fig. 1

has been demonstrated to show potent inhibitory activity against cysteine proteinases in tissues when given orally.⁶⁾ Further, the long-term administration of **1a** to inherited muscular dystrophic hamsters prevented the development of necrotic changes in the myocardium, accompanied with a marked decrease in calcium deposition and prolonged life span.⁷⁾ These effects were presumed to be due to the potent inhibitory activity against cysteine proteinases. Therefore, there has been a growing expectation that this drug may be practically useful as a therapeutic agent for muscular dystrophy.

On the other hand, the development of a method suitable for industrial production of **1a** is necessary. We report herein efficient synthetic methods for **1a** and its diastereomers (**1b—d**), and the effect of the stereochemistry on the inhibitory activity.

As shown in Fig. 1, **1a** consists of *L-trans*-epoxysuccinic acid (**3a**; 2*S*, 3*S*), *L*-leucine and isoamylamine. Although there are some reports on the preparation of *D-trans*-epoxysuccinic acid (**3b**; 2*R*, 3*R*) by stereoselective synthesis⁸⁾ or fermentation,⁹⁾ little work has been done on the preparation of the *L*-isomer (**3a**). Ohashi and Harada¹⁰⁾ reported the optical resolution of *DL-trans*-epoxysuccinic acid (**4**) with (–)-ephedrine by diastereomeric salt formation. Mori and Iwasawa,¹¹⁾ and Seebach and Wasmuth¹²⁾ have reported a stereoselective synthesis of the diethyl ester of **3a** from *D*-tartaric acid and (–)-malic acid, respectively. However, the resolution seems to be available only on a laboratory scale, and the stereoselective syntheses were considered to be expensive because of the complex processes involved. Therefore, we tried to find a new resolving agent (for **4**) available for industrial use. Compound **4** was prepared by epoxidation of fumaric acid according to the method of Payne and Williams.¹³⁾

As a result of studies with various optically active amines, five compounds were found to be useful for the resolution of **4**, as shown in Table I.

D- α -Phenylglycine amide and dehydroabiethylamine gave **3a** in low yield. Though (–)-ephedrine¹⁰⁾ was superior to the above two reagents, it was inferior to arginine in terms of optical purity and yield. When *L*-phenylalanine amide was compared with *L*-arginine, the former was inferior in optical purity though the former was superior in yield. The optical purity of **3a** obtained by using *L*-phenylalaninol was at the same level as that obtained by using *L*-arginine, though the yield was much lower. In terms of economy, *L*-arginine is preferable to *L*-phenylalaninol. Consequently, *L*-arginine was selected for the practical resolution of **4**. The *D*-isomer (**3b**) was also obtained in high optical purity by the same procedure using *D*-arginine. As shown in Chart 1, diethyl *L-trans*-epoxysuccinate (**5a**) was synthesized from **3a** in good yield.

However, the extraction of **3a** from the aqueous solution was so troublesome that the direct esterification of the diastereomeric salt (**6a**) was tried by the use of 3.0 eq of sulfuric acid without isolation of **3a**. This method turned out to be much more efficient than the two-step method.

TABLE I. Resolution of *DL-trans*-Epoxy succinic Acid (**4**) by Using Various Optically Active Amines

Resolving agent	<i>L-trans</i> -Epoxy succinic acid (3a)	
	$[\alpha]_D$	Yield (%)
<i>L</i> -Phenylalaninol	+121.0°	40.0
<i>L</i> -Phenylalanine amide	+109.8°	68.0
<i>D</i> - α -Phenylglycine amide	+110.8°	32.2
Dehydroabiethylamine	+116.0°	26.2
<i>L</i> -Arginine	+122.2°	54.7
(–)-Ephedrine ¹⁰⁾	+117.8°	48.0

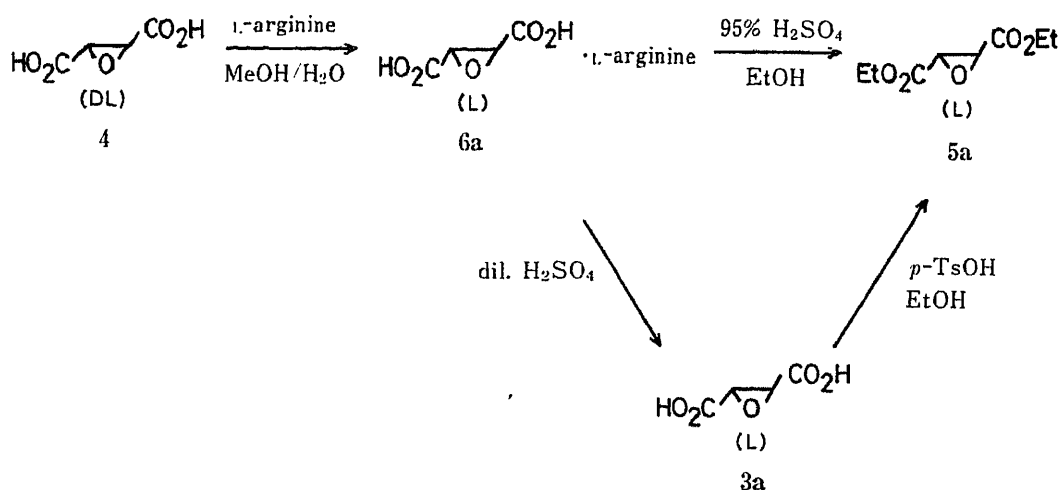


Chart 1

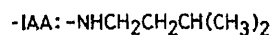
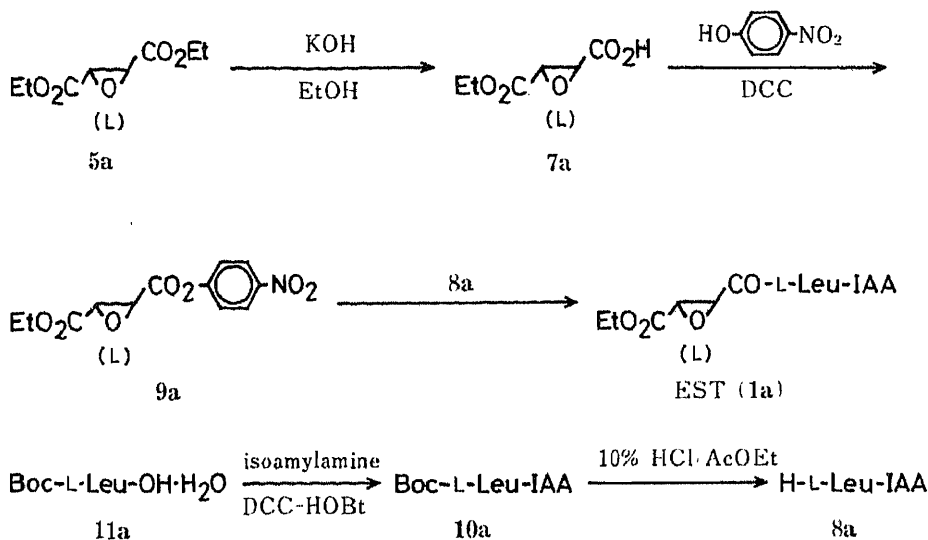


Chart 2

Compound **1a** was prepared from the diethyl ester (**5a**) and L-leucine according to the scheme shown in Chart 2. The diethyl ester (**5a**) was hydrolyzed to the half ester (**7a**) and then coupled with L-leucine isoamylamide (H-L-Leu-IAA) (**8a**). Among many possible methods, the active ester method using *p*-nitrophenol (HONp) was finally selected for this reaction because of the extremely low formation of by-products. The active ester (**9a**) was easily prepared from the half ester (**7a**) and HONp by using *N,N'*-dicyclohexylcarbodiimide (DCC) in good yield. Compound **8a** was prepared from *N*-(*tert*-butoxycarbonyl)-L-leucine isoamylamide (Boc-L-Leu-IAA) (**10a**)¹⁴⁾ by using a conventional method of peptide chemistry.

This synthetic route (shown in Chart 2) was expected to be suitable for industrial production since no special purification step, such as column chromatography, was necessary in any reaction step.

The physical properties of **1a** and its isomers (**1b—d**) prepared by similar procedures are summarized in Table II. The chemical shifts of the epoxy ring protons, the melting point and

TABLE II. Physical Data for EST (**1a**) and Its Diastereomers (**1b—d**)

Compound	Configuration		$[\alpha]_D^{20}$ ^{a)}	mp (°C)	Chemical shift of epoxy ring protons (ppm)	
	<i>t</i> -ES ^{b)}	Leu ^{c)}				
1a	L	L	+51.7 ^a	126.2	3.48	3.69
1b	L	D	+93.4 ^a	133.5	3.55	3.69
1c	D	L	-92.6 ^a	133.4	3.55	3.69
1d	D	D	-50.0 ^a	123.8	3.48	3.69

a) ($c=1.00$, EtOH). b) *trans*-Epoxy succinic acid moiety. c) Leucine moiety.

TABLE III. Rate Constant for Inactivation of Papain

Compound	Configuration		Rate constant ^{c)} (M ⁻¹ , min ⁻¹)
	<i>t</i> -ES ^{a)}	Leu ^{b)}	
1a	L	L	277
1b	L	D	58
1c	D	L	102
1d	D	D	25

a) *trans*-Epoxy succinic acid moiety. b) Leucine moiety. c) The rate constants were measured according to the method of Barrett *et al.*¹⁷⁾

the specific rotation showed that **1d** and **1b** were the antipodes of **1a** and **1c**, respectively.

To examine the contribution of the stereochemistry of the *trans*-epoxy succinic acid and leucine moieties to the inhibitory activity against cysteine proteinases, we measured the rate constants of **1a** and its isomers (**1b—d**) for the inactivation of papain. As shown in Table III, the stereochemistry strongly influenced the inhibitory activity. Compound **1a** reacted with papain faster than the other three isomers. The reactivity of the D-D isomer (**1d**), which showed the lowest rate, was approximately one-tenth of that of **1a** (L-L isomer). The configuration of the leucine moiety seems to play an important role in the binding of **1a** to papain rather than that of the epoxy succinic acid group, based on a comparison of the rate constants of **1b**, **1c** and **1a**. It was suggested that the L-L isomer (**1a**) has the best conformation for approach to the active site of papain, and its epoxy ring may be located closer to the active thiol group as compared with the epoxy rings of the other three isomers. The *in vitro* and *in vivo* inhibitory activities of **1a** for cysteine proteinases were reported in the previous paper.⁶⁾

Experimental

Melting points were determined with a Yanagimoto micro melting point apparatus and are uncorrected. Infrared (IR) spectra were measured with a JASCO DS-701G spectrophotometer. Proton nuclear magnetic resonance (¹H-NMR) spectra were taken on a Varian XL-200 spectrometer using tetramethylsilane or sodium trimethylsilyl propionate-*d*₄ as an internal standard. Chemical shifts are given on the δ scale. Optical rotations were obtained with a JASCO DIP-140 or JASCO DIP-360 digital polarimeter. Mass spectra (MS) were recorded on a Shimadzu LKB-9000 spectrometer.

Examples of Optical Resolution of DL-*trans*-Epoxy succinic Acid (4)—a) Optical Resolution with L-Phenylalanine Amide: A mixture of **4** (0.396 g, 3.0 mmol) in 95% MeOH (1.0 ml) and L-phenylalanine amide¹⁵⁾ (0.492 g, 3.0 mmol) in 95% MeOH (2.0 ml) was kept at room temperature overnight. The separated crystals were collected by suction. Yield, 0.372 g of acidic salt (83.8%). mp 176—177°C. $[\alpha]_D^{17}$ +64.6° ($c=0.90$, MeOH). *Anal.* Calcd for C₁₃H₁₆N₂O₆: C, 73.75; H, 9.69; N, 3.74. Found: C, 73.95; H, 9.54; N, 3.65.

A solution of the above salt (0.354 g, 1.54 mmol) in 5 ml of water was applied to a column of Dowex 50 × 8 (H-

form, 100–200 mesh, 0.5×7 cm) and the column was washed with water until the effluent become neutral. The effluent was evaporated to dryness under reduced pressure to give the crude (+)epoxy acid, 0.154 g. Recrystallization from dioxane and *n*-hexane gave **3a** as colorless prisms of mp 176–177 °C (lit.¹⁰ mp 188 °C). Yield, 0.128 g (81.1%). $[\alpha]_D^{25} + 109.8^\circ$ ($c = 0.82$, EtOH). The overall yield of optical resolution was 68.0%.

b) Optical Resolution with L-Phenylalaninol: L-Phenylalaninol¹⁶ (7.55 g, 50 mmol) in 20 ml of EtOH was added to a solution of **4** (6.60 g, 50 mmol) in 20 ml of hot EtOH (80 °C) at 80 °C. The mixture was allowed to cool to room temperature and then kept at 5 °C overnight. The crystals were collected by suction and washed with cold EtOH. Recrystallization of this salt from MeOH (43 ml) gave 4.61 g of neutral salt (42.5%), mp 167–169.5 °C. $[\alpha]_D^{18} + 39.8^\circ$ ($c = 0.6$, MeOH). Anal. Calcd for $C_{22}H_{30}N_2O_7$: C, 60.81; H, 6.96; N, 6.45. Found: C, 60.79; H, 6.99; N, 6.43.

The above salt (4.61 g, 11 mmol) was treated with an ion-exchange column by the same procedure as in a). Colorless prisms 1.32 g of **3a** (94.3%). mp 171–172 °C. $[\alpha]_D^{20} + 121^\circ$ ($c = 1.20$, EtOH). The overall yield of optical resolution was 40.0%.

c) Optical Resolution with L-Arginine: L-Arginine (234.9 g, 1.35 mol) in warm water (650 ml) was added gradually to a stirred solution of **4** (178 g, 1.35 mol) in MeOH (2600 ml), and the mixture was allowed to stand overnight at room temperature. The precipitate formed was filtered by suction and washed with MeOH–water (4 : 1, 1000 ml) to give crude **6a** (201.2 g). Recrystallization of **6a** from MeOH–water (2 : 1, 3000 ml) gave pure **6a** as colorless prisms. Yield, 170.2 g (82.5%). mp 172 °C (dec.). $[\alpha]_D^{22} + 54.7^\circ$ ($c = 1.00$, H₂O). Anal. Calcd for $C_{10}H_{18}N_4O_7$: C, 39.21; H, 5.92; N, 18.29. Found: C, 39.17; H, 5.90; N, 18.46. IR (KBr): 3340, 3140, 1650, 1490, 1390, 1330, 1260, 1170 cm^{-1} . ¹H-NMR (D₂O) δ : 1.54–2.02 (4H, m, $-CH_2CH_2-$), 3.22 (2H, t, $J = 6$ Hz, $-NHCH_2-$), 3.48 (2H, s, epoxy ring), 3.84 (1H, t, $J = 6$ Hz, $-CH<$).

The corresponding D,D-isomer (**6b**) was obtained as colorless prisms by the same procedure as described above. Yield, (84.0%). $[\alpha]_D^{26} - 54.0^\circ$ ($c = 1.00$, H₂O).

Compound **6a** (73.1 g) was added to a stirred solution of dilute H₂SO₄ (95% H₂SO₄–H₂O, 1 : 10, 330 ml) under ice-cooling. The mixture was saturated with sodium chloride, and then extracted with acetone–AcOEt (7 : 3, 400 ml \times 3). The combined extract was washed with brine (40 ml \times 3), dried over MgSO₄, and then concentrated *in vacuo*. Crude **3a** obtained was crystallized from dioxane–*n*-hexane (95 : 5) to give colorless needles. Yield, 20.9 g (66.3%). mp 178–180 °C. $[\alpha]_D^{26} + 122.2^\circ$ ($c = 1.01$, EtOH). IR (KBr): 3080, 1685, 1405, 1295, 1235, 1080 cm^{-1} . ¹H-NMR (D₂O) δ : 3.77 (2H, s, epoxy ring). Anal. Calcd for $C_4H_4O_5$: C, 36.37; H, 3.06. Found: C, 36.52; H, 3.27.

By the same procedure as described above, the D-isomer (**3b**) was obtained as colorless needles. Yield, (67.0%). $[\alpha]_D^{26} - 121.6^\circ$ ($c = 1.00$, EtOH).

Diethyl L-trans-Epoxy succinate (5a)—Method A: A stirred suspension of **6a** (107.1 g, 0.35 mol) in EtOH (1050 ml) was treated dropwise with 95% H₂SO₄ (102.9 g, 1.05 mol) at room temperature, and then the mixture was stirred under reflux for 4.5 h. The solvent was evaporated off *in vacuo* and the residue was poured into ice-water (200 ml), then extracted with AcOEt (300 ml \times 3). The extract was washed with saturated aqueous NaHCO₃ (200 ml \times 2) and brine (200 ml \times 2) successively, then dried over MgSO₄ and filtered by suction. After evaporation of the solvent, the residue was purified by fractional distillation to provide **5a** as a colorless oil. Yield, 50.4 g (76.6%). bp 78–80 °C/0.9 mmHg (lit.¹¹ bp 98–99 °C/3 mmHg). $[\alpha]_D^{26} + 110.5^\circ$ ($c = 1.12$, EtOH). IR (neat): 2980, 1740, 1370, 1325, 1275, 1195, 1025 cm^{-1} . ¹H-NMR (CDCl₃) δ : 1.31 (6H, t, $J = 7$ Hz, $-CH_3 \times 2$), 3.66 (2H, s, epoxy ring), 4.28 (4H, dq, $J = 7, 2$ Hz, $-CH_2 \times 2$).

By the same procedure as described above, the D-isomer (**5b**) was obtained as a colorless oil. Yield, (72.3%). $[\alpha]_D^{26} - 109.4^\circ$ ($c = 1.00$, EtOH).

Method B: *p*-Toluenesulfonic acid monohydrate (1.73 g, 0.009 mol) was added to a stirred suspension of **3a** (40 g, 0.3 mol) in EtOH (350 ml), and the mixture was refluxed for 7 h, then the solvent was evaporated off *in vacuo*. The resulting residue was dissolved in benzene (500 ml) and washed with saturated aqueous NaHCO₃ (250 ml), water (250 ml) and brine (250 ml) successively, and dried over MgSO₄. The solvent was evaporated off *in vacuo* and the residue was purified by fractional distillation to give **5a** as a colorless oil. Yield, 44 g (78%). bp 77–79 °C/0.9 mmHg. $[\alpha]_D^{25} + 109.3^\circ$ ($c = 1.00$, EtOH).

Ethyl p-Nitrophenyl L-trans-Epoxy succinate (9a)—A solution of 85% KOH (6.72 g, 0.1 mol) in EtOH (67 ml) was added dropwise to a stirred solution of **5a** (18.8 g, 0.1 mol) in EtOH (150 ml) at 4–6 °C. The reaction mixture was stirred for 1 h under ice-cooling and then for 4 h at room temperature. After evaporation of the solvent *in vacuo* below 50 °C, water (50 ml) was added to the residue and the solution was washed with AcOEt (50 ml \times 2). The aqueous layer was acidified (pH = 2) by using 6 N HCl under ice-cooling and extracted with AcOEt (70 ml \times 3). The extract was washed with brine (70 ml \times 2), dried over MgSO₄ and filtered. Evaporation of the filtrate *in vacuo* gave the crude half ester (**7a**) (13.1 g) as a colorless oil.

N,N'-Dicyclohexylcarbodiimide (12.9 g, 0.0625 mol) in AcOEt (26 ml) was added dropwise to a stirred solution of the crude **7a** (10.0 g) and *p*-nitrophenol (8.69 g, 0.0625 mol) in AcOEt (55 ml) at 4–5 °C, and the mixture was stirred for 3 h under ice-cooling and for 1 h at room temperature.

The precipitate of *N,N'*-dicyclohexylurea formed was filtered off and washed with AcOEt (20 ml). The combined filtrate and washings were concentrated *in vacuo* and the residue was crystallized from AcOEt–*n*-hexane to give pure **9a** as pale yellow needles. Yield, 14.1 g (65.8% from **5a**). mp 86–87 °C. $[\alpha]_D^{20} + 114.8^\circ$ ($c = 1.00$, AcOEt). Anal. Calcd

for $C_{12}H_{11}NO_7$: C, 51.24; H, 3.95; N, 4.98. Found: C, 51.38; H, 3.95; N, 5.05. IR (KBr): 1755, 1735, 1515, 1340, 1305, 1195, 1170, 1020, 860, 855 cm^{-1} . 1H -NMR (DMSO- d_6) δ : 1.26 (3H, t, $J=8$ Hz, $-OCH_2CH_3$), 4.06 (1H, d, $J=2$ Hz, epoxy ring), 4.08 (1H, d, $J=2$ Hz, epoxy ring), 4.24 (2H, q, $J=8$ Hz, $-OCH_2CH_3$), 7.58 (2H, d, $J=8$ Hz, aromatic), 8.36 (2H, d, $J=8$ Hz, aromatic).

By the same procedure as described above, the D-isomer (**9b**) was obtained as pale yellow needles. Yield, (67.1% from **5b**). $[\alpha]_D^{26} -114.1^\circ$ ($c=1.01$, AcOEt).

EST (1a)—L-Leucine isoamylamide (**8a**) (7.12 g, 0.035 mol) in AcOEt (13 ml) was added dropwise to a stirred solution of the active ester (**9a**) obtained by the above procedure (10.0 g, 0.035 mol) in AcOEt (100 ml) at room temperature, and stirring was continued for 4 h at the same temperature. The precipitate formed was filtered off and the filtrate was washed with 2% aqueous NaOH (30 ml \times 5), brine (40 ml), 5% HCl (40 ml) and brine (40 ml \times 4) successively, and dried over $MgSO_4$. The solvent was evaporated off *in vacuo* and the residue was crystallized from EtOH to give pure **1a** as colorless fine needles. Yield, 9.08 g (74.6%). mp 126.2 $^\circ C$. $[\alpha]_D^{20} +51.7^\circ$ ($c=1.00$, EtOH). Anal. Calcd for $C_{17}H_{30}N_2O_5$: C, 59.63; H, 8.83; N, 8.18. Found: C, 59.78; H, 8.60; N, 7.95. IR (KBr): 3290, 2960, 1755, 1642, 1555, 900 cm^{-1} . 1H -NMR ($CDCl_3$) δ : 0.85—1.04 (12H, m, $-CH_3 \times 4$), 1.32 (3H, t, $J=7$ Hz, $-OCH_2CH_3$), 1.41 (2H, q, $J=7$ Hz, $-NHCH_2CH_2-$), 1.47—1.76 (4H, m, $-CH_2 \times 2$, $\overset{CO}{HN} > CHCH_2-$), 3.11—3.41 (2H, m, $-NHCH_2-$), 3.48 (1H, d, $J=2$ Hz, epoxy ring), 3.69 (1H, d, $J=2$ Hz, epoxy ring), 4.27 (2H, dq, $J=7, 2$ Hz, $-OCH_2CH_3$), 4.35—4.50 (1H, m, $-NHCH_2-$), 6.16—6.30 (1H, m, $-CONHCH_2-$), 6.80 (1H, d, $J=8$ Hz, $-CONHCH_2-$).

By the same procedures as described above, **1b**, **1c** and **1d** were obtained as colorless fine needles by using the active ester (**9a** or **9b**) and leucine isoamylamide (**8a** or **8b**).

1b: Yield, (69.8%). mp 133.5 $^\circ C$. $[\alpha]_D^{20} +93.4^\circ$ ($c=1.00$, EtOH). IR (KBr): 3300, 3240, 2950, 1760, 1640, 1563, 900 cm^{-1} . 1H -NMR ($CDCl_3$) δ : 0.86—1.08 (12H, m, $-CH_3 \times 4$), 1.32 (3H, t, $J=7$ Hz, $-OCH_2CH_3$), 1.39 (2H, q, $J=7$ Hz, $-NHCH_2CH_2-$), 1.48—1.76 (4H, m, $-CH_2 \times 2$, $\overset{CO}{HN} > CHCH_2-$), 3.13—3.40 (2H, m, $-NHCH_2-$), 3.55 (1H, d, $J=2$ Hz, epoxy ring), 3.69 (1H, d, $J=2$ Hz, epoxy ring), 4.27 (2H, dq, $J=7, 2$ Hz, $-OCH_2CH_3$), 4.32—4.48 (1H, m, $-NHCH_2-$), 5.94—6.12 (1H, m, $-CONHCH_2-$), 6.68 (1H, d, $J=8$ Hz, $-CONHCH_2-$).

1c: Yield, (70.5%). mp 133.4 $^\circ C$. $[\alpha]_D^{20} -92.6^\circ$ ($c=1.00$, EtOH).

1d: Yield, (73.6%). mp 123.8 $^\circ C$. $[\alpha]_D^{20} -50.0^\circ$ ($c=1.00$, EtOH).

Boc-L-Leucine Isoamylamide (10a)—*N,N'*-Dicyclohexylcarbodiimide (10.32 g, 0.05 mol) in AcOEt (20 ml) was added dropwise to a stirred solution of Boc-L-leucine monohydrate (**11a**) (12.47 g, 0.05 mol), isoamylamine (4.36 g, 0.05 mol) and 1-hydroxybenzotriazole (6.76 g, 0.05 mol) in AcOEt (35 ml) while keeping the temperature at 3—8 $^\circ C$, and the mixture was stirred for 1.5 h at the same temperature and then for 2.5 h at room temperature. The precipitate of *N,N'*-dicyclohexylurea formed was filtered off and washed with AcOEt (40 ml). The combined filtrate and washings were washed with 5% HCl (100 ml), brine (100 ml), saturated aqueous $NaHCO_3$ (100 ml) and brine (100 ml) successively.

The organic layer was dried over $MgSO_4$ and filtered. The filtrate was evaporated *in vacuo*. The residue was dissolved in *n*-hexane (50 ml) and insoluble materials were filtered off and washed with small amounts of *n*-hexane. The filtrate and washings were concentrated *in vacuo* to give **10a** as a colorless solid, which could be used for the next step without further purification. Yield, 14.45 g (96.1%). An analytical sample was obtained by recrystallization from MeOH—water (2:1) after purification by silica gel column chromatography (Wako gel C-200, AcOEt—*n*-hexane, 1:3). mp 88—90 $^\circ C$. $[\alpha]_D^{24} -24.6^\circ$ ($c=1.00$ EtOH). Anal. Calcd for $C_{16}H_{32}N_2O_3$: C, 63.95; H, 10.76; N, 9.32. Found: C, 64.28; H, 10.37; N, 9.40. MS m/z : 300 (M^+). IR (KBr): 3240, 2960, 1690, 1640, 1555, 1520, 1310, 1240, 1165 cm^{-1} . 1H -NMR ($CDCl_3$) δ : 0.92 (12H, m, $-CH_3 \times 4$), 1.30—1.80 (15H, m, *tert*-Bu, $-CH_2CH_2 \times 2$), 3.27 (2H, m, $-CONHCH_2-$), 4.07 (1H, m, $-CONHCH_2-$), 4.96 (1H, d, $J=8$ Hz, $-NH$ Boc), 6.22 (1H, m, $-CONHCH_2-$).

By the same procedure as described above, the D-isomer (**10b**) was obtained from Boc-D-leucine monohydrate (**11b**) as a colorless solid. Yield, (97.0%). mp 87—89 $^\circ C$. $[\alpha]_D^{24} +24.0^\circ$ ($c=1.02$, EtOH).

L-Leucine Isoamylamide (8a)—Compound **10a** (18.5 g, 0.062 mol) was dissolved in 10% HCl—AcOEt (65 ml) and the mixture was stirred for 2.5 h at room temperature. After evaporation of the solvent, water (50 ml) was added to the residue and the solution was washed with AcOEt (50 ml). The aqueous layer was alkalified (pH > 10) with 25% aqueous NaOH and extracted with AcOEt (50 ml \times 1, 25 ml \times 2). The extract was washed with brine, dried over $MgSO_4$ and filtered by suction. The filtrate was evaporated *in vacuo* to give crude **8a** as a pale yellow oil (12.3 g, 99.6%), which could be used for the next step without further purification. IR (neat): 3280—2940, 1640, 1530, 1465, 1365 cm^{-1} . 1H -NMR ($CDCl_3$) δ : 0.88—1.05 (12H, m, $-CH_3 \times 4$), 1.22—1.86 (8H, m, $-CH_2CH_2 \times 2$, $-NH_2$), 3.22—3.46 (3H, m, $-CONHCH_2-$, H_2NCH_2-), 7.12—7.36 (1H, m, $-CONH-$).

The corresponding D-isomer (**8b**) was obtained from **10b** by the same procedure as described above, as a pale yellow oil. Yield, (99.3%).

Acknowledgment We wish to thank Miss. Y. Yoshimori and Mr. A. Kobayashi for their technical assistance.

References and Notes

- 1) M. Tamai, T. Adachi, K. Oguma, K. Kashiwagi, K. Hanada, S. Omura, and M. Ozeki, *J. Biochem. (Tokyo)*, **90**, 255 (1981).
- 2) K. Suzuki, *J. Biochem. (Tokyo)*, **93**, 1305 (1983).
- 3) S. Hashida, T. Towatari, E. Kominami, and N. Katunuma, *J. Biochem. (Tokyo)*, **88**, 1805 (1980).
- 4) N. C. Kar and C. M. Pearson, *Clin. Chim. Acta*, **73**, 293 (1976).
- 5) R. J. Pennington and J. E. Robinson, *Enzymol. Biol. Clin.*, **9**, 175 (1968).
- 6) M. Tamai, K. Matsumoto, S. Omura, I. Koyama, Y. Ozawa, and K. Hanada, *J. Pharmacobio-Dyn.*, **9**, 672 (1986).
- 7) M. Tamai *et al.*, unpublished data.
- 8) R. Kune and R. Zell, *Chem. Ber.*, **59**, 2514 (1926).
- 9) a) J. H. Birkinshaw, A. Bracken, and Raistic, *Biochem. J.*, **39**, 70 (1945); b) K. Sakaguchi, T. Inoue, and Y. Tada, *Nippon Nogeikagaku Kaishi*, **13**, 241 (1937); c) M. W. Miller, *J. Med. Chem.*, **6**, 233 (1963).
- 10) I. Ohashi and K. Harada, *Bull. Chem. Soc. Jpn.*, **40**, 2977 (1967).
- 11) K. Mori and H. Iwasawa, *Tetrahedron*, **36**, 87 (1980).
- 12) D. Seebach and D. Wasmuth, *Helv. Chim. Acta*, **63**, 197 (1980).
- 13) G. P. Payne and P. H. Williams, *J. Org. Chem.*, **24**, 54 (1959).
- 14) D. H. Rich and F. G. Salituro, *J. Med. Chem.*, **26**, 904 (1983).
- 15) F. Bergel and M. A. Peutherer, *J. Chem. Soc.*, **1964**, 3973.
- 16) H. Seki, K. Koga, H. Matsuo, S. Ohki, I. Matsuno, and S. Yamada, *Chem. Pharm. Bull.*, **13**, 995 (1965).
- 17) A. J. Barret, A. A. Kembhavi, M. A. Brown, H. Kirshke, C. G. Night, M. Tamai, and K. Hanada, *Biochem. J.*, **201**, 189 (1982).

[Chem. Pharm. Bull.]
35(3) 1105—1108(1987)

Tannins and Related Compounds. LII.¹⁾ Studies on the Constituents of the Leaves of *Thujopsis dolabrata* SIEB. et ZUCC.

GEN-ICHIRO NONAKA,^a YUKO GOTO,^b JUN-EI KINJO,^b
TOSHIHIRO NOHARA,^b and ITSUO NISHIOKA*^a

Faculty of Pharmaceutical Sciences, Kyushu University,^a 3-1-1 Maidashi, Higashi-ku,
Fukuoka 812, Japan and Faculty of Pharmaceutical Sciences, Kumamoto University,^b
5-1 Oe-honmachi, Kumamoto 862, Japan

(Received July 17, 1986)

From the leaves of *Thujopsis dolabrata* SIEB. et ZUCC. (Cupressaceae), four new flavanonol glycosides, the 3-*O*- β -D-xylopyranosides (1 \rightarrow 4) of (+)-taxifolin, (-)-taxifolin, (+)-epitaxifolin and (-)-epitaxifolin, together with (+)-catechin (5), (-)-epicatechin (6) and thirteen oligomeric procyanidins (7—19), were isolated and their chemical structures were characterized by spectroscopic and chemical investigations.

Keywords—*Thujopsis dolabrata*; Cupressaceae; flavanonol glycoside; taxifolin xyloside; oligomeric procyanidin

The leaves of *Thujopsis dolabrata* SIEB. et ZUCC. (Cupressaceae) are used as a folk medicine for treatment of diabetes. With regard to the constituents of the title plant, detailed examinations on essential oils and flavonoids have been reported. We have now investigated the leaves of this plant, and have isolated four flavanonol xylosides (1—4), together with (+)-catechin (5), (-)-epicatechin (6), and thirteen oligomeric procyanidins (7—19). This paper deals with the isolation and structure elucidation of these compounds.

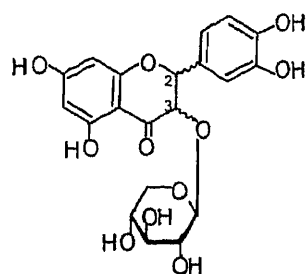
The methanolic extract of the title plant was subjected to a combination of Sephadex LH-20, MCI gel CHP 20P and Bondapak C₁₈ chromatographies with various solvent systems to yield compounds 1—19. Compounds 5—19 were identified as (+)-catechin, (-)-epicatechin, procyanidins B-1, B-2, B-4, B-5, B-6, B-7, C-1 and C-2,²⁾ gambiridin C,³⁾ epicatechin-(4 β \rightarrow 8)-epicatechin-(4 β \rightarrow 8)-catechin,^{2c)} epicatechin-(4 β \rightarrow 6)-epicatechin-(4 β \rightarrow 8)-catechin,⁴⁾ epicatechin-(4 β \rightarrow 8)-epicatechin-(4 β \rightarrow 6)-catechin,^{2c)} and catechin-(4 α \rightarrow 8)-epicatechin-(4 β \rightarrow 8)-catechin,⁵⁾ respectively, by comparison of their physical and spectral data of with those of authentic samples.

Compound 1, an amorphous powder, $[\alpha]_D -8.4^\circ$, was positive to the ferric chloride reagent (dark green) and negative to the anisaldehyde-sulfuric acid reagent. The ultraviolet (UV) maxima at 291 and 330 (sh) nm were suggestive of a flavanone analogue. The proton nuclear magnetic resonance (¹H-NMR) spectrum of 1 showed aliphatic signals at δ 5.28, 4.70 (each 1H, d, $J=9$ Hz) ascribable to the flavanone H-2 and H-3, respectively, the coupling pattern indicating them to be in a *trans* relationship. Five aromatic proton signals appeared at δ 5.96 (2H, br s), 6.85 (2H, br s) and 7.04 (1H, s). In addition, the carbon-13 nuclear magnetic resonance (¹³C-NMR) spectrum exhibited the signals of a pentosyl moiety at δ 64.7, 70.0, 72.1, 76.6 and 102.2. The enzymatic hydrolysis of 1 yielded D-xylose, R_f 0.67 (on thin layer chromatography (TLC)), $[\alpha]_D +19.2^\circ$, and an aglycone (20), colorless needles, mp 218—220 °C, $[\alpha]_D +17.3^\circ$, the latter of which was found to be identical with an authentic sample of (+)-taxifolin with respect to the physical constants and ¹H-NMR spectrum. The maximum (291 nm) in the UV spectrum of 1 showed a bathochromic shift (14 nm) upon addition of

AlCl_3 , and subsequent addition of HCl caused a further bathochromic shift (6 nm). On the other hand, addition of NaOAc caused a bathochromic shift of 37 nm. The ^{13}C -NMR spectrum of **1** showed shifts of the C-2 (-1.7), C-3 (+0.9) and C-4 (-3.2) signals compared with those of **20**. Thus, the location of the xylosyl moiety was established to be at the C-3 position of the taxifolin moiety. The configuration at the anomeric center was determined to be β on the basis of the coupling constant ($J=7\text{ Hz}$) of the anomeric proton signal. Compound **1** was therefore characterized as (+)-taxifolin 3-*O*- β -D-xylopyranoside.

Compound **2**, an amorphous powder, $[\alpha]_{\text{D}} -122.2^\circ$, was positive to the FeCl_3 reagent. The UV spectrum of **2** showed a curve similar to that of **1**. The ^{13}C -NMR spectrum suggested the presence of a xylopyranosyl moiety. On enzymatic hydrolysis with crude hesperidinase, compound **2** furnished D-xylose and an aglycone (**21**), colorless needles, mp 219–221 °C, $[\alpha]_{\text{D}} -20.6^\circ$. The ^1H - and ^{13}C -NMR spectra of **21** were coincident with those of **20**, but the circular dichroism (CD) spectrum showed a reversed Cotton curve, as shown in Fig. 1. Thus, compound **21** was characterized as (-)-taxifolin. The location of the sugar linkage to the flavanonol moiety and the mode of the glycosidic linkage were determined in the same way as described for **1**. Compound **2** therefore could be represented as (-)-taxifolin 3-*O*- β -D-xylopyranoside.

Compound **3**, an amorphous powder, $[\alpha]_{\text{D}} +2.3^\circ$, and compound **4**, an amorphous powder, $[\alpha]_{\text{D}} -93.3^\circ$, were positive to the FeCl_3 reagent. The UV spectra of these compounds were also analogous to that of **1**. The signals at δ 5.46 and 4.46 (each 1H, d, $J=3\text{ Hz}$) in the ^1H -NMR spectrum of **3** could be assigned to H-2 and H-3, respectively, the coupling constants of which indicated the *cis*-configuration. The ^{13}C -NMR spectra of **3** and **4** suggested the occurrence of a D-xylosyl residue in each molecule. Hydrolysis with crude hesperidinase gave D-xylose and an aglycone (**22**), $[\alpha]_{\text{D}} +58.8^\circ$, whose ^1H -NMR spectrum showed signals due to H-2 and H-3 at δ 5.46 (d, $J=3\text{ Hz}$) and 4.46 (d, $J=3\text{ Hz}$), respectively.



1: 2*R*,3*R* 3: 2*S*,3*R*
2: 2*S*,3*S* 4: 2*R*,3*S*

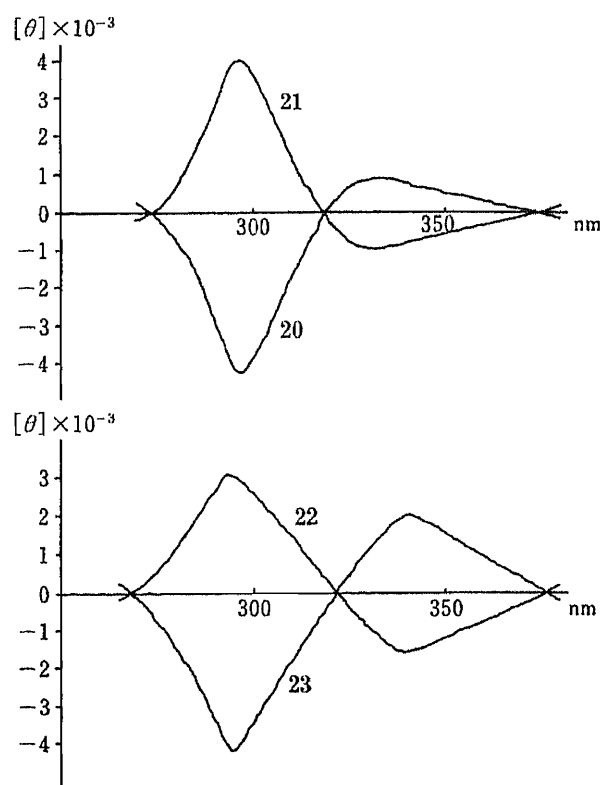


Fig. 1. CD Spectra of Compounds 20–23

The absolute configurations at C-2 and C-3 were deduced by comparing the CD spectrum of **22** with those of **20** and **21**. That is, the CD spectrum of **22** showed positive and negative Cotton effects at 295 and 341 nm, respectively, the signs and positions being in good agreement with those of **21**, while the signs were opposite in the case of **20**. Therefore, the configuration at C-2 in **22** was determined to be the same (*S*-series) as that in **21**, establishing the structure of **22** to be (2*S*, 3*R*)-3,3',4',5,7-pentahydroxyflavanone (designated as (+)-epitaxifolin). The location of the xylosyl linkage in **3** was determined in the same way as described for **1**.

Compound **4** showed two doublet signals (each $J=4$ Hz) at δ 5.56 and 4.69 arising from H-2 and H-3, respectively, indicating these positions to be in the *cis* relationship. Hydrolysis of **4** afforded xylose and an aglycone (**23**), $[\alpha]_D -59.5^\circ$. The $^1\text{H-NMR}$ spectrum of **23** was superimposable on that of **22**, but the CD spectrum showed opposite signs, confirming that **23** is an enantiomer of **22**. Therefore, compound **23** could be represented as (2*R*, 3*S*)-3,3',4',5,7-pentahydroxyflavanone (named (–)-epitaxifolin). The xylosyl moiety in **4** was concluded to be combined with C₃-OH of **23** on the basis of a $^{13}\text{C-NMR}$ comparison between **4** and **23** and a similar UV spectral comparison (with addition of AlCl_3 or NaOAc).

Experimental

Melting points were determined on a Yanagimoto micro-melting point apparatus and are uncorrected. Optical rotations were taken with a JASCO DIP-4 digital polarimeter. Field desorption (FD-) and fast atom bombardment mass spectrum (FAB-MS) were obtained with a JEOL JMS DX-300 instrument. $^1\text{H-}$ and $^{13}\text{C-NMR}$ spectra were recorded on JEOL PS-100 and JEOL FX-100 spectrometers, respectively, using tetramethylsilane as an internal standard, and chemical shifts are given in the δ scale. Column chromatography was carried out with Sephadex LH-20 (25–100 μm , Pharmacia Fine Chemical Co., Ltd.), MCI gel CHP 20P (75–150 μm , Mitsubishi Chemical Industries, Ltd.), Bondapak C₁₈/Porasil B (37–75 μm , Waters Associates, Inc.) and Kieselgel 60 (70–230 mesh, Merck). TLC was conducted on precoated Kieselgel 60 F₂₅₄ plates (0.2 mm, Merck) and spots were located by ultraviolet illumination and by spraying FeCl_3 and anisaldehyde–sulfuric acid reagent. TLC for sugar was performed on Avicel SF cellulose plates (Funakoshi) with the upper layer of *n*-BuOH–pyridine–water (6:2:3) + pyridine (1) and spots were visualized with aniline hydrogen phthalate reagent. CD spectra were taken with a JASCO J-20C spectrometer.

Isolation—The fresh leaves (3.3 kg) of *Thujopsis dolabrata* were extracted twice with refluxing MeOH. The extract was concentrated, and the brown residue was defatted with *n*-hexane. The insoluble residue was then partitioned between *n*-BuOH and water. Evaporation of the aqueous layer gave a residue (139 g), which was chromatographed on Sephadex LH-20 with aqueous MeOH containing increasing amounts of MeOH (water→60% MeOH→70% MeOH→80% MeOH→MeOH) to give fractions I–VII. Fraction IV was subjected to MCI gel ($\text{H}_2\text{O}\rightarrow\text{MeOH}$), Sephadex LH-20 (60% aq. MeOH), and Bondapak C₁₈ ($\text{H}_2\text{O}\rightarrow\text{MeOH}$) chromatographies to afford **1** (89 mg), **2** (48 mg), **3** (30 mg) and **4** (47 mg). Fractions V–VII were each subjected to a combination of Sephadex LH-20, MCI gel and Bondapak C₁₈ chromatographies in the same way as above to give **5** (700 mg), **6** (28 mg), **7** (94 mg), **8** (40 mg), **9** (56 mg), **10** (29 mg), **11** (27 mg), **12** (34 mg), **13** (26 mg), **14** (27 mg), **15** (12 mg), **16** (112 mg), **17** (49 mg), **18** (25 mg) and **19** (34 mg).

(+)-Taxifolin 3-O- β -D-Xylopyranoside (1)—An amorphous powder, $[\alpha]_D^{21} -8.4^\circ$ ($c=1.00$, acetone). $^1\text{H-NMR}$ (acetone- d_6 + D_2O) δ : 3.16–4.14 (6H, m, xylosyl-H₆), 4.70 (1H, d, $J=9$ Hz, H-3), 5.28 (1H, d, $J=9$ Hz, H-2), 5.96 (2H, br s, H-6,8), 6.85 (2H, br s, H-5',6'), 7.04 (1H, s, H-2'). $^{13}\text{C-NMR}$ (acetone- d_6 + D_2O) δ : 64.6 (C-5'), 70.0 (C-4'), 72.1 (C-2'), 74.0 (C-3), 76.6 (C-3'), 82.8 (C-2), 96.1 (C-8), 97.0 (C-6), 102.0 (C-10), 102.2 (C-1'), 115.4, 116.0 (C-2',5'), 120.2 (C-6'), 128.2 (C-1'), 145.8 (C-3'), 146.6 (C-4'), 163.3 (C-9), 164.7 (C-5), 168.3 (C-7), 194.9 (C-4). UV $\lambda_{\text{max}}^{\text{MeOH}}$ nm (log ϵ): 291 (4.43), 330 (sh) (3.86), $\lambda_{\text{max}}^{\text{MeOH}+\text{AlCl}_3}$ nm (log ϵ): 305 (4.38), 380 (sh) (3.43), $\lambda_{\text{max}}^{\text{MeOH}+\text{AlCl}_3+\text{HCl}}$ nm (log ϵ): 311 (4.38), 380 (sh) (3.50), $\lambda_{\text{max}}^{\text{MeOH}+\text{NaOAc}}$ nm (log ϵ): 298 (sh) (3.84), 328 (4.60).

(+)-Taxifolin (20)—A mixture of compound **1** (40.9 mg) and crude hesperidinase in water (5 ml) was incubated for 1 h at 37°C. Usual work-up gave products which were subjected to Sephadex LH-20 column chromatography with MeOH to give **20** (19.3 mg) and D-xylose (13 mg). Compound **20**, colorless needles, mp 218–220°C, $[\alpha]_D^{20} +17.3^\circ$ ($c=0.57$, acetone), $^1\text{H-NMR}$ (acetone- d_6) δ : 4.51–4.65 (2H, m, H-3 and OH), 5.02 (1H, d, $J=11$ Hz, H-2), 5.92–6.00 (2H, m, H-6,8), 6.79–6.97 (2H, m, H-5',6'), 7.06 (1H, d, $J=2$ Hz, H-2'), 7.80–10.0 (4H, m, arom.H). $^{13}\text{C-NMR}$ (acetone- d_6) δ : 73.1 (C-3), 84.5 (C-2), 96.1 (C-8), 97.1 (C-6), 102.0 (C-10), 115.8 (C-2',5'), 120.8 (C-6'), 129.8 (C-1'), 145.7 (C-3'), 146.6 (C-4'), 164.1 (C-9), 165.0 (C-5), 167.9 (C-7), 198.1 (C-4). CD ($c=0.0397$, MeOH): $[\theta]_{274}^0$ 0, $[\theta]_{297}^0 -4.28 \times 10^3$, $[\theta]_{318}^0$ 0, $[\theta]_{332}^0 +9.01 \times 10^2$, $[\theta]_{375}^0$ 0. D-Xylose, $[\alpha]_D^{21} +19.2^\circ$ ($c=0.51$, H_2O), was identical with a standard sample on TLC (R_f 0.67).

(-)-**Taxifolin 3-O-β-D-Xylopyranoside (2)**—An amorphous powder, $[\alpha]_D^{21} - 122.2^\circ$ ($c=1.00$, acetone). $^1\text{H-NMR}$ (acetone- $d_6 + \text{D}_2\text{O}$) δ : 3.10–3.64 (5H, m, xylosyl- H_5), 4.57–4.87 (2H, m, H-1'',3), 5.26 (1H, d, $J=9$ Hz, H-2), 5.98 (2H, br s, H-6,8), 6.84 (2H, br s, H-5',6'), 7.02 (1H, br s, H-2'). $^{13}\text{C-NMR}$ (acetone- $d_6 + \text{D}_2\text{O}$) δ : 65.2 (C-5'), 70.2 (C-4'), 73.4 (C-2'), 75.5 (C-3), 76.9 (C-3'), 82.7 (C-2), 96.1 (C-8), 97.1 (C-6), 101.7 (C-10), 104.3 (C-1'), 115.6, 115.8 (C-2',5'), 120.4 (C-6'), 128.5 (C-1'), 145.7 (C-3'), 146.4 (C-4'), 163.4 (C-9), 164.8 (C-5), 168.4 (C-7), 195.8 (C-4). UV $\lambda_{\text{max}}^{\text{MeOH}}$ nm (log ϵ): 291 (4.58), 330 (sh) (3.94), $\lambda_{\text{max}}^{\text{MeOH} + \text{AlCl}_3}$ nm (log ϵ): 299 (4.51), 385 (sh) (3.50), $\lambda_{\text{max}}^{\text{MeOH} + \text{AlCl}_3 + \text{HCl}}$ nm (log ϵ): 310 (4.52), 385 (sh) (3.39), $\lambda_{\text{max}}^{\text{MeOH} + \text{NaOAc}}$ nm (log ϵ): 290 (sh) (4.17), 329 (4.73).

(-)-**Taxifolin (21)**—Compound **2** (25.5 mg) was hydrolyzed with crude hesperidinase in the same way as described for **1** to give (-)-taxifolin (**21**) (10.1 mg) and D-xylose (9.8 mg). Compound **21**, colorless needles, mp 219–221 °C, $[\alpha]_D^{20} - 20.6^\circ$ ($c=0.32$, acetone). $^1\text{H-NMR}$ (acetone- d_6) δ : 4.51–4.65 (2H, m, H-3 and OH), 5.02 (1H, d, $J=11$ Hz, H-2), 5.92–6.00 (2H, m, H-6,8), 6.79–6.97 (2H, m, H-5',6'), 7.06 (1H, d, $J=2$ Hz, H-2'), 7.80–10.0 (4H, m, arom. H). $^{13}\text{C-NMR}$ (acetone- d_6) δ : 72.9 (C-3), 84.4 (C-2), 96.0 (C-8), 97.0 (C-6), 101.3 (C-10), 115.8 (C-2',5'), 120.6 (C-6'), 129.3 (C-1'), 145.7 (C-3'), 146.5 (C-4'), 163.9 (C-9), 164.4 (C-5), 168.0 (C-7), 195.5 (C-4). CD ($c=0.092$, MeOH): $[\theta]_{274}^0$, $[\theta]_{297}^0 + 4.02 \times 10^3$, $[\theta]_{318}^0$, $[\theta]_{332}^0 - 9.77 \times 10^2$, $[\theta]_{375}^0$.

(+)-**Epitaxifolin 3-O-β-D-Xylopyranoside (3)**—An amorphous powder, $[\alpha]_D^{24} + 2.3^\circ$ ($c=0.25$, acetone). $^1\text{H-NMR}$ (acetone + D_2O) δ : 3.04–4.22 (5H, m, xylosyl- H_5), 4.30 (1H, $J=6$ Hz, anomeric H), 4.46 (1H, d, $J=3$ Hz, H-3), 5.46 (1H, d, $J=3$ Hz, H-2), 5.94–6.02 (2H, m, H-6,8), 6.80 (1H, d, $J=8$ Hz, H-5'), 6.94 (1H, dd, $J=2, 8$ Hz, H-6'), 7.14 (1H, d, $J=2$ Hz, H-2'). $^{13}\text{C-NMR}$ (acetone- $d_6 + \text{D}_2\text{O}$) δ : 65.9 (C-5'), 70.2 (C-4'), 73.6 (C-2'), 76.1 (C-3), 77.8 (C-3'), 81.1 (C-2), 96.1 (C-8), 97.0 (C-6), 101.9 (C-10), 103.9 (C-1'), 115.8 (C-2',5'), 120.1 (C-6'), 127.7 (C-1'), 145.6 (C-3'), 146.2 (C-4'), 163.4 (C-9), 164.9 (C-5), 168.0 (C-7), 194.2 (C-4). UV $\lambda_{\text{max}}^{\text{MeOH}}$ nm (log ϵ): 291 (4.43), 330 (sh) (3.83), $\lambda_{\text{max}}^{\text{MeOH} + \text{AlCl}_3}$ nm (log ϵ): 301 (4.38), 385 (sh) (3.42), $\lambda_{\text{max}}^{\text{MeOH} + \text{AlCl}_3 + \text{HCl}}$ nm (log ϵ): 310 (4.40), 385 (sh) (3.51), $\lambda_{\text{max}}^{\text{MeOH} + \text{NaOAc}}$ nm (log ϵ): 288 (sh) (4.02), 330 (4.60).

(+)-**Epitaxifolin**—Compound **22** (8 mg) together with D-xylose was obtained by enzymic hydrolysis of **3** (19 mg) in the same way as described for **1** and **2**. Compound **22**, an amorphous powder, $[\alpha]_D^{20} + 58.8^\circ$ ($c=0.26$, acetone). $^1\text{H-NMR}$ (acetone- d_6) δ : 4.46 (1H, d, $J=2$ Hz, H-3), 5.46 (1H, d, $J=2$ Hz, H-2), 5.94–6.02 (2H, m, H-6,8), 6.80 (1H, d, $J=8$ Hz, H-5'), 6.92 (1H, dd, $J=2, 8$ Hz, H-6'), 7.10 (1H, d, $J=2$ Hz, H-2'). CD ($c=0.0658$, MeOH): $[\theta]_{268}^0$, $[\theta]_{295}^0 + 3.19 \times 10^3$, $[\theta]_{322}^0$, $[\theta]_{341}^0 - 1.52 \times 10^3$, $[\theta]_{378}^0$.

(-)-**Epitaxifolin 3-O-β-D-Xylopyranoside (4)**—An amorphous powder, $[\alpha]_D^{21} - 93.3^\circ$ ($c=0.89$, acetone + H_2O). $^1\text{H-NMR}$ (acetone- $d_6 + \text{H}_2\text{O}$) δ : 3.10–3.80 (5H, m, xylosyl- H_5), 4.62 (1H, d, $J=6$ Hz, anomeric H), 4.69 (1H, d, $J=4$ Hz, H-3), 5.56 (1H, d, $J=4$ Hz, H-2), 5.95–6.02 (2H, m, H-6,8), 6.76 (1H, d, $J=8$ Hz, H-5'), 6.90 (1H, dd, $J=2, 8$ Hz, H-6'), 7.10 (1H, d, $J=2$ Hz, H-2'). $^{13}\text{C-NMR}$ (acetone- $d_6 + \text{D}_2\text{O}$) δ : 65.9 (C-5'), 70.2 (C-4'), 73.6 (C-2'), 76.1 (C-3), 77.8 (C-3'), 81.1 (C-2), 96.1 (C-8), 97.0 (C-6), 101.9 (C-10), 103.9 (C-1'), 115.8 (C-2',5'), 120.1 (C-6'), 127.7 (C-1'), 145.6 (C-3'), 146.2 (C-4'), 163.4 (C-9), 164.9 (C-5), 168.0 (C-7), 194.2 (C-4). UV $\lambda_{\text{max}}^{\text{MeOH}}$ nm (log ϵ): 291 (4.40), 330 (sh) (3.79), $\lambda_{\text{max}}^{\text{MeOH} + \text{AlCl}_3}$ nm (log ϵ): 298 (4.38), 385 (sh) (3.24), $\lambda_{\text{max}}^{\text{MeOH} + \text{AlCl}_3 + \text{HCl}}$ nm (log ϵ): 306 (4.40), 385 (sh) (3.35), $\lambda_{\text{max}}^{\text{MeOH} + \text{NaOAc}}$ nm (log ϵ): 288 (sh) (4.18), 330 (4.78).

(-)-**Epitaxifolin (23)**—Compound **4** (26 mg) gave upon enzymic hydrolysis compound **23** (12 mg) and D-xylose. Compound **23**, an amorphous powder, $[\alpha]_D^{20} - 59.5^\circ$ ($c=0.13$, acetone + H_2O). $^1\text{H-NMR}$ (acetone- d_6) δ : 4.28 (1H, br s, H-3), 5.43 (1H, d, $J=2$ Hz, H-2), 5.95–6.02 (2H, m, H-6,8), 6.80 (1H, d, $J=8$ Hz, H-5'), 6.92 (1H, dd, $J=2, 8$ Hz, H-6'), 7.10 (1H, $J=2$ Hz, H-2'), CD ($c=0.0789$, MeOH): $[\theta]_{268}^0$, $[\theta]_{295}^0 - 4.18 \times 10^3$, $[\theta]_{322}^0$, $[\theta]_{341}^0 + 2.03 \times 10^3$, $[\theta]_{378}^0$.

Acknowledgement We are grateful to Dr. K. Murakami of the Faculty of Pharmaceutical Sciences, Tokushima University for collection of materials.

References and Notes

- 1) Part LI: G. Nonaka, K. Ishimaru, M. Watanabe, I. Nishioka, T. Yamauchi, and A. S. C. Wan, *Chem. Pharm. Bull.*, **35**, 217 (1987).
- 2) a) R. S. Thompson, D. Jacques, E. Haslam, and R. J. N. Tanner, *J. Chem. Soc., Perkin Trans. 1*, **1972**, 1387; b) G. Nonaka, O. Kawahara, and I. Nishioka, *Chem. Pharm. Bull.*, **30**, 4277 (1982); c) G. Nonaka, F.-L. Hsu, and I. Nishioka, *J. Chem. Soc., Chem. Commun.*, **1981**, 781.
- 3) G. Nonaka and I. Nishioka, *Chem. Pharm. Bull.*, **28**, 3145 (1980).
- 4) F.-L. Hsu, G. Nonaka, and I. Nishioka, *Chem. Pharm. Bull.*, **33**, 3293 (1985).
- 5) S. Morimoto, G. Nonaka, and I. Nishioka, Abstracts of Papers, The 102nd Annual Meeting of the Pharmaceutical Society of Japan, Osaka, April 1982, p. 555.

[Chem. Pharm. Bull.]
35(3)1109—1117(1987)

Studies on the Glycosides of *Epimedium grandiflorum* MORR. var. *thunbergianum* (MIQ.) NAKAI. I

TOSHIO MIYASE,^{*,a} AKIRA UENO,^a NOBUO TAKIZAWA,^b
HIROMI KOBAYASHI^b and HIROKO KARASAWA^b

Shizuoka College of Pharmacy,^a 2-2-1, Oshika, Shizuoka 422, Japan and Central Research Laboratories, Yomeishu Seizo Co., Ltd.,^b Nakaminowa, Minowa-cho, Kamiina-gun, Nagano 399-46, Japan

(Received September 4, 1986)

A new phenolic glycoside, icariside A₁ (IV), and six new terpenic glycosides, icariside B₁ (V), B₂ (VI), C₁ (VII), C₂ (VIII), C₃ (IX), and C₄ (X), have been isolated from *Epimedium grandiflorum* MORR. var. *thunbergianum* (MIQ.) NAKAI, together with three known glycosides, salidroside (I), thalictoside (II) and benzyl glucoside (III). The structures of IV—X were established on the basis of chemical evidence and spectral data.

Keywords—*Epimedium grandiflorum* var. *thunbergianum*; 9,10-dihydrophenanthrenol glycoside; ionone derivative; sesquiterpene glycoside; icariside A; icariside B; icariside C

The aerial parts of *Epimedium grandiflorum* MORR. var. *thunbergianum* (MIQ.) NAKAI have been used since ancient times as a tonic in China and Japan. The constituents of this plant were investigated by Takemoto *et al.* (flavonoids and lignans)¹⁾ and Tomita and Ishii (alkaloid).²⁾

Our interest has been directed to the reinvestigation of the constituents of the aerial parts, with the aim of isolating some biologically active substances.³⁾ In this paper, we wish to describe the isolation of seven new glycosides, icariside A₁ (IV), B₁ (V), B₂ (VI), C₁ (VII), C₂ (VIII), C₃ (IX), and C₄ (X), along with three known glycosides, salidroside (I), thalictoside (II), and benzyl glucoside (III). The structures of these compounds were determined on the basis of chemical evidence and spectroscopic studies.

Salidroside (I) was identified by direct comparison [thin layer chromatography, infrared (IR), proton nuclear magnetic resonance (¹H-NMR), and carbon-13 nuclear magnetic resonance (¹³C-NMR) spectra] with an authentic sample.⁴⁾

Thalictoside (II), C₁₄H₁₉NO₈, mp 138—139 °C was identified by comparison of various data (mp, IR, ¹H-NMR) with reported values.⁵⁾

Benzyl glucoside (III), C₁₃H₁₈O₆·1/4H₂O, [α]_D -59.2 °, was obtained as colorless needles, mp 123—124 °C. The ¹H-NMR spectrum exhibited AB-type signals due to a benzylic methylene at δ 4.85 (1H, *J* = 12 Hz) and 5.17 (1H, *J* = 12 Hz), a doublet signal due to an anomeric proton at δ 5.01 (1H, *J* = 7 Hz) and multiplet signals due to aromatic protons at δ 7.25—7.65 (5H). These data led us to conclude the structure of this compound to be III, previously synthesized by Bonner *et al.* (lit. mp 121 °C).⁶⁾ This is the first isolation of III from this plant.

Icariside A₁ (IV), C₂₄H₃₀O₁₀, [α]_D -22.9 °, was obtained as colorless needles, mp 220—222 °C. The ultraviolet (UV) spectrum showed absorption maxima at 280 (4.27), 302 (4.17) and 312 (4.19) nm (log ε). The ¹H-NMR spectrum exhibited a broad singlet signal due to benzylic methylene protons at δ 2.68 (4H), four singlet signals due to methoxyl protons at δ 3.84, 3.87, 3.91 and 4.11 (each 3H), a doublet signal due to an anomeric proton at δ 5.75

(1H, $J=7$ Hz) and three singlet signals due to aromatic protons at δ 6.92, 7.43 and 8.31 (each 1H). From these data, IV was assumed to be a 9,10-dihydrophenanthrene derivative having four methoxyl groups and a glucosyl residue.⁷⁾ The ¹³C-NMR spectrum exhibited four methoxyl carbon signals at δ 56.1, 56.5, 60.8 and 61.5, the latter two signals might be due to *ortho*-disubstituted methoxyl groups because of the downfield shifts.⁸⁾ Acid hydrolysis afforded glucose as the sugar moiety and enzymatic hydrolysis afforded an aglycone IVa. Acetylation of IVa afforded a monoacetate IVb and methylation of IVa afforded a methyl ether IVc. In the ¹H-NMR spectrum of IVa, two aromatic proton signals (δ 6.66 and 6.76) were long-range-coupled with a benzylic methylene proton signal at δ 2.71 (4H, brs) and another one was deshielded at δ 7.97.⁷⁾ Nuclear Overhauser effects (NOE) were observed at the proton signals at δ 6.76 (21%) and 7.97 (24%) on irradiation at the methoxyl signals. From these data, IVa was assumed to be 7-hydroxy-2,3,4,6-tetramethoxy-9,10-dihydrophenanthrene, previously isolated from *Combretum psidioides*.⁹⁾ The identities of IVa, IVb and IVc were established by comparison of the physical and spectral data (mp, UV, ¹H-NMR) with reported data. Therefore, the structure of icariside A₁ was concluded to be IV.

Icariside B₁ (V), C₁₉H₃₀O₈ · 1/2H₂O, $[\alpha]_D - 73.5^\circ$, was obtained as an amorphous powder. The UV spectrum showed an absorption maximum at 232 (4.16) nm (log ϵ) and the IR spectrum showed the presence of hydroxyl groups (3450 cm⁻¹), an allenic structure (1945 cm⁻¹) and a conjugated ketone group (1670 cm⁻¹). The ¹H-NMR spectrum exhibited four singlet methyl signals at δ 1.09 (3H), 1.51 (6H), 2.21 (3H), the last one being due to a methyl ketone, a carbinol proton signal at δ 4.95 (1H, m), an anomeric proton signal at δ 5.12 (1H, d, $J=7$ Hz) and an olefinic proton signal at δ 5.92 (1H, s). Acid hydrolysis afforded glucose as the sugar moiety and enzymatic hydrolysis afforded an aglycone Va. In the ¹H-NMR spectrum, a carbinol proton signal was observed at δ 4.32 (m, $W_{1/2} = 17.5$ Hz). From these data, Va was assumed to be grasshopper ketone, previously isolated from *Romalea microptera*.¹⁰⁾ The identity of Va was established by comparison of the physical and spectral data (mp, UV, IR, ¹H-NMR) with reported data. In the ¹³C-NMR spectrum of Va, two carbinol carbon signals were observed at δ 63.8 (d) and 72.3 (s). The former was shifted downfield by 8.2 ppm in the ¹³C-NMR spectrum of V, but the latter was shifted downfield by only 1.0 ppm. Therefore, the glucosidation position was decided to be at C-3. These results led us to conclude the structure of icariside B₁ to be V.

Icariside B₂ (VI), C₁₉H₃₀O₈ · 1/2H₂O, $[\alpha]_D - 102.1^\circ$, was obtained as colorless needles, mp 172.5—174.0 °C. The UV spectrum showed an absorption maximum at 230 (4.06) nm (log ϵ)

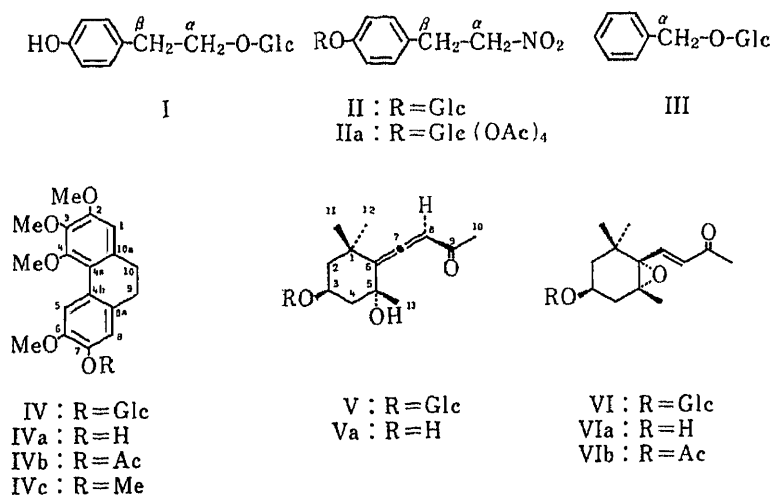
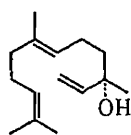
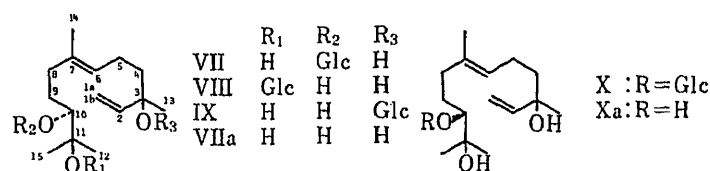
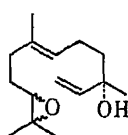


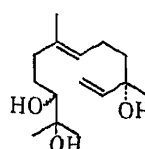
Chart 1



XI



XII



XIII

Chart 2

TABLE I. ¹H-NMR Chemical Shifts and Coupling Constants

Proton No.	V ^{a)}	V _a ^{b)}	VI ^{a)}	VI ^{c)}
3	4.95 (1H, m)	4.32 (1H, m, $W_{1/2} = 17.5$ Hz)	7.21 (1H, d, $J = 15$ Hz)	4.84 (1H, m, $W_{1/2} = 18$ Hz)
7			6.51 (1H, d, $J = 15$ Hz)	6.92 (1H, d, $J = 15$ Hz)
8	5.92 (1H, s)	5.87 (1H, s)		6.25 (1H, d, $J = 15$ Hz)
10	2.21 (3H, s)	2.19 (3H, s)	2.29 (3H, s)	2.22 (3H, s)
11	$\left\{ \begin{array}{l} 1.09 (3H, s) \\ 1.51 (6H, s) \end{array} \right.$	$\left\{ \begin{array}{l} 1.16 (3H, s) \\ 1.39 (3H, s) \\ 1.43 (3H, s) \end{array} \right.$	$\left\{ \begin{array}{l} 0.96 (3H, s) \\ 1.13 (6H, s) \end{array} \right.$	$\left\{ \begin{array}{l} 0.99 (3H, s) \\ 1.19 (3H, s) \\ 1.22 (3H, s) \end{array} \right.$
12				
13				
Anomeric	5.12 (1H, d, $J = 7$ Hz)		4.95 (1H, d, $J = 7$ Hz)	
OAc				1.97 (3H, s)

Run at 89.55 MHz in a) pyridine-*d*₅ b) CDCl₃ c) CCl₄ solution.

and the IR spectrum showed the presence of hydroxyl groups ($3500, 3400\text{ cm}^{-1}$) and a conjugated ketone group (1685 cm^{-1}). The ¹H-NMR spectrum exhibited four singlet methyl signals at $\delta 0.96$ (3H), 1.13 (6H), 2.29 (3H), the last one being due to a methyl ketone, an anomeric proton signal at $\delta 4.95$ (1H, d, $J = 7$ Hz) and a pair of *trans* olefinic proton signals at $\delta 6.51$ (1H, d, $J = 15$ Hz) and 7.21 (1H, d, $J = 15$ Hz). In the ¹³C-NMR spectrum, three oxygen-bearing carbon signals were observed at $\delta 67.1$ (s), 69.9 (s), 71.5 (d), and the former two signals were assigned to epoxy carbons. Acid hydrolysis afforded glucose as the sugar moiety and enzymatic hydrolysis afforded an aglycone VIa, which was acetylated immediately, to give an acetate VIb. The ¹H-NMR spectrum of VIb exhibited an acetyl methyl signal at $\delta 1.97$ (3H, s) and a carbinol proton signal at $\delta 4.84$ (1H, m, $W_{1/2} = 18$ Hz) suggesting that VIb has an equatorial acetoxy group. From these data, VIb was assumed to be 3β -acetoxy- $5\alpha,6\alpha$ -epoxy- β -ionone, previously synthesized from a constituent of *Nicotiana tabacum* L.¹¹⁾ The identity of VIb was established by comparison of the physical and spectral data [mp, $[\alpha]_D$, UV, IR, ¹H-NMR, circular dichroism (CD)] with reported data. These results led us to conclude the structure of icariside B₂ to be VI.

Icariside C₁ (VII), C₂₁H₃₈O₈, $[\alpha]_D -22.5^\circ$, was obtained as an amorphous powder. The IR spectrum showed the presence of hydroxyl groups (3450 cm^{-1}) and double bonds (1645 cm^{-1}). The ¹H-NMR spectrum exhibited three singlet methyl signals at $\delta 1.36, 1.46, 1.49$, a vinyl methyl signal at $\delta 1.66$ (brs), an anomeric proton signal at $\delta 5.16$ (1H, d, $J = 8$ Hz), an olefinic proton signal at $\delta 5.51$ (1H, br t, $J = 7$ Hz) and three olefinic proton signals at $\delta 5.16$ (1H, dd, $J = 11, 2$ Hz), 5.52 (1H, dd, $J = 18, 2$ Hz), 6.17 (1H, dd, $J = 18, 11$ Hz)

TABLE II. ^{13}C -NMR Chemical Shifts

Carbon No.	V ^{a)}	Va ^{b)}	VI ^{d)}
Aglycone moiety			
1	36.3	36.1	35.1
2	47.1 ^{c)}	48.8 ^{e)}	44.8
3	72.0	63.8	71.5 ^{c)}
4	48.1 ^{c)}	49.0 ^{e)}	37.8
5	71.3	72.3	67.1
6	119.8	118.8	69.9
7	197.8	198.2	143.0
8	100.6	100.8	133.3
9	209.6	209.6	197.1
10	26.5	26.4	27.7 ^{d)}
11	29.3 ^{d)}	29.1 ^{d)}	29.0 ^{d)}
12	31.1 ^{d)}	30.9 ^{d)}	22.5 ^{d)}
13	32.0 ^{d)}	31.8 ^{d)}	20.0
Sugar moiety			
1	103.1		103.2
2	75.4		75.3
3	78.6 ^{e)}		78.7 ^{e)}
4	71.7		71.8 ^{e)}
5	78.3 ^{e)}		78.4 ^{e)}
6	62.8		62.8

Run at 22.5 MHz in a) pyridine-*d*₅, b) CDCl₃ solution. c—e) Assignments may be interchanged in each column.

which were due to a vinyl group. In the ^{13}C -NMR spectrum, twenty-one carbon signals were observed, including six signals due to a glucopyranosyl moiety. Acid hydrolysis afforded glucose as the sugar moiety and enzymatic hydrolysis afforded an aglycone VIIa, colorless oil, $[\alpha]_{\text{D}} - 13.4^{\circ}$. The ^1H -NMR spectrum of VIIa exhibited a carbinol proton signal at δ 3.76 (1H, dd, $J = 10, 2$ Hz), while the ^{13}C -NMR spectrum of VIIa exhibited fifteen carbon signals including three carbinol carbon signals at δ 72.4 (s), 72.7 (s), 78.5 (d). From a comparison of these spectral data with those of nerolidol,¹²⁾ VIIa was assumed to be 3,7,11-trimethyl-1,6-dodecadien-3,10,11-triol. The identity of VIIa was established by chemical synthesis of XIII from (+)-nerolidol (XI).¹³⁾ Compound XIII was obviously a mixture of 10*S* and 10*R* from the synthetic process, but the two isomers were not distinguishable in the ^1H - and ^{13}C -NMR spectra. Thus, in order to decide the stereochemistry at C-10, the Cotton effect of the α -glycol in the presence of a shift reagent Eu(fod)₃ was examined. The CD spectrum of VIIa showed a positive Cotton effect, $[\theta]_{305} + 41322$, and a negative Cotton effect, $[\theta]_{285} - 27716$, suggesting C-10 to be *S*.¹⁴⁾ In the ^{13}C -NMR spectrum of VIIa, three carbinol carbon signals were observed at δ 72.4 (s), 72.7 (s), 78.5 (d). The last one was shifted downfield at δ 90.7 (d) in the ^{13}C -NMR spectrum of VII, so the glucosidation position was decided to be C-10. These results led us to conclude the structure of icariside C₁ to be VII.

Icariside C₂ (VIII), C₂₁H₃₈O₈ · 1/2H₂O, $[\alpha]_{\text{D}} - 19.3^{\circ}$, was obtained as an amorphous powder. The IR and ^1H -NMR spectra were very similar to those of VII. Acid hydrolysis afforded glucose as the sugar moiety and enzymatic hydrolysis afforded an aglycone VIIa. On comparison of the ^{13}C -NMR spectra of VIII and VIIa, the signal of C-10 (δ 76.9) of VIII was shifted upfield by 1.6 ppm and that of C-11 (δ 80.9) was shifted downfield by 8.2 ppm. Therefore, the structure of icariside C₂ was concluded to be VIII, with a glucosyl residue at C-11.

Icariside C₃ (IX), C₂₁H₃₈O₈ · 1/2H₂O, $[\alpha]_{\text{D}} - 34.7^{\circ}$, was obtained as an amorphous

TABLE III. ^1H -NMR Chemical Shifts and Coupling Constants

Proton No.	VII	VIII	IX	X
1a	5.52 (1H, dd, $J=18, 2$ Hz)	5.54 (1H, dd, $J=17, 2$ Hz)	5.39 (1H, dd, $J=18, 1.5$ Hz)	5.58 (1H, dd, $J=17, 2$ Hz)
1b	5.16 (1H, dd, $J=11, 2$ Hz)	5.17 (1H, dd, $J=10, 2$ Hz)	5.23 (1H, dd, $J=11, 1.5$ Hz)	5.18 (1H, dd, $J=10, 2$ Hz)
2	6.17 (1H, dd, $J=18, 11$ Hz)	6.17 (1H, dd, $J=17, 10$ Hz)	6.28 (1H, dd, $J=18, 11$ Hz)	6.18 (1H, dd, $J=17, 10$ Hz)
6	5.51 (1H, br t, $J=7$ Hz)	<i>a)</i>	<i>a)</i>	<i>a)</i>
10				
12 } 13 } 15 }	{ 1.36 (3H, s) 1.46 (3H, s) 1.49 (3H, s)	{ 1.49 (6H, s) 1.51 (3H, s)	{ 1.48 (3H, s) 1.52 (3H, s) 1.58 (3H, s)	{ 1.35 (3H, s) 1.43 (3H, s) 1.48 (3H, s)
14	1.66 (3H, br s)	1.67 (3H, br s)	1.65 (3H, br s)	1.67 (3H, br s)
Anomeric	5.16 (1H, d, $J=8$ Hz)	5.23 (1H, d, $J=7$ Hz)	4.95 (1H, d, $J=8$ Hz)	5.01 (1H, d, $J=8$ Hz)

Proton No.	VIIa	XIII	Xa
1a	5.56 (1H, dd, $J=18, 2$ Hz)	5.53 (1H, dd, $J=17, 2$ Hz)	5.56 (1H, dd, $J=17, 2$ Hz)
1b	5.17 (1H, dd, $J=11, 2$ Hz)	5.16 (1H, dd, $J=11, 2$ Hz)	<i>a)</i>
2	6.17 (1H, dd, $J=18, 11$ Hz)	6.17 (1H, dd, $J=17, 11$ Hz)	6.17 (1H, dd, $J=17, 11$ Hz)
6	5.45 (1H, br t, $J=7$ Hz)	5.43 (1H, br t, $J=7$ Hz)	<i>a)</i>
10	3.76 (1H, dd, $J=10, 2$ Hz)	3.74 (1H, dd, $J=10, 2$ Hz)	3.77 (1H, dd, $J=10, 2$ Hz)
12 } 13 } 15 }	{ 1.48 (3H, s) 1.49 (3H, s) 1.53 (3H, s)	{ 1.48 (6H, s) 1.51 (3H, s)	{ 1.49 (3H, s) 1.50 (3H, s) 1.54 (3H, s)
14	1.71 (3H, br s)	1.69 (3H, br s)	1.70 (3H, br s)

Run at 89.55 MHz in pyridine- d_5 solution. *a)* Overlapped with H_2O .

TABLE IV. ^{13}C -NMR Chemical Shifts

Carbon No.	VII	VIII	IX	X	VIIa	XIII
Aglycone moiety						
1	111.3	111.4	114.8	111.2	111.2	111.9
2	147.1	147.1	144.6	147.2	147.2	147.1
3	72.5 ^{a)}	72.5	80.1	72.4 ^{a)}	72.4 ^{a)}	73.1 ^{a)}
4	43.5	43.4	42.3	43.4	43.4	43.4
5	23.5	23.4	23.0	23.4	23.4	23.7
6	128.5	125.8	125.1	125.8	125.3	125.6
7	135.2	135.3	135.5	135.2	135.5	135.7
8	30.7	30.6	30.8	31.2	30.9	31.0
9	36.7	37.6	37.6	36.5	37.7	37.9
10	90.7	76.9	78.9 ^{a)}	90.3	78.5	78.7
11	73.6 ^{a)}	80.9	72.7	72.0 ^{a)}	72.7 ^{a)}	73.4 ^{a)}
12	24.3 ^{b)}	21.6 ^{a)}	26.0 ^{b)}	25.2 ^{b)}	26.0 ^{b)}	26.1 ^{b)}
13	28.6	28.6	23.6	28.4	28.5	28.7
14	16.4	16.4	16.3	16.1	16.3	16.8
15	26.8 ^{b)}	24.2 ^{a)}	26.1 ^{b)}	27.0 ^{b)}	26.1 ^{b)}	26.6 ^{b)}
Sugar moiety						
1	106.8	98.8	99.8	106.1		
2	76.2	75.4	75.4	75.5		
3	78.8 ^{c)}	78.8 ^{b)}	78.5 ^{a)}	78.6 ^{c)}		
4	71.8	71.8	72.0	71.8		
5	78.3 ^{c)}	78.2 ^{b)}	78.1 ^{a)}	78.5 ^{c)}		
6	62.9	62.8	63.1	62.7		

Run at 22.5 MHz in pyridine- d_5 solution. a—c) Assignments may be interchanged in each column.

powder. The IR and ^1H -NMR spectra were similar to those of VII and VIII. Acid hydrolysis afforded glucose as the sugar moiety and enzymatic hydrolysis afforded an aglycone VIIa. In the ^{13}C -NMR spectrum of IX, the signal of C-3 (δ 80.1) was shifted downfield by 7.7 ppm, while those of C-2 (δ 144.6), C-4 (δ 42.3) and C-13 (δ 23.6) were shifted upfield by 2.6, 1.1 and 4.9 ppm, respectively, compared with those of VIIa. Therefore, the structure of icariside C₃ was concluded to be IX, with a glucosyl residue at C-3.

Icariside C₄ (X), C₂₁H₃₈O₈ · 1/2H₂O, $[\alpha]_{\text{D}} + 3.4^\circ$, was obtained as an amorphous powder. The ^1H - and ^{13}C -NMR spectra were very similar to those of VII, though C-11 and C-12 showed small differences in the chemical shifts. Therefore, X was assumed to be an epimer of VII at C-10. The aglycone Xa obtained by enzymatic hydrolysis of X gave the same IR and ^1H -NMR spectra as a synthetic product, XIII. The CD spectrum of Xa in the presence of Eu(fod)₃ showed a negative Cotton effect, $[\theta]_{305} - 32768$, and a positive one, $[\theta]_{284} + 20480$, opposite to those in the case of VIIa. Thus, the stereochemistry at C-10 was decided to be R and the structure of icariside C₄ to be X.

This is the first report of the isolation of a dihydrophenanthrene derivative and terpenic glycosides from *Epimedium* species. Studies on the structures of other minor glycosides (polar) are in progress.

Experimental

Melting points were taken on a Yanaco MP-500 micromelting point apparatus and are uncorrected. Optical rotations were determined with a JASCO DIP-140 digital polarimeter. IR spectra were run on a JASCO A-202 IR spectrometer and UV spectra on a Shimadzu UV-360 recording spectrometer. Mass spectra (MS) were measured on a JEOL JMS-100 mass spectrometer. CD spectra were recorded on a JASCO J-20A spectropolarimeter. ^1H - and ^{13}C -NMR spectra were recorded on a JEOL FX-90Q NMR spectrometer (89.55 and 22.5 MHz, respectively). Chemical

shifts are given on the δ scale with tetramethylsilane as an internal standard (s, singlet; d, doublet; t, triplet; m, multiplet; br, broad). Gas chromatography (GC) was done on a Hitachi K53 gas chromatograph. High-performance liquid chromatography (HPLC) was done on a Kyowa Seimitsu model K880 instrument.

Isolation—Aerial parts of *E. grandiflorum* MORR. var. *thunbergianum* (MIQ.) NAKAI (15 kg), collected in summer 1985, in Niigata prefecture, Japan, were extracted twice with hot water. The extract was absorbed on Amberlite XAD-2 and the resin was eluted with methanol after being washed with water. After repeated chromatography of the methanol eluate (420 g) on silica gel with a chloroform–methanol system and HPLC (column: Develosil ODS-10, 20 \times 250 mm) with a water–acetonitrile system, ten glycosides were isolated.

Salidroside (I): Amorphous powder (50 mg). IR $\nu_{\max}^{\text{KBr}} \text{cm}^{-1}$: 3420, 1670, 1620, 1600, 1525, 1445, 1380, 1260, 1250, 1165, 1130, 1075, 910. $^1\text{H-NMR}$ (pyridine- d_5) δ : 3.02 (2H, t, $J=7$ Hz, H_2 - β), 4.94 (1H, d, $J=7$ Hz, H-1'), 7.17 (4H, brs, H-2, H-3, H-5, H-6). $^{13}\text{C-NMR}$ (pyridine- d_5) δ : 36.0 (C- β), 62.8 (C-6'), 71.1 (C-4'), 71.7 (C- α), 75.2 (C-2'), 78.5, 78.6 (C-3'/C-5'), 104.7 (C-1'), 116.2 (C-3, C-5), 129.5 (C-1), 130.5 (C-2, C-6), 157.3 (C-4).

Thalictoside (II): Colorless needles from methanol–ethyl acetate (330 mg), mp 138–139 °C. *Anal.* Calcd for $\text{C}_{14}\text{H}_{19}\text{NO}_8$: C, 51.06; H, 5.82; N, 4.25. Found: C, 50.78; H, 5.65; N, 4.07. IR $\nu_{\max}^{\text{KBr}} \text{cm}^{-1}$: 3520, 1620, 1550, 1520, 1385, 1240, 1105, 1075, 1050, 1015. $^1\text{H-NMR}$ (pyridine- d_5) δ : 3.23 (2H, t, $J=7$ Hz, H_2 - β), 4.84 (2H, t, $J=7$ Hz, H_2 - α), 5.60 (1H, d, $J=7$ Hz, H-1'), 7.22 (2H, d, $J=9$ Hz, H-3, H-5), 7.31 (2H, d, $J=9$ Hz, H-2, H-6). $^{13}\text{C-NMR}$ (pyridine- d_5) δ : 32.7 (C- β), 62.4 (C-6'), 71.3 (C-4'), 74.9 (C-2'), 76.8 (C- α), 78.5, 78.8 (C-3'/C-5'), 102.2 (C-1'), 117.3 (C-3, C-5), 130.1 (C-1, C-2, C-6), 157.8 (C-4).

Benzyl Glucoside (III): Colorless needles from methanol–ethyl acetate (390 mg), mp 123–124 °C, $[\alpha]_{\text{D}}^{25} - 59.2^\circ$ ($c=0.67$, methanol). *Anal.* Calcd for $\text{C}_{13}\text{H}_{18}\text{O}_6 \cdot 1/4\text{H}_2\text{O}$: C, 56.82; H, 6.79. Found: C, 56.66; H, 6.53. IR $\nu_{\max}^{\text{KBr}} \text{cm}^{-1}$: 3450, 1640, 1505, 1460, 1420, 1375, 1160, 1110, 1085, 1055, 1030. $^1\text{H-NMR}$ (pyridine- d_5) δ : 4.85 (1H, d, $J=12$ Hz, H- α), 5.01 (1H, d, $J=7$ Hz, H-1'), 5.17 (1H, d, $J=12$ Hz, H- α'), 7.25–7.65 (5H, m, H-2, H-3, H-4, H-5, H-6). $^{13}\text{C-NMR}$ (pyridine- d_5) δ : 62.7 (C-6'), 70.8 (C- α), 71.6 (C-4'), 75.0 (C-2'), 78.3 (C-3', C-5'), 103.8 (C-1'), 127.7 (C-4), 128.1 (C-2, C-6), 128.5 (C-3, C-5), 138.8 (C-1).

Icariside A₁ (IV): Colorless needles from methanol (1.4 g), mp 220–222 °C, $[\alpha]_{\text{D}}^{25} - 22.9^\circ$ ($c=0.59$, methanol). *Anal.* Calcd for $\text{C}_{24}\text{H}_{30}\text{O}_{10}$: C, 60.24; H, 6.32. Found: C, 60.14; H, 6.29. UV $\lambda_{\max}^{\text{MeOH}}$ nm (log ϵ): 216 (4.53), 233 (sh, 4.36), 272 (sh, 4.21), 280 (4.27), 302 (4.17), 312 (4.19). IR $\nu_{\max}^{\text{KBr}} \text{cm}^{-1}$: 3520, 3420, 1615, 1595, 1525, 1460, 1405, 1265, 1220, 1115, 1080, 1050, 1045. $^1\text{H-NMR}$ (pyridine- d_5) δ : 2.68 (4H, brs, H_2 -9, H_2 -10), 3.84, 3.87, 3.91, 4.11 (each 3H, s, OMe), 5.75 (1H, d, $J=7$ Hz, H-1'), 6.92 (1H, s, H-1), 7.43 (1H, s, H-8), 8.31 (1H, s, H-5). $^{13}\text{C-NMR}$ (pyridine- d_5) δ : 29.6, 30.9 (C-9/C-10), 56.1, 56.5 (methoxyl at C-2/C-6), 60.8, 61.5 (methoxyl at C-3/C-4), 62.5 (C-6'), 71.4 (C-4'), 75.0 (C-2'), 78.7, 79.0 (C-3'/C-5'), 102.6 (C-1'), 112.4, 112.7, 112.9 (C-1/C-5/C-8), 122.6, 125.8 (C-8a/C-10a), 131.6 (C-4a), 134.7 (C-3), 143.1 (C-4b), 148.4, 148.7 (C-6/C-7), 150.8, 152.1 (C-2/C-4).

Icariside B₁ (V): Amorphous powder (525 mg), $[\alpha]_{\text{D}}^{25} - 73.5^\circ$ ($c=1.00$, methanol). *Anal.* Calcd for $\text{C}_{19}\text{H}_{30}\text{O}_8 \cdot 1/2\text{H}_2\text{O}$: C, 57.71; H, 7.90. Found: C, 57.56; H, 7.76. UV $\lambda_{\max}^{\text{MeOH}}$ nm (log ϵ): 232 (4.16). IR $\nu_{\max}^{\text{KBr}} \text{cm}^{-1}$: 3450, 1945, 1670, 1460, 1370, 1245, 1170, 1160, 1080, 1030, 955. $^1\text{H-}$ and $^{13}\text{C-NMR}$: Tables I and II.

Icariside B₂ (VI): Colorless needles from methanol–ethyl acetate (510 mg), mp 172.5–174.0 °C, $[\alpha]_{\text{D}}^{25} - 102.1^\circ$ ($c=0.97$, methanol). *Anal.* Calcd for $\text{C}_{19}\text{H}_{30}\text{O}_8 \cdot 1/2\text{H}_2\text{O}$: C, 57.71; H, 7.90. Found: C, 57.92; H, 7.66. UV $\lambda_{\max}^{\text{MeOH}}$ nm (log ϵ): 230 (4.06). IR $\nu_{\max}^{\text{KBr}} \text{cm}^{-1}$: 3500, 3400, 1685, 1390, 1365, 1250, 1170, 1125, 1085, 1045, 1025, 990, 905. $^1\text{H-}$ and $^{13}\text{C-NMR}$: Tables I and II.

Icariside C₁ (VII): Amorphous powder (1.12 g), $[\alpha]_{\text{D}}^{25} - 22.5^\circ$ ($c=1.00$, methanol). *Anal.* Calcd for $\text{C}_{21}\text{H}_{38}\text{O}_8$: C, 60.27; H, 9.15. Found: C, 60.27; H, 9.14. IR $\nu_{\max}^{\text{KBr}} \text{cm}^{-1}$: 3450, 1645, 1470, 1455, 1415, 1385, 1370, 1170, 1150, 1075, 1030, 965, 925, 900. $^1\text{H-}$ and $^{13}\text{C-NMR}$: Tables III and IV.

Icariside C₂ (VIII): Amorphous powder (420 mg), $[\alpha]_{\text{D}}^{25} - 19.3^\circ$ ($c=0.96$, methanol). *Anal.* Calcd for $\text{C}_{21}\text{H}_{38}\text{O}_8 \cdot \text{H}_2\text{O}$: C, 57.78; H, 9.24. Found: C, 57.81; H, 8.97. IR $\nu_{\max}^{\text{KBr}} \text{cm}^{-1}$: 3450, 1645, 1470, 1455, 1415, 1390, 1375, 1160, 1080, 1040, 1020, 925. $^1\text{H-}$ and $^{13}\text{C-NMR}$: Tables III and IV.

Icariside C₃ (IX): Amorphous powder (315 mg), $[\alpha]_{\text{D}}^{25} - 34.7^\circ$ ($c=0.88$, methanol). *Anal.* Calcd for $\text{C}_{21}\text{H}_{38}\text{O}_8 \cdot 1/2\text{H}_2\text{O}$: C, 59.00; H, 9.19. Found: C, 59.26; H, 9.09. IR $\nu_{\max}^{\text{KBr}} \text{cm}^{-1}$: 3450, 1640, 1455, 1415, 1390, 1375, 1160, 1075, 1040, 1030, 925. $^1\text{H-}$ and $^{13}\text{C-NMR}$: Tables III and IV.

Icariside C₄ (X): Amorphous powder (35 mg), $[\alpha]_{\text{D}}^{25} + 3.4^\circ$ ($c=0.87$, methanol). *Anal.* Calcd for $\text{C}_{21}\text{H}_{38}\text{O}_8 \cdot 1/2\text{H}_2\text{O}$: C, 59.00; H, 9.19. Found: C, 59.16; H, 9.12. IR $\nu_{\max}^{\text{KBr}} \text{cm}^{-1}$: 3350, 1645, 1390, 1370, 1315, 1270, 1230, 1180, 1160, 1140, 1105, 1010, 990, 920, 870. $^1\text{H-}$ and $^{13}\text{C-NMR}$: Tables III and IV.

Acetylation of Thalictoside (II)—Thalictoside (II, 10 mg) was dissolved in pyridine and acetic anhydride (each 0.3 ml), and the reaction mixture was left at room temperature. The reagents were evaporated off *in vacuo* and the residue was recrystallized from methanol to give a tetraacetate (IIa, 8 mg) as colorless crystals, mp 165–166 °C. IR $\nu_{\max}^{\text{KBr}} \text{cm}^{-1}$: 1755, 1620, 1560, 1525, 1440, 1380, 1230, 1100, 1070, 1050; 910. $^1\text{H-NMR}$ (CDCl_3) δ : 2.05, 2.06, 2.07, 2.09 (each 3H, s, OAc), 3.28 (2H, t, $J=7$ Hz, H_2 - β), 4.60 (2H, t, $J=7$ Hz, H_2 - α), 6.98 (2H, d, $J=9$ Hz, H-3, H-5), 7.16 (2H, d, $J=9$ Hz, H-2, H-6).

Enzymatic Hydrolysis of Icariside A₁ (IV)—A solution of icariside A₁ (IV, 13 mg) in water (2 ml) was treated with β -glucosidase (50 mg) at 37 °C for a day. The reaction mixture was diluted with water and extracted with ethyl acetate 3 times. Ethyl acetate was evaporated off and the residue was recrystallized from methanol to give colorless

needles (IVa, 6 mg), mp 179—180 °C. $[\alpha]_D^{25} 0^\circ$ ($c=1.56$, chloroform). UV $\lambda_{\max}^{\text{MeOH}}$ nm (log ϵ): 215 (4.61), 233 (sh, 4.59), 273 (sh, 4.19), 281 (4.26), 301 (4.13), 313 (4.13). IR ν_{\max}^{KBr} cm^{-1} : 3430, 1610, 1580, 1520, 1450, 1415, 1405, 1345, 1330, 1265, 1210, 1180, 1150, 1065, 1040, 850. MS m/z : 316 (M^+ , 100), 301 ($M^+ - \text{CH}_3$, 34), 286 ($M^+ - 2 \times \text{CH}_3$, 6), 270 (16), 151 (17). $^1\text{H-NMR}$ (CDCl_3) δ : 2.71 (4H, brs, H_2 -9, H_2 -10), 3.77, 3.93, 3.95, 4.00 (each 3H, s, OMe), 5.73 (1H, s, OH), 6.66 (1H, brs, H-8), 6.76 (1H, brs, H-1), 7.97 (1H, s, H-5). $^{13}\text{C-NMR}$ (CDCl_3) δ : 29.3, 30.3 (C-9/C-10), 55.8, 56.1 (methoxyl at C-2/C-6), 60.1, 61.2 (methoxyl at C-3/C-4), 110.3, 111.0, 111.2 (C-1/C-5/C-8), 120.2 (C-8a), 125.1 (C-10a), 130.5 (C-4a), 135.0 (C-3), 139.0 (C-4b), 147.2, 147.3, 147.6 (C-4/C-6/C-7), 150.5 (C-2).

Acetylation of IVa—IVa (8 mg) was acetylated in the same way as II. A monoacetate IVb (6 mg) was obtained as colorless needles, mp 143—144 °C after recrystallization from methanol. UV $\lambda_{\max}^{\text{MeOH}}$ nm (log ϵ): 218 (4.56), 233 (sh, 4.37), 273 (sh, 4.19), 280 (4.24), 294 (sh, 4.12), 310 (4.17). IR ν_{\max}^{KBr} cm^{-1} : 1785, 1615, 1590, 1525, 1470, 1455, 1415, 1405, 1370, 1340, 1290, 1265, 1250, 1220, 1200, 1110, 1065, 1040, 950, 910, 890. $^1\text{H-NMR}$ (CDCl_3) δ : 2.36 (3H, s, OAc), 2.73 (4H, brs, H_2 -9, H_2 -10), 3.77 (3H, s, OMe), 3.94 (9H, s, OMe \times 3), 6.75, 6.77 (each 1H, brs, H-1/H-8), 8.03 (1H, s, H-5). $^{13}\text{C-NMR}$ (CDCl_3) δ : 20.8 (OAc), 29.1, 30.0 (C-9/C-10), 55.9, 56.2 (methoxyl at C-2/C-6), 60.4, 61.0 (methoxyl at C-3/C-4), 110.9 (C-1), 111.8 (C-5), 117.5 (C-8), 124.6, 126.4 (C-8a/C-10a), 131.3 (C-4a), 134.2 (C-3), 142.1 (C-8b), 144.3 (C-7), 147.3, 148.1 (C-6/C-4), 151.4 (C-2), 169.3 (C=O).

Methylation of IVa—A mixture of IVa (5 mg), dimethyl sulfate (0.2 ml) and anhydrous potassium carbonate (100 mg) in dry acetone (2 ml) was refluxed for 3 h with stirring. After removal of the precipitate by filtration, the filtrate was concentrated to a syrup, which was chromatographed on a thin layer plate (Kiesel gel GF₂₅₄; benzene-acetone (95:5)) to yield a methyl ether (IVc, 3 mg) as colorless needles (methanol), mp 108—109 °C. UV $\lambda_{\max}^{\text{MeOH}}$ nm (log ϵ): 216 (4.58), 233 (sh, 4.20), 273 (sh, 4.03), 281 (4.11), 301 (4.01), 312 (4.00). IR ν_{\max}^{KBr} cm^{-1} : 1610, 1520, 1495, 1465, 1415, 1400, 1265, 1245, 1220, 1190, 1130, 1085, 1055, 1005. $^1\text{H-NMR}$ (CDCl_3) δ : 2.74 (4H, brs, H_2 -9, H_2 -10), 3.79, 3.90, 3.94 (each 3H, s, OMe), 3.95 (6H, s, OMe \times 2), 6.62, 6.72 (each 1H, brs, H-1/H-8), 8.02 (1H, s, H-5). $^{13}\text{C-NMR}$ (CDCl_3) δ : 29.4, 30.6 (C-9/C-10), 55.9, 56.0 (1C) and (2C), methoxyl at C-2/C-6/C-7), 60.5, 61.1 (methoxyl at C-3/C-4), 107.7 (C-8), 111.0, 111.1 (C-1/C-5), 120.9 (C-8a), 125.2 (C-10a), 130.4 (C-4a), 134.2 (C-3), 141.6 (C-4b), 147.3, 147.4 (C-4/C-6), 151.5, 151.7 (C-2/C-7).

Enzymatic Hydrolysis of Icariside B₁ (V)—A solution of icariside B₁ (V, 27 mg) in water (2 ml) was treated with cellulase (30 mg) at 37 °C for 5 h. After being diluted with water the reaction mixture was passed through an Amberlite XAD-2 column, which was washed with water. The methanol eluate was purified by HPLC (Develosil ODS-10, 20 \times 250 mm; $\text{H}_2\text{O}-\text{CH}_3\text{CN}$ (77:23)) to give an aglycone (Va, 11.5 mg) as colorless needles (acetone-benzene), mp 134—136 °C, $[\alpha]_D^{25} -63.0^\circ$ ($c=1.15$, methanol). UV $\lambda_{\max}^{\text{MeOH}}$ nm (log ϵ): 232 (4.15). IR ν_{\max}^{KBr} cm^{-1} : 3350, 1945, 1680, 1595, 1465, 1370, 1240, 1190, 1165, 1150, 1070, 1045, 990, 955, 860, 820. ^1H - and ^{13}C -NMR: Tables I and II.

Enzymatic Hydrolysis of Icariside B₂ (VI)—A solution of icariside B₂ (VI, 9 mg) in water (0.5 ml) was treated with β -glucosidase (10 mg) at 37 °C for 13 h. The reaction mixture was worked up in the same way as described for IV to give an aglycone (VIa, 5 mg) as an amorphous powder. This was acetylated in the usual way with pyridine and acetic anhydride (each 3 drops) to give VIb (4 mg) as colorless needles (ether-hexane), mp 129—130 °C, $[\alpha]_D^{25} -104.7^\circ$ ($c=0.25$, chloroform). CD ($c=0.039$, methanol) $[\theta]$ (nm): -37326 (232). UV $\lambda_{\max}^{\text{MeOH}}$ nm (log ϵ): 230 (4.09). IR ν_{\max}^{KBr} cm^{-1} : 1740, 1685, 1390, 1375, 1270, 1255, 1170, 1050, 1045, 1000, 915. MS m/z : 266 (M^+ , trace), 191 (7), 175 (4), 163 (5), 149 (8), 135 (10), 124 (24), 123 (100). $^1\text{H-NMR}$: Table I.

Enzymatic Hydrolysis of Icarisides C₁ (VII), C₂ (VIII) and C₃ (IX)—A solution of icariside C₁ (VI, 34 mg) in water (1 ml) was treated with cellulase (30 mg) at 37 °C overnight. The reaction mixture was worked up in the same manner as described for VI. The methanol eluate was purified by HPLC (Develosil ODS-10, 20 \times 250 mm; $\text{H}_2\text{O}-\text{CH}_3\text{CN}$ (63:37)) to give an aglycone (VIIa, 11 mg) as a colorless oil. $[\alpha]_D^{25} -13.4^\circ$ ($c=1.08$, methanol). IR $\nu_{\max}^{\text{CHCl}_3}$ cm^{-1} : 3450, 1610, 1460, 1380, 1165, 1080, 1000, 930. CD ($c=0.010$, carbon tetrachloride with equimolar $\text{Eu}(\text{fod})_3$): +41322 (305), -27716 (285). From VIII (14 mg), VIIa (5 mg) was obtained in the same manner. $[\alpha]_D^{25} -12.2^\circ$ ($c=0.49$, methanol). CD ($c=0.010$, carbon tetrachloride with equimolar $\text{Eu}(\text{fod})_3$): +35840 (305), -23040 (284). From IX (14 mg), VIIa (2.8 mg) was obtained in the same manner. $[\alpha]_D^{25} -13.4^\circ$ ($c=0.19$, methanol). CD ($c=0.010$, carbon tetrachloride with equimolar $\text{Eu}(\text{fod})_3$): +31530 (305), -22220 (284). $^1\text{H-NMR}$: Table III.

Enzymatic Hydrolysis of Icariside C₄ (X)—A solution of icariside C₄ (X, 13 mg) was treated in the same manner as described for VII to give an aglycone (Xa, 7 mg) as a colorless oil. $[\alpha]_D^{25} +44.5^\circ$ ($c=0.64$, methanol). IR $\nu_{\max}^{\text{CHCl}_3}$ cm^{-1} : 3450, 1610, 1460, 1380, 1160, 1080. CD ($c=0.010$, carbon tetrachloride with equimolar $\text{Eu}(\text{fod})_3$): -32768 (305), +20480 (284). $^1\text{H-NMR}$: Table III.

Acid Hydrolysis of Glycosides IV, V, VI, VII, VIII, IX and X—A solution of a glycoside (*ca.* 0.1 mg) in 10% sulfuric acid (2 drops) was heated in a boiling water bath for 30 min. The solution was passed through an Amberlite IRA-45 column and concentrated to give a residue, which was reduced with sodium borohydride (*ca.* 1 mg) for 1 h at room temperature. The reaction mixture was passed through an Amberlite IR-120 column and the eluate was concentrated to dryness. Boric acid was removed by co-distillation with methanol and the residue was acetylated with acetic anhydride and pyridine (1 drop each) at room temperature overnight. The reagents were evaporated off *in vacuo*. From each glycoside, glucitol acetate was detected by GC. Conditions: column, 1.5% OV-17, 3 mm \times 1 m; column temperature, 200 °C; carrier gas, N_2 ; t_R 4.8 min.

Synthesis of 3,7,11-Trimethyl-1,6-dodecadien-3,10,11-triol (XIII)—*m*-Chloroperbenzoic acid (2.5 g) was added to a stirred solution of (+)-nerolidol (XI, 2.8 g) in dichloromethane (25 ml) and saturated aqueous sodium hydrogen carbonate (25 ml). The mixture was stirred for 17 h at room temperature, then the dichloromethane layer was washed with saturated aqueous sodium chloride and dried over sodium sulfate. Removal of the solvent afforded a crude product, which was chromatographed on silica gel using benzene-acetone (9:1) as the eluent to give 10,11-epoxynerolidol (XII, 2.6 g) as a colorless oil. A solution of XII (850 mg) in 0.1 N sulfuric acid (33 ml) and tetrahydrofuran (33 ml) was stirred for 5.5 h at room temperature. The reaction mixture was diluted with water and passed through an Amberlite XAD-2 column. After washing of the column with water, the methanol eluate was purified by HPLC (Develosil ODS-10, 20 × 250 mm; H₂O-CH₃CN (70:30)) to give 3,7,11-trimethyl-1,6-dodecadien-3,10,11-triol (XIII, 150 mg) as a colorless oil. *Anal.* Calcd for C₁₅H₂₈O₃: C, 70.27; H, 11.01. Found: C, 70.24; H, 11.03. IR ν_{\max}^{KB} cm⁻¹: 3450, 1610, 1460, 1380, 1165, 1080, 1000, 930. ¹H- and ¹³C-NMR: Tables III and IV.

Acknowledgement We wish to thank Prof. T. Shimizu, Shinshu University, for his valuable advice on judging the species of the plant. We also thank Mr. T. Tsuneya, Shiono Koryo Kaisha Ltd., for providing (+)-nerolidol, and the staff of the Central Analytical Laboratory of this college for elemental analyses and measurement of MS.

References and Notes

- 1) T. Takemoto, K. Daigo and Y. Tokuoka, *Yakugaku Zasshi*, **95**, 312 (1975); *idem, ibid.*, **95**, 321 (1975); *idem, ibid.*, **95**, 557 (1975); *idem, ibid.*, **95**, 698 (1975); *idem, ibid.*, **95**, 825 (1975).
- 2) M. Tomita and H. Ishii, *Yakugaku Zasshi*, **77**, 212 (1957).
- 3) R. Hashimoto, *Jikken Yakubutsugaku Zasshi*, **14**, 195 (1937).
- 4) H. Karasawa, H. Kobayashi, N. Takizawa, T. Miyase and S. Fukushima, *Yakugaku Zasshi*, **106**, 721 (1986).
- 5) H. Iida, T. Kikuchi, K. Kobayashi and H. Ina, *Tetrahedron Lett.*, **1980**, 759.
- 6) T. G. Bonner, E. J. Bourne and S. McNally, *J. Chem. Soc.*, **1962**, 761.
- 7) R. M. Letcher and L. R. M. Nhamo, *J. Chem. Soc. (C)*, **1971**, 3070.
- 8) G. C. Levy, "Topics in Carbon-13 NMR Spectroscopy," Vol. 2, John Wiley & Sons, Inc., New York, 1976, p. 108.
- 9) R. M. Letcher and L. R. M. Nhamo, *J. Chem. Soc., Perkin Trans. 1*, **1972**, 2941.
- 10) J. Meinwald, K. Erickson, M. Hartshorn and T. Eisner, *Tetrahedron Lett.*, **1968**, 2959; S. Isoe, S. Katsumura, S. B. Hyeon and T. Sakan, *ibid.*, **1971**, 1089.
- 11) A. J. Aasen, S. O. Almogvist and C. R. Enzell, *Beitra. Tabakforsch.*, **8**, 366 (1976); K. Mori, *Tetrahedron*, **30**, 1065 (1974).
- 12) G. C. Levy, "Topics in Carbon-13 NMR Spectroscopy," Vol. 2, John Wiley & Sons, Inc., New York, 1976, p. 92.
- 13) T. Kametani, H. Kurobe, H. Nemoto and K. Fukumoto, *J. Chem. Soc., Perkin Trans. 1*, **1982**, 1085; K. Nakanishi, D. A. Schooley, M. Koreeda and J. Dillon, *J. Chem. Soc., Chem. Commun.*, **1971**, 1235.
- 14) J. J. Pertridge, V. Toome and M. R. Uskokovic, *J. Am. Chem. Soc.*, **98**, 3739 (1976).

[Chem. Pharm. Bull.]
35(3)1118-1127(1987)

Determination of Corticoids Using Pyrrole. V. Studies on the Colored Products

HIROSHI TOKUNAGA,* MASAYUKI TANNO, and TOSHIO KIMURA

*National Institute of Hygienic Sciences, 1-18-1, Kamiyoga,
Setagaya-ku, Tokyo 158, Japan*

(Received July 15, 1986)

The mechanism of the color reaction and the structures of the colored products of cortisone (**1a**) and deoxycorticosterone (**2a**) with pyrrole were elucidated. In the presence of cupric acetate, **1a** and **2a** were converted to the oxidation products (**1b** and **2b**) which have a glyoxal side chain at C(17). For studying the chemical structures of the colored products derived from corticoids, phenylglyoxal (**3a**) was used as a model compound with a glyoxal side chain. By reacting **3a** with pyrrole in hydrochloric acid, di(2-pyrrolyl)benzoylmethane (**3b**) was produced as an intermediate in the formation of the colored product. Compound **3b** was changed to [5-(2-pyrrolyl)-2(2*H*)-pyrrolylidene](2-pyrrolyl)benzoylmethane (**3d**) by reaction with pyrrole in the presence of cupric acetate and hydrochloric acid. Compound **3d** in dichloromethane gave the absorption maximum at 480 nm. Corticoids **1b** and **2b** were converted to the colored products, 21-[5-(2-pyrrolyl)-2(2*H*)-pyrrolylidene]-21-(2-pyrrolyl)-4-pregnene-3,11,20-trione (**1e**) and 21-[5-(2-pyrrolyl)-2(2*H*)-pyrrolylidene]-21-(2-pyrrolyl)-4-pregnene-3,20-dione (**2e**), by reaction with pyrrole under the above conditions. Corticoids **1e** and **2e** in dichloromethane gave absorption maxima at 510 and 480 nm, respectively. Corticoid **1e** showed fluorescence at 562 nm with excitation at 516 nm.

Keywords—corticoid; cortisone; deoxycorticosterone; phenylglyoxal; color reaction; pyrrole; fluorescent reaction; ¹³C-NMR

Corticoids are hormones secreted by the adrenal cortex, and are administered for treatment of various diseases such as Cushing's syndrome, adrenal insufficiency, Addison's disease, *etc.*

In our previous papers,¹⁾ we reported a new colorimetric and fluorometric method for the determination of corticoids in pharmaceutical preparations and serum. The color reaction includes two steps. In the first step, the ketol side chain at C(17) of the corticoid was oxidized to a glyoxal side chain in the presence of cupric acetate. In the second step, reaction of the glyoxal group with pyrrole proceeded in the presence of cupric acetate and hydrochloric acid. The colored mixture was measured colorimetrically at about 580 nm in the case of mineralocorticoids and at about 600 nm in the case of glucocorticoids. The products obtained from glucocorticoids also showed fluorescence at about 620 nm with excitation at about 600 nm. This paper describes the structural elucidation of the colored products produced from corticoids.

In order to confirm the production of a glyoxal side chain at C(17), a solution of **1a** was bubbled with air in the presence of cupric acetate and then the oxidation product (**1b**) was condensed with *o*-phenylenediamine in the manner reported by Lewbart and Mattox.²⁾ The product (**1c**) (Table I) has absorption maxima at 238, 310, and 320 nm corresponding to those of quinoxaline.

The carbon-13 nuclear magnetic resonance (¹³C-NMR) signal of **1c** are summarized in Table II.

All the carbon signals of **1c** were assigned on the basis of the data for cortisone acetate (**4**)

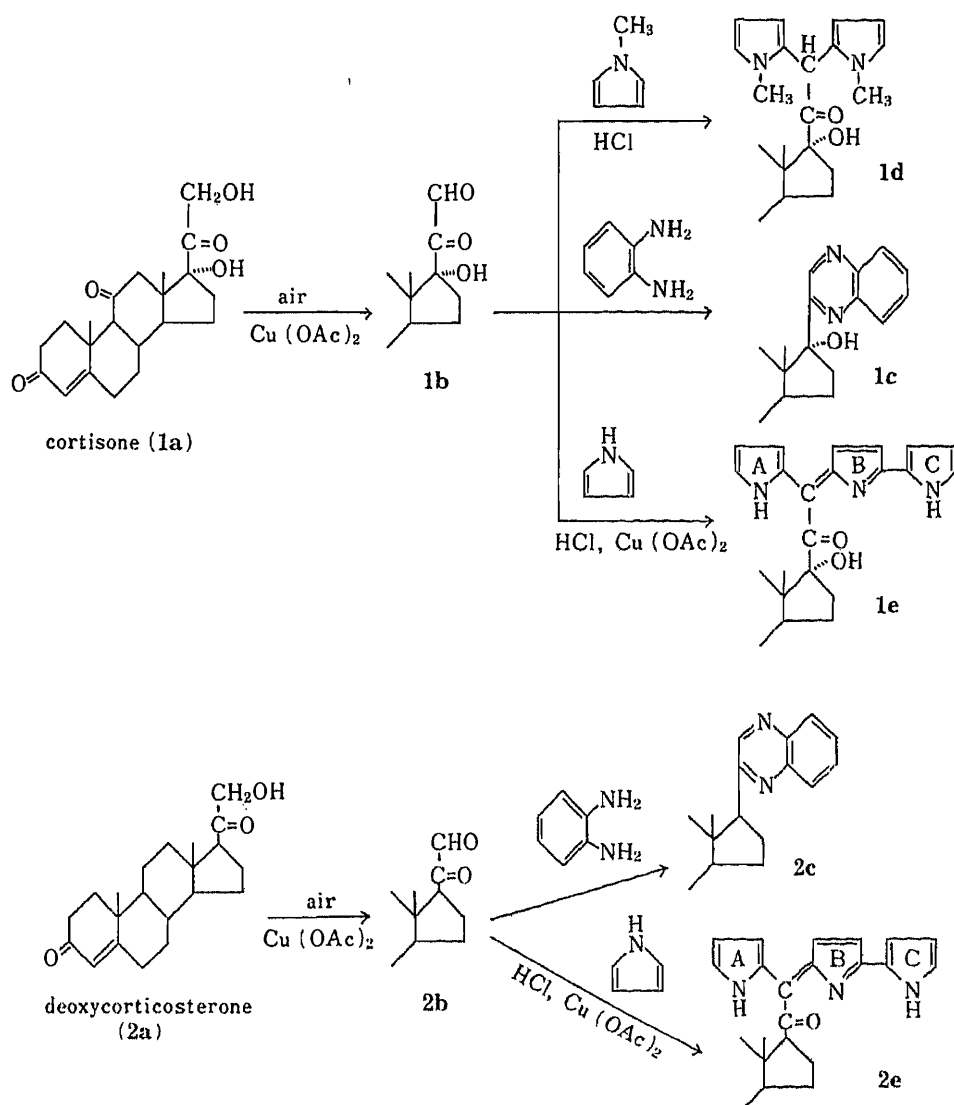


Chart 1

and quinoxaline (5).³⁾ Deoxycorticosterone (2a) was also oxidized by cupric acetate. The product was an oily substance, whereas 1b was a colorless powder. The reaction of the oxidation product with *o*-phenylenediamine was carried out to confirm the formation of the glyoxal side chain at C(17). The product (2c) shows absorption maxima at 238, 310, and 320 nm (Table I). The ¹³C-NMR data are shown in Table II. We concluded that the oxidation product formed from 2a had a glyoxal side chain, as shown in Chart 1.

In order to clarify the structure of the colored product, we employed phenylglyoxal (3a) as a model compound with a glyoxal side chain, because acetaldehyde and benzaldehyde did not show coloration on reacting with pyrrole in the presence of cupric acetate and hydrochloric acid.^{1a)} It has been reported⁴⁾ that the aldehyde group reacted with pyrrole at the α -position in hydrochloric acid, yielding a 2,2'-dipyrrole compound. Reaction of 3a under the same conditions gave a colorless reaction mixture. This mixture reacted further with pyrrole in the presence of cupric acetate, giving a coloration. We presumed that the colorless product would be formed first from 3a and pyrrole in hydrochloric acid without cupric acetate. The mass spectrum (MS) of the colorless product (3b) gave the molecular ion peak at m/z 250 (Table III). Its infrared (IR) spectrum showed new absorptions due to a pyrrole ring

TABLE I. Physical Data for Compounds Tested

Compd.	mp (°C)	IR ^{a)} (cm ⁻¹)	Absorption max. ^{b)} (nm)	ϵ^c
1b · CH ₃ OH	121—134 (dec.)	3436 (OH) 1702 (C=O) 1652 (C=O)	238	26000
1c	240—243 (dec.)	3444 (OH) 1706 (C=O) 1670 (C=O)	238 310 320	53300 7800 9000
2c	260—262 (dec.)	1674 (C=O) 1616	238 310 320	53300 7400 8500
1d	254—248 (dec.)	3400 (OH) 1710 (C=O) 1646 (C=O)	228	33600
3b	64—67	3392 (NH) 1676 (C=O) 1596, 1580 1558	240 280	15600 2700
3c · 1/5 H ₂ O	143—146	2812 (N-CH ₃) 1694 (C=O) 1596, 1580	238 282	22000 2600
3d · 1/3 H ₂ O	181—189	3424 (NH) 1666 (C=O) 1602 (polyene) 1582, 1554	238 280 480	14400 6400 18500
1e · 1/2 C ₆ H ₆		3400 (OH, NH) 1706 (C=O) 1668 (C=O) 1622 (polyene) 1568, 1534	284 510	16100 40900
2e		3432 (NH) 1660 (C=O) 1602 (polyene)	238 280 480	3400 10400 29900

a) IR spectra were measured by the KBr disc method. b) Absorption maxima were measured in CH₂Cl₂. c) Molar extinction coefficient.

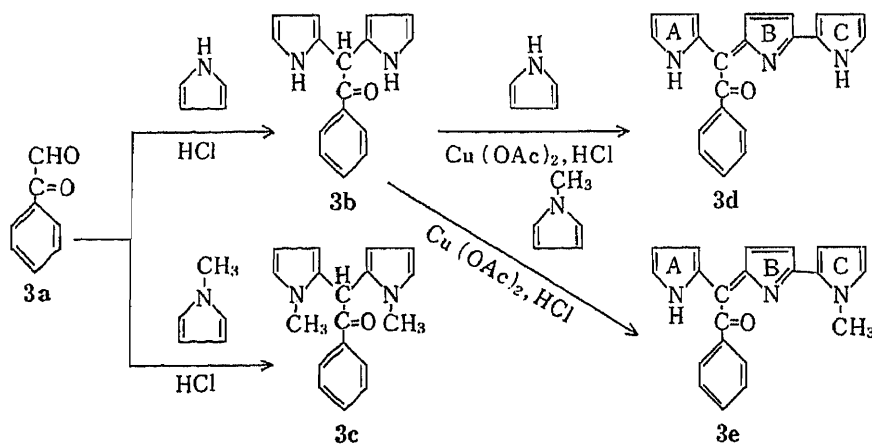


Chart 2

TABLE II. ^{13}C -NMR Data for Cortisone Acetate (4), 1c, 2c, and Quinoxaline (5) in CDCl_3

Carbon	4 ³⁾	1c	2c	5 ³⁾	1d
Steroid					
1	34.8	35.1	35.8		34.5
2	33.7	34.4	32.9		33.9
3	199.6	199.4	199.1		199.5
4	124.5	124.2	123.9		124.8
5	170.4	168.6	170.8		168.7
6	32.2	32.1	32.1		32.3
7	32.3	33.4	32.9		32.4
8	36.5	36.8	36.0		36.6
9	62.5	62.4	56.2		62.6
10	38.2	37.9	38.7		38.3
11	208.7	209.6	20.9		209.2
12	49.8	49.5	38.1		45.5
13	51.2	52.8	53.9		52.1
14	49.8	49.5	45.6		50.1
15	23.2	23.4	24.5		23.4
16	35.0	35.1	35.8		34.8
17	88.8	83.8	56.5		89.6
18	15.4	16.2	13.3		16.1
19	17.2	17.0	17.4		17.3
20	204.3				207.6
21	67.3				45.6
-OCOCH ₃	168.4				
-OCOCH ₃	20.4				
Quinoxaline					
2		155.5	156.6	144.8	
3		143.4	146.3	144.8	
5		130.1	129.6	129.6	
6		128.7	128.8	129.4	
7		128.8	129.1	129.4	
8		129.7	129.3	129.6	
9		140.2	141.4	142.8	
10		141.1	142.2	142.8	
Pyrrole					
A-2					127.4
A-3					107.0
A-4					110.5
A-5					123.7
B-2					126.4
B-3					106.9
B-4					108.8
B-5					123.5
N-CH ₃					33.8

at 1580 and 1558 cm^{-1} , respectively. The chemical shifts of **3b** are summarized in Table IV.

Cushley *et al.*⁵⁾ assigned the carbon signals of pyrrole derivatives as shown in Table IV. The signals of carbonyl and tertiary carbons of **3b** were at 198.1 and 45.1 ppm and the chemical shift of the quaternary carbon at the α -position of pyrrole was 127.9 ppm. From the above results **3b** was concluded to have the structure shown in Chart 2.

Compound **3a** was also reacted with 1-methylpyrrole in hydrochloric acid. As shown in Table III, the MS of **3c** gave the molecular ion peak at m/z 278 and $\text{C}_{11}\text{H}_{13}\text{N}_2$ ion peak at m/z 173. All the carbon signals of **3c** are assigned in Table IV. The structure of **3c** was elucidated

TABLE III. Physical Data for Compounds Tested

Compd.	Formula	MS (<i>m/z</i>)	Analysis (%) Found (Calcd)		
			C	H	N
1b·CH ₃ OH	C ₂₁ H ₂₆ O ₅ ·CH ₃ OH	358 (M ⁺ - CH ₃ OH)	67.73 (67.67)	7.62 (7.74)	
1c	C ₂₇ H ₃₀ N ₂ O ₃	430 (M ⁺)	75.47 (75.32)	7.02 (7.02)	6.42 (6.51)
2c	C ₂₇ H ₃₂ N ₂ O	400 (M ⁺)	80.07 (80.96)	7.96 (8.05)	6.89 (6.99)
1d	C ₃₁ H ₃₈ N ₂ O ₄	173 (M ⁺ - C ₂₀ H ₂₈ O ₄)	73.93 (74.08)	7.35 (7.62)	5.43 (5.20)
3b	C ₁₆ H ₁₄ N ₂ O	250 (M ⁺)	76.65 (76.78)	5.68 (5.64)	10.96 (11.19)
3c·1/5 H ₂ O	C ₁₈ H ₁₈ N ₂ O·1/5 H ₂ O	278 (M ⁺ - 1/5 H ₂ O)	76.55 (76.68)	6.46 (6.58)	9.85 (9.94)
3d·1/3 H ₂ O	C ₂₀ H ₁₅ N ₃ O·1/3 H ₂ O	173 (M ⁺ - C ₇ H ₅ O)	75.12 (75.22)	4.78 (4.94)	12.91 (13.16)
1e·1/2 C ₆ H ₆	C ₃₃ H ₃₅ N ₃ O ₄ ·1/2 C ₆ H ₆	313 (M ⁺ - 1/3 H ₂ O)	75.05 (74.98)	6.41 (6.64)	7.57 (7.28)
2e	C ₃₃ H ₃₇ N ₃ O ₂		77.97 (78.07)	7.45 (7.35)	7.90 (8.28)

TABLE IV. ¹³C-NMR Data for 3b, 3c, 3d, the Pyrrole (6), the 1-Methylpyrrole (7), and the Bipyrrrole (8) in CDCl₃

Carbon	3b	3c	3d	6 ^{s)}	7 ^{s)}	8 ^{s)}
Benzyl						
1	133.4	132.9	133.1			
2	128.8	128.7	128.7			
3	128.7	128.6	128.3			
4	136.6	136.7	137.7			
5	128.7	128.7	128.3			
6	128.8	128.6	128.7			
C=O	198.1	195.8	194.6			
C-H, C=	45.1	45.8	130.3			
Pyrrole						
A-2	127.5	127.9	126.8 ^{a)}	120.9	124.3	129.4
A-3	107.5	107.0	111.3 ^{b)}	110.7	111.2	106.0
A-4	108.4	110.0	119.2	110.7	111.2	111.5
A-5	118.5	123.1	123.7 ^{c)}	120.9	124.3	120.2
B-2	127.5	127.9	147.7			129.4
B-3	107.5	107.0	135.4 ^{d)}			106.9
B-4	108.4	110.0	134.0 ^{d)}			111.5
B-5	118.4	123.1	162.1			120.2
C-2			127.8 ^{a)}			
C-3			111.6 ^{b)}			
C-4			114.7			
C-5			124.6 ^{c)}			
N-CH ₃		34.1			34.1	

a-d) The assignments may be reversed, but those given are preferred.

as shown in Chart 2.

When **3b** was allowed to stand in the presence of cupric acetate and hydrochloric acid without pyrrole, the mixture did not give the coloration. However, when **3b** was brought into contact with pyrrole under the same conditions as described above, the reaction mixture was colored. The alkaline and acidic solutions had absorption maxima at 480 and 580 nm, respectively. Compound **3c** was also reacted with pyrrole in the presence of cupric acetate and hydrochloric acid, but the reaction mixture was colorless. It appears that **3b** is an intermediate in the color reaction and that the addition of pyrrole is essential for this color reaction. As shown in Tables I and III, the MS of the colored product (**3d**) obtained from **3b** gave the molecular ion peak at m/z 313, and **3d** in dichloromethane had the absorption maximum at 480 nm. Its IR spectrum in the range of $1600\text{--}1700\text{ cm}^{-1}$ showed a new and strong absorption at 1602 cm^{-1} due to polyene. The results suggested that the colored product might have a benzoyl group, three pyrrole groups and conjugated double bonds. The chemical shifts of **3d** are shown in Table IV. In a comparison of its signals with those of **3b**, the signal at 45.8 ppm due to a tertiary carbon was absent in the spectrum of **3d**, suggesting that a new double bond existed between the tertiary carbon and the α -position of pyrrole on **3b**. Compound **3d** might have three tautomeric forms as indicated in Chart 3.

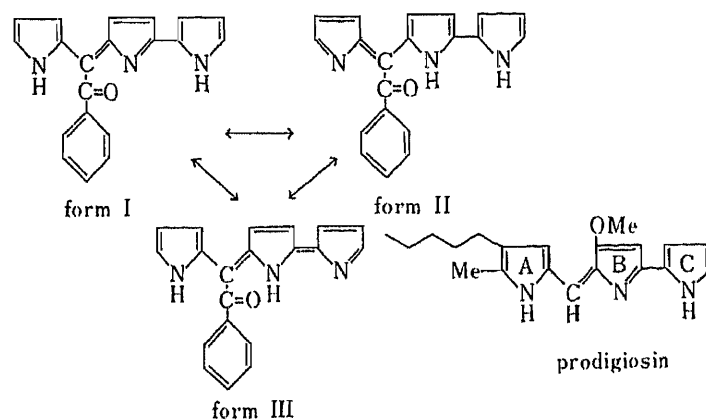


Chart 3

To further examine the structure of **3d**, reaction of **3b** with 1-methylpyrrole instead of pyrrole was undertaken. The product (**3e** in Chart 2) gave a new absorption maximum at 476 nm and its MS had the molecular ion peak at m/z 327. On comparing the absorption maximum of **3d** with that of **3e**, both wavelengths were in agreement. Therefore, **3d** should not take the form III tautomeric in Chart 3 because **3e** containing 1-methylpyrrole could not have a tautomeric structure such as form III. We next took account of the chemical shifts of prodigiosin (**9**), a red bacterial pigment, having a methoxybipyrrole-methene skeleton, as shown in Chart 3, and of Zn(II) porphyrin (**10**). In the ^{13}C -NMR spectrum of **10**, Abraham *et al.* assigned the three signals at 149.3, 131.7, and 104.3 ppm to the α - and β -carbon of pyrrole and meso carbon.⁶⁾ Cusheley *et al.* reported the assignment of carbon signals of **9** as demonstrated in Table V.⁵⁾

If **3d** takes the form II structure, all carbon signals of the pyrrole rings should appear below 149 ppm, based on the signals of **10**. However, a signal at 162.1 ppm was present in the case of **3d**. The tautomeric structure of **3d** should therefore be form I. The signals at 147.7 and 162.1 ppm were assigned to the B-2 and B-5 carbons on the pyrrole B ring. The two signals at 135.4 and 134.0 ppm were assigned to the tertiary carbons by reference to the β -carbon signals of **10**. The other signals due to carbons on the pyrrole A and C rings were assigned on the basis of the data for **8**, **9**, and **10**, as shown in Table IV. Compound **3d** is concluded to have

TABLE V. ^{13}C -NMR Data for **1e**, **2e**, **3d**, and Prodigiosin (**9**) in CDCl_3

Carbon	1e	2e	3d	9^d
Steroid				
16	34.8	35.5		
17	61.1	56.2		
18	16.6	12.8		
19	17.3	17.3		
C=O (20)	204.0	205.2		
meso (C=)	160.6 ^{a)}	128.6	130.3	118.7
Pyrrole				
A-2	128.4	127.8	126.8	130.1
A-3	117.8	117.9	119.2	123.8
A-4	112.5	111.1	111.3	126.9
A-5	123.7	124.7	123.7	139.6
B-2	165.9 ^{a)}	147.3	147.7	140.7
B-3	126.3 ^{b)}	136.3	135.4	171.9
B-4	125.2 ^{b)}	135.1	134.0	98.2
B-5	167.8 ^{a)}	161.9	162.1	162.4
C-2	124.7	128.3	127.8	131.4
C-3	113.6	114.6	114.7	115.3
C-4	112.1	111.1	111.6	112.6
C-5	118.5	126.5	124.6	125.4
Alkyl				
OCH ₃				61.0
1'				28.3
2'				32.9
3'				34.5
4'				25.2
5'				16.7
A-5-CH ₃				12.7

a, b) The assignments may be reversed, but those given are preferred.

the form I structure and the reaction of **3a** with pyrrole proceeds as shown in Chart 2.

To examine the intermediate of the colored product obtained from **1b** (like **3b** in Chart 2), **1b** was reacted with pyrrole in hydrochloric acid. However, it was difficult to separate and purify the colorless product. Thus, we synthesized **1d** as a colorless powder from **1b** and 1-methylpyrrole in hydrochloric acid, as shown in Chart 1. Its MS gave the fragment ion peak at m/z 173 which corresponded to that of **3c** ($\text{C}_{11}\text{H}_{13}\text{N}_2$ ion). The chemical shifts are shown in Table III.

A comparison of the spectrum of **1d** with that of **4** revealed nine new signals due to two 1-methylpyrroles and one signal due to tertiary carbon at C(21), like that of **3c**. On the basis of the ^{13}C -NMR data of **3c** and **4**, all the carbon signals of **1d** were assigned. The result suggested that an intermediate such as **3b** is involved in the coloration of corticoids with pyrrole.

After oxidation of **2a**, the oxidation product (**2b**) was reacted with pyrrole in the same way as **3d**. The colored product (**2e**) gave absorption maxima at 280 and 480 nm in acidic and alkaline solutions, respectively, like **3d**. As shown in Table III, the IR spectrum of **2e** showed a new and strong absorption at 1602 cm^{-1} (polyene). The new carbon signals were in reasonable agreement with those of **3d**. For the assignment of all the carbon signals as shown in Table V, **2e** should have a structure resembling the form I tautomer in Chart 3.

Corticoid **1b** was treated with pyrrole in the same way as **3d**. The reaction mixture in an acidic medium gave the absorption maximum at 600 nm and showed fluorescence at 620 nm with excitation at 598 nm. In alkaline solution, its absorption maximum changed to 510 nm

and its fluorescence to 562 nm with excitation at 516 nm. The change of the absorption maxima of the reaction mixture in acidic and alkaline media corresponded to that from **3d** and **2e**. The chromophore of **1e** may thus be similar to that of **3d** and **2e**. The absorption maxima of the reaction mixtures obtained from glucocorticoids differed from those obtained from mineralocorticoids.^{1a,b)} The differences of the absorption maxima were about 20 nm. The structural difference between glucocorticoids and mineralocorticoids is the presence or absence of the hydroxy group of the steroidal skeleton at C(17). Thus, there may be some the interaction between the chromophore and the hydroxy group, such as a hydrogen bond. The IR spectrum of **1e** showed strong polyene absorption at 1622 cm^{-1} (Table II) which differed to that of **2e** or **3d** (1602 cm^{-1}). The ^{13}C -NMR signals of **1e** are shown in Table V. On the basis of the data for **2e** and **10**, the signals of the A-2, A-3, A-4, and A-5 carbons on pyrrole A ring were assigned at 128.4, 112.5, 117.8, and 123.7 ppm, respectively, and those of C-2, C-3, C-4, and C-5 on the pyrrole C ring at 124.7, 113.6, 112.1, and 118.5 ppm, respectively. The five residual signals (167.8, 165.9, 160.6, 126.3, and 125.2 ppm) due to B-2, B-3, B-4, B-5, and C(21) of **1e** obviously differed from those of **2e**. In a comparison of the signals of the steroidal skeleton with those of **1d**, a difference of the C(17) signals (61.1 and 89.6 ppm) was observed. In the case of **2e**, the C(17) signal appeared at 56.2 ppm. The results suggested that the deshielding effect of the hydroxy group on C(17) of **1e** was reduced because of hydrogen bond formation between the chromophore and the hydroxy group. Loewenstein and Margalit reported a change of the methyl carbon signal caused by hydrogen bond formation between methyl isocyanate and methanol.⁶⁾ A comparison of the methyl carbon signal of methyl isocyanate with that of acetonitrile showed that the chemical shift of the methyl carbon of the former compound moved to higher field as the amount of methanol was varied from 0.4 mol per mol of methyl isocyanate to none (methyl isocyanate alone). The difference was 25 ppm. Thus, the signals of B-2 and B-5 should be shifted to low field because of the hydrogen bond formation. From a stereochemical model of **1e**, which has a hydrogen bond, the seven-membered ring, which was newly formed due to the hydrogen bond between the hydroxy group at C(17) and the lone pair of the nitrogen atom on the pyrrole B ring, takes a planar structure with respect to the pyrrole B ring. The result suggested that the signals due to B-3 and B-4 of **1e** should be shifted to high field (such as 125.2 and 126.3 ppm) in comparison with the signals at 135.1 and 136.3 ppm of **2e** because of the strong π electron shielding effect owing to the formation of the planar structure. If the structure of phenolphthalein (a pH indicator) is compared with that of fluorescein (having fluorescence), the structural difference is the absence and presence of an ether linkage between two benzene rings. As fluorescein, having the ether linkage, has a planar structure involving two benzene rings, this might account for the fluorescence.⁷⁾ By analogy, this supports the planar structure of **1e** involving the seven-membered ring and pyrrole B ring. On the basis of the existence of the hydrogen bond and planar structure, the signals of B-2, B-3, B-4, B-5, and C(21) were assigned at 165.9, 125.2, 126.3, 167.8, and 160.6 ppm as shown in Table V.

From the present study, we concluded that the color reaction of corticoids such as **1a** and **2a** proceeds by the mechanisms shown in Charts 1 and 2. Corticoids **1a** and **2a** were oxidized in the presence of cupric acetate to form a glyoxal side chain (**1b** and **2b**). Corticoids **1b** and **2b** were reacted with pyrrole in the presence of cupric acetate and hydrochloric acid. In the first step, **1b** and **2b** were condensed with two pyrroles in hydrochloric acid and consequently dipyrrole compounds such as **3b** were formed. Secondly, the dipyrrole compounds were further reacted with a pyrrole in the presence of cupric acetate and hydrochloric acid. The colored products, such as **1e** and **2e**, had absorption maxima at 480 and 510 nm, respectively. Corticoid **1e** was fluorescent because of the formation of a hydrogen bond between the chromophore and the hydroxy group at C(17).⁸⁾

Experimental

All melting points were taken on a micro hot-stage apparatus and are uncorrected. ^{13}C -NMR spectra were recorded on a JEOL FX NMR spectrometer at 200 MHz using tetramethylsilane as an internal standard. MS were obtained on a JEOL JMS-DX33 mass spectrometer equipped with a JEOL JMA-DA5000 computer, employing a direct injection method. The apparatus used for the high-performance liquid chromatography (HPLC) was a Hitachi 655 liquid chromatograph equipped with a variable-wavelength UV monitor monitoring the absorbance at 254 nm and with a Shimadzu C-R1B Chromatopac. HPLC was carried out on a LiChrosorb Si 60 ($5\ \mu\text{m}$, $25 \times 0.4\ \text{cm}$ i.d.; E. Merck AG, Darmstadt) column under the ambient conditions at a flow rate of 1 ml/min. For column chromatography and thin-layer chromatography (TLC), Silica gel 60 (0.062–0.2 mm; E. Merck AG, Darmstadt) and pre-coated TLC plates with Silica gel F₂₅₄ (E. Merck AG, Darmstadt) were used, respectively. Absorption spectra were measured with a Hitachi 557 dual-wavelength, double-beam spectrophotometer. The apparatus for IR spectrometry was a Hitachi 270-30 IR spectrophotometer.

17,21-Dihydroxy-21-methoxypregn-4-ene-3,11,20-trione (1b)—Corticoid **1a** (400 mg) was dissolved in 0.5 M methanolic cupric acetate solution (100 ml). Air was bubbled into the solution for 50 min. After addition of H_2O , the reaction product was extracted twice with CH_2Cl_2 (80 ml). After being washed with H_2O , the extract was dried over anhydrous Na_2SO_4 . After evaporation, the oily residue was crystallized from $\text{MeOH-H}_2\text{O}$. The product was recrystallized with $\text{MeOH-H}_2\text{O}$ to give **1b** (285 mg) as a colorless powder.

17 β -(2-Quinoxaliny)-17-hydroxy-3,11-dioxo-4-androstene (1c)—Corticoid **1b** (200 mg) was dissolved into MeOH (5 ml) and NaHSO_3 (0.08 g) in H_2O (30 ml) was added to the solution. After heating of the mixture for 5 min, *o*-phenylenediamine (0.08 g) in H_2O (50 ml) was added and the whole was heated for 30 min. The precipitate was collected by filtration and then recrystallized from $\text{MeOH-H}_2\text{O}$ to give **1c** (0.131 g) as colorless needles.

2-(3-Oxopregn-4-ene-17 β -yl)quinoxaline (2c)—Corticoid **2a** (0.66 g) was dissolved in 1 M methanolic cupric acetate solution (100 ml) and treated by procedures similar to those described for **1b**. NaHSO_3 (0.13 g) in H_2O (30 ml) was added to the oily residue and the synthetic procedures for **1c** were followed. Recrystallization of the crude product with MeOH gave **2c** (0.366 g) as colorless prisms.

21-Bis(1,1-dimethyl-2-pyrrolyl)-17-hydroxy-3,11,20-trioxopregn-4-ene (1d)—Corticoid **1b** (140 mg) was dissolved in MeOH (40 ml), then 2.5% methanolic 1-methylpyrrole solution (20 ml) and HCl-MeOH (7:13, 80 ml) were added to the solution. The mixture was reacted for 30 min at 40°C . The reaction mixture was processed in the same manner as described for **1b**. The residue was subjected to TLC using $\text{CH}_2\text{Cl}_2\text{-MeOH}$ (96:4) as a developing solvent. Elution of the adsorbent corresponding to the spot (R_f 0.37) with $\text{CH}_2\text{Cl}_2\text{-MeOH}$ and recrystallization of the crude product from tetrahydrofuran-hexane gave **1d** (60 mg) as a colorless powder.

Di(2-pyrrolyl)benzoylmethane (3b)—Compound **3a** (100 mg) was treated by the same procedure as used for **1d** but with pyrrole instead of 1-methylpyrrole. The oily residue was subjected to column chromatography on silica gel ($3 \times 2\ \text{cm}$ i.d.) using $\text{CH}_2\text{Cl}_2\text{-hexane}$ (8:2). The fraction containing the desired substance was collected and evaporated. Recrystallization of the oily residue from benzene-hexane (2:8) gave **3b** (22 mg) as yellow needles.

Bis(1-methyl-2-pyrrolyl)benzoylmethane (3c)—Compound **3a** (250 mg) was treated as described for the preparation of **3b**, but with 1-methylpyrrole and $\text{CH}_2\text{Cl}_2\text{-hexane}$ (6:4) instead of pyrrole and $\text{CH}_2\text{Cl}_2\text{-hexane}$ (8:2). Recrystallization from $\text{CH}_2\text{Cl}_2\text{-hexane}$ (1:5) gave **3c** (160 mg) as yellow needles.

[5-(2-Pyrrolyl)-2(2H)-pyrrolylidene](2-pyrrolyl)benzoylmethane (3d)—Compound **3a** (134 mg) was dissolved in MeOH (100 ml). Then 2.5% methanolic pyrrole solution (17 ml) and HCl-MeOH (3:7, 94 ml) containing 94 mg of cupric acetate were added and the mixture was reacted for 30 min. After addition of H_2O , the reaction product was isolated by the procedure described for **3b**. Recrystallization from benzene-hexane (1:9) gave **3d** (11 mg) as a brown powder.

21-[5-(2-Pyrrolyl)-2(2H)-pyrrolylidene]-21-(2-pyrrolyl)-4-pregnene-3,11,20-trione (1e)—Corticoid **1b** (60 mg) was dissolved in MeOH (90 ml). Then 2.5% methanolic pyrrole solution (20 ml) and HCl-MeOH (3:7, 70 ml) containing 35 mg of cupric acetate were added. After 40 min at 40°C , the reaction mixture was treated by the procedure described for **3d**. The residue was subjected to HPLC on LiChrosorb Si 60 ($5\ \mu\text{m}$) using $\text{CH}_2\text{Cl}_2\text{-MeOH}$ (98.5:1.5) as the mobile phase. The desired fraction (t_R 7.1 min) was collected, and evaporated. Recrystallization of the product from benzene-hexane gave **1e** (3.3 mg) as a red powder.

21-[5-(2-Pyrrolyl)-2(2H)-pyrrolylidene]-21-(2-pyrrolyl)-4-pregnene-3,20-dione (2e)—Corticoid **2a** (330 mg) was treated as described for **1b**. The oily residue was dissolved in MeOH (100 ml). This solution (30 ml) was treated with 2.5% methanolic pyrrole solution (18 ml) and HCl-MeOH (3:7, 60 ml) containing 60 mg of cupric acetate. After standing for 50 min, the reaction mixture was processed as described above using $\text{CH}_2\text{Cl}_2\text{-MeOH}$ (99.4:0.6) instead of CH_2Cl_2 . The desired fraction (t_R 7.9 min) was collected and evaporated. Recrystallization of the product from benzene-hexane gave **2e** (19 mg) as an orange powder.

Acknowledgments We are grateful to Dr. A. Tanaka, the head of the Division of Biochemistry and Reference Standards in our Institute, and Dr. T. Yamaha, Japan Health Sciences Foundation, for their encouragement throughout this work.

References and Notes

- 1) a) H. Tokunaga, T. Kimura, and J. Kawamura, *Bunseki Kagaku*, **25**, 392 (1976); b) *Idem, ibid.*, **26**, 154 (1977); c) *Idem, Yakugaku Zasshi*, **100**, 200 (1980); d) *Idem, Chem. Pharm. Bull.*, **30**, 2228 (1982).
- 2) M. L. Lewbart and V. R. Mattox, *Anal. Chem.*, **33**, 559 (1961).
- 3) L. F. Johnson and W. V. Jankouski, "Carbon-13 NMR Spectra," A Wiley-Interscience Publication, New York, 1972, p. 282, 373, 492.
- 4) M. Ohta, "Fukusokan Kagaku," Vol. 1, Baifuukan, Tokyo, 1957, p. 37.
- 5) R. J. Cushley, R. J. Sykes, C. K. Shaw, and H. H. Wasserman, *Can. J. Chem.*, **53**, 148 (1975).
- 6) R. J. Abraham, H. Person, and K. M. Smith, *Tetrahedron Lett.*, **11**, 877 (1976).
- 7) A. Loewenstein and Y. Margalit, *J. Phys. Chem.*, **69**, 4152 (1965).
- 8) M. Watanabe, "Keikou Bunseki," Hirokawa Publ. Co., Tokyo, 1970, p. 21.

[Chem. Pharm. Bull.]
35(3)1128—1137(1987)

Selective Cytotoxicity of Drug–Monoclonal Antibody Conjugates against Murine Bladder Tumor Cells

SUSUMU IWASA,*^a EIKO KONISHI,^a KOICHI KONDO,^a
TOHRU SUZUKI,^b HIDEYUKI AKAZA,^c
and TADA0 NIJIMA^c

Central Research Division, Takeda Chemical Industries, Ltd.,^a Yodogawa-ku, Osaka 532,
Japan, Department of Urology, Medical College of Dokkyo,^b Shimotoga-gun,
Tochigi 321-02, Japan and Department of Urology,
Faculty of Medicine, University of Tokyo,^c
Bunkyo-ku, Tokyo 113, Japan

(Received June 11, 1986)

Antitumor agents including mitomycin C (MMC) and methotrexate (MTX) were coupled to monoclonal antibodies against murine bladder tumor cell line MBT-2 for the purpose of enhancing their drug activity. MMC was conjugated with antibody through two carriers, periodate-oxidized dextran and dithiopyridylated serum albumin, and MTX was conjugated with antibody either directly or through dithiopyridylated serum albumin or poly-L-lysine *via* an amide bond. These conjugates were assayed for growth inhibitory effect on MBT-2 bladder tumor cells, MCA clone 15 embryo cells and P388 leukemic cells. The cytotoxicity tests demonstrated that drug–antibody immune conjugates were 10 to 100 times more cytotoxic against antibody-reactive MBT-2 cells than nonimmune drug conjugates and showed a similar level of cytotoxicity against antibody-nonreactive cells to that of the nonimmune conjugates. This selective cytotoxicity was also confirmed by competitive inhibition of unconjugated antibody, showing a dependency on antibody binding to the target cell surface antigens. The targeting effect was further assessed by evaluating the suppression of tumor growth subsequent to *in vitro* treatment of MBT-2 cells with immune conjugates. Half of the mice receiving cells treated with immune conjugates survived more than 40 d after inoculation, while none or one of 7 mice receiving cells treated with unconjugated drug, antibody alone or nonimmune conjugates survived at 40 d after inoculation.

Keywords—mitomycin C; methotrexate; drug–monoclonal antibody conjugate; selective cytotoxicity; murine bladder tumor cell; cell surface antigen

The idea of targeting cytotoxic agents was proposed by Ehrlich at the beginning of the century,¹⁾ but such a goal has become feasible only with the recent advent of monoclonal antibody production.²⁾ Monoclonal antibodies, because of their purity and specificity, and the ability to obtain them in large quantities, represent very attractive carriers for tumor therapeutic agents.³⁾ Many cytotoxic agents coupled with monoclonal antibodies have been proposed and investigated for cancer chemotherapy with various degrees of success.⁴⁾

Among them, immunotoxins prepared by coupling biological toxins to antibodies have received much attention because of their enormous cytotoxic potential.⁵⁾ Such an approach would, however, appear to require absolute tumor specificity of monoclonal antibodies in order not to damage normal tissues, and it is probably unrealistic to expect to obtain such truly tumor-specific antibodies. An alternative is to couple conventional chemotherapeutic drugs which have acceptable side effects. Such antibody-targeted drugs would be expected to provide either improved therapeutic effects or reduced side effects. Several researchers reported successful conjugates prepared by direct coupling of drugs to antibodies,⁶⁾ but this type of conjugate has the drawback that there are only a small number of functional groups

available per antibody molecule which can be used for chemical coupling without significant loss of antibody binding activity. Then a carrier molecule was used to which the drug was attached and which in turn was linked to the antibody in order to obtain a higher molar ratio of drug to antibody. Dextran,^{4a,7)} serum albumin^{4b,8)} and synthetic polypeptides such as poly-L-glutamic acid⁹⁾ were used for this purpose.

We have developed two monoclonal antibodies to the cell surface antigens of chemically-induced transitional cell carcinomas of mouse urinary bladder.¹⁰⁾ The tumor cell line was initiated from primary FANFT (*N*-[4-(5-nitro-2-furyl)-2-thiazolyl]formamide)-induced murine bladder tumors arising in C3H/He mice and established as a stable cell line MBT-2, which is useful as an *in vitro* model for bladder cancer. In the present study we have conjugated these monoclonal antibodies with mitomycin C (MMC) and methotrexate (MTX), which are widely used in cancer chemotherapy, but the utility of which is limited by several side effects including severe bone marrow depression and gastrointestinal damage. Dextran, human serum albumin (HSA) and poly-L-lysine (PLL) were chosen as carrier molecules because of their good biological stability in aqueous solutions, and MMC or MTX molecules were coupled to monoclonal antibodies through the carriers. This paper describes the selective cytotoxicity of these drug-antibody conjugates against murine bladder tumor cells.

Experimental

Target Cells—Three established murine cell lines (MBT-2,¹¹⁾ MCA clone 15¹²⁾ and P388) were used in the present study. MBT-2 and embryonal MCA clone 15 cell lines were grown as monolayers in Eagle's minimum essential medium supplemented with 10% newborn calf serum (NCS) and passaged routinely after detachment with 0.1% trypsin in calcium- and magnesium-free phosphate-buffered saline.

P388 leukemia cells were maintained by weekly transplantation of tumor cells into the peritoneal cavity of female DBA/2 mice. P388 cells were grown in RPMI 1640 medium supplemented with 10% NCS *in vitro*.

Cell Extracts for Binding Assay—Various tissues from C3H/He mice were washed with 0.02 M phosphate-buffered saline (PBS; pH 7.3) and chopped up with scissors. After addition of lysing buffer containing 1 mM NaHCO₃ and 1 mM phenylmethylsulfonylfluoride,¹³⁾ the material was homogenized on ice, followed by centrifugation for 3 min at 500 × *g* at 5 °C. The supernatant fraction was further centrifuged for 20 min at 20000 × *g* and the pellet was sonicated in 0.02 M Tris-HCl buffer (pH 8.0) containing 0.1 M NaCl, 1 mM ethylenediaminetetra acetic acid (EDTA) and 0.5% Nonidet P-40 in a cell disruptor. The lysate was spun for 20 min at 100000 × *g* and the supernatant, which contained solubilized membrane proteins, was stored at -80 °C.¹⁴⁾

Binding Assays—Enzyme-linked immunosorbent assays (ELISA) were carried out for the measurement of antibody activity. Protein from cell extracts in PBS was plated (50 μg per well) on a flat-bottomed microplate with 96 wells (Nunc Co., Denmark) and left at 5 °C overnight. The plate was washed twice with PBS and allowed to stand at 5 °C overnight with 100 μl of PBS containing 1% bovine serum albumin (BSA) to reduce nonspecific binding. Then 50 μl of spent hybridoma medium or control medium was added. The plate was incubated at room temperature for 2 h, after which the medium was aspirated off, and the plate was washed. Subsequently, 100 μl of horseradish peroxidase (HRP)-labeled rabbit anti-mouse immunoglobulin G (IgG; Miles-Yeda Ltd., Israel) in 1% BSA-PBS was added at the dilution of 1:10000. The plate was incubated for another 2 h at room temperature and washed three times. Then 0.1 M citrate buffer (pH 5.5) containing 0.04 M *o*-phenylenediamine and 6 mM H₂O₂ as substrates was added to the attached cell material and the plate was incubated at room temperature for 20 min. After addition of 4 N H₂SO₄ to stop the reaction, optical density was measured at 492 nm by using a Titertek Multiskan (Flow Laboratories Inc., Virg., U.S.A.).

Cultured cells in 100 μl of growth medium (25000 cells/well) were plated in a flat-bottomed sterile tissue culture microplate with 96 wells (Nunc Co.) and incubated overnight to allow the cells to become adherent. After washing with Hank's balanced salt solution (HBSS), the plate was used for the binding assays described above.

Mixed Hemadsorption (MHA) Assay—MHA assays for the detection of antibodies against cell surface antigens were performed by a slight modification of the method of Tachibana *et al.*¹⁵⁾ To prepare indicator cells, sheep red blood cells (SRBC) in PBS were incubated with an equal volume of 1:100 diluted mouse anti-SRBC serum for 1 h at room temperature. The mixture was washed three times with PBS, resuspended in PBS at the original SRBC concentration, and treated with an equal volume of 1:40 diluted rabbit anti-mouse IgG for 2 h at room temperature. The doubly-sensitized SRBC were washed three times with PBS and resuspended in 0.2% BSA-HBSS at the concentration of 0.25%.

Aliquots of 100 μl of target cell suspension were inoculated into wells of a microplate to give 10000 cells/well and

the plate was incubated overnight. After removal of non-adherent cells by washing with 0.2% BSA-HBSS, serially diluted antibody solutions (50 μ l/well) were added and incubated for 2 h at room temperature. After washing of the plate with 0.2% BSA-HBSS, 50 μ l of indicator SRBC suspension (0.25%) was added to each well and incubation was continued for another 2 h at room temperature. Non-adherent SRBC were removed by gentle aspiration, followed by observation under a phase-contrast microscope.

Monoclonal Antibodies—An antibody, designated 1-3C6-9, was obtained from a hybridoma produced by fusing spleen cells from a C3H/He mouse immunized against MBT-2 cell extracts with P3-X63-Ag8-U1 mouse myeloma,¹⁶⁾ and another antibody, designated 7-4B6-2, was obtained by the same method from spleen cells of a hybrid mouse (C3H/He, female \times Balb/c, male) immunized against cultured MBT-2 cells.

Binding of MMC to Monoclonal Antibody—MMC (Kyowa Hakkō Co., Tokyo, Japan) was conjugated with monoclonal antibody through two different carriers, dextran and HSA.

Dextran Conjugate: Dextran T-500, mean molecular weight 510000 (Pharmacia Fine Chemicals, Sweden), was oxidized to polyaldehyde dextran (PAD) with sodium periodate, extensively dialyzed against water, lyophilized and stored at 4°C.¹⁷⁾ The PAD was incubated with MMC at a molar ratio of 1:200 in a minimum volume of 0.1 M phosphate buffer (PB; pH 8.9) with stirring for 30 min at room temperature. Immunoglobulin in 0.1 M PB (pH 8.0) was then added to the reaction mixture at a 2:1 molar ratio to the PAD used and incubation was continued at 5°C for a further 20 h. The conjugate was separated from any free drug by Sephadex G-25 gel filtration.

Albumin Conjugate: HSA was first incubated with a 3-fold molar excess of *N*-succinimidyl-3-(2-pyridyldithio)propionate (SPDP; Pharmacia Fine Chemicals).¹⁸⁾ After incubation at room temperature for 40 min, the reaction mixture was subjected to Sephadex G-25 column chromatography using 0.02 M PB (pH 5.3) as the eluent. Then MMC in 0.1 M PB (pH 6.0) and solid 1-ethyl-3-(3-dimethylaminopropyl)carbodiimide hydrochloride (ECDI; Wako Pure Chemicals, Osaka, Japan) were added to the dithiopyridylated HSA (HSA-DTP) in molar ratios of 80:1:200 (MMC-HSA-ECDI). After incubation at 5°C for 2 d the reaction was terminated by applying the mixture to a Sephadex G-25 column. MMC-HSA-DTP thus synthesized was reduced with dithiothreitol (DTT) at a final concentration of 10 mM for 30 min and applied to a Sephadex G-25 column pre-equilibrated with 0.1 M PB (pH 6.0) containing 5 mM EDTA.

Monoclonal antibody was maleimidated with *N*-succinimidyl-4-(*N*-maleimidomethyl)cyclohexane-1-carboxylate (Zieben Chemicals Co., Tokyo, Japan) as described elsewhere,¹⁹⁾ and added to the reduced MMC-HSA conjugate. The reaction mixture was then concentrated to a small volume using a collodion bag and incubated overnight at 5°C, followed by Ultrogel AcA-34 column chromatography using PBS as the eluent.

Binding of MTX to Monoclonal Antibody—MTX (Fluka AG, Switzerland) was conjugated with monoclonal antibody directly and through two different carriers, HSA and PLL.

Direct Coupling: MTX was activated with *N*-hydroxysuccinimide and dicyclohexylcarbodiimide in dimethylformamide, and added to the antibody solution in 0.02 M PB (pH 8.0). After incubation at 5°C overnight, the conjugate was separated from free drug by Sephadex G-25 gel filtration.

Albumin Conjugate: The active ester of MTX described above was added to HSA-DTP in a molar ratio of 50:1 and incubated at room temperature for 3 h. After centrifugation, the supernatant was subjected to Sephadex G-25 column chromatography, followed by reduction with DTT. The reduced MTX-HSA conjugate was coupled with maleimidated monoclonal antibody and purified by Ultrogel AcA-34 column chromatography, as described above.

PLL Conjugate: PLL, molecular weight 30000—70000 (Sigma Chemical Co., Mo., U.S.A.), was first dithiopyridylated with SPDP and to the resulting PLL-DTP (containing one DTP residue per 120 lysine residues) was added the active ester of MTX in a molar ratio of 1:5 (MTX-lysine residues of PLL). After incubation at room temperature for 3 h, MTX-PLL-DTP conjugate was separated by Sephadex G-25 gel filtration, and then coupled with monoclonal antibody by the same method as used in the preparation of the albumin conjugate.

Cytotoxicity Tests—*In Vitro* Studies: MBT-2 of MCA clone 15 cells in 1 ml of growth medium (2000 cells/well) were plated in a sterile tissue culture plate with 24 flat-bottomed wells (Flow Laboratories Inc.) and incubated overnight to allow the cells to become adherent. The drug or conjugate was filtered through a 0.22 μ m Millex filter (Millipore Corp., Mass., U.S.A.) and various dilutions in 1 ml of growth medium were added to the wells, after which the plate was incubated for 45—100 min at 37°C. After washing of the plate twice with HBSS, 1 ml of fresh medium was added to each well and the plate was cultured at 37°C for 5—6 d. The cell growth was judged by counting the cells with a hemocytometer (TOA Microcell Counter CC-108, Kobe, Japan).

In Vivo Studies: MBT-2 cells that had been treated with conjugate or various controls were tested for their ability to grow after transplantation into mice and the effect of the conjugate was evaluated in terms of the prolongation of survival time in the recipient mice. The pretreatment was carried out by incubating 2.5×10^6 cells with the drug or conjugates (50 μ g as free MMC) and the cells were intraperitoneally injected into C3H/He mice at 2.0×10^5 cells/mouse after washing with PBS.

Results

Specificity and Affinity of Monoclonal Antibody

Binding studies by ELISA performed during the initial screening of hybridomas indicated that antibodies formed by hybridomas 1-3C6-9 and 7-4B6-2 bind preferentially to the surface of MBT-2 cells from transitional cell bladder carcinomas. Both monoclonal antibodies showed little or no reactivity to other tissue extracts including spleen, thymus, liver, lung, kidney, colon, stomach and urinary bladder extracts from normal C3H/He mice.

To further investigate the antibody specificity and affinity, MHA assays were performed. In these assays, antibody 1-3C6-9 showed definite reactivity to MBT-2 cells at the concentration of 0.5–2.0 $\mu\text{g/ml}$, but not to MCA clone 15 or P388 cells. Antibody 7-4B6-2 had a higher affinity for MBT-2 cells than 1-3C6-9, while the former antibody showed slight cross-reactivity to MCA clone 15 cells. The binding activity to MBT-2 cells was not significantly inhibited in the presence of various tissue extracts or even after adsorption with lymphoid and liver cells from normal C3H/He mice.

These two monoclonal antibodies of 1-3C6-9 and 7-4B6-2 were determined to be an IgG_{2a} and an IgM, respectively, by using class- or subclass-specific antisera.

Characterization of Drug–Antibody Conjugates

MMC–Antibody Conjugates—MMC molecules were linked to 1-3C6-9 IgG and 7-4B6-2 IgM monoclonal antibodies through PAD. The degree of substitution by MMC of the dextran was estimated to be one molecule per approximately 50–60 glucose units, and thus 26 and 180 molecules of MMC were indirectly linked to one antibody molecule of 1-3C6-9 and 7-4B6-2, respectively (Table I). The antibody activity of MMC–PAD–antibody conjugates was determined by ELISA using cultured MBT-2 cells as target antigen and the two conjugates showed 14 and 27% of the binding activity of the respective original antibody.

HSA was also used as a linker between MMC and antibody. HSA was first substituted by SPDP and determined to contain 2.1 dithiopyridyl (DTP) residues per molecule of HSA. The HSA–DTP was further substituted with MMC using ECDI and the product showed a molar ratio of 10:1 of MMC to HSA. After reduction with DTT, MMC-substituted HSA was added to maleimidated IgM monoclonal antibody 7-4B6-2 in a 24:1 molar ratio. The pooled conjugate fractions obtained by Ultrogel Aca-34 column chromatography have a probable formula of (MMC₁₀–HSA)₈–(7-4B6-2) with a molar ratio of 78:1 of MMC to antibody, though some free antibody would be present in this preparation. This MMC–HSA–antibody conjugate retained 71% of the reactivity to cultured MBT-2 cells of the original antibody 7-4B6-2 (Table I).

TABLE I. Composition and Antibody Activity of Drug–Monoclonal Antibody (Ab) Conjugates

Conjugates	Molar ratio of drug/Ab	% antibody activity ^{a)}
MMC–PAD–(1-3C6-9)	26	14
MMC–PAD–(7-4B6-2)	180	27
MMC–HSA–(7-4B6-2)	78	71
MTX–(7-4B6-2)	31	15
MTX–HSA–(7-4B6-2)	160	15
MTX–PLL–(7-4B6-2)	180	18

a) The reactivity to MBT-2 cells was expressed as % activity of the original antibody in each case. (1-3C6-9), IgG_{2a}Ab; (7-4B6-2), IgMAB.

MTX-Antibody Conjugates—In the direct conjugation of MTX and antibody 7-4B6-2, approximately 31 drug molecules were linked to an antibody molecule and the antibody activity of the conjugate was 15% of that of the original antibody (Table I).

Dithiopyridylated HSA was coupled with the active ester of MTX and the product with a molar ratio of 29:1 of MTX-HSA was added to maleimidated antibody 7-4B6-2 in a 20:1 molar ratio. The MTX-HSA-antibody conjugate showed an approximate molar ratio of 160:1 of MTX to antibody and retained 15% of the reactivity to cultured MBT-2 cells of the original antibody.

PLL was also dithiopyridylated with SPDP, followed by coupling with the active ester of MTX. The conjugate has a probable empirical formula of $\text{MTX}_{27}\text{-PLL-DTP}_{2,3}$ on the assumption that the molecular weight of PLL used here is 40000. The MTX-PLL conjugate was further coupled to IgM monoclonal antibody 7-4B6-2 with retention of 18% of the antibody activity of the original antibody and the molar ratio of MTX to antibody in the MTX-PLL-(7-4B6-2) conjugate was estimated to be approximately 180.

In Vitro Cytotoxicity

MMC-Antibody Conjugates—MMC-PAD-(1-3C6-9) conjugate was tested for cytotoxic activity against MBT-2 (bladder tumor), MCA clone 15 (embryo) and P388 (leukemia) cell lines. MMC-PAD conjugate without immunoglobulin molecules and MMC-PAD-normal IgG (NIgG) with no reactivity to MBT-2 cells were also prepared and used as controls in the cytotoxicity test. The target cells were incubated at 37 °C for 80 min with MMC or its conjugates, and further cultivated in fresh growth medium for 5 d. In a cytotoxicity test against antibody-reactive target cells (MBT-2), MMC-PAD-(1-3C6-9) conjugate was 3 times more active than free MMC, while nonimmune conjugates including MMC-PAD and MMC-PAD-NIgG were 3 to 5 times less active than free MMC, when the concentrations giving 50% inhibition of cell growth (IC_{50} in Table II) were compared. MMC-PAD-(1-3C6-9) showed significant cytotoxicity at a low dose of 12 ng/ml, and 200–500 ng/ml of nonimmune conjugates was required in order to show a similar level of cytotoxic effect. In a test against antibody-nonreactive cells (MCA clone 15 and P388), MMC-PAD-(1-3C6-9) demonstrated a similar level of cytotoxicity to that of nonimmune conjugates, which was 2–3 times less than that of free MMC in the MCA clone 15 system and almost the same in the P388 system (Table II).

In order to further investigate the selective cytotoxicity of MMC-PAD-(1-3C6-9), antibody-reactive MBT-2 cells were incubated with the conjugate in the presence of free antibody 1-3C6-9 for 60 min. The antibody solution at 5 $\mu\text{g/ml}$ inhibited the cytotoxicity of 56 and 167 ng/ml as free MMC of the immune conjugate by 86 and 29%, respectively. As free monoclonal antibody had little or no effect on cell growth at concentrations of less than 50 $\mu\text{g/ml}$, the decreased cytotoxicity was supposed to result from the inhibitory effect of free

TABLE II. Cytotoxicity of MMC and Its Dextran Conjugates against MBT-2, MCA Clone 15 and P388 Cell Lines

Sample	IC_{50}^a ($\mu\text{g/ml}$ as free MMC)		
	MBT-2	MCA clone 15	P388
MMC	0.48	0.21	0.57
MMC-PAD	2.2	0.50	0.58
MMC-PAD-NIgG	1.5	0.54	0.56
MMC-PAD-MoAb	0.16	0.48	0.51

a) 50% inhibition of cell growth. MoAb, monoclonal antibody 1-3C6-9 against MBT-2 cells.

antibody on the binding of the immune conjugate to MBT-2 cell surface antigens.

HSA conjugate of antibody 7-4B6-2 was also subjected to a cytotoxicity test against MBT-2 and MCA clone 15 cells. MMC-HSA-DTP conjugate, an intermediate in the preparation of MMC-HSA-antibody, was used as a control, as well as free MMC. The target cells were incubated at 37°C for 45 min with test samples and cultivated in fresh growth medium for 6 d (Table III). In a test against MBT-2 cells, MMC-HSA-(7-4B6-2) conjugate showed more than 10 times higher cytotoxicity than nonimmune conjugate MMC-HSA-DTP, although the former conjugate had the same inhibitory effect as the latter conjugate on MCA clone 15 cell growth. Moreover, the cytotoxic effect of the immune conjugate was 10 to 15 times that of free MMC and the covalent coupling of specific antibody to MMC was found to considerably increase its cytotoxicity. This increased cytotoxicity of MMC-HSA-antibody conjugate was diminished in the presence of free antibody, as was that of MMC-PAD-antibody conjugate described above, and these results suggest that the cytotoxicity of the antibody conjugates was dependent upon antibody binding to the target cells.

MTX-Antibody Conjugates—MTX-antibody conjugates were also tested for *in vitro* cytotoxicity against MBT-2 bladder tumor cells. Nonimmune conjugates MTX-HSA-DTP and MTX-PLL-DTP were used as controls. The target cells were exposed to these drug solutions at 37°C for 100 min, washed and cultivated in fresh growth medium for several days. Immune conjugates including MTX-(7-4B6-2) showed about 10 times higher cytotoxicity than free MTX, while nonimmune conjugates were 4 to 10 times less toxic to MBT-2 cells (Table IV). Since unconjugated antibody 7-4B6-2 was not toxic at concentrations which were equivalent to those in the immune conjugates, the immune conjugates showed the increased cytotoxicity through antibody binding to the target cells. These results mean that

TABLE III. Cytotoxicity of MMC and Its Albumin Conjugates against MBT-2 and MCA Clone 15 Cell Lines

Sample	IC ₅₀ ^{a)} (μg/ml as free MMC)	
	MBT-2	MCA clone 15
MMC	3.3	1.1
MMC-HSA-DTP	3.0	0.63
MMC-HSA-MoAb	0.29	0.65

a) Described in Table II.

TABLE IV. Cytotoxicity of Various MTX-Antibody Conjugates against MBT-2 Cell Lines

Sample	IC ₅₀ ^{a)} (μg/ml as free MTX)	Ratio ^{b)}
MTX	0.81	1
MoAb	>20 ^{c)}	<0.04
MTX-MoAb	0.091	8.9
MTX-HSA-DTP	3.3	0.25
MTX-HSA-MoAb	0.073	11
MTX-PLL-DTP	8.5	0.095
MTX-PLL-MoAb	0.080	10

a) Described in Table II. b) IC₅₀ of each sample was divided by that of free MTX. c) Expressed as antibody amount (μg/ml).

TABLE V. The Effect of Previous Treatment^{a)} of MBT-2 Cells with MMC-Antibody Conjugates on Tumor Growth *in Vivo*

Sample	Life span (d)		Survivors at 40 d
	Median value	Mean \pm S.D.	
Control (saline)	21	21.0 \pm 2.9	0/7
MoAb (7-4B6-2)	22	22.4 \pm 3.4	0/7
MMC	30	31.9 \pm 7.8 ^{b)}	1/7
MMC-PAD	24	24.1 \pm 6.3	0/7
MMC-PAD-NIlgG	31	33.4 \pm 6.3 ^{b)}	1/7
MMC-PAD-MoAb	>40	>40 ^{b)}	4/7
MMC-HSA-DTP	23	23.1 \pm 4.3	0/7
MMC-HSA-MoAb	38	>40 ^{b)}	3/7

a) MBT-2 cells were treated at room temperature for 60 min *in vitro* with various conjugates and injected intraperitoneally into C3H/He mice. Each group consisted of 7 mice. b) Significantly different from the control ($p < 0.01$).

immune conjugates were 40 to 100 times more active than nonimmune conjugates as targeting drugs.

In Vivo Cytotoxicity

Immune conjugates including MMC-PAD-(7-4B6-2) and MMC-HSA-(7-4B6-2) were tested for effect on tumor cell growth *in vivo*. MBT-2 cells were treated with the conjugates at room temperature for 60 min, and then the cells were transplanted intraperitoneally into syngeneic C3H/He mice. Life span and survival of mice receiving 2×10^5 cells are shown in Table V. The median survival times of control mice and the mice receiving cells treated with antibody alone were 21 and 22 d, respectively. In the group of mice receiving cells treated with free MMC a 1.5-fold prolongation of life span was observed, but there was little prolongation in the group of mice receiving cells treated with MMC-PAD and MMC-HSA-DTP conjugates. The nonimmune conjugate MMC-PAD-NIlgG showed some cytotoxic effect, but the highest survival rate was observed in the groups of mice receiving cells treated with the immune conjugates MMC-PAD-(7-4B6-2) and MMC-HSA-(7-4B6-2). These two groups showed median survival times of >40 and 38 d, respectively. Four and three out of 7 mice receiving cells treated with MMC-PAD-(7-4B6-2) and MMC-HSA-(7-4B6-2) survived even at 40 d after inoculation, respectively, and these results suggest that the cells treated with the immune conjugates had only a slight tumorigenic capacity.

Discussion

Hellström *et al.*¹³⁾ established two hybridomas secreting antibodies to antigens that are more strongly expressed in mouse transitional-cell bladder carcinomas than in other mouse tumors or normal tissues. We have also cloned two hybridomas, 1-3C6-9 and 7-4B6-2, secreting antibodies which preferably bind to a stable cell line of mouse bladder tumor. Although the monoclonal antibodies were not strictly specific for bladder carcinoma, since binding to cells from some control tissues or to embryonal cells was detected, they were employed to assess the therapeutic applicability of drug coupling with monoclonal antibody directed against tumor cell surface antigens.

Several kinds of drug-antibody conjugates were prepared with or without using dextran, albumin and polylysine as carriers in the present study. In the direct coupling of MTX and IgM antibody 7-4B6-2 without carriers, the extent of substitution was 31 mol of drug per mol

of antibody and the MTX-(7-4B6-2) conjugate showed selective cytotoxicity against MBT-2 cells while retaining 15% of the antibody activity of unconjugated antibody. Another preparation of MTX-(7-4B6-2) conjugate with a molar ratio of 45:1 of MTX to antibody showed less than 1% of the reactivity to MBT-2 cells of unconjugated antibody, and demonstrated little targeting effect, although the data are not shown here. In the direct conjugation, a high molar ratio of drug to antibody resulted in significant loss of antibody-binding activity. On the other hand, conventional chemotherapeutic drugs such as MMC, MTX or daunomycin, are less toxic than biological toxins and therefore a high molar ratio of drug to antibody is desirable from this viewpoint. Tsukada *et al.*⁷⁾ and Pimm *et al.*^{4a)} reported that 20–50 molecules of daunomycin or adriamycin could be coupled to one IgG antibody molecule through a dextran bridge. Conjugation of MMC to IgG and IgM antibodies here was effected through a dextran bridge to give molar ratios of 26 and 180, respectively, resulting in sufficiently cytotoxic conjugates (Table I). The Schiff base linkages formed between MMC or antibody and dextran were not reduced with sodium borohydride since the reduction caused significant loss of antibody activity, although Tsukada *et al.*,⁷⁾ Pimm *et al.*,^{4a)} and Levi-Schaffer *et al.*²⁰⁾ adopted a reduction procedure. Even so, chemical coupling of antibody to dextran caused 70–80% reduction in its antibody activity toward MBT-2 cells. The release of MMC from the dextran conjugates thus formed was less than 10% of the original content in the conjugates during incubation in PBS at 37 °C for 80 min. The released MMC probably made only a slight contribution to the cytotoxic activity of the conjugates. HSA and PLL were also used as carriers since the conjugates can be synthesized more controllably, giving defined products, as indicated by Garnet *et al.*^{4b)} and Ryser and Shen,²¹⁾ respectively. In the preparation of MMC-HSA-antibody conjugate, MMC was coupled with monoclonal antibody through an albumin molecule with a good retention of antibody activity, although the substitution of HSA by MMC was smaller than that in the dextran conjugates (Table I). The smaller MMC substitution in the MMC-HSA-antibody conjugates obtained here was probably due to the use of only a 2.5-fold excess of ECDI when MMC was coupled to HSA-DTP molecules. Kojima *et al.*²²⁾ coupled MMC molecules effectively to the carboxyl group of ϵ -aminocaproic acid which was introduced onto dextran as a spacer. They introduced one molecule of MMC per approximately 14–17 glucose units by using a 35-fold molar excess of ECDI. In the preparation of MTX-HSA and MTX-PLL conjugates, the active ester method resulted in high substitution of HSA and PLL by MTX. More than 25 MTX molecules were introduced into one carrier molecule under mild conditions.

The degree of maleimidation of an antibody molecule had a marked effect on the composition of the drug-carrier-antibody conjugate. Highly maleimidated IgM antibody 7-4B6-2 which had 30–50 maleimide residues per mol of antibody gave an insoluble polymerized conjugate. In particular, considerable precipitation was observed during the coupling procedure of MTX-PLL conjugate and maleimidated antibody. It was probably accelerated by the fact that the antibody used here was an IgM. In the present study, therefore, we introduced only 13 maleimide residues into one antibody molecule and coupled the maleimidated antibody with drug-substituted carrier molecules. Such small substitution with maleimide residues probably means that some free antibody remains in the drug-carrier-antibody preparations, and this might lower the targeting effect. Further study is planned on the conjugation procedures between drug and antibody.

In cytotoxicity tests, we adopted 45–100 min exposure of target cells to drug or conjugate. Overnight or one-day incubation with drug or conjugate obscured the selective cytotoxicity of antibody-targeted drugs, and the immune conjugates showed a level of cytotoxicity similar to that of nonimmune conjugates. On short exposure, antibody-targeted drugs were more cytotoxic than free drugs to antibody-reactive MBT-2 cells, while they had almost the same activity on antibody-nonreactive MCA clone 15 or P388 cells as free drugs

and nonimmune conjugates.

The cytotoxic action of immune conjugates on MBT-2 cells was significantly diminished by the coexistence of free antibody. At the two levels of 56 and 167 ng as free MMC, MMC-PAD-(1-3C6-9) conjugate showed 28 and 34% cell growth inhibition, but the addition of 5 μ g of monoclonal antibody 1-3C6-9 diminished the degree of cell growth inhibition to 4 and 24%, respectively. Fifty-six and 167 ng of the conjugate as free MMC contained approximately 1 and 3 μ g of antibody, respectively, and so 5 μ g of free antibody strongly competed with the two levels of the immune conjugate for binding to MBT-2 cell surface antigens. These results suggest that the higher toxicity of the immune conjugate against MBT-2 cells depends upon the specificity of the antibody used for the preparation of the conjugate. MMC-HSA-(7-4B6-2) conjugate also showed selective cytotoxicity against MBT-2 bladder tumor cells and its action was diminished in the presence of free antibody 7-4B6-2. Covalent coupling of MMC to HSA had little effect on its cytotoxic action against MBT-2 cells, but further antibody attachment resulted in about 10-fold increased activity over free MMC (Table II).

The growth of the tumor cells subsequent to *in vitro* treatment with the immune conjugates was prevented in more than 50% of the recipient mice. The treatment with the nonimmune conjugates including MMC-PAD and MMC-HSA-DTP had little effect on prolongation of the life span of the recipient mice and all the mice used died within 40 d after inoculation. About half of the mice receiving cells treated with the immune conjugates, however, survived even at 40 d after inoculation. Thus the selective cell-killing effect was also confirmed by interference with the transplant capability of tumor cells.

Akaza *et al.*²³⁾ reported a lectin-targeted bleomycin conjugate which was effective as an intravesical chemotherapeutic agent for murine bladder tumor. Here, we have developed antibody-targeted drug conjugates using MMC and MTX, and examined them as potential chemotherapeutic agents against murine bladder tumor. The results indicated that the immune conjugates could be useful as selective chemotherapeutic agents against bladder tumor and may be suitable for intravesical treatment.

Acknowledgement We are grateful to Prof. M. S. Soloway of the University of Tennessee for his kind gift of MBT-2 cells. We also thank Drs. M. Fujino and I. Imada for their encouragement and support during the course of this study.

References

- 1) P. Ehrlich, "The Collected Works of Paul Ehrlich," Pergamon Press, New York, 1956, pp. 442-447.
- 2) G. Köhler and C. Milstein, *Nature* (London), **256**, 495 (1975).
- 3) H. Koprowski, Z. Steplewski, K. Michell, M. Herlyn, D. Herlyn, and P. Fuhrer, *Somat. Cell Genet.*, **5**, 957 (1979).
- 4) a) M. V. Pimm, J. A. Jones, M. R. Price, J. G. Middle, M. J. Embleton, and R. W. Baldwin, *Cancer Immunol. Immunother.*, **12**, 125 (1982); b) M. C. Garnett, M. J. Embleton, E. Jacobs, and R. W. Baldwin, *Int. J. Cancer*, **31**, 661 (1983); c) K. Imai, T. Nakanishi, T. Noguchi, A. Yachi, and S. Ferrone, *Cancer Immunol. Immunother.*, **15**, 206 (1983); d) G. Jung, W. Köhnlein, and G. Lüders, *Biochem. Biophys. Res. Commun.*, **101**, 599 (1981).
- 5) a) E. S. Vitetta, K. A. Krolick, M. M. Inaba, W. Cushley, and J. W. Uhr, *Science*, **219**, 644 (1983); b) M. I. Bernhard, K. A. Foon, T. N. Oeltmann, M. E. Key, K. M. Hwang, G. C. Clarke, W. L. Christensen, L. C. Hoyer, M. G. Hanna, Jr., and R. K. Oldham, *Cancer Res.*, **43**, 4420 (1983); c) K. Kishida, Y. Masuho, M. Saito, T. Hara, and H. Fujii, *Cancer Immunol. Immunother.*, **16**, 93 (1983).
- 6) a) E. Hurwitz, R. Lezy, R. Maron, M. Wilchek, R. Arnon, and M. Sela, *Cancer Res.*, **35**, 1175 (1975); b) T. Ghose and A. H. Blain, *J. Natl. Cancer Inst.*, **55**, 1353 (1975); c) G. F. Rowland, C. A. Axton, R. W. Baldwin, J. P. Brown, J. R. F. Corvalan, M. J. Embleton, V. A. Gore, I. Hellström, K. E. Hellström, E. Jacobs, C. H. Marsden, M. V. Pimm, R. G. Simmonds, and W. Smith, *Cancer Immunol. Immunother.*, **19**, 1 (1985).
- 7) Y. Tsukada, W. K-D. Bischof, N. Hibi, H. Hirai, E. Hurwitz, and M. Sela, *Proc. Natl. Acad. Sci. U.S.A.*, **79**, 621 (1982).
- 8) N. Umemoto, Y. Kato, K. Hara, K. Seto, and T. Takahashi, *Proc. Jpn. Cancer Assoc.*, **42**, 159 (1983).
- 9) Y. Tsukada, Y. Kato, N. Umemoto, K. Hara, and H. Hirai, *Proc. Jpn. Cancer Assoc.*, **42**, 159 (1983).

- 10) M. S. Soloway and S. Masters, *Proc. Amer. Assoc. Cancer Res.*, **20**, 256 (1979).
- 11) M. S. Soloway, *Cancer Res.*, **37**, 2918 (1977).
- 12) C. A. Reznikoff, D. W. Brankow, and C. Heidelberger, *Cancer Res.*, **33**, 3231 (1973).
- 13) I. Hellström, N. Rollins, S. Settle, P. Chapman, W. H. Chapman, and K. E. Hellström, *Int. J. Cancer*, **29**, 175 (1982).
- 14) J. P. Brown, R. G. Woodbury, C. E. Hart, I. Hellström, and K. E. Hellström, *Proc. Natl. Acad. Sci. U.S.A.*, **78**, 539 (1981).
- 15) T. Tachibana, P. Worst, and E. Klein, *Immunology*, **19**, 809 (1970).
- 16) M. L. Gefter, D. H. Margulies, and M. D. Scharff, *Somat. Cell Genet.*, **3**, 231 (1977).
- 17) R. L. Foster, *Experientia*, **31**, 773 (1975).
- 18) J. Carlsson, H. Drevin, and R. Axén, *Biochem. J.*, **173**, 723 (1978).
- 19) E. Ishikawa, M. Imagawa, S. Hashida, S. Yoshitake, Y. Hamaguchi, and T. Ueno, *J. Immunoassay*, **4**, 209 (1983).
- 20) F. Levi-Schaffer, A. Bernstein, A. Meshorer, and R. Arnon, *Cancer Treat. Rep.*, **66**, 107 (1982).
- 21) H. J. P. Ryser and W. C. Shen, *Proc. Natl. Acad. Sci. U.S.A.*, **75**, 3867 (1978).
- 22) T. Kojima, M. Hashida, S. Muranishi, and H. Sezaki, *J. Pharm. Pharmacol.*, **32**, 30 (1980).
- 23) H. Akaza, K. Koseki, K. Kobayashi, T. Nijima, M. S. Soloway, M. Iwabuchi, and Y. Muraoka, *J. Jpn. Urolog. Soc.*, **75**, 211 (1984).

[Chem. Pharm. Bull.]
[35(3)1138—1143(1987)]

Correlation between Tumor Cell Cytotoxicity and Serine Protease Activity of Peritoneal Macrophages from Mice Treated with Bakers' Yeast Mannans

YOSHIO OKAWA, YUTAKA OZEKI, KO SUZUKI, KAZUHIKO SAKAI,
SHIGEO SUZUKI and MASUKO SUZUKI*

Tohoku College of Pharmacy, Komatsushima 4-4-1,
Sendai, Miyagi 983, Japan

(Received July 4, 1986)

Peritoneal exudate cells (PEC) from C3H/He mice given bakers' yeast mannans, WNM and WAM025, showed marked cytolytic activity against MM46 tumor cells *in vitro*. Because the cytotoxicity of the PEC was strongly inhibited by actinomycin D, it was assumed that the cytolytic factor was a proteinous material(s). Of the macrophages and polymorphonuclear leucocytes (PMN) separated from the PEC, only the former cells were found to display cytolytic activity. Quinacrine, a phospholipase A₂ inhibitor, and sodium azide, a myeloperoxidase inhibitor, did not reduce the cytotoxicity of macrophages from mice treated with acidic mannan (WAM025). In contrast, diisopropylfluorophosphate, a serine protease inhibitor, inhibited the cytolysis of the MM46 target cells by WAM025-treated macrophages. Chymostatin, a chymotrypsin inhibitor, and elastatinal, an elastase inhibitor, also inhibited the cytolytic effect. It is therefore concluded that serine proteases secreted into the medium from the macrophages activated by mannans participated in the cytolytic destruction of neoplastic cells.

Keywords—mannan; cytotoxicity; macrophage; serine protease; tumoricidal effect

Macrophage activation for nonspecific tumoricidal activity against target tumor cells can be induced by various immunopotentiators. In our previous reports, it was found that mannan of bakers' yeast was able to enhance the immunological response of mice to transplanted tumor cells and to lethal infection with pathogenic microbes.¹⁻⁴⁾ In order to identify the competent cells in acidic mannan (WAM025)-treated peritoneal exudate cells (PEC), we carried out an *in vitro* cytolysis assay by macrophages and polymorphonuclear leucocytes (PMN) separated from the PEC by the Percoll gradient centrifugation technique.⁵⁾ The results indicated that WAM025-treated macrophages were able to display a marked cytolytic effect, while PMN from the same source did not show the effect. Because the chemical entity involved in the cytolysis of tumor cells by WAM025-treated macrophages remained to be identified, we attempted to characterize the cytolytic factor elicited in mouse macrophages by the administration of the yeast mannans.

The relevancy of serine protease release to tumoricidal activity of macrophages has been reported in mice treated with BCG^{6,7)} and *Nocardia rubra* cell-wall skeleton.⁸⁾ However, the real cytolytic factors of antitumor polysaccharide-treated macrophages have not been elucidated to date, although many reports have been published on identifying various lytic factors produced by cytolytically activated macrophages such as oxygen intermediates,^{9,10)} lysosomal enzymes,^{11,12)} proteases,^{6,7)} complement component C3,¹³⁾ tumor necrotic factor,¹⁴⁾ prostaglandins,¹⁵⁾ and myeloperoxidase.¹⁶⁾ Therefore, the present study was designed to investigate the possible role of serine proteases in the cytolysis of target tumor cells by antitumor mannan-induced macrophages.

Materials and Methods

Mice—Male 6- to 8-week-old C3H/HeSlc mice were obtained from the Shizuoka Cooperative for Experimental Animals, Shizuoka, Japan.

Mannans—The preparation of mannan was conducted in accordance with our previous descriptions.^{1,17)} Briefly, the bulk mannan of bakers' yeast (a wild type strain of *Saccharomyces cerevisiae*) obtained by extraction of the parent cells with hot water followed by fractional precipitation with Fehling's solution was fractionated by diethylaminoethyl (DEAE)-Sephadex column chromatography. The mannan subfractions eluted with water and 0.25 M NaCl were designated as WNM and WAM025, respectively. Lentinan was purchased from Ajinomoto Co., Inc, Tokyo.

Treatment of Mice—Mice were injected intraperitoneally (i.p.) with mannans (WNM and WAM025) at 150 mg/kg/d, for 5 d. Lentinan (50 mg/kg/d) was injected i.p. into mice for 5 d. Assays were performed at 6 d after the first polysaccharide administration.

Preparation of Peritoneal Phagocytes—PEC from mice injected i.p. with the polysaccharides were collected by washing the peritoneal cavity of mice with Hanks' balanced salt solution (Hanks' BSS, pH 7.2). For the experiment on individual types of phagocytes, macrophages and PMN in PEC were separated by Percoll-gradient centrifugation according to the description in the previous paper.⁵⁾ The homogeneity of macrophages and PMN was found to be more than 98% by May-Giemsa staining.

Assay of Cytolysis—Cytolytic activity was examined as described previously⁵⁾ in accordance with the report by Hashimoto and Sudo.¹⁸⁾ Namely, a solution of ³H-uridine in 10 μ l of physiological saline was added to a cell suspension containing 1×10^7 MM46 tumor cells and the radioactivity was adjusted by the addition of physiological saline to 1 μ Ci/ml. After incubation for 24 h, the cells were sedimented by centrifugation at $250 \times g$ for 10 min, and then washed 3 times with RPMI 1640 medium containing 10% FBS (10% FBS-RPMI 1640 medium). The macrophages and PMN, each $1-2 \times 10^6$ cells, were mixed with the target cells (1×10^4) in round-bottomed wells (7-mm diameter) of a microplate (NUNC, Roskilde, Denmark). The mixture was incubated in 0.2 ml of 10% FBS-RPMI 1640 medium at 37 °C for 24 h in the presence of 5% CO₂. The cells were harvested on glass filter papers, and counted by means of a Beckman LS-7800 liquid scintillation counter. The extent of target cell cytolysis was calculated from the following equation:

$$\text{cytolysis (\%)} = 100 \times (A - B) / A$$

where A is (tumor cell only(cpm) - background(cpm)) and B is (test sample-treated tumor cell(cpm) - background(cpm)). Inhibition of target cell cytolysis was calculated from the following equation:

$$\text{inhibition (\%)} = 100 \times (A - B) / A$$

where A is cytolysis in the absence of inhibitor (%) and B is cytolysis in the presence of inhibitor (%).

Quantification of Neutral Proteases—Macrophages (3×10^5 cells/well) separated by Percoll-gradient centrifugation of PEC obtained after polysaccharide administration were incubated at 37 °C for 24 h in 10% FBS-RPMI 1640 medium in flat-bottomed wells of a microplate (NUNC, Roskilde, Denmark), in the presence or absence of diisopropylfluorophosphate (DFP) (0.2-2 mM). After centrifugation, the neutral protease activity of the supernatant was assayed by measuring the release of trichloroacetic acid (TCA)-soluble peptides from casein according to the reported method¹⁹⁾ with a slight modification as follows. Each incubation mixture contained 200 μ l of 2% substrate solution, 100 μ l of 0.5 M phosphate buffer, pH 7.2, and 80-90 μ l of the enzyme solution. After incubation at 37 °C for 1 or 2 h, 4 ml of 5% (w/v) TCA was added. The preparations were removed by filtration through Toyo No. 3 filter paper and the absorbance at 275 nm of the filtrate was read. One unit of the enzyme was expressed as the activity causing an increase in absorbance of 0.01 per min.

Inhibitors—Actinomycin D, quinacrine and sodium azide were purchased from Nakarai Chemicals, Ltd, Kyoto. DFP was purchased from Sigma Chemical Co., St. Louis, Mo., U.S.A. The inhibitor solutions were prepared by dissolving the chemicals in RPMI 1640 medium daily. Chymostatin and elastatinal were obtained from the Protein Research Foundation, Minoh, Osaka; stock solutions (10 mg/ml) in dimethyl sulfoxide, were prepared.

Results and Discussion

The cytolytic activities of PEC obtained from WNM- and WAM025-treated mice were assayed against MM46 tumor cells, in the presence or absence of actinomycin D. Table I shows that the PEC from mice treated with either mannan displayed a marked cytolytic effect. It has been reported by Ito *et al.*⁸⁾ that actinomycin D inhibited the ability of *Nocardia rubra* cell wall skeleton (N-CWS)-induced macrophages to cytolize target tumor cells, indicating

TABLE I. Effect of Actinomycin D on Cytotoxicity to MM46 Tumor Cells of PEC from Mice Given Mannans

PEC treated with ^{a)}	Concentration of actinomycin D ($\mu\text{g/ml}$)	Average cytolysis ^{b)} (%)	Inhibition (%)
Untreated		3	
WNM	0	25	—
WNM	1	10	60
WAM025	0	23	—
WAM025	1	5	78

a) PEC were harvested from mice injected i.p. with polysaccharide as described under Materials and Methods. Cytolysis was performed at 37°C for 24 h in 5% CO₂. b) Ratio of the number of effector cells to that of tumor cells was 100:1 in the presence or absence of actinomycin D (0.1 and 1.0 $\mu\text{g/ml}$).

TABLE II. Cytolysis of MM46 Tumor Cells by Macrophages and Polymorphonuclear Leucocytes from Mice Given WAM025 and Lentinan

Cells treated with ^{a)}	Average cytolysis ^{b)} (%)	
	Macrophages	PMN
Untreated	0	—
WAM25	20	0
Lentinan	26	0

a) PEC were obtained from mice injected i.p. with polysaccharide, and were separated into macrophages and PMN by Percoll-gradient centrifugation. Cytolysis was performed at 37°C for 24 h in 5% CO₂. b) Ratio of the number of effector cells to that of tumor cells was 100:1.

that protein synthesis may be required for the cytotoxicity exhibited by N-CWS-induced macrophages. Actinomycin D at 0.1 and 1 $\mu\text{g/ml}$ significantly inhibited cytolysis by all treated PEC, the inhibition being 78%. It was therefore assumed that some proteinous substance(s) produced by the macrophages might be responsible for cytotoxicity of PEC from mice treated with both mannans.

The cytolytic activities of macrophages and PMN obtained from PEC of WAM025- and lentinan-treated mice were assayed against MM46 tumor cells (Table II). The number of PMN from PEC of WNM-treated mice was almost the same as that of the control group. Therefore, this polysaccharide was not used in this experiment. It was clear that macrophages from the nontreated mice and PMN from the WAM025- and lentinan-treated mice were unable to exhibit cytolytic activity against the tumor cells, while the macrophages from treated mice showed a marked cytolytic effect.

As proteinous factors produced by activated macrophages, phospholipase A₂, via the production of prostaglandins D₂ and E₂ (possessing antitumor activity),¹⁵⁾ and myeloperoxidase (mediating cell killing as the active component of H₂O₂-myeloperoxidase-chloride system)¹⁶⁾ have the ability to destroy tumor cells. To determine the possible role of WAM025-induced phospholipase A₂ and/or myeloperoxidase, peritoneal macrophages were assayed with ³H-uridine-labeled MM46 tumor cells in the presence of quinacrine²⁰⁾ or sodium azide,²¹⁾ at doses which did not show detectable cytotoxicity of the effector cells. These substances did not exhibit any inhibitory effect on the cytolytic activity of WAM025-induced macrophages, as shown in Table III. Thus, it was unlikely that phospholipase A₂ and myeloperoxidase of the macrophages were responsible for the cytolysis. It also seems likely that active oxygens are not responsible for the cytolytic effect, because PMN did not show the effect.⁵⁾ Adams *et al.*^{6,7)} demonstrated that cytolytically activated macrophages secreted a potent, tumor specific lytic substance (CF) whose activity was principally due to a neutral serine protease and was reduced by inhibitors of neutral proteases. Interestingly, they²²⁾ also reported that the direct binding of BCG-activated macrophages to target tumor cells triggered secretion of CF. The effect of DFP, an inhibitor of serine protease, on the cytolytic activity of WAM025-induced macrophages was examined. DFP at 2 mM significantly inhibited the cytolysis of WAM025-induced macrophages (67% inhibition). To test the possibility that DFP is toxic to the macrophages, macrophages from WAM025-administered mice were cultured with or without DFP at 2 mM for up to 48 h. However, the viability (tested by trypan blue exclusion) and morphology showed no significant alterations. In order to determine whether serine proteases

TABLE III. Effect of Several Enzyme Inhibitors on Cytotoxicity to MM46 Tumor Cells of Macrophages from Mice Given WAM025

Macrophages treated with ^{a)}	Inhibitor	Concentration	Cytolysis ^{b,c)} (%)	Inhibition (%)
WAM025			20 ± 0.5	—
WAM025	DFP	0.2 mM	21 ± 0.4	5
WAM025	DFP	2 mM	7 ± 0.06	67
WAM025	Chymostatin	2 µg/ml	20 ± 1.1	0
WAM025	Chymostatin	20 µg/ml	16 ± 0.5	20
WAM025	Chymostatin	200 µg/ml	10 ± 0.04	50
WAM025	Elastatinal	2 µg/ml	21 ± 1.7	5
WAM025	Elastatinal	20 µg/ml	12 ± 0.1	40
WAM025	Elastatinal	200 µg/ml	4 ± 0.2	80
WAM025	Quinacrine	1 µM	21 ± 0.7	5
WAM025	Quinacrine	10 µM	35 ± 3.6	-75
WAM025	Sodium azide	1 mM	20 ± 0.02	0
WAM025	Sodium azide	10 mM	20 ± 0.7	0

a) Mice were given i.p. injection of WAM025 (150 mg/kg/d) on days 0–4. Macrophages were separated by Percoll-gradient centrifugation of PEC from mice on day 5, and were incubated at 37 °C for 24 h in 5% CO₂. b) Ratio of the number of effector cells to that of tumor cells was 100:1, in the presence or absence of several inhibitors. c) Mean ± S.D. of 3 experiments.

TABLE IV. Effect of DFP on the Cytotoxicity to MM46 Tumor Cells of Culture Supernatant of Macrophages from Mice Given WAM025

Culture supernatants of macrophages treated with ^{a)}	Concentration of DFP (mM)	Cytolysis ^{b,c)} (%)	Inhibition (%)
WAM025	0	28 ± 3	—
WAM025	0.2	6 ± 0.2	79
WAM025	2	0.6 ± 0.05	98

a) Mice were given i.p. injection of WAM025 (150 mg/kg/d) on days 0–4. Macrophages (5×10^5 cells/well) were separated by Percoll-gradient centrifugation of PEC from mice on day 5, and were incubated at 37 °C for 24 h in 5% CO₂, with/without DFP. The supernatants were obtained by centrifugation. b) The supernatants (each 80 µl) were mixed with the target cells (1×10^4) in wells. The mixture was incubated at 37 °C for 24 h in 5% CO₂. c) Mean ± S.D. of 3 experiments.

were involved in this activity, we examined the effect of chymostatin, an inhibitor of chymotrypsin, and elastatinal, an inhibitor of elastase, on the cytolytic activity of the polysaccharides-treated macrophages. Treatment of the macrophages with chymostatin and elastatinal, 200 µg/ml, caused inhibition of 50 and 80%, respectively, of the cytolytic activity.

To examine the role of serine proteases in the supernatant of the macrophages on the cytolytic effect against the same tumor cells, the macrophages were incubated with DFP in a similar manner to that described in Table III. As shown in Table IV, DFP at 0.2 and 2 mM inhibited the cytolytic activity of the culture supernatants, (79 and 98% inhibition, respectively). The cytotoxicity of the culture supernatant obtained by incubation with macrophages and DFP (Table IV) was lower than that in the case of direct incubation with macrophages in the presence of DFP (Table III). This might be due to some decrease of serine protease activity during prolonged incubation with DFP under the conditions in Table IV.

To examine the production of proteases in the medium, mice were given i.p. injection of WNM and WAM025 on days 0–4. Macrophages (3×10^5 cells/well) were separated by

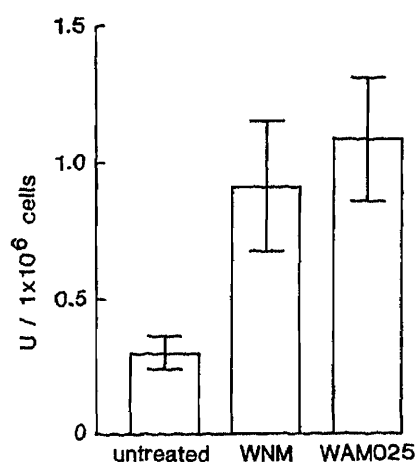


Fig. 1. Neutral Protease Activity of Culture Supernatants of Macrophages in Mice Given Mannans

PEC were obtained from mice injected i.p. with mannans as described under Materials and Methods. Macrophages (3×10^5 cells/well) separated by Percoll-gradient centrifugation of PEC were incubated at 37°C for 24 h in 5% CO_2 . After centrifugation, the neutral protease activity in the supernatant was measured.

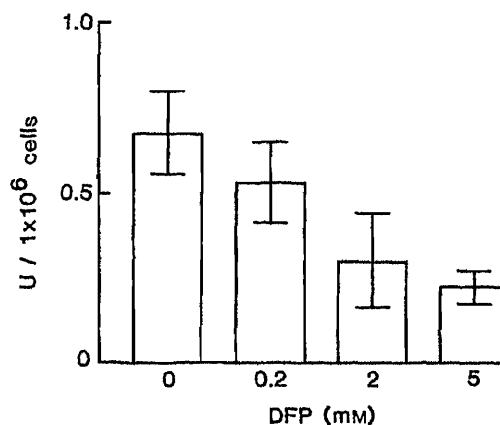


Fig. 2. Effect of DFP on Neutral Protease Activity of Culture Supernatants of Macrophages in Mice Given WAM025

PEC were obtained from mice injected i.p. with WAM025 (150 mg/kg/d) on days 0–4. Macrophages (3×10^5 cells/well) separated by Percoll-gradient centrifugation of PEC in mice on day 5 were incubated at 37°C for 24 h in 5% CO_2 , in the presence of DFP. After centrifugation, the neutral protease activity of the supernatant was measured.

Percoll-gradient centrifugation of PEC from the mice on day 5, and were incubated at 37°C for 24 h in 5% CO_2 . After centrifugation, the neutral protease activities in the supernatant were measured. As shown in Fig. 1, the neutral protease activities from macrophages treated with WNM and WAM025 were increased about 3.0 and 3.5 times as compared with untreated macrophages. This finding indicates that these polysaccharides can enhance the release of neutral protease activity from mouse macrophages. The above observations also indicate the importance of the role of secreted serine proteases in the cytotoxicity. To examine this role, the inhibitory effect of DFP on the protease activity was assayed after 24 h cultivation of WAM025 treated macrophages. The protease activity of the culture supernatant was measured (Fig. 2). DFP (2–5 mM) significantly inhibited the serine protease activity of the supernatant (about 80% inhibition).

Chymotrypsin and elastase are well known as typical serine proteases. It appears that the cytotoxicity is mediated by these serine proteases secreted into the medium by macrophages from mice treated with antitumor polysaccharides.

Recently, a linear β -1,3-glucan from *Alcaligenes faecalis*, TAK, was reported to induce tumoricidal activity of PMN^{23,24} by releasing hydrogen peroxide, but this did not seem to be the case in the present experiments (Table II). Recently, Schmidt *et al.*²⁵ found that the lysis of target tumor cells by NK cells was closely related to the exocytosis of ³⁵S-labeled proteoglycan from the NK cells. Thus, it is conceivable that many cells in addition to macrophages have various cytolytic activities on target tumor cells by releasing cytolytic substances.

Because WAM025 contains protein, *N*-acetylglucosamine, and phosphorus, comprising phosphomannan–protein complex(es),¹⁷ whereas WNM consists of a simple polysaccharide with a very small amount of protein,¹ the mannan moiety alone may play some important role in evoking the tumoricidal effect, including the induction of serine protease activities, in macrophages from mice treated with both mannans, WNM and WAM025. In other words, the production of serine proteases by the macrophages seems to be one of the key processes in

the antitumor effect of yeast mannans. The mechanism of serine protease production might be similar to those in macrophages treated with BCG^{6,7)} and N-CWS.⁸⁾ Kitagawa *et al.*²⁶⁾ reported that enzymatically active membrane-bound serine proteases were essential for human PMN and macrophages to initiate and maintain O₂⁻ production in response to stimuli. Our previous paper⁵⁾ and the present data showed that superoxide release from the PMN was clearly, higher than that from the macrophages, but the PMN did not show any tumoricidal activity. Thus, it is suggested that serine protease-producing activity of macrophages is not always related to the active oxygen releasing activity of the same cells.

References

- 1) S. Suzuki, M. Suzuki, H. Hatsukaiwa, H. Sunayama, T. Suzuki, M. Uchiyama, F. Fukuoka, M. Nakanishi and S. Akiya, *Gann*, **60**, 273 (1969).
- 2) Y. Okawa, Y. Okura, K. Hashimoto, T. Matsumoto, S. Suzuki and M. Suzuki, *Carbohydr. Res.*, **108**, 328 (1982).
- 3) K. Hashimoto, Y. Okawa, K. Suzuki, Y. Okura, S. Suzuki and M. Suzuki, *J. Pharmacobio-Dyn.*, **6**, 668 (1983).
- 4) Y. Okawa, Y. Okura, K. Hashimoto, K. Suzuki, S. Suzuki and M. Suzuki, *J. Pharmacobio-Dyn.*, **8**, 942 (1985).
- 5) K. Sakai, S. Suzuki and M. Suzuki, *J. Pharmacobio-Dyn.*, **7**, 943 (1984).
- 6) D. O. Adams, *J. Immunol.*, **124**, 286 (1980).
- 7) D. O. Adams, K. J. Kao, R. Farb and S. V. Pizzo, *J. Immunol.*, **124**, 293 (1980).
- 8) M. Ito, H. Suzuki, N. Nakano, N. Yamashita, E. Sugiyama, M. Maruyama, K. Hoshino and S. Yano, *Gann*, **74**, 128 (1983).
- 9) C. F. Nathan, S. C. Silverstein, L. H. Brukner and Z. A. Cohn, *J. Exp. Med.*, **149**, 100 (1979).
- 10) P. Mavrier and T. S. Edgington, *J. Immunol.*, **132**, 1980 (1984).
- 11) J. B. Hibbs, Jr., *Science*, **184**, 468 (1974).
- 12) C. Bucana, L. C. Hoyer, B. Hobbs, S. Breesman, M. McDaniel and M. G. Hanna, Jr., *Cancer Res.*, **36**, 4444 (1976).
- 13) J. Hamuro, U. Hadding and D. Britter-Suermann, *Immunology*, **34**, 695 (1978).
- 14) D. N. Mannel, R. N. Moore and S. E. Mergenhagen, *Infect. Immun.*, **30**, 523 (1980).
- 15) M. Fukushima, T. Kato, R. Ueda, K. Ota, S. Narumiya and O. Hayaishi, *Biochem. Biophys. Res. Commun.*, **105**, 956 (1982).
- 16) S. J. Weiss and A. Slivka, *J. Clin. Invest.*, **69**, 255 (1982).
- 17) Y. Okubo and S. Suzuki, *Carbohydr. Res.*, **62**, 135 (1978).
- 18) Y. Hashimoto and H. Sudo, *Gann*, **62**, 139 (1971).
- 19) Y. Suzuki and T. Murachi, *J. Biochem. (Tokyo)*, **82**, 215 (1977).
- 20) T. Yorino and P. J. Bentley, *Nature (London)*, **271**, 79 (1978).
- 21) F. Dallegri, A. Ballestrero, G. Frumento and F. Patrone, *Immunology*, **55**, 639 (1985).
- 22) W. J. Johnson, C. C. Whisnant and D. O. Adams, *J. Immunol.*, **127**, 1787 (1981).
- 23) K. Morikawa, R. Takeda, M. Yamazaki and D. Mizuno, *Cancer Res.*, **45**, 1496 (1985).
- 24) K. Morikawa, S. Kamegaya, M. Yamazaki and D. Mizuno, *Cancer Res.*, **45**, 3482 (1985).
- 25) R. E. Schmidt, R. P. MacDermott, G. Bartley, M. Bertovich, D. A. Amato, K. F. Austen, S. F. Schlossman, R. L. Stevens and J. Ritz, *Nature (London)*, **318**, 289 (1985).
- 26) S. Kitagawa, F. Takaku and S. Sakamoto, *J. Clin. Invest.*, **65**, 74 (1980).

[Chem. Pharm. Bull.]
35(3)1144—1150(1987)

Studies on Biological Activities of Melanin from Marine Animals. V. Anti-inflammatory Activity of Low-Molecular-Weight Melanoprotein from Squid (Fr. SM II)

TSUTOMU MIMURA,^{*,a} SUSUMU ITOH,^a KAZUTAKE TSUJIKAWA,^a
HIROSHI NAKAJIMA,^a MIKIO SATAKE,^b YASUHIRO KOHAMA^a
and MASARU OKABE^a

Faculty of Pharmaceutical Sciences, Osaka University,^a Yamadaoka 1-6, Suita, Osaka 565,
Japan and The Central Research Laboratory of Nippon Suisan Co., Ltd.,^b
Kitanocho, Hachiohji, Tokyo 192, Japan

(Received July 18, 1986)

Low-molecular-weight melanoprotein obtained from *Ommastrephes bartrami* LESUEL (Fr. SM II) was subjected to an anti-inflammatory screening procedure and was shown to have a potent inhibitory activity against carrageenin-induced rat paw edema. Fr. SM II was then studied with various acute inflammatory models and appeared to suppress the enhanced capillary permeability of mouse ear induced by xylene and the acceleration of vascular permeability induced by compound 48/80. Using the carboxymethylcellulose pouch method, both leucocyte emigration and protein exudation into the pouch fluid were potently inhibited by Fr. SM II. Fr. SM II was also effective in subacute inflammation induced by the felt pellet and the croton oil granuloma pouch methods. Thus, in addition to its anti-ulcerogenic activity, Fr. SM II also has anti-inflammatory activity.

Keywords—squid melanin; anti-inflammatory activity; carrageenin-induced paw edema; capillary permeability; CMC pouch; felt pellet-induced granuloma; croton oil granuloma pouch

The authors have reported that low-molecular-weight melanoprotein from *Ommastrephes bartrami* LESUEL (Fr. SM II) has anti-ulcerogenic activity based on its inhibition of gastric juice secretion.¹⁾ The mechanism of anti-ulcerogenic activity of this melanoprotein was reported in previous papers.^{2,3)}

In the present paper, the anti-inflammatory activity of Fr. SM II was examined using carrageenin-induced rat paw edema. We also examined the anti-inflammatory mechanism of Fr. SM II using both acute and subacute inflammatory models.

Materials and Methods

Preparation of Fr. SM II—Fr. SM II was obtained from the ink bags of *Ommastrephes bartrami* LESUEL as described in a previous paper.¹⁾ Briefly, the ink bags were chopped into pieces and the suspension was homogenized in a Waring blender, then extracted by adding 1 N NaOH to the homogenate at pH 9.0. The extract was filtered through a double gauze layer and the filtrate was dialyzed against distilled water. The undialyzable fraction (crude melanin) was separated into high- (Fr. SM I) and low- (Fr. SM II) molecular-weight fractions by gel filtration on a Sephadex G-100 column equilibrated with 0.1 M phosphate buffer (pH 7.0) containing 0.5 M NaCl.

Carrageenin-Induced Rat Paw Edema—According to the methods described by Vanarman *et al.*⁴⁾ and Winter *et al.*⁵⁾ male SD rats (purchased from Japan Kearsy Co.) weighing 150–170 g were fasted for 24 h prior to experiments but were supplied with water *ad libitum*. Carrageenin (Picnin-A, Zushikagaku) was suspended in 0.9% NaCl to make a 1.5% (w/v) suspension. The right hind paw was inoculated with 0.1 ml of the prepared carrageenin suspension while the left hind paw was given saline. At an indicated time, the volume difference between the carrageenin-inoculated and saline-injected paws was recorded as the amount of edema, and the swelling percentage was calculated on the basis of the volume of the saline-injected paw. Saline was given intraperitoneally 30 min before the carrageenin

injection. Dexamethasone (Sigma) as a positive control was given subcutaneously 30 min before the carrageenin injection.

Vascular Permeability Test Using Mouse Ear—According to the method described by Fujimura *et al.*,⁶⁾ male ddY mice weighing 15–20 g were injected with 5% pontamine sky blue (0.1 ml/10 g b.w.; PSB) through the vein. Immediately after the injection, the left ear was pinched for 5 s between two felt pads which were soaked in xylene beforehand. Fifteen minutes later, both ears were removed and placed between two plates (10 × 45 mm), each of which had a hole (6 mm diameter) in its center. The plates were then placed in a cuvette and the optical density (OD) value of the bluish color in the left ear was measured at 630 nm (the right ear was used as a blank). The dye concentration was calculated from a calibration curve and expressed as pontamine sky blue concentration. Thirty minutes prior to the stimulation, the sample to be tested was administered intraperitoneally to the mouse. Dexamethasone, used as a positive control, was administered subcutaneously.

Capillary Permeability Test with Various Phlogists—According to the methods of Thomas and West⁷⁾ and Crunkhorn and Willis,⁸⁾ male SD rats weighing 150–180 g were fasted and had their backs shaved 24 h prior to experiments, but were supplied with water *ad libitum*. Histamine 2HCl (Wako Pure Chemical Ind., Ltd.), serotonin creatinine sulfate (Seikagaku Kogyo Co., Ltd.), bradykinin (Seikagaku Kogyo Co., Ltd.), prostaglandin E₂ (PG E₂) (Sigma) and compound 48/80 (Sigma) solutions were prepared at concentrations of 1 mg/ml, 100 µg/ml, 50 µg/ml, 10 µg/ml and 1 mg/ml, respectively. Then 0.1 ml of a phlogist and saline was administered intradermally at two points in the left and right back, respectively. Immediately after that, the rats were injected intravenously with 1% Evans blue (1 ml/kg, Nakarai Co., Ltd.). Thirty minutes later, the rats were killed and skinned. The capillary permeability was expressed by the multiplying major and minor axes of the blue area caused by the phlogist. The sample was administered intraperitoneally 30 min prior to the injection of the phlogist.

Anti-inflammatory Activity Test Using the Carboxymethylcellulose (CMC) Pouch Method—According to the method described by Ishikawa *et al.*,⁹⁾ carboxymethylcellulose was dissolved in 0.9% NaCl to make a 2% solution. Nitrogen gas (5 ml) was injected subcutaneously into the backs of male rats weighing 130–150 g, and the next day, CMC solution was injected into the N₂ gas sac. For the measurement of leucocyte number and protein content in the CMC fluid, 0.2 ml of the pouch fluid was collected in a tuberculin syringe at 1.5, 3.0, 4.5 and 6.0 h after the injection of the CMC solution. Leucocytes from 0.1 ml of the pouch fluid were stained with 0.05% brilliant cresyl blue in saline and were counted with a hemocytometer. The remaining pouch fluid (0.1 ml) was used for the determination of protein concentration using the Folin–Lowry method. The sample was administered intraperitoneally 30 min prior to the administration of the CMC solution.

Felt Pellet-Induced Granuloma—Felt pellet-induced granuloma was basically prepared according to the methods reported by Robert and Eezanic¹⁰⁾ and Nakamura and Shimizu.¹¹⁾ Nine male rats of SD strain weighing 150–180 g were used for each group. Felt pellets, weighing 35 ± 1 mg (0.5–0.6 cm in diameter) each, were prepared from a felt plate 0.6 cm thick and sterilized in an autoclave for 30 min at 120 °C. Two of the pellets were implanted into the subcutaneous space of the scapular region under pentobarbiturate anesthesia and 0.1 ml of 4000 U/ml penicillin was injected subcutaneously. On the eighth day of the implantation, the felt pellets, along with the surrounding inflammatory tissue, were removed from the animals. The removed granulomas were dried at 60 °C until they reached constant weight. The increase in weight was determined by subtracting the original weight of the felt pellet. Liver, spleen, adrenal glands and thymus were also weighed immediately after excision and were expressed as the weight per 100 g body weight. The sample was administered intraperitoneally at 24 h intervals for 8 d. As a positive control, dexamethasone was administered subcutaneously.

Croton Oil Granuloma Pouch—The procedure employed was basically the same as that of Serie¹²⁾ and Itoga and Miyake.¹³⁾ Male rats of SD strain weighing 150–180 g were used. A pouch was formed by injecting 20 ml of N₂ gas into the subcutaneous space of the back under pentobarbiturate anesthesia. Then 1 ml of 1% croton oil (Wako Pure Chemical Ind., Ltd.) dissolved in sesame oil (Nakarai Chem.) was injected into the pouch and 0.1 ml of 4000 U/ml penicillin was injected subcutaneously. On the eighth day of the injection, the animals were sacrificed and the wet weights of the pouch and the exudate were measured. Liver, spleen, adrenal glands and thymus were also weighed immediately after the incision and were expressed as weight per 100 g body weight. The sample was administered intraperitoneally at 24 h intervals for 8 d. As a positive control, dexamethasone was administered subcutaneously.

Statistics—The significance of differences between drug-treated and control animals was evaluated by means of Student's test.

Results

Effect of Fr.SM II on Carrageenin-Induced Paw Edema

Fr.SM II depressed the paw edema dose-dependently when administered intraperitoneally (Fig. 1) or intravenously (Fig. 2). It is noteworthy that there was no difference in the inhibitory activity between the two methods of administration. Therefore, we employed

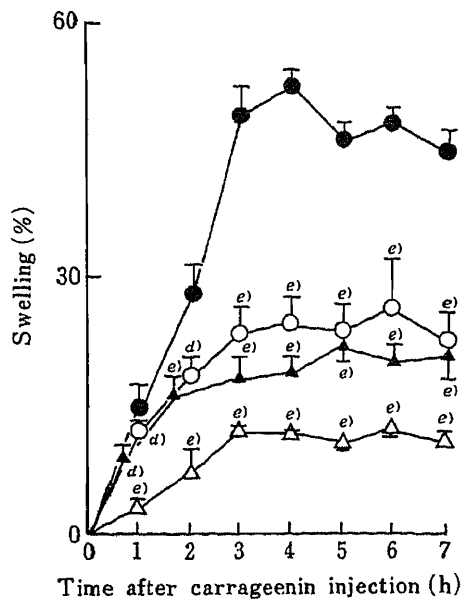


Fig. 1. Effect of Fr. SM II on Carrageenin-Induced Paw Edema in Rats (i.p.)

●, control;^{a)} ○ Fr. SM II^{b)} 10 mg/kg, ▲ 20 mg/kg, △ dexamethasone^{c)} 1 mg/kg. a) Saline. b) Sample was administered intraperitoneally 30 min prior to the carrageenin injection. c) Sample was administered subcutaneously 30 min prior to the carrageenin injection. All values represent mean \pm S.E. ($n=8$). Significantly different from the control group: d) $p < 0.05$, e) $p < 0.001$.

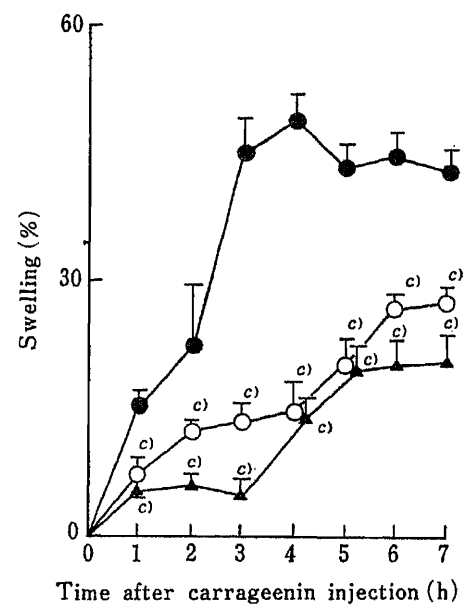


Fig. 2. Effect of Fr. SM II on Carrageenin-Induced Paw Edema in Rats (i.v.)

● Control;^{a)} ○ Fr. SM II^{b)} 10 mg/kg, ▲ 20 mg/kg. a) Saline. b) Sample was administered intravenously 30 min prior to the carrageenin injection. All values represent mean \pm S.E. ($n=8$). Significantly different from the control group: c) $p < 0.001$.

TABLE I. Effect of Fr. SM II on Enhanced Capillary Permeability Induced by Xylene in Mice

Treatment	Dose (mg/kg)	Vascular permeability (PSB ^{d)} mg/dl)
Control ^{a)}		4.12 \pm 0.35
Fr. SM II ^{b)}	10	4.65 \pm 0.40
	20	2.91 \pm 0.15 ^{e)}
Dexamethasone ^{c)}	1	2.41 \pm 0.16 ^{f)}

a) Saline. b) Sample was administered intraperitoneally 1 h prior to the intravenous administration of PSB. c) Sample was administered subcutaneously 1 h prior to the intravenous administration of PSB. d) PSB; pontamine sky blue. All values represent mean \pm S.E. ($n=8$). Significantly different from the control group: e) $p < 0.01$, f) $p < 0.001$.

TABLE II. Effect on Accelerated Capillary Permeability Induced by Various Phlogists in Rat Skin

Treatment	Dose (mg/kg)	Colored area (mm ²)				
		Histamine	Serotonin	Bradykinin	PG E ₂	Compound 48/80
Control ^{a)}		126.0 \pm 10.6	275.2 \pm 29.1	93.0 \pm 6.8	58.6 \pm 5.0	441.1 \pm 24.3
Fr. SM II ^{b)}	10	137.9 \pm 6.3	274.8 \pm 26.1	86.2 \pm 6.2	53.6 \pm 7.6	397.6 \pm 23.4
	20	126.1 \pm 5.9	268.4 \pm 34.1	112.5 \pm 6.7	60.8 \pm 3.7	315.6 \pm 17.1 ^{c)}

a) Saline. b) Sample was administered intraperitoneally 30 min prior to the injection of Evans blue solution. All values represent mean \pm S.E. ($n=8$). Significantly different from the control group: c) $p < 0.001$.

intraperitoneal administration in the following experiments.

Effects of Fr.SM II in the First Phase of Inflammation

Fr.SM II at a dose of 20 mg/kg significantly depressed the accelerated vascular permeability of the ear induced by xylene (Table I).

Fr.SM II at a dose of 20 mg/kg significantly depressed the acceleration of the vascular permeability in the back induced by compound 48/80, but not those produced by serotonin and PG E₂. Fr.SM II slightly increased the acceleration of vascular permeability induced by histamine and bradykinin (Table II).

Effect of Fr.SM II in the Second Phase of Inflammation

In the CMC pouch method, which represents the second inflammatory phase, Fr.SM II at doses of 10 and 20 mg/kg significantly suppressed leucocyte emigration at 4.5 h after the injection of CMC solution and significantly suppressed protein exudation from 3 h after that time (Tables III and IV).

Effect of Fr.SM II on the Subacute Inflammatory Models

Felt pellet-induced granuloma was employed as one of the subacute inflammatory

TABLE III. Effect of Fr. SM II on Leucocyte Emigration into the Pouch Fluid in the CMC Pouch Method

Treatment	Dose (mg/kg)	Leucocyte count in 1 mm ³ of pouch fluid ($\times 10^3$)				(h)
		1.5	3.0	4.5	6.0	
Control ^{a)}		7.40 \pm 0.30	8.14 \pm 0.39	10.31 \pm 0.39	6.73 \pm 0.54	
Fr. SM II ^{b)}	10	7.31 \pm 0.44	8.81 \pm 0.19	8.67 \pm 0.50 ^{c)}	6.31 \pm 0.33	
	20	7.12 \pm 0.59	8.50 \pm 0.48	8.27 \pm 0.32 ^{d)}	6.96 \pm 0.67	

a) Saline. b) Sample was administered intraperitoneally 30 min prior to the CMC administration. All values represent mean \pm S.E. ($n=8$). Significantly different from the control group: c) $p<0.05$, d) $p<0.01$.

TABLE IV. Effect of Fr. SM II on Protein Exudation into the Pouch Fluid in the CMC Pouch Method

Treatment	Dose (mg/kg)	mg of protein 1 ml of pouch fluid				(h)
		1.5	3.0	4.0	6.0	
Control ^{a)}		14.89 \pm 1.18	22.29 \pm 1.18	28.31 \pm 1.62	43.23 \pm 2.11	
Fr. SM II ^{b)}	10	12.35 \pm 0.75	19.14 \pm 1.16	23.68 \pm 2.15	28.53 \pm 1.67 ^{c)}	
	20	14.02 \pm 0.10	17.17 \pm 1.12 ^{d)}	21.84 \pm 1.17 ^{d)}	27.67 \pm 1.02 ^{d)}	

a) Saline. b) Sample was administered intraperitoneally 30 min prior to the CMC administration. All values represent mean \pm S.E. ($n=8$). Significantly different from the control group: c) $p<0.05$, d) $p<0.01$.

TABLE V. Effect of Successive Administration of Fr. SM II on Granuloma Formation Induced by Felt Pellet in Rats

Treatment	Daily dose (mg/kg)	Granuloma formed by felt pellet (mg)
Control ^{a)}		35.8 \pm 1.1
Fr. SM II ^{b)}	5	35.7 \pm 1.2
	10	29.8 \pm 1.4 ^{d)}
Dexamethasone ^{c)}	0.5	7.8 \pm 0.9 ^{e)}

a) Saline. b) Sample was administered intraperitoneally for 8 d. c) Sample was administered subcutaneously for 8 d. All values represent mean \pm S.E. ($n=18$). Significantly different from the control group: d) $p<0.01$, e) $p<0.001$.

TABLE VI. Effect of Successive Administration of Fr. SM II on Various Wet Organ Weights in Rats with Felt Pellet Granuloma Pouch

Treatment	Daily dose (mg/kg)	Adrenal ^{d)}	Relative wet organ weights		Liver ^{e)}
			Thymus ^{d)}	Spleen ^{d)}	
Control ^{a)}		7.9 ± 0.6	194.3 ± 11.2	298.1 ± 18.5	4.3 ± 0.1
Fr. SM II ^{b)}	5	8.9 ± 0.8	185.7 ± 11.5	292.9 ± 20.8	4.7 ± 0.2
	10	11.1 ± 0.5 ^{g)}	180.8 ± 6.3	452.2 ± 9.7 ^{h)}	4.7 ± 0.1 ^{f)}
Dexamethasone ^{c)}	0.5	4.0 ± 0.2 ^{g)}	28.3 ± 4.0 ^{h)}	95.8 ± 7.4 ^{h)}	5.2 ± 0.0 ^{h)}

a) Saline. b) Sample was administered intraperitoneally for 8 d. c) Sample was administered subcutaneously for 8 d. d) mg/100 g final body wt. e) g/100 g final body wt. All values represent mean ± S.E. (n=9). Significantly different from the control group: f) $p < 0.05$, g) $p < 0.01$, h) $p < 0.001$.

TABLE VII. Effect of Successive Administration of Fr. SM II on Granuloma Formation and Exudate in the Granuloma Pouch Method in Rats

Treatment	Daily dose (mg/kg)	Pouch fluid (ml)	Pouch wall (g)
Control ^{a)}		14.75 ± 1.73	4.54 ± 0.45
Fr. SM II ^{b)}	5	15.69 ± 2.40	4.15 ± 0.69
	10	9.31 ± 1.24 ^{d)}	2.64 ± 0.38 ^{e)}
Dexamethasone ^{c)}	0.5	0.00 ± 0.00 ^{f)}	1.62 ± 0.36 ^{f)}

a) Saline. b) Sample was administered intraperitoneally for 8 d. c) Sample was administered subcutaneously for 8 d. All values represent mean ± S.E. (n=9). Significantly different from the control group: d) $p < 0.05$, e) $p < 0.01$, f) $p < 0.001$.

TABLE VIII. Effect of Successive Administration of Fr. SM II on Various Wet Organ Weights in Rats with Granuloma Pouch

Treatment	Daily dose (mg/kg)	Adrenal ^{d)}	Relative wet organ weights		Liver ^{e)}
			Thymus ^{d)}	Spleen ^{d)}	
Control ^{a)}		8.7 ± 0.2	191.9 ± 11.8	367.9 ± 17.3	4.7 ± 0.1
Fr. SM II ^{b)}	5	11.7 ± 0.8 ^{g)}	144.0 ± 14.2 ^{f)}	420.4 ± 15.4 ^{f)}	4.5 ± 0.2
	10	11.2 ± 0.5 ^{h)}	165.3 ± 6.9	336.9 ± 13.9	4.8 ± 0.1
Dexamethasone ^{c)}	0.5	5.4 ± 0.4 ^{h)}	63.5 ± 6.5 ^{h)}	103.0 ± 8.3 ^{h)}	6.7 ± 0.6 ^{h)}

a) Saline. b) Sample was administered intraperitoneally for 8 d. c) Sample was administered subcutaneously for 8 d. d) mg/100 g final body wt. e) g/100 g final body wt. All values represent mean ± S.E. (n=9). Significantly different from the control group: f) $p < 0.05$, g) $p < 0.01$, h) $p < 0.001$.

models. Fr.SM II significantly suppressed the granuloma formation at doses of 5 and 10 mg/kg. Dexamethasone showed significant suppression at a dose of 0.5 mg/kg (Table V). The weights of various organs at the end of the experiments are summarized in Table VI. Fr.SM II significantly increased the weights of the adrenal glands, spleen and liver. Dexamethasone significantly decreased the weights of the spleen, thymus and adrenal glands and increased that of the liver.

The granuloma pouch method was employed as another subacute inflammatory model. Fr.SM II significantly suppressed the pouch fluid accumulation and the granuloma formation at a dose of 10 mg/kg. Dexamethasone was much more effective (Table VII). The organ weights at the conclusion of the experiments are shown in Table VIII. Fr.SM II significantly increased the weights of the adrenal glands and spleen, but decreased that of the thymus, while

dexamethasone significantly decreased those of the spleen, thymus and adrenal glands and increased that of the liver.

Discussion

Melanin is a high-molecular-weight compound formed by oxidative polymerization of various forms of quinones, which originate from tyrosine and exist as melanoproteins after being combined with proteins in the cytosol. Since melanoprotein has an indefinite molecular weight and a random sequence of constituent units, there have been few reports concerning its biosynthesis or physiological significance. Recently, it was reported that the melanins of *Str. bottropensis* (GIS),^{14,15)} *Octopus vulgaris* CUVIER (OM)¹⁶⁾ and *Ommastrephes bartrami* LESUEL (Fr.SM II)¹⁻³⁾ exhibit anti-ulcer activity as evaluated in terms of the inhibition of gastric juice secretion.

In this paper, we examined the anti-inflammatory activity of Fr.SM II, and found that Fr.SM II suppressed carrageenin-induced rat paw edema when given either by intraperitoneal or intravenous administration (Figs. 1 and 2). In our previous report,¹⁾ it was demonstrated that the intraperitoneal administration of Fr.SM II caused no squirming and no stimulation of peritoneal capillary permeability in mice. Therefore, in the following experiments, Fr.SM II was administered intraperitoneally.

According to Vineger *et al.*¹⁷⁾ and Dirosa *et al.*,^{18,19)} carrageenin-induced rat paw edema can be classified into three steps. The first step (from 0.5 to 1.5 h) is mediated by histamine and/or serotonin, the second (from 1 to 2 h) by bradykinin and the third (after 2 h) by prostaglandins (PGs). As shown in Figs. 1 and 2, the first step of carrageenin-induced paw edema was significantly inhibited by Fr.SM II, so it was assumed that the fraction affected the histamine- and/or the serotonin-related process. Since Fr.SM II had anti-inflammatory activity in the carrageenin-induced paw edema, its effects on other experimental inflammatory models were also examined.

In general, the inflammation process can be divided into three phases. During the first phase, tissue damage caused by local stimulants and an enhancement of the vascular permeability takes place. Next, an emigration of leucocytes is observed. The third phase is characterized by granuloma formation and tissue regeneration.

Fr.SM II suppressed the non-specifically enhanced vascular permeability caused by xylene, and at the same time, suppressed the enhancement of vascular permeability caused by compound 48/80 (Table II). The latter compound is known to affect mast cells, causing release of chemical mediators such as histamine, serotonin and the eosinophilic chemotactic factor of anaphylaxis (ECF-A). Therefore, it was assumed that Fr.SM II inhibited the release of these chemical mediators from the mast cells.

Moreover, Fr.SM II inhibited the emigration of leucocytes and the exudation of protein into the CMC pouch fluid, which corresponds to the second phase of inflammation. It was supposed that the effect was based on a lowering of the vascular permeability, which leads to inhibition of the leakage of protein through the vessels and results in inhibition of leucocyte emigration.

Moreover, Fr.SM II was effective in subacute inflammation, which was caused by felt pellet granuloma and the croton oil granuloma pouch, as well as acute inflammation. In the subacute inflammatory models, the toxicity of the tested sample has to be considered. As shown in Tables VI and VIII, the weights of the adrenal glands and spleen increased but that of the thymus decreased. From these results, the authors considered that Fr.SM II had showed little toxicity on successive administration. However, the reason for the changes in the thymus and adrenal glands is not clear, and we intend to carry out a histological investigation of the effect of Fr.SM II on these organs.

Although the physiological significance of the anti-inflammatory activity of melanin must await further investigation, it is clear that Fr.SM II has anti-inflammatory activity in addition to anti-ulcer activity.

References

- 1) T. Mimura, K. Maeda, H. Hariyama, S. Aonuma, M. Satake and T. Fujita, *Chem. Pharm. Bull.*, **30**, 1381 (1982).
- 2) T. Mimura, K. Maeda, T. Terada, Y. Oda, K. Morishita and S. Aonuma, *Chem. Pharm. Bull.*, **33**, 2052 (1985).
- 3) T. Mimura, K. Maeda, Y. Oda, T. Terada, K. Yoshida and S. Aonuma, *Chem. Pharm. Bull.*, **33**, 2061 (1985).
- 4) C. G. Vanarman, A. J. Begany, L. M. Miller and H. H. Bless, *J. Pharmacol. Exp. Ther.*, **150**, 328 (1965).
- 5) C. A. Winter, E. A. Risley and G. W. Nuss, *Proc. Soc. Exp. Biol. Med.*, **111**, 544 (1962).
- 6) H. Fujimura, S. Tsurumi and M. Hayashi, *Folia Pharmacol. Jpn.*, **64**, 379 (1968).
- 7) G. Thomas and G. B. West, *Br. J. Pharmacol.*, **50**, 231 (1974).
- 8) P. Crunkhorn and A. L. Willis, *Br. J. Pharmacol.*, **41**, 57 (1971).
- 9) H. Ishikawa and Y. Mori, *Eur. J. Pharmacol.*, **7**, 201 (1969).
- 10) A. Robert and J. E. Eezanic, *Acta Endocrinol.*, **25**, 105 (1957).
- 11) H. Nakamura and M. Shimizu, *Eur. J. Pharmacol.*, **27**, 198 (1974).
- 12) H. Serie, *Proc. Soc. Exp. Biol. Med.*, **82**, 328 (1953).
- 13) E. Itoga and Y. Miyake, *Folia Pharmacol. Jpn.*, **66**, 316 (1970).
- 14) T. Mimura, N. Muto, J. Tanaka, H. Oshita, N. Onishi and S. Aonuma, *Chem. Pharm. Bull.*, **25**, 897 (1977).
- 15) T. Mimura, N. Muto, Y. Oda, N. Tanaka and S. Aonuma, *Chem. Pharm. Bull.*, **26**, 998 (1978).
- 16) T. Mimura, K. Maeda, H. Tsujibo, M. Satake and T. Fujita, *Chem. Pharm. Bull.*, **30**, 1508 (1982).
- 17) R. Vineger, W. Schreiber and R. Hugo, *J. Pharmacol. Exp. Ther.*, **166**, 96 (1969).
- 18) M. Dirosa and D. A. Willoughby, *J. Pharm. Pharmacol.*, **24**, 89 (1972).
- 19) M. Dirosa and L. Sorretina, *Br. J. Pharmacol.*, **38**, 214 (1970).

[Chem. Pharm. Bull.]
35(3)1151—1156(1987)

Interaction between Semi-alkaline Proteinase and Protease Inhibitors of Rabbit Serum

SHINICHI KOBAYASHI,^a FUSAYO YAMADA,^a MASANORI SASAKI,^{*a}
KIKUO ASAHINA,^a and MAMORU SUGIURA^b

Niigata College of Pharmacy,^a 5829 Kamishinei-cho, Niigata 950-21, Japan
and Gifu Pharmaceutical University,^b Mitahora-higashi
5-6-1, Gifu 502, Japan

(Received July 30, 1986)

Interactions *in vitro* and *in vivo* between semi-alkaline proteinase (SAP) and protease inhibitors of rabbit serum were studied. As a result of the purification of SAP inhibitors from rabbit serum, the caseinolytic activity of SAP was found to be inhibited by α_1 -macroglobulin (α_1 M) and α_1 -proteinase inhibitor (α_1 PI). SAP was stoichiometrically bound to α_1 M at a molar ratio of 1:1 and the proteolytic activity remained constant at 16% of the original activity even in the presence of excess α_1 M. In contrast, the proteolytic activity of SAP decreased linearly with increase in the amount of α_1 PI, but a 10-fold molar excess of α_1 PI was needed for complete inhibition.

The disappearance rate of intravenously injected ¹²⁵I-labeled SAP (¹²⁵I-SAP) from rabbit serum was also investigated by using high-performance liquid chromatography (HPLC). Serum levels of ¹²⁵I-SAP decreased biexponentially after a single injection. The results of gel-permeation HPLC of rabbit serum on a TSK G-3000 SW column indicated that SAP was mainly bound to α -macroglobulins and that α -macroglobulin-SAP complex was cleared from the blood circulation with a half-life of 10 min.

Keywords—semi-alkaline proteinase; rabbit serum; serum protease inhibitor; high-performance liquid chromatography

Semi-alkaline proteinase (SAP) from *Aspergillus melleus* is now used clinically as an oral anti-inflammatory drug, but the mechanism of its action is still obscure. To understand the pharmacological effect of SAP, detailed pharmacokinetic studies are necessary. Our previous papers dealt with the quality of commercial SAP preparations and showed that they were not pharmaceutically equivalent.^{1,2)} An assay method for SAP in biological fluids, however, is still required for the evaluation of biological equivalence of SAP preparations.

Enzyme activity measurement is not useful for determining the concentration of the protease in biological fluids, because the enzyme activity is easily affected by the endogenous proteases, activators and inhibitors. Thus, radioimmunoassay (RIA) procedures are being developed for the quantitative measurement of the protease in biological fluids.³⁻⁵⁾ However, several investigators have reported that the immunoreaction in the RIA is inhibited by some high-molecular-weight protease inhibitors such as α_2 -macroglobulin in the biological fluids.⁶⁻⁸⁾

Recently, high-performance liquid chromatography (HPLC) has been widely used for the separation of proteins and peptides.⁹⁻¹²⁾ In the present paper, we attempted to determine the ¹²⁵I-labelled SAP (¹²⁵I-SAP) and ¹²⁵I-SAP-protease inhibitor complexes in rabbit serum by using HPLC, and to apply the HPLC method to studies on the interactions *in vitro* and *in vivo* between SAP and protease inhibitors of rabbit serum.

Materials and Methods

Materials—Carrier-free Na^{125}I (2 mCi) and Enzymobeads were purchased from New England Nuclear and Bio-Rad Laboratories, respectively. Sephacryl S-200, DEAE-Sephacel and Sephadex G-25 were obtained from Pharmacia Fine Chemicals.

Purification of SAP—Purification of SAP from *Aspergillus melleus* was performed as previously described.¹³⁾ The molecular weight of SAP was estimated to be 3.4×10^4 by gel filtration and sedimentation analysis.

Radioiodination of SAP—A 2% glucose solution (20 μl) was added to a mixture containing 20 μl of SAP (0.22 mg), 50 μl of 0.2 M phosphate buffer (pH 6.77), 50 μl of Bio-Rad enzymobeads and 12.5 μl of Na^{125}I (0.25 mCi). After standing at 25°C for 1 h, the reaction mixture was chromatographed on Sephadex G-50 equilibrated with 15 mM Tris-HCl buffer (pH 8.0) containing 1 mM CaCl_2 . Fractions containing radiolabeled protein were pooled. The specific activity of ^{125}I -labeled SAP (^{125}I -SAP) was about 0.26 $\mu\text{Ci}/\mu\text{g}$ and no loss of its proteolytic activity was observed.

Inhibitory Assay Method—SAP (10 μg) and protease inhibitor in a final volume of 0.5 ml of 50 mM Tris-HCl buffer (pH 8.0) were incubated at 37°C for 10 min prior to the addition of 2.5 ml of 1.2% casein in 0.1 M phosphate buffer (pH 7.0). The reaction mixture was further incubated at 37°C for 10 min, then the enzyme reaction was terminated by the addition of 2.5 ml of solution containing 0.11 M trichloroacetic acid, 0.22 M sodium acetate and 0.33 M acetic acid, and the absorbance of the filtrate was measured at 280 nm. One inhibitory unit was defined as the amount of protease inhibitor which inhibited 1.0 μg of SAP under the above conditions.

Ultrafiltration—A Diaflo pressure dialysis apparatus (model 52) with a YM-10 membrane (Amicon Corp.) was used for ultrafiltration of pooled rabbit serum.

Purification of Protease Inhibitors from Rabbit Serum—Rabbit blood was allowed to clot spontaneously at room temperature and 50 ml of rabbit serum thus obtained was concentrated to 20 ml by ultrafiltration. The concentrated serum was applied to a column (3.0 \times 96 cm) of Sephacryl S-200 equilibrated with 50 mM phosphate buffer (pH 7.0) containing 0.1 M NaCl. Two peaks with SAP inhibitory activity were eluted from the column (cf. Fig. 1). The first peak was purified further by chromatographies on DEAE-Sephacel and Zn-chelate Sepharose 4B.^{14, 15)} The obtained inhibitor gave a single protein band on polyacrylamide gel electrophoresis and the molecular weight was calculated to be 8.2×10^5 by sodium dodecyl sulfate-polyacrylamide gel electrophoresis (SDS-PAGE) and gel filtration on Sepharose CL-6B. The final preparation was purified about 22.4-fold from the rabbit serum with a recovery of 56%. The second peak was purified further by chromatographies on Cibacron-Blue Sepharose 4B, DEAE-Sephacel and Sephadex G-100. The purified inhibitor showed a single band on disc polyacrylamide gel electrophoresis and its molecular weight was estimated to be 6.2×10^4 by SDS-PAGE. The final preparation represented a 59.6-fold purification with a recovery of 47%.

Animal Experiment—Male rabbits (2.90–3.15 kg) were given KI in their drinking water for five days to prevent uptake of iodine by the thyroid and fasted for 24 h prior to the experiment. ^{125}I -SAP (3×10^7 cpm/rabbit) was injected into a marginal ear vein of rabbits at a dose of 0.5 mg/kg. Blood was obtained from the vein of the other ear at timed intervals after injection and the serum was separated by centrifugation for analysis.

Chromatographic Conditions—HPLC was performed on a Hitachi 638-80 liquid chromatograph equipped with a TSK GEL G-3000 SW column (7.5 \times 600 mm, Toyo Soda). As a mobile phase, 0.2 M phosphate buffer (pH 7.0) containing 0.1% SDS was used at a flow rate of 0.5 ml/min.

HPLC Separation of Rabbit Serum—A 50 μl aliquot of serum was injected into the HPLC instrument and fractions of 1.0 ml were collected. The radioactivity of each fraction was counted in an Aloka Autowell γ -System ARC-500.

Results and Discussion

Effect of Protease Inhibitors of Rabbit Serum on the Caseinolytic Activity of SAP

As it appeared that administered SAP was trapped by protease inhibitors in biological fluids, the interaction between SAP and the protease inhibitors of rabbit serum *in vitro* was investigated. As shown in Fig. 1, rabbit serum was fractionated on a Sephacryl S-200 column, and the SAP inhibitory activity of each fraction was assayed. Two peaks with SAP inhibitory activity emerged from the column (fraction numbers 55 and 85). The inhibitors were purified as described in "Materials and Methods".

It is well known that rabbit serum contains two immunologically distinct α -macroglobulins, α_1 -macroglobulin and α_2 -macroglobulin, and that rabbit α_1 -macroglobulin is antigenically related to human α_2 -macroglobulin.¹⁶⁻¹⁸⁾ Our preparation gave a single precipitin line against anti-human α_2 -macroglobulin antibody (data not shown). Therefore, this purified

inhibitor was identified as α_1 -macroglobulin (α_1 M) based on the molecular weight and immunological character. As the second inhibitor eluted in gel-filtration on Sephacryl S-200 was bound to pancreatic trypsin and chymotrypsin at a molar ratio of approximately 1 : 1, the purified inhibitor was considered to be α_1 -proteinase inhibitor (α_1 PI) as judged from the molecular weight and protease inhibition spectrum.

Figure 2 shows the effects of rabbit α_1 M and α_1 PI on the caseinolytic activity of SAP. When the molar ratio of α_1 M to SAP was increased, the residual activity decreased linearly to 16% of the control, and then leveled off. At this saturation point, the binding molar ratio of α_1 M to SAP was calculated to be 1 : 1. It is well known that human α_2 M-protease complexes retain enzymic activity for low-molecular-weight substrates, but the hydrolysis of large substrates tends to be sterically hindered.¹⁹⁾ The binding of SAP to the rabbit α_1 M results in a reduction, but not total absence of caseinolytic activity, indicating that the inhibition of enzymic activity results from the steric hindrance of access of casein to bound SAP.

In contrast, the caseinolytic activity of SAP decreased linearly with the amount of added α_1 PI, but a 10-fold molar excess of α_1 PI was needed for the complete inhibition of caseinolytic activity of SAP. The binding stoichiometry of SAP to α_1 M was not the same as that of other proteases. Berthillier *et al.*¹⁷⁾ reported that 2 mol of trypsin or chymotrypsin was bound to

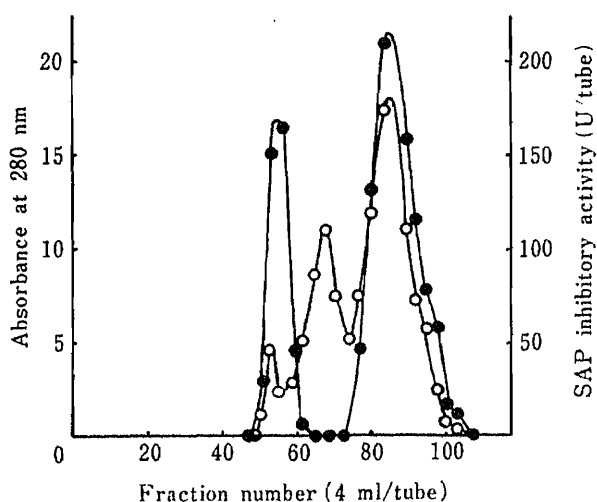


Fig. 1. Chromatography of Rabbit Serum on Sephacryl S-200

Rabbit serum was fractionated by gel filtration on a Sephacryl S-200 column, and the fractions were assayed for absorbance at 280 nm (○) and SAP inhibitory activity (●).

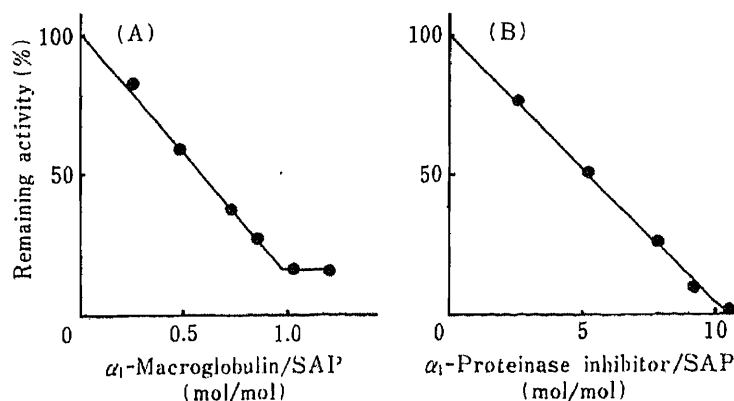


Fig. 2. Effect of Rabbit α_1 -Macroglobulin (A) and α_1 -Proteinase Inhibitor (B) on the Caseinolytic Activity of SAP

SAP (10 μ g) was preincubated with various amounts of α_1 M or α_1 PI in 0.5 ml of 50 mM Tris-HCl buffer (pH 8.0) at 37 °C for 10 min and then the residual caseinolytic activity was measured.

1 mol of rabbit α_1 M. A similar variability has been observed in the binding ratio of the various proteinase-human α_2 macroglobulin complexes.²⁰⁻²²⁾

Separation of ^{125}I -SAP and ^{125}I -SAP-Protease Inhibitor Complexes Using HPLC

HPLC fractionation was carried out on a TSK G-3000 SW column for the separation and quantification of ^{125}I -SAP and ^{125}I -SAP-protease inhibitor complexes. ^{125}I -SAP was incubated with the purified α_1 M or α_1 PI at 37°C for 10 min, and the mixture was subjected to HPLC. As shown in Fig. 3, ^{125}I -SAP- α_1 M complex (fraction numbers 17), ^{125}I -SAP- α_1 PI complex (fraction numbers 22) and ^{125}I -SAP (fraction numbers 26) were well separated from each other. Thus, the HPLC fractionation method was found to be useful for the determination of ^{125}I -SAP and ^{125}I -SAP-protease inhibitor complexes separately on the basis of their elution volumes.

Interaction between ^{125}I -SAP and Rabbit Serum *in Vitro*

The interaction between ^{125}I -SAP and rabbit serum was studied by HPLC fractionation of mixtures of ^{125}I -SAP and different amounts of serum. The ^{125}I -SAP was incubated with 2 μl (30% saturation of SAP-inhibiting capacity of serum) or 10 μl (100% saturation) of rabbit serum at 37°C for 10 min and then the reaction mixture was subjected to HPLC. As shown in Fig. 4, the radioactivity appeared in three fractions. The first peak was eluted with the α -macroglobulins fraction, the second was eluted with unbound SAP fraction and the final one was eluted with degraded products of SAP. When a large amount of serum was added, the radioactivity of the α -macroglobulins fraction increased. However, no peak corresponding to ^{125}I -SAP- α_1 PI complex was observed. When mixtures of ^{125}I -SAP, purified α_1 M and α_1 PI (molar ratio of 1:0.3:3 or 1:1.5:15) were analyzed as described in Fig. 4, the radioactivity was mainly observed in α_1 M fraction and unbound SAP fraction, but the radioactivity of α_1 M fraction increased on increasing the amount of inhibitors (data not shown). These results indicated that SAP has a higher affinity for α -macroglobulins than for α_1 PI in rabbit serum.

Serum Levels of ^{125}I -SAP after Intravenous Administration to Rabbits

The disappearance of ^{125}I -SAP injected intravenously was studied by using HPLC

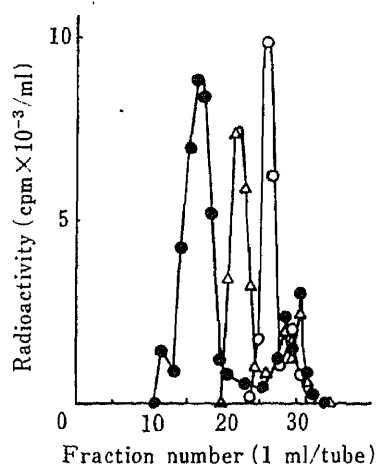


Fig. 3. HPLC Profiles of α_1 M-SAP Complex, α_1 PI-SAP Complex and SAP

^{125}I -SAP (0.5 μg) was incubated with α_1 M (60 μg) or α_1 PI (10 μg) at 37°C for 10 min. SAP (O), α_1 M-SAP complex (●) and α_1 PI-SAP complex (Δ) were independently subjected to HPLC after formation of the complex. Fractions of the eluate were collected and counted for radioactivity.

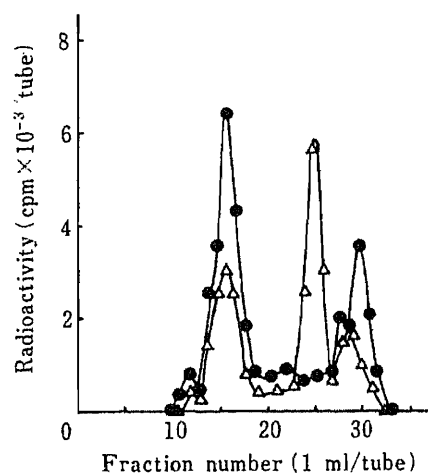


Fig. 4. HPLC Profiles of Mixtures of SAP and Rabbit Serum

^{125}I -SAP (0.5 μg) was incubated with 2 μl (Δ) or 10 μl (●) of rabbit serum at 37°C for 10 min prior to HPLC fractionation.

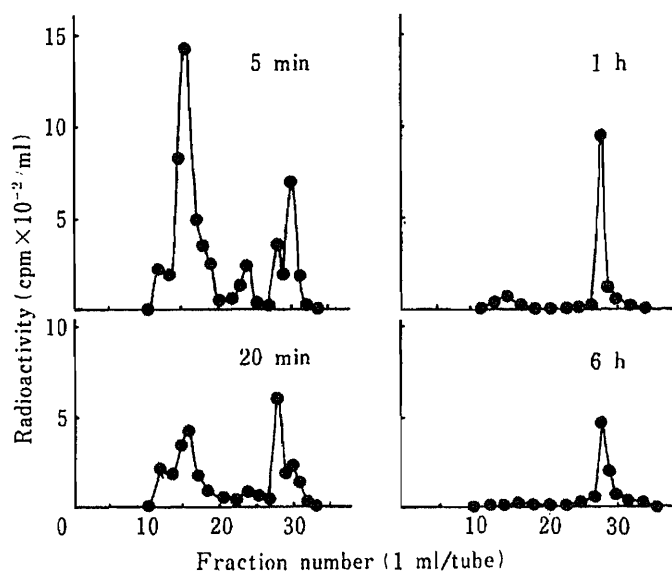


Fig. 5. Elution Profiles of Rabbit Serum after Intravenous Injection of 0.5 mg of ^{125}I -SAP per kg

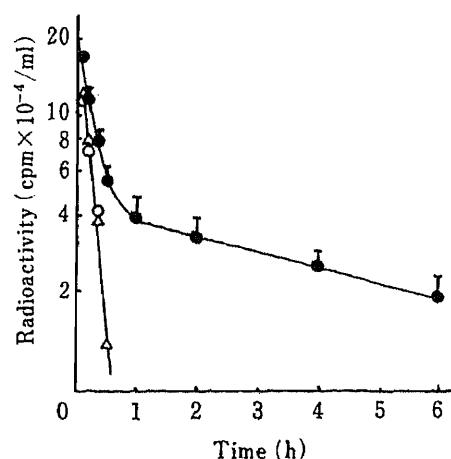


Fig. 6. Rabbit Serum Levels of Radioactivity after Intravenous Injection of 0.5 mg of ^{125}I -SAP per kg

The α -phase (Δ) was determined by subtracting the extrapolated values of the β -phase from the initial data points represented by the closed symbols (\bullet). Radioactivity of α -macroglobulin-SAP complex (\circ) was measured after separation by HPLC. Each point represents the mean \pm S.E. of three rabbits.

fractionation. Figure 5 shows the elution profiles of rabbit serum following the intravenous administration of 0.5 mg of ^{125}I -SAP per kg. Radioactivity in the serum 5 min after dosing appeared mainly in both α -macroglobulins and low-molecular fractions, and α -macroglobulins contained 75% of the applied radioactivity. The radioactivity in the α -macroglobulins fraction gradually diminished with time and disappeared 1 h after the administration. The radioactivity eluted around fraction number 28 (degradation products of SAP) gradually increased, reached a maximum almost 1 h after the administration, and then decreased.

Figure 6 shows the time course of the total radioactivity of rabbit serum after intravenous administration of ^{125}I -SAP. The curve for disappearance of radioactivity followed a biphasic pattern with half lives of 10 min in the α -phase and 5 h in the β -phase. The radioactivity derived from α -macroglobulins fraction in rabbit serum was measured by HPLC fractionation and the results are included in Fig. 6. The rate of decrease in ^{125}I -SAP- α -macroglobulin complex coincided with that of the fast disappearance phase. These results suggest that the administered ^{125}I -SAP exists mainly in α -macroglobulins-bound form in the rabbit serum at the early stage and then low-molecular-weight metabolites begin to appear with time. The results of our pharmacokinetic study of SAP were similar to those obtained by Katayama and Fujita²³⁾ in experiments with elastase. They reported that the serum levels of elastase declined biexponentially with half-lives of 13.6 min and 5.5 h after intravenous administration of ^{131}I -elastase to rats.

Since the HPLC method presented here enables the measurement of ^{125}I -SAP and ^{125}I -SAP-protease inhibitor complexes in rabbit serum on the basis of their elution volumes and can be applied to study the disappearance of ^{125}I -SAP-protease inhibitor complex and degradation products of SAP in rabbit serum, it should be useful for pharmacokinetic studies of SAP.

References and Notes

- 1) M. Sasaki, S. Kobayashi, K. Shimada, R. Iinuma, S. Kiryu, and M. Sugiura, *Chem. Pharm. Bull.*, **33**, 748 (1985).
- 2) S. Kobayashi, M. Sasaki, and M. Sugiura, *Yakuzaigaku*, **45**, 34 (1985).
- 3) R. S. Temler and J.-P. Felber, *Biochim. Biophys. Acta*, **445**, 720 (1976).
- 4) C. Largman, J. W. Brodrick, M. C. Geokas, and J. H. Johnson, *Biochim. Biophys. Acta*, **543**, 450 (1978).
- 5) K. Katayama and T. Ooyama, *Chem. Pharm. Bull.*, **28**, 3422 (1980).
- 6) M. C. Geokas, C. Largman, J. W. Brodrick, J. H. Johnson, and M. Fassett, *J. Biol. Chem.*, **254**, 2775 (1979).
- 7) K. Miyata, M. Tuda, and K. Tomoda, *Anal. Biochem.*, **101**, 332 (1980).
- 8) C. M. O'Connor, M. D. O'Donnell, and K. F. McGeeney, *Clin. Chim. Acta*, **114**, 29 (1981).
- 9) T. Imamura, K. Konishi, M. Yokoyama, and K. Konishi, *J. Biochem. (Tokyo)*, **86**, 639 (1979).
- 10) N. Ui, *Anal. Biochem.*, **97**, 65 (1979).
- 11) F. E. Regnier and K. M. Gooding, *Anal. Biochem.*, **103**, 1 (1980).
- 12) Y. Kato, K. Komiya, H. Sasaki, and T. Hashimoto, *J. Chromatogr.*, **193**, 29 (1980).
- 13) S. Kobayashi, M. Sasaki, S. Kiryu, and M. Sugiura, *Chem. Pharm. Bull.*, **32**, 3105 (1984).
- 14) L. Sundberg and J. Porath, *J. Chromatogr.*, **90**, 87 (1974).
- 15) T. Kureki, F. Lawrence, and M. Laskowski Sr., *Anal. Biochem.*, **99**, 415 (1979).
- 16) J. J. Picard and J. F. Heremans, *Biochim. Biophys. Acta*, **71**, 554 (1963).
- 17) G. Berthillier, R. Got, and G. Bertagnolio, *Biochim. Biophys. Acta*, **170**, 140 (1968).
- 18) B. H. Berne, S. Dray, and K. L. Knight, *Proc. Soc. Exp. Biol. Med.*, **138**, 531 (1971).
- 19) A. J. Barrett and P. M. Starkey, *Biochem. J.*, **133**, 709 (1973).
- 20) P. O. Ganrot, *Acta Chem. Scand.*, **21**, 602 (1967).
- 21) H. Rinderknewcht, R. M. Fleming, and M. C. Geokas, *Biochim. Biophys. Acta*, **377**, 158 (1975).
- 22) A. J. Barrett and P. M. Starkey, *Biochem. J.*, **133**, 709 (1973).
- 23) K. Katayama and T. Fujita, *Biochim. Biophys. Acta*, **288**, 181 (1972).

[Chem. Pharm. Bull.]
35(3)1157—1161(1987)

Chronic Effect of *Salviae Miltiorrhizae Radix* on Renal Tissue Blood Flow and Blood Pressure in Uremic Rats

TAKAKO YOKOZAWA,* HAE YOUNG CHUNG, and HIKOKICHI OURA

Department of Applied Biochemistry, Research Institute for Wakan-Yaku,
Toyama Medical and Pharmaceutical University,
Sugitani, Toyama 930-01, Japan

(Received August 2, 1986)

The chronic effect of oral administration of *Salviae Miltiorrhizae Radix* extract on renal tissue blood flow and blood pressure was investigated in uremic rats. Chronic administration of the aqueous extract from *Salviae Miltiorrhizae Radix* to rats significantly increased renal tissue blood flow by 32 and 38% on days 12 and 24, respectively. Blood pressure measured by the tail-cuff method was significantly decreased by 4–8% on the 6th, 18th, and 24th d. The uremia-alleviating action of *Salviae Miltiorrhizae Radix* extract is discussed on the basis of the present results.

Keywords—*Salviae Miltiorrhizae Radix*; uremic rat; renal tissue blood flow; blood pressure

It has previously been shown that the aqueous extract from *Salviae Miltiorrhizae Radix* was effective in rats with uremia induced by an adenine diet, during the course of screening 15 crude drugs used in traditional Chinese medicine for renal diseases and hemostasis.¹⁾ Furthermore, we have reported that the oral administration of *Salviae Miltiorrhizae Radix* extract to adenine-fed rats resulted in significant decreases of serum urea nitrogen, creatinine, methylguanidine, and guanidinosuccinic acid and increases in the excretion of urinary urea and creatinine, which suggested that *Salviae Miltiorrhizae Radix* might alleviate the uremic state by improving renal function.^{2–4)} In the present study, further investigations were carried out to determine the effects of chronic administration of this preparation on two parameters of renal function, *i.e.*, renal blood flow and blood pressure.

Materials and Methods

Animals and Treatments—Male Wistar rats of 10 weeks of age, initially weighing 280–300 g, were used in the experiment. The animals were fed *ad libitum* on an 18% casein diet containing 0.75% adenine. The 18% casein diet had the following composition (in 100 g): casein 18 g, α -cornstarch 57.9 g, sucrose 15 g, soybean oil 2 g, salt mixture⁵⁾ 4 g, vitamin mixture⁵⁾ 1 g, cellulose powder 2 g, and choline chloride 0.1 g. To this diet, adenine was added at the level of 0.75 g/100 g of the diet. The adenine feeding procedure produced experimental chronic renal failure, as reported previously.^{6–9)} During the adenine feeding period, *Salviae Miltiorrhizae Radix* extract was allowed *ad libitum* at a concentration of 1 mg/ml in water, while control rats were given tap water. The dose of *Salviae Miltiorrhizae Radix* extract was about 30 mg/rat/d during the experimental period. There were no statistically significant differences between the control and *Salviae Miltiorrhizae Radix* extract-treated groups with regard to body weight or food intake.

Extraction of *Salviae Miltiorrhizae Radix*—Roots of *Salviae Miltiorrhizae Radix* (*Salvia Miltiorrhiza* BUNGE), produced in China, and supplied by Tochimoto Tenkaido Co., Ltd., Osaka, Japan, were finely powdered and extracted with distilled water at 100 °C for 40 min (roots: water = 1 : 10, w/v), as described previously.¹⁾ The aqueous extract was filtered through 4 layers of gauze and the filtrate was freeze-dried under reduced pressure to leave a brown residue in a yield of about 25%.

Measurement of Blood Flow in Renal Tissue—Renal blood flow was determined with a needle-type bipolar electrode electrolytic organ rheometer (Biomedical Science Co., Ishikawa, Japan), by applying a hydrogen gas clearance method.^{10,11)} The procedure was as follows: rats were anesthetized by intraperitoneal administration of 30 mg/kg body weight of sodium pentobarbital (Abbott Laboratories, North Chicago, Ill., U.S.A.) and laparoto-

mized. Then, a needle-type electrode was obliquely inserted into the renal cortex 1—2 mm below the renicapsule, while plate-type Ag—AgCl electrodes were implanted under the skin. Electrodes A and B were used for the determination of hydrogen concentration and the generation of hydrogen gas, respectively. From electrode B a current of 10 μ A was applied to the renal cortex for 40 s, and the change in the polarocurrent of hydrogen gas generated was recorded. The half-life of the approximate index from each figure was then applied to the calculation of renal blood flow using the equation given below. Apparent blood flow based on the diffusion of hydrogen gas was obtained postmortem from the diffusion data.

$$\frac{69.3}{\text{half-life obtained from clearance curve (min)}} = \text{apparent blood flow based on the diffusion of hydrogen gas in the body (ml/100 g renal tissue/min)}$$

Measurement of Blood Pressure—For the determination of blood pressure, a RAT USM-105-R-type automatic sphygmotonomograph (Ueda Manufacturing Co., Tokyo, Japan) was used. Systolic blood pressure was determined in the rats without anesthesia.

Statistics—The significance of differences between the control and *Salviae Miltiorrhizae Radix* extract-treated groups was tested by the use of Student's *t*-test.

Results

Chronic Effect of *Salviae Miltiorrhizae Radix* Extract on Renal Blood Flow

Figure 1 compares the relative renal blood flow in rats of the three groups. On day 6, renal tissue blood flow in the control rats fed an adenine diet was significantly decreased by 17% as compared with normal rats, while renal tissue blood flow in the adenine-fed rats treated with *Salviae Miltiorrhizae Radix* extract tended to be slightly higher than in the control rats. On day 12, a significant fall of renal tissue blood flow in control rats was observed as compared with normal rats. At this time, treatment with *Salviae Miltiorrhizae Radix* extract significantly increased renal tissue blood flow by 32% from 73.1 ml/100 g tissue/min to 96.2 ml/100 g tissue/min ($p < 0.05$). When renal tissue blood flow in *Salviae Miltiorrhizae Radix* extract-treated rats was compared with that of normal rats, there was almost no difference. On day 24, a large decrease of renal tissue blood flow in control rats was noted in comparison with normal rats. At the same time, *Salviae Miltiorrhizae Radix* extract significantly increased the renal tissue blood flow by 38% from 56.6 ml/100 g tissue/min to 78.1 ml/100 g tissue/min ($p < 0.01$). Figure 2 shows representative examples of hydrogen gas clearance curves (left) and semi-logarithmic plots of these clearance curves (right) at 24 d after oral administration. Chronic administration of *Salviae Miltiorrhizae Radix* extract increased the rate of hydrogen gas clearance in renal tissue.

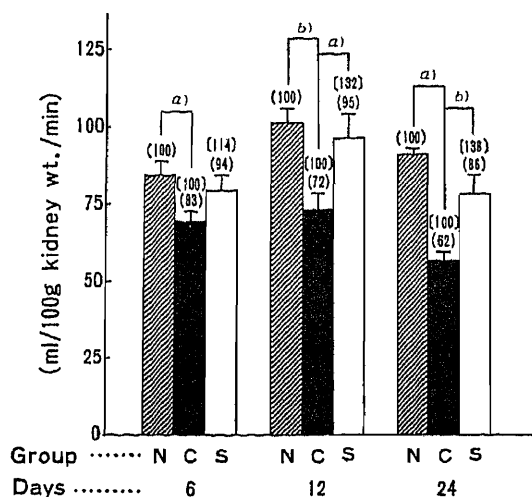


Fig. 1. Chronic Effect of *Salviae Miltiorrhizae Radix* Extract on Renal Tissue Blood Flow

N, normal rats; C, uremic rats (control group); S, uremic rats (*Salviae Miltiorrhizae Radix* extract-treated group).

Values are means \pm S.E. of 6 rats. Figures in parentheses are percentages of the normal or control value. a) Significantly different from the normal or control value, $p < 0.05$, b) $p < 0.01$.

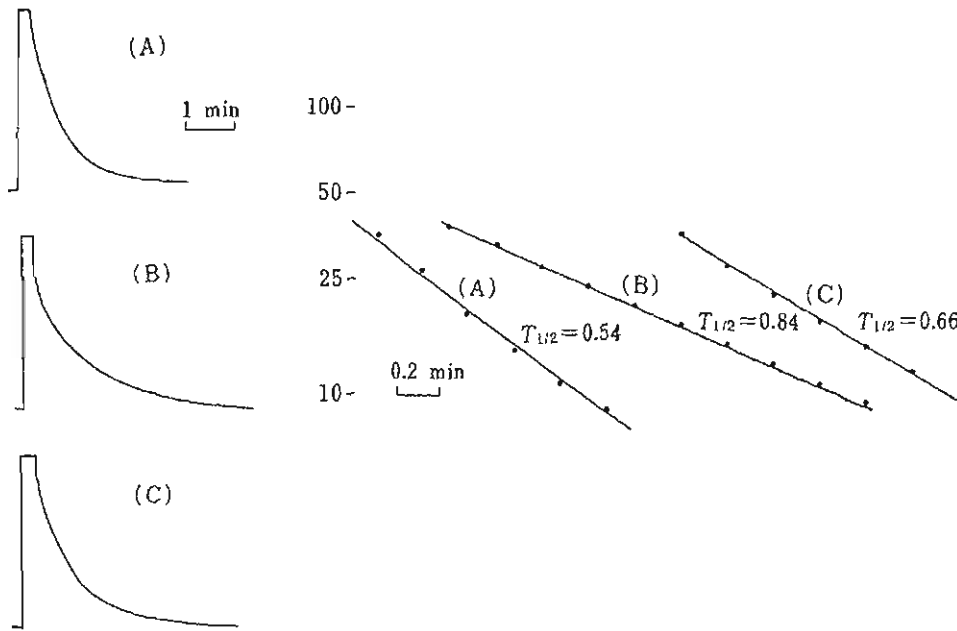


Fig. 2. Representative Examples of Hydrogen Gas Clearance Curves (Left) and Their Semi-Logarithmic Plots (Right)

A, normal rat; B, uremic rat (control group); C, uremic rat (*Salviae Miltiorrhizae Radix* extract-treated group).

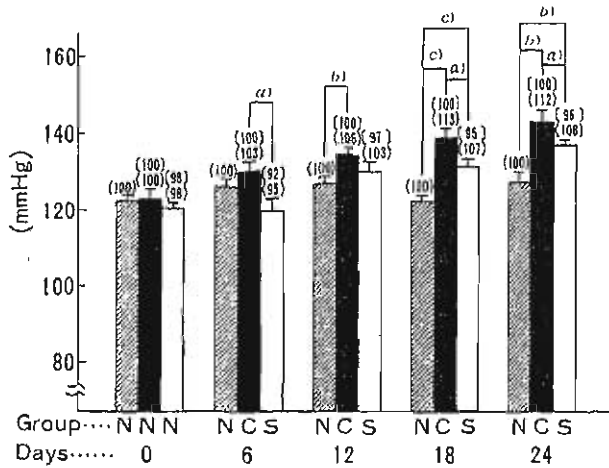


Fig. 3. Chronic Effect of *Salviae Miltiorrhizae Radix* Extract on Blood Pressure

N, normal rats; C, uremic rats (control group); S, uremic rats (*Salviae Miltiorrhizae Radix* extract-treated group).

Values are means \pm S.E. of 6 rats. Figures in parentheses are percentages of the normal or control value. a) Significantly different from the normal or control value, $p < 0.05$, b) $p < 0.01$, c) $p < 0.001$.

Chronic Effect of *Salviae Miltiorrhizae Radix* Extract on Blood Pressure

As shown in Fig. 3, there were no significant differences in blood pressure among the 3 groups on day 0 prior to administration of adenine. After the administration of adenine for 6 d, blood pressure was increased by 3% but there were no statistically significant differences as compared with normal rats. The administration of *Salviae Miltiorrhizae Radix* extract significantly decreased blood pressure by 8% from 129.9 to 119.5 mmHg ($p < 0.05$). On day 12 of adenine administration, blood pressure was significantly higher in control rats than in normal rats, but slightly lower in *Salviae Miltiorrhizae Radix* extract-treated rats (not significant). On day 18, blood pressure in control and *Salviae Miltiorrhizae Radix* extract-treated rats was significantly higher than that of normal rats. However, in extract-treated rats, blood pressure was decreased significantly by 5% ($p < 0.05$). On day 24 of adenine or extract administration, increases in blood pressure paralleling those on day 18 were noted. Blood

pressure in *Salviae Miltiorrhizae Radix* extract-treated rats was significantly lower than in control rats (137.0 mmHg vs. 143.0 mmHg, decrease rate 4%, $p < 0.05$).

Discussion

It is widely accepted that in renal failure, the renal blood flow naturally falls progressively. Decrease in the renal blood flow is accelerated by complications such as cardiac insufficiency, dehydration, electrolyte disorders, *etc.*, in addition to the changes in the kidneys themselves, and renal blood flow has a direct influence on the glomerular filtration rate.¹²⁾ On the other hand, patients with renal failure frequently have complicating hypertension. Generally, it is known that hypertension is caused by an increase of extracellular fluid and that it can also be associated with the renin-angiotensin-aldosterone system and vasopressor amines. At the same time, the existence of the prostaglandins, kinin-kallikrein system as an anti-vasopressor factor, and depressor substances has been proved.¹³⁾

In the present experiment, adenine-fed rats showed a decrease in renal blood flow on the 6th, 12th, and 24th d of 17–38% compared with normal rats. However, chronic treatment with *Salviae Miltiorrhizae Radix* extract increased the renal blood flow by 14–38%. This finding is also supported by a recent report that *Salviae Miltiorrhizae Radix* improves the circulation of the capillary blood vessels and increases coronary blood flow.¹⁴⁾

Renal blood flow is adjusted not only neurologically and humorally, but also by autoregulation.¹⁵⁾ These neurological and humoral factors are also associated with blood pressure.¹⁶⁾ In this study, therefore, we investigated the effect of *Salviae Miltiorrhizae Radix* extract on blood pressure, and it was found to significantly decrease the blood pressure in uremic rats. This result agrees with a report that *Salviae Miltiorrhizae Radix* has hypotensive activity clinically.¹⁷⁾ These observations imply that neurological and humoral factors responsible for lowering blood pressure may mediate an increase in renal blood flow. These effects of *Salviae Miltiorrhizae Radix* were in agreement with those which have been observed in rats given the traditional Chinese prescription “onpi-tô (wen-pi-tang)” composed of *Rhei Rhizoma*, *Ginseng Radix*, *Glycyrrhizae Radix*, *Zingiberis Rhizoma*, and *Aconiti Japonici Tuber*.¹⁸⁾

On the other hand, renal vascular resistance has generally been calculated by dividing the mean blood pressure by renal blood flow.¹⁹⁾ In the present experiment, renal vascular resistance in *Salviae Miltiorrhizae Radix* extract-treated rats was decreased by 20–30% compared with control rats. The fall in renal vascular resistance together with the increase of renal blood flow and decrease of blood pressure during *Salviae Miltiorrhizae Radix* extract administration is of interest. It may be that the diminished renal vascular resistance and the attendant increase in renal blood flow would be large enough to increase the glomerular filtration rate. It can thus be postulated that the increased renal blood flow produced by *Salviae Miltiorrhizae Radix* extract may contribute to the increases in the urinary excretion of uremic toxins such as urea, creatinine, electrolytes, and so forth, reported previously.³⁾

Though renal blood flow is an important determinant of renal function, it remains to be seen whether the observed increase in renal blood flow and decrease of renal vascular resistance produced by *Salviae Miltiorrhizae Radix* extract affects the renal elimination of uremic toxins. Further studies are therefore in progress in our laboratory to define more accurately the relative contributions of parameters of renal function to the observed improvement of uremic states by *Salviae Miltiorrhizae Radix* extract.

References

- 1) H. Oura, T. Yokozawa, and H. Y. Chung, *J. Med. Pharm. Soc. for WAKAN-YAKU*, 2, 434 (1985).
- 2) T. Yokozawa, H. Y. Chung, and H. Oura, *J. Med. Pharm. Soc. for WAKAN-YAKU*, 2, 446 (1985).

- 3) T. Yokozawa, H. Y. Chung, and H. Oura, *J. Med. Pharm. Soc. for WAKAN-YAKU*, **3**, 10 (1986).
- 4) H. Y. Chung, T. Yokozawa, and H. Oura, *Chem. Pharm. Bull.*, **34**, 3818 (1986).
- 5) A. E. Harper, *J. Nutr.*, **68**, 405 (1959).
- 6) T. Yokozawa, H. Oura, H. Nakagawa, and T. Okada, *Nippon Nôgeikagaku Kaishi*, **56**, 655 (1982).
- 7) T. Yokozawa, P. D. Zheng, and H. Oura, *Agric. Biol. Chem.*, **47**, 2341 (1983).
- 8) H. Oura, T. Yokozawa, P. D. Zheng, and F. Koizumi, *Igaku No Ayumi*, **130**, 729 (1984).
- 9) T. Yokozawa, P. D. Zheng, H. Oura, and F. Koizumi, *Nephron*, **44**, 230 (1986).
- 10) T. Harada, S. Miyagata, and H. Sakamoto, *Jpn. J. Nephrol.*, **26**, 745 (1984).
- 11) K. Koshu, S. Endo, A. Takaku, and T. Saito, *Neurological Surgery*, **9**, 1261 (1981).
- 12) S. Asano, "Renal Disease," ed. by K. Oshima, S. Asano, Y. Yoshitoshi, and Y. Ueda, Igaku Shoin, Tokyo, 1972, p. 990.
- 13) E. Kuwano and K. Arakawa, *Biomedicine & Therapeutics*, **14**, 337 (1985).
- 14) Microcirculation Research Group, Department of Pathophysiology, Shanghai First Medical College, *Chin. Med. J.*, **4**, 191 (1978).
- 15) N. K. Hollenberg, "Renal Disease," ed. by S. D. Black and N. F. Jones, Blackwell Scientific Publications, London, 1979, p. 30.
- 16) A. Golden, "The Kidney," ed. by A. Colden and J. Maher, The Williams and Wilkins Company, Baltimore, 1971, p. 6.
- 17) "Kanyaku No Rinsyo Ohyo," ed. by Chuzan Igakuin, Ishiyaku Shutsupan, Tokyo, 1980, p. 257.
- 18) P. D. Zheng, T. Yokozawa, H. Oura, and T. Nakada, *J. Med. Pharm. Soc. for WAKAN-YAKU*, **3**, 37 (1986).
- 19) D. M. Gomez, *J. Clin. Invest.*, **30**, 1143 (1951).

[Chem. Pharm. Bull.]
35(3)1162-1168(1987)

The Chemical Structure of an Antitumor Polysaccharide in Fruit Bodies of *Grifola frondosa* (Maitake)

HIROAKI NANBA,* ATSUKO HAMAGUCHI and HISATORA KURODA

Laboratory of Microbiology, Kobe Women's College of Pharmacy,
Motoyama, Higashinada, Kobe 658, Japan

(Received August 27, 1986)

A polysaccharide was extracted from fruit bodies of *Grifola frondosa* (maitake), and the chemical structure and antitumor activity were studied. The extracted polysaccharide could be hydrolyzed by β -glucanase into glucose, indicating it to be a β -glucan. The sample gave methyl 2,3,4,6-tetra-*O*-, methyl 2,4,6-tri-*O*-, methyl 2,3,4-tri-*O*- and methyl 2,4-di-*O*-methylglucoside in the molar ratio of 4:2:1:4 on methylation. In the carbon-13 nuclear magnetic resonance spectrum, the signals of C-6' (related to (1-6) bonding) and C-3' (related to (1-3) bonding) were observed in addition to those of free C-6 and C-3. These results indicate that the major chain is made up of β -1,6-linked glucose residues with branches of β -1,3-linked glucose. This glucan inhibited the growth of Sarcoma 180 tumor in ICR mice.

Keywords—*Grifola frondosa* (maitake); β -1,6 glucan; antitumor glucan; antitumor activity

Polysaccharides consisting of a β -1,3 glucopyranoside main chain with β -1,6-linked glucose branches have been isolated from various fungi belonging to *Basidiomycetes*. It has been reported that such polysaccharides possess antitumor activities.¹⁻⁴⁾ Furthermore, Kohno *et al.* obtained TC-13 polysaccharide possessing antitumor activity from *Actinomycetes*.⁵⁾ Recently, Miyazaki *et al.* obtained a 6-branched β -1,3 glucan from *Grifola frondosa*.⁶⁾ However, in the present investigation, we obtained an apparently different polysaccharide from *G. frondosa*.

Materials and Methods

Extraction of Polysaccharide—The process used for extracting polysaccharide from the powdered fruit bodies, which is illustrated in Fig. 1, is based on that described by Chihara for extraction of lentinan from shiitake (*Lentinus edodes*).⁷⁾ The powder (500 g) was mixed with 5000 ml of deionized water. The mixture was heated at 100°C for 10 h and centrifuged (at 6000 rpm for 10 min), then the supernatant and an equal volume of EtOH were combined and left at 4°C for 12 h. The precipitate was separated and dissolved in deionized water. Then, 25% cetyltrimethylammonium hydroxide (CTA-OH) was added dropwise with stirring until the pH exceeded 12 and the mixture was allowed to stand at 4°C for 12 h to obtain about 14 g of pellet. This pellet was treated with 20% and then 50% acetic acid to remove the acid-soluble fraction. About 3 g of substance insoluble in the acids was obtained. It was treated with 6% NaOH to separate the alkali-soluble fraction. The solution was then combined with 4 volumes of EtOH to precipitate polymers. The pellet thus obtained was dissolved in water and the solution was treated with a 2:1 mixture of CHCl₃ and MeOH to remove protein. The solution was again treated with 4 volumes of EtOH. The resulting pellet was a light brown powder, which was insoluble in cold water, was positive for the anthrone reaction, and contained about 22% protein, as determined by Lowry's method. Based on these results, this substance was considered to be a proteoglycan.

Carbon-13 Nuclear Magnetic Resonance (¹³C-NMR) Spectrum—A solution was prepared from 10 mg of sample, 0.8 ml of heavy water and NaOH to make 0.2M, and the spectrum was taken on a Varian XL-200 (50.3 MHz) at 40°C with acetonitrile as the standard.

Methanolysis—To determine the constituent monosaccharide, 1 mg of the proteoglycan was methanolized in 1 ml of 5% (w/w) HCl in MeOH solution at 100°C for 6 h in a sealed tube. The product was diluted with toluene-EtOH (1:1), and the mixture was dried under reduced pressure to remove HCl. After trimethylsilylation, it was

analyzed by gas liquid chromatography (GLC).

Enzymatic Digestion—(i) α - and β -Glucosidase: The sample (1 mg) was dissolved in 1.5 ml of 1/15 M phosphate buffer containing 0.1 mg of either α -glucosidase (pH 6.8) or β -glucosidase (pH 5.25) and incubated at 37°C.

(ii) *exo*- β -1,3 Glucanase: The enzyme (0.1 mg) and the sample (1 mg) were dissolved in 1 ml of 1/10 M McIlvaine buffer (pH 5.0). The mixture was incubated at 50°C for 24 h then supplemented with an equal volume of enzyme solution and further incubated for another 48 h. This enzyme has been purified from a culture solution of *Tricoderma* spp. in our laboratory.

Methylation Analysis—In order to investigate the modes of linkages of monomer units in the polysaccharides, the sample was methylated by Hakomori's method.⁸⁾ After complete methylation, 2 ml of 5% (w/w) HCl-MeOH solution was added, and the methylated products were hydrolyzed at 100°C in a sealed tube. The methylated sugars were analyzed by GLC using a Shimadzu NGS column.

Smith Degradation—Smith degradation was performed in order to determine whether the 1,6 linkage exists in the main chain or as branches. The sample (5 mg) was dissolved in 1 ml of water, and this solution, 20 ml of 0.1 M acetic acid-sodium acetate buffer (pH 4.6) and 30 ml of 0.1 M sodium metaperiodate were combined. The mixture was diluted with deionized water to make 100 ml. The solution was stirred at 4°C for 144 h in the dark. After completion of the reaction, 1 g of sodium borohydride was added, and the reaction mixture was allowed to stand for 30 h at 25°C. The solution was adjusted to pH 4.0 with 6 N acetic acid and evaporated *in vacuo*. The residue was washed 3 times with 3 ml of MeOH. The precipitate was dissolved in water, and adjusted to pH 1.0 with 1 M sulfuric acid. The solution was allowed to stand for 24 h at 25°C, then filtered. The filtrate was evaporated and the residue was dissolved in 1 ml of water. The solution was submitted to gel filtration on a Sepharose CL-4B column (1.5 × 23 cm) to determine the molecular weight distribution.

Sedimentation Velocity—The sedimentation pattern and velocity was measured at 60000 rpm by using an analytical ultracentrifuge (Hitachi 282 with RA-60H rotor, single cell) equipped with the Schlieren's method.

Antitumor Activity—(i) Transplantation Method: Sarcoma 180 tumor cells from the peritoneal cavity of male ICR mice (7 weeks old) were suspended in Hanks' solution and 2×10^6 cells were injected subcutaneously in the axillary region of male ICR mice (5 weeks old).

(ii) Administration of Sample and Measurement of Tumor Size: Given amounts of the sample were injected into the peritoneal cavity of mice daily for 10 d starting from either the 1st or the 9th day after the implantation of the tumor cells. The solid tumor was removed and weighed on the 13th day after the treatment was completed. The inhibition ratio (%) was calculated as follows. $[1 - (\text{weight of tumor mass from animals treated with drug} \div \text{weight of tumor mass from animals receiving no treatment})] \times 100$.

(iii) Disc Electrophoresis of the Serum: Mice were treated intraperitoneally with 1 or 10 mg/kg of the sample, and every 6 h, the blood was withdrawn from the caudal vein. The serum was separated, 10 μ l was applied to a polyacrylamide gel plate (pH 8.2), and electrophoresis was carried out at a current of 5 mA.

Results and Discussion

The results of chromatography of the sample, purified by the process shown in Fig. 1, on a Sepharose CL-4B column are illustrated in Fig. 2. The sample gave two fractions, MT-1a and MT-1b. The molecular weight of the former is about 1.8×10^5 while that of the latter is approximately 3×10^4 . Both of them were proteoglycans containing about 18.2 and 50% protein, respectively. MT-1a, containing less protein, was further separated into 4 subfractions on a diethylaminoethyl (DEAE)-Sepharose CL-6B column as shown in Fig. 3. MT-2 and MT-2' were eluted from the column with 1/15 M phosphate buffer (pH 7.2) and MT-3 and MT-3' were eluted with the same buffer containing 0.25 M NaCl. MT-2, which consists mainly of polysaccharides passing through the column without retention, and MT-3, containing a considerable amount of protein, were dialyzed and further chromatographed on a Sephadex G-25 column to remove salts. The desalted MT-2 and MT-3 fractions contained 0.6 and 6.6% protein, respectively. MT-2 showed an apparent molecular weight of 2×10^6 , but this might reflect association of lower-molecular-weight species. The purified major fraction MT-2 gave a single peak ($s_{20,w} = 6.09$) on ultracentrifugal analysis, suggesting that the substance eluted in this fraction is a polysaccharide essentially uniform in molecular weight. In order to identify the constituent monosaccharides, MT-2 was trimethylsilylated after methanolysis. The GLC gave only glucose, indicating that the polysaccharide is a glucan. When the polysaccharide was treated with α - and β -glucosidase, only β -glucosidase could hydrolyze it into glucose, and it was hydrolyzed by a highly specific *exo*- β -1,3-glucanase from *Tricoderma*, as shown in

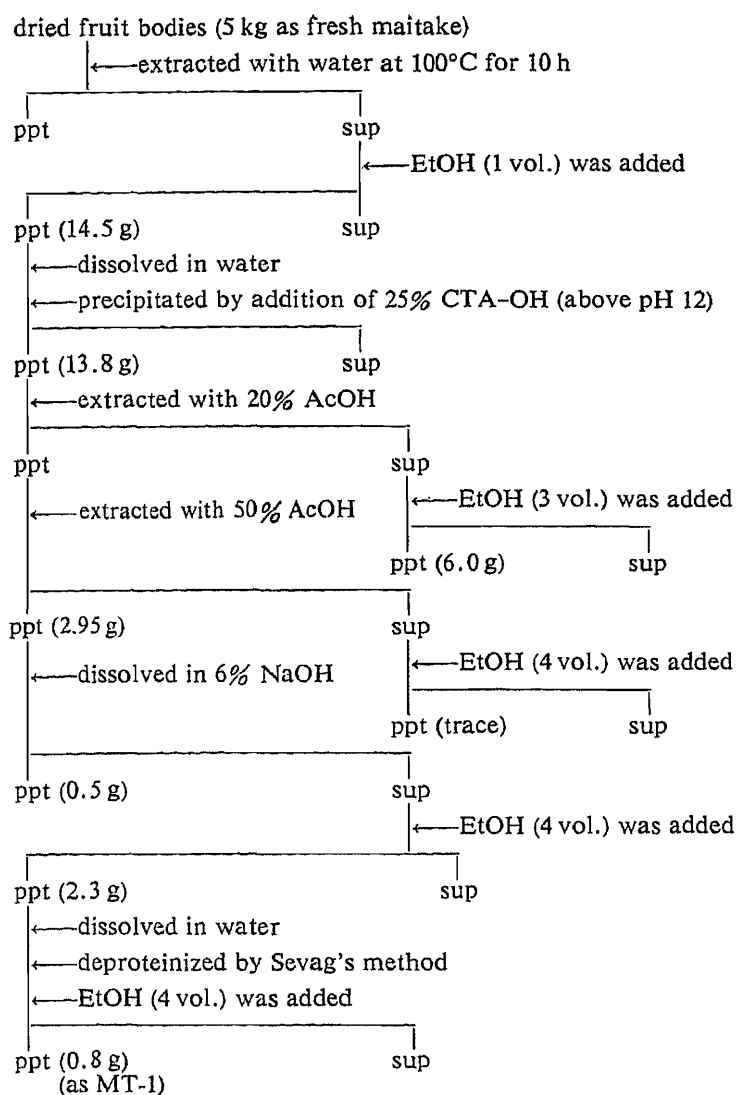
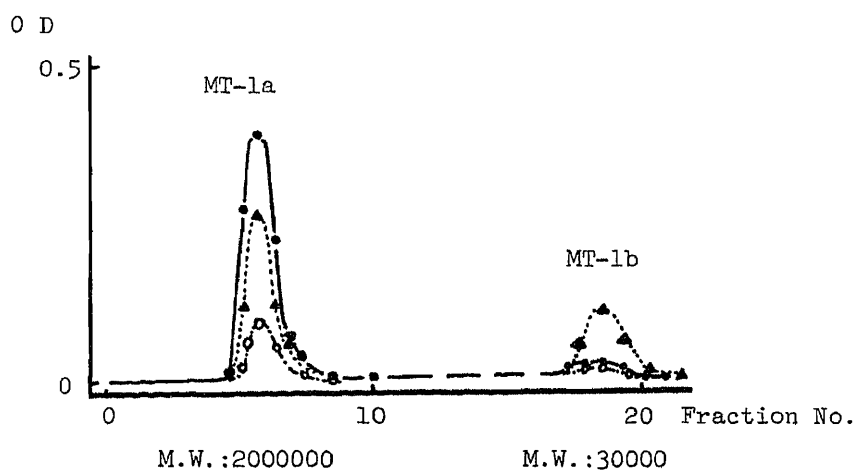
Fig. 1. Extraction of Polysaccharides from *G. frondosa*

Fig. 2. Elution Profile of MT-1 from a Sepharose CL-4B Column

Column, 2.5 × 45 cm; 5.25 ml/fraction.

●—●, 620 nm; ▲—▲, 280 nm; ○—○, 750 nm.

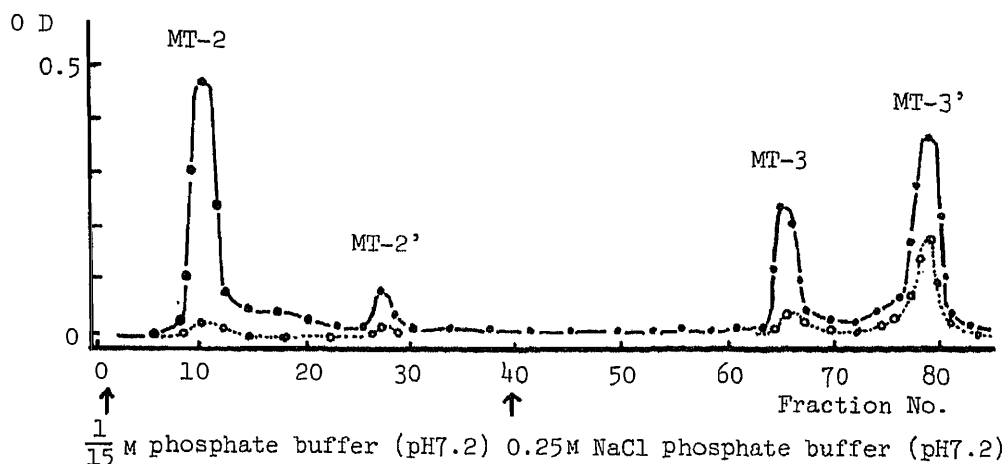


Fig. 3. Elution Profile of MT-1a from a DEAE-Sepharose CL-6B Column

Column, 3.0 × 32 cm; 8.3 ml/fraction.

●—●, 620 nm; ○---○, 280 nm.

TABLE I. Susceptibilities of MT-1a, MT-2 and MT-3 to Glucosidases

Enzyme	Liberated glucose (mg) ^{a)}		
	MT-1a	MT-2	MT-3
α-Glucosidase	—	—	—
β-Glucosidase	0.16	0.21	0.13
exo-β-1,3 Glucanase	0.45	0.43	0.36

a) Glucose liberated (mg) from 1.00 mg of sample.

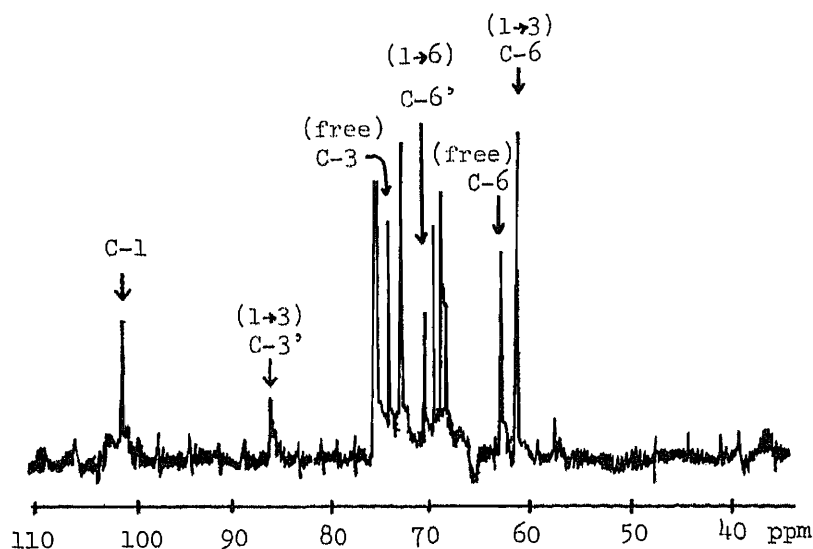
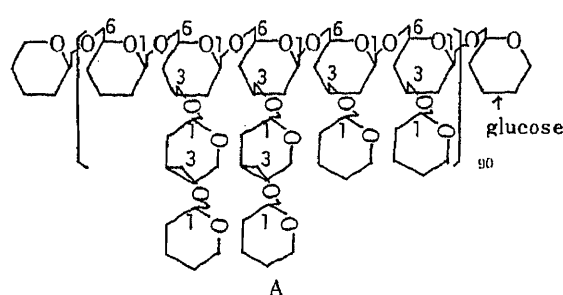


Fig. 4. ¹³C-NMR Spectrum of MT-2

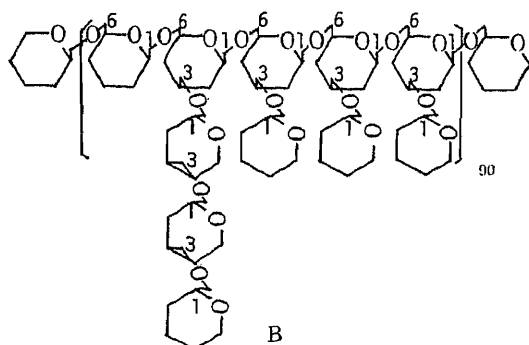
Table I. After a 24 h incubation, about 45% of glucose residues were liberated, indicating that at least 45% of glucose residues are included in chains made up of β-1,3-linked glucose units with non-reducing terminal glucose units. Furthermore, in the ¹³C-NMR spectrum, as shown in Fig. 4, the signals of C-6' (70.7 ppm) (related to (1→6) bonding) and C-3' (87.4 ppm) (related

TABLE II. Gas Liquid Chromatographic Analyses of Methylated MT-2 and MT-3

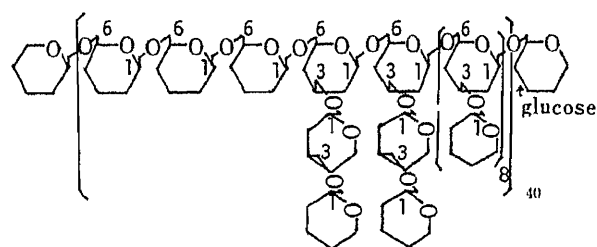
Methyl glucopyranoside of	Molar ratio	
	MT-2	MT-3
2,3,4,6-Tetra- <i>O</i> -Me-glucose	4.00	5.00
2,4,6-Tri- <i>O</i> -Me-glucose	1.97	1.00
2,3,4-Tri- <i>O</i> -Me-glucose	1.00	1.87
2,4-Di- <i>O</i> -Me-glucose	4.00	5.00



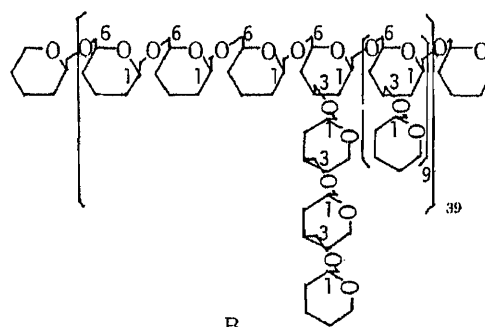
A



B



A



B

Fig. 5-a. Probable Structures of MT-2

Fig. 5-b. Probable Structures of MT-3

to (1-3) bonding) were observed in addition to free C-6 and C-3, suggesting that MT-2 is a β -glucan with 1,6- and 1,3-bonding. Subsequently, the sample was methylated and analyzed to examine the mode of linkage. As shown in Table II, MT-2 gave methyl 2,3,4,6-tetra-*O*-, methyl 2,4,6-tri-*O*-, methyl 2,3,4-tri-*O*- and methyl 2,4-di-*O*-methylglucopyranosides in the molar ratio of 4:2:1:4. In MT-3, the molar ratio was 5:1:2:5. These results mentioned above indicate that the polysaccharides in both MT-2 and MT-3 are highly branched and made up of chains of glucose units with β -1,3 and β -1,6 linkages. The yield of MT-2 was 0.62 g from 5 kg of dried fruit bodies of maitake and that of MT-3 was 0.27 g. In order to clarify whether the 1,6 linkages are present in the main chain or the branches, Smith degradation was carried out. Gel filtration on a Sepharose CL-4B column following the degradation revealed that the molecular weight of MT-2 was reduced from 1.8×10^5 to less than 3×10^4 . As 1,3- or 1,3,6-linked glucose chains are resistant to periodate oxidation, the reduction of molecular weight of MT-2 indicates that the 1,6-linked glucose units from the main chain. Based on the results mentioned above, as shown in Fig. 5-a and Fig. 5-b. It is concluded that the MT-2 is made up of β -1,6-linked glucose residues with β -1,3-linked glucose branches.

Generally, polysaccharides isolated from various fungi of *Basidiomycetes* are C-6-branched β -1,3-linked glucans.^{1-3,7)} Recently, Miyazaki *et al.* reported that the neutral glucan extracted from *G. frondosa* contained mainly α -1,4 and 6-branched β -1,3 linkages and

TABLE III. Antitumor Activities of MT-1a and MT-2 against Sarcoma 180 Transplanted in ICR Mice

Agent	Doses (mg/kg/d × 10)	From 1st day after transplantation		From 9th day after transplantation	
		Tumor wt. (g)	TIR (%)	Tumor wt. (g)	TIR (%)
Saline	—	3.4 ± 1.5	—	4.9 ± 0.7	—
MT-1a	1	0.7 ± 0.5 ^{a)}	79.9	0.7 ± 0.7	86.6
	10	1.1 ± 0.2 ^{a)}	69.1	0.7 ± 0.6 ^{b)}	86.0
	20	1.1 ± 0.6 ^{b)}	69.4	3.9 ± 0.1 ^{a)}	20.6
MT-2	1	0.7 ± 0.3 ^{b)}	80.2	—	—
PS-K	300	7.1 ± 0.3	-4.7	5.3 ± 0.3 ^{b)}	-7.1
Lentinan	1	2.9 ± 0.8 ^{b)}	33.6	2.3 ± 2.6	54.4

t-Test: a) $p < 0.01$, b) $p < 0.05$. Mice: 8—10 × 2.

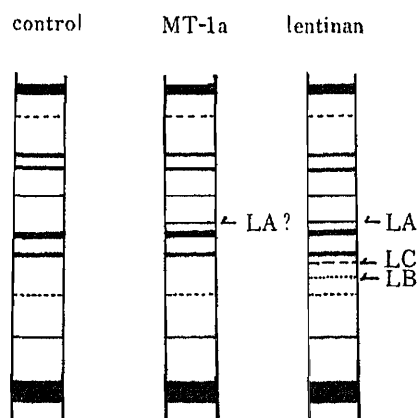


Fig. 6. Disc-Electrophoretograms of Sera from MT-1a-Inoculated Mouse (after 72 h)

the acidic glucan contained β -1,6 and 6-branched β -1,3 linkages.⁶⁾ However, the authors have obtained a highly branched polysaccharide different from the glucan which was isolated from the same fungus by Miyazaki *et al.* The structures of our polysaccharides remain to be fully clarified; Fig. 5 shows some possibilities for MT-2 and MT-3. Yadomae *et al.* found that 6-branched β -1,3-linked neutral and acidic glucans showed potent antitumor activity against Sarcoma 180 solid tumor.⁶⁾ Therefore, the antitumor activities of this C-3-branched β -1,6-linked polysaccharide were investigated as mentioned above. Mice were treated with MT-1a and MT-2 from the 1st or 9th day after implantation of Sarcoma 180. The results are given in Table III. When mice were treated with 1—20 mg/kg/d of MT-1a daily for 10 d starting from the 1st day after the implantation, the inhibition rates ranged from 69.1 to 79.9%. The rates were 86.0 and 86.6% when 1 mg and 10 mg/d of MT-1a were started from the 9th day after implantation, respectively. These results suggest that the antitumor activity of MT-1a is more potent than that of lentinan (prepared in our laboratory from *L. edodes*) employed as a positive control. The relation of antitumor activity of polysaccharides with chemical structure mostly remains to be elucidated, but, among β -1,3-linked glucans with 1,6-glucoside branches, such as scleroglucan,¹⁰⁾ schizophyllan,³⁾ grifolan¹³⁾ and lentinan, lentinan, which is most highly branched, is most active. The present glucan possesses antitumor activity more potent than that of lentinan, possibly partly because the degree of branching is greater than that of lentinan. As a part of studies to elucidate the mechanism of antitumor activity of the glucan, sera were taken from ICR mice at various intervals after administration of MT-1a and

analyzed by polyacrylamide gel electrophoresis. According to Chihara *et al.*¹¹⁾ LA, LC and LB proteins in the α - and β -regions of the serum increase transiently when animals are treated with lentinan, which shows antitumor action through activation of cellular immunity. When 1—10 mg of MT-1a was administered, a new protein appeared at the position corresponding to LA protein after 24 h and the band became most intense after 72 h as shown in Fig. 6. The significance of the new serum protein remains to be studied, but it has been reported that the synthesis of this protein is also induced by immunopotentiators such as zymosan,¹¹⁾ picibanil¹²⁾ and grifolan.⁴⁾ In conclusion, the authors have isolated a highly branched peptide-polysaccharide from fruit bodies of *G. frondosa*; it comprises about 0.6% protein and has a β -1,6-linked glucan main chain with 1,3-linked branches. It inhibits the growth of an allogeneic tumor in mice through the activation of cellular immunity. The effect on a syngeneic tumor and the influence on macrophages, natural killer cells and T cells will be reported shortly.

Acknowledgement The authors wish to thank Dr. Kanichi Mori and Mr. Tetsuro Toyomasu, Mushroom Research Institute of Japan, for supplying Maitake.

References

- 1) Y. Y. Maeda, J. Hamuro, Y. O. Yamada, K. Ishimura and G. Chihara, "Immunopotential," ed. by G. E. W. Wolstenholme and J. Knight, Elsevier, Excerpta Medica, North Holland, 1973, p. 259.
- 2) G. Chihara, Y. Y. Maeda, J. Hamuro, T. Sasaki and F. Fukuoka, *Nature* (London), **222**, 687 (1969).
- 3) N. Komatsu, S. Okubo, S. Kikumoto, K. Kimura, G. Saito and S. Sasaki, *Gann*, **60**, 137 (1969).
- 4) N. Ohno, K. Iino, T. Takeyama, I. Suzuki, K. Sato, S. Oikawa and T. Miyazaki, *Chem. Pharm. Bull.*, **33**, 3395 (1985).
- 5) M. Kohno, S. Abe, M. Tamazaki and D. Mizuno, *Gann*, **73**, 488 (1982).
- 6) N. Ohno, K. Iino, I. Suzuki, S. Oikawa, K. Sato, T. Miyazaki and T. Yadomae, *Chem. Pharm. Bull.*, **33**, 1181 (1985).
- 7) G. Chihara, J. Hamuro, Y. Arai and F. Fukuoka, *Cancer Res.*, **30**, 2776 (1970).
- 8) S. Hakomori, *J. Biochem.* (Tokyo), **55**, 205 (1964).
- 9) G. Chihara, J. Hamuro, Y. Y. Maeda, Y. Arai and F. Fukuoka, *Cancer Res.*, **30**, 2776 (1970).
- 10) J. Johnson, Jr., S. Kirkwood, M. Misaki, T. E. Nelson, J. V. Scaletti and F. Smith, *Chem. Ind.* (London), **1963**, 820.
- 11) Y. Y. Maeda, G. Chihara and K. Ishimura, *Nature* (London), **252**, 250 (1974).
- 12) T. Torikai, O. Itoh, S. Toyoshima and T. Osawa, *Gann*, **69**, 657 (1978).
- 13) N. Ohno, M. Hayashi, I. Iino, I. Suzuki, S. Oikawa, K. Sato, Y. Suzuki and T. Yadomae, *Chem. Pharm. Bull.*, **34**, 2149 (1986).

[Chem. Pharm. Bull.]
35(3)1169—1175(1987)

Inhibitory Effects of Tannic Acid on the Respiratory Chain of *Photobacterium phosphoreum*

KIYOSHI KONISHI,^{*,a} HIROKAZU ADACHI,^b KIYOSHI KITA,^c
and ISAMU HORIKOSHI^b

*Department of Biochemistry, Faculty of Medicine,^a Department of Hospital Pharmacy,^b
Toyama Medical and Pharmaceutical University, Sugitani, Toyama 930-01, Japan
and Department of Parasitology, Juntendo University,^c
School of Medicine, Hongo, Tokyo 113, Japan*

(Received September 10, 1986)

Tannic acid inhibited the growth of *Photobacterium phosphoreum* in liquid culture and also decreased the viability, expressed in terms of the colony forming activity.

The activity of glucose dependent oxygen consumption of whole cells was inhibited by tannic acid. It was found that the activity of reduced nicotinamide adenine dinucleotide (NADH) oxidase of the sonicated membrane of *Photobacterium phosphoreum* decreased when tannic acid was added to the assay system. The results suggested that the targets of tannic acid action were NADH dehydrogenase and the terminal oxidase.

The inhibitory effect of tannic acid on the terminal oxidase was compared in the cases of purified terminal oxidase (cytochrome b560-d complex) and sonicated membrane vesicles. The oxidase activities toward ubiquinol-1 and *N,N,N',N'*-tetramethyl-*p*-phenylenediamine dihydrochloride (TMPD) in the presence of ascorbate were both inhibited by tannic acid in both sonicated membrane and purified cytochrome b560-d complex. The inhibition of ubiquinol-1 oxidase activity in sonicated membrane was biphasic and noncompetitive in both phases. The inhibition of the ubiquinol-1 oxidase activity of purified terminal oxidase was monophasic and noncompetitive. On the other hand, the inhibition of TMPD oxidase activity in the presence of ascorbate in both membrane vesicles and purified enzyme was uncompetitive. Thus, the mechanisms of inhibition of the two kinds of oxidase activity by tannic acid were different.

Keywords—tannic acid; cytochrome b560-d; *Photobacterium phosphoreum*; terminal oxidase; respiratory chain

We have previously purified to near homogeneity and characterized the terminal oxidase complex of *Photobacterium phosphoreum*.¹⁾ This enzyme contains two polypeptides (54000 and 41000), with protoheme and heme d as prosthetic groups. Moreover, the purified oxidase showed *N,N,N',N'*-tetramethyl-*p*-phenylenediamine dihydrochloride (TMPD)-dependent oxygen consumption in the presence of ascorbate or ubiquinol-1 as a substrate, and the enzyme is involved in the pathway of oxidative phosphorylation.

Tannic acid contained in Chinese nutgall is a polyphenol and is composed of glucose and gallic acid.²⁻⁵⁾ The known pharmaceutical effects of this compound are astringency and antimicrobial action.³⁾ However, the antimicrobial effect has not yet been studied from a biochemical viewpoint.

In this work, we found that the growth of *Photobacterium phosphoreum* was inhibited by tannic acid and that the targets of tannic acid in the respiratory chain were reduced nicotinamide adenine dinucleotide (NADH) dehydrogenase and the terminal oxidase (cytochrome b560-d complex). In order to understand the mechanism of action of this acid, we carried out some kinetic studies of the enzymes that were affected by tannic acid.

Materials and Methods

Organism—Strain IAM12085 of *Photobacterium phosphoreum* was obtained from the Institute of Applied Microbiology, The University of Tokyo, and was grown in the medium described previously.⁶⁾ Inocula of 10 ml of seed culture were incubated in 2-l volumes of medium in 5-l glass containers at 25 °C for 20 h with vigorous aeration by shaking, and cells were harvested in the middle of the exponential phase of growth. The yield was 5 g wet weight of cells/l. The cells were stored at –20 °C before use.

Preparation of Cytochrome b560-d Complex—The procedures for solubilization and purification of the cytochrome b560-d complex were as described previously.¹¹⁾

Preparation of Sonicated Membrane—The frozen cell pellet was thawed and suspended with buffer A (10 mM Tris-HCl (pH 7.0), 10 mM MgCl₂). The suspension was sonicated with a Tomy Seiko UR-200P ultrasonic disruptor with cooling in an ice bath. The sonicated lysate was centrifuged at 20000 × *g* for 1 h, and the supernatant obtained was centrifuged at 100000 × *g* for 1 h. The precipitate was washed twice with buffer A by centrifugation. The membrane vesicle preparation obtained was used for the experiments.

Assay of Oxidase Activity—Ubiquinol-1 oxidase activity was assayed as described previously.⁷⁻⁹⁾ A mixture (20 μl) of cytochrome b560-d complex (1 μg), phospholipids (acetone washed soybean phospholipids, asolectin 2 mM), and 50 mM Tris-HCl (pH 7.5) was incubated at 4 °C for 5 min, and the activity was measured at 25 °C by recording the increase of absorbance of ubiquinol-1 at 278 nm. The activities for oxidation of NADH, and oxidation of TMPD in the presence of ascorbate were measured according to the methods of Kasahara and Anraku,¹⁰⁾ and Kita *et al.*,⁷⁾ respectively, using a Clark type oxygen electrode (Rank Brothers, Rank oxygen electrode). The NADH oxidase activity of whole cells was assayed after preincubation of the cells in the assay chamber for 30 min.

Assay of NADH Dehydrogenase Activity—Assay of NADH-menadione dehydrogenase activity was carried out by the method described previously.¹¹⁾ The concentrations of NADH and menadione were 150 and 200 μM, respectively.

Other Method—Protein was determined by the method of Lowry *et al.*¹²⁾ with bovine serum albumin as a standard.

Chemicals—Ubiquinol-1 was a generous gift from Eisai Co., Ltd. Five lots of tannic acid purchased from 4 companies were used in our experiment (No. 1, Wako Pure Chemical lot No. KWP7592; No. 2, Wako Pure Chemical lot No. EPR7215; No. 3, Nakarai Chemicals lot No. M4R1112; No. 4, Kanto Chemical lot No. 001H5101; No. 5, Sigma-lot No. 64F-0049).

Only the data obtained with tannic acid No. 1 are presented in this paper, but the results with other tannic acids were almost the same (data not shown).

Results

Effect on the Growth of *Photobacterium phosphoreum*

First of all, we examined the effect of tannic acid on the growth of *P. phosphoreum* in liquid culture (Fig. 1). The doubling time of cell growth increased about 1.5-fold when 100 μg/ml of tannic acid was added to the culture medium. The final growth yield of cells decreased drastically above 200 μg/ml of tannic acid. There was no effect on the growth in the presence of tannic acid at concentrations below 10 μg/ml. The cells could not grow at all at about 250 μg/ml of inhibitor. Similar results were obtained in plate cultivation (Fig. 2). Cells were not viable in the presence of more than 500 μg/ml of the inhibitor. No effect was observed in the presence of tannic acid at below 10 μg/ml. It is clear that tannic acid is a potent inhibitor of the growth of *Photobacterium phosphoreum*.

To determine whether the inhibitory effect of tannic acid is bacteriocidal, bacteriostatic, or bacteriolytic, we examined the growth curve of cells after addition of the inhibitor. When 200 μg/ml of tannic acid was added to the culture medium, the increase of turbidity of the culture (monitored by measuring the absorbance at 650 nm) was interrupted and the turbidity remained unchanged for at least 5 h. The viable cell count (based on the ability to form colonies) showed a similar pattern (data not shown). These results indicated that the type of inhibitory effect was bacteriostatic.

The effect of tannic acid on bacterial growth was essentially the same among 5 lots from 4 companies (see Materials and Methods).

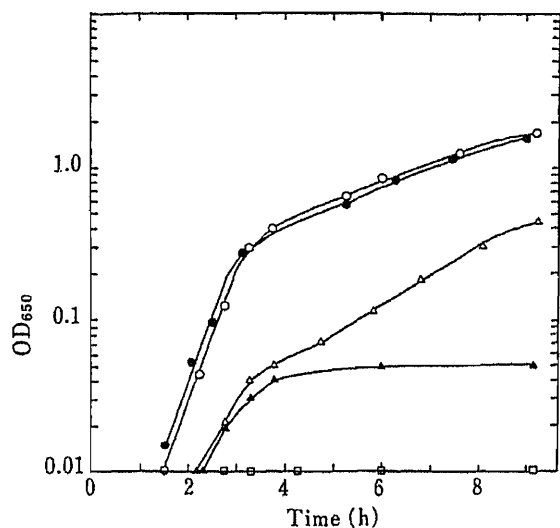


Fig. 1. Effect of Tannic Acid on the Growth of *P. phosphoreum* in Liquid Culture

Tannic acid was added at 0 time to the culture medium: (●), 10 $\mu\text{g/ml}$; (△), 100 $\mu\text{g/ml}$; (▲), 200 $\mu\text{g/ml}$; (□), 250 $\mu\text{g/ml}$; (○), control (no addition). The conditions of culture are described in Materials and Methods.

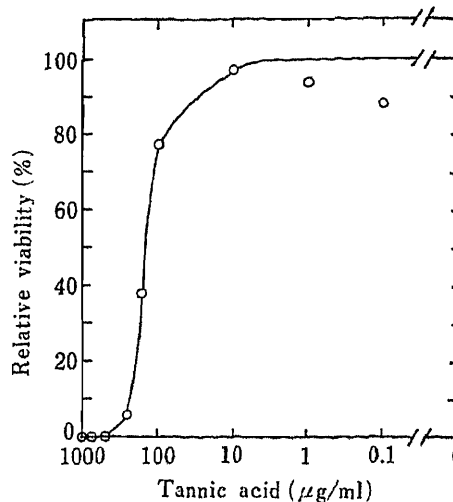


Fig. 2. Effect of Tannic Acid on the Viability of *P. phosphoreum*

The cultivation was carried out on plates at 25°C for 48 h. The number of colonies was counted, and relative viability was expressed as the ratio of the number of colonies in the presence of tannic acid to the control.

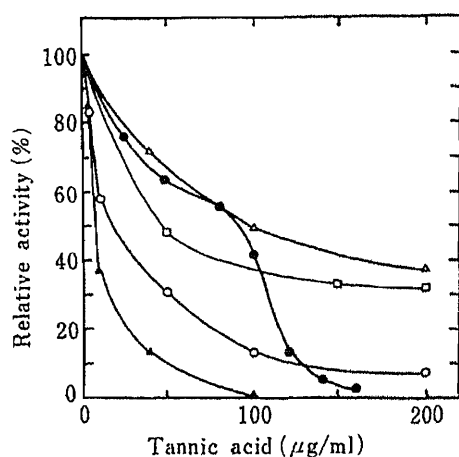


Fig. 3. Inhibition by Tannic Acid of the Electron Transfer Activities of *P. phosphoreum*

Whole cells were used for NADH oxidase activity assay (□). Other activities were assayed with sonicated membranes. (▲), NADH oxidase; (○), NADH dehydrogenase; (●), ubiquinol-1 oxidase; (△), TMPD+ascorbate oxidase. NADH dehydrogenase activity was determined by NADH-menadione assay.¹¹⁾ NADH oxidase activity was assayed with a Clark type electrode by the reported method.¹⁰⁾ In each assay, the enzyme preparation was incubated with the indicated concentration of tannic acid at 25°C for 5 min.

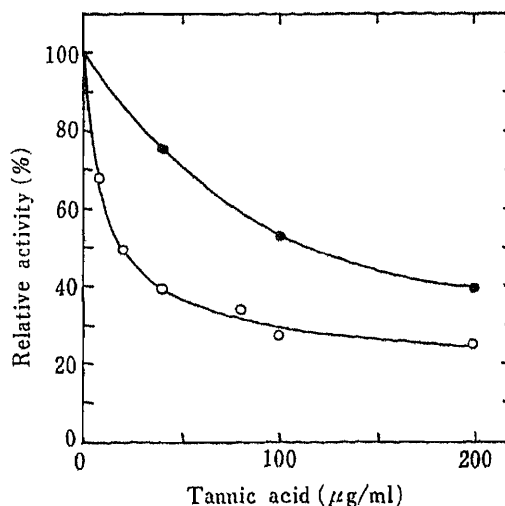


Fig. 4. Inhibition by Tannic Acid of the Electron Transfer Activities of Purified Cytochrome b560-d Complex of *P. phosphoreum*

The assay procedures were the same as described in the legend to Fig. 3. The ubiquinol-1 oxidase (○) and TMPD+ascorbate oxidase activities (●) were measured.

Effect on the Electron Transfer Activities of the Respiratory Chain

As shown in Fig. 1 and Fig. 2, tannic acid was an effective inhibitor of the growth of *P. phosphoreum*. The respiratory chain is one of the primary systems which regulate growth, so

we studied various activities of the respiratory chain of *P. phosphoreum* in an *in vitro* assay system. In the case of whole cells, glucose-dependent oxidase activity was not inhibited in the presence of 200 $\mu\text{g}/\text{ml}$ of tannic acid, if preincubation of whole cells with the inhibitor was omitted before the assay (data not shown). This result indicates that it is difficult for tannic acid to pass through the outer membrane, peptide glycan, or inner membrane of whole cells. The inhibitor was probably taken up slowly by simple diffusion into cells. Indeed, after incubation for 30 min, the oxidase activity was inhibited by tannic acid (Fig. 3).

In order to avoid this complication, we used sonicated membrane for this experiment. Figure 3 shows that tannic acid quite effectively inhibited NADH dehydrogenase and NADH oxidase, and less effectively inhibited TMPD oxidase activity (in the presence of ascorbate) and ubiquinol-1 oxidase activity of the respiratory chain. At the concentration of 50 $\mu\text{g}/\text{ml}$, tannic acid inhibited about 90% of NADH oxidase activity, about 70% of NADH dehydrogenase activity, and about 30% of TMPD oxidase activity. Since the NADH oxidase activity includes the activities of NADH dehydrogenase and ubiquinol oxidase, the site of inhibition should be either NADH dehydrogenase or cytochrome b560-d complex. NADH dehydrogenase of *P. phosphoreum* has not been characterized well. NADH–menadione (Fig. 3) and NADH–ferricyanide (data not shown) were detected in sonicated membrane vesicles in this experiment. The NADH dehydrogenase activity was activated by addition of KCN in the absence of tannic acid, but was decreased by addition of KCN in the presence of the inhibitor. We do not know the reason for this at present. In the following study, we examined only the

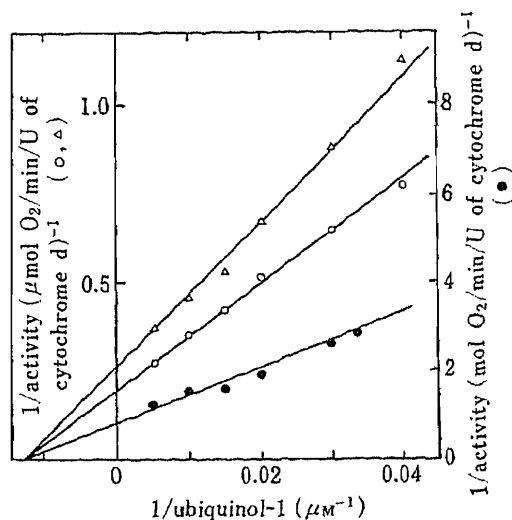


Fig. 5. Double-Reciprocal Plot of the Effect of Tannic Acid on Ubiquinol-1 Oxidase Activity in Membrane Vesicles of *P. phosphoreum*

The assay mixture, in a total volume of 1 ml, contained 0.1 mg of membrane, 50 mM Tris-HCl (pH 7.5), various concentrations of ubiquinol-1, and/or tannic acid. (O), no addition; (Δ), in the presence of 20 $\mu\text{g}/\text{ml}$ tannic acid; (\bullet), 120 $\mu\text{g}/\text{ml}$ tannic acid. The plot is typical of noncompetitive inhibition. The K_i values were calculated to be 58.2 $\mu\text{g}/\text{ml}$ in the presence of low concentrations of tannic acid and 40.0 $\mu\text{g}/\text{ml}$ in the presence of higher concentrations of tannic acid. The K_m for ubiquinol-1 was 76.9 mM, and this was not altered by addition of tannic acid. One activity unit (U) was equal to 0.001 absorbance unit at 645 nm, and 1 mg of membrane vesicles contained 2.46 U of cytochrome d.

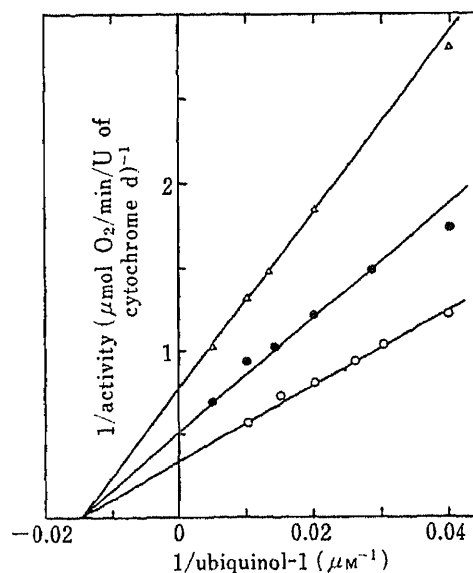


Fig. 6. Double-Reciprocal Plot of the Effect on Ubiquinol-1 Oxidase Activity of Purified Cytochrome b560-d Complex

The conditions of assay were the same as in the legend to Fig. 5. (O), no addition; (\bullet), in the presence of 10 $\mu\text{g}/\text{ml}$ tannic acid; (Δ), 25 $\mu\text{g}/\text{ml}$ tannic acid. The plot is typical of noncompetitive inhibition, like Fig. 5. The K_i value was calculated to be 18.8 $\mu\text{g}/\text{ml}$ and K_m for ubiquinol-1 was 69.0 mM, which was not altered by the addition of tannic acid. One milligram of purified enzyme contained 28.8 U of cytochrome d.

terminal oxidase.

Effect on the Electron Transfer Activities of the Purified Terminal Oxidase

The terminal oxidase of *P. phosphoreum* was purified and characterized as previously described.¹⁾ This purified terminal oxidase, a cytochrome b560-d complex, was used in the studies of the inhibitory effect of tannic acid. Phospholipids were essential for full activation of the purified enzyme, and the ubiquinol oxidase or TMPD + ascorbate oxidase activity was measured in the presence of 3 mM asolection, soybean phospholipids. The ubiquinol oxidase activity was more sensitive to tannic acid than the activity of TMPD + ascorbate oxidase (Fig. 4). This result was similar to that obtained with the sonicated membrane at relatively high concentrations of tannic acid (Fig. 3). The inhibition pattern of ubiquinol-1 oxidase activity by the inhibitor was monophasic, different from that in sonicated membrane. The concentrations required for 50% inhibition of the activity (ID_{50}) estimated from the dose response curve (Fig. 4) were 105 $\mu\text{g/ml}$ (TMPD+ascorbate) and 20 $\mu\text{g/ml}$ (ubiquinol oxidase), respectively.

Enzyme Kinetics

We next studied the inhibition kinetics of ubiquinol oxidase by tannic acid at various concentrations of ubiquinol-1. As shown in Fig. 3, the inhibitory pattern of ubiquinol-1 oxidase activity on the membrane was biphasic. To examine the difference between the two phases of inhibition, we studied the kinetics of the oxidase at about 20% and 80% inhibition. The kinetic pattern in the presence of 20 $\mu\text{g/ml}$ tannic acid was similar to that in the presence of 120 $\mu\text{g/ml}$, showing that the K_m value did not change in the presence of the inhibitor. The results are illustrated in a double-reciprocal plot in Fig. 5, which clearly indicates that tannic acid is a noncompetitive inhibitor of ubiquinol-1 oxidase activity. We then performed similar experiments on the ubiquinol-1 oxidase activity of purified cytochrome b560-d complex (Fig. 6). The inhibition constant was 69 $\mu\text{g/ml}$, which was close to the ID_{50} value estimated from the dose-response curve. The K_m value did not change in the presence of the inhibitor.

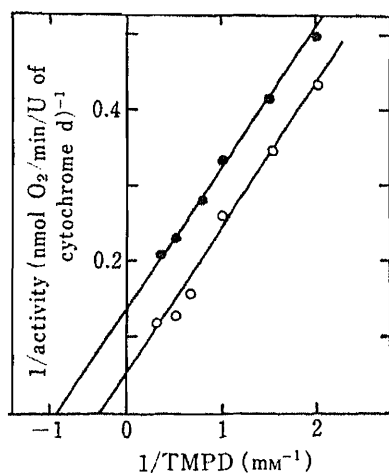


Fig. 7. Double-Reciprocal Plot of the Effect of Tannic Acid on TMPD Oxidase Activity in Membrane Vesicles of *P. phosphoreum* in the Presence of Ascorbate

The assay was carried out with an oxygen electrode. The assay mixture, in a total volume of 1 ml, contained 1.0 mg of membrane, 50 mM Tris-HCl, 5 mM ascorbate, various concentrations of TMPD, and/or tannic acid. (○), no addition; (●), in the presence of 40 $\mu\text{g/ml}$ tannic acid; (△), 100 $\mu\text{g/ml}$ tannic acid.

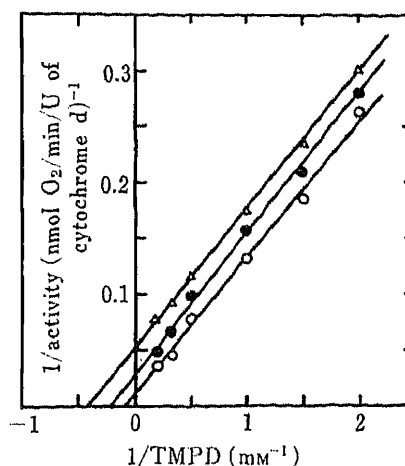


Fig. 8. Double-Reciprocal Plot of the Effect on TMPD Oxidase Activity of Purified Cytochrome b560-d Complex of *P. phosphoreum* in the Presence of Ascorbate

The conditions of assay were the same as in the legend to Fig. 7. (○), no addition; (●), in the presence of 40 $\mu\text{g/ml}$ tannic acid; (△), 100 $\mu\text{g/ml}$ tannic acid.

The effect of tannic acid on TMPD + ascorbate oxidase activity was also examined (Fig. 3). The kinetics of inhibition by tannic acid of TMPD + ascorbate oxidase activity in sonicated membrane was uncompetitive, as shown in Fig. 7, and this was different from the case of ubiquinol-1 oxidase. A similar result was obtained with purified cytochrome b560-d complex (Fig. 8).

Discussion

We showed that tannic acid inhibits the growth of *P. phosphoreum*. One of the inhibitory sites is probably the respiratory chain, based on the results of glucose oxidase assay on whole cells and NADH oxidase assay on sonicated membrane (Fig. 3). The inhibition of glucose oxidase activity was observed only when preincubation with inhibitor was carried out, and the uptake of inhibitor by the cells was probably a limiting step. NADH dehydrogenase activity was also sensitive to the inhibitor, but no further study was carried out at this time. Experiments on the dehydrogenase activity are in progress. Tannic acid also inhibited the ubiquinol-1 oxidase activity and TMPD oxidase activity in the presence of ascorbate, indicating that the terminal oxidase was one of the sites of action of tannic acid.

In *E. coli*, it was reported that the only terminal oxidase present in the early exponential phase of growth was cytochrome b562-o complex and that cytochrome b558-d complex was also synthesized in the late exponential phase or early stationary phase.^{7,8)} The K_m and V_{max} values of ubiquinol oxidase activity in membrane vesicles at the early exponential phase were the same as those of the purified oxidase, cytochrome b562-o complex, but the values of the oxidase activity in the membrane at the late exponential phase were between those of purified cytochrome b562-o and cytochrome b558-d. The cytochrome b560-d of *P. phosphoreum* was probably the only terminal oxidase over the growth phase, because the K_m and V_{max} values of the oxidase activity were the same on the membrane and in a purified sample.¹⁾

It is interesting that the inhibition pattern of ubiquinol oxidase activity on membrane vesicles is biphasic. Both phases were examined kinetically, and only V_{max} varied in the presence of the inhibitor, indicating that this inhibition is noncompetitive. In the presence of low concentrations of inhibitor, the pattern of inhibition of ubiquinol-1 oxidase was the same as that of TMPD + ascorbate oxidase. Inhibition of the ubiquinol-1 oxidase activity of the purified enzyme at relatively low concentrations was monophasic. The TMPD + ascorbate oxidase activities of sonicated membrane and purified cytochrome b560-d were also decreased by the addition of the inhibitor, and uncompetitive-type inhibition was observed. It is possible that this inhibitor does not interact with the free enzyme (E) or substrate (S), but interacts with ES complex. If this is correct, the inhibitor may bind to substrate-reduced cytochrome b560-d complex.

Various lots of tannic acid were used (see Materials and Methods), and their inhibitory activities on growth and on oxidase activity on membrane vesicles were almost the same (data not shown). These results indicate that the major compound(s) contained in all the tannic acid preparations exhibit the activities.

Commercial tannic acid is a very complex and non-uniform mixture. We therefore attempted the isolation and purification of components of commercial tannic acid. Several partially purified compounds were obtained. However, gallic acid, digallic acid, and minor components of higher molecular weight did not have inhibitory activity. The other components which were partially purified have almost the same activity as the commercial preparation (data not shown). Complete purification and characterization are in progress in our laboratory.

References

- 1) K. Konishi, M. Ouchi, K. Kita, and I. Horikoshi, *J. Biochem. (Tokyo)*, **99**, 1227 (1986).
- 2) E. Haslam, *J. Chem. Soc. (C)*, **1967**, 1734.
- 3) I. Nishioka, *Yakugaku Zasshi*, **103**, 125 (1983).
- 4) M. Nishizawa, T. Yamagishi, G. Nonaka, and I. Nishioka, *J. Chem. Soc., Perkin Trans. 1*, **1983**, 961.
- 5) M. Nishizawa, T. Yamagishi, G. Nonaka, and I. Nishioka, *J. Chem. Soc., Perkin Trans. 1*, **1982**, 2963.
- 6) H. Watanabe, N. Mimura, A. Takimoto, and T. Nakamura, *J. Biochem. (Tokyo)*, **77**, 1147 (1975).
- 7) K. Kita, K. Konishi, and Y. Anraku, *J. Biol. Chem.*, **259**, 3375 (1984).
- 8) K. Kita, K. Konishi, and Y. Anraku, *J. Biol. Chem.*, **259**, 3368 (1984).
- 9) K. Kita, M. Kasahara, and Y. Anraku, *J. Biol. Chem.*, **257**, 7933 (1982).
- 10) M. Kasahara and Y. Anraku, *J. Biochem. (Tokyo)*, **72**, 777 (1972).
- 11) J. W. Thomson and B. M. Shapiro, *J. Biol. Chem.*, **256**, 3077 (1981).
- 12) O. H. Lowry, N. J. Rosebrough, A. L. Farr, and R. J. Randall, *J. Biol. Chem.*, **193**, 265 (1951).

[Chem. Pharm. Bull.]
35(3)1176—1182(1987)

The *in Vitro* Effects of Tannic Acid on Rat Liver Mitochondrial Respiration and Oxidative Phosphorylation

HIROKAZU ADACHI,^{*,a} KIYOSHI KONISHI,^b KAZUO TORIIZUKA,^c
and ISAMU HORIKOSHI^a

*Department of Hospital Pharmacy,^a Department of Biochemistry, Faculty of Medicine,^b
and Department of Sino-Japanese (Kampo) Medicine,^c Toyama Medical
and Pharmaceutical University, Sugitani, Toyama 930-01, Japan*

(Received September 10, 1986)

The *in vitro* effects of tannic acid on the membrane structure and function of rat liver mitochondria were investigated. The respiratory control ratio (RCR) decreased by about 50% on addition of 50 $\mu\text{g/ml}$ tannic acid to highly coupled mitochondria, but the adenosine-5'-diphosphate/oxygen (ADP/O) ratio was constant. The uncoupler-induced respiration was also inhibited in the same manner as the RCR. Moreover, the respiratory control disappeared and the ADP/O ratio could not be measured at concentrations of tannic acid above 100 $\mu\text{g/ml}$. On the other hand, the oxygen consumption rate of succinate-dependent respiration decreased on addition of more than 100 $\mu\text{g/ml}$ tannic acid (50% inhibitory concentration (IC_{50})=150 $\mu\text{g/ml}$ tannic acid) to mitochondria. These findings suggest that tannic acid at lower concentrations inhibits the electron transport system to decrease the RCR, but does not impair the membrane, retaining the coupled reaction, while at higher concentrations it impairs the structural integrity of mitochondrial membranes, and directly inhibits the electron transport system.

Tannic acid inhibited the succinate oxidase, reduced nicotinamide adenine dinucleotide (NADH) oxidase, succinate dehydrogenase, and NADH dehydrogenase activities of submitochondrial particles (SMP). The IC_{50} values of tannic acid toward these enzyme systems were estimated to be 35, 45, 30, and 15 $\mu\text{g/ml}$, respectively. Tannic acid competitively inhibited succinate dehydrogenase and NADH dehydrogenase. However, it did not show significant inhibition of the cytochrome oxidase activity of SMP. It is thus concluded that tannic acid exerts its effect on mitochondrial respiration and oxidative phosphorylation through action on the membrane and on both succinate dehydrogenase and NADH dehydrogenase of mitochondria.

Keywords—tannic acid; mitochondria; dehydrogenase; respiratory control; submitochondrial particle

Introduction

Tannin, a general term for water-soluble polyphenols included in plants, is a major component in various oriental medicinal plants. Tannic acid, which is a kind of tannin (also called Chinese gallotannin), is readily available as a commercial reagent prepared from Chinese nutgall. This compound possesses protein-aggregating, astringent, and antibacterial actions.¹⁾ As regards toxicity, it was reported that tannic acid might be absorbed from the gastrointestinal tract, denuded surfaces, and mucous membranes and then cause severe centrilobular necrosis of the liver.²⁻⁴⁾ We have recently observed that tannic acid exerted its antibacterial effects on *Photobacterium phosphoreum* through inhibition of nicotinamide adenine dinucleotide (NADH) dehydrogenase and the terminal oxidase of the respiratory chain.⁵⁾ From these results, we supposed that tannic acid might influence the respiratory chain of mitochondria in animal cells. In this work, the *in vitro* effects of tannic acid on rat liver mitochondria were investigated.

Materials and Methods

Preparation of Mitochondria—Rat liver mitochondria were prepared according to the method of Hogeboom⁶⁾ with some modification. Wistar rats (male, 250–300 g weight), purchased from Sankyo Labo. Co., were used in this study. In order to obtain intact mitochondria with high respiratory control and normal adenosine-5'-diphosphate/oxygen (ADP/O) ratio, we chose the following procedure for the preparation of the rat liver mitochondria. The liver was quickly excised and thoroughly washed with ice-cold 0.25 M sucrose following decapitation of the rat. The liver was minced into small pieces with a pair of sharp, chilled scissors. The finely minced tissue was gently homogenized with a loose-fitted Potter–Elvehjem homogenizer in 0.25 M sucrose, 0.1 mM ethylenediamine tetraacetic acid (EDTA), and 5 mM Tris–HCl, pH 7.4 (solution A), at the rate of 10 ml/g of liver. The homogenate was centrifuged at $700 \times g$ for 10 min. The supernatant obtained was centrifuged at $7000 \times g$ for 10 min. The precipitate was washed once with solution A by centrifugation, and then washed twice with 0.25 M sucrose, adjusted with KOH to pH 7.4 (solution B), by repeating the above centrifugations. The final mitochondrial pellet was suspended in a minimal volume of solution B. The above procedures were carried out at 4 °C.

Preparation of Submitochondrial Particles (SMP)—The rat liver SMP was prepared according to the method of Gregg⁷⁾ with some modification. The isolated mitochondria were sonicated with a Tomy Seiko UR-200p ultrasonic disrupter in 50 mM phosphate buffer, pH 7.4, with cooling in ice water. The treated suspension was centrifuged at $7000 \times g$ for 10 min to remove undisturbed mitochondria, and the supernatant thus obtained was then centrifuged at $100000 \times g$ for 1 h. The packed pellet was suspended in 50 mM phosphate buffer, pH 7.4, 50% glycerol by gentle homogenization. The SMP were stored at –20 °C before use.

Tannic Acid—Tannic acid mainly used in this study was purchased from Wako Pure Chemical Industries (Lot No. KWP7592). In order to check the difference of activities of tannic acids from various makers, several other tannic acids were used (Nakarai Chemicals, Lot No. M4R1112; Kanto Chemical, Lot No. 001H5101; Sigma Chemical, Lot No. 64F-0049; Wako Pure Chemical, Lot No. EPR7215). Tannic acid was adjusted with NaOH to pH 7.0 before use.

Assay of Electron Transport Activity of Mitochondria—The succinate-dependent respiration rate of mitochondria was determined polarographically in an oxygen monitor equipped with a Clark type oxygen electrode as described by Estabrook.⁸⁾ Freshly prepared mitochondria were incubated in the reaction chamber containing 1 ml of assay mixture (125 mM sucrose, 20 μ M cytochrome c, 50 mM KCl, 6 mM MgCl₂, 20 μ M rotenone, and 15 mM phosphate buffer, pH 7.0) at 25 °C for 3 min before addition of 10 mM succinate. The substrate-induced oxygen consumption was plotted on a strip chart recorder, and then 400 μ M ADP was added to the assay system to stimulate the respiration to state 3. After the consumption of ADP the respiration will change to state 4. The respiratory control ratio (RCR) was expressed as the ratio of the respiration rate of state 3 to that of state 4.

Succinate Oxidase and NADH Oxidase Activity of SMP—Substrate (10 mM succinate or 4 mM NADH) was added to the assay mixture (0.7 mg of SMP, tannic acid, 20 μ M cytochrome c, 1 mM EDTA, and 0.1 M phosphate buffer, pH 7.4) at 25 °C, and oxidase activity was determined polarographically.

Cytochrome Oxidase Activity of SMP—Ascorbate (16 mM, adjusted to pH 7.4) as the electron donor was added to the assay mixture (0.7 mg of SMP, tannic acid, 20 μ M cytochrome c, and 0.1 M phosphate buffer, pH 7.4) at 25 °C, and oxidase activity was determined polarographically.

Succinate Dehydrogenase and NADH Dehydrogenase Activities of SMP—Substrate (20 mM succinate or 1 mM NADH) was added to the assay mixture (0.7 mg of SMP, tannic acid, 0.06 mM 2,6-dichloroindophenol (DCIP), and 0.3 mM KCN) at 25 °C, and the dehydrogenase activity was determined spectrophotometrically by measuring the absorbance change of DCIP at 600 nm.

Effect of Tannic Acid on Redox Behavior of Cytochromes b and c, +c—In order to investigate the effect of tannic acid on electron transport between cytochrome b and cytochrome c₁ + c in succinate oxidoreductase, we employed the following procedure. In the control experiment, an excess amount of sodium succinate was added to the suspension containing SMP (3.0 mg/ml), and the succinate reduced-minus-oxidized difference spectrum was recorded on an Aminco DW-2C spectrophotometer. In the inhibitory experiment, 30 μ g/ml tannic acid was added to the same suspension before the addition of an identical amount of sodium succinate. The complete reduction of cytochromes was carried out by the addition of sodium dithionite.

Other Methods—Various polyphenols included in commercial tannic acid were fractionated by Sephadex LH-20 (Pharmacia Fine Chemical) column chromatography according to the method of Nishioka *et al.*⁹⁾

The protein concentration was determined by the method of Lowry *et al.*¹⁰⁾ with bovine serum albumin as a standard.

Results

The Effects on the Respiratory Control and Oxidative Phosphorylation of Mitochondria

Addition of ADP induced an approximately fivefold increase in the rate of succinate-dependent respiration (Fig. 1). However, in the presence of 50 μ g/ml tannic acid this

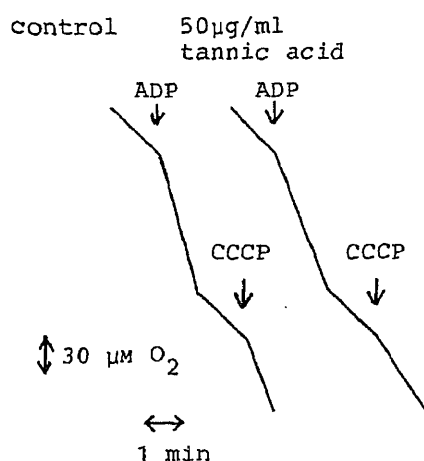


Fig. 1. Inhibitory Effect of Tannic Acid on Succinate-Dependent Respiration of Rat Liver Mitochondria

Mitochondria (1.42 mg of protein/ml) were preincubated in the assay mixture (125 mM sucrose, 20 μ M cytochrome c, 50 mM KCl, 6 mM $MgCl_2$, 20 μ M rotenone, and 15 mM phosphate buffer) for 3 min at 25 $^{\circ}$ C in the presence or absence of tannic acid before addition of 10 mM succinate. ADP (400 μ M) and CCCP (100 nM) were added as indicated. Oxygen uptake was measured with a Clark-type oxygen electrode.

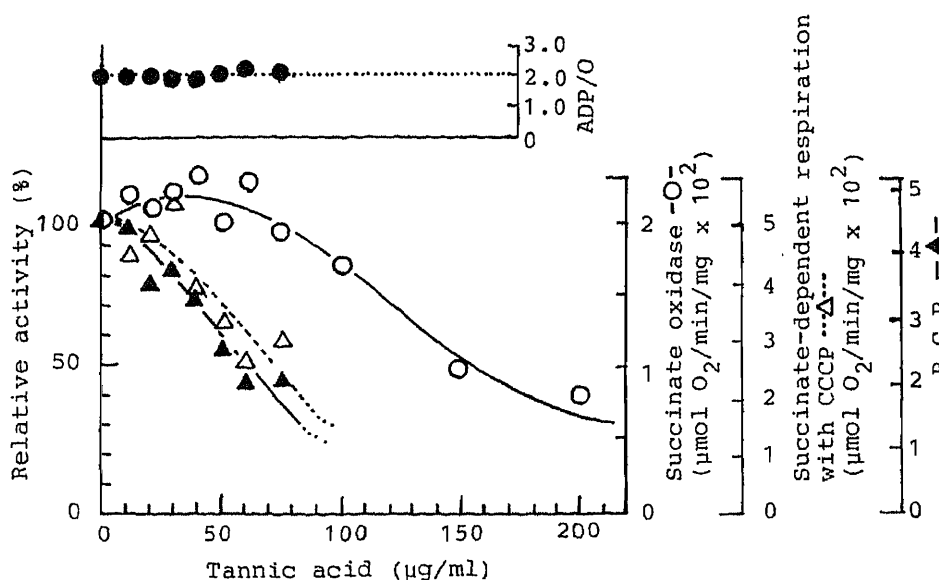


Fig. 2. Effects of Tannic Acid on the Respiratory Control of Rat Liver Mitochondria

(O), Succinate oxidase; (\blacktriangle), respiratory control ratio; (\triangle), succinate-dependent respiration in the presence of 0.1 μ M CCCP. The control succinate oxidase activity of 0.020 μ mol O_2 /min/mg of mitochondria was taken as 100%. Conditions were the same as for Fig. 1 except that the indicated concentrations of tannic acid were used.

respiratory control ratio decreased to about 50%. This effect was found to be dose-dependent. On addition of more than 100 μ g/ml tannic acid, this respiratory control disappeared (Fig. 2). On the other hand, the ratio between the amount of ADP added and the oxygen consumed in state 3 (ADP/O ratio) was maintained at about 2.0 in the presence of tannic acid until its respiratory control disappeared (Fig. 2). The increase in oxygen consumption rate with an uncoupler, carbonyl cyanide *m*-chlorophenylhydrazone (CCCP), was inhibited by up to 100 μ g/ml tannic acid (Figs. 1, 2). This inhibitory pattern is similar to that of RCR. Moreover, succinate-dependent electron transport activity was inhibited by more than 100 μ g/ml of tannic acid and its 50% inhibitory concentration (IC_{50}) was about 150 μ g/ml (Fig. 2). We also found that the substrate-induced respiration (state 4) was slightly increased by low concentrations of tannic acid.

The Effect of Tannic Acid on the Electron Transport Activities of the Respiratory Chain of SMP

In view of the findings that tannic acid inhibited the succinate-dependent respiratory

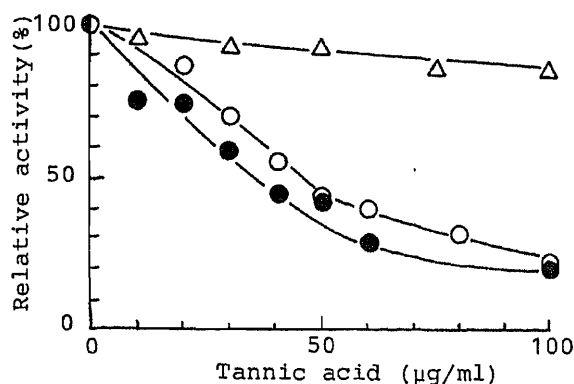


Fig. 3. Effects of Tannic Acid on Various Oxidase Activities of the Rat Liver Submitochondrial Particles

(●), Succinate oxidase; (○), NADH oxidase; (△), cytochrome oxidase. The control activities were 0.068, 0.032, and 0.023 $\mu\text{mol O}_2/\text{min}/\text{mg}$ of protein, respectively. The activities of submitochondrial particles (0.7 mg of protein/ml) were assayed with an oxygen electrode.

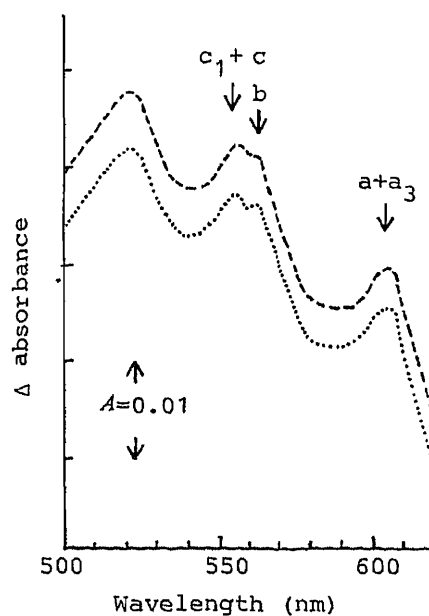


Fig. 4. Effects of Tannic Acid on the Succinate Reduced-Minus-Oxidized Difference Spectra of the Submitochondrial Particles

The spectra were recorded with an Aminco DW-2C dual wavelength spectrophotometer at 20°C. The sample cuvette contained 3 mg of submitochondrial particles in 1 ml of assay mixture. (---), control experiment; (····), inhibition experiment in the presence of 30 $\mu\text{g}/\text{ml}$ tannic acid.

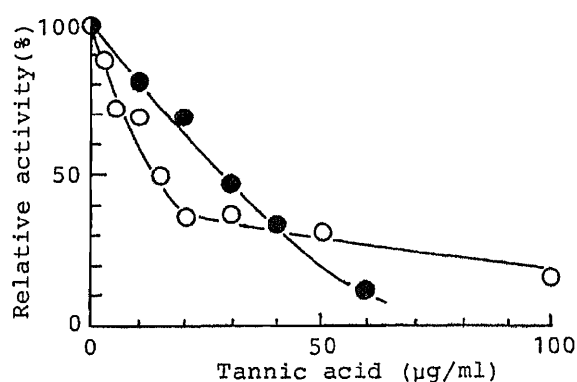


Fig. 5. Effects of Tannic Acid on NADH and Succinate Dehydrogenase Activities of the Submitochondrial Particles

(●), Succinate dehydrogenase; (○), NADH dehydrogenase. The control activities were 0.035 and 0.39 $\mu\text{mol DCIP}/\text{min}/\text{mg}$ of protein, respectively.

activity of mitochondria, we investigated the effects of tannic acid on SMP to determine the inhibitory site of tannic acid on the respiratory chain. As shown in Fig. 3, tannic acid inhibited succinate oxidase and NADH oxidase activities (IC_{50} : 35 and 45 $\mu\text{g}/\text{ml}$, respectively), but did not significantly inhibit cytochrome oxidase activity. The results obtained suggested that the crossover point was prior to the cytochrome oxidase. We found that the spectral features of both cytochromes b and $c_1 + c$ in the succinate reduced-minus oxidized difference spectrum of SMP were not changed after incubation with tannic acid (Fig. 4). It appears that tannic acid does not inhibit the electron transport between cytochromes b and $c_1 + c$, and thus the crossover point is prior to cytochrome b. Furthermore, it was shown that tannic acid inhibited succinate dehydrogenase and NADH dehydrogenase activities (Fig. 5) (IC_{50} : 30 and 15 $\mu\text{g}/\text{ml}$, respectively). The above results suggest that the inhibitory sites of tannic acid on the respiratory chain are both succinate dehydrogenase and NADH dehydrogenase.

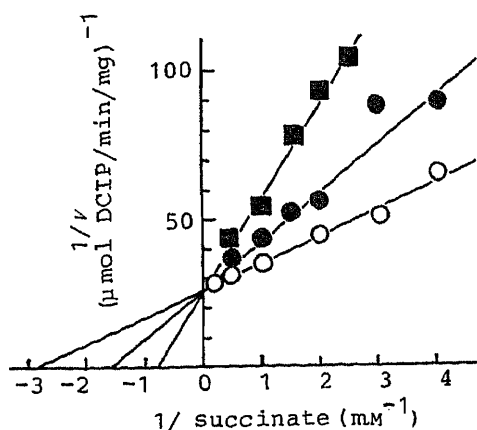


Fig. 6. Double Reciprocal Plot of the Effect of Tannic Acid on Succinate Dehydrogenase Activity of the Submitochondrial Particles

The concentrations of tannic acid were 0 (○), 5 (●), and 10 $\mu\text{g/ml}$ (■).

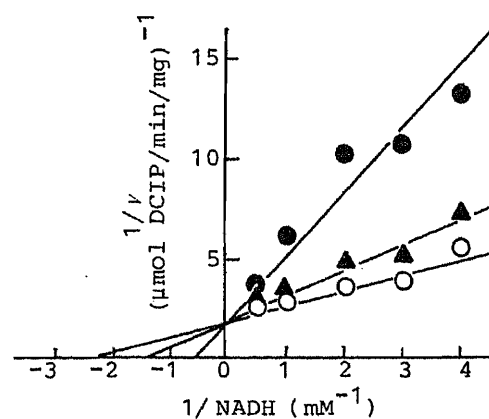


Fig. 7. Double Reciprocal Plot of the Effect of Tannic Acid on NADH Dehydrogenase Activity of the Submitochondrial Particles

The concentrations of tannic acid were 0 (○), 0.5 (▲), and 5 $\mu\text{g/ml}$ (●).

Enzyme Kinetics

Since the inhibitory effects of tannic acid on the respiratory chain were found to be located at succinate dehydrogenase and NADH dehydrogenase, we performed some kinetic studies to establish the mechanism of inhibition by tannic acid. The results are illustrated by double-reciprocal plots in Figs. 6 and 7, indicating that tannic acid is a competitive inhibitor of both succinate dehydrogenase and NADH dehydrogenase.

Discussion

When succinate was used as a substrate, the respiratory control ratio and the ADP/O ratio of prepared mitochondria were about 4.5 and 1.9, respectively. These data indicated that the mitochondrial preparation was highly coupled and active in oxidative phosphorylation. When tannic acid was present in the assay medium, the RCR was decreased and this effect was dose-dependent, but the ADP/O ratio was constant. The decrease of RCR was caused by the alteration of state 3 respiration, since the state 4 respiration did not change greatly with tannic acid at concentrations below 75 $\mu\text{g/ml}$, and the inhibition of state 3 respiration was not released by the addition of uncoupler CCCP. These findings suggest that tannic acid inhibits the electron transport system of mitochondria, but does not much impair the membrane barrier, and does not inhibit coupled oxidative phosphorylation.

We found that the succinate-dependent respiration (state 4) was slightly increased by tannic acid, suggesting that the respiration was somewhat uncoupled due to leakiness of the mitochondrial membrane to ions induced by the inhibitor. Although this effect might be similar to that of an uncoupler of oxidative phosphorylation,¹¹⁾ it was very small and probably did not significantly affect the ADP/O ratio.

At high concentrations of tannic acid (above 100 $\mu\text{g/ml}$), the respiratory control was not observed, the ADP/O ratio could not be measured, and the succinate-dependent electron transport system was inhibited. These data indicate that tannic acid impairs the mitochondrial membrane and then directly inhibits the exposed electron transfer system. The inhibitory sites of tannic acid on the electron transport system are considered to be both succinate dehydrogenase and NADH dehydrogenase. This conclusion is supported by the findings that the succinate- and NADH-supported respiratory systems were inhibited by tannic acid but

cytochrome oxidase was not influenced, and the crossover point was prior to cytochrome b from the difference spectral data. In fact, both the dehydrogenases of SMP were inhibited competitively by tannic acid (Figs. 5, 6), even though this inhibitor is not obviously structurally related to succinate and NADH. As a similar example, pyrophosphate, which is not structurally related of succinate, is a strong competitive inhibitor of succinate dehydrogenase.¹²⁾ It is not yet clear how tannic acid reacts with the dehydrogenases.

The orientation of the mitochondrial inner membrane is opposite to that of SMP (inside-out), and in the case of mitochondria, there is an outer membrane outside of the inner membrane which carries the respiratory chain components. Regardless of these differences, the inhibitory effect of tannic acid on uncoupler-induced activity or state 3 respiration activity of mitochondria ($IC_{50} = 65$ and $40 \mu\text{g/ml}$, respectively; determined from the data in Fig. 2) was similar to that on succinate oxidase of SMP ($IC_{50} = 35 \mu\text{g/ml}$).

As described above, the decrease of RCR was caused by the decrease of state 3 respiration while state 4 respiration remained almost constant in the presence of the inhibitor. One possible explanation is that tannic acid may hardly be taken up by mitochondria in the presence of membrane potential (state 4 respiration).

From the above results, we may draw the following conclusions. At lower concentrations of tannic acid, it inhibits the electron transport of mitochondria to decrease the respiratory control ratio but does not inhibit the coupled reaction in oxidative phosphorylation. At higher concentrations, tannic acid breaks the membrane barrier of mitochondria to dissipate the coupled reaction, and then competitively inhibits succinate dehydrogenase and NADH dehydrogenase.

Tannic acid prepared from Chinese nutgall is readily available from commercial sources, but this contains many structural analogues composed of glucose and gallic acid, and the composition of polyphenols may differ from lot to lot. Therefore, we investigated the effects of five different lots of tannic acid purchased from four companies on the NADH dehydrogenase activity of SMP. Their IC_{50} values were almost the same (15 — $30 \mu\text{g/ml}$) (data not shown). Furthermore, we tried to fractionate tannic acid by Sephadex LH-20 column chromatography and obtained 15 fractions, although it is difficult to isolate each polyphenol from tannic acid. Three of the 15 fractions separated by the chromatography had no inhibitory effect. On the other hand, the others (12 fractions) had strong inhibitory activities against succinate oxidase of SMP and their IC_{50} values were 21 — $44 \mu\text{g/ml}$, similar to that of the whole tannic acid. One of the former 3 fractions was the first fraction eluted from the column and contained mainly gallic acid and digallic acid. The other two were the last-but-one fraction and the final fraction, and contained mostly high-molecular-weight polyphenol. No inhibitory effect was observed with pure gallic acid, which is consistent with the above result. The isolation and characterization of each polyphenol are in progress in our laboratory.

References

- 1) I. Nishioka, *Yakugaku Zasshi*, **103**, 125 (1983).
- 2) D. W. Wells, H. D. Humphrey, and J. J. Coll, *New. Engl. J. Med.*, **226**, 629 (1942).
- 3) J. M. Barnes and R. J. Rossiter, *Lancet*, **2**, 218 (1943).
- 4) J. Z. Krezanoski, *Radiology*, **87**, 655 (1966).
- 5) K. Konishi, H. Adachi, K. Kita, and I. Horikoshi, *Chem. Pharm. Bull.*, **35**, 1169 (1987).
- 6) G. H. Hogeboom, "Methods in Enzymology," Vol. 1, ed. by S. P. Colowick and N. O. Kaplan, Academic Press, New York, 1955, pp. 16—19.
- 7) C. T. Gregg, "Methods in Enzymology," Vol. 10, ed. by R. W. Estabrook and M. E. Pullman, Academic Press, New York, 1967, pp. 181—185.
- 8) R. W. Estabrook, "Methods in Enzymology," Vol. 10, ed. by R. W. Estabrook and M. E. Pullman, Academic

-
- Press, New York, 1967, pp. 41—47.
- 9) M. Nishizawa, T. Yamagishi, G. Nonaka, and I. Nishioka, *J. Chem. Soc., Perkin Trans. 1*, **1982**, 2963.
 - 10) O. H. Lowry, N. J. Rosebrough, A. L. Farr, and R. J. Randall, *J. Biol. Chem.*, **193**, 265 (1951).
 - 11) W. G. Hanstein, *Biochim. Biophys. Acta*, **456**, 129 (1976).
 - 12) D. V. Dervartanian and C. Veeger, *Biochim. Biophys. Acta*, **92**, 233 (1964).

[Chem. Pharm. Bull.]
[35(3)1183—1188(1987)]

Novel Preparation of Decylenediamine-dextran T70 and Inhibitory Activity toward Dihydrofolate Reductase of Decylenediamine-dextran T70-Methotrexate Conjugate

HIRAKU ONISHI* and TSUNEJI NAGAI

*Faculty of Pharmaceutical Sciences, Hoshi University,
Ebara 2-4-41, Shinagawa-ku, Tokyo 142, Japan*

(Received May 13, 1986)

The previously reported method for the preparation of decylenediamine-dextran T70 (T70-C₁₀) was improved, and several chemical properties of the polymer support were examined. Methotrexate (MTX) was conjugated to T70-C₁₀ by using 1-ethyl-3-(3-dimethylaminopropyl)-carbodiimide hydrochloride. The T70-C₁₀-MTX conjugate (T70-C₁₀-MTX) and T70-C₁₀ carrying adsorbed MTX (T70-C₁₀-adsorbed MTX) were dialyzed in order to examine the nature of the adsorption of MTX on T70-C₁₀-MTX. Before and after dialysis, the activity of these derivatives was assayed in terms of the binding affinity to dihydrofolate reductase. A more stable T70-C₁₀ was obtained by using more severe reaction conditions in the Schiff's base formation between diaminodecane (C₁₀) and oxidized dextran T70 and in the subsequent reduction. Conjugation was successful and the separation by gel-filtration (Sephadex G50) was good. The chemical properties of T70-C₁₀ and T70-C₁₀-MTX were consistent and similar to those of the previous preparations. From the dialysis experiment, T70-C₁₀-MTX was estimated to have about 5 to 6% of the inhibitory activity of free MTX.

Keywords—conjugation; T70-C₁₀-MTX; T70-C₁₀-adsorbed MTX; dialysis; activity; DHFR fluorescence

Introduction

The modification of antitumor agents with macromolecules might make it possible to obtain persistent and high local concentrations of the inhibitor at the tissue or cellular level.^{1,2)} Hydrolyzable macromolecules or hydrolyzable conjugation bonds would permit slow release of the active agent.³⁾ Moreover, in utilizing degradable macromolecules, it is important that the antitumor drug should be modified in such a way that effective binding to the target molecule is still possible.⁴⁾ Such modifications should reduce the acute toxicity which follows the administration of a large amount of free drug. Further, injecting or implanting macromolecule-drug conjugates into the body cavities or tissues where malignant cells might remain after surgical operation would be useful for maintaining local therapeutic potency and for preventing the recurrence of cancer.

In the previous work, decylenediamine-dextran T70 was found to be useful for the conjugation of methotrexate (MTX) and mycophenolic acid (MPA).⁵⁾ However, the previous preparation procedure gave only a small amount of the products and the polymer support was not completely stable. Thus, the preparation of the polymer support was reexamined. Further, the possibility that free MTX might be adsorbed on the polymer support had to be examined. In this work, the effectiveness of T70-C₁₀-MTX conjugate was studied in detail, by measuring the inhibitory activities of T70-C₁₀-MTX and T70-C₁₀ carrying adsorbed MTX toward dihydrofolate reductase (DHFR) before and after dialysis.

Experimental

Material—Dextran T70 (T70), with a molecular weight of 70000 was purchased from Tokyo Kasei Industrial Co. MTX and DHFR from chicken liver were obtained from Sigma Chemicals Co. All other chemicals were commercial reagent-grade products.

Preparation of Spacer-Introduced Dextran—The previously reported method for the preparation of T70-C₁₀ was changed as follows. The binding reaction time of oxidized dextran T70 (T70-CHO) and diaminodecane (C₁₀) was increased to 6 h and the pH was adjusted to about 9.0 with NaOH and HCl solutions. The subsequent reduction of the Schiff's base was executed under more severe conditions than before. Namely, about ten times as much NaBH₄ as before was added, and the reaction time was changed to 22 h, while the pH was maintained at about 9.5 with NaOH and HCl solutions. Finally, T70-C₁₀ was obtained as powder by lyophilization after sufficient dialysis against H₂O. These procedures are shown in Chart 1.

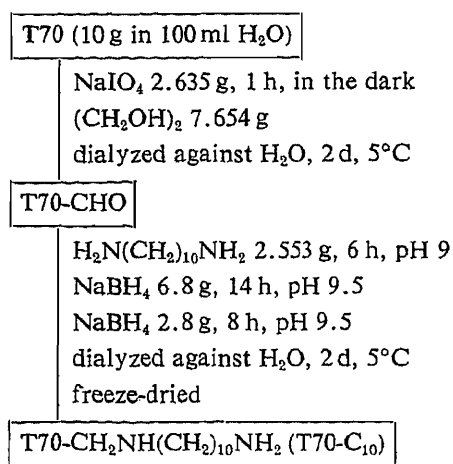


Chart 1. Preparation of the Polymer Support, T70-C₁₀

Characterization of T70-C₁₀—The result of elementary analysis was as follows: C, 42.66; H, 6.65; N, 0.97%. The molecular weight distribution was investigated by gel-filtration (Sephadex G50) by using a 50 mM NaCl aqueous solution for elution. The absorbance of each fraction at 260 nm was measured, then the fraction was lyophilized and the product was weighed. The formation of the effective polymer support, T70-CH₂NH(CH₂)₁₀NH₂, was checked by measuring the reactivity to ninhydrin; 1 ml of the sample solution and 0.5 ml of ninhydrin aqueous solution (1% (w/v)) were mixed, heated in a boiling water bath for 5 min and assayed colorimetrically at 570 nm. As for the macromolecular fractions, the amounts of bound spacer (C₁₀) were calculated from the weight and nitrogen ratio obtained by elementary analysis.

Further, the stability of T70-C₁₀ was investigated under conditions similar to those of the conjugation reaction, that is, stirring for 24 h at pH 6.0. Subsequently, the molecular weight distribution was checked by gel-filtration (Sephadex G50) with a 50 mM NaCl aqueous solution as the eluent. Each fraction was weighed and checked for reactivity to ninhydrin, content of C₁₀ and ultraviolet (UV) absorption at 260 nm.

To confirm the binding of C₁₀ to T70-CHO and the subsequent reduction of the Schiff's base by NaBH₄, Fehling tests were carried out on T70-C₁₀ and T70-CHO at several concentrations as reported previously.⁵⁾

Preparation of T70-C₁₀-MTX Conjugate and T70-C₁₀ Carrying Adsorbed MTX—T70-C₁₀ (300 mg) was dissolved in 10 ml of purified water, and MTX (5 mg) and 1-ethyl-3-(3-dimethylaminopropyl)carbodiimide hydrochloride (EDC) (300 mg) were added. The pH was adjusted to about 6.0 with 1 N NaOH and 1 N HCl. The mixture was stirred for 24 h in the dark at room temperature. The polymer conjugate, T70-C₁₀-MTX, was obtained from the macromolecular fractions after gel-filtration (Sephadex G50). T70-C₁₀-MTX, was estimated spectrophotometrically at 260 nm and the spectrum of the macromolecular fraction was compared with that of intact MTX.

An aqueous solution (10 ml) of T70-C₁₀ (300 mg) and MTX (5 mg) without EDC was stirred for 24 h at pH 6.0 in the dark at room temperature, and T70-C₁₀ carrying adsorbed MTX (T70-C₁₀·adsorbed MTX) was obtained from the macromolecular fractions after gel-filtration.

The amount of MTX contained in T70-C₁₀-MTX and that in T70-C₁₀·adsorbed MTX were calculated from their ultraviolet absorptions at 260 nm in a 0.1 N NaOH aqueous solution and the weight of the macromolecular fractions used (No. 10—13). The void volume and the total volume corresponded to fractions No. 10 and No. 28, respectively. The fraction size was 5 ml, and the amount of sample loaded was 5 ml (see Fig. 4).

Dialysis Experiment—Seamless cellulose tubing supplied by Union Carbide Corporation was used throughout this work. The pore diameter was 24 Å.

Walpole's buffer (pH 2.3) was used as the dialysis medium. T70-C₁₀-MTX and T70-C₁₀·adsorbed MTX were dialyzed by the same procedure. The amount of MTX removed was checked from the UV absorption of the remaining sample at 260 nm and its spectrum in a 0.1 N NaOH aqueous solution.

T70-C₁₀-MTX and T70-C₁₀·adsorbed MTX were prepared at the same concentration (w/v) in purified water, and dialyzed under the following conditions. T70-C₁₀-MTX (3 ml) and T70-C₁₀·adsorbed MTX (3 ml) were packed so that the tube surface areas were almost equal. Dialysis was carried out in a 3 l flask with magnetic stirring at 800 rpm at 4 °C. Walpole's buffer (2.4 l) was used as a dialysis medium for 24 h, then it was replaced with purified water (2.5 l) and dialysis was continued for 24 h. Finally, the medium was replaced with fresh purified water (2.5 l) and further stirred for 24 h. After dialysis, the volume of each sample was measured. The UV absorption spectra of all samples before and after dialysis were compared in a 0.1 N NaOH aqueous solution. These samples were used for the activity study of T70-C₁₀-MTX.

Activity Study of T70-C₁₀-MTX—The activity measurement was based on the fact that the specific binding of MTX causes quenching of DHFR fluorescence quantitatively.⁶⁾ All experiments were conducted at room temperature in 15 ml of Bistris buffer, pH 7.0, containing 500 mM KCl. DHFR was prepared at the concentration of 0.5 μM. T70-C₁₀-MTX and T70-C₁₀·adsorbed MTX before dialysis were prepared to give MTX concentrations of 0.7, 1.4 and 2.8 μM. T70-C₁₀ was used at the same concentration (w/v) as T70-C₁₀·adsorbed MTX. The samples after dialysis were prepared similarly. DHFR solution (1.5 ml) and the substrate solution (1.5 ml) were mixed and the fluorescence at 320 nm (excited at 288 nm) was measured after 2 min.^{7,8)} The inhibitory activity of the substrate was calculated as the ratio of the quenching of the DHFR fluorescence by the substrate to that by free MTX.

Results and Discussion

The elementary analysis of T70-C₁₀ indicated that it contained 59.7 mg of diaminododecane (C₁₀) per gram, so that the degree of substitution with C₁₀ in T70-C₁₀ was one molecule per 14–15 glucose units. The Fehling reaction showed that essentially no aldehyde groups remained in T70-C₁₀. Namely, the formation of T70-C₁₀ was effectively accomplished.

The gel-filtration pattern of T70-C₁₀ (Fig. 1) indicated that the molecular weight of T70-C₁₀ is at least 10000, judging from the characteristics of the Sephadex G50 column. The macromolecular fractions, No. 12–16, contained 74.1% of the total eluted T70-C₁₀ by weight. The content of C₁₀ in each fraction ranged from 7 to 8% of eluted T70-C₁₀, being similar to that of the previously obtained T70-C₁₀. In the ninhydrin reaction test of native T70-C₁₀

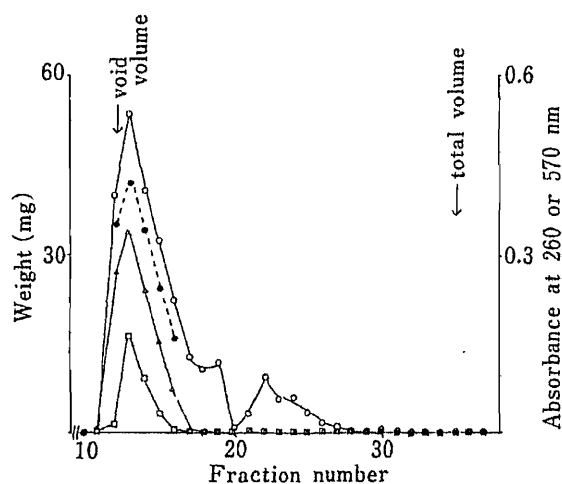


Fig. 1. Elution Profiles of T70-C₁₀ Checked by Several Methods on Sephadex G50 Gel-Filtration with a 50 mM NaCl Aqueous Solution

○, weight; △, absorbance at 260 nm; □, absorbance at 570 nm after ninhydrin reaction; ●, weight of contained C₁₀ (× 10).

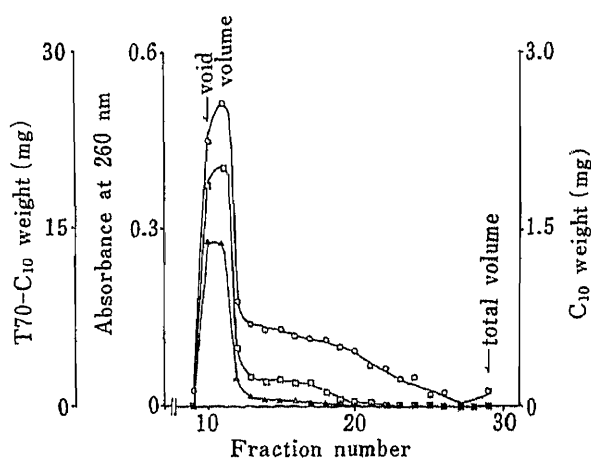


Fig. 2. Elution Profiles of T70-C₁₀ Checked by Several Methods on Sephadex G50 Gel-Filtration with a 50 mM NaCl Aqueous Solution after the Stability Test

○, weight; △, absorbance at 260 nm; □, weight of contained C₁₀.

Only the macromolecular fractions showed strong positive reactivity to ninhydrin.

(5.6 mg/ml of 50 mM NaCl (pH 7–8)), the absorbance at 570 nm was 2.836. The high reactivity to ninhydrin in the macromolecular fractions indicated that the polymer support, T70-CH₂NH(CH₂)₁₀NH₂, was formed effectively. Further, the elution patterns in terms of absorbance at 260 nm and reactivity to ninhydrin gave similar profiles to that by weight. These results suggested that T70-C₁₀ was macromolecular and structurally uniform. After a stability test in a pH 6.0 aqueous solution for 24 h, the gel-filtration pattern was similar to that of the original T70-C₁₀ (Fig. 2). The relationship of absorbance at 260 nm to the ninhydrin reactivity, weight and content of C₁₀ in each fraction was similar to that before the stability test. Thus, T70-C₁₀ obtained in this study was found to be a stable polymer.

T70-C₁₀-MTX conjugate (T70-C₁₀-MTX) and T70-C₁₀ carrying adsorbed MTX (T70-C₁₀·adsorbed MTX) were obtained from the macromolecular fractions, No. 10–13, after gel-filtration (Fig. 3). In the case of T70-C₁₀·adsorbed MTX, MTX was eluted throughout the range. With T70-C₁₀-MTX, a small peak appeared at the fraction No. 25 in the low-molecular fractions but the UV absorption spectrum was not that of MTX. Thus, MTX was supposed to be bound to the polymer support almost completely through an amide bond in T70-C₁₀-MTX.

The ultraviolet spectra of the obtained derivatives, the polymer support and free MTX were all available (Fig. 4), and the spectra of T70-C₁₀-MTX and T70-C₁₀·adsorbed MTX appeared to correspond to the summation of the spectrum of the polymer support and that of MTX. Thus, the content of MTX in each derivative was calculated as shown in Table I.

The results of the activity study of T70-C₁₀-MTX and T70-C₁₀·adsorbed MTX before dialysis and of T70-C₁₀ are shown in Fig. 5. T70-C₁₀ had no binding affinity for DHFR. Namely, the polymer support was inactive. T70-C₁₀·adsorbed MTX showed the same activity as free MTX at the equivalent content of MTX. Thus, MTX adsorbed by T70-C₁₀ was considered to be separated quickly from the polymer support and then to interact with

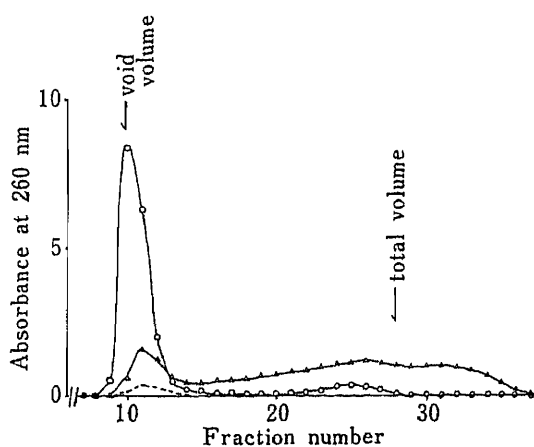


Fig. 3. Elution Profiles on Sephadex G50 Gel-Filtration with a 50 mM NaCl Aqueous Solution

○, T70-C₁₀ + MTX + EDC; △, T70-C₁₀ + MTX.
The elution profile of T70-C₁₀ alone is shown by the broken line.

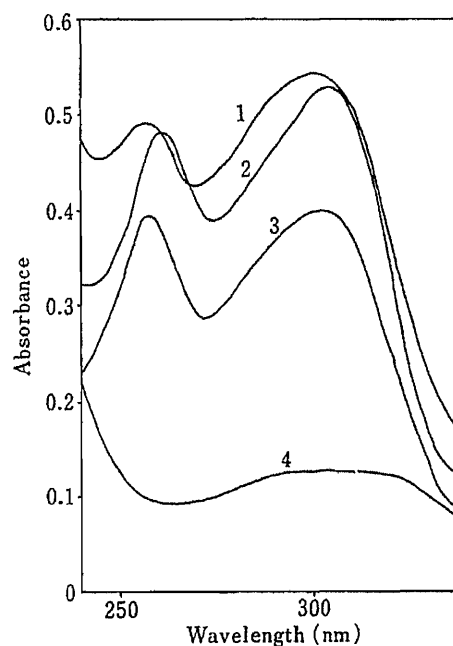


Fig. 4. Absorption Spectra of MTX Derivatives in 0.1 N NaOH

1, T70-C₁₀·adsorbed MTX (1.8 mg/ml); 2, T70-C₁₀-MTX (4.2×10^{-1} mg/ml); 3, MTX (8.4×10^{-3} mg/ml); 4, T70-C₁₀ (1.9 mg/ml)

TABLE I. Bound Drug Amounts and UV Absorption Parameters of MTX Derivatives

Compound	Bound drug amounts ($\mu\text{M/g}$)	λ_{max} (I) (nm)	λ_{max} (II) (nm)
MTX		258	302
T70-C ₁₀ ·adsorbed MTX	13.5	258	301
T70-C ₁₀ -MTX	67.4	261	304

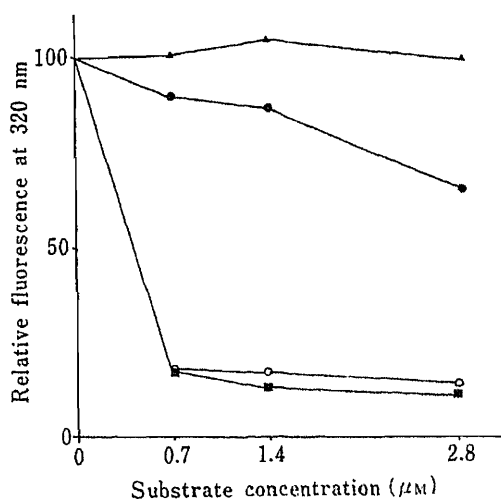


Fig. 5. Quenching of Fluorescence

▲, T70-C₁₀; ●, T70-C₁₀-MTX; ■, T70-C₁₀·adsorbed MTX; ○, MTX

Concentration is given as that of MTX for MTX derivatives. T70-C₁₀ was used at the same concentration (w/v) as T70-C₁₀·adsorbed MTX.

DHFR.

The UV absorption spectra before and after dialysis are shown in Fig. 6. After dialysis, the volume of the samples was maintained at about 3.0 ml. Therefore, the absorbances before and after dialysis represent the contents of the polymer support and MTX, respectively. Since only a small decrease in the UV absorption was observed for T70-C₁₀-MTX, most of the MTX was concluded to remain in the conjugate. On the other hand, the UV absorption of T70-C₁₀·adsorbed MTX was considerably reduced by dialysis and the spectrum after dialysis showed almost the same profile as that of T70-C₁₀. This suggests that the polymer support was stable under the above dialysis conditions. The activities of the samples before and after dialysis are shown in Fig. 7. The activity of T70-C₁₀·adsorbed MTX was corrected to that at the same concentration (w/v) of T70-C₁₀-MTX. The activities of T70-C₁₀-MTX before and after dialysis were 8.7 and 5.9%, respectively compared with that of free MTX. If the ultraviolet absorption of the sample after dialysis is adjusted to that before dialysis, the activity of T70-C₁₀-MTX after dialysis would be 7.1%. The small difference between the activity before dialysis and that after might be due to adsorbed MTX or the remaining low-molecular conjugate. The activities of T70-C₁₀·adsorbed MTX before and after dialysis were 19.5 and 0.5% at the same concentration (w/v) as T70-C₁₀-MTX. Thus, adsorbed MTX was removed almost completely by dialysis. As for T70-C₁₀-MTX after dialysis, the activity of the remaining free MTX would be at most 0.5%, if any. Consequently, T70-C₁₀-MTX could be estimated to have 5.4–5.9% activity. This value is a little greater than those of the MTX derivatives of Whiteley,⁹⁾ Harding¹⁰⁾ and Shen and Ryser.⁴⁾ Sirotnak *et al.* indicated that the γ -carboxyl group of the glutamic acid residue of MTX does not have to be free for inhibitory activity, on the basis of a structure-activity relationship study.¹¹⁾ The lower inhibitory activity of T70-C₁₀-MTX as compared with free MTX is considered to be owing to the steric hindrance by the bulky polymer support, assuming that the γ -carboxyl group undergoes

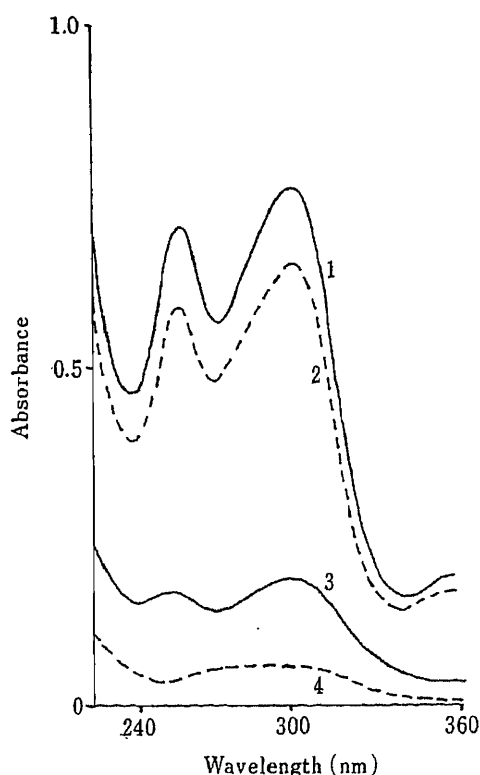


Fig. 6. Spectra of T70-C₁₀-MTX and T70-C₁₀·adsorbed MTX before and after Dialysis

1, T70-C₁₀-MTX before dialysis; 2, T70-C₁₀-MTX after dialysis; 3, T70-C₁₀·adsorbed MTX after dialysis; 4, T70-C₁₀·adsorbed MTX before dialysis.

T70-C₁₀·adsorbed MTX before dialysis was used at the same concentration (w/v) as T70-C₁₀-MTX.

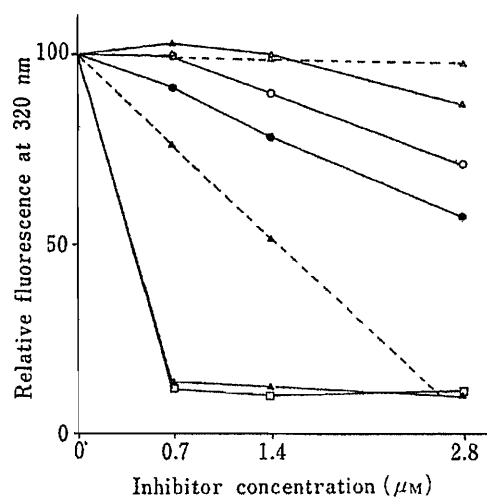


Fig. 7. Quenching of Fluorescence

—●—, T70-C₁₀-MTX before dialysis; —○—, T70-C₁₀-MTX after dialysis; —▲—, T70-C₁₀·adsorbed MTX before dialysis; —△—, T70-C₁₀·adsorbed MTX after dialysis; —□—, MTX; ---▲---, T70-C₁₀·adsorbed MTX before dialysis, corrected to correspond to the same concentration (w/v) as T70-C₁₀-MTX; ---△---, T70-C₁₀·adsorbed MTX after dialysis, corrected to correspond to the same concentration (w/v) as T70-C₁₀-MTX.

amidation with the polymer support preferentially. Nevertheless, T70-C₁₀-MTX is considered to be a potent inhibitor of DHFR.

References and Notes

- 1) Y. Takakura, S. Matsumoto, M. Hashida, and H. Sezaki, *Cancer Res.*, **44**, 2505 (1984).
- 2) C. D. Duve, T. D. Barsy, B. Poole, A. Trouet, P. Tulkens, and F. V. Hoof, *Biochem. Pharmacol.*, **23**, 2495 (1974).
- 3) A. Kato, Y. Takakura, M. Hashida, T. Kimura, and H. Sezaki, *Chem. Pharm. Bull.*, **30**, 2951 (1982).
- 4) W.-C. Shen and H. J.-P. Ryser, *Mol. Pharmacol.*, **16**, 614 (1979).
- 5) H. Onishi and T. Nagai, *Chem. Pharm. Bull.*, **34**, 2561 (1986).
- 6) B. T. Kaufman and V. F. Kemerer, *Arch. Biochem. Biophys.*, **179**, 420 (1977).
- 7) S. M. J. Dunn and R. W. King, *Biochemistry*, **19**, 766 (1980).
- 8) P. J. Cayley, S. M. J. Dunn, and R. W. King, *Biochemistry*, **20**, 874 (1981).
- 9) J. M. Whiteley, *Ann. N. Y. Acad. Sci.*, **186**, 29 (1971).
- 10) N. G. L. Harding, *Ann. N. Y. Acad. Sci.*, **186**, 270 (1971).
- 11) F. M. Sirotnak, P. L. Chello, J. I. Degraw, J. R. Piper, and J. A. Montgomery, "Molecular Actions and Targets for Cancer Chemotherapeutic Agents," Academic Press, Inc., New York, 1981, p. 349.

[Chem. Pharm. Bull.]
35(3)1189—1195(1987)

Studies on the Uptake Mechanism of Liposomes by Perfused Rat Liver. II. An Indispensable Factor for Liver Uptake in Serum

HIROSHI KIWADA,*¹⁾ TAKAAKI MIYAJIMA and YURIKO KATO

Faculty of Pharmaceutical Sciences, Science University of Tokyo, 12 Ichigaya
Funagawara-machi, Shinjuku-ku, Tokyo 162, Japan

(Received July 28, 1986)

Participating factors in the uptake of liposomes by the liver were examined in a small-volume circulating perfusion system. The volume of the perfusate was 23 ml, which corresponds to the blood volume of the rat. It is considered that this system is suitable for examining the factors participating in the uptake *in vivo*. An indispensable factor for the uptake was found in fresh serum, and the uptake proportionally depended on the amount of the factor in serum. The properties of the factor were investigated with serum pretreated in various ways. The experiment with preheated serum indicated that the factor is very heat-sensitive and may be a protein. When serum was dialyzed with a cellulose membrane, the activity penetrated through the membrane, and its molecular weight was concluded to be below 17000 daltons. The sum of the activities on both sides of the membrane in equilibrium dialysis was almost equal to that in fresh serum. This strongly suggests that the factor does not participate cooperatively with other factors in the uptake. The uptake activity disappeared when serum was incubated with liposomes at 38 °C for 5 min in advance. The interaction of the factor with liposomes appears to be very fast and irreversible.

Correspondence of the uptake by the liver and elimination from the perfusate in the perfusion system to the *in vivo* behavior after i.v. injection was also examined. Correspondence of the uptake was observed, but the elimination kinetics from perfusate and blood were different. It is suggested that the uptake is dominated by the factor described here, but the elimination kinetics is partially affected by other factor(s).

Keywords—liposome; perfused liver; uptake; clearance; serum participating factor; dialysis; opsonin; interaction; heat-sensitivity

Introduction

It is generally accepted that substantial fractions of intravenously injected liposomes are rapidly taken up by the liver.²⁾ This is a problem to be overcome in the case of usage of liposomes for sustained release of a drug or targeting to other organs or tissues. It is necessary to control the uptake of liposomes by the liver. However, the detailed mechanism of the liver uptake of liposomes is still uncertain.

As reported in the previous paper,³⁾ we studied the uptake mechanism of liposomes by single perfusion of rat liver. Large liposomes (reverse-phase evaporation vesicles (REV), about 0.1—0.2 μm in diameter) were able to pass through the liver without any interaction or interference and there was little uptake by the liver during perfusion with phosphate-buffered saline (containing no blood components). On the other hand, small liposomes (small unilamellar vesicles (SUV), about 0.06 μm in diameter) showed uptake corresponding to about 0.25 μmol of total lipid (about a half of injected liposomes) without any participation of blood components. These results suggest that the uptake mechanism of REV may be different from that of SUV, and opsonization by or interaction with the blood components may be indispensable for the uptake of REV by the liver. If REV can escape opsonization or interaction, they may be able to pass through the liver freely and it may be possible to design

drug carriers that can circulate through the whole body for a long time. Therefore, it is necessary to examine the indispensable factor(s) in blood.

Although liver perfusion is considered to be the most suitable method for examining the participating factor(s) in the uptake of liposomes from blood by the liver, very few studies have been reported in this area. Tyrrell *et al.*⁴⁾ studied the effect of serum protein fractions on liposome-cell interactions in the perfused rat liver, and reported that the α - and β -globulin fractions of bovine serum enhanced the uptake of anionic liposomes into the perfused rat liver. However, the protein fractions were not from fresh rat blood and they used a large volume of perfusate compared with the rat blood volume. Therefore, their results did not necessarily reflect the *in vivo* uptake profiles of liposomes by the liver. Hildenbrandt and Aronson⁵⁾ reported that the uptake of asialoglycopholin-liposomes by the perfused rat liver required Ca^{2+} . Smith *et al.*⁶⁾ studied the kinetics of uptake of liposomes by perfused rat liver. They showed that the uptake was gradual, reaching a plateau of 60% of the initial load after 20 min of perfusion, and it was significantly lower in livers obtained from silica-treated animals. However, they did not refer to the blood components affecting the uptake.

In this experiment, we designed a circulating liver perfusion system with a small volume of perfusate, corresponding to the blood volume of a rat. The participating factor in the uptake of liposomes was examined with fresh rat blood or blood components as the perfusate, and the uptake profile was kinetically compared with that *in vivo* after intravenous injection of liposomes.

Experimental

Materials—Hydrogenated egg-phosphatidylcholine was a gift from Nippon Fine Chemicals Co., Ltd. (Osaka, Japan). Dicetylphosphate and cholesterol were purchased from Nakarai Chem. Ltd. (Kyoto, Japan) and $[4\text{-}^{14}\text{C}]$ -cholesterol was from New England Nuclear (Boston, Mass). All other chemicals were of reagent grade or better.

Preparation of Liposomes—The liposomes used in this experiment were composed of hydrogenated egg-phosphatidylcholine, dicetylphosphate and cholesterol in a molar ratio of 4:1:4, and they contained appropriate radioactivity of $[^{14}\text{C}]$ cholesterol as a liposomal marker. The liposomes (multilamellar vesicles (MLV)) were prepared as described in a previous paper⁷⁾ and sized by extrusion through a polycarbonate membrane having a pore size of $0.4\ \mu\text{m}$.⁸⁾

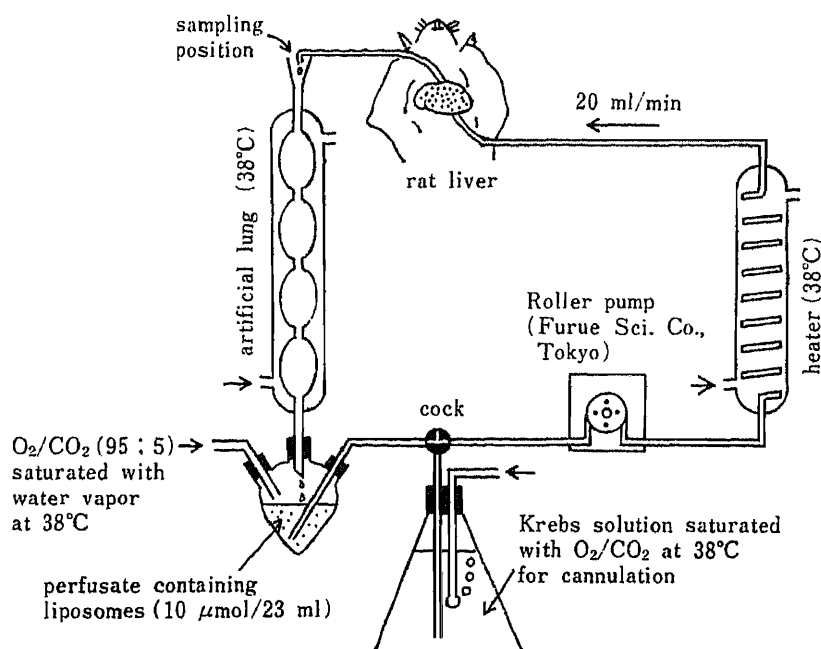


Fig. 1. Illustration of the Perfusion System Used in the Present Experiment

Perfusion System—The liver of a Wistar male rat (body weight 300 ± 15 g) was perfused *in situ* with Krebs–Henseleit acid carbonate-buffered solution (Krebs solution, pH 7.4, composed of 118.5 mM NaCl, 4.75 mM KCl, 2.54 mM CaCl_2 , 1.19 mM KH_2PO_4 , 2.43 mM MgSO_4 and 25.0 mM NaHCO_3) which was saturated with O_2/CO_2 (95:5), from the portal vein to the inferior *vena cava* according to the method of Tyrrell *et al.*⁴⁾ at 38 °C. At 5 min after the start of perfusion, the perfusate was changed to the small-volume perfusate (23 ml, corresponding to the blood volume of a rat) containing liposomes (10 μmol as total lipids) and circulating perfusion at 38 °C was started as illustrated in Fig. 1. The flow rate of the perfusate was 20 ml/min and an Allihn type condenser was used as an artificial lung.

Perfusate—The perfusate used in circulating perfusion was based on Krebs solution. In the case of whole blood, 10 ml of blood freshly drained from the carotid artery of a rat with 200 units of heparin was diluted with Krebs solution to 23 ml and used. In the case of serum, an appropriate volume of fresh rat serum was diluted with Krebs solution to 23 ml.

Animal Experiment and Sample Treatment—In the perfusion study, at an appropriate time after starting circulating perfusion, 0.1 ml of perfusate was sampled at the top of the artificial lung shown in Fig. 1. After 12 min, the perfusion was stopped and the liver was isolated and homogenized. In the *in vivo* study, a Wistar male rat (body weight 300 ± 15 g) was cannulated in the femoral artery and femoral vein as described in a previous paper.⁹⁾ Liposome suspension was injected through the cannula inserted in the vein. At an appropriate time after injection, 0.1 ml of blood was collected from the cannula inserted in the artery. At 12 min after the injection, the animal was sacrificed, and the liver was isolated and homogenized. Radioactivity of [^{14}C]cholesterol as a liposomal marker in the sample was counted after treatment as follows. In the perfusion with no blood cells, 0.1 ml of perfusate was transferred into a liquid scintillation vial, and 0.9 ml of water and 10 ml of liquid scintillation cocktail (Scintisol EX-H, Wako Pure Chem. Co., Osaka, Japan) were added. Then the radioactivity was counted with a liquid scintillation counter (Aloka LSC-673, Tokyo, Japan). In the case of the *in vivo* study and perfusion with whole blood, 0.5 ml of 30% H_2O_2 and 0.5 ml of 2 N KOH solution in isopropanol were added to 0.1 ml of blood or perfusate in a liquid scintillation vial, and treated as described in a previous paper.⁹⁾ The volume of the liver homogenate was adjusted to 50 ml with water and 1 ml of the diluted homogenate was transferred into the liquid scintillation vial, and treated as described in the previous paper.¹⁰⁾

Pretreatment of Serum—Freshly obtained serum was used. However, in order to examine the factor in serum participating in the uptake of liposomes by the liver, dialyzed serum or preheated serum was used in some experiments. Serum was dialyzed in cellulose tubing (Sanko Pure Chem. Co., Tokyo) against 2 l of Krebs solution at 4 °C for 2 d and the solution was changed 3 or 4 times during the dialysis. Equilibrium dialysis was carried out in an equilibrium dialysis cell with two chambers separated by a cellulose membrane (Sanko Pure Chem. Co.); the volume of each chamber was 6 ml. Serum was placed in one chamber and Krebs solution in the other, and the cell was shaken for 2 d at 4 °C. In the experiment with preheated serum, serum which had been incubated at 45, 56 or 60 °C for 30 min was used.

Results and Discussion

Uptake of Liposomes by Perfused Liver

Time courses of liposomes in the perfusate during circulating liver perfusion with Krebs solution, whole blood and serum are shown in Fig. 2. When whole blood was used as the perfusate, fresh blood was diluted with Krebs solution (10 ml of whole blood in 23 ml of perfusate; hematocrit 20%) for convenience of perfusion. The concentration of serum was 5.4 ml/23 ml of perfusate, taking into account the serum volume in 10 ml of blood.

As shown in Fig. 2, a rapid decrease of radioactivity in the perfusate was observed in the initial phase in all experiments. This is due to the dilution with the Krebs solution remaining in the liver before the circulating perfusion even after correction for the dead volume of the tubing used in the system. Thereafter, no disappearance of radioactivity was observed in the perfusate of Krebs solution. On the other hand, substantial activity disappeared from the perfusate containing whole blood or serum, though no significant difference was found between whole blood and serum. Remaining radioactivity in the liver after 12 min of perfusion is shown in Fig. 3 in the experiments. About 8% of the radioactivity used in the perfusion with Krebs solution was found in the liver at the end of perfusion. On the other hand, remaining radioactivity with whole blood and serum amounted to 27.4% and 30.0%, respectively. The difference between the results with Krebs solution and whole blood or serum is significant ($p < 0.01$) and that between whole blood and serum is not ($p > 0.05$). These results suggested

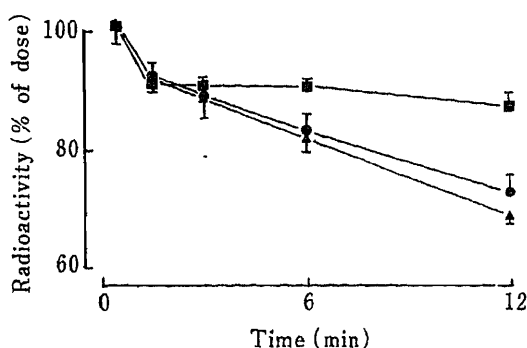


Fig. 2. Elimination of Liposomal Radioactivity from Perfusate

The perfusate consisted of Krebs solution alone (■), or 5.4 ml of serum (●) or 10 ml of blood (▲) in 23 ml of Krebs solution, and it contained 10 μ mol of liposomes (as total lipids). Each value represents the mean \pm S.D. of three experiments.

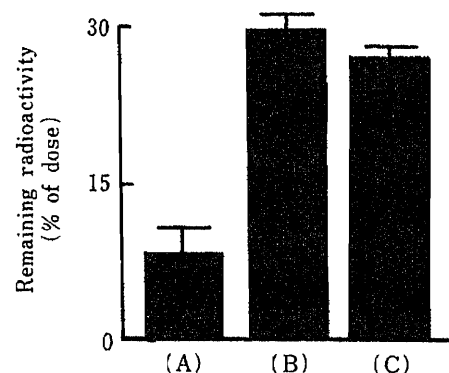


Fig. 3. Liposomal Radioactivity Remaining in the Liver after Perfusion

The perfusate was consisted of Krebs solution alone (A), or 5.4 ml of serum (B) or 10 ml of blood (C) in 23 ml of Krebs solution and it contained 10 μ mol of liposomes (as total lipids). Each value represents the mean \pm S.D. of three experiments.

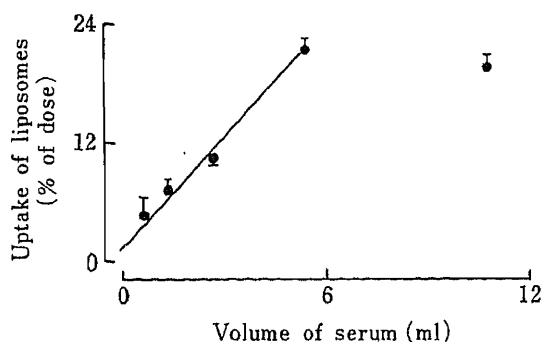


Fig. 4. Effect of Volume of Serum Contained in the Perfusate on the Liver Uptake of Liposomes

Each value represents the mean \pm S.D. of three experiments.

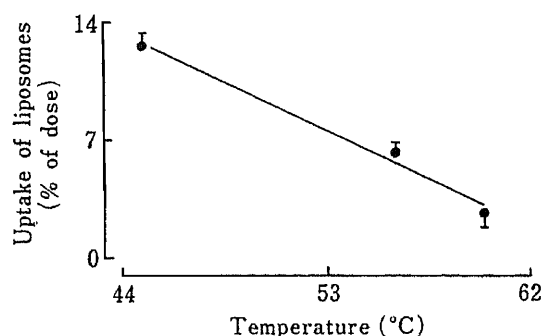


Fig. 5. Effect of Preheating Temperature of Serum on the Liver Uptake of Liposomes

The volume of serum was 5.4 ml, the preheating time was 30 min, and the liposomal content was 10 μ mol. Each value represents the mean \pm S.D. of three experiments.

that some component(s) in the serum is essential for the uptake of liposomes by the liver, and blood cells are not required for the uptake in the present system. The observed radioactivity in the liver after the perfusion with Krebs solution seems to be due to the remaining perfusate containing liposomes in the liver at the end of perfusion, corresponding to the blood volume in rat liver. Therefore, all later data on the uptake of liposomes by the liver are expressed as corrected values by subtracting the radioactivity in the perfusate remaining in the liver vessels.

Effect of Serum Concentration

The effect of serum volume contained in the perfusate on the uptake of liposomes by the liver was examined. Amount of liposomal radioactivity taken up by the liver (corrected for the perfusate volume remaining in the liver) after perfusion with perfusate containing 0.68, 1.53, 2.7, 5.4 and 10.8 ml of serum are shown in Fig. 4 as percentages of the initial load. The uptake showed a linear increase up to 5.4 ml of serum. This result indicates that the uptake activity is proportional to the amount of the factor in serum. However, at 10.8 ml of serum the uptake did not increase as expected, apparently because of saturation in this system. The saturation

may be caused by restriction of oxygen supply, flow rate of perfusate, temperature or other biological factors. Suppression of physical functions of the liver might also be the reason for the saturation because of the effects of the cannulation and/or the perfusion procedure.

Effect of Preheating of Serum

The heat stability of the factor participating in the uptake of liposomes by the perfused liver was examined. The results are shown in Fig. 5 in terms of the percentage found in the liver after perfusion. With non-treated serum 21.6% of the dose was taken up by the liver, as shown above. On the other hand, with serum preheated at 44 °C for 30 min, 12.7% of the load was found in the liver, and the uptake activity decreased to about 60% of that of fresh serum. The activity linearly decreased with increase of preheating temperature, as shown in Fig. 5. The results obtained in this experiment showed that the participating factor in serum is very heat-sensitive, and may be a protein or peptide.

Effect of Dialysis of Serum

Fractionation of the serum proteins by salting-out with ammonium sulfate⁽¹⁾ was attempted in order to elucidate the properties of the participating factor. However, uptake activity was not observed in any fraction. Two possible reasons were considered for the loss of the activity. One is irreversible denaturation of a protein having the uptake activity during the salting-out processes with ammonium sulfate. The other is leakage of the activity through the cellulose membrane during dialysis for desalting. The effect of dialysis of the serum was examined, and the results are shown in Fig. 6. The uptake after perfusion with serum dialyzed at 4 °C for 2 d was very low compared with that with fresh serum, as shown in Fig. 6 ($p < 0.01$). On the other hand, with serum left at 4 °C for 2 d, uptake corresponding to that with fresh serum was observed ($p > 0.05$).

After equilibrium dialysis at 4 °C for 2 d, experiments with the media in both chambers of the dialysis cell were carried out. The uptake with the medium from the chamber filled with serum was decreased (16.9%) although not significantly ($p > 0.05$), and corresponding activity was found on the other side (filled with Krebs solution). The sum of the uptake with both

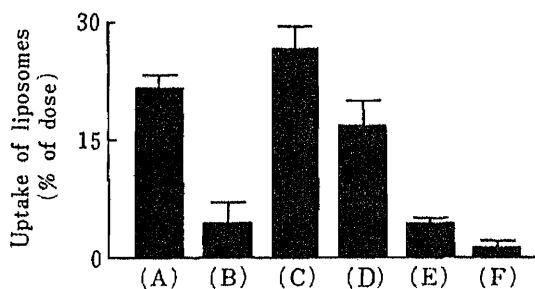


Fig. 6. Effects of Dialysis and Incubation with Liposomes on the Liver Uptake of Liposomes

- (A): with fresh serum (control).
 (B): with serum dialyzed in cellulose tubing at 4 °C for 2 d.
 (C): with serum left at 4 °C for 2 d.
 (D): with medium from the serum side after equilibrium dialysis at 4 °C for 2 d.
 (E): with medium from the Krebs solution side after the equilibrium dialysis.
 (F): with serum incubated with non-labeled liposomes (10 μ mol of total lipids) at 38 °C for 5 min in advance.

The volume of serum corresponded to 5.4 ml and liposomal content to 10 μ mol (as total lipids). Each value represents the mean \pm S.D. of three experiments.

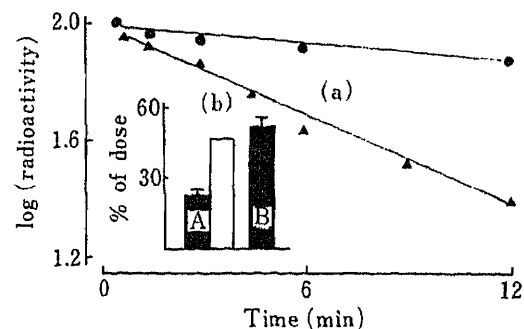


Fig. 7. Comparisons of Elimination and Liver Uptake of Liposomes *in Vivo* and *in Situ*

(a): Semilogarithmic plots of elimination of liposomes from perfusate containing 5.4 ml of fresh serum (●) and from blood (▲) after intravenous injection.

(b): Uptake of liposomes by the liver after perfusion (A) and i.v. injection (B). The open column shows the value corrected for the *in vivo* serum content (see the text).

Liposomal dose was 10 μ mol (as total lipids) and each value represents the mean \pm S.D. of three experiments.

media is almost equal to that with fresh serum. The uptake with the medium in the Krebs solution chamber was significantly higher than that with Krebs solution ($p < 0.01$) without the correction for perfusate in the liver. The results suggest that the serum factor participating in the uptake of liposomes by the liver penetrated through the cellulose membrane. The cut-off limit of the membrane was 17000 daltons (Da). Therefore, the molecular weight of the factor may be below 17000 Da. As components in serum having an opsonic activity, immunoglobulin G (IgG),¹²⁾ complement,¹³⁾ fibronectin,¹⁴⁾ and C-reactive protein (CRP)¹⁵⁾ are known, but these have large molecular weights. The fact that the sum of the activities in the two chambers of the equilibrium dialysis cell was equal to that with fresh serum suggests that the factor participates independently of other components in serum, since multiple components participating in the uptake would not be expected to show the same permeability in dialysis. If components with different permeabilities participate cooperatively, the sum of activities in the two chambers should be lower than that with fresh serum, and should be restored when the two solutions are mixed.

Effect of Preincubation with Liposomes

Interaction of the factor with liposomes was also examined. The uptake activity with serum which was incubated with nonlabeled liposomes (10 μ mol of total lipid) at 38 °C for 5 min almost disappeared, as shown in Fig. 6. This result shows that the factor interacted with liposomes like opsonin, not with liver cells, and it does not activate the cells. The interaction of the factor with liposomes is very rapid and is irreversible. However, it is uncertain whether the interaction involves binding of the component to the liposomes or consumption by transformation of the factor interacting with the liposomes.

Correspondence to *in Vivo* Behavior of Liposomes

The correspondence of the results obtained in the perfusion experiments to the *in vivo* behavior of liposomes after intravenous injection was examined. Eliminations from perfusate and blood and uptakes by the liver are shown in Fig. 7. It seems that the elimination from blood is faster than that from perfusate (Fig. 7-a) and liver uptake is greater *in vivo* (Fig. 7-b). However direct comparison of these two cases is unreasonable, because the perfusate was not 100% blood but diluted serum (5.4 ml of serum in 23 ml of perfusate) for technical reasons in the perfusion system. A proportional increase of uptake with increase of the volume of serum contained in the perfusate was observed in the perfusion experiment as mentioned above (Fig. 4). Though the linearity was not maintained at high serum concentration (10.8 ml/23 ml), if the saturation is due to functional suppression of the liver in the present system for the reasons mentioned above, the intact liver would be expected to show more uptake with pure serum. If the linearity is extrapolated to the volume of serum in 100% whole blood (12 ml), the liver uptake is expected to be 48.1% as shown in Fig. 7-b by the open column. This value corresponds quite well to the *in vivo* uptake (51.4%), and it is assumed that the factor found in the perfusion experiment may proportionally participate even in *in vivo* uptake of liposomes by the liver.

The semilogarithmic plots of time courses of the two cases in Fig. 7 showed linear decreases. The half-lives were calculated from the slopes as 27.0 and 5.78 min *in situ* and *in vivo*, respectively. These values are not consistent even if the correction of serum volume is considered. Therefore, other factors may affect the rate of elimination of liposomes, besides the factor found in the perfusion experiment, *e.g.* blood flow in other organs, uptake by other organs, oxygen supply, interaction with blood cells, *etc.*

Conclusion

The results of the present study on the uptake mechanism of liposomes by rat liver with

the small-volume circulating perfusion system may be summarized as follows.

- 1) An indispensable factor for the uptake of liposomes is present in serum.
- 2) The uptake proportionally depends on the amount of the factor.
- 3) The factor is a heat-sensitive proteinous substance.
- 4) The molecular weight of the factor is less than 17000 Da and it may participate in the uptake independently of other factors.
- 5) The interaction of the factor with liposomes is very rapid and is irreversible.
- 6) The factor may be dominant in the *in vivo* uptake by the liver.

It is not clear whether the interaction involves binding of the factor on the liposomal surface, as in the case of opsonin, activation of liposomes with consumption of the factor, as in the case of complement, alteration of the liposomal properties (*e.g.* aggregation), or others. More detailed studies on the interaction of the factor with liposomes, identification of the factor and a kinetic study on the correlation of *in vivo* and *in situ* uptakes are in progress.

References and Notes

- 1) Present address: *Faculty of Pharmaceutical Sciences, University of Tokushima, 1-78-1 Shomachi, Tokushima 770, Japan.*
- 2) D. A. Tyrrell, T. D. Heath, C. M. Colley and B. E. Ryman, *Biochim. Biophys. Acta*, **457**, 259 (1976); T. Tanaka, T. Taneda, H. Kobayashi, K. Okumura, S. Muranishi and H. Sezaki, *Chem. Pharm. Bull.*, **23**, 3069 (1975).
- 3) H. Kiwada, S. Obara, H. Nishiwaki and Y. Kato, *Chem. Pharm. Bull.*, **34**, 1249 (1986).
- 4) D. A. Tyrrell, V. J. Richardson and B. E. Ryman, *Biochim. Biophys. Acta*, **497**, 469 (1977).
- 5) G. R. Hildenbrandt and N. N. Aronson, *Biochim. Biophys. Acta*, **631**, 499 (1980).
- 6) J. E. Smith, P. Pirson and R. E. Sinden, *Ann. Trop. Med. Parasitol.*, **77**, 379 (1983).
- 7) H. Kiwada, H. Niimura, Y. Fujisaki, S. Yamada and Y. Kato, *Chem. Pharm. Bull.*, **33**, 753 (1985).
- 8) H. Kiwada, H. Niimura and Y. Kato, *Chem. Pharm. Bull.*, **33**, 2475 (1985).
- 9) Y. Sato, H. Kiwada and Y. Kato, *Chem. Pharm. Bull.*, **34**, 4244 (1986).
- 10) H. Kiwada, J. Sato, S. Yamada and Y. Kato, *Chem. Pharm. Bull.*, **34**, 4253 (1986).
- 11) E. J. Cohn, T. L. McMeekin, J. L. Oncley, J. M. Newell and W. L. Hughes, *J. Am. Chem. Soc.*, **62**, 3386 (1940).
- 12) M. J. Hsu and R. L. Juliano, *Biochim. Biophys. Acta*, **729**, 411 (1982).
- 13) F. Roerdink, N. M. Wassef, E. C. Richardson and C. R. Alving, *Biochim. Biophys. Acta*, **734**, 33 (1983).
- 14) F. A. Blumenstoch, T. M. Saba and J. E. Kaplan, *Dev. Hematol. Immunol.*, **5**, 119 (1982).
- 15) S. Nakayama, C. Mold, H. Gewurz and T. W. Du Clos, *J. Immunol.*, **129**, 2435 (1982).

[Chem. Pharm. Bull.]
35(3)1196—1200(1987)

Effect of Probenecid on Disposition of Cefpiramide in Rat. The Application of Population Pharmacokinetics

KIYOSHI YAMAOKA,* YOSHITAKA YANO, OSAMU SAKURAI,
and HISASHI TANAKA

*Faculty of Pharmaceutical Sciences, Kyoto University,
Sakyo-ku, Kyoto 606, Japan*

(Received August 1, 1986)

The effect of probenecid on the disposition of cefpiramide was studied in rats. Cefpiramide (50 mg/kg) was injected into rats through a femoral vein. Probenecid (75 or 150 mg/kg) was administered simultaneously with cefpiramide. The plasma concentration of cefpiramide and the amount excreted into the bile were monitored with a high-performance liquid chromatograph (HPLC). Population pharmacokinetics with Akaike's information criterion (AIC) was applied to analyze the effect of probenecid on the disposition of cefpiramide. The result of the AIC method was compared with that of the χ^2 test. It was concluded that probenecid exclusively inhibits the biliary excretion of cefpiramide. The presence of probenecid does not influence the volume of distribution of cefpiramide or the non-biliary elimination rate. The administration of 75 mg/kg of probenecid markedly suppresses the biliary excretion of cefpiramide. However, the effect of 150 mg/kg of probenecid on the elimination rate of cefpiramide is almost the same as that of 75 mg/kg.

Keywords—probenecid; cefpiramide; population pharmacokinetics; MULTI (ELS); bile excretion; MULTI; extended least-squares

Introduction

Cefpiramide (Fig. 1) is a new semisynthetic cephalosporin antibiotic which has a broad spectrum and high activity against gram-positive and gram-negative bacteria including *Pseudomonas aeruginosa*.¹⁾ Cefpiramide shows much longer plasma half-lives in rabbits, dogs and rhesus monkeys²⁾ and humans³⁾ as compared with other cephalosporin antibiotics. This antibiotic has the peculiarity that the major elimination route is not the urinary excretion but biliary excretion as the intact drug.²⁾ Cefpiramide, therefore, is considered to be a potentially useful in research on membrane transport.

It is well known that the administration of probenecid with many penicillins and cephalosporins results in prolongation of the half-lives of these drugs in the body.⁴⁾ The pharmacological action of probenecid is believed to be inhibition of the renal tubular secretion of organic acids⁵⁾ which are mainly eliminated through the urinary excretion. It is of interest in connection with our understanding of membrane transport to investigate the effect of probenecid on cefpiramide elimination.

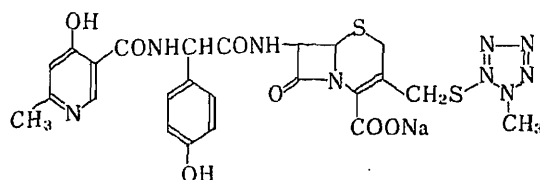


Fig. 1. Structure of Cefpiramide

Population pharmacokinetics, which deals with plural time courses altogether, has attracted growing attention since the proposal of Sheiner *et al.*⁶⁾ The theoretical basis of population pharmacokinetics is an extended nonlinear least-squares method. This analysis has usually been used in the field of clinical pharmacokinetics.^{7,8)} The present report is concerned with an attempt to apply population pharmacokinetics to the evaluation of the pharmacodynamic effect of probenecid on the disposition of cefpiramide in rats. Akaike's information criterion (AIC) is shown to be effective in the population pharmacokinetic analysis.

Experimental

Reagents and Materials—Cefpiramide was a gift from Yamanouchi Pharmaceutical Co., Ltd. (Tokyo, Japan). Probenecid was provided by Sigma Chemical Company (MO, U.S.A.). Heparin was obtained from Novo Ind. (Denmark). Sodium pentobarbital solution (Nenbutal for animal injection, Abbott Lab., IL, U.S.A.) was used to anesthetize rats. Trichloroacetic acid for the precipitation of protein was obtained from Wako Pure Chem. Ind. Ltd. (Osaka, Japan). Acetonitrile and the other chemicals for high-performance liquid chromatographic (HPLC) analysis were commercial products of reagent grade. Water was purified by distillation. The prepared mobile phase for HPLC was degassed before use.

Determination of Cefpiramide by HPLC—A high-performance liquid chromatograph (LC-3A, Shimadzu Co., Kyoto, Japan) equipped with a variable-wavelength UV detector (SPD-2A, Shimadzu Co., Kyoto, Japan) was used with a stationary phase of Chemcosorb 7-ODS-H (50 × 4.6 mm i.d., Chemco Co., Osaka, Japan). A short precolumn (50 × 4.6 mm i.d.) packed with LiChrosorb RP-2 (E. Merck Co.) was attached to guard the main column. The detection wavelength was set at 254 nm. The flow rate of the mobile phase was set at 1.5 ml/min. The peak area was recorded with a Chromatopac C-R1B (Shimadzu, Kyoto, Japan). Column temperature was 30 °C. The mobile phase composition for the analysis of cefpiramide in plasma and bile was phosphate buffer (pH = 7.0, 1/15 M)-acetonitrile (85:15 v/v). The pretreatments before HPLC injection are described in the following section.

Rat Experiments—Under anesthesia by i.p. administration of pentobarbital (30–40 mg/kg), male Wistar rats weighing 200–250 g received 50 mg/kg cefpiramide alone (treatment I), 50 mg/kg cefpiramide with 75 mg/kg probenecid (treatment II), or 50 mg/kg cefpiramide with 150 mg/kg probenecid (treatment III). Cefpiramide and probenecid dissolved in warm pH 7.4 isotonic phosphate buffer (2.54% NaH₂PO₄·2H₂O–4.41% Na₂HPO₄·12H₂O) were rapidly injected into a femoral vein. Blood samples (0.2 ml) were collected from a jugular vein at 5, 10, 15, 20, 40, 60 and 120 min after the injection. Test tubes used to collect blood were heparinized. After centrifugation of the blood at 3000 rev/min for 5 min, 25 μl of 0.1 M phosphate buffer (pH 7.4) and 450 μg of a 5% aqueous solution of trichloroacetic acid were added to 25 μl of plasma. After centrifugation and precipitation of protein, 5 μl of the supernatant was injected into the liquid chromatograph. Rats were opened with a midline incision and the bile duct was cannulated with PE-50 polyethylene tubing (Clay Adams, NJ, U.S.A.), before the injection of cefpiramide and probenecid into a femoral vein. Bile samples were collected at 30, 60, 90 and 120 min after the injection of cefpiramide and probenecid. The collected bile was diluted with 0.1 M phosphate buffer (pH 7.4) to 2 ml. Then 450 μl of an aqueous solution of 5% trichloroacetic acid was added to the bile sample. After centrifugation of the sample at 3000 rev/min for 5 min, 5 μl of supernatant was injected into the liquid chromatograph. Calibration curves for plasma and bile samples were freshly prepared by spiking plasma and bile with appropriate amounts of cefpiramide.

Data Analysis—Prior to application of the extended nonlinear least-squares (ELS) method, the plasma and bile data on cefpiramide were evaluated by MULTI, which is based on an ordinary nonlinear least-squares (OLS)⁹⁾ approach, in order to reduce the number of population model candidates. Since all time courses of plasma concentration excepting that of one rat showed monoexponential decrease on the testing by AIC, a one-compartment model was adopted for the analysis of plasma and bile data. When both plasma and bile data for a rat were available, the simultaneous least-squares method was applied using the following equations:

$$C_p = D/V_d \exp(-k_e t) \quad (1)$$

$$F_b = F_b^\infty (1 - \exp(-k_e t)) \quad (2)$$

where C_p is plasma concentration, D is the dose, k_e is the elimination rate constant, F_b is the biliary recovery ratio of cefpiramide, and F_b^∞ is the recovery ratio at infinite time. The biliary excretion rate constant k_b and non-biliary elimination constant k_{nb} are calculated by means of the following equations.

$$k_b = F_b^\infty k_e \quad (3)$$

$$k_{nb} = (1 - F_b^\infty)k_e \quad (4)$$

The estimated pharmacokinetic parameters were compared among treatments I, II and III by the one-way analysis of variance (ANOVA) with a paired *t*-test. With reference to the results of ANOVA, some population pharmacokinetic models were constructed for the time course data of treatments I, II and III. The effect of probenecid on the disposition of cefpiramide was evaluated by using MULTI(ELS), which is based on the extended least-squares method.¹⁰⁾ The results of the AIC method for extended least-squares were compared with those of the χ^2 test.⁹⁾

Results and Discussion

Figure 2 presents the time course of plasma concentration of cefpiramide without probenecid (treatment I), with 75 mg/kg probenecid (treatment II) and with 150 mg/kg probenecid (treatment III). When the data points of treatments II (Δ) and III (\square) are too close, those of treatment III are shifted to the right in Fig. 2. Figure 3 shows the time course of the biliary recovery ratio F_b . It appears that the presence of probenecid inhibits the elimination of cefpiramide from the plasma and the excretion into the bile. Table I shows the pharmacokinetic parameters estimated by MULTI and the results of ANOVA. The volume of distribution (V_d) and the non-biliary elimination rate constant (k_{nb}) are independent of the presence of probenecid. Nakagawa *et al.*³⁾ showed that 60% and 35% of administered

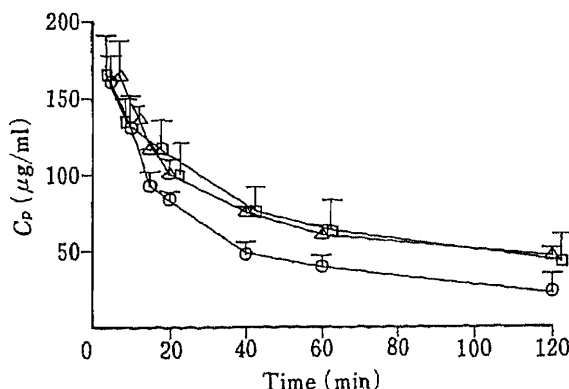


Fig. 2. Time Courses of Cefpiramide Plasma Concentrations with Probenecid Treatments I, II and III

O, treatment I; Δ , treatment II; \square , treatment III.

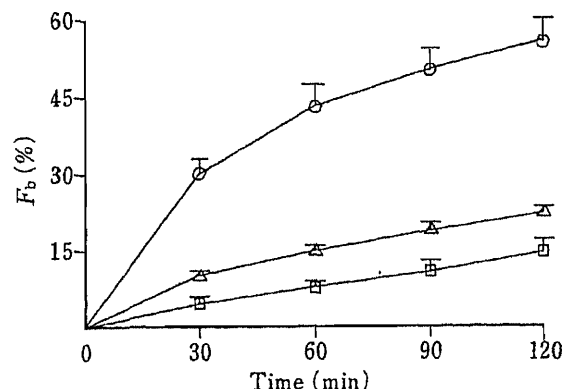


Fig. 3. Time Courses of Cefpiramide Biliary Excretions with Probenecid Treatments I, II and III

O, treatment I; Δ , treatment II; \square , treatment III.

TABLE I. Pharmacokinetic Parameters of Cefpiramide without Probenecid and with Probenecid (75 and 150 mg/kg) by Ordinary Least-Squares Method

Treatment	(N_p)	V_d (ml/kg)	k_e (/h)	(N_b)	F_b^{ss} (%)	k_b (/h)	k_{nb} (/h)
I	(3) mean	294	0.0310	(3)	53.9	0.0168	0.0142
	S.D.	44	0.0056				
II	(4) mean	317	0.0161	(2)	25.0	0.00441	0.0135
	S.D.	35	0.0037				
III	(5) mean	324	0.0187	(4)	13.1	0.00269	0.0182
	S.D.	44	0.0069				
ANOVA (5%)		NS	S		S	S	NS
Paired <i>t</i> -test (5%)			I \neq II		I \neq II	I \neq II	
			I \neq III		I \neq III	I \neq III	
			II = III		II \neq III	II = III	

N_p , number of rats for which plasma data are available; N_b , number of rats for which bile data are available; V_d , volume of distribution; k_e , elimination rate constant; F_b^{ss} , recovery ratio of cefpiramide into bile; k_b , biliary excretion rate constant, k_{nb} , non-biliary elimination rate constant; NS, not significant at the 5% level; S, significant at the 5% level.

cefpiramide are excreted into the bile and the urine of rats, respectively. Therefore, k_{nb} approximately represents the urinary excretion rate constant. ANOVA shows that the differences of k_e , F_b^∞ and k_b among the treatments are significant at the 5% level. The following paired t -test at the 5% significance level revealed that the values of k_e , F_b^∞ and k_b decrease in the presence of probenecid. The difference of k_e (or k_b) between treatments II and III is insignificant, but the difference of F_b^∞ between treatments II and III is significant. Based on the results of OLS, the four population models were selected.

Model 1

The population time course data of treatments I, II and III are expressed by the following population model.

$$C_p = D/(V_d + \eta_V) \exp(-(k_e + \eta_k)t) + \varepsilon_C \quad (5)$$

$$F_b = (F_b^\infty + \eta_F)(1 - \exp(-(k_e + \eta_k)t) + \varepsilon_F \quad (6)$$

where C_p is plasma concentration, F_b is the recovery ratio in the bile, D is the dose, V_d is the volume of distribution, η_V is the inter-individual variation around V_d , k_e is elimination rate constant, η_k is the inter-individual variation around k_e , F_b^∞ is the bile recovery ratio at infinite time, η_F is the inter-individual variation around F_b^∞ , ε_C is the intra-individual variation of plasma concentration, and ε_F is the intra-individual variation of bile recovery ratio. In model 1, the population parameters are assumed to be the same among the treatments (*i.e.* probenecid has no influence on the disposition of cefpiramide).

Model 2

F_b^∞ and k_e of treatment I are different from those of treatments II and III. These parameters are the same between treatments II and III.

Model 3

The value of k_e of treatment I is different from those of treatments II and III. The values of F_b^∞ are different between treatments I and II, and between treatments II and III. This model corresponds to the results of ANOVA.

Model 4

Both k_e and F_b^∞ are different among treatments I and II, and treatments II and III.

The variances of the inter-individual variations and the intra-individual variations are assumed to be the same among the treatments. Table II presents the results of MULTI(ELS). Model 3 gives the minimum AIC, and this result agrees with that of ANOVA. Sheiner *et al.* proposed the χ^2 test for the selection of a population model.⁶⁾ The difference of Ob between models 1 and 2 is 17.9, which is greater than the critical value of 10.6 ($p < 0.005$, degree of freedom 2). The difference of Ob between models 2 and 3 is 22.0, which is greater than the critical value of 7.88 ($p < 0.005$, degree of freedom 1). The difference of Ob between models 3 and 4 is 0.5, which is less than the critical value. Therefore, the χ^2 test selects model 3 as the best model, which coincides with the result of the AIC method. The estimated population

TABLE II. The Values of Objective Function (Ob) and AIC for Population Models by Extended Nonlinear Least-Squares Method

	Model 1	Model 2	Model 3	Model 4
Ob	697.4	679.5	657.5	657.0
AIC	713.4	699.5	679.4	681.0
Number of parameters	8	10	11	12

TABLE III. The Estimated Population Mean Parameters and Variances of Inter- and Intra-individual Variations

$V_d = 312$ (ml/kg), $\omega^2(V_d) = 654$ (ml ² /kg ²)
k_e (I) = 0.0247 (/min), k_e (II) = k_e (III) = 0.0156 (/min)
$\omega^2(k_e) = 4.98 \times 10^{-5}$ (/min ²)
F_b^∞ (I) = 57.6 (%), F_b^∞ (II) = 26.3 (%), F_b^∞ (III) = 14.8 (%)
$\omega^2(F_b^\infty) = 8.55$ (% ²)
$\sigma^2(C_p) = 293$ ($\mu\text{g}^2/\text{ml}^2$)
$\sigma^2(F_b) = 1.70$ (% ²)

I, II and III specify treatments I, II and III, respectively. ω^2 and σ^2 specify the variances of inter- and intra-individual variations, respectively.

parameters are given in Table III.

It is concluded that probenecid exclusively inhibits the excretion of cefpiramide into the bile of rats. Probenecid is believed to inhibit the active transport of organic acids through the renal tubular membrane.⁵⁾ Therefore, the present result raises the possibility that the excretion of cefpiramide into the bile includes an active transport process in the liver. The volume of distribution and the urinary excretion rate of cefpiramide are not affected by the presence of probenecid.

Biliary data could not be obtained for some rats in the present report. The ordinary least-squares method cannot estimate the parameters for biliary excretion in this case. However population pharmacokinetics can be used to evaluate groups of time courses where some data are deficient.

References

- 1) M. Fukasawa, H. Noguchi, T. Okuda, T. Komatsu, and K. Yano, *Antimicrob. Agents Chemother.*, **23**, 195 (1983).
- 2) H. Matsui, K. Yano, and T. Okuda, *Antimicrob. Agents Chemother.*, **22**, 213 (1982).
- 3) K. Nakagawa, M. Koyama, H. Matsui, C. Ikeda, K. Yano, N. Nakatsuru, K. Yoshinaga, and T. Noguchi, *Antimicrob. Agents Chemother.*, **25**, 221 (1984).
- 4) W. D. Conway and S. Melethill, *J. Pharm. Sci.*, **63**, 1551 (1974).
- 5) D. E. Smith and H. S. H. Lau, *J. Pharmacokinet. Biopharm.*, **11**, 31 (1983).
- 6) L. B. Sheiner, B. Rosenberg, and V. V. Marathe, *J. Pharmacokinet. Biopharm.*, **5**, 445 (1977).
- 7) L. B. Sheiner and S. L. Beal, *J. Pharmacokinet. Biopharm.*, **8**, 553 (1980).
- 8) S. Vozeh, G. Katz, V. Steiner, and F. Follath, *Eur. J. Clin. Pharmacol.*, **23**, 445 (1982).
- 9) K. Yamaoka, Y. Tanigawa, T. Nakagawa, and T. Uno, *J. Pharmacobio-Dyn.*, **4**, 879 (1981).
- 10) K. Yamaoka, H. Tanaka, K. Okumura, M. Yasuhara, and R. Hori, *J. Pharmacobio-Dyn.*, **9**, 161 (1986).

[Chem. Pharm. Bull.]
35(3)1201—1206(1987)

Preparation and *in Vitro* Evaluation of Sustained-Release Suppositories Containing Microencapsulated Indomethacin

TOSHIAKI NAKAJIMA,^{*,a} YASUJI TAKASHIMA,^a KIN-ICHI IIDA,^a
HARUMI MITSUTA^a and MASUMI KOISHI^b

Research Center, Taisho Pharmaceutical Co., Ltd.,^a 1-403, Yoshino-cho, Omiya, Saitama 330,
Japan and Faculty of Pharmaceutical Sciences and Institute of Colloid and
Interface Science, Science University of Tokyo,^b 12 Ichigaya
Funagawara-machi, Shinjuku-ku, Tokyo 162, Japan

(Received August 13, 1986)

Microencapsulation of indomethacin (IM) was carried out by a simple coacervation method using ethylcellulose. To control the release of IM, its surface was modified by dry-blending it with a carboxy-vinyl polymer (Hiviswako 104, HW) by pulverization in an automatic ceramic mortar before encapsulation. Suppositories containing intact IM and microencapsulated IM (IM-MC) were prepared by the fusion method. Dissolution and release testing of the IM-MC and of the suppositories were carried out by the methods of JPX and Muranishi *et al.*, respectively. The dissolution rate of microencapsulated intact IM decreased as the content of the coacervation-inducing agent, polyethylene (PE), was increased. The release rate profile of the suppositories containing these microcapsules did not show an apparent zero-order release, and the release rate was rapid without PE. When the PE content was 1% (w/v), the release rate was too slow and a large portion of IM remained in the IM-MC. On the other hand, suppositories containing microencapsulated HW-modified IM (HW/IM = 1/1) showed an apparent zero-order release profile and about 100% of the IM in the IM-MC was released.

These results showed that the surface modification of IM with HW before encapsulation is a good method to prepare sustained-release suppositories containing IM-MC.

Keywords—microcapsule; suppository; indomethacin; ethylcellulose; coacervation; carboxy-vinyl polymer; surface modification; sustained release

The advantages of suppositories over other forms of drug administration are reduced side effects from gastrointestinal irritation and the avoidance of both disagreeable taste and first-pass effects. Sustained-release suppositories are preferable to conventional suppositories because they reduce the frequency of drug administration. There are several reports¹⁻⁶⁾ on the preparation of sustained-release suppositories with various additives and structure-altering devices, and there are several papers on indomethacin (IM) microcapsules,⁷⁻¹⁵⁾ but little work has been done on the use of microcapsules in sustained-release suppositories.^{16,17)} Therefore, the use of microcapsules in sustained-release suppositories was investigated.

Among the methods of microencapsulation using ethylcellulose as a wall material,¹⁸⁻²⁵⁾ the simple coacervation method was chosen, and the IM surface was modified with carboxy-vinyl polymer (Hiviswako 104, HW), which served as a core material controlling IM release. Sustained-release suppositories were evaluated by *in vitro* release testing.

Experimental

Materials—IM was purchased from Sumitomo Chemical Co., Ltd.; the average particle size was 20 μm as measured by a particle size distribution analyzer (granulometer model 715, CILAS Co., Ltd.). Ethylcellulose (N-100NF, viscosity, 90—100 cP, ethoxy content, 48.0—49.5%), polyethylene (Sun Wax 131P, M.W. 3500) and HW

were obtained from Hercules Co., Ltd., Sanyo Kasei Co., Ltd., and Wako Pure Chemical Industries Ltd., respectively. All other chemicals were reagent-grade commercial products. Ethylcellulose and polyethylene are abbreviated as EC and PE, respectively.

Preparation of IM Microcapsules—The preparation was carried out according to the method of Samejima *et al.*¹⁸⁾ Cyclohexane solution (300 ml), containing PE (0, 0.7, 1.0% (w/v)), the coacervation-inducing agent, was placed in a 500 ml three-necked round-bottomed flask. The flask, equipped with an air-tight stirrer having three blades, a thermometer and a reflux condenser, was set in a water bath. While stirring at 324 rpm, 6–18 g of EC was added at room temperature. To form a homogeneous solution, the water bath temperature was maintained at 80–82 °C. Then 12–24 g of either IM or surface-modified IM was suspended in the solution. With continued stirring for 60 min, the system was cooled to 40 °C, and then cooled quickly to 25 °C. The microcapsules (IM-MC) that formed were recovered by decantation, washed with cyclohexane and dried under reduced pressure.

Surface Modification of IM—This procedure was carried out according to the method of Koishi *et al.*²⁶⁾ IM (30 g) and HW (15 or 30 g) were mixed using an automatic ceramic mortar (Yamato-Nitto, Labomill, UT-21, Yamato Kagaku Co., Ltd.) for 1 h at room temperature.

Size Distribution of Microcapsules—After drying of the microcapsules, they were sieved by a mechanical shaker (Tutui Rika Co., Ltd.) using a JIS standard sieve for 10 min.

Determination of IM Content—Microcapsules (25 mg) were dissolved in a solution (50 ml) consisting of equal volumes of ethanol and 0.2 M phosphate buffer solution (pH 7.2). After extraction with a sonicator for 30 min, the residues were removed on filter paper. The above-mentioned solution was added to the filtrate (1 ml) to make 20 ml. The IM content was assayed spectrophotometrically at 318 nm (Shimadzu spectrophotometer, model UV 240). The microcapsules with particle sizes from 177 μm to 250 μm were used in subsequent experiments. The EC content was calculated by means of the following equation: $\text{EC}(\%) = [(\text{IM-MC}) - \text{IM} - \text{HW}] \times 100 / (\text{IM-MC})$ where MC, IM and HW represent the weight of each substance. The weight of HW was calculated from its ratio to IM. The EC contents were 60.6 ± 1.6 (S.D.)% and 20.1 ± 0.9 (S.D.)% respectively.

Dissolution of IM from Microcapsules—Dissolution of IM from the microcapsules was tested by the JPX II method at 37 °C; stirring was maintained at 100 rpm. The dissolution medium was 900 ml of 0.2 M phosphate buffer (pH 7.2). Microcapsules (36 mg IM) were dispersed in the dissolution medium. At appropriate times, 5 ml of the test solution was removed and filtered through a Millipore filter (pore size 0.45 μm), and 5 ml of fresh dissolution fluid was added to maintain the original volume. The IM concentration was assayed spectrophotometrically at 318 nm.

Preparation of IM Suppositories—The suppository formula is shown in Table I. The suppositories were made by the fusion method. The bases (45 g) were fused in a beaker on an oil bath at 70 °C and cooled to 50 °C. Then, intact IM or IM-MC (1.5 g IM) was added to the bases and dispersed by stirring for 30 min. The fused bases containing intact IM or IM-MC were poured into suppository molds, which were quickly placed in a refrigerator at 5 °C.

Release of IM from Suppositories—Suppository IM release was measured according to a modification of the method of Muranishi *et al.*²⁷⁾ The suppository release apparatus was obtained from Toyama Industries Co., Ltd. The test solution was the same medium as used in the IM-MC dissolution test. A suppository, along with 3 ml of the test solution, was placed in a cylindrical cell equipped with a Millipore filter (pore size 3.0 μm). The cell was connected with the releasing-fluid glass vessel contained 300 ml of the test solution. The apparatus was maintained at 37 °C. At appropriate times, 1 ml of the releasing fluid was removed and diluted with a mixture of equal volumes of ethanol and 0.2 M phosphate buffer (pH 7.2); one ml of fresh released fluid was added to the vessel to maintain the original volume. The IM concentration was assayed spectrophotometrically at 318 nm.

Observation of the Surface and the Cross Section of Microcapsules with a Scanning Electron Microscope—

TABLE I. Suppository Formula

Component	mg
IM-MC	50.0 ^{a)}
Glycerine	120.0
Dibutylhydroxytoluene	0.8
Distilled water	30.0
Hydrogenated castor oil	6.0
POE ^{b)} (40) monostearate	30.0
Macrogol 1540	13.0
Macrogol 4000	1186.2
Macrogol 6000	64.0
Total	1500.0

a) IM content. b) POE: polyoxyethylene.

Microcapsules were coated with gold vapor using an ion coater (model I B-3, Nissei Industry Co., Ltd.) and observed under a scanning electron microscope (model S-450, Hitachi Co., Ltd.).

Results and Discussion

Electron Microphotographs of Intact IM, IM-MC and the Cross Section of IM-MC

Electron microphotographs of intact IM, IM-MC and the cross section of IM-MC are shown in Fig. 1. The photograph of the cross section of IM-MC showed that these microcapsules were multinuclear microcapsules, because the boundary between the core and the wall materials was not clear.

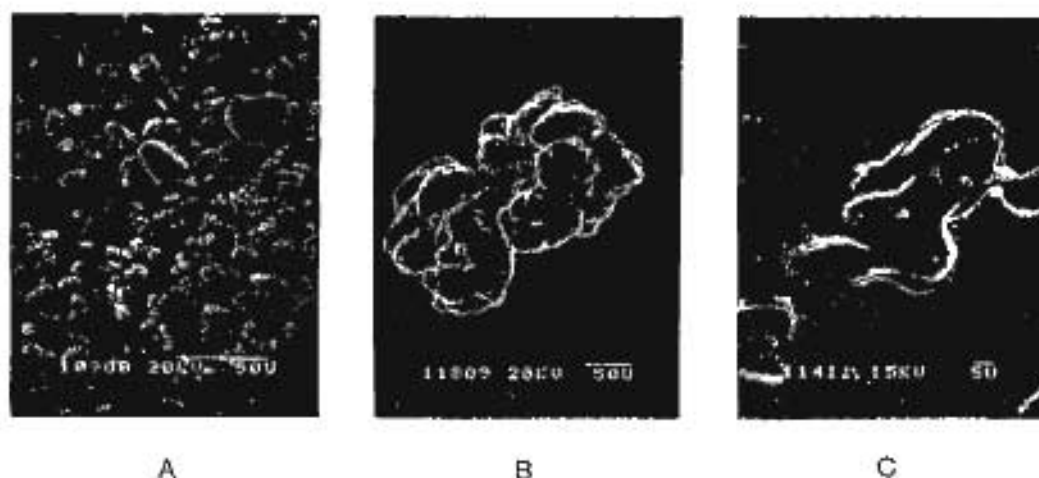


Fig. 1. Scanning Electron Micrographs of Intact IM, IM-MC and a Cross Section of IM-MC

A: intact IM. B: IM-MC. C: cross section of IM-MC. Scale: A: $\times 500$; B: $\times 1000$; C: $\times 3000$.

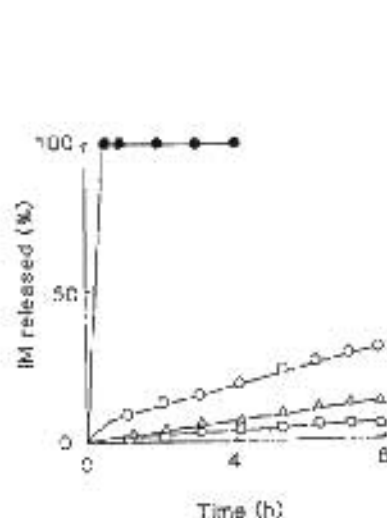


Fig. 2. Dissolution of IM from IM-MC at Various Levels of PE Content

PE content (w/v): \circ , 0%; \triangle , 0.7%; \square , 1.0%. BC content (w/v): 60%. \bullet , intact IM.

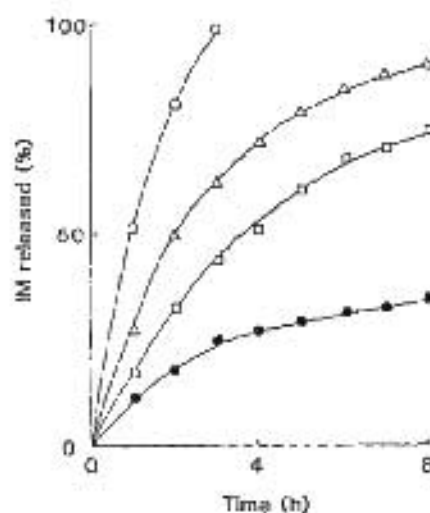


Fig. 3. Release of IM from Suppositories Containing IM-MC and the Effect of the PE Content on IM Release

Suppository containing intact IM: \circ . Suppository containing IM-MC (BC 60%): \triangle , \square , \bullet . PE content (w/v): \triangle , 0%; \square , 0.7%; \bullet , 1.0%.

Dissolution of IM from IM-MC

The results of the dissolution test of IM from IM-MC are shown in Fig. 2. The dissolution rates of IM were very slow and decreased with increasing PE content. PE may make the IM-MC wall smooth and tight.¹⁸⁾

Release of IM from Suppositories Containing Intact IM and IM-MC

The results of release tests from suppositories containing intact IM and IM-MC are shown in Fig. 3. The release rates of IM from suppositories decreased as the PE content increased, in accordance with the results in the dissolution test of IM from IM-MC. The release rates of IM from suppositories containing IM-MC prepared without PE or with 0.7% (w/v) PE were fast compared with the dissolution rate of IM from IM-MC; the times required to dissolve 50% of the IM from IM-MC (t_{50}) were 2 and 4 h, respectively. It is possible that a part of the IM in the IM-MC dissolved in the base of the suppository during preparation.

Surface Modification of IM

In animal tests, a zero-order release profile is generally required to sustain a plasma IM

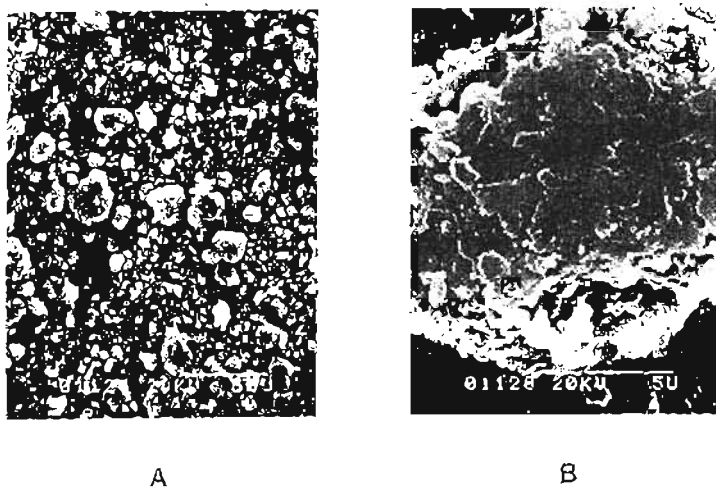


Fig. 4. Surface Modification of IM with HW in an Automatic Ceramic Mortar
HW/IM = 1/1 (w/w). Scale: A, $\times 500$; B, $\times 5000$.

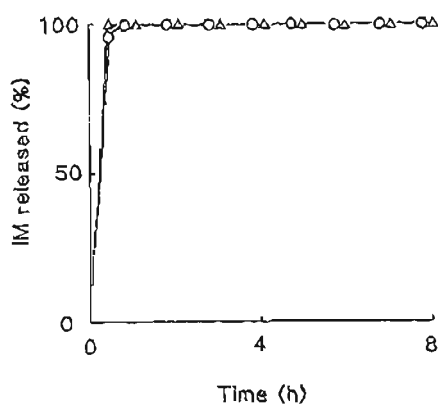


Fig. 5. Dissolution of IM from HW-Modified IM-MC [EC 20%, PE 1% (w/v)]
O: HW/IM = 1/2 (w/w). Δ : HW/IM = 1/1 (w/w).

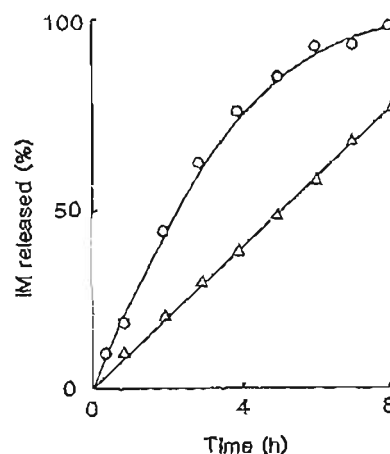


Fig. 6. Release of IM from Suppositories Containing HW-Modified IM-MC [EC 20%, PE 1% (w/v)]
O: HW/IM = 1/2 (w/w). Δ : HW/IM = 1/1 (w/w).

level. Suppositories containing IM-MC which directly microencapsulated intact IM did not show a zero-order release profile in the release test. Koishi *et al.*²⁸⁾ reported that the release of a drug from a wax matrix was improved by the addition of an acrylic polymer, and also reported^{29,30)} that powder surface wettability could be varied by powder/powder dry blending. Thus, surface modification of IM with HW by dry blending was investigated with the aim of forming fluid channels in the MC in order to improve IM release. Electron microphotographs of this modification, involving dry blending of IM and HW (1/1, w/w) with an automatic ceramic mortar for 1 h, are shown in Fig. 4. The strong adhesion of HW to the IM surface indicated that this IM surface modification procedure was effective. When HW-modified IM was immersed in cyclohexane, stirred for 30 min at 324 rpm and dried, electron microphotographs taken appeared the same as those taken when HW-modified IM had not been washed with cyclohexane.

Dissolution of IM from HW-Modified IM-MC

The results of the dissolution tests of HW-modified IM-MC are shown in Fig. 5. The ratio of HW to IM (HW/IM, w/w) was 0.5 to 1. Approximately 100% of the IM was released from both microcapsules after 1 h. This indicates that the IM located in the microcapsule center was dissolved and completely released *via* fluid channels formed after HW dissolved.

Release of IM from Suppositories Containing HW-Modified IM-MC

The results of the release test from suppositories containing HW-modified IM-MC are shown in Fig. 6. The suppositories containing HW-modified IM-MC (HW/IM = 1/2) did not show a zero-order release profile except when the HW/IM ratio was 1/1. The suppository release rates were slow compared with the dissolution rates from microcapsules. It is possible that the dissolution fluid in the case of microcapsules (900 ml) was enough to dissolve HW, forming fluid channels, but in the case of the suppositories, the 3 ml of release fluid in the inner cell was insufficient for fluid channel formation. Therefore, in the suppositories HW dissolution and microcapsule fluid channel formation occurred gradually. In addition, the high fluid viscosity in the inner cell from the swollen or gelled HW, which could be eluted from the microcapsules, would make IM release from the suppositories slow. When the HW/IM ratio was 1/2, the suppositories did not show a zero-order release pattern because of insufficient fluid viscosity. Since the total amount of rectal fluid in animals such as rabbits is small, it can be expected that IM plasma levels will be sustained if suppositories are used.

Comparison between Surface Modification and Physical Mixtures of HW and IM as Core Materials

A physical mixture of equal amounts of HW and IM (1/1, w/w) was microencapsulated with ethylcellulose by the method described above. The IM released from these suppositories was compared with that from suppositories containing HW-modified IM-MC. The results are

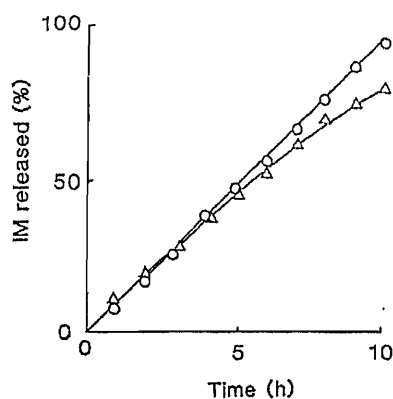


Fig. 7. Release of IM from Suppositories Containing Microcapsules [EC 20%, PE 1% (w/v)]

MC core materials were as follows. ○: HW-modified IM (HW/IM = 1/1) (w/w). △: physical mixture of IM and HW (HW/IM = 1/1) (w/w).

shown in Fig. 7. When a physical mixture was prepared, a zero-order release profile was observed initially, but the release rate decreased with time. On the other hand, suppositories containing HW-modified IM-MC showed a zero-order release profile that did not decrease for 9 h, and approximately 100% of the IM was released. It was considered that in the physical mixture of HW and IM, both HW and IM might be localized: in some microcapsules there might be no HW in the center although IM is present. On the other hand, when surface modification was used, HW and IM were considered not to be localized in the microcapsules, and fluid channels formed allowing the release of the IM.

The findings indicate that the surface modification of IM with HW before microencapsulation with ethylcellulose is a good method to obtain a sustained-release suppository containing microcapsules.

References

- 1) H. Enomoto, T. Ichiba, and T. Sumi, Japan Patent Kokai 83140012 (1983) [*Chem. Abstr.*, **99**, 181504 (1983)].
- 2) M. Himeji, Japan Patent Kokai 8173018 (1981) [*Chem. Abstr.*, **95**, 156583 (1981)].
- 3) Y. Watanabe, K. Yokoyama, M. Yamaji, F. Tanaka, and M. Matsumoto, *Yakugaku Zasshi*, **105**, 278 (1985).
- 4) S. Kobayashi and H. Matsumoto, Japan Patent Kokai 7946826 (1979).
- 5) T. Nishihata, H. Wada, and A. Kamada, *Int. J. Pharmaceut.*, **27**, 245 (1985).
- 6) S. Miyazaki, C. Yokouchi, T. Nakamura, N. Hashiguchi, W. M. Hou, and M. Takada, *Chem. Pharm. Bull.*, **34**, 1801 (1986).
- 7) J. S. Rowe and J. E. Carless, U. K. Patent 2075458 (1981) [*Chem. Abstr.*, **96**, 91669 (1981)].
- 8) L. D. Morse, U. S. Patent 3557279 (1971) [*Chem. Abstr.*, **74**, 67738 (1971)].
- 9) Y. Takeda, N. Nambu, and T. Nagai, *Chem. Pharm. Bull.*, **29**, 264 (1981).
- 10) E. Zour and J. M. Lausier, *J. Microencapsulation*, **1**, 47 (1984).
- 11) C. Cristallini, G. E. de Grassi, L. Guardines, and R. Gaussmann, *Appl. Biochem. Biotechnol.*, **10**, 267 (1984).
- 12) H. Suryakusuma and H. W. Jun, *J. Pharm. Pharmacol.*, **36**, 497 (1984).
- 13) Y. Pongpaibul, J. C. Price and C. W. Whitworth, *Drug Dev. Ind. Pharm.*, **10**, 1597 (1984).
- 14) T. Kondo and M. Koishi, "Microcapsule," Sankyo-Shuppan, Tokyo, 1977.
- 15) P. B. Deasy, "Microencapsulation and Related Drug Processes," Marcel Dekker, Inc., New York, 1984.
- 16) T. Umeda, A. Matsuzawa, T. Yokoyama, K. Kuroda, and T. Kuroda, *Chem. Pharm. Bull.*, **31**, 2793 (1983).
- 17) M. Masaki, Japan Patent Kokai 8140608 (1981) [*Chem. Abstr.*, **95**, 30431 (1981)].
- 18) M. Samejima, G. Hirata, and Y. Koida, *Chem. Pharm. Bull.*, **30**, 2894 (1982).
- 19) K. P. R. Chowdary and G. N. Rao, *Indian J. Pharm. Sci.*, **46**, 213 (1984).
- 20) R. Sjöqvist, H. Nyqvist, J. Sjövall, and D. Westerlund, *J. Microencapsulation*, **2**, 123 (1985).
- 21) K. Uno, Y. Ohara, M. Arakawa, and T. Kondo, *J. Microencapsulation*, **1**, 3 (1984).
- 22) R. Senjkovic and I. Jalsenjak, *J. Microencapsulation*, **1**, 241 (1984).
- 23) M. Itoh and M. Nakano, *Chem. Pharm. Bull.*, **28**, 2816 (1980).
- 24) S. Kasai and M. Koishi, *Chem. Pharm. Bull.*, **25**, 314 (1977).
- 25) S. Goto, T. Uchida, and T. Aoyama, *J. Pharmacobio-Dyn.*, **8**, 270 (1985).
- 26) M. Koishi, *Nippon Gomu Kyokaishi*, **56**, 466 (1983).
- 27) S. Muranishi, Y. Okubo, and H. Sezaki, *Yakuzaigaku*, **39**, 1 (1979).
- 28) H. Emori, T. Ishizaka, and M. Koishi, *J. Pharm. Sci.*, **73**, 910 (1984).
- 29) M. Koishi, *Hyomen*, **18**, 25 (1980).
- 30) M. Koishi, K. Yano, and T. Ishizaka, *J. Pharmacobio-Dyn.*, **5**, s-9 (1982).

[Chem. Pharm. Bull.]
35(3)1207—1213(1987)

Kinetic Study on the Isothermal Transition of Bromovalerylurea Polymorphs in the Solid State at High Temperature¹⁾

NORIAKI OHNISHI, TERUYOSHI YOKOYAMA,* YOSHIFUMI KIYOHARA,
YOSHIKI KITA, and KOJI KURODA

*Hospital Pharmacy, Kobe University School of Medicine,
Kusunoki-cho, Chuo-ku, Kobe 650, Japan*

(Received August 20, 1986)

The kinetics of the solid-state isothermal transition of bromovalerylurea polymorphic forms (I, II and III) at high temperature were investigated by means of differential scanning calorimetry. Kinetic analysis according to the method of Hancock and Sharp indicated that the transition of form I to form II follows the one-dimensional diffusion mechanism. The activation energy for this transition calculated from the Arrhenius plots was 826.2 kJ/mol. On the other hand, it was found that the transition of form III to form I conforms with the mechanism of random nucleation and two-dimensional growth of nuclei (Avrami-Erofeev equation). This activation energy was estimated to be 185.2 kJ/mol. It was concluded that the mechanism and the value of activation energy were both different between the two kinds of isothermal transitions of bromovalerylurea polymorphic forms.

Keywords—bromovalerylurea polymorphism; isothermal transition; kinetic analysis; differential scanning calorimetry; X-ray powder diffractometry

In the previous papers,²⁻⁴⁾ we investigated the kinetics and mechanisms of the isothermal transition of polymorphic forms in the solid state. It was confirmed that the kinetics and mechanisms of the isothermal transition were different among drugs and among polymorphic forms of the same drug.

Watanabe⁵⁾ reported that bromovalerylurea had two polymorphic forms (forms I and II). Furthermore, Kiwada *et al.*⁶⁾ found a new polymorphic form (form III) of bromovalerylurea, and reported that form II was the most stable and form III was the most unstable at higher temperature.

This paper is concerned with the kinetics of the isothermal transition of bromovalerylurea polymorphic forms (forms I, II and III) in the solid state at high temperature, based on differential scanning calorimetry.^{7,8)}

Experimental

Materials—Bromovalerylurea was a commercial product (Lot No. 2761EN) of JP X grade (Nihon Shinyaku Co., Ltd.). All other chemicals were reagent-grade commercial products.

Preparation of Polymorphic Forms—1) Form I: Form I was prepared by the method of Watanabe⁵⁾ as follows. Bromovalerylurea (5 g) was dissolved in 200 ml of methanol at 64–65 °C and recrystallized at room temperature. The resulting crystals were collected by filtration and dried at 30 °C in a vacuum.

2) Form II: Form II was obtained by heating form I at about 130 °C for 1 h under a flow of dried nitrogen gas.

3) Form III: Form III was obtained by a modification of the method of Kiwada *et al.*⁶⁾ as follows. Form I (10 g) was dissolved in 40 ml of methanol at 64–65 °C and maintained in a freezer at –20 °C for about 1 week. The resulting crystals were collected by filtration and dried at 30 °C in a vacuum.

Forms I, II and III thus obtained were passed through a 200 or 300 mesh sieve. All crystalline forms were stored at 4 °C in a desiccator and then used for experiments.

Identification of Polymorphic Forms—Each polymorphic form passed through a 200 mesh sieve was identified

by X-ray powder diffractometry (Rigaku Denki, Miniflex, Ni-filter, Cu- K_{α} radiation, 35 kV, 20 mA). The X-ray powder diffraction patterns of the three polymorphic forms were in agreement with those reported by Kiwada *et al.*,⁶⁾ respectively.

Thermal Analysis—Thermal analysis was carried out with a differential scanning calorimeter (DSC; Perkin-Elmer, model DSC-2C) and a thermogravimeter (TG; Perkin-Elmer, model TGS-2).

Preparation of Calibration Curve for Form I or Form III by DSC—Known quantities of form I (passed through a 200 mesh sieve) or form III (passed through a 300 mesh sieve) were accurately weighed into aluminum pans. Thermograms of these samples were run at a heating rate of 5°C/min (for form I) or 20°C/min (for form III) with a sensitivity of 4.2 mJ/s (for form I) or 8.4 mJ/s (for form III). Dry nitrogen gas was passed at 20 ml/min during all DSC experiments. The area under the transition peak of form I to form II at 130°C (Fig. 1a) or that of form III to form I at 111°C (Fig. 1c) was measured in units of $\mu\text{V}\cdot\text{s}$ with a Chromatopac (Shimadzu, C-RIA). As can be seen in Fig. 2, each calibration curve gave a straight line (form I, $r=0.996$; form III, $r=0.997$).

Kinetic Study of Isothermal Transition—Form I or form III (5 ± 0.5 mg) was accurately weighed into aluminum pans. The samples were then placed at selected constant temperatures (± 0.1 °C) for a suitable period in the analyzer unit of the DSC. Thermograms for each sample were run under the same conditions as described in the case of preparation of the calibration curves, and the area under the transition peak was measured. The residual fractions ($1-\alpha$) of form I or form III were calculated from the appropriate calibration curve.

Scanning Electron Microscopy—Changes of crystal shapes during the isothermal transition of polymorphic forms were observed with a scanning electron microscope (Nihon Denshi, JSM-T20).

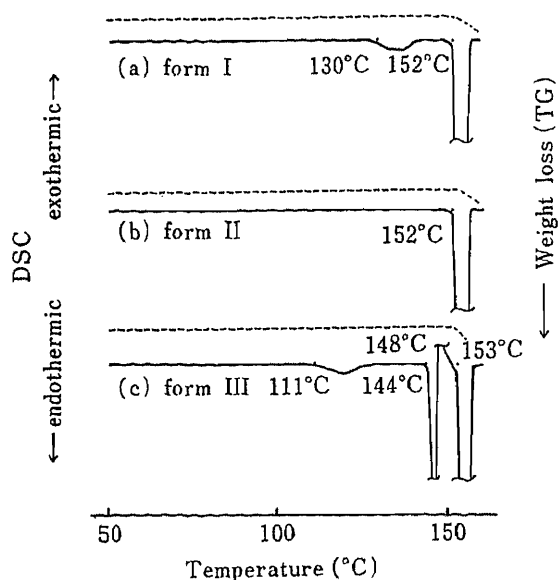


Fig. 1. DSC-TG Curves of Bromovalerylurea Polymorphic Forms

—, DSC curves; ---, TG curves. Heating rate: 5°C/min for forms I and II; 20°C/min for form III.

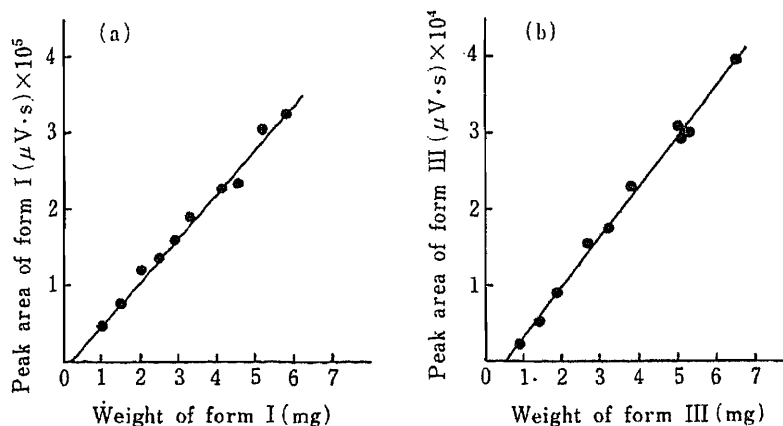


Fig. 2. Calibration Curves for Bromovalerylurea Form I and Form III by DSC

(a) Form I: $Y=57752X-9019.6$ ($r=0.996$); heating rate, 5°C/min; sensitivity, 4.2 mJ/s.
 (b) Form III: $Y=6537.9X-3044.2$ ($r=0.997$); heating rate, 20°C/min; sensitivity, 8.4 mJ/s.

Results and Discussion

DSC and TG Curves of Polymorphic Forms

The DSC and TG curves (heating rate: forms I and II, 5 °C/min; form III, 20 °C/min) of the three polymorphic forms are shown in Fig. 1.

Form I gave a characteristic thermogram with two endothermic peaks; one at 130 °C corresponded to the solid-state transition of form I to form II, and the other at 152 °C was attributed to fusion accompanied with decomposition of form II (Fig. 1a). Form II showed only one endothermic peak at 152 °C due to fusion accompanied with decomposition (Fig. 1b). Form III exhibited a small endothermic peak at 111 °C, attributable to transition of form III to form I, and sharp endo- and exothermic peaks at about 144–148 °C corresponding to fusion of form I and recrystallization to form II, with a large endothermic peak at 153 °C due to fusion accompanied with decomposition of form II (Fig. 1c). In this case, the X-ray powder diffraction pattern of form I obtained by recrystallization from methanol was identical with that of form I obtained on transition of form III by heating. The polymorphic transformation pathway of the metastable form III during heating was III→I→II, without direct transition of form III to form II.

None of the polymorphic forms showed any decrease in weight until the melting point during heating.

The Isothermal Transition of Form I to Form II

Figure 3 shows the isothermal transition curves of form I to form II at 117, 118, 119 and 120 °C. The four curves were all exponential and this isothermal transition appeared to be temperature-dependent.

The kinetic analysis of the isothermal transition of form I to form II was carried out according to the method of Hancock and Sharp.⁹⁾ and the m value for this transition was estimated, based on Eq.1:

$$\ln[-\ln(1-\alpha)] = \ln B + m \cdot \ln t \quad (\alpha = 0.15 - 0.5) \quad (1)$$

where m is the intrinsic value for various theoretical equations of solid-state decomposition, α

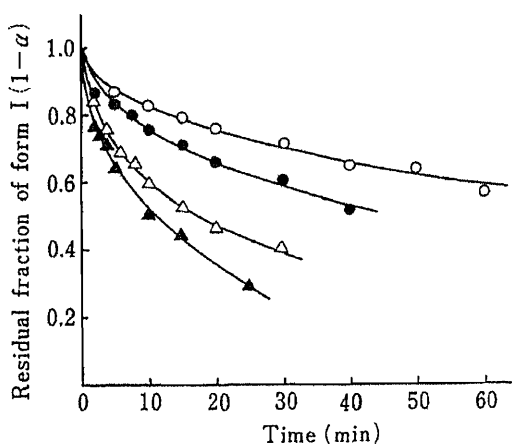


Fig. 3. Residual Fraction of Form I during the Isothermal Transition to Form II of Bromovalerylurea

○, 117 °C; ●, 118 °C; △, 119 °C; ▲, 120 °C.

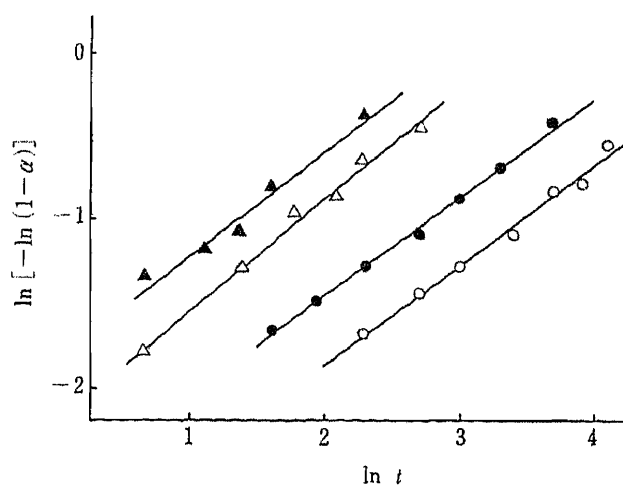


Fig. 4. Plots of $\ln[-\ln(1-\alpha)]$ versus $\ln t$ for the Isothermal Transition of Form I to Form II of Bromovalerylurea ($\alpha = 0.15 - 0.5$)

○, 117 °C ($m = 0.597$, $r = 0.994$); ●, 118 °C ($m = 0.585$, $r = 0.997$); △, 119 °C ($m = 0.670$, $r = 0.996$); ▲, 120 °C ($m = 0.620$, $r = 0.984$).

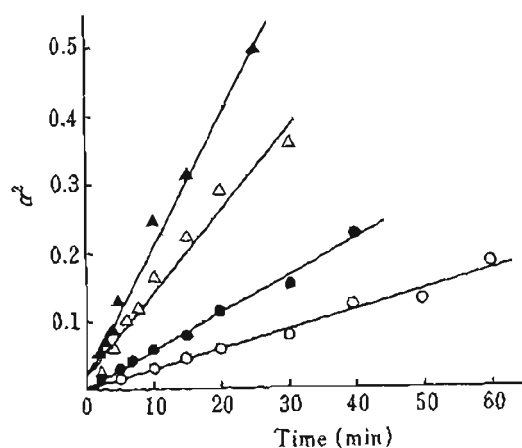


Fig. 5. Plots of α^2 versus t for the Isothermal Transition of Form I to Form II of Bromovalerylurea

○, 117°C ($r=0.990$); ●, 118°C ($r=0.996$); △, 119°C ($r=0.984$); ▲, 120°C ($r=0.995$).

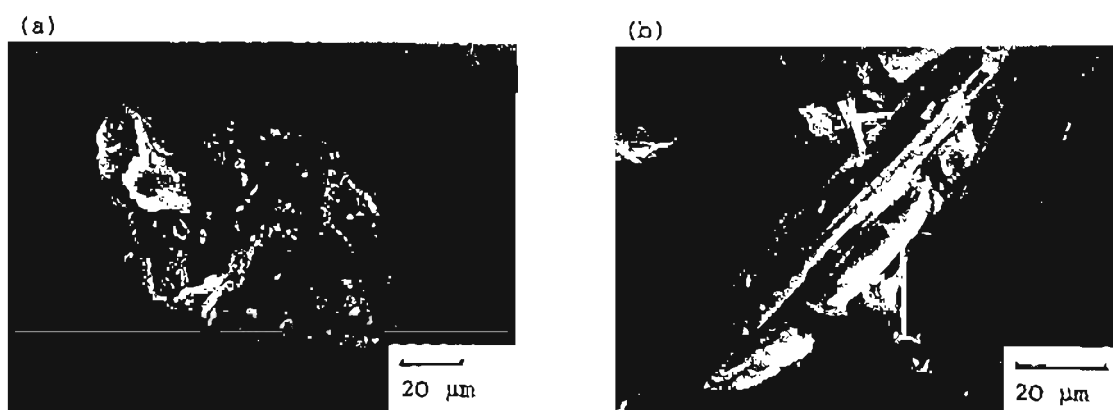


Fig. 6. Scanning Electron Microphotographs of Bromovalerylurea Crystals during the Isothermal Transition of Form I to Form II at 120°C

(a) form I before heating ($\times 500$), (b) after 60 min ($\times 750$).

is the fraction of transition, t is the heating time and B is a constant. The relationship between the theoretical equations and the m value was discussed in the previous paper.⁴⁾

The m value for the isothermal transition of form I to form II was estimated to be 0.62 ± 0.04 (mean \pm S.D.; $n=4$), as shown in Fig. 4. These results suggest that this transition proceeds by the one-dimensional diffusion mechanism ($\alpha^2 = k \cdot t$, $m=0.62$).⁸⁻¹⁰⁾ The plots of α^2 against t at any temperature were linear, as shown in Fig. 5. The apparent transition rate constant (k) at 120°C calculated from the slope of the straight line (Fig. 5) was about 7 times higher than that at 117°C.

From the results of observation with a scanning electron microscope, it was found that the crystalline shapes during the isothermal transition of form I to form II apparently changed, as shown in Fig. 6; the leaflet (parallelogramic) crystals of form I were transformed into needle crystals of form II. These results correspond well with the thermomicroscopic observations reported by Kiwada *et al.*⁶⁾

The Isothermal Transition of Form III to Form I

The isothermal transition curves of form III to form I at 75, 77.5, 80 and 82.5°C are shown in Fig. 7. It was confirmed, by means of X-ray powder diffractometry, that form III did not directly transform to form II during heating at the temperatures described above. The transition rates were relatively lower at the earlier period of transition and then increased rapidly at any temperature.

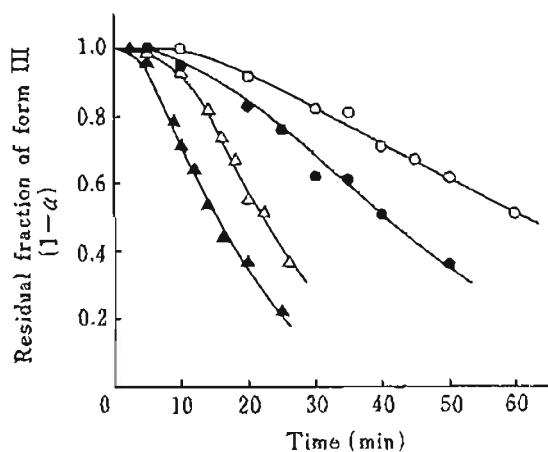


Fig. 7. Residual Fraction of Form III during the Isothermal Transition to Form I of Bromovalerylurea

○, 75°C; ●, 77.5°C; △, 80°C; ▲, 82.5°C.

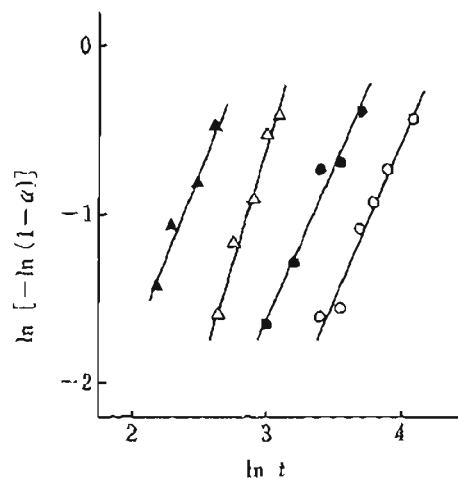


Fig. 8. Plots of $\ln[-\ln(1-\alpha)]$ versus $\ln t$ for the Isothermal Transition of Form III to Form I of Bromovalerylurea ($\alpha=0.15-0.5$)

○, 75°C ($m=1.84, r=0.984$); ●, 77.5°C ($m=1.80, r=0.981$); △, 80°C ($m=2.69, r=0.994$); ▲, 82.5°C ($m=2.03, r=0.988$).

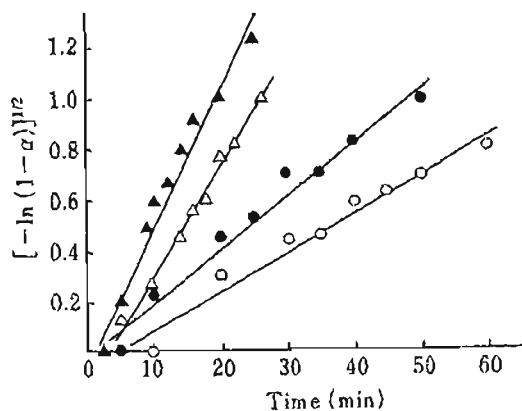


Fig. 9. Plots of $[-\ln(1-\alpha)]^{1/2}$ versus t for the Isothermal Transition of Form III to Form I of Bromovalerylurea

○, 75°C ($r=0.980$); ●, 77.5°C ($r=0.988$); △, 80°C ($r=0.996$); ▲, 82.5°C ($r=0.979$).

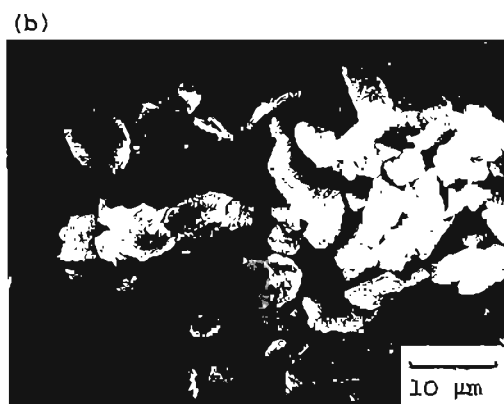
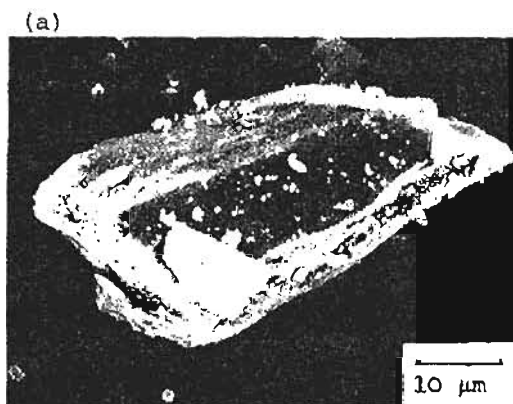


Fig. 10. Scanning Electron Microphotographs of Bromovalerylurea Crystals during the Isothermal Transition of Form III to Form I at 82.5°C

(a) form III before heating ($\times 1500$), (b) after 40 min ($\times 1500$).

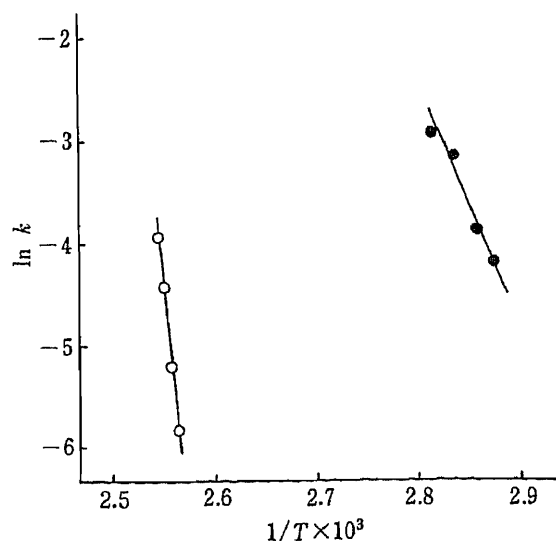


Fig. 11. Arrhenius Plots for the Isothermal Transition of Bromovalerylurea Polymorphic Forms

O, form I→form II ($r = -0.996$); ●, form III→form I ($r = -0.983$).

As shown in Fig. 8, the m value for the isothermal transition of form III to form I was calculated to be 2.09 ± 0.41 (mean \pm S.D.; $n=4$) according to the same method as described previously. Accordingly, this transition may conform with the mechanism of random nucleation and two-dimensional growth of nuclei (Avrami-Erofeev equation, $[-\ln(1-\alpha)]^{1/2} = k \cdot t$; $m=2.00$).⁹⁻¹¹) The plots of $[-\ln(1-\alpha)]^{1/2}$ against t at four temperatures showed good linearity (Fig. 9). The value of k at 82.5 °C was about 4 times that at 75 °C. This transition mechanism is similar to that of carbamazepine polymorphic form I to form III²⁾ and benoxaprofen polymorphic form I to form II.¹⁾

Figure 10 shows scanning electron microphotographs of bromovalerylurea crystals during the isothermal transition of form III to form I at 82.5 °C. It was confirmed that the columnar crystals of form III were transformed into smaller parallelogramic crystals of form I. In this case, the occurrence and growth of nuclei of form I within a crystal of form III were not clearly observed on scanning electron microphotographs.

Activation Energy for Isothermal Transitions

The activation energy for the isothermal transition of form I to form II was calculated to be 826.2 kJ/mol from the slope of the Arrhenius plots, as shown in Fig. 11. This value appeared to be very high. This high activation energy may be related to the energy required to unpack the crystal structure, which is very rigid. More research is needed to explain the high value of this activation energy.

On the other hand, the activation energy for the isothermal transition of form III to form I was calculated to be 185.2 kJ/mol in the same manner as described above (Fig. 11). The activation energy for the isothermal transition of form I to form II was thus about 4 times higher than that of form III to form I. It was concluded that the mechanism and the value of activation energy were both different between the two kinds of isothermal transitions of bromovalerylurea polymorphic forms.

Acknowledgement The authors are grateful to Prof. Yoshihisa Matsuda of Kobe Women's College of Pharmacy for the use of a scanning electron microscope.

References and Notes

- 1) This paper forms Part XVII of "Studies on Drug Nonequivalence." The preceding paper, Part XVI: T. Yokoyama, N. Ohnishi, T. Umeda, T. Kuroda, Y. Kūta, K. Kuroda, and Y. Matsuda, *Chem. Pharm. Bull.*, **34**,

-
- 917 (1986).
- 2) T. Umeda, N. Ohnishi, T. Yokoyama, K. Kuroda, T. Kuroda, E. Tatsumi, and Y. Matsuda, *Yakugaku Zasshi*, **104**, 786 (1984).
 - 3) T. Umeda, N. Ohnishi, T. Yokoyama, T. Kuroda, Y. Kita, K. Kuroda, E. Tatsumi, and Y. Matsuda, *Chem. Pharm. Bull.*, **33**, 2073 (1985).
 - 4) T. Umeda, N. Ohnishi, T. Yokoyama, T. Kuroda, Y. Kita, K. Kuroda, E. Tatsumi, and Y. Matsuda, *Chem. Pharm. Bull.*, **33**, 3422 (1985).
 - 5) A. Watanabe, *Yakugaku Zasshi*, **58**, 565 (1938).
 - 6) H. Kiwada, K. Takami, and Y. Kato, *Chem. Pharm. Bull.*, **28**, 1351 (1980).
 - 7) M. A. Moustafa and J. E. Carless, *J. Pharm. Pharmacol.*, **21**, 359 (1969).
 - 8) E. G. Shami, P. D. Bernardo, E. S. Rattie, and L. J. Ravin, *J. Pharm. Sci.*, **61**, 1318 (1972).
 - 9) J. D. Hancock and J. H. Sharp, *J. Am. Ceram. Soc.*, **55**, 74 (1972).
 - 10) S. R. Byrn, "Solid-State Chemistry of Drugs," Academic Press Inc., New York, 1982, p. 59.
 - 11) S. F. Hulbert, *J. Brit. Ceram. Soc.*, **6**, 11 (1969).

[Chem. Pharm. Bull.]
35(3)1214-1222(1987)

Partition Characteristics and Retention of Anti-inflammatory Steroids in Liposomal Ophthalmic Preparations

KADZUYA TANIGUCHI,* NORIKO YAMAZAWA, KADZUE ITAKURA,
KATSUHIKO MORISAKI and SHIN'ICHI HAYASHI

*The Research and Development Division, Rohto Pharmaceutical Co., Ltd.,
Tatsumi Nishi 1-8-1, Ikuno-ku, Osaka 544, Japan*

(Received August 20, 1986)

Liposome preparations containing dexamethasone or its ester derivatives were formulated as eye drops. Steroids were efficiently incorporated into the liposomes; the incorporation ratio was not affected by the period of sonication or the addition of stearylamine or dicetylphosphate, but was decreased by the addition of cholesterol. The incorporation ratio appears to be governed by partition equilibrium between the lipid membrane and the aqueous phase. A theoretical interpretation of the findings was attempted by using partition theory. No release of dexamethasone palmitate from liposomes was detected, but a small portion of other steroids was rapidly released when the liposome preparation was diluted with a buffer solution. The amount of steroid released from the liposomes may also be governed by the partition equilibrium.

Keywords—eye drop; liposome; anti-inflammatory steroid; incorporation; release profile; partition theory; ultrafiltration; dexamethasone; ester derivative

The topical application of eye drops is a convenient and useful therapeutic method for the treatment of various ocular diseases. An ophthalmic preparation should be a clear aqueous solution to avoid temporary blurred vision and local irritation by particulate foreign matter. However, ocular drug availability as eye drops is very low due to rapid clearance of the drops from the precorneal area, and water-soluble drugs are hardly absorbed by the cornea.¹⁾ For instance, it was reported that corneal absorption of pilocarpine from a solution is terminated within only 5 min following instillation.²⁾ Thus, an effective and safe ophthalmic preparation appears to be quite difficult to make. Many attempts to overcome these problems have been made using various delivery systems such as ointment,³⁾ viscous solution,⁴⁾ gels,⁵⁾ or Ocucert.⁶⁾ Recently, the use of liposomes has also been reported,⁷⁾ but whether a liposomal preparation will provide any therapeutic advantage remains in question.

The topical instillation of anti-inflammatory steroids is commonly carried out in the therapy of serious ophthalmic inflammation such as iritis or choroiditis. The dosage form should be an aqueous suspension since the steroids are poorly water-soluble or a water-soluble derivative solution. Various problems may be encountered in making such a preparation. A higher concentration of a fluoromethorone suspension did not improve the aqueous humor drug concentration,⁸⁾ and as the particle size of dexamethasone suspension increased, the drug concentration in the cornea or aqueous humor decreased.⁹⁾ Furthermore, Leibowitz *et al.*¹⁰⁾ reported that unless the corneal epithelium is damaged, dexamethasone sodium phosphate, a water-soluble derivative of dexamethasone is not absorbed by the cornea.

It thus appears that a more sophisticated preparation which increases the ophthalmic availability and prolongs the interval between doses is necessary to make steroidal therapy safer and more effective. Gregoriadis¹¹⁾ has suggested the carrier potential of liposomes for lipid-soluble substances, and a number of studies¹²⁾ concerning the application of liposomes

containing anti-inflammatory steroid have been reported, mainly for the treatment of rheumatoid arthritis. In the field of ophthalmology, Singh and Mezei¹³⁾ reported that liposomes increased the ocular tissue concentration of triamcinolone acetonide. However, the details of the mechanism or factors affecting this improvement in availability have yet to be established.

In the present work, to estimate the usefulness of liposomes for steroid therapy in ophthalmology, we formulated various liposome preparations containing dexamethasone or its ester derivatives as eye drops, and investigated the factors affecting the incorporation of steroids. In addition, the release profiles of drugs from liposomes were studied. The mechanisms involved are discussed.

Materials and Methods

Materials—Dexamethasone (DM) and dexamethasone acetate (DA) were obtained from Roussel Uclaf (Paris, France), and dexamethasone valerate (DV) and dexamethasone palmitate (DP) were synthesized by the method of Show *et al.*¹⁴⁾ Synthesized steroids were identified by thin layer chromatography (TLC), infrared (IR) and nuclear magnetic resonance (NMR) examinations. Egg yolk lecithin (EYL) and dipalmitoyl phosphatidylcholine (DPPC), whose purity was in excess of 99%, were obtained from Sigma Chemicals (St. Louis, U.S.A.). All other chemicals were of reagent grade and were obtained commercially.

Preparation of Liposomes—Suitable amounts of phosphatidylcholine and steroid were dissolved in chloroform, and cholesterol, stearylamine (SA) or dicetylphosphate (DCP) were added as required. The organic solvent was evaporated under vacuum to a thin lipid film. The film was dried and suspended in pH 7.4 isotonic phosphate buffer by Vortex mixing followed by ultrasonic radiation, usually for 2.5 min, using an Ohtake 5202 sonicator under nitrogen. The liposomes containing DPPC were prepared at 70 °C, and the others were prepared at 0 °C. After standing for a period of 1 h at room temperature, the liposome suspension was filtered with polycarbonate membrane filter of 1 μm pore size (Nuclepore Corp., Pleasanton, U.S.A.) to remove foreign matters such as metal particle formed during sonication.

Evaluation of Liposome-Steroids Interaction—The liposome preparations were ultrafiltered using a micropartition system, MPS-1 (Amicon, Mass, U.S.A.), and the steroid concentration in the preparation (C_T) and that in the ultrafiltrate (C_W) were assayed by high performance liquid chromatography (HPLC). The steroid concentration before membrane filtration (C_S) was also determined. Recovery of the steroid in the membrane filtrate (FR) was,

$$FR(\%) = \left(\frac{C_T}{C_S} \right) \cdot 100 \quad (1)$$

C_W was considered to be free steroid concentration, since phosphatidylcholine was not detected in the ultrafiltrate. Thus, the incorporation ratio in the liposomes (IR) was,

$$IR(\%) = \left(\frac{C_T - C_W}{C_T} \right) \cdot 100 \quad (2)$$

and the distribution ratio of the steroid (DR) was,

$$DR = \frac{C_T - C_W}{C_W} \quad (3)$$

Dexamethasone Uptake into the Liposomes—The EYL liposomes free of the steroids were prepared by the previous method, and DM solution was prepared in ethanol at a concentration of 25 mM. Then 50 μl of the DM solution were added to 10 ml of the empty liposome suspensions, and the final DM concentration was adjusted to 50 μg/ml. After periodic incubation at 37 °C, the free DM concentration was estimated by ultrafiltration (MPS-1).

Release Experiment—Following preincubation at 37 °C for 1 h, the liposome preparation was diluted with phosphate buffered saline (pH 7.4) prewarmed at 37 °C, and immediately after dilution, it was incubated at 37 °C. The initial steroid concentration in the preparation (C_T) and that in the aqueous phase (C_W) were determined before dilution. The free steroid concentration was monitored by periodical ultrafiltration of samples. Retention of the steroid in the liposomes was,

$$\text{remaining ratio} = \frac{C_T/N - C_N}{(C_T - C_W)/N} \quad (4)$$

$$\text{percent remaining} = (\text{remaining ratio}) \cdot 100$$

where N is the dilution ratio and C_N is the steroid concentration in the ultrafiltrate of the samples.

Analytical Methods—The steroids were determined by HPLC on an apparatus (LC-6A, Shimadzu, Kyoto) equipped with a variable wavelength ultraviolet (UV) detector (SPD-6A, Shimadzu). The stationary phase used was a Nucleosil 10C₁₈ (Macherey-Nagel, Dueren, Germany) packed column (4 × 300 mm), and 95% methanol in water for DP or 70% methanol in water containing 1% acetic acid for other steroids was used as the mobile phase, at a flow rate of 1.0 ml/min. Chromatograms of the standard solution were obtained and calibration lines were constructed on the basis of peak area measurements. Phosphatidylcholine was assayed using a Wako Phospholipid B-Test (Wako Chemicals, Osaka) based on a colorimetric reaction. No disturbance of the colorimetric reaction due to the presence of the steroids was detected.

Results and Discussion

Factors Affecting Steroid Incorporation into Liposomes

The physicochemical properties of the steroids used in this study are shown in Table I. The ester derivatives showed higher partition coefficients to chloroform and lower solubilities in the buffer than DM. DP was almost insoluble in the buffer and the partition coefficient was so high that it could not be determined exactly. Other steroids showed amphiphilic properties. However, DM, which had the highest hydrophilicity, showed a maximum solubility of only 80 μg/ml in the buffer solution.

Though the interaction of drugs and liposomes has been evaluated by gel filtration¹⁵⁾ or ultracentrifugation,¹⁶⁾ some problems were encountered when using these methods in the preliminary experiments. Steroid leakage during gel filtration was unavoidable, and a portion of the liposomes remained in the supernatant following ultracentrifugation. On the other hand, there were no problems such as adsorption, release of the steroid or appearance of phosphatidylcholine in the filtrate when the micropartition system was used for estimating

TABLE I. Physicochemical Properties of Dexamethasone and Its Ester Derivatives

Compound	Molecular weight	Melting point (°C)	PC _{CHCl₃} ^{a)}	Solubility ^{b)} (μg/ml)
Dexamethasone	392.45	262—264	9.0	80.5
Dexamethasone acetate	452.52	226—229	657	29.6
Dexamethasone valerate	493.58	214—217	8780	1.3
Dexamethasone palmitate	630.88	55—60	—	0.052

a) Partition coefficient between chloroform and water. b) Solubility in pH 7.4 buffer solution at 37°C.

TABLE II. Effect of Sonication Time on the Incorporation of Various Steroids in Liposomes

Sonication time (min)	Distribution volume (%) ^{a)}	Filtration ratio (%) ^{b)} ± S.D.				Incorporation ratio (%) ± S.D.			
		DM	DA	DV	DP	DM	DA	DV	DP
2.5	1.5	101.3	99.6	100.2	101.6	90.5	94.7	99.5	(100)
		±2.6	±1.5	±0.9	±1.5	±1.3	±0.3	±0.0	
5.0	1.3	101.5	100.6	98.0	100.8	91.8	95.5	99.5	(100)
		±2.0	±1.6	±0.9	±1.5	±0.8	±0.2	±0.1	
10.0	1.0	100.7	102.1	99.3	99.3	92.2	96.0	99.6	(100)
		±0.4	±2.9	±2.7	±0.6	±0.3	±0.6	±0.0	
20.0	0.7	100.5	101.4	99.5	100.5	92.0	95.7	99.6	(100)
		±2.0	±2.1	±0.3	±0.4	±1.5	±0.2	±0.0	

a) Determined by the method of Oku *et al.*¹⁷⁾ b) Recovery of the steroids in the filtrate after polycarbonate membrane (1 μm) filtration.

free steroid concentration in the liposome suspension.

The effect of the sonication period on the incorporation of various steroids is shown in Table II. The concentrations of EYL and the steroid were fixed at 16 and 0.5 mM, respectively, in the following experiments. No steroid loss during membrane filtration was observed in any system. The incorporation ratio increased with increasing lipophilicity of the steroids. Even DM, which showed the lowest lipophilicity, provided a high incorporation ratio of more than 90% and DP was confirmed to be completely incorporated into the liposomes. From a practical standpoint, the amount of the steroids in the inner aqueous phase may be small enough to be neglected, because of the low free concentration of steroids and the small distribution volume of the liposomes. Liposome diameter appeared to become smaller with increasing time of sonication, since the turbidity and distribution volume decreased. However, the incorporation ratio was not affected by the sonication period. Thus, the steroids may be incorporated mainly into the lipid bilayer, and the incorporation ratio may depend on the properties of the lipid constituting the liposome membrane and not on the shape or size of the liposomes.

The effects of cholesterol on free steroid concentration are shown in Fig. 1. The free concentrations of various steroids except DP increased with the addition of cholesterol. This is in agreement with the previous reports that the penetration of hydrocortisone decreases upon addition of cholesterol to DPPC monolayer systems,¹⁸⁾ and the addition of cholesterol to lipid dispersion decreases the uptake of hydrocortisone and other steroids by the membrane.¹⁹⁾ Even when cholesterol was added to the liposomal membrane, free DP could

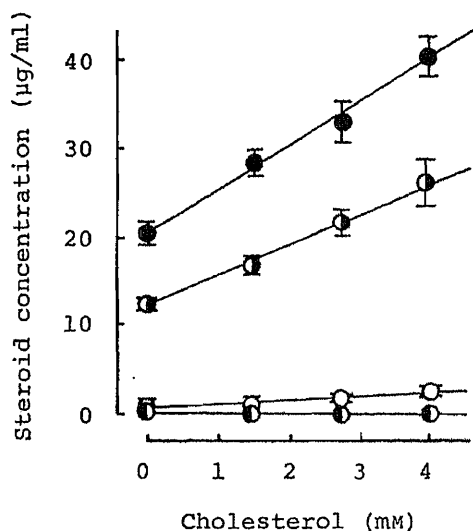


Fig. 1. Effect of Cholesterol on Free Steroid Concentration in the Liposome Preparation

Each preparation contained 16mM EYL and 0.5 mM steroid. ●, DM; ◐, DA; ○, DV; ◑, DP.

TABLE III. Effect of Lipid Composition on the Incorporation of Steroids in Liposomes

Composition of liposomes	Incorporation ratio (%) ± S.D.			
	DM	DA	DV	DP
EYL : steroid = 16 : 0.5	90.5 ± 1.3	94.7 ± 0.3	99.5 ± 0.0	(100)
EYL : SA : steroid = 16 : 2 : 0.5	91.2 ± 0.5	94.5 ± 0.2	99.5 ± 0.0	(100)
EYL : DCP : steroid = 16 : 2 : 0.5	90.5 ± 1.1	94.9 ± 0.6	99.5 ± 0.1	(100)
DOPC : steroid = 16 : 0.5	92.1 ± 0.4	95.8 ± 0.6	99.7 ± 0.0	(100)
DPPC : steroid = 16 : 0.5 ^{a)}	78.5 ± 1.4	91.0 ± 0.2	99.3 ± 0.0	(100)

a) Prepared at 70°C. Others were prepared at 0°C.

not detected. Cleary and Zats¹⁸⁾ suggested that since hydrocortisone has a polar group at each end of the molecule, a horizontal orientation is favored, so that all polar groups remain hydrated. On the other hand, Fildes and Oliver²⁰⁾ suggested that cortisone-21-palmitate is anchored in the phospholipid bilayer by an acyl side chain. Thus, it is likely that the incorporation mode of DP differs from those of other steroids.

Table III shows the incorporation ratio of steroids into various liposomes. DP was completely incorporated in all cases. As far as other steroids were concerned, the incorporation ratio was unaffected by the addition of SA or DCP, which rendered the liposomal surface electrically charged. The ratio was affected by the species of phosphatidylcholine. It is considered that the addition of SA or DCP may not induce any transition in the inner structure of the lipid membrane, while the membrane structure consisting of saturated phosphatidylcholine is so rigid that the number of binding sites of amphiphilic steroids in the liposomes may be reduced.

Mechanism of Incorporation

The influence of additional DM concentration on liposome-steroid interaction is illustrated in Fig. 2. The liposomes consisted of EYL and DM, and the concentration of EYL was fixed at 16 mM. The free DM concentration increased linearly with additional DM concentration up to 2 mM, but further addition had no effect. This plateau level coincided with the solubility of DM in the buffer. When free DM became saturated, the recovery of DM in the membrane filtrate dropped while EYL was entirely recovered in the filtrate. This steroid loss may be caused by crystallization. However, the incorporation ratio of DM was always 90% irrespective of additional DM concentration. This suggests the existence of a partition equilibrium of the steroid between the liposomes and the aqueous phase.

To confirm this hypothesis, the uptake of DM by empty liposomes was investigated. Free DM concentration after the addition of DM to the liposome suspension is shown in Fig. 3. It was much lower than that following the addition of DM only 5 min later. This steady-state

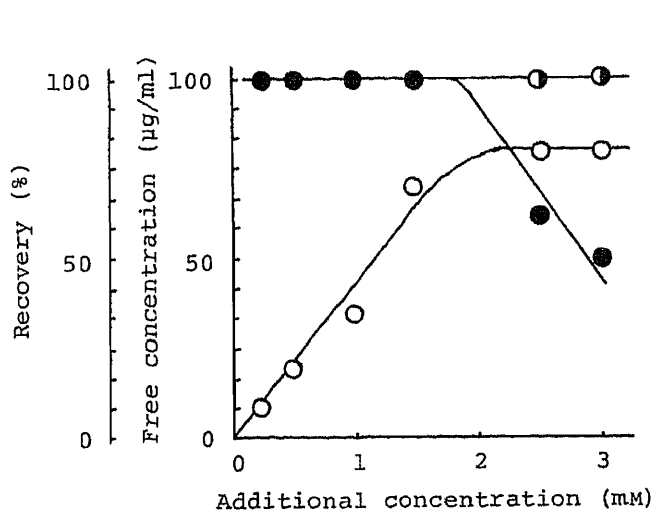


Fig. 2. Influence of Additional Dexamethasone Concentration on Free Steroid Concentration and Recovery of Phosphatidylcholine or Dexamethasone in the Polycarbonate Membrane Filtrate

○, free dexamethasone concentration; ●, dexamethasone recovery in polycarbonate membrane filtrate; ◐, phosphatidylcholine recovery in polycarbonate membrane filtrate.

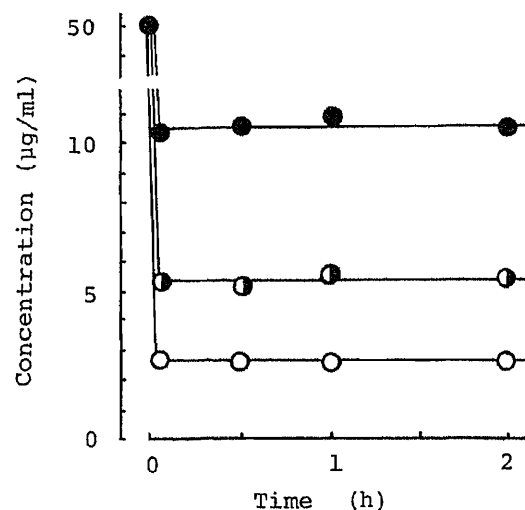


Fig. 3. Free Dexamethasone Concentration Profile after Addition of the Steroid Solution to the Various Empty Liposome Suspensions

○, 32 mM EYL; ◐, 16 mM EYL; ●, 8 mM EYL.

free concentration decreased with increase in EYL concentration. Thus, additional DM may be rapidly taken up by the liposomes, possibly by the partition of DM to the liposomal membrane.

If a partition equilibrium is established, the partition coefficient (PC) may be defined as,

$$PC = \frac{C_L}{C_W} = \frac{X_L \cdot V_W}{X_W \cdot V_L} = \text{constant} \quad (5)$$

where C_L is the steroid concentration in the lipid membrane, C_W is that in the aqueous phase, X_L and X_W are the steroid amounts in the liposomes and the aqueous phase, respectively, and V_L and V_W are the volume ratios of the liposomes and the aqueous phase, respectively. The DR is,

$$DR = \frac{X_L}{X_W} = \frac{C_L \cdot V_L}{C_W \cdot V_W} = PC \cdot \left(\frac{V_L}{1 - V_L} \right) \quad (6)$$

Since $V_L \ll 1$ and $V_L = W_L/A$ where W_L is the lipid concentration in the liposome suspension and A is specific gravity of the lipid, Eq. 6 becomes,

$$DR = \left(\frac{PC}{A} \right) \cdot W_L \quad (7)$$

The correlation of the distribution ratio in the liposome preparations determined by Eq. 3 with the additional concentration of EYL is shown in Fig. 4. The distribution ratio of each steroid increased linearly with EYL concentration, which is in agreement with the theoretical relation between DR and W_L in Eq. 7.²¹⁾ It is thus confirmed that the incorporation ratio of steroids such as DM, DA or DV may be governed by partition equilibrium. The partition coefficient of DA and that of DV are 2 times and 20 times greater than that of DM, respectively, from the slopes of the lines in Fig. 3.

As far as DP was concerned, neither free steroid nor crystal could be observed in any

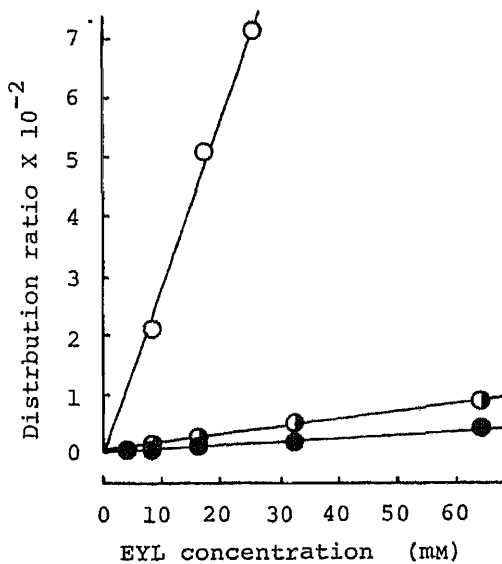


Fig. 4. Relationship between Distribution Ratio of the Steroid and Phosphatidylcholine Concentration in the Liposome Preparation

Each liposome preparation consisted of EYL and steroid, and contained 0.5mM steroid. ●, DM; ◐, DA; ○, DV.

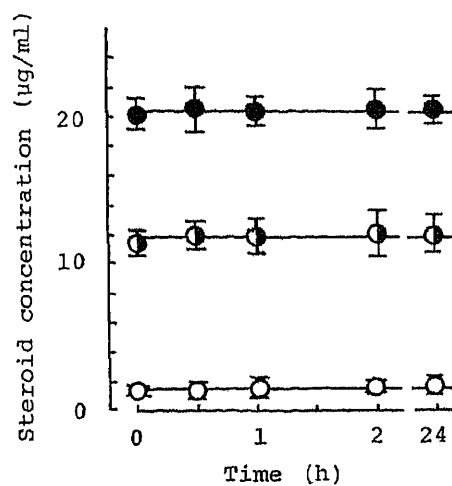


Fig. 5. Free Steroid Concentration in the Liposome Preparations after Incubation at 37°C without Dilution

Each preparation contained 16mM EYL and 0.5 mM steroid. ●, DM; ◐, DA; ○, DV.

system. DP was considered to be completely incorporated into the liposomes as one of the components constituting the membrane structure, such as cholesterol.

Release of Steroids from Liposomes

Arrowsmith *et al.*²²⁾ reported that the *in vitro* release of steroids from liposomes proceeds by first-order kinetics once an initial phase of rapid loss is terminated, but the details of the initial phase were not discussed.

The free steroid concentration in the liposome preparation following incubation at 37°C is shown in Fig. 5 to confirm the stability of steroid incorporation. The free concentration of each steroid was quite stable for 24 h.

The release profiles of the steroids following dilution are shown in Fig. 6. A part of the steroids was rapidly released within 5 min and after that no further release occurred within 24 h. The percentage of steroids remaining in the liposomes at the steady state increased with the lipophilicity of the steroid, and decreased with increasing dilution ratio. Considering that this rapid release may be caused by transition of the equilibrium as a result of dilution, we carried out the following theoretical analysis.

The volume ratio of the lipid (V_L) was so small that the volume ratio of the aqueous phase (V_W) could be considered as unity. From Eq. 5, the steroid amount in the liposomes (X_L) is,

$$X_L = PC \cdot (X_T - X_L) \cdot \frac{V_L}{1 - V_L} \quad (8)$$

where X_T is the total amount in the liposome preparation. Since V_L is sufficiently small, Eq. 8 becomes,

$$X_L = \frac{PC \cdot V_L}{1 + PC \cdot V_L} \cdot X_T \quad (9)$$

Thus, the steroid amounts in the liposomes before dilution, X_0 , and after dilution, X_N , are,

$$X_0 = \frac{PC \cdot V_L}{1 + PC \cdot V_L} \cdot X_T \quad (10)$$

$$X_N = \frac{PC \cdot (V_L/N)}{1 + PC \cdot (V_L/N)} \cdot X_T \quad (11)$$

where N is the dilution ratio. The remaining ratio in the liposomes, R_N , is,

$$R_N = \frac{X_N}{X_0} = \frac{1 + PC \cdot V_L}{N + PC \cdot V_L}$$

$$\frac{1}{R_N} = \frac{1}{1 + PC \cdot V_L} N + \frac{PC \cdot V_L}{1 + PC \cdot V_L} \quad (12)$$

The correlation between the reciprocal value of the remaining ratio in the steady state determined experimentally by applying Eq. 4, and the dilution ratio is shown in Fig. 7. A linear correlation appears to exist for each steroid. This is in close agreement with the theoretical relation in Eq. 12. Thus it is confirmed that release of the steroid from the liposomes may occur during transition of the equilibrium. As long as the preparation is not diluted or the free steroid concentration is not decreased, the steroid will not be released from the liposomes.

Drugs instilled as eye drops rapidly disappear from the precorneal area.²³⁾ If it is possible for liposomes to be retained at the precorneal area for a reasonable period of time, they might serve as a good drug vehicle. However, even if liposomes remain at the precorneal area, drugs

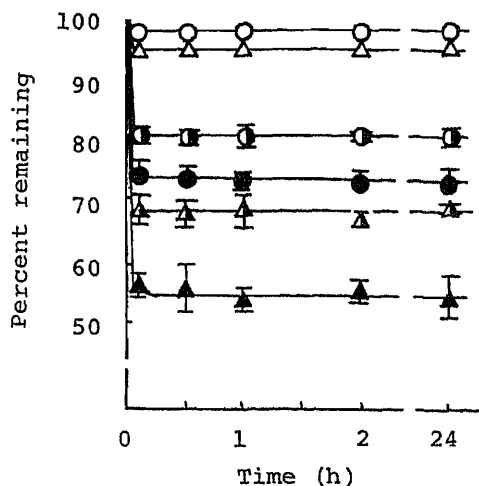


Fig. 6. *In Vitro* Release Profile of the Steroids from the Liposomes after Dilution with PBS (pH 7.4)

●, DM ($\times 5$); ○, DA ($\times 5$); ○, DV ($\times 5$); ▲, DM ($\times 10$); ▲, DA ($\times 10$); ▲, DV ($\times 10$).

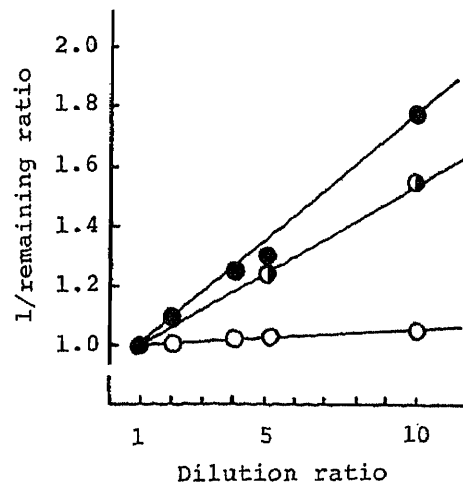


Fig. 7. Relationship between Reciprocal Value of the Remaining Ratio of the Steroids in the Liposomes after Dilution and the Dilution Ratio

●, DM; ○, DA; ○, DV.

slowly released from the liposomes may not be absorbed by the ocular tissue due to rapid clearance by tear flow. The liposome preparation containing DP, which is completely incorporated into liposomes and not released, may not be satisfactory, unless the liposomes can be directly taken up into the cornea or DP can be transferred directly from the liposome membrane to the cell membrane, as in the case of cholesterol.²⁴⁾ It is doubtful whether a considerable amount of drug can be absorbed in such a manner. Incorporated steroids except DP may be released by dilution of the preparation with tears or clearance of free steroids. Free steroids in the precorneal layer may possibly be retained for a longer period. Besides, a liposome preparation, in contrast to other drug delivery systems, can be easily self-administered by patients. Accordingly, liposome preparations containing steroids such as DM, DA or DV could prove to be useful ophthalmic delivery systems for treatment of various eye inflammations.

References and Notes

- 1) K. Kishida, *Nihon Ganka Kiyo*, **25**, 798 (1974); K. G. Swan and N. G. White, *Am. J. Ophthalmol.*, **25**, 1043 (1972).
- 2) J. W. Sieg and J. R. Robinson, *J. Pharm. Sci.*, **65**, 1816 (1976).
- 3) A. Kupferman, M. V. Pratt, K. Suckewer and H. M. Leibowitz, *Arch. Ophthalmol.*, **91**, 373 (1974).
- 4) J. W. Chrai and J. R. Robinson, *J. Pharm. Sci.*, **63**, 1218 (1974).
- 5) R. D. Shoenwald and J. J. Boltralic, *Invest. Ophthalmol. Visual Sci.*, **18**, 61 (1979).
- 6) K. T. Richardson, *Arch. Ophthalmol.*, **93**, 74 (1975).
- 7) R. E. Stratford, D. C. Yang, M. A. Redell and V. H. L. Lee, *Int. J. Pharmaceut.*, **13**, 263 (1983); G. Smolin, M. Okumoto, S. Feilar and D. Condon, *Am. J. Ophthalmol.*, **91**, 220 (1981); S. Benita, J. D. Plencassange, G. Cave, D. Drouin, P. L. H. Dong and D. Sincholle, *Journal of Microencapsulation*, **1**, 203 (1984).
- 8) J. W. Sieg and J. R. Robinson, *J. Pharm. Sci.*, **64**, 931 (1975).
- 9) R. D. Shoenwald and P. Stewart, *J. Pharm. Sci.*, **69**, 391 (1980).
- 10) V. C. William, A. Kupferman and H. M. Leibowitz, *Arch. Ophthalmol.*, **88**, 308 (1972).
- 11) A. D. Gregoriadis, *New Engl. J. Med.*, **295**, 704 (1976).
- 12) J. T. Dingle, J. T. Godon, G. L. Hazleman and C. G. Knight, *Nature (London)*, **271**, 372 (1978); S. Shinozawa, Y. Araki and T. Oda, *Res. Commun. Chem. Pathol. Pharmacol.*, **24**, 223 (1979); M. de Silva, B. L. Hazleman, D. P. Page Thomas and P. Wright, *Lancet*, **8130**, 1320 (1979).
- 13) K. Singh and M. Mezei, *Int. J. Pharmaceut.*, **16**, 339 (1983).

- 14) I. H. Show, C. G. Knight, D. P. Page Thomas, N. C. Phillips and J. T. Dingle, *Br. J. Exp. Path.*, **60**, 142 (1979).
- 15) N. Muranushi, Y. Nakajima, M. Kinugawa, S. Muranishi and H. Sezaki, *Int. J. Pharmaceut.*, **4**, 281 (1980).
- 16) I. H. Show, C. G. Knight and J. T. Dingle, *Biochem. J.*, **158**, 473 (1976).
- 17) N. Oku, D. A. Kendall and R. C. MacDonald, *Biochim. Biophys. Acta*, **691**, 332 (1982).
- 18) G. W. Cleary and J. L. Zatz, *J. Pharm. Sci.*, **66**, 975 (1977).
- 19) R. S. Snart and M. J. Wilson, *Nature (London)*, **215**, 964 (1967).
- 20) F. J. T. Fildes and J. E. Oliver, *J. Pharm. Pharmacol.*, **30**, 337 (1978).
- 21) H. Sasaki, personal communications.
- 22) M. Arrowsmith, J. Hadgraft and I. W. Kellaway, *Int. J. Pharmaceut.*, **14**, 191 (1983).
- 23) S. Mishima, A. Aaset, S. D. Klyce and J. L. Baum, *Invest. Ophthalmol.*, **5**, 264 (1966).
- 24) B. Bloj and D. B. Zilversmit, *Biochemistry*, **16**, 3943 (1977).

[Chem. Pharm. Bull.]
35(3)1223—1227(1987)]

Barium Sulfate Crystals in Parenteral Solutions of Aminoglycoside Antibiotics

TOSHINOBU AOYAMA* and MASAYOSHI HORIOKA

*Hospital Pharmacy, Kyushu University Hospital, Maidashi 3-1-1,
Higashi-ku, Fukuoka 812, Japan*

(Received September 8, 1986)

Particulate matter in micromonicin, sisomicin and tobramycin injection solutions sealed in glass ampules was identified as barium sulfate crystals by using scanning electron microscopy and energy dispersing X-ray analysis. Barium sulfate crystals isolated from these solutions occurred as single or agglomerated crystals which were 0.5—2.0 μm long in maximum dimension. Barium sulfate crystal formation in usual ampules tended to increase with increasing temperature of sterilization, but that in surface-treated ampules did not increase during sterilization at high temperature.

Keywords—particulate matter; contamination; barium sulfate; glass ampule; aminoglycoside antibiotics; scanning electron microscopy; energy dispersing X-ray analysis

In 1963 and 1964, Garvan and Gunner¹⁾ reported that large volume parenteral solutions often contained a variety of foreign particulate matter in alarmingly large quantities, and they claimed that the use of a rubber closure gave rise to specific contaminants. Further, a Symposium on Safety of Large Volume Parenteral Solutions sponsored by the FDA²⁾ in 1966 emphasized the importance of foreign particulate matter present in injectable solutions. Since then, an increasing number of reports have described the presence of such particulate matter and the consequent safety problem.³⁻¹²⁾ A requirement that certain small volume injections meet particulate matter standards became official in USP on January 1, 1986.

A recent report⁹⁾ states that barium sulfate was found in injectable solutions sealed in glass ampules when sulfate or an oxidant such as sodium sulfite is contained in the products. This paper deals with the formation of barium sulfate crystals as a reaction product between aminoglycoside antibiotics and glass ampules.

Experimental

Opening of Ampule—In order to avoid detachment of glass fragments into the product solution at the time of ampule opening, the inner pressure of the ampule was made higher than atmospheric pressure by heating up to 70 °C according to the method of Sommerville and Gibson¹¹⁾ and then the ampule was opened.

Sampling of Product Solution in Ampule and Preparation of Test Sample Solution—A commonly used glass syringe which is substantially free from foreign particulate matter production was transferred into a 150 ml clean glass container for foreign particle counting, and then made up to 100 ml with ultra-clean distilled water, filtered through a 0.22 μm pore-size membrane filter.

Sterilizing Conditions and Count of Foreign Particulate Matter—Four conditions, 126 °C for 15 min, 121 °C for 20 min, 115 °C for 30 min, and 100 °C for 60 min, were employed to observe the influence of sterilizing conditions on the appearance of foreign particulate matter in solution. Commercial micromonicin solution was filtered through a 0.45 μm Millipore filter and sealed in fresh ampules. A commonly used ampule and a surface-treated (ammonium sulfate) ampule were used in this test.

Count of Foreign Particulate Matter—A polyethylene magnetic stirrer (2.0cm length) was placed in a measurement container containing the sample solution, and the container was housed in a measuring apparatus,

HIAC PC-305 automatic particle counter (HIAC/Royco Instrument Division, Pacific Scientific Co., Ltd., California, U.S.A.). The solution was stirred gently for 2 min and vacuum-degassed for 3 min. Measurement was done four times on each sample solution (10 ml). The first value was discarded, and the last three were averaged to obtain the mean value.

Scanning Electron Microscopy (SEM)—The remaining sample solution after HIAC measurement was collected, made up to 100 ml, and passed through a 13 mm diameter Millipore filter with a pore size of 0.45 μm . The residue was washed with 200 ml of ultra-clean distilled water and dried at 30 °C. The dry filter was fixed on an aluminum stub (1 \times 1 cm) with double-sided adhesive tape, gold-coated by a usual method using an Eiko IB-3 ion coater (Eiko Engineering Co., Ltd., Tokai-mura, Ibaragi, Japan), and inspected with a Hitachi-Akashi MSM-4 scanning electron microscope (Hitachi Co., Ltd., Tokyo, Japan).

Identification of BaSO₄—Sample solution which might contain BaSO₄ on the basis of SEM was filtered through a Nucleopore filter and the residue was washed, dried and coated with carbon at 150 Å thickness with a Hitachi HUS-5B high vacuum evaporator (Hitachi Co., Ltd., Tokyo, Japan) at 30 Å and 1×10^{-6} Torr. This sample was examined under a Hitachi S-45 scanning electron microscope (Hitachi Co., Ltd.) at 20 kV, and simultaneously subjected to energy dispersing X-ray analysis (EDX) (Horiba Seisakusho, Tokai-mura, Ibaragi, Japan) at 10 eV for 100 s.

TABLE I. Particle Counts in Aminoglycoside Injections

Sample	Lot. No.	Particle diameter (μm)				
		2	5	10	20	
Blank		63	10	0.8	0.8	
Micronomicin	120 mg/ampule	107AAJ ^{a)}	13028	514	27	0
	60 mg/ampule	011AAJ ^{a)}	12213	729	12	0.5
Treated ampule	120 mg/ampule	—	258	40	11	0
Sisomicin (A)	75 mg/ampule	28A003	205	65	19	2.5
	(B) 75 mg/ampule	Y003A ^{a)}	435	95	24	2.5
Tobramycin	60 mg/ampule	1036 ^{a)}	3388	683	53	0.8
		0017	570	138	30	5.8
Gentamicin	60 mg/ampule	1516	838	180	23	6.8
		0514	423	90	25	3.3

Particle counts: per ampule by HIAC PC-305. ^{a)} BaSO₄ was identified. Values are means of 9 ampules.

TABLE II. Particle Counts in Micronomicin Ampule (120 mg/ampule) Sterilized under Various Conditions

Sample	Sterilization	Particle diameter (μm)			
		2	5	10	20
Blank		63	10	0.8	0.8
Usual ampule	100 °C 1 h	847	124	27	0
	115 °C 30 min	1215 ^{a)}	215	41	7.5
	121 °C 20 min	1487 ^{a)}	246	59	14
	126 °C 15 min	1447 ^{a)}	292	98	17
Treated ampule	100 °C 1 h	483	169	67	12
	115 °C 30 min	593	140	30	3.1
	121 °C 20 min	576	130	67	3.8
	126 °C 15 min	563	136	61	12

Values are means of 9 ampules. ^{a)} BaSO₄ was identified.

Results and Discussion

Count of Foreign Particulate Matter in Aminoglycoside Antibiotics Sealed in Ampules

As reported in Table I, micromonicin preparation was found to contain a relatively large amount of particulate matter in comparison with the other preparations. Two sisomicin preparations are commercially available from two companies, A and B, and the product from

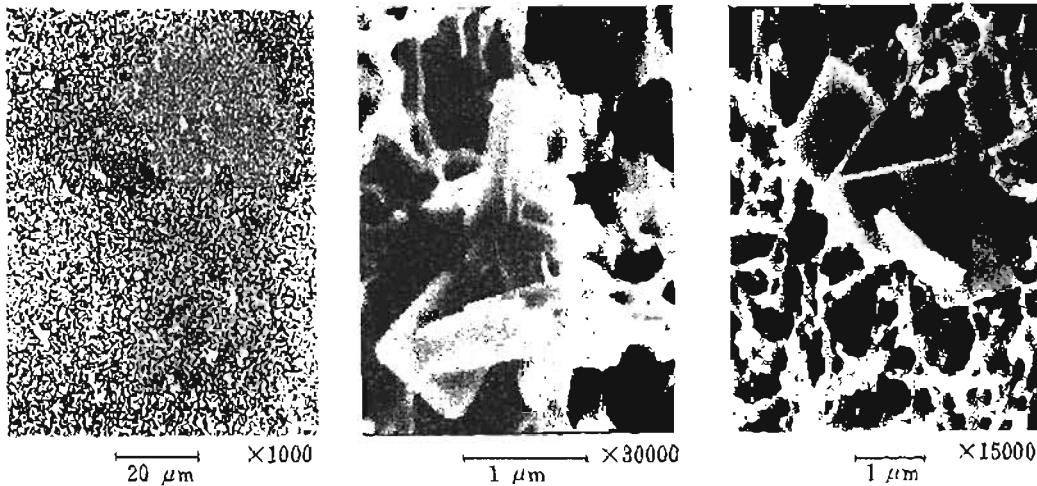


Fig. 1. Particulate Matter ($BaSO_4$) in Micromonicin Ampule

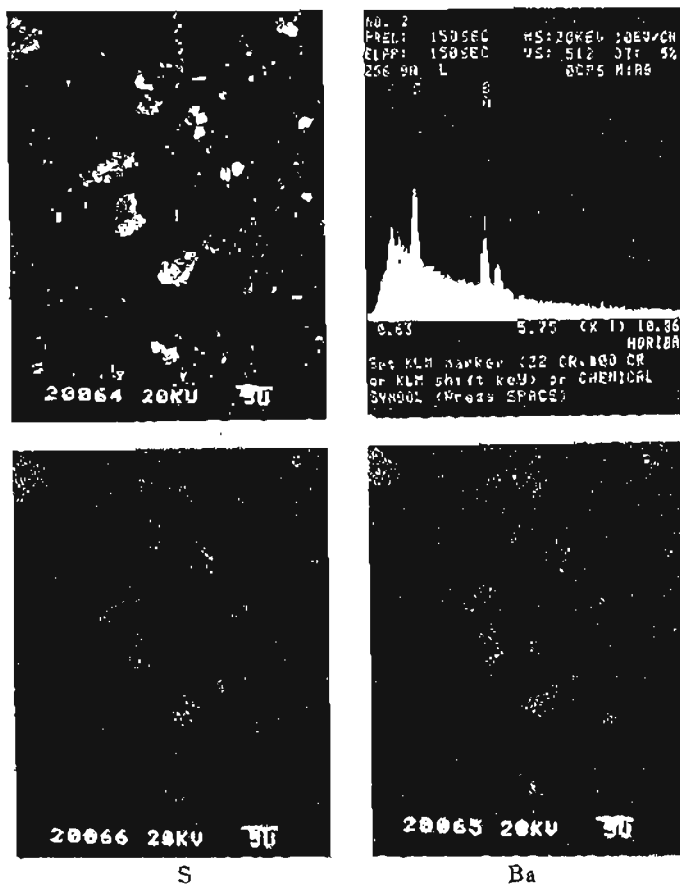


Fig. 2. SEM and EDX of $BaSO_4$ in Micromonicin Ampule

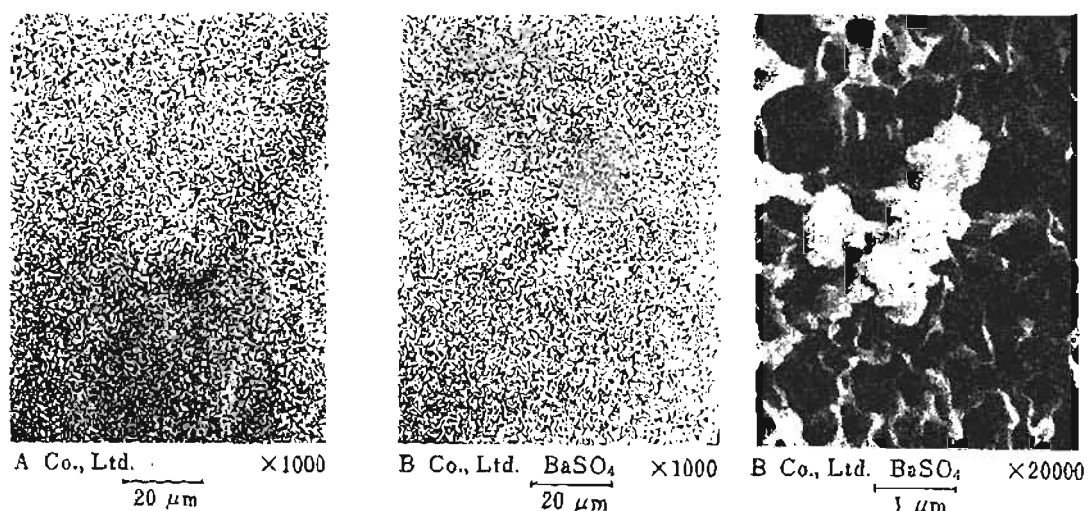


Fig. 3. Particulate Matter in Sisomicin Ampule

company B contained a larger amount of particulate matter than that from company A. Particulate matter count varied from batch to batch in the case of tobramycin preparation.

Count of Foreign Particulate Matter and Effect of Sterilization Conditions

The relation between particulate matter content and sterilization temperature for micronomicin is shown in Table II. In view of the fact that the count of particulate matter in usual ampules tends to increase with increasing temperature, the count is considered to depend on the Ba content of the ampule. The count of particulate matter for surface-treated ampules did not increase at high temperature. Recently the Parenteral Drug Association¹²⁾ has recommended the use a barium-free container, *e.g.*, type KG-33 from Kinble, for injectable products, especially those containing SO_4^{2-} , although it is also desirable to employ a lower temperature of sterilization, aseptic procedures and container-surface treatment.

Foreign Particulate Matter in Solution of Aminoglycoside Antibiotics Sealed in Ampules

Particulate matter in ampules was collected on filters and inspected by SEM. As illustrated in Fig. 1, a number of crystalline particulates were found, in accordance with the report of Boddapati *et al.*⁹⁾ Although their particulates were in the size range from 8–30 μm , ours were as small as 0.5–2.0 μm . The EDX result verifying the presence of Ba and S supports the view that these crystalline particles are crystals of BaSO_4 (Fig. 2).

Sisomicin preparation, an imported product, is commercially available from two companies. The preparation from company B was found to contain agglomerated crystals (Fig. 3) which were presumably BaSO_4 crystals in view of the EDX result. Tobramycin preparation contained crystals of BaSO_4 in one batch, but gentamicin preparation did not. The nature of the particles formed might depend upon the sterilization conditions, the material of the ampule and the nature of the product itself.

References and Notes

- 1) J. M. Garvan and B. W. Gunner, *Med. J. Aust.*, **2**, 140 (1963); *idem, ibid.*, **2**, 1 (1964).
- 2) National Symposium Proceedings, Safety of Large Volume Parenteral Solutions, Food and Drug Administration, Washington, D.C., 1966.
- 3) S. Turco and N. M. Davis, *New Engl. J. Med.*, **287**, 1204 (1972); *idem, Hosp. Pharm.*, **8**, 137 (1973).
- 4) J. Y. Masuda and J. H. Beckerman, *Am. J. Hosp. Pharm.*, **30**, 72 (1973); *idem, ibid.*, **31**, 1189 (1974).
- 5) P. P. DeLuca, R. Rapp, B. Bivins, H. McKean, and W. Griffen, *Am. J. Hosp. Pharm.*, **32**, 1001 (1975).

-
- 6) W. E. Evans, L. F. Barker, and J. V. Simone, *Am. J. Hosp. Pharm.*, **33**, 1160 (1976).
 - 7) T. Rebagy, R. Rapp, B. Bivin, and P. P. DeLuca, *Am. J. Hosp. Pharm.*, **33**, 433 (1976).
 - 8) T. Rebagy and P. P. DeLuca, *Am. J. Hosp. Pharm.*, **33**, 443 (1976).
 - 9) S. Boddapati, L. D. Butler, S. Im, and P. P. DeLuca, *J. Pharm. Sci.*, **69**, 608 (1980).
 - 10) M. J. Pikal and J. E. Lang, *J. Parent. Drug Assoc.*, **32**, 162 (1978).
 - 11) T. G. Sommerville and M. Gibson, *Pharm. J.*, **211**, 128 (1973).
 - 12) Technical Method Bulletin No. 3, Glass Containers for Small Volume Parenteral Products: Factors for Selection and Test Methods for Identification, Parenteral Drug Association Inc., Philadelphia, U.S.A., 1982.

[Chem. Pharm. Bull.]
35(3)1228-1233(1987)

Effect of Cholesterol on Liposome Stability to Ultrasonic Disintegration and Sodium Cholate Solubilization

TOSHIHISA YOTSUYANAGI,* HOTAKA HASHIMOTO,
MOTOKAZU IWATA and KEN IKEDA

*Faculty of Pharmaceutical Sciences, Nagoya City University,
Mizuho-ku, Nagoya 467, Japan*

(Received October 2, 1986)

Liposome disintegration by either ultrasonic vibration or sodium cholate solubilization was investigated as a function of cholesterol (CH) content in the egg phosphatidylcholine (PC) liposome membrane. Turbidity changes were used as an indication of the membrane stability to these stresses. First-order disintegration constants (k_u for ultrasonic stress and k_s for sodium cholate solubilization) were calculated to evaluate the membrane stability. A plot of k_u against membrane CH content gave a sigmoidal curve on which inflection points occurred at about 15 mol% and 33 mol% CH. In contrast, the plot of k_s against membrane CH content gave a biphasic curve with only one inflection point at about 17 mol% CH. These results can be explained in terms of the molecular packing model of phospholipids and CH proposed by Presti *et al.* (*Biochemistry*, **21**, 3831 (1982)). Disintegration by ultrasonic stress was little affected by the accumulation of CH-rich domains up to 15 mol% CH, but disintegration by sodium cholate was abruptly suppressed in the same CH content range. These results indicate that the mechanisms of disintegration of CH-rich domains and interfacial boundary phospholipid are entirely different between the two stresses.

In the liposome disintegration by sodium cholate, it was suggested that the penetration-saturation step of the surfactant molecule into the bilayer is rate-determining for pure PC liposomes, while the lamellar-micellar transition step is rate-determining for CH-rich liposomes.

Keywords—liposome stability; cholesterol; egg phosphatidylcholine liposome; ultrasonic vibration; sodium cholate; turbidity change; disintegration mechanism

The physical integrity of liposomes is affected by a variety of external stresses such as ultrasonic vibration, surfactants and freezing.¹⁻⁶⁾ Ultrasonic vibration, used for the size reduction of vesicles, transforms large multilamellar liposomes into small vesicles. An explanation of this rearrangement process has been given.⁷⁾ The destruction of liposomal structures by bile salt surfactants may be one of the important factors influencing drug carrier activity after oral administration.^{3,4)}

The ability of liposomes to resist degradation by externally applied stresses depends on lipid composition, in particular cholesterol (CH), and also vesicle size and surface charge.⁸⁾ We studied the disintegration of phosphatidylcholine (PC)/CH liposomes caused by ultrasonic vibration and sodium cholate solubilization. The time course of vesicle disintegration was followed by measuring the turbidity changes. Disintegration rate constants obtained from turbidity measurement were used to evaluate the stability of liposomes to these externally applied forces.

Experimental

Materials—PC was extracted from egg yolk and purified by column chromatography on silicic acid (Mallinckrodt, St. Louis).⁹⁾ Sodium cholate was purchased from Katayama Chem. Co. (Osaka), and recrystallized from acetic acid as cholic acid. CH and all other chemicals were of reagent grade.

Preparation of Liposomes—Liposomes were prepared essentially by the method of Bangham *et al.*¹⁰ In short, the required amounts of PC and CH (0–57 mol%) were taken in a round-bottomed flask, and dried to give a thin film. Tris buffer (pH 7.4, I.S. 0.1 with NaCl) was added to make a final PC concentration of 1×10^{-3} M based on phosphorus,¹¹ and the mixture was shaken gently then dispersed in a vortex mixer for 3 min.

Disintegration Rate of Liposomes by Ultrasonic Vibration—Turbidities of the multilamellar liposomes (MLV) prepared above varied significantly even for liposomes of identical lipid composition. Therefore liposome samples were briefly sonicated (probe-type sonifier, model UR 200P, 20 kHz, Tomy Seiko Co., Tokyo) for 2.5 min to obtain reproducible initial turbidities. This preliminary sonication was uniformly applied to all of the liposomes containing 0–57 mol% CH. The resulting suspensions were allowed to equilibrate at room temperature for 30 min, which was taken to be $t=0$ for the calculations of disintegration kinetics. Ultrasonic vibration was continuously applied for various periods to each sample, the volume of which was always maintained at 10 ml in a 50 ml glass centrifuge tube under a nitrogen stream at 40°C. The samples were left standing for 30 min at room temperature, then turbidity measurements were carried out in a 1 cm quartz cell at 400 nm, using a Hitachi 124 spectrophotometer.

Disintegration Rate of Liposomes by Sodium Cholate—The disintegration kinetics of liposomes in sodium cholate solution was also followed by measuring the turbidity changes. Turbidity was monitored at 660 nm by a stopped-flow apparatus (model RA-401, Union Giken, Osaka) equipped with a UV-VIS detector.⁵ Liposomes were first subjected to ultrasonic vibration to give various initial turbidities for the cholate disintegration studies. An equal volume of the liposome suspension containing 3×10^{-4} M phosphorus was quickly mixed with a 0.02 M sodium cholate solution (Tris buffer, pH 7.4, I.S. 0.1, 25°C).

The concentrations of lipid and surfactant are diluted to half in the cell of the apparatus. Accordingly, the initial turbidity was presumed to be half of the original turbidity.

Turbidity reduction by ultrasonic vibration or surfactant solubilization was treated as a pseudo-first-order process, and first-order liposome disintegration rate constants, k_u and k_s , respectively, were obtained from the turbidity measurements; k_u was calculated from the initial slope of the plots shown in Fig. 1, and k_s was obtained from the linear plots of turbidity disappearance.

Results and Discussion

Disintegration Behavior under Ultrasonic Vibration

The sonication system used for the disintegration of liposomes gave reproducible turbidity changes ($\pm 5\%$ scattering). Unlike the disintegration of vesicles in surfactant solution, in which the bilayer was assumed to be disintegrated by successive stripping of shells from the vesicles, yielding mixed micelles, ultrasonic vibration merely tears the vesicles into smaller bilayer fragments and ultimately finer vesicles. These small vesicles contribute to the total turbidity of the suspension. Because of this, turbidity reduction at the early stages of disintegration was used to calculate k_u values. The rate constant (k_u) was assumed to represent membrane stability to ultrasonic stress: the smaller the rate constant, the more resistant the bilayer membrane.

Figure 1 shows the turbidity reductions of CH containing liposomes. At less than 17 mol% CH, linearity was generally poor for long sonication times. As the CH content increased to more than 33 mol%, the reduction showed an initial slow stage and a subsequent faster stage. Decreasing the sonication stress by using a bath-type sonicator, instead of a probe, prolonged the initial slow stage significantly.² The reason for this is not clear.

The k_u values were calculated from the initial slope, and also from the terminal linear portion at CH contents of more than 33 mol%. Figure 2 shows a plot of k_u vs. mol% CH in the liposomes. The sigmoidal shape of the k_u vs. mol% CH plot had three distinct regions. These regions are defined by the two inflection points at about 15 mol% CH and about 33 mol% CH. From 0 to 15 mol% CH, the membrane stability remained almost unchanged (stage I). From 15 mol% CH to 33 mol% CH, a rather sharp increase in membrane stability occurred (stage II). Increasing CH beyond 33 mol% caused only a moderate increase in membrane stability (stage III). At stage III there was little difference between the increments of the stability obtained from the initial and terminal slopes of the turbidity reductions (Fig. 1).

Presti *et al.*¹² proposed a model for the molecular packing of CH and phospholipids in membranes. According to their model, phases are formed as a function of the CH content in

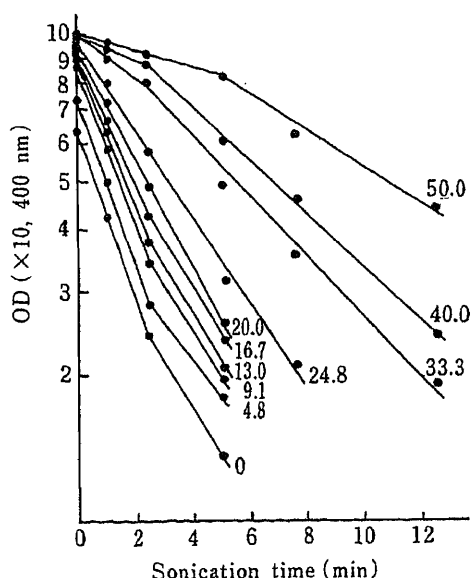


Fig. 1. First-Order Plots of the Turbidity Change due to Liposome Disintegration by Ultrasonic Vibration

The PC concentration is constant at 1×10^{-3} M. Numbers indicate CH content (mol%). All liposome suspensions were subjected to a prior sonication of 2.5 min. Points are the mean values of 3–5 determinations and were reproducible better than $\pm 5\%$.

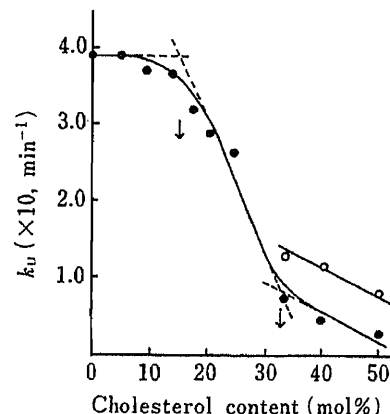


Fig. 2. The Effect of CH Content on the Disintegration Constant (k_u) of Liposomes by Ultrasonic Vibration

k_u was calculated from the initial slope (●—●). k_u was also obtained from the subsequent linear portion for liposomes containing 33.3, 40.0 and 50.0 mol% CH (○—○). PC concentration, 1×10^{-3} M. ↓ shows an inflection point at which the membrane stability anomalously changes.

the bilayer: under 20 mol% CH, CH-rich domains are formed and surrounded by a continuous phospholipid domain or phase. At about 20 mol% CH, the continuous PC domain disappears, but interfacial boundary phospholipid remains, separating the CH-rich domains. Further increasing the membrane CH causes the fraction of interfacial boundary phospholipid to gradually diminish and become zero at *ca.* 33.3 mol%. Uncomplexed phospholipid molecules finally disappear at 50 mol% CH.

Based on this model, the relationship between k_u and mol% CH can be interpreted as follows. The membrane stability, *i.e.* k_u , changed very little in stage I, where CH-rich domains are present but do not occupy a large fraction of the membrane. The inflection point observed at 15 mol% CH, which probably corresponds to the first critical ratio in Presti's model, reflects a critical ratio under which the contribution of the CH-rich domains produced in the continuous PC phase to the stability is still minor in the egg PC liposomes. In stage II, the stability increased dramatically with increasing CH content. This is a reasonable reflection of an accumulation of the CH-rich domains, in other words, a decrease of the interfacial boundary phospholipid. The second inflection point observed at 33 mol% CH coincides with the second critical point (33.3 mol% CH) in the model, at which the bilayer contains only CH-rich domains. Further incorporation (> 33 mol%) of the sterol into liposomes results in a mild increase in membrane stability (stage III) where the CH-rich domains are transformed to the 1:1 hydrogen-bonded complexes up to about 50 mol% CH. Membranes containing 50 mol% CH are stabilized about four-fold compared to CH free membranes. This also suggests strong interactions among resulting PC/CH 1:1 complexes. It is therefore reasonable to consider that tearing of bilayers by sonication occurs mainly in the free phospholipid domain.

The ultrasonic velocity has been considered to be a good measure of the mechanical properties of membranes.^{13,14)} In the liquid-crystalline state of dipalmitoylphosphatidylcholine (DPPC) liposomes, the limiting value of ultrasonic velocity shows an abrupt increase

in the region of 15 to 30 mol% CH. The k_u values also start changing abruptly near 15 mol% CH. When egg PC liposomes are used instead of DPPC liposomes, it seems that the stabilizing effect of CH against ultrasonic vibration is not sensitive to the fatty acid composition of phospholipids but rather to the disappearance of interfacial boundary phospholipid. It is noteworthy that a macroscopic mechanical property represented by the ultrasonic disintegration rate constant (k_u) is consistent with Presti's model.

Disintegration Behavior in Sodium Cholate

A mechanistic sequence for the disintegration of liposomes by surfactants has been proposed, in which the mode of action of sodium cholate was classified into type B.¹⁵⁾ We reported previously that the turbidity disappearance of pure PC liposomes clearly followed first-order kinetics despite the presence of polydispersed vesicles in terms of size.⁵⁾ An explanation was given for the linearity of the first-order plots by introducing the average size factor ($\bar{\phi}$). The reduction rate of the total turbidity (T_{tot}) is expressed by

$$-\frac{dT_{\text{tot}}}{dt} = \bar{k} \sum_{i=j}^m \frac{A_i - A_{i-1}}{A_i} A_i n_i \quad (m > j) \quad (1)$$

where \bar{k} is the size-independent disintegration rate constant, A_i is the scattering coefficient of the i -th vesicle, n_i is the number of the i -th vesicle, and m and i denote the size classes of the largest and the j -th vesicles sensitive to the turbidity changes at a certain wavelength. The absorbance ($T = An$) of a dispersed system containing monodispersed particles is given by^{16,17)}

$$T = \frac{\ln(I_0/I)}{L} = K\pi a^2 n \quad (2)$$

$$K = K_0 \left(\frac{a}{\lambda} \right)^p \quad (3)$$

where I_0 and I are the intensities of the incident and transmitted light, respectively. a is the particle radius, L is the length of scattering path, K and K_0 are the total scattering coefficient and the size-independent component of the scattering coefficient, respectively, and p is the exponent of the wave-length (λ). The term $(A_i - A_{i-1})/A_i$ in Eq. 1 can be therefore represented based on Eqs. 2, 3 and $T = An$ as

$$\phi_i = \frac{A_i - A_{i-1}}{A_i} = \frac{a_i^{p+2} - a_{i-1}^{p+2}}{a_i^{p+2}} \quad (4)$$

If ϕ_i , which is intrinsically size-dependent, is defined as an average size factor ($\bar{\phi}$), Eq. 1 can be represented as a first-order kinetic equation with regard to T_{tot} , *i.e.*

$$\begin{aligned} -\frac{dT_{\text{tot}}}{dt} &= \bar{k} \bar{\phi} \sum_{i=j}^m A_i n_i \quad (m > j) \\ &= \bar{k}_a T_{\text{tot}} \end{aligned} \quad (5)$$

Accordingly, the experimentally obtained first-order disintegration rate constant (\bar{k}_a) contains an average size factor $\bar{\phi}$, which may be useful to characterize the disintegration behaviors of dispersed systems with different size distributions.

The turbidity changes of liposomes containing 0–57 mol% CH followed first-order kinetics. Figure 3 shows the pseudo-first-order rate constant (k_s) obtained as a function of the initial turbidity and CH content at the constant sodium-cholate concentration of 0.01 M. The egg-PC/bile salt molar ratio was maintained at 0.1 throughout, *i.e.* excess of bile salt. The k_s value depended on the initial turbidities, which reflect different size distributions of vesicles, even when the composition of PC and CH was fixed, and the curves appeared to be generally biphasic. Values of k_s for PC liposomes (CH free) were most sensitive to the initial turbidity.

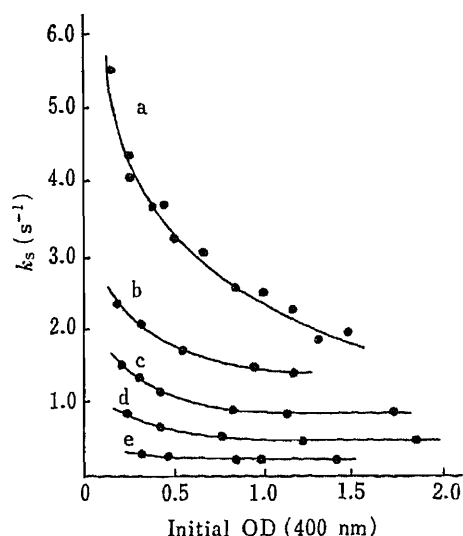


Fig. 3. Effects of Initial Turbidity and CH Content on the Disintegration Constant (k_s) in Sodium Cholate Solution

The concentrations of PC and sodium cholate were always maintained at 3×10^{-3} and 2.0×10^{-2} M, respectively. CH content (mol%): 0 (a), 9.2 (b), 14.0 (c), 29.6 (d) and 57.1 (e). The temperature was 25 °C.

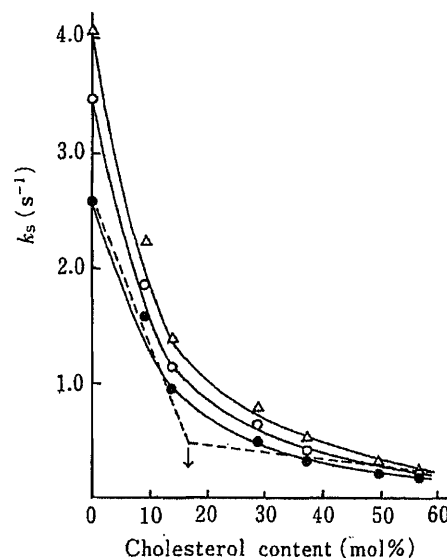


Fig. 4. The Effect of CH Content on the Disintegration Constant (k_s) at Different Initial Turbidities

Initial turbidity: 1.0 (●), 0.5 (○) and 0.25 (△). ↓ shows an inflection point at which the membrane stability anomalously changes.

Incorporating CH into the membrane decreased the biphasic nature of the curve (Fig. 3); at about 50 mol% CH, k_s was little affected by the initial turbidity.

In connection with the theory described earlier, the dependency of k_s on the initial turbidity reflects the difference of the size factor; the relationship $k_s = \bar{k}_a = \bar{k} \bar{\phi}$ holds because \bar{k} is assumed to be a size-independent disintegration constant for a single bilayer. However, as the CH-rich domains were accumulated, the dependency of k_s on the initial turbidity gradually diminished, suggesting that the size factor $\bar{\phi}$ apparently becomes rather constant despite the fact that various initial turbidities were used. These results (Fig. 3) raise the question of why $k_s = \bar{k} \bar{\phi}$ does not always hold for PC/CH membranes as the CH content increases, because we previously estimated ϕ_i to increase 2.5 times as the vesicle size decreased by half in radius in model calculations⁵⁾ and such changes of ϕ_i should be intrinsically applicable irrespective of CH content. Therefore, the physical meaning of the parameter \bar{k} involved in k_s may differ between the pure PC liposomes and the CH-rich liposomes. This discrepancy could be accounted for by a stepwise disintegration mechanism of the bilayer. Step I is the penetration-saturation step of bile salt molecules followed by step II, the lamellar-micellar phase transition step.

As shown in Fig. 4, the relationship between CH content and k_s was biphasic when the initial turbidity was maintained at 1.0 O D. The same tendency was also seen with other initial turbidities (0.25 and 0.5). Accumulation of CH-rich domains in the membrane is responsible for the abruptly increasing stability up to about 17 mol%, and as interfacial boundary phospholipid appears, the membrane shows relatively minor increments of the stability. It was also noted that the k_s dependency showed an inflection point at about 17 mol% irrespective of the initial turbidity. It seems likely that with CH-rich liposomes (*e.g.* 1:1 molar ratio) the amount of the surfactant molecule that penetrates into the bilayer is limited and the transition rate is slowed.

Accordingly, the larger the bilayer in radius, the slower the integration rate. If the \bar{k} reflects the lamellar-micellar phase transition rate for the CH-rich liposomes, it seems

probable that $k_s = \bar{k} \bar{\phi} \simeq \text{constant}$ in consequence of the mutual compensation of the changes in the two parameters, \bar{k} and $\bar{\phi}$. With CH-free liposomes, the penetration-saturation step is rate-determining and \bar{k} is a size-independent parameter; it was assumed previously that the dependency of k_s on the initial turbidity is due to changes of $\bar{\phi}$. Furthermore, the size of the mixed micelles decreases readily. Although the consistency of the theory and results should be further examined, we assume that the disintegration rate of the pure PC liposomes is mainly governed by the former step and with increasing CH content in the membrane the latter step becomes predominant.

In conclusion, there is a marked difference between the liposome stabilities to ultrasonic vibration (physical stress) and the disintegrating action of cholic acid (chemical stress) as a function of the CH content. The role of CH incorporated in egg PC liposomes is often said to be to make the bilayer membrane "more solid-like," but the amounts of CH used are not always rationalized in the literature. The observed variation of the membrane stability may provide useful criteria for compounding CH in liposomes and in assessing their response to external stresses.

Acknowledgements This study was supported in part by a Grant-in-Aid for Scientific Research (No. 59570925, No. 60571023) from the Ministry of Education, Science and Culture, Japan.

References

- 1) D. Chapman, D. J. Fluck, S. A. Penkett and G. G. Shipley, *Biochim. Biophys. Acta*, **163**, 255 (1968).
- 2) T. Yotsuyanagi, M. Nonomura and K. Ikeda, *J. Parenteral Sci. Technol.*, **35**, 271 (1981).
- 3) M. H. Richards and C. R. Gardner, *Biochim. Biophys. Acta*, **543**, 508 (1978).
- 4) R. N. Rowland and J. F. Woodley, *Biochim. Biophys. Acta*, **620**, 400 (1980).
- 5) T. Yotsuyanagi, J. Mizutani, M. Iwata and K. Ikeda, *Biochim. Biophys. Acta*, **731**, 304 (1983).
- 6) G. J. Morris and J. J. McGrath, *Cryobiology*, **18**, 390 (1981).
- 7) W. Helfrich, *Phys. Lett.*, **50A**, 115 (1974).
- 8) J. J. Collins and M. C. Phillips, *J. Lipid Res.*, **23**, 291 (1982).
- 9) A. E. Brandt and W. E. M. Lands, *Biochim. Biophys. Acta*, **144**, 605 (1967).
- 10) A. D. Bangham, M. M. Standish and J. C. Watkins, *J. Mol. Biol.*, **13**, 238 (1965).
- 11) H. Eibl and W. E. M. Lands, *Anal. Biochem.*, **30**, 51 (1969).
- 12) F. T. Presti, R. J. Pace and S. I. Chan, *Biochemistry*, **21**, 3831 (1982).
- 13) S. Mitaku, A. Ikegami and A. Sakanishi, *Biophys. Chem.*, **8**, 295 (1978).
- 14) A. Sakanishi, S. Mitaku and A. Ikegami, *Biochemistry*, **18**, 2636 (1979).
- 15) A. Helenius and K. Simons, *Biochim. Biophys. Acta*, **415**, 29 (1975).
- 16) G. F. Lothian and F. P. Chappel, *J. Appl. Chem.*, **1**, 475 (1951).
- 17) S. R. Reddy and H. S. Fogler, *J. Colloid Interface Sci.*, **79**, 101 (1981).

[Chem. Pharm. Bull.]
35(3)1234—1237(1987)

**Chemical and Pharmaceutical Studies on Medicinal Plants in Paraguay. I.
Isolation and Identification of Lens Aldose Reductase Inhibitor
from "Tapecué," *Acanthospermum australe* O.K.¹⁾**

MINEO SHIMIZU,*^a SYUNJI HORIE,^a MUNEHISA ARISAWA,^a TOSHIMITSU HAYASHI,^a
SHOICHI SUZUKI,^a MASAO YOSHIZAKI,^a MASARU KAWASAKI,^a
SATOSHI TERASHIMA,^a HIDEKI TSUJI,^a SYUJI WADA,^a
HAJIME UENO,^a NAOKATA MORITA,^a
LUIS H. BERGANZA,^b ESTIBAN FERRO^b
and ISABEL BASUALDO^b

*Faculty of Pharmaceutical Sciences, Toyama Medical and Pharmaceutical University,^a
2630 Sugitani, Toyama 930-01, Japan and Facultad de Ciencias Químicas,
Universidad Nacional de Asunción,^b Casilla de Correo 1055,
Asunción, Paraguay*

(Received July 23, 1986)

The EtOH extract of "Tapecué," *Acanthospermum australe*, was found to have a potent inhibitory activity towards rat lens aldose reductase (AR). From the active fraction of the extract, 5,7,4'-trihydroxy-3,6-dimethoxyflavone was isolated. It was found to have higher activity ($IC_{50} = 1 \times 10^{-7}$ M) than quercitrin, which is a known inhibitor of AR ($IC_{50} = 1.8 \times 10^{-6}$ M in our bioassay).

Keywords—*Acanthospermum australe*; Compositae; 5,7,4'-trihydroxy-3,6-dimethoxyflavone; aldose reductase inhibitor; rat lens

There is a traditional system of medicine, "Medico de Yuyo," employing medicinal plants in Paraguay. In screening tests for biological activities of these plants "Tapecué," *Acanthospermum australe* (Compositae), showed weak inhibitory effects on β -glucuronidase activity and on the growth of KB cells and high inhibitory activity towards rat lens aldose reductase (AR). This paper deals with the isolation and identification of chemical constituents in "Tapecué," and identification of the active component inhibiting rat lens AR, which plays a significant role in the reduction of aldose to alditol under abnormal conditions such as diabetes.

"Tapecué" is an important crude drug which has traditionally been used for the treatment of blood stagnation, rheumatism and arthritis by internal administration, and of swelling and bleeding by external application in "Medico de Yuyo." Various diterpenes,²⁾ acanthospermal A, tridecapenta-3,5,7,9,11-yne-1-ene, thymol, isothymol, *etc.* have been isolated from this plant³⁾ but no studies in relation to the biological activity have been reported. Chemical and pharmacological studies of another plant of the same genus, *Acanthospermum glabratum*⁴⁾ have revealed no AR inhibitory activity.

EtOH:H₂O (7:3) extract (A) was suspended in water and extracted with *n*-hexane, CHCl₃ and *n*-BuOH successively to afford *n*-hexane extract (B), CHCl₃ extract (C), *n*-BuOH extract (E) and residue (F) (Fig. 1.)

The extract E (Table I), which was most active, was applied to a column of polyamide, and elution with MeOH:H₂O (3:2) followed by MeOH and CHCl₃ gave four fractions (fr. 1—4) (Fig. 1).

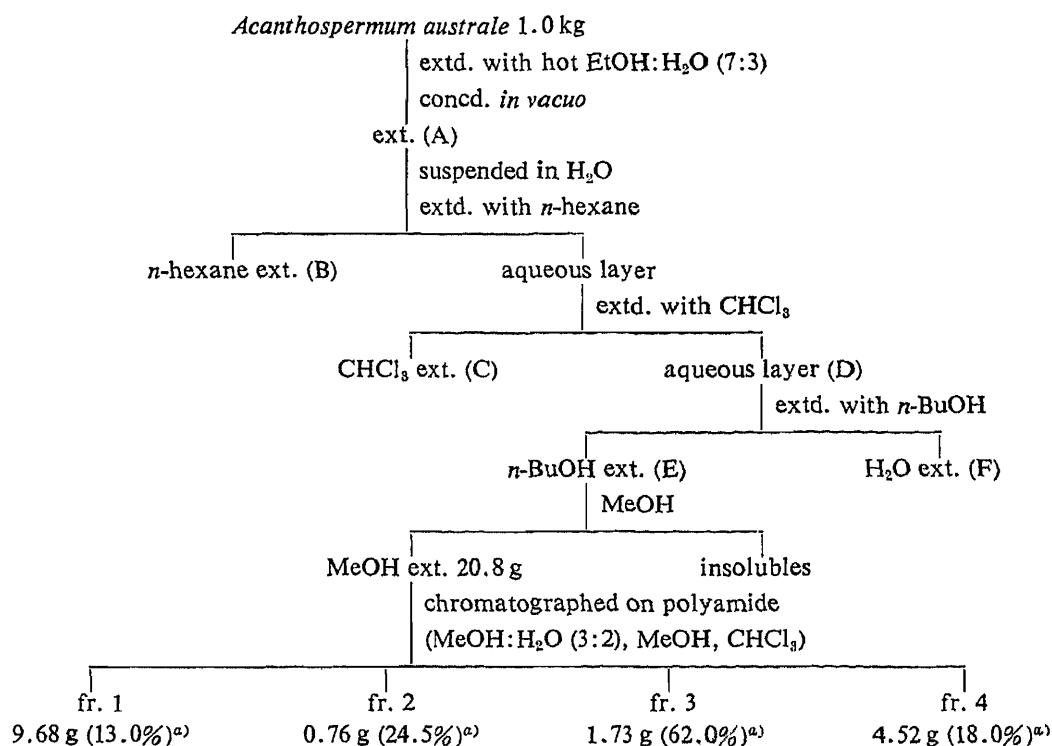


Fig. 1. Fractionation of Biologically Active Constituents of *Acanthospermum australe*

a) Values in parentheses indicate the inhibitory activities towards crude rat lens aldose reductase at the concentration of 1 $\mu\text{g/ml}$.

TABLE I. Inhibition of Crude Rat Lens Aldose Reductase by Extracts from *Acanthospermum australe* and Compounds 1–6

Extract	IC ₅₀ (μg)	Yield (%)	Compound	IC ₅₀ (μM)
A	2.3	100	1	0.1
B	20.0	13	2	—
C	4.0	14	3	3.2
D	2.6	—	4	9.2
E	1.5	29	5	4.8
F	13.0	43	6	—
			Quercitrin ^{a)}	1.8

a) Quercitrin was assayed previously, and was tested again as a reference in this study.

Three crystalline compounds **1**, **2** and **3** were obtained from fr. 3, which exhibited higher activity than other fractions, by gel-filtration and silica gel column chromatography. Compounds **4**, **5** and **6** were obtained from fr. 2 and fr. 4.

Compound **1**, yellow needles, exhibited a positive reduction test for flavonoids. Infrared (IR) and ultraviolet (UV) spectra of **1** showed the characteristic absorption patterns of flavonoids. In the proton nuclear magnetic resonance (¹H-NMR) spectrum of **1**, peaks due to four aromatic protons appeared as A₂B₂ type signals attributable to B ring protons. Another aromatic proton signal at 6.6 ppm assigned to the C-8 proton and a 6H singlet at 3.8 ppm attributed to two methoxyl groups were observed. The presence of three hydroxyl groups at C-5, C-7 and C-4' in **1** was determined by analysis of the UV spectrum.⁵⁾ From the above results, **1** was concluded to be 5,7,4'-trihydroxy-3,6-dimethoxyflavone⁶⁾ and this identification

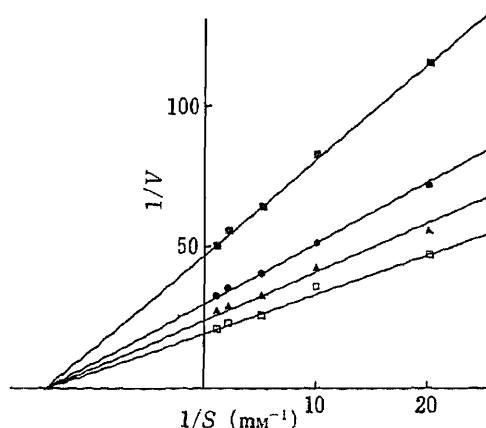


Fig. 2. Lineweaver-Burk Plots of Lens AR Activity

Enzyme activity was measured at each substrate concentration in the presence and absence of inhibitors. Key: (□) control, (●) in the presence of 10^{-7} M 1, (▲) 5×10^{-8} M 1 and (■) 10^{-6} M quercitrin. The substrate is glyceraldehyde (S) and the velocity units (V) are changes in $OD_{340}/200$ s.

was confirmed by comparison of the physical and spectral data with those of an authentic sample.

Compounds 2, 3, 4 and 5 were identified as trifolin, hyperin, rutin and quercetin, respectively, by comparison of the physical and spectral data with those of authentic samples.

Compound 6, a pale yellow powder, exhibited a negative reduction test for flavonoids and a positive color reaction to $FeCl_3$ and was concluded to be caffeic acid from the physical and spectral data.

Inhibitory Effect on Crude Rat Lens AR

Compound 1, which has not previously been tested for inhibitory activity towards AR, exhibited the highest activity ($IC_{50} = 1.0 \times 10^{-7}$ M) among compounds 1–6 and was about 18 times more potent than quercitrin ($IC_{50} = 1.8 \times 10^{-6}$ M) (Table I).

According to Okuda *et al.*,⁷⁾ axillarin and LARI 1 are the most potent inhibitors of aldose reductase known so far ($IC_{50} = 5.2 \times 10^{-8}$ and 4.2×10^{-8} M), respectively, being at least 6 times more potent than quercitrin (3.1×10^{-7} M). Some flavonoids showed varying activities depending on the solvent used,⁸⁾ and different values of IC_{50} of quercitrin were found by Varma *et al.*⁹⁾ and Okuda *et al.*,⁷⁾ and in this work, so the comparative potency of compounds should be estimated under the same conditions. As judged from the relative potencies (IC_{50}) of compound 1, axillarin and quercitrin, 1 might be as potent as or more potent than axillarin.

We concluded that compound 1 is mainly responsible for the rat lens AR inhibitory activity of this plant.

Kinetics of Inhibition by Compound 1

Kinetic studies were conducted with 1 in order to determine the type of inhibition and the inhibition constant (K_i). The Lineweaver-Burk plots are shown in Fig. 2. Compound 1 was found to be a non-competitive inhibitor at the concentrations of 1.0×10^{-7} and 5.0×10^{-8} M, as was seen in the cases of quercitrin⁷⁾ and axillarin,⁷⁾ but it did not show the same type of inhibition at the concentration of 5.0×10^{-7} M. Okuda *et al.*⁷⁾ reported that many uncompetitive inhibitors display non-competitive inhibition at low concentrations and switch to uncompetitive inhibition at higher concentrations. In our experiment, 1 showed a similar action. The K_i value of 1 for lens AR was 2.05×10^{-7} M.

The inhibitory effect of 1 on lens AR was also checked in the presence of a large amount of bovine serum albumin (BSA). Compound 1 showed almost the same degree of inhibition in the presence and absence of BSA, suggesting that 1 inhibits the activity of lens AR even in the presence of other proteins.

Experimental

The melting point is uncorrected. IR and UV spectra were obtained with Hitachi 260-10 and Hitachi 220S spectrometers. ¹H-NMR spectra were taken with a Hitachi R-24B (60 MHz) spectrometer with tetramethylsilane as an internal standard, and chemical shifts are given in δ (ppm). Mass spectra (MS) were obtained on a JEOL-JMS-D 200 instrument. Paper partition chromatography (PPC) was performed on Toyo filter paper No 51B employing the descending technique with AcOH:H₂O (15:85) and *tert*-BuOH:AcOH:H₂O (3:1:1) (TBA) as developing solvents, and the spots were detected under a UV lamp. Thin layer chromatography (TLC) was performed on Kieselgel 60F₂₅₄ plates (Merck); spots were detected under a UV lamp and by heating after spraying 10% H₂SO₄.

Plant Materials—“Tapecué” was purchased from local dealers in Asunción, Paraguay and identified as *Acanthospermum australe* O.K. (aerial part) by Dr. H. Koyama, Faculty of Science, Kyoto University.

Bioassay—Crude AR was obtained from the supernatant fraction of the homogenate of rat lens according to the method of Kador and Sharpless.¹⁰ One unit was defined as the amount catalyzing the oxidation of 1 μ mol of reduced nicotinamide adenine dinucleotide phosphate per minute. Samples (1.4–2.0 units) were stored frozen until needed. The inhibitory effects of extract A–F and the isolated compounds on AR were assayed by the method previously reported.⁹ Samples were dissolved in dimethylsulfoxide, which was found to have no effect on the enzyme activity at below 0.1% concentration.

Extraction and Fractionation—Dried powder (1 kg) of “Tapecué” was extracted with hot EtOH:H₂O (7:3) (1 h \times 3). The EtOH:H₂O (7:3) solution was concentrated *in vacuo* to give the extract A (118 g). Extract A (100 g) was suspended in H₂O (600 ml) and extracted with *n*-hexane (500 ml \times 3), CHCl₃ (800 ml \times 3) and *n*-BuOH (670 ml \times 3) successively to yield the biologically active extract E (29 g). The MeOH solubles (20.8 g) of E (21 g) was chromatographed on polyamide (Waco C-200, 280 g, 5 \times 50 cm). Elution with MeOH:H₂O (3:2), MeOH and CHCl₃ gave fr. 1 (9.68 g), fr. 2 (0.76 g), fr. 3 (1.73 g) and fr. 4 (4.52 g). The most biologically active fr. 3 was subjected to gel-filtration (Toyopearl HW-40F) and silica gel column chromatography to give compounds 1 (13 mg), 2 (2 mg) and 3 (41 mg). From fr. 2, compounds 4 (21 mg) and 5 (7 mg) were obtained by column chromatography (silica gel and Sephadex LH 20). Compound 6 (110 mg) was obtained from fr. 4.

Compound 1 (5,7,4'-Trihydroxy-3,6-dimethoxyflavone)—Yellow needles, mp 199–200 °C (CHCl₃/MeOH). PPC *R*_f 0.34 (15% AcOH), 0.86 (TBA). Mg+HCl: orange; Zn+HCl: red-violet. MS *m/z*: 330 (M⁺), 315. UV $\lambda_{\text{max}}^{\text{EtOH}}$ nm (log ϵ): 341 (4.22), 270 (4.14). IR $\nu_{\text{max}}^{\text{KBr}}$ cm⁻¹: 3450, 1660, 1610.

Compounds 2–6—2, mp 236 °C (MeOH), 3, mp 233–234 °C (EtOH), 4, mp 192–195 °C (MeOH/H₂O), 5, mp > 300 °C, and 6, mp 220–222 °C (MeOH/H₂O), were identical with authentic trifolin, hyperin rutin, quercetin and caffeic acid, respectively.

Acknowledgement This work is a part of a joint study between Japan and the Republic of Paraguay on medicinal plants in Paraguay supported by both governments through the Japan International Cooperation Agency (JICA). We wish to thank Prof. T. J. Mabry, University of Texas at Austin, Texas, U.S.A., for providing 5,7,4'-trihydroxy-3,6-dimethoxyflavone. We also wish to thank Dr. H. Koyama, Faculty of Science, Kyoto University, for identification of *Acanthospermum australe* O.K.

References and Notes

- 1) This work was presented in part at the 106th Annual Meeting of the pharmaceutical Society of Japan, Chiba, April 1986.
- 2) W. Herz and P. S. Kalyanaraman, *J. Org. Chem.*, **40**, 3486 (1975); F. Bohlmann, J. Jakupovic, A. Dhar, R. King and H. Robinson, *Phytochemistry*, **20**, 1081 (1981).
- 3) F. Bohlman, H. G. Schmeda and J. Jakupovic, *Planta Medica*, **50**, 37 (1984).
- 4) A. A. Saleh, G. A. Cordell and N. R. Farnsworth, *J. Natural Products*, **39**, 456 (1976); H. Lotter, H. Wagner, A. A. Saleh, G. A. Cordell and N. R. Farnsworth, *Z. Naturforsch. Teil C*, **34C**, 677 (1979); A. A. Saleh, G. A. Cordell and N. R. Farnsworth, *J. Chem. Soc., Perkin Trans. 1*, **1980**, 1090.
- 5) T. J. Mabry, K. R. Markham, M. B. Thomas, “The Systematic Identification of Flavonoids,” Springer-Verlag, New York, 1970, Chapter IV–VII; K. R. Markham, “Techniques of Flavonoid Identification,” Academic Press, 1982, Chapter 3.
- 6) H. Rosler, A. E. Star and T. J. Mabry, *Phytochemistry*, **10**, 450 (1971); A. A. Saleh, G. A. Cordell and N. R. Farnsworth, *J. Natural Products*, **39**, 456 (1976).
- 7) J. Okuda, I. Miwa, K. Inagaki, T. Horie and M. Nakayama, *Biochemical Pharmacology*, **31**, 3807 (1982).
- 8) M. Shimizu, T. Itoh, S. Terashima, T. Hayashi, M. Arisawa, N. Morita, S. Kurokawa, K. Itoh and Y. Hashimoto, *Phytochemistry*, **23**, 1885 (1984).
- 9) S. D. Varma and J. H. Kinoshita, *Biochemical Pharmacology*, **25**, 2505 (1976); P. F. Kador, J. H. Kinoshita, W. H. Tung and L. T. Chylack, Jr., *Invest. Ophthalmol. Visual Sci.*, **19**, 980 (1980).
- 10) P. F. Kador and N. E. Sharpless, *Biophys. Chem.*, **8**, 81 (1978).

[Chem. Pharm. Bull.]
35(3)1238—1242(1987)

Adsorption of Hydrogen Sulfide, Dimethyl Sulfide, and Their Binary Mixtures into Pores of N-Containing Activated Carbon

SHOZO TSUTSUI* and SEIKI TANADA

Faculty of Pharmaceutical Sciences, Kinki University, Kowakae 3-4-1,
Higashi-Osaka, Osaka 577, Japan

(Received June 25, 1986)

The adsorption behavior of gas mixtures composed of hydrogen sulfide and dimethyl sulfide in the pores of N-containing activated carbon (N-CAC) was investigated on the basis of adsorption isotherms of the pure components and binary gas mixtures. Hydrogen sulfide and dimethyl sulfide were mainly adsorbed into smaller micropores and into larger micropores, respectively. The adsorption capacity of N-CAC for hydrogen sulfide was increased by 25—35% as compared with that of raw activated carbon (R-AC). The adsorption capacity of N-CAC for dimethyl sulfide was decreased by 20% as compared with that of R-AC. The experimental adsorption isotherms of binary gas mixtures at different molar ratios agreed closely with the theoretical adsorption isotherms on N-CAC. However, the experimental adsorption isotherms of the binary gas mixtures did not agree with the theoretical adsorption isotherms on R-AC and the amounts adsorbed on R-AC were very much smaller than the theoretical ones. These results indicated that adsorption of each component on N-CAC did not interfere with that of the other component, and that hydrogen sulfide and dimethyl sulfide entered micropores of different sizes in N-CAC. It was concluded that N-CAC is a characteristic adsorbent having a greater adsorption capacity for hydrogen sulfide in these binary gas mixtures. It seemed that adsorption of the binary gas mixtures was mainly competitive on R-AC and selective on N-CAC.

Keywords—binary gas mixture; hydrogen sulfide; dimethyl sulfide; N-containing activated carbon; selective adsorption; experimental adsorption isotherm; theoretical adsorption isotherm

Malodorous gas mixtures are often discharged into the atmosphere as wastes from industrial facilities such as sewage disposal plants, fish and animal processing plants, *etc.*, and the concentration and composition ratio of these substances, which may also be toxic even at relatively low concentration, usually fluctuate greatly with time. Thus, it is important to find selective adsorbents which can remove the undesirable components specifically. However, only a few reports are available on adsorption of binary malodorous gas mixtures.¹⁾ Lewis *et al.*²⁾ and Danner and Choi³⁾ have reported on the adsorption of mixed hydrocarbon gases on activated carbon and zeolite. They found that data on the adsorption isotherms of the pure components are very helpful to clarify the occurrence of competitive or preferential adsorption of a binary gas mixture.^{2,3)}

This report describes the adsorption behavior of hydrogen sulfide and dimethyl sulfide gas mixtures at different molar ratios in the pores of N-containing activated carbon (N-CAC)^{4,5)} having a greater adsorption ability for hydrogen sulfide.

Experimental

Materials—Hydrogen sulfide gas was of certified grade from Seitetsu Kagaku Co., and its purity was indicated to be 99.9%. Dimethyl sulfide gas with a purity of better than 98.0% was obtained from Seitetsu Kagaku Co. Activated carbon No. 1 (raw activated carbon (R-AC)) was obtained commercially from Wako Pure Chemical Inds. Ltd. (SDE 6318). Activated carbon No. 2 (N-CAC) was prepared by impregnating activated carbon No. 1 with 20% methylol melamine urea alcohol solution.⁶⁾ The particle size of these adsorbents was 32—48 mesh. The procedure for

measurement of pore volume was described previously.⁷⁾

Procedure for Pure Component Adsorption—Adsorption isotherms of hydrogen sulfide and dimethyl sulfide on activated carbon were determined in an all-glass vacuum system similar to that described previously.⁸⁾

Procedure for Binary Mixture Adsorption—Adsorption isotherms of hydrogen sulfide and dimethyl sulfide gas mixtures (1:3, 1:1, and 3:1) were measured at 30 °C and at equilibrium pressures up to approximately 100 Torr.

Results and Discussion

Adsorption of Pure Hydrogen Sulfide and Dimethyl Sulfide

Figure 1 shows the adsorption isotherms of pure hydrogen sulfide and dimethyl sulfide on R-AC and N-CAC at 30 °C. The amount of hydrogen sulfide adsorbed on N-CAC was increased by 25–35% as compared with R-AC in the range up to 50 Torr and by 10–20% as compared with R-AC in the range up to 175 Torr. On the other hand, the amount of dimethyl sulfide adsorbed on N-CAC was decreased by approximately 20% as compared with R-AC in the range up to 175 Torr. Dubinin⁹⁾ pointed out that the pore structure of an adsorbent can be divided into three classes *i.e.*, micropores (radius < 15–16 Å), transitional pores (15–16 < radius < 1000–2000 Å), and macropores (radius > 1000–2000 Å). Later, Dubinin¹⁰⁾ further classified the finest pores of adsorbent with equivalent radii up to 15–16 Å into

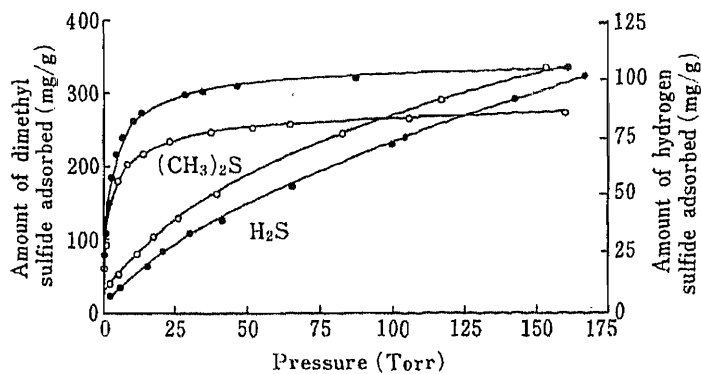


Fig. 1. Adsorption Isotherms of Hydrogen Sulfide and Dimethyl Sulfide on R-AC and N-CAC

●, R-AC; ○△, N-CAC.

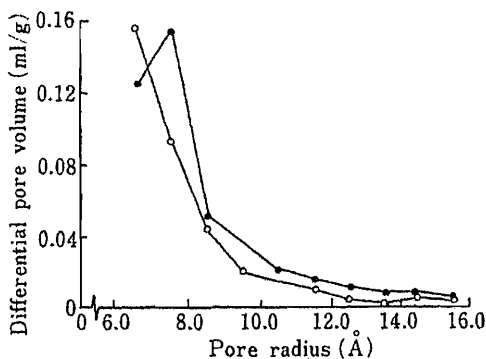


Fig. 2. Differential Pore Size Distribution Curves of R-AC and N-CAC

●, R-AC; ○, N-CAC.

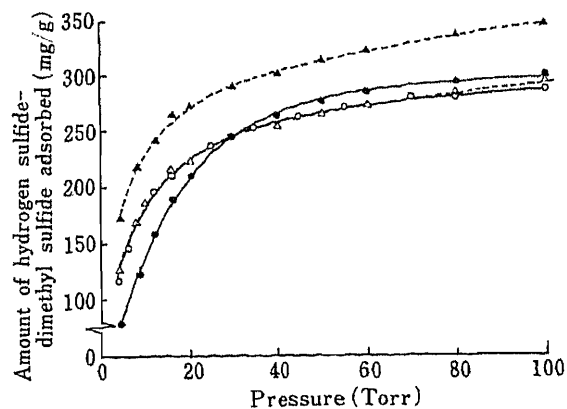


Fig. 3. Experimental and Theoretical Adsorption Isotherms of Hydrogen Sulfide-Dimethyl Sulfide Gas Mixture (1:1) on R-AC and N-CAC

— experimental data; --- theoretical data: ●▲, R-AC; ○△, N-CAC.

micropores (radius $< 6-7 \text{ \AA}$) and supermicropores ($6-7 < \text{radius} < 15-16 \text{ \AA}$). Figure 2 shows the differential pore size distribution curves of R-AC and N-CAC in the range up to 15 \AA . The differential pore volume of N-CAC having pore radii smaller than 6.5 \AA was 20% greater than that of R-AC. On the other hand, the differential pore volume of N-CAC with pore radii of $7.0-8.5 \text{ \AA}$ was much less than that of R-AC. The relationship between the amount adsorbed and differential pore size distribution can best be explained by assuming that hydrogen sulfide and dimethyl sulfide were mainly adsorbed into micropores (radius $< 6-7 \text{ \AA}$) and into supermicropores ($6-7 < \text{radius} < 15-16 \text{ \AA}$), respectively, in the range of low pressures.

Adsorption of Binary Mixtures of Hydrogen Sulfide and Dimethyl Sulfide

Figure 3 shows experimental and theoretical adsorption isotherms of hydrogen sulfide and dimethyl sulfide gas mixture (1 : 1) on R-AC and N-CAC at 30°C . Theoretical adsorption isotherms of the binary mixture were calculated from the experimental adsorption isotherms of the pure components by using the law of partial pressures. The experimental adsorption isotherm of the binary gas mixture (1 : 1) on N-CAC agreed closely with the theoretical adsorption isotherm in the range up to 100 Torr. However, there was poor agreement in the case of R-AC; the amounts adsorbed on R-AC were very much smaller than the theoretical ones. Nishida *et al.*¹⁾ reported that the amount of hydrogen sulfide and methanethiol gas mixture (1 : 1) adsorbed on activated carbon was much less than the theoretical amount. Nishida *et al.* pointed out that hydrogen sulfide and methanethiol were competitively adsorbed on activated carbon.¹⁾ Lewis *et al.*,²⁾ and Danner and Choi³⁾ reported that in the adsorption of a binary mixture of hydrocarbons on activated carbon and zeolite, each

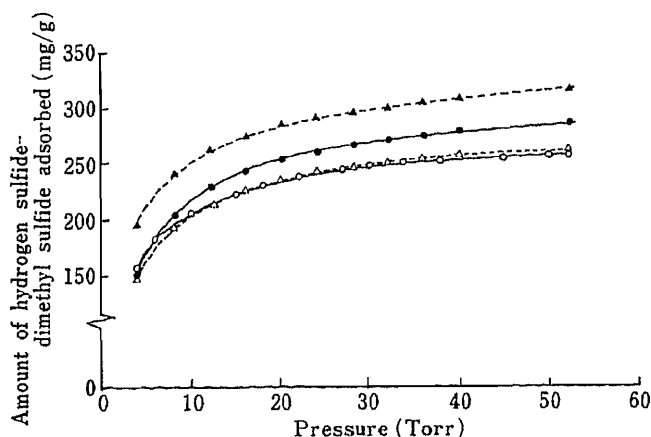


Fig. 4. Experimental and Theoretical Adsorption Isotherms of Hydrogen Sulfide-Dimethyl Sulfide Gas Mixture (1 : 3) on R-AC and N-CAC

— experimental data; --- theoretical data; ●▲, R-AC; ○△, N-CAC.

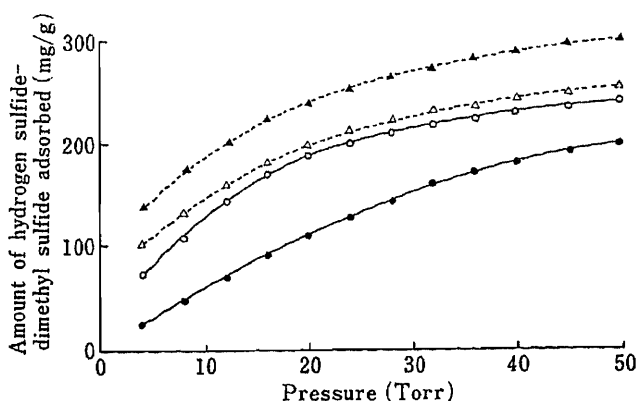


Fig. 5. Experimental and Theoretical Adsorption Isotherms of Hydrogen Sulfide-Dimethyl Sulfide Gas Mixture (3 : 1) on R-AC and N-CAC

— experimental data; --- theoretical data; ●▲, R-AC; ○△, N-CAC.

component interfered with the adsorption of the other. Our results on the adsorption behavior of a binary gas mixture (1 : 1) on N-CAC were different from theirs, but our results on R-AC agreed with theirs.¹⁻³⁾ Our results indicate that in the adsorption of a binary gas mixture of hydrogen sulfide and dimethyl sulfide on N-CAC, each component did not interfere with the adsorption of the other component, and that hydrogen sulfide and dimethyl sulfide selectively entered micropores of different size in N-CAC. Moreover, the characteristic sizes obtained by using the Dubinin-Radushkevich equation¹¹⁾ for hydrogen sulfide on R-AC and N-CAC were 4.32 and 3.66 Å,⁵⁾ respectively. The characteristic sizes for dimethyl sulfide on R-AC and N-CAC were 4.79 and 5.16 Å, respectively. The characteristic size of micropores is an average radius which corresponds to the characteristic point of the adsorption isotherm. R-AC showed little difference between the characteristic sizes for hydrogen sulfide and dimethyl sulfide. However, N-CAC showed a considerable difference. This difference in the case of N-CAC can best be explained by assuming that hydrogen sulfide and dimethyl sulfide enter mainly smaller micropores and larger micropores, respectively, and that hydrogen sulfide and dimethyl sulfide did not mutually interfere in adsorption on N-CAC in the low-pressure range. It was concluded that N-CAC is an adsorbent having a new character, because the adsorption behavior of a binary gas mixture on N-CAC was clearly different from those reported by Nishida *et al.*,¹⁾ and Lewis *et al.*,²⁾ and Danner and Choi.³⁾ Figure 4 shows experimental and theoretical adsorption isotherms of hydrogen sulfide and dimethyl sulfide gas mixture (1 : 3) on R-AC and N-CAC at 30 °C. The experimental adsorption isotherm on N-CAC approximately agreed with the theoretical adsorption isotherm in the range up to 60 Torr. However, the amounts adsorbed on R-AC were much smaller than the theoretical ones. These results indicated that each component in the binary gas mixture did not interfere with the adsorption of the other when dimethyl sulfide was predominant in the gas mixture. Figure 5 shows the experimental and theoretical adsorption isotherms of hydrogen sulfide and dimethyl sulfide gas mixture (3 : 1) on R-AC and N-CAC at 30 °C. The experimental amounts of gas mixture adsorbed on N-CAC were decreased by 10—25% as compared with the theoretical ones, and those on R-AC were decreased by 40—80% as compared with the theoretical ones in the range up to 50 Torr. This result indicated that when hydrogen sulfide was predominant in the binary gas mixture, each component in the binary gas mixture did not interfere markedly with the adsorption of the other on N-CAC and selectively entered micropores of different size. These results (Figs. 3—5) indicate that N-CAC is a characteristic new adsorbent whose adsorption properties do not depend markedly on the

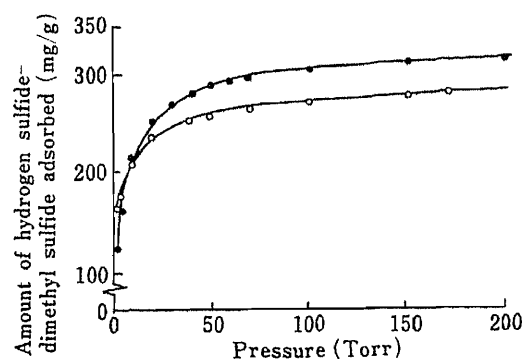


Fig. 6. Adsorption Isotherms of Hydrogen Sulfide-Dimethyl Sulfide Gas Mixture (1 : 3) on R-AC and N-CAC

●, R-AC; ○, N-CAC.

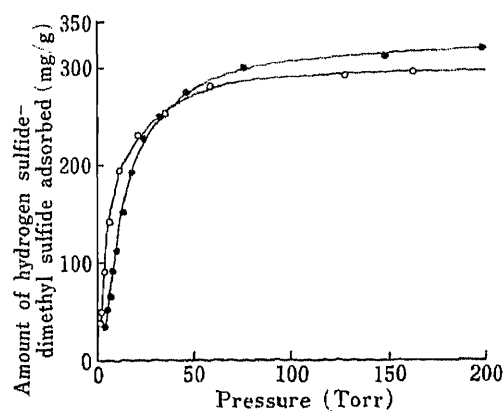


Fig. 7. Adsorption Isotherms of Hydrogen Sulfide-Dimethyl Sulfide Gas Mixture (1 : 1) on R-AC and N-CAC

●, R-AC; ○, N-CAC.

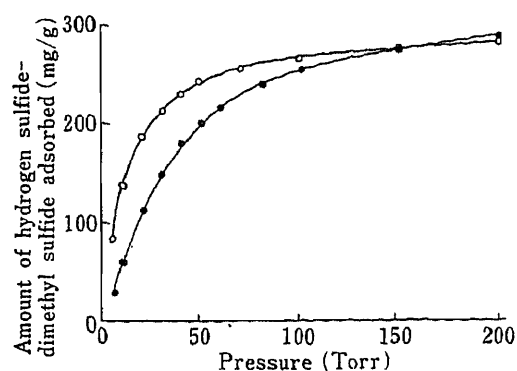


Fig. 8. Adsorption Isotherms of Hydrogen Sulfide-Dimethyl Sulfide Gas Mixture (3:1) on R-AC and N-CAC

●, R-AC; ○, N-CAC.

composition ratio of hydrogen sulfide and dimethyl sulfide gas mixtures.

Figures 6, 7, and 8 show adsorption isotherms of hydrogen sulfide and dimethyl sulfide gas mixtures (1:3, 1:1, and 3:1, respectively) on R-AC and N-CAC at 30 °C. The adsorption capacity of N-CAC for the 1:3 mixture was larger than that of R-AC in the range up to 5 Torr. The adsorption capacity of N-CAC for the 1:1 mixture was also larger than that of R-AC in the range up to 35 Torr. The same was also true for the 3:1 mixture up to 150 Torr. The results indicate that each component of the gas mixture was adsorbed more competitively on R-AC with increase in the molar ratio of hydrogen sulfide in gas mixture. On N-CAC, however, each adsorbate did not interfere with the adsorption of the other component, and hydrogen sulfide and dimethyl sulfide entered micropores of different sizes. It was concluded that N-CAC is a characteristic adsorbent having greater adsorption capacity for hydrogen sulfide from gas mixtures composed of hydrogen sulfide and dimethyl sulfide at different molar ratios.

Acknowledgement The authors are grateful to Dr. K. Boki and Mr. T. Nakamura of this institute for helpful discussions.

References

- 1) K. Nishida, M. Yamakawa, and M. Takahashi, *Akushu No Kenkyu*, **12**, 10 (1984).
- 2) W. K. Lewis, E. R. Gilliland, B. Chertow, and W. P. Cadogan, *Ind. Eng. Chem.*, **42**, 1319 (1950).
- 3) R. P. Danner and E. C. Choi, *Ind. Eng. Chem. Fundam.*, **17**, 248 (1978).
- 4) K. Boki, S. Tanada, T. Kita, and K. Sakaguchi, *Experientia*, **37**, 815 (1981).
- 5) K. Boki, S. Tanada, and T. Miyoshi, *Jpn. J. Hyg.*, **38**, 877 (1983).
- 6) S. Tanada, K. Boki, K. Sakaguchi, M. Kitakouji, K. Matsumoto, and Y. Yamada, *Chem. Pharm. Bull.*, **29**, 1736 (1981).
- 7) K. Boki, *Jpn. J. Hyg.*, **32**, 482 (1972).
- 8) S. Tanada and K. Boki, *Chem. Pharm. Bull.*, **23**, 2703 (1974).
- 9) M. M. Dubinin, "Chemistry and Physics of Carbon," Vol. 2, ed. by P. L. Walker, Jr., Marcel Dekker, New York, 1966, pp. 51-120.
- 10) M. M. Dubinin, *J. Colloid Interface Sci.*, **46**, 351 (1978).
- 11) M. M. Dubinin and L. V. Radushkevich, *Dokl. Akad. Nauk SSSR*, **55**, 331 (1947).

[Chem. Pharm. Bull.]
35(3)1243—1248(1987)

Effect of Pluronic Gels on the Rectal Absorption of Indomethacin in Rabbits¹⁾

SHOZO MIYAZAKI,* TSUGUYA NAKAMURA, CHIZUKO YOKOUCHI,
and MASAHIKO TAKADA

*Faculty of Pharmaceutical Sciences, Higashi-Nippon-Gakuen University,
Ishikari-Tohgetsu, Hokkaido 061-02, Japan*

(Received July 30, 1986)

Indomethacin gel preparations made by dissolving the drug in Pluronic aqueous gels were administered rectally to rabbits and the drug plasma levels were determined. When indomethacin gel preparations with 20% (w/w) Pluronic F-127 were given to rabbits, the plasma concentration reached the maximum level 0.5 h after administration. On the other hand, the 25% (w/w) Pluronic F-127 gel preparation did not show a sharp peak of plasma concentration and produced a sustained-release effect. The 30% (w/w) gel preparation also gave a sustained-release effect, but it was not a desirable preparation because its $[AUC]_0^{10}$ was only half that of a commercial suppository. Pluronic F-108 and Pluronic F-98 did not give a sustained-release effect at the concentration of 25% (w/w).

Damage to the mucosal membrane by Pluronic F-127 was rarely found in the rectum. In addition, the individual differences in drug plasma levels following rectal administration of the 25% (w/w) Pluronic F-127 gel preparation were small compared with those of other preparations.

These results suggest that the 25% (w/w) Pluronic F-127 gel is most suitable for use as a vehicle for rectal administration of indomethacin with prolonged action and with reduced side effects.

Keywords—Pluronic F-127; Pluronic F-108; Pluronic F-98; indomethacin; gel preparation; sustained release; rectal administration; rectal absorption; rabbit

The possible use of Pluronic F-127 gel as a vehicle for drug delivery has been examined.²⁾ Pluronic F-127 consists of approximately 70% ethylene oxide and 30% propylene oxide with an average molecular weight of 11500. The unique characteristic of this copolymer is reverse thermal gelation; concentrated solutions (20—40% w/w) of the copolymer are fluid at refrigerator temperature (4—5 °C), but are soft gels at body temperature.³⁾ This suggests that when poured onto the skin or injected into a body cavity, the preparation will form a solid artificial barrier and sustained-release depot. In recent years, Pluronic F-127 has been evaluated as a vehicle for novel dosage forms, either for dermatological use^{3,4)} or topical ophthalmic application.⁵⁾ Since Pluronic F-127 has low toxicity and is inexpensive, it might be suitable for use in the preparation of other dosage forms of commercial drugs.

Indomethacin has been widely used as a non-steroidal drug having anti-inflammatory and anti-pyretic effects. However, when given by the usual oral administration route, indomethacin may produce gastrointestinal side effects. In order to minimize such side effects, rectal administration of the drug has been attempted.⁶⁾ Furthermore, sustained-release suppositories of indomethacin were prepared to obtain desirable plasma concentrations, since a high plasma level of the drug has an adverse effect on the nervous system.⁷⁾

In the previous paper,⁸⁾ it was suggested that indomethacin preparations based on Pluronic F-127 aqueous gel may be practically useful as a rectal preparation with prolonged action and reduced side effects. The purpose of the present study was to investigate in more detail the rectal absorption of indomethacin from Pluronic gels in rabbits.

Experimental

Materials—Indomethacin was obtained from Sigma Chemical Co., St. Louis. Pluronics were a gift from Asahi Denka Kogyo Co., Tokyo and BASF Wyandotte Co., Parsippany, and were used as received (Pluronic F-127, Pluronic F-108, and Pluronic F-98).

Preparation of Pluronic Gels—All Pluronic formulations were prepared on a weight percentage basis by the cold process. An appropriate amount of Pluronic was slowly added to cold phosphate buffer at pH 7.2 in a vial containing a magnetic stirring bar with gentle mixing. The container was left overnight in a refrigerator to ensure complete dissolution. With time, a clear, viscous solution formed. Indomethacin was dissolved in each gel at a concentration of 0.8% (w/v).

Measurement of Drug Release from Pluronic Gels—Indomethacin release rates were measured by using a plastic dialysis cell containing a membrane barrier (Visking Co., type 36/32).²⁾ The drug concentration of the sample was determined with a spectrophotometer at 266 nm. All experiments were carried out in triplicate and average values were plotted.

Rectal Absorption—White male rabbits weighing 3.3–3.8 kg were fasted for 36 h prior to the experiments but allowed free access to water. Pluronic gel preparation was administered into the rectum 3–5 cm above the anus through a stomach sonde needle for rats (KN-348, Natsume Seisakusho, Tokyo) fitted on a glass syringe: the gel was chilled prior to filling the syringe to facilitate this procedure. Indomethacin gel preparation was given as 3 ml of Pluronic gel containing 25 mg of the drug. At predetermined intervals, 1 ml of blood was collected from the ear vein and centrifuged at 3000 rpm for 10 min. The plasma concentration of indomethacin was determined chromatographically by the method of Skellern and Salole⁹⁾ with slight modifications.⁸⁾

Morphological Studies on Rectal Tissue in Rats—Male, Wistar rats weighing 200 g were fasted for 18 h prior to experiments but allowed free access to water. The Pluronic F-127 gel without drug (0.4 ml) was administered to the rat rectum. After 1 and 6 h, the rectum was isolated, rinsed with a saline solution, fixed in 10% formalin and cut into slices. The slices were stained with hematoxylin-eosin, and observed under a light microscope (model PM-10-A, Olympus, Tokyo).

Results

In Vitro Release Experiment

The effects of Pluronic F-127 concentration on the drug release kinetics are illustrated in

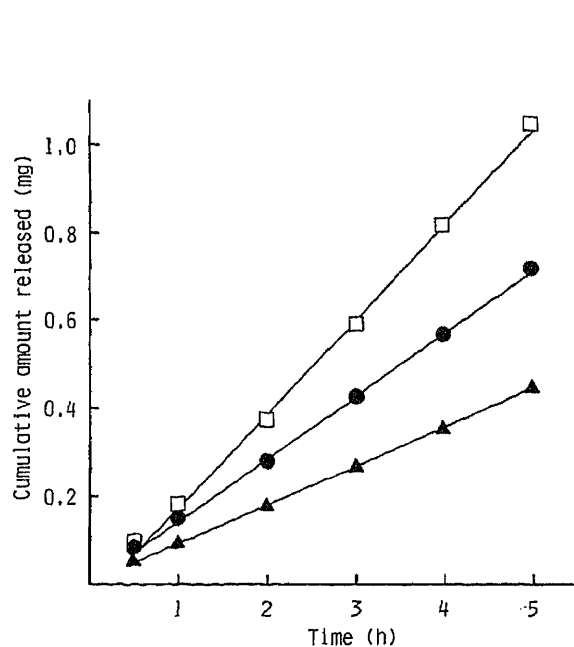


Fig. 1. Effect of Pluronic F-127 Concentration on Indomethacin Release at 37°C

□, 20%; ●, 25%; ▲, 30% (w/w) Pluronic F-127 gels.

The concentration of indomethacin was 0.8% (w/v). Each value represents the mean of 3 experiments.

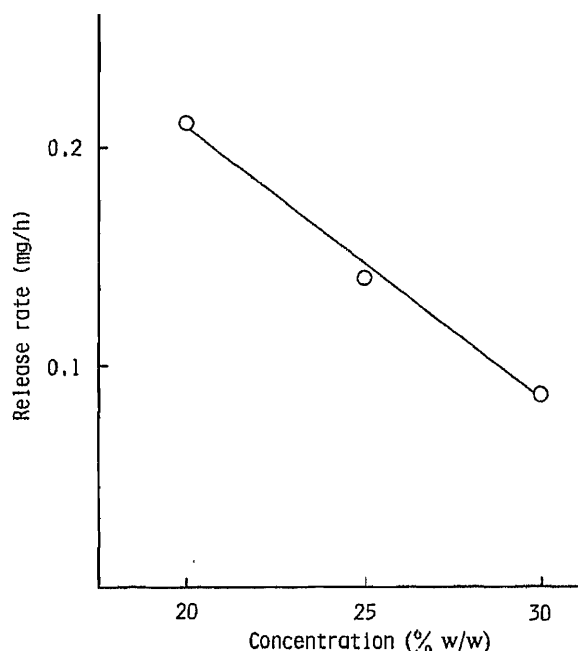


Fig. 2. The Relationship between the Release Rate of Indomethacin and the Concentration of Pluronic F-127 at 37°C

Fig. 1, which shows the cumulative amount of indomethacin released *versus* time. The apparent release rate (k) was determined by measuring the slopes (mg/h) of the lines by the least-squares method. A plot of the k values as a function of vehicle concentration was linear (Fig. 2). The release rate decreased as the concentration of Pluronic F-127 in the vehicle increased. The reason for the decreased release rate may be an increase in the viscosity of the vehicle. It was reported that the higher the Pluronic F-127 concentration, the greater the yield strength³⁾ or rigidity of the gels.¹⁰⁾ Since the gels are micellar, it may also be assumed that micellar solubilization contributed to the decrease in drug release.⁴⁾ Further studies will be required to obtain a complete understanding of the mechanism.

In the previous paper,⁸⁾ concentrated solutions of Pluronic F-98 and Pluronic F-108 were also transformed from low viscosity transparent solutions to soft gels on heating from 5 to 37°C. Thus, indomethacin release from Pluronic F-127 gels was compared to that from the

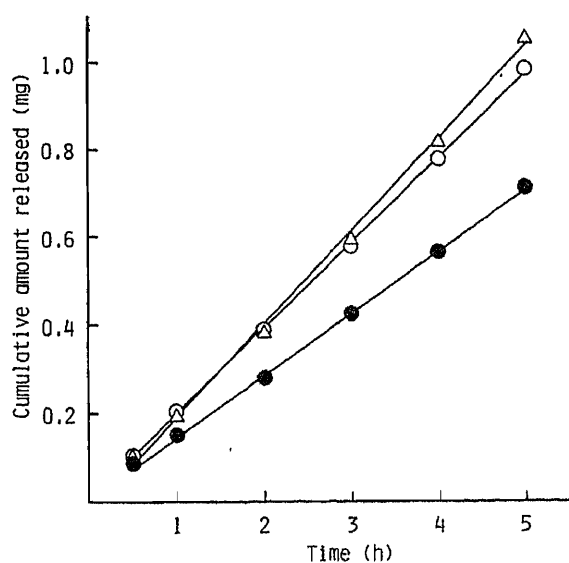


Fig. 3. Release of Indomethacin from 25% (w/w) Pluronic Gels at 37°C

●, Pluronic F-127 gels; ○, Pluronic F-108 gels; △, Pluronic F-98 gels.

The concentration of indomethacin was 0.8% (w/v). Each value represents the mean of 3 experiments.

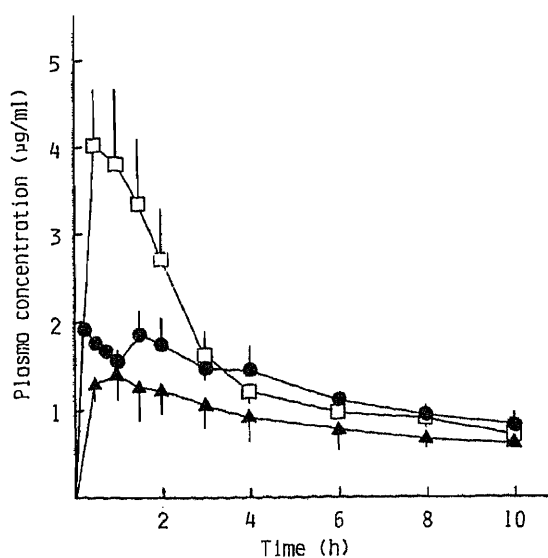


Fig. 4. Effect of Pluronic F-127 Concentration on Indomethacin Absorption after Rectal Administration to Rabbits

□, 20%; ●, 25%; ▲, 30% (w/w) Pluronic F-127 gels.

Each preparation contained 25mg of the drug. Each value represents the mean \pm S.E. of 4 rabbits.

TABLE I. Comparison of T_{max} , C_{max} , and $[AUC]_0^{10}$ Values between Pluronic Gel Preparations and Commercial Suppository

Form	Gel concn. (% w/w)	T_{max} (h)	C_{max} ($\mu\text{g/ml}$) ^{b)}	$[AUC]_0^{10}$ ($\mu\text{g}\cdot\text{h/ml}$) ^{b)}
Pluronic F-127	20	0.5—1.5	4.28 ± 0.69^c	15.57 ± 1.98
Pluronic F-127	25	0.5—2.0	1.93 ± 0.16^d	12.71 ± 1.28
Pluronic F-127	30	1.0—2.0	1.57 ± 0.32^d	8.82 ± 2.29^e
Pluronic F-98	25	0.5—2.0	2.11 ± 0.10^d	8.63 ± 0.75^f
Pluronic F-108	25	0.5	2.68 ± 0.21^d	12.42 ± 1.04
Commercial suppository ^{g)}	—	0.25—0.75	9.29 ± 0.63	15.57 ± 1.27

a) The area under the curve (AUC) was calculated by means of the trapezoidal method. b) Each value represents the mean \pm S.E. of 4 rabbits. c) Significantly different from the commercial suppository; $p < 0.005$, d) $p < 0.001$, e) $p < 0.1$, f) $p < 0.01$, g) reference 8.

other Pluronics at the concentration of 25% (w/w) (Fig. 3); the rates of release were F-98 = F-108 > F-127. This order seems to be the reverse of the order of viscosity of the gels at 37°C.¹⁰⁾

Plasma Concentrations of Indomethacin after Rectal Administration

The plasma levels of indomethacin after rectal administration of Pluronic F-127 gel preparation at various concentrations are shown in Fig. 4. Table I summarizes the parameters of bioavailability, with the previous results⁹⁾ using commercial indomethacin suppositories.

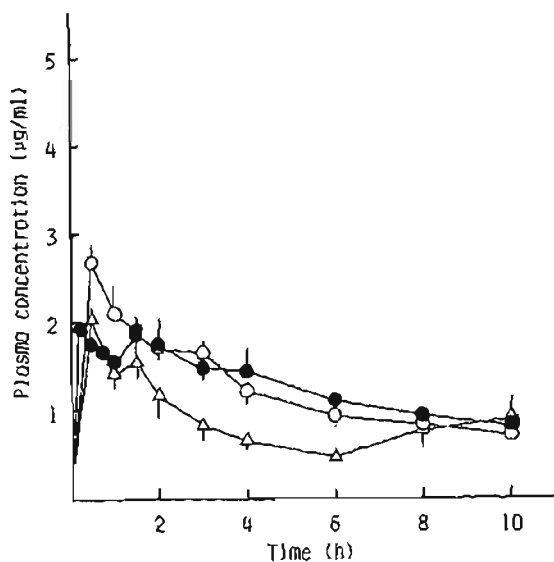
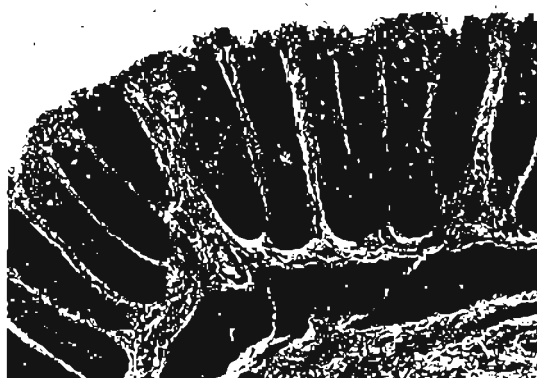


Fig. 5. Rectal Absorption of Indomethacin from 25% (w/w) Pluronic Gels in Rabbits

●, Pluronic F-127; ○, Pluronic F-108; △, Pluronic F-98.

Each preparation contained 25mg of the drug. Each value represents the mean \pm S.E. of 4 rabbits.



(A)



(B)



(C)

Fig. 6. Histological Observation of Rectal Mucosa at 0 h (A), 1 h (B), and 6 h (C) after Rectal Administration of 25% (w/w) Pluronic F-127 Gel without Indomethacin in Rats ($\times 240$)

Figure 4 shows that absorption of indomethacin from the 20% (w/w) gel preparation was rapid, and the mean maximum plasma concentration (C_{max}) was 4.28 $\mu\text{g/ml}$ at 0.5 h, which was lower than that (9.29 $\mu\text{g/ml}$) of the commercial suppository. Then indomethacin was eliminated rapidly from the plasma. On the other hand, the 25% (w/w) Pluronic F-127 gel preparation did not give a sharp peak of plasma concentration, but produced a sustained plateau plasma level of indomethacin from 0.5 to 4 h without a lag time, and the plasma level of indomethacin maintained for over 10 h. In the case of 30% (w/w) Pluronic gel, a low and plateau plasma level of indomethacin was maintained for over 10 h. As shown in Table I, however, the 30% (w/w) gel preparation is unfavorable because its $[AUC]_0^{10}$ value was only half that of the commercial suppositories. The mean $[AUC]_0^{10}$ value after administration of 25% (w/w) gel preparation was 80.6% of that of the commercial suppository, and there was no significant difference in extent of bioavailability between the two.

Indomethacin gel formulations prepared from Pluronic F-98 and Pluronic F-108 (25% w/w) were administered rectally to rabbits and the drug plasma levels were compared with those after rectal administration of the 25% (w/w) Pluronic F-127 (Fig. 5). The gel preparations of Pluronic F-98 and Pluronic F-108 showed peak plasma concentrations of 2.11 and 2.68 $\mu\text{g/ml}$, respectively, after 0.5 h, and later the concentration decreased rapidly. These Pluronic gels did not give a sustained-release effect.

Morphological Studies on Rectal Tissue in Rats

In order to examine the rectal mucosal damage caused by the Pluronic F-127 gels, Pluronic F-127 gels without indomethacin was administered into the rectum of rats. As illustrated in the photographs in Fig. 6, no mucosal damage caused by the Pluronic F-127 gel was observed as compared with the control. This result indicates that Pluronic is suitable for use as a vehicle for rectal administration.

Discussion

As a part of an investigation into the potential use of Pluronic F-127 gels as sustained-release depot preparations, we studied the *in vitro* and *in vivo* release characteristics of indomethacin from various gel formulations. In the *in vitro* release experiments, the effect of the gel concentration was evident; the higher the concentration of the gel, the slower indomethacin release was (Fig. 1). As is evident from Fig. 4, the results of *in vivo* absorption experiments at various concentrations coincide with the *in vitro* ones. That is, the 20% (w/w) Pluronic F-127 gel produced a sharp peak of plasma concentration and did not give a sustained-release effect. At higher concentrations (25 and 30% w/w), where drug release was slower, indomethacin absorption was also slower and the plasma level was maintained for longer. However, the 30% (w/w) gel preparation is not desirable, because its $[AUC]_0^{10}$ value was only half (56%) that of the commercial suppository, indicating that the extent of bioavailability was small. The 25% (w/w) Pluronic F-108 and Pluronic F-98 did not give a sustained-release effect (Fig. 5). On the basis of the release experiments (Fig. 3), some differences in the blood levels after rectal administration of the F-98 or F-108 gels and the F-127 gel would be expected. However, the results obtained in this study indicate that there are no distinct differences in the blood levels. The low plasma levels of the F-98 or F-108 gels appear to be attributable to their higher osmotic pressure and/or greater hydrophilicity than the F-127 gels, but further work is required to clarify this point.

The 25% (w/w) Pluronic F-127 gel preparation gave a plateau level of drug in the plasma after rectal administration without producing a sharp peak of plasma concentration. Therefore, it was considered that this Pluronic gel preparation is a suitable dosage form for reducing the incidence of side effects and the frequency of administration.

In particular, Pluronic F-127 is desirable because it has low toxicity. The toxicological properties of this series of block polymers have been studied, and the results indicate that Pluronic F-127 is one of the least toxic of commercially available block polymers.³⁾ Although one must take into consideration the membrane damage due to some surfactants, which is undesirable, damage to the mucosal membrane by Pluronic F-127 was rarely found in rat rectum (Fig. 6). Malik *et al.*¹¹⁾ reported that Pluronic F-68 has no effect on the membrane. In addition, the individual differences on rectal administration of the 25% (w/w) Pluronic F-127 gel preparation seemed to be small compared with those of other preparations.

These results suggest that indomethacin preparations based on Pluronic F-127 aqueous gel given by rectal administration may have clinical potential. There are several dosage forms available for the rectal delivery of drugs: suppositories, rectal gelatin capsules, and enemas.⁶⁾ Pluronic F-127 gel is potentially useful for sustained-drug release when given in the form of enemas.

Pluronic F-127 gel possess several properties which appear to be particularly suitable for the formulation of enema dosage forms. There is no practical difficulty in administration of the gel preparation, since the gelation is reversible, and this reversible sol-gel property allows a cool solution to flow into the rectum. Since it is water-soluble, Pluronic gel can be easily removed by washing in water.

The preparation of gels based on Pluronic F-127 is a very simple matter. One may use either a "cold" or a "hot" technique.³⁾ Once the Pluronic is completely dissolved, ingredients may be added.

Another advantage of using Pluronic F-127 is its general applicability to most drugs; water-insoluble material become solubilized in the surfactant micelles (the Pluronic gels are known to contain a large population of micelles^{4,12)}).

Acknowledgements We are grateful to Asahi Denka Kogyo Co. and BASF Wyandotte Co. for supplying Pluronics. We are also indebted to Mr. Norio Hashiguchi of Higashi-Nippon-Gakuen University for his assistance.

References and Notes

- 1) Pharmaceutical Application of Biomedical Polymers, Part XXII. Part XXI: S. Miyazaki, N. Hashiguchi, W.-M. Hou, C. Yokouchi, and M. Takada, *Chem. Pharm. Bull.*, **34**, 3384 (1986).
- 2) S. Miyazaki, S. Takeuchi, C. Yokouchi, and M. Takada, *Chem. Pharm. Bull.*, **32**, 4205 (1984).
- 3) I. R. Schmolka, *J. Biomed. Mater. Res.*, **6**, 571 (1972).
- 4) P. C. Chew-Chow and S. G. Frank, *Int. J. Pharm.*, **8**, 89 (1981).
- 5) S. C. Miller and M. D. Donovan, *Int. J. Pharm.*, **12**, 147 (1982).
- 6) A. G. Boer, F. Moolenaar, L. G. J. Heede, and D. D. Breimer, *Clin. Pharmacokinet.*, **7**, 285 (1982).
- 7) T. Umeda, A. Matsuzawa, T. Yokoyama, K. Kuroda, and T. Kuroda, *Chem. Pharm. Bull.*, **31**, 2793 (1983).
- 8) S. Miyazaki, C. Yokouchi, T. Nakamura, N. Hashiguchi, W.-M. Hou, and M. Takada, *Chem. Pharm. Bull.*, **34**, 1801 (1986).
- 9) G. G. Skellern and E. G. Salole, *J. Chromatogr.*, **114**, 483 (1975).
- 10) S. C. Miller and B. R. Drabik, *Int. J. Pharm.*, **18**, 269 (1984).
- 11) S. N. Malik, D. H. Canaham, and M. W. Gouda, *J. Pharm. Sci.*, **64**, 987 (1975).
- 12) D. Attwood, J. H. Collett, and C. J. Tait, *Int. J. Pharm.*, **26**, 25 (1985).

[Chem. Pharm. Bull.]
35(3)1249—1254(1987)

Syntheses and Properties of Dipeptides Containing γ -Aminobutyric Acid or Its Analogues at the C-Terminal¹⁾

KAZUHARU IENAGA,^{*,a} KUNIIHIKO HIGASHIURA^a and HIROSHI KIMURA^b

Institute of Bio-Active Science, Nippon Zoki Pharmaceutical Co., Ltd.^a

Kinashi, Yashiro-cho, Kato-gun, Hyogo 673-14, Japan and

Department of Anatomy, Shiga University of Medical

Science,^b Seta, Otsu 520-21, Japan

(Received July 14, 1986)

Twelve dipeptides (1—12) containing γ -aminobutyric acid (GABA: H- γ Abu-OH: 37) at the C-terminal were synthesized. Another six dipeptides (13—18) containing GABA analogues such as γ -amino- β -hydroxybutyric acid [GABOB: H- γ Abu(2OH)-OH: 38], β -alanine (39) and ϵ -aminocaproic acid (EACA: ϵ Acp: 40) at the C-terminal were also synthesized. Their properties are presented, together with preliminary findings on the immuno-crossreactivity with antiserum against GABA.

Keywords—dipeptide; γ -aminobutyric acid (GABA); GABA analogue; immunohistochemistry; immuno-crossreactivity; absorption test

Many neuroscientific studies have suggested that gamma-aminobutyric acid (GABA) is a chemical neurotransmitter in the nervous system of vertebrates.^{2,3)} Neuroanatomically, GABAergic neurons have been visualized by immunohistochemical methods, conventionally by using antisera against glutamic acid decarboxylase (an enzyme synthesizing GABA)⁴⁾ and recently by using antisera against GABA itself.^{5,6)} The latter method seems much better than the former, because it can directly detect the transmitter molecule. Since, however, the reliability of the method depends upon the specificity of anti-GABA serum, the immunological crossreactivity of the antiserum should be as low as possible with various other compounds that may also be present in the nervous system.

In our immunohistochemical study using an anti-GABA serum, which was proven to have very low immuno-crossreactivities with many other amino acids,⁷⁾ we noticed that some dipeptides containing GABA at the C-terminal showed quite high immunoreactivities with the anti-GABA serum. Rat brain sections, for example, that were incubated with the antiserum used as the first antibody in a usual immunohistochemical procedure, revealed numerous neuronal structures stained positively for GABA-like immunoreactivity.⁷⁾ When the antiserum had been preincubated with a crossreactive compound, the staining intensity of GABA-like immunoreactivity was decreased or even completely abolished. All the C-terminal GABA-containing dipeptides listed in Chart 1 were crossreactive on this criterion (Fig. 1). Interestingly enough, when the antiserum was absorbed with some dipeptides containing GABA at the N-terminal, such as homocarnosine, no such effect was seen.

A similar phenomenon has been reported with antisera against another amino acid, taurine. Namely, Kimura *et al.*⁸⁾ observed that some naturally occurring dipeptides, that contained taurine at the C-terminal, had very high immuno-crossreactivities with antisera against taurine. Although no precise knowledge is yet available concerning the immunorecognition sites of the antigens of interest, it is very likely that many unknown dipeptides containing antigenic amino acids at the C-terminal may also have strong crossreactivity with anti-amino acid sera. However, only a few dipeptides containing GABA at the C-terminal

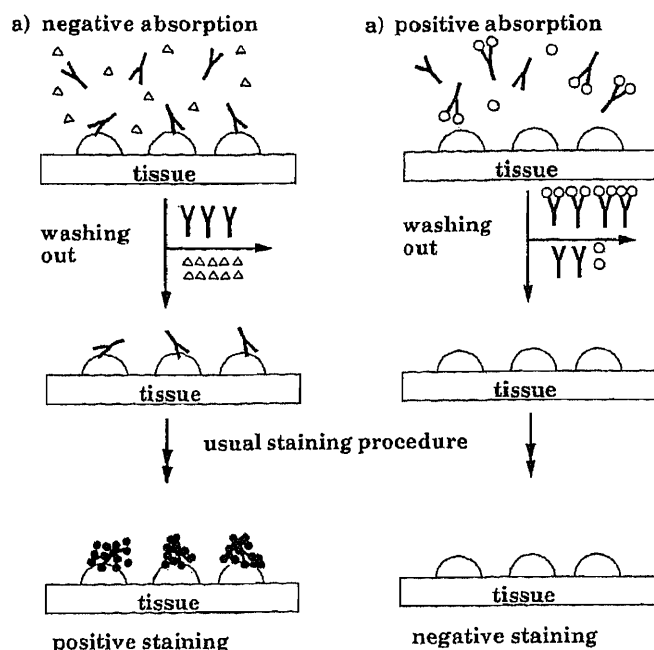


Fig. 1. Illustration of Absorption Test for Immunohistochemistry

Q, antigen; Y, antibody; ••, oxidized diaminobenzidine; Δ, immuno-inactive compound; O, immuno-active compound.

have been synthesized.⁹⁾ Further, dipeptides containing such GABA analogues as β -Ala, GABOB and EACA have not been reported so far.

In the present study, we synthesized eighteen dipeptides (1—18), aiming to analyze systematically their immuno-crossreactivity with GABA antiserum. We present here the details of the syntheses and some immunochemical and physicochemical properties of these unique dipeptides.

Eighteen dipeptides (1—18) were synthesized by the routes shown in Chart 2. Two methods using active esters were chosen for the first condensation step, and protecting groups were easily removed in a usual manner. The first method using *N*-hydroxy-5-norbornene-2,3-dicarboximide (HONB) with *N,N'*-dicyclohexylcarbodiimide (DCC) was carried out according to Fujino *et al.*¹⁰⁾ In the second method, *N,N'*-disuccinimidyl carbonate (DSC) was used to form active esters, Z-X-ONSu,¹¹⁾ and unprotected GABA or an analogue was used as the C-terminal component. Dipeptide benzyl esters containing a proline residue (Z-Pro-Y-OBzl) were difficult to purify. In contrast, Z-Pro-Y-OH was easily obtained as a pure crystalline

H-X- γ Abu-OH

X: Gly (1) Ala (2) Val (3) Leu (4) Ile (5) Pro (6) Hyp (7)

Ser (8) Thr (9) Phe (10) Tyr (11) Asp (12)

H-X- γ Abu(2OH)-OH

H-X- β Ala-OH

H-X- ϵ Acp-OH

X: Phe (13) Pro (14)

X: Phe (15) Pro (16)

X: Phe (17) Pro (18)

Z-X- γ Abu-OBzl

X: Gly (19) Ala (20) Val (21) Leu (22) Ile (23) Hyp (24)

Ser (25) Thr (26) Phe (27) Tyr(OBzl) (28) Asp(OBzl) (29)

Z-X- γ Abu-OH

Z-X- γ Abu(2OH)-OBzl

Z-X- γ Abu(2OH)-OH

X: Pro (30)

X: Phe (31)

X: Pro (32)

Z-Phe- β Ala-OH

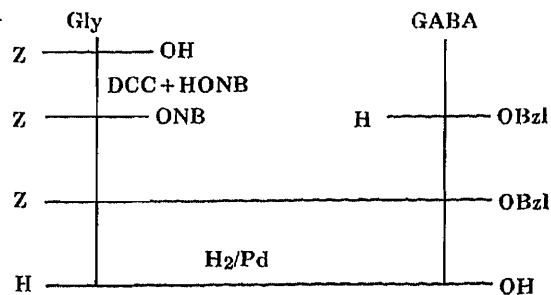
Z-Pro- ϵ Acp-OH

X: Phe (33) Pro (34) X: Phe (35) Pro (36)

H- γ Abu-OH (37) H- γ Abu(2OH)-OH (38) H- β Ala-OH (39) H- ϵ Acp-OH (40)

Chart 1

method A



method B

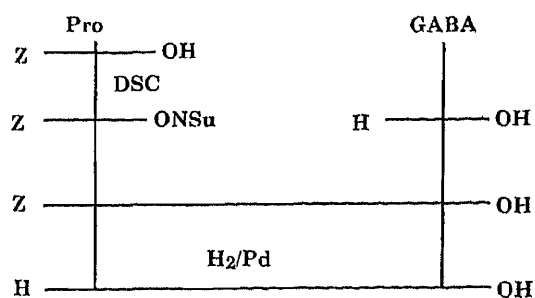


Chart 2

TABLE I. Specific Optical Rotation Values at the Sodium D Line of Neutral Dipeptides and Their Amino Acid Components^{a)} at 20–25 °C

Compd.	Dipeptides (H-X-Y-OH) [α] _D (c=1, H ₂ O)	Amino acid components (H-X-OH)	
		[α] _D (c=1–5, H ₂ O)	[α] _D (c=1–5, aq. HCl)
2	+15.1 ^c	+1.8 ^c	+14.6 ^o
3	+40.7 ⁿ	+5.6 ^c	+28.3 ⁿ
4	+31.6 ^c	–11.0 ^c	+28.3 ⁿ
5	+28.6 ^c	+12.4 ^c	+39.5 ^u
6	–47.3 ^o	–86.2 ^o	–60.4 ^u
14	–31.9 ⁿ	–86.2 ^o	–60.4 ^u
16	–50.8 ⁿ	–86.2 ^o	–60.4 ^o
18	–47.6 ⁿ	–86.2 ^o	–60.4 ⁿ
7	–35.8 ⁿ	–76.0 ^o	–50.5 ^o
8	+12.5 ^o	–7.5 ^o	+15.1 ^o
9	+19.2 ^u	–28.5 ^o	–15.0 ^o
10	+54.1 ^c	–34.5 ^o	–4.5 ^o
13	+60.3 ^o	–34.5 ^o	–4.5 ^o
15	+63.4 ⁿ	–34.5 ^o	–4.5 ^o
17	+42.9 ^c	–34.5 ^o	–4.5 ^o
11	+44.6 ^o	^{b)}	–10.5 ^o

^{a)} "Data for Biochemical Research," ed. by R. M. C. Dawson, D. Elliott, W. H. Elliott and K. M. Jones, Clarendon Press, Oxford, 1974. ^{b)} Insoluble.

solid, so that dipeptides containing proline were synthesized by the latter method.

Specific optical rotation values of sixteen neutral dipeptides (2–18) and their amino acid components are shown in Table I. The [α]_D values of the dipeptides, except Ser, Phe and Tyr derivatives (8, 10, 11, 13, 15, 17), were similar to those of the amino acids located at the N-

TABLE II. Proton Magnetic Resonance Spectra of Dipeptides (H-X-Y-OH) and C-Terminal Amino Acids (H-Y-OH)

	Signals of N-terminal moiety (-X-)	Signals of C-terminal moiety (-Y-)
1	3.77 (2H, s)	1.77 (tt, $J=7.5$, 7, β H), 2.25 (t, $J=7.5$, α H), 3.25 (t, $J=7$, γ H)
2	1.50 (3H, d, $J=7$), 4.02 (1H, q, $J=7$)	1.78 (tt, $J=7$, 7, β H), 2.29 (t, $J=7$, α H), 3.24, 3.27 (dt, $J=7$, 14, γ H)
3	1.01 (3H, d, $J=7$), 1.02 (3H, d, $J=7$), 2.12—2.24 (1H, m), 3.72 (1H, d, $J=7$)	1.80 (tt, $J=7$, 7, β H), 2.31 (t, $J=7$, α H), 3.24, 3.30 (dt, $J=7$, 14, γ H)
4	0.94 (3H, d, $J=6$), 0.96 (3H, d, $J=6$), 1.58—1.75 (3H, m), 3.94 (1H, t, $J=7$)	1.81 (tt, $J=7$, 7, β H), 2.36 (t, $J=7$, α H), 3.22, 3.32 (dt, $J=7$, 14, γ H)
5	0.92 (3H, t, $J=7$), 0.98 (3H, d, $J=7$), 1.17—1.29 (1H, m), 1.45—1.56 (1H, m), 1.89—2.00 (1H, m), 3.79 (1H, t, $J=6$)	1.80 (tt, $J=7$, 7, β H), 2.34 (t, $J=7$, α H), 3.23, 3.31 (dt, $J=7$, 14, γ H)
6	1.97—2.11 (3H, m), 2.36—2.49 (1H, m), 3.34—3.77 (2H, m), 4.32 (1H, dd, $J=7$, 8)	1.79 (tt, $J=7$, 7, β H), 2.29 (t, $J=7$, α H), 3.24, 3.29 (dt, $J=7$, 14, γ H)
7	2.15 (1H, ddd, $J=3.5$, 10, 14), 2.47 (1H, dddd, $J=2$, 2, 8, 14), 3.41 (1H, ddd, $J=2$, 2, 12.5), 4.53 (1H, dd, $J=8$, 10), 4.68—4.72 (1H, m)	1.80 (tt, $J=7$, 7, β H), 2.33 (t, $J=7$, α H), 3.25, 3.31 (dt, $J=7$, 14, γ H)
8	3.91 (1H, dd, $J=6$, 12.5), 3.97 (1H, dd, $J=4$, 12.5), 4.07 (1H, dd, $J=4$, 6)	1.79 (tt, $J=7.5$, 7.5, β H), 2.29 (t, $J=7$, 5, α H), 3.27 (t, $J=7.5$, γ H)
9	1.29 (3H, d, $J=6.5$), 3.79 (1H, d, $J=6$), 4.12 (1H, dq, $J=6$, 6.5)	1.81 (tt, $J=7$, 7, β H), 2.37 (t, $J=7$, α H), 3.28 (t, $J=7$, γ H)
10	3.09 (1H, dd, $J=9$, 13), 3.23 (1H, dd, $J=6$, 13), 4.12 (1H, dd, $J=6$, 9), 7.24—7.42 (5H, m)	1.46—1.63 (m, β H), 1.94—2.11 (m, α H), 2.98, 3.25 (dt, $J=7$, 14, γ H)
11	3.00 (1H, dd, $J=9$, 14), 3.16 (1H, dd, $J=6$, 14), 4.06 (1H, dd, $J=6$, 9), 6.86 (2H, d, $J=8$), 7.13 (2H, d, $J=8$)	1.48—1.61 (m, β H), 1.97—2.13 (m, α H), 2.97, 3.29 (dt, $J=7$, 14, γ H)
12	2.95 (1H, dd, $J=7$, 18), 3.01 (1H, dd, $J=6$, 18), 4.27 (1H, dd, $J=6$, 7)	1.81 (tt, $J=7$, 7, β H), 2.40 (t, $J=7$, α H), 3.23, 3.33 (dt, $J=7$, 13.5, γ H)
37		1.90 (tt, $J=7.5$, 7.5, β H), 2.34 (t, $J=7.5$, α H), 3.01 (t, $J=7.5$, γ H)
13	3.10—3.29 (2H, m), 4.17—4.23 (1H, m), 7.25—7.45 (5H, m)	2.09—2.32 (m, α H), 3.10—3.29 (m, γ H), 3.88—4.35 (m, β H)
14	2.01—2.11 (3H, m), 2.41—2.54 (1H, m), 3.30—3.48 (2H, m), 4.37 (1H, dd, $J=7$, 8)	2.41—2.54, 2.58—2.65 (m, α H), 3.30—3.48 (m, γ H), 4.13—4.22 (m, β H)
38		2.46 (dd, $J=7$, 15, α H), 2.51 (dd, $J=5$, 15, α H), 2.96 (dd, $J=9$, 13, γ H), 3.17 (dd, $J=3$, 13, γ H), 4.19—4.26 (m, β H)
15	3.10 (1H, dd, $J=9$, 14), 3.21 (1H, dd, $J=6$, 14), 4.15 (1H, dd, $J=6$, 9), 7.20—7.43 (5H, m)	2.34 (ddd, $J=5$, 8, 17, α H), 2.44 (ddd, $J=5$, 6, 17, α H), 3.25 (ddd, $J=5$, 8, 14, β H), 3.45 (ddd, $J=5$, 6, 14, β H)
16	2.10—2.18 (3H, m), 2.38—2.47 (1H, m), 3.35—3.46 (2H, m), 4.35 (1H, dd, $J=7$, 8)	2.64 (t, $J=6.5$, α H), 3.49, 3.57 (dd, $J=6.5$, 13, β H)
39		2.58 (t, $J=6.5$, α H), 3.18 (t, $J=6.5$, β H)
17	3.08 (1H, dd, $J=9$, 13), 3.22 (1H, dd, $J=6$, 13), 4.12 (1H, dd, $J=6$, 9), 7.20—7.45 (5H, m)	0.97—1.07 (m, γ H), 1.22—1.34 (m, δ H), 1.48 (tt, $J=7$, 7, β H), 2.30 (t, $J=7$, α H), 2.91—3.00, 3.15—3.23 (m, ϵ H)
18	1.96—2.11 (3H, m), 2.39—2.49 (1H, m), 3.35—3.48 (2H, m), 4.33 (1H, t, $J=7.5$)	1.30—1.38 (m, γ H), 1.49—1.60 (m, δ H), 1.60 (tt, $J=8$, 8, β H), 2.38 (t, $J=8$, α H), 3.19, 3.29 (dt, $J=7$, 14, ϵ H)
40		1.29—1.38 (m, γ H), 1.55 (tt, $J=7.5$, 7.5, δ H), 1.62 (tt, $J=7.5$, 7.5, β H), 2.20 (t, $J=7.5$, α H), 2.24 (t, $J=7.5$, ϵ H)

δ values ex *tert*-BuOH (1.23), J in Hz, measured in 0.1 N DCl/D₂O.

terminal under acidic conditions. However, no relationship was apparent between the values of the dipeptides and those of the amino acids under neutral conditions (around pH 7). The values seemed to depend not on the total charge of molecules, but on the charge of the hetero atom next to the carbonyl group: CO-NH-, CO-OH or CO-O⁻.

Table II shows the δ and J values of dipeptides (1—18) in 0.1 N DCl, taken from the proton nuclear magnetic resonance (¹H-NMR) spectra. Signals derived from GABA were characteristic. The chemical shifts of α H, β H and γ H of the GABA residue in these peptides were similar to those of GABA itself.

The peptide containing Gly (1) had one kind of γ H proton signal, while most of the other peptides (2—7, 10—12) had two kinds of γ H proton signals. Two other peptides (8, 9), however, containing Ser and Thr, respectively, also showed only one kind of γ H proton signal.

All of the dipeptides studied in this paper possessed more or less strong immunological absorption capability as mentioned above. A quantitative evaluation of the immunocrossreactivity of the anti-GABA serum is in progress.

Experimental

Melting points of all compounds are uncorrected. ¹H-NMR spectra were obtained by using *tert*-butanol (1.23 ppm) as an internal standard with a Bruker AM-400 spectrometer. Optical rotations were measured with a JASCO DIP-140 spectrometer.

Immunostaining Procedure—The avidin-biotin-complex (ABC) method¹²⁾ was used as an immunohistochemical procedure. Immunostaining for GABA-like immunoreactivity was carried out in rat brain tissues according to the procedure described by Kimura and Tanaka.⁶⁾ For absorption tests, only the first step of the staining procedure was modified. Namely, a 0.3% Triton-X solution (100 μ l), in which a test sample (3.3 mg or none) was dissolved, was added to a diluted solution of anti-GABA serum (1 ml; 1 : 10000). The absorption ability of the sample was judged from the staining intensity compared with that of the non-absorbed control.

Method A—a) Z-Hyp- γ Abu-OBzl (24): DCC (4.54 g) was added to a solution of Z-Hyp-OH (4.78 g) and HONB (4.34 g) in THF (100 ml) at 0 °C, and the mixture was stirred at the same temperature for an additional 1 h, then at room temperature for 1 h. Z-Hyp-ONB was formed, and the resulting DCU was filtered off. The filtrate was concentrated *in vacuo*. The oily residue was dissolved in dioxane (100 ml), and to this solution, GABA-OBzl *p*-toluene sulfonate (7.31 g) and triethylamine (2.02 g) were added at room temperature. After stirring of the mixture for 20 h followed by evaporation *in vacuo*, the oily residue was dissolved in ethyl acetate (100 ml). The solution was washed successively with water, 5% aqueous sodium hydrogen carbonate, brine, 10% aqueous citric acid and brine. After being dried over sodium sulfate, the organic layer was evaporated to dryness *in vacuo*. The crystalline residue was recrystallized from ethyl acetate-ether (15 ml : 50 ml) to yield pure Z-Hyp- γ Abu-OBzl (24) (7.15 g, 81%), mp 72—73 °C, $[\alpha]_D -15.0^\circ$ ($c=1$, DMF).

Eleven other protected dipeptides (19—23, 25—30) were similarly synthesized: Z-Gly- γ Abu-OBzl (19) (84%), mp 83.5—85 °C; Z-Ala- γ Abu-OBzl (20) (88%), mp 99.5—100.5 °C, $[\alpha]_D +6.4^\circ$ ($c=1$, DMF); Z-Val- γ Abu-OBzl (21) (78%), mp 114.5—116 °C, $[\alpha]_D +10.1^\circ$ ($c=1$, DMF); Z-Leu- γ Abu-OBzl (22) (50%), mp 73—74 °C, $[\alpha]_D -3.8^\circ$ ($c=1$, DMF); Z-Ile- γ Abu-OBzl (23) (56%), mp 106.5—109 °C, $[\alpha]_D +6.7^\circ$ ($c=1$, DMF); Z-Ser- γ Abu-OBzl (25) (61%), mp 137—138 °C, $[\alpha]_D +17.5^\circ$ ($c=1$, DMF); Z-Thr- γ Abu-OBzl (26) (95%), mp 94.5—95.5 °C, $[\alpha]_D +2.0^\circ$ ($c=1$, DMF); Z-Phe- γ Abu-OBzl (27) (70%), mp 133—134 °C, $[\alpha]_D -8.9^\circ$ ($c=1$, DMF); Z-Tyr(OBzl)- γ Abu-OBzl (28) (92%), mp 138—139 °C, $[\alpha]_D -13.0^\circ$ ($c=1$, DMF); Z-Asp(OBzl)- γ Abu-OBzl (29) (87%), mp 111—112 °C, $[\alpha]_D -6.5^\circ$ ($c=1$, DMF); Z-Phe- γ Abu (2OH)-OBzl (32) (70%), mp 122—123 °C, $[\alpha]_D -10.8^\circ$ ($c=1$, DMF).

b) H-Gly- γ Abu-OH (1): Hydrogenation of Z-Gly- γ Abu-OBzl (19) (4.6 g) over a Pd catalyst in the usual manner in a mixed solvent of MeOH-AcOH-H₂O (30 ml : 10 ml : 5 ml), followed by removal of the catalyst and evaporation of the solvent, gave a residue. The residue was dissolved in a mixed solvent of EtOH and toluene (20 ml : 30 ml), and the solution was evaporated to dryness to give a colorless solid. Recrystallization from H₂O-EtOH gave pure H-Gly- γ Abu-OH (1), (2.05 g, 85%), mp 212—215 °C (dec.). *Anal.* Calcd for C₆H₁₂N₂O₃: C, 44.99; H, 7.55; N, 17.49. Found: C, 44.97; H, 7.62; N, 17.41.

Ten other dipeptides (2—11, 13) were similarly obtained: H-Ala- γ Abu-OH (2) (87%), mp 215—218 °C (dec.). *Anal.* Calcd for C₇H₁₄N₂O₃: C, 48.26; H, 8.10; N, 16.08. Found: C, 48.26; H, 8.04; N, 15.98; H-Val- γ Abu-OH (3) (69%), mp 202—203 °C. *Anal.* Calcd for C₉H₁₈N₂O₃: C, 53.44; H, 8.97; N, 13.85. Found: C, 53.78; H, 9.02; N, 14.00; H-Leu- γ Abu-OH (4) (73%), mp 179.5—180.5 °C. *Anal.* Calcd for C₁₀H₂₀N₂O₃: C, 55.55; H, 9.47; N, 13.07. Found: C, 55.53; H, 9.32; N, 12.95; H-Ile- γ Abu-OH (5) (56%), mp 152—154 °C (amorphous); H-Hyp- γ Abu-OH (7) (75%),

mp 210—211 °C. *Anal.* Calcd for $C_9H_{16}N_2O_4$: C, 49.99; H, 7.46; N, 12.96. Found: C, 49.85; H, 7.87; N, 12.66; H-Ser- γ Abu-OH (8) (82%), mp 188—191 °C (dec.). *Anal.* Calcd for $C_7H_{14}N_2O_4$: C, 44.20; H, 7.42; N, 14.73. Found: C, 43.91; H, 7.78; N, 14.82; H-Thr- γ Abu-OH (9) (52%), mp 136 °C (dec.). *Anal.* Calcd for $C_8H_{16}N_2O_4$: C, 47.05; H, 7.90; N, 13.72. Found: C, 47.25; H, 7.99; N, 13.89; H-Phe- γ Abu-OH (10) (82%), mp 173.5—174.5 °C. *Anal.* Calcd for $C_{13}H_{18}N_2O_3$: C, 62.38; H, 7.25; N, 11.19. Found: C, 62.03; H, 7.38; N, 10.95; H-Tyr- γ Abu-OH (11) (72%), mp 68—71 °C (amorphous). H-Asp- γ Abu-OH (12) (83%), mp 216—218 °C (dec.), $[\alpha]_D + 12.6^\circ$ ($c=1$, 0.1 N NaOH). *Anal.* Calcd for $C_8H_{14}N_2O_5$: C, 44.03; H, 6.47; N, 12.84. Found: C, 44.00; H, 6.61; N, 12.59; H-Phe- γ Abu(2OH)-OH (13) (75%), mp 177—179 °C. *Anal.* Calcd for $C_{13}H_{18}N_2O_4$: C, 58.63; H, 6.81; N, 10.52. Found: C, 58.41; H, 6.90; N, 10.42.

Method B—a) Z-Pro- γ Abu-OH (31): Z-Pro-ONSu (1.73 g) in acetonitrile (30 ml) was added to a solution of GABA (0.52 g) and TEA (0.51 g) in water-acetonitrile (10 ml : 10 ml) at room temperature. After stirring of the mixture for 20 h and evaporation *in vacuo*, the residue was dissolved in a mixed solvent of 1 N aq. HCl (20 ml) and ethyl acetate (50 ml). The organic layer was separated, washed with brine and extracted with 5% aqueous sodium hydrogen carbonate (30 ml \times 3). The extract was washed with ethyl acetate (30 ml \times 2) and acidified with 6 N aq. HCl. The separated oil was extracted with ethyl acetate (30 ml \times 3) and the organic solution was washed with brine (30 ml), dried over sodium sulfate and evaporated *in vacuo*. The oily residue was triturated with petroleum ether. The crystalline product was recrystallized from ethyl acetate-ether (55 ml : 30 ml) to give pure Z-Pro- γ Abu-OH (31) (0.89 g, 53%), mp 73—75 °C, $[\alpha]_D - 29.5^\circ$ ($c=1$, H_2O).

Five other protected dipeptides (33—37) were similarly synthesized: Z-Pro- γ Abu (2OH)-OH DCHA (33) (84%), mp 128—130 °C, $[\alpha]_D - 18.7^\circ$ ($c=1$, DMF); Z-Phe- β Ala-OH (34) (82%), mp 136—137 °C, $[\alpha]_D - 11.5^\circ$ ($c=1$, DMF); Z-Pro- β Ala-OH (35) (83%), mp 134—136 °C, $[\alpha]_D - 31.7^\circ$ ($c=1$, DMF); Z-Phe- ϵ Acp-OH (36) (46%), mp 126—128 °C, $[\alpha]_D - 10.2^\circ$ ($c=1$, DMF); Z-Pro- ϵ Acp-OH (37) (92%), mp 92—94 °C, $[\alpha]_D - 26.2^\circ$ ($c=1$, DMF).

b) H-Pro- γ Abu-OH (6): Hydrogenation of 31 (4.0 g) was carried out as in method A b) to give pure H-Pro- γ Abu-OH (6), (1.50 g, 63%), mp 202—205 °C (dec.). *Anal.* Calcd for $C_9H_{18}N_2O_3$: C, 53.98; H, 8.06; N, 13.99. Found: C, 53.71; H, 8.17; N, 13.66.

Five other dipeptides (14—18) were similarly obtained: H-Pro- γ Abu(2OH)-OH (14) (91%), mp 210—212 °C. *Anal.* Calcd for $C_9H_{16}N_2O_4$: C, 49.99; H, 7.46; N, 12.96. Found: C, 50.03; H, 7.70; N, 13.14; H-Phe- β Ala-OH (15) (88%), mp 218—220 °C (dec.). *Anal.* Calcd for $C_{12}H_{16}N_2O_3$: C, 61.00; H, 6.83; N, 11.86. Found: C, 61.13; H, 6.93; N, 11.94; H-Pro- β Ala-OH (16) (54%), mp 218—219 °C (dec.). *Anal.* Calcd for $C_8H_{14}N_2O_3$: C, 51.60; H, 7.58; N, 15.04. Found: C, 51.47; H, 7.73; N, 15.08; H-Phe- ϵ Acp-OH (17) (92%), mp 130—132 °C (dec.). *Anal.* Calcd for $C_{15}H_{22}N_2O_3$: C, 64.73; H, 7.97; N, 10.06. Found: C, 64.56; H, 8.18; N, 10.04; H-Pro- ϵ Acp-OH (18) (59%), mp 182—183 °C. *Anal.* Calcd for $C_{11}H_{20}N_2O_3$: C, 57.87; H, 8.83; N, 12.27. Found: C, 58.00; H, 9.09; N, 12.50.

References and Notes

- 1) Amino acids, peptides and their derivatives, except Gly, β Ala, γ Abu, γ Abu(2OH) and ϵ Acp, are of the L-configuration. Abbreviations used are those recommended by the IUPAC-IUB Commission on Biochemical Nomenclature: *Biochemistry*, 5, 2485 (1966); *ibid.*, 6, 362 (1967); *ibid.*, 11, 1726 (1972). Z = benzyloxycarbonyl, Boc = *tert*-butoxycarbonyl, Bzl = benzyl, DCC = *N,N'*-dicyclohexylcarbodiimide, HONB = *N*-hydroxy-5-norbornene-2,3-dicarboximide, DSC = *N,N'*-disuccinimidyl carbonate, THF = tetrahydrofuran, DCU = dicyclohexyl urea; DMF = *N,N*-dimethylformamide, TEA = triethylamine.
- 2) E. Roberts, T. N. Chase and D. B. Tower, "GABA in Nervous System Function," ed. by E. Roberts, T. N. Chase and D. B. Tower, Raven Press, New York, 1976, pp. 1—6.
- 3) P. L. McGeer and E. G. McGeer, "Basic Neurochemistry," 3rd ed., ed. by G. T. Siegel, R. W. Albers, B. W. Agranoff and R. Katzman, Little Brown and Co., Boston, 1981, pp. 233—253.
- 4) W. H. Oertel, D. E. Schmechel, E. Mugnaini, M. L. Tappaz and I. J. Kopin, *Neuroscience*, 6, 2715 (1981).
- 5) O. P. Ottersen and J. Storm-Mathisen, *J. Comp. Neurol.*, 229, 374 (1984).
- 6) H. Kimura and T. Tanaka, *Neuroscience*, in press.
- 7) B. Onteniente, H. Tago, H. Kimura and T. Maeda, *J. Comp. Neurol.*, 248, 422 (1986).
- 8) Y. Tomida, H. Kimura, S. Ida and K. Kuriyama, *Bull. Jpn. Neurochem. Soc.*, 24, 193 (1985).
- 9) A. P. Fosker and H. D. Law, *J. Chem. Soc.*, 1965, 7305.
- 10) M. Fujino, S. Kobayashi, M. Obayashi, T. Fukuda, S. Shinagawa and O. Nishimura, *Chem. Pharm. Bull.*, 22, 1857 (1974).
- 11) H. Ogura, T. Kobayashi, K. Shimizu, K. Kawabe and K. Takeda, *Tetrahedron Lett.*, 1979, 4745.
- 12) S. M. Hsu, L. Raine and H. Fanger, *J. Histochem. Cytochem.*, 29, 557 (1981).

[Chem. Pharm. Bull.]
35(3)1255—1261(1987)

Studies on Stable Diazoalkanes as Potential Fluorogenic Reagents. III.¹⁾ 4-Diazomethyl-2(1*H*)-quinolinones

KEIICHI ITO* and JUNKO MARUYAMA

Hokkaido Institute of Pharmaceutical Sciences,
Katsuraoka-cho, Otaru-shi 047-02, Japan

(Received July 22, 1986)

A series of 4-diazomethyl-2(1*H*)-quinolinones **4a–f** was prepared, and the physical and chemical properties were compared with those of the known 4-diazomethylcoumarins. In view of their easy accessibility, high stability and reactivity, these new diazoalkanes are expected to be practical reagents for the fluorescence labeling of carboxylic acids, although the fluorescence intensities of the labeled esters are less than those of the esters with the corresponding coumarin reagents.

Keywords—stable diazoalkane; diazomethyl-2-quinolinone; carboxylic acid; fluorescence labeling; fluorescence quantum yield

Stable but reactive diazoalkanes bearing an intrinsic function capable of introducing a fluorophore into non-fluorescent compounds through facile reactions can serve as practical reagents for use in high-performance liquid chromatographic detection of acidic substances such as carboxylic acids, alcohols, *etc.*²⁾ As an extension of our recent studies on diazomethyl-substituted coumarins³⁾ and benzo-fused coumarins¹⁾ aimed at developing such fluorescent

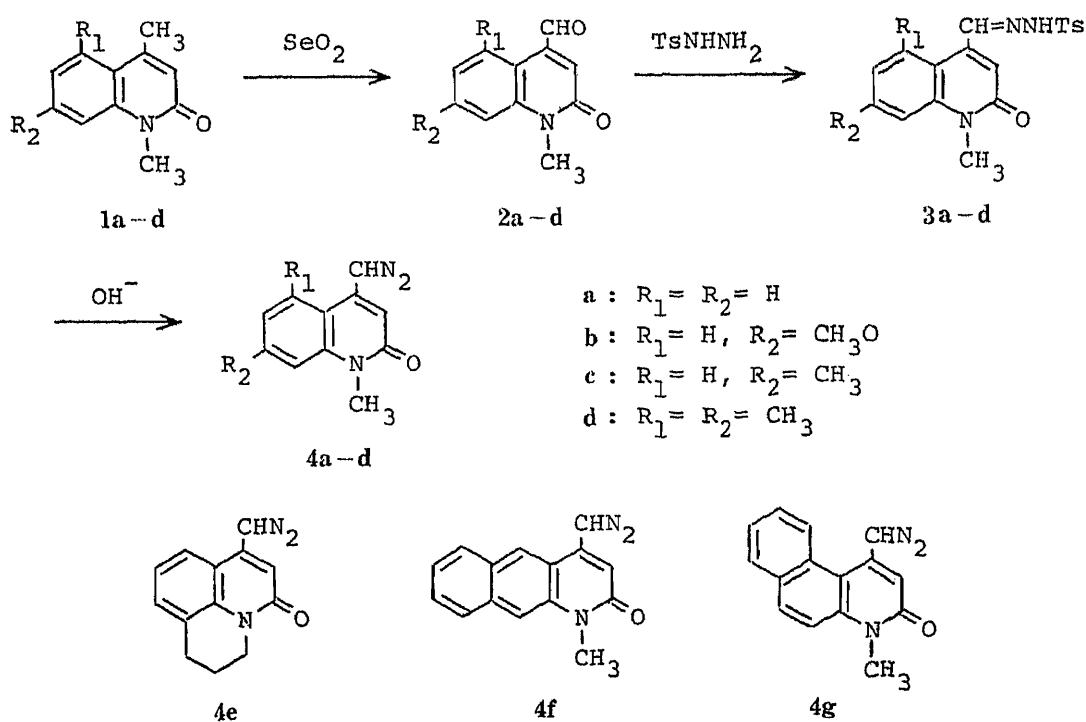


Chart 1

TABLE I. Preparation of 4-Diazomethyl-2(1*H*)-quinolinones 4

Starting material No.	Reaction ^{a)} 2→3		Reaction ^{a)} 3→4		Product No.
	Reaction time (h)	Yield ^{b)} (%)	Reaction time (h)	Yield (%)	
2a	3.5	93	5	76	4a
2b	7	98	8	98	4b
2c	4	99	4.5	86	4c
2d	6	95	4	76	4d
2e	5	82	3.5	99	4e
2f	4	88	1 ^{c)}	93	4f
2g	6	95	0.75	53	4g

a) See the experimental section. b) Yield of crude product. c) Reaction carried out at 40°C.

labels, we have now synthesized 4-diazomethyl derivatives **4a—d** of 1-methyl-2(1*H*)-quinolinone, which is isosteric to coumarin, together with the analogous tricyclic derivatives **4e—g**, as shown in Chart 1. The products were compared with the reported coumarin derivatives^{1,3)} with respect to stability, reactivity and fluorogenic properties to examine their availability as practical reagents.

The preparation of the new diazoalkanes was readily carried out in good yields as shown in Chart 1 and Table I. Treatment of 4-formyl-1-methyl-2(1*H*)-quinolinones **2a—d** (obtained by oxidation of the corresponding 4-methyl derivatives **1** with selenium dioxide) with *p*-toluenesulfonylhydrazine in ethanol at room temperature gave almost pure precipitates of the tosylhydrazones **3a—d**. Conversion of **3a—d** into the desired diazoalkanes **4a—d** was achieved by treatment with 0.2N sodium hydroxide according to Cava, *et al.*⁴⁾ The above procedure was also successfully applied to the preparation of **4e—g**.

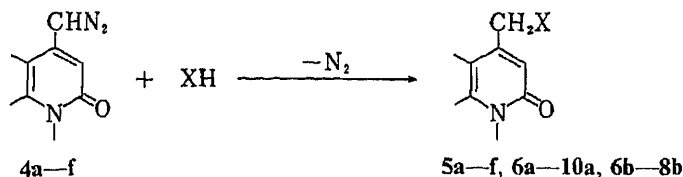
All of the diazo compounds obtained are almost non-fluorescent yellow or orange crystals. Characteristic infrared (IR) absorption bands due to a diazo group and proton nuclear magnetic resonance (¹H-NMR) signals due to diazomethyl and C³-H protons, together with the microanalysis data, shown in Table II, were consistent with the expected structures of **4a—g**. The presence of a substituent at the C⁵ position in **4d** and **4g** causes the low-field shifts of the diazomethyl proton signals relative to that of the parent **4a** ($\Delta\delta$: 0.32 ppm for **4d**, 0.43 ppm for **4g**) in the ¹H-NMR spectra, as was reported previously⁵⁾ for the corresponding 4-methyl proton signals of **1d** and **1g**. Low-field shifts of the 4-formyl proton signals of **2d** and **2g** are likewise observed ($\Delta\delta$: both 0.39 ppm). Similarly to the 4-diazomethylcoumarin reagents, the present diazomethyl derivatives **4a—g** are stable enough to be stored at room temperature for a year in a desiccator without any detectable decomposition. Even in a refluxing solvent such as chloroform, ethanol or tetrahydrofuran (THF) most of the diazo compounds are stable, with the exception of **4d** and **4g**. However, a significant decrease in ultraviolet (UV) absorption was observed for **4a** at λ_{\max} 230 and 332 nm after standing in ethanol without detection from light, as was similarly observed for 4-diazomethylcoumarin.³⁾ The possible photodegradation of **4** was not further investigated.

The diazomethyl derivatives **4a—f** reacted smoothly with carboxylic acids to give 2(1*H*)-quinolinon-4-ylmethyl esters (**5a—f**, **6a—8a**, **6b—8b**) in fairly good yields by refluxing an equimolar mixture in chloroform for 1—2 h with addition of silica gel catalyst,⁶⁾ as shown in Table III. Reactions of methanesulfonic acid (without catalyst) and methanol (with fluoroboric acid catalyst) with **4a** are also listed in Table III. For the labeling of acetic acid (0.2 mmol scale) without addition of silica gel catalyst, the use of one molar excess of the diazo reagent and refluxing for 4 h were needed to complete the reaction.

TABLE II. 4-Diazomethyl-2(1*H*)-quinolinones 4

No.	Appearance (Recrystn. solvent)	mp (dec.) (°C)	Formula (<i>m/z</i> M ⁺)	Analysis (%)			IR $\nu_{\text{CHN}_2}^{\text{KBr}}$ cm ⁻¹	¹ H-NMR (CDCl ₃) δ ppm		
				Calcd (Found)				NCH ₃ (3H, s), CHN ₂ (1H, s), C ³ -H (1H, s) others		
				C	H	N				
4a	Orange prisms (THF)	147—149	C ₁₁ H ₉ N ₃ O (199)	66.31 (66.59)	4.55 4.46	21.10 21.03)	2061	3.67 7.12—7.66 (4H, m, Ar-H)	5.34	6.23
4b	Orange prisms (CH ₃ CN)	152—154	C ₁₂ H ₁₁ N ₃ O ₂ (229)	62.87 (63.04)	4.84 4.81	18.33 18.36)	2066	3.65 3.92 (3H, s, OCH ₃), 6.75—6.84 (2H, m, C ^{6,8} -H), 7.31 (1H, d, <i>J</i> =8.5 Hz, C ⁵ -H)	5.27	6.12
4c	Orange plates (CH ₃ CN)	151—153	C ₁₂ H ₁₁ N ₃ O (213)	67.59 (67.96)	5.20 5.22	19.71 19.60)	2060	3.66 2.49 (3H, s, CCH ₃), 6.97—7.30 (3H, m, Ar-H)	5.30	6.17
4d	Pale brown prisms ^{a)}	b)	C ₁₃ H ₁₃ N ₃ O (227)	68.70 (68.73)	5.77 5.92	18.49 18.08)	2060	3.67 2.42 (3H, s, C ⁷ -CH ₃), 2.70 (3H, s, C ⁵ -CH ₃), 6.83 (1H, s, C ⁶ -H), 7.05 (1H, s, C ⁸ -H)	5.66	6.25
4e	Yellow prisms (Benzene)	140—142	C ₁₃ H ₁₁ N ₃ O (225)	69.32 (69.49)	4.92 4.93	18.66 18.50)	2071	— 2.08 (2H, m, C ⁹ -H), 2.98 (2H, t, C ⁸ -H), 4.18 (2H, t, C ¹⁰ -H), 7.00—7.36 (3H, m, Ar-H)	5.33	6.25
4f	Orange leaves (Benzene)	151—153	C ₁₅ H ₁₁ N ₃ O (249)	72.27 (72.55)	4.45 4.47	16.86 16.80)	2072	3.75 7.36—7.93 (6H, m, Ar-H)	5.47	6.28
4g	Yellow Prisms ^{a)}	b)	C ₁₅ H ₁₁ N ₃ O (249)	72.27 (72.46)	4.45 4.72	16.86 16.31)	2028	3.83 7.50—7.92 (5H, m, Ar-H), 8.64 (1H, d, <i>J</i> = 8.1 Hz, C ¹⁰ -H)	5.77	6.46 ^{c)}

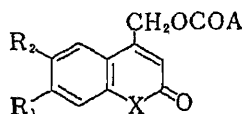
a) Not recrystallized. b) Changed to a white powder on heating. c) C²-H.

TABLE III. Reactions^{a)} of 4 with Acidic Substances XH

Diazo reagent No.	XH	Catalyst	Reaction time (h)	Product	Yield ^{b)} (%)
4a	CH ₃ COOH	SiO ₂	2	5a	75
4a	CH ₃ COOH	None	2	5a	62
4b	CH ₃ COOH	SiO ₂	2	5b	79
4c	CH ₃ COOH	SiO ₂	2	5c	77
4d	CH ₃ COOH	SiO ₂	2 ^{c)}	5d	51
4e	CH ₃ COOH	SiO ₂	2	5e	78
4f	CH ₃ COOH	SiO ₂	2	5f	68
4a	<i>n</i> -C ₁₅ H ₃₁ COOH	SiO ₂	1	6a	83
4a	C ₆ H ₅ COOH	SiO ₂	1	7a	57
4a	C ₆ H ₅ CH=CHCOOH	SiO ₂	1	8a	62
4a	CH ₃ SO ₃ H	None	1 ^{c)}	9a	80
4a	CH ₃ OH	HBF ₄	3 ^{c)}	10a	61
4b	<i>n</i> -C ₁₅ H ₃₁ COOH	SiO ₂	1	6b	87
4b	C ₆ H ₅ COOH	SiO ₂	1	7b	63
4b	C ₆ H ₅ CH=CHCOOH	SiO ₂	1	8b	75

a) Carried out in refluxing CHCl₃. See the experimental section. b) Isolated yield. c) Reaction carried out at room temperature.

TABLE IV. Comparison of Fluorescence Quantum Yields



R ₁	R ₂	A	Quantum yield ^{a)}	
			X=NCH ₃	X=O
H	H	CH ₃	0.011	0.020 ^{c)}
CH ₃ O	H	CH ₃	0.024	0.080 ^{c)}
CH ₃	H	CH ₃	0.012	0.050 ^{c)}
	Benzo ^{b)}	CH ₃	0.022	0.0035 ^{d)}
CH ₃ O	H	<i>n</i> -C ₁₅ H ₃₁	0.025	0.100 ^{c)}
CH ₃ O	H	C ₆ H ₅	0.022	0.120 ^{c)}

a) Determined in EtOH, relative to quinine sulfate (0.55). b) Benzene ring fused at the 6-7 positions. c) Data reported in ref. 3. d) Data reported in ref. 1.

In conclusion, the accessibility, stability and reactivity of the present diazo compounds 4 as practical labeling reagents are comparable to those of the known 4-diazomethyl-coumarins.^{1,3)} However, the fluorescence intensities of the esters labeled with 4 are generally less than those of the esters with the corresponding coumarin reagents, as shown in Table IV. It should be, also noted that the linearly benzo-fused quinolinonylmethyl acetate 5f is moderately fluorescent, although the corresponding coumarinylmethyl acetate is almost non-fluorescent.

Experimental

All melting points were determined on a Yanaco micro melting point apparatus and are uncorrected. IR spectra were determined using a Hitachi 215 grating spectrophotometer. ¹H-NMR spectra were recorded on a JEOL JNM-FX-100 spectrometer (100 MHz). Mass spectra (MS) were taken on a Shimadzu LKB-900B spectrometer. UV spectra were obtained in EtOH with a Hitachi 200-10 spectrophotometer. Fluorescence (F) spectra were measured in non-fluorescent EtOH on a Shimadzu RF-503 spectrofluorometer. Relative fluorescence quantum yields were determined according to the method of Parker and Rees⁷⁾ using quinine sulfate in 0.1 N H₂SO₄ as the standard.

7-Methoxy-1,4-dimethyl-2(1H)-quinolinone (1b)—Prepared from 7-methoxy-4-methyl-2(1H)-quinolinone⁸⁾ with iodomethane as usual. Leaves from hexane, mp 92–93°C. ¹H-NMR (CDCl₃) δ: 2.40 (3H, s, C⁴-H), 3.64 (3H, s, NCH₃), 3.91 (3H, s, OCH₃), 6.42 (1H, s, C³-H), 6.77 (1H, s, C⁸-H), 6.81 (1H, d, *J*=8.4 Hz, C⁶-H), 7.58 (1H, d, *J*=8.4 Hz, C⁵-H). *Anal.* Calcd for C₁₂H₁₃NO₂: C, 70.91; H, 6.45; N, 6.89. Found: C, 70.97; H, 6.30; N, 6.75.

4-Formyl-2(1H)-quinolinones 2a–g—Compounds 2a–g were obtained by heating a mixture of 4-methyl-

TABLE V. 2(1H)-Quinolinon-4-ylmethyl Esters and Ether 5–10

No.	mp (°C) (Recrystn. solvent)	Formula	Analysis (%)			IR ν _{CO} ^{KB} cm ⁻¹	UV		F (EtOH) ^{a)}		
			Calcd (Found)				λ _{max} ^{EtOH} nm (log ε)	λ _{max} ^{ex} nm	λ _{max} ^{em} nm	Quantum yield ^{b)} × 10 ³	
C	H	N									
5a	119–120 ^{c)} (Hexane)	C ₁₃ H ₁₃ NO ₃	67.52 (67.65)	5.67 (5.58)	6.06 (6.14)	1749 1663	230 (4.60), 270 (3.80), 276 (3.78), 330.5 (3.84)	274 332	387	11	
5b	152–154 ^{d)} (iso-PrOH)	C ₁₄ H ₁₅ NO ₄	64.36 (64.29)	5.79 (5.82)	5.36 (5.35)	1744 1646	229 (4.45), 255 (3.82), 287.5 (3.66), 328 (4.08), 341 (4.00)	289 331	377	24	
5c	143–145 ^{e)} (iso-PrOH)	C ₁₄ H ₁₅ NO ₃	68.55 (68.56)	6.16 (6.04)	5.71 (5.84)	1747 1657	231 (4.56), 275.5 (3.84), 329.5 (3.93)	333	385	12	
5d	156–158 ^{f)} (iso-PrOH)	C ₁₅ H ₁₇ NO ₃	69.48 (69.28)	6.61 (6.63)	5.40 (5.52)	1739 1650	229 (4.44), 234 (4.44), 251 (4.07), 285 (3.86), 328 (3.75)	289 332	399	8.1	
5e	130–132 ^{e)} (iso-PrO ₂)	C ₁₅ H ₁₅ NO ₃	70.02 (70.18)	5.88 (5.91)	5.44 (5.42)	1747 1648	235 (4.48), 248 (4.15), 275.5 (3.75), 332.5 (3.72)	279 336	395	11	
5f	173–175 ^{e)} (iso-PrOH)	C ₁₇ H ₁₅ NO ₃	72.58 (72.77)	5.37 (5.23)	4.98 (5.10)	1749 1659	255.5 (4.56), 266.5 (4.57), 267.5 (4.49), 316.5 (3.98), 329.5 (4.08), 377 (3.54)	267 331 379	458	22	
6a	70–72 ^{f)} (MeOH)	C ₂₇ H ₄₁ NO ₃	75.83 (75.57)	9.66 (9.46)	3.28 (3.42)	1746 1727 1640	229.5 (4.40), 269.5 (3.61), 275 (3.59), 330 (3.64)	275 333	390	6.6	
7a	133–135 ^{f)} (MeOH)	C ₁₈ H ₁₅ NO ₃	73.70 (73.90)	5.15 (5.09)	4.78 (4.84)	1724 1658	270.5 (3.82), 330.5 (3.81)	275 334	388	8.9	
8a	154–156 ^{e)} (iso-PrOH)	C ₂₀ H ₁₇ NO ₃	75.22 (75.20)	5.37 (5.41)	4.39 (4.44)	1724 1710 1657	222.5 (4.60), 229 (4.56), 244 (4.15), 276.5 (4.38), 330 (3.80)	276 333	389	8.3	
9a	113–114 ^{e)} (THF)	C ₁₂ H ₁₃ NO ₄ S	53.93 (53.99)	4.90 (4.81)	5.24 (5.07)	1613	229.5 (4.32), 269 (3.56), 275.5 (3.55), 329.5 (3.54)	275 331	385	<1	
10a	91–93 ^{e)} (Hexane)	C ₁₂ H ₁₃ NO ₂	70.91 (70.49)	6.45 (6.28)	6.89 (7.14)	1644	228 (4.53), 269 (3.73), 275.5 (3.71), 329 (3.83)	274 331	384	12	
6b	73–74 ^{e)} (MeOH)	C ₂₈ H ₄₃ NO ₄	73.48 (73.12)	9.47 (9.44)	3.06 (3.39)	1732 1640	229 (4.39), 254.5 (3.73), 285 (3.59), 328 (4.03), 341 (3.94)	290 332	377	25	
7b	147–149 ^{f)} (EtOH)	C ₁₉ H ₁₇ NO ₄	70.57 (70.06)	5.30 (5.47)	4.33 (4.07)	1723 1645	228 (4.67), 253.5 (3.91), 281 (3.75), 327.5 (4.13), 340.5 (4.04)	286 333	377	22	
8b	140–141 ^{f)} (iso-PrOH)	C ₂₁ H ₁₉ NO ₄	72.19 (72.34)	5.48 (5.50)	4.01 (3.80)	1718 1656	258 (4.25), 279.5 (4.41), 327.5 (4.12), 341 (4.03)	322	377	16	

a) Fluorescence: ex, excitation; em, emission. b) Relative to quinine sulfate⁷⁾ (0.55); ex, 320 nm. c) Needles. d) Yellow plates. e) Pale yellow prisms. f) Prisms. g) Plates.

2(1*H*)-quinolinones **1a**–**g** and SeO₂ at 180–200 °C according to the previously reported method.⁹⁾ Except for the known compounds, **2a**,⁹⁾ **2c**,¹⁰⁾ and **2e**,⁹⁾ chromatography over silica gel was necessary for the isolation of pure products.

4-Formyl-7-methoxy-1-methyl-2(1*H*)-quinolinone (**2b**): Prepared from 7-methoxy-1,4-dimethyl-2(1*H*)-quinolinone (**1b**). Yellow needles from benzene, mp 181–182 °C. Yield, 65%. ¹H-NMR (CDCl₃) δ: 3.72 (3H, s, NCH₃), 3.93 (3H, s, OCH₃), 6.83–6.99 (3H, m, C^{3,6,8}-H), 8.75 (1H, d, *J* = 9.2 Hz, C⁵-H), 10.07 (1H, s, CHO). *Anal.* Calcd for C₁₂H₁₁NO₃: C, 66.35; H, 5.10; N, 6.45. Found: C, 66.44; H, 5.12; N, 6.31.

4-Formyl-1,5,7-trimethyl-2(1*H*)-quinolinone (**2d**): Prepared from 1,4,5,7-tetramethyl-2(1*H*)-quinolinone⁵⁾ (**1d**). Brown prisms from benzene, mp 167–169 °C. Yield, 84%. ¹H-NMR (CDCl₃) δ: 2.47 (3H, s, C⁷-CH₃), 2.53 (3H, s, C⁵-CH₃), 3.71 (3H, s, NCH₃), 6.77, 6.96 (1H × 2, 2s, C^{6,8}-H), 7.09 (1H, s, C³-H), 10.51 (1H, s, CHO). *Anal.* Calcd for C₁₃H₁₃NO₂: C, 72.54; H, 6.09; N, 6.51. Found: C, 71.98; H, 6.00; N, 6.48.

4-Formyl-1-methyl-2(1*H*)-benzo[*g*]quinolinone (**2f**): Prepared from 1,4-dimethyl-2(1*H*)-benzo[*g*]quinolinone⁵⁾ (**1f**). Orange prisms from THF, mp 205–207 °C. Yield, 79%. ¹H-NMR (CDCl₃) δ: 3.78 (3H, s, NCH₃), 7.10 (1H, s, C³-H), 7.45–8.00 (5H, m, Ar-H), 9.32 (1H, s, C⁵-H), 10.11 (1H, s, CHO). *Anal.* Calcd for C₁₅H₁₁NO₂: C, 75.93; H, 4.67; N, 5.90. Found: C, 76.00; H, 4.72; N, 6.03.

1-Formyl-4-methyl-3(4*H*)-benzo[*f*]quinolinone (**2g**): Prepared from 1,4-dimethyl-3(4*H*)-benzo[*f*]quinolinone⁵⁾ (**1g**). Yellow prisms from acetonitrile–hexane, mp 180–182 °C. Yield, 60%. ¹H-NMR (CDCl₃) δ: 3.90 (3H, s, NCH₃), 7.06 (1H, s, C²-H), 7.55–8.15 (6H, m, Ar-H), 10.51 (1H, s, CHO). *Anal.* Calcd for C₁₅H₁₁NO₂: C, 75.93; H, 4.67; N, 5.90. Found: C, 75.79; H, 4.41; N, 5.76.

Preparation of 4-Diazomethyl-2(1*H*)-quinolinones 4a–g—4-Diazomethyl-1-methyl-2(1*H*)-quinolinone (4a)
—A suspension of **2a** (3.74 g, 20 mmol) and *p*-toluenesulfonylhydrazine (4.10 g, 22 mmol) in EtOH (50 ml) was vigorously stirred at room temperature for 3.5 h. The collected and dried precipitate (crude **3a**, 6.61 g, 93%) was suspended in CH₂Cl₂ (300 ml), and 0.2*N* NaOH (300 ml) was added dropwise at 10 °C. The reaction mixture was stirred vigorously at room temperature for 5 h, then the organic layer was separated and the water layer was extracted with CH₂Cl₂ (100 ml × 3). The combined CH₂Cl₂ solution was washed with water (50 ml) and dried over anhydrous MgSO₄. Evaporation of the solvent *in vacuo* followed by recrystallization of the residual solid from THF gave **4a** as orange prisms (2.82 g, 71% from **2a**), mp 147–149 °C (dec.).

Compounds **4b**–**g** were obtained by procedures similar to that described for **4a**: reaction times and yields are shown in Table I, and physical and analytical data are listed in Table II. Compounds **4d** and **4g** were unstable on warming, and hence were not recrystallized.

Reaction of 4-Diazomethyl-2(1*H*)-quinolinones 4a–f with Acidic Substances. Esterification of Acetic Acid with 4a
—Method A: A mixture of **4a** (880 mg, 4.4 mmol), AcOH (240 mg, 4 mmol) and silica gel (Wakogel C-200, 800 mg) in CHCl₃ (20 ml) was vigorously stirred under reflux for 2 h, whereupon N₂ gas evolution was observed. The reaction mixture was filtered to remove the silica gel, washed with CHCl₃ and concentrated *in vacuo* to afford 1-methyl-2(1*H*)-quinolinon-4-ylmethyl acetate (**5a**), which was recrystallized from hexane as needles, mp 119–120 °C (lit.¹¹⁾ mp 117–117.5 °C). Yield, 75% (694 mg). ¹H-NMR (CDCl₃) δ: 2.20 (3H, s, CH₃CO), 3.73 (3H, s, NCH₃), 5.36 (2H, s, CH₂), 6.80 (1H, s, C³-H), 7.33–7.69 (4H, m, Ar-H). The same reaction without addition of silica gel gave **5a** in 62% yield.

The reaction of AcOH with **4b**–**f** and those of other acidic substances with **4a**–**b** were carried out by procedures similar to that described above, except that no silica gel was added in the reaction of methanesulfonic acid and two drops of 40% HBF₄ were added in place of silica gel in the reaction of methanol; reaction times and yields are shown in Table III, and physical and analytical data for the products are listed in Table V.

Method B: A mixture of **4a** (80 mg, 0.4 mmol) and AcOH (12 mg, 0.2 mmol) was refluxed in CHCl₃ (2 ml) for 4 h. Compound **5a** was observed as the sole product by thin-layer chromatography, and the yield (90%) was determined by the titration method as reported previously.³⁾

The microscale reaction of AcOH with **4b**–**f** was carried out by the same procedure. Yields of the products were as follows: 92% with **4b**; 94% with **4c**; 50% with **4d** carried out at room temperature; 90% with **4e**; 85% with **4f**.

Acknowledgement The authors are indebted to the staff of the Center for Instrumental Analysis, Hokkaido University, for elemental analyses.

References

- 1) Part II: K. Ito and J. Maruyama, *Chem. Pharm. Bull.*, **34**, 390 (1986).
- 2) N. Nimura and T. Kinoshita, *Anal. Lett.*, **13**(3A), 191 (1980); A. Takadate, T. Tahara, H. Fujino and S. Goya, *Chem. Pharm. Bull.*, **30**, 4120 (1982); Sankyo Co., Ltd., Japan Kokai Tokkyo Koho JP 60 56985 [85 56985] (1985) [*Chem. Abstr.*, **103**, 87858 (1985)].
- 3) K. Ito and J. Maruyama, *Chem. Pharm. Bull.*, **31**, 3014 (1983).
- 4) M. P. Cava, R. L. Litle and D. R. Napier, *J. Am. Chem. Soc.*, **80**, 2257 (1958).
- 5) K. Ito, J. Maruyama and T. Shimamori, *J. Heterocycl. Chem.*, **23**, 1207 (1986).

-
- 6) K. Ito and J. Sawanobori, *Synth. Commun.*, **12**, 665 (1982).
 - 7) C. A. Parker and W. T. Rees, *Analyst*, **85**, 587 (1960).
 - 8) E. Späth and O. Brunner, *Ber.*, **57B**, 1243 (1924).
 - 9) D. J. Cook, R. W. Sears and D. Dock, *Proc. Indian Acad. Sci.*, **58**, 145 (1949).
 - 10) D. J. Cook, R. S. Yungmans, T. R. Moore and B. E. Hoogenboom, *J. Org. Chem.*, **22**, 211 (1957).
 - 11) A. M. Nadzan and K. L. Reinhardt, Jr., *J. Am. Chem. Soc.*, **99**, 4647 (1977).

[Chem. Pharm. Bull.]
35(3) 1262—1265(1987)

A Convenient One-Pot Synthesis of Carboxylic Acid Anhydrides Using 1,1'-Oxalyldiimidazole¹⁾

TOKUJIRO KITAGAWA,* HIROKO KURODA, and HIDEAKI SASAKI

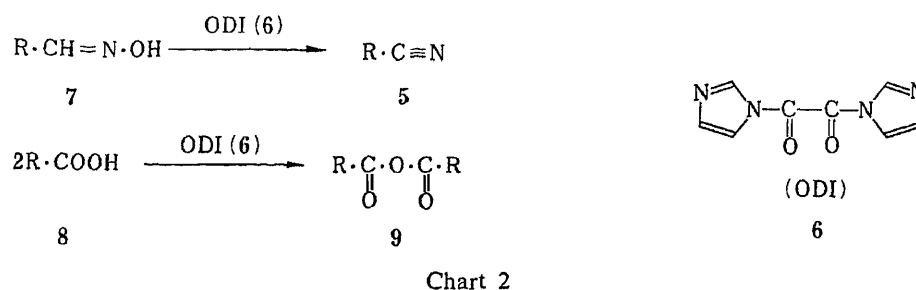
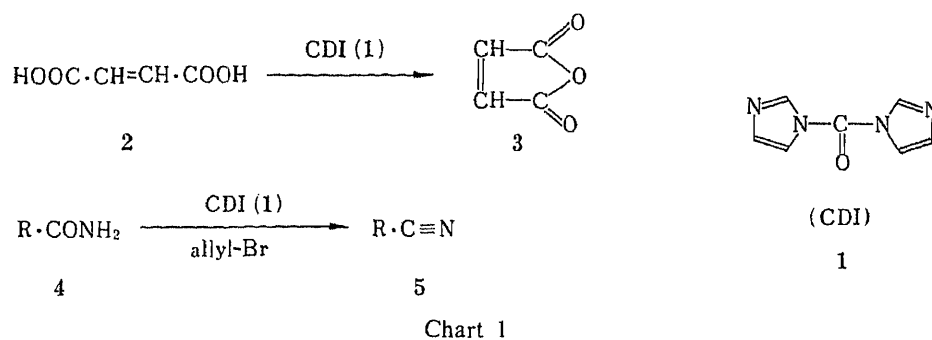
Faculty of Pharmaceutical Sciences, Kobe Gakuin University,
Ikawadani, Nishi-ku, Kobe 673, Japan

(Received July 30, 1986)

Aliphatic, aromatic, and heteroaromatic carboxylic acids (5a—i) react with 1,1'-oxalyldiimidazole (6) in acetonitrile under reflux in the presence of methanesulfonic acid (12) to give the corresponding carboxylic acid anhydrides (9a—i) in 30—98% yields.

Keywords—dehydration; carboxylic acid anhydride; *N*-acylimidazole; 1,1'-carbonyldiimidazole; 1,1'-oxalyldiimidazole

It is well known that 1,1'-carbonyldiimidazole (1)²⁾ is a useful dehydrating reagent. For example, the reaction between maleic acid (2) and 1 in tetrahydrofuran has been shown to afford maleic acid anhydride (3) in 88% yield.³⁾ More recently, Iizuka and co-workers have also reported that carboxamides (4) react with 1 in the presence of allyl bromide to give the corresponding nitriles (5) in good yield.⁴⁾ Compound 1, though commercially available, is too expensive to utilize on a large scale. Furthermore, the toxicity of phosgene, used for the preparation of 1, means that preparation of 1 in the laboratory is quite troublesome. On account of these shortcomings, we were prompted to examine the possibility that 1,1'-oxalyldiimidazole (6)⁵⁾ in place of 1 may be generally effective as a dehydration reagent. As a result of our study on the reactivity of 6, we have reported recently that 6 can be conveniently

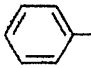
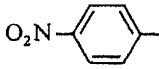
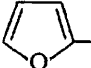
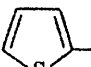
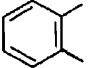
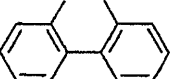


used for the dehydration of aldehyde oximes (7) to the corresponding nitriles (5) under mild and neutral conditions.⁶ As a continuation of our work on the utility of 6, we sought a convenient synthesis of carboxylic acid anhydrides (9).

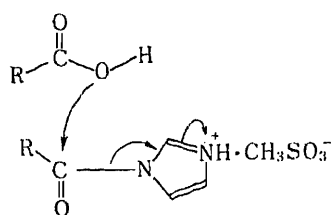
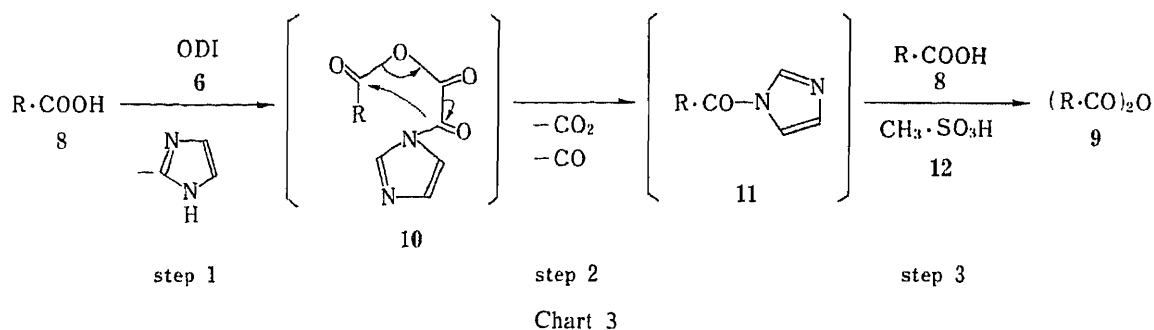
In this short communication we would like to report another successful application of a readily available dehydration reagent, 6, for the transformation of carboxylic acids (8) into 9. Thus, the reaction of benzoic acid (5b) (1 eq) with 6 (1 eq) in acetonitrile was carried out at 40°C for 2 h, with liberation of carbon dioxide and carbon monoxide, to provide the corresponding *N*-acylimidazole intermediate (11), which subsequently reacted with a second molecule of the acid 8 (1 eq) under refluxing conditions for 3 h in the presence of methanesulfonic acid (12) to afford benzoic anhydride (9b) in 98% yield. Similarly, heteroaromatic compounds, 2-furoic and 2-thenoic acids (8d and 8e) were converted to the desired carboxylic acid anhydrides (9d and 9e) in 66% and 71% yields, respectively. A dicarboxylic acid, phthalic acid (8h) was intramolecularly dehydrated with 6 to give phthalic anhydride (9h) in 84% yield. An advantage of 6 as a dehydrating reagent is that 9 can be isolated very easily; the removal of the by-products, imidazole, methanesulfonic acid, and/or imidazolium methanesulfonate is achieved simply by washing the reaction mixture with water. Representative results are summarized in Table I.

As shown in Chart 3, the reaction probably proceeds *via* the formation of a mixed acid anhydride intermediate (10) from the reaction of the carboxylic acid 8 with 6 at 40°C, and subsequently concerted eliminations of CO₂, CO, and imidazole occur to afford the corresponding *N*-acylimidazole 11 through step 2. At step 3, 11 reacts with a second molecule

TABLE I. Preparation of Carboxylic Acid Anhydrides ((RCO)₂O; 9)
Using 1,1'-Oxalyldiimidazole (ODI; 6)

Compd. No. 9a-i	R	Reaction time (h)		Yield ^{a)} (%)	mp (°C) ^{b)}		IR $\nu_{\text{max}}^{\text{KBr}} \text{ cm}^{-1}$ >C=O	
		Steps 1 and 2, at 40°C	Step 3 under reflux		Found	Reported		
a	CH ₃ (CH ₂) ₁₄ -	1	3	94	61—63 ^{c)}	62.5—63.5 ^{h)}	1803	1740
b		2	3	98	41—42 ^{d)}	41—42 ^{g)}	1788	1725
c		1	2	56	188—190 ^{f)}	189—190 ^{g)}	1797	1728
d		1	2	66	71—72 ^{f)}	71—73 ¹⁰⁾	1791	1734
e		1	2	71	59—61 ^{f)}	60.5—61.5 ¹¹⁾	1761	1701
f	-CH ₂ ·CH ₂ -	1	3	39	119—120 ^{g)}	118—119 ¹²⁾	1866	1782
g	-CH ₂ ·CH ₂ ·CH ₂ -	1	2	30	55—56 ^{h)}	52—55 ¹³⁾	1806	1755
h		2	2	84	132—133 ^{e)}	133 ^{10a)}	1854	1764
i		3	2	42	218—220 ^{e)}	217 ¹⁴⁾	1764	1734

a) Yield of the products (9a—i) after purification. Compounds (9a—i) were characterized by comparison of their melting point and IR data with those of authentic samples. b) All melting points are uncorrected. c) Recrystallized from *n*-hexane. d) Recrystallized from benzene-pet. ether. e) Recrystallized from benzene. f) Recrystallized from benzene-cyclohexane. g) Recrystallized from ethyl acetate. h) Recrystallized from ether.



of **8** in refluxing acetonitrile in the presence of **12** to provide the corresponding carboxylic acid anhydride (**9**) as the final product.

Thin layer chromatography (TLC) monitoring showed that there was no detectable benzoic anhydride **9b** when the reaction of benzoic acid (**8b**) with **6** was performed under the above-mentioned reaction conditions without **12** at step 3. This finding suggests that the formation of *N*-acylimidazolium methanesulfonate from the reaction of **11** with **12** as shown in Chart 4 is essential to enhance the leaving ability of the imidazole ring from **11**, so that concerted nucleophilic attack of **8** on the carbon atom of the acyl group of **11** can take place smoothly to form the corresponding **9**.

Thus, in conclusion 1,1'-oxalyldiimidazole (**6**) can be conveniently used for the direct conversion of carboxylic acids **8** to the corresponding carboxylic acid anhydrides **9** under mild reaction conditions.

Experimental⁷⁾

Carboxylic Acid Anhydrides (9a–e) from Monocarboxylic Acids (8a–e)—General Procedure: Compound **6** (5 mmol) was added to a solution of a carboxylic acid **8** (5 mmol) in acetonitrile (30 ml). The mixture was stirred at 40°C for the time listed in Table I (steps 1 and 2). After cooling to room temperature, the same carboxylic acid **8** (5 mmol) was further added in one portion, and a solution of **12** (10 mmol) in acetonitrile (10 ml) was added dropwise at room temperature. The resultant mixture was stirred under reflux for the time listed in Table I (step 3). On cooling to room temperature again, the mixture afforded a white precipitate. This was filtered off, and the filtrate was evaporated *in vacuo*. The residue thus obtained was poured into ice water and extracted with two 50 ml portions of ethyl acetate. The extract was washed with water, and dried over anhydrous sodium sulfate, then the organic solvent was removed *in vacuo* to give the crude product (**9**), which was further purified by recrystallization (see Table I).

Cyclic Carboxylic Acid Anhydrides (9f–i) from Dicarboxylic Acids (8f–i)—General Procedure: Compound **6** (2 mmol) was added to a solution of a dicarboxylic acid (**8**) (4 mmol) in acetonitrile (30 ml). The resultant mixture was stirred at 40°C for the time listed in Table I (steps 1 and 2), then allowed to cool to room temperature. A solution of **12** (10 mmol) in acetonitrile (10 ml) was added dropwise at room temperature. The reaction mixture was stirred under reflux for the time listed in Table I (step 3). The white precipitate was filtered off, and the filtrate was worked up as described for **9a–e** to give the crude cyclic product (**9**), which was further purified by recrystallization (see Table I).

Acknowledgment This work was supported in part by a Grant-in-Aid for Scientific Research (No. 61226013) from the Ministry of Education, Science and Culture, Japan.

References and Notes

- 1) A part of this work was presented at the Annual Meeting of the Pharmaceutical Society of Japan at Chiba, April 1986.
- 2) a) H. A. Staab and K. Wendel, *Chem. Ber.*, **93**, 2910 (1960); b) *Idem*, "Organic Syntheses," Vol. 48, ed. by P. Yates, John Wiley and Sons, Inc., New York, 1968, p. 44; c) Leading references: A. H. Staab, *Angew. Chem. Int. Ed. Engl.*, **1**, 351 (1962); S. Ohta and M. Okamoto, *Yuki Gosei Kagaku Kyokai Shi*, **41**, 38 (1983); T. Kamijio, R. Yamamoto, H. Harada, and K. Iizuka, *Chem. Pharm. Bull.*, **30**, 4242 (1982); T. Kamijio, H. Harada, and K. Iizuka, *Chem. Pharm. Bull.*, **32**, 5044 (1984).
- 3) H. A. Staab, G. Walther, and W. Rohr, *Chem. Ber.*, **95**, 2073 (1962).
- 4) T. Kamijio, H. Harada, and K. Iizuka, *Chem. Pharm. Bull.*, **32**, 2560 (1984).
- 5) 1,1'-Oxalyldiimidazole (ODI; **6**), a known compound, is easily prepared on a laboratory scale from 1-(trimethylsilyl)imidazole [L. Birkofer, P. Richter, and A. Ritter, *Chem. Ber.*, **93**, 2804 (1960)] and oxalyl chloride in benzene at room temperature [W. Walter and M. Radke, *Justus Liebigs Ann. Chem.*, **1979**, 1756].
- 6) T. Kitagawa, H. Sasaki, and N. Ono, *Chem. Pharm. Bull.*, **33**, 4014 (1985).
- 7) IR spectra were measured on a Hitachi model 270-30 infrared spectrophotometer.
- 8) Y. Kita, S. Akai, M. Yoshigi, Y. Nakajima, H. Yasuda, and Y. Tamura, *Tetrahedron Lett.*, **25**, 6027 (1984).
- 9) R. Mestres and C. Palomo, *Synthesis*, **1981**, 218.
- 10) a) J. Cabre-Castellvi, A. Palomo-Coll, and A. L. Palomo-Coll, *Synthesis*, **1981**, 616; b) H. Adkins and Q. E. Thompson, *J. Am. Chem. Soc.*, **71**, 2242 (1949).
- 11) M. C. Ford and D. Mackay, *J. Chem. Soc.*, **1957**, 4620.
- 12) L. F. Fieser and E. L. Martin, "Organic Syntheses," Coll. Vol. II, ed. by A. H. Blatt, John Wiley and Sons, Inc., New York, 1943, p. 560.
- 13) W. E. Bachmann, S. Kushner, and A. C. Stevenson, *J. Am. Chem. Soc.*, **64**, 974 (1942).
- 14) R. C. Roberts and T. B. Johnson, *J. Am. Chem. Soc.*, **47**, 1396 (1925).

[Chem. Pharm. Bull.]
35(3)1266-1269(1987)

Studies on Peptides. CXLIX.^{1,2)} Solid-Phase Synthesis of a Rabbit Stomach Peptide by Application of a New Polymer Support and a New Deprotecting Procedure

NOBUTAKA FUJII,^a YOSHIO HAYASHI,^a KENICHI AKAJI,^a SUSUMU FUNAKOSHI,^a
MASAHARU SHIMAMURA,^b SADA O YUGUCHI,^c LAWRENCE H. LAZARUS,^d
and HARUAKI YAJIMA*.^a

Faculty of Pharmaceutical Sciences, Kyoto University,^a Sakyo-ku, Kyoto 606, Japan,
Fiber Research Laboratories, Toray Industries, Inc.,^b Sonoyama, Otsu 520,
Japan, Showa Industry Co., Ltd.,^c Moriyama, Shiga 524,
Japan and National Institute of Environmental Health
Sciences,^d Research Triangle Park,
N.C. 27709, U.S.A.

(Received September 19, 1986)

A newly found rabbit stomach peptide, H-Pyr-Val-Asp-Pro-Asn-Ile-Gln-Ala-OH, was synthesized by the solid-phase method. A new polymer support, cross-linked polystyrene-polypropylene composite fiber (IONEX), was employed to facilitate multiple washing processes in chain elongation reactions. β -Cycloheptyl aspartate, Asp(OChp), was employed for the first time in this solid-phase peptide synthesis. In the final step of the synthesis, the peptide was cleaved from the resin, together with other protecting groups employed, by treatment with 1M trimethylsilyl trifluoromethanesulfonate-thioanisole in trifluoroacetic acid. The deprotected peptide was found to be identical with the sample obtained from the natural source.

Keywords—rabbit stomach peptide synthesis; new polymer support; polystyrene-polypropylene composite fiber; β -cycloheptyl aspartate; trimethylsilyl trifluoromethanesulfonate deprotection; trifluoromethanesulfonic acid deprotection

Recently, Lazarus *et al.*³⁾ isolated a physalaemin-like immunoreactive peptide from the rabbit stomach (PHLIP-8) and its sequence, H-Pyr-Val-Asp-Pro-Asn-Ile-Gln-Ala-OH, was determined by mass-spectrometric analysis. In order to confirm this sequence, we synthesized this heptapeptide by the solid phase method (Fig. 1).

General methods employed here are essentially the same as described by Merrifield.⁴⁾ However, several modifications have been made. As a support, a chloromethylated fiber-resin, cross-linked polystyrene-polypropylene composite fiber (IONEX),⁵⁾ was adopted. This fiber (Fig. 2) has a higher mechanical strength and larger surface areas per unit of weight than the usual polystyrene-divinylbenzene bead-resin and its volume is not changed by organic solvents, such as methylene chloride, DMF and MeOH. The latter property facilitates the multiple washing procedures required for solid-phase peptide synthesis. A new amino

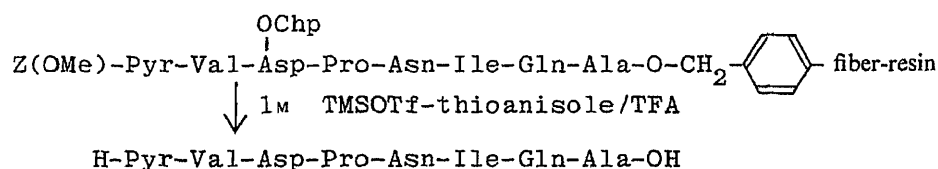


Fig. 1. Application of the TMSOTf Deprotecting Procedure to Solid-Phase Peptide Synthesis

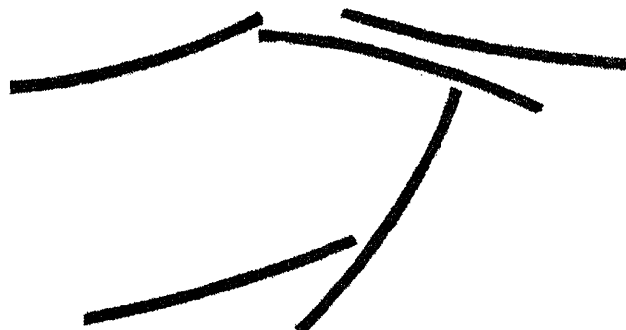


Fig. 2. Microscopic Picture of IONEX Composite Fibers

Fiber length 1 mm, diameter 35–40 μm .

acid derivative, Asp(OChp),⁶⁾ was employed for the first time in solid-phase synthesis in combination with a new deprotecting reagent. In the final step of the synthesis, the octapeptide was cleaved from the resin, together with other protecting groups, Z(OMe) and Chp, by treatment with 1 M trimethylsilyl trifluoromethanesulfonate (TMSOTf)-thioanisole/TFA.⁷⁾ Recently, we found that this reagent cleaved various Bzl and Tos-type protecting groups, and even the Chp group more readily than 1 M TFMSA-thioanisole/TFA.⁸⁾ The deprotected peptide was purified by gel-filtration, followed by preparative high performance liquid chromatography (HPLC) on a TSK-GEL LS-410KG column using isocratic elution with acetonitrile in 0.1% TFA aq. Alternatively, TFMSA deprotection was performed for comparison. The time required for TMSOTf deprotection was 60 min, while TFMSA deprotection required 120 min. The yield in the former experiment was 27.4% from the peptide resin, while that in the latter case was 15.8%. Both purified products exhibited an identical retention time, when examined by analytical HPLC on a Nucleosil 5C18 column. Identity of the synthetic peptide with the natural peptide was established by mass-fragmentation studies.³⁾

By means of the above experiments, we confirmed the sequence of the natural peptide. In addition, this is the first example of application of the TMSOTf deprotecting procedure to solid-phase peptide synthesis. Establishment of the utility of the fiber-resin will require the accumulation of further results, especially in relation to syntheses of larger and more complex peptides.

Experimental

An automated solid-phase synthesizer, Vega Biotech. Coupler 250C was employed. HPLC was conducted with a Waters 204 compact model. Optical rotation and ultraviolet (UV) absorption were measured with a Union PM 101 instrument and a Hitachi model 100-20 spectrometer, respectively. R_f values on thin layer chromatography (TLC), performed on silica gel (Kieselgel G, Merck), refer to the following solvent systems: R_{f1} *n*-BuOH-AcOH-pyridine-H₂O (4:1:1:2) and R_{f2} *n*-BuOH-AcOH-AcOEt-H₂O (1:1:1:1).

Solid-Phase Synthesis—Z(OMe)-Ala-OCH₂-fiber-resin (Ala content = 0.61 mmol/g) was prepared by coupling Z(OMe)-Ala-OH to chloromethylated IONEX (Lot. No. A-503) by the standard procedure.⁴⁾ Starting with 1.0 g of the Z(OMe)-Ala-resin, each of derivatized amino acids, corresponding to the sequence of PHLIP-8, was condensed successively onto the resin, *i.e.*, Z(OMe)-Gln-OH, Z(OMe)-Ile-OH, Z(OMe)-Asn-OH, Z(OMe)-Pro-OH, Boc-Asp(OChp)-OH, Z(OMe)-Val-OH, and Z(OMe)-Pyr-OH. The Gln and Asn residues were introduced by the Np method⁹⁾ and the rest of the residues by the symmetrical anhydride procedure.¹⁰⁾ N²-Deprotection, neutralization and washing were performed according to the schedule of Chang *et al.*¹¹⁾ Washing the resin was easily performed. Since this resin has a pale brown color, the ninhydrin¹²⁾ test was not accurate enough, so after two coupling reactions, a part of the resin was subjected to acid hydrolysis to ensure the satisfactory incorporation of the respective amino acids. Thus, 1.38 g of protected PHLIP-8-resin was obtained.



Fig. 3. HPLC of the Rabbit Stomach Peptide (PHLIP-8)

A mixture of the two samples obtained in (a) and in (b) was injected (6 μ g each).

Deprotection—(a) The peptide resin (0.1 g) was suspended in 1 M thioanisole/TFA (1 ml, 16 eq), and TMSOTf (to a final concentration of 1 M) and *m*-cresol (0.19 ml, 30 eq) were added. The mixture was stirred in an ice-bath for 60 min, then the solution was filtered and the resin was washed with TFA (2 ml). The filtrate and the washing were combined and concentrated *in vacuo* at a bath temperature below 15°C, then dry ether was added and the resulting powder was collected by centrifugation. The deprotected peptide was dissolved in ice-chilled 5% NH_4OH (2 ml) containing NH_4F (10 eq) at pH 8.0 to ensure the hydrolysis of trimethylsilyl compounds. After 10 min, the solution was neutralized with 1 N AcOH and applied to a column of Sephadex G-10 (2.8 \times 85 cm), which was eluted with 0.01 M NH_4HCO_3 buffer (pH 7.8). The solvent of the desired fractions (10.5 ml each, tube Nos. 19–26, monitored by using the Folin-Lowry test¹³) was removed by lyophilization to give a fluffy powder; yield 25 mg (47%). Subsequent purification of the crude product (6 mg each) was performed by reverse-phase HPLC on a TSK-GEL LS-410KG column (21.5 \times 300 mm), by isocratic elution with 17% acetonitrile in 0.1% TFA aq. at a flow rate of 6.0 ml/min. The eluate corresponding to the main peak (retention time of 40.2 min, monitored by UV absorption measurement at 233 nm) was collected. The rest of the sample was similarly purified and the solvent of the combined eluates was removed by lyophilization to give a white fluffy powder; yield 14.5 mg (27.4%, based on the starting loading of Ala onto the resin); $[\alpha]_D^{30} - 114.6^\circ$ ($c=0.1$, 0.01 M NH_4HCO_3), a single spot on TLC, R_f 0.36, R_f 0.48. HPLC on a Nucleosil 5C18 column (4 \times 150 mm), with 17% acetonitrile in 0.1% TFA aq. as the mobile phase at a flow rate of 0.8 ml/min, resulted in a single peak with a retention time of 9.5 min. Amino acid ratios in a 6 N HCl hydrolysate (numbers in parentheses are theoretical): Asp 1.96 (2), Glu 1.94 (2), Pro 0.93 (1), Ala 1.00 (1), Ile 0.97, Val 0.94 (recovery of Ala, 81%).

(b) The peptide resin (0.50 g) suspended in 1 M thioanisole/TFA (10 ml) was similarly treated with TFMSA (to a final concentration of 1 M) in the presence of *m*-cresol (0.5 ml, 30 eq) in an ice-bath for 60 min, then at room temperature for 60 min. The deprotected peptide was treated with 5% NH_4OH (3 ml), then purified by gel-filtration on Sephadex G-10, followed by HPLC on a TSK-GEL LS-410KG column as described above; yield 41.8 mg (15.8% from the peptide resin); R_f and R_f were identical with those of the sample obtained in (a). A mixture of the samples obtained in (a) and (b) emerged from a Nucleosil 5C18 column (4 \times 150 mm) as a single peak (retention time, 9.5 min), when eluted with 17% acetonitrile in 0.1% TFA aq. at a flow rate of 0.8 ml/min (Fig. 3). Synthetic PHLIP-8 yielded a mass fragmentation pattern identical with that of the natural peptide as reported.³) Amino acid ratios in a 6 N HCl hydrolysate: Asp 2.04, Glu 1.94, Pro 1.05, Ala 1.00, Ile 0.96, Val 0.94, (recovery of Ala, 88%). *Anal.* Calcd for $\text{C}_{37}\text{H}_{58}\text{N}_{10}\text{O}_{14} \cdot \text{H}_2\text{O}$: C, 50.21; H, 6.83; N, 15.82. Found: C, 50.42; H, 6.70; N, 16.08.

References and Notes

- 1) Part CXLVIII: N. Fujii, O. Ikemura, S. Funakoshi, H. Matsuo, T. Segawa, Y. Nakata, A. Inoue, and H. Yajima, *Chem. Pharm. Bull.*, **35**, 1076 (1987).
- 2) The following abbreviations are used: Bzl=benzyl, Z(OMe)=*p*-methoxybenzyloxycarbonyl, Pyr=pyroglutamyl, Chp=cycloheptyl, DMF=dimethylformamide, TFA=trifluoroacetic acid, TFMSA=trifluoromethanesulfonic acid.
- 3) W. E. Wilson, D. J. Harvan, C. Hamm, L. H. Lazarus, D. G. Klapper, H. Yajima, and Y. Hayashi, *Int. J. Peptide Protein Res.*, **28**, 58 (1986).
- 4) R. B. Merrifield, *J. Am. Chem. Soc.*, **85**, 2149 (1963).
- 5) T. Yoshioka and M. Shimamura, *Bull. Chem. Soc. Jpn.*, **56**, 3726 (1983); *idem, ibid.*, **57**, 334 (1984); *idem, ibid.*, **59**, 77, 399 (1986); T. Yoshioka, *ibid.*, **58**, 2618 (1985).
- 6) N. Fujii, M. Nomizu, S. Futaki, A. Otaka, S. Funakoshi, K. Akaji, K. Watanabe, and H. Yajima, *Chem. Pharm. Bull.*, **34**, 864 (1986).
- 7) N. Fujii, A. Otaka, O. Ikemura, K. Akaji, S. Funakoshi, Y. Hayashi, Y. Kuroda, and H. Yajima, *J. Chem. Soc., Chem. Commun.*, in press.

-
- 8) H. Yajima, N. Fujii, H. Ogawa, and H. Kawatani, *J. Chem. Soc., Chem. Commun.*, **1974**, 107; H. Yajima and N. Fujii, "The Peptides, Analysis, Synthesis, Biology," Vol. 5, ed. by E. Gross and J. Meienhofer, Academic Press, New York, 1983, p. 65.
 - 9) M. Bodanszky and V. du Vigneaud, *J. Am. Chem. Soc.*, **81**, 5688 (1959).
 - 10) J. Blake and C. H. Li, *Int. J. Peptide Protein Res.*, **7**, 495 (1975).
 - 11) J. K. Chang, M. Shimizu, and S. S. Wang, *J. Org. Chem.*, **41**, 3255 (1976).
 - 12) E. Kaiser, R. L. Colescott, C. D. Bossinger, and P. I. Cook, *Anal. Biochem.*, **34**, 595 (1951).
 - 13) O. H. Lowry, N. J. Rosebrough, A. L. Farr, and R. J. Randall, *J. Biol. Chem.*, **193**, 265 (1951).

[Chem. Pharm. Bull.]
[35(3)1270—1274(1987)]

Synthesis and Biological Activities of 2,3-Dimethyl-1,4-benzoquinones Having Alkylthio and Arylthio Side Chains

KOICHI MORI,* KYOKO TAKAHASHI, TAKEO KISHI
and HIROTERU SAYO

Faculty of Pharmaceutical Sciences, Kobe-Gakuin University,
Ikawadani, Nishi-ku, Kobe 673, Japan

(Received August 25, 1986)

New 2,3-dimethyl-1,4-benzoquinones having an alkylthio or arylthio side chain at the 5-position and two alkylthio side chains at the 5- and 6-position were synthesized as possible antimetabolites of coenzyme Q. These compounds were tested for inhibition of coenzyme Q in mitochondrial succinoxidase and reduced nicotinamide adenine dinucleotide (NADH)-oxidase systems, and were found to show greater inhibition of the NADH-oxidase system than of the succinoxidase system. 5,6-Di-octylthio-2,3-dimethyl-1,4-benzoquinone showed greater inhibitory activities than 5-alkylthio-2,3-dimethyl-1,4-benzoquinones. 5-Arylthio-2,3-dimethyl-1,4-benzoquinones showed potent inhibitory activities towards both enzyme systems.

Keywords—coenzyme Q analog; 5-alkylthio-2,3-dimethyl-1,4-benzoquinone; 5-arylthio-2,3-dimethyl-1,4-benzoquinone; succinoxidase; NADH-oxidase; 5,6-dialkylthio-2,3-dimethyl-1,4-benzoquinone

Coenzyme Q (ubiquinone, CoQ) has a 2,3-dimethoxy-5-methyl-6-multiprenyl-1,4-benzoquinone structure, and has been reported to play an important role in the electron transport system in the mitochondria. Many kinds of coenzyme Q analogs that act as antagonists have been synthesized.¹⁻¹⁰⁾ They inhibit succinoxidase and reduced nicotinamide adenine dinucleotide (NADH)-oxidase *in vitro* and show antitumor activity *in vivo*.^{4,5)} Alkyl- or arylthio derivatives of 2,3-dimethoxy-1,4-benzoquinone,^{6,7)} 5-methyl-2,3-dimethoxy-1,4-benzoquinone,^{6,8)} 2-hydroxy-1,4-naphthoquinone,⁹⁾ and 6-hydroxy-quinolinequinone¹⁰⁾ were obtained by the reaction of quinones with thiols in ethanol. Studies of the biological activities of these analogs have indicated that an alkylthio side chain with a long carbon chain and an arylthio side chain are the effective substituents of CoQ antagonists. This paper describes the synthesis and biological activities of new 2,3-dimethyl-1,4-benzoquinones having an alkylthio or arylthio side chain at the 5-position and two alkylthio side chains at the 5- and 6-positions.

Results and Discussion

Synthesis of 2,3-Dimethyl-1,4-benzoquinones Having Alkylthio and Arylthio Side Chains

New 5-alkylthio and 5-arylthio-2,3-dimethyl-1,4-benzoquinones were prepared by treat-

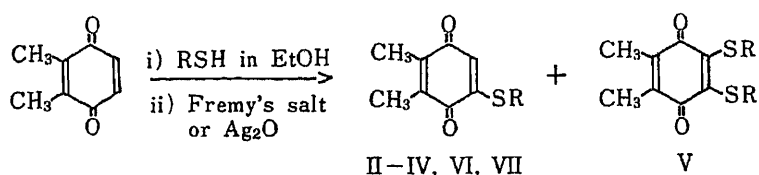


Chart 1

ing 2 eq of 2,3-dimethyl-1,4-benzoquinone (I) in ethanol with a hexane solution of 1 eq of the alkyl or arylthiol by the method shown in Chart 1. The addition of the thiol to the quinone (I) proceeded readily, and the reaction mixture containing the alkylthio- or arylthio-hydroquinone was oxidized with Fremy's salt to give the quinone (II—IV, VI, or VII). The

TABLE I. Effects of Quinones on Succinoxidase and NADH-Oxidase Activities in Beef Heart Mitochondria

Compd. (No.)	Succinoxidase			NADH-oxidase		
	Concentration ^{a)}	Relative enzyme activity ^{b)}	Antimetabolite CoQ index ^{c)}	Concentration ^{a)}	Relative enzyme activity ^{b)}	Antimetabolite CoQ index ^{c)}
None	—	100	—	—	100	—
Standard	6	55		4	61	
inhibitor ^{d)}	8	56	5	6	54	4
	10	49		8	41	
5-RS-2,3-Dimethyl-1,4-benzoquinones						
R						
<i>n</i> -C ₁₈ H ₃₇ (II)	500	95		100	95	
			> 287	200	88	> 291
				500	78	
<i>n</i> -C ₁₂ H ₂₅ (III)	500	84		250	51	
	1000	83	> 575	500	42	151
				1000	38	
<i>n</i> -C ₈ H ₁₇ (IV)	250	73		10	76	
	500	62	552	50	70	105
	1000	49		250	42	
				400	10	
Di- <i>n</i> -C ₈ H ₁₇ (V)	100	69		50	83	
	500	54	345	100	65	87
	1000	40		250	28	
β -C ₁₀ H ₇ (VI)	100	65		10	62	
	200	51	132	50	27	10
	500	45		100	12	
	1000	32		500	16	
C ₆ H ₅ (VII)	10	82		25	74	
	50	62		50	30	
	100	47	49	100	14	20
	500	7				
5-RS-2,3-Dimethoxy-1,4-benzoquinones ^{e)}						
R						
<i>n</i> -C ₁₈ H ₃₇	500	96		500	99	
β -C ₁₀ H ₇	1000	91	> 425	1000	98	> 567
	16	68		8	84	
	20	59	11	16	50	9
	28	46		24	33	
	40	32				
2-RS-1,4-Naphthoquinones ^{f)}						
R						
<i>n</i> -C ₁₈ H ₃₇	100	99	> 37	100	100	> 49
β -C ₁₀ H ₇	80	78		20	85	
	120	64	> 73	30	72	28
	200	57		60	48	

a) nmol in a flask. b) Percentage of specific activity in the presence of inhibitor to that of the control. c) The mark (>) means that antimetabolite CoQ index is greater than the number shown. d) 7-*n*-Dodecylthio-6-hydroxy-5,8-quinolinequinone. e) Ref. 6. f) Ref. 9.

reactions gave overall yields of 34—48% based on the amount of I. 5,6-Di-*n*-octylthio-2,3-dimethyl-1,4-benzoquinone (V) was also obtained from the reaction of I and *n*-octanethiol under similar conditions.

Inhibition of Succinoxidase and NADH-Oxidase Systems

The newly synthesized quinones were evaluated in mitochondrial succinoxidase and NADH-oxidase systems for inhibition of coenzyme Q₁₀ (CoQ₁₀). 7-*n*-Dodecylthio-6-hydroxy-5,8-quinolinequinone was used as a standard inhibitor. To compare the inhibitory activities of the quinones, the inhibitory activities are expressed as antimetabolite CoQ₁₀ indices³⁾ for approximately 50% inhibition of enzyme activity. This index is calculated on the basis of nmol of the inhibitor per nmol of CoQ₁₀. The results are summarized in Table I. It can be seen that these quinones caused a slightly greater inhibition of the NADH-oxidase system than of the succinoxidase system. A dependence of the inhibitory effects for both enzyme systems on the length of the alkylthio side chain was observed, and the 5-*n*-octylthio group was slightly more effective in both enzyme systems than *n*-dodecylthio and *n*-octadecylthio groups. Moreover, 5,6-di-*n*-octylthio-2,3-dimethyl-1,4-benzoquinone (V) showed more potent inhibitory activities than 5-alkylthio-2,3-dimethyl-1,4-benzoquinones (II—IV). Two 5-arylthio-2,3-dimethyl-1,4-benzoquinones (VI, VII) exhibited potent inhibitory activities towards both enzyme systems. On the other hand, in order to evaluate the effect of the presence of the 2,3-dimethyl group on the activities, the inhibitory effects of II and VI were compared with those of 5-*RS*-2,3-dimethoxy-1,4-benzoquinones⁶⁾ and 2-*RS*-1,4-naphthoquinones⁹⁾ (Table I). Table I shows that VI and 5- β -naphthylthio-2,3-dimethoxy-1,4-benzoquinone caused greater inhibitions of both enzyme systems than 2- β -naphthylthio-1,4-naphthoquinone. In the case of *n*-octadecylthio analogs, all three kinds of quinones showed weak inhibitory activities in both enzyme systems. From these results, it is considered that the 5-arylthio-2,3-dimethyl-1,4-benzoquinone moiety is effective for the inhibition of succinoxidase and NADH-oxidase. Further investigations should be done on shorter-chain homologs of 5,6-dialkylthio-2,3-dimethyl-1,4-benzoquinone.

Experimental

Melting points were determined on a Yanagimoto micro melting point apparatus, and are uncorrected. Infrared (IR) spectra were taken in KBr with a Hitachi 260-30 spectrophotometer. Nuclear magnetic resonance (NMR) spectra were measured with a Hitachi R-22 NMR spectrometer in CDCl₃ with tetramethylsilane (TMS) as an internal standard. Chemical shifts are given as δ values (ppm): s, singlet; t, triplet; br, broad; m, multiplet. Mass spectra (MS) were measured with a Hitachi M-60 mass spectrometer. Beef heart mitochondria were isolated by the usual procedures.¹³⁾ The final mitochondrial pellet, which was a mixture of heavy and light particles, was suspended in 0.25 M sucrose and was used immediately or kept frozen until used. Phospholipid micelles were prepared by sonication of commercial soybean phospholipids (Asolectin)¹⁴⁾ and used instead of mitochondrial phospholipids. Protein was determined by the Lowry method.¹⁵⁾ The amount of CoQ₁₀ in the mitochondrial preparation was determined by the modified Craven's assay¹⁶⁾ after extraction with pentane.¹⁷⁾ The mitochondria contained 2.61 nmol of CoQ₁₀/mg of mitochondrial protein.

Synthesis of 5-Alkylthio-2,3-dimethyl-1,4-benzoquinones (II, III)—A solution of *n*-octadecanethiol (590 mg) in *n*-hexane (20 ml) was added dropwise to a solution of I (277 mg) in EtOH (20 ml) at room temperature under stirring. After being stirred for 3 h, the reaction mixture was evaporated to dryness under reduced pressure. The residue was purified by column chromatography on silica gel with *n*-hexane–benzene (1 : 1) as the eluent. The first eluate afforded di-*n*-octadecylsulfide (424 mg). The second eluate was concentrated under reduced pressure and diluted with MeOH (10 ml). A solution of Fremy's salt (2.4 g), 1 N sodium acetate (1.4 ml) and H₂O (40 ml) was added to the MeOH solution. After being stirred for 20 min, the reaction mixture was extracted with Et₂O. The extract was concentrated to a volume of 20 ml and Ag₂O was added in order to oxidize the residual hydroquinone. The insoluble material was removed by filtration. The filtrate and the third eluate were combined and evaporated to dryness under reduced pressure. The residue was recrystallized from *n*-hexane to afford 5-*n*-octadecylthio-2,3-dimethyl-1,4-benzoquinone (II). Yield 424 mg (36.2%). NMR (CDCl₃) δ : 0.87 (3H, s, CH₂–CH₃), 1.0—1.8 (32H, br, (CH₂)₁₆), 2.02 (6H, s, CH₃ on the ring), 2.73 (2H, t, SCH₂), 6.32 (1H, s, H on the ring). Compound I (367 mg) and *n*-dodecanethiol (544 mg) were

TABLE II. Physicochemical Data for 5-RS-2,3-dimethyl-1,4-benzoquinones

Compd. No.	R	Yield (%)	mp (°C)	Formula	Analysis (%)		MS (M ⁺)	IR (cm ⁻¹ , KBr)
					Calcd	Found		
					C	H		
II	<i>n</i> -C ₁₈ H ₃₇	36.2	78.5—79	C ₂₆ H ₄₄ O ₂ S	74.23 (74.06)	10.45 (10.70)	420	2920 (C—H) 1660 (C=O)
III	<i>n</i> -C ₁₂ H ₂₅	46.4	69—70	C ₂₀ H ₃₂ O ₂ S	71.38 (71.56)	9.58 (9.79)	336	2910 (C—H) 1660 (C=O)
IV	<i>n</i> -C ₈ H ₁₇	34.7	61.5—62	C ₁₆ H ₂₄ O ₂ S	68.53 (68.33)	8.63 (8.74)	280	2920 (C—H) 1660 (C=O)
V ^{a)}	Di- <i>n</i> -C ₈ H ₁₇	6.2	31—31.5	C ₂₄ H ₄₀ O ₂ S	67.88 (67.64)	9.49 (9.63)	424	2920 (C—H) 1650 (C=O)
VI	β-C ₁₀ H ₇	48.2	123—124	C ₁₈ H ₁₄ O ₂ S	73.45 (73.25)	4.79 (4.73)	294	1665 (C=O) 1575 (C=C)
VII	C ₆ H ₅	46.5	90—91	C ₁₄ H ₁₂ O ₂ S	68.83 (68.84)	4.95 (4.68)	244	1650 (C=O) 1575 (C=C)

a) 5,6-Di-*n*-octylthio-2,3-dimethyl-1,4-benzoquinone.

reacted in a manner similar to that described for the synthesis of II to afford 5-*n*-dodecylthio-2,3-dimethyl-1,4-benzoquinone (III). However, the oxidation procedure with Ag₂O was unnecessary in this case. Yield 422 mg (46.4%). NMR (CDCl₃) δ: 0.87 (3H, s, CH₂-CH₃), 1.0—1.8 (20H, br, (CH₂)₁₀), 2.02 (6H, s, CH₃ on the ring), 2.73 (2H, t, SCH₂), 6.32 (1H, s, H on the ring). The physicochemical data are summarized in Table II.

Synthesis of 5,6-Dialkylthio-2,3-dimethyl-1,4-benzoquinone (V)—A solution of *n*-octanethiol (350 mg) in *n*-hexane (10 ml) was added dropwise to a solution of I (280 mg) in EtOH (20 ml) at room temperature under stirring. The reaction mixture was treated in the usual manner and the residue was purified by column chromatography on silica gel with *n*-hexane-benzene (1:1) as the eluent. The eluates were separated into three fractions; fraction 1 (colorless), fraction 2 (brown color), fraction 3 (brown color). Fraction 1 was concentrated to dryness to give di-*n*-octylsulfide. Fraction 2 was concentrated under reduced pressure and the residue was purified by column chromatography on alumina with *n*-hexane-benzene (3:2) as the eluent. The eluate was concentrated under reduced pressure and the residue was recrystallized from 80% EtOH to afford V. Yield 539 mg (6.2%). NMR (CDCl₃) δ: 0.87 (6H, s, CH₃), 1.0—1.8 (24H, br, (CH₂)₆), 2.01 (6H, s, CH₃), 2.73 (2H, t, SCH₂), 6.34 (1H, s, H on the ring). Fraction 3 was concentrated under reduced pressure and the residue was recrystallized from petroleum ether to afford 5-*n*-octylthio-2,3-dimethyl-1,4-benzoquinone (IV). Yield 200 mg (34.7%). NMR (CDCl₃) δ: 0.87 (3H, s, CH₂-CH₃), 1.0—1.8 (12H, br, (CH₂)₆), 2.01 (6H, s, CH₃ on the ring), 2.73 (2H, t, SCH₂), 6.34 (1H, s, H on the ring). The physicochemical data are summarized in Table II.

Synthesis of 5-Arylthio-2,3-dimethyl-1,4-benzoquinones (VI, VII)—A solution of β-naphthalenethiol (257 mg) in Et₂O (10 ml) was added dropwise to a solution of I (199 mg) in EtOH (10 ml) at room temperature under stirring. The mixture was stirred for 3 h until the solution became colorless. The reaction mixture was treated in the usual manner and the residue was purified by column chromatography on silica gel with benzene-*n*-hexane (1:1) as the eluent. The eluate was concentrated under reduced pressure and the residue was recrystallized from *n*-hexane to afford VI. Yield 207 mg (48.2%). NMR (CDCl₃) δ: 1.96 (3H, s, CH₃), 2.04 (3H, s, CH₃), 5.84 (1H, s, H), 7.3—8.2 (7H, m, C₁₀H₇). Compound I (241 mg) and benzenethiol (231 mg) were reacted in a manner similar to that described for the synthesis of VI to afford 5-phenylthio-2,3-dimethyl-1,4-benzoquinone (VII). Yield 201 mg (46.5%). NMR (CDCl₃) δ: 1.99 (3H, s, CH₃), 2.05 (3H, s, CH₃), 5.84 (1H, s, H), 7.45 (5H, s, C₆H₅). The physicochemical data are summarized in Table II.

Inhibition of Mitochondrial Succinoxidase and NADH-Oxidase Systems—Succinoxidase and NADH-oxidase activities were determined manometrically in a Gilson differential respirometer.¹³⁾ A total of 2.6 ml of the reaction mixture in the main compartment of each 15 ml flask contained: 1.0 ml of 0.1 M Tris-HCl buffer (pH 7.6); 0.5 ml of 1 M sucrose; 0.1 ml of 0.8 mM ethylenediaminetetraacetic acid (EDTA); 0.05 ml of Asolectin (20 mg/ml); 0.25 mg of the standard inhibitor dissolved in ethanol; 0.1 ml of 2% cytochrome c; mitochondrial enzyme (0.667 mg of protein for the succinoxidase assay and 0.659 mg of protein for the NADH-oxidase assay). Then, 0.2 ml of 0.75 M succinate or 0.075 M NADH was put in the side arm and 0.2 ml of 6 N KOH was put in the center well. The reaction was initiated by addition of the substrate from the side arm into the reaction mixture, and the activity was determined at 30 °C.

References

- 1) L. Yu, F. D. Yang and C. A. Yu, *J. Biol. Chem.*, **260**, 963 (1985).
- 2) L. Q. Gu, L. Yu and C. A. Yu, *Biochem. Biophys. Res. Commun.*, **113**, 477 (1983).
- 3) T. H. Porter and K. Folkers, *Angew. Chem. Int. Ed. Engl.*, **13**, 559 (1974).
- 4) A. Begeiter, *Biochem. Pharmacol.*, **34**, 2629 (1985).
- 5) T. H. Porter, T. Kishi and K. Folkers, *Acta Pharm. Suec.*, **16**, 74 (1979).
- 6) T. H. Porter, T. Kishi, H. Kishi and K. Folkers, *J. Bioorganic Chem.*, **7**, 333 (1978).
- 7) J. Vorkapic-Furac, T. Kishi, H. Kishi, T. H. Porter and K. Folkers, *Acta Pharm. Suec.*, **14**, 171 (1977).
- 8) R. J. Wilhelm, U. Iwamoto, C. B. Bogentoft, T. H. Porter and K. Folkers, *J. Med. Chem.*, **17**, 893 (1974).
- 9) T. H. Porter, C. S. Tsai, T. Kishi, H. Kishi and K. Folkers, *Acta Pharm. Suec.*, **15**, 97 (1978).
- 10) T. H. Porter, C. M. Bowman and K. Folkers, *J. Med. Chem.*, **16**, 115 (1973).
- 11) K. Okamoto, E. Mizuta, K. Kamiya and I. Imada, *Chem. Pharm. Bull.*, **33**, 3756 (1985).
- 12) K. Okamoto, M. Matsumoto, M. Watanabe, M. Kawada, T. Iwamoto and I. Imada, *Chem. Pharm. Bull.*, **33**, 3745 (1985).
- 13) P. V. Blair, *Methods Enzymol.*, **10**, 78 (1967).
- 14) S. Fleisher and B. Fleisher, *Methods Enzymol.*, **10**, 406 (1967).
- 15) O. H. Lowry, N. J. Rosebrough, A. L. Farr and R. J. Randall, *J. Biol. Chem.*, **193**, 265 (1951).
- 16) F. L. Crane and R. Barr, *Methods Enzymol.*, **18**, 137 (1971).
- 17) L. Szarkowska, *Arch. Biochem. Biophys.*, **113**, 519 (1966).

[Chem. Pharm. Bull.]
35(3)1275—1280(1987)]

Anti-thrombic Actions of 70% Methanolic Extract and Cinnamic Aldehyde from Cinnamomi Cortex

HIDEAKI MATSUDA,* REIKO MATSUDA, SEIYA FUKUDA,
HIDEMI SHIOMOTO, and MICHINORI KUBO

Faculty of Pharmaceutical Sciences, Kinki University, 3-4-1,
Kowakae, Higashiosaka, Osaka 577, Japan

(Received June 5, 1986)

The anti-thrombic activities of a 70% methanolic extract (CMe) from Cinnamomi Cortex on blood coagulation and fibrinolysis were investigated. CMe prevented the hepatic venous thrombosis in high butter diet-treated rats, and the decreases of blood platelets and fibrinogen in normal rats induced by endotoxin. CMe also inhibited the blood platelet aggregation induced by collagen, arachidonic acid and adenosine diphosphate (ADP) and the conversion of fibrinogen to fibrin induced by thrombin in *in vitro* experiments. Cinnamic aldehyde, a major essential oily component of CMe were showed stronger inhibitory activity than that of CMe on the blood coagulation. These results suggest that Cinnamomi Cortex has anti-thrombic activities.

Keywords—crude drug; *Cinnamomum cassia*; cinnamic aldehyde; thrombosis; blood platelet aggregation; thrombin; disseminated intravascular coagulation

Cinnamomi Cortex (the cortex of *Cinnamomum cassia* BLUME) is frequently used as a crude drug for treatment of inflammation, headache and pyrexia in the traditional Chinese system of medicine. Cinnamomi Cortex is also a main component in Keishi-Bukuryo-gan, which is used for Oketsu syndrome. We reported that Keishi-Bukuryo-gan possesses anti-thrombic activity.¹⁾ The possibility arises that Cinnamomi Cortex may be effective against disseminated intravascular coagulation (DIC).

The purpose of the present investigation was to study the preventive effect of Cinnamomi Cortex on experimental DIC induced by endotoxin in rats, as well as on blood platelet aggregation and the conversion of fibrinogen to fibrin (*in vitro* models).

Materials and Methods

Materials—A 70% methanolic extract (CMe, yield 21.6%) was prepared from Cinnamomi Cortex. The sources of other materials were as follows: cinnamic aldehyde (Kishida Chemical Co. Ltd., Japan), endotoxin (*Escherichia coli* 055: B5, Difco Lab., U.S.A.), dextran sulfate (Pharmacia Fine Chemicals, Sweden), adenosine diphosphate·2Na (ADP, Sigma Chemical Co., U.S.A.), collagen, arachidonic acid and aspirin (Sigma Chemical Co., U.S.A.).

Animals—Male Wistar-King strain rats weighing 150–200 g and male JW strain rabbits weighing 2–2.5 kg were used for the experiments. They were fed a standard diet (Nihon Clea, Japan) for a minimum period of 7 d and then fasted for 24 h before the start of the experiments.

Endotoxin-Induced DIC in High Butter Diet-Treated Rats—Endotoxin-induced DIC model was prepared according to Renaud.²⁾ Rats were fed on a high butter diet (salt-free butter (30%), cholesterol (15%) and bile powder (2 g) in a laboratory chow) for 15 weeks. CMe (200 or 500 mg/kg) was orally administered to those rats for 7 d before the intravenous injection of endotoxin (0.1 mg/kg). The animals were killed by decapitation 8 h after the injection of endotoxin, and the livers were quickly removed and subjected to microscopic examination for hepatic infarcts. The results of histological observation were rated as follows: 3, severe hepatic infarct; 2, moderate; 1, slight; 0, undetectable.

Endotoxin-Induced DIC in Normal Rats—Experimental DIC was induced by a modification of the method of

Schoendorf *et al.*³¹ CMe (50, 200 or 500 mg/kg) and cinnamic aldehyde (0.1 or 0.5 mm/kg) were administered orally to rats 1 h before the injection of endotoxin (0.1 mg/kg) into the tail vein. Blood samples were withdrawn from the heart into plastic syringes at 4 h after the injection of endotoxin, while the rats were anesthetized with pentobarbital. As anticoagulants, 0.01 M sodium ethylenediaminetetraacetic acid (EDTA) was used for platelet counts and a 1:9 volume of 3.8% sodium citrate for prothrombin time and fibrinogen determinations.

Blood platelets were counted with an automatic blood cell counter (Coulter counter, mode S-Plus, Coulter Co., U.S.A.). Fibrinogen was determined according to the method of Quick.⁴³ The prothrombin time was measured with a COAG-A-Mate dual-channel device (General Diagnostic, Warner-Lambert Co., U.S.A.). Fibrin degradation product (FDP) was determined by means of the latex aggregation test (FDPL test U, Teikoku Zoki, Japan).

Euglobulin Lysis Time (ELT) in Normal Rats—Whole blood samples were collected in plastic syringes from the heart of rats anesthetized with pentobarbital at 1 h after the oral administration of CMe (50, 200 or 500 mg/kg) or cinnamic aldehyde (0.1 or 0.5 mm/kg). One-tenth volume of 3.8% sodium citrate was added to the blood sample and the mixture was centrifuged at 4000 rpm at 4 °C for 10 min. Using the plasma thus obtained, ELT was measured in the manner reported by Kaulla and Schultz.³¹ After addition of 9.8 ml of precooled water, the plasma was incubated at 4 °C for 5 min in a stream of CO₂ gas, then centrifuged at 4000 rpm for 10 min. The resulting precipitates were dissolved in 0.7 ml of 1/15N phosphate buffer solution, then 40 μ l of thrombin solution (125 U/ml) was added. The coagulating plasma was incubated at 37 °C, and the ELT was measured.

Whole blood samples obtained from the heart at 30 min after intravenous injection of dextran sulfate (1 or 10 mg/kg) were treated in the same manner as mentioned above, and the ELT was measured.

Blood Platelet Aggregation Test—Whole blood samples were collected from pentobarbital-anesthetized rabbits. Nine ml of the blood of rabbit and 1 ml of sodium citrate (3.8%) was transferred into a plastic tube, and centrifuged at 1000 rpm for 10 min to obtain platelet-rich plasma (PRP). PRP was removed with a siliconized pipet, and stored in a plastic test tube with a screw cap. The remaining red cell precipitate of the blood samples was further centrifuged at 3000 rpm for 30 min to give platelet-poor plasma (PPP), which was used as a maximal transmittance standard.

The platelet aggregation test described by Born and Cross⁶¹ was performed with collagen (500 μ g/ml), arachidonic acid (50 mM) and ADP (2 μ M) as aggregating agents. A 0.2 ml aliquot of PRP was placed in a test tube and the content was stirred at 1200 rpm for 3 min at 37 °C, then a 10 μ l aliquot of a test solution was added. After 3 min, an aggregating agent was added to the reaction mixture. Changes in the light transmittance of the reaction mixture were continuously recorded with a Husm system platelet aggregometer (Rika Electric Co., Japan) and the transmission at the maximal aggregation after the addition of an aggregating agent was recorded. Platelet aggregation was expressed as the percent increase in the transmittance taking the transmittance of a control mixture containing no test solution as zero. An anti-platelet aggregating agent, aspirin, was used as a standard drug.

Thrombin-Induced Conversion of Fibrinogen to Fibrin—Fibrinogen (500 mg) was dissolved in 100 ml of 0.05 M NaCl containing 0.05 M Tris-acetate buffer (pH 7.4). A test solution (0.1 ml) was added to 1.8 ml of the fibrinogen solution with stirring. After 1 min, 0.1 ml of thrombin solution (0.2 U/ml) was added to the mixture and the whole was gently stirred until a fibrin clot appeared. The time required for clotting was recorded. An anti-thrombin agent, heparin, was used as a standard drug.

Results

Endotoxin-Induced DIC in High Butter Diet-Treated Rats

In high butter diet-fed rats, intravenous injection of endotoxin induced hepatic infarct



Fig. 1. Hepatic Vein Thrombosis Induced by Endotoxin (0.1 mg/kg) in a Hyperlipemic Rat

TABLE I. Effect of CMe from Cinnamomi Cortex on the Endotoxin-Induced DIC in High Butter Diet-Treated Rats

Treatment	Dose (mg/kg)	Route	No. of rats	Hepatic infarct score ^{a)}				Mean \pm S.E.
				3	2	1	0	
Control		<i>p.o.</i>	15	6	5	2	2 ^{b)}	2.0 \pm 0.3
CMe	200	<i>p.o.</i>	15	3	2	5	5	1.2 \pm 0.3
	500	<i>p.o.</i>	15	1	2	4	8	0.7 \pm 0.2 ^{c)}

Each value is the mean \pm S.E. a) Hepatic infarct score: 3, severe hepatic infarct; 2, moderate; 1, slight; 0, undetectable. b) Number of rats. c) Significantly different from the control, $p < 0.01$.

TABLE II. Effects of CMe and Cinnamic Aldehyde from Cinnamomi Cortex and Aspirin on the Endotoxin-Induced DIC in Normal Rats

Treatment	Dose	Route	No. of rats	Blood platelets ($\times 10^4/\text{mm}^3$)	Fibrinogen (mg/dl)	Prothrombin time (s)	FDP ($\mu\text{g}/\text{ml}$)
Normal		<i>p.o.</i>	10	115 \pm 4	201 \pm 20	11.6 \pm 0.2	0.1 \pm 0.1
Control		<i>p.o.</i>	10	62 \pm 7	127 \pm 21	13.9 \pm 1.0	1.6 \pm 0.4
CMe	50 (mg/kg)	<i>p.o.</i>	10	68 \pm 5	138 \pm 12	13.9 \pm 0.8	1.5 \pm 0.3
	200 (mg/kg)	<i>p.o.</i>	10	71 \pm 3	154 \pm 18	14.3 \pm 0.7	1.1 \pm 0.3
	500 (mg/kg)	<i>p.o.</i>	10	88 \pm 5	172 \pm 8 ^{a)}	13.3 \pm 0.4	1.0 \pm 0.1
Cinnamic aldehyde	0.1 (mM/kg)	<i>p.o.</i>	10	71 \pm 5	147 \pm 16	13.1 \pm 0.4	1.2 \pm 0.2
	0.5 (mM/kg)	<i>p.o.</i>	10	86 \pm 6 ^{a)}	161 \pm 5 ^{a)}	13.3 \pm 0.4	1.1 \pm 0.2
Normal		<i>p.o.</i>	10	92 \pm 12	240 \pm 17	13.4 \pm 0.3	0.3 \pm 0.1
Control		<i>p.o.</i>	10	32 \pm 4	77 \pm 12	16.9 \pm 0.5	1.9 \pm 0.5
Aspirin	0.5 (mM/kg)	<i>p.o.</i>	10	48 \pm 3 ^{a)}	108 \pm 10	15.4 \pm 1.0	1.7 \pm 0.5
	1.0 (mM/kg)	<i>p.o.</i>	10	64 \pm 3 ^{b)}	140 \pm 8 ^{b)}	14.9 \pm 0.8	1.8 \pm 0.7

Each value is the mean \pm S.E. Significantly different from the control, a) $p < 0.05$, b) $p < 0.01$.

with partial or straggling thrombus and hemorrhage (Fig. 1). Table I showed that CMe (500 mg/kg) significantly inhibited the formation of hepatic infarct in high butter diet- and endotoxin-treated rats.

Endotoxin-Induced DIC in Normal Rats

It was shown that DIC could be induced by injection of endotoxin (0.1 mg/kg) into the tail vein, resulting in decreases of blood platelets and fibrinogen, prolongation of prothrombin time and an increase of FDP. Before the injection of endotoxin, CMe (50, 200 or 500 mg/kg) or cinnamic aldehyde (0.1 or 0.5 mM/kg) was administered, and its preventive effect against the endotoxin-induced DIC was examined (Table II).

The blood platelet count was $115 \pm 4 \times 10^4/\text{mm}^3$ in normal rats injected with saline only. It was reduced to $62 \pm 7 \times 10^4/\text{mm}^3$ in rats injected with endotoxin (0.1 mg/kg). When rats were given CMe (500 mg/kg) or cinnamic aldehyde (0.5 mM/kg), the reduction of the blood platelet count by endotoxin was significantly smaller.

The level of fibrinogen was 201 ± 20 mg/dl in normal rats given saline only. The level decreased to 127 ± 20 mg/dl in DIC rats. The decrease of fibrinogen levels was significantly less in rats given CMe (500 mg/kg) or cinnamic aldehyde (0.5 mM/kg).

Prothrombin time was 11.6 ± 0.2 s in the normal rats, while it was prolonged to 13.9 ± 1.0 s in the DIC rats. No shortening of prothrombin time was observed in rats given CMe (50, 200 or 500 mg/kg) or cinnamic aldehyde (0.1 or 0.5 mM/kg), as compared with the control.

The FDP level was 0.1 ± 0.1 $\mu\text{g}/\text{ml}$ in normal rats injected with saline only. The level

TABLE III. Effects of CMe and Cinnamic Aldehyde from Cinnamomi Cortex and Dextran Sulfate on the ELT in Rats

Treatment	Dose	Route	No. of rats	ELT (min)
Normal (water)		<i>p.o.</i>	10	108 ± 13
CMe	200 (mg/kg)	<i>p.o.</i>	10	104 ± 24
	500 (mg/kg)	<i>p.o.</i>	10	110 ± 22
Cinnamic aldehyde	0.1 (mM/kg)	<i>p.o.</i>	10	99 ± 15
	0.5 (mM/kg)	<i>p.o.</i>	10	107 ± 13
Normal (saline)		<i>i.v.</i>	10	115 ± 23
Dextran sulfate	1 (mg/kg)	<i>i.v.</i>	10	62 ± 11
	10 (mg/kg)	<i>i.v.</i>	10	36 ± 4 ^{a)}

Each value is the mean ± S.E. a) Significantly different from the normal, $p < 0.01$.

TABLE IV. Effects of CMe and Cinnamic Aldehyde from Cinnamomi Cortex and Aspirin on Collagen-Induced Blood Platelet Aggregation

Treatment	Concentration	% inhibition
CMe	20 ($\mu\text{g/ml}$)	5.1
	50 ($\mu\text{g/ml}$)	13.2
	100 ($\mu\text{g/ml}$)	29.2
Cinnamic aldehyde	0.1 (mM)	0.7
	0.25 (mM)	13.1
	0.5 (mM)	55.9
	1.0 (mM)	83.3
Aspirin	0.01 (mM)	8.1
	0.05 (mM)	28.0
	0.1 (mM)	56.0
	0.2 (mM)	76.9

Each value is the mean of 5 experiments.

TABLE V. Effects of CMe and Cinnamic Aldehyde from Cinnamomi Cortex and Aspirin on Arachidonic Acid-Induced Blood Platelet Aggregation

Treatment	Concentration	% inhibition
CMe	50 ($\mu\text{g/ml}$)	7.5
	100 ($\mu\text{g/ml}$)	26.0
Cinnamic aldehyde	0.1 (mM)	3.6
	0.25 (mM)	21.2
	0.5 (mM)	53.4
	1.0 (mM)	82.9
Aspirin	0.01 (mM)	13.2
	0.025 (mM)	20.2
	0.05 (mM)	72.4
	0.1 (mM)	91.4

Each value is the mean of 5 experiments.

increased to $1.6 \pm 0.4 \mu\text{g/ml}$ in the DIC rats. When CMe (50, 200 or 500 mg/kg) or cinnamic aldehyde (0.1 or 0.5 mM/kg) was administered to rats 1 h before the injection of endotoxin, the FDP levels were not reduced.

A clear preventive effect of aspirin (used as a standard drug) was recognized on blood platelets and fibrinogen, but not on prothrombin time or FDP.

ELT in Normal Rats

As shown in Table III, ELT was 108 ± 13 min in the normal rats orally given water only. When 10 mg/kg dextran sulfate (as a standard drug) was injected into rats, the ELT was significantly shortened to 36 ± 4 min. It was not shortened when 200 or 500 mg/kg of CMe or 0.1 or 0.5 mM/kg of cinnamic aldehyde was given.

Collagen-Induced Blood Platelet Aggregation

As shown in Table IV, the incubation of CMe (50 to 100 $\mu\text{g/ml}$) with PRP weakly inhibited the blood platelet aggregation induced by collagen. Cinnamic aldehyde (1.0 mM), as well as the active control agent, aspirin, showed an inhibitory effect on blood platelet aggregation induced by collagen.

Arachidonic Acid-Induced Blood Platelet Aggregation

As shown in Table V, CMe (100 $\mu\text{g/ml}$) showed weak inhibition of arachidonic acid-

TABLE VI. Effects of CMe and Cinnamic Aldehyde from Cinnamomi Cortex and Aspirin on ADP-Induced Blood Platelet Aggregation

Treatment	Concentration	% inhibition
CMe	20 ($\mu\text{g/ml}$)	0.2
	50 ($\mu\text{g/ml}$)	8.3
	100 ($\mu\text{g/ml}$)	24.2
Cinnamic aldehyde	0.25 (mM)	9.1
	0.5 (mM)	21.9
	1.0 (mM)	44.1
Aspirin	0.5 (mM)	4.7
	1.0 (mM)	9.2

Each value is the mean of 5 experiments.

TABLE VII. Effects of CMe and Cinnamic Aldehyde from Cinnamomi Cortex and Heparin on Conversion of Fibrinogen to Fibrin Induced by Thrombin

Treatment	Concentration	Clotting time of fibrinogen (s)
Control		150 ± 3
CMe	20 ($\mu\text{g/ml}$)	154 ± 5
	50 ($\mu\text{g/ml}$)	162 ± 3^a
	100 ($\mu\text{g/ml}$)	175 ± 4^b
Cinnamic aldehyde	0.1 (mM)	158 ± 7
	0.5 (mM)	175 ± 2^b
	1.0 (mM)	181 ± 4^b
Heparin	10 (U/ml)	189 ± 3^b

Each value is the mean \pm S.E. of 5 experiments. Significantly different from the control, a) $p < 0.05$, b) $p < 0.01$.

induced blood platelet aggregation. Cinnamic aldehyde and the active control agent, aspirin, both showed potent inhibition of blood platelet aggregation induced by arachidonic acid.

ADP-Induced Blood Platelet Aggregation

As shown in Table VI, CMe (100 $\mu\text{g/ml}$) inhibited blood platelet aggregation induced by ADP. Cinnamic aldehyde also had an inhibitory effect, but aspirin did not.

Thrombin-Induced Conversion of Fibrinogen to Fibrin

As shown in Table VII, the clotting time of the control without addition of any test solution was 150 ± 3 s. The clotting time was prolonged significantly by incubation with 10 U/ml of heparin, an anti-thrombic agent, before addition of thrombin. CMe at a concentration of 50 or 100 $\mu\text{g/ml}$ inhibited the conversion of fibrinogen to fibrin. Cinnamic aldehyde at a concentration of 0.5 or 1.0 mM also significantly prolonged the clotting time.

Discussion

CMe of Cinnamic Cortex inhibited the hepatic venous thrombosis in high butter diet-treated rats, and the decreases of blood platelets and fibrinogen induced by endotoxin in normal rats. CMe also inhibited collagen-, arachidonic acid- and ADP-induced blood platelet aggregation and thrombin-induced conversion of fibrinogen to fibrin *in vitro*.

However, CMe had no effect on euglobulin lysis time in rats. Cinnamic aldehyde, major essential oily component which is contained in CMe prepared from Cinnamomi Cortex, showed greater inhibitory activity than CMe on the blood coagulation *in vitro* and endotoxin-induced DIC in normal rats.

Consequently, cinnamic aldehyde seems to be an active principle of CMe.

Among the five crude drugs (Moutan Cortex, Cinnamomi Cortex, Paeoniae Radix, Persicae Semen and Hoelen) that make up Keishi-Bukuryo-gan, Moutan Cortex extract was previously shown in exhibit anti-thrombic activity.^{7,8)} In the present study, Cinnamomi Cortex was also found to have such activity.

References

- 1) M. Kubo, H. Matsuda, T. Nagao, T. Tani, K. Namba, and S. Arichi, *Proc. Symp. WAKAN YAKU*, **16**, 171 (1983).

- 2) S. Renaud, *Angiology*, **20**, 657 (1969).
- 3) T. H. Schoendorf, M. Rosenberg, and F. K. Beller, *Am. J. Path.*, **65**, 51 (1971).
- 4) A. J. Quick, "Hemorrhagic Diseases," 1st, Lea and Febiger, Philadelphia, 1957, p. 379.
- 5) K. N. Kaulla and R. L. Schultz, *Am. J. Clin. Path.*, **29**, 104 (1958).
- 6) G. V. R. Born and M. J. Cross, *J. Physiol. (London)*, **168**, 178 (1963).
- 7) M. Kubo, H. Matsuda, S. Izumi, T. Tani, S. Arichi, M. Yoshikawa, and I. Kitagawa, *Shoyakugaku Zasshi*, **36**, 70 (1982).
- 8) M. Kubo, H. Matsuda and R. Matsuda, *Shoyakugaku Zasshi*, **38**, 307 (1984).

[Chem. Pharm. Bull.]
35(3)1281-1284(1987)

Colorimetric Determination of Salicylaldehyde with 1,3-Diphenyl-2-thiohydantoin

RIKA NONOYAMA,^a TOSHIKO NAITO,^a MIYUKI TAKAYANAGI,^b
SHOJI GOTO,^b and TAMOTSU YASHIRO*^a

*Faculty of Pharmaceutical Sciences, Nagoya City University,^a 3-1, Tanabe-dori,
Mizuho-ku, Nagoya 467, Japan and Aichi Prefecture Red Cross Blood Center,^b
3-2-2, San-nomaru, Naka-ku, Nagoya 460, Japan*

(Received September 5, 1986)

A spectrophotometric method for determination of salicylaldehyde (SA) with 1,3-diphenyl-2-thiohydantoin (DPTH) is described. The method is based on the formation of a pigment having an absorption maximum at around 510 nm from SA in acetone in the presence of sodium hydroxide. This method is simple and allows the determination of SA in the concentration range of 0.2–10 $\mu\text{M}/\text{ml}$.

Keywords—salicylaldehyde; 1,3-diphenyl-2-thiohydantoin; spectrophotometry

In the field of clinical chemistry, monoamine oxidase activity is often measured as a good indicator of liver function impairment.^{1,2)} However, the most common assay method, the benzylamine method,³⁾ is time-consuming. This method may be improved by the use of 2-hydroxybenzylamine, a benzylamine derivative. Therefore, we studied the determination of salicylaldehyde (SA) which is considered to be the product of oxidation of 2-hydroxybenzylamine by monoamine oxidase.

Many methods have been reported for the determination of SA, including those based on titrimetry,^{4,5)} chromatography,⁶⁾ gravimetry,⁷⁾ and colorimetry.⁸⁾ However, these methods have various disadvantages with regard to sensitivity or specificity, requirement of special equipment, and troublesome procedures. Among them colorimetry is the most convenient.

Recently we developed⁹⁾ an analytical method for formaldehyde using 1,3-diphenyl-2-thiohydantoin (DPTH) and sodium hydroxide. We have extended this method to the determination of SA, because it was recognized that the reaction between DPTH and formaldehyde or SA proceeded in the same manner.

Experimental

Reagents and Apparatus—SA, 2-hydroxy-3-methoxybenzaldehyde (HMBA-3), 2-hydroxy-5-methoxybenzaldehyde (HMBA-5), and 2-hydroxy-1-naphthaldehyde (HNA) were purchased from Wako Pure Chemicals (Osaka). β -Resorcyraldehyde (β -RA) and pyridoxal were from Nakarai (Kyoto) and Sigma (St. Louis), respectively. DPTH was synthesized according to the method of Shirai *et al.*¹⁰⁾ All other chemicals were of reagent grade.

DPTH solution (44 mM) was prepared by dissolving 600 mg of DPTH in 50 ml of acetone. This solution was stable for at least one week when stored at room temperature in the dark. Standard solutions used to obtain the calibration curve were prepared by diluting freshly distilled SA in ethanol, to give SA concentrations up to 10 $\mu\text{M}/\text{ml}$.

Visible adsorption spectra and absorbances were measured with a spectrophotometer (model Spectra-20, Beckman) using 10 \times 2 mm cells.

Procedure—To 2.5 ml of DPTH solution in a test tube, 1.0 ml of the test or SA standard solution, containing 0.2–10 $\mu\text{M}/\text{ml}$ of SA, and 0.3 ml of 0.17 M sodium hydroxide were added successively. The mixture was allowed to stand for 30 min at 25 \pm 5°C. To prepare the blank, the same procedure was followed except that the 1.0 ml of test sample was replaced by 1.0 ml of ethanol. The absorbances of the test, standard, and blank solutions were measured at the wavelength of 510 nm, using acetone as a reference.

Results

Optimization of the Conditions for Color Formation

Figure 1 shows the absorption spectrum of the reaction mixture at SA and DPTH. Several solvents, such as acetone, ethanol, isopropanol, and others, were examined, and acetone was selected because of the high solubility of DPTH. DPTH concentrations in the range of 22–60 mM were tested, and 44 mM gave almost maximal absorbance for SA. Sodium hydroxide was selected to facilitate the color reaction according to the literature.^{9,11} Its concentration was set at 0.17M, because sodium hydroxide was precipitated at higher concentrations.

Coloration with Other Substrates

Since other aldehydes analogous to SA were expected to be colored under the established conditions, their reactivity was tested under the standard conditions. Table I compares the absorbances of the reaction mixtures obtained. HMBA-3 and HMBA-5 gave about 65% of the absorbance of SA at the same concentration as that of SA, but the absorbances of other aldehydes were less than this. Interestingly, salicylic acid gave no absorbance.

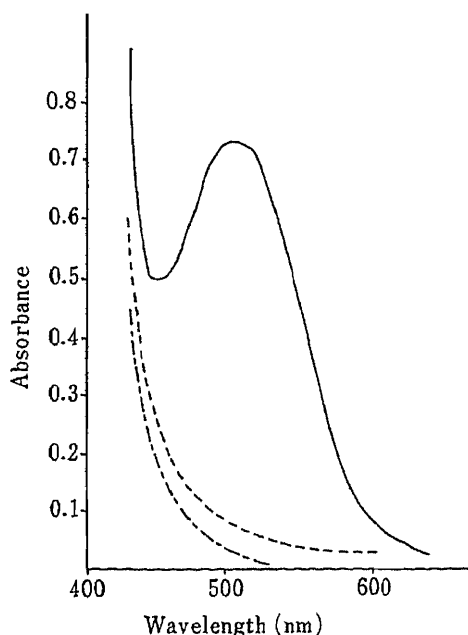


Fig. 1. Absorption Spectra of Reaction Mixtures in the Visible Region under the Proposed Conditions Using Acetone as a Reference

Salicylaldehyde concentrations were 0 (reagent blank; ----) and 6.7 (— and - - -) $\mu\text{M}/\text{ml}$. 1,3-Diphenyl-2-thiohydantoin (DPTH) was not contained in one case (· · · ·).

TABLE I. Absorbances of Reaction Mixtures Obtained from Various Aldehydes and 1,3-Diphenyl-2-thiohydantoin under the Standard Conditions

Aldehyde	Absorbance	Relative absorbance to SA (%)
2-Hydroxy-3-methoxybenzaldehyde (HMBA-3)	0.475	66
2-Hydroxy-5-methoxybenzaldehyde (HMBA-5)	0.450	63
β -Resorcyaldehyde (β -RA)	0.200	28
2-Hydroxy-1-naphthaldehyde (HNA)	0.135	19
Vaniline	0	0
Pyridoxal	0	0
Salicylaldehyde (SA)	0.720	100
Salicylic acid	0	0

Concentration of each aldehyde was 7.5 $\mu\text{M}/\text{ml}$.

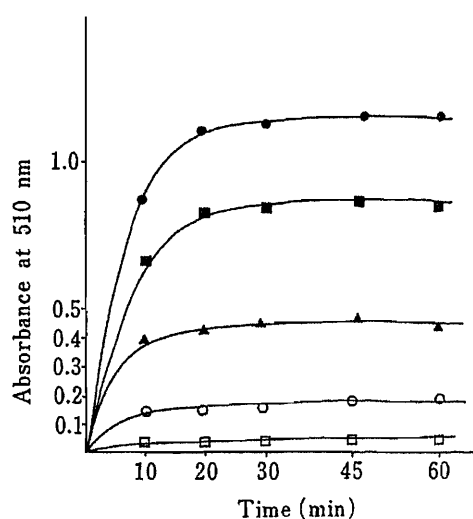


Fig. 2. Time Course of Color Formation

Salicylaldehyde concentrations were 1.0 (○), 3.8 (▲), 7.6 (□ and ■), and 10.0 (●) $\mu\text{M}/\text{ml}$. 1,3-Diphenyl-2-thiohydantoin (DPTH) was not contained in one case (□).

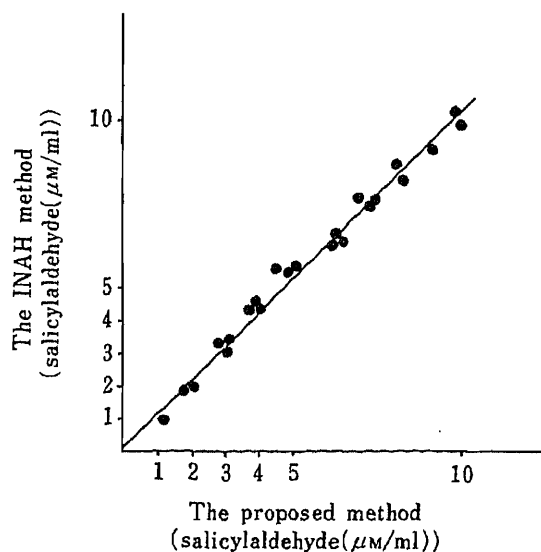


Fig. 3. Correlation between the Results Obtained by the Proposed Method and the INAH Method

TABLE II. Reproducibility and Precision of the Proposed Method for the Determination of Salicylaldehyde

	Salicylaldehyde ($\mu\text{M}/\text{ml}$)			C.V. ($\%$) ^{b)}
	Added	Measured		
		Mean	S.D. ^{a)}	
Within-assay ($n=10$)	3.8	3.6	0.1	1.8
	7.6	7.5	0.2	2.1
Between-assay ($n=14$)	3.8	3.9	0.2	4.8

a) Standard deviation. b) Coefficient of variation ($\%$).

Effect of Reaction Time

The color reaction between DPTH and SA was studied at $25 \pm 5^\circ\text{C}$. Figure 2 illustrates the time-course of coloration at $25 \pm 5^\circ\text{C}$ for various DPTH concentrations. Under the conditions mentioned above, absorbance peaked within 30 min, and remained unchanged for 30 min thereafter.

Accuracy and Precision

The calibration curve was linear in the range of 0.2–10 $\mu\text{M}/\text{ml}$ of SA, but at lower concentrations large errors were observed. The values of standard deviation, in both within- and between-assay modes are shown in Table II.

Figure 3 shows the SA concentrations of identical sample solutions, prepared by diluting freshly distilled SA in ethanol, measured by the proposed method and the isonicotinoic acid hydrazine method⁸⁾ (the INAH method), adopted because of its simplicity. The results of these two methods showed a good correlation ($n=23$, $r=0.99$), and the regression equation was $y=0.99x+0.01$.

Discussion

Recently, Sinnhuber *et al.* showed¹²⁾ that in the color reaction between 2-thiobarbituric acid (TBA) and malonaldehyde (MA), two molecules of TBA were coupled with one molecule of MA to produce the pigment. The red pigment from DPTH and formaldehyde was also considered to be produced in a similar manner.⁹⁾ The color reaction under the present conditions was presumed to proceed as follows: DPTH was coupled with SA in the presence of sodium hydroxide, and the phenolic hydrogen of the coupled compound derived from SA was removed by sodium hydroxide to give anionic-type structure which is responsible for the color.

Under the proposed conditions, SA was the most sensitive among the aldehydes examined in this study (Table I). In the absence of HMBA-3 and HMBA-5, our present method is considered to be very useful for determining the concentration of SA with good reproducibility and a simple procedure. This method may therefore be applicable to the determination of monoamine oxidase activity in the clinical field.

References

- 1) C. M. McEwen, Jr. and D. C. Harrison, *J. Lab. Clin. Med.*, **65**, 546 (1965).
- 2) C. M. McEwen, Jr. and D. O. Castell, *J. Lab. Clin. Med.*, **70**, 36 (1967).
- 3) C. M. McEwen, Jr. and J. D. Cohen, *J. Lab. Clin. Med.*, **62**, 766 (1963).
- 4) W. M. D. Bryant, J. Mitchell, Jr., and D. M. Smith, *J. Am. Chem. Sci.*, **62**, 3504 (1940).
- 5) H. R. Roe and J. Mitchell, Jr., *Anal. Chem.*, **23**, 1758 (1951).
- 6) J. H. Dhout and C. DeRooy, *Analyst*, **86**, 74 (1961).
- 7) H. A. Iddles, A. W. Low, B. D. Rosen, and R. I. Hart, *Ind. Eng. Chem. Anal. Ed.*, **11**, 102 (1939).
- 8) M. H. Hashmi, R. H. Ahmad, A. A. Ayaz, and F. Azan, *Anal. Chem.*, **37**, 1027 (1965).
- 9) M. Takayanagi, Y. Morishima, S. Goto, I. Hasegawa, T. Fukuda, M. Usami, T. Naito, and T. Yashiro, *Anal. Sci.*, **1**, 181 (1985).
- 10) H. Shirai, T. Yashiro, and I. Miwa, *Ann. Rep. Pharm. Nagoya City Univ.*, **14**, 63 (1966).
- 11) Z. A. Placer, L. L. Cushman, and B. C. Johnson, *Anal. Biochem.*, **16**, 359 (1966).
- 12) R. O. Sinnhuber, T. C. Yu, and T. H. Yu, *Food Res.*, **23**, 626 (1958).

[Chem. Pharm. Bull.]
35(3)1285—1288(1987)

The Chemical Structure of an Antitumor Polysaccharide in Mycelia of *Cochliobolus miyabeanus*

HIROAKI NANBA* and HISATORA KURODA

Laboratory of Microbiology, Kobe Women's College of Pharmacy,
Motoyama, Higashinada, Kobe 658, Japan

(Received August 27, 1986)

The chemical structure and antitumor activities of a polysaccharide from mycelia of *Cochliobolus miyabeanus* (*Ascomycetes*) were examined. The polysaccharide extracted with 4N acetic acid was purified by Sepharose CL-4B and diethylaminoethyl (DEAE)-Sepharose column chromatography; 0.3 g of this antitumor glucan (As-I) was obtained from 100 g of dried mycelia. The purified polysaccharide (As-I) contains 99.1% sugar and 0.9% protein and its molecular weight was approximately 1.2×10^6 . The chemical structure of As-I was determined by methylation, Smith degradation and carbon-13 nuclear magnetic resonance analyses. The results suggested that As-I has a 1,3-linked main chain with branches from the 6 position of some glucose residues. As-I (0.5 mg/kg/d) caused tumor growth inhibition in the allogeneic system of ICR mice-Sarcoma 180 tumor (50% inhibition ratio) when given by intraperitoneal injection.

Keywords— β -1,3 glucan; antitumor polysaccharide; antitumor activity; *Cochliobolus miyabeanus*

Antitumor polysaccharides have been found in fungi of *Basidiomycetes* spp. They are β -1,3 glucan to which β -1,6 glucan side chains are attached, and they have potent activity.¹⁻³⁾ Previously, the authors reported that a major polysaccharide in cell walls of hyphae of *Cochliobolus miyabeanus* (*Ascomycetes*) is a β -1,3 glucan with branches of 1,6-linked glucose units.⁴⁾ In this paper, a polysaccharide resembling the previous one in structure was isolated from hyphae, and its antitumor activity was evaluated.

Materials and Methods

Growth of Mycelia—The hyphae of fungi (ATCC 38724) were cultured in a potato liquid medium containing 2% sucrose. After cultivation for 148 h, the growing mycelia were collected and washed with water.

Extraction and Purification of Polysaccharide—The crushed mycelia were heated with 4N AcOH at 1.2 atmospheres pressure for 60 min in an autoclave. The supernatant was shaken with an equal volume of CHCl_3 ; MeOH (9:1) to remove protein and EtOH was added to the mixture to make a final concentration of 80%. The pellet obtained was designated as fraction A-S. A-S was purified by Sepharose CL-4B column chromatography and further purified by ion-exchange chromatography on a diethylaminoethyl (DEAE)-Sepharose CL-6B column to give two fractions. One fraction (As-I) was eluted with 0.0125 M Tris-HCl buffer (pH 7.2) and the other (As-II) with the same buffer containing 0.5 M NaCl. As-I contained less than 0.9% protein.

Methanolysis—As-I (5 mg) was dissolved in 5% MeOH-HCl, heated at 125 °C for 6 h in a sealed tube, and analyzed by gas liquid chromatography (GLC) (Shimadzu SE-30 column packing) after trimethylsilylation.

Enzymatic Analysis—As-I (1 mg/ml) and α - or β -glucosidase (1 mg/ml) prepared in 0.01 M McIlvaine buffer (pH 6.15) were incubated at 30 °C for 48 h. After removal of the enzyme protein, liberated glucose was determined by the use of glucose oxidase.

Methylation Analysis—As-I (15 mg) was methylated by Hakomori's method,⁵⁾ and the methylated product was converted into methylated alditol acetate derivatives by the conventional method and analyzed by GLC (NGS column, Shimadzu).

Nuclear Magnetic Resonance Analysis—As-I (25 mg) was dissolved in D_2O containing 0.01 N KOH and the carbon-13 nuclear magnetic resonance (^{13}C -NMR) spectrum was obtained at 40 °C with a Varian XL-200

(50.3 MHz). The INEPT method was employed for assignment.

Smith Degradation—In order to determine whether the 1,6-substituted glucose residues in the As-I glucose chain are present in the main chain or as side chains, the sample was submitted to Smith degradation. As-I (5 mg) in 20 ml of acetic acid–sodium acetate buffer (pH 4.6) and 30 ml of 0.1 M sodium metaperiodate was diluted with distilled water to make 100 ml. The solution was shaken for 144 h at 4 °C in the dark, and 1 g of sodium borohydride was added. The reaction mixture was allowed to stand for 30 min and then adjusted to pH 4.0 with 6 N acetic acid. The solution was dried and the residue was washed with MeOH. The resulting pellet was dissolved in water, adjusted to pH 1.0 with 1 N H₂SO₄ and left at 25 °C for 24 h. After neutralization, the solution was submitted to gel filtration on a Sepharose CL-4B column.

Ultracentrifugal Sedimentation Analysis—As-I was examined for homogeneity, and the sedimentation coefficient was measured, in a single sector cell by the Schlieren method with an analytical ultracentrifuge (Hitachi model 282). The sample was centrifuged at 20 °C and 60000 rpm.

Preparation of Lentinan-like Polysaccharide—The lentinan-like polysaccharide was extracted from the powdered fruit bodies of shiitake (*Lentinus edodes*) according to the method of Chihara *et al.*⁶⁾

Assay for Antitumor Activity—Sarcoma 180 tumor cells (2×10^6) were implanted subcutaneously in the right axillary region of male ICR mice (5 weeks old). The mice were given As-I intraperitoneally at various doses daily for 10 d from 24 or 216 h after tumor implantation. Tumor masses were extirpated after 28 d and weighed, and the inhibition of tumor growth was determined. Separately, ICR mice (5 weeks old) into which 2×10^6 P-388 tumor cells had been inoculated intraperitoneally, were given As-I daily for 10 d at various doses. The longevity of the treated animals was evaluated in terms of the time required for half of the animals to die.

Disk Electrophoresis of Serum—Mice were given As-I at 0.5–1.0 mg/kg/d intraperitoneally and blood was sampled from the caudal vein periodically. A 0.5 ml portion of the serum was applied to 10% polyacrylamide gel (pH 8.6) and analyzed by disc electrophoresis (5–7 mA/tube). The gel was stained with amidoschwarz 10B and examined.

Results and Discussion

The high polymer extracted with hot 4 N AcOH was chromatographed on a column of Sepharose CL-4B. Since it contained protein, the polymer fraction (M.W. approximately 1.2×10^6) was further purified on a DEAE-Sepharose CL-6B column. Two fractions, As-I and As-II, were separately eluted with 0.0125 M Tris–HCl buffer (pH 7.2) and the same buffer containing 0.5 M NaCl, respectively. As-I was further purified on the same column to remove low-molecular-weight substances. The purified As-I was proved to be homogeneous by

TABLE I. Gas Chromatographic Analysis of Methylated Alditol Acetates Derived from As-I

Sugar (as alditol acetate)	Molar ratio
1,3,5-Tri- <i>O</i> -Ac-2,4,6-tri- <i>O</i> -Me-glucitol (1,3 bond)	3.01
1,3,5,6-Tetra- <i>O</i> -Ac-2,4-di- <i>O</i> -Me-glucitol (1,3,6-bond)	1.00
1,5-Di- <i>O</i> -Ac-2,3,4,6-tetra- <i>O</i> -Me-glucitol (non-)	1.03

TABLE II. ¹³C-NMR Chemical Shifts of 1,3- and 1,6-Linked Glucans

Carbon atom	Laminarin (1,3-)	Lentinan (1,3- and 1,6-)	As-I
C-1	105.3	104.9	105.1
C-2	74.2	74.4	74.4
C-3	87.1	87.3	86.9
C-4	70.4	70.5	69.8
C-5	76.8	75.1	76.3
C-6	62.3	62.3	62.4
C-6' ^{a)}	—	70.9	71.1

a) C-6': C-6 at the branch point of β-1,3 glucosidic linkage.

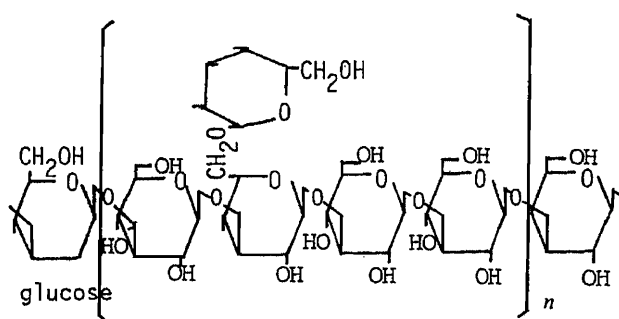


Fig. 1. Chemical Structure of (As-I) from Mycelia of *Cochliobolus miyabeanus*

TABLE III. Antitumor Activity of As-I against Sarcoma 180 in ICR (Crj: CD-1) Mice

Sample	Dose (mg/kg)	No. of mice	Average of tumor (g)	Inhibition ratio (%)
Control	—	40	7.34 ± 0.25 ^{b)}	0.0
I As-I	1.0	20	6.37 ± 0.77 ^{b)}	13.2
	0.5	26	3.69 ± 1.11 ^{c)}	49.7
	0.1	25	5.42 ± 0.96 ^{b)}	26.2
	0.5	27	4.61 ± 1.21 ^{b)}	37.1
II As-I	0.1	25	5.51 ± 0.96 ^{d)}	24.9
	1.0	20	4.29 ± 1.09 ^{b)}	41.5
I lentinan	0.5	21	4.20 ± 0.73 ^{b)}	42.8
	1.0	15	4.45 ± 1.24 ^{d)}	39.4
II lentinan	0.5	16	5.21 ± 2.01 ^{d)}	28.8

I: daily injection for 9 d from the 1st day after tumor implantation. II: daily injection for 9 d from the 9th day after tumor implantation. *t*-Test: a) $p < 0.05$, b) $p < 0.01$, c) $p < 0.001$.

ultracentrifugal analysis.

Thus, As-I is a proteoglycan consisting of 0.9% protein and 99.1% polysaccharide. The sedimentation coefficient measured in 1% solution, $s_{20,w}$, was 1.20 S. As-I was methanolized in 5% MeOH-HCl at 125°C for 6 h in a sealed tube. After methanolysis, the sample was trimethylsilylated and analyzed by GLC. Only glucose was identified, indicating that As-I is a glucan. In order to investigate the intramolecular linkages, As-I was treated with α - or β -1,3-glucanase. The glucose was liberated from this glucan only by *exo*- β -1,3 glucanase. Thus, As-I is identified as a β -glucan possessing non-reducing terminal units joining by 1,3-linkages. As-I (20 mg) was methylated thoroughly by Hakomori's method and analyzed by GLC after methanolysis. As shown in Table I, 1,3,5-tri-*O*-Ac-2,4,6-tri-*O*-Me-glucitol (arising from 1,3-disubstituted glucose), 1,3,5,6-tetra-*O*-Ac-2,4-di-*O*-Me-glucitol (from 1,3,6-trisubstituted glucose), and 1,5-di-*O*-Ac-2,3,4,6-tetra-*O*-Me-glucitol (from non-reducing terminal glucoses) were detected in the molar ratio of 3.0:1.0:1.0. This indicates that this polysaccharide comprises a β -1,3 glucan chain with 1,6-linked branches. As-I was further analyzed by ¹³C-NMR spectroscopy. As shown in Table II, the ¹³C-NMR spectrum showed a signal at 71.9 ppm, which is to be attributed to C-6' and was not found with laminarin, a β -1,3 glucan. Smith degradation did not cause a marked reduction of the molecular weight. The chemical structure illustrated in Fig. 1 is therefore proposed for As-I. This chemical structure resembles those of shizophyllan and lentinan. All these polysaccharides, however, were isolated from fungi of *Basidiomycetes*, and this is the first report of such a polysaccharide from a typical Japanese rice plant disease pathogen of *Ascomycetes*. Structurally similar polysaccharides isolated from fungi belonging to *Basidiomycetes* can inhibit the growth of not only allogeneic

tumors, but also certain types of syngeneic tumors.^{1,2,7)} First, using an allogeneic system of ICR mice-Sarcoma 180 the antitumor activity of As-I was evaluated. As shown in Table III, in mice receiving 0.5 mg/kg/d of As-I daily for 9 d, the tumor growth was inhibited by 49.7%. The inhibitory effect is comparable to that of a lentinan-like substance employed as a positive control. When the tumor-bearing mice were treated daily for 9 d from the 9th day after tumor implantation, the inhibition rate was 37.1%. However, As-I was entirely ineffective against P-388 leukemia.

These results suggest that, in general, branched β -glucans such as lentinan exert their antitumor action through activation of cellular immunity. Furthermore, serum were taken from mice at various times after injection of As-I and analyzed by polyacrylamide gel electrophoresis. As found by Chihara *et al.*,⁸⁾ LA, LC and LB proteins in the α - and β -regions of the serum increased transiently when animals were treated with lentinan, which activates cellular immunity against tumors.^{9,10)} When 0.5 mg of As-I had been administered, a new protein appeared in the position corresponding to LC protein after 48 h and the band became very marked after 72 h. The significance of the new serum protein remains to be established. In conclusion, we isolated a polysaccharide from the hyphae of *Cochliobolus miyabeanus*, (*Ascomycetes*), and showed that it has a 1,3-linked main chain with 1,6-linked branches. The antitumor activity against an allogeneic tumor is comparable to that of lentinan, a structural analogue isolated from shiitake (*Lentinus edodes*, *Basidiomycetes*).

References

- 1) G. Chihara, J. Hamuro, Y. Y. Maeda, Y. Arai and F. Fukuoka, *Nature* (London), **225**, 943 (1970).
- 2) J. Hamuro, Y. Y. Maeda, Y. Arai, F. Fukuoka and G. Chihara, *Chem. Biol. Interact.*, **3**, 69 (1971).
- 3) K. Iino, N. Ohno, I. Suzuki, T. Miyazaki, T. Yadomae, S. Oikawa and K. Sato, *Carbohydr. Res.*, **141**, 111 (1985).
- 4) H. Nanba and H. Kuroda, *Chem. Pharm. Bull.*, **22**, 1895 (1974).
- 5) S. Hakomori, *J. Biochem.* (Tokyo), **55**, 205 (1964).
- 6) G. Chihara, J. Hamuro, Y. Y. Maeda, Y. Arai and F. Fukuoka, *Cancer Res.*, **30**, 2776 (1970).
- 7) N. Komatsu, S. Okumoto, K. Kimura, G. Saito and S. Sasaki, *Gann*, **60**, 137 (1969).
- 8) Y. Y. Maeda, G. Chihara and K. Ishimura, *Nature* (London), **252**, 250 (1974).
- 9) J. Hamuro, M. Röllinghoff and G. Wagner, *Cancer Res.*, **38**, 3080 (1978).
- 10) S. Haba, T. Hamaoka, K. Takatsu and M. Kitagawa, *Int. J. Cancer*, **18**, 93 (1976).

[Chem. Pharm. Bull.]
35(3)1289—1293(1987)

Potentiating Effect of β -Glucan from *Cochliobolus miyabeanus* on Host-Mediated Antitumor Activity in Mice

HIROAKI NANBA* and HISATORA KURODA

Laboratory of Microbiology, Kobe Women's College of Pharmacy,
Motoyama, Higashinada, Kobe 658, Japan

(Received August 27, 1986)

The polysaccharide As-I, a β -1,3 glucan possessing 1,6-linked side chains, isolated from mycelia of *Cochliobolus miyabeanus* (*Ascomycetes*), inhibited the growth of Sarcoma 180 solid tumor in ICR mice. As-I also inhibited the growth of solid tumors of IMC-carcinoma in CDF₁ mice by 32% and that of solid tumors of MM-46 carcinoma in C3H mice by 99.3% at 0.1 mg/kg/d (10 times). However, As-I has no direct cytotoxic activity against tumor cells. The effect of As-I on macrophages was studied, because branched β -1,3 glucans may stimulate cellular immunity. As-I activated macrophage spreading and phagocytosis of tumor cells. Accordingly, the antitumor activity of As-I might be host-mediated, like that of other β -1,3 glucans.

Keywords—*Cochliobolus miyabeanus*; β -1,3 glucan; antitumor activity; macrophage activation; phagocytic activity

In the previous paper,¹⁾ we described the isolation of β -glucan possessing 1,6-linked side chains from the mycelia of *Cochliobolus miyabeanus* (*Ascomycetes*) and showed that it inhibited the growth of Sarcoma 180 solid tumor in ICR mice. According to Chihara *et al.*,²⁾ small doses of lentinan isolated from shiitake (*Lentinus edodes*), the chemical structure of which resembles that of this glucan, caused some regression of various syngeneic tumors in mice and its combined use with chemotherapeutic agents prolonged the survival of mice bearing syngeneic tumors. In the present investigation, the β -glucan obtained from the mycelia of *Cochliobolus miyabeanus* inhibited the growth of syngeneic tumors and activated macrophages.

Materials and Methods

Animals—Male mice of ICR (4 weeks old), C3H, CDF₁, BALB/C and C57BL/6N (6 weeks old) strains purchased from Charles River Japan were raised for 1 week before being used for tests.

Tumors—MM-46 tumor cells were transplanted into male C3H mice, IMC-carcinoma cells into CDF₁ mice, Meth-A fibrosarcoma cells into BALB/C mice, B-16 melanoma and Lewis Lung carcinoma into C57BL/6N mice and Sarcoma 180 cells into ICR mice, in the axilla. In all experiments, 2×10^6 tumor cells were transplanted s.c.

Collection of Macrophages from the Peritoneal Cavity—The peritoneal cavity of a mouse was washed with Hanks' solution and the washings were centrifuged at 1200 rpm for 10 min. Cells from the pellet were suspended in RPMI 1640 medium and 1.0×10^6 cells per well were inoculated onto a 24-well plastic plate (Linbro, Flow Lab.). The plate was incubated at 35°C in a 5% CO₂ atmosphere. As macrophages were firmly adherent after 30 min in culture, non-adherent cells were removed by washing with Hank's solution 3 times. A 1 ml portion of RPMI 1640 medium was added to each well and the macrophages were incubated in a 5% CO₂ atmosphere as above. The cells were fixed for 2 h with glutaraldehyde and 3 times more in MeOH, followed by staining with Giemsa. The number of spreading cells was determined by examining 200 cells per sample at random.³⁾ For the evaluation of phagocytic activity, 1×10^7 fluorescein-*Listeria* or latex particles were added to glass-adherent cells, and 60 min later, extracellular *Listeria* or latex particles were rinsed away with phosphate buffered saline (PBS). The number of intracellular particles per 200 cells was counted to assess the phagocytic activity.⁴⁾

Preparation of Fluorescein *Listeria*—*Listeria* were inoculated into nutrient broth medium containing 0.1 ml of fluorescein solution and cultured at 37°C for 16 h. After centrifugation (1500 rpm, 20 min), the bacterial sediment was

washed and heated at 98 °C for 15 min. The bacteria were suspended in saline.

Results and Discussion

A dose of 0.5 or 1.0 mg/kg/d of As-I was injected i.p. into mice daily for 9 d, starting at 24 h after the implantation of Sarcoma 180 tumor cells. The solid tumor masses were removed and weighed 30 d after the implantation. The extents of tumor growth inhibition were 49.7% and 26.2%, respectively, while the extent of inhibition at 0.5 mg/kg/d of lentinan was 42.8%. On the other hand, glycoprotein consisting of 61% protein and 39% glucan from mycelia showed essentially no antitumor action at 0.5 mg/kg/d.

The dependence of the antitumor effect of As-I on the period of administration was next examined. The inhibition was 51.8% when As-I was injected i.p. daily for 9 d starting at 24 h after the tumor implantation, and it was still as high as 37.1% when As-I was injected daily 9 times from 1 week after the tumor implantation. As-I, however, showed no antitumor activity at all when daily injection for 3 d was repeated 3 times at 3-d intervals after the implantation, when 4.5 mg was injected at once immediately after the implantation, or when 2.25 mg of As-I was injected twice. These results indicate that As-I should be administered (i.p.) successively for a certain period in certain doses in order to exert antitumor action.

The effects of As-I on syngeneic tumors were examined. In mice in which Meth-A fibrosarcoma (in BALB/C mice), Lewis Lung carcinoma or B-16 melanoma (in C57BL/6N mice) were implanted i.p., no prolongation of the survival was found in terms of the time required for half of the mice in a group to die. In contrast, As-I inhibited the growth of solid tumors of IMC-carcinoma in CDF₁ mice by 32% and that of solid tumors of MM-46 carcinoma in C3H mice by as much as 95.2% (25% complete regression) and 99.3% (75% complete regression) at 0.1 and 0.5 mg/kg/d, respectively as shown, in Table I. These results show that As-I is effective against some syngeneic tumors. However, the tumor growth recurred when the mice were left without treatment for 3 weeks after the disappearance of the tumor. Whether or not the antitumor activities of As-I depend on cytotoxic activity or immunostimulating activity was studied. MM-46 carcinoma cells were collected from the peritoneal cavity of tumor-bearing C3H mice and harvested by centrifugation at 1200 rpm for 10 min. Isolated tumor cells were suspended in Hanks' solution with 50 µg/ml As-I to give a concentration of 3×10^6 cells/ml. The suspension was incubated in a 5% CO₂ atmosphere for periods ranging from 0 to 90 min. After the incubation, the cells were collected and rinsed in Hanks' solution. Then 2×10^6 cells were implanted (s.c.) into C3H mice, and after 32 d the tumor mass was removed and weighed. No significant difference was observed between tumors arising from cells treated with As-I and those from intact cells receiv-

TABLE I. Antitumor Effects of As-I against Various Syngeneic Tumors

Tumor	Antitumor activity	
	Ascites type ^{a)}	Solid type ^{b)}
Meth-A fibrosarcoma in BALB/C mouse	+11.5	23.8 ^{e)}
B-16 melanoma in C57BL/6N mouse	-5.8	21.3
Lewis lung carcinoma in C57BL/6N mouse	+13.2	10.4
IMC carcinoma in CDF ₁ mouse	+17.4	32.0 ^{b)}
MM-46 carcinoma in C3H mouse	+26.8	95.2 (25% complete regression) ^{c, f)}
	+29.5	99.3 (75% complete regression) ^{d, e)}

a) ILS of median survival (%). b) Inhibition (%). c, d) As-I administered on days 1-9 (c, 0.5 mg/kg; d, 0.1 mg/kg). t-Test: e) $p < 0.05$, f) $p < 0.01$.

TABLE II. Spreading Rate of Macrophages Treated with As-I

Sample	Dose ($\mu\text{g/ml}$)	Spreading rate
Saline (control)	—	1.00
As-I	10	1.98 ^{a)}
	100	1.55 ^{b)}
Laminarin	10	1.14
	100	0.97 ^{a)}
Lentinan	10	2.17 ^{b)}
	100	1.77 ^{b)}

Spreading rate = No. of spreading cells/total cells. *t*-Test: a) $p < 0.05$, b) $p < 0.01$.

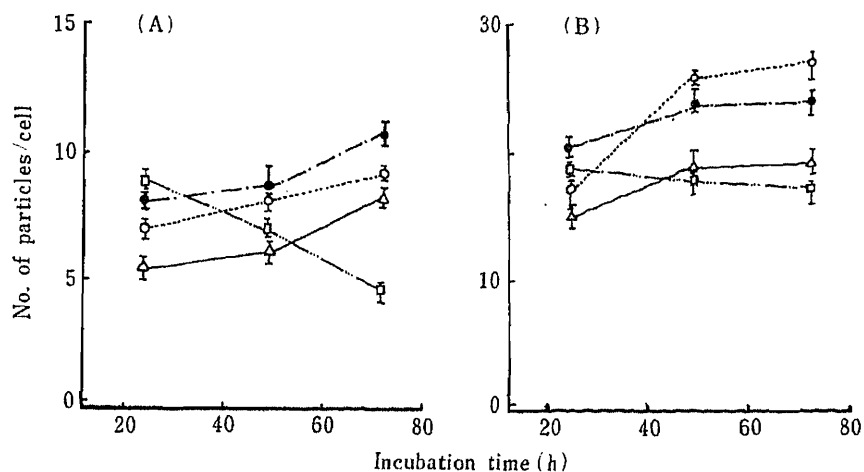


Fig. 1. Phagocytic Activities of (A) Latex Particles and (B) Fluorescein-*Listeria* by Macrophages

○, 10 $\mu\text{g/ml}$ As-I; ●, 50 $\mu\text{g/ml}$ As-I; □, 50 $\mu\text{g/ml}$ lentinan; Δ, control (saline).

ing no treatment. This indicates that tumor cells treated with As-I were capable of growing. Namely, this result suggests that As-I exerts no direct cytotoxic action against tumor cells. The effect of As-I on macrophages was next studied, because the antitumor activity of As-I required a certain period after treatment for its manifestation, and structurally related lentinan can activate cellular immunity.⁵⁻⁷⁾ The activation of macrophages was assessed in terms of spreading rate. Macrophages were collected 24 h after subcutaneous injection of As-I into the femoral region of ICR mice. The macrophages were fixed and stained, and spreading ones were counted. Being adherent to glass and extended to form a distinctive shape, activated macrophages are readily distinguishable from non-activated ones. The number of spreading macrophages approximately doubled after treatment with 10 $\mu\text{g/ml}$ As-I. Laminarin, which has no antitumor action, could not activate macrophages (Table II).

In order to determine whether the activation of macrophages involves direct action of As-I or is an indirect function mediated by other cells (*e.g.* T lymphocytes, NK cells), the effect of As-I on phagocytosis of fluorescein-*Listeria* and latex particles was studied *in vitro*. To increase the yields of macrophages, 3.0 ml of 1.5% methylcellulose (MC, 4000 cP), an inducer, was injected into the peritoneal cavity of ICR mice. In peritoneal cells harvested one day after the injection, neutrophils were dominant, while macrophages were not mature and resembled monocytes. After 3-4 d, however, the yield of mature macrophages increased to about 20 times that for untreated mice. After cultivation, the macrophages induced by methylcellulose

TABLE III. Phagocytosis of Latex Particles

Sample	Dose ($\mu\text{g/ml}$)	Phagocytic enhancement ratio (after 48 h)
Saline	—	1.00
As-I	5.0	2.04 ^{b)}
	10.0	1.31 ^{a)}
	50.0	1.40 ^{b)}
Laminarin	5.0	1.11
	10.0	0.96 ^{a)}
	50.0	1.16 ^{a)}
Lentinan	5.0	1.91 ^{b)}
	10.0	1.47 ^{b)}
	50.0	0.91 ^{a)}

t-Test: a) $p < 0.05$, b) $p < 0.01$.

TABLE IV. Phagocytosis of Latex Particles

Sample	Dose ($\mu\text{g/ml}$)	Resident M ϕ			MC-elicited M ϕ		
		Phagocytic enhancement rate (%)	$0 < X < 10^a$ (%)	$10 < X^a$ (%)	Phagocytic enhancement rate (%)	$0 < X < 10^a$ (%)	$10 < X^a$ (%)
Saline (control)	—	1.00	60.0	8.0	1.00	61.7	10.7
As-I	5.0	1.85 \pm 0.19	51.6	25.4	1.89 \pm 0.30	57.7	21.0
Laminarin	5.0	1.21 \pm 0.18	21.2	4.3	1.14 \pm 0.33	15.6	3.7
Lentinan	5.0	2.22 \pm 0.55	61.3	24.3	2.34 \pm 0.93	51.0	30.0

a) M ϕ phagocytizing 1 to 9 latex particles, or 10 or more particles.

(MC macrophages) were transferred to RPMI 1640 medium containing As-I at 1—50 $\mu\text{g/ml}$ and phagocytosis of latex particles or fluorescein-*Listeria* was assessed after incubation for 42—78 h. As shown in Fig. 1A, the phagocytosed latex particles increased in number in macrophages treated with As-I, especially after incubation for 80 h. Phagocytosis of fluorescein-*Listeria* also increased (Fig. 1B). Maximum phagocytosis was observed when 1×10^6 cells/well were exposed to As-I at 5 $\mu\text{g/ml}$ for 48 h as shown in Table III. Table IV summarizes the effects of As-I on the latex phagocytic activity of macrophages obtained without inducing agents and those induced with methylcellulose. The treatment with As-I approximately doubled (1.9) the phagocytic activity in both cases. In other words, although methylcellulose increased the yield of macrophages about 20 times, the macrophages so induced were activated by As-I just as well as those from the untreated source. When the effects of As-I on the phagocytic activity of macrophages were studied *in vivo*, macrophages were harvested 48—144 h after i.p. administration of 100 μg of As-I to ICR mice and phagocytic action towards fluorescein-*Listeria* was assessed. The phagocytosis was approximately doubled 144 h after administration of As-I, in agreement with the results obtained in the absence of T cells and complement *in vitro*. Based on these results, it is considered that As-I directly activates macrophages even in the absence of T cells and complement.^{8,9)} A non-antitumor polysaccharide, laminarin, did not exhibit such activities.

In summary, As-I, extracted from mycelia of *Cochliobolus miyabeanus* (*Ascomycetes*) and structurally similar to, but less branched than, lentinan, is able to inhibit allogeneic and syngeneic tumors *in vivo*. However, As-I did not inhibit the growth of transplants in mice when

the tumor cells to be implanted were preliminarily exposed to As-I *in vitro*. Accordingly, the antitumor activity of As-I might be host-mediated like that of lentinan. It was confirmed that in macrophages cultured after collection from the peritoneal cavity, both phagocytic activity and spreading were approximately doubled by As-I, suggesting a stimulation of non-specific phagocytic activity of macrophages *in vitro*. Moreover, macrophages harvested from the peritoneal cavity of mice treated with As-I phagocytosed latex and *Listeria* particles as effectively as those directly treated with As-I *in vitro* did. Similar results have been obtained with β -glucans extracted from fruit bodies and mycelia of *Basidiomycetes*, but such activity has not been found in polysaccharides from *Ascomycetes* except for As-I from *Cochliobolus miyabeanus*. Our next paper will deal with the effects of As-I on activated macrophages, cytotoxic cells, natural killer cells and killer cells.

References

- 1) H. Nanba and H. Kuroda, *Chem. Pharm. Bull.*, **35**, 1285 (1987).
- 2) J. Zakny, G. Chihara and J. Facht, *Int. J. Cancer*, **25**, 371 (1980).
- 3) M. Robinovitch, R. E. Manejias, M. Russo and E. E. Abbey, *Cellular Immunology*, **29**, 86 (1974).
- 4) J. Imanishi, Y. Yokota, T. Kishida, T. Mukainaka and A. Matsuo, *Acta Virol.*, **19**, 52 (1975).
- 5) J. Hamuro, M. Röllinghoff and H. Wagner, *Cancer Res.*, **38**, 3080 (1978).
- 6) J. Hamuro, M. Röllinghoff and H. Wagner, *Immunol.*, **38**, 328 (1978).
- 7) Y. Y. Maeda and G. Chihara, *Gann*, **64**, 351 (1973).
- 8) A. G. Ehlenberger and V. Nussenzweig, *J. Exp. Med.*, **145**, 375 (1977).
- 9) J. Hamuro, U. Hadding and D. Bitter-Suermann, *Immunol.*, **34**, 695 (1978).

[Chem. Pharm. Bull.]
35(3)1294—1298(1987)]

Application of Nifedipine Sustained-Release Suppositories to Healthy Volunteers¹⁾

NORIAKI OHNISHI, TERUYOSHI YOKOYAMA,* TSUNEO UMEDA,
YOSHIFUMI KIYOHARA, TSUTOMU KURODA,
YOSHIKI KITA, and KOJI KURODA

*Hospital Pharmacy, Kobe University School of Medicine,
Kusunoki-cho, Chuo-ku, Kobe 650, Japan*

(Received June 25, 1986)

Double layer suppositories (D-15) of nifedipine (NF), prepared by using a solid dispersion system of polyethylene glycol 4000 as a water-soluble carrier and cellulose acetate phthalate as a poorly water-soluble carrier, were administered to healthy volunteers, and their sustained-release characteristics, bioavailability and clinical utility were investigated. It was found that D-15 was able to maintain a therapeutically effective level of NF from 30 min to 10h without causing an excessively high peak level and offered good bioavailability. From the results of pharmacokinetic analysis by using the compartment model method, it appeared that the plasma concentration-time course after rectal administration of D-15 is satisfactorily accounted for by a one-compartment model with first-order release and absorption steps. The value of release rate constant of D-15 obtained was smaller than that of absorption rate constant, and the sustained-release effect was apparently attributed to the slow release of NF from the suppository.

The plasma level of NF rapidly decreased as removing D-15, and the plasma level showed hardly any irregularities arising from the removal and the renewal of suppositories.

Accordingly, it was concluded that D-15 is an effective sustained-release dosage form and represents a convenient mode of therapy with reduced frequency of drug administration and reduced risk of side-effects.

Keywords—nifedipine; sustained-release suppository; cellulose acetate phthalate-polyethylene glycol matrix; solid dispersion; rectal administration; pharmacokinetic analysis

Nifedipine (NF), a calcium channel blocker, is increasingly used in the treatment of hypertension and angina pectoris.²⁾ However, NF is inactivated rapidly through oxidative biotransformation, resulting in a short duration of action.³⁾ Therefore, several sustained-release dosage forms of NF have recently been developed in an attempt to reduce the frequency of drug administration and the incidence and intensity of side-effects.^{4,5)} A few studies on rectal sustained-release dosage forms of NF have been carried out.^{6,7)} Kleinbloesem *et al.*⁸⁾ reported that NF could be given rectally through an osmotic pump system at zero-order rate for 24 h.

In the previous paper,⁷⁾ we reported that double layer suppositories of NF prepared by using a solid dispersion system of polyethylene glycol 4000 (PEG) as a water-soluble carrier and cellulose acetate phthalate (CAP) as a poorly water-soluble carrier show a sustained-release effect and good bioavailability in rabbits.

In this paper, the double layer suppositories of NF reported previously⁷⁾ were administered to healthy volunteers, and their bioavailability and clinical utility were investigated.

Experimental

Materials—NF (Lot No. 2044100) was a gift from Sawai Pharmaceutical Co., Ltd. PEG and CAP were

purchased from Wako Pure Chemical Ind., Ltd. All other chemicals were reagent-grade commercial products.

Preparation of Suppositories—(1) Conventional Suppositories (C-0): C-0 was prepared by the fusion method using PEG alone as a base according to the previous paper.⁷⁾

(2) Double Layer Suppositories (D-15): D-15 was prepared by the use of 15% (w/w) CAP-PEG matrix as a base according to the previous paper.⁷⁾ D-15 included NF only in the outside layer of the suppositories.

The content of NF in all suppositories was 10 mg.

Administration Experiment—Our volunteers were five healthy men aged 25 to 43 years (mean age: 32 years) and weighing 52 to 65 kg (mean body weight: 57 kg). All volunteers gave their consent after receiving full verbal and written information about purpose and risks of the study.

Each administration experiment was performed for a group comprising three volunteers, who were randomly selected from all volunteers. The interval between the various parts of the experiment was at least 2 weeks in all volunteers. None was on any medication during the course of the experiment, and all volunteers could move around freely during the experiments.

Blood samples (3–4 ml) were drawn from a forearm vein before and at 0.5, 1, 2, 3, 4, 6, 8 and 10 h after rectal administration. The plasma was immediately separated after centrifugation and frozen at -4°C until assay.

Assay of NF—Plasma concentrations of NF were determined according to the previous paper.⁷⁾

Data Analysis—The computer simulations of plasma concentration–time courses were carried out using the MULTI program⁹⁾ with a personal computer (NEC, PC-9801VM). The nonlinear least-squares algorithm used was the Simplex method at the preliminary fitting, and the converged values were further analyzed by the modified Marquardt method.

Results and Discussion

Plasma Levels of NF after Rectal Administration

Figure 1 shows the plasma concentration–time curves of NF after rectal administration of C-0 and D-15. The absorption of NF after administration of C-0 was very fast, and the mean maximum plasma concentration was 80.1 ng/ml at 1 h. Subsequently, the plasma level declined rapidly to a value below 10 ng/ml at 8 h after administration (Fig. 1). On the other hand, the administration of D-15 resulted in a plateau plasma level in the range of 20–35 ng/ml from 30 min to 10 h (Fig. 1).

Aoki *et al.*¹⁰⁾ reported that the lowest therapeutically effective level of NF may be in the range from 20 to 30 ng/ml, and Stern *et al.*¹¹⁾ reported that the minimum toxic concentration of NF is not necessarily constant, but adverse effects such as headache and flushing may be

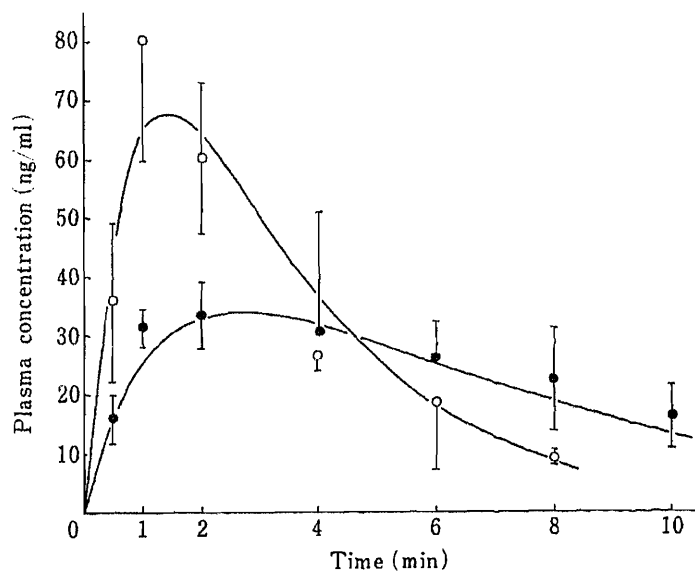


Fig. 1. Plasma Concentrations of NF after Rectal Administration of C-0 and D-15 to Healthy Volunteers

○, C-0; ●, D-15.

Each point represents the mean \pm S.D. ($n=3$).

observed at plasma concentrations exceeding 50–70 ng/ml. In our experiments, all volunteers experienced side-effects such as headache, flushing or dizziness after administration of C-0, in particular at the time of peak plasma level. However, no marked side-effects were observed during administration of D-15.

From these results, it was concluded that D-15 is a suitable dosage form for obtaining a desirable level of NF for a long time.

Pharmacokinetic Analysis

The plasma concentration–time course of NF after intravenous administration to rabbits or man follows a two-compartment model.^{3,12,13} On the other hand, it is known that the plasma concentration–time course after oral administration is consistent with a one-compartment model with a first-order absorption step because of the fusion of compartments, even though the plasma concentration–time course after intravenous administration is explained by a two-compartment model.¹⁴

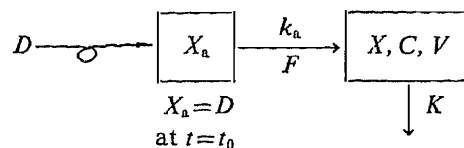
Therefore, the pharmacokinetic analysis of the plasma concentration–time course of NF after rectal administration of C-0 was performed according to a one-compartment model with a first-order absorption step, as shown in Fig. 2 (model A). The calculated plasma concentration–time curve fitted well with the observed plasma data, as can be seen in Fig. 1. These results suggest that the plasma concentration–time course after rectal administration of C-0 follows a one-compartment model with a first-order absorption step.

Furthermore, the curve fitting of the plasma concentration–time course data after rectal administration of D-15 was carried out by using a one-compartment model with two consecutive first-order steps in order to clarify the release rate of NF from a suppository, as shown in Fig. 2 (model B). The computer analysis was done by simultaneous fitting of the equation for both C-0 and D-15. The calculated plasma concentration–time curve was successfully fitted to the observed plasma data (Fig. 1). From these results, it appears that the plasma concentration–time course after rectal administration of D-15 is satisfactorily accounted for by a one-compartment model with first-order release and absorption steps. The pharmacokinetic parameters obtained are listed in Table I.

The value of absorption rate constant (k_a) or elimination rate constant (K) was not significantly different between C-0 and D-15, and the value of release rate constant (k_r) was smaller than that of k_a . From these results, it was concluded that the sustained-release effect achieved by D-15 is apparently attributable to the slow release of NF from a suppository.

model A one-compartment model with first-order absorption

$$C_p = H \cdot [e^{-K(t-t_0)} - e^{-k_a(t-t_0)}] \quad (k_a > K)$$



model B one-compartment model with two consecutive first-order input steps

$$C_p = P \cdot e^{-k_a(t-t_0')} + Q \cdot e^{-K(t-t_0')} + R \cdot e^{-k_r(t-t_0')} \\ (P+Q+R=0, k_a > K > k_r)$$

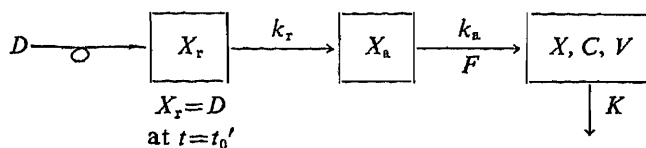


Fig. 2. Pharmacokinetic Compartment Models Used for NF

D , dose administered; F , fraction of drug absorbed; X_r , amount of drug in release site; X_a , amount of drug in absorption site; X , amount of drug in the body; C , plasma concentration of drug; V , apparent volume of distribution; k_r , release rate constant; k_a , absorption rate constant; K , elimination rate constant; t_0 , t_0' , lag time.

TABLE I. Pharmacokinetic Parameters^{a)} of NF after Rectal Administration of C-0 and D-15 to Healthy Volunteers

Parameter	C-0	D-15
Dose (mg)	10	10
Number of volunteers	3	3
Age (years)	32.0 ± 9.6	33.0 ± 9.2
Body weight (kg)	58.0 ± 6.6	55.3 ± 2.9
<i>H</i> (ng/ml)	166.2 ± 93.8	—
<i>P</i> (ng/ml)	—	4.17 ± 0.44
<i>Q</i> (ng/ml)	—	-294.3 ± 49.5
<i>R</i> (ng/ml)	—	290.2 ± 49.1
<i>k_s</i> (h ⁻¹)	1.199 ± 0.284	1.051 ± 0.072
<i>K</i> (h ⁻¹)	0.366 ± 0.035	0.402 ± 0.024
<i>k_r</i> (h ⁻¹)	—	0.288 ± 0.040
[AUC] ₀ [∞] (ng·h/ml) ^{b)}	295.0 ± 104.6	285.3 ± 51.6

a) No lag times were observed from the results of pharmacokinetic analysis. Each value represents the mean ± S.D. b) Calculated by the trapezoidal rule with extrapolation to infinity.

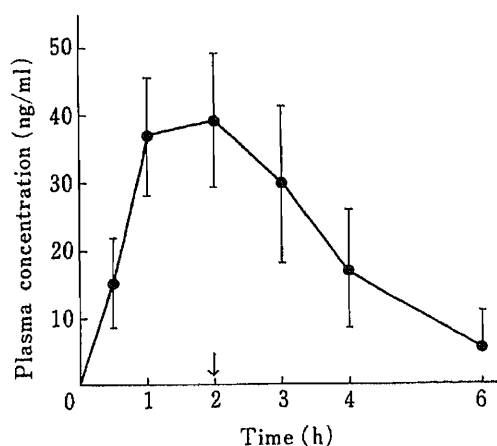


Fig. 3. Effect of Removal of D-15 on the Plasma Level of NF

The arrow shows the time of removal (↓). Each point represents the mean ± S.D. (*n* = 3).

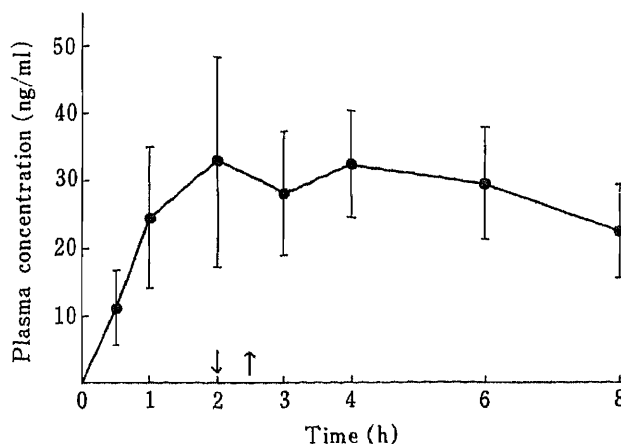


Fig. 4. Effect of Renewal of D-15 on the Plasma Level of NF

The arrows show the times of removal (↓) and reinsertion (↑). Each point represents the mean ± S.D. (*n* = 3).

On the other hand, the areas under the plasma concentration–time curves (AUC) of C-0 and D-15 were almost the same.

Removal and Renewal of D-15

One serious disadvantage of oral sustained-release preparations is the lack of flexibility on administration.¹⁵⁾ In the case of an oral sustained-release dosage form, it is difficult to respond to changes in the condition of a patient, because its action is maintained for 8–12 h once it is administered.

Figure 3 shows the effect of removal of D-15 at 2 h after administration on the plasma concentration–time course. When the suppository was removed, the plasma level of NF rapidly decreased. These results suggest that D-15 is much safer than oral sustained-release preparations.

The effect of renewal of D-15 on the plasma concentration–time course is shown in Fig. 4; *i.e.*, D-15 was removed at 2 h after administration and then a new D-15 was inserted after

30 min. The plasma level curve showed hardly any irregularity in spite of the removal and renewal of suppositories. These results indicate that, even when the suppository is eliminated due to defecation and so on, readministration of a new D-15 provides a therapeutically effective level of NF for a long time without causing an excessively high peak level. However, this dosage form might be unsuitable for patients with serious diarrhea.

In this administration experiment, no pain or discomfort in the rectal loop was encountered.

Conclusion

The rectal administration of D-15 to healthy volunteers resulted in a therapeutically effective level of NF from 30 min to 10 h without causing an excessively high peak level, and bioavailability was good. Therefore, it appears that the administration of D-15 containing 10 mg of NF will be sufficiently effective in the treatment of hypertension if D-15 is taken twice daily. In addition, this dosage form may be useful to prevent the frequent crises of angina pectoris early in the morning if D-15 is given before bedtime.

Accordingly, it was concluded that D-15 should represent a convenient mode of therapy with reduced frequency of administration and reduced risk of side-effects.

References and Notes

- 1) This paper forms Part VI of "Studies on Sustained-Release Dosage Forms." The preceding paper, Part V: N. Ohnishi, T. Yokoyama, T. Umeda, Y. Kiyohara, T. Kuroda, Y. Kita, and K. Kuroda, *Chem. Pharm. Bull.*, **34**, 2999 (1986).
- 2) G. Mabuchi, H. Kikuchi, and E. Kimura, *Shinzo*, **3**, 1352 (1971).
- 3) K. D. Raemisch and J. Sommer, *Hypertension, Supp. II*, **5II-18** (1983).
- 4) N. Kohri, K. Mori, K. Miyazaki, and T. Arita, *J. Pharm. Sci.*, **75**, 57 (1986).
- 5) A. Hasegawa, H. Nakagawa, and I. Sugimoto, *Chem. Pharm. Bull.*, **33**, 1615 (1985).
- 6) N. Hamakawa, T. Koga, K. Ushimaru, M. Gogo, and S. Sugiyama, Abstracts of Papers, the 35th Meeting of the Kinki Branch, Pharmaceutical Society of Japan, Kyoto, November 1985, p. 56.
- 7) T. Umeda, T. Yokoyama, N. Ohnishi, T. Kuroda, Y. Kita, K. Kuroda, and S. Asada, *Chem. Pharm. Bull.*, **33**, 3953 (1985).
- 8) C. H. Kleinbloesem, P. van Brummelen, J. A. van de Linde, P. J. Voogd, and D. D. Breimer, *Clin. Pharmacol. Ther.*, **36**, 396 (1984).
- 9) K. Yamaoka, Y. Tanigawara, T. Nakagawa, and T. Uno, *J. Pharmacobio-Dyn.*, **4**, 879 (1981).
- 10) K. Aoki, K. Sato, Y. Kawaguchi, and M. Yamamoto, *Eur. J. Clin. Pharmacol.*, **23**, 197 (1982).
- 11) Z. Stern, E. Zylber-Katz, and M. Levy, *Int. J. Clin. Pharmacol., Therapy and Toxicology*, **22**, 198 (1984).
- 12) C. H. Kleinbloesem, P. van Brummelen, J. A. van de Linde, P. J. Voogd, and D. D. Breimer, *Clin. Pharmacol. Ther.*, **35**, 742 (1984).
- 13) T. Kuroda, T. Yokoyama, T. Umeda, N. Ohnishi, K. Kuroda, and S. Asada, *Kobe J. Med. Sci.*, **31**, 117 (1985).
- 14) J. Zhu, K. Katayama, M. Kakemi, and T. Koizumi, *Yakugaku Zasshi*, **106**, 221 (1986).
- 15) S. Iguchi, S. Goto, K. Nagai, and S. Hayashi, "Shinsogoyakuzaigaku <II>," Ishiyakushuppan Co., Ltd., Tokyo, 1982, p. 198.

[Chem. Pharm. Bull.]
[35(3)1299—1303(1987)]

Contribution of N^4 -Acetylsulfadimethoxine to the Interaction of Sulfadimethoxine with Ketoprofen in Rabbits

YORISHIGE IMAMURA,* HIROYUKI MORI, and MASAKI OTAGIRI

Faculty of Pharmaceutical Sciences, Kumamoto University,
5-1, Oe-honnachi, Kumamoto 862, Japan

(Received August 30, 1986)

The contribution of N^4 -acetylsulfadimethoxine (N^4 -AcSDM), a major metabolite of sulfadimethoxine (SDM), to the serum protein binding and pharmacokinetic interactions between SDM and ketoprofen (KPF) was investigated in rabbits. When SDM and KPF were intravenously co-administered, KPF indirectly reduced the serum protein binding of SDM through the interaction of KPF with N^4 -AcSDM, and significantly increased the total body clearance (Cl_{tot}) and steady-state volume of distribution (V_{dss}) of SDM. In addition, the co-administration of N^4 -AcSDM was found to increase Cl_{tot} and V_{dss} of SDM. These results indicate that N^4 -AcSDM contributes substantially to the serum protein binding and pharmacokinetic interactions between SDM and KPF in rabbits.

Keywords—sulfadimethoxine; ketoprofen; drug-metabolite interaction; N^4 -acetylsulfadimethoxine; serum protein binding; pharmacokinetic parameter; protein binding displacement

Several investigators have demonstrated that a metabolite can contribute to drug-drug interaction.¹⁻³ For example, when warfarin and chloral hydrate were co-administered, a major metabolite of chloral hydrate, trichloroacetic acid, reduced the serum protein binding of warfarin and enhanced its anti-coagulant activity.¹ In addition, probenecid indirectly reduced the serum protein binding of sulfadimethoxine (SDM) through the interaction of probenecid with N^4 -acetylsulfadimethoxine (N^4 -AcSDM),² a major metabolite of SDM.⁴ However, the contribution of metabolites to drug-drug interaction has not yet been fully examined. The purpose of the present study was to elucidate the contribution of N^4 -AcSDM to the serum protein binding and pharmacokinetic interactions between SDM and ketoprofen (KPF) in rabbits.

Experimental

Materials—SDM was purchased from Daiichi Pharmaceutical Co., Tokyo. KPF was kindly supplied by Kaken Pharmaceutical Co., Tokyo. N^4 -AcSDM was synthesized from SDM by the method of Uno *et al.*⁵ All other chemicals were of reagent grade.

Animal Experiments—Male albino rabbits weighing 2.5–3.5 kg were used in a cross-over design. An interval of at least 10 d was taken to minimize the residual or cumulative effect of the preceding dose. SDM at a dose of 50 mg/kg was administered intravenously as a bolus to rabbits. KPF or N^4 -AcSDM at a dose of 25 mg/kg was administered intravenously as a bolus immediately after SDM administration. The injections of SDM, KPF and N^4 -AcSDM were prepared by dissolving the drugs in saline solution containing the same molar amount of NaOH. Blood samples were collected from the ear vein. The blood was centrifuged at 3000 rpm for 15 min and the serum or plasma was separated.

Protein Binding Experiments—*In vivo* and *in vitro* protein binding experiments were carried out by means of the ultrafiltration method described previously.⁶ The *in vivo* protein binding of SDM was determined for the serum obtained at 2 h after intravenous bolus administration of SDM alone or in combination with KPF. The *in vitro* protein binding of SDM was determined for the serum prepared by the addition of SDM with or without KPF or N^4 -AcSDM.

Pharmacokinetic Analysis—The plasma SDM concentration data were analyzed by statistical moment

analysis to obtain values for the total body clearance (Cl_{tot}) and steady-state volume of distribution (V_{dss}) of SDM according to the following equation⁷:

$$Cl_{tot} = D/AUC \quad (1)$$

$$V_{dss} = D \cdot MRT/AUC \quad (2)$$

where D is the dose, AUC is the area under the plasma SDM concentration-time curve from zero to infinite time and MRT is the mean residence time. AUC was determined by means of the trapezoidal rule until the last data point (C_t) with the area to infinity being calculated as C_t/β . The elimination rate constant (β) was obtained from the log-linear regression line of the SDM concentration time curve. The values of AUC and MRT were calculated by using a microcomputer.

Analytical Methods—SDM concentrations in serum, plasma and ultrafiltrate samples were measured by the method of Bratton and Marshall.⁸ Total SDM (SDM + metabolites) in serum was measured by the same method after hydrolysis (0.5 N HCl, 100 °C) for 1 h. N^4 -AcSDM concentration in serum or plasma was estimated by subtracting SDM from total SDM concentration, since no metabolite other than N^4 -AcSDM was detected in serum or plasma by the extraction method of Rieder.⁹

Statistical Analysis—Statistical significance of differences between means was determined by the paired Student's t -test. A p -value of 0.05 or less was considered to be significant.

Results and Discussion

Serum Protein Binding Interaction

The effect of KPF on the *in vivo* and *in vitro* bindings of SDM to rabbit serum was examined. As shown in Fig. 1, KPF markedly reduced the *in vivo* binding of SDM to rabbit serum. On the other hand, KPF had little effect on the *in vitro* binding of SDM to rabbit serum (Fig. 2). It is noteworthy that KPF reduces only the *in vivo* binding of SDM to rabbit serum.

Our previous paper²) showed that N^4 -AcSDM strongly displaces SDM from its protein binding sites. Since N^4 -AcSDM is the major metabolite of SDM in rabbits,⁴) it may contribute to the *in vivo* protein binding interaction between SDM and KPF. As shown in Fig. 3, the co-administration of KPF was found to increase the serum concentration of N^4 -AcSDM at 2 h after intravenous bolus administration of SDM. This finding implies that KPF indirectly reduces the *in vivo* serum protein binding of SDM, by causing an increase in the

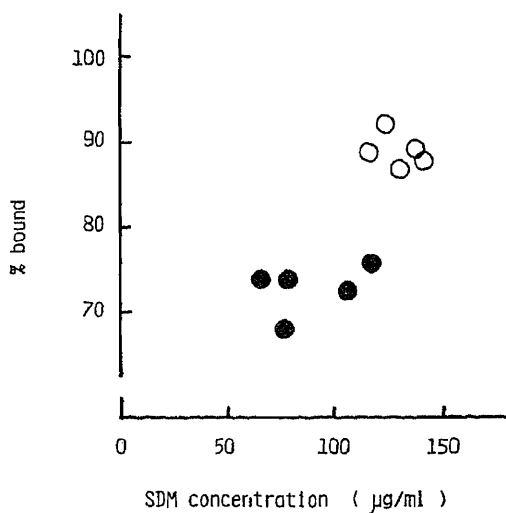


Fig. 1. Effect of KPF on the *in Vivo* Binding of SDM to Rabbit Serum

The *in vivo* protein binding of SDM was determined for the serum obtained at 2 h after intravenous bolus administration of SDM alone (O) or in combination with KPF (●).

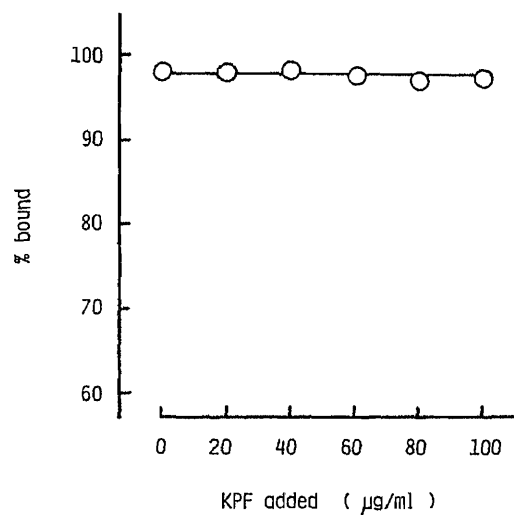


Fig. 2. Effect of KPF on the *in Vitro* Binding of SDM to Rabbit Serum

The *in vitro* protein binding of SDM was determined for the serum prepared by the addition of SDM (100 µg/ml) with or without KPF.

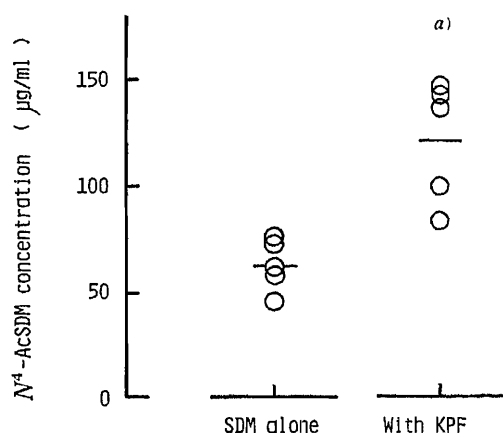


Fig. 3. Serum Concentration of N^4 -AcSDM at 2 h after Intravenous Bolus Administration of SDM Alone or in Combination with KPF to Rabbits

The horizontal bars indicate the mean values.
a) Significantly different from SDM alone ($p < 0.01$).

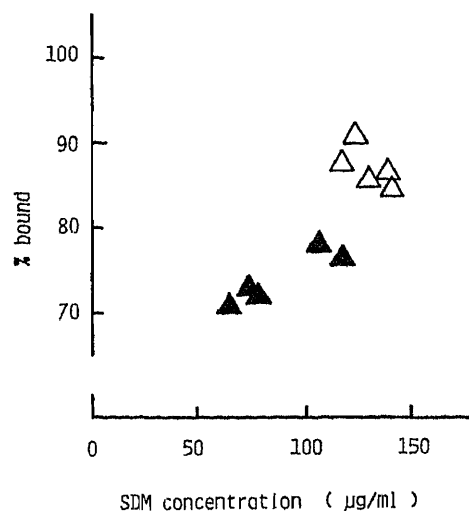


Fig. 4. *In Vitro* Binding of SDM to Rabbit Serum in the Presence of N^4 -AcSDM at the Same Concentration as that Found at 2 h after Intravenous Bolus Administration of SDM Alone (Δ) or in Combination with KPF (\blacktriangle) to Rabbits

serum concentration of N^4 -AcSDM.

To elucidate further the mechanism of the *in vivo* protein binding interaction between SDM and KPF, we examined the *in vitro* binding of SDM to rabbit serum in the presence of N^4 -AcSDM at the same concentration as that found at 2 h after intravenous bolus administration of SDM alone or in combination with KPF. As shown in Fig. 4, the *in vitro* serum protein binding of SDM in the presence of N^4 -AcSDM was closely similar to the *in vivo* serum protein binding of SDM shown in Fig. 1. Therefore, it is concluded that N^4 -AcSDM plays an important role in the *in vivo* protein binding interaction between SDM and KPF in rabbits. A similar mechanism has been observed in the *in vivo* protein binding interaction between SDM and phenylbutazone in rabbits.¹⁰⁾

It is well-known that nonsteroidal anti-inflammatory drugs such as KPF and bucolome depress the renal excretion of drugs or metabolites which are actively secreted by the tubules.^{11,12)} Since N^4 -AcSDM is actively secreted by the tubules,¹³⁾ unlike SDM, KPF may cause the increase in the serum concentration of N^4 -AcSDM by depressing its renal excretion.

Pharmacokinetic Interaction

Figure 5 shows the time course of the plasma concentrations of SDM and N^4 -AcSDM after intravenous bolus administration of SDM alone or in combination with KPF. The co-administration of KPF markedly decreased the plasma concentration of SDM, while the co-administration of KPF markedly increased the plasma concentration of N^4 -AcSDM. In addition, the pharmacokinetic parameters were derived from the SDM plasma concentration data. As shown in Table I, the co-administration of KPF significantly increased Cl_{tot} and V_{dss} of SDM. Recently, the displacement of one drug from its protein binding sites by another has been reported to induce increases in Cl_{tot} and/or V_{dss} of the drug.^{14,15)} For example, Arimori *et al.* reported that penicillins displace phenytoin from its protein binding sites, and significantly increase Cl_{tot} and V_{dss} of phenytoin.¹⁵⁾ Thus, the increases in Cl_{tot} and V_{dss} of SDM induced by KPF may be explained on the basis of the displacement of SDM from its protein binding sites by N^4 -AcSDM.

To confirm the contribution of N^4 -AcSDM to the pharmacokinetic interaction between

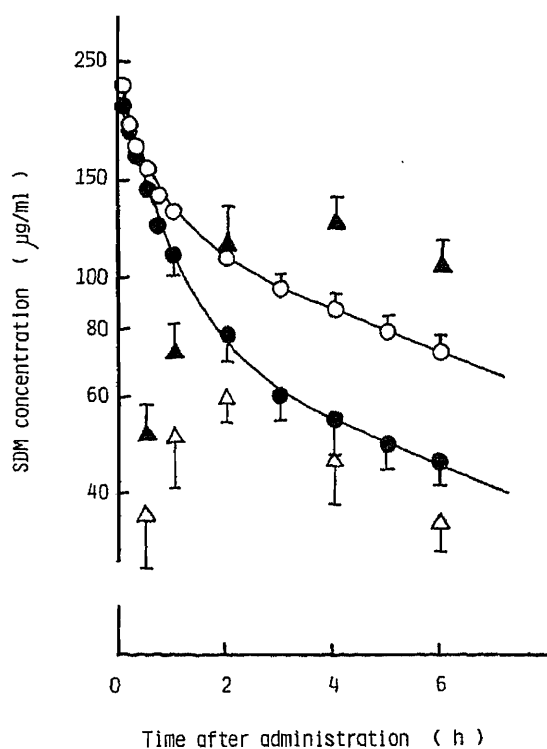


Fig. 5. Time Course of Plasma Concentration of SDM and N^4 -AcSDM after Intravenous Bolus Administration of SDM Alone or in Combination with KPF to Rabbits

Each point represents the mean \pm S.E. of 5 rabbits.
 —○—, plasma concentration of SDM (SDM alone);
 —●—, plasma concentration of SDM (with KPF);
 —△—, plasma concentration of N^4 -AcSDM (SDM alone);
 —▲—, plasma concentration of N^4 -AcSDM (with KPF).

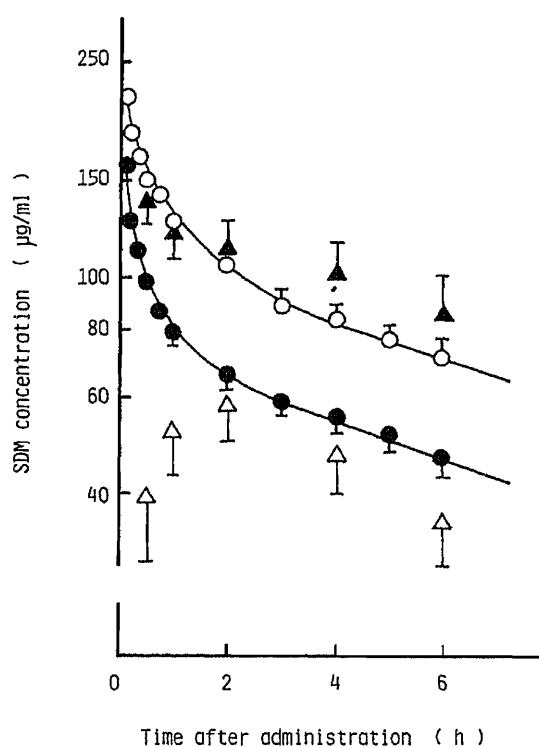


Fig. 6. Time Course of Plasma Concentration of SDM and N^4 -AcSDM after Intravenous Bolus Administration of SDM Alone or in Combination with N^4 -AcSDM to Rabbits

Each point represents the mean \pm S.E. of 5 rabbits.
 —○—, plasma concentration of SDM (SDM alone);
 —●—, plasma concentration of SDM (with N^4 -AcSDM);
 —△—, plasma concentration of N^4 -AcSDM (SDM alone);
 —▲—, plasma concentration of N^4 -AcSDM (with N^4 -AcSDM).

TABLE I. Pharmacokinetic Parameters of SDM after Intravenous Bolus Administration of SDM Alone or in Combination with KPF to Rabbits

Parameter	SDM alone	With KPF
Cl_{tot} (ml/h/kg)	35.4 ± 3.2	$52.1 \pm 6.2^a)$
V_{dss} (ml/kg)	358 ± 13	$526 \pm 43^a)$

Each value represents the mean \pm S.E. of 5 rabbits.
 a) Significantly different from SDM alone ($p < 0.05$).

TABLE II. Pharmacokinetic Parameters of SDM after Intravenous Bolus Administration of SDM Alone or in Combination with N^4 -AcSDM to Rabbits

Parameter	SDM alone	With N^4 -AcSDM
Cl_{tot} (ml/h/kg)	35.9 ± 1.6	$51.9 \pm 4.4^a)$
V_{dss} (ml/kg)	384 ± 8	$620 \pm 11^b)$

Each value represents the mean \pm S.E. of 5 rabbits.
 a) Significantly different from SDM alone ($p < 0.01$).
 b) Significantly different from SDM alone ($p < 0.001$).

SDM and KPF, we examined whether the co-administration of N^4 -AcSDM decreases the plasma concentration of SDM after intravenous bolus administration. As expected, the co-administration of N^4 -AcSDM markedly decreased the plasma concentration of SDM (Fig. 6), resulting in significant increases in Cl_{tot} and V_{dss} of SDM (Table II). Interestingly, the co-administration of N^4 -AcSDM, in contrast to that of KPF, caused a marked decrease in the plasma concentration of SDM at the early stage (distribution phase) after intravenous bolus administration. These observations indicate that N^4 -AcSDM contributes to the pharmacokinetic interaction between SDM and KPF in rabbits.

References

- 1) E. K. Seller and J. Koch-Weser, *New Engl. J. Med.*, **15**, 827 (1970).
- 2) Y. Imamura, H. Mori, and H. Ichibagase, *Chem. Pharm. Bull.*, **31**, 274 (1983).
- 3) O. Sugita, Y. Sawada, Y. Sugiyama, T. Iga, and M. Hanano, *Drug Metab. Dispos.*, **12**, 131 (1984).
- 4) J. W. Bridges, M. R. Kibby, S. R. Walker, and R. T. Williams, *Biochem. J.*, **109**, 851 (1968).
- 5) T. Uno and M. Ueda, *Yakugaku Zasshi*, **80**, 1785 (1960).
- 6) Y. Imamura, M. Sonoda, K. Arimori, and H. Ichibagase, *Chem. Pharm. Bull.*, **27**, 463 (1979).
- 7) L. Z. Benet and R. L. Galeazzi, *J. Pharm. Sci.*, **68**, 1071 (1979).
- 8) A. C. Bratton and E. K. Marshall, *J. Biol. Chem.*, **128**, 537 (1939).
- 9) J. Rieder, *Chemotherapy*, **17**, 1 (1972).
- 10) Y. Imamura, H. Nakamura, and M. Otagiri, *J. Pharmacobio-Dyn.*, **9**, 694 (1986).
- 11) K. Chiba, S. Nishimura, S. Kikuchi, N. Higuchi, S. Miyazaki, and M. Takada, *Chem. Pharm. Bull.*, **33**, 5100 (1985).
- 12) M. Takada, S. Akuzu, A. Misawa, R. Hori, and T. Arita, *Chem. Pharm. Bull.*, **22**, 542 (1974).
- 13) T. Arita, R. Hori, M. Takada, S. Akuzu, and A. Misawa, *Chem. Pharm. Bull.*, **20**, 570 (1972).
- 14) H. Y. Yu, Y. Sawada, Y. Sugiyama, T. Iga, and M. Hanano, *J. Pharm. Sci.*, **70**, 323 (1981).
- 15) K. Arimori, M. Nakano, M. Otagiri, and K. Uekama, *Biopharm. Drug Dispos.*, **5**, 219 (1984).

[Chem. Pharm. Bull.]
35(3)1304-1307(1987)

Determination of Ticlopidine in Rabbit Plasma by High-Performance Liquid Chromatography

SOICHI ITOH,^{*,a} SHINJI SUZUKI,^a SHUICHI ANDO,^a YUMIKO FUNATSU,^a
MASARU YAMAZAKI,^a KAZUHISA TANABE,^b
and MASAYOSHI SAWANOI^c

*Faculty of Pharmaceutical Sciences, Osaka University,^a Yamadaoka 1-6, Suita, Osaka 565, Japan,
Osaka University Hospital,^b 1-50 Fukushima 1-chome, Fukushima-ku, Osaka 553, Japan,
and Hospital Attached to the Research Institute for Microbial Diseases,
Osaka University,^c Yamadaoka 3-1, Suita, Osaka 565, Japan*

(Received September 18, 1986)

A method for determination of ticlopidine in plasma by high-performance liquid chromatography was established. The plasma samples (0.2 ml) were extracted with hexane. After evaporation, the hexane extracts were redissolved in the mobile phase containing phenobarbital as an internal standard, and an appropriate volume was injected onto a column of Cosmosil 5C8 (150 × 4 mm, i.d.); mobile phase, acetonitrile–10 mM phosphate buffer of pH 4.0 (30:70 v/v); flow rate, 1.0 ml/min; spectrophotometric detection at 230 nm. Ticlopidine and the internal standard were separated from interfering plasma components by this method. The peak height ratio of ticlopidine to the internal standard was proportional to the ticlopidine concentration in the range from 0.1 to 2.0 μg/ml.

Keywords—ticlopidine; HPLC; rabbit plasma; human plasma; oral administration; intravenous administration

Ticlopidine hydrochloride (TP·HCl), 5-(*o*-chlorobenzyl)-4,5,6,7-tetrahydrothieno[3,2-*c*]pyridine hydrochloride, is a potent anti-thrombotic agent.¹⁻³⁾ Usually anti-thrombotic therapy with a drug such as TP·HCl is a long-term process, and it is important to monitor not only the anti-thrombotic effect but also drug concentration in plasma. Although TP·HCl has been used in the treatment of thromboembolism, cerebral infarction and transient ischemic attack,⁴⁾ the relationship between the anti-thrombotic effect and the behavior of TP in plasma after administration is still unclear. This may be due to the lack of a sensitive and simple assay for TP in plasma.

Several analytical methods^{5,6)} have been developed for the quantitative determination of TP in plasma. The reported gas chromatographic (GC) method⁵⁾ seems to be unsuitable for routine analysis because of the need for time-consuming pretreatment such as repeated back-extraction, and the sensitivity is not sufficient for studies with small animals such as rabbits, dogs and rats. For a 0.2 ml plasma sample, the quantitation limit of the GC method was about 0.2 μg/ml in our laboratory. Therefore, we developed a high-performance liquid chromatographic (HPLC) method to determine TP in rabbit and human plasma.

Experimental

Materials—TP·HCl was a gift from Daiichi Seiyaku Co., Ltd. Other chemicals were of reagent grade.

Apparatus and Conditions—The HPLC apparatus consisted of a Hitachi 635S liquid chromatograph and a Hitachi 635M UV monitor (Hitachi Seisakusho, Tokyo). The column was a stainless-steel tube (150 × 4 mm, i.d.) packed with Cosmosil 5C8 (Nakarai Chemical, Kyoto). The mobile phase consisted of 30% acetonitrile in 10 mM phosphate buffer (pH 4.0). The flow rate was set at 1.0 ml/min. The eluate was monitored at 230 nm. Operations were

carried out at room temperature. TP concentration was determined by the method of peak height ratios.

Calibration Curve—An appropriate volume (10–200 μ l) of the methanolic TP·HCl stock solution was added to a glass-stoppered test tube. After removal of the methanol under reduced pressure, TP was redissolved in 0.2 ml of plasma by mixing thoroughly. Concentrations of 0.1, 0.3, 0.5, 1.0 and 2.0 μ g/ml in plasma were prepared. Then 0.5 ml of 1 N NH_4OH was added to each sample (0.2 ml) of plasma and the solution was extracted with 6 ml of *n*-hexane for 10 min using a mechanical shaker. After 10 min of centrifugation at $1200 \times g$, 5 ml of the organic layer was transferred into a 15-ml glass test tube and evaporated to dryness under reduced pressure at room temperature. The residue was redissolved in 60 μ l of the mobile phase of HPLC containing phenobarbital (PB) (5 μ g/ml) as an internal standard. A 50 μ l aliquot of the solution was injected into the HPLC column.

Determination of Plasma Concentration—Male albino rabbits, weighing 2.3–3.2 kg, were used. Food was withheld for 24 h prior to use, and water was permitted *ad libitum*. For oral administration, TP·HCl (300 mg/body) was administered *via* a stomach tube as an aqueous solution (60 mg/ml). For intravenous injection, TP·HCl (50 mg/body) was injected into the marginal vein of one ear as a 50 mg/ml aqueous solution. Blood samples (0.5 ml) were collected in heparinized glass centrifuge tubes from the marginal vein of the contralateral ear prior to drug administration and at intervals for 6 h. After immediate centrifugation, the plasma was transferred to a 10 ml glass-stoppered test tube and TP was extracted in the same way as described for preparation of the calibration curve.

Results and Discussion

Chromatograms

Figure 1 shows typical chromatograms obtained from blank rabbit and human plasma, rabbit plasma withdrawn after oral administration of TP·HCl, and human plasma containing 1.0 μ g/ml of TP·HCl. Chromatograms from blank rabbit plasma (Fig. 1a) and human plasma (Fig. 1c) did not contain any interfering peak showing a retention time similar to those of TP and PB. The retention times of TP and PB were 7.9 and 5.5 min, respectively.

Calibration Curve and Recovery

The calibration curve for determination of TP in rabbit plasma was linear over 0.1–2.0 μ g/ml and the regression equation was as follows: $y = 0.647x + 6.36 \times 10^{-3}$ ($r = 0.9998$), where y is the peak height ratio to PB and x is the TP concentration (μ g/ml) in plasma. The detection limit was 0.04 μ g/ml at a signal-to-noise ratio of 5:1. The coefficient of variation ($n = 3$) was less than 4% (Table I). The extraction recovery of TP from the rabbit plasma was 93% as well as from the human plasma, and did not change between 0.2 and 0.5 ml sample volume. The plasma samples were stable for at least 2 weeks when stored at -20°C .

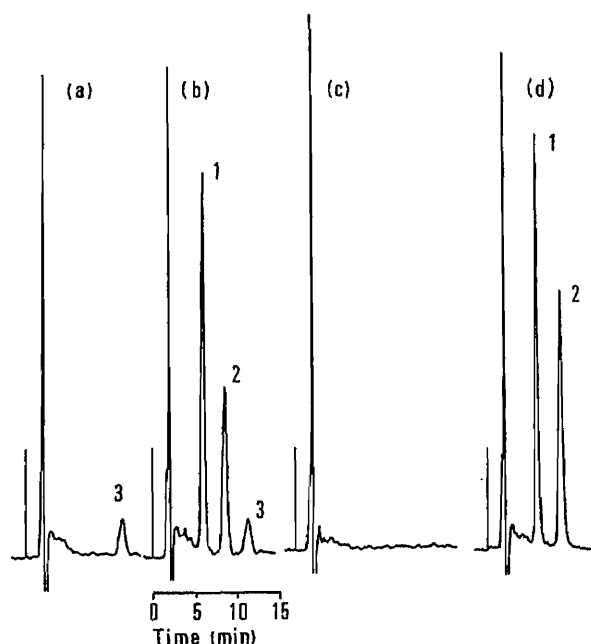


Fig. 1. Typical Chromatograms Obtained from Various Plasma Samples

(a), blank rabbit plasma; (b), rabbit plasma obtained after oral administration of TP·HCl (300 mg/body); (c), blank human plasma; (d), human plasma containing TP·HCl (0.2 μ g) and internal standard. 1, internal standard; 2, TP; 3, unknown peak.

TABLE I. Reproducibility of the Analysis of Ticlopidine in Rabbit Plasma

Added amount of TP·HCl ($\mu\text{g/ml}$)	Found ^{a)}	
	Mean \pm S.E.	C.V. %
0.1	0.104 \pm 0.002	3.7
0.3	0.302 \pm 0.006	0.6
0.5	0.505 \pm 0.012	1.0
1.0	1.002 \pm 0.005	0.2
2.0	1.997 \pm 0.011	0.1

a) Mean \pm S.E. and coefficient of variation (C.V.) of three determinations.

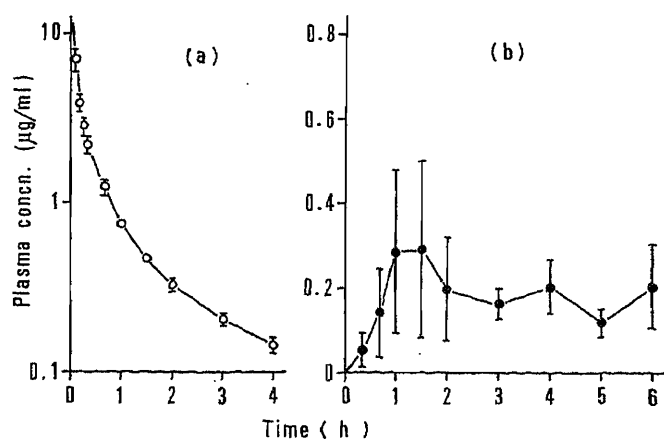


Fig. 2. Plasma Concentration-Time Courses of Ticlopidine Following Intravenous and Oral Administrations of Ticlopidine Hydrochloride in Rabbits

(a), intravenous administration (50 mg/body, $n=8$); (b), oral administration (300 mg/body, $n=5$). Each point represents the mean \pm S.E.

Determination of Plasma TP

The present method was applied to determination of plasma TP in rabbits. The plasma concentrations of TP after intravenous and oral administrations of TP·HCl are shown in Fig. 2. After intravenous administration, plasma TP declined rapidly and the pharmacokinetic parameters calculated on the basis of a linear two-compartment model, $C_0 = Ae^{-\alpha t} + Be^{-\beta t}$, were as follows: A , $9.34 \pm 1.55 \mu\text{g/ml}$; α , $11.09 \times 10^{-2} \pm 1.45 \times 10^{-2} \text{ min}^{-1}$; β , $9.13 \times 10^{-3} \pm 0.74 \times 10^{-3} \text{ min}^{-1}$; $T_{1/2}(\beta)$, $80.3 \pm 7.8 \text{ min}$. After oral administration, the variation in the plasma concentration of TP was much larger than that after intravenous administration and the maximum plasma concentration ranged between 0.07 and $0.57 \mu\text{g/ml}$. In a few cases, the plasma concentration was still increasing at the end of the experiment, indicating that the absorption process was still going on. The reason for the variability in intestinal absorption of TP·HCl is not clear.

The HPLC method is convenient for determining TP in plasma and the sensitivity is 5 times higher than that of the GC method. Under the experimental conditions which we used, the TP peak was well separated from the peaks of other plasma components. Although in this study we did not assay human plasma after administration TP·HCl, the results in Fig. 1 and Table I showed that the method should be applicable to TP in human plasma as well as in rabbit plasma. It was reported⁴⁾ that the maximum concentration of TP in human plasma after oral administration (500 mg/body) is about $1.9 \mu\text{g/ml}$, and that dose is about 2.5–5 times larger than the usual dosage. Assuming that the plasma concentration is proportional to the dose administered, the HPLC method seems to be sufficiently sensitive for use within the therapeutic concentration range.

This simple HPLC method should be valuable for monitoring the plasma concentration of TP in patients and for examining the relationship between TP concentration in plasma and

anti-thrombotic effect.

References

- 1) S. Ashida and Y. Abiko, *Thromb. Haemost.*, **41**, 436 (1979).
- 2) S. Ashida and Y. Abiko, *Thromb. Haemost.*, **40**, 542 (1978).
- 3) M. Tomikawa, S. Ashida, K. Kakihata, and Y. Abiko, *Thromb. Res.*, **12**, 1157 (1978).
- 4) Daiichi Seiyaku Co., Ltd., "Panaldine® Tablets, Interview Form," Tokyo, Japan.
- 5) A. Tuong, A. Bouyssou, J. Paret, and T. G. Cuong, *Eur. J. Drug Metab. Pharmacokinet.*, **6**, 91 (1981).
- 6) T. Takegoshi, K. Ono, K. Matsubayashi, F. Hashimoto, and M. Sano, *Oyoyakuri*, **19**, 349 (1980).

Communications to the Editor

[Chem. Pharm. Bull.]
[35(3)1308—1310(1987)]

ABSOLUTE CONFIGURATION OF (-)-LUSITANINE, A NEW LUPIN ALKALOID
in MAACKIA SPECIES

Kazuki Saito,^a Takaaki Yoshino,^a Shi Tsai,^a Shigeru Ohmiya,^b
Hajime Kubo,^b Hirotaka Otomasu,^b and Isamu Murakoshi^{*,a}

Faculty of Pharmaceutical Sciences, Chiba University,^a Yayoi-cho 1-33,
Chiba 260, Japan and Faculty of Pharmaceutical Sciences, Hoshi
University,^b Ebara 2-4-41, Shinagawa-ku, Tokyo 142, Japan

A new lupin alkaloid, (-)-lusitanine (I), has been isolated from the fresh stems of Maackia amurensis var. burgeri and M. tashiroi (Leguminosae), together with other types of the alkaloids. Its absolute configuration has also been established as (1R,6R)-5-(E)-acetamidomethylidenequinolizidine (I) on the basis of chemical transformation into its dihydro-derivatives II ((1R,5R,6R)-(+)-acetamidomethylquinolizidine) and III ((1R,5S,6R)-(-)-acetamidomethylquinolizidine) and of their spectral evidence.

KEYWORDS — lupin alkaloid; quinolizidine alkaloid; (-)-lusitanine(1R,6R); (+)-lusitanine(1R,6S); absolute configuration; Maackia amurensis; Maackia tashiroi; Leguminosae; (+)-acetamidomethylquinolizidine(1R,5R,6R); (-)-acetamidomethylquinolizidine(1R,5S,6R)

During the course of our studies of the lupin alkaloids in leguminous plants which grow mainly in Japan, a new lupin alkaloid, (-)-lusitanine (I), has been isolated from the 75% EtOH extracts of the freshly harvested young stems of Maackia amurensis var. burgeri(Maxim.) and M. tashiroi Makino (Leguminosae) as colourless needles, mp 185-186°, $[\alpha]_D^{23} -4.6^\circ$ (c=0.60, EtOH), together with other types of the alkaloids such as (+)-13 β -hydroxymamanine,¹⁾ ammodendrine and so on.²⁾

The planar structure of (-)-lusitanine (I) was readily proved by the MS, IR, mp, ¹H-NMR and ¹³C-NMR data⁶⁾ to be the same structure as (+)-lusitanine which had previously been isolated from the flourishing aerial parts of Genista lusitanica (= Echinospartum lusitanicum(L.)Rothm (Leguminosae) by Wicky and Steinegger.^{3,4,5)}

However, the data on the optical rotation of I showed an opposite value compared with (+)-lusitanine, $[\alpha]_D^{27} +6.9^\circ$ (c=2.50, EtOH), suggesting that I is the enantiomer of (+)-lusitanine (IV) reported by Wicky *et al.*⁴⁾

The absolute configuration of (+)-lusitanine (IV) has never been confirmed but it has tentatively been proposed to be 1R,6R in the stereostructure shown as a figure.⁵⁾

We report herein the absolute configuration of (-)-lusitanine and

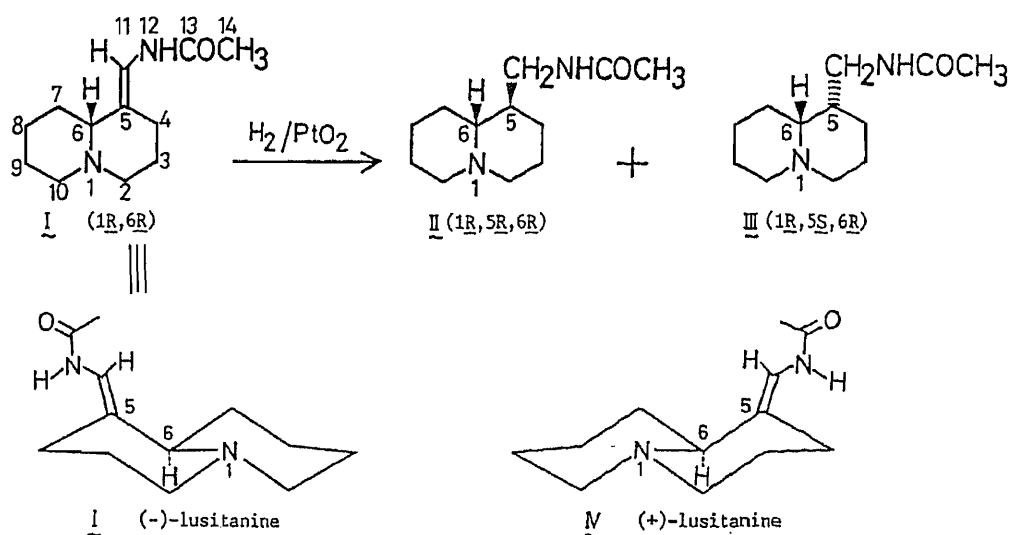


Chart 1. Stereostructures of (-)-lusitanine(I) and (+)-lusitanine(IV)

(+)-lusitanine as I and IV, respectively, based upon the chemical transformation of (-)-lusitanine (I) into (+)-acetamidomethylquinolizidine (II: 1R,5R,6R) and (-)-acetamidomethylquinolizidine (III: 1R,5S,6R). (-)-Lusitanine (I) was converted to a mixture of the diastereomers II and III in the presence of PtO₂ by a method of Wicky *et al.*⁴⁾ These were separated from each other by silica gel column chromatography using the solvent system of cyclohexene-diethylamine (9:1/v) with increasing Et₂NH content, and purified by recrystallization from petr. ether.

The structures of II and III were established carefully by analyzing the IR, MS, ¹H-NMR and ¹³C-NMR data.^{7,8)} II was completely identified as (1R,5R,6R)-(+)-acetamidomethylquinolizidine by comparing its IR, mp and [α]_D data with the authentic samples which had already been stereospecifically synthesized from (+)-epilupinine(1R,5S,6R) and (-)-anagryne(7R,9R,11R) by Okuda, Kataoka and Tsuda.⁹⁾

The value of optical rotation of II, [α]_D²³ +53.1° (c=0.16, EtOH), derived from (-)-lusitanine (I), also is very close to these values, [α]_D²⁰ +56.7° (c=0.74, EtOH) and [α]_D²⁰ +56.4° (c=0.71, EtOH), of the authentic samples⁹⁾ prepared from (+)-epilupinine and (-)-anagryne, respectively.

From this information, it is concluded that the absolute configuration of II is 1R,5R,6R as shown in Chart 1. Consequently, the stereostructure for (-)-lusitanine (I), isolated from the *Maackia* species, can now be defined as in I: (1R,6R)-5(E)-acetamidomethylidenequinolizidine.

These results led us to define the absolute configuration of (+)-lusitanine (IV), separated from the *Genista* species,³⁻⁵⁾ as shown in Chart 1, i.e. 1R,6S. Thus, the absolute configuration of (-)-acetamidomethylquinolizidine (III) has also been confirmed to be 1R,5S,6R as shown in Chart 1.

Full details of the basic ingredients in the *Maackia* species will be published elsewhere.¹⁰⁾

ACKNOWLEDGEMENTS We are grateful to Professor S. Okuda, Institute of Applied Microbiology, University of Tokyo, for his valuable advice during the course of this work. We also are indebted to Dr. F. Ikegami, Medicinal Plant Gardens, Chiba University, and to Mr. M. Otomasu, Kumamoto, for cordially providing the plant materials.

REFERENCES AND NOTES

- 1) K. Saito, S. Tsai, S. Ohmiya, H. Kubo, H. Otomasu and I. Murakoshi, Chem. Pharm. Bull., **34**, 3982 (1986).
- 2) I. Murakoshi, K. Saito, S. Tsai, S. Ohmiya, H. Otomasu and H. Kubo, The 106th Annual Meeting of Pharmaceutical Society of Japan at Chiba, April, 1986, Meeting Abstracts, p. 184.
- 3) E. Steinegger and K. Wicky, Pharm. Acta Helv., **40**, 610 (1965).
- 4) K. Wicky and E. Steinegger, Pharm. Acta Helv., **40**, 658 (1965).
- 5) K. Wicky and D. Schumann, Pharm. Acta Helv., **57**, 215 (1982).
- 6) (-)-lusitanine (I): MS m/z: 208 (M^+), 179, 166 (base peak), 136, 110. IR ν_{\max}^{KBr} cm^{-1} : 3330, 1662 (-CONH-), 2800, 2775, 2750 (Bohlmann bands). $^1\text{H-NMR}$ (400 MHz, CDCl_3) δ : 7.12 (1H, d, $J=11$, -CONH-), 6.67 (1H, d, $J=11$, 11-H), 2.88 (2H, m, 2- and 10-Heq), 2.47 (1H, d, $J=13$, 4-Heq), 2.28 (1H, d, $J=11$, 6-H), 2.17 (1H, dt, $J=12, 3$), 2.08 (1H, dt, $J=11, 4$), 2.06 (3H, s, 14-H). $^{13}\text{C-NMR}$ (CDCl_3) δ : 167.9 (s, C(13)), 121.0 (s, C(5)), 116.0 (d, C(11)), 64.2 (d, C(6)), 57.0 (t, C(2)), 56.4 (t, C(10)), 27.8 (t, C(7)), 25.4 (t, C(9)), 25.1 (t, C(8)), 24.2 (t, C(3)), 23.3 (q, C(14)).
- 7) II: needle, mp 147-148 $^\circ$ (lit.⁹) 147-148 $^\circ$, $[\alpha]_{\text{D}}^{23} +53.1^\circ$ (c=0.16, EtOH), MS m/z: 210 (M^+), 168 (M-COCH₂), 152 (M-NHCOCH₃), 138 (M-CH₂NHCOCH₃, base peak). IR $\nu_{\max}^{\text{CHCl}_3}$ cm^{-1} : 2840, 2810, 2760 (Bohlmann bands), 1665, 1515. $^1\text{H-NMR}$ (270 MHz, CDCl_3) δ : 5.30 (1H, br, 12-H), 3.36 (1H, ddd, $J=13.8, 5.4, 4.0$, 11-H), 3.17 (1H, ddd, $J=13.8, 6.9, 6.9$, 11-H), 1.96 (3H, s, 14-H). $^{13}\text{C-NMR}$ (CDCl_3) δ : 170.1 (s, C(13)), 65.4 (d, C(6)), 56.9 (t, C(2)), 56.6 (t, C(10)), 41.8 (d, C(5)), 41.7 (t, C(11)), 29.8 (t, C(7)), 29.2 (t, C(4)), 25.6 (t, C(9)), 25.0 (t, C(8)), 24.6 (t, C(3)), 23.3 (q, C(14)).
- 8) III: needle, mp 97-98 $^\circ$, $[\alpha]_{\text{D}}^{23} -33.5^\circ$ (c=0.17, EtOH), MS: same as those of II. IR ν_{\max}^{KBr} cm^{-1} : 2860, 2800, 2760 (Bohlmann bands), 1640, 1550. $^1\text{H-NMR}$ (270 MHz, CDCl_3) δ : 7.44 (1H, br, 12-H), 3.48 (1H, ddd, $J=13.8, 5.5, 3.1$, 11-H), 3.40 (1H, ddd, $J=13.8, 6.7, 3.7$, 11-H), 1.96 (3H, s, 14-H). $^{13}\text{C-NMR}$ (CDCl_3) δ : 169.8 (s, C(13)), 64.8 (d, C(6)), 57.4 (t, C(10)), 57.0 (t, C(2)), 41.1 (t, C(11)), 36.4 (d, C(5)), 29.9 (t, C(7)), 29.6 (t, C(4)), 25.8 (t, C(9)), 24.9 (t, C(8)), 23.4 (q, C(14)), 22.0 (t, C(3)).
- 9) S. Okuda, H. Kataoka and K. Tsuda, Chem. Pharm. Bull., **13**, 491 (1965).
- 10) I. Murakoshi, K. Saito, S. Tsai, T. Yoshino, F. Ikegami, S. Ohmiya, H. Kubo, and H. Otomasu, in preparation.

(Received December 26, 1986)

 Communications to the Editor

[Chem. Pharm. Bull.]
35(3)1311—1314(1987)

 TOTAL SYNTHESIS OF *PROTEUS MIRABILIS* LIPID A¹⁾

Kiyoshi Ikeda, Toshio Takahashi, Hiroshi Kondo,
and Kazuo Achiwa*

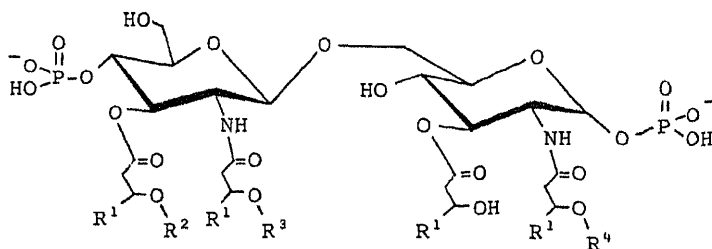
Shizuoka College of Pharmacy, 2-2-1 Oshika, Shizuoka 422, Japan

We describe a total synthesis of *Proteus mirabilis* lipid A via a new common key disaccharide intermediate bearing two amino and six hydroxyl groups which are chemically differentiated.

KEYWORDS — total synthesis; *proteus mirabilis* lipid A; disaccharide intermediate; chemical differentiation

The lipid As have received much attention.²⁾ Especially, Shiba's group has synthesized the biologically active constituents of lipopolysaccharide (LPS) of Gram-negative bacteria, *Salmonella* mutant (1a),³⁾ *Escherichia coli* (1b)⁴⁾ and *Salmonella minnesota* (1c).⁵⁾ They used the elegant two-fragment condensation method. Also, a formal synthesis of 1a was realized by us using the novel disaccharide intermediate bearing two amino and six hydroxyl groups which were chemically differentiated.⁶⁾

Here we describe a short synthesis of a new common key disaccharide intermediate (2) and the first total synthesis of *Proteus mirabilis* lipid A (1e) from 2.



1a: $R^1 = \text{CH}_3(\text{CH}_2)_{10}-$, $R^2 = R^3 = R^4 = \text{H}$
(*Salmonella* mutant)

1b: $R^1 = \text{CH}_3(\text{CH}_2)_{10}-$, $R^2 = \text{CH}_3(\text{CH}_2)_{12}\text{CO}-$, $R^3 = \text{CH}_3(\text{CH}_2)_{10}\text{CO}-$, $R^4 = \text{H}$
(*Escherichia coli*)

1c: $R^1 = \text{CH}_3(\text{CH}_2)_{10}-$, $R^2 = \text{CH}_3(\text{CH}_2)_{12}\text{CO}-$, $R^3 = \text{CH}_3(\text{CH}_2)_{10}\text{CO}-$, $R^4 = \text{CH}_3(\text{CH}_2)_{14}\text{CO}-$
(*Salmonella minnesota*)

1d: $R^1 = \text{CH}_3(\text{CH}_2)_{10}-$, $R^2 = \text{CH}_3(\text{CH}_2)_{12}\text{CO}-$, $R^3 = \text{CH}_3(\text{CH}_2)_{12}\text{CO}-$, $R^4 = \text{H}$
(*Proteus mirabilis*)

1e: $R^1 = \text{CH}_3(\text{CH}_2)_{10}-$, $R^2 = \text{CH}_3(\text{CH}_2)_{12}\text{CO}-$, $R^3 = \text{CH}_3(\text{CH}_2)_{12}\text{CO}-$, $R^4 = \text{CH}_3(\text{CH}_2)_{14}\text{CO}-$
(*Proteus mirabilis*)

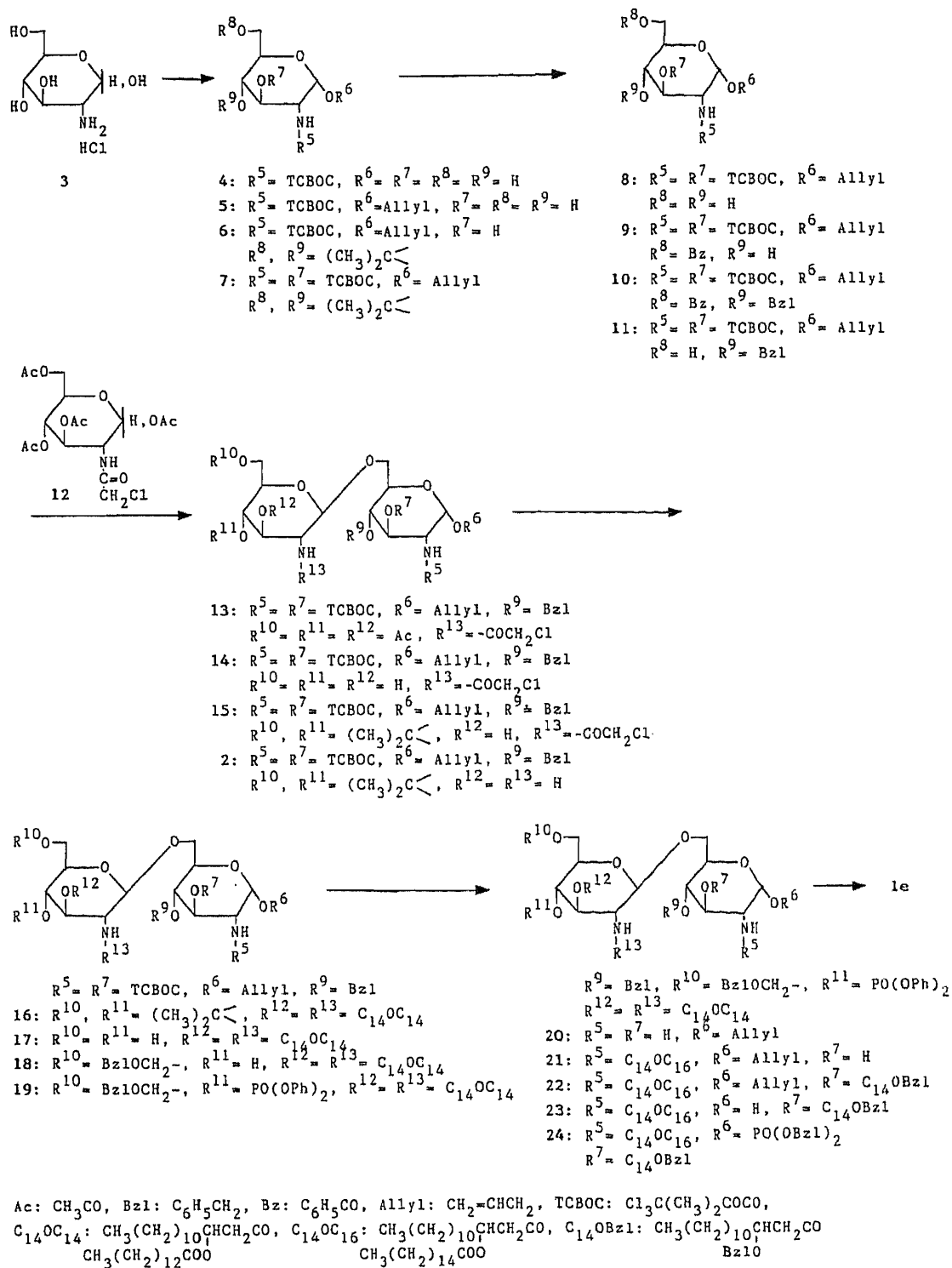
The synthesis route to 1e, using the readily available disaccharide (2) as a key intermediate, was constructed as shown in chart 1.

The reducing glucosamine part of 2 was prepared as follows. The primary protection of the amino group of D-glucosamine hydrochloride (3) with the 2,2,2-trichloro-1,1-dimethylethoxycarbonyl (TCBOC) group afforded 4⁷⁾ [87%, mp 141-142°C, $[\alpha]_D^{24} +37.0^\circ$ (c=1.00, MeOH)]. The following glycosidation of N-TCBOC-glucosamine (4) in 2% dry HCl in allyl alcohol at 100°C for 1.5 h gave the α -allyl glycoside (5)⁷⁾ [62%, mp 143-146°C, $[\alpha]_D^{25} +91.7^\circ$ (c=1.00, MeOH)], which was then converted into 4,6-isopropylidene derivative (6)⁷⁾ with 2,2-dimethoxypropane-TsOH in DMF at room temperature for 5 h [82%, mp 129-131°C, $[\alpha]_D^{21} +63.9^\circ$ (c=1.34, CHCl₃)]. Acylation of the free hydroxyl group of 6 with TCBOC-Cl in pyridine containing a catalytic amount of 4-dimethylaminopyridine (DMAP) at room temperature for 11 h gave 7⁷⁾ [94%, mp 65-67°C, $[\alpha]_D^{21} +50.4^\circ$ (c=1.01, CHCl₃)]. The isopropylidene group of 7 was then removed by hydrolysis with 90% acetic acid at 90°C for 15 min to yield 8⁷⁾ [83%, mp 74-77°C, $[\alpha]_D^{24} +55.3^\circ$ (c=1.00, CHCl₃)]. Selective benzylation of 8 with benzoyl chloride in pyridine-CH₂Cl₂ at 0°C for 7 h afforded the 6-benzoyl compound (9)⁷⁾ [77%, mp 69-70°C, $[\alpha]_D^{21} +52.0^\circ$ (c=1.01, CHCl₃)]. Then 9 was benzylated with benzyl trichloroacetimidate and a catalytic amount of trifluoromethanesulfonic acid in CH₂Cl₂ at room temperature for 48 h to yield 10⁷⁾ [83%, mp 50-51°C, $[\alpha]_D^{19} +49.7^\circ$ (c=0.30, CHCl₃)]. And 10 was then debenzoylated with aqueous NH₄OH-MeOH (1:10) to give 11⁷⁾ [57%, mp 41°C, $[\alpha]_D^{21} +53.8^\circ$ (c=1.06, CHCl₃)], which is the reducing glucosamine component in the disaccharide synthesis.

Coupling of the two component, 11 and 12 in the presence of FeCl₃ and N,N,N',N'-tetramethylurea (TMU) and Molecular Sieves 4A in CH₂Cl₂ at room temperature for 48 h gave a β (1+6)-disaccharide (13)^{7,8)} [80%, mp 102-104°C, $[\alpha]_D^{20} +32.8^\circ$ (c=1.41, CHCl₃)], which was deacetylated with aqueous NH₄OH-MeOH (1:10) to give 14⁷⁾ [76%, mp 153-154°C, $[\alpha]_D^{27} +31.6^\circ$ (c=1.00, CHCl₃)]. The two hydroxyl groups on position 4' and 6' were reprotected by conversion into the isopropylidene derivative (15)⁷⁾ [69%, mp 117-118°C, $[\alpha]_D^{20} +17.7^\circ$ (c=0.55, CHCl₃)]. Then the N-chloroacetyl group was removed with thiourea and diisopropylethylamine in THF refluxing for 5 h to give the general key intermediate (2)⁷⁾ [95%, mp 88-89°C, $[\alpha]_D^{20} +23.1^\circ$ (c=0.31, CHCl₃)].

For the successful completion of this approach to the total synthesis of 1e, the free amino and hydroxyl groups of 2 were acylated with (R)-3-tetradecanoyloxytetradecanoic acid in the presence of dicyclohexylcarbodiimide (DCC) and a catalytic amount of DMAP in CH₂Cl₂ at room temperature for 17 h to give 16⁷⁾ [98%, mp 132-134°C, $[\alpha]_D^{19} +11.8^\circ$ (c=1.41, CHCl₃)]. Removal of the isopropylidene group of 16 with 90% acetic acid at 90°C for 15 min afforded 17⁷⁾ [75%, mp 88-90°C, $[\alpha]_D^{20} +15.1^\circ$ (c=0.68, CHCl₃)], whose 6'-hydroxyl group was selectively protected with benzyloxymethyl chloride and TMU in CH₂Cl₂ to give 18⁷⁾ [54%, mp 94-96°C, $[\alpha]_D^{20} +14.6^\circ$ (c=1.28, CHCl₃)]. The phosphorylation of 18 with diphenylphosphoryl chloride in the presence of pyridine and DMAP in CH₂Cl₂ at room temperature for 2 h gave 19⁷⁾ [87%, syrup, $[\alpha]_D^{20} +20.8^\circ$ (c=0.74, CHCl₃)]. Treatment of 19 with zinc-acetic acid at room temperature for 24 h gave 20⁷⁾ [89%, syrup, $[\alpha]_D^{23} +22.9^\circ$ (c=0.68, CHCl₃)]. The free amino group of 20 was acylated with (R)-3-hexadecanoyloxytetradecanoic acid and DCC in CH₂Cl₂ at room temperature for 22 h to give 21⁷⁾ [78%, mp 53-55°C, $[\alpha]_D^{23} +15.0^\circ$ (c=0.57, CHCl₃)].

Chart 1.



The remaining hydroxyl group of **21** was acylated with (R)-3-benzyloxytetradecanoic acid and DCC in the presence of DMAP in CH_2Cl_2 to give **22**⁷⁾ [70%, mp 48-49°C, $[\alpha]_{\text{D}}^{23} +18.9^\circ$ (c=2.18, CHCl_3)]. The allyl glycoside was in turn isomerized with iridium complex and the resultant 1-propenyl glycoside was treated with iodine in aqueous THF to give **23**⁷⁾ [87%, syrup, $[\alpha]_{\text{D}}^{22} +12.6^\circ$ (c=0.89, CHCl_3)]. The glycosidic hydroxyl group was then phosphorylated with n-BuLi and dibenzylphosphoryl chloride in THF at -70°C and the reaction product (**24**) was immediately hydrogenolyzed, first with Pd-black to remove the benzyl groups and then with platinum dioxide to cleave the phenyl esters of 4'-phosphate group in THF-MeOH (10:1). The final product was isolated by means of a silica gel column (CHCl_3 -MeOH- H_2O - Et_3N = 20:5:1:0.05). After acidic precipitation, lyophilization from dioxane afforded **1e**^{7,9-11)} [10% yield from **23**, mp 60-62°C, $[\alpha]_{\text{D}}^{23} +4.6^\circ$ (c=0.22, CHCl_3)].

Further application of this method to the synthesis of KDO-KDO-lipid **As**¹²⁾ is actively under way.

References and Notes

- 1) Lipid A and Related Compounds. X., Part IX.: Reference 6h.
- 2) M. Imoto, S. Kusumoto, T. Shiba, H. Naoki, T. Iwashita, E. T. Rietschel, H. -W. Wollenweber, C. Galanos, and O. Lüderitz, *Tetrahedron Lett.*, **24**, 4017 (1983); U. Seydel, B. Lindner, H. -W. Wollenweber, and E. T. Rietschel, *Eur. J. Biochemistry*, **24**, 2736 (1985).
- 3) M. Imoto, H. Yoshimura, M. Yamamoto, T. Shimamoto, S. Kusumoto, and T. Shiba, *Tetrahedron Lett.*, **25**, 2667 (1984).
- 4) M. Imoto, H. Yoshimura, N. Sakaguchi, S. Kusumoto, and T. Shiba, *Tetrahedron Lett.*, **26**, 1545 (1985).
- 5) H. Yoshimura, M. Imoto, Y. Tsuji, S. Kusumoto, and T. Shiba, The 50th Annual Meeting Abstract of Chemical Society of Japan (1986), Part II, p 971.
- 6) a) T. Takahashi, C. Shimizu, S. Nakamoto, K. Ikeda, and K. Achiwa, *Chem. Pharm. Bull.*, **33**, 1760 (1985); b) S. Nakamoto, T. Takahashi, K. Ikeda, and K. Achiwa, *ibid.*, **33**, 4098 (1985); c) T. Shimizu, S. Akiyama, T. Masuzawa, Y. Yanagihara, S. Nakamoto, K. Ikeda, and K. Achiwa, *ibid.*, **33**, 4621 (1985); d) K. Ikeda, S. Nakamoto, T. Takahashi, and K. Achiwa, *Carbohydr. Res.*, **145**, C5 (1986); e) T. Takahashi, S. Nakamoto, K. Ikeda, and K. Achiwa, *Tetrahedron Lett.*, **27**, 1819 (1986); f) S. Nakamoto, and K. Achiwa, *Chem. Pharm. Bull.*, **34**, 2302 (1986); g) T. Shimizu, S. Akiyama, T. Masuzawa, Y. Yanagihara, S. Nakamoto, and K. Achiwa, *ibid.*, **34**, 2310 (1986); h) Idem, *ibid.*, in press (1986); i) T. Shimizu, S. Akiyama, T. Masuzawa, Y. Yanagihara, S. Nakamoto, T. Takahashi, K. Ikeda, and K. Achiwa, *ibid.*, in press (1986).
- 7) Satisfactory analytical and spectral data were obtained for this compound.
- 8) The configuration of glycosidic linkage at C-1' of **13** was assigned as β by ^{13}C NMR data which appeared at δ 100.2 with $^1\text{J}_{\text{CH}} = 161$ Hz for C-1'.
- 9) The molecular weight of **1e** was confirmed by positive ion FAB-mass spectrometry, which showed an $(\text{M}+\text{NET}_3)^+$ ion at m/z 2164.7, and $(\text{M}+\text{NET}_3+\text{Na})^+$ ion at m/z 2186.8.
- 10) We thank to Mr Kazuo Tanaka of JEOL L.T.D. for recording and measuring the FAB-mass spectrum.
- 11) The compound (**1e**) possesses biological activities (pyrogenicity, lethal toxicity). cf. T. Shimizu, S. Akiyama, T. Masuzawa, Y. Yanagihara, K. Ikeda, T. Takahashi, H. Kondo, and K. Achiwa, *Microbiol. Immunol.*, **31** (1987) in press.
- 12) R. Christian, G. Schultz, P. Waldstätten, F. M. Unger, *Tetrahedron Lett.*, **25**, 3433 (1984); b) U. Zähringer, B. Lindner, U. Seydel, E. T. Rietschel, H. Naoki, F. M. Unger, M. Imoto, S. Kusumoto, and T. Shiba, *Tetrahedron Lett.*, **26**, 6321 (1985).

(Received December 27, 1986)

Communications to the Editor

[Chem. Pharm. Bull.]
35(3)1315-1318(1987)]

EVIDENCE THAT T-KININ DOES NOT MEDIATE PAW SWELLING INDUCED BY
CARRAGEENIN: STUDIES WITH PLASMA HIGH MOLECULAR WEIGHT KININOGEN AND
LOW MOLECULAR WEIGHT KININOGEN DEFICIENT RATS

Sachiko Oh-ishi, Izumi Hayashi, Iku Utsunomiya, Masahiko Hayashi,
Kohji Yamaki, Akiko Yamasu and Takeshi Nakano^a

Department of Pharmacology, School of Pharmaceutical Sciences,
Kitasato University, Minatoku, Tokyo 108, Japan and
School of Medicine^a, Sagamihara 228 Japan

Paw swelling induced by carrageenin was compared in Brown Norway Kitasato rats (normal) and Brown Norway Katholiek rats, deficient in HMW and LMW kininogens. The increase in the paw volume of the former after the carrageenin injection was about 50-70% of the initial volume, whereas that of the latter was about 10%. Pretreatment with captopril, a kininase inhibitor, enhanced the edema significantly in the former but had no effect in the latter. The T-kininogen level in the plasmas of both strains increased gradually and peaked on the 2nd day at 10 times of the control level. But the paw swelling peaked at 4-5 hours after the carrageenin injection. These results indicate that bradykinin but not T-kinin induces paw swelling by plasma exudation.

KEYWORDS—— HMW-kininogen; T-kininogen; captopril; T-kinin; paw edema; carrageenin

T-kinin, isoleucyl-seryl-bradykinin, was identified as a peptide released by trypsin from a distinct kininogen of rats.¹⁾ The kininogen was named T-kininogen²⁾ and was differentiated from the classical HMW and LMW kininogens, since it did not release any kinin by the action of either plasma kallikrein or glandular kallikrein.^{3,4)} It has been reported that the plasma level of T-kininogen increases following inflammatory stimuli or injection of bacterial lipopolysaccharide (LPS).⁵⁻⁷⁾ The content of the mRNA encoding T-kininogen in the liver also increased after rats received LPS.⁸⁾

This is proof that neither T-kinin nor T-kininogen play a role in the paw swelling of rats induced by the intradermal injection of carrageenin in rats congenitally deficient in plasma HMW and LMW kininogens.⁹⁾

Inbred strains of male Brown Norway Kitasato (B/N-Ki) rats, 12-15 weeks old with normal plasma kininogens, and Brown Norway Katholiek (B/N-Ka) rats deficient in plasma HMW and LMW kininogens, but with normal levels of T-kininogen,^{3,4)} were injected in the right paw with 0.1 ml sterile saline solution of 1% carrageenin (lambda-carrageenin, Sigma). The paw volume was measured with a mercury

plethysmograph before and at 1, 2, 3, 5, 24 h after the carrageenin injection.¹⁰⁾ The B/N-Ka and B/N-Ki rats were each divided into two groups; one group of each strain received intravenously 10 mg/kg captopril (kindly supplied from Sankyo co.,Ltd.). The other groups received saline 30 min before the carrageenin injection. Blood samples were drawn from the subclavian vein before the carrageenin injection, and rats from each group were exsanguinated at the indicated times after the carrageenin injection. Plasma was obtained from the citrated blood as previously described.⁴⁾ T-kininogen and HMW-kininogen were measured by radioimmunoassay using ¹²⁵I-labeled kininogen as previously described.⁶⁾

Table I clearly indicates that the B/N-Ka rats show less swelling and thus HMW kininogen has an important role in the induction of plasma leakage. This coincides with our previous result of carrageenin-induced pleurisy,¹¹⁾ in that B/N-Ka rat showed less pleural fluid accumulation than the normal strain, B/N-Ki and Sprague-Dawley rats. The result also agrees with Damas *et al.*¹²⁾ who report a role of the plasma kallikrein-kinin system in urate crystal-induced paw edema in kininogen-deficient rats. These results also demonstrate that T-kininogen may not have any role in the paw swelling, since the level of T-kininogen in B/N-Ka rat plasma is the same as that in B/N-Ki rat plasma, and it increased in the same way it did in B/N-Ki rats as shown in Fig. 1. Pretreatment with captopril in B/N-Ki rats enhanced paw swelling at 1-2 hr, indicating that bradykinin may be released from HMW-kininogen by plasma kallikrein activation, as previously reported for sprague-Dawley rat.¹¹⁾ Pretreatment with captopril may inhibit kininase and cause bradykinin to stay longer at the site to induce more swelling. As shown in Fig. 2, the plasma levels of HMW kininogen in B/N-Ka rats

Table I. Percentage increase in paw volumes in Brown Norway Kitasato (B/N-Ki) and Brown Norway Katholiek (B/N-Ka) rats after carrageenin injection with or without pretreatment of captopril (10 mg/kg)

	Hours after carrageenin injection				
	1	2	3	5	24
B/N-Ki (vehicle) (n = 12)	30.4 ± 3.2	45.5 ± 4.7	50.2 ± 5.1	48.8 ± 3.4	21.7 ± 2.1
B/N-Ki (captopril)* (n = 10)	69.0 ± 5.8	*61.9 ± 6.7	59.9 ± 7.5	56.5 ± 4.7	21.7 ± 2.6
B/N-Ka (vehicle) (n = 12)	10.8 ± 1.7	6.8 ± 1.1	8.0 ± 1.2	11.8 ± 2.1	9.3 ± 1.2
B/N-Ka (captopril) (n = 11)	9.0 ± 2.0	6.2 ± 1.5	7.5 ± 2.2	8.1 ± 1.2	5.7 ± 1.4

Data are means with standard errors. n: number of rats used. *: statistically significant at 5%.

were 1/30 - 1/50 as high as those in B/N-Ki rats and showed no change during inflammation. The B/N-Ka rats showed no enhancement with captopril, indicating that T-kinin may not be released from T-kininogen at the paw site. If T-kinin has been released the effect would be enhanced, since exogenous T-kinin caused the same degree of vascular permeability increase in rats as bradykinin does.¹¹⁾ T-kinin was also inactivated with rat plasma as bradykinin and captopril partly prevented the inactivation (Data not shown).

Furthermore, the plasma level of T-kininogen increased at 24 h after the carrageenin injection, when the paw swelling had already decreased. The peak swelling was at about 5 h and at that time the T-kininogen level had not yet increased. The time lag in the increase of T-kininogen also indicates no role of T-kinin, if any release, for the increased vascular permeability during paw swelling. The profiles and increased levels of T-kininogen in both strains were almost the same, also indicating that the different degree of swelling did not reflect the level of T-kininogen but HMW kininogen (Fig. 2), since the level of HMW kininogen in B/N-Ka rats was less than 1/30 of that of normal rats. All of these results indicate that neither T-kinin nor T-kininogen has any direct role in the paw swelling, while bradykinin may be released from the HMW kininogen to induce vascular permeability increase in the paw. This is quite different from the report of Barlas *et al.*¹³⁾, who found that in rats, T-kinin is released in the granuloma induced by carrageenin. Thus the question remains: What is the role of the increased level of T-kininogen?

ACKNOWLEDGEMENTS This work was partly supported by the Naito Foundation. The authors are grateful to Ms. Kazuko Hozumi (Department of Physiology, School of Hygiene) and Mr. Tatsuo Suzuki (Kitasato Institute) for breeding and taking care of Brown Norway Katholiek rats.

REFERENCES

- 1) H. Okamoto and L.M. Greenbaum, *Biochem. Biophys. Res. Commun.*, **112**, 701 (1983)
- 2) H. Okamoto and L.M. Greenbaum, *Life Sci.*, **32**, 2007 (1983)
- 3) I. Hayashi, T. Ino, H. Kato, S. Iwanaga, T. Nakano and S. Oh-ishi, *Thromb. Res.*, **36**, 509 (1984)
- 4) I. Hayashi, S. Oh-ishi, H. Kato, K. Enjyoji, S. Iwanaga and T. Nakano, *Thromb. Res.*, **39**, 313 (1985)
- 5) A. Barlas, H. Okamoto and L.M. Greenbaum, *Biochem. Biophys. Res. Commun.*, **129**, 280 (1985)
- 6) I. Hayashi, S. Oh-ishi, K. Enjyoji, H. Kato and S. Iwanaga, *Chem. Pharm. Bull.*, **34**, 3502 (1986)
- 7) J. Damas and A. Adam, *Mol. Phys.*, **8**, 307 (1985)
- 8) R. Kageyama, N. Kitamura, H. Ohkubo and S. Nakanishi, *J. Biol. Chem.*, **260**, 12060 (1985)
- 9) J. Damas and A. Adam, *Experientia* **36**, 586 (1980)
- 10) S. Oh-ishi and A. Sakuma, *Japan. J. Pharmacol.*, **20**, 337 (1970)
- 11) S. Oh-ishi, I. Hayashi, M. Hayashi, K. Yamaki, A. Yamasu, T. Nakano, I. Utsunomiya and Y. Nagashima, *Agents Actions*, **18**, 450 (1986)
- 12) J. Damas, G. Remacle-Volon and A. Adam, *Naunyn-schmied. Arch. Pharm.*, **325**, 76 (1984)
- 13) A. Barlas, K. Sugio and L.M. Greenbaum, *FEBS Lett.*, **190**, 268 (1985)

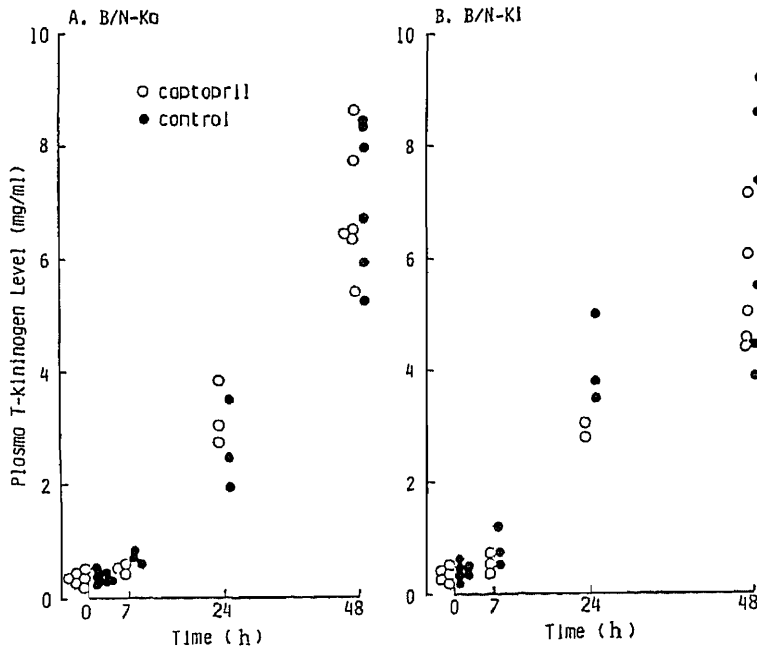


Fig. 1. Plasma T-kininogen levels in Brown Norway Katholiek (B/N-Ka)(A) and Brown Norway Kitasato (B/N-Ki)(B) rats following the carrageenin injection.

Intravenous injection of captopril, 10 mg/kg (o), or vehicle (o) were administered 30 min prior to the carrageenin injection.

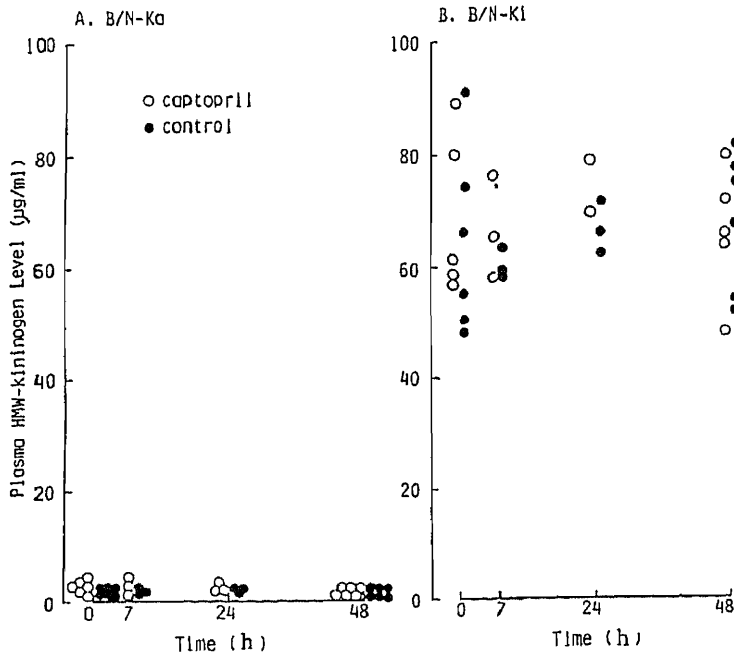


Fig. 2. Plasma HMW-kininogen levels in B/N-Ka (A) and B/N-Ki (B) rats following carrageenin injection into the paw.

Symbols are the same as in Fig. 1.

(Received January 22, 1987)

Communications to the Editor

[Chem. Pharm. Bull.]
35(3)1319—1321(1987)]

A NEW METHOD FOR INTRODUCING THE 2,2-DICHLOROETHYL GROUP AT THE 3 POSITION OF THE 2-QUINOLONE SYSTEM, AND THE SYNTHESIS OF DICTAMNINE¹⁾

Masayuki Sato, Katsuhiko Kawakami, and Chikara Kaneko*
Pharmaceutical Institute, Tohoku University,
Aobayama, Sendai 980, Japan

A novel method is described for the introducing the 2,2-dichloroethyl group at the 2-quinolone ring. The method from 4-substituted 2-quinolone consists of 1) photoaddition of the quinolone to 1,1-dichloroethylene, 2) base treatment of the cross adduct giving a bicyclobutane, and 3) conversion of the latter to the final product with hydrogen chloride. By applying this reaction to 4-methoxy-2-quinolone, a short-step synthesis of dictamnine is accomplished.

KEYWORDS — photo [2+2] cycloaddition; 2,2-dichloroethylation; furo[2,3-*b*]quinoline; dictamnine; 1,1a-methanocyclopropa[*c*]quinoline; cyclobuta[*c*]quinoline; 2-quinolone

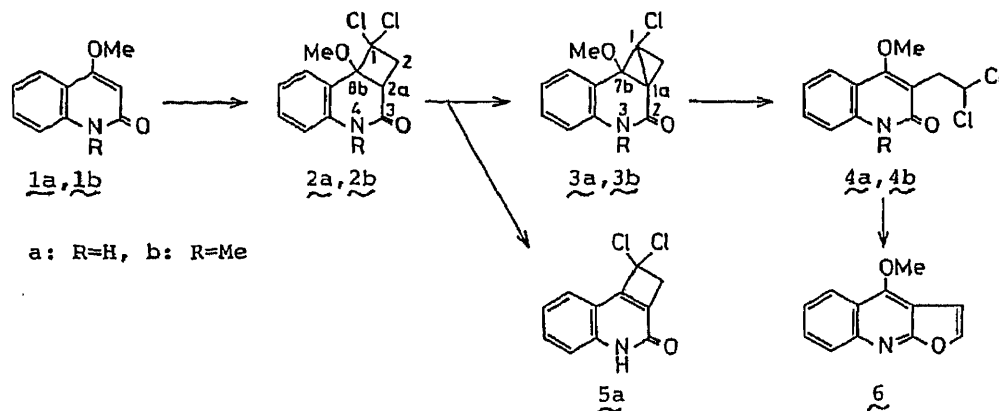
Photochemical cyclobutanation of a cyclic enone system, coupled with subsequent C-C bond fission in the strained four-membered ring, provides a useful method for the construction of a variety of complex carbon frameworks.^{2,3)} Our continuing studies concerning the application of this method to heteroaromatic compounds^{4,5)} have led us to examine the chemical behaviour of the cross adducts obtained from 2-quinolones and 1,1-dichloroethylene, with an expectation that the cyclobutanes thus formed would undergo C-C bond formation between 1- and 2a-positions to give highly strained bicyclobutane derivatives.

Here, we wish to report the reaction of the cross adduct obtained by photoaddition of 4-substituted 2-quinolones to 1,1-dichloroethylene with a base to give the bicyclobutane derivatives *via* expected C-C bond formation and their further reactions. The scope of the bicyclobutane formation and the application of this reaction to the synthesis of dictamnine are also reported.

A solution of 1.75 g (0.01 mol) of 4-methoxy-2-quinolone (**1a**) and 19.2 g (0.2 mol) of 1,1-dichloroethylene in methanol (1000 ml) was irradiated with a 400-W high-pressure mercury lamp through a Pyrex filter at room temperature for 1.5 h. Concentration of the reaction mixture gave 2.57 g (95%) of the cross adduct (**2a**: mp 158-159 °C)⁶⁾ as a sole product. The regiochemistry of the adduct was determined unequivocally by its NMR spectrum showing an ABX pattern [δ 2.76 (H_{2-endo}, dd, *J*=12 and 8 Hz), 3.24 (H_{2-exo}, dd, *J*=12 and 8 Hz), and 3.50 (H_{2a}, t, *J*=8 Hz)].⁶⁾

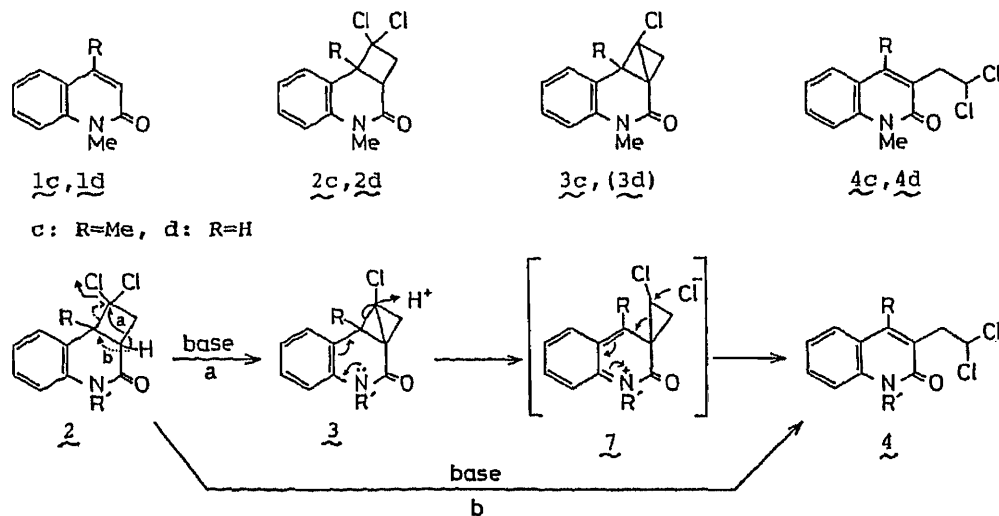
Treatment of **2a** with base (*tert*-BuOK/tetrahydrofuran, room temperature, 3 h) gave two products (**3a**: mp 213-215 °C and **5a**: mp 213-215 °C) in the respective yields of 65 and 12%. From NMR spectra, the major product (**3a**)⁷⁾ was revealed to be 1-chloro-7b-methoxy-1a,7b-dihydro-1,1a-methano-1H-cyclopropa[*c*]quinolin-2-(3H)-

one and the latter to be a simple cyclobutane-fused quinolone formed by base-catalyzed elimination of methanol. The formation of **3a** proceeds through the ring closure of **2a** via intramolecular S_N2 displacement of the C_1 -Cl bond by an attack of the carbanion at the 2a position. Treatment of **3a** with dry hydrogen chloride in dichloromethane (room temperature, a few min) afforded 3-(2,2-dichloroethyl)-4-methoxy-2-quinolone (**4a**: mp 197-198 °C)⁸⁾ in a quantitative yield.



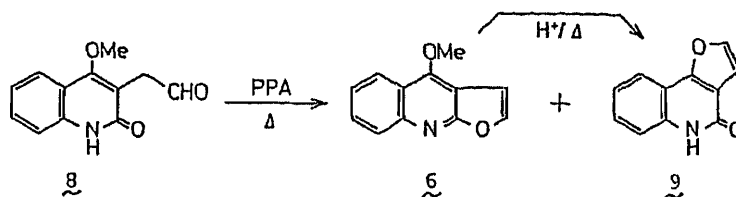
The same sequence of reactions applied to 1-methyl-2-quinolones (**1b** and **1c**) also afforded dichloroethyl derivatives (**4b**: mp 119-120 °C and **4c**: mp 122-123 °C) via the corresponding bicyclobutane derivatives (**3b**: mp 80-82 °C and **3c**: oil⁹⁾) as isolable intermediates.

Though each step in the above transformation proceeded with almost quantitative yields,¹⁰⁾ the adduct (**2d**) obtained from 1-methyl-2-quinolone (**1d**) directly afforded under the same basic conditions the dichloroethyl compound in 20% yield (**4d**: mp 84-85 °C) as the only isolable product. In this case, none of the corresponding bicyclobutane (**3d**) was detected. These facts clearly indicate that the presence of a substituent at the 8b position in the adduct (**2**) may play an important role in the formation of the bicyclobutane system (**3**), and the effects can be attributed to the steric strain in the adduct (**2**) which facilitates the formation of a central bond in the bicyclobutane (**3**). The conversion of **3** to **4** is best explained by assuming the spiro compound (**7**) as an intermediate. An alternative mechanism involving **2** as the intermediate (e.g. **3**→**2**→**4**) is denied by the inert-



ness of 2 under these acidic conditions.

The 1-unsubstituted 3-(2,2-dichloroethyl)-2-quinolones thus obtained may be useful synthons for furo[2,3-b]quinolines, when one considers that the 2,2-dichloroethyl group can function as a masked formylmethyl group. Actually when 4a was treated with potassium carbonate in acetone (reflux, 3 h), dictamnine (6: mp 131-132 °C, lit.¹¹) mp 132-133 °C), a furoquinoline alkaloid of *Dictamnus albus* Linn. and *Skimmia repens* Nakai; Rutaceae, was obtained in 75% yield as a sole product. The most efficient synthesis of this alkaloid so far reported involves cyclization of 3-formylmethyl-4-methoxy-2-quinolone (8), obtained from 4-methoxy-3-(3-methylbut-2-enyl)-2-quinolone by ozonolysis, with polyphosphoric acid.¹² However, the high temperature (ca. 180 °C) in acidic medium required for the cyclization step inevitably results in the concomitant formation of the angular compound (9).¹²



Elucidation of the detailed mechanism in each step in the above sequence and the scope of the reaction is now under investigation to develop a general method for synthesizing furo[2,3-b]quinoline and its derivatives.

ACKNOWLEDGEMENT This work was supported by a Ministry of Education, Science and Culture, Grant-in-Aid for Special Project Research No. 61123005.

REFERENCES AND NOTES

- 1) This paper forms Part 34 of "Cycloadditions in Synthesis." For Part 33: M. Sato, N. Katagiri, M. Muto, T. Haneda, and C. Kaneko, *Tetrahedron Lett.*, **27**, 6091 (1986).
- 2) S. W. Baldwin, "Org. Photochem." (A. Padwa, ed.), Marcel Dekker, N.Y. p. 122 (1982).
- 3) C. Kaneko, *Kagaku Sosetsu*, No.47, 107 (1985).
- 4) C. Kaneko and T. Naito, *Heterocycles*, **19**, 2183 (1982).
- 5) T. Naito and C. Kaneko, *J. Synth. Org. Chem. Jpn*, **42**, 51 (1984).
- 6) All new compounds were identified by either elemental analysis or by high-resolution mass spectra, and the structures were supported by acceptable spectral data.
- 7) ¹H-NMR (CDCl₃) of 3a, δ: 2.75 (1H, d, J=3 Hz), 3.13 (3H, s, Me), 3.24 (1H, d, J=3 Hz), 6.95-7.75 (4H, m, Ar-H), 10.10 (1H, br s, NH), ¹³C-NMR (CDCl₃) of the N-methyl derivative (3b), δ: 29.7 (q, N-Me), 31.9 (s, C-1a or C-1), 39.4 (t, CH₂) 40.4 (s, C-1 or C-1a), 54.5 (q, O-Me), 93.5 (s, C-7b), 115.0 (d), 117.2 (s, C-7a), 122.9 (d), 126.9 (d), 130.3 (d), 139.4 (s, C-3a), 163.4 (s, C-3).
- 8) ¹H-NMR signals of 2,2-dichloroethyl group in 4a appeared at δ 3.70 (2H, d, J=6 Hz) and 6.62 (1H, t, J=6 Hz) as a typical AX₂ pattern.
- 9) The ¹H-NMR signals of the geminal protons in 3c appeared at δ 2.44 and 3.13 as two sets of doublets (J=3 Hz).
- 10) None of the cyclobutaquinolones (5b or 5c) was obtained in the base-catalyzed cyclization reaction of 2b or 2c.
- 11) M. F. Grundon and N. J. McCorkindale, *J. Chem. Soc.*, **1957**, 2177.
- 12) J. F. Collins, G. A. Gray, M. F. Grundon, D. M. Harrison, and C. G. Spyropoulos, *J. Chem. Soc. Perkin Trans. I*, **1973**, 94.

(Received January 22, 1987)

Communications to the Editor

[Chem. Pharm. Bull.]
35(3)1322-1325(1987)

TIN-THALL REACTION, A VERSATILE METHOD FOR CROSS COUPLING
TIN COMPOUNDS WITH THALLIUM COMPOUNDS¹⁾

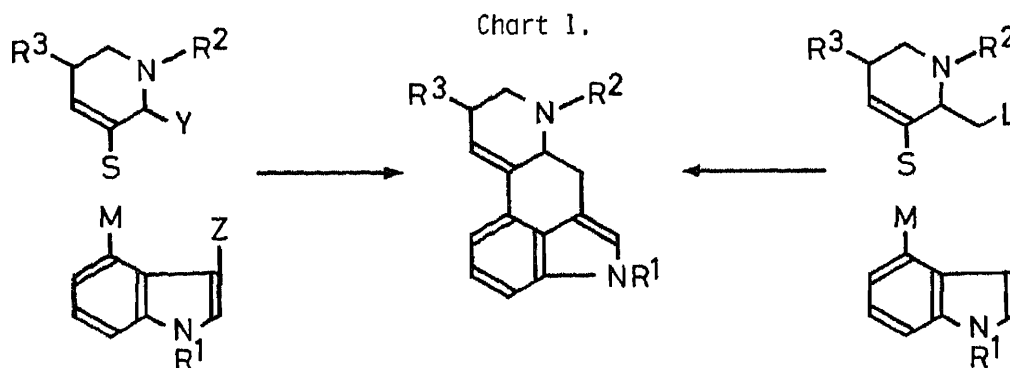
Masanori Somei,* Fumio Yamada, and Katsumi Naka

Faculty of Pharmaceutical Sciences, Kanazawa University, Kanazawa 920, Japan

A new cross coupling reaction between tin compounds and thallium compounds is developed and its versatility is demonstrated by the convenient synthesis of various 4-substituted indoles.

KEYWORDS ——— tin-thall reaction; thallation-palladation; cross coupling; 4-substituted indole; thallium compound; tin compound; palladium acetate; 4-(3-pyridyl)-3-indolecarbaldehyde

Our short step synthesis strategy for ergot alkaloids shown in Chart 1 led us to examine various known cross coupling reactions that have possibilities for incorporating pyridine derivatives²⁾ and cyclic compounds²⁾ into the 4-position of the indole nucleus. This survey resulted in the successful development of thallation-palladation³⁾ and boronation-thallation methods.^{2,3)} In our continuing work in search of an effective cross coupling reaction working directly at the 4-position of the indole nucleus, we have now found a new palladium-catalyzed reaction between tin and thallium compounds, designated the tin-thall reaction, as a version of the thallation-palladation method.³⁾ It has the advantage of being carried out in the presence of air and moisture.



The reaction of (3-formylindol-4-yl)thallium bis-trifluoroacetate⁴⁾ (2), prepared in 72% yield from 3-indolecarbaldehyde (1), with (3-pyridyl)trimethyltin⁵⁾ in the presence of a catalytic amount of palladium acetate in refluxing *N,N*-dimethylformamide produced 57% yield of 4-(3-pyridyl)-3-indolecarbaldehyde (3)^{2,6)} together with 1 and 4-methyl-3-indolecarbaldehyde (4) in 28% and 3% yields, respectively (Chart 2). Under similar reaction conditions, 4 was produced in 33% yield, together with 48% yield of 1, by treating 2 with tetramethyltin. 4-Phenyl-3-indolecarbaldehyde²⁾ (5) was also prepared in 54% yield in addition to 36% yield of 1 by

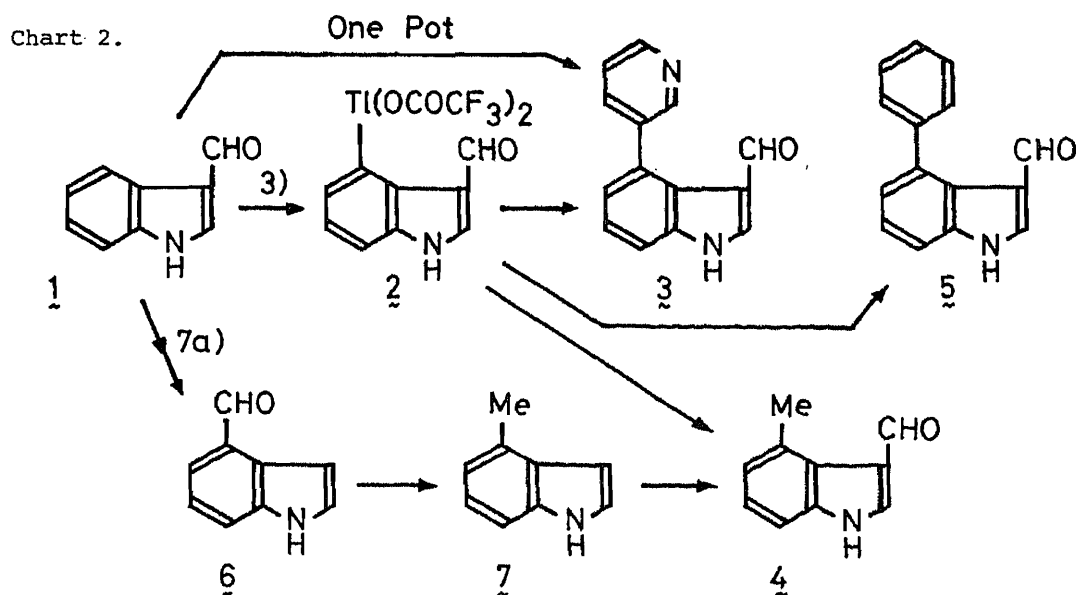
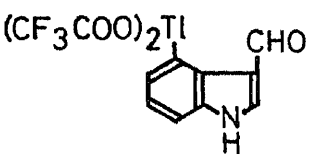
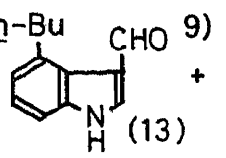
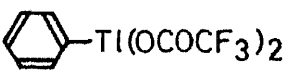
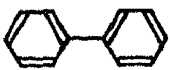
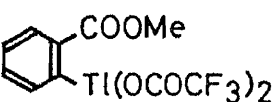
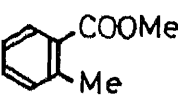
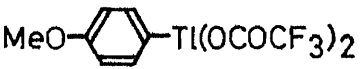

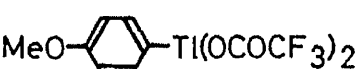
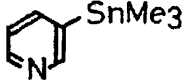
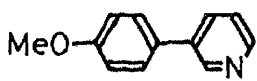


Table. The Palladium-Catalyzed Tin-Thall Reaction

Run	Thallium Compounds	Tin Compounds	Products (%)
1		$(n\text{-Bu})_4\text{Sn}$	 9) + 1) (13) (53)
2		Ph_4Sn	 10) (84)
3		Me_4Sn	 11) (38)
4		Ph_4Sn	 10) (49)
5			 11) (40)

treating 2 with tetraphenyltin.

The tin-thall reaction can be carried out in a one-pot procedure and the desired compounds are obtained directly from the starting materials. For example, after thallation of 1 with thallium tris-trifluoroacetate in trifluoroacetic acid, the solvent was removed under reduced pressure to give crude 2, which was treated without purification with (3-pyridyl)trimethyltin to afford 3, 1, and 4 in 45, 25, and 6% yields, respectively. The one-pot procedure and recycling of the recovered starting material make the present reaction profitable.

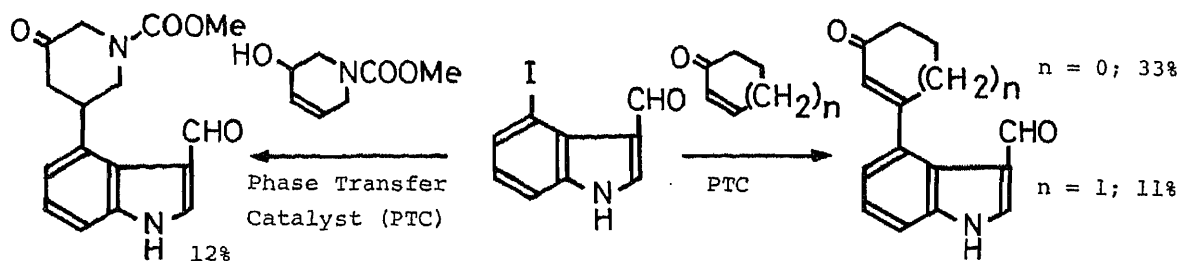
The structures of 3 and 5 were verified by direct comparison with authentic samples, prepared according to our reported procedure.²⁾ The structure of 4 was unequivocally proved by the following alternative synthesis. 4-Indolecarbaldehyde⁷⁾ (6) was converted to 4-methylindole⁸⁾ (7) in 90% yield by the Wolff-Kishner reduction using hydrazine, potassium hydroxide, and ethylene glycol. The subsequent Vilsmeier reaction applied to 7 afforded 4 in 66% yield.

Further applications of the tin-thall reaction and their results are summarized in the Table. As can be seen, variation of the substituent on both the tin and thallium compounds seems to have significant effect on the reaction, although the yields have not been optimized.

Investigations for establishing optimum reaction conditions such as changing solvents, reaction temperatures, catalysts, species of tin compounds, etc., are currently in progress.

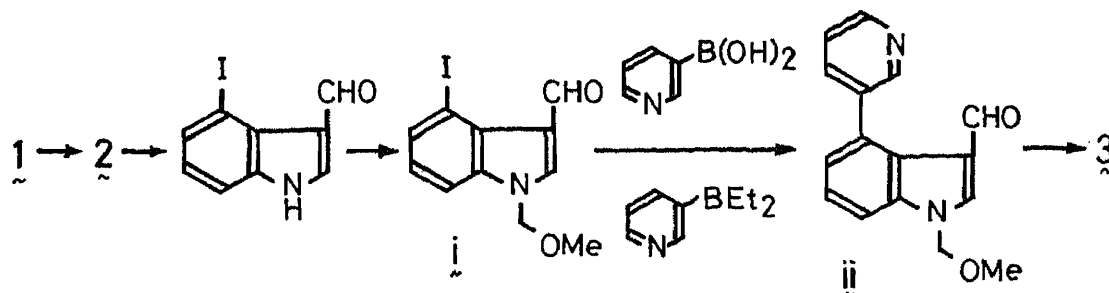
REFERENCES AND NOTES

- 1) This report is part XL of a series entitled "The Chemistry of Indoles." Part XXXIX: M. Somei, Y. Saida, T. Funamoto, and T. Ohta, Chem. Pharm. Bull., submitted. B-2969.
- 2) M. Somei, H. Amari, and Y. Makita, Chem. Pharm. Bull., 34, 3971 (1986); M. Somei, Advances in Pharmaceutical Sciences, The Research Foundation for Pharmaceutical Sciences, Vol. 1, 45 (1985); M. Somei, Yuki Gosei Kagaku Kyokai Shi, 40, 387 (1982). For example, the best results so far obtained were with the following improved Heck reactions: M. Somei, T. Hasegawa, T. Suzuki, and M. Wakida, The 105th Annual Meeting of Pharmaceutical Society of Japan, Kanazawa, April 1985, p679.



- 3) M. Somei, T. Hasegawa, and C. Kaneko, Heterocycles, 20, 1983 (1983).
- 4) M. Somei, F. Yamada, M. Kunimoto, and C. Kaneko, Heterocycles, 22, 797 (1984); R.A. Hollins, L.A. Colnago, V.M. Salim, and M.C. Seidl, J. Heterocycl. Chem., 16, 993 (1979). See also reference 3.
- 5) Y. Yamamoto and A. Yanagi, Chem. Pharm. Bull., 30, 1731 (1982).
- 6) Quite recently, we have newly found that both Suzuki's¹²⁾ and Terashima's¹³⁾

methods work well if the indole nitrogen is protected in advance. Thus, the 4-iodo-1-methoxymethyl-3-indolecarbaldehyde (i) reacted with 3-pyridylboronic acid or (3-pyridyl)diethylborane in the presence of a catalytic amount of palladium acetate to give 1-methoxymethyl-4-(3-pyridyl)-3-indolecarbaldehyde (ii) in 68% and 78% yields, respectively. However, the overall yield of 3 from 1 became insufficient to warrant further studies of total synthesis because of the inevitable extra three steps, iodination, protection, and deprotection. Therefore, we believe that the present tin-thall reaction is adequate to meet our end. Detailed results will be presented in due course.



- 7) a) F. Yamada and M. Somei, *Heterocycles*, in press, 26, No. 5 (1987); b) N. Hatanaka, N. Watanabe, and M. Matsumoto, *ibid.*, 24, 1987 (1986); c) M. Somei, F. Yamada, Y. Karasawa, and C. Kaneko, *Chem. Lett.*, 1981, 615; d) M. Somei, Y. Karasawa, and C. Kaneko, *ibid.*, 1980, 813; e) A.P. Kozikowski, H. Ishida, and Y.-Y. Chen, *J. Org. Chem.*, 45, 3350 (1980).
- 8) A.D. Batcho and W. Leimgruber, *Org. Synth.*, 63, 214 (1985); R.D. Clark and D. B. Repke, *J. Heterocycl. Chem.*, 22, 121 (1985); R.J. Sundberg and J.P. Laurino, *J. Org. Chem.*, 49, 249 (1984); M. Natsume and H. Muratake, *Tetrahedron Lett.*, 1979, 3477.
- 9) The structure of this compound was determined based on the spectral data.
- 10) These compounds were identified upon direct comparison with the commercial samples.
- 11) M. Ishikura, M. Kamada, and M. Terashima, *Heterocycles*, 22, 265 (1984); T. Yamazaki, M. Makimo, T. Yamamoto, K. Tsuji, H. Zenda, and T. Kosuge, *Yakugaku Zasshi*, 98, 914 (1978).
- 12) W.J. Thompson and J. Gaudino, *J. Org. Chem.*, 49, 5237 (1984); M. Miyaura, K. Yamada, and A. Suzuki, *Tetrahedron Lett.*, 1979, 3437.
- 13) M. Ishikura, I. Oda, and M. Terashima, *Heterocycles*, 23, 2375 (1985) and references cited therein.

(Received February 13, 1987)